RA
5.1.26

CVC-H02921-2 P024480



AJR

American
Journal of
Roentgenology

2

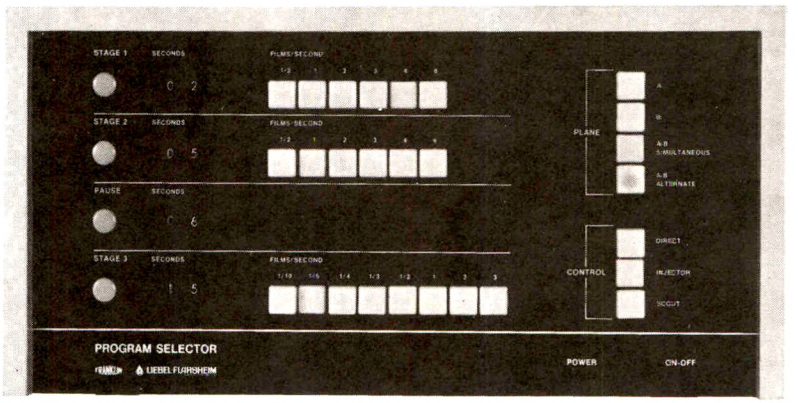
April 1976

developed for todays' angiographic needs

L-F'S NEW SOLID STATE PROGRAM SELECTOR

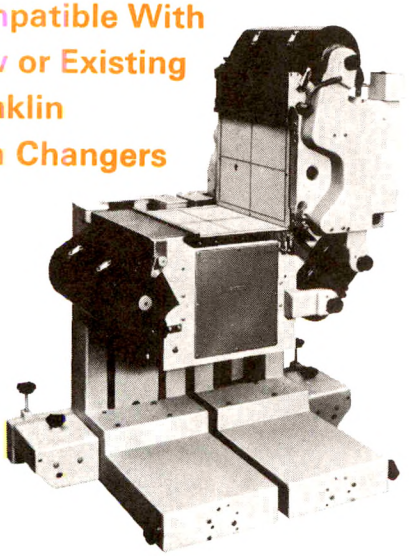
for use with Franklin Film Changers

- Precise, digital time settings, coupled with solid state pulse generators for accuracy
- Back-lighted, color-coded push button operation
- Trouble-free printed circuits
- Integrated circuit components



IMPROVED FUNCTIONAL FLEXIBILITY . . .

Compatible With New or Existing Franklin Film Changers



- Expanded film speeds for each stage . . . down to one film in 10 seconds on 3rd stage.
- Separate pause timer between 2nd and 3rd stages
- Instant program reset
- "Scout" film mode
- Separate handswitch
- Last film automatically advances into Receiver

LIEBEL-FLARSHEIM
SYBRON CORPORATION
111 East Amity Road, Cincinnati, Ohio 45215 U.S.A.

Volume 126

P24,430

AMERICAN JOURNAL OF ROENTGENOLOGY

EDITOR MELVIN M. FIGLEY
ASSISTANT EDITOR ROSALIND H. TROUPIN
ASSOCIATE EDITORS LUTHER W. BRADY
KENNETH L. KRABBENHOFT
E. FREDERICK LANG
RUSSELL H. MORGAN
EDITOR EMERITUS TRAIAN LEUCUTIA

INCLUDING DIAGNOSTIC RADIOLOGY, RADIATION ONCOLOGY, NUCLEAR MEDICINE ULTRASONOGRAPHY AND RELATED BASIC SCIENCES

CONSULTING EDITORIAL BOARD

KENT ELLIS
E. ROBERT HEITZMAN
DONALD L. KING
JOHN A. KIRKPATRICK, JR.
EUGENE C. KLATTE
JOHN G. McAFEE
THOMAS H. NEWTON
ROBERT G. PARKER
STEWART R. REUTER
WILLIAM B. SEAMAN
ROBERT J. SHALEK
JOHN STORER
MICHEL M. TER-POGOSSIAN
JOSEPH P. WHALEN
DAVID M. WITTEN

OFFICIAL JOURNAL
AMERICAN ROENTGEN RAY SOCIETY
AMERICAN RADIUM SOCIETY

The American Journal of Roentgenology is issued monthly by Charles C Thomas, Publisher, 301-327 East Lawrence Ave., Springfield, Illinois 62717. Correspondence regarding subscriptions, advertisements and other business should be addressed to the Publisher. Annual subscription prices: United States and U. S. Possessions $30.00, Pan America, Canada and others $35.00. Printed by the George Banta Co., Menasha, Wisconsin. Copyright © 1976 by American Roentgen Ray Society. Second-class postage paid at Springfield, Illinois and at additional mailing offices. Printed in U.S.A.

AMERICAN ROENTGEN RAY SOCIETY

OFFICERS 1975–76

President: Ted F. Leigh.
President Elect: Seymour F. Ochsner.
1st Vice President: Edward B. Singleton.
2nd Vice President: Sidney W. Nelson.
Secretary: James F. Martin.
Treasurer: Joseph D. Calhoun.
Honorary President: C. L. Sherratt.

COMMITTEES 1975–76

Executive Council: T. F. Leigh, S. F. Ochsner, E. B. Singleton, J. F. Martin, J. D. Calhoun, M. M. Figley, T. Leucutia, H. C. Carlson, R. C. Pfister, R. A. Gagliardi, M. P. Capp, E. Gedgaudas, G. A. Kling, C. B. Holman, W. B. Seaman, E. C. Klatte, J. P. Tampas, J. L. Gwinn, C. E. Bickham, H. L. Friedell, Chairman.

Finance and Budget Committee: J. J. Stein, C. E. Bickham, R. McLelland, J. L. Gwinn, H. C. Carlson, Chairman.

Publication Committee: E. R. Heitzman, J. V. Rogers, K. Ellis, F. F. Ruzicka, Jr., R. A. Gagliardi, Chairman.

Editorial Policy Committee: M. M. Figley, E. F. Lang, L. W. Brady, K. L. Krabbenhoft, R. H. Morgan, E. R. Heitzman, J. V. Rogers, K. Ellis, F. F. Ruzicka, R. A. Gagliardi, Chairman.

Program Committee: T. F. Leigh, J. F. Martin, H. L. Friedell, M. M. Figley, R. A. Gagliardi, R. C. Pfister, E. Gedgaudas, G. A. Kling, M. P. Capp, S. F. Ochsner, Chairman.

Advisory Committee on Education and Research: G. W. Hartman, L. F. Rogers, E. Gedgaudas, A. E. James, M. P. Capp, Chairman.

Scientific Exhibits Committee: B. G. Brogdon, R. J. Alfidi, R. C. Pfister, Chairman.

Instruction Courses: Director, E. Gedgaudas, Associate Director, H. O. Peterson.

Representatives on the American Board of Radiology: R. W. McConnell, J. F. Roach, S. W. Nelson.

Representative on the Board of Chancellors and Council of the American College of Radiology: W. B. Seaman.

ANNUAL MEETING: September 20–24, 1976, Washington, D. C., Washington Hilton Hotel.

SCIENTIFIC PROGRAM: Seymour Ochsner, *President Elect*, Ochsner Clinic, New Orleans, La.

MANAGER ANNUAL MEETING: George A. Kling, Harper Hospital, Detroit, Mich.

MEMBERSHIP: Hymer Friedell, Chairman, Executive Council,
Case Western Reserve University, Cleveland, Ohio 44106.

BUSINESS OFFICE: Keith W. Gundlach, Comptroller, American College of Radiology,
20 North Wacker Drive, Chicago, Illinois 60606.

AMERICAN RADIUM SOCIETY

OFFICERS: 1975–76

President: Felix N. Rutledge.
President Elect: Luther W. Brady.
1st Vice President: Elliott Strong.
2nd Vice President: Alfred Sherman.
Secretary: Richard H. Jesse.
Treasurer: Fred W. George, III.

COMMITTEES 1975–76

Executive Committee: V. A. Marcial, F. N. Rutledge, L. W. Brady, E. Strong, R. H. Jesse, A. I. Sherman, F. George, A. Raventos, Chairman.

Public Relations Committee: W. J. Taylor, R. G. Parker, W. G. Cosbie, J. M. W. Gibson, Chairman.

Publication Committee: K. L. Krabbenhoft, A. F. Schroeder, L. W. Brady, Chairman.

Scientific Program Committee: L. W. Brady, D. Johnson, A. S. Ketcham, F. N. Rutledge, Chairman.

Janeway Lecture Committee: A. S. Ketcham, S. H. Levitt, L. W. Brady, Chairman.

Local Arrangements Committee: J. M. W. Gibson, Chairman.

Representatives on the American Board of Radiology: J. J. Stein, E. Richard King, R. M. Scott.

Representative on the Board of Chancellors of the American College of Radiology: J. A. del Regato.

Liaison Representative on the National Council on Radiation Protection and Measurements: Lawrence W. Davis.

ANNUAL MEETING: May 9–14, 1976, Vancouver, British Columbia, Bayshore Inn.

SCIENTIFIC PROGRAM: Felix N. Rutledge, *President*, Houston, Texas

LOCAL ARRANGEMENTS: John M. W. Gibson, Vancouver, British Columbia

MEMBERSHIP: Richard H. Jesse, *Secretary*, M. D. Anderson Hospital and Tumor Institute,
Houston, Texas 77025.

BUSINESS OFFICE: Richard H. Jesse, 6723 Bertner Avenue, M.D. Anderson Hospital and Tumor Institute,
Houston, Texas 77025.

CONTENTS OF VOLUME 126

VOL. 126 JANUARY 1976 NO. 1

DIAGNOSTIC RADIOLOGY

Introduction of Caldwell Lecturer, 1975. *Harold G. Jacobson, M.D.* . . . 3
Iatrogenic Lesions of the Skeleton: Caldwell Lecture, 1975. *Ronald O. Murray, M.B.E., M.D.* . . . 5
Idiopathic Multicentric Osteolysis. *Terry Tyler, M.D., and H. D. Rosenbaum, M.D.* . . . 23
Myositis Ossificans Circumscripta: A Benign Lesion with a Malignant Differential Diagnosis. *Amy Beth Goldman, M.D.* . . . 32
Lesions Resembling Gout in Patients with Rheumatoid Arthritis. *Arnold S. Rappoport, M.B., J. Leland Sosman, M.D., and Barbara N. Weissman, M.D.* . . . 41
Bronchopulmonary Foregut Malformations: A Unifying Etiological Concept. *Kenneth B. Heithoff, M.D., Shashikant M. Sane, M.D., Hugh J. Williams, M.D., Charles J. Jarvis, M.D., John Carter, M.D., Peter Kane, M.D., and William Brennom, M.D.* . . . 46
Neuroepithelial (Colloid) Cysts: Pathogenesis and Unusual Features. *Enrique Palacios, M.D., Behrooz Azar-Kia, M.D., Michael Shannon, M.D., and Albert V. Messina, M.D.* . . . 56
Optimal Tomographic Technique to Demonstrate Common Bile Duct Stones: an *In Vitro* Study. *Gerald R. Smith, M.D., John W. Loop, M.D., and T. Noel K. Allan, M.B.B.S.* . . . 63
Successful Intravenous Cholecystocholangiography in the Jaundiced Patient Using Meglumine Iodoxamate (Cholovue). *Alan H. Robbins, M.D., Sinnadurai Earampamoorthy, M.D., Raymond S. Koff, M.D., Louis T. Di Fazio, Ph.D., Elizabeth A. Wickis, and Arthur N. Gertler, M.D.* . . . 70
Griffiths' Point: Critical Anastomosis at the Splenic Flexure: Significance in Ischemia of the Colon. *Morton A. Meyers, M.D.* . . . 77
Angiography and Ultrasonography: A Comparative Study of Abdominal Aortic Aneurysms. *William E. Wheeler, M.D., Michael C. Beachley, M.D., and Klaus Ranniger, M.D.* . . . 95
Coarctation of the Aorta: Roentgenographic Assessment after Operative Correction. *Arthur B. Simon, M.D., and Harvey L. Neiman, M.D.* . . . 101

RADIATION ONCOLOGY

External and Interstitial Radiation Therapy of Carcinoma of the Oral Tongue: A Review of 32 Years' Experience. *Karen K. Fu, M.D., J. Warner Ray, M.D., Eric K. Chan, R. T., and Theodore L. Phillips, M.D.* . . . 107
Comparison of Split-Course Radiation Therapy and Continuous Radiation Therapy for Unresectable Bronchogenic Carcinoma: 5 Year Results. *Robert E. Lee, M.D., David T. Carr, M.D., and Donald S. Childs, Jr., M.D.* . . . 116
Mediastinal Hodgkin's Disease. *Jerome M. Vaeth, M.D., Steven A. Moskowitz, M.D., and Jerold P. Green, M.D.* . . . 123
Elective Irradiation with the Electron Beam after Mastectomy for Breast Cancer. *Norah DuV. Tapley, M.D., and Eleanor D. Montague, M.D.* . . . 127
Treatment Selection in Primary Breast Cancer: Pathologic Considerations. *H. Stephen Gallager, M.D.* . . . 135
Treatment, Results and Prognostic Factors in Stage I and II Sarcomas of the Corpus Uteri. *Vitune Vongtama, M.D., John R. Karlen, M.D., Steven M. Piver, M.D., Yoshiaki Tsukada, M.D., and Robert H. Moore, M.S.* . . . 139
Irradiation of Endometrial Cancer in Patients with Medical Contraindication to Surgery or with Unresectable Lesions. *Robert C. Landgren, M.D., Gilbert H. Fletcher, M.D., Luis Delclos, M.D., and J. Taylor Wharton, M.D.* . . . 148
Experience with Twice-a-Day Fractionation in Clinical Radiotherapy. *Leonard J. Shukovsky, M.D., Gilbert H. Fletcher, M.D., Eleanor D. Montague, M.D., and H. Rodney Withers, M.D.* . . . 155
Volume and Time Factors in Interstitial Gamma-Ray Therapy. *H. T. Barkley, Jr., M.D., and G. H. Fletcher, M.D.* . . . 163
Low Energy Radionuclides for Permanent Interstitial Implantation. *B. S. Hilaris, M.D., J. H. Kim, M.D., and N. Tokita, M.D.* . . . 171

NUCLEAR MEDICINE

Gallium-67 Scans in Children with Solid Tumors. *Philip B. Lepanto, M.D., Jeffrey Rosenstock, M.D., Philip Littman, M.D., Abass Alavi, M.D., Milton Donaldson, M.D., and David E. Kuhl, M.D.* . . . 179

Officers . . . 187
Editorial:
Changing of the Guard . . . 188
News Items . . . 190
Book Review . . . 192
Books Received . . . 192
Society Proceedings . . . 193
Abstracts of Radiologic Literature . . . 200

VOL. 126 FEBRUARY 1976 NO. 2

RADIATION ONCOLOGY

Ovarian Cancer: Multifacet Disease; Multifarious Therapy and Therapists; Janeway Lecture, 1975. *George C. Lewis, Jr., M.D.* . . . 205
Combination of Conservative Surgery and Irradiation for Cancer of the Breast. *Gilbert H. Fletcher, M.D., Eleanor Montague, M.D., and Alvah J. Nelson, III, M.D.* . . . 216
Squamous Cell Carcinoma of the Oral Tongue and Floor of Mouth: Evaluation of Interstitial Radium Therapy. *Luis Delclos, M.D., Robert D. Lindberg, M.D., and Gilbert H. Fletcher, M.D.* . . . 223
Combined Radiation Therapy and 5-Fluorouracil for Advanced Squamous Cell Carcinoma of the Oral Cavity and Oropharynx: a Randomized Study. *Theodore C. M. Lo, M.D., Albert L. Wiley, Jr., M.D., Ph.D., Fred J. Ansfield, M.D., James H. Brandenburg, M.D., Hugh L. Davis, Jr., M.D., Frank F. Gollin, M.D., Robert O. Johnson, M.D., Guillermo Ramirez, M.D., and Halvor Vermund, M.D., Ph.D.* . . . 229
Carcinoma of the Oropharynx: Results of Megavoltage Radiation Therapy in 305 Patients. *Stephen A. Weller, M.D., Don R. Goffinet, M.D., Richard L. Goode, M.D., and Malcolm A. Bagshaw, M.D.* . . . 236
Non-Randomized Comparison of Preoperative Irradiation and Surgery *versus* Irradiation Alone in the Management of Carcinoma of the Tonsil. *Carlos A. Perez, M.D., Fransiska A. Lee, M.D., Lauren V. Ackerman, M.D., Joseph H. Ogura, M.D., and William E. Powers, M.D.* . . . 248
Initial Comparative Response to Peak Pions and X-Rays of Normal Skin and Underlying Tissue Surrounding Superficial Metastatic Nodules. *Morton M. Kligerman, M.D., G. West, M.D., John F. Dicello, Ph.D., C. J. Sternhagen, M.D., J. E. Barnes, Ph.D., R. Kenneth Loeffler, M.D., Frances Dobrowolski, H. T. Davis, Ph.D., James N. Bradbury, Ph.D., Thomas F. Lane, Donald F. Petersen, Ph.D., and Edward A. Knapp, Ph.D.* . . . 261
Initial Evaluation of Reduced Fractionation in the Irradiation of Malignant Epithelial Tumors. *Maurice Greenberg, M.D., Donald R. Eisert, M.D., and James D. Cox, M.D.* . . . 268
Patterns of Failure in Intracranial Astrocytomas after Irradiation: Analysis of Dose and Field Factors. *Omar M. Salazar, M.D., Philip Rubin, M.D., Joseph V. McDonald, M.D., and Michael L. Feldstein, Ph.D.* . . . 279
Pharmaco-Kinetics of Current Skeletal-Seeking Radiopharmaceuticals. *G. T. Krishnamurthy, M.B.B.S., R. J. Huebotter, B.A., M. Tubis, Ph.D., and W. H. Blahd, M.D.* . . . 293
Cancer of the Undescended or Maldescended Testis. *Mostafa A. Batata, M.D., Willet F. Whitmore, Jr., M.D., Basil S. Hilaris, M.D., Nobuhiko Tokita, M.D., and Harry Grabstald, M.D.* . . . 302
Effect of Therapeutic Irradiation on the Immune Responses. *James M. Slater, M.D., Ernest Ngo, M.D., and Benjamin H. S. Lau, Ph.D.* . . . 313

DIAGNOSTIC RADIOLOGY

The Spectrum of Osteoblastoma. *Richard A. McLeod, M.D., David C. Dahlin, M.D., and John W. Beabout, M.D.* . . . 321
Non-Rheumatic Acute Mitral Insufficiency Caused by Ruptured Chordae Tendineae. *Edward Buonocore, M.D., James J. Acker, M.D., and Hu A. Blake, M.D.* . . . 336
Hemochromatosis: A Disease Often Silent But Not Invisible. *Pamela S. Jensen, M.D.* . . . 343
Biliary Ascariasis in Children. *B. J. Cremin, F.R.A.C.R., and R. M. Fisher, M.B.* . . . 352
Intestinal Malrotation in Adults: Roentgenographic Assessment with Emphasis on Isolated Complete and Partial Nonrotations. *Emil J. Balthazar, M.D.* . . . 358
Arteriography of Retroperitoneal Lymphoma. *David C. Levin, M.D., David H. Gordon, M.D., Mahesh Kinkhabwala, M.D., and Joshua A. Becker, M.D.* . . . 368
Roentgenology-Pathology Correlative Study of Neovascularity. *Stephen L. Gammill, M.D., Frederick H. Shipkey, M.D., Elliot H. Himmelfarb, M.D., Louis S. Parvey, M.D., and Jack G. Rabinowitz, M.D.* . . . 376
Complications of Percutaneous Transaxillary Catheterization for Arteriography and Selective Chemotherapy. *Ruza Antonovic, M.D., Josef Rösch, M.D., and Charles T. Dotter, M.D.* . . . 386
Analysis of Cecal Vasculature in the Search for Vascular Malformations. *Jeanne W. Baer, M.D., and Stephen Ryan, M.D.* . . . 394
Computerized Reconstructive Tomography Applied to Breast Pathology. *David F. Reese, M.D., J. Aidan Carney, M.B., John J. Gisvold, M.D., Philip R. Karsell, M.D., and Stephen A. Kollins, M.D.* . . . 406
Efficacy of Pneumogynecography in the Diagnosis of Meyer-Rokitansky-Küster-Hauser Syndrome. *Spas A. Spasov, M.D., Stoyan I. Dokumov, M.D., Lubomir A. Diankov, M.D., Ivo M. Balkov, M.D., and Anton M. Sarkanyatz, M.D.* . . . 413
Retrocecal Appendicitis Presenting with Air in the Subhepatic Space. *Roger K. Harned, M.D.* . . . 416
Pulmonary Metastases from Intracerebral Meningioma: Diagnosis by Percutaneous Needle Aspiration Biopsy. *Anthony G. Peck, M.D., Carolyn G. Dedrick, M.D., and Priscilla D. Taft, M.D.* . . . 419
Hazards of the Intensive Care Unit. *Carl E. Ravin, M.D., Charles E. Putman, M.D., and Theresa C. McLoud, M.D.* . . . 423
A Device to Measure Roentgenographic Structures. *Gilles Hudon, M.D., Richard Moore, Ph.D., Sung Kim, M.S., and Kurt Amplatz, M.D.* . . . 432

Officers . . . 438
Editorial
The James Picker Foundation for Radiologic Research. MMF . . . 439
In Memoriam
Fernando G. Bloedorn, M.D., 1913–1975. *Gilbert H. Fletcher, M.D.* . . . 441
Charles Hanson Peterson, M.D., 1904–1975. *James G. Snead, M.D., John A. Martin, M.D., and Charles D. Smith, M.D.* . . . 444
Fifty-eighth Annual Meeting of the American Radium Society. *Felix N. Rutledge, M.D.* . . . 446
Fifty-eighth Annual Meeting of the American Radium Society: Preliminary Program . . . 447
News Items . . . 450
Books Received . . . 455
Society Proceedings . . . 456
Abstracts of Radiologic Literature . . . 463

VOL. 126 MARCH 1976 NO. 3

RADIATION ONCOLOGY

The Role of the Clinician in Community Cancer Control Activities. *Victor A. Marcial* 471
Radiation Therapy for Testicular Tumors Metastasizing to the Lungs. *Theodore C. M. Lo, M.D., and Yung H. Son, M.D.* 475
Radiation Therapy in the Treatment of Glioblastoma. *Yasuto Onoyama, M.D., Mitsuyuki Abe, M.D., Eizo Yabumoto, M.D., Tsutomu Sakamoto, M.D., Takehiro Nishidai, B.Sc., and Sumio Suyama, B.Sc.* 481
Growth Analysis of Pulmonary Metastases from Salivary Gland Tumors. *Frank G. Twardzik, M.D., and David M. Sklaroff, M.D., F.A.C.R.* 493
Concepts for Treatment of Micrometastases Developed in Murine Systems. *Frank M. Schabel, Jr., Ph.D.* 500

DIAGNOSTIC RADIOLOGY

Optimal Visualization of Esophageal Varices. *Edward M. Cockerill, M.D., Roscoe E. Miller, M.D., Stanley M. Chernish, M.D., Gordon C. McLaughlin, III, M.D., and Bruce E. Rodda, Ph.D.* 512
Involvement of the Gastric Antrum in Ménétrier's Disease. *Major William W. Olmsted, USAF, MC, Major Philip H. Cooper, MC, USA, and Major John E. Madewell, MC, USA* 524
Normal Pancreas and Splenic Variants Simulating Suprarenal and Renal Tumors. *A. K. Raja Rao, M.D., and Terry M. Silver, M.D.* 530
Fat Thickness in the Neonatal Small Left Colon Syndrome. *Lawrence R. Kuhns, M.D., Paul E. Berger, M.D., Andrew K. Poznanski, M.D., and John F. Holt, M.D.* 538
Rhabdomyosarcoma in the Pediatric Age Group. *Ned B. Hornback, M.D., and Homayoon Shidnia, M.D.* 542
Postadrenalectomy Pituitary Adenoma (Nelson's Syndrome) in Childhood: Clinical and Roentgenologic Detection. *Lionel W. Young, M.D., Gerald H. K. Lim, M.B., B.S., Gilbert B. Forbes, M.D., and Michael F. Bryson, M.D.* 550
Changing Clinical and Roentgenographic Patterns of Necrotizing Enterocolitis. *Jack G. Rabinowitz, M.D., and Robert L. Siegle, M.D.* 560
Arteriographic Manifestations of Pheochromocytoma. *Richard Christenson, M.D., Clyde W. Smith, M.D., and Henry Burko, M.D.* 567
Embolic Occlusion of the Superior and Inferior Divisions of the Middle Cerebral Artery with Angiographic-Clinical Correlation. *L. Reed Altemus, M.D., Glenn H. Roberson, M.D., C. Miller Fisher, M.D., and Michael Pessin, M.D.* 576
Cerebral Blood Volume Alterations During Fractional Pneumoencephalography. *Karsten Voigt and Torgny Greitz* 582
Frontal Ventricular Dimensions on Normal Computed Tomography. *Francis J. Y. Hahn, M.D., and Kwan Rim, Ph.D.* 593
Bronchography in Patients with Hemoptysis. *John V. Forrest, M.D., Stuart S. Sagel, M.D., and Gary H. Omell, M.D.* 597
Isolated Rotatory Subluxation of the Carpal Navicular. *Terry M. Hudson, M.D., William J. Caragol, M.D., and Jeremy J. Kaye, M.D.* 601
The Notched Articular Process of C7 (Dorsalization of C7). *Kenneth R. Kattan, M.D.* 612
Spinal Neurofibromatosis. *Norman E. Leeds, M.D., and Harold G. Jacobson, M.D.* 617

ULTRASOUND

Demonstration and Dimensional Analysis of the Normal Pancreas with Gray-Scale Echography. *Kai Haber, M.D., Atis K. Freimanis, M.D., and W. Michael Asher, M.D.* 624

CASE REPORTS

Intra- and Extracerebral Arachnoid Cyst: An Atypical Roentgenographic Presentation. *Richard E. Latchaw, Major, USAF, MC, and Joseph Nadell, Major, USAF, MC* 629
Radiation-Induced Renovascular Hypertension. *Gerald E. Staab, M.D., Charles J. Tegtmeyer, M.D., and William C. Constable, M.B., Ch.B., D.M.R.T.* 634
Postesophageal Narrowing Associated with Barrett Esophagus. *Alan E. Oestreich, M.D.* 638
Multichambered Bladder Anomalies. *Alexander A. Cacciarelli, M.D., Bruce Lucas, M.D., and William H. McAlister, M.D.* 642
Localized Nodular Synovitis of the Knee: A Report of Two Cases with Abnormal Arthrograms. *Thomas G. Goergen, M.D., Donald Resnick, M.D., and Gen Niwayama, M.D.* 647

Officers 651
Editorial:
Guidelines for the Modern Cardiac Catheterization-Angiocardiographic Laboratory: Report of the Inter-Society Commission for Heart Disease Resources. *Herbert L. Abrams* 652
News Items 654
Book Review 656
Books Received 656
Society Proceedings 658
Abstracts of Radiologic Literature 665

CONTENTS OF VOLUME 126

VOL. 126 APRIL 1976 NO. 4

DIAGNOSTIC RADIOLOGY

Virus Diseases of Bone. Do They Exist? The Neuhauser Lecture. *Frederic N. Silverman, M.* 677
Loss of Colonic Haustration in Progressive Systemic Sclerosis. *William Martel, M.D., Stanley F. Chang, M.D., and Murray R. Abell, M.D.* 704
Roentgen Findings in Aorto-Enteric Fistulae. *George M. Wyatt, M.D., Michael I. Rauchway, M.D., and Harold B. Spitz, M.D.* 714
Multiple Benign Ureteral Fibrous Polyps. *Felix A. Hughes, III, M.D., and Charles S. Davis, Jr., M.D.* 723
Cavitating Lung Nodules and Pneumothorax in Children with Metastatic Wilms' Tumor. *E. George Kassner, M.D., Harold S. Goldman, M.D., and Alberto Elguezabal, M.D.* 728
The Spotted Nephrogram of Renal Scleroderma. *Jeffrey Winograd, M.D., Daniel H. Schimmel, M.D., and Alphonse J. Palubinskas, M.D.* 734
The Role of Emergency Excretory Urography in Evaluation of Blunt, Abdominal Trauma. *Eugene J. McDonald, Jr., M.D., Melvyn Korobkin, M.D., Richard P. Jacobs, M.D., and Hideyo Minagi, M.D.* 739
Arthrography in Total Hip Prosthesis Complications. *Martin I. Gelman, M.D.* 743
The Grooves of the Distal Articular Surface of the Femur—A Normal Variant. *R. Brent Harrison, M.D., Mary Beth Wood, M.D., and Theodore E. Keats, M.D.* 751
Chiba Percutaneous Transhepatic Cholangiography: A Valuable Method for Visualizing the Nondilated Biliary Tract. *Joseph Tabrisky, M.D., Rabbe L. Lindstrom, M.D., Laurence G. Hanelin, M.D., and William F. Pfisterer, M.D.* 755
Organizing a Community Department for Academic Radiology. *D. William Sherrick, M.D., P. F. Mahon, M.D., David B. Lewis, M.D., and Erwin M. Janzen, M.D.* 761
Computerized Tomography (CT) in Acute Head Trauma. *Jorge Merino-deVillasante, M.D., and Juan M. Taveras, M.D.* 765
Individualized Computer Tomography of the Skull with the EMI Scanner Using the 160×160 Matrix. *Steven H. Cornell, M.D., Jacob J. Musallam, M.D., Ching L. Chiu, M.D., and James H. Christie, M.D.* 779
Computed Tomography of the Normal and Infarcted Myocardium. *Douglass F. Adams, Samuel J. Hessel, Philip F. Judy, Jay A. Stein, and Herbert L. Abrams* 786
The Value of Repeat Cerebral Arteriography in the Evaluation of Trauma. *Eugene J. McDonald, Jr., M.D., David P. Winestock, M.D., and Julian T. Hoff, M.D.* 792
Caudal Dislocation of the Pons in the Adult Arnold-Chiari Malformation: An Angiographic Evaluation. *Meredith Weinstein, M.D., and Thomas H. Newton, M.D.* 798
Angiographic Manifestations of Bilateral Wilms' Tumor. *Barry T. Katzen, M.D., and Melvin Markowitz, M.D.* 802
The Abdominal Angiographic Spectrum of Tuberous Sclerosis. *William R. Compton, M.D., Patrick D. Lester, M.D., Myo M. Kyaw, M.D., and Jack A. Madsen, M.D.* 807
The Complication Rate of Catheter Angiography by Direct Puncture Through Aorto-Femoral Bypass Grafts. *Ronald L. Eisenberg, M.D., Richard L. Mani, M.D., and Eugene J. McDonald, Jr., M.D.* 814
Systemic Arterial Supply to Normal Basilar Segments of the Left Lower Lobe. *Donald R. Kirks, M.D., Peter E. Kane, M.D., Edward A. Free, M.D., and Hooshang Taybi, M.D.* 817
Iatrogenic Embolization of the Superior Mesenteric Artery: Arteriographic Observations and Clinical Implications. *Adam Lande, M.D., and Morton A. Meyers, M.D.* 822
Partial Mesenteric Arterial Occlusion with Subsequent Ischemic Bowel Damage Due to Pitressin Infusion. *Cameron Roberts, M.D., and Frank E. Maddison, M.D.* 829

NUCLEAR MEDICINE

Radionuclide Imaging in Skeletal Inflammatory and Ischemic Disease in Children. *Massoud Majd, M.D., and Robert S. Frankel, M.D.* 832
"Doughnut" Sign in Brain Scanning. *Yavuz A. Tarcan, M.D., William Fajman, M.D., Joseph Marc, M.D., and David Berg, D.O.* 842

ULTRASONOGRAPHY

Ultrasonic Evaluation of the Unilateral Nonvisualized Kidney. *John P. Marangola, M.D., Patrick J. Bryan, F.R.C.R., and Farhad Azimi, M.D.* 853

RADIATION ONCOLOGY

Factors that Modify the Radio-Response of Cancer of the Nasopharynx. *Joseph Bohorquez, M.D.* 863
Definitive Treatment of Carcinoma of the Rectum by Intracavitary Radiation Therapy. *Gwynn Jelden, M.D., Ranjit Dhaliwal, M.D., Antonio Rodriguez-Antunez, M.D., Edward Chernak, B.S., R. Turnbull, M.D., Victor Fazio, M.D., and Frank Weakley, M.D.* 877
Serial Studies of Immunocompetence in Head and Neck Cancer Patients Undergoing Radiation Therapy. *Stefano Stefani, M.D., Ronald Kerman, Ph.D., and Joseph Abbate, M.D.* 880
Hemangiopericytoma: Report of Three Cases Regarding Role of Radiation Therapy. *Harbans Lal, M.D., B. Sanyal, M.D., G. C. Pant, M.D., B. L. Rastogi, M.D., N. N. Khanna, M.S., and K. N. Udupa, M.S.* 887

CASE REPORTS

Congenital Absence of the Ductus Venosus: With Direct Connection Between the Umbilical Vein and the Distal Inferior Vena Cava. *John C. Leonidas, M.D., and Richard A. Fellows, M.D.* 892
Aneurysmal Bone Cyst of the Orbit with Unusual Angiographic Features. *A. M. O'Gorman, M.B., and T. H. Kirkham, F.R.C.S.* 896
Vertebral Sarcoidosis: A Case Report and Review of the Literature. *Philip A. Brodey, M.D., Stephen Pripstein, M.D., Gerald Strange, M.D., and Nevea D. Kohout, M.D.* 900
Extra-Abdominal Desmoid of the Axillary Tail Mimicking Breast Carcinoma. *Lester Kalisher, M.D., John A. Long, M.D., and Robert G. Peyster, M.D.* 903

Officers 907
Editorial:
Is Nuclear Medicine in Trouble? John G. McAfee 908
News Items 910
Book Reviews 913
Books Received 915
Society Proceedings 917
Abstracts of Radiologic Literature 924

Vol. 126 May 1976 No. 5

DIAGNOSTIC RADIOLOGY

Cannon Lecture: Islet Cell Tumors and the Alimentary Tract. *R. M. Zollinger* 933

Angiography in Crohn's Disease Revisited. *F. Brahme and J. Hildell* 941

Hepatic Angiography in Ulcerative Colitis and Crohn's Disease. *L. Ekelund, A. Lunderquist, H. Dencker, and M. Åkerman* 952

Megacystis-Microcolon–Intestinal Hypoperistalsis Syndrome: A New Cause of Intestinal Obstruction in the Newborn. Report of Radiologic Findings in Five Newborn Girls. *W. E. Berdon, D. H. Baker, W. A. Blanc, B. Gay, T. V. Santulli, and C. Donovan* 957

Multiple "Bull's-eye" Lesions in Gastric Lymphoma. *N. R. Dunnick, G. S. Harell, and B. R. Parker* 965

Vascular Impressions of the Gut Secondary to Chronic Vascular Occlusive Disease. *L. Menuck and M. Coel* 970

A New Concept of Ascitic Fluid Distribution. *A. V. Proto, E. J. Lane, and J. P. Marangola* 974

Glucagon and Barium Enema Examinations: A Controlled Clinical Trial. *R. K. Harned, C. B. Stelling, S. Williams, and G. L. Wolf* 981

Spontaneous Internal Drainage of Pancreatic Pseudocysts. *J. L. Clements, Jr., E. L. Bradley, III, and S. B. Eaton, Jr.* 985

Lumbar Epidural Venography in the Diagnosis of Disc Herniations. *R. Gershater and R. C. Holgate* 992

Transfemoral Lumbar Epidural Venography. *M. H. Miller, S. F. Handel, and J. D. Coan* 1003

Epidural Venography: Diagnosis of Herniated Lumbar Intervertebral Disc and Other Disease of the Epidural Space. *G. F. Drasin, R. H. Daffner, R. F. Sexton, and W. C. Cheatham* 1010

The Cardiac Pacemaker: A Different Twist. *C. J. Tegtmeyer and J. M. Deignan* 1017

Iliocaval Thrombi in Pulmonary Thromboembolic Disease. *J. C. Rudikoff, P. R. Clapp, and E. J. Ferris* 1019

Venography in Penetrating Injuries of the Extremities. *A. J. Gerlock, Jr., E. R. Thal, and W. H. Snyder, III* 1023

Selective Arterial Embolization for Control of Hemorrhage in Pelvic Malignancy: Femoral and Brachial Catheter Approaches. *F. J. Miller, Jr., R. Mortel, W. J. Mann, and A. E. Jahshan* 1028

Peripheral Embolization Complicating Bilateral Renal Infarction with Gelfoam. *J. Woodside, H. Schwarz, and P. Bergreen* 1033

Crossed Renal Ectopia: Angiographic Findings in Six Cases. *Z. J. Rubinstein, M. Hertz, N. Shahin, and V. Deutsch* 1035

Angiographically Induced Renal Failure and Its Radiographic Detection. *R. A. Older, J. P. Miller, D. C. Jackson, I. S. Johnsrude, and W. M. Thompson* 1039

Arthrographic Evaluation of Injuries of the First Metacarpophalangeal Joint: Gamekeeper's Thumb. *D. Resnick and L. A. Danzig* 1046

Isolated Fracture of the Medial Portion of the Lateral Mass of the Atlas: A Previously Undescribed Entity. *E. G. Barker, Jr., J. Krumpelman, and J. M. Long* 1053

Concomitant Dislocation and Intraarticular Foreign Body: A Rare Complication of the Charnley Total Hip Arthroplasty. *R. E. Campbell and J. P. Marvel, Jr.* 1059

Embryogenesis of the Human Occipital Bone. *R. Shapiro and F. Robinson* 1063

Film Screening by Physician Assistants in Diagnostic Radiology. *E. G. Barker, Jr., H. D. Rosenbaum, A. C. Selke, Jr., D. Henderson, and J. H. Hildner* 1069

NUCLEAR MEDICINE

^{99m}Tc-Diphosphonate Uptake in Neuroblastoma. *W. McCartney, M. L. Nusynowitz, B. E. F. Reimann, J. Prather, and B. Mazat* 1077

RADIATION ONCOLOGY

Adjuvant Chemoimmunotherapy in Advanced Lesions of the Head and Neck. *F. R. Eilber and D. L. Morton* 1082

Immunotherapy of Malignancies: Current Status. *F. R. Eilber, E. C. Holmes, D. L. Morton, K. P. Ramming, and F. C. Sparks* 1088

Editorial: CT and the Planners. *T. F. Meaney* 1095

News Items 1098

Society Proceedings 1100

Abstracts of Radiologic Literature 1107

Vol. 126 June 1976 No. 6

DIAGNOSTIC RADIOLOGY

Hickey Lecture: New Frontier for Radiology: Computed Tomography. *G. G. Evens* 1117
Breast Patterns as an Index of Risk for Developing Breast Cancer. *J. N. Wolfe* 1130
Radiographic Visualization of Left Ventricular Aneurysms on Lateral Chest Film. *R. D. Kittredge, B. Gamboa, and H. G. Kemp* 1140
The Chest X-ray in Acute Left Ventricular Power Failure: An Aid to Determining Prognosis of Patients Supported by Intraaortic Balloon Pumping. *P. N. Cascade, A. Kantrowitz, W. J. Wajszczuk, and M. Rubenfire* 1147
Abnormal Left Ventricular Catheter Motion: An Ancillary Angiographic Sign of Left Atrial Myxoma. *J. M. Rausch, R. T. Reinke, K. L. Peterson, and C. B. Higgins* 1155
Evaluation of Routine Double Contrast Views of the Anterior Wall of the Stomach. *M. R. Goldsmith, R. E. Paul, Jr., W. E. Poplack, J. P. Moore, H. Matsue, and S. Bloom* 1159
Intussusception of the Appendix in Children. *G. O. Atkinson, B. B. Gay, Jr., and D. Naffis* 1164
Plain Film Findings of Gastric Volvulus Herniating into the Chest. *L. Menuck* 1169
Chondrosarcoma of the Esophagus. *I. Yaghmai and G. G. Ghahremani* 1175
Localized Giant Pseudopolyposis in Ulcerative Colitis. *J. W. Keating, Jr., and H. J. Mindell* 1178
Clinical and Radiographic "Reankylosis" Following Hip Surgery in Ankylosing Spondylitis. *D. Resnick, I. L. Dwosh, T. G. Goergen, R. F. Shapiro and R. D'Ambrosia* 1181
Medial Deviation of the Upper Pole Calyx on the Intravenous Urogram as an Indication of Vesicoureteral Reflux. *R. B. Harrison, S. S. Howards, and B. R. Thomas* 1189
Ultrasound Diagnosis of Posttransplant Renal Lymphocele. *J. F. Phillips, H. L. Neiman, and T. L. Brown* 1194
Pseudotumor of the Kidney: A Sequel to Regional Glomerulonephritis. *T. A. Depner, K. G. Ryan, and H. Yamauchi* 1197
Tortuosity of the Cavernous Carotid Arteries Causing Sellar Expansion Simulating Pituitary Adenoma. *R. D. Anderson* 1203
Serial Cerebral Angiography in Stereoscopic Magnification. *M. Takahashi, Y. Tamakawa, K. Goto, and M. Kosaka* 1211
Radiologic Changes in the Thymoma-Hypogammaglobulinemia Syndrome. *R. E. Moffat* 1219
Cerebro-Costo-Mandibular Syndrome: Long Term Follow-up of a Patient and Review of the Literature. *H. J. Williams and S. M. Sane* 1223
Intestinal Perforation Secondary to Nasojejunal Feeding Tubes. *R. L. Siegle, J. G. Rabinowitz, and C. Sarasohn* 1229
Lesion Conspicuity, Structured Noise, and Film Reader Error. *H. L. Kundel and G. Revesz* 1233
A Circular Test Pattern for Evaluating X-ray Tube Focal Spots. *G. H. Zeman, G. U. V. Rao, and R. J. Doyle* 1239

NUCLEAR MEDICINE

Lack of Gallium Uptake in Primary Hepatic Amyloidosis. *T. G. Goergen, A. Taylor, and N. Alazraki* 1246
Incidentally Detected Thrombosed Vein during ^{67}Ga Citrate Scanning. *C. H. Park, F. J. Miller, A. Lipton, and H. Harvey* 1249

RADIATION ONCOLOGY

Electron Beam Therapy in Head and Neck Tumors. *D. A. Tobin, W. Hall, and R. M. Scott* 1251
Surgical Treatment of Advanced Carcinoma of the Floor of the Mouth. *O. M. Guillamondegui and R. H. Jesse* 1256
Central Axis Depth Dose for a 2.5 MV Van de Graaff Generator. *D. W. Anderson, D. E. Raeside, R. I. Adams, and M. R. Goede* 1260

SPECIAL SECTION: International Bone Mineralization Conference Abstracts 1266

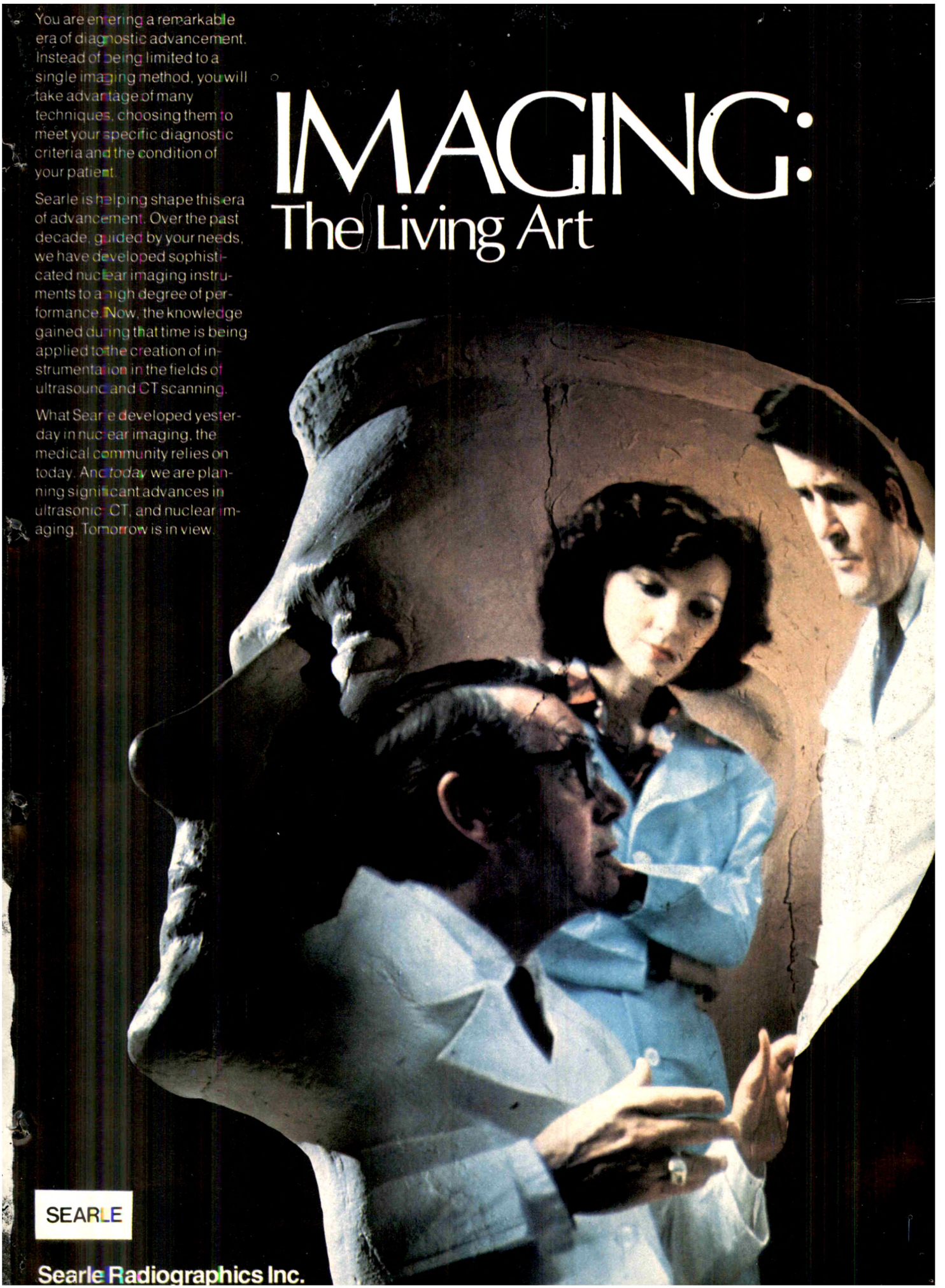
Editorial: Bone Mineral Measurement. *J. P. Whalen* 1315
77th ARRS Meeting Announcement and Preliminary Program 1316
Memorial: Paul A. Bishop 1325
News 1327
Literature Abstracts 1331
Volume Index 1339

IMAGING: The Living Art

You are entering a remarkable era of diagnostic advancement. Instead of being limited to a single imaging method, you will take advantage of many techniques, choosing them to meet your specific diagnostic criteria and the condition of your patient.

Searle is helping shape this era of advancement. Over the past decade, guided by your needs, we have developed sophisticated nuclear imaging instruments to a high degree of performance. Now, the knowledge gained during that time is being applied to the creation of instrumentation in the fields of ultrasound and CT scanning.

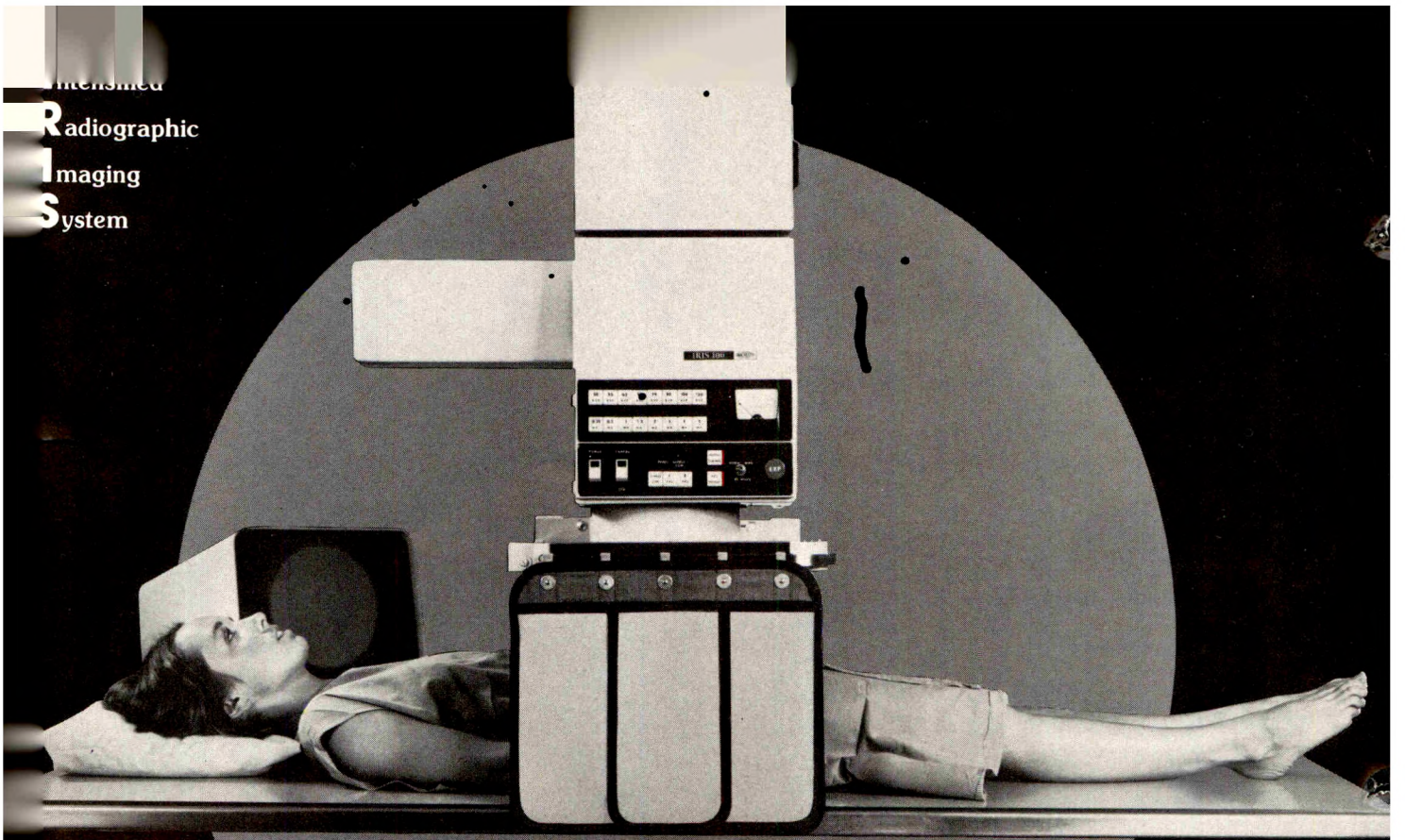
What Searle developed yesterday in nuclear imaging, the medical community relies on today. And today we are planning significant advances in ultrasonic, CT, and nuclear imaging. Tomorrow is in view.



SEARLE

Searle Radiographics Inc.

Intensified
Radiographic
Imaging
System



IRIS 100 adds television fluoroscopy and 100mm spotfilming to your present x-ray room.

Machlett's IRIS 100 system is a sound investment — both for the diagnostician and for the hospital — because it provides the most modern television fluoroscopy/spotfilming capabilities without the need for buying a whole new x-ray room. By improving the radiologist's productivity, moreover, IRIS 100 enables him to apply his much needed skills to a greater patient load.

While its cost is attractive, the real reasons for selecting IRIS 100 for your x-ray room are far more important:

Image Sharpness Machlett's Cesium Iodide Image Intensifier tube with its three focusing grids assures bright, sharp images both on film and on the television screen.

Short F-R-F Time Machlett's "sliding mirror" image distributor lets you quietly shift from fluoroscopy to spot radiography and back to fluoroscopy in *less than one second*.

Rapid Filming The Old Delft "Anodica" camera takes 100mm films singly or sequentially at 1-per-second or 2-per-second rates. Exposures are short enough to freeze peristaltic motion. Phototiming assures uniform film densities.

Human-Engineered Controls Controls are conveniently placed and designed for operation with gloved hands. Warning lights and interlocks eliminate such human errors as exposure without film.

Positive Patient ID The 100mm camera will not operate without the patient identification card in place. Film is identified at the time it is exposed.

For the whole story on IRIS 100, contact your x-ray equipment dealer or

MACHLETT

Machlett Laboratories, Incorporated
A Raytheon Company
1063 Hope Street
Stamford, Connecticut 06907
(203) 348-7511

See the IRIS 100 in Machlett's booth at the RSNA Meeting.

AMERICAN JOURNAL OF ROENTGENOLOGY

EDITOR MELVIN M. FIGLEY
ASSISTANT EDITOR ROSALIND H. TROUPIN
ASSOCIATE EDITORS LUTHER W. BRADY
KENNETH L. KRABBENHOFT
E. FREDERICK LANG
RUSSELL H. MORGAN
EDITOR EMERITUS TRAIAN LEUCUTIA

INCLUDING DIAGNOSTIC RADIOLOGY, RADIATION ONCOLOGY, NUCLEAR MEDICINE, ULTRASONOGRAPHY AND RELATED BASIC SCIENCES



CONSULTING EDITORIAL BOARD

KENT ELLIS
E. ROBERT HEITZMAN
DONALD L. KING
JOHN A. KIRKPATRICK, JR.
EUGENE C. KLATTE
JOHN G. McAFEE
THOMAS H. NEWTON
ROBERT G. PARKER
STEWART R. REUTER
WILLIAM B. SEAMAN
ROBERT J. SHALEK
JOHN STORER
MICHEL M. TER-POGOSSIAN
JOSEPH P. WHALEN
DAVID M. WITTEN



OFFICIAL JOURNAL
AMERICAN ROENTGEN RAY SOCIETY
AMERICAN RADIUM SOCIETY



The American Journal of Roentgenology is issued monthly by Charles C Thomas, Publisher, 301–327 East Lawrence Ave., Springfield, Illinois 62717. Correspondence regarding subscriptions, advertisements and other business should be addressed to the Publisher. Annual subscription prices: United States and U. S. Possessions $30.00, Pan America, Canada and others $35.00. Printed by the George Banta Co., Menasha, Wisconsin. Copyright © 1976 by American Roentgen Ray Society. Second-class postage paid at Springfield, Illinois and at additional mailing offices. Printed in U.S.A.

GUIDELINES FOR AUTHORS

The AMERICAN JOURNAL OF ROENTGENOLOGY publishes original and timely contributions to the advancement of radiologic diagnosis and treatment. Although the content is predominantly clinical in origin, laboratory investigations are accepted when their relevance to clinical practice is demonstrable. Contributions are reviewed by two outside consultants and are accepted on condition that they are submitted only to this Journal and that they will not be reprinted or translated without consent of the Editor. Statements within an article are the responsibility of the authors and not the Journal or its publisher.

Address all manuscripts and correspondence to the Editor, Dr. Melvin M. Figley, 403 Pacific National Bank Building, 4545 15th Avenue N.E., Seattle, Washington 98105.

Manuscript Form

Manuscripts should be typed double-spaced throughout, including references, tables, and footnotes. Tables, footnotes, and figure legends should be on separate sheets, and a separate title page should be provided. In addition to the original typewritten copy, a duplicate copy complete with figures, tables, and references is required.

Figures should be submitted as 5″×7″ glossy prints, untrimmed and unmounted. Identifying information (author name, figure number, and indication of the top of the figure) should be attached to the back of each figure with a gummed label. Line illustrations and graphs should be drawn in black ink on white background. Labels on all figures should be of professional quality and sufficiently large to be easily read when reduced in size.

References should be cited in the text by number (e.g., [3, 4]). The bibliography should be arranged in the numerical order that references are cited in the text and typed double-spaced throughout. Data for each reference should be arranged according to the uniform style on bibliographic citations adopted by many biomedical journals. Abbreviations for titles of medical periodicals should conform to those published in *Index Medicus*. Examples:

1. Miller RE, Chernish SM, Skulas J, Rosenak BD, Rodda BE: Hypotonic roentgenography with glucagon. *Am J Roentgenol* 121:264–274, 1974
2. Boijsen E: Superior mesenteric angiography, in *Angiography*, edited by Abrams H, Boston, Little, Brown, 1971, pp 1091–1119

Organization

Title page. Titles should be brief and specific. Include full names and addresses of all authors and acknowledgment of grant support when appropriate.

Abstract. A description of the purpose, methods, results, and conclusions of the study is required. It should be informative to a reader who has not read the text of the article.

Key indexing words. Five to 10 words or short phrases should be supplied to enable cross-indexing of the article.

Introduction. Clearly state the purpose of the investigation including necessary background facts.

Materials and methods. Describe the protocol clearly so that an experienced worker can understand what was done. Use standard abbreviations as presented in the *Council of Biology Editors Style Manual*, 3d edition.

Results. Present results in logical sequence.

Discussion. Interpret the results to lend meaning and importance to the observations. If hypotheses and speculation are included, they must be labeled as such. When results differ from those of previous investigators, an attempt should be made to explain the discrepancy.

References. Only include those references which provide adequate background and present fairly any opposing evidence and concepts. Accuracy of reference data is the responsibility of the author.

Legends. Legends should be brief but should provide sufficient description to interpret the figure.

Special Communications

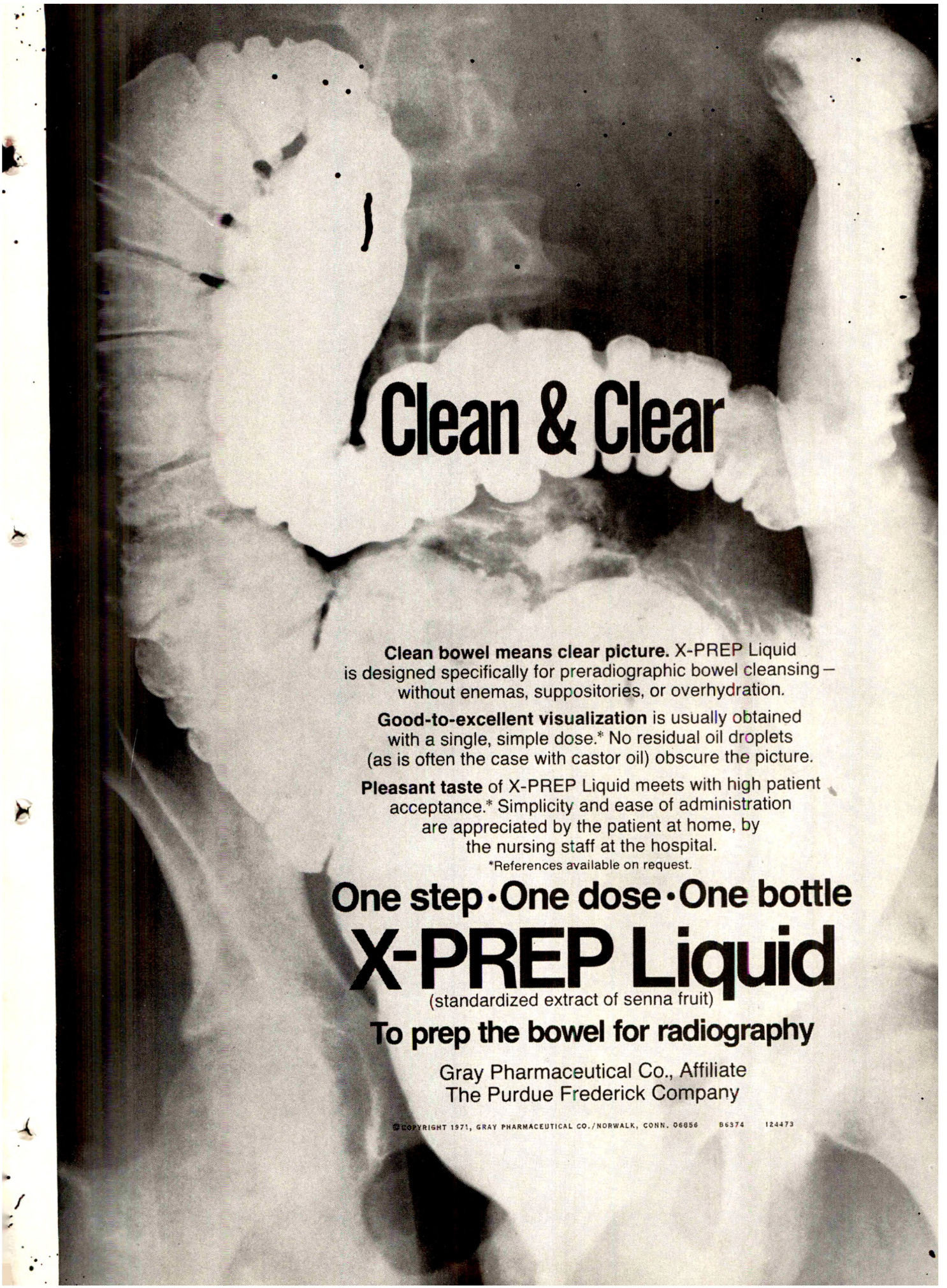
Case Reports. Concise case reports are accepted if they present unusual experiences that are medically important and educational. Clarity and brevity are essential.

Technical notes. Brief descriptions of new techniques or significant modifications of older ones which are directly applicable to clinical practice will be accepted.

Letters to the Editor. Letters should be limited to between 250 and 500 words. Criticism of published articles should be objective and constructive. Letters may also discuss matters of general interest to radiologists.

Proofs and Reprints

Copy-edited manuscripts are sent to the author for checking prior to typesetting. Galley proofs will be sent for correction of typographical errors only. The corrected proof, copy-edited manuscript, and the reprint order should be returned directly to the Editor. If the author fails to return proof by the date specified, it may be necessary to publish without the author's approval.



Clean bowel means clear picture. X-PREP Liquid is designed specifically for preradiographic bowel cleansing—without enemas, suppositories, or overhydration.

Good-to-excellent visualization is usually obtained with a single, simple dose.* No residual oil droplets (as is often the case with castor oil) obscure the picture.

Pleasant taste of X-PREP Liquid meets with high patient acceptance.* Simplicity and ease of administration are appreciated by the patient at home, by the nursing staff at the hospital.

*References available on request.

One step • One dose • One bottle

X-PREP Liquid

(standardized extract of senna fruit)

To prep the bowel for radiography

Gray Pharmaceutical Co., Affiliate
The Purdue Frederick Company

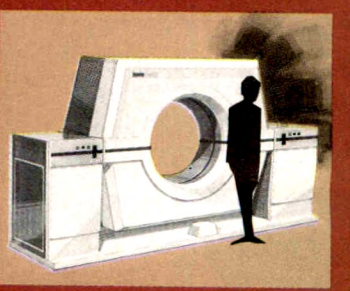
©COPYRIGHT 1971, GRAY PHARMACEUTICAL CO./NORWALK, CONN. 06856 B6374 124473

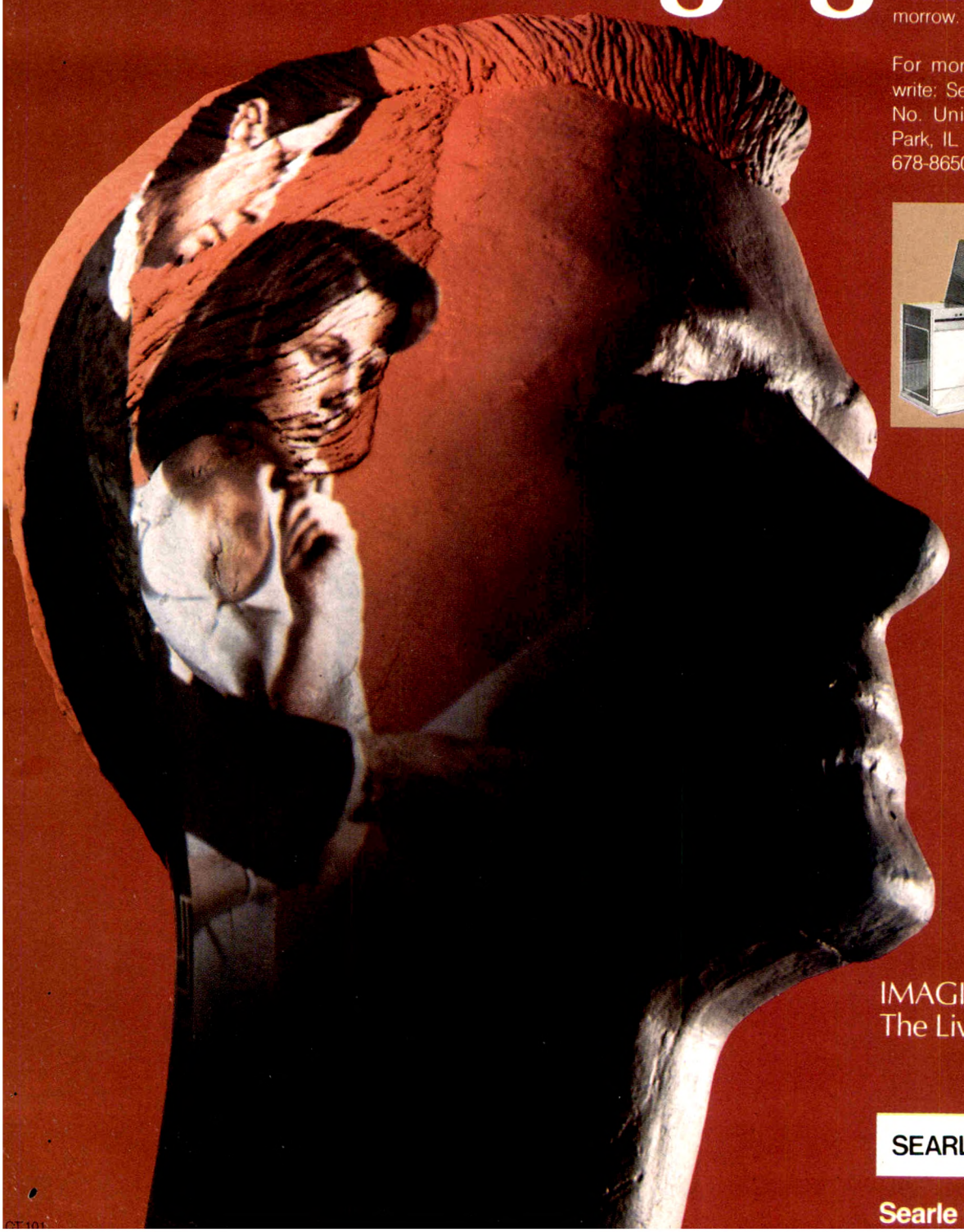
Designed for better CT imaging

Searle will soon introduce a new X-ray CT imager. This highly sophisticated instrument uses advanced mechanical and electronic technology to make CT imaging of the future a practical reality today.

This new system is now being evaluated and will be released for sale when its reliability, speed, and diagnostic superiority have been established. What Searle is developing today, the medical community relies on tomorrow.

For more information, call or write: Searle CT Systems, 4233 No. United Parkway, Schiller Park, IL 60176. Telephone (312) 678-8650.





IMAGING:
The Living Art

SEARLE

Searle CT Systems

CT 101

Pfizer Medical Systems, Inc. announces 57,600 reasons why the ACTA-SCANNER®

provides superior resolution and image clarity in whole body computerized tomographic scanning



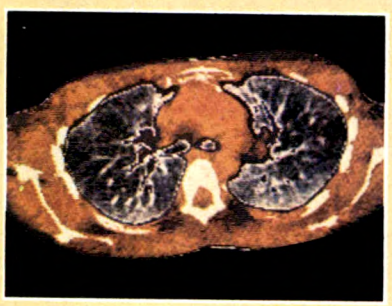
ACTA-SCANNER

WHOLE BODY COMPUTERIZED TOMOGRAPHIC SCANNER

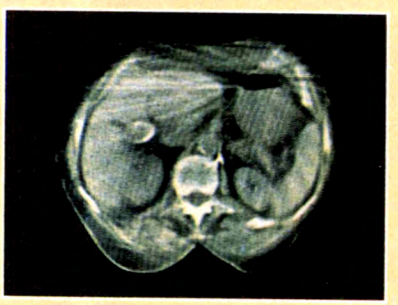
The new matrix improves image quality

Up to 57,600 absorption values are now actually measured for translation into the finished ACTA-scan with the recently developed 320 matrix.

This means a large, high-resolution display (1.5 mm) with greater clarity and true detail—important in extracranial scanning.



Thoracic 320 Scan. (Normal Chest)

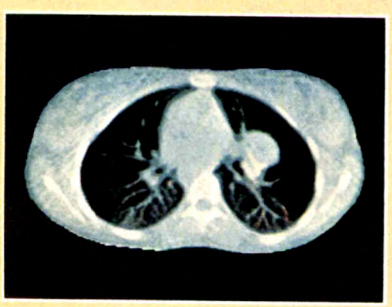


Abdominal 320 Scan. "Porcelain" Gallbladder

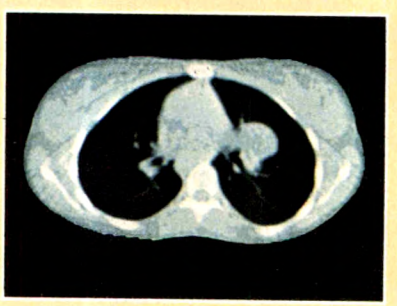
Multiple windows let you see more

With the Pfizer ACTA-Scanner, multiple windows can be imposed upon the image, allowing tissues with great density differences to be viewed at the same time in a single ACTA-scan.

This capability greatly facilitates interpretation of scans in the thoracic and abdominal areas.



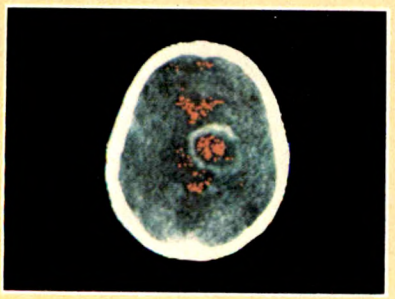
Thoracic scan with multiple windows. Mass in right lung.



Same area as scanned at left, without imposition of the multiple window capability.

And you can enlarge selected areas

A special cursor—or movable dot—allows the operator of the ACTA-Scanner to enlarge selected areas of interest by a factor of 2 in diameter (4 in area).

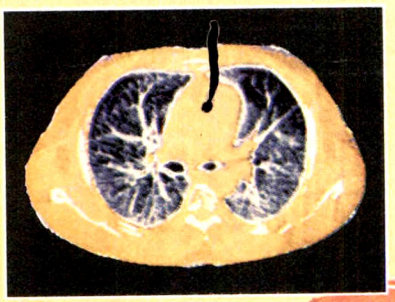


Pituitary Adenoma

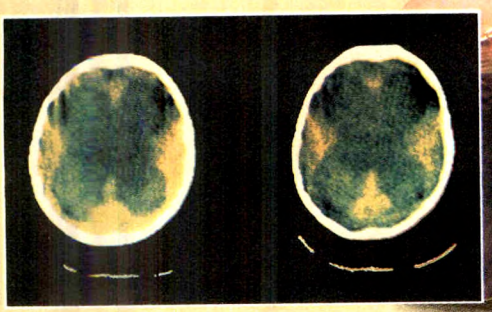


Pituitary Adenoma. Instantaneous enlargement of pathologic area

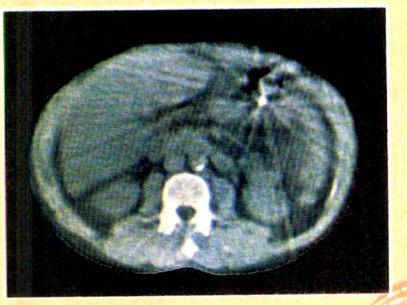
Pathology in virtually any part of the body can be visualized and evaluated. •



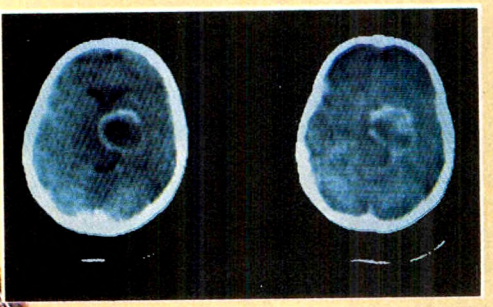
Thoracic 320 Scan.
(Normal Chest)



Marked Hydrocephalus



Abdominal 320 Scan.
(Barium Deposits)



Pituitary Adenoma

Pfizer MEDICAL SYSTEMS, INC.
A SUBSIDIARY OF PFIZER INC.

ACTA-SCANNER®

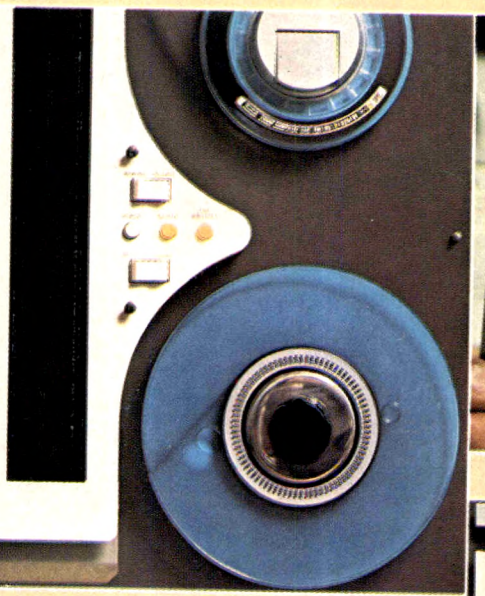
WHOLE BODY COMPUTERIZED TOMOGRAPHIC SCANNER

A revolutionary innovation in diagnostic radiology maintained by an original concept of service...and backed by the full resources of a great medical organization

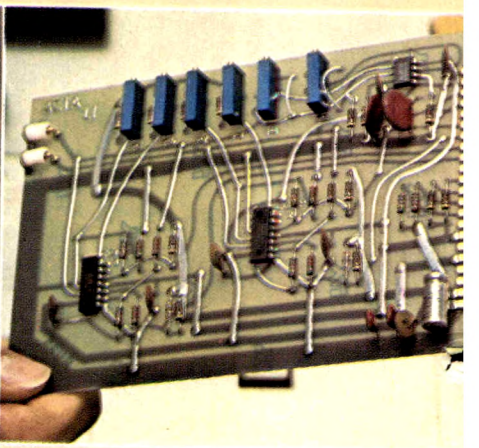
The Pfizer Medical Systems Field Engineer is an integral component of the ACTA-Scanner Service Program.



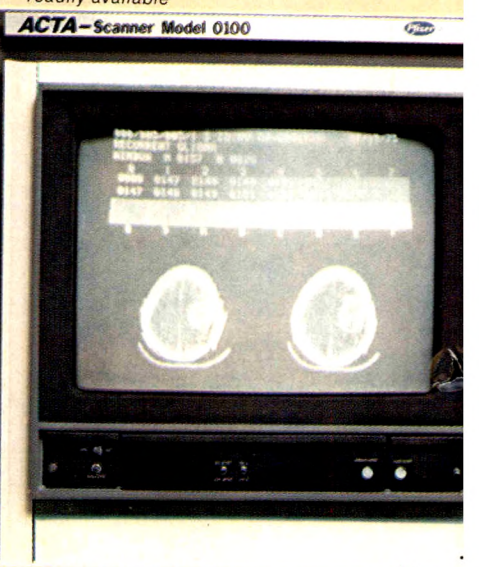
Field engineer readily available



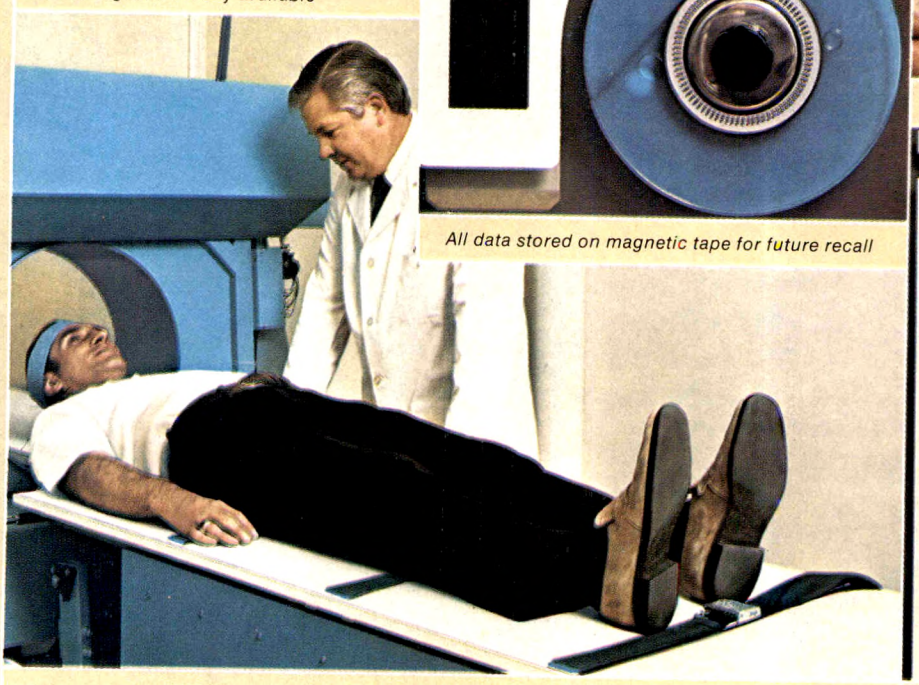
All data stored on magnetic tape for future recall



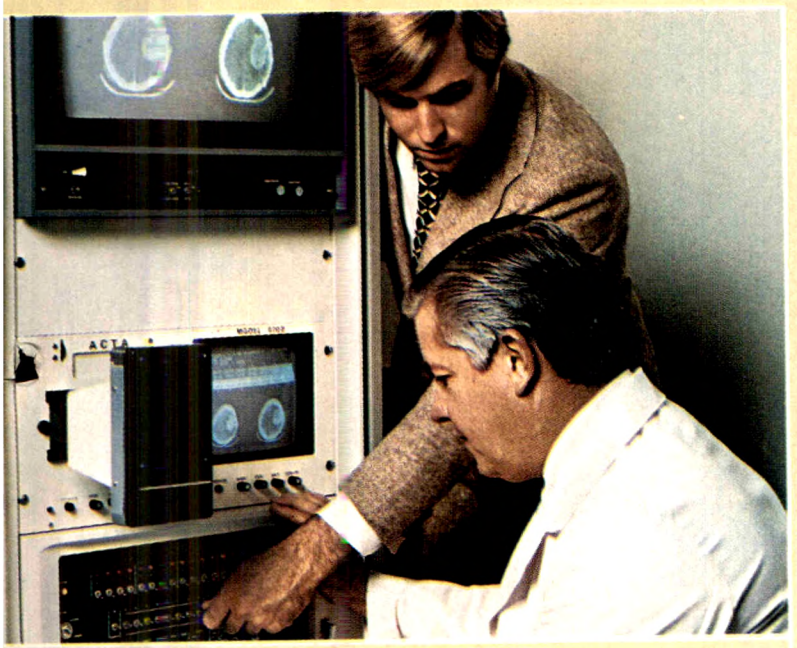
Replacement parts, if needed, are readily available



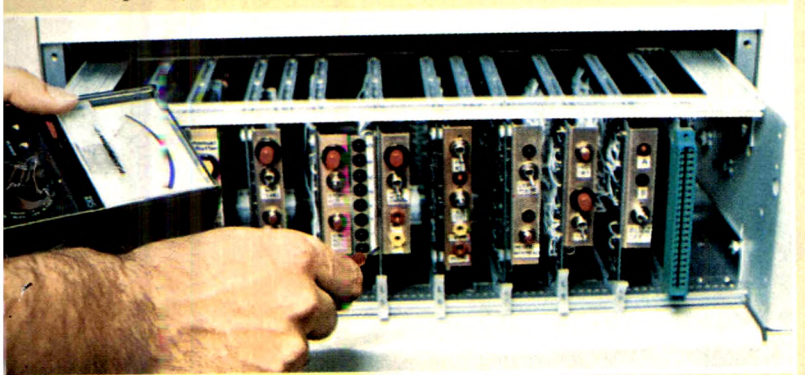
Instant display following completion of scan



Minimal patient preparation before scan



Field engineer provides continued updating on capabilities



Frequent visits by field engineer keep ACTA-Scanner at peak performance

Automation with Representation

A team of highly qualified field engineers is on standby duty to respond to your needs when necessary.

Warranty: No charges for all parts and service support during normal working hours. Any necessary maintenance can be done at night or during nonpeak hours, as requested.

Continuous inspection: Frequent visits, at your convenience, will be made to assure optimum performance.

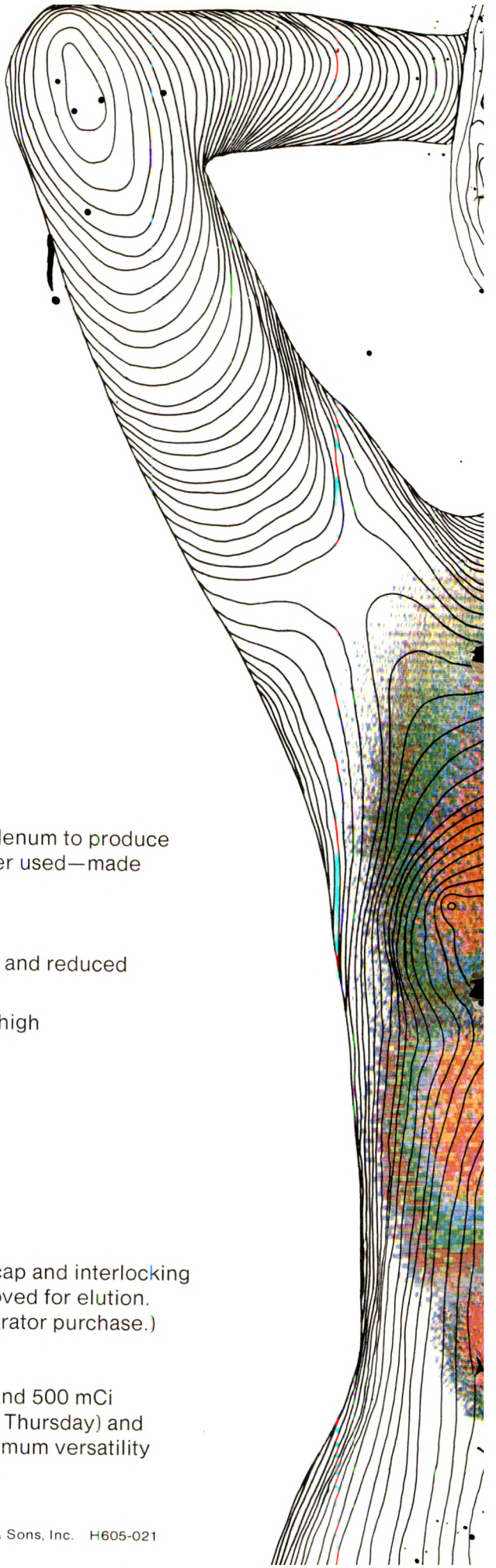
Direct link to research and development: Your representative will keep you apprised of the activities of the Pfizer physicists and x-ray and computer experts who are dedicated to providing ever greater performance and more features on your ACTA-Scanner.

Pfizer MEDICAL SYSTEMS, INC.
A SUBSIDIARY OF PFIZER INC.

WHAT'S NOW SQUIBB?

On the current nuclear medicine scene





MINITEC® (Technetium 99m) Generator

The Technetium 99m Generator using fission product molybdenum to produce technetium 99m. MINITEC is unlike any generator you've ever used—made small to make sense.

Designed for easy handling

- MINITEC has its own handle for easy lifting, easy carrying and reduced hand exposure
- Weighs only 24½ lbs., less than 5″ in diameter, under 8½″ high

Designed for easy elution

- Sets up in seconds
- Elutes in only 3 minutes after eluent vial has emptied

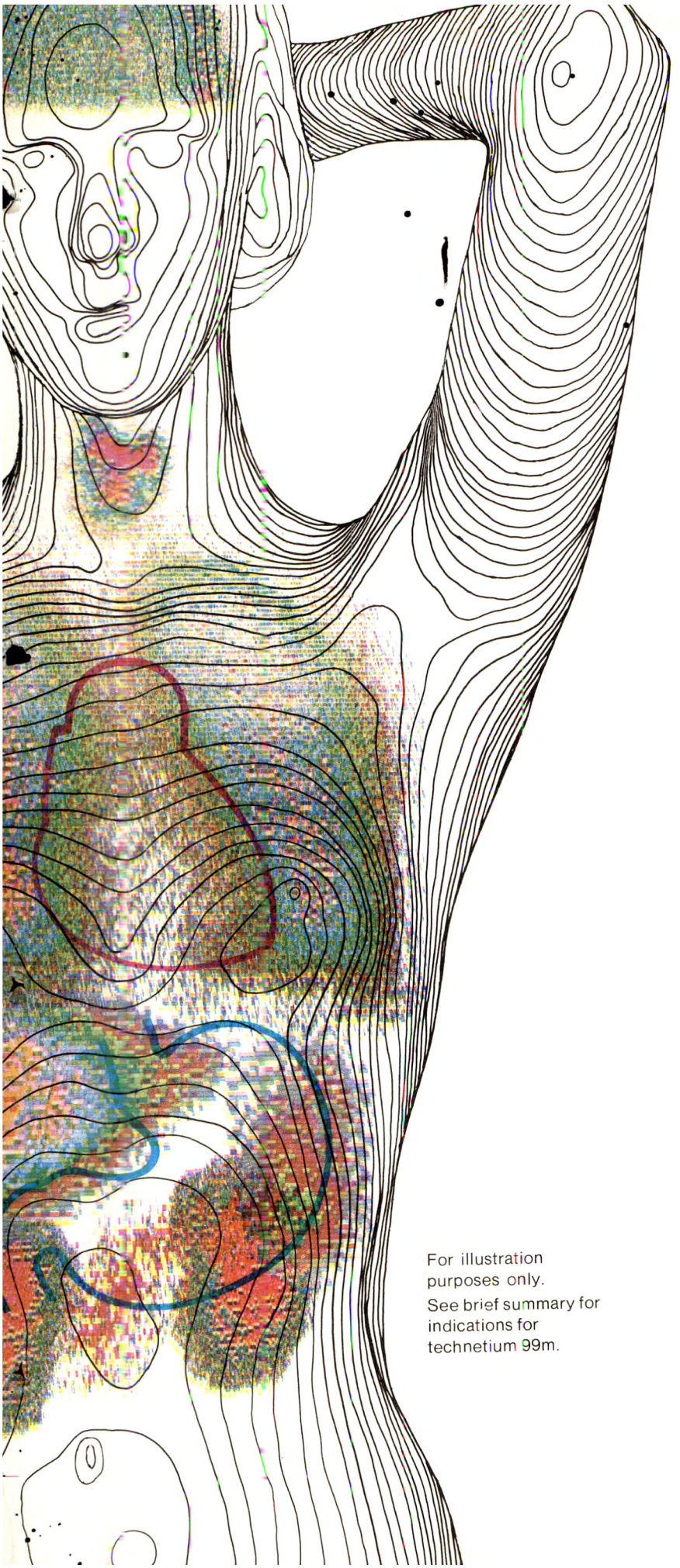
Designed for safety

- No exposed tubing when eluting
- 1⅝″ lead surrounds the MINITEC column
- 1½″ of extra lead protection from MAXI-SHIELD™. Base, cap and interlocking half rings easily assembled on site . . . only the cap is removed for elution. (You get MAXI-SHIELD free with your first MINITEC Generator purchase.)

Designed for convenience

- MINITEC Generator is available in 50,100, 200, 300, 400 and 500 mCi potencies. Delivery on Monday AM (precalibrated through Thursday) and Wednesday (precalibrated through Monday) provides maximum versatility to satisfy technetium requirements of your lab's work load.

© 1975 E. R. Squibb & Sons, Inc. H605-021



For illustration purposes only.

See brief summary for indications for technetium 99m.

Minitec®
(Technetium 99m)
Generator

Minitec® (Technetium 99m) Generator provides a means of obtaining a sterile, non-pyrogenic supply of technetium 99m (^{99m}Tc) as sodium pertechnetate ^{99m}Tc.

Indications: Sodium pertechnetate ^{99m}Tc is indicated for brain imaging, thyroid imaging, salivary gland imaging, blood pool imaging, and placenta localization.

Contraindications: At present, there are no known contraindications to the use of sodium pertechnetate ^{99m}Tc.

Warnings: Radiopharmaceuticals should be used only by physicians who are qualified by specific training in the safe use and safe handling of radionuclides, produced by nuclear reactor or cyclotron, and whose experience and training have been approved by the appropriate federal or state agency authorized to license the use of radionuclides.

This radiopharmaceutical should not be administered to women who are pregnant or who may become pregnant or during lactation unless the information to be obtained outweighs the possible potential risks from the radiation exposure involved. Ideally, examinations using radiopharmaceuticals, especially those elective in nature, of a woman of childbearing capability should be performed during the first few (approximately 10) days following the onset of menses.

Since radioactive pertechnetate is secreted in milk during lactation, formula-feedings should be substituted for breast-feedings.

Important: Since material obtained from the generator may be intended for intravenous administration, aseptic technique must be strictly observed in all handling. Only the eluent provided should be used to elute the generator. Do not administer material eluted from the generator if there is any evidence of foreign matter.

Precautions: As in the use of any other radioactive material, care should be taken to insure minimum radiation exposure to the patient consistent with proper patient management and to insure minimum radiation exposure to occupational workers.

At the time of administration, the solution should be crystal clear.

Adverse Reactions: At present, adverse reactions have not been reported following the use of sodium pertechnetate ^{99m}Tc.

For complete prescribing information, consult package insert.

How Supplied: Minitec (Technetium 99m) Generator is available in potencies of 50, 100, 200, 300, 400, and 500 mCi. Supplied with the generator are vials of eluent containing 5 ml. of a sterile, non-pyrogenic solution of 0.9% sodium chloride in water for injection. Also supplied is suitable equipment for eluting, collecting, and assaying the technetium 99m.

Medotopes®

SQUIBB HOSPITAL DIVISION
E. R Squibb & Sons, Inc.
Princeton, N.J. 08540



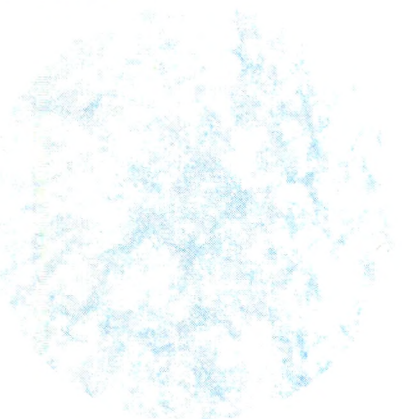
This 48-year-old gravida-1 woman has no palpable abnormalities in her breasts. Routine Xeroradiograph shows prominent duct pattern, with a faint mass-like density distorting the architectural pattern in the left breast.

Pathological findings: 6 mm adenocarcinoma with no positive axillary lymph node involvement.

Should she wait until she can feel it?

This woman is asymptomatic, yet she has breast cancer.

3X magnification.



At this time, the likelihood of metastatic disease is slight. Left undetected, however, this tiny lesion will develop into a palpable mass with the possibility of lymph node involvement greatly increased.

The ten-year survival rate for women with localized breast cancers is 76 percent. When nodes are involved, only 36 percent survive.

More and more physicians are referring high-risk female patients (over 35, strong family history of carcinoma, previous biopsy or mastectomy, nulliparity) for routine mammography. And the majority of radiologists who are experienced in mammography are finding that Xeroradiography, with its heightened local contrast and extraordinary soft-tissue detail, makes it easier to identify very early or occult carcinomas.

The earlier cancer is detected, the greater the range of options available to the physician and patient. And, needless to say, the greater the opportunity to save the patient's life.

Xeroradiography is now the most widely used method of early detection.

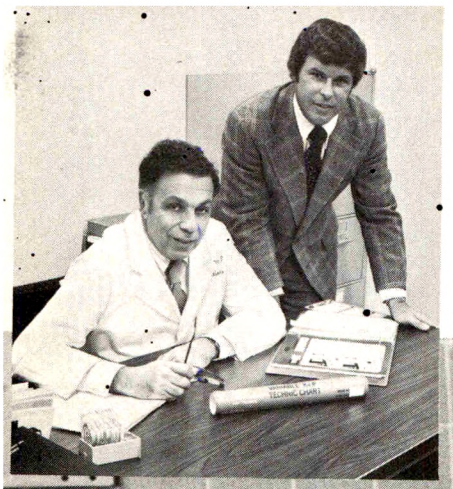
Write for information to Xerox Corporation, Xeroradiography Physician Information, P.O. Box 5786, Pasadena, California 91107.

CP 24,430

XEROX

XEROX® is a trademark of XEROX CORPORATION.

Du Pont consultation saving $12,300 at



Leon Love, M.D., Chairman, Radiology Department, Foster G. McGaw Hospital, Loyola University Medical Center, Maywood, Illinois.
Ted Bauerle, Du Pont Senior Technical Representative.

In May 1974, Ted Bauerle, Du Pont Senior Technical Representative, called in Jack Stevens, a Du Pont Medical X-ray Specialist, to consult with the radiological staff at Loyola.

Jack and Don Falduto, Chief Technologist, conducted a Repeat Analysis of 2,301 discarded films, classifying them by cause for rejection.

Then, based on Du Pont recommendations, the Radiology Department instituted corrective programs to reduce repeats.

After just one year, significant improvements have been made, according to Leon Love, M.D., Chairman of the Department.

A second Repeat Analysis showed only 702 discarded films. Projecting these figures annually, the Department realized a $12,300 savings from the 69% reduction in repeats.

Savings like these are typical of the results which can be achieved when Du Pont works with a Radiology Department to increase efficiency and improve radiographic quality.

In the words of Marianne Troy, R.T., Adminis-

helped reduce repeats 69%, Loyola University Medical Center.



trative Assistant for Radiology, "Du Pont was the catalyst in making us aware of our repeat problems and what corrective action might be taken.

"As a result of our own programs, we now have repeats at a controllable level. Our next goal is to strive for even better performance and radiographic quality."

It's all part of Du Pont's commitment: personal involvement and quality in everything we do and sell to provide reduced operating costs and better patient care.

Personal Involvement: the key to extra quality in radiologic systems.

DU PONT

REG. U.S. PAT. & TM. OFF.

SILVER
IS OUR ONLY BUSINESS
(and has been since 1937)

IF YOU PROCESS . . .
X-RAY FILM

OUR TOTAL SILVER RECOVERY SERVICE

MEANS MONEY TO YOUR DEPARTMENT.

We Purchase

* Outdated or damaged unexposed x-ray film
* Exposed x-ray film
* Silver chip, flake and sludge

Write or call for full information

CALL TOLL FREE
(800) 323-4503
Ill. residents call (312) 473-4800

McELROY
INTEGRITY LEADERSHIP
INC.

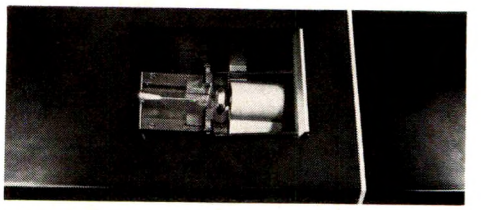
A subsidiary of AgMet, Inc.
2730 Commonwealth
North Chicago, Illinois 60064

CintiChem™
Automated ^{99m}Tc Unit-Dose Delivery System

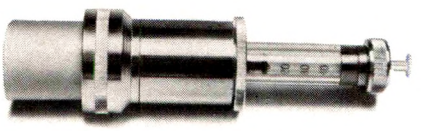
Systematically safer.



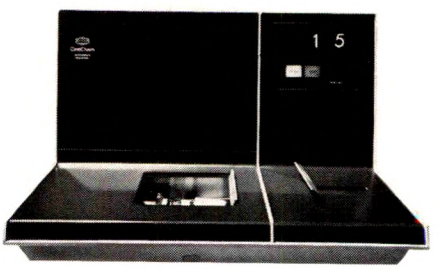
Organ-specific agents for optimum imaging of brain, kidney, bone and lung, and for glomerular filtration rate studies, are provided in kits containing 10 unit-dose vials. Each kit is single step, requiring only addition of technetium to produce the scanning agent.



Preselected amount of ^{99m}Tc activity is automatically dispensed into vial, then diluted with saline to 1.3 ml. Entire dispense/dilute cycle is automatic and shielded, and is completed within 75 seconds.



Unit-dose vial is entered only once for technetium delivery, once for agent withdrawal. Shielded syringe assembly automatically centers disposable syringe with vial. A 1.0-ml patient injection is reproducibly withdrawn into syringe.



Dispenser fully automates isotope measurement, reagent transfer and dose calibration. Eliminates time-consuming manual steps, computations and potential radiation exposure.

UNION CARBIDE

Delivering the future in imaging agents:

The CINTICHEM System, a total unit-dose ^{99m}Tc delivery system...

- ☐ Simplifies radionuclide delivery
- ☐ Improves dosage accuracy and reproducibility
- ☐ Reduces radiation burden
- ☐ Permits precise, contaminant-free administration of agents
- ☐ Reduces labor and cost per test
- ☐ Simplifies record keeping and calculations

The CINTICHEM System includes: an automated technetium dispenser, a high-yield molybdenum 99/technetium 99m generator, organ-specific kits and a unique unit-dose shielded syringe assembly. All integrated for the preparation of sterile, pyrogen-free radiodiagnostic agents—precisely, reliably and with greatly reduced radiation burden to the user.

The CINTICHEM Dispenser automatically delivers a preselected amount of ^{99m}Tc activity (TcO_4^- in saline) into a single-use unit-dose vial. Vial contents are transferred to a disposable syringe via a shielded syringe assembly that permits reproducible withdrawal of a 10-ml patient dose.

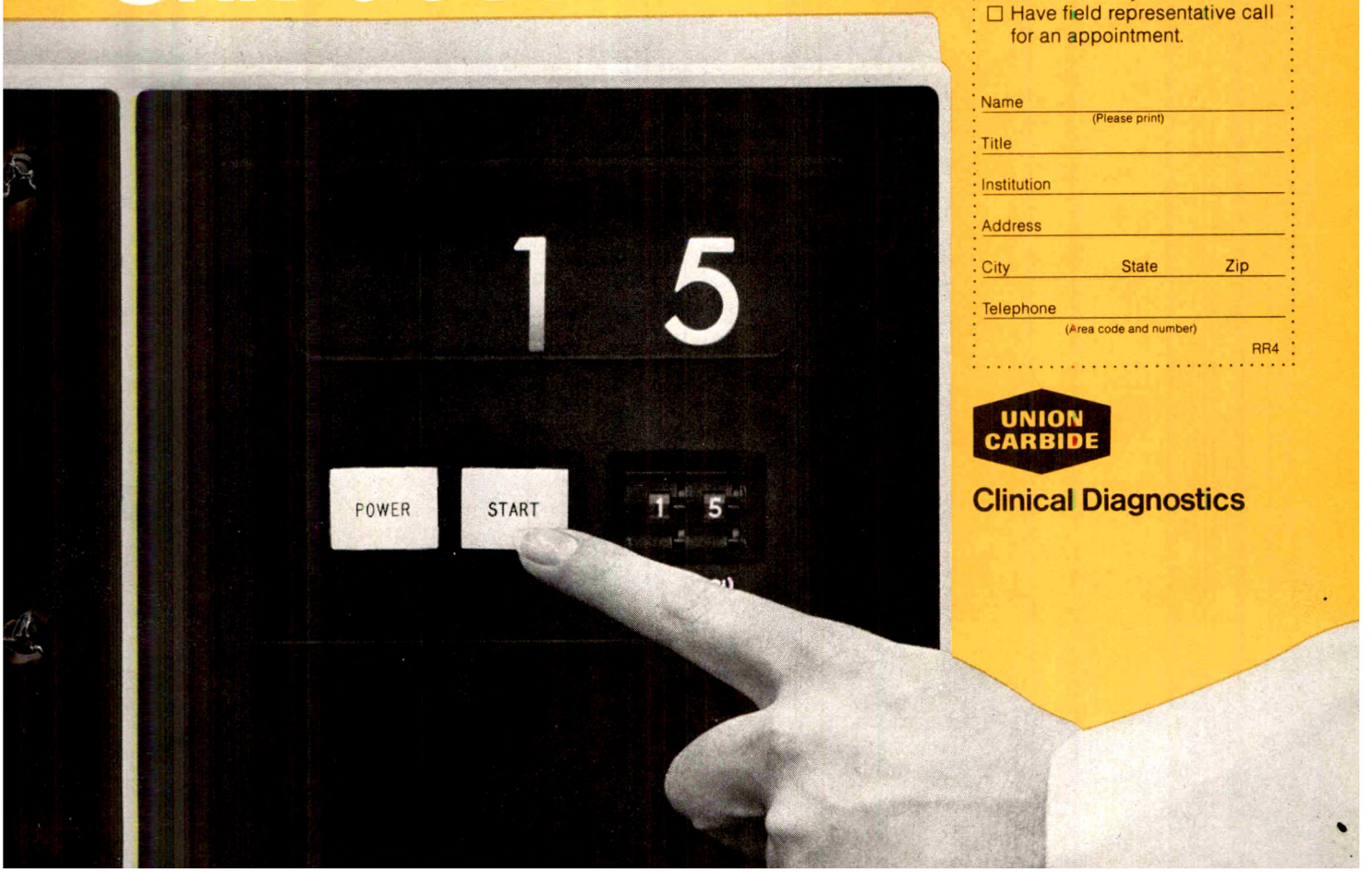
The CINTICHEM Generator is an optimized, advanced-technology ^{99m}Tc generator. It offers exceptionally high yields and is available in 500-, 1,000-, 1,500- and 2,000-mCi sizes. (Sodium pertechnetate ^{99m}Tc in isotonic saline.)

A series of organ-specific CINTICHEM Agents incorporates optimum current formulations for organ specificity. Each kit contains 10 unit-dose vials. (Kits containing five multidose vials are also available.) Each kit is single step. Requires only the addition of technetium to produce the imaging agent. And the CINTICHEM Dispenser performs this step automatically.

Kits currently available include: DTPA (diethylene triamine pentaacetic acid [calcium trisodium salt]). For brain and kidney imaging, and glomerular filtration rate (GFR) studies. Unit dose contains 3.3 mg $CaNa_3$ DTPA, 0.17 mg $SnCl_2$-$2H_20$, pH adjusted to 4 with HCl. HEDSPA (1-hydroxy-ethylidene-1,1 disodium phosphonate). For bone imaging. Unit dose contains 0.75 mg HEDSPA, 0.08 mg stannous ion as tartrate, pH adjusted to 4 with HCl. MAA (macroaggregated albumin). For lung perfusion studies. Unit dose contains 0.11 mg MAA (0.3-1.3 $\times 10^6$ particles), 0.09 mg stannous tartrate, isotonic saline. HCl and Na0H may be present for pH adjustment. Additional radiopharmaceuticals will also be offered.

Let us send detailed data on the CINTICHEM System. Simply return the coupon and we'll come back with a glimpse into the future.

Unit-dose.



CintiChem™
Systematically safer.

Union Carbide Corporation
Clinical Diagnostics
401 Theodore Fremd Avenue
Rye, New York 10580

- ☐ Send brochure on the CINTICHEM System.
- ☐ Have field representative call for an appointment.

Name _____
(Please print)
Title _____
Institution _____
Address _____
City _____ State _____ Zip _____
Telephone _____
(Area code and number)
RR4

UNION CARBIDE
Clinical Diagnostics

Clysodrast®
(BISACODYL TANNEX)

The safe and certain barium additive

Helps you be sure of what you see



Clysodrast is a unique colonic evacuant. It mixes with barium enemas to give radiologists the only form of tannic acid* available for safe, high-resolution barium enema studies. And a growing body of experimental evidence has shown the diagnostic benefits of Clysodrast added to a barium suspension.[1,2,3] This combination provides unmatched mucosal visualization for superior roentgenologic diagnoses.

SAFETY YOU CAN COUNT ON

Only tannic acid really prepares the colon and produces the even, thin-film deposition of barium sulfate that a radiologist needs for maximum clarity. Clysodrast combines tannic acid with the contact laxative bisacodyl, for optimum effectiveness. And Clysodrast comes in accurately measured, 2.5 Gm. packets to avoid the danger of accidental overdose. With Clysodrast, results are consistently safe and uniform, too. No patient has ever suffered hepatic necrosis as a result of Clysodrast being used within the dosage limits indicated in the instructions.[4,5,6] And it has been used in well over 2 million barium enema procedures since 1970 alone, usually with no more side effects than a water enema produces.[7,8]

Clysodrast is recommended for double contrast studies with an appropriate form of barium sulfate, such as Barotrast.® It is also indicated for the preparation of patients for radiologic examinations of the colon, sigmoidoscopy and proctologic examinations, when used as directed.

USE CLYSODRAST, FOR SURE

Clysodrast provides radiologists with the assurance of high resolution barium studies no other product can provide. Find out for yourself how Clysodrast can help you see for sure. Contact your local X-ray supplies dealer.

See summary of prescribing information on adjoining page.

*Bisacodyl tannex

Also see your X-ray supplies dealer for Oratrast,® Barotrast® and Esophotrast.®

INDICATIONS: CLYSODRAST (bisacodyl tannex) may be indicated for the preparation of patients for radiologic examinations of the colon, sigmoidoscopy and proctologic examinations.

CONTRAINDICATIONS: CLYSODRAST is contraindicated in patients under the age of 10 because the possibility of absorption of tannic acid has not been adequately studied in this age group to warrant a conclusion of safety. CLYSODRAST is also contraindicated in cases with known or suspected extensive ulcerative lesions of the colon.

WARNING: Usage in Pregnancy. Safe use of CLYSODRAST has not been established with respect to the adverse effects upon fetal development. Therefore, it should not be used in women of child-bearing potential, particularly during early pregnancy, except where, in the judgment of the physician, the potential benefits outweigh the possible hazards.

PRECAUTIONS: Tannic acid, one of the active ingredients of CLYSODRAST, is hepatotoxic if absorbed in sufficient quantity. Deaths have been reported from hepatic damage due to tannic acid used in barium enema examination. Thus, CLYSODRAST should be used with caution in a regimen where multiple enemas are administered. Certain patients, because of age, debility, or underlying disease, require more gentle preparation than the routine castor oil and CLYSODRAST preparation. It is important that the instructions for preparation and administration be followed in detail, and that the recommended dosages not be exceeded.

ADVERSE REACTIONS: The following adverse reactions have been reported: Cramping, weakness, nausea and fainting.

DOSAGE AND ADMINISTRATION: It is important that the entire medical history and condition of the patient be considered in deciding the dosage regimen. Traumatizing procedures, such as repetition of enemas (with or without CLYSODRAST) should be kept at the minimum necessary to achieve the desired result.

CLEANSING ENEMA: Prepare the cleansing enema by dissolving the contents of one packet (2.5 Gm.) of CLYSODRAST in one liter of lukewarm water and administer.

BARIUM ENEMA: Prepare the barium enema by dissolving the contents of one or not more than two packets (2.5 Gm. or 5.0 Gm.) of CLYSODRAST in one liter of barium suspension. If more than one liter of barium suspension is prepared, it is important that the concentration of CLYSODRAST (bisacodyl tannex) never exceed 0.5 percent (2 packets per liter).

The total dosage of CLYSODRAST for any one complete colonic examination, including the cleansing enema, should not exceed 7.5 Gm. (3 packets). No more than 10 Gm. (4 packets) of CLYSODRAST should be administered to any individual within a 72-hour period.

HOW SUPPLIED: CLYSODRAST is supplied in packets containing 1.5 mg. of 4,4′–(diacetoxydiphenyl)–(pyridyl-2)–methane complexed with 2.5 Gm. of tannic acid, N.F. These packets are supplied in cartons of 25 and 50 packets.

CAUTION: U.S. Federal law prohibits dispensing without prescription.



A Colonic Evacuant

Clysodrast®
(bisacodyl tannex)

Barnes-Hind Pharmaceuticals, Inc.
Sunnyvale, California 94086

1. Goldman, L., *Clinical Medicine*, Vol. 28, pg. 28, 1971
2. Hamilton, *American Journal of Roentgenology*, 1946
3. Janower, M. L., *Radiology*, Vol. 85, pg. 887, 1965
4. Burhenne, et al, *American Journal of Roentgenology*, Vol. 96, pg. 510, 1966
5. Lucke, et al, *Canadian Medical Association*, Vol. 89, pg. 1111, 1963
6. McAlister, et al, *Radiology*, Vol. 80, pg. 765, 1963
7. Steinbach, et al, *American Journal of Roentgenology*, Vol. 87, pg. 644, 1962
8. Thomas, *American Journal of Roentgenology*, Vol. 89, pg. 889, 1963

CHARLES C THOMAS • PUBLISHER

HEALTH PROTECTION OF RADIATION WORKERS *by* **W. Daggett Norwood**, *Hanford Environmental Health Foundation, Richland, Washington.* Using simple terms, this volume provides basic facts on ionizing radiation, its measurement and dosimetry. Acute and chronic, somatic and genetic effects are discussed with emphasis on prevention. Radiation protection standards and regulations are outlined, and methods for maintaining these standards are described. Diagnosis and treatment of radiation injury from external radiation and/or internally deposited radionuclides are considered generally as well as specifically for each radioisotope. The medical supervision of radiation workers, radiation accidents, atomic power plants and medicolegal problems are also covered. *'75, 468 pp., 16 il., 16 tables, $27.50*

ROENTGEN EXAMINATIONS IN ACUTE ABDOMINAL DISEASES (3rd Ed.) *by* **J. Frimann-Dahl**, *Ulleval Hospital, Oslo, Norway.* This new Third Edition is completely revised with 133 new black and white illustrations and two new color illustrations. Written for radiologists and students in diagnostic radiology, this book also serves as a guide and support for surgeons in the important and difficult field of emergency medicine. This book is principally concerned with roentgen anatomy of the abdomen and unusual or normal variations. The diagnosis of the most important acute abdominal diseases is also covered, including lesion diagnosis on plain films and lesions observable by repeat examinations. *'74, 632 pp., 614 il. (4 in color), $29.50*

BRONCHIAL CARCINOMA *by* **Thomas W. Shields**, *Northwestern Univ. Medical School, Chicago. Sections on Immunologic Features and Immunotherapy by* **Roy E. Ritts, Jr.** In this monograph, the incidence and etiology of the disease are discussed and the pathologic, clinical and roentgenographic features of these tumors are presented. Appropriate diagnostic studies are emphasized to classify the extent of the patient's disease. The indications and contraindications of surgical resection, radiation therapy, chemotherapy and immunotherapy are outlined. *'74, 200 pp., 48 il., 22 tables, $12.75*

Prepaid orders sent postpaid, on approval

301-327 EAST LAWRENCE
SPRINGFIELD • ILLINOIS • 62717

Angiography of Posterior Fossa Tumors

by SAMUEL M. WOLPERT, M.B.B.Ch., D.M.R.D.

This volume is aimed at elucidating and teaching the complexities of the vertebral angiogram to the student, based on a thorough knowledge of the normal vascular anatomy. A series of colored line diagrams depicting the pathology in a didactic manner is utilized together with a readable and detailed text.

CONTENTS: Historical Aspects of Vertebral Angiography. Techniques of Vertebral Angiography. Clinical and Pathological Aspects of Posterior Fossa Tumors, by Bennett M. Stein, M.D.C.M., F.A.C.S. Normal Angiographic Anatomy of Posterior Fossa. Prepontine and Cerebellopontine Angle Tumors. Pontine and Mesencephalic Tumors. Fourth Ventricle Tumors. Vermian and Hemispheric Tumors. Differential Diagnosis of Posterior Fossa Tumors.

1976, 208 pp., 167 illus. (7 in color), $23.50/£12.20 ISBN 0-8089-0924-x

SECOND EDITION

Clinical Scintillation Imaging

edited by LEONARD M. FREEMAN and PHILIP M. JOHNSON

CONTENTS: **Fundamental Considerations:** *B. Cassen*, The Evolution of Scintillation Imaging. *J. G. McAfee and G. Subramanian*, Radioactive Agents for Imaging. *R. N. Beck*, Instrumentation and Information Portrayal. *G. V. Taplin et al.*, The Scintillation Image. *M. D. Blaufox and E. S. Himelstein*, Dynamic Function: Rapid-Sequence Imaging. *P. N. Goodwin*, Radiation Safety for Patient and Personnel. **Clinical Considerations:** *F. J. Bonte and J. P. Kriss*, Cardiovascular Imaging. *R. A. Holmes and E. V. Staab*, The Central Nervous System. *L. M. Freeman*, The Kidney. *P. M. Johnson*, The Liver. *G. L. DeNardo and S. J. DeNardo*, The Lung. *R. E. O'Mara and N. D. Charkes*, The Osseous System. *T. P. Hyanie III and A. Miale, Jr.*, The Pancreas. *S. M. Larsen and W. B. Nelp*, The Placenta. *P. M. Johnson and R. P. Spencer*, The Spleen. *H. L. Atkins*, The Thyroid. *F. S. Mishkin and L. M. Freeman*, Progress in Scintillation Imaging. *P. B. Hoffer and A. Gottschalk*, Prospective.

1975, 848 pp., 300 illus., $55.00/£27.50 ISBN 0-8089-0859-6

Diagnostic Use of Ultrasound

by BARRY B. GOLDBERG, MORRIS N. KOTLER, MARVIN C. ZISKIN, and ROBERT D. WAXHAM

CONTENTS: *M. C. Ziskin*, Basic Principles. *M. C. Ziskin*, Instrumentation. *B. B. Goldberg*, Head and Neck. *B. B. Goldberg*, Chest. *M. N. Kotler*, Echocardiography: Valves, Chambers, and Pericardium. *M. N. Kotler*, Echocardiography: Valves, Chambers, and Cogenital Heart Disease. *B. B. Goldberg*, Abdominal Ultrasonography: Retroperitoneal Structures. *B. B. Goldberg*, Abdominal Ultrasonography: Intraperitoneal Structures. *B. B. Goldberg*, Gynecology. *B. B. Goldberg*, Obstetrics. *R. D. Waxham*, Doppler Ultrasound.

1975, 480 pp., illus., $30.00/£15.00 ISBN 0-8089-0879-0

N.B.: Postage plus 50¢ handling charge on all orders not accompanied by payment.
Prices are subject to change without notice.

GRUNE & STRATTON
A Subsidiary of Harcourt Brace Jovanovich, Publishers
111 FIFTH AVENUE, NEW YORK, N. Y. 10003
24-28 OVAL ROAD, LONDON NW1 7DX

Name_____

No._____

Date_____

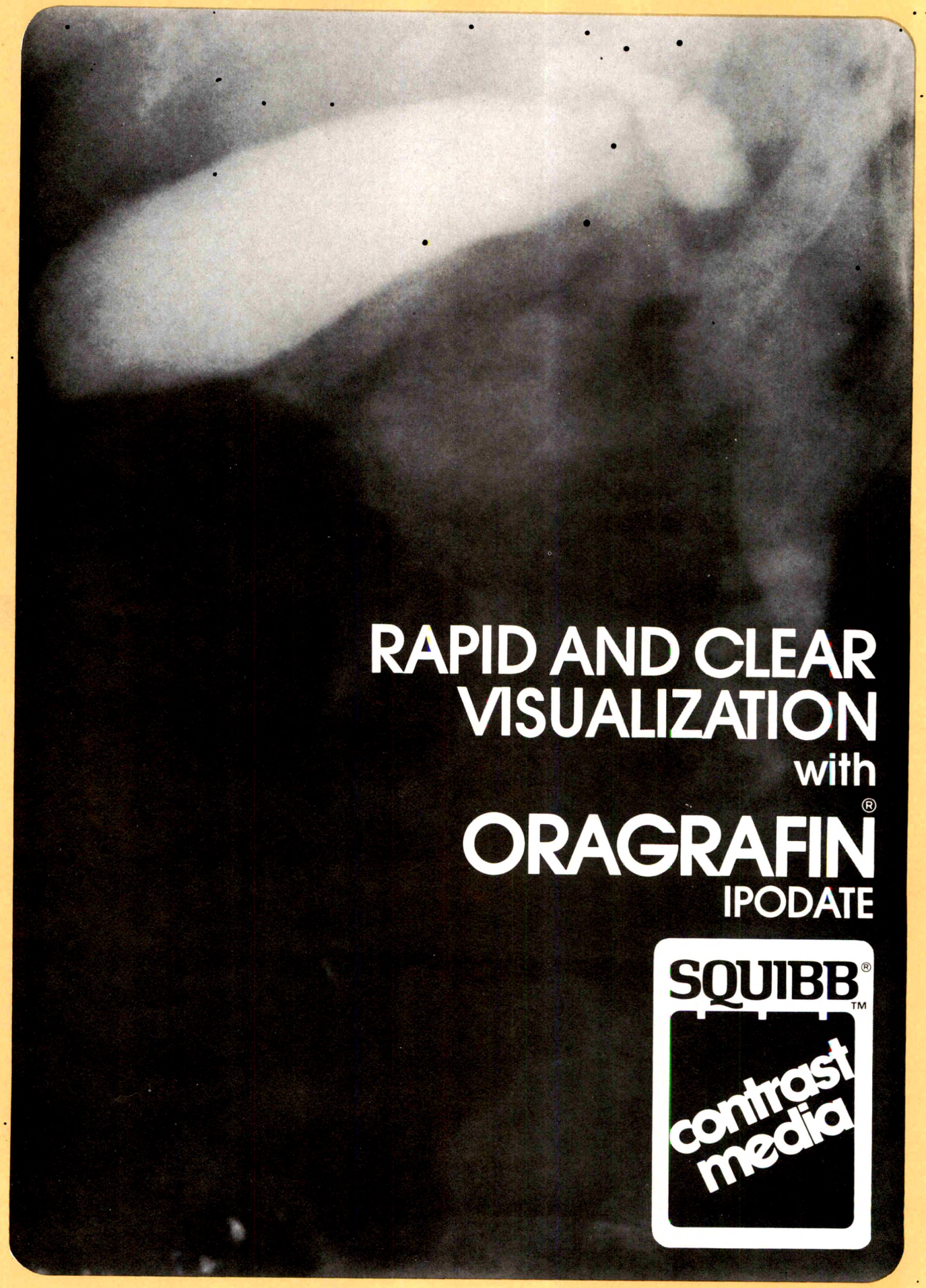
Dr._____

Remarks_____

_____

_____

The
Reason
is
Clear...
Effectiveness


RAPID AND CLEAR
VISUALIZATION
with
ORAGRAFIN®
IPODATE
SQUIBB®
contrast media

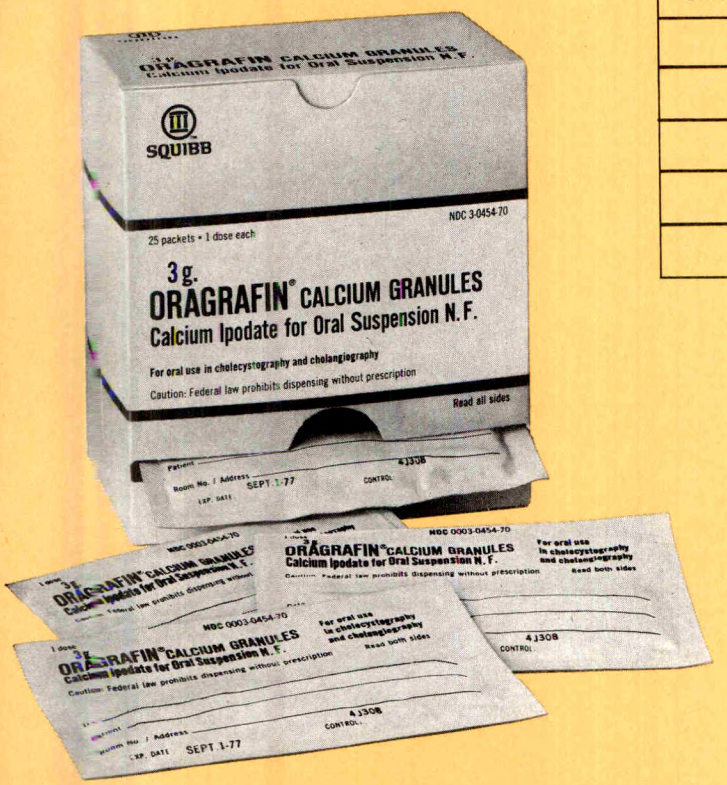
- Visualization of the ducts occurs in 1 to 3 hours and of the gallbladder within 5 hours or less with Oragrafin Calcium Granules (Calcium Ipodate for Oral Suspension N.F.).
- The gallbladder is opacified approximately 10 hours after ingestion of Oragrafin Sodium Capsules (Sodium Ipodate Capsules N.F.).
- Rapid absorption often permits visualization of even poorly functioning gallbladders. An unprepared patient can be studied the same day.
- When patients cannot take capsules, the granules are a convenient, palatable alternative.
- Both salts are usually well tolerated.

Dosage Schedules

FOR ROUTINE OVERNIGHT PROCEDURES Sodium Ipodate Capsules and/or Calcium Ipodate for Oral Suspension			
	Gallbladder Films		Films of the Gallbladder and Biliary Ducts
11 P.M.	6 Capsules (or 12 Capsules)	OR 1 packet of Granules (or 2 packets)	6 Capsules (or 1 packet of Granules, if preferred) and
next morning, 8 A.M.			1 packet of Granules
9 A.M.	Visualization of gallbladder	Visualization of gallbladder	Visualization of ducts and gallbladder
10 A.M.			
11 A.M.			

FOR RAPID, SAME-DAY PROCEDURES Calcium Ipodate for Oral Suspension	
Films of Gallbladder and Ductal System	
8 A.M.	2 packets of Granules
9 A.M.	Visualization of ducts
10 A.M.	Optimal visualization of ducts
1 P.M.	Visualization of gallbladder

See next page for complete prescribing information.





ORAGRAFIN®
CALCIUM GRANULES
Calcium Ipodate for Oral Suspension N.F.

ORAGRAFIN®
SODIUM CAPSULES
Sodium Ipodate Capsules N.F.

the reason is clear

ORAGRAFIN®
CALCIUM GRANULES
Calcium Ipodate for Oral Suspension N.F.

ORAGRAFIN®
SODIUM CAPSULES
Sodium Ipodate Capsules N.F.

DESCRIPTION
Oragrafin Calcium Granules (Calcium Ipodate for Oral Suspension N.F.) and Oragrafin Sodium Capsules (Sodium Ipodate Capsules N.F.) are oral radiopaque media for cholangiography and cholecystography. *Calcium* ipodate is available in single-dose foil packets providing 3 g. calcium ipodate as granules dispersed in flavored sucrose. When mixed with water, the granules produce a pleasantly-flavored suspension. *Sodium* ipodate is available in capsules providing 500 mg. sodium ipodate per capsule.

The organically bound iodine content of calcium ipodate and sodium ipodate is 61.7% and 61.4%, respectively.

ACTIONS
Calcium ipodate and sodium ipodate are absorbed from the gastrointestinal tract, excreted by the liver into the bile, and stored and concentrated in the gallbladder. The calcium salt, which is absorbed somewhat faster than the sodium salt, appears in the ducts as early as 30 minutes after ingestion. Optimal concentration of either salt in the hepatic and biliary ducts occurs within 1 to 3 hours after ingestion in nearly all cases; rarely, maximal opacification may be delayed for as much as 5 hours. Adequate opacification of the ducts usually persists for about 45 minutes. The ducts may be visualized in patients who have undergone cholecystectomy.

The gallbladder is optimally opacified approximately 10 hours after ingestion of either salt. Diagnostically adequate filling, however, often takes place within 5 hours or less after ingestion, particularly with the calcium salt. Thus, studies of ducts and gallbladder may be carried out in as little as 5 hours when necessary or desirable. In this connection, it should be pointed out that both salts have been administered to unprepared patients as well as to previously prepared patients, with no significant difference in results.

INDICATIONS
Calcium ipodate and sodium ipodate are indicated for cholecystography. They may also be used for cholangiography, although they are not considered the drugs of choice.

CONTRAINDICATIONS
Both preparations are contraindicated in persons who are hypersensitive to ipodate salts.

WARNINGS
A history of sensitivity to iodine *per se* or to other iodinated compounds is not an absolute contraindication to the use of these preparations, but calls for extreme caution in administration.

Usage in Pregnancy
The safety of these preparations for use during pregnancy has not been established; therefore, they should be used in pregnant patients only when, in the judgment of the physician, their use is deemed essential to the welfare of the patient.

PRECAUTIONS
Increasing the dosage above that recommended increases the possibility of hypotension.

Anuria may result when these preparations are administered to patients with combined renal and hepatic disease or severe renal impairment.

Renal toxicity has been reported in a few patients with liver dysfunction who were given oral cholecystographic agents followed by urographic agents. Administration of urographic agents should therefore be postponed in any patient with a known or suspected hepatic or biliary disorder who has recently taken a cholecystographic contrast agent.

Gastrointestinal disorders which interfere with absorption and liver disorders which interfere with excretion may result in non-visualization of the hepatic and biliary ducts and the gallbladder.

Contrast agents may interfere with some chemical determinations made on urine specimens; therefore, urine should be collected before administration of the contrast media or two or more days afterwards.

Thyroid function tests, if indicated, should be performed prior to the administration of these preparations since iodine containing contrast agents may alter the results of these tests.

ADVERSE REACTIONS
Sodium ipodate and calcium ipodate are usually well tolerated. Unwanted effects such as mild and transient nausea, vomiting, or diarrhea sometimes occur but the incidence can be reduced by restricting the dosage to 3 g. and administering only the Granules to patients who may be prone to gastrointestinal reactions. Headache, dysuria, or abdominal pains may occur infrequently as transient disturbances.

Hypersensitivity reactions may include urticaria, serum sickness-like reactions (fever, rash, arthralgia), other skin rashes, and, rarely, anaphylactoid shock. They are more likely to occur in individuals with a history of allergy, asthma, hay fever, or urticaria, and in those who have previously demonstrated hypersensitivity to iodine compounds.

DOSAGE AND ADMINISTRATION
The Capsules should be taken with as little water as possible. They may be swallowed in rapid succession or slowly over the course of ½ hour or more, depending on patient preference.

The Granules should be stirred vigorously into a small amount of water (¼ glass or less) and swallowed immediately. If lukewarm rather than cold water is used, the patient will find the suspension quite palatable and there will be less likelihood of nausea.

A total dose of 6 g. (12 Capsules or 2 packets of Granules) per 24 hour period should not be exceeded.

When an upper gastrointestinal barium study is scheduled, prior administration of either salt will not interfere. Either salt may also be used in conjunction with an intravenous cholangiographic agent.

The recommended dosage and patient preparation for cholangiography and/or cholecystography are as follows:

Routine Cholecystography
On the day before the examination, the patient may, if feasible, eat a high-fat lunch so that the gallbladder will evacuate and refill with opacified bile. The evening meal, which should be light and fat-free, should be eaten 2 hours before the contrast medium is taken. The contrast agent should be administered 10 to 12 hours before the roentgenologic examination. The usual dose is 6 Capsules (providing 3 g. sodium ipodate), although up to 12 Capsules may be given; 1 to 2 packets of Granules may be used instead. No other food or drink except small amounts of water should be taken before the examination. A mild laxative or other cathartic may be given, but is not generally necessary.

Roentgenologic examination of the gallbladder is performed the next morning in the usual manner, employing the standard positions. An immediate study of the wet films will determine any need for repositioning of the patient. Administration of a fat meal or other cholecystokinetic agent provides good dynamic studies of gallbladder function. If a barium meal examination is also to be performed, the fat meal may be given simultaneously with or following the barium meal. Gallbladder function studies are then made after the barium meal examination is completed.

Cholangiography
No prior preparation of the patient is necessary. For this procedure, the Granules should be used. They are administered one hour before cholangiography. Although only one packet (providing 3 g. calcium ipodate) may suffice, two packets (6 g.) are usually necessary for visualization of the ducts.

Beginning one hour after ingestion of the Granules, and at 15-minute intervals thereafter, films should be taken, preferably with the aid of tomography or laminography. With proper positioning of the patient, residual contrast medium in the gastrointestinal tract is not likely to be a problem, particularly with the more rapidly absorbed calcium salt. Optimal visualization of the ducts is generally achieved between 1½ and 2½ hours after ingestion of the medium.

Combined Cholangiography and Cholecystography
Preparation of the patient and administration of dosage should be as outlined under *Routine Cholecystography*, with a dosage of 6 Capsules or, if preferred, one packet of Granules taken on the evening before examination. On the following morning, one hour before the examination, one additional packet of Granules should be administered.

Beginning one hour after the morning dose, and at 15-minute intervals thereafter, films should be made, preferably with the use of tomography or laminography. While the gallbladder will have concentrated the evening dose of the medium, the additional morning dose will provide opacification of the ducts, and simultaneous visualization may be achieved. When satisfactory films have been obtained, a fat meal may be administered to provide gallbladder function studies.

Rapid Combined Cholangiography and Cholecystography
No prior preparation of the patient is necessary. On the day of examination, the patient should be given two packets of Granules. Beginning one hour later, examination of the ducts should be performed as described under *Cholangiography*. If the gallbladder has not opacified sufficiently by the time the cholangiographic examination is completed, further cholecystograms may be taken after 2 or 3 hours. Dynamic studies of gallbladder function may be carried out in the usual manner.

HOW SUPPLIED
Oragrafin Calcium Granules (Calcium Ipodate for Oral Suspension N.F.), single-dose foil packets; boxes of 25 packets (3 g. calcium ipodate per packet). Oragrafin Sodium Capsules (Sodium Ipodate Capsules N.F.), boxes of 25 vials (6 capsules each vial); bottles of 100; and Unimatic® single-dose packages of 100.

SQUIBB®

The Reason is Clear

contrast media™

SQUIBB HOSPITAL DIVISION
E.R. Squibb & Sons, Inc.

© 1975 E. R. Squibb & Sons, Inc. H655-033

AMERICAN JOURNAL OF ROENTGENOLOGY

VOL. 126 APRIL, 1976 NO. 4

VIRUS DISEASES OF BONE. DO THEY EXIST?*

THE NEUHAUSER LECTURE

By FREDERIC N. SILVERMAN, M.D.†
CINCINNATI, OHIO

THIS is a very personal experience. The invitation to give the Neuhauser Lecture of the Society for Pediatric Radiology is one that I received with considerable ambivalence. On the one hand, my warmth of feeling for our Society and our first President welcomed the opportunity for expression; on the other, the responsibility of linking a presentation of my composition with names so deservedly prestigious was disconcerting. What could I offer that might justify my acceptance of this responsibility? This certainly was not the time to indulge my fascination with the esoterica of skeletal dysplasias. A review of Dr. Neuhauser's Curriculum Vitae and extensive bibliography finally gave me some direction.

Many of you may not know that Dr. Neuhauser was well on the way to become an orthopedic surgeon before he responded to the allure of Pediatric Radiology. So it seemed appropriate to explore some subject related to the skeletal system, even though Dr. Neuhauser himself seemed to avoid it in his own writings. He waited until his eleventh publication to establish his mastery in this field, writing a classic article on progressive diaphyseal dysplasia[82] which subsequently was recognized as Engelmann disease, and currently, craniodiaphyseal dysplasia. But Dr. Neuhauser's interests lay in other areas of esoterica. I refer particularly to his scholarly investigation, with his colleagues, of an unusual pulmonary disease which he designated as lycoperdonosis, after the causal agent, *Lycoperdon pyriforme* or *Lycoperdon gemmatum*, also known as the common puffball.[110] Since I have no expertise to explore the culinary art in which Dr. Neuhauser's erudition was also displayed in this fascinating contribution, I thought it would be appropriate to combine a consideration of bone disease with unusual causal agents, and the subject of viral disease of bone immediately came to mind. However, like the preparation of mushrooms described by Dr. Neuhauser,[110] this is another subject about which I knew nothing. So, with a trust, hopefully justified, in the tolerant attitude of the members of the Society for Pediatric Radiology toward exploration of uncertain areas of medical interest, I elected to learn about viral diseases of bone, if they exist, and to share what I learned with you. Let me emphasize at the onset that my literature search had to be limited both by time and by my blind gropings as a non-virologist in

* Presented at the Eighteenth Annual Meeting of the Society for Pediatric Radiology, Atlanta, Georgia, September 28–29, 1975.
From the Division of Roentgenology, Children's Hospital Medical Center, University of Cincinnati College of Medicine, Cincinnati, Ohio.
† Professor, Pediatrics and Radiology and Director, Division of Roentgenology.

a field that makes skeletal dysplasias seem simple.

There is a mixed reception in current textbooks to the concept of viral diseases of bone. Caffey *et al.*[17] state that "osteitis due to viral infections has not been conclusively proved." The lesions reported in smallpox are ascribed to secondary infection by pyogenic organisms from the skin. Aegerter and Kirkpatrick[3] state that bone infections of viral origin are so rare that insufficient material is available for adequate and conclusive descriptions of the process. Jaffe[61] however, clearly accepts smallpox virus as the causal agent of osteomyelitis which can be differentiated from bacterial osteomyelitis, and also recognizes osteomyelitis due to *vaccina* virus. Other viral diseases have been reported in association with roentgenographically demonstrable bone lesions[11] (rubella, cytomegalic inclusion disease, varicella, lymphogranuloma venereum, infectious mononucleosis) and some bone diseases of, as yet, unknown cause have had advocates of their viral etiology[25,34,78] (infantile cortical hyperostosis, cat scratch disease, etc.).

The varying points of view seem to be based on several opposing arguments:

1. Bone lesions in the course of viral diseases are caused by secondary bacterial invaders and not by the virus *per se*;—to which is opposed
2. Bacterial cultures have been sterile in several carefully investigated instances, while virus or virus particles "typical" for the agent of the clinical disease (apart from the bone lesion) have been identified;—to which there is the riposte
3. The presence of virus in a lesion merely indicates the fact of viremia; it does not prove that the virus is the cause of the lesion;—to which, the reply
4. The clinical course of the viral bone disease is different from that of bacterial bone disease;—to which, etc., etc., etc.

Let us examine the evidence on which these arguments are based and if we cannot come to any conclusions, perhaps we can ask some questions and indicate areas or directions to explore for answers,—or for more questions.

CLINICAL EXPERIENCES

Variola (Smallpox)

It might be appropriate to refresh our memories that the eruption of smallpox usually appears after an incubation period of about twelve days after exposure and a three to four day period of prodromal fever, during which a viremia carries virus throughout the body. When the skin eruption appears, the virus disappears from the blood and the temperature tends to regress.

Reported complications of smallpox have included heart failure and terminal pneumonia, and occasionally osteomyelitis. It was generally considered that bacterial complications of smallpox could be incriminated as the principle cause of death, particularly after the pustular phase. It is now believed that the mortality in smallpox is chiefly related to the amount of virus in the blood during the first two days of the infection (*i.e.*, before the appearance of the rash!) Even in the absence of antibiotics, pneumonias found in fatal cases yield the virus on culture and are sterile with respect to bacteria. Occasionally, there is an encephalitis like that of measles, varicella, or vaccinia.

Osteomyelitis variolosa is a term coined by Chiari[24] to designate nonsuppurative lesions he observed in the bone marrow of patients dying of smallpox during an epidemic in Prague in the winter of 1891–92. The lesions were found in 19 of 22 patients dying as early as two days and as late as two months after the skin eruption. Chiari had previously observed non-suppurative lesions in the testes of patients dying of smallpox which he called orchitis variolosa.[23–a, 23–b] He expected to find similar lesions in the bone marrow because patients complained so frequently of bone

pain in various stages of the disease; he did not record bone or joint involvement *per se*. Bacterial cultures were usually sterile and microscopic organisms were so infrequent that they were considered secondary invaders.

Bancroft,[7] in a detailed clinical description of an epidemic in Boston in 1902–1903 involving about 1,200 cases, stated that "purulent inflammation of the elbow joint was seen in the third week of the disease in two cases. Acute, non-suppurative arthritis was common." Musgrave and Sison[79] and Musgrave *et al.*[80] reported 18 instances of disturbances of bone growth, deformity, and even ankylosis following skeletal involvement during smallpox in childhood in the Philippine Islands. All cases had been infected prior to the age of 14 years. The clinical and roentgenographic features were unlike those expected with suppurative pyogenic osteomyelitis or arthritis (Fig. 1; and 2).

Similar late deformities after smallpox infection were reported by physicians encountering instances of smallpox in the United States. Brown and Brown,[14] reported a six year old girl who had deformity secondary to "destruction of the epiphyseal line" at the wrists. A 20 year old with similar changes was reported in the same paper. These authors pointed to the absence of scars or sinuses in the area of bone and joint deformity as different from the sequels to pyogenic osteomyelitis. That same year, Sheldon[100] added two more instances of late joint deformity after osteoarticular involvement in smallpox. Sheldon was concerned about the joint fusion representing sequels to a peculiar "oriental" form of the disease, (prior reports involved non-white individuals) but he was reassured about the non-racial nature of the infectious process by the almost contemporaneous report of Brown and Brown. In 1926, Huenekens and Rigler[60] described an acute episode of osteoarticular smallpox ("osteomyelitis variolosa") in a four year old boy who had pain and swelling of the wrists and elbows when admitted four days after the onset of a typical variolar eruption. Twelve days after the onset, the knees became swollen and tender. Roentgenographic examination showed symmetrical lesions on the metaphyseal side of epiphyseal lines in affected areas. The authors noted the predilection for areas of active

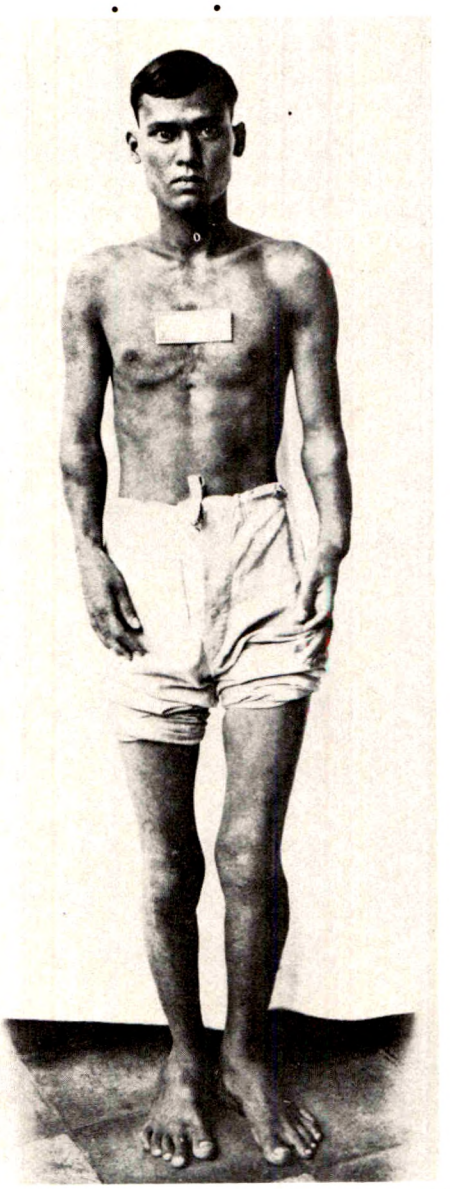


Fig. 1. Deformities following childhood smallpox. Both elbows and forearms are affected; note left hand and wrist and asymmetrical deformities of lower extremities. From Musgrave and Sison.[79]

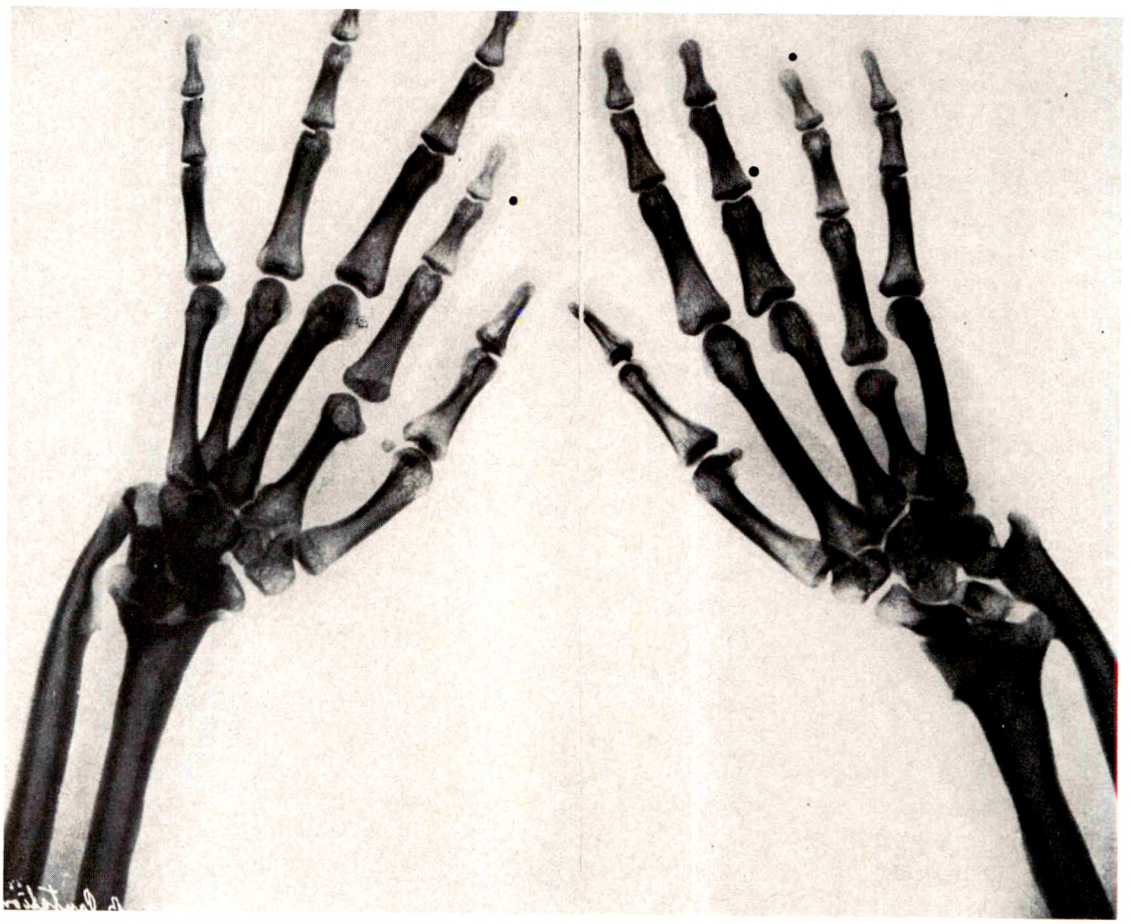


FIG. 2. Roentgenogram of hands and wrists of patient in Figure 1. Note carpal deformities and asymmetrical shortening of metacarpal bones. From Musgrave and Sison.[79]

growth as well as the absence of suppuration. A short follow-up period (eleven months) showed irregularity of growth in some bones but a gradual return to function.

Other reports confirmed the clinical character of osteoarticular involvement in smallpox and emphasized the subsequent deformities to the extent of recommending inquiry for a past history of smallpox whenever obscure deformities and growth inequalities of the extremities were seen (Eikenbary and LeCocq[41]). Chatterjee[21] stated that arthritis was the most serious complication of smallpox. In an epidemic in India comprising 2,341 cases, 10 out of the 115 children under ten years of age developed arthritis. In every case, the elbows were affected. The onset was usually three to four weeks after the onset of the disease. Only in the area of histopathology was there any dissenting opinion. Bras[13] in a comprehensive paper on the morbid anatomy of smallpox based on 177 cases was unable to confirm the bone marrow lesions which Chiari called osteomyelitis variolosa. He indicated that his postmortem examinations were done much sooner after death than were Chiari's. Nevertheless, when Cockshott and MacGregor reported their experiences in 1958 and 1959,[27,28] they were able to list 134 instances of osteomyelitis variolosa in addition to their 15 carefully studied cases. On the basis of these data, they suggested that 0.25–0.5 percent of all patients during an epidemic, and two to

five percent of affected children, would be expected to have osteoarthritic signs and symptoms. A latent interval between onset of the rash and the joint symptoms usually occurred and varied between one to six weeks. In 80 percent of patients, an elbow was affected; in 20 percent, hands and wrists; ankles and feet in 18 percent; and knees, hips and shoulders less frequently. In over 50 percent, more than one site was involved, and symmetry of involvement was striking. Joints, or groups of joints, were affected in an irregular sequence at intervals of one or two days.

Swelling around the affected joint was usually the first sign (Fig. 3); pain was generally mild and often there seemed to be merely a disinclination to move the affected extremity. Effusions were moderate in amount when found and the joint was surrounded by tender, fusiform swellings which extended as boggy sheaths over the adjacent bones. Hand and foot swellings (Fig. 4) resembled those in the hand-foot syndrome, but none of the affected patients showed evidence of sickling. Large effusions sometimes drained spontaneously, forming sinuses. Fluid removed from joints was generally sterile; elementary bodies of variola were detected in the joint fluid from four of the cases.

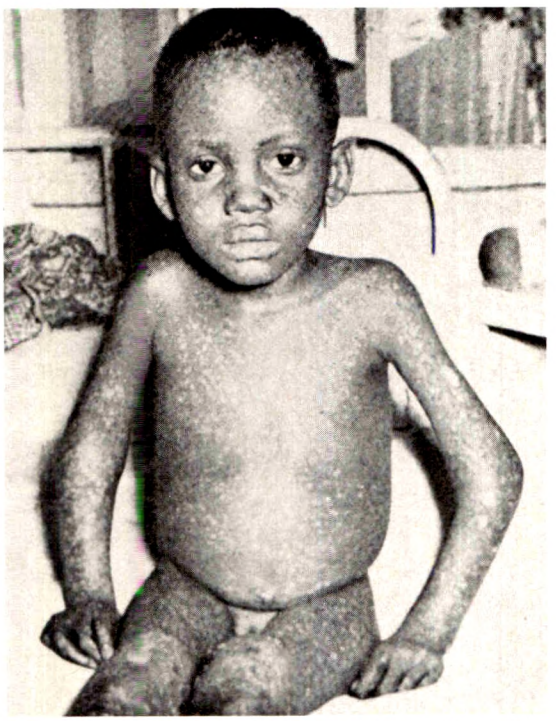


Fig. 3. Bilateral elbow swelling in child still showing cutaneous lesions of smallpox. With permission from Cockshott and MacGregor.[27]



Fig. 4. Swelling of hand in smallpox with dactylitis. With permission from Cockshott and MacGregor.[28]

Roentgenographic studies showed early soft tissue swelling around the affected joint. The earliest osseous change was a radiolucent band in the metaphysis (Fig. 5). The calcified cartilaginous plate occasionally seemed totally disconnected from the remainder of the bone. A thin shell of periosteal new bone subsequently formed extending along the shaft away from the affected joint. This gradually (over a period of months) became incorporated with the shaft and, though it could remodel and disappear, often left spurs at the sites of capsular attachment (Fig. 6). Epiphyses not infrequently were totally destroyed so that bone fusion across joints occurred, with focal excavations in the bony continuum where the epiphyses had been. In some instances, the epiphysis was com-

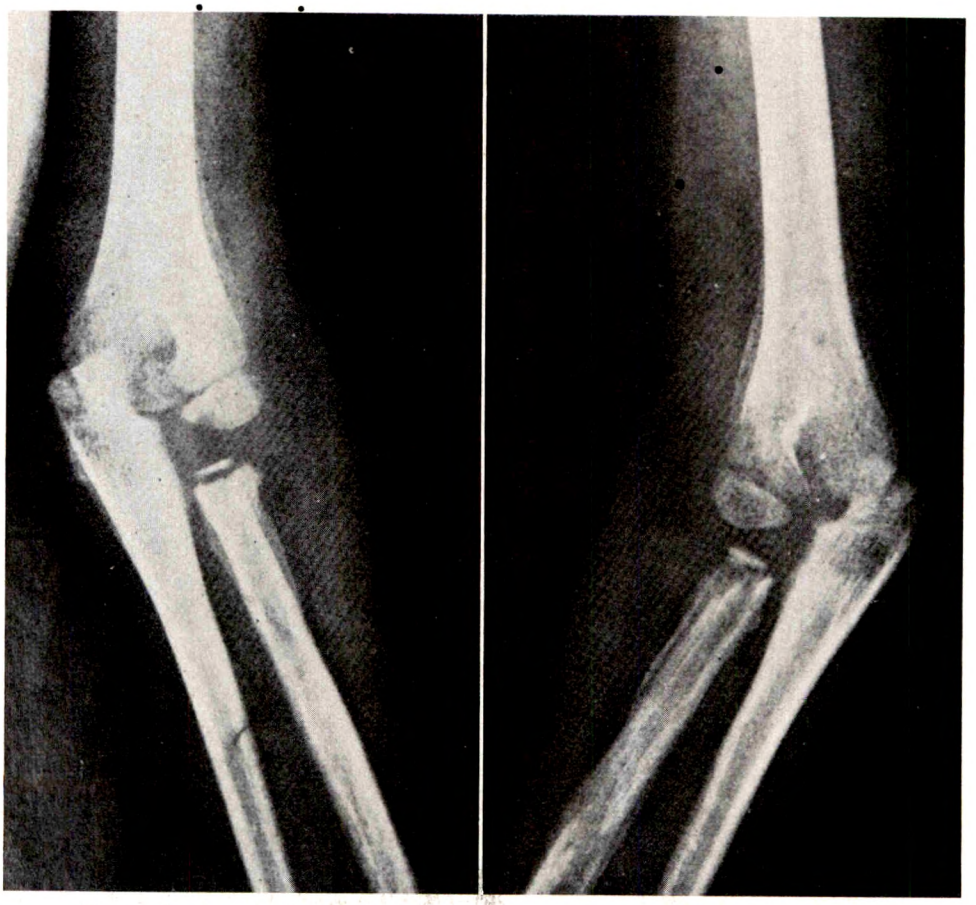


Fig. 5. Symmetrical elbow lesions in osteomyelitis variolosa in seven year old girl. With permission from Cockshott and MacGregor.[27]

pletely separated from the shaft and, with its ossification center, persisted as a foreign body in the soft tissues until resorption occurred. Subsequent growth of affected bones was commonly retarded; when tubular bones of the hands or feet were affected, bizarre, acquired brachydactyly often resulted (Fig. 7). And in most instances, these osseous mutilations took place with surprisingly little impact on the clinical status of the patient. The prostration and systemic reaction that are customary with comparable bone destruction in pyogenic osteomyelitis were almost totally lacking. Ultimately, resolution proceeded to surprising degrees of recovery even with residual deformity, apparently unaffected by treatment.

These observations of Cockshott and MacGregor[27–29] have since been confirmed by Davidson *et al.*,[33] Eeckels *et al.*,[40] and Gupta and Srivastava.[52] Bacteriologic and viral cultures of material obtained by biopsy in three instances[40] were sterile. Histologic and microroentgenographic studies were similar in all three patients and different from what would have been expected in pyogenic infection of bone. Purulent exudate was not present; instead, bone necrosis and resorption, medullary fibrosis, and a striking diminution in numbers of osteoclasts were noted. Vascular lesions were present, characterized by intimal proliferation leading to obliteration of the lumen.

Vaccinia

With vaccination it is likely the virus

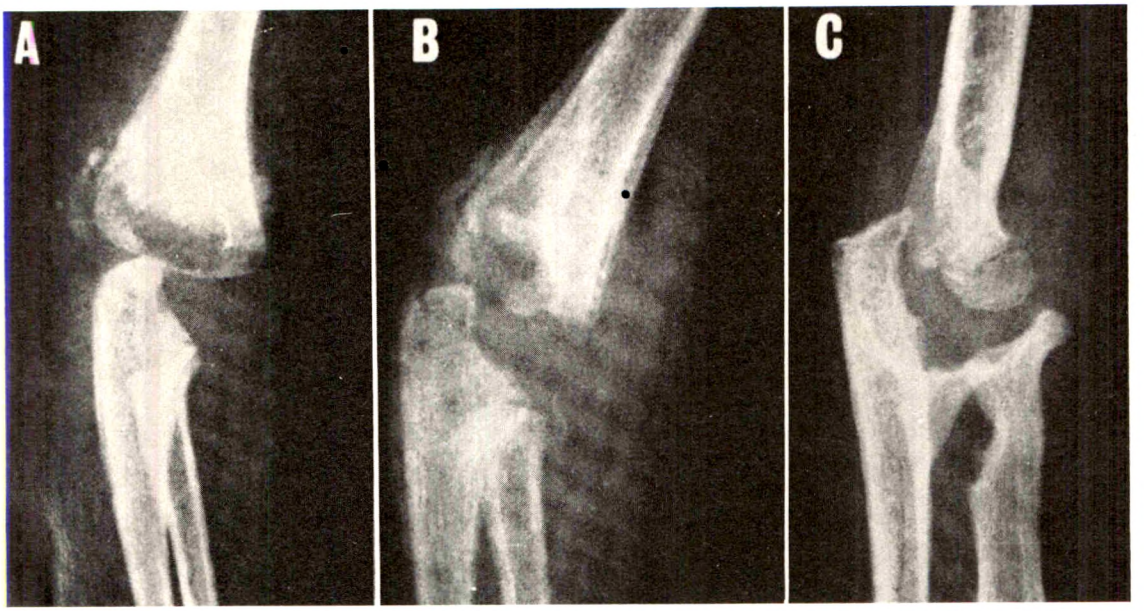


Fig. 6. Serial changes in elbow in osteomyelitis variolosa. (*A*) Acute phase. (*B*) Further disorganization of the joint three weeks later. (*C*) Flail joint, two years later. With permission from Cockshott.[29]

enters the blood stream, but only rarely does generalized infection occur. The viruses of variola and vaccinia have close biologic relationships and consequently, if bone lesions can occur in association with the more virulent smallpox virus, bone lesions with vaccinia infection are possible but are not unexpectedly infrequent.

Delano and Butler[34] reported a child of three months who developed fever, irritability, tender swellings of the feet, and pseudo-paralysis of the right arm ten days after "successful" vaccination on the left arm. Following a nine day period of improvement, the constitutional symptoms recurred. The patient gradually improved over the next four and one-half months and had no sequels. Roentgenograms at the time of the foot swellings showed new bone formation along the fifth metatarsal shafts bilaterally. During the recurrence, both clavicles and one scapula showed hyperostotic reaction and the authors felt they were describing a case of infantile cortical hyperostosis in association with vaccinia. However, they postulated that the vaccinia and the infantile cortical hyperostosis were causally related.

Another publication (Cochran *et al.*[26]) links signs and symptoms ordinarily characteristic for infantile cortical hyperostosis with vaccination. In this patient, a three and one-half week old infant, with an even more typical clinical course for infantile cortical hyperostosis, material obtained from biopsy of the scapula and overlying muscle, negative for bacteria, produced typical vaccinia pox on chorioallantoic membrane of embryonated eggs. Vaccination had been accomplished four weeks prior to the onset of skeletal disease and was followed by a "severe" reaction which took three weeks to subside. The biopsy from which the vaccinia virus was recovered was done 67 days after the initial vaccination.

A report of vaccinal bone disease without implication of associated disorder was that of Sewall.[99] This concerned a 17 month girl examined because of swelling of the distal portion of the left forearm and of the forehead, five months after a successful vaccination characterized by a "severe" reaction. The forearm swelling was first noted two weeks after the vaccination, and penicillin was given occasionally over the next

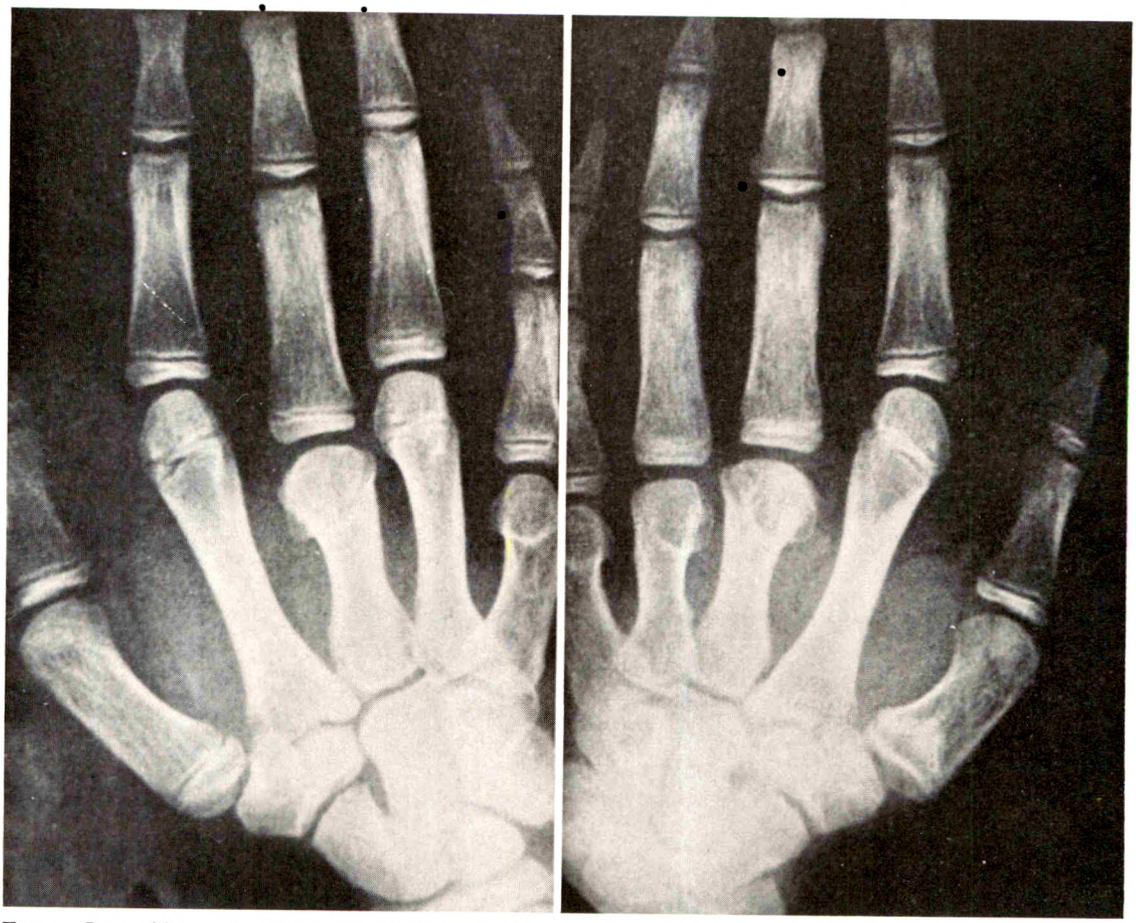


FIG. 7. Late, bizarre brachymetacarpalia secondary to premature epiphyseal union as a complication of osteomyelitis variolosa affecting the hands. Compare with Figure 2. With permission from Cockshott.[29]

two weeks because of fever. By one month after the vaccination, the clinical symptoms had disappeared but the arm swelling persisted, and one month later an asymptomatic swelling appeared on the forehead. Roentgenographic examination revealed destruction of the distal two-thirds of the right ulna with involucrum formation. In the frontal bone, an ill-defined area of demineralization about the size of a lemon was noted, and an eccentrically located density within it suggested sequestrum formation. White granular material removed at biopsy from the ulna, five and one-half months after the vaccination, did not have features of pyogenic osteomyelitis and did contain vaccinia virus. Bacterial cultures were sterile. Virus identification was accomplished by production of typical lesions on chorioallantoic membrane as well as typical intracytoplasmic inclusions. Typical skin lesions were produced in rabbits, and the infective material could be neutralized by anti-vaccinia anti-serum. Because of these findings, and the absence of clinical signs of acute pyogenic osteomyelitis, the lesions were attributed to persistent infection in the bone with vaccinia virus.

Other instances of isolation of vaccinia virus from patients with bone lesions are recorded. Barbero *et al.*[9] reported the case of a five and one-quarter year old boy who developed slowly progressive enlargement of a primary vaccination site in the arm with necrosis of the affected soft tissues (Fig. 8). Roentgenograms (Fig. 9) two and one-half months after vaccination showed a periosteal reaction about the fourth meta-

carpal bone but no other lesion. Biopsy of the bone after failure of response to usual antibacterial therapy disclosed yellow gray granulation tissue, negative for bacterial growth, but containing vaccinia virus. The patient did not have circulating antibodies to vaccinia and recovered after treatment with hyperimmune gamma globulin. In this instance, a defect in humeral immunity apparently was associated with persistence of virus in bone and other tissues in association with local tissue destructive changes.

Elliott[42] described the case of a five year old girl who developed metaphyseal irregularity of the humerus at the elbow and exuberant irregular subperiosteal new bone formation five weeks after vaccination. Microbiologic proof of the viral cause for the bone lesion is lacking in this case. The roentgenographic features are not those of infantile cortical hyperostosis and resemble more the response to a mechanical injury.

Varicella (Chickenpox)

Reports of bone involvement in varicella are practically non-existent in spite of the frequency of this disease in childhood. Two fatal cases of bone marrow involvement in varicella with virus isolation and positive serologic studies were reported by Cheatham *et al.*[22] In both cases, immunosuppression had been induced: in the first instance, by roentgen-radiation and chemotherapy in a child with metastatic neuroblastoma; and in the second, by steroid treatment of acute rheumatic fever. Similar observations were noted by Feldman *et al.*[45] in a study of 77 patients with malignancy who developed varicella; 60 were under active treatment at the time. Four of the 60 died; bone marrow lesions with focal necrosis and eosinophilic intranuclear inclusions were found in the two patients who came to necropsy.

Arthritis associated with varicella infection was reported by Ward and Bishop[118] in a five year old female who developed a knee joint effusion. The viral nature was not proved, but the patient's brother and



Fig. 8. Local extension of vaccinia (vaccinia gangrenosa) in patient with immunodeficiency disorder. With permission from Barbero *et al.*[9]

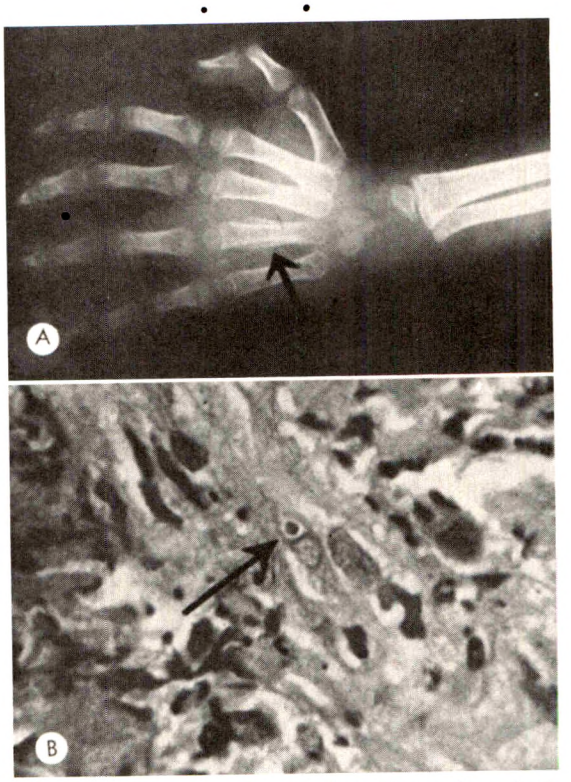


Fig. 9. (*A*) Endosteal and periosteal reaction of 4th metacarpal bone in same child as in Figure 8, two and one-half months after vaccination. Material removed at biopsy was sterile for bacteria but contained vaccinia virus.

(*B*) Photomicrograph of tissue removed from 4th metacarpal bone; arrow indicates typical Guarnieri body of vaccinia virus infection. With permission from Barbero *et al.*[9]



Fig. 10. "Celery stalk" linear markings in metaphyses of newborn infant with congenital rubella involvement of bone. This is the case presented by Dr. B. J. Reilly in 1964. Neonatal jaundice, congenital heart disease and deafness. Rubella titer high at two years. (Courtesy of Dr. B. J. Reilly, Toronto.)

sister developed varicella two weeks later, and the arthritis subsided simultaneously with the subsidence of the varicella. In a five year follow-up, no other explanation for the "arthritis" was provided. In the absence of a history of trauma, the authors felt that this was probably an infectious arthritis.

Rubella (German Measles)

Rubella infection as a cause of arthritis has been known for some time. Chambers and Bywaters[20] reported five instances of clinical arthritis in association with acute rubella affecting the small joints of the hands, and of the wrists and knees, predominantly in adult females. Synovial fluid from affected joints was quite different from that in rheumatoid arthritis, showing mononuclear rather than polymorphonuclear pleocytosis. Reports of arthralgias and clinical arthritis following natural rubella have appeared, and in some instances, the episodes were recurrent.[62,66] After live, attenuated, rubella virus became available for active immunization, the complication of acute arthritis was noted in children injected with the virus.[108,109,114] A little over one percent of the children developed recurrent joint symptoms. The knee was most commonly affected, but symptoms in smaller joints (wrists, hands, fingers) were also noted. Recovery of wild rubella virus from affected joint fluid after natural rubella,[55] and of the attenuated virus after vaccination[83,120] has been recorded. Recently, Ogra *et al.*[84] reported that rubella antibody levels were high, not only in rubella-vaccine arthritis, but also in a significant proportion of patients with juvenile rheumatoid arthritis. They found rubella virus antigen in synovial fluid in 33 percent of the patients with juvenile rheumatoid arthritis and suggested a possible role of rubella virus infection in this disease.

Roentgenographically visible bone lesions due to intra-uterine rubella infection were described by Dr. Bernard Reilly to this Society at the 1964 meeting (Fig. 10), but the relationship was not accepted until the following year when several papers were published, almost simultaneously, showing identical changes. Rudolph and his associates[94,95] incriminated wild rubella virus, transmitted *in utero*, as the cause of "characteristic" metaphyseal lesions in long bones of newborn infants. The roentgenographic features consisted of symmetrical alteration of the trabecular pattern of the metaphyses, especially in the region of the knees. Linear areas of radiolucency and increased bone density, with a longitudinal axis parallel to the long axis of the bone, abutted on irregular provisional zones of calcification at the junction with the epiphyseal cartilage. Radiolucent bands parallel to the growth plate were present in many bones, including those with the linear streaking. Periosteal reaction was specifically stated to be absent. If the child recovered from the intrauterine viral infection, return to normal trabecular architec-

ture and bone appearance was observed; in infants who failed to thrive, in whom it was subsequently shown that infection persisted, the osseous abnormalities persisted with increasing density of the juxta-epiphyseal region. Beak-like projections of the bone were noted during healing at the metaphyseal ends. The bone changes tended to parallel in their severity, the clinical severity of the disseminated viral infection. Histologic examination (Fig. 13) of bone from infants dying of the disease revealed variation in the thickness of the zone of mature cartilage cells adjacent to the epiphyseal line; multiple poorly calcified fragments of acellular cartilage and osteoid were found. The numbers of metaphyseal bony trabeculae were reduced in comparison with normal and there was a reduction in the amount of calcified bone and osteoid around the cartilaginous cores. These latter persisted far into the diaphyses. The deficiency in osteoid apparently occurred in the face of what was considered excessive osteoblastic activity characterized by large numbers of cells on the surfaces of the bone spicules. Positive cultures for rubella virus were obtained from several sites including bone marrow.

Practically simultaneous reports from many centers appeared as a consequence of the careful study of the 1964–1965 rubella epidemic in the United States and elsewhere.[31,54,68,86–88,91,92,104,124] Brandner[12] subsequently described localized periosteal reaction in rubella (Fig. 14), a feature which he felt helpful to distinguish the "distinctive" bone lesions in rubella (and cytomegalic inclusion disease) from the special but different lesions of syphilis, and from the non-specific lesions which occur in syphilis and other systemic disorders.

Marshall *et al.*[75] reported a proved instance of neonatal rubella infection (age three weeks) with virus recovery persisting up to eight months and with typical roentgenographic bone lesions, in whom a clavicular lesion was also found. This presented as an area of rarefaction which over a period of three months developed sclerosis and thickening. At one year, the clavicle was normal.



Fig. 11. Magnification photograph of metaphysis of humerus in intrauterine rubella infection. Note focal areas of osteoporosis which correspond to the metaphyseal lucencies in roentgenograms. With permission from Reed.[93]

A detailed study of the histology of bone lesions in congenital rubella was made by Reed.[93] In brief, he confirmed the metaphyseal features described in previous reports but suggested that the radiolucent streaks in roentgenograms resulted from focal areas of osteoporosis rather than poorly mineralized osteoid (Fig. 11). He considered these to result from an insult to the complex bone-forming mechanism as a consequence of the viremia. Pointing to a slowing of cell growth in tissue cultures infected by rubella virus, he suggested slowing of certain (cartilage) cell clones which could lead to focal failure of bone matrix formation (Fig. 12). Strauss,[111] in the study of an infected 19 week old fetus had previously noted a spotty delay in resorption of cartilage in the zone of provisional calcification. This led to retarded

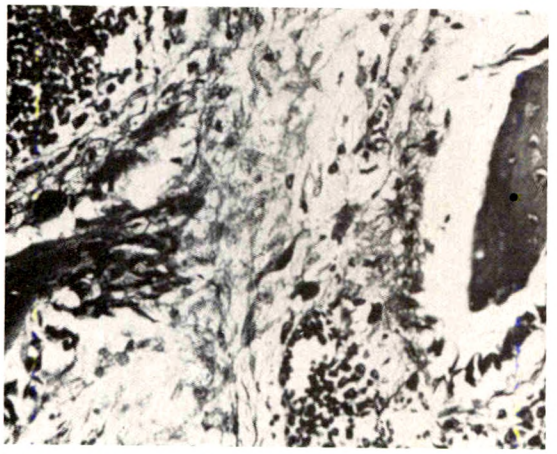


Fig. 12. Microscopic section in intrauterine rubella bone disease. Osteoblasts surround the spicule of metaphyseal bone; the marrow ground substance shows myxofibromatous changes, with large, fusiform fibroblasts. With permission from Reed.[93]

ossification of the preparatory cartilage with abnormal orientation of some bony trabeculae in the metaphysis. Strauss did not note any evidence of osteomyelitis or periostitis in her material, but Reed[93] did note scattered periosteal mononuclear infiltrations in tissues examined within about three weeks of birth.

Naeye and Blanc[81] based the clinical and radiologic features on a growth disturbance secondary to viral inhibition of cell multiplication. They provide evidence of a subnormal number of cells in many body organs. Töndury and Smith[115] invoked cell damage and necrosis without inflammatory or fibrotic response in infected fetuses to explain the findings. These authors also described destructive lesions in dental buds, but made no mention of osseous lesions.

Support for viral action on chondrocytes was provided by London *et al.*[69] who studied the mechanism for growth retardation in rabbits congenitally infected with rubella virus. They concluded that rubella virus has a predilection for cartilaginous tissue in congenitally infected rabbits, and consequently could be responsible for the growth retardation "by interfering with the maturation of the individual chondrocytes," to slow ossification and retard bone growth.

Sekeles and Ornoy[98] confirmed the thinning of the layer of hypertrophic cartilage, thinning and disorganization of metaphyseal trabeculae, and reduced numbers of osteoblasts and osteoclasts in a series of fetuses aborted between four and six months because of maternal rubella (Fig. 13). They reported abundant plasma cells in the metaphyses, and in and around blood vessels in the cartilaginous epiphyses, and in subperiosteal locations (Fig. 14). They suggested that the "excessive osteoblastic and osteoclastic activity" in prior reports might actually represent misinterpretation of this form of inflammatory cellular response. Singer and associates,[103] in a study of 18 fatal cases of rubella, obtained viral cultures from many tissues, including bone, when viremia could not be demonstrated. They felt that this precluded the contamination of tissues from the contained blood and represented the actual localization of virus in the areas sampled. A review of the bony manifestations of congenital rubella, based on 165 cases available in the literature, has been published by Saidi and Chagnon.[97]

Cytomegalic Inclusion Disease

Prior to the recognition of radiographically demonstrable bone lesions in neonatal rubella, Sacrez and associates[96] pointed out that neonatal cytomegalic inclusion disease infection could manifest changes in the long bones. The lesions were described as demineralization of the metaphyses at the knee with linear streaking and irregularity of the epiphyseal line. The initial enthusiasm for "characteristic" roentgenographic changes in the bones of neonates infected with rubella was tempered when Graham *et al.*[51] rediscovered Sacrez's report and presented another instance of bone changes in severe cytomegalic inclusion disease in an infant from whom rubella infection was excluded while cytomegalic virus was easily cultured. Metaphyseal radiolucency, streaking, and irregularity of the zone of provisional calcification were identical to the features in rubella babies on the first

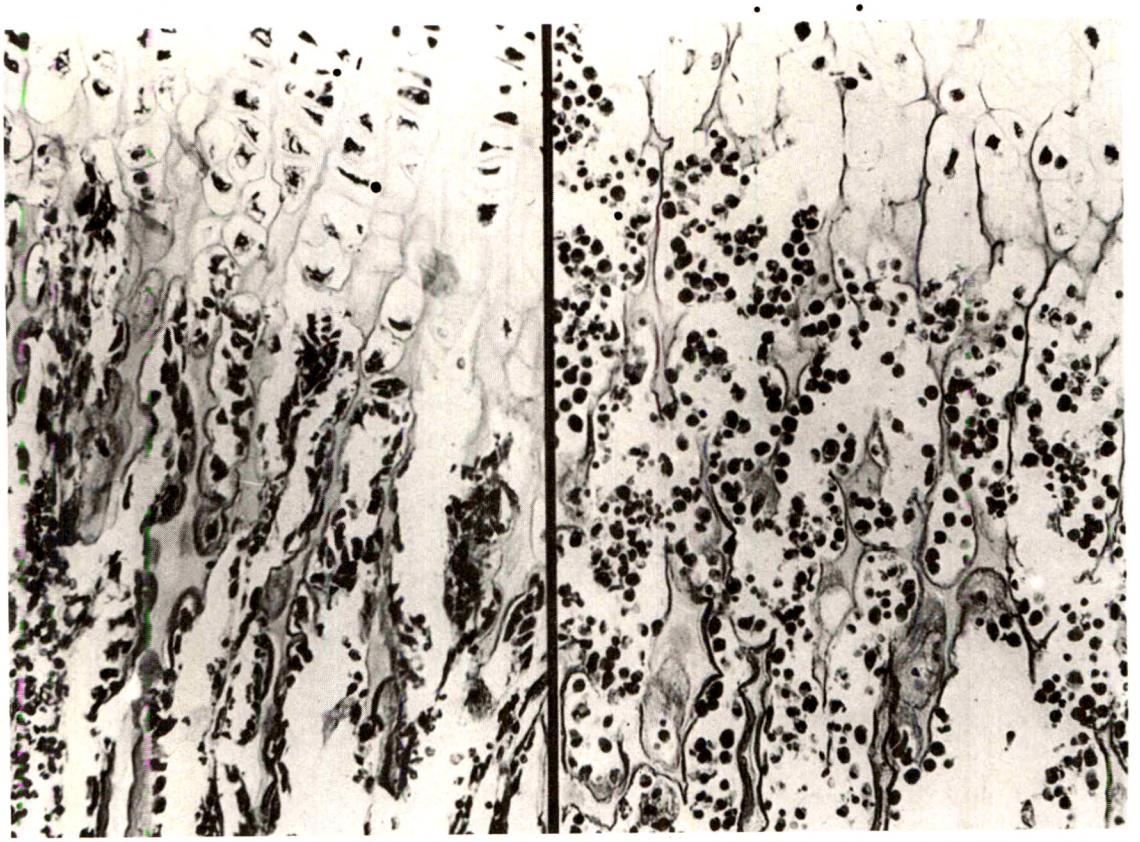


Fig. 13. Comparison of metaphyses in six month fetus without rubella (left) and six month aborted fetus with congenital rubella (right). Note relative paucity of trabeculae and marrow infiltration with plasma cells in affected fetus. (Courtesy of Dr. A. Ornoy, The Hebrew University, Hadassah Medical School, Jerusalem, Israel.)

day of life, but faded by ten days and were completely gone when the patient was examined at five weeks. The patient died at 66 days.

The implication of these reports was that the roentgenographic changes were not characteristic for rubella but required a differential diagnosis which included cytomegalic inclusion disease, congenital syphilis, and hypophosphatasia. Other intrauterine causes, especially infections, were anticipated to be found causing similar nondiagnostic changes. Graham's observations were confirmed by Merton and Gooding[77] and later by McCandless *et al.*[70] The general opinion persisted that the bone changes were due to the viral infection, but the disturbance of endochondral bone formation was considered quite different from an osteomyelitis.

Lymphogranuloma Venereum

Lymphogranuloma venereum is not a viral disease but the infective agent is an intracellular parasite which produces intracytoplasmic "elementary bodies" resembling the intracellular inclusions in cells infected with true viruses. Bone lesions have been described, exclusively, so far as I have been able to ascertain, in adults, with features resembling a low grade chronic pyogenic osteomyelitis. In fact, secondary infection is not uncommon; but those who have carefully studied the condition believe that the presence of the organism in the absence of true pyogenic reaction (the lesions in the bone as well as the lymph nodes are granulomatous) supports the opinion that the organism causing the cutaneous and lymph node disease also causes the bone lesion. The observation of

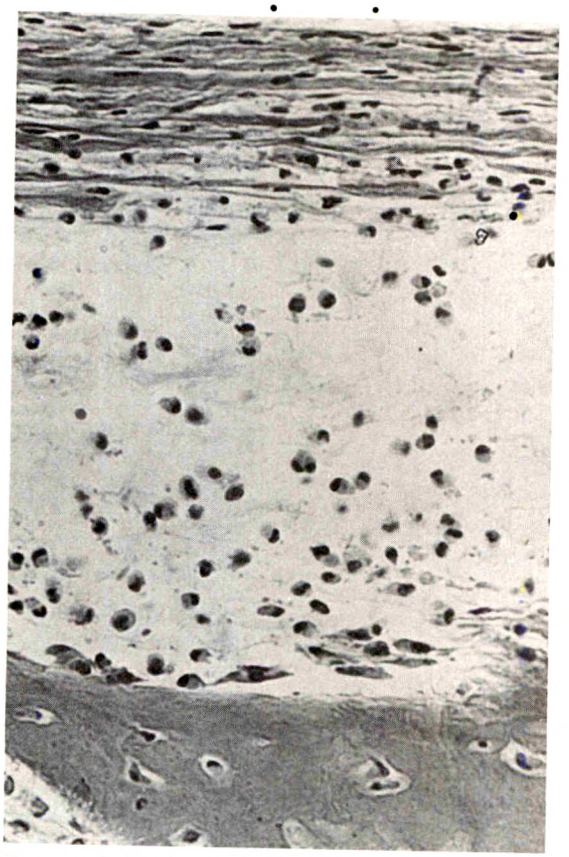


Fig. 14. Subperiosteal infiltration with plasma cells in aborted fetus with congenital rubella. (Courtesy of Dr. A. Ornoy, The Hebrew University, Hadassah Medical School, Jerusalem, Israel.)

bone lesions in the extremities, thoracic skeleton, and skull in the absence of cutaneous ulcerations is thought to favor bone infection *via* the blood stream. Further support comes from instances in which the skin lesion was secondary to a lesion in the underlying bone. Wright and Logan[125] noted the rarity of osseous changes in association with lymphogranuloma venereum but were able to report three personal cases. Sheldon *et al.*[101] reported an instance in which the organism was cultured as well as seen in biopsy sections from a bone lesion under a large ulcer in the upper leg (Fig. 15, *A* and *B*), and cited nine prior instances of bone involvement, including those in Wright and Logan's publication.

Infectious Mononucleosis

It is now generally accepted that infectious mononucleosis is a viral disease and that the etiologic agent is probably an infective agent related to, if not identical with, a form of the Epstein-Barr virus (EBV) a member of the herpesvirus group. The Epstein-Barr virus has also been implicated in the cause of Burkitt's lymphoma. Tamir *et al.*[112] reported positive antibody titers to EBV in 21 of 22 children with infectious mononucleosis, supporting the strong association.

Abebonojo[2] reported a well documented case of monoarticular arthritis in the course of infectious mononucleosis for which no cause other than the primary disorder could be found. Reports of actual bone lesions are extremely rare. Burrows,[16] however, did report the case of a nine year old boy with an acceptable diagnosis of infectious mononucleosis who complained of tenderness

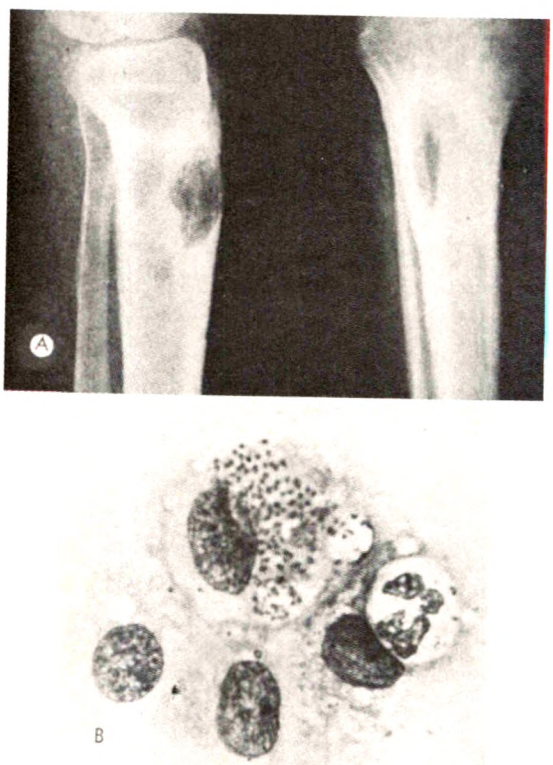


Fig. 15. (*A*) Destructive bone lesion with some sclerotic reaction in lymphogranuloma venereum. (*B*) Tissue removed at biopsy, sterile for bacteria, shows typical intracellular Bedsoniae ("large virus particles"). With permission from Sheldon *et al.*[101]

over both ulnas and the upper tibias with no signs or symptoms of joint involvement. Roentgenologic examination demonstrated thin lamellated periosteal reaction in the areas of tenderness. Bacterial and viral studies were negative but there was some elevation of serum globulins. The combination of periosteal reaction and dysproteinemia bore some resemblance to the cases described by Goldbloom *et al.*[50]

Coxsackie Virus Infection

Notwithstanding the almost ubiquitous distribution of these infective agents and their known potential for tissue damage, bone lesions caused by Coxsackie virus do not seem to have been described. Freudenberg *et al.*[48] reported a newborn infant with congenital contractures of both hip joints presumably secondary to congenital Coxsackie virus infection.

CONDITIONS AFFECTING BONE OF UNKNOWN, BUT POSSIBLY VIRAL, CAUSE

Infantile Cortical Hyperostosis (Caffey disease).

The association of Caffey disease with vaccinia infection has been noted above.[26,34] Caffey *et al.*[17] include the condition in their textbook under infections of bone on the basis that although the cause is unknown, many patients have severe and protracted fever, an elevated erythrocyte sedimentation rate, and occasionally cellular pleural or extra-pleural exudate in association with contiguous costal hyperostosis. Cellular infiltration in the periosteum early in the disease also suggests the possibility of infection.[44] We would agree with Caffey that the question of cause (or causes) must be left open, but in the context of this review, also suggest that the suspicion of a viral agent must stand high in the list of possibilities. A viral infection could explain the tendency of the disease to occur in clusters in both time and space. As has been noticed in the case of rubella and cytomegalic inclusion disease, an intrauterine transmission is possible. Such transmission is in accord with the cases reported of prenatal demonstration of the bone lesions,[8,10] lesions present at birth, and the almost invariable onset prior to the sixth month of age.[17] Even the familial instances of infantile cortical hyperostosis[25,117] could favor an infectious basis. Tuberculosis was considered a familial disease until a causative organism was found and its pathway of transmission was clearly defined. The apparent immunity to recurrence after the initial course of the disease is not unlike the immunity following other viral diseases. The usual antibacterial therapeutic agents have no effect on the course of the disease, as is common in viral infections. In several instances, alterations in the serum proteins have been noted (Fig. 16); such changes not uncommonly represent responses to infection, and may include specific antibodies to a causal agent capable of reacting with causal agent antigen if it were only known.

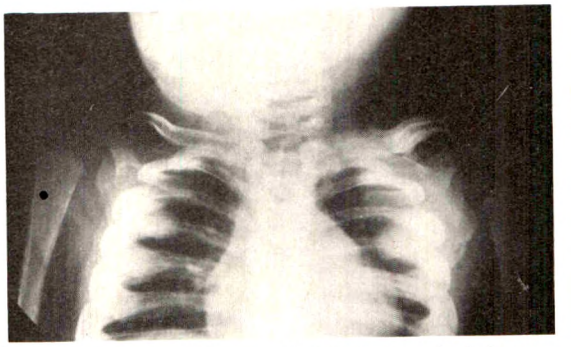


FIG. 16. Caffey disease (infantile cortical hyperostosis). Typical costal, clavicular, scapular and mandibular involvement in three month old boy with classical clinical features. Alpha 2 globulins were appreciably elevated at time of this examination, but had returned to normal by $7\frac{1}{2}$ months when roentgenograms were also normal.

Temperley *et al.*[113] indicated that elevations of gamma globulins in infantile cortical hyperostosis are consistent with an *in utero* viral infection, representing a residual response to a disease which may even then have run its course. Altered serum proteins may also indicate an altered immune status. Two instances of infantile cortical hyperostosis in association with an immunodeficient disease were reported by McEnery and Nash.[71] Both children suf-

fered from the Wiskott-Aldrich syndrome; in one, there was a history of mandibular swelling in the mother when she was 15 years of age which had been diagnosed as Caffey disease. For both children, the authors hypothesized that the immunologic defect predisposed to whatever is the causal agent for infantile cortical hyperostosis, and speculated on the frequency of the association of infantile cortical hyperostosis in other less obvious forms of the immunodeficiency disease. In the absence of a bacterial cause for the typical infantile cortical hyperostosis in this severe immunologic defect, a viral cause seems possible.

Other Hyperostotic Disorders of Possible Viral Origin

Other conditions of unknown origin with cortical hyperostotic manifestations bear certain similarities to infantile cortical hyperostosis and merit mention here. Goldbloom and associate's[50] patients were mentioned in relation to infectious mononucleosis. These children, with fever, pain and tenderness in the bones, developed subperiosteal new bone in the tubular bones, and also in the mandible. An elevation of gamma globulins as well as transient disturbance of other plasma proteins occurred in both patients.

Melhem *et al.*[76] reported two instances in which soft tissue swelling followed by extensive cortical hyperostoses in limb bones was associated with elevated serum phosphate levels (hyperphosphatemia). Other laboratory studies were not remarkable and biopsy in one instance showed vascular connective tissue between the trabeculae of subperiosteal new bone formation with some round cell infiltration but no diagnostic features. Some similarities did exist with Goldbloom's patients, but the clinical course and the roentgenologic findings were not unlike those seen in the condition described by Soriano.[105,106] This author reported a bizarre form of cortical hyperostosis of unknown cause associated with severe disability and delayed spontaneous recovery except for residual bony deformity. The autopsy specimens are also not unlike those seen in avian osteopetrosis.

These unusual forms of cortical hyperostotic disorders are included because they all have features which suggest an infectious origin and yet in none has an infectious cause been found; virus infection is a possibility.

Cat Scratch Disease

The fascinating history of the discovery of this disease of unknown cause has been described by Carithers[19] and an encyclopedic review has been published by Warwick.[119] No infectious agent has been found for the disease; a viral agent has been suspected. In 1954, Adams and Hindman[1] reported an osteolytic lesion of the ilium in a five year old boy with a fluctuant cervical lymph node from which biopsy showed multiple granulomas with central necrosis compatible with cat scratch disease. The appearance of the ilium was comparable to that produced by an eosinophilic granuloma, or a granulomatous process. Biopsy of the lesion, which was sterile on culture for bacteria and fungi, showed "vascular fibroplastic tissue infiltrated with small lymphocytes . . . rare nodular aggregates of large mononuclear cells were present. . . ." The patient reacted positively to antigen for the diagnosis of cat scratch disease obtained from two sources. The bone lesion slowly resolved, and complete healing was observed nine months later.

In 1959, Collipp and Koch[30] reported a similar bone lesion in a four year old boy who had a swollen cervical lymph node. A skin test with cat-scratch antigen was positive. On the 26th day of illness, the cervical lymph node was fluctuant and material obtained at drainage was sterile but gave a positive reaction when injected into another patient known to have had cat scratch disease. On the 28th day of illness there was a destructive lesion in the femoral neck with slight periosteal reaction

(Fig. 17). A needle biopsy of the lesion done on the 41st day obtained sterile material, granulomatous in nature, with central necrosis surrounded by epithelioid cells and lymphocytes compatible with the diagnosis of cat-scratch disease. The patient subsequently improved clinically and roentgenologically, but a defect was still present in the femoral neck five months later.

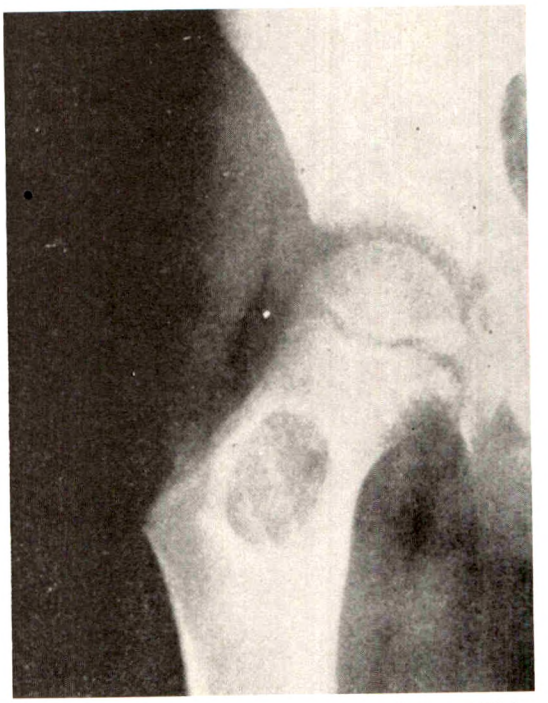


Fig. 17. Bone lesion in cat-scratch disease. With permission from Collipp and Koch.[30]

ANIMAL AND LABORATORY STUDIES

Avian Osteopetrosis

The experiments of nature which are studied clinically need to be complemented by experiments deliberately designed to answer questions which cannot be answered by investigations in humans. A considerable body of knowledge has accumulated concerning viral bone disease in birds and other laboratory species. The best known is avian osteopetrosis. Originally described by Pugh[90] in Great Britain as a sporadic disease of fowl characterized by symmetrical thickening of the shafts of the long bones, it has been shown to be an experimentally transmittable disease *via* a filterable agent obtained from infected birds. The disease can be produced by injecting filtered plasma, whole blood, or suspensions of bone marrow cells from birds with active bone lesions into day old chicks (Fig. 18). The first reaction is periosteal proliferation which is followed by subperiosteal new bone formation and in some by a defect in mineralization at the ends of the bones (Fig. 19). The thickening of the compacta (cortex) results in bone that is wider and more dense than normal with a narrow medullary cavity. The calvarium and the mandible may be affected (Fig. 20). Unlike Caffey disease, however, spontaneous recovery does not take place, and thus some affected birds die early while others live two years or more dying as a result of profound anemia due to occlusion of marrow spaces by endosteal bone. In 20 percent of experimentally affected birds, soft tissue tumors occurred; the virus responsible for osteopetrosis (Fig. 21) could conceivably have activated latent leukosis virus in these birds.

Holmes[56,57] states "It seems likely that the virus exerts its effects directly on the skeleton, with a predilection initially for the long bone periosteum causing new bone formation, primarily in the long bone diaphyses but later throughout the skeleton." Simpson and Sanger[102] note that the condition differs from human osteopetrosis which results from a failure to remove primary spongiosa within the shaft; avian "osteopetrosis" results from excessive subperiosteal spongy bone (Fig. 22). The affected osteoblasts and osteocytes apparently form bone faster than normal. These authors suggest the roentgenologic and histologic changes in avian osteopetrosis are closer to those occurring in Caffey disease, Engelmann disease, and Ribbing disease than to those in human osteopetrosis.

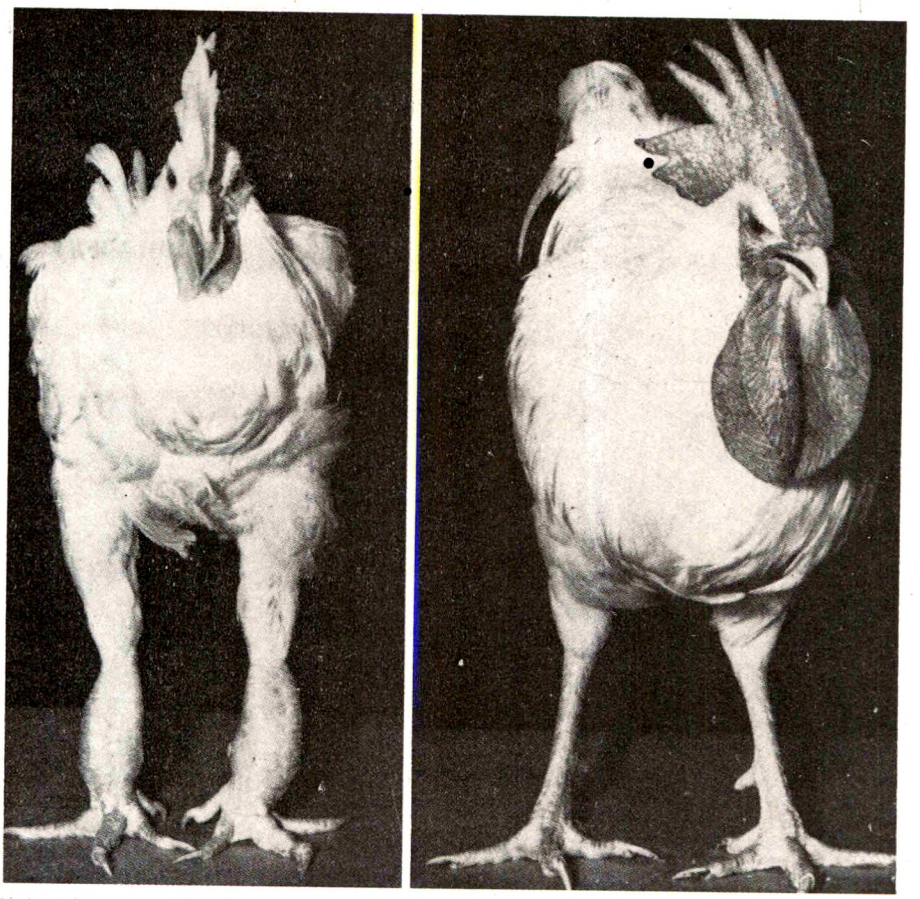


Fig. 18. Marked bony swelling in avian osteopetrosis. Both chickens are 183 days old; the one on the left was injected with leukosis virus at one day of age. With permission from Simpson and Sanger.[102]

Laboratory Induced Virus Diseases With Bone Changes

Buddingh,[15] noting that vaccine virus found in inoculated animals was as generally distributed as were the lesions, described changes which occurred when the chick embryo was injected. Bone marrow was second only to liver in titratable viral activity, and the periosteal tissues were consistently involved by perivascular collections of large mononuclear cells. Buddingh stated "Every section studied which contained bone structures showed evidence of involvement of the periosteum throughout the entire course of the disease." In addition, extreme involvement of synovial surfaces of the joints was noted. Inclusion bodies in connective tissue cells of both periosteum and synovia indicated proliferation of virus in these cells. Buddingh felt that the distribution and nature of the lesions closely corresponded to the findings in human disease, but that the relative volume of the inoculum was greater in the experimental model.

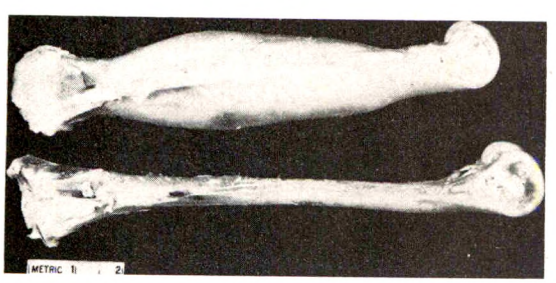


Fig. 19. Experimental osteopetrosis of tibia. Seventy-five day old chicken with 70 day old normal control. With permission from Simpson and Sanger.[102]

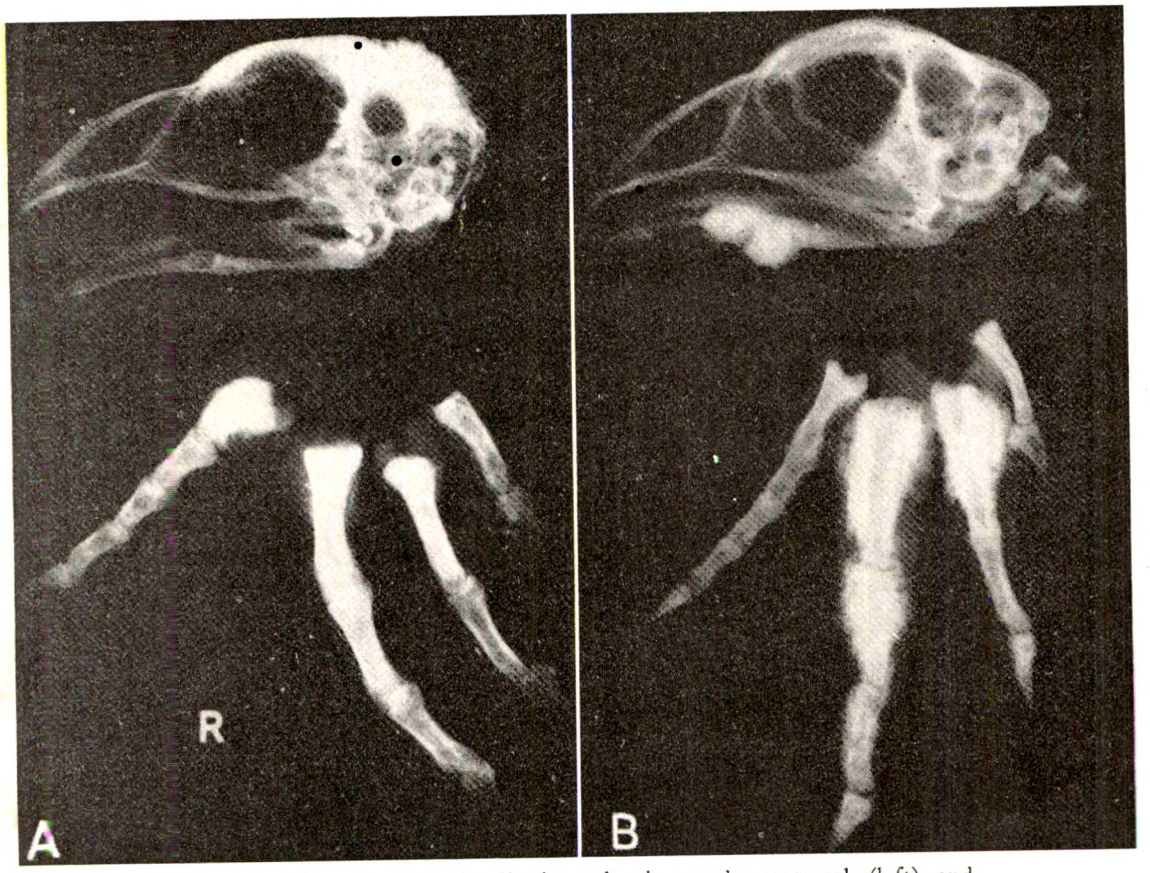


Fig. 20. Avian osteopetrosis affecting calvarium and metatarsals (left), and mandible and metatarsals (right). With permission from Holmes.[56]

Lillie and Armstrong[67] studied generalized vaccinia in rabbits. Citing Chiari[24] in relation to necrotic bone cells in involved trabeculae in the marrow lesions of variola, as well as previous reports of vaccinal osteomyelitis, they suggested that the vaccinal lesions and the variolar lessions represented the same osteomyelitic process.

Dalldorf[32] described an osteolytic virus (OLV) found in human cancer and transplantable in laboratory animals which had an effect principally on bones and teeth. Subsequently, Ferm and Kilham[46] injected suckling hamsters with several closely related viruses including H-1 (see below) and OLV, and reported skeletal changes.

Markowa[72] reported an instance of acute osteitis, presumably viral, in a seven year old boy with an encephalitic syndrome. Subsequently, he showed growth of tick-borne encephalitis virus in bone and associated skeletal changes after intraosseous inoculation in mice.

Heggie[53] studied embryonic hamster bone in tissue culture in which H-1 virus was inoculated. H-1 virus is a small infective agent containing deoxyribonucleic acid (DNA) originally recovered from certain rat and human tumors, and found to produce bone and dental changes (among others) when injected into suckling hamsters. As viral replication increased in the culture, infected bones changed shape in comparison with non-infected ones, increased less in weight, and showed histologic evidence of damage to bone-forming cells in the periosteum. Hoover and Griesemer[58] inoculated kittens intravenously with feline herpesvirus and produced osteolytic lesions which could be correlated with

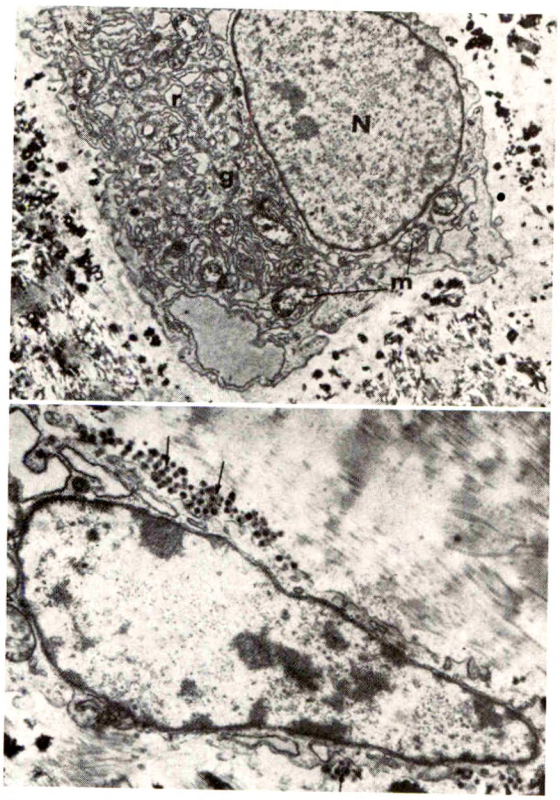


Fig. 21. Electromicroscopic comparison of normal osteoblast (above) and osteoblast from an affected bone in avian osteopetrosis (below). Viral particles are present in the intracellular osteoid adjacent to the osteoblast, in close proximity to the plasma membrane of an osteoblast and its nucleus with margination of chromatin. N= (nucleus); r= (endoplasmic reticulum); m= (mitochondria); and g= (Golgi apparatus). With permission from Simpson and Sanger.[102]

intranuclear inclusion bodies, viral antigen, viral particles, and infectious virus. Necrotic lesions of bone (Fig. 23) were found in the growth regions of numerous bones and cellular degeneration and necrosis were present in the primary spongiosa of long bones. Intranuclear inclusion bodies occurred in many types of cells including osteoclasts, osteoblasts, and periosteal cells. Necrotic osteocytes were seen but intranuclear inclusions were not observed in these. Areas of periosteal necrosis were present (Fig. 24). Osteolytic lesions were restricted to regions of osteogenesis.

Viruses and Bone Tumors

Oncogenic viruses in animals have been under intensive study. Support for viral causation of bone neoplasia in mice, rats and hamsters, comes from the apparent induction of tumors,[35] the finding of virus particles in human[37] and animal tumors,[74] biochemical studies of the nucleoproteins in affected cells,[5,38] and immunologic evidence for antibodies to tumor cells.[36,89] It has been suggested that malignant transformation of cells following ionizing irradiation may be related to viruses latent within the cells until activated by the physical agent.[63,117] "Latency" of viruses may actually represent a virus-host equilibrium. The possibility of viral causes for human cancer has been the focus for many investigations,[18,123,138] but unequivocal evidence of viral causation for human cancer has not yet been forthcoming.[49]

DISCUSSION

The question to which we have addressed our inquiry is whether or not viral diseases of bone exist. If the answer is yes, we must

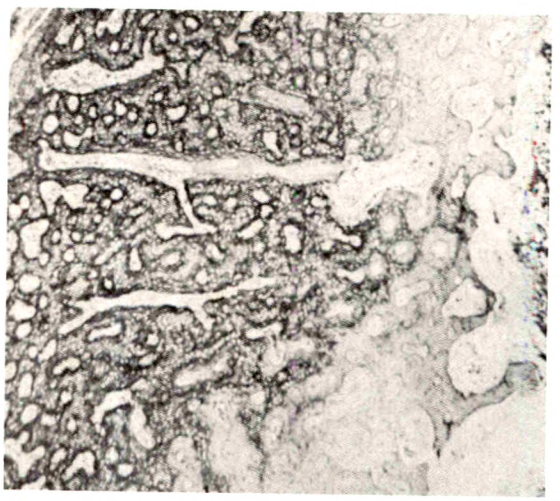


Fig. 22. Histologic cross section of bone affected by avian osteopetrosis. The normal compact bone is to the right, spongy subperiosteal new bone is on the left. A minute portion of affected periosteum is seen in the upper left corner. With permission from Simpson and Sanger.[102]

ask what are they and why are they not better known? Are bones resistant to viral infection, and if so, does this resistance have any preventive or therapeutic implications with respect to other viral diseases? Are there other conditions which should be investigated for viral factors in their occurrence? And can roentgenographic examination add new dimensions to viral diseases in which clinical signs are lacking in the skeletal system? Even more basic, is there a need for more histologic (including electron microscopic) investigation of skeletal structures in "routine" necropsy material, and for efforts to identify viral agents in bone from biopsy as well as necropsy specimens?

The experimental studies cited leave little doubt that viruses can have pathologic effects on growing bone which represent induced viral disease of bone. The question of whether or not they act directly



Fig. 23. Necrotic primary spongiosum in tibia of kitten six days after intravenous inoculation with feline herpesvirus. Note widespread pyknosis and karyorrhexis of bone cells. From Hoover and Griesemer.[58]

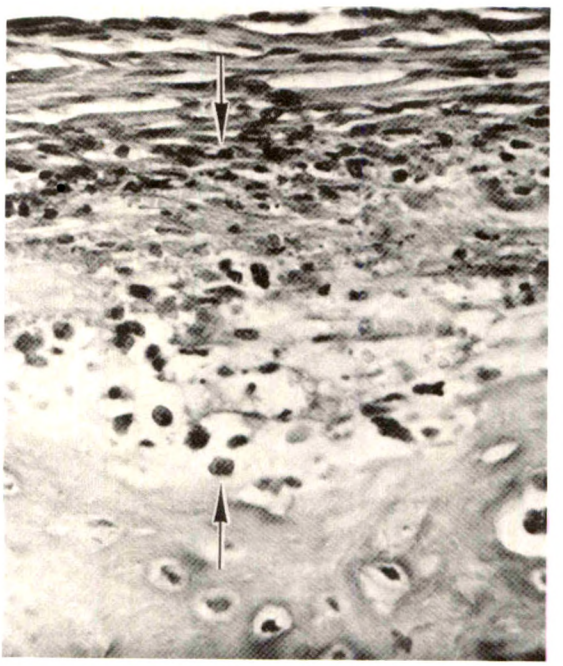


Fig. 24. Periosteal and subperiosteal necrosis (between arrows) in femur of kitten six days after intravenous inoculation with feline herpesvirus. Compare with Figure 14. From Hoover and Griesemer.[58]

or through intermediary factors (vascular, chemical, metabolic, etc.) is immaterial; in the presence of virus, reproducible alterations of bone occur which are different from the changes occurring in health. Therefore, virus diseases of bone do exist in the laboratory.

Likewise, smallpox does cause bone disease as described so clearly by the authors whose personal observations have provided the material for this presentation. The repetitive pattern of clinical signs and roentgenographic features described by most observers,[21,27–29,40,41,52,79,80] suggests a common causal agent different from the usual bacterial osteomyelitis which demonstrates a different, and also repetitive, constellation of clinical and roentgenographic signs. Even the case described by Huenekens and Rigler[60] in which roentgenographic features were relatively mild would not be expected to be caused by pyogenic complication considering that the disease occurred prior

to the era of specific antibacterial therapy when pyogenic osteomyelitis ran a quite different clinical course than it does today.

The association of vaccinia infection with clinical and roentgenologic signs of infantile cortical hyperostosis,[26,34] if causally related, may indicate only that vaccinia virus is one of several which can cause infantile cortical hyperostosis. There may be a latent virus which can be activated by vaccinia, among other agents. The current interest in "slow virus" infection may have an appropriate field to explore in Caffey disease. However, we cannot overlook the role of size of viral inoculum in the disease, as stated by Buddingh.[15]

The bone lesions of rubella and cytomegalic inclusion disease are usually attributed to "nutritional" effects of infection. Bone lesions are not necessarily a new manifestation of rubella; they have probably only been newly recognized. Cooper *et al.*[31] cite a personal communication from Dr. G. W. Mellin to the effect that typical changes were seen in films of patients with congenital rubella syndrome in 1951 and 1955. The enormous capacity of bones to remodel (*viz.*, disappearance of lesions within weeks to months) could easily obscure the true incidence of bone involvement. Infants infected early *in utero* might have gone through the sequence of bone disease and recovery by the time they were presented to medical scrutiny.

The current activity in exploration of the Epstein-Barr and other herpesviruses offers to provide new understanding of conditions like infectious mononucleosis, and *via* lymphoma studies, other less benign hematologic disorders. Coupled with appropriate use of clinical roentgenographic procedures, they may lead to better understanding of Caffey disease, cat scratch disease, and conditions like generalized fibromatosis of the newborn, cherubism, hyperphosphatasemia, and other disorders of unknown cause affecting bone. One might even ask if congenital pseudarthroses could be a suitable subject for this type of study, in view of the evidence that virus proliferated in healing osseous wounds of adult hamsters, interfering with callus formation and subperiosteal osteogenesis.[43]

The review by Altshuler and Russell[4] on chronic intrauterine infection suggests that careful study of the placenta for evidence of viral disease may indicate infants in whom investigation for virus disease of bone may be especially rewarding. An increased frequency of careful examination of the skeletal system in routine necropsies can be assisted significantly in the recognition of virus diseases of bone by electron microscopy techniques. The rapid diagnosis of small pox by electron microscopy has been current for some time[39] and the diagnosis of other viral diseases, *e.g.*, gastroenteritis, ocular infections, respiratory infections, etc., is now a routine function in some electron microscopy laboratories.[6,85]

In the background stands the challenge of neoplastic disease of bone in relation to viruses. Many orthodox microbiologic concepts derived from studies of bacteria do not apply in the field of virology. The limitations of Koch's third and fourth postulates with respect to experimental transmission of disease in humans are real. Dalldorf[32] indicates that the first two are also of little value to the virologist. The virus cannot be grown *in vitro* in the absence of living material; and the lesions induced by a virus inoculated into an experimental animal may bear little resemblance to the primary disease. A virus which may cause a recognizable disease in one species of animal may produce a neoplasm in another.[59,126]

To summarize the literature which has been reviewed on the subject of viral infections and bone disease, we can say there is good evidence for bone involvement in smallpox and a strong suggestion that it also occurs in vaccinia. Bone changes are not described in varicella although evidence of the presence of virus within the marrow has been established and a possible instance of arthritis has been reported. Almost specific, roentgenologically demonstrable bone lesions are seen in a high per-

centage of infants affected with transplacental rubella, and definite involvement of joints occurs in natural rubella as well as in the modified form of the disease that is induced for vaccination purposes. Roentgenologically demonstrable bone lesions after infancy have not been reported in rubella. In cytomegalic inclusion disease of newborn infants (acquired intragestationally as in rubella) roentgenologically demonstrable lesions are seen which are indistinguishable from those due to rubella. Lymphogranuloma infection can be associated with bone lesions; periosteal reaction has been described in infectious mononucleosis. Infantile cortical hyperostosis and cat scratch fever are conditions in which bone lesions occur but a cause, viral or otherwise, has not been established. Avian osteopetrosis is a distinct viral disease of bone and several forms of virus, including H-1 and feline herpesvirus, can produce skeletal lesions in experimental animals, but roentgenographic features of this involvement have not yet been described. The role of viruses in the production of bone tumors is suggested but unproved.

The pediatric radiologist is in an advantageous position to contribute to the as yet unanswered questions. Viruses appear to have a predilection for actively proliferating cells, and actively proliferating cells are found more commonly in the infant and child than in the adult. If we can exercise the same intellectual curiosity and sharing of these discoveries which the exercise produces as Dr. Neuhauser did in his exploration of a disease produced by the common puffball—lycoperdonosis—we too may have an opportunity to expand the knowledge of human health and disease.

Division of Roentgenology
Children's Hospital Medical Center
University of Cincinnati College of Medicine
Cincinnati, Ohio 45229

REFERENCES

1. Adams, W. C., and Hindman, S. M. Cat-scratch disease associated with osteolytic lesion. *J. Pediat.*, 1954, *44*, 665–669.
2. Adebonojo, F. O. Monoarticular arthritis: unusual manifestation of infectious mononucleosis. *Clin. Pediat.*, 1972, *11*, 549–550.
3. Aegerter, E. E., and Kirkpatrick, J. A., Jr. Orthopedic Diseases: Physiology, Pathology, Radiology. Third edition. W. B. Saunders Company, Philadelphia, 1968.
4. Altshuler, G., and Russell, P. Human placental villitides: review of chronic intrauterine infection. *Curr. Top. Path.*, 1975, *60*.
5. Bader, J. P., and Steck, T. L. Analysis of ribonucleic acid of murine leukemia virus. *J. Virol.*, 1969, *4*, 454–459. (Cited by Dmochowski *et al.*)[37]
6. Banatvala, J. E., Chrystie, I. L., and Flower, A. J. E. Rapid diagnosis of virus infections. *Lancet*, 1975, *2*, 79–80.
7. Bancroft, I. R. Clinical observations on variola. *J. Med. Res.*, 1904, *11*, 322–344.
8. Barba, W. P., II, and Freriks, D. J. Familial occurrence of infantile cortical hyperostosis *in utero*. *J. Pediat.*, 1953, *42*, 141–150.
9. Barbero, G. J., Gray, A., McNair Scott, T. F., and Kempe, C. H. Vaccinia gangrenosa treated with hyperimmune vaccinal gamma globulin. *Pediatrics*, 1955, *16*, 609–618.
10. Bennett, H. S., and Nelson, T. R. Prenatal cortical hyperostosis. *Brit. J. Radiol.*, 1953, *26*, 47–49.
11. Blattner, R. J. Bone and joint involvement in virus disease. *J. Pediat.*, 1965, *67*, 144–147.
12. Brandner, M. Die Bedeutung der metaphysären Ossifikationsstörungen im Säuglingsalter mit besonderer Berücksichtingung der infektiösen Fetopathien. *Fortschr. a. d. Geb. de Rèntgenstrahlen u. d. Nuklearmedizin*, 1973, *118*, 531–537.
13. Bras, G. Morbid anatomy of smallpox. *Docum. Med. geog. et trop.* (Amst.) 1952, *4*, 303–351.
14. Brown, W. L., and Brown, C. B. Osteomyelitis variolosa. *J.A.M.A.*, 1923, *81*, 1414–1416.
15. Buddingh, G. J. Study of generalized vaccinia in the chick embryo. *J. Exper. Med.*, 1936, *63*, 227–240.
16. Burrows, F. G. Transient periosteal reaction in illness diagnosed as infectious mononucleosis. *Radiology*, 1971, *98*, 291–292.
17. Caffey, J., *et al.* Pediatric X-ray Diagnosis. Sixth edition. Year Book Medical Publishers, Inc., Chicago, 1972.
18. Camiel, M. R., Alexander, L. L., and Benninghoff, D. L. Hypothesis for viral oncogenesis of Gardner's syndrome. *J. Nat. Med.*, 1971, *63*, 272–275.
19. Carithers, H. A. Cat-scratch disease. *A.M.A., Am. J. Dis. Child.*, 1970, *119*, 200–203.
20. Chambers, R. J., and Bywaters, E. G. Rubella

synovitis. *Ann. Rheum. Dis.*, 1963, *22*, 263–268.

21. Chatterjee, R. N. Incidence of arthritis in smallpox. *Indian M. Gaz.*, 1950, *85*, 49–54.
22. Cheatham, W. J., Weller, T. H., Dolan, T. F., Jr., and Dower, J. C. Varicella: report of two fatal cases with necropsy, virus isolation and serologic studies. *Am. J. Path.*, 1956, *32*, 1015–1035.
23. Chiari, H. (A)-Ueber Orchitis variolosa. *Ztschr. f. Heilk.*, 1886, *7*, 385–406.[24] (B)-Weitere Beitrage zur Lehre von der Orchitis variolosa. *Ztschr. f. Heilk.*, 1889, *10*, 340–352.[24]
24. Chiari, H. Ueber osteomyelitis variolosa. *Beitr. z. path. Anat. u. z. allg. Path.*, 1893, *13*, 13–31.
25. Clemett, A. R., and Williams, J. H. Familial occurrence of infantile cortical hyperostosis. *Radiology*, 1963, *80*, 409–416.
26. Cochran, W., Connolly, J. H., and Thompson, I. D. Bone involvement after vaccination against smallpox. *Brit. M. J.*, 1963, *2*, 285–287.
27. Cockshott, P., and MacGregor, M. Osteomyelitis variolosa. *Quart J. Med.*, 1958, *27*, 369–387.
28. Cockshott, P., and MacGregor, M. Natural history of osteomyelitis variolosa. *J. Fac. Radiologists*, 1959, *10*, 57–63.
29. Cockshott, W. P. Osteomyelitis variolosa. *Z. Tropenmed. Parasit.*, 1965, *16*, 199–206.
30. Collipp, P. J., and Koch, R. Cat scratch fever associated with osteolytic lesion. *New England J. Med.*, 1959, *260*, 278–280.
31. Cooper, L. Z., Green, R. H., Krugman, S., Giles, G., and Mirick, G. S. Neonatal thrombocytopenic purpura and other manifestations of rubella contracted *in utero*. *A.M.A., Am. J. Dis. Child.*, 1965, *110*, 416–427.
32. Dalldorf, G. Viruses and human cancer. *Bull. N. Y. Acad. Med.*, 1960, *36*, 795–803.
33. Davidson, J. C., Palmer, P. E. S., and Bulawayo, P. E. Osteomyelitis variolosa. *J. Bone & Joint Surg.*, 1963, *45*-B, 687–693.
34. Delano, P. J., and Butler, C. D. Etiology of infantile cortical hyperostosis. Am. J. Roentgenol. & Rad. Therapy, 1947, *58*, 633–636.
35. Dmochowski, L. Studies on relationship of RNA viruses to origin of leukemia and solid tumors of animals and man. *Bibl. Haematol.*, 1973, *39*, 1194–1207.
36. Dmochowski, L. Personal communication.
37. Dmochowski, L., Georgiades, J., East, J. L., Allen, P. T., and Bowen, J. M. Virus retrieval studies in human neoplasia. *Bibl. Haematol.* #40, Comp. Leuk. Res., 1973, Leukemogenesis. Edited by Y. Ito and R. M. Dutcher. Karger, Basel, 1975, pp. 431–449.
38. East, J. L., Allen, P. T., Knesek, J. E., Chan, J. C., Bowen, J. M., and Dmochowski, L. Structural rearrangement and subunit composition of RNA from released Soehner-Dmochowski murine sarcoma virions. *J. Virol.*, 1973, *11*, 709–720.
39. Editorial. Rapid diagnosis of viral disease. *Lancet*, 1975, *1*, 1411.
40. Eeckels, R., Vincent, J., and Seynhaeve, V. Bone lesions due to smallpox. *Arch. Dis. Childhood*, 1964, *39*, 591–597.
41. Eikenbary, C. F., and LeCocq, J. F. Osteomyelitis variolosa; report of three cases. *J.A.M.A.*, 1931, *96*, 584–587.
42. Elliott, W. D. Vaccinal osteomyelitis. *Lancet*, 1959, *2*, 1053–1055.
43. Engler, W. O., Baer, P. N., and Kilham, L. Effects of rat virus on healing osseous wounds. *A.M.A. Arch. Path.*, 1966, *82*, 93–98.
44. Eversole, S. L., Jr., Holman, G. H., and Robinson, R. A. Hitherto undescribed characteristics of pathology of infantile cortical hyperostosis (Caffey's disease). *Bull. Johns Hopkins Hosp.*, 1957, *101*, 80–99.
45. Feldman, S., Hughes, W. T., and Daniel, C. B. Varicella in children with cancer: seventy-seven cases. *Pediatrics*, 1975, *56*, 388–397.
46. Ferm, V. H., and Kilham, L. Skeletal studies of virus induced dwarfism. *Growth*, 1965, *29*, 7–16.
47. Fournier, F., Sarragne, M., Rouffet, A., Leaute, J.-B., and Chany, C. Mécanisme d'action de facteurs tissulaires inhibant l'état antiviral établi par l'interféron. *C. R. Acad. Sci.* (Paris), 1974, *278*, 1915–1918.
48. Freudenberg, E., Roulet, F., and Nicole, R. Kongenitale Infektion mit Coxsackie-Virus, *Ann. Paediat.*, 1952, *178*, 150–161.
49. Gellhorn, A. Background and promise of tumor virology, immunology and chemotherapy and a challenge to radiotherapy. Janeway Memorial Lecture. Am. J. Roentgenol. Rad. Therapy & Nuclear Med., 1973, *117*, 489–501.
50. Goldbloom, R. B., Stein, P. B., Eisen, A., McSheffrey, J. B., Brown, B. St. J., and Wiglesworth, F. W. Idiopathic periosteal hyperostosis with dysproteinemia: new clinical entity. *New England J. Med.*, 1966, *274*, 873–878.
51. Graham, C. B., Thal, A., and Wassum, C. S. Rubella-like bone changes in congenital cytomegalic inclusion disease. *Radiology*, 1970, *94*, 39–43.
52. Gupta, S. K., and Srivastava, T. P. Roentgen features of skeletal involvement in smallpox. *Australasian Radiol.*, 1973, *17*, 205–211.
53. Heggie, A. D. Pathogenesis of H-1 virus infec-

tion of embryonic hamster bone in organ culture. *J. Exp. Med.*, 1971, *133*, 506–519.
54. Highman, J. H. Congenital osseous rubella. *Clin. Radiol.*, 1967, *18*, 445–449.
55. Hildebrandt, H. M., and Maassab, H. F. Rubella synovitis in 1 year-old patient. *New England J. Med.*, 1966, *274*, 1428–1430.
56. Holmes, J. R. Radiological changes in avian osteopetrosis. *Brit. J. Radiol.*, 1961, *34*, 368–377.
57. Holmes, J. R. Avian osteopetrosis. *Nat. Cancer Inst. Monograph*, 1964, *17*, 63.
58. Hoover, E. A., and Griesemer, R. A. Bone lesions produced by feline herpes virus. *Lab. Invest.*, 1971, *25*, 457–464.
59. Huebner, R. J., Rowe, W. P., and Lane, W. T. Oncogenic effects in hamsters of human adenovirus types 12 and 18. *Proc. Nat. Acad. Sc. U. S.*, 1962, *48*, 2051–2058.
60. Huenekens, E. J., and Rigler, L. G. Osteomyelitis variolosa: report of case observed during acute stage. *J.A.M.A.*, 1926, *87*, 295–298.
61. Jaffe, H. L. Metabolic, Degenerative, and Inflammatory Diseases of Bones and Joints. Lea & Feiberger, Philadelphia, 1972.
62. Kantor, T. G., and Tanner, M. Rubella, arthritis and rheumatoid arthritis. *Arthritis & Rheum.*, 1962, *5*, 378–383.
63. Kaplan, H. S. On natural history of murine leukemias. *Cancer Res.*, 1967, *27*, 1325–1340.
64. Kilroy, A. W., Schaffner, W., Fleet, W. F., Jr., Lefkowitz, L. B., Jr., Karzon, D. T., and Fenischel, T. M. Two syndromes following rubella immunizations: clinical observations and epidemiological studies. *J.A.M.A.*, 1970, *214*, 2287–2292.
65. Latarjet, R. Sur l'étiologie virale de certains ostéosarcomes ostéogènes: revue critique. *Bull. Cancer*, 1971, *58*, 277–286.
66. Lee, P. R., Barnett, A. F., Scholer, J. F., Bryner, S., and Clark, W. H. Rubella arthritis: study of 20 cases. *Calif. Med.*, 1960, *93*, 125–128.
67. Lillie, R. L., and Armstrong, C. The pathology of generalized vaccinia in rabbits. USPHS, NIH Bulletin No. 156, Aug., 1930.
68. Lindquist, J. M., Plotkin, S. A., Shaw, L., Gilden, R. V., and Williams, M. L. Congenital rubella syndrome as systemic infection: studies of affected infants born in Philadelphia, U.S.A. *Brit. M. J.*, 1965, *2*, 1401–1406.
69. London, W. T., Fuccilo, D. A., Anderson, B., and Sever, J. L. Concentration of rubella virus antigen in chondrocytes of congenitally infected rabbits. *Nature*, 1970, *226*, 172–173.
70. McCandless, A. E., Davis, C., and Hall, E. G. Bone changes in congenital cytomegalic inclusion disease. *Arch. Dis. Childhood*, 1975, *50*, 160–162.
71. McEnery, G., and Nash, F. W. Wiskott-Aldrich syndrome associated with idiopathic infantile cortical hyperostosis (Caffey's disease). *Arch. Dis. Childhood*, 1973, *48*, 818–821.
72. Markowa, J. Acute osteitis of undetermined origin with neuro-infection. *J. Bone & Joint Surg.*, 1961, *43*-B, 95–99.
73. Markowa, J. Osteitis produced experimentally in mice by virus of tick-borne encephalitis. *J. Bone & Joint Surg.*, 1962, *44*-B, 722–734.
74. Marquart, K.-H. Virus-like particles in 224 Ra-induced murine osteosarcomas. *Beitr. Pathol.*, 1974, *152*, 116–126.
75. Marshall, W. C., Hayes, K., and Chrispin, A. R. Correspondence: unusual bone abnormality in congenital rubella. *Brit. M. J.* 1967, *3*, 47.
76. Melhem, R. E., Najjar, S. S., and Khachadurian, A. K. Cortical hyperostosis with hyperphosphatemia: new syndrome? *J. Pediat.*, 1970, *77*, 986–990.
77. Merton, D. F., and Gooding, C. A. Skeletal manifestations of congenital cytomegalic inclusion disease. *Radiology*, 1970, *95*, 333–334.
78. Mollaret, P., Reilly, J., Bastin, R., and Tournier, P. Récherches virologiques dans la lymphoreticulose benigne d'inoculation. *C. R. Soc. Biol.*, 1950, *144*, 1495.
79. Musgrave, W. E., and Sison, A. G. Bone lesions of smallpox. *Philippine J. Sc.*, 1910, *5*, 553–557.
80. Musgrave, W. E., Sison, A. G., and Crowell, B. C. Bone lesions of smallpox; second report; pathological report. *Philippine J. Sc.*, 1913, *8*, 67–76.
81. Naeye, R. L., and Blanc, W. Pathogenesis of congenital rubella. *J.A.M.A.*, 1965, *194*, 1277–1283.
82. Neuhauser, E. B. D., Shwachman, H., Wittenborg, M. H., and Cohen, J. Progressive diaphyseal dysplasia. *Radiology*, 1948, *51*, 11–22.
83. Ogra, P. L., and Herd, J. K. Arthritis associated with induced rubella infection. *J. Immunol.*, 1971, *107*, 810–813.
84. Ogra, P. L., Ogra, S. S., Chiba, Y., Dzierba, J. L., and Herd, J. K. Rubella virus infection in juvenile rheumatoid arthritis. *Lancet*, 1975, *1*, 1157–1161.
85. Pennington, T. H., Follett, E. A. C., and Timbury, M. C. Rapid diagnosis of virus infections. *Lancet*, 1975, *2*, 182.
86. Peters, E. R., and Davis, R. L. Congenital rubella syndrome: cerebral mineralizations and subperiosteal new bone formation as expressions of this disorder. *Clin. Pediat.*, 1966, *5*, 743–746.
87. Phillips, C. A., Behbehani, A. M., Johnson,

L. W., and Melnick, J. L. Isolation of rubella virus: epidemic characterized by rash and arthritis. *J.A.M.A.*, 1965, *191*, 615–618.

88. Poole, C. A., Greenberg, L. A., and Mackey, E. A. Late osseous manifestations of rubella syndrome: case report and discussion. *J. Canad. A. Radiologists*, 1966, *17*, 206–210.
89. Priori, E. S., Wilbur, J. R., and Dmochowski, L. Immunofluoroescence tests of sera of patients with osteogenic sarcoma. *J. Nat. Cancer Inst.*, 1971, *46*, 1299–1308.
90. Pugh, L. P. Sporadic diffuse osteoperiostitis of fowls. *Vet. Rec.*, 1927, *7*, 189–190.
91. Rabinowitz, J. G., Wolf, B. S., Greenberg, E. I., and Rausen, A. R. Osseous changes in rubella embryopathy (congenital rubella syndrome). *Radiology*, 1965, *85*, 494–500.
92. Rausen, A. R., London, R. D., Mizrahi, A., and Cooper, L. Z. Generalized bone changes and thrombocytopenic purpura in association with intrauterine rubella. *Pediatrics*, 1965, *36*, 264–268.
93. Reed, G. B., Jr. Rubella bone lesions. *J. Pediat.*, 1969, *74*, 208–213.
94. Rudolph, A. J., Singleton, E. B., Rosenberg, H. S., Singer, E. B., and Phillips, C. A. Osseous manifestations of congenital rubella syndrome. *A.M.A. Am. J. Dis. Child.*, 1965, *110*, 428–433.
95. Rudolph, A. J., Yow, M. D., Phillips, A., Desmond, M. M., Blattner, R. J., and Melnick, J. L. Transplacental rubella infection of newly born infants. *J.A.M.A.*, 1965, *191*, 843–845.
96. Sacrez, R., Fruhling, L., Korn, R., Juif, J.-G., Francfort, C., and Geiger, R. Trois observations de maladie des inclusions cytomegaliques. *Arch. franc. pediat.*, 1960, *17*, 129–142.
97. Saidi, M., and Chagnon, J. Les manifestations osseuses de la rubéole congénitale. *Union Med. Can.*, 1971, *100*, 1771–1774.
98. Sekeles, E., and Ornoy, A. Osseous manifestations of gestational rubella in young human fetuses. *Am. J. Obstet. & Gynec.*, 1975, *122*, 307–312.
99. Sewall, S. Vaccinia osteomyelitis; report of case with isolation of vaccinia virus. *Bull. Hosp. Joint Dis.*, 1949, *10*, 59–63.
100. Sheldon, F. B. Bone lesions of smallpox. Am. J. Roentgenol. & Rad. Therapy, 1923, *10*, 35–41.
101. Sheldon, W. H., Thebaut, B. R., Heyman, A., and Wall, M. J. Osteomyelitis caused by granuloma inguinale; report of case with cultivation of Donovan body in yolk sac of developing chick embryo. *Am. J. M. Sc.*, 1945, *210*, 237–245.
102. Simpson, C. F., and Sanger, V. L. Review of avian osteopetrosis: comparisons with other bone diseases. *Clin. Orthop.*, 1968, *58*, 271–281.
103. Singer, D. B., Rudolph, J., Rosenberg, H. S., Rawls, W. E., and Boniuk, M. Pathology of congenital rubella syndrome. *J. Pediat.*, 1967, *71*, 665–675.
104. Singleton, E. B., Rudolph, A. J., Rosenberg, H. S., and Singer, G. B. Roentgenographic manifestations of rubella syndrome in newborn infants. Am. J. Roentgenol., Rad. Therapy & Nuclear Med., 1966, *97*, 82–91.
105. Soriano, M. Periostitis deformans. *Ann. Rheumat. Dis.*, 1952, *11*, 154–161.
106. Soriano-Jimenez, M. Las lesiones oseas y articulares da la periostitis deformans. Publication of Clinica Medica B d'la Faculdad de Medicina de Barcelona, 1956.
107. Southard, M. E. Roentgen findings in chickenpox pneumonia; review of literature and report of five cases. Am. J. Roentgenol., Rad. Therapy & Nuclear Med., 1956, *76*, 533–539.
108. Spruance, S. L., and Smith, C. B. Joint complications associated with derivatives of HPV-77 rubella virus vaccine. *A.M.A. Am. J. Dis. Child.*, 1971, *122*, 105–111.
109. Spruance, S. L., Klock, L. E., Jr., Bailey, A., Ward, J. R., and Smith, C. B. Recurrent joint symptoms in children vaccinated with HPV-77 DK-12 rubella vaccine. *J. Pediat.*, 1972, *80*, 413–417.
110. Strand, R., Neuhauser, E. B. D., and Sornberger, C. F. Lycoperdonosis. *New England J. Med.*, 1967, *277*, 89–91.
111. Strauss, L. Rubella symposium. *J. Pediat.*, 1965, *67*, 989–990.
112. Tamir, D., Benderly, A., Levy, J., Ben-Porath, E., and Vansover, A. Infectious mononucleosis and Epstein-Barr virus in childhood. *Pediatrics*, 1974, *53*, 330–335.
113. Temperley, I. J., Douglas, S. J., and Rees, J. P. Raised immunoglobulin levels and thrombocytosis in infantile cortical hyperostosis. *Arch. Dis. Childhood*, 1972, *47*, 982–983.
114. Thompson, G. R., Ferreyra, A., and Brackett, R. G. Acute arthritis complicating rubella vaccination. *Arthritis Rheum.*, 1971, *14*, 19–26.
115. Töndury, G., and Smith, D. W. Fetal rubella pathology. *J. Pediat.*, 1966, *68*, 867–879.
116. VanBuskirk, F. W., Tampas, J. P., and Peterson, O. S., Jr. Infantile cortical hyperostosis: inquiry into its familial aspects. Am. J. Roentgenol., Rad. Therapy & Nuclear Med., 1961, *85*, 613–632.
117. Vaughan, J. M. The Effects of Irradiation on the Skeleton. Oxford University Press, Oxford, 1973.

118. Ward, J. R., and Bishop, B. Varicella arthritis. *J.A.M.A.*, 1970, *212*, 1954–1956.

119. Warwick, W. J. Cat-scratch syndrome, many diseases or one disease? *Prog. in Med. Virol.*, 1967, *9*, 256–301.

120. Weibel, R. E., Stokes, J., Jr., Buynak, E. B., and Hilleman, M. R. Live rubella vaccines in adults and children: HPV-77 and Merck-Benoit strains. *A.M.A., Am. J. Dis. Child.*, 1969, *118*, 226–229.

121. Weinmann, J. P., and Sicher, H. Bone and Bones. C. V. Mosby Company, St. Louis, 1947.

122. Whalen, J. P., Winchester, P., Krook, L., O'Donohue, N., Dische, R., and Nunez, E. Neonatal transplacental rubella syndrome. Its effect on normal maturation of the diaphysis. Am. J. Roentgenol., Rad. Therapy & Nuclear Med., 1974, *121*, 166–172.

123. Willems, D., Billiau, A., Sobis, H., and Mulier, J. C. Evidence for human oncogenic virus. *Acta Orthop. Belg.*, 1973, *39*, 772–776.

124. Williams, H. J., and Carey, L. S. Rubella embryopathy: roentgenologic features. Am. J. Roentgenol., Rad. Therapy & Nuclear Med., 1966, *97*, 92–99.

125. Wright, L. T., and Logan, M. Osseous changes associated with lymphogranuloma venereum. *Arch. Surg.*, 1939, *39*, 108–121.

126. Yabe, Y., Trentin, J. J., and Taylor, G. Cancer induction in hamsters by human type 12 adenovirus. *Proc. Soc. Exp. Biol. Med.*, 1962, *111*, 343–344.

LOSS OF COLONIC HAUSTRATION IN PROGRESSIVE SYSTEMIC SCLEROSIS*

By WILLIAM MARTEL, M.D.,† STANLEY F. CHANG, M.D.,†
and MURRAY R. ABELL, M.D.‡
ANN ARBOR, MICHIGAN

ABSTRACT:

Complete loss of colonic haustration was observed in six cases of progressive systemic sclerosis. Varying degrees of haustral loss or sacculation were noted in twelve others. An increase in colonic length was characteristic and, occasionally, there was slight to moderate generalized dilatation. Correlation of these findings with the microscopic appearance of the colon showed that muscular atrophy and fibrous replacement were consistent findings, varying in degree. Although the data are insufficient to permit definite conclusions, it is suggested that these changes may be responsible for colonic lengthening and loss of haustration. Attention is drawn to the importance of not confusing this appearance with other conditions, particularly chronic ulcerative colitis.

ALTHOUGH sacculation of the colon is a well known feature of progressive systemic sclerosis,[8–10,17] loss of colonic haustration is not widely recognized as a manifestation of this disease. Recognition of this association is important to avoid confusion with other conditions which may exhibit loss of haustration. This report concerns the roentgenologic and microscopic findings in the colon in 20 patients, eight of whom came to necropsy. Six patients had severe loss of colonic haustration on barium enema examination, twelve had varying degrees of haustral loss or colonic sacculation and two had no colonic abnormality.

MATERIAL AND METHOD

Severe loss of colonic haustration was observed in five cases of progressive systemic sclerosis at the University of Michigan Medical Center from 1969 to 1975. This observation prompted a study of the colon in these cases and 15 others with this disease. The latter were derived as follows. Nine were selected from the files of the Department of Radiology because they had "abnormal barium enema examinations." An additional six were selected from a group of 13 necropsied patients with proved scleroderma because barium enema examinations were available for retrospective study. Necropsy had also been performed in one of the original five cases and one of the nine cases selected from the files of the Department of Radiology (Cases 2 and 14, respectively). The medical records and roentgenograms were reviewed in all 20 cases and the microscopic appearance of the colon was studied in retrospect in the eight patients in whom necropsy had been performed. The pathologic material was obtained by random sections of the colon at the time of necropsy. All cases were classified into four groups according to the predominant roentgenologic abnormality in the colon as follows: Group I, ahaustral; Group II, relatively ahaustral; Group III, sacculation, characteristic of scleroderma; and Group IV, normal. The roentgenologic appearance of the colon in each case was correlated with clinical and roentgenologic manifestations of the disease and microscopic findings in the colon. Necropsy was done in all cases within eight hours of death and within four hours for five of the eight. Hematoxylin and eosin, Masson's trichrome, and silver reticulin stains were done on tissue sections from each colon. The histologic changes in the mucosa, muscularis mucosae, sub-

* From the Departments of Radiology†, and Pathology,‡ The University of Michigan Medical Center, Ann Arbor, Michigan.

TABLE I

CLINICAL AND ROENTGENOLOGIC FEATURES IN 20 CASES OF PROGRESSIVE SYSTEMIC SCLEROSIS

Case	Group	Age at Onset	Duration Before Barium Enema Examination	Pathologic Data	Raynaud's Phenomenon	Roentgenologic Abnormalities				
						Duodenum	Small Bowel	Esophagus	Hands	Lungs
1	I	22	1	–	+	+	+	+	–	–
2	I	50	3	Skin bx	–	–	+	+	n.f.	–
3	I	22	30	–	+	–	+	+	+	+
4	I	39	8	Necropsy	+	–	±	+	n.f.	–
5	I	27	22	–	+	–	+	+	+	+
6	I	35	37	Skin bx	+	+	+	+	+	+
7	II	23	1	Skin bx	+	+	+	+	+	–
8	II	47	8	Necropsy	+	–	+	+	+	+
9	II	16	29	Necropsy	+	+	+	+	+	+
10	II	37	3	Necropsy	±	+	n.f.	+	n.f.	+
11	II	48	9	–	+	–	–	+	+	–
12	II	58	2	Necropsy	+	+	+	+	–	±
13	III	39	10	–	+	–	–	+	n.f.	–
14	III	48	4	–	+	–	–	+	–	–
15	III	42	7	–	+	–	+	+	–	–
16	III	27	12	–	+	–	–	+	+	–
17	III	39	13	Necropsy	+	–	–	+	–	+
18	III	30	4	–	+	±	–	+	–	–
19	IV	34	3	Necropsy	+	–	–	–	+	+
20	IV	63	2	Necropsy	+	–	–	–	+	+

bx = biopsy.
n.f. = no films.
Duration = in years.

mucosa, muscularis propria, and myenteric plexus were assessed, and their severity graded on a scale of +1 to +4.

RESULTS

There were six patients in Group I, including the five who were originally observed, six in Groups II and III respectively, and two in Group IV (Table I). The ages of the patients at the time of initial symptoms of the disease, duration of disease prior to colon examination and roentgenologic evidence of involvement of other segments of the alimentary tract, hands and lungs were documented (Table I). There was no significant difference in ages at the time of colon examination or at onset of disease between these patients. All with colonic abnormalities had esophageal involvement and virtually all in Group I had characteristic changes in the small intestine. The hands and lungs were affected in the two patients with a normal colon but other portions of the alimentary tract were not examined. Cases 1 and 7 had the disease for only one year prior to the roentgenologic demonstration of colonic abnormality. The majority had severe disease of long duration. Seventeen had a clearly documented history of Raynaud's phenomenon. This was questionable in one case and was not mentioned in two others. The diagnosis of scleroderma was verified histologically by skin biopsy in three of the twelve patients in whom necropsy was not performed. The clinical picture was typical of the disease in the remaining nine. All had characteristic roentgenologic lesions in the esophagus, and the small intestine was affected in four, the fingers in four, and the lungs in two.

These patients had relatively few intestinal symptoms, despite severe involvement of the alimentary tract. The clinical indication for barium enema examination in most cases was to evaluate the extent of visceral involvement rather than in-

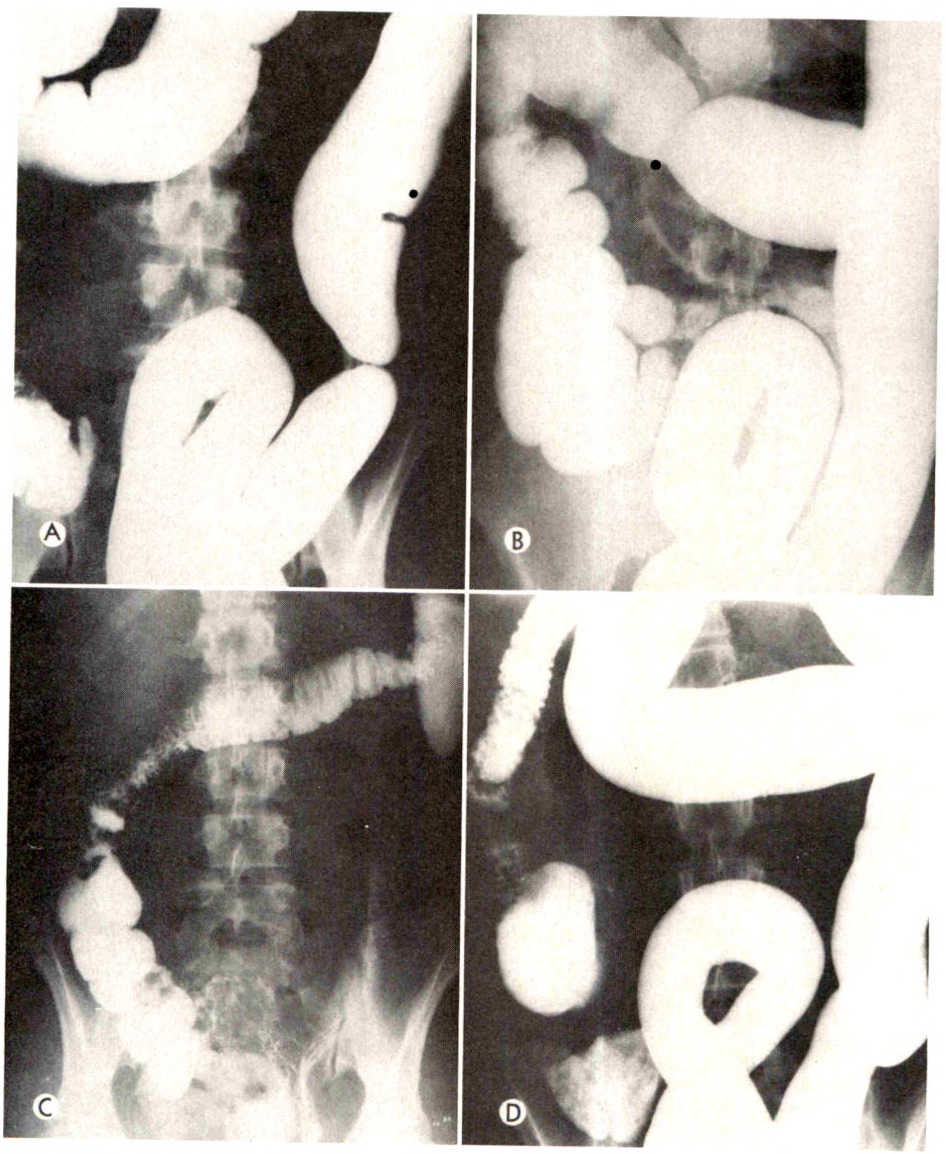


Fig. 1. Case 1. (*A*) 1965. Loss of colonic haustration, one year after the onset of symptoms of progressive systemic sclerosis. (*B* and *C*) 1968. Pre- and postevacuation films showing ahaustrum-like appearance in the ascending colon and a normal over-all mucosal pattern. (*D*) 1974. Loss of haustration is again evident, associated with slight dilatation in the transverse segment. The ascending colon and cecum contain feces and are not fully distended. Additional views at this time showed the ascending colon moderately dilated with some saccule formation and minimal haustration. Note colonic redundancy, presumably due to elongation.

testinal symptomatology. Constipation and diarrhea were occasionally noted but these symptoms were neither severe nor chronic. Continuous cathartic therapy was not employed in any case and bloody stools or melena were not observed. Various medications had been employed, including potassium para-aminobenzoic acid (POTABA), reserpine, myocholine, and dibenzylene. None of these medications was given consistently with the exception of POTABA.[18] However, in one patient in Group 1 (Case 1) the loss of colonic haustration was evident prior to the initiation of POTABA therapy.

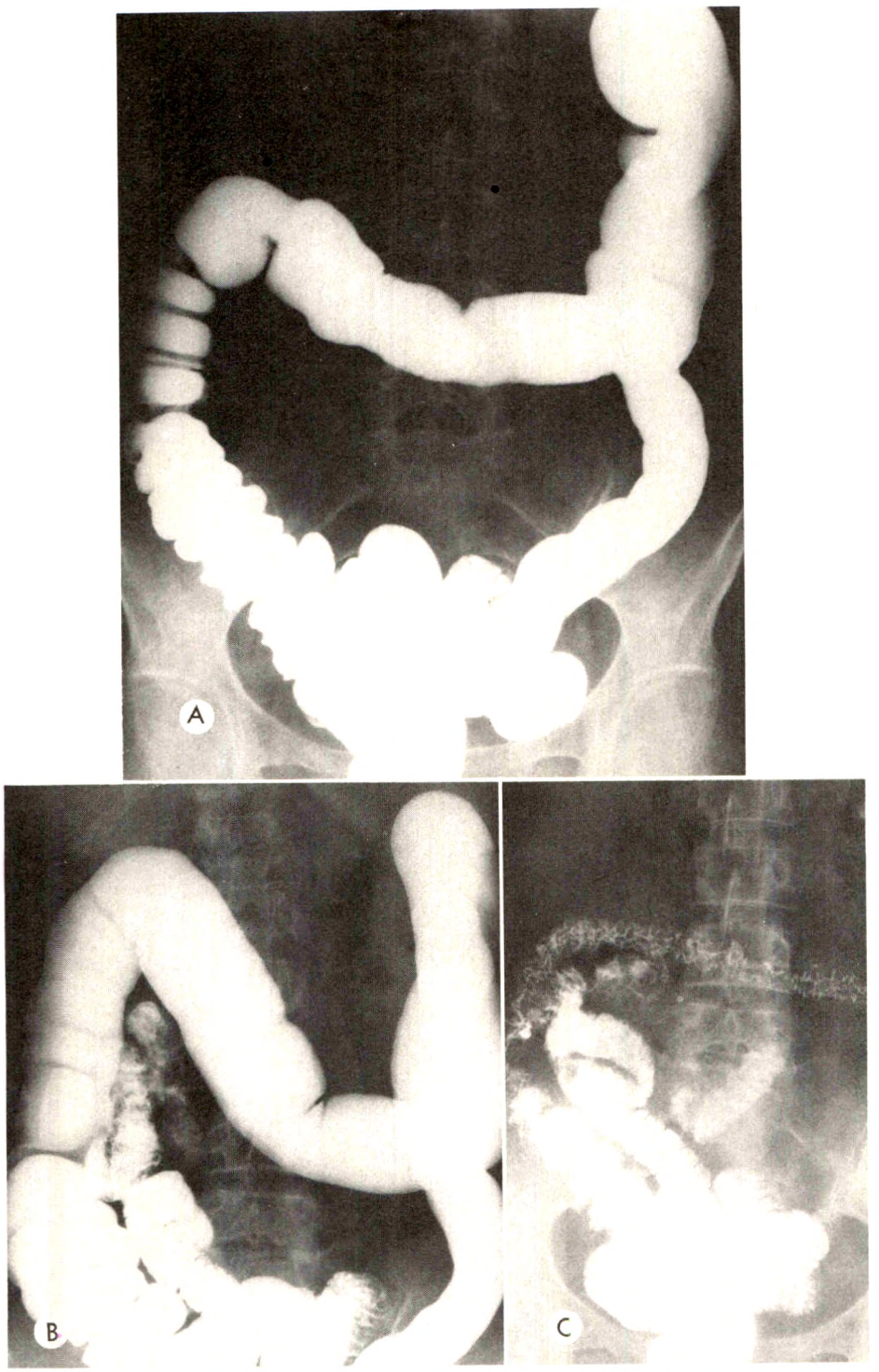


Fig. 2. Case 3. (*A*) 1966. Colonic haustration is essentially absent except in the ascending colon. (*B* and *C*) 1967. Pre- and postevacuation films. Loss of haustration is again evident but the mucosal pattern is normal. The patient had intermittent, moderate constipation at this time which did not require continuous cathartic therapy.



FIG. 3. Case 4. Complete loss of haustration and redundancy of the colon, eight years after onset of disease. Necropsy three years later showed 4+ atrophy and fibrosis of the muscularis propria. Irregular filling defects in the transverse colon and splenic flexure were due to fecal material.

Loss of haustration was most obvious roentgenologically in the transverse and descending portions of the colon. Although haustration was usually diminished in the ascending colon, it tended to persist in this segment, even when completely absent in the transverse colon (Fig. 1*B*; 2, *A* and *B*). Redundancy of the colon, associated with elongation, was a significant feature, particularly in Groups I and II (Fig. 1; 5; and 6). This was difficult to evaluate in view of the wide variation in the length of the normal colon. Nevertheless, it was conspicuous in six patients (Cases 1, 4, 6, 9, 10, 12) and was less marked and of equivocal significance in seven others. There was generalized, minimal to moderate dilatation of the colon in four patients (Cases 1, 2, 6, 10) (Fig. 5). In no case was the colon foreshortened or clearly reduced in caliber. It was often difficult to evaluate the presence of colonic sacculation in those cases where there was loss of haustration. Nevertheless, sacculation, superimposed on partial or complete loss of haustration seemed to be evident in at least three patients (Cases 5, 11, 12). In these cases the saccules seemed to differ from haustra in that the separation between saccules tended to be shallow, the saccules themselves varied in orientation and diameter and the wall opposite the saccules was devoid of haustration (Fig. 6).

Table II shows the correlation of the roentgenologic and microscopic changes in the colon in the eight patients in whom necropsy was performed. Of the eight, one proved to be in Group I, four in Group II, one in Group III, and two in Group IV. The interval between roentgenologic examination of the colon and necropsy was one year or less in five of the eight. The only consistent histologic findings were atrophy and fibrosis of the muscularis propria (Table II). These were patchy, variable in



FIG. 4. Case 5. There is loss of colonic haustration. Note the large wide-mouthed sacculations at the superior aspect of the transverse colon (arrows).



Fig. 5. Case 6. (*A*) 1966. The colon is redundant and slightly dilated. The haustra are poorly developed in the transverse colon. Note the sacculation in the sigmoid and descending colon (arrows). (*B* and *C*) 1974. Posteroanterior and anteroposterior views. There are dilatation and marked lengthening of the colon. The transverse colon (large arrows) is ahaustral. Sacculation is evident in the sigmoid and descending segments (small arrows). Note absence of haustra on wall opposite these saccules.

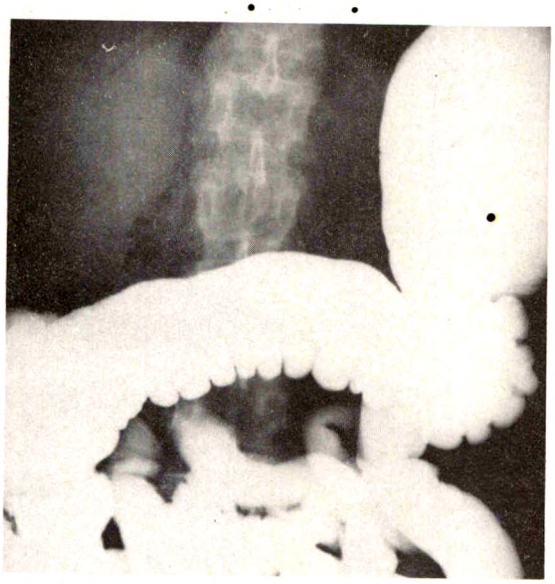


FIG. 6. Case 12. Sacculation is prominent at the inferior aspect of the transverse colon. The separations between the individual saccules are shallow and the latter vary in orientation and diameter. The superior aspect is devoid of haustration. Note colonic redundancy.

severity, and involved both muscular coats. In one patient (Case 4), the changes were severe, resulting in considerable loss of muscle mass (Fig. 7). In four patients (Cases 10, 12, 17, 19) atrophy was of moderate severity but in only one of these was there an equivalent degree of fibrosis. The changes were minimal in the remaining patients. Hypertrophy of the nerves of the myenteric plexus with perineural fibrosis was marked in one case (Fig. 8), moderate in two, and minimal or absent in the others. There were no mucosal changes of chronic idiopathic ulcerative colitis. Non-specific subserosal fibrosis was present in two patients. Vascular sclerosis in the form of intimal fibrosis was minimal and non-specific; there was no vasculitis.

DISCUSSION

Atrophy and fibrous replacement of the smooth muscle of the alimentary tract is a

TABLE II

CORRELATION OF ROENTGENOLOGIC AND MICROSCOPIC CHANGES IN COLON IN EIGHT CASES OF PROGRESSIVE SYSTEMIC SCLEROSIS*

Case	Roentgenologic Features	Interval Between Barium Enema Examination and Necropsy	Mucosal Ulceration	Hypertrophy Muscularis Mucosae	Submucosal Fibrosis	Atrophy Muscularis Propria	Fibrosis Muscularis Propria	Hypertrophy Myenteric Plexus	Serosal Reaction
4	Ahaustral	2 yr 10 mos	No	+	+	++++	++++	o	o
8	Relatively ahaustral	9 yr 5 mos	Acute superficial ulcers	o	o	+	±	o	o
9	Relatively ahaustral	1 yr	No	o	o	+	±	+	o
10	Relatively ahaustral c sacculation	2 da	Chronic cecal ulcer	+	+	++	++	++	+
12	Relatively ahaustral c sacculation	3 mos	No	o	o	++	+	+	o
17	Sacculation	8 yr	No	o	o	++	+	++	++
19	Normal	3 mos	No	o	o	++	+	+++	o
20	Normal	8 mos	No	o	o	+	±	+	o

* Grading: +1 to +4 according to severity.
± equivocal significance.
o not present.

hallmark of progressive systemic sclerosis. This was quite remarkable in one case and was a significant feature in four others which came to necropsy, suggesting that it is a factor in causing the ahaustral pattern.

The colon contains a complete outer longitudinal muscle layer which is thickened into three bands, the taeniae coli. These are most prominent in the ascending and transverse segments. Sectioning of the longitudinal muscle apparently causes loss of haustration and elongation of the bowel in that segment.[12] The colonic lengthening seemed to be associated with loss of haustration. This supports the view that the latter is due to alteration in the muscle fibers of the taeniae.

It has been suggested that the wide-mouthed sacculation of the colon, typical of this disease,[8,9,17] represents a gradual "blow out" phenomenon, secondary to focal fibrous replacement of muscle. Indeed Heinz *et al.*[10] showed that there were atrophy and fibrous replacement of muscle at sites of sacculation. On this basis, one may postulate that loss of haustration is due to more complete and continuous fibrous replacement of the muscularis propria. This was suggested by the more severe muscular atrophy and fibrosis in Case 4. However, our pathologic findings are not altogether conclusive. The fact that this



Fig. 7. Case 4. Full thickness section of wall of colon. Mucosa with dark-staining muscle of muscularis mucosae in upper field. Severe atrophy of muscularis propria which is faintly stained due to marked loss of muscle cytoplasm. Masson's trichrome stain ×40.

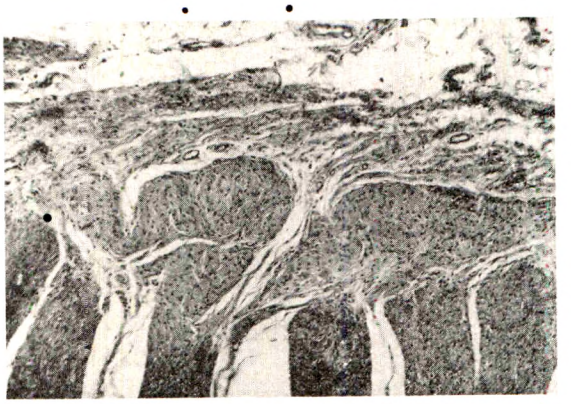


Fig. 8. Case 19. Marked hypertrophy of myenteric plexus with perineural fibrosis across center of field. Marked atrophy of outer muscular coat above the plexus. H & E ×120.

was a retrospective study in which there was random sampling of the colon is important. It is significant, for example, that the microscopic sections in Case 19 showed definite atrophy and fibrosis of the muscularis propria but the colon appeared normal on roentgenologic examination. It is possible that other factors play a role. A complex microscopic meshwork of connective tissue invests both the circular and longitudinal muscle and forms connections between them.[13] Alterations in this connective tissue network may cause a functional imbalance between the actions of the circular and longitudinal muscle layers. The significance of hyperplasia of the myenteric plexus is not clear. Its occurrence in patients who did not have an abnormal haustral pattern (Case 19), and its absence in others who did, suggests that it does not cause the latter. Such hyperplasia has previously been noted, both in the esophagus and colon,[7] but has apparently not been emphasized. It may be secondary to perineural fibrosis or, possibly, it is related to the presence of abnormal neurohumeral substances. This is apparently not related to the severity of the muscular atrophy and fibrosis. This, too, could reflect the method of sampling the colon. Such hyperplasia was noted in a case of cathartic colon in which there was also hypertrophy of the muscularis mucosae.[1] However, the significance of such hyperplasia is also uncer-

tain in this condition inasmuch as Clain *et al.*[4] also observed thickening of the muscularis mucosae in such a case, but in this instance the myenteric plexus was normal. Dabich *et al.*[5] have suggested that in progressive systemic sclerosis there is an underlying autonomic disorder associated with derangement in the degradation of serotonin and norepinephrine. Inasmuch as vasculitis has been repeatedly documented in the wall of the bowel,[17] it is conceivable that loss of haustration is an indirect result of repeated episodes of focal mural necrosis. There was no evidence for this in our pathologic material, however. There was no evidence that the loss of haustration was related to drug therapy. Inasmuch as three patients in Group I had multiple barium enema examinations, years apart, all showing loss of colonic haustration, the latter probably represents a fixed morphologic alteration. Nevertheless, it would be of interest to employ a drug such as reserpine to determine whether this loss of haustration is reversible.

Loss on colonic haustration has previously been noted in this disease but it has apparently not been emphasized. Peachey *et al.*[14] observed loss of haustration in four cases. They noted localized and generalized colonic dilatation but lengthening of the colon was not described. In one case Harper and Jackson[9] observed a transformation from colonic sacculation to dilatation and atony. Hale and Schatzki,[8] in describing the roentgenologic appearance of the gastrointestinal tract in scleroderma, noted two cases in which there were alterations in the transverse colon with superimposed sacculation. They stated, "in many respects the appearance was similar to that seen in ulcerative colitis and reexamination two weeks later showed no change. Sigmoidoscopy failed to show evidence of ulcerative colitis." In this regard two case reports of "chronic ulcerative colitis" occurring in scleroderma are of interest.[2,6] Review of these raises a question as to whether these patients did indeed have chronic ulcerative colitis. Intestinal malabsorption, associated with diarrhea, is a recognized complication of this disease[3,11] and vasculitis may in some instances lead to colonic infarction[17] and rectal bleeding. In view of these considerations, it is important that radiologists not be confused by a loss of haustral pattern, should it occur, and erroneously diagnose ulcerative colitis in such cases.

Conditions which should be included in the differential diagnosis of "loss of colonic haustration" are chronic ulcerative colitis, cathartic colon, amyloidosis, and Fabry's disease. All of our cases with colonic abnormality had involvement of the esophagus and small bowel. This suggests that if the latter structures are normal, the diagnosis of progressive systemic sclerosis is unlikely. None of our cases had foreshortening or significant narrowing of the colon, features which one might expect in advanced stages of ulcerative colitis, associated with loss of haustration. In cathartic colon, the changes are most marked in the proximal portion, particularly the ascending segment and terminal ileum. In this condition the ascending and transverse segments tend to be foreshortened and dilated, as well as ahaustral, and the terminal ileum is often dilated. Amyloidosis may cause complete loss of haustration but rarely is this an isolated finding, and there is usually evidence of involvement of the small intestine and other viscera. Loss of haustration has been described in Fabry's disease (glycosphingolipid lipidosis),[15] but the clinical findings secondary to involvement of the kidneys, heart, skin, and central nervous system are so characteristic that, for practical purposes, this does not present a problem in differential diagnosis.

Occasionally, individuals, usually elderly and otherwise normal, exhibit unexplained loss of haustration in the transverse and descending portions of the colon. In these cases the haustral loss is usually slight or moderate. This raises a question as to the significance of "relative loss of haustration" in cases in Group II. Although this could have been a coincidental finding in

some instances, we are proposing that complete loss of haustration as shown in Group 1 cases (Fig. 1), particularly when it occurs in young or middle-aged individuals, is significant and due to morphologic or functional alterations in the colon due to the disease itself. This view is supported by the sequential changes in Case 6 over an eight year interval (Fig. 5). The fact that there was fairly complete evacuation of the barium in some individuals in Group 1 (Cases 1, 2), does not, in our opinion, necessarily preclude our concept of such alterations in the colon. Patients with quiescent chronic ulcerative colitis characteristically exhibit a similar loss of haustration but usually retain the ability to evacuate the colon on barium enema examination.

William Martel, M.D.
Department of Radiology
University of Michigan Medical Center
Ann Arbor, Michigan 48104

The authors are indebted to Drs. Chris Zarafonetis and Lyubica Dabich for making these patients available.

REFERENCES

1. Abell, M. R., and Martel, W. Microscopic and radiologic findings in cathartic colon: report of case. To be published.
2. Bicks, R. O., Goldgraber, M. B., and Kirsner, J. B. Generalized scleroderma associated with chronic ulcerative colitis. *Am. J. Med.*, 1958, *24*, 447–453.
3. Bluestone, R., MacMahon, M., and Dawson, J. M. Systemic sclerosis and small bowel involvement. *Gut*, 1969, *10*, 185–193.
4. Clain, J., Novis, B. H., Bank, S., Kahn, L. B., and Marks, I. N. Cathartic colon with unusual histological features. *S. Afr. Med. J.*, 1974, *48*, 216–218.
5. Dabich, L., Bookstein, J. J., Zweifler, A. J., and Zarafonetis, C. J. D. Digital arteries in patients with scleroderma. *A.M.A. Arch. Int. Med.*, 1972, *130*, 708–714.
6. DeLuca, V. A., Jr., Spiro, H. M., and Thayer, W. R. Ulcerative colitis and scleroderma. *Gastroenterology*, 1965, *49*, 433–438.
7. Goetz, R. H., and Berne, M. B. Pathology of progressive systemic sclerosis (generalized scleroderma) with special reference to changes in viscera. *Clin. Proc.*, 1945, *4*, 337–392.
8. Hale, C. H., and Schatzki, R. Roentgenological appearance of gastrointestinal tract in scleroderma. Am. J. Roentgenol. & Rad. Therapy, 1944, *51*, 407–420.
9. Harper, R. A. K., and Jackson, D. C. Progressive systemic sclerosis. *Brit. J. Radiol.*, 1965, *38*, 825–834.
10. Heinz, E. R., Steinberg, A. J., and Sackner, M. A. Roentgenographic and pathologic aspects of intestinal scleroderma. *Ann. Int. Med.*, 1963, *59*, 822–826.
11. Hoskins, L. C., Norris, H. T., Gottlieb, L. S., and Zamcheck, N. Functional and morphologic alterations of gastrointestinal tract in progressive systemic sclerosis (scleroderma). *Am. J. Med.*, 1962, *33*, 459–470.
12. Meyers, M. A., Volberg, F., Katzen, B., and Abbot, G. Haustral anatomy and pathology: new look. *Radiology*, 1973, *108*, 497–504.
13. Pace, J. L., and Williams, I. Organization of muscular wall of human colon. *Gut*, 1969, *10*, 352–349.
14. Peachey, R. D. G., Creamer, B., and Pierce, J. W. Sclerodermatous involvement of stomach and small and large bowel. *Gut*, 1969, *10*, 285–292.
15. Robinson, J. C., and Teitelbaum, S. L. Stercoral ulceration and perforation of sclerodermatous colon: report of two cases and review of literature. *Dis. Colon & Rectum*, 1974, *17*, 622–632.
16. Rowe, J. W., Gilliam, J. I., and Warthin, T. A. Intestinal manifestations of Fabry's disease. *Ann. Int. Med.*, 1974, *81*, 628–631.
17. Sackner, M. A. Scleroderma. Grune & Stratton, New York, 1966, pp. 69–73.
18. Zarafonetis, C. J. D. Antifibrotic therapy with POTABA. *Am. J. Med. Sc.*, 1964, *248*, 550–561.

ROENTGEN FINDINGS IN AORTO-ENTERIC FISTULAE*

By GEORGE M. WYATT, M.D., MICHAEL I. RAUCHWAY, M.D., *and* HAROLD B. SPITZ, M.D.
CINCINNATI, OHIO

ABSTRACT:

Six cases of aorto-enteric fistulas are discussed. In three patients the aorta ruptured into the duodenum and in three there was rupture into the esophagus. Aorto-enteric fistula is usually caused by atherosclerosis, but may also be due to syphilis or tuberculosis. Following insertion of an aortic graft, fistula is usually the result of breakdown of the anastomosis. Gastrointestinal bleeding usually heralds the problem. The roentgen signs of rupture are pressure on the esophagus or intestine, bleeding into the wall or lumen, and demonstration of the fistula. The abnormal connection may not be demonstrable by aortography. These signs permit early diagnosis and subsequent possible life saving surgical correction.

RUPTURE of the aorta into a portion of the alimentary tract is indeed a dramatic medical event. That this need not be immediately lethal to the patient is of great importance in establishing diagnostic criteria that may permit life saving surgical correction of this condition.

In this paper three patients will be discussed in whom the aorta ruptured into the duodenum. These cases will serve as a reminder of the more frequent clinical situations encountered. In addition, three patients in whom there was aorto-esophageal perforation will be presented. This situation is more rare and not previously reported in the roentgenological literature. Roentgen findings in all the patients will be discussed with special emphasis on the roentgen signs of aorto-esophageal perforation.

REPORT OF CASES

Case I. D.L. A 64 year old male was admitted following the sudden onset of weakness and massive hematemesis. Three years prior to admission an atherosclerotic abdominal aortic aneurysm had been resected and an aortic homograft had been inserted (Fig. 1).

An emergency upper gastrointestinal series revealed extrinsic pressure on the gastric antrum from a hematoma in the retrogastric space. A linear opacity of barium was visualized in the area of the descending duodenum which possibly lay in the area of communication between the ruptured suture line of the graft and the duodenum (Fig. 2). The duodenal folds were effaced and the duodenal bulb and loop were filled with clot (Fig. 3). Extrinsic pressure was also seen on the third portion of the duodenum. Following completion of this study the patient had an episode of projectile hematemesis. Emergency surgery was performed revealing aneurysmal dilatation of the aortic homograft with rupture into the third portion of the duodenum. The aneurysm was repaired locally and the duodenum resected with an end to end anastomosis.

Case II. This 73 year old woman entered the

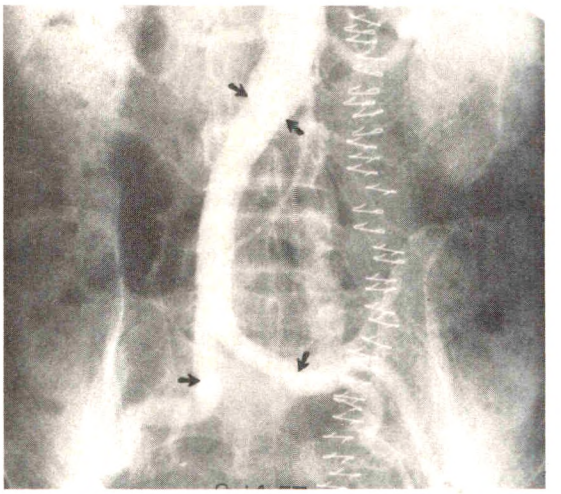


Fig. 1. The bifurcation graft is demonstrated by aortography. The anastomoses (arrows) are intact with no extravasation.

* From the Department of Radiology, Cincinnati General Hospital, University of Cincinnati Medical Center, Cincinnati, Ohio.

hospital in stupor. A blood sugar of 710 mgm percent was found. Following intravenous fluids and insulin she began to awaken. Physical examination revealed a non-tender but distended abdomen. The liver margin was depressed by 4 cm. Four days after admission a nasogastric tube was passed for persistent abdominal distention and coffee ground material was aspirated from the tube. The patient improved. The abdomen was soft and bowel sounds were normal. She complained of abdominal fullness. Twelve days after admission she developed fever, tachycardia and shortness of breath, and mild abdominal tenderness developed on the following day. The upper gastrointestinal series revealed an aneurysm with calcification in the wall (Fig. 4). There was extrinsic pressure on the distal third portion of the duodenum. The folds of the duodenum in this area were effaced (Fig. 5). There was no definite ulceration seen and there was no filling of the clotted aneurysm with barium. The hematocrit fell from 39 to 30. Massive hematemesis ensued with further drop in hematocrit to 24. The patient developed cardiac arrest but was resuscitated. Shock developed and the patient died 18 days after admission.

Case III. C.B. This 62 year old white male was admitted on September 6, 1973, with the complaint of twelve hours of rectal bleeding, the fifth such episode in the preceding ten months. The past history included an aorto-femoral bypass graft and superior mesenteric artery jump graft in 1968 for arteriosclerotic vascular disease. An episode of rectal bleeding in August, 1973 necessitated operative inter-

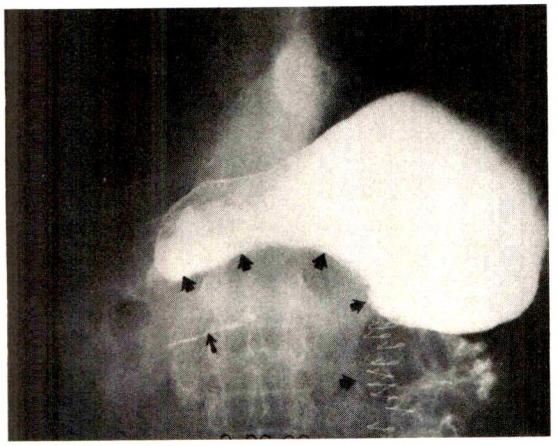


Fig. 2. A linear opacity of barium (small arrow) is visualized in the area of the descending duodenum which possibly lies in the tract between the ruptured suture line of the graft and the duodenum. There is extrinsic pressure on the gastric antrum and third portion of the duodenum (large arrows) from hematoma in the retrogastric space.

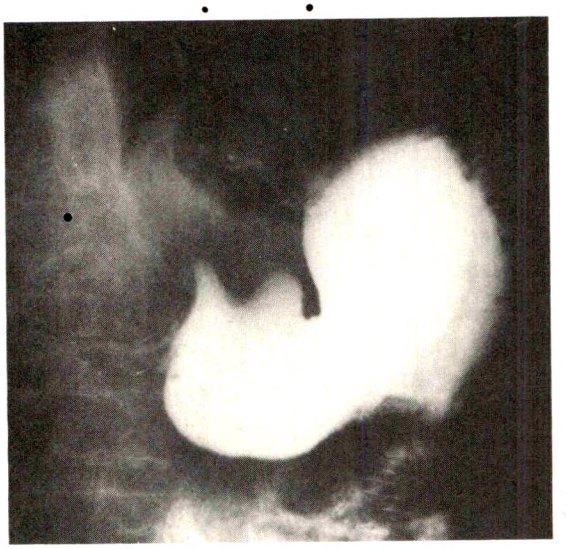


Fig. 3. The duodenal folds are effaced and the duodenal bulb and loop are filled with clot.

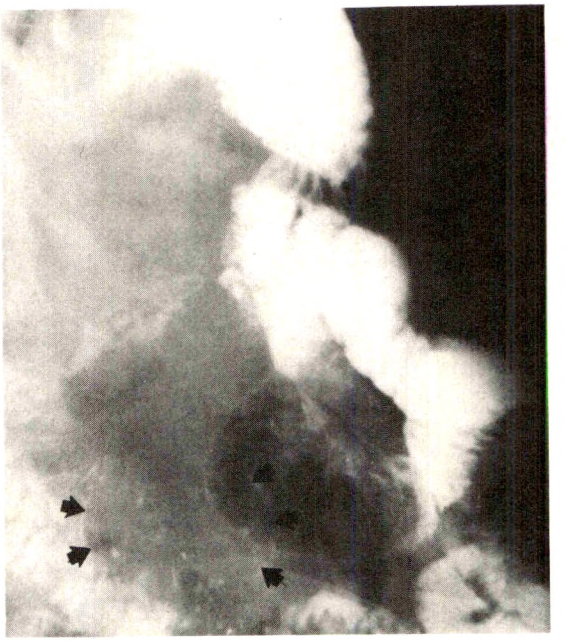


Fig. 4. An aneurysm with calcification in the wall (arrows) is seen in an area of extrinsic pressure on the third portion of the duodenum. The folds of the duodenum in this area are effaced. There is no definite ulceration seen and there is no filling of the aneurysm with barium.

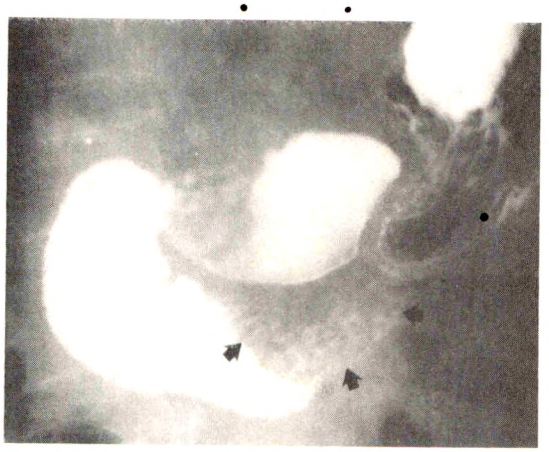


Fig. 5. The spot film clearly demonstrates the extrinsic pressure on the third portion of the duodenum (arrows).

vention, and exploration of the duodenum failed to demonstrate a bleeding site. The graft was examined and felt to be intact. A right colectomy was performed. During the final admission in September, 1973 massive hematemesis prompted re-exploration. An aortoduodenal fistula was found and oversewn. The patient died one month later. The autopsy demonstrated infection of the graft site and peritonitis.

The roentgen evaluation of this patient included an anteroposterior and lateral abdominal aortogram which failed to demonstrate a bleeding site (Fig. 6). An upper gastrointestinal series at the time of the original bleeding episode showed extrinsic pressure in the third portion of the duodenum (Fig. 7). On the final admission a repeat anteroposterior abdominal aortogram showed the graft to have a scalloped wall (Fig. 8) which was interpreted as a post-surgical change, since the area had been recently explored at the time of the right colectomy. Again no extravasation of contrast material was seen.

Of particular interest in this case is the fact that the graft itself was the site of rupture into the duodenum, rather than at the anastomosis.

Case iv. L.S. An 81 year old female was admitted to the hospital with severe chest and back pain of 24 hours' duration. A large aneurysm of the descending thoracic aorta was demonstrated on chest roentgenograms (Fig. 9). A clinical diagnosis of ruptured aortic aneurysm with bleeding into the left pleural space was made. She was treated conservatively with multiple thoracenteses and blood transfusions. An upper gastrointestinal series revealed a hiatus hernia and displacement of the esophagus to the right by a large aneurysm (Fig. 10). The patient was discharged and re-admitted six weeks later with hematemesis associated with lower chest and upper abdominal pain radiating to the back. An upper gastrointestinal series revealed gross irregularity of the mucosa

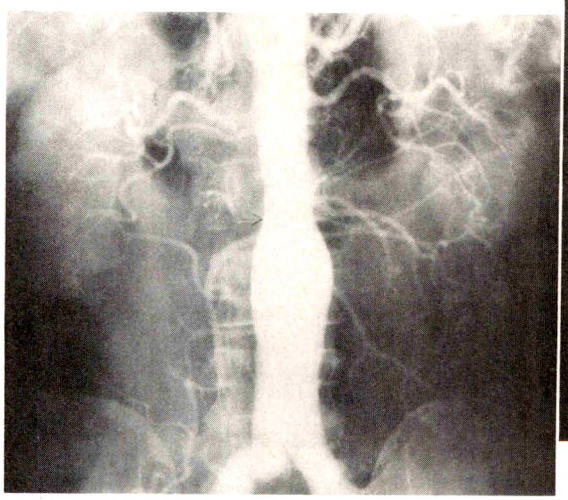


Fig. 6. An anteroposterior and lateral abdominal aortogram failed to demonstrate a bleeding site. The arrow indicates the anastomotic site.

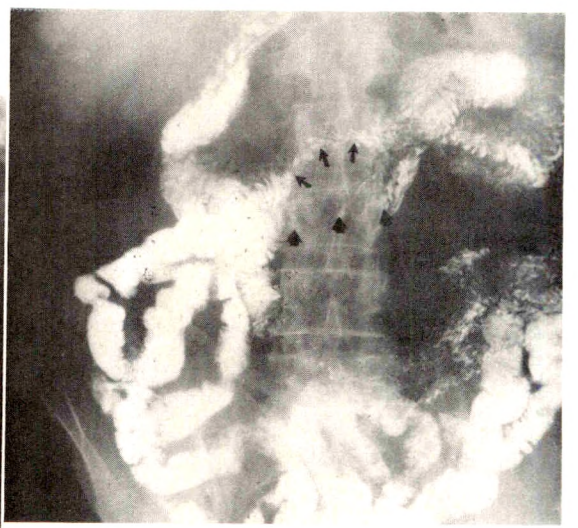


Fig. 7. The upper gastrointestinal series at the time of the original gastrointestinal bleeding episode shows extrinsic pressure on the third portion of the duodenum (large arrows). A jejunal loop is also slightly displaced (small arrows).

of the distal esophagus as well as the previously described displacement (Fig. 11). A spot film showed barium extravasation from the distal esophagus and mixture of the barium with the laminated clot in the aneurysm (Fig. 12). There was also a collection of barium in the mediastinum, outside both the area of the aneurysm and the esophagus indicating a perforation of the ulcerated esophagus into the mediastinum as well as into the aneurysm. Three days after this the patient died.

Autopsy revealed three aneurysms of the descending thoracic aorta. The largest measured $6\frac{1}{2} \times 5$ cm and it communicated posteriorly with the esophagus. The second aneurysm was on the left side of the aorta and was believed to have been the cause of the left hemothorax on the first admission. The right pleural cavity contained 1,200 cc of fluid and was covered by a thin gray chalky material thought to be barium.

Case v. L.W. A 78 year old male was admitted to the hospital with a three day history of inability to swallow fluids and food. There was intractable singultus. An aneurysm of the descending aorta had been present since 1959

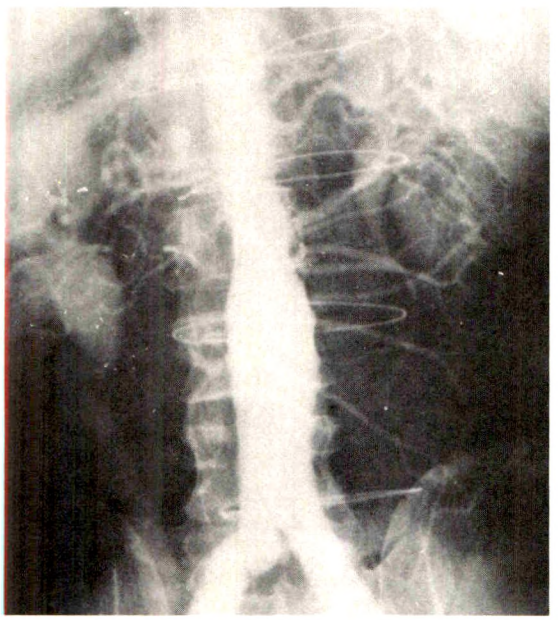


Fig. 8. On the final admission a repeat anteroposterior abdominal aortogram showed the graft to have a scalloped wall which was interpreted as a post surgical change, since the area had been recently explored at the time of the right colectomy. Again no extravasation of contrast material was seen.

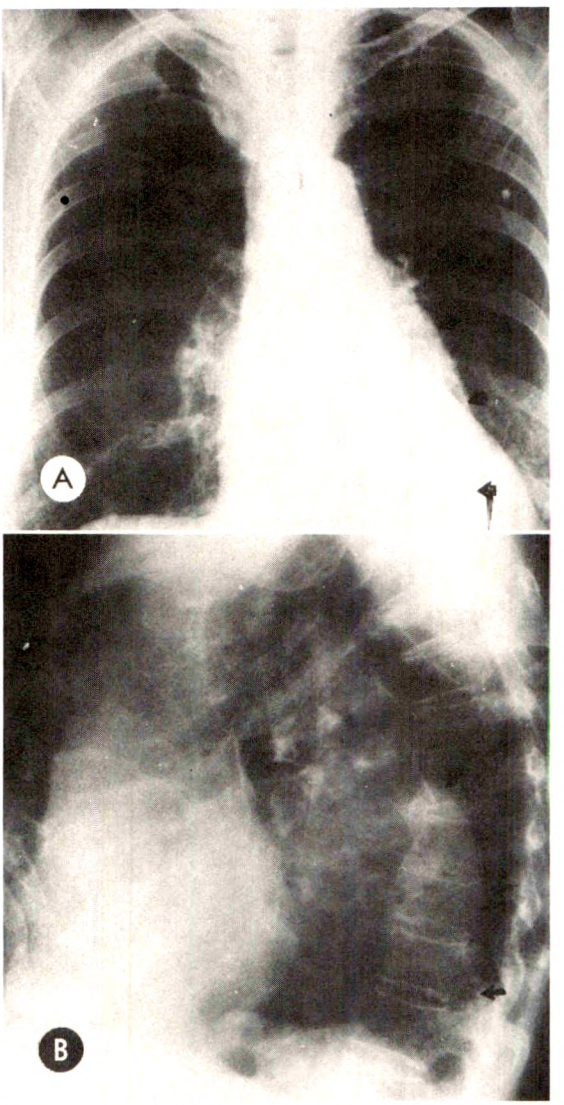


Fig. 9. (*A* and *B*) Posteroanterior and lateral chest roentgenograms on March 15, 1974 demonstrate a large, fusiform aneurysm (arrows) of the descending aorta beginning above the carina and extending below the diaphragm.

(Fig. 13). An upper gastrointestinal series three months prior to admission showed displacement of the esophagus to the right by the large calcified aneurysm unchanged from an examination in 1962 (Fig. 14). The serological test for syphilis was positive. An upper gastrointestinal series three days after admission revealed extravasation of barium from the esophagus into the aneurysm and mixture of the barium with the laminated clot. There was also a collection of barium in the mediastinum

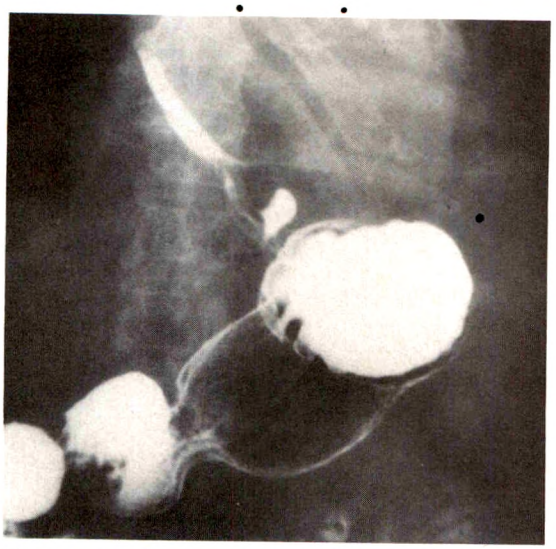


Fig. 10. At the time of the initial bleeding episode the barium study shows displacement of the esophagus to the right by the large aneurysm and a small hiatus hernia, but no mucosal irregularity and no abnormality other than the displacement.

which was outside the aneurysm and the esophagus (Fig. 15). Esophagoscopy demonstrated an extrinsic mass impinging on the esophagus. A thoracic aortogram revealed the neck of the clotted aneurysm but there was no extravasation of contrast material (Fig. 16). Massive hematemesis occurred on the ninth hospital day. The patient underwent emergency thoracotomy which revealed a 7 cm aneurysm arising from the anterior surface of the aorta. The aneurysm displaced the esophagus far to the right and a communication between the two structures was identified. Repair was attempted but the patient expired during the procedure.

Case vi. D.C. The patient was admitted with a chief complaint of repeated episodes of vomiting of large amounts of blood. She had been in good health until one year prior to admission when she began to experience intermittent epigastric pain radiating around the costal margin. An upper gastrointestinal series at that time was reported as entirely normal.

Hematemesis began three days prior to admission and the patient was admitted from the receiving unit in shock. The initial hemoglobin determination was 11.4 grams which fell to 8.0 grams during hospitalization. An upper gastrointestinal series demonstrated complete obstruction of the esophagus at the level of the

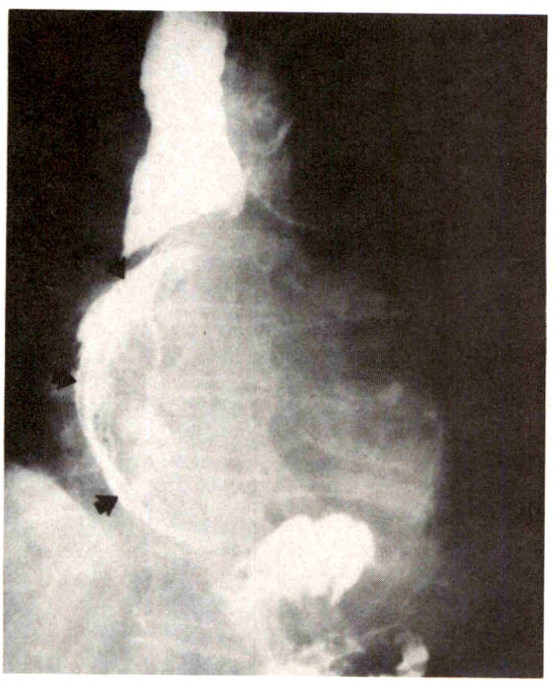


Fig. 11. The upper gastrointestinal series on April 1, 1974 shows gross irregularity of the mucosa of the distal esophagus (arrows) as well as the displacement.



Fig. 12. A spot film of the distal esophagus shows barium extravasation from the esophagus and mixture of the barium with the laminated clot in the aneurysm. There is also a collection of barium in the mediastinum (arrows), outside both the area of the aneurysm and the gastrointestinal tract, indicating a perforation of the ulcerated esophagus into the mediastinum as well as into the aneurysm.

aortic arch and a large oval soft tissue mass could be seen in the posterior mediastinum and along the course of the esophagus and aorta (Fig. 17). A spot film suggested an intramural lesion (Fig. 18). The roentgenographic impression was either carcinoma of the esophagus or an aneurysm eroding into the esophagus.

The patient expired approximately 36 hours after admission. At autopsy the mid-portion of the esophagus was filled with recent and old blood clots. A large perforation, irregular in outline and approximately 2×3 cm in size, was noted on the posterior wall of the esophagus. Along the thoracic aorta a large break in the continuity of the wall measuring 4×2 cm was noted, representing an aneurysmal sac which had ruptured into the esophagus.

DISCUSSION

In a recent review of 131 cases of aorto-enteric fistula reported by Reckless *et al.*,[3] atherosclerosis was found to be the most common cause, being reported in 61 percent of the patients. Other etiologies in this group included syphilis, tuberculosis, and mycotic aneurysms in about equal percentages. In 17 percent of the group, the etiology was not reported. The average age of patients in this group was 60 years.

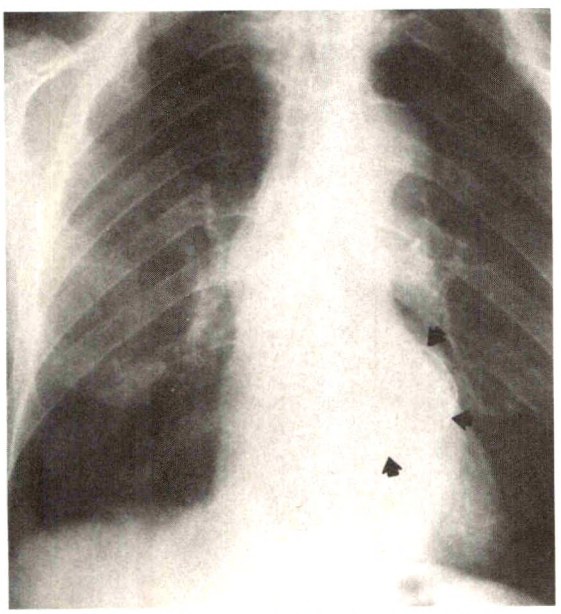


Fig. 13. A curvilinear calcification (arrows) is seen in the wall of a saccular aneurysm of the descending aorta.

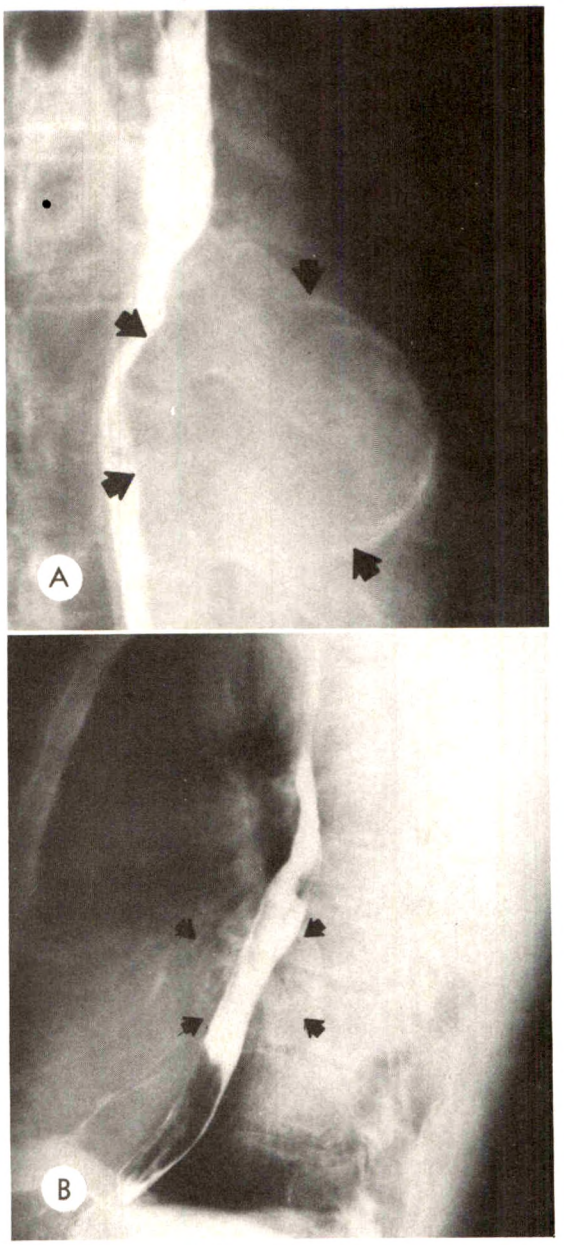


Fig. 14. (*A* and *B*) Extrinsic pressure on the esophagus by the aneurysm (arrows) is demonstrated.

Atherosclerosis as the cause occurred in older patients, the average age being 67 years. Seventy-seven percent of these cases occurred in males. In this series the most common site of the fistula was the third portion of the duodenum which accounted for 57 percent of the cases. The other portions of the duodenum accounted for an additional 24 percent of cases raising the

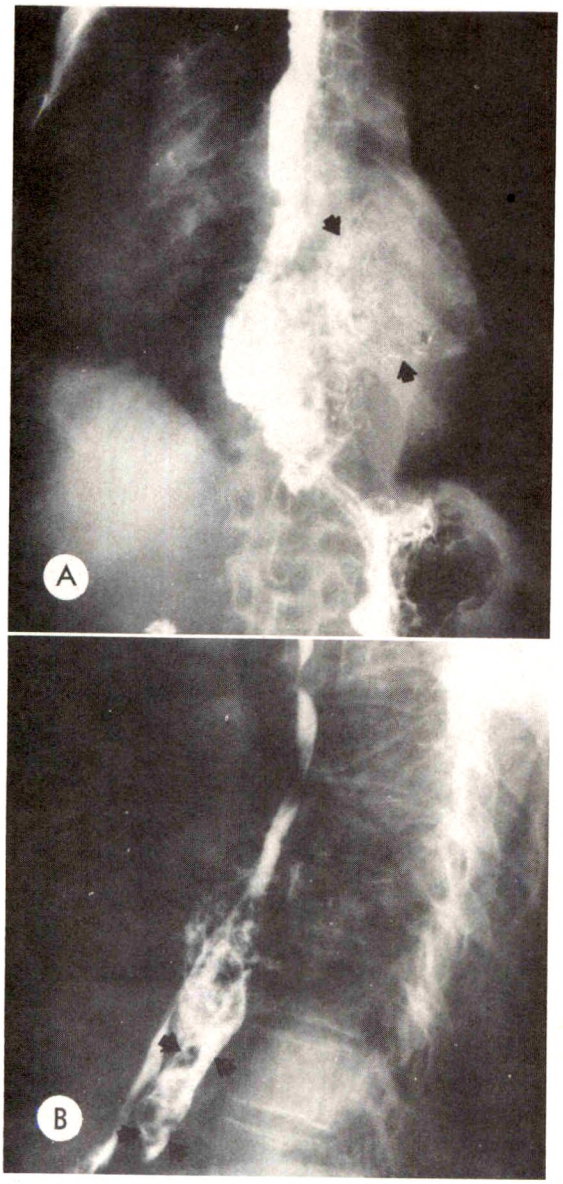


Fig. 15. Barium study at the time of bleeding shows barium mixed with the laminated clot in the aneurysm (arrows, *A*) and a mediastinal collection outside the aneurysm (arrows, *B*).

total number of aorto-enteric fistulas into the duodenum to 81 percent. The stomach, small bowel, and large bowel were about equal in incidence as sites of fistula in the remaining 18 percent.

The third portion of the duodenum is fixed and closely opposed to the anterior wall of the aorta and this probably is the reason for the high incidence of fistulas at this site. It seems likely that due to the fixation there is pressure necrosis of the duodenum at this site, and the enteric secretion then digests away the wall of the aneurysm to produce the fistulous communication.

In another series[1] in which the natural history of 230 aneurysms was studied, there were 79 syphilitic thoracic aneurysms that resulted in death. Three of these ruptured into the esophagus. There were eight fatal arteriosclerotic aneurysms, one of which ruptured into the esophagus and one into the duodenum.

Ferris *et al.*[2] reported that 46 aorto-duodenal fistulas following aortic grafts had been reported up until 1965. These fistulas are usually the result of breakdown at the anastomosis between the atherosclerotic aorta and the graft. Gastrointestinal bleeding, abdominal pain, and back pain

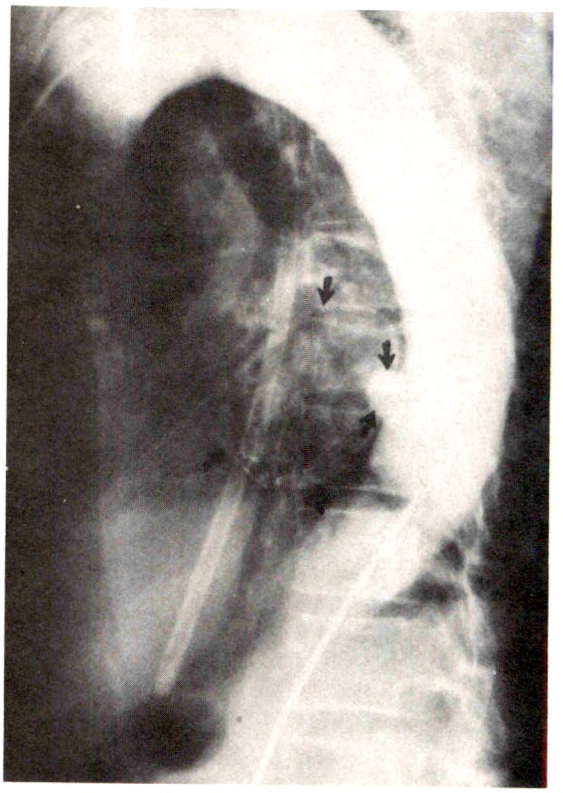


Fig. 16. The thoracic aortogram demonstrates the neck of the aneurysm and the calcification in the wall (arrows) but no extravasation of contrast material is seen.

were the most frequent presenting symptoms. Hematemesis was present in 40 percent, melena in 40 percent, abdominal pain in 48 percent, lumbar back pain in 22 percent and a palpable abdominal mass on admission in 56 percent. In some of these patients gastrointestinal bleeding was not detected until after admission.

Of interest is the elapsed time from the initial gastrointestinal bleed to death or surgery. Of 115 patients,[3] this interval was less than six hours in 30 patients, seventeen had an interval of 6–24 hours, 31 an interval of one to seven days and 37 patients an interval greater than one week.

Although the surgical treatment of this abnormality is attended by a high operative mortality rate, as high as 50 percent, and the complication rate of vascular surgery in an area of infection is also very high, there is no reported case of survival of this condition without operative treatment. Eight of 18 patients in one series survived.[3]

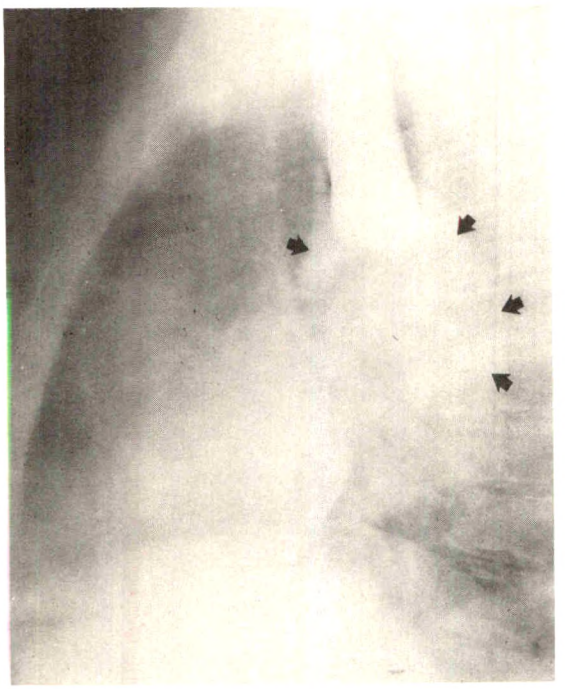


FIG. 17. A barium swallow demonstrates complete obstruction of the esophagus at the level of the aortic arch and a large oval soft tissue mass could be seen in the posterior mediastinum and along the course of the esophagus and aorta (arrows).

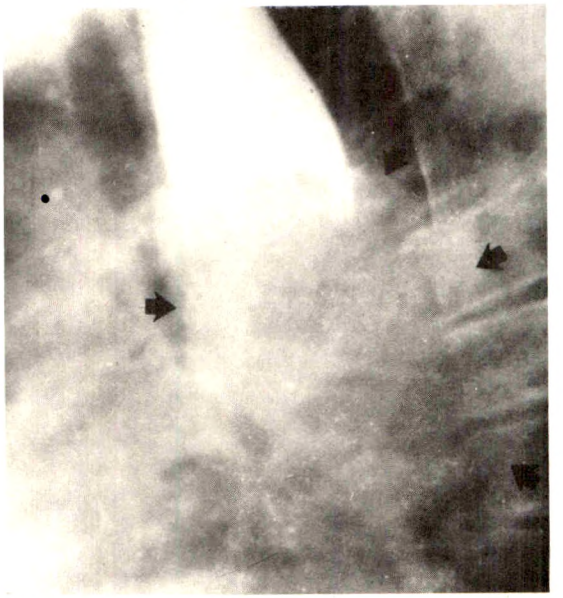


FIG. 18. The spot film shows the intramural type defect as well as the soft tissue density of the aneurysmal mass (arrows).

The roentgen signs demonstrated by the fistulas into the duodenum in our three cases included primarily extrinsic pressure on the third portion of the duodenum. In one case the entire duodenum was filled with clot and the tract between the duodenum and the ruptured graft was filled with barium. In the other cases there was effacement of the duodenal folds in the area of extrinsic pressure. This combination of findings in a patient with severe upper gastrointestinal bleeding should certainly raise the question of a fistulous communication. The failure to demonstrate the bleeding point by angiography should not exclude this possibility. Both anteroposterior and lateral aortograms should be obtained if angiography is done.

The signs of aorto-enteric fistulas into the esophagus are dramatic. In two of our cases there was mixture of the barium with the laminated clot in the aneurysm. In addition there was loculation of barium outside both the aneurysm and the esophagus in the mediastinum. In one case there was obstruction of the flow of barium in the esophagus by what appeared to be an intramural defect, namely a sharply demarcated

defect with undercut margins. In all of our cases there was an aneurysm present in the area of the defects with calcification in the wall, making aorto-enteric fistula the most likely explanation for the esophageal abnormality.

George M. Wyatt, M.D.
Department of Radiology
Cincinnati General Hospital
College of Medicine
University of Cincinnati Medical Center
234 Goodman Street
Cincinnati, Ohio 45267

REFERENCES

1. Cranley, J. J., Herrmann, L. G., and Preuninger, R. M. Natural history of aneurysms of aorta. *A.M.A. Arch. Surg.*, 1954, *69*, 185–197.
2. Ferris, E. J., Koltay, M. R. S., Koltay, O. P., and Sciammas, F. D. Abdominal aortic and iliac graft fistulae; unusual roentgenographic findings. Am. J. Roentgenol., Rad. Therapy & Nuclear Med., 1965, *94*, 416–420.
3. Reckless, J. P. D., McColl, I., and Taylor, G. W. Aorto-enteric fistulae: uncommon complication of abdominal aortic aneurysms. *Brit. J. Surg.*, 1972, *59*, 458–460.

Vol. 126, No. 4

MULTIPLE BENIGN URETERAL FIBROUS POLYPS*

By FELIX A. HUGHES, III, M.D.,†‡ *and* CHARLES S. DAVIS, Jr., M.D.§
VIRGINIA BEACH, VIRGINIA

ABSTRACT:

Two cases of benign fibrous polyps of the ureter are reported with emphasis on the uroradiological features and methods of evaluation in the diagnosis of benign mesodermal tumors of the ureter. The apparently excellent results from conservative surgery make the recognition and preoperative roentgenologic diagnosis of this entity mandatory.

DESPITE the increasing frequency of reports and articles in the urologic literature concerning benign mesodermal tumors of the ureter, little mention of benign fibrous polyps and their frequence has occurred in the roentgenologic literature. Two cases of multiple benign ureteral polyps are discussed with particular emphasis on the roentgenologic appearance. Recognition of this entity is important for the radiologist if only to alert his urologist colleague to the possible benign nature of the ureteral lesions which may make ureteronephrectomy unnecessary. Multiple cases have now been treated using a conservative surgical approach without evidence of malignant transition or recurrence.[4]

REPORT OF CASES

Case I. G.C., a 31 year old white male, was admitted with left flank pain of recent onset. Laboratory data included microscopic hematuria, but otherwise were normal. Pertinent urologic past history revealed spontaneous passage of left ureteral calculi five years prior to his current admission.

Uroradiologic work-up included an excretory urogram (IVP), cystoscopy, and a left retrograde pyelogram as well as fluoroscopic examination and videotape recording of the left ureter utilizing a small catheter placed in the ureter at cystoscopy (Fig. 1, *A–C*). Multiple smooth walled pedunculated tumors which exhibited all the criteria of benignity were demonstrated as well as obstruction and deformity of the lower calyceal system secondary to associated calyceal and renal calculi.

The patient underwent a left ureteral exploration with surgical demonstration of the benign polyps (Fig. 2, *A*). Frozen section confirmed the benign nature of the mesodermal tumors (Fig. 2, *B*) and an excisional biopsy of the polyps was performed as well as a partial left nephrectomy for the associated renal lithiasis and severe secondary inflammatory changes.

The postoperative course has been benign. A follow-up IVP demonstrated no recurrence of the ureteral tumors.

Comment. This case is complicated by the association of the polyps with renal and ureteral calculi. Similar association was not found in the reviewed urological literature. Unfortunately, an IVP performed in Europe five years earlier was unavailable for review.

Case II. R.S., a 42 year old white male, presented with gross painless hematuria. Laboratory findings included microscopic pyuria as well as the hematuria, but were otherwise unremarkable.

Uroradiologic work-up included an IVP and left retrograde pyelogram (Fig. 3, *A* and *B*). There was partial obstruction to the upper one-third of the left ureter and a suggestion of a filling defect on the IVP which was confirmed on the retrograde pyelogram.

The patient underwent a left ureteral exploration with an excisional biopsy of the benign polyps. The surgical specimen and frozen section microscopic examination confirmed the benign nature of the multiple fibrous polyps and the conservative surgical approach was completed. One polyp measured 2.2 cm in length while the second was 1.8 cm long.

There was an uneventful postoperative course and a recent follow-up IVP demon-

* From the Departments of Radiology† and Urology,§ General Hospital of Virginia Beach, Virginia Beach, Virginia.
‡ Assistant Clinical Professor of Radiology, Medical College of Virginia, Richmond, Virginia.

UNIVERSITY COLLEGE OF MEDICINE LIBRARY

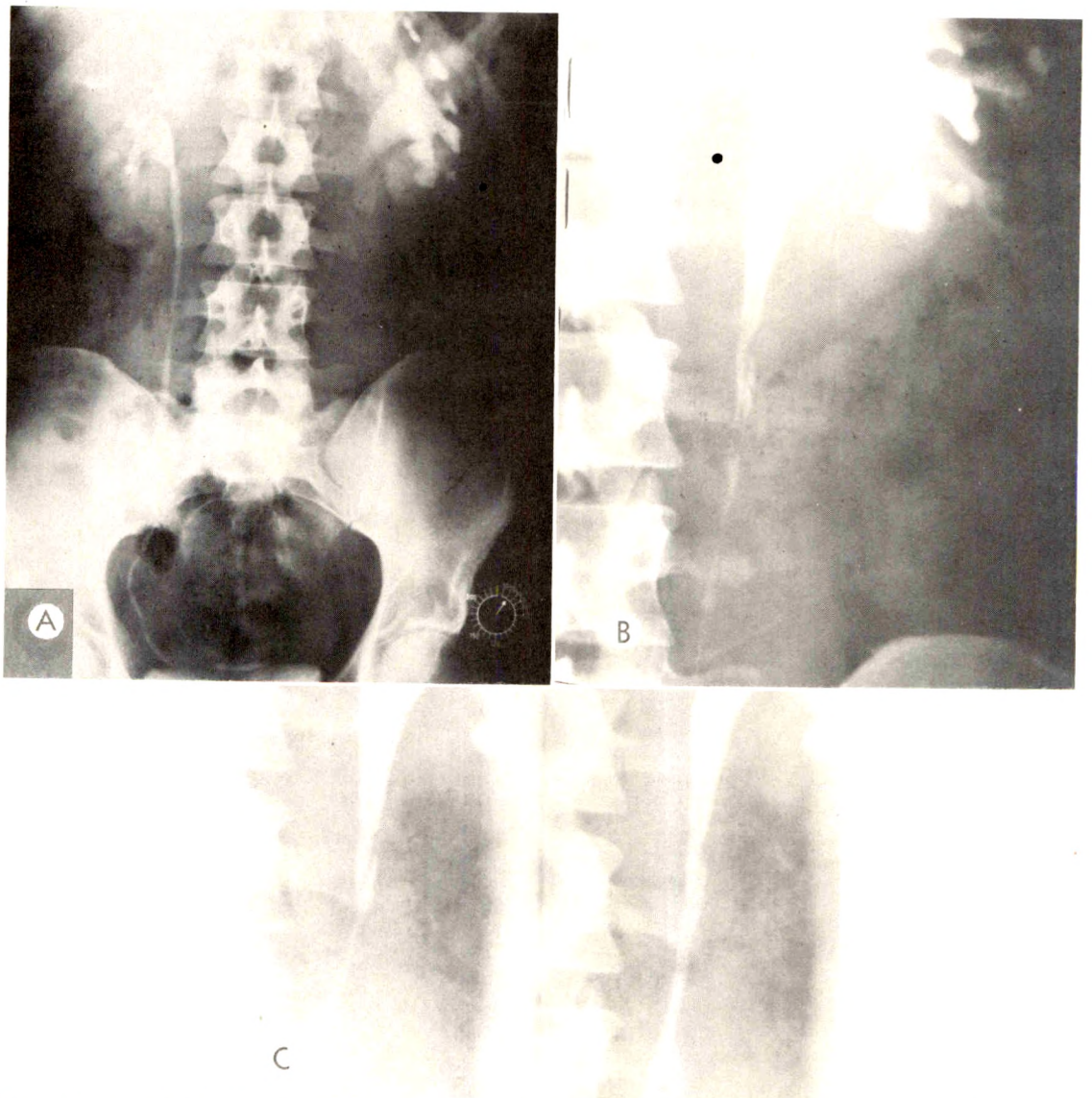


Fig. 1. Case 1. (*A*) Initial excretory urogram demonstrates bilateral renal function with partial obstructive changes on the left as well as a suggestion of a ureteral filling defect in the upper one-third of the ureter. (*B*) Left retrograde pyelography confirms the presence of persistent filling defects within the ureter as well as demonstration of the renal and calyceal calculi in the lower one-third of the left kidney with associated calyceal deformity and infundibular obstruction. (*C*) Fluoroscopic spot films clearly demonstrate the multiplicity, intraluminal position, pliability, mobility, and pedicle attachment of the benign fibrous polyps.

strated prompt bilateral renal function with healing of the surgical incision near the left ureteropelvic junction.

Comment. The initial pyuria was felt to be due to associated prostatitis. There is a relatively high incidence of associated urinary tract infection and benign fibrous polyps in the literature.[3]

DISCUSSION

Microscopically, non-epithelial benign ureteral tumors are characterized by a surface layer of normal transitional epithelial cells and a stroma composed predominantly of various cells of mesodermal origin.[1,17] Fibrous polyps are the most common in this category of tumors which include

fibro-epitheliomas, fibromas, fibrolipomas, leiomyomas, fibromyomas, vascular fibrous tumors, vascular epithelial polyps, cavernous hemangiomas and lymphangiomas.[6,15] No significant epithelial cellular atypia is present. Once this diagnosis is established by surgical biopsy and frozen section, a conservative approach can be taken by the urologist. Local resection, as the excisional biopsies in these cases, or segmental ureterotomy with reanastomosis and preservation of the upper urinary tract is adequate for permanent therapy.

Clinically, there is a wide spectrum of symptomatology and laboratory presentation of benign ureteral polyps. This is somewhat in contradistinction to malignant epithelial ureteral tumors where the triad of hematuria, colicy pain, and a palpable mass are generally seen. There is a definite predilection for a younger population in any composite series of benign ureteral polyps. Indeed, there is a case report of a benign fibrous polyp in the newborn,[16] as well as multiple cases in children,[4,5] but the fourth and fifth decade appears to be the most common age group.

Hematuria is present in over half of the reported cases of ureteral polyps, but surprisingly multiple cases without gross or even microscopic hematuria have been reported.[2,8,13,14] Because of the relative infrequency of total ureteral obstruction, only scattered reports of clinically palpable masses or hydronephrotic kidneys are found. Interestingly, the most common symptom, non-specific flank pain generally of a non-colicy nature, is intermittent and may be present for many years before an adequate uroradiologic work-up is provided.[5,13,14] Certainly, there is no pathognomonic symptom nor clinical sign to suggest the diagnosis, making the roentgenologic appraisal all the more significant.

In the reviewed reported cases,[2–5,8,9,12–14,16] the most common roentgenologic finding was a long, narrow, generally smooth, ureteral filling defect with easy flow of contrast material around the lesion. As in the two cases reported above, the lesions were most common in the upper one-third of the ureter with a definite predilection for males and a seemingly disproportionate number of cases involving the left ureter.[5,8,13,14] As a rule, the routine excretory urogram or an infusion pyelogram was adequate for diagnosis because of the lack of obstructive uropathy or significant renal damage even with relatively large lesions. In cases of significant obstruction, retrograde pyelograms were necessary to visualize the filling defects. One case of bilateral filling defects found to be benign fibrous polyps has been reported.[5]

Roentgenographic priority should be given to optimum visualization of the filled ureter. Although the serpiginous intralumi-

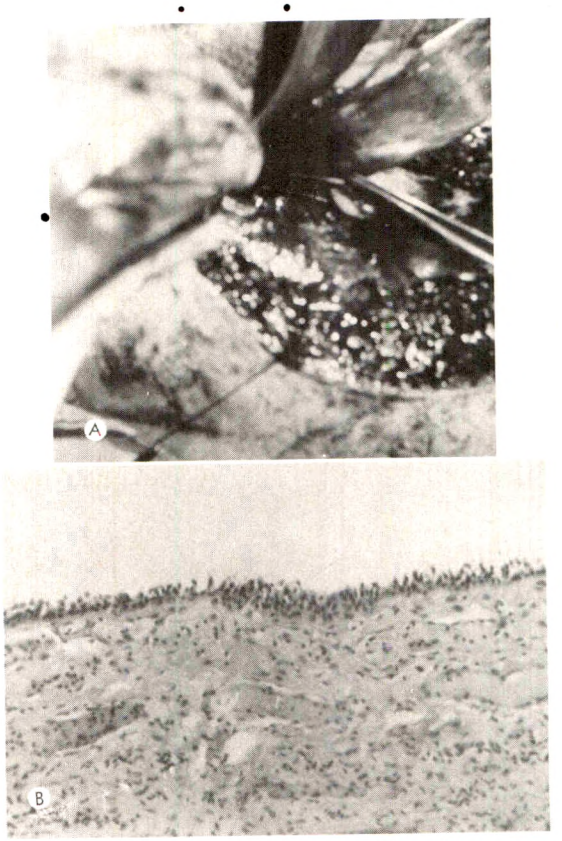


Fig. 2. Case 1. (*A*) Surgical exploration of the upper third of the left ureter with demonstration of one of the long fibrous ureteral polyps (arrows). (*B*) Microscopic appearance of the frozen section of this polyp. Normal transitional epithelium covering a stroma of congested fibrovascular tissue is well seen. (Final pathological diagnosis: Multiple benign ureteral fibrous polyps.)

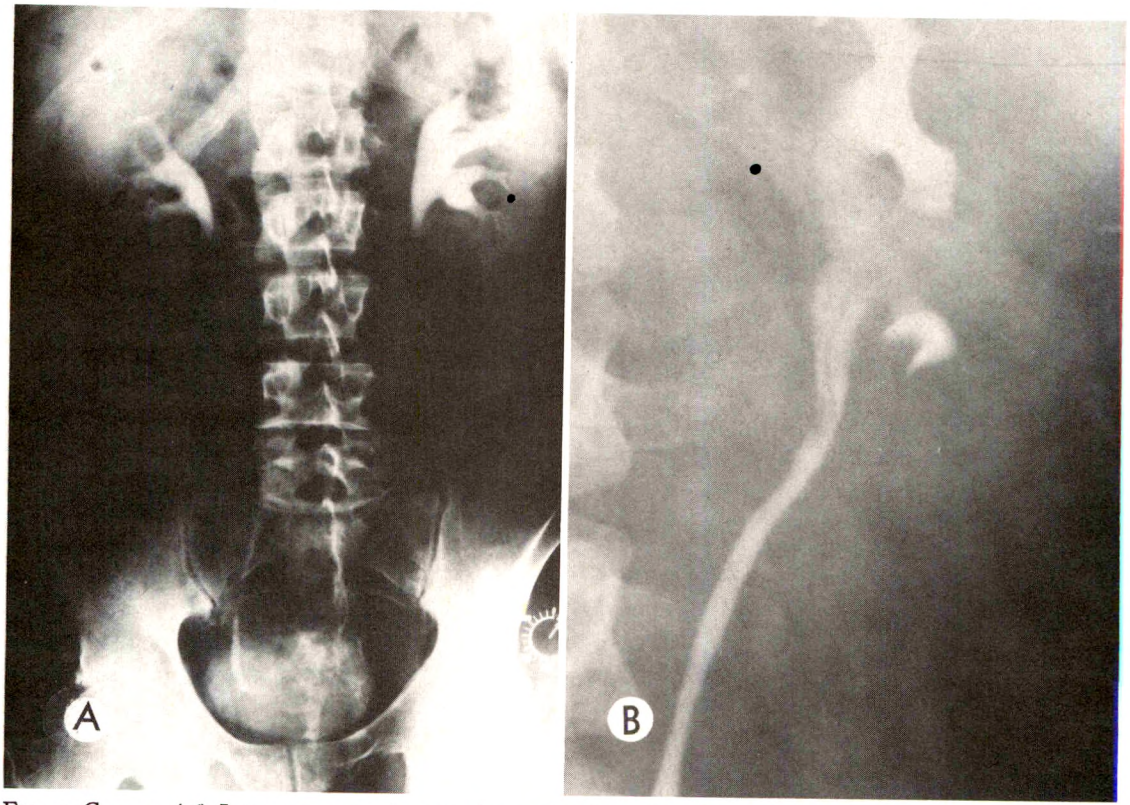


Fig. 3. Case II. (*A*) Intravenous pyelogram demonstrating mild obstructive changes in the upper urinary tract with a suggestion of a ureteral filling defect on the left. (*B*) Left retrograde pyelogram demonstrates the multiple intraluminal filiform ureteral filling defects with attachment of the pedicles of the polyps near the left ureteropelvic junction. Movement of the polyps within the renal pelvis was also shown.

nal filling defects may be suspected or well demonstrated on a routine excretory urogram, maximum distention of the ureter is generally afforded by drip infusion hydration pyelography. Using these techniques which can be enhanced with tomography, fluoroscopy with spot filming, or recording motion with videotape or cine studies, the criteria for benignity outlined below can best be appreciated. Another modification in technique, as discussed in Case I above, is the utilization of an indwelling ureteral catheter inserted following (bulb) retrograde pyelography. Roentgenologic control of ureteral filling and maximum distention of the involved portion of the ureter are possible allowing for optimum demonstration of the lesion.

Roentgenologic findings that strongly suggest the diagnosis of benign fibrous polyps include:

1. There are space occupying filling defects within the lumen of the ureter which are smooth walled or have a smooth contour. These may be bifid, multibranched or single, but are definitely intraluminal. The polypoid tumors are generally long, at least a centimeter in length.

2. Separation of the polyps from the ureteral mucosal wall is generally possible, particularly when the techniques allowing for maximum distention of the contrast filled ureter are used. Easy flow of the contrast material around the polyp and identification of a rim of contrast medium around the lesion establish the lack of fixation. Not infrequently, attachment of the pedicle of the fibrous polyp to the ureteral wall can be demonstrated.

3. Lack of rigidity, and the presence of mobility and pliability of the polyp are important and can be shown by change in position during the examination.[13]

4. Multiplicity of the lesions and location

of the polypoid filling defects in the upper third of the ureter, particularly in the region of the ureteropelvic junction also favor benignity. It has long been taught that malignant epithelial tumors are more common in the lower ureter.[1,15]

5. Lack of significant upper urinary tract obstruction and relatively little renal damage or diminished function even with relatively large ureteral filling defects are also significant findings. However, cases of complete obstruction with significant hydronephrosis as well as obstruction secondary to intussusception have both been reported.[2,7,9]

Retrograde pyelography continues to have a place in the diagnosis of ureteral tumors, either benign or malignant, particularly where significant obstruction or renal damage has occurred.

Selective angiography may be useful in the diagnosis of ureteral tumors, especially if there is significant hematuria and suspicion of a vascular lesion or evidence of total obstruction, or when a poorly functioning kidney is present. Angiography on a routine basis, however, for the work-up of benign fibrous polyps, would not appear feasible particularly if suitable effort to maximize ureteral distention is utilized.

Again, the importance of roentgenologic appreciation for the apparent increasing incidence of fibrous polyps of the ureter is stressed. Preoperative suspicion of benignity can lead to conservative surgery and the preservation of the upper urinary tract.

Felix A. Hughes, III, M.D.
Department of Radiology
General Hospital of Virginia Beach
1060 First Colonial Road
Virginia Beach, Virginia 23454

The authors would like to express their appreciation to Mr. Robert Cox and Mr. Jim Glascow of Dupont Corporation for their kind technical assistance in the preparation of this paper.

REFERENCES

1. Abeshouse, B. S. Primary benign and malignant tumors of ureter. *Am. J. Surg.*, 1956, *91*, 237–271.
2. Bose, B., and Williams, J. P. Benign polypoidal tumor of ureter. *Brit. J. Surg.*, 1971, *58*, 149–151.
3. Cavallo, T., and Crocker, D. W. Benign tumor of ureter: case report. *J. Nat. M. A.*, 1972, *64*, 421–423.
4. Colgon, J. R., Skaist, L. E., and Morrow, J. W. Benign ureteral tumors in childhood: case report and plea for conservative management. *J. Urol.*, 1973, *109*, 308–310.
5. Crum, P. M., Sayegh, E. S., Sacher, E. C., and Wescott, J. W. Benign ureteral polyps. *J. Urol.*, 1969, *102*, 678–682.
6. Emmett, J. L., and Witten, D. M. Clinical Urology. Volume II: Tumors of Renal Pelves and Ureter. Third edition. W. B. Saunders Company, Philadelphia, 1971, pp. 1145–1151.
7. Gerdes, G., and Nordqvist, L. Intussusception of ureter caused by primary benign tumor. *Acta. chir. scandinav.*, 1966, *132*, 397–402.
8. Hudson, H. C., and Howland, R. L. Primary benign ureteral tumor of mesodermal origin. *J. Urol.*, 1971, *105*, 794–796.
9. Knackstedt, J., Pirozynski, W., and Oliver, J. A. Benign fibroepithelial polyps of ureter. *Brit. J. Urol.*, 1971, *43*, 284–288.
10. Lambeth, J. T., and Ranniger, K. Angiographic demonstration of a benign tumor of ureter. *Radiology*, 1965, *91*, 929–930.
11. Lang, E. K. Arteriographic diagnosis of primary and secondary tumors of ureter or ureter and renal pelvis. *Radiology*, 1969, *93*, 799–805.
12. Neal, J. M., and Arbuckle, L. D. Benign fibrous polyp of ureter: case report. *J. Urol.*, 1972, *108*, 230–232.
13. Pinto, R. S., Fauver, E., and Anderson, J. R. Benign fibroepithelioma of ureter. *Urology*, 1974, *3*, 747–749.
14. Roen, P. R., and Kandalaft, S. Primary benign mesodermal ureteral tumor. *J. Urol.*, 1966, *96*, 890–891.
15. Scott, W. W., and McDonald, D. F. Tumors of ureter. In: Urology. Edited by M. F. Campbell, and J. H. Harrison, Volume 2. Third edition. W. B. Saunders Company, Philadelphia, 1970, pp. 987–992.
16. Soderdahl, D. W., and Schuster, S. R. Benign ureteral polyp in newborn. *J.A.M.A.*, 1969, *207*, 1714–1715.
17. Vest, S. A. Conservative surgery in certain benign tumors of ureter. *J. Urol.*, 1945, *53*, 97–130.

CAVITATING LUNG NODULES AND PNEUMOTHORAX IN CHILDREN WITH METASTATIC WILMS' TUMOR*

By E. GEORGE KASSNER, M.D.,† HAROLD S. GOLDMAN, M.D.,‡ *and* ALBERTO ELGUEZABAL, M.D.§
BRONX AND BROOKLYN, NEW YORK

ABSTRACT:

Lung metastases evolved into large thin-walled cysts in two children with Wilms' tumor. Histologic examination of one lesion suggested that invasion of a small bronchus or bronchiole, leading to ball-valve obstruction, was responsible. One patient also experienced recurrent pneumothorax, probably on the same basis.

The formation of thin-walled cysts has not previously been observed with metastatic Wilms' tumor. Pneumothorax is a rare complication of metastatic Wilms' tumor.

CAVITATION of pulmonary metastases is very rare in children. This phenomenon has been reported in three children with metastatic Wilms' tumor.[3,5] We have observed two children with Wilms' tumor in whom pulmonary metastases evolved into large thin-walled cysts. One of these patients had recurrent episodes of pneumothorax, a complication that has rarely been associated with metastatic Wilms' tumor.[4]

REPORT OF CASES

CASE 1. (Jewish Hospital and Medical Center of Brooklyn.) A.R. had a right nephrectomy for Wilms' tumor at two and one-half years of age. Tumor was present in the renal vein. Lung metastases were not detected in the initial chest roentgenogram. A course of actinomycin D was begun and 3,000 rads were delivered to the tumor bed using Co-60 teletherapy. Six months after nephrectomy a pulmonary metastatic nodule was seen in the right lower lobe. Alternating courses of actinomycin D and vincristine were administered and 300 rads were delivered to a small field encompassing the nodule. Sixteen months after nephrectomy another small pulmonary metastatic deposit appeared in the lingula and 300 rads were delivered to this lesion. After nine months without change the nodule in the right lung began to enlarge and was excised with a cuff of tumor-free lung.

A second course of radiation therapy was administered to a small field that encompassed the metastasis in the left lung (Fig. 1*A*). After 750 rads of a planned tumor dose of 2,250 rads had been delivered, a cavity was noted within the metastasis (Fig. 1*B*). This cavity continued to enlarge and the heart was displaced to the right (Fig. 1, *C* and *D*). The patient had a cough and was easily fatigued but he was not in acute distress. Radiation therapy was stopped after 1,050 rads and lingulectomy was performed, 16 months after the appearance of the metastatic deposit in the left lung and 25 months after nephrectomy.

The resected lung specimen consisted of a collapsed empty sac, which measured 4 cm in diameter, partially surrounded by a solid tumor which measured 5×3.5×2 cm. Where it did not abut the tumor mass, the cyst wall was 1–2 mm thick.

Microscopically the tumor was a typical Wilms' tumor; the sarcomatous component predominated and there were a few scattered epithelial areas. Tumor completely surrounded the cyst and extended either to the lining epithelium, if present (Fig. 2, *A* and *B*), or to the lumen in areas where the lining epithelium was absent. In most areas the cyst was lined with respiratory epithelium. There were foci of squamous metaplasia or flattened cuboidal epithelium. Where lining epithelium was absent the cyst wall was composed of a thin layer of tumor covered externally by subpleural

* From the Departments of Radiology of the State University of New York, Downstate Medical Center,† and the Albert Einstein Medical Center, Bronx, New York,‡ and the Department of Pathology of The Jewish Hospital and Medical Center of Brooklyn.§

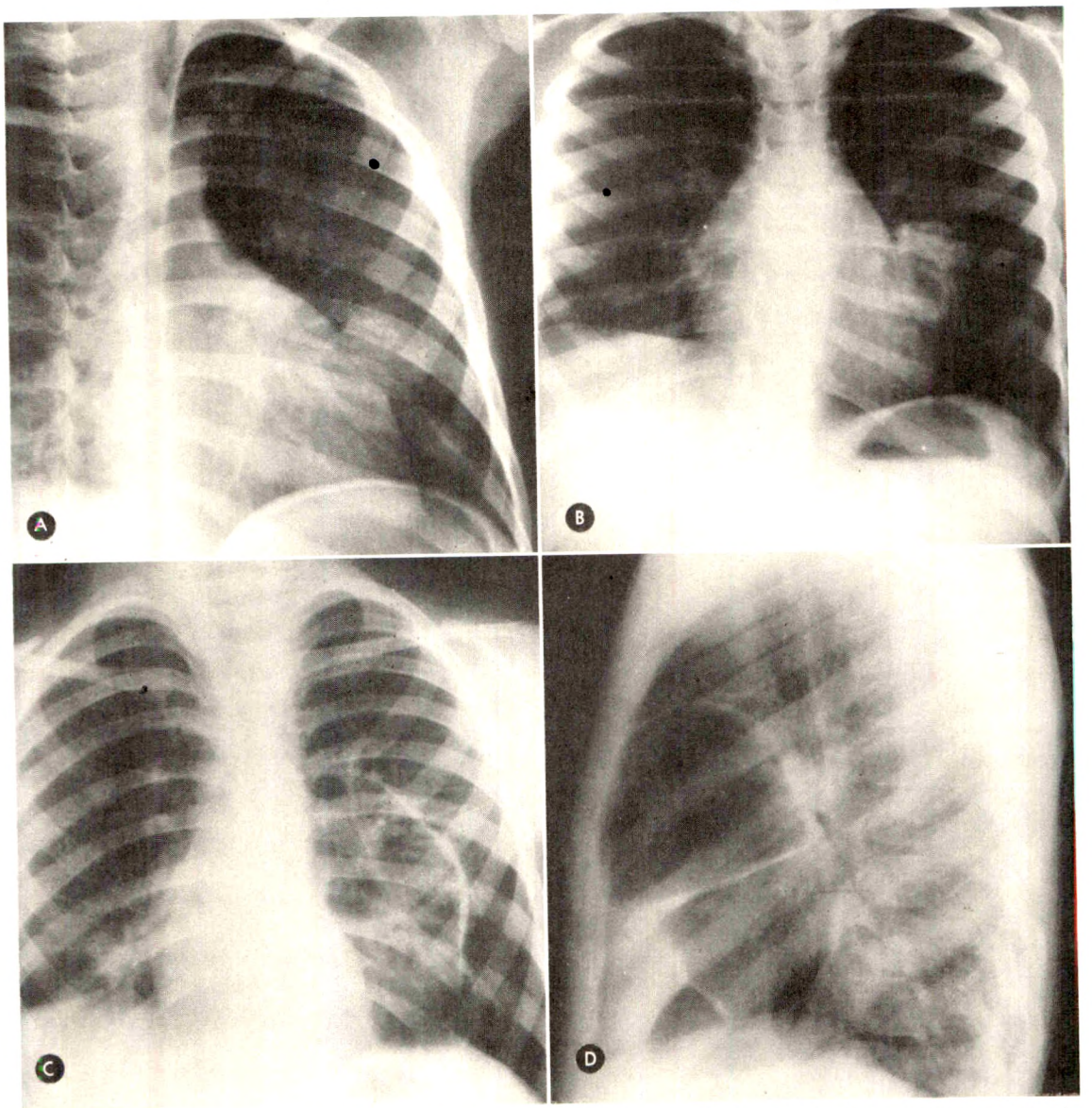


Fig. 1. Case 1. (*A*) March 7. Twenty degree right anterior oblique projection of the chest shows a metastatic nodule in the lingula. (*B*) April 18. A cavity is visible within the nodule. (The changes on the right—basilar parenchymal infiltrate, pleural thickening and elevation of the hemidiaphragm—are the residua of previous surgery.) (*C* and *D*) May 26. A large thin-walled cyst with several "septa" has developed at the site of the nodule. The heart is displaced to the right. On the lateral projection the solid portion of the tumor is visible anteriorly. Lingulectomy was performed the following day.

fibrous tissue and pleura. Tumor did not penetrate the pleura. Cartilage was not seen in the cyst wall.

Necrosis, bizarre nuclei or other radiation changes were not present in the tumor. There was no evidence of acute radiation pneumonitis, vasculitis or fibrosis in the surrounding lung parenchyma. The only features that were probably related to radiation therapy were prominence of the endothelial cells of some vessels and squamous metaplasia in a few bronchi.

Subsequently tumor recurred in the left lung, mediastinum, pleura and abdomen. He died at five and one-half years of age, 38 months after nephrectomy. Permission for autopsy was not obtained.

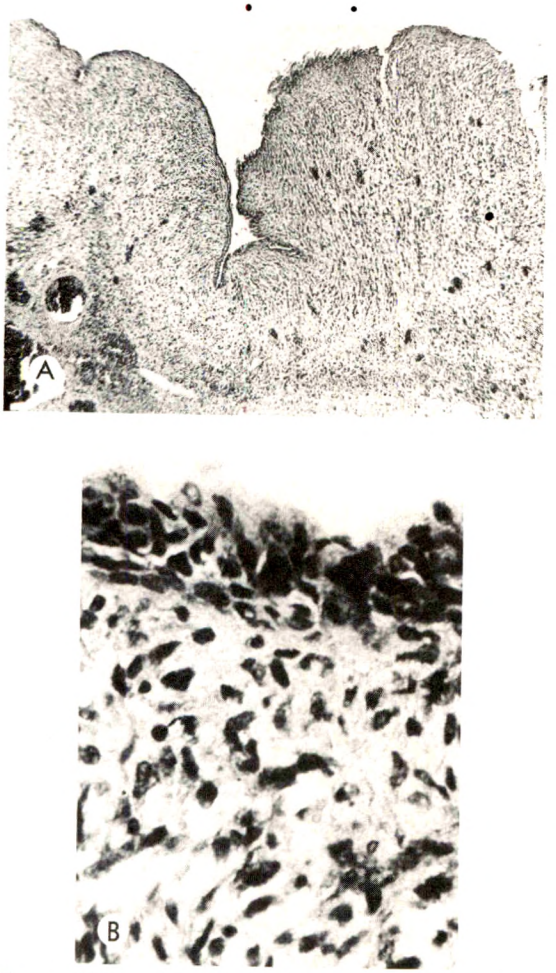


FIG. 2. Case I. (*A*) Photomicrograph of the excised metastatic nodule, showing an area in which the cyst abuts the main tumor mass. Tumor is visible just beneath the lining epithelium of the cyst. Two types of epithelium are present in this field: respiratory epithelium on the right and flattened cuboidal epithelium on the left. (H & E, 300× magnification.) (*B*) High power. The cyst lining consists of respiratory epithelium. Tumor is present just beneath the epithelium. (H & E, 750× magnification.)

CASE II. (Albert Einstein Medical Center.) M.C. had a left nephrectomy for locally invasive Wilms' tumor at three years of age. There was no evidence of pulmonary metastases. Actinomycin D was administered and, because the tumor had ruptured during surgery, 3,300 rads were delivered to the entire abdomen using Co-60 teletherapy: the right kidney was shielded after 1,500 rads. Several subsequent courses of actinomycin D were given. Twenty-four months after nephrectomy he was readmitted with a four day history of right chest pain. A chest roentgenogram showed a pneumothorax on the right and metastatic deposits in both lungs (Fig. 3*A*). A chest tube was inserted and actinomycin D and vincristine were begun. A tumor dose of 1,600 rads was delivered by moving strip technique (eight fractions in ten days) to opposing fields that included both entire lungs. Cavitation of several metastatic deposits was observed about three weeks after the completion of radiation therapy (Fig. 3*B*). Some evolved into thin-walled cysts (Fig. 3*C*).

He was re-admitted several times for treatment of recurrent right-sided pneumothorax. Several cysts in the right lung reached enormous size (Fig. 3*D*). He died at home at six years and five months of age, 38 months after nephrectomy. Autopsy was not performed.

DISCUSSION

Necrosis due to inadequate blood supply —often cited as the major cause of cavitation in lung metastases[2]—rarely if ever accounts for cavitation in small nodules or cavities in which the wall is extremely thin (1–2 mm).[6] Breakdown of tumor usually results in cavities with thick, irregular walls which do not enlarge rapidly nor reach great size.[2] Tumor necrosis does not adequately explain the rapid formation of large thin-walled cysts that occurred in our patients.

Anderson and Pierce[1] described six papatients with carcinomas of the bronchus which had the roentgenographic appearance of thin-walled cysts. Grossly, the cyst walls were smooth, gray, and shiny. Inflammation, if present, was minimal. Microscopically, the cyst walls consisted of fibrous tissue and squamous cell carcinoma. The lining consisted of malignant cells or squamous metaplastic epithelium, with malignant tumor just beneath the surface. In some instances, parts of the cavity wall were formed of compressed lung. Occasionally there was continuity between tumor in the cavity and the nodule of growth in an adjacent bronchus.

Anderson and Pierce attributed the morphology of these tumors to a ball-valve

mechanism:* Growth of tumor into a small bronchus caused partial obstruction and led to cystic distention of distal air sacs. Subsequent growth of tumor into the cyst formed a secondary lining layer of tumor cells. Rupture of the lining of tumor cells by increases in intracavitary pressure accounted for the portions of the cyst that were lined by respiratory epithelium or compressed lung.

The resected metastasis in our patient with Wilms' tumor (Case 1) was morphologically similar to these cases of bronchial carcinoma. A ball-valve mechanism, resulting from growth of tumor into small bronchi or bronchioles, satisfactorily explains the initial cavitation and subsequent evolution into thin-walled cysts that characterized the metastatic deposits in both of our patients. Although both children had received radiation therapy and chemotherapy, we believe that these changes in the metastatic deposits were the result of tumor growth rather than the consequence of therapy.

No single explanation satisfactorily accounts for all instances of pneumothorax that have been associated with lung metastases.[4,10,11] Most are probably due to the formation of malignant bronchopleural fistulas.[11] This mechanism was documented in one of the rare instances in which pneumothorax and cavitation were observed in the same patient. Kew[7] described a teenager with a solitary subpleural metastasis of osteogenic sarcoma that underwent cavitation. At thoracotomy, the pleura was carefully inspected. When the anesthetic bag was pumped, gas escaped from a small hole in the pleura overlying the cavity. Both the cavity and the pleural defect were lined with tumor.

Lodmell and Capps[9] adapted the "air-block" theory of the Macklins to explain cases in which pleural invasion by tumor was not present. They suggested that peripheral tumor nodules sometimes caused partial bronchiolar obstruction. Intercommunication between alveoli of adjacent lobules usually prevented the development of excessive local pressures, but in some patients strategically-placed tumor nodules produced a ball-valve effect. Relatively small changes in intra-alveolar pressure, *e.g.*, with coughing and sneezing, could result in dissection of air along vascular sheaths and, in some instances, lead to pneumomediastinum and pneumothorax. Lodmell and Capps cited the presence of interstitial emphysema and subpleural blebs in one of their patients as evidence in support of this concept.

Regression of tumor and radiation therapy do not appear to predispose patients with lung metastases to pneumothorax.[8,12] Our patient (Case 11) had his first episode of pneumothorax before radiation therapy to the lung was begun.

E. George Kassner, M.D.
Department of Radiology
State University of New York
Downstate Medical Center
450 Clarkson Avenue
Box 45
Brooklyn, New York 11203

* Dodd and Boyle[6] have proposed that certain properties of squamous epithelium account for the thin-walled cavitary form of bronchial carcinoma and for thin-walled cystic metastases of squamous cell carcinoma. As the growing tumor breaks into alveoli, malignant squamous epithelium is likely to come in contact with air; the process of cornification is facilitated and respiratory motion assists in stripping the keratinized surface layers from cavity walls. Meanwhile, growth progresses peripherally, so that the size of the cavity increases while its wall maintains a relatively constant thickness. In some instances, a ball-valve mechanism—manifest on serial roentgenograms as an alternately smooth and crenated appearance of the external wall—may assist in the growth of thin-walled cystic neoplasms.

Dodd and Boyle suggested that inherent properties of the normal primary tissue might account for thin-walled cystic metastases that occasionally occur with other tumors. We are not aware of any property of embryonal tissue that would explain this phenomenon in metastatic Wilms' tumor.

REFERENCES

1. Anderson, H. J., and Pierce, J. W. Carcinoma of bronchus presenting as thin-walled cysts. *Thorax*, 1954, *91*, 100–105.
2. Chaudhuri, M. R. Cavitary pulmonary metastases. *Thorax*, 1970, *25*, 375–381.
3. Coussement, A. M., and Gooding, C. A. Cavitating pulmonary metastatic disease in children. Am. J. Roentgenol., Rad. Therapy & Nuclear Med., 1973, *117*, 833–839.
4. D'Angio, G. J., and Iannaccone, G. Spontane-

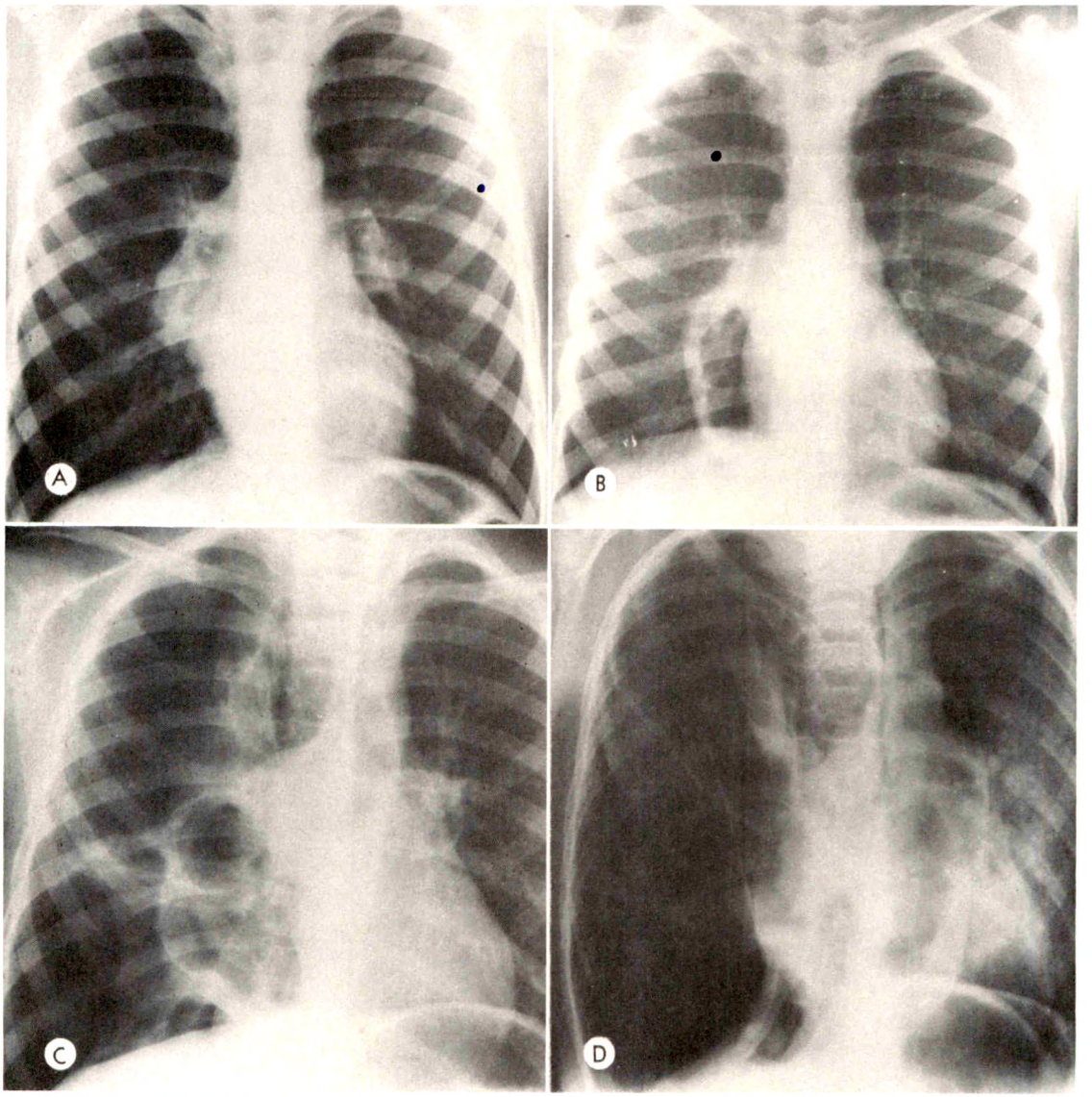


Fig. 3. Case 11. (*A*) September 21. Metastatic deposits are present in the hilar lymph nodes and in the mid-zones of both lungs. A small pneumothorax is present on the right. (*B*) November 3. The right lung has re-expanded. Nodules in both lungs have undergone cystic change. (*C*) November 20. There is a large pneumothorax on the right; a portion of the right lower lobe is adherent to the parietal pleura. Numerous thin-walled cysts are present in both lungs. (*D*) May 17 (five weeks before death). Numerous giant thin-walled cysts have almost totally replaced the right lung and there is a marked mediastinal shift to the left. Several thin-walled cysts are visible on the left. There is a small pneumothorax on the left. Solid masses of tumor are present in the mediastinum and in both lungs.

ous pneumothorax as complication of pulmonary metastases in malignant tumors. Am. J. Roentgenol., Rad. Therapy & Nuclear Med., 1961, *86*, 1092–1102.

5. Deck, F. W., and Sherman, R. S. Excavation of metastatic nodules in lung: roentgenographic considerations. *Radiology*, 1959, *72*, 30–34.

6. Dodd, G. D., and Boyle, J. J. Excavating pulmonary metastases. Am. J. Roentgenol., Rad. Therapy & Nuclear Med., 1961, *85*, 277–293.

7. Kew, M. C. Cavitating pulmonary metastasis associated with spontaneous pneumothorax. *Lancet*, 1966, *86*, 571–574.

8. Laucius, J. F., Brodovsky, H. S., and Howe, C. D. Spontaneous pneumothorax and pneumomediastinum as complications of sarcoma. *J. Thoracic & Cardiovasc. Surg.*, 1972, *64*, 467–471.
9. Lodmell, E. A., and Capps, S. C. Spontaneous pneumothorax associated with metastatic sarcomas. *Radiology*, 1949, *52*, 88–93.
10. Sherman, R. S., and Brant, E. E. X-ray study of spontaneous pneumothorax due to cancer metastases to lungs. *Dis. Chest*, 1953, *26*, 328–337.
11. Spittle, M. F., Heal, J., Harmer, C., and White, W. F. Association of spontaneous pneumothorax with pulmonary metastases in bone tumors of children. *Clin. Radiol.*, 1968, *19*, 400–403.
12. Stolzenberg, J. G., and Clements, J. P. Bilateral simultaneous pneumothorax during radiation therapy for metastatic disease from osteogenic sarcoma: case report and review of literature. *Radiol. Clin. Biol.*, 1970, *39*, 437–442.

THE SPOTTED NEPHROGRAM OF RENAL SCLERODERMA*

By JEFFREY WINOGRAD, M.D.,† DANIEL H. SCHIMMEL, M.D.,‡
and ALPHONSE J. PALUBINSKAS, M.D.
SAN FRANCISCO, CALIFORNIA

ABSTRACT:

The renal angiographic findings in our two patients with scleroderma and recent onset of hypertension included minor changes in the distal interlobar and arcuate arteries and a nephrogram displaying diffuse, spotty lucencies. Although the spotted nephrogram is occasionally seen in cases of severe nephrosclerosis, we believe that, in the absence of major arterial changes in the arcuate and distal interlobar arteries, it is virtually diagnostic of renal scleroderma.

THE various roentgenographic manifestations of scleroderma on plain films and barium contrast studies have been well described.[3,6,13] However, we have found only two reports concerning angiographic findings of renal scleroderma.[4,11] We wish to report the renal angiographic findings in two patients with scleroderma and recent onset of hypertension, and to describe particularly the nephrographic appearance, which we believe may be distinctive of, but not unique to, scleroderma kidney.

REPORT OF CASES

Case I. A 54 year old Caucasian woman was hospitalized because of a ten month history of increasing skin tightness and recently discovered hypertension. Her blood pressure at the time of admission was 190/120 mm Hg. The skin over her hands, arms, and upper chest was tight and her nose appeared pinched. Urinalysis showed 2+ protein and occasional red blood cells and white blood cells. Blood urea nitrogen was 50 mg/dl and creatinine was 2.7 mg/dl.

Findings were normal on plain chest roentgenogram, excretory urogram, barium enema study, and, except for decreased esophageal motility, roentgenograms of the upper gastrointestinal tract. A renal arteriogram, performed because of the hypertension, showed normal-sized kidneys with only minor changes in the distal interlobar and arcuate arteries; the nephrogram, however, appeared spotted (Fig. 1, *A* and *B*).

Subsequent to the arteriogram, renal biopsy was performed on one kidney; results substantiated the diagnosis of scleroderma.

The patient was treated with antihypertensive and diuretic medications. At the time of discharge from the hospital, her blood pressure had stabilized to 180/90 mm Hg, blood urea nitrogen was 42 mg/dl, and creatinine was 1.9 mg/dl.

Case II. A 51 year old Caucasian woman was referred to our hospital because, despite antihypertensive medication, she had a rapid increase in previously mild hypertension, persistent headaches, and blurred vision. She also gave a history suggestive of Raynaud's phenomenon. Prior to admission her blood pressure was 220/130 mm Hg, blood urea nitrogen 13 mg/dl, and creatinine 2.0 mg/dl.

The patient's blood pressure on admission was 200/105 mm Hg. Inspection of the eyegrounds revealed hemorrhages and exudates. The skin over the fingers was hard and waxy. Blood urea nitrogen was 38 mg/dl and creatinine 2.4 mg/dl. Anti-nuclear antibody and lupus erythematosus preparations gave negative results. A chest roentgenogram showed cardiomegaly with congestive heart failure. Excretory urography demonstrated a right kidney measuring 9.9 cm in length and a left kidney 12.5 cm. Renal arteriography showed ab-

* From the Department of Radiology, University of California School of Medicine, San Francisco, California.
† Present Address: Department of Radiology, St. Mary's Hospital, Waterbury, Connecticut.
‡ Fellow in Diagnostic Radiology.
Supported in part by National Institutes of Health Training Grant GM 01272 from the National Institute of General Medical Sciences.

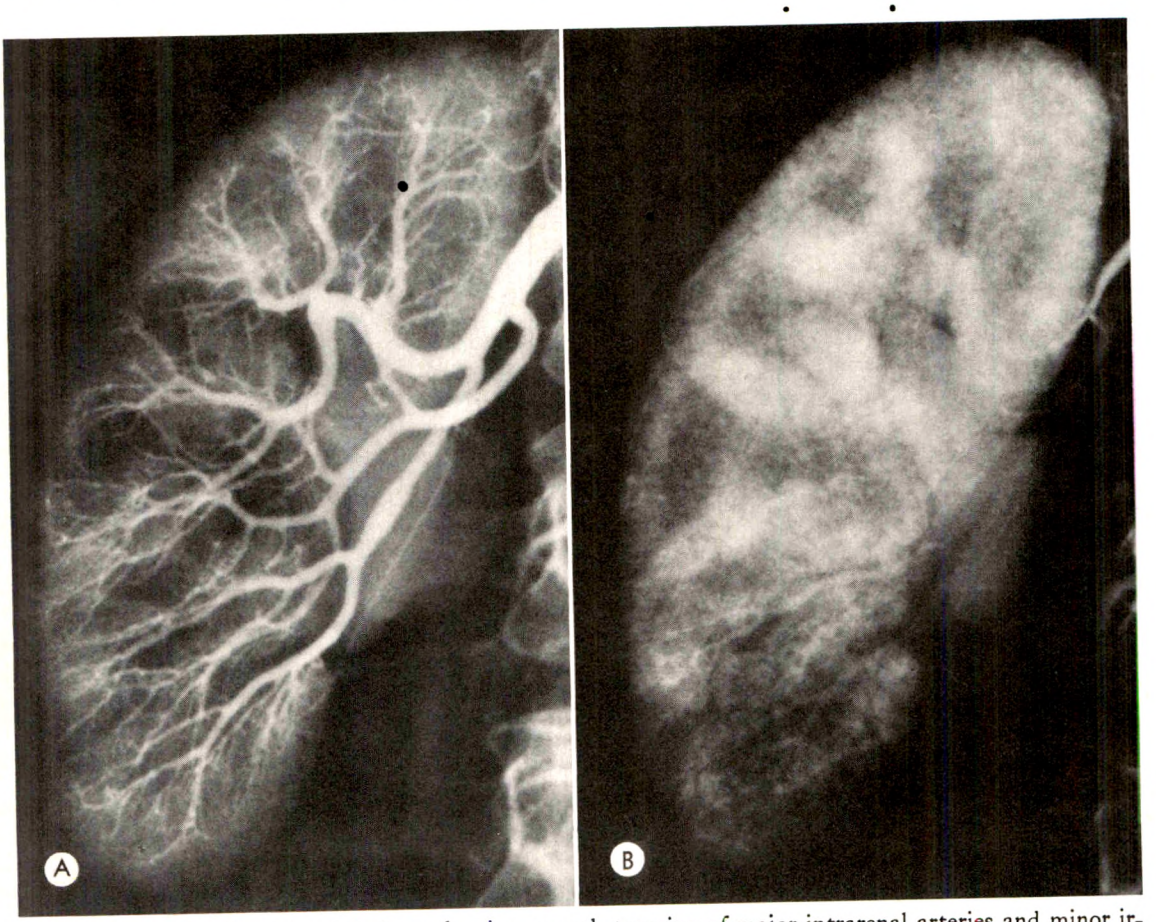


Fig. 1. Case 1. (*A*) Late arterial phase showing smooth tapering of major intrarenal arteries and minor irregularities of distal interlobar and arcuate vessels. Arterial vessels are somewhat decreased in caliber. (*B*) Nephrogram demonstrating striking, diffuse, spotty lucencies. The corticomedullary junction is preserved although blurred. Note persistent filling of arteries in lower pole, indicating marked slowing of flow.

normal kidneys bilaterally with decreased caliber of interlobar arteries and a peculiarly spotted nephrogram (Fig. 2, *A* and *B*).

Renal and skin biopsies were suggested but not performed as it was believed they would not contribute to the patient's management.

The patient was treated with diuretics. At the time of her discharge from the hospital, her blood urea nitrogen was 29 mg/dl, creatinine 2.5 mg/dl, and creatinine clearance 28 ml/min.

CLINICAL PRESENTATION

Scleroderma has been reported to occur within the age range of 3 to 83 years. The age of onset, however, is most often between the fourth and sixth decades.[4] Women are affected three to ten times as frequently as men.[17] Involvement of the kidneys in scleroderma is of major clinical importance. In one series[4] of 210 patients with scleroderma, renal scleroderma was the leading cause of mortality (42 percent). Evidence of renal involvement appears about two years following the clinical onset of scleroderma, although cases have been reported of renal disease antedating the skin lesions.[2,4,9] Clinical signs of renal involvement occur in 15 to 45 percent[4,17] of cases and consist of proteinuria, azotemia, and hypertension. The hypertension presents itself in one of two clinical patterns: (1) malignant hypertension of abrupt onset in previously normotensive patients, or (2) moderately elevated blood pressure, which can be intermittent or persistent, with sudden onset of oliguric renal failure. Malignant hypertension is of major clinical

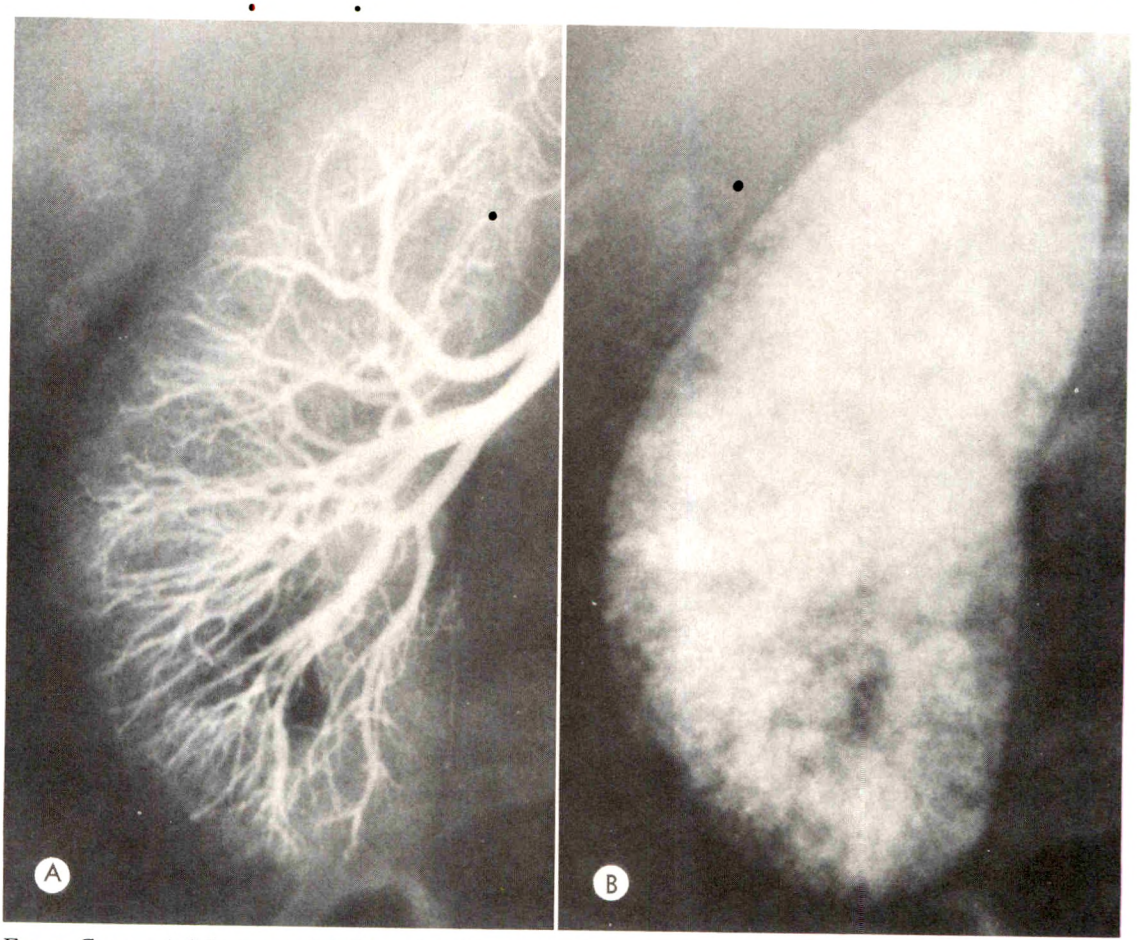


Fig. 2. Case II. (*A*) Late arterial phase showing mildly reduced caliber of intrarenal arteries but with regular tapering. Occasional tortuosities of distal interlobar and arcuate arteries are evident. Note crowding of interlobar arteries in inferior pole, possibly from shrinkage of parenchyma. (*B*) Capillary phase showing nonhomogeneous nephrogram with spotty lucencies of roughly equal size. Loss of corticomedullary junction and reduced density of peripheral cortex are demonstrated.

significance—in the series of Cannon *et al.*,[4] mentioned above, it was associated with an 80 percent mortality.

Our two patients fit the general profile, being in their early 50's with the physical manifestations of scleroderma preceding the onset of their hypertension and renal disease. It is interesting that in one patient (Case II) the skin changes were not appreciated until her hypertension became evident.

PATHOLOGICAL FINDINGS

Kidneys with scleroderma display many of the pathological changes seen in kidneys with advanced malignant hypertension; these changes include fibrinoid changes and arterial hyperplasia of smaller arteries and arterioles with glomerular sclerosis.[1,15,16,18] Some authorities maintain that these two entities cannot be differentiated on a purely histologic basis.[5,9] Recent reports, however, have focused on abnormalities that do appear to distinguish nephrosclerosis from scleroderma.[4,7] Most important is the consistent finding in scleroderma of involvement of interlobular arteries (50–500μ in diameter) with marked proliferation of concentric intimal cells in a mucoid ground substance. The changes in malignant hypertension, on the other hand, are found primarily in smaller arteries (50–150μ in

diameter) and arterioles, and they are not of the same character. Other findings described in scleroderma and not in malignant hypertension are adventitial fibrosis around interlobar, arcuate, and interlobular arteries; specific types of glomerular abnormalities; and a greater degree of cortical ischemia and focal cortical necrosis.[4]

The biopsy specimen obtained in one of our patients (Case 1) showed narrowing of arterioles and marked narrowing of interlobular arteries due to intimal thickening. Ischemic changes were also seen in the glomeruli. These were similar to the changes that have been described in scleroderma, but the pathologist did not distinguish them from those seen in malignant hypertension.

DISCUSSION

Lester and Koehler[11] studied two patients with advanced renal scleroderma who arteriographically manifested irregular arterial narrowing, tortuosity of interlobular arteries, a prolonged arterial phase, and absence of a nephrogram. Cannon *et al.*[4] studied 19 of their 94 patients with renal scleroderma arteriographically and found varying degrees of narrowing within renal arteries of all calibers, blurring or absence of the corticomedullary junction, narrowing and obliteration of interlobular arteries, and delayed transit of contrast medium through the kidney. In addition, they saw nonhomogeneity of the nephrogram, suggesting focal areas of cortical ischemia or necrosis. Our two patients also showed the minor degrees of tortuosity of distal interlobar and arcuate arteries, changes in definition of the corticomedullary junction, slowing of arterial flow, and nonhomogeneity of the nephrogram.

Most remarkable was the spotted nephrogram characterized by focal lucencies scattered throughout the kidneys without evidence of any major arterial changes. A similar nephrogram has been seen by Mena and associates[12] who described a pattern of fine lucencies in the nephrograms of two patients with severe arteriolar nephrosclerosis. The arterial systems in those patients, however, were markedly different from those in our patients and showed the classic changes of severe nephrosclerosis, *i.e.*, prominence and slight ectasia of proximal renal arteries and abrupt pruning of distal interlobar and arcuate vessels. Hollenberg *et al.*[10] reported arteriographic findings in 91 patients with essential hypertension. In the more severely symptomatic patients, they frequently saw patchy, cortical nephrograms with various degrees of loss of the corticomedullary junction. These patients also displayed marked tortuosity of interlobar and arcuate vessels with abrupt pruning and "step ladder" caliber changes. Halpern[8] presented a case of malignant nephrosclerosis with findings on the nephrogram similar to those we found, but the arterial changes were pronounced. We thus find that a spotted nephrogram without major changes in the renal arteries is significant and probably diagnostic of renal scleroderma.

It is likely that hypertension is not the cause of the pathologic and roentgenologic changes seen in the kidneys of our hypertensive scleroderma patients; identical changes have also been found in normotensive scleroderma patients.[4,5,14] The changes, however, tend to be more advanced in the patients with hypertension. In fact both of our patients had been hypertensive for only a short period of time, yet demonstrated marked nephrographic abnormalities. We believe that the pronounced constriction of interlobular arteries produces the focal cortical ischemia and spotty lucencies in the nephrogram in scleroderma and in malignant nephrosclerosis. In scleroderma this constriction is a primary process that subsequently produces the hypertension; in malignant nephrosclerosis, the constriction is a secondary process resulting from prolonged hypertension—a condition that concomitantly produces arteriographically visible proximal arterial ectasia and severe interlobar arterial narrowing.[8] Therefore, it is reasonable that a spotted nephrogram may ap-

pear in scleroderma without major arterial abnormalities, whereas in malignant nephrosclerosis, major arterial changes must be present with the nephrographic changes.

Alphonse J. Palubinskas, M.D.
Department of Radiology, 380-M
University of California School of Medicine
San Francisco, California 94143

REFERENCES

1. Barnett, A. J. Scleroderma (Progressive Systemic Sclerosis). Publication 925 of American Lecture Series. Charles C Thomas, Springfield, Ill., 1974.
2. Biegelman, P. M., Goldner, F., Jr., and Bayles, T. B. Progressive systemic sclerosis (scleroderma). *New England J. Med.*, 1953, *249*, 45–58.
3. Boyd, J. A., Patrick, S. I., and Reeves, R. J. Roentgen changes observed in generalized scleroderma: report of sixty-three cases. *A.M.A. Arch. Int. Med.*, 1954, *94*, 248–258.
4. Cannon, P. J., Hassar, M., Case, D. B., Casarella, W. J., Sommers, S. C., and Leroy, E. C. Relationship of hypertension and renal failure in scleroderma (progressive systemic sclerosis) to structural and functional abnormalities of renal cortical circulation. *Medicine*, 1974, *53*, 1–46.
5. D'Angelo, W. A., Fries, J. F., Masi, A. T., and Schulman, L. E. Pathologic observations in systemic sclerosis (scleroderma): study of fifty-eight autopsy cases and fifty-eight matched controls. *Am. J. Med.*, 1969, *46*, 428–440.
6. Gondos, B. Roentgen manifestations in progressive systemic sclerosis (diffuse scleroderma). Am. J. Roentgenol., Rad. Therapy & Nuclear Med., 1960, *84*, 235–247.
7. Guseva, N. G., Much, E. S., and Sysoev, V. F. Microangiopathy and microcirculatory disorders in progressive systemic sclerosis: Part 1. Methodology in microcirculation. *Bibl. Anat.*, 1973, *11*, 347–351.
8. Halpern, M. Angiography in chronic renal disease and renal failure. *Radiol. Clin. North America*, 1972, *10*, 467–494.
9. Hamburger, J., as cited by Cannon *et al.*[4]
10. Hollenberg, N. K., Epstein, M., Basch, R. I., and Merrill, J. P. "No man's land," of renal vasculature. *Am. J. Med.*, 1969, *47*, 845–859.
11. Lester, P. D., and Koehler, P. R. Renal angiographic changes in scleroderma. *Radiology*, 1971, *99*, 517–521.
12. Mena, E., Bookstein, J. J., and Gikas, P. W. Angiographic diagnosis of renal parenchymal disease. *Radiology*, 1973, *108*, 523–532.
13. Meszaros, W. T. Regional manifestations of scleroderma. *Radiology*, 1958, *70*, 313–325.
14. Progressive systemic sclerosis and pulmonary hypertension. Case records of Massachusetts General Hospital (Case 2-1972). *New England J. Med.*, 1972, *286*, 91–99.
15. Rodnan, G. P. Progressive systemic sclerosis (diffuse scleroderma). Chapter 20. In: Modern Trends in Rheumatology. Edited by A. G. S. Hill. Butterworths, London, 1966.
16. Sommers, S. C. Hypertension and kidney disease. *Prog. Cardiovasc. Dis.*, 1965, *8*, 210–234.
17. Tuffanelli, D. L., and Winkelman, R. K. Systemic scleroderma: clinical study of 727 cases. *A.M.A. Arch. Dermatol.*, 1961, *84*, 359–371.
18. Winkelman, R. K. Classification and pathogenesis of scleroderma. *Mayo Clin. Proc. Staff Meet.*, 1971, *46*, 83–91.

VOL. 126, NO. 4

THE ROLE OF EMERGENCY EXCRETORY UROGRAPHY IN EVALUATION OF BLUNT, ABDOMINAL TRAUMA*

By EUGENE J. McDONALD, JR., M.D., MELVYN KOROBKIN, M.D., RICHARD P. JACOBS, M.D., *and* HIDEYO MINAGI, M.D.
SAN FRANCISCO, CALIFORNIA

ABSTRACT:

In our hospital, patients seen for blunt, abdominal trauma have an "emergency" urogram. The results of our review of 209 such patients with complete urographic evaluations indicate that (1) the clinical examination, urinalysis, and plain abdominal roentgenogram do not reliably allow one to predict which patients would show urographic abnormalities and (2) the clinical management of these patients is rarely altered by the knowledge of the results of the urogram.

THE incidence of blunt trauma to the kidney has increased over the last decade, in large part because of the increasing number of motor vehicle accidents.[1,2] Although it is agreed that prompt recognition and appropriate treatment of the renal injury are of paramount importance, the proper approach to evaluation of such injury is still controversial.[1,5,9,13]

As a result of the rapid rise in the cost of medical care, considerable interest is presently being focused on the efficacy of certain diagnostic roentgenographic examinations. Bell and Loop[2] and Roberts and Shopfner[10] recently published studies indicating that routine skull roentgenograms in the evaluation of head trauma have little or no effect on the course of treatment in the vast majority of patients. In our institution excretory urography is routinely employed in assessing victims of blunt, abdominal trauma. We wanted to determine if the findings on the excretory urogram bear significantly on subsequent choice of treatment.

MATERIAL AND METHOD

We reviewed the medical records and roentgenograms of all patients at our hospital who underwent excretory urography during the course of evaluation of blunt, abdominal trauma from April, 1973, through October, 1974. Excluded from the analysis were those whose need for immediate surgical intervention precluded complete urographic evaluation. Patients included in the study, therefore, were in sufficiently stable clinical condition to permit thorough study by routine excretory urography. This group comprised 209 patients. All plain abdominal roentgenograms and urograms were examined and the findings tabulated.

RESULTS

Table 1 relates the results of excretory urography to those of the urinalyses, clinical examinations, and the findings on the plain abdominal roentgenograms for all 209 patients. Because the presence of hematuria was the primary indication for urography in the overwhelming majority of patients, it is not surprising that all 18 patients with an abnormal urogram had gross or microscopic hematuria—indeed, 177 out of the 191 patients with normal urographic findings also had hematuria. Pain in the abdomen and the costovertebral angle was more frequently associated (89 percent) with urographic abnormalities, but this was of no predictive value because such pain occurred commonly (39 percent) when

* From the Departments of Radiology, San Francisco General Hospital and University of California School of Medicine, San Francisco, California.

TABLE I

UROGRAPHIC RESULTS *versus* URINALYSIS, CLINICAL EXAMINATION, AND PLAIN ABDOMINAL ROENTGENOGRAM

	Normal Urogram	Abnormal Urogram
Urinalysis		
normal	14 (7.3%)	0 (0%)
abnormal	177 (92.7%)	18 (100%)
microscopic hematuria	157 (82.2%)	12 (66.7%)
gross hematuria	20 (10.5%)	6 (33.3%)
Total	191	18
Clinical examination		
normal	114 (59.7%)	6 (33.3%)
abnormal	77 (40.3%)	12 (66.7%)
abdominal pain	54 (28.3%)	12 (66.7%)
costovertebral angle pain	21 (11.0%)	4 (22.2%)
hypotension	11 (5.8%)	2 (11.2%)
Total	191	18
Findings on plain film of abdomen		
normal	113 (59.2%)	12 (66.7%)
abnormal	78 (40.8%)	6 (33.3%)
bone fracture	68 (35.6%)	5 (27.8%)
ileus	25 (13.1%)	2 (5.6%)
soft tissue mass	1 (0.5%)	1 (5.6%)
Total	191	18

no urographic abnormalities were seen. Plain roentgenograms of the abdomen also failed to predict which patients would have abnormal urograms: 78 of the 84 patients with abnormal plain roentgenograms showed normal urographic findings and 12 of the 125 patients with normal plain roentgenograms showed abnormal urographic findings.

Table II gives the specific findings in the 18 patients exhibiting urographic abnormalities. The most frequent observed urographic abnormality was that of diminished volume of contrast material excreted from the kidney suspected of injury (Fig. 1, *A* and *B*). This finding in the absence of other urographic abnormalities is considered to indicate renal contusion.

TABLE II

UROGRAPHIC FINDINGS IN THE 18 PATIENTS WITH AN ABNORMAL EXCRETORY UROGRAM

Finding	Occurrence
Renal or ureteral displacement	5
Decreased volume	11
Clots	6
Extravasation	4

Management of the patients with urographic abnormalities is shown in Table III. Half of the patients were treated conservatively (Fig. 2, *A* and *B*). Eight of the other nine patients underwent laparotomy solely to exclude intraperitoneal damage. Exclusion of intraperitoneal damage and evaluation of renal injury were the reasons for laparotomy in the remaining patient.

The results of laparotomy are shown in Table IV. All nine patients had a retroperitoneal hematoma. A nephrectomy was necessary in the one patient in whom the hematoma was surgically explored. Two patients continued to have gross hematuria for three to five days and therefore had repeat urography. Because of the hematuria and because repeat urograms indicated a fractured kidney, both patients underwent retroperitoneal exploration. One required nephrectomy, the other recovered

uneventfully after drains were placed in the retroperitoneum. Because these were delayed complications they are not discussed further; we are confining our study to the contribution of the emergency, initial urogram.

DISCUSSION

There has been a distinct trend around the world toward a conservative approach to the management of traumatic renal injuries.[4,6–8,12] The vast majority of patients with renal trauma recover without the necessity of renal surgery and without serious sequelae. Indeed, in the clinically stable patient the only urographic abnormalities that would require prompt surgical management are disruptions of the renal pedicle or ureter.[3,7,9,11] Neither of these injuries was found to occur in our large series.

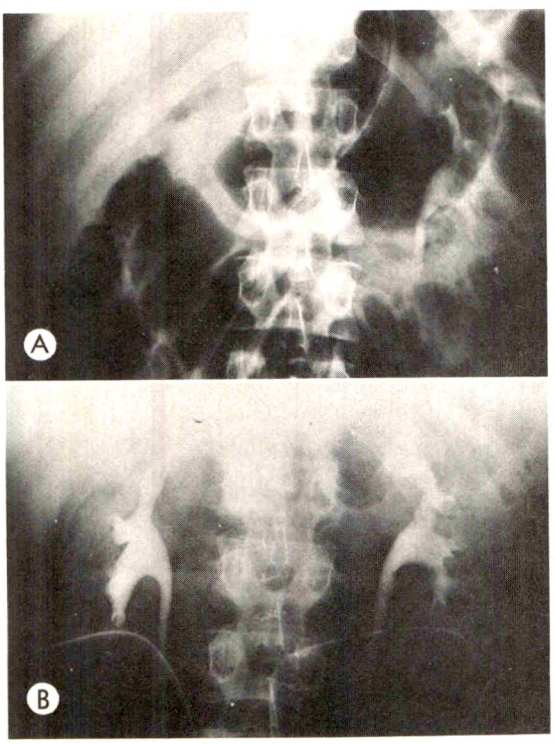


Fig. 1. (*A*) Two hours after blunt trauma to the right abdomen, excretory urogram shows severely decreased excretion of contrast material on the right, the most common urographic abnormality associated with such trauma. (*B*) Repeat urogram two weeks later demonstrates normal, symmetric excretion of contrast material by the kidneys. Outline of compression device can be seen.

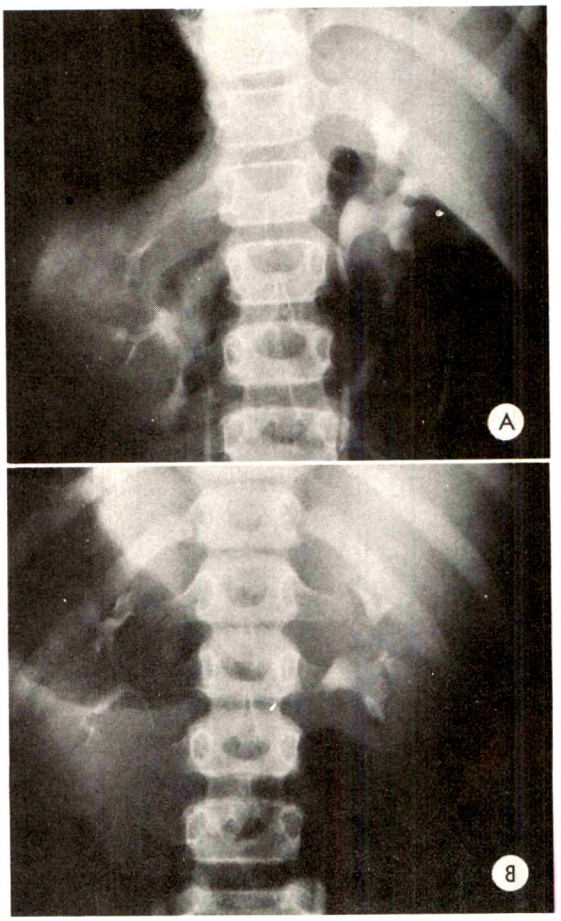


Fig. 2. (*A*) Soon after a fall, this child was found to have a fracture of the left kidney, with extravasation of contrast material seen on the excretory urogram. The renal injury was treated conservatively. (*B*) Two weeks after trauma, the urogram shows no abnormalities.

We found that abnormalities shown by the emergency urogram had remarkably little influence on patient management. Only nine of the 18 patients with an abnormal

Table III

MANAGEMENT OF THE 18 PATIENTS WITH UROGRAPHIC ABNORMALITIES

Conservative	9	
Laparotomy	9	
to exclude intraperitoneal damage		8
to exclude intraperitoneal damage and evaluate fractured kidney		1

TABLE IV

RESULTS OF LAPAROTOMY IN NINE PATIENTS

Liver laceration and retroperitoneal hematoma	2
Liver laceration, retroperitoneal hematoma, and nephrectomy	1
Retroperitoneal hematoma only	6

urogram underwent subsequent surgery, and in eight of these nine the reason for the laparotomy was only to exclude the damage to an intraperitoneal viscus—not to evaluate the urographically identified abnormal kidney. In the remaining patient the reason for laparotomy was to evaluate both the damaged kidney and a suspected intraperitoneal injury. Therefore, the result of excretory urography directly influenced emergency management of only one (5.5 percent) of the 18 patients with urographic abnormalities, in other words, only one (0.5 percent) of the 209 patients in our study. We conclude that an emergency urogram is unnecessary in a clinically stable patient with blunt, abdominal trauma.

We cannot, however, argue against excretory urography for patients requiring laparotomy. The main purpose of such preoperative urograms would be to determine the presence and status of the kidneys.[13]

Eugene J. McDonald, Jr., M.D.
Department of Radiology, M-380
University of California
San Francisco, California 94143

REFERENCES

1. Banowski, L. H., Wolfel, D. A., and Lackner, L. H. Considerations in diagnosis and management of renal trauma. *J. Trauma*, 1970, *10*, 587–597.
2. Bell, R. S., and Loop, J. W. Utility and futility of radiographic skull examination for trauma. *New England J. Med.*, 1971, *284*, 236–239.
3. Carlton, C. E., Jr., Scott, R., Jr., and Goldman, M. Management of penetrating injuries of kidney. *J. Trauma*, 1968, *8*, 1071–1083.
4. Cass, A. S., and Ireland, G. W. Comparison of conservative and surgical management of more severe degrees of renal trauma in multiple injured patients. *J. Urol.*, 1973, *109*, 8–10.
5. Elkin, M., Ming, C-H, and de Paredes, R. G. Roentgenologic evaluation of renal trauma with emphasis on renal angiography. Am. J. Roentgenol., Rad. Therapy & Nuclear Med., 1966, *98*, 1–26.
6. Glenn, J. F., and Harvard, B. M. Injured kidney. *J.A.M.A.*, 1960, *173*, 1189–1195.
7. Hessel, S. J., and Smith, E. G. Renal trauma: comprehensive review and radiologic assessment. *CRC Crit. Rev. Clin. Radiol. & Nuclear Med.*, 1974, *5*, 251–293.
8. Javadpour, N., Guinan, P., and Bush, I. M. Renal trauma in children. *Surg., Gynec. & Obst.*, 1973, *136*, 237–240.
9. Nation, E. F., and Massey, B. D. Renal trauma: experience with 258 cases. *J. Urol.*, 1963, *89*, 775–778.
10. Roberts, F., and Shopfner, C. E. Plain skull roentgenograms in children with head trauma. Am. J. Roentgenol., Rad. Therapy & Nuclear Med., 1971, *284*, 230–239.
11. Salvatierra, O. Management of urologic injuries (trauma rounds). *West. J. Med.*, 1975, *122*, 257–261.
12. Scott, R., Jr., Carlton, C. E., Ashmore, A. J., and Duke, H. H. Initial management of nonpenetrating renal injuries: clinical review of 111 cases. *J. Urol.*, 1963, *90*, 535–539.
13. Solheim, K., Resch, F., and Kordt, K. F. Closed renal injuries. *Injury*, 1972, *3*, 185–195.

Vol. 126, No. 4

ARTHROGRAPHY IN TOTAL HIP PROSTHESIS COMPLICATIONS*

By MARTIN I. GELMAN, M.D.
SALT LAKE CITY, UTAH

ABSTRACT:

Previous reports have stressed the value of hip arthrography primarily in determining the presence of loosening of the total hip prosthesis. Although loosening is a common complication and frequently associated with infection, other complications producing a painful hip prosthesis exist and are demonstrable by arthrography. Since the etiologies of these are as diversely different as the treatment, the hip arthrogram is advocated as an integral part of the diagnostic approach to the patient with a painful hip prosthesis in order to assess the specific complication and determine the therapeutic approach.

ARTHROGRAPHY for evaluation of total hip replacement complications was introduced in 1971 by Salvati *et al.*,[5] and in 1973, Anderson and Staple[1] described total hip replacement arthrography using subtraction technique. These authors stressed the usefulness of this procedure mainly in determining loosening of the prosthesis. Since 1972 we have utilized subtraction hip arthrography in evaluation of the painful hip prosthesis and have been impressed not only with its value in determining the presence of loosening but also in assessing the other possible complications that may occur, such as soft tissue abscesses and fistulous tracts, irreducible or persistent dislocation, trochanteric bursitis, and fractures.

The purpose of this report is to amplify the usefulness of hip arthrography including subtraction technique in evaluation of the painful hip prosthesis, present the complications that may be demonstrated, and illustrate its value as a preoperative diagnostic examination.

TECHNIQUE OF ARTHROGRAPHY

The technique used is basically that of Salvati *et al.*[5] with a few modifications. An anteroposterior roentgenogram of the hip is obtained with the foot internally rotated as well as a frog-leg lateral. Using fluoroscopic image amplification, a metallic marker is placed on the skin over the mid point of the neck of the femoral component. This point is marked on the skin with indelible ink and the metallic marker removed. The inguinal ligament as well as the femoral artery should be palpated to make sure the mark is below the ligament and lateral to the artery. The skin is cleansed with Betadine, draped and locally infiltrated with one percent Xylocaine in the area of the ink mark. A No. 20 gauge disposable spinal needle is directed straight down to the metal prosthesis under fluoroscopic guidance. Metal-to-metal contact will be felt when the needle point encounters the femoral prosthesis. Having the patient roll into an oblique position will allow observation of the needle point. If fluid is present, as much of it as possible is aspirated. If no fluid can be aspirated, normal saline (without bacteriostatic agent) is injected and aspirated and sent to the laboratory for smear, culture, and sensitivity of aerobic as well as anaerobic organisms. A few drops of Renografin-60 or 76 are then injected and if these flow away from the needle point, the needle is properly positioned. The patient may have to roll into an oblique position in order to observe the contrast material separated from the prosthesis. If the contrast material

* From the Department of Radiology, University of Utah Medical Center, Salt Lake City, Utah.

pools around the needle point, the needle must be repositioned. When the needle is properly positioned the lower leg and foot are immobilized with sandbags and a head clamp. An anteroposterior roentgenogram is then made with the needle in place. Under fluoroscopic guidance, contrast material is injected through a connector tube until the capsular space is well filled or the patient complains of a pressure sensation, using approximately 15 to 20 ccs of contrast material or more. A second anteroposterior roentgenogram is then made, making certain the hip remains immobile, and these two films are used for the subtraction study. The large volume of contrast material provides adequate filling of the capsular space and insures seepage of contrast material between the methacrylate and bone or between the prosthesis and bone due to the increased pressure, since the subtraction study precludes exercise of the hip before the first two roentgenograms are obtained. The needle is then removed and the hip is passively or actively exercised. Anteroposterior views with and without traction are obtained as well as a frog-leg lateral.

THE NORMAL ARTHROGRAM

In the normal arthrogram, contrast medium remains confined by a thick pseudocapsule which usually forms within four to five months following surgery. This pseudocapsule creates a space limited by the rim of the acetabular cup and the base of the neck of the femoral component. Contrast material should not be observed beyond this space.[5]

Case I. A 54 year old man had a left total hip replacement for post-traumatic degenerative arthritis. Since the operation he complained of left hip pain and limitation of motion. The pain was primarily superficial and about the incision. Physical examination showed marked tenderness over the left hip incision with some pain on internal rotation and flexion and a slight degree of limitation of motion. Arthrography demonstrated no evidence of loosening of the prosthesis and both antegrade and retrograde filling of the regional lymphatics occurred (Fig. 1, *A* and *B*). The hip pain was determined to be cutaneous in origin and not related to the hip prosthesis.

Comment. Several hip arthrograms have demonstrated antegrade and retrograde lymphatic filling. This has occurred in the absence of demonstrable infection in an otherwise normal hip prosthesis and is probably related to a combination of increased pressure during injection as well as alteration of the lymphatic bed by previous operation.

THE ABNORMAL ARTHROGRAM

The abnormal arthrogram demonstrates contrast medium beyond the pseudocapsular space. Seepage of contrast material between the methyl methacrylate and bone, whether in the acetabular or femoral components, indicates loosening.

Case II. A 62 year old male had a left total hip prosthesis implanted for degenerative arthritis with subsequent postoperative hip infection which cleared with antibiotics and suction drainage. He remained asymptomatic for approximately one year after which he developed pain. An arthrogram demonstrated loosening of the acetabular and femoral components with a fistulous tract adjacent to the acetabular component (Fig. 2, *A–C*). *Staphylococcus aureus* was cultured from the hip aspirate and the components were removed to accomplish a Girdlestone procedure.

Comment. Loosening may be due to mechanical failure or infection. If the lucent zone which frequently normally develops adjacent to the acetabular and femoral components increases to a width greater than 2 mm after the sixth postoperative month, infection must be strongly considered.[2] Arthrography, however, will establish this diagnosis considerably earlier. In addition, subtraction films should be an integral part of the examination since they frequently demonstrate findings not readily appreciated on the routine arthrogram as illustrated by this case.

Case III. A 50 year old man had a right total hip replacement approximately one year previ-

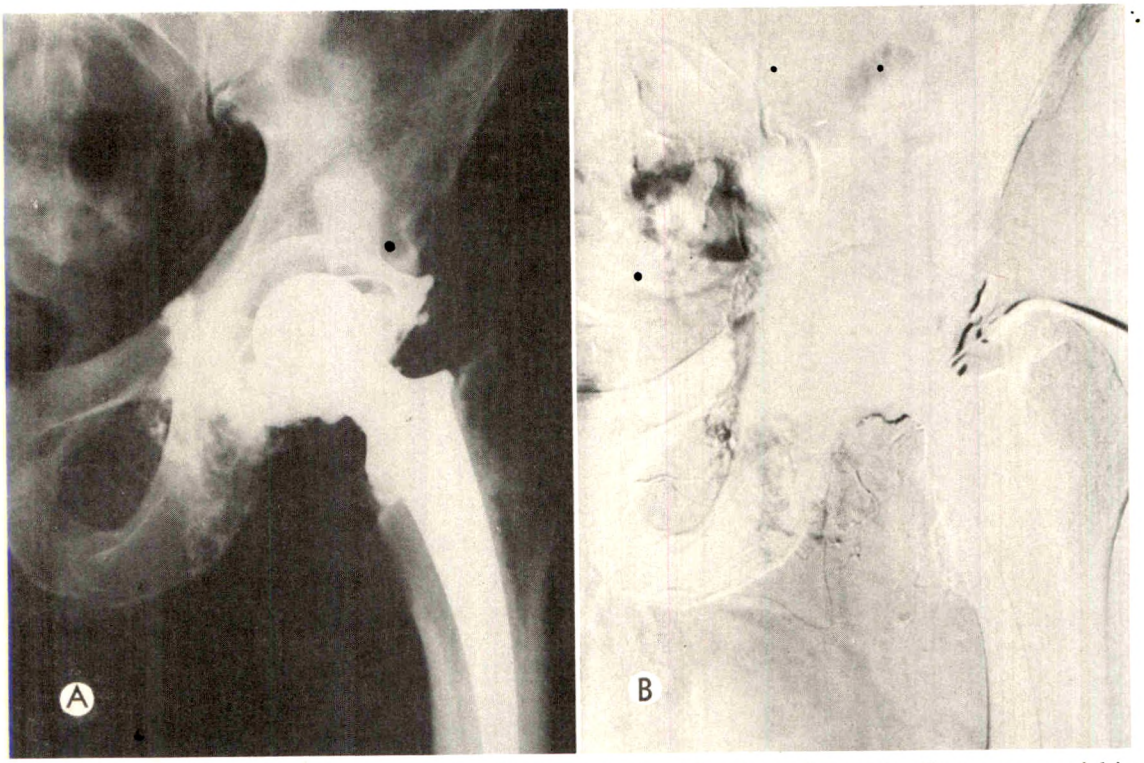


FIG. 1. (*A* and *B*) Normal arthrogram of total hip prosthesis with subtraction study. Contrast material is confined to pseudocapsular space. Filling of lymphatic system is most likely related to increased pressure during injection as well as alteration of lymphatic bed from previous surgery.

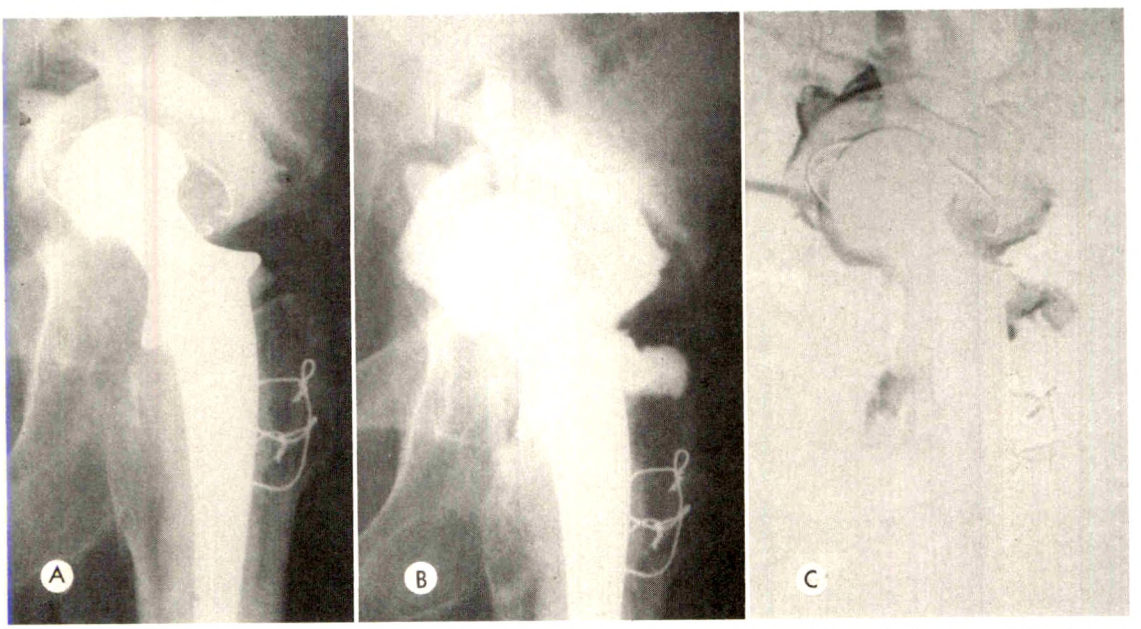


FIG. 2. (*A*) Routine anteroposterior view of the left hip shows a malpositioned acetabular cup with a lucent zone between the methyl methacrylate and bone. (*B*) Arthrogram demonstrates fistulous tract extending from acetabular component into pelvis in addition to loosening of femoral component. (*C*) Subtraction study yields additional information by delineating the acetabular component loosening at methacrylate-bone interface, which was obscured by barium impregnated methyl methacrylate, as well as by showing the femoral component loosening.

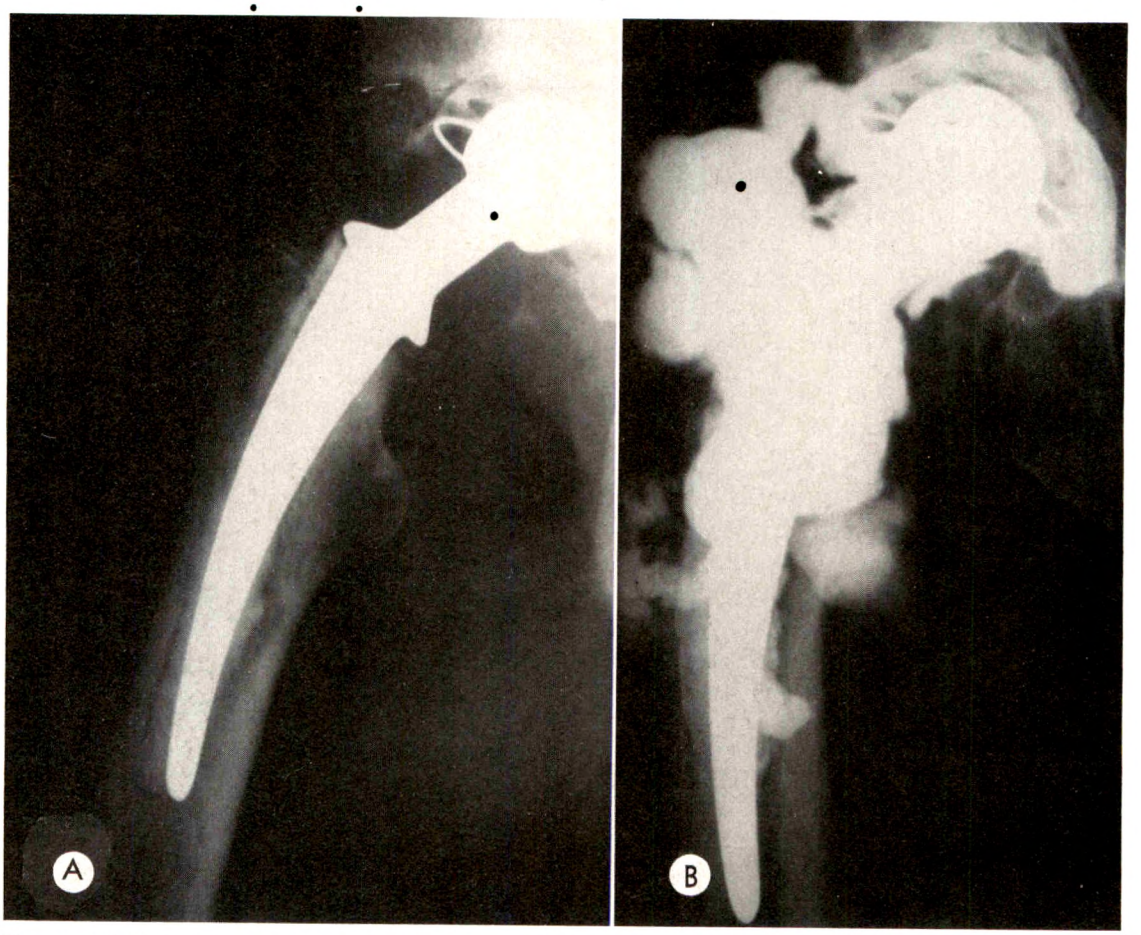


Fig. 3. (*A*) Lucent zones are noted adjacent to the acetabular and femoral components. (*B*) Arthrogram demonstrates contrast material filling the lucent zones indicating loosening as well as fistulous tracts between the bone and soft tissue.

ously. This was complicated by persistent pain and postoperative drainage despite reoperation and irrigation. An arthrogram was done and demonstrated loosening of the acetabular and femoral components as well as fistulous communications with the bone and adjacent soft tissues (Fig. 3, *A* and *B*). At surgery both prosthetic components were loose and pockets of pus were found along the anterior portion of the femoral shaft extending into the thigh. Cultures grew out *Staphylococcus aureus*. The components were removed and suction irrigation continued until negative cultures were obtained (approximately 10th postoperative day). Drainage stopped approximately three weeks after the operation at which time nonweight-bearing ambulation was begun.

Comment. Abscess cavities or fistulous tracts may occur with infection. Their demonstration by arthrography is of considerable importance in allowing the orthopedic surgeon to plan the extent of operative exposure as well as provide adequate drainage.

Case iv. A 70 year old female with rheumatoid arthritis treated with cortisone for several years, had a right total hip replacement. Her postoperative course was complicated by anemia requiring multiple blood transfusions. While ambulating during physical therapy she avulsed her right greater trochanter and this was followed by massive hemorrhage into the thigh and a right sciatic palsy. Diffuse bleeding also occurred and was attributed to heparin with which the patient was being treated for cerebral thrombosis. Multiple attempts to relocate the hip were made but were unsuccessful. Roentgenograms revealed dislocation of the

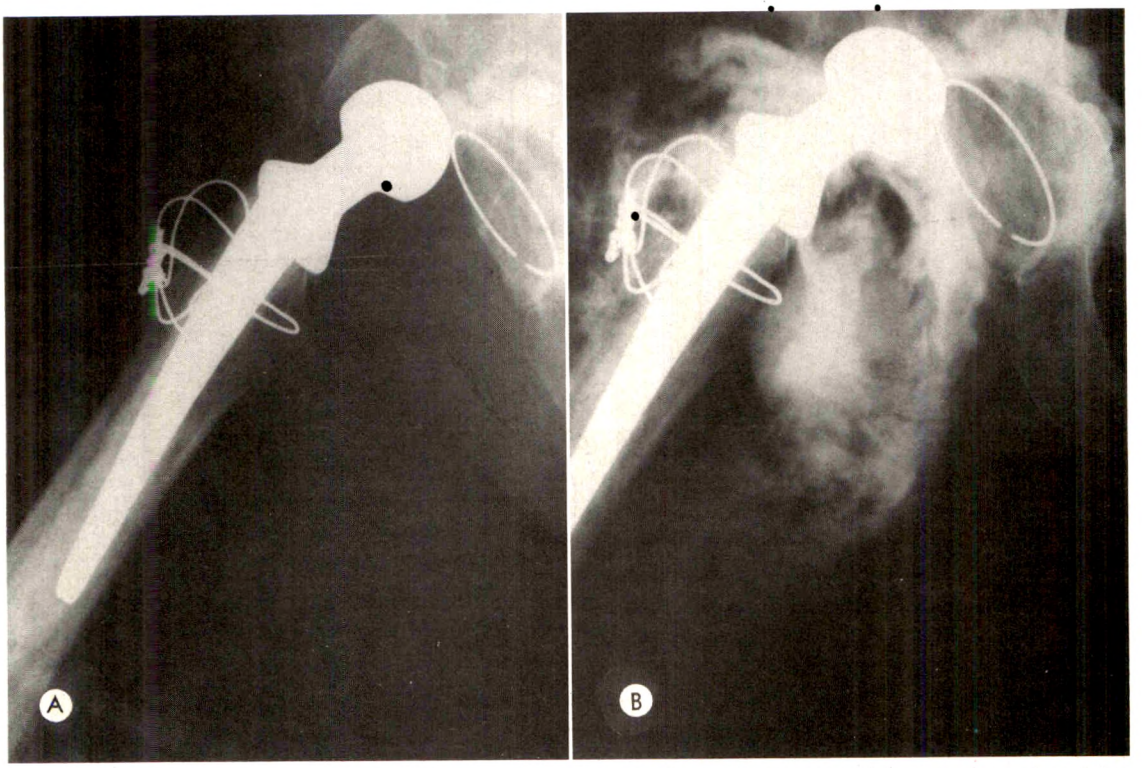


Fig. 4. (*A*) The femoral component is dislocated superiorly and laterally and there is a comminuted avulsion fracture of the greater trochanter. (*B*) Arthrogram demonstrates large cystic appearing collection of contrast material communicating with the pseudocapsular space, with mottled appearance and filling defects. At surgery this represented a large hematoma with clotted blood.

femoral component and a comminuted avulsion fracture of the greater trochanter (Fig. 4*A*). A hip arthrogram was performed demonstrating no loosening. Fifteen hundred ccs of thick, dark blood were aspirated and a large cavity communicating with the joint space was demonstrated containing irregular and mottled filling defects representing clotted blood (Fig. 4*B*). An exploration of the right hip revealed a very large hematoma with fibrin clots which had completely encompassed the sciatic nerve and compressed it. The abductor muscles were markedly necrotic precluding reattachment to the greater trochanter. The hematoma and fibrin were evacuated and the dense fibrin sheath incised and dissected away from the sciatic nerve. The greater trochanter was reapproximated to the femoral shaft and secured. There was no evidence of loosening or infection. Relocation of the femoral component within the acetabular cup was achieved once the hematoma was evacuated.

Comment. Arthrography may be helpful in evaluating persistent dislocation in the presence of well positioned acetabular and femoral components. Dislocation may be early or late. If early, it is usually associated with postoperative hematoma, lack of pseudocapsule formation, or both; whereas late dislocation is more frequently associated with a malpositioned acetabular component or instability created by a fracture through the greater trochanter.[3,4] Hematoma, whether postoperative or posttraumatic may dissect into the adjacent soft tissues and maintain communication with the neocapsular space causing increased intracapsular pressure and persistent dislocation. The cause is probably related to lack of formation of a pseudocapsule allowing direct communication of the joint space with the hematoma. Surgical evacuation and drainage allow the femoral head to return to the acetabular cup with restoration of stability to the joint.

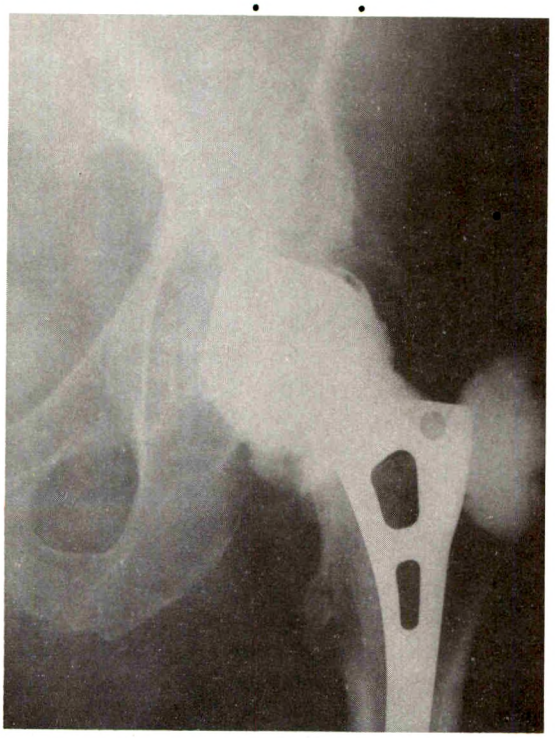


Fig. 5. Arthrogram demonstrates no loosening but filling of the bursa over the greater trochanter.

Postoperative drains will help reduce hematoma formation in the uncomplicated total hip replacement thereby reducing the incidence of dislocation in the immediate postoperative period.

Case v. A 62 year old male had bilateral Ring hip prostheses implanted three years ago on the right and two years ago on the left for degenerative arthritis. He developed an aching pain over the lateral aspect of the left hip which became progressively worse. The clinical impression was a failing left hip prosthesis and a total hip replacement was anticipated. An arthrogram was performed and 3 ccs of cloudy yellow fluid aspirated which on culture yielded no growth. No loosening was demonstrated; however, there was filling of the bursa over the greater trochanter suggesting a trochanteric bursitis (Fig. 5). Symptomatic treatment plus physical therapy resulted in marked diminution of symptoms and the patient eventually became asymptomatic.

Comment. This case effectively illustrates the value of hip arthrography in determining the necessity for surgery. The clinician thought the patient had a loosened prosthesis and ordered the arthrogram as a preoperative examination; however, pain in the patient with a total hip prosthesis does not always mean loosening. A more conservative approach was indicated by the results of the arthrogram which allowed appropriate therapy to be instituted.

Case vi. A 50 year old male was seen in the Orthopedic Clinic for evaluation of pain in the left hip. He had had a total hip prosthesis implanted approximately three years previously for degenerative arthritis. Routine roentgenograms showed an ununited fracture of the greater trochanter with breaks in the stabilization wires (Fig. 6*A*). An arthrogram was performed and demonstrated extravasation of contrast material into the fracture site as well as medially along the flange of the base of the neck of the femoral component (Fig. 6, *B* and *C*). Operative restabilization of the greater trochanter was carried out and the patient recovered without incident.

Comment. Routine roentgenograms effectively demonstrated the fracture of the greater trochanter and stabilization wires as well as heterotopic bone formation. Although there was no evidence of bony union at the fracture site, fibrous union could not be excluded. The arthrogram demonstrated contrast material in the fracture site indicating nonunion and also eliminated loosening of the prosthesis as a diagnostic possibility. These findings allowed the orthopedic surgeon to limit his surgical approach to restabilization of the greater trochanter with subsequent recovery of the patient.

The significance of contrast medium between the flange of the base of the neck of the femoral component and the adjacent bone is not known at this time. It may be related to resorption of bone at sites of greater stress; however, if not associated with evidence of loosening more inferiorly, we currently regard it as a finding of doubtful clinical significance.

Discussion

The patient with a painful total hip pros-

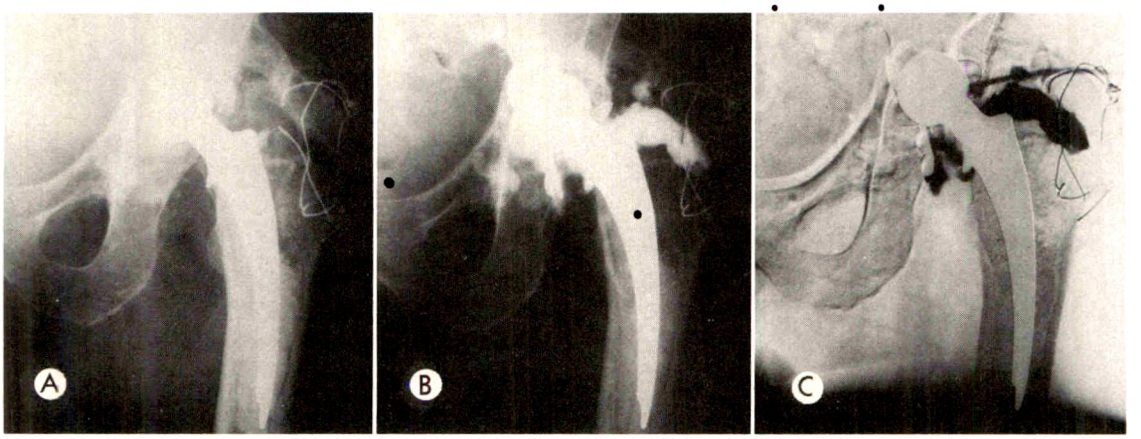


Fig. 6. (*A*) There is a fracture through the greater trochanter without evidence of bony union as well as fractures through the stabilization wires. Heterotopic bone formation is also present. (*B* and *C*) Arthrogram with subtraction technique demonstrates contrast material in the fracture site indicating nonunion rather than fibrous union. Contrast material is noted between flange at base of neck and bone.

thesis presents a diagnostic dilemma to the orthopedic surgeon and radiologist. Routine roentgenograms frequently show a lucent zone between the methyl methacrylate surrounding the acetabular component and the bony acetabulum which may be normal. Interval roentgenograms may show progressive widening of this lucent zone confirming the suspected loosening; however, in a patient with pain, it is highly desirable to determine the etiology as soon as possible. Since this lucent zone may not widen even in the presence of loosening, rather than temporizing with interval roentgenograms, arthrography is advocated to establish a definitive diagnosis.

Analysis of fluid aspirated at the time of arthrography is very helpful in determining loosening secondary to infection. The absence of purulent fluid does not exclude infection as the cause and sterile saline (without bacteriostatic agent) aspirations of the pseudocapsular space should be obtained for aerobic and anaerobic cultures.

When infection is the cause of loosening, abscess formation and fistulous tracts may be present, communicating with the pseudocapsular space. Their demonstration by arthrography is important since adequate surgical drainage must be instituted for recovery to occur.

Dislocation most frequently occurs secondary to a malpositioned prosthesis or to an avulsion fracture of the greater trochanter and its stabilization wires which results in increased instability. In the early postoperative period the hip prosthesis may dislocate because of lack of a pseudocapsule since complete formation of the pseudocapsule requires approximately five months. Failure to reduce a dislocated hip prosthesis indicates increased intra-articular pressure which may be secondary to a collection of blood. Arthrography may assess the integrity of the pseudocapsule, demonstrate a hematoma communicating with the pseudocapsular space as well as the filling defects representing clotted blood, and furnish fluid from the pseudocapsular space for analysis.

Although pain in a patient with a total hip prosthesis frequently indicates loosening, we have observed several cases where the arthrogram has implicated other causes, necessitating a different type of treatment. Filling of the trochanteric bursa indicates a trochanteric bursitis which is a nonsurgical cause for hip pain in a patient with a total hip prosthesis. Symptomatic treatment as well as physical therapy usually results in full recovery. Fractures through the greater trochanter may be ununited or

fibrous union may be present. If contrast material is observed in the fracture site on arthrography, nonunion is demonstrated and motion at the fracture site may be the cause of the patient's pain. Reapproximation of the fracture fragment and stabilization wires will promote bony union.

Department of Radiology
University of Utah Medical Center
50 North Medical Drive
Salt Lake City, Utah 84112

The author expresses his appreciation to Dr. David G. Bragg for his review of the manuscript and to Mrs. LeVern Jarrad for her patience and help in the preparation of the manuscript.

REFERENCES

1. Anderson, L., and Staple, T. Arthrography of total hip replacement using subtraction technique. *Radiology*, 1973, *109*, 470–474.
2. Bergstrom, B., Lidgren, L., and Lindberg, L. Radiographic abnormalities caused by postoperative infection following total hip arthroplasty. *Clin. Orthopedics*.. 1974, *99*, 95–102.
3. Dolinskas, C., Campbell, R. E., and Rothman, R. H. Painful Charnley total hip replacement. Am. J. Roentgenol., Rad. Therapy & Nuclear Med., 1974, *121*, 61–68.
4. Mullins, M. F., Sutton, R. N., and Lodwick, G. S. Complications of total hip replacement: roentgen evaluation. Am. J. Roentgenol., Rad. Therapy & Nuclear Med., 1974, *121*, 55–60.
5. Salvati, E., Freiberger, R., and Wilson, P. Arthrography for complications of total hip replacement. *J. Bone & Joint Surg.*, 1971, *53*-A, 701–709.

VOL. 126, NO. 4

THE GROOVES OF THE DISTAL ARTICULAR SURFACE OF THE FEMUR—A NORMAL VARIANT*

By R. BRENT HARRISON, M.D.,† MARY BETH WOOD, M.D.,‡
and THEODORE E. KEATS, M.D.§
• CHARLOTTESVILLE, VIRGINIA

THE distal articular surface of the femur articulates with the patella anteriorly and with the tibia posteriorly and inferiorly. These anterior and inferior articulations are separated by shallow grooves (Fig. 1; and 2). The groove in the lateral condyle is usually better defined and extends laterally and forward from the front part of the intercondyloid fossa and expands to form a triangular depression.[1] The anterior part of the lateral meniscus rests in this depression when the knee is extended. The groove of the medial condyle is present only on the medial aspect of the condyle and receives the anterior portion of the medial meniscus when the knee is fully extended.

These grooves are frequently seen on the axial projection (sunrise) and lateral views and may simulate compression fractures (Fig. 3) or osteochondritis dissecans (Fig. 4; and 5).

Keats[2] recognized these irregular areas as normal variants and termed them a "transition zone" (Fig. 6). The appearance of the groove on the axial projection (sunrise) view obviously depends on the depth of the groove and also on the angle of the x-ray beam (Fig. 2).

As with all normal variants, the significance lies in knowing these grooves exist and recognizing their variable appearance

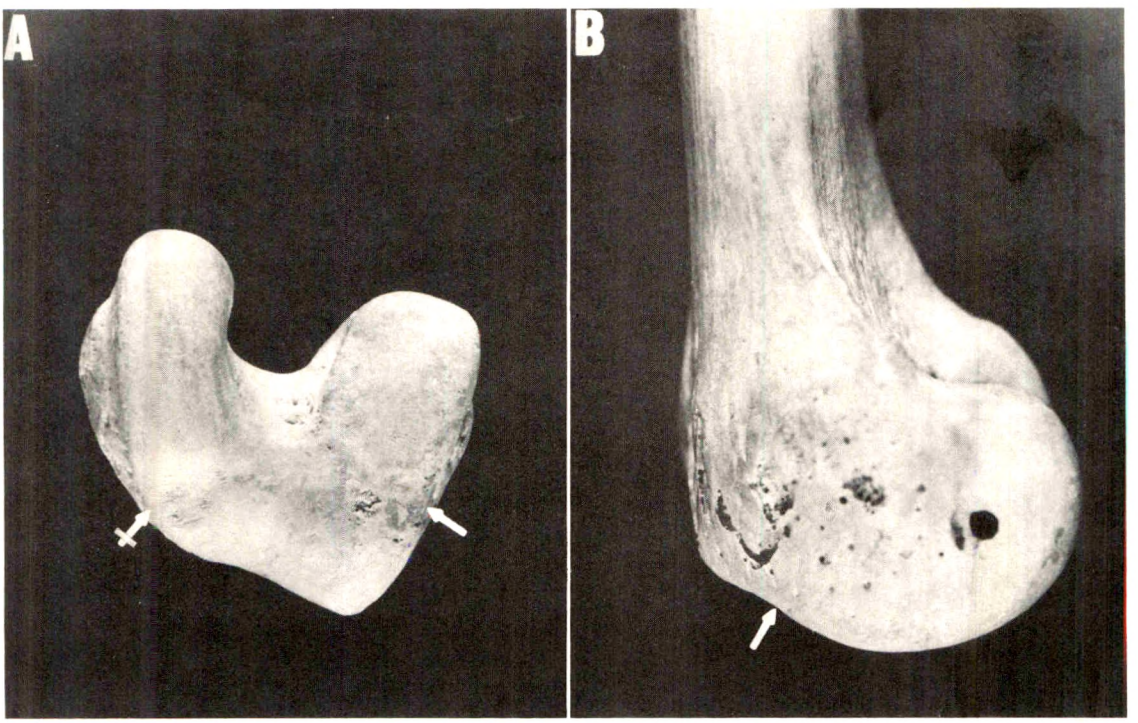


FIG. 1. Photographs of femur demonstrate grooves in the lateral (↔) and medial (→) condyles.

* From the Department of Radiology, University of Virginia Medical Center, Charlottesville, Virginia.
† Assistant Professor. ‡Resident. §Professor and Chairman.

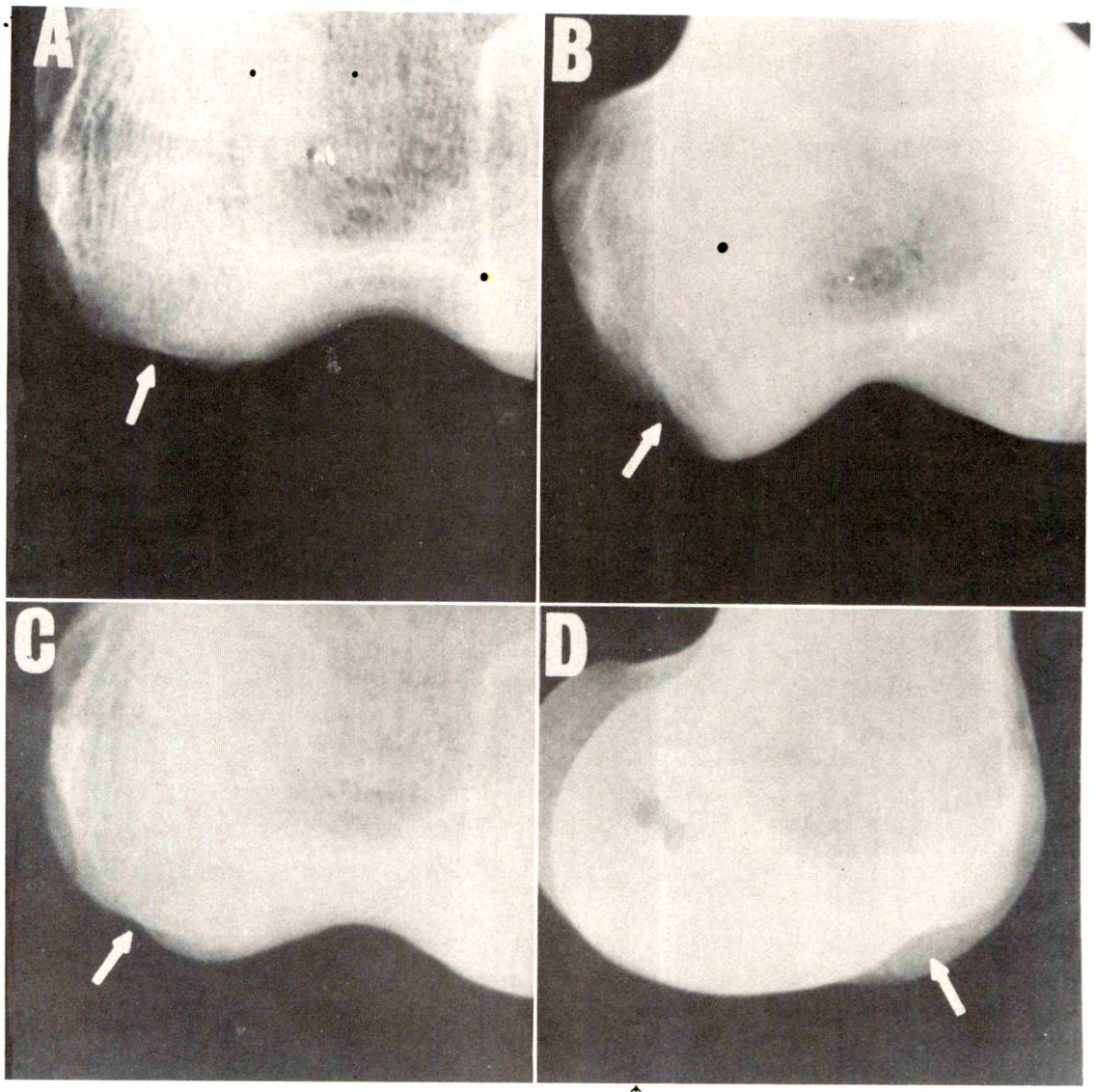


FIG. 2. Spot film roentgenograms of specimen femur show change in appearance of groove in medial condyle with change in the angle of the roentgen-ray beam.

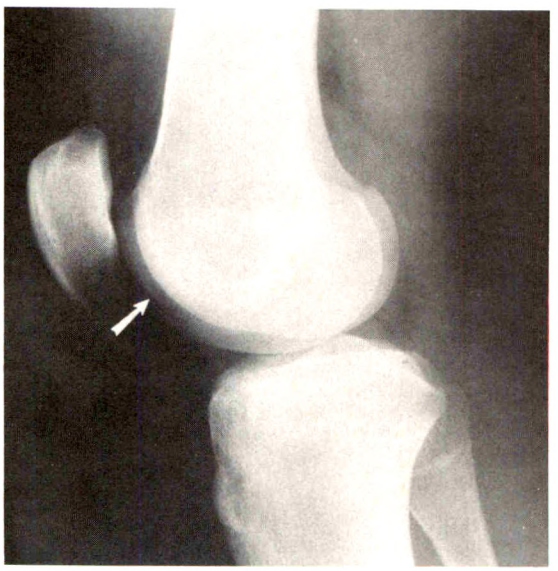


FIG. 3. Groove in the medial condyle mimics compression fracture in the lateral view.

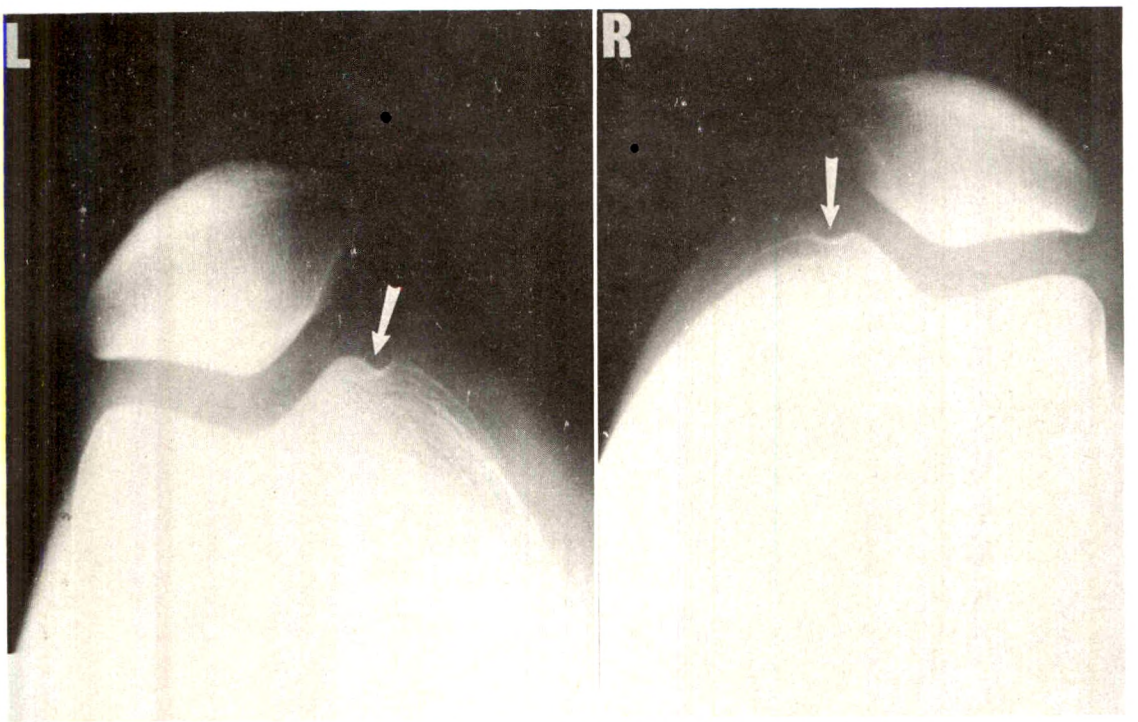


Fig. 4. Deep grooves in both medial condyles simulate osteochondritis dissecans in the axial projection (sunrise) view.

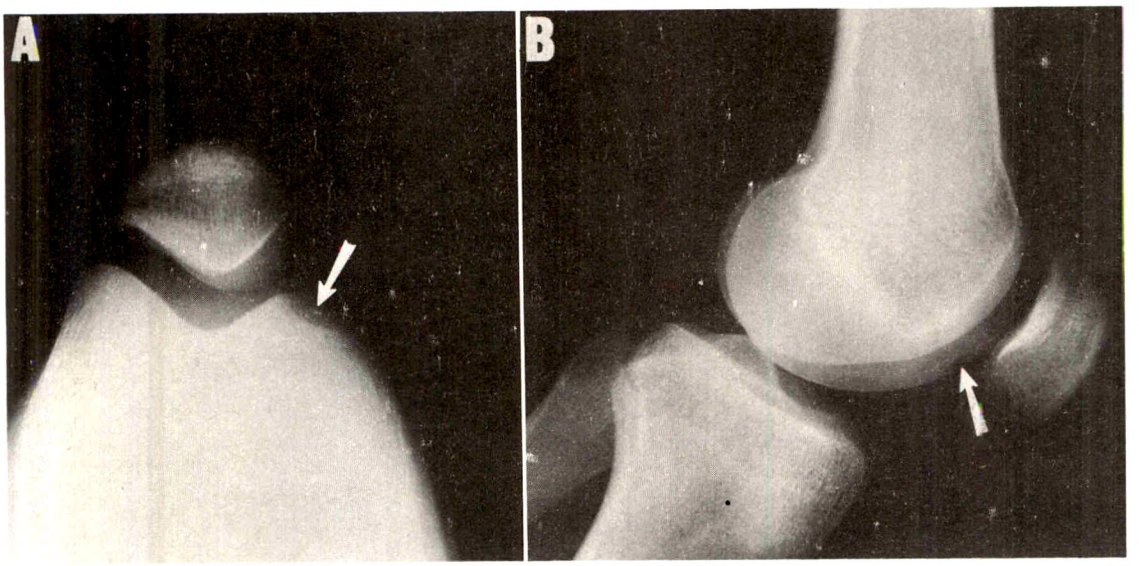


Fig. 5. Groove in medial condyle simulates osteochondritis dissecans in the lateral view.

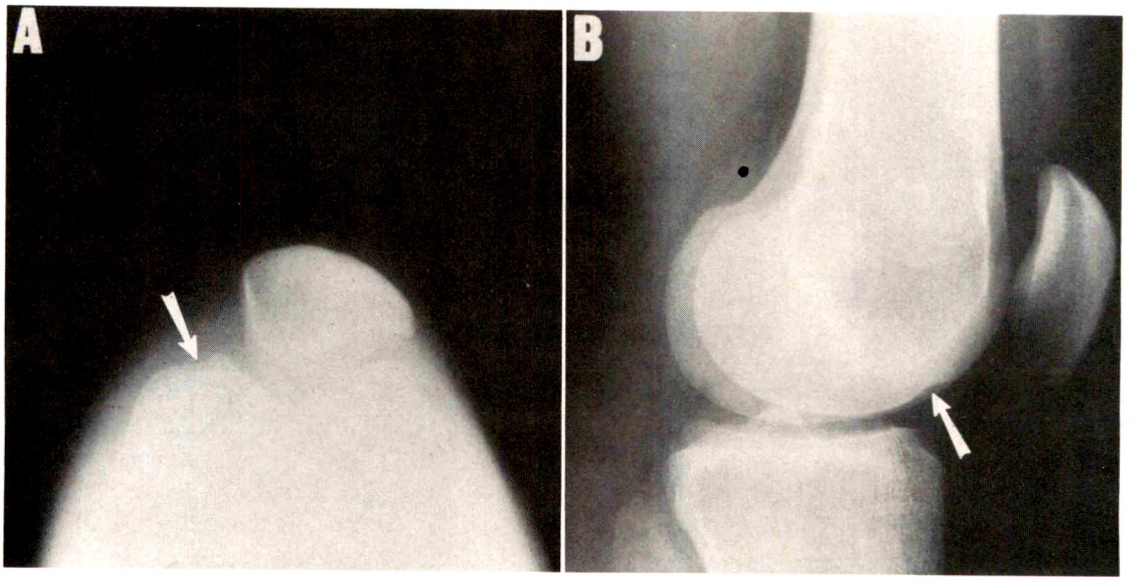


Fig. 6. Groove in the medial condyle appears as shallow depression or "transition zone" as described by Keats.[2]

on the roentgenogram to obviate their misinterpretation as a pathologic process.

R. Brent Harrison, M.D.
Department of Radiology
University of Virginia Medical Center
Charlottesville, Virginia 22901

REFERENCES

1. Gray's Anatomy of the Human Body. 28th edition. Edited by C. M. Goss. Lea & Febiger, Philadelphia, 1966.
2. Keats, T. E. An Atlas of Normal Roentgen Variants. Year Book Medical Publisher, Inc., Chicago, 1973.

Vol. 126, No. 4

CHIBA PERCUTANEOUS TRANSHEPATIC CHOLANGIOGRAPHY*

A VALUABLE METHOD FOR VISUALIZING THE NONDILATED BILIARY TRACT

By JOSEPH TABRISKY, M.D., RABBE L. LINDSTROM, M.D., LAURENCE G. HANELIN, M.D., *and* WILLIAM F. PFISTERER, M.D.
TORRANCE, CALIFORNIA

ABSTRACT:

Percutaneous transhepatic cholangiography with the Chiba needle has had remarkable results in cannulating small bile ducts. We have roentgenographically visualized a nondilated biliary system in the first five out of seven cases attempted. Including our series, there have been 71 successful Chiba studies in 107 nondilated or presumed normal biliary tracts with only one questionable major complication. The technique is simple to learn, particularly in comparison with endoscopic retrograde cholangiography. Since the incidence of complications is low, surgical standby should seldom be necessary. The value of the Chiba percutaneous transhepatic cholangiogram is described *via* four unusual case reports.

PERCUTANEOUS transhepatic cholangiography (PTC) is generally recognized as the definitive method short of surgical exploration for the diagnosis of lesions that obstruct the biliary tract. Unfortunately this procedure must have the close cooperation of a surgical team because of the potential complications of bile leakage and hemorrhage. Moreover, bile ducts that are normal or small in size usually cannot be demonstrated. This problem is important since some lesions do not dilate the biliary ducts and therefore defy detection by standard PTC. Although the unsuccessful demonstration of bile ducts by PTC has been considered *prima facie* evidence for a nondilated biliary tract, the clinician frequently feels insecure with a diagnosis derived from negative rather than positive data.

The PTC procedure as modified by Japanese investigators utilizes a long, thin, sheathless (Chiba) needle which can traverse large volumes of liver.[7] Their experience, confirmed by others,[8] reveals greater than 60 percent visualization in nondilated biliary tracts or nonsurgical hepatobiliary disease. Major complications have been less frequently reported than in series which utilize the larger, sheathed needles.[2,5,7]

Recently, the advent of endoscopic retrograde cholangiography (ERC) has enhanced the preoperative diagnosis of the etiology of jaundice.[3,4] Although complications from this technique are minor, the skill of the endoscopist is critical to the success of the procedure.[1,2,6] ERC requires considerable practice before one achieves reasonable proficiency in cannulating the ampulla of Vater. Situations can develop when an endoscopist familiar with ERC is not available, ERC is technically impossible, or the bile ducts proximal to the obstruction cannot be discerned.

Our paper discusses the value of the Chiba PTC as a diagnostic method when information cannot be obtained by ERC or other techniques.

REPORT OF CASES

CASE 1. A 65 year old male was hospitalized on June 5, 1975, because of the sudden onset of right upper quadrant pain. He had a bleeding duodenal ulcer treated by a subtotal gastrectomy with a Billroth II anastomosis in 1954 and

* From the Department of Radiology, Harbor General Hospital-UCLA School of Medicine, Torrance, California.

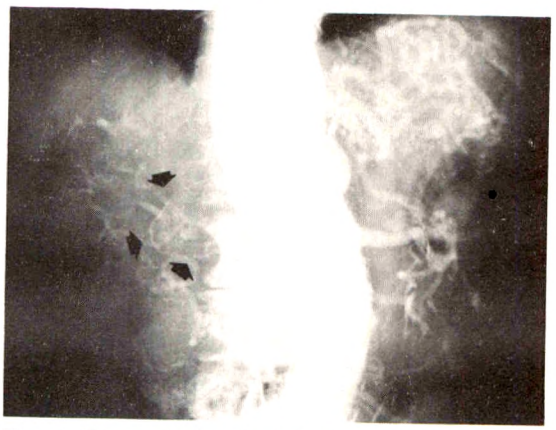


FIG. 1. Case 1. A rim of calcium (black arrows) represents a hepatic artery aneurysm which extends far to the right of the vertebrae. Note the abdominal aortic and splenic arterial aneurysms. The hepatic vessels are not opacified by the contrast medium.

a cholecystectomy in 1955 as a consequence of cholelithiasis.

The patient was afebrile on admission and had normal liver function tests. Ten days later he became febrile coincident with blood cultures positive for gram negative bacteria. Liver function tests became abnormal: total serum bilirubin 3.8 mg per 100 ml (normal: 0.1–1.2 mg per per 100 ml), alkaline phosphatase 259 IU (normal: 36–42 IU), and LDH 237 IU (normal: 109–193 IU). He also had a hepatic artery aneurysm which was calcified and easily observed on an abdominal roentgenogram (Fig. 1).

His precarious clinical state required an exact definition of the nature and extent of the lesion causing the presumed obstructive jaundice. Since ERC was technically impossible because of the previous Billroth II procedure, the Chiba PTC was considered to have the best chance of roentgenographically visualizing the biliary system.

Only a small hepatic area was accessible to a percutaneous puncture since bowel was interposed between the flank and the liver and the hepatic artery aneurysm bulged ominously to the right of the mid-line. The Chiba PTC was accomplished *via* an anterior approach at the mid-clavicular line just inferior to the 12th rib. The needle was angled laterally in order to avoid the hepatic aneurysm. On the second attempt a superior bile duct in the right hepatic lobe was cannulated. A short segmental stricture of a distal posterior divisional bile duct was noted, and a possible intrahepatic mass shifted the main left and right hepatic ducts inferiorly (Fig. 2*A*). A radiolucent stone partially obstructed the distal common bile duct (CBD) (Fig. 2*B*). The entire common duct was displaced to the right by the huge hepatic artery aneurysm.

Subsequently, the stone was removed and a T-tube inserted into the common bile duct. The possible intrahepatic mass could not be investigated at surgery due to the patient's critical

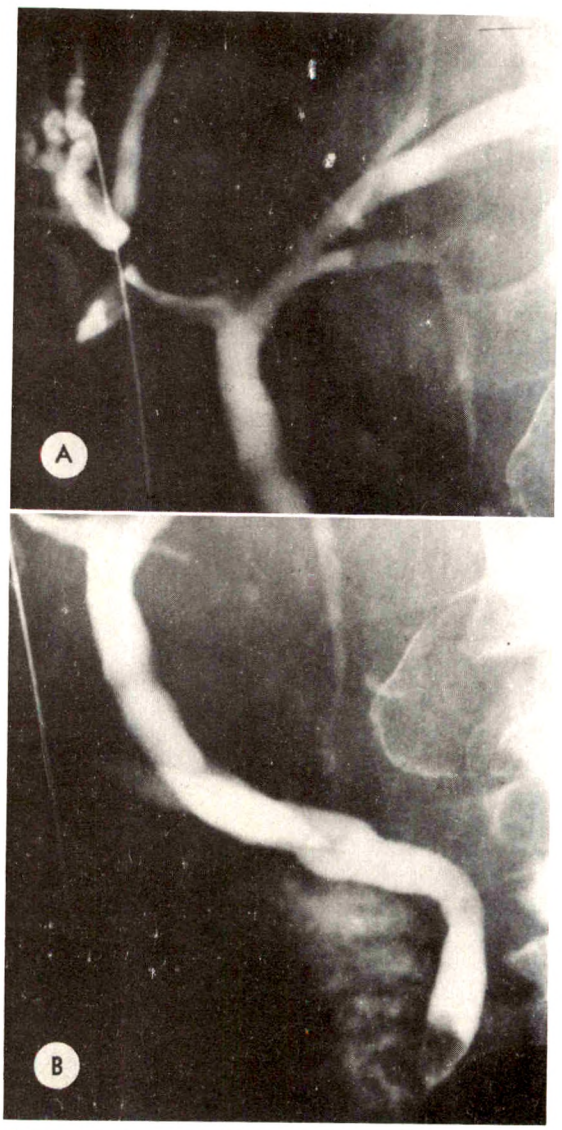


FIG. 2. Case 1. (*A*) Chiba needle enters a superior biliary radicle. There is a stricture of the posterior divisional duct. Note the extrinsic pressure pushing the main right and left hepatic ducts inferiorly. (*B*) A radiolucent stone is evident in the distal CBD. The proximal common duct is displaced to the right by the calcified hepatic artery aneurysm.

condition. He promptly defervesced postoperatively and his liver functions tests returned to normal.

Case II. A 63 year old male was hospitalized on June 28, 1975, because of a one month history of mid epigastric pain. One week prior to admission the patient noted that his pain radiated to the right upper quadrant and that his stools were lighter in color.

In November, 1974, he had had an episode of similar pain. Oral cholecystography at that time resulted in non-visualization of the gallbladder. Since his symptoms rapidly resolved the patient did not return for follow-up. There was no history of hepatitis, alcoholism, nor exposure to drugs or industrial toxins.

Shortly after admission the patient became febrile. Blood studies revealed: total serum bilirubin 3.9 mg per 100 ml, alkaline phosphatase 377 IU, and LDH 159 IU. Intravenous cholangiography was not attempted since the serum bilirubin elevation indicated the high probability of failure. Because of the presumptive diagnosis of ascending cholangitis due to choledocholithiasis, an emergency operation was deemed necessary. A Chiba PTC was performed to delineate the presence, number, and position of the probable stones. The cholangiogram revealed strictures at the origin of the main hepatic ducts and a radiolucent stone in the distal CBD (Fig. 3). The cystic duct and gallbladder could not be outlined. The CBD was slightly dilated and contained linear radiolucencies consistent with poor mixing of contrast medium and viscous bile. The main hepatic ducts and their radicles were small and devoid of filling defects.

At operation, the stone described by cholangiography was removed. However, the gallbladder and cystic duct were totally absent, presumably due to a congenital defect. A T-tube was inserted into the CBD and the patient had an uneventful recovery.

Case III. A 46 year old female was hospitalized on April 16, 1975, because of nausea, vomiting, and abdominal pain localized to the right upper quadrant. A gastric adenocarcinoma involving the fundus and distal esophagus was discovered in 1970. Since then she had a partial gastrectomy and esophagectomy (1970) and another resection with colon interposition for recurrent tumor (1972). In September, 1974, an exploratory laparotomy for partial obstruction at the colonic-jejunal anastomosis revealed poorly differentiated adenocarcinoma involving the anastomosis and adjacent lymph nodes. Resection of the lesion along with 30 cm of small bowel, a jejunojejunostomy and postoperative irradiation through an anterior abdominal portal were accomplished.

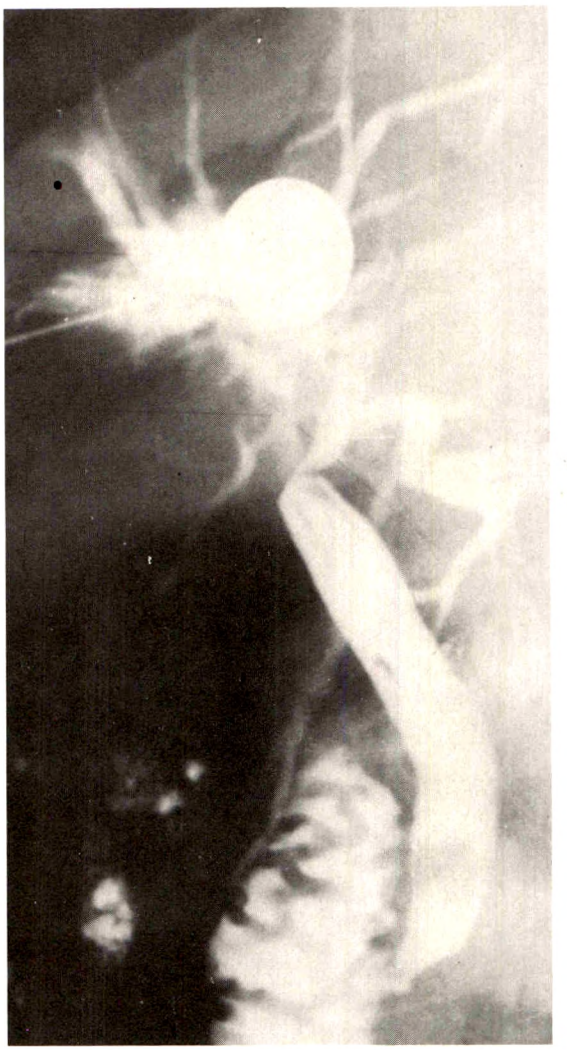


Fig. 3. Case II. The intrahepatic ducts are small. There is a stricture at the origin of the main hepatic ducts and dilatation of the CBD. Radiolucent streaks in the CBD were interpreted as viscous bile which could not mix with the contrast medium. A radiolucent stone is present in the distal CBD. Neither the cystic duct nor gallbladder could be demonstrated.

The patient had serum hepatitis in 1970. She was a known alcoholic with an admitted consumption of more than three whiskey drinks per day. A cholecystectomy for cholelithiasis had been performed at least 20 years ago.

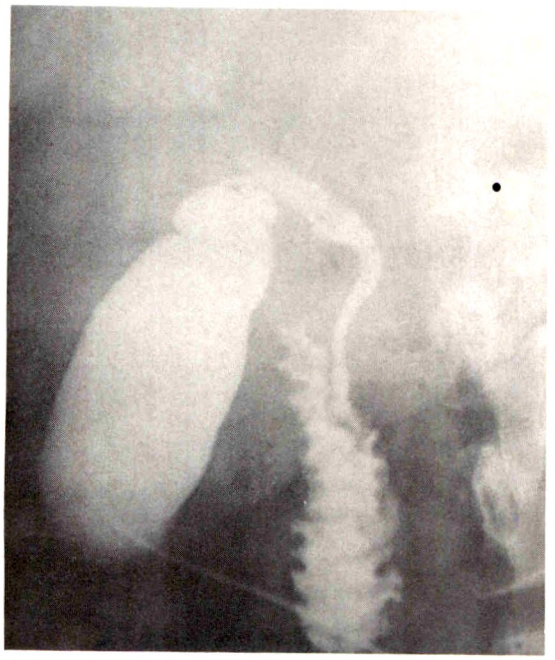


Fig. 4. Case iv. An intraoperative transcholecystocholangiogram shows a normal gallbladder, cystic duct, and common bile duct. The common hepatic duct was interpreted as normal. Faint streaming of the contrast medium into the right hepatic duct resulted in inadequate delineation of the intrahepatic biliary tract.

The upper gastrointestinal and small bowel series were normal except for the obvious surgical changes; no recurrent tumor was observed. A Tc^{99m} sulfur colloid scan demonstrated hepatosplenomegaly and increased bone marrow uptake but no focal liver defects. A diagnosis of active alcoholic hepatitis was made from a percutaneous liver biopsy.

During her hospitalization the serum bilirubin determinations rose from 12.3 to 21 mg per 100 ml. Alkaline phosphatase levels ranged from 51.6 to 59.5 IU, LDH from 173 to 194 IU, and SGOT from 200 to 237 IU. She spiked daily temperature elevations to 101°F.

The progressive increase in serum bilirubin, persistent fever, pain in right upper quadrant, and past history of cholelithiasis suggested the remote, although significant, possibility of choledocholithiasis with obstructive jaundice. The active alcoholic hepatitis was a prime cause for the jaundice but a common duct stone or strategic focus of tumor might be present and contributing to her hepatic failure.

Intravenous cholangiography and ERC were technically impossible, the former because of the hepatocellular dysfunction and the latter due to the surgically altered anatomy. A Chiba PTC was attempted as the lowest risk procedure to obviate laparotomy and as the best method for cannulating nondilated bile ducts. An entirely normal biliary system without obstruction was demonstrated. As a result the patient was spared surgery and treated medically for alcoholic hepatitis. She recovered sufficiently to be discharged from the hospital.

Case iv. A 40 year old male was hospitalized on April 19, 1974, following a motorcycle accident. He had a liver laceration which coursed superior to the gallbladder and dissected deeply into the inferior liver edge. The patient had an uneventful recovery except for persistently abnormal liver functions: total serum bilirubin 1.6 mg per 100 ml, alkaline phosphatase 259 IU, and LDH 257 IU.

On October 9, 1974, he was re-admitted with pruritus and jaundice. Pertinent laboratory findings were: total serum bilirubin 5.9 mg per 100 ml, alkaline phosphatase 293 IU, and LDH 183 IU. There was non-visualization of the biliary tract by intravenous cholangiography. The rose bengal scan was interpreted as showing partial obstruction of the biliary tree due to delayed emptying of the isotope into the bowel. ERC was technically unsuccessful. PTC with a standard large sleeve catheter failed to show a bile duct despite multiple attempts resulting in the presumption that there was a nondilated biliary tree. Percutaneous biopsy of the right hepatic lobe represented only intrahepatic cholestasis.

At exploratory laparotomy on November 4, 1974, an operative transcholecystocholangiogram showed a normal common bile duct although the proximal hepatic and intrahepatic ducts were not satisfactorily visualized (Fig. 4). A large pancreatic pseudocyst was drained *via* a cholecystojejunostomy. Persistent fever and pruritus prompted a second laparotomy at which a small subhepatic abscess was drained and no other lesion noted.

Despite multiple intravenous cholangiograms, an intraoperative cholecystocholangiogram, two laparotomies, a standard PTC, and an ERC, visualization of the porta hepatis and intrahepatic ducts could not be accomplished. The severe pruritus suggested a degree of obstruction that was not confirmed by any standard test. Consequently, to obviate hazardous re-exploration, the Chiba technique was attempted to visualize roentgenographically the intrahepatic ducts and porta hepatis.

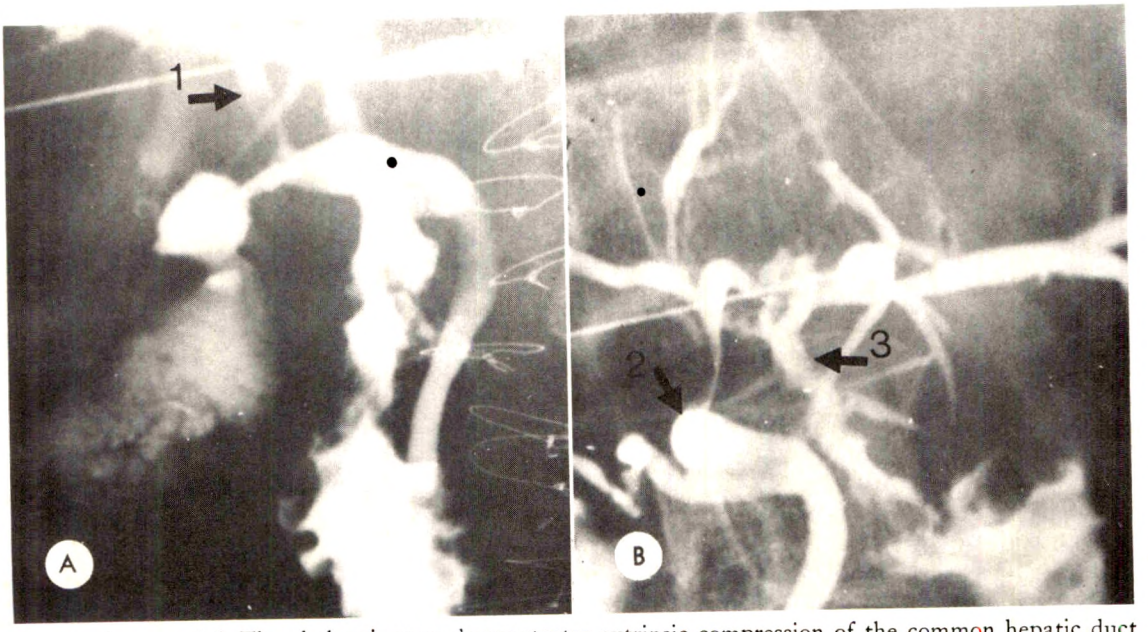


Fig. 5. Case IV. (*A*) The cholangiogram demonstrates extrinsic compression of the common hepatic duct (arrow 1). Note the normal common bile duct and cystic duct. (*B*) The Chiba needle enters a branch leading to the left main hepatic duct. The narrowed common hepatic duct is observed proximal to the pseudo-dilatation (arrow 2) caused by a projectional artifact. The left hepatodocho-duodenal fistula (arrow 3) is well outlined on this oblique view.

A small left hepatic duct was entered and the resultant cholangiogram demonstrated a fistulous tract between the proximal left hepatic duct and the descending duodenum. The intrahepatic ducts were not dilated and the common hepatic duct distal to the junction of the main hepatic ducts was compressed by a smooth extrinsic pressure defect (Fig. 5, *A* and *B*). The contrast medium preferentially drained through the fistula into the duodenum.

On the basis of the Chiba cholangiogram the patient was considered to have adequate drainage of the biliary tract *via* the left hepatodocho-duodenal fistula. Rapid amelioration of his pruritus as well as a decrease in serum bilirubin occurred after the institution of phenobarbital and cholestyramine therapy.

DISCUSSION

Many difficulties still exist in making a preoperative diagnosis in jaundiced patients. Oral and intravenous cholangiography are frequently useless. Liver function studies may suggest biliary obstruction rather than primary hepatocellular dysfunction but cannot delineate the anatomic lesion. PTC which utilizes the larger, sheathed needle has a variable and often poor success rate when there is little or no dilatation of the biliary tract. Moreover, significant complications can occur from the procedure thus necessitating surgical stand-by.[2,5] Although ERC is often diagnostic, it requires a skill that can be acquired only with considerable practice. ERC cannot be performed if the ampulla of Vater is anatomically inaccessible.

The Chiba PTC is a simple technological advance that obviates surgical stand-by and allows an excellent chance of roentgenographically visualizing the nondilated as well as the dilated biliary system. The 23-gauge needle, developed at Chiba University in Japan, is made of flexible steel and contains a stylet but not an outer sheath. The small cross-sectional size of the needle reduces the area of the puncture wound and the diameter of the tract. These facts probably account for the decreased complications and a better chance to cannulate nondilated intrahepatic bile ducts.

The first patient, with bowel interposed

in the right flank lateral to the liver, hepatic artery aneurysm, and a Billroth II anastomosis, could be studied by PTC only through a small anterior portal. The Chiba technique allowed the strategic cannulation of a biliary radicle that probably would have been inaccessible to the larger sheath needle.

The second patient who had acute ascending cholangitis required an emergency PTC. Although the CBD was dilated, the intrahepatic ducts were not. The Chiba needle entered and permitted roentgenographic visualization of the small intrahepatic biliary system. At surgery, in addition to choledocholithiasis, the diagnosis of agenesis of the gallbladder and cystic duct was first appreciated. Since other anomalies of the biliary tract commonly co-exist, the preoperative Chiba examination allayed the concern that more than one surgical lesion might be present.

The third patient had known gastric adenocarcinoma and active alcoholic hepatitis but had survived three operations for her disease during the past five years. There was a remote possibility that a surgically correctable lesion was causing the deterioration of her hepatic function. The Chiba PTC proved conclusively that an obstructive lesion did not exist, thereby preventing a laparotomy with a potentially high mortality rate.

The fourth case was a diagnostic enigma. Despite the use of every available method of investigation including laparotomy, ERC, and intraoperative cholangiography, the etiology of his intrahepatic cholestasis eluded detection. An inference of a nondilated biliary system was made because a large needle PTC was unsuccessful in demonstrating bile ducts. The Chiba study finally delineated the anatomic lesions of common hepatic duct stenosis and left hepatodocho-duodenal biliary fistula. Consequently the patient was spared needless surgery and received appropriate medical therapy.

Although our experience is admittedly small, we have been able to demonstrate five of seven (71 percent) nondilated biliary systems and have had no major complications in the 13 procedures performed. Our results in the nondilated biliary tract parallel those of Okuda *et al.*[7] and Redeker *et al.*[8] Summarizing the three series, there have been 71 successful cholangiograms in 107 nondilated or presumed normal biliary tracts with only one major complication. This was a hepatobronchial fistula which, according to the clinical history, might have developed prior to the examination.[7] Transient febrile episodes that were self-limited or rapidly controlled by antibiotics were considered minor complications. The technique, relatively easy to learn, seems valuable as a primary procedure or alternative to ERC.

Joseph Tabrisky, M.D.
Department of Radiology—Box 27
Harbor General Hospital
1000 West Carson Street
Torrance, California 90509

REFERENCES

1. Geisse, G., Melson, G. L., Tedesco, F. J., Kelly, J. J., and Stanley, R. J. Stenosing lesions of biliary tree. Am. J. Roentgenol., Rad. Therapy & Nuclear Med., 1975, *123*, 378–385.
2. Gothlin, J., and Tranberg, K. Complications of percutaneous transhepatic cholangiography (PTC). Am. J. Roentgenol., Rad. Therapy & Nuclear Med., 1973, *117*, 426–431.
3. Kasugai, T., Kuno, N., Kizu, M., Kobayashi, S., and Hattori, K. Endoscopic pancreatocholangiography I. *Gastroenterology*, 1972, *63*, 217–226.
4. Kasugai, T., Kuno, N., Kizu, M., Kobayashi, S., and Hattori, K. Endoscopic pancreatocholangiography II. *Gastroenterology*, 1972, *63*, 227–234.
5. Lane, E. K. Transhepatic cholangiography. *Radiology*, 1974, *112*, 283–290.
6. Morrissey, J. F. Cannulate or not to cannulate. *Gastroenterology*, 1972, *63*, 351–352.
7. Okuda, K., Tanikawa, K., and Emura, T. Nonsurgical, percutaneous transhepatic cholangiography: diagnostic significance in medical problems. *Am. J. Digest. Dis.*, 1974, *19*, 21–36.
8. Redeker, A. G., Karvountzis, G. G., Richman, R. H., and Masumasa, H. Percutaneous transhepatic cholangiography. *J.A.M.A.*, 1975, *231*, 386–387.

Vol. 126, No. 4

ORGANIZING A COMMUNITY DEPARTMENT FOR ACADEMIC RADIOLOGY*

By D. WILLIAM SHERRICK, M.D.,† P. F. MAHON, M.D.,‡
DAVID B. LEWIS, M.D.,§ *and* ERWIN M. JANZEN, M.D.§
SPRINGFIELD, ILLINOIS

WITH the current emphasis on community based medical schools and the extension of traditional schools into community hospitals, the opportunity to develop an academic Department of Radiology may present itself to radiologists in private practice. Presented with this challenge and unencumbered by previous tradition, the radiologists in Springfield, Illinois, have developed what we consider to be a very workable organizational structure. Our organization allows us to continue the independent practice of radiology and to meet the needs of the academic Radiology program. This is a recounting of the evolution of the Radiology Department within the guidelines established for development of the new Southern Illinois University School of Medicine.

CHRONOLOGY OF EVENTS

In 1965 the Illinois State Legislature passed a bill to create additional facilities for medical education and the Board of Higher Education was directed to establish a commission to survey the status of education in health fields in Illinois. This commission (The Campbell Commission) published its results in June of 1968 and recommended that Southern Illinois University School of Medicine be established with the preclinical year to be spent on the Carbondale Campus of Southern Illinois University and the clinical training years in Springfield, Illinois. Richard H. Moy, M.D. was appointed Dean of Southern Illinois University School of Medicine in December of 1969.

Two community hospitals with a total bed capacity of approximately 1,300 provide excellent medical facilities for the 90,000 inhabitants of Springfield. The medical population served by these two large community hospitals approaches 300,000. Affiliation agreements were signed between the two hospitals and Southern Illinois University School of Medicine. The medical school does not own nor operate a teaching hospital, and the clinical teaching is performed in the affiliated hospitals.

The locally practicing physicians were encouraged to participate in the formation of a teaching program and to form search committees to aid in the recruitment of full time faculty. A limited number of full time academic faculty has been recruited and part time and volunteer clinical faculty provide significant teaching in all major departments.

The Charter Class of the new medical school began basic science instruction in Carbondale in June of 1973 and an Advanced Standing Class of third year medical students entered clinical training in Springfield in October of 1973. In the Spring of 1975 Southern Illinois University School of Medicine received full accreditation and graduated its first M.D.'s.

ORGANIZING RADIOLOGY DEPARTMENT

One of the basic guidelines of the Campbell Commission Report was for new medical schools to make maximum use of existing manpower and physical resources. The radiologists have attempted to follow this premise in the organization of their academic Department of Radiology.

We will begin our saga of the evolution of the academic Department of Radiology in 1970. At that time two groups of radiologists were practicing in Springfield, one at each of the community hospitals, and while

* From the Department of Radiology, Southern Illinois University School of Medicine, Springfield, Illinois.
† Chairman and Clinical Professor. ‡Assistant Chairman and Clinical Professor. §Clinical Professor.

good personal relationships existed between the radiologists, each group was organized into separate service corporations. The eight radiologists practiced general radiology including radiation therapy, nuclear medicine and all branches of diagnostic radiology.

The radiologists agreed to accept the commitment to provide the radiology teaching for the academic program and to form the academic faculty of the Department of Radiology. Our first need was for a formal structure to unite the radiologists into a single faculty. Merger of the two medical service corporations was considered but was not feasible for multiple reasons.

When actual merger was abandoned, it was decided to create a third corporation termed University Radiologists, S.C. University Radiologists would contract with the Southern Illinois University School of Medicine for payment of a negotiated number of full time equivalent faculty. During the planning years, before the arrival of medical students, the number of full time equivalents in the Department of Radiology was small. Currently, with students in attendance, there are 5.7 full time equivalent academic faculty within the Department of Radiology. All of the radiologists are shareholders in University Radiologists and this corporation provides a formal organizational structure for the faculty. Operating within a corporate structure was familiar to the radiologists and was easily adapted to the academic program. The Board of Directors of University Radiologists is the policy making board for the academic Radiology program and monthly meetings provide a forum for discussion of academic matters.

The number of full time equivalents to deliver the academic program in Radiology is discussed and negotiated with the Associate Dean of Medical Education. The mutually agreed upon number of full time equivalent faculty is then compensated at academic faculty rates through an annual contract between Southern Illinois University School of Medicine and University Radiologists, S.C. The total compensation for the full time equivalent academic faculty is paid in monthly installments to University Radiologists, S.C. and the disbursement of those funds is determined by the Board of Directors.

Organizing the faculty into a corporation provided a legal entity to recruit additional radiologists. Since 1970, seven additional faculty members have been recruited. Those radiologists who practice at both of the affiliated hospitals, such as the two new radiation therapists and the radiation physicist, are employed by University Radiologists, S.C. The four diagnostic radiologists recruited are hired by the medical service corporations and practice at one of the affiliated hospitals.

The hiring of the radiation therapists by University Radiologists, S.C. requires that this corporation also serve as the business corporation for radiation therapy. Fringe benefits including pension and profit sharing plans, malpractice and other forms of insurance are provided for the therapists and physicist through University Radiologists, S.C.

The Board of Directors of University Radiologists consists of two members from each of the two radiologic service corporations, a radiation therapist, the assistant chairman and the chairman of the academic Department of Radiology. This representation on the Board helps to prevent fragmentation of radiology into separate departments of diagnosis and therapy. There are currently, between the two hospitals, fifteen faculty members in the Department of Radiology (University Radiologists, S.C.).

When the radiologists agreed to accept the teaching commitment for the academic program in Radiology they also agreed to subspecialize with each faculty member concentrating his efforts and interest in well defined fields. Subspecialization applies to community needs as well as the individual group needs. Recruitment was

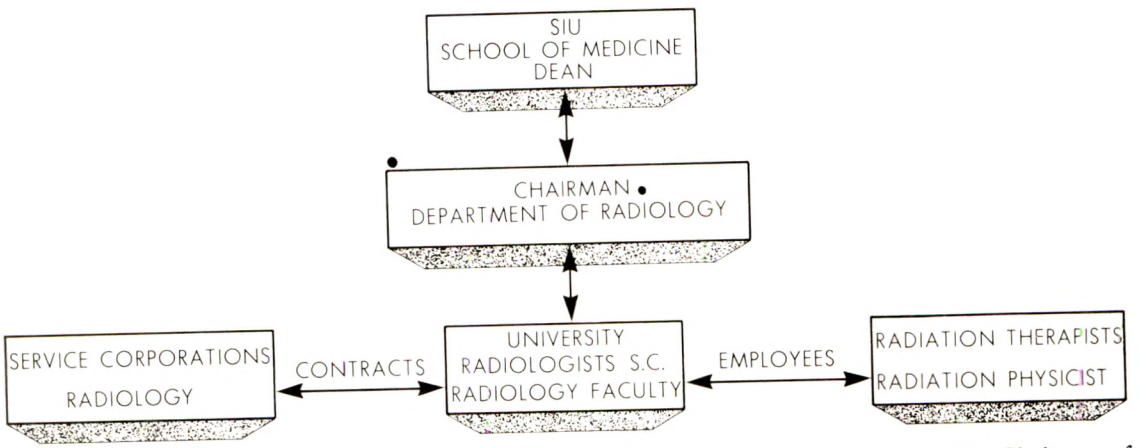


Fig. 1. Diagram of the organizational structure of the academic Department of Radiology. The Chairman of the Department serves as the President of University Radiologists. In time, the radiation therapists may elect to form their own service corporation in radiation therapy and relate in the same way to University Radiologists as the diagnostic radiology corporations.

also designed to supplement subspecialty requirements within the department. To date, there has been no turnover in the radiology faculty and the subspecialty requirements have been well fulfilled by the older faculty members as well as the more recently recruited faculty.

Initially, we elected to appoint acting co-chairmen from each hospital for the administration of the Department during its early developmental years. During this period we considered recruiting radiologists known for their ability as teachers to aid in the delivery of the radiology program. "Teaching" radiologists were difficult to locate and recruit and our decision was to accept the teaching responsibility with no full time academicians within the department.

In 1973 a chairman and an assistant chairman were named for the Department of Radiology. The chairman provides a communication link between the Medical School Dean and the faculty. In addition to the usual duties of this position, the chairman also serves as the President of the Board of Directors of University Radiologists, S.C. In this role the chairman becomes the implementor of policy decisions made by the Board. This dual role of the chairman is not dissimilar to the role of other chairmen, but the duties and responsibilities are better defined when the faculty is organized into a corporation. The chairman has less autonomy in the corporate structure but has the distinct advantage of regular input by senior faculty members who make up the Board of Directors.

Our organization of the academic Department of Radiology has proved to be practical and workable for our needs (Fig. 1). In establishing this organization we have benefited from the constant support of the Dean of the Southern Illinois University School of Medicine and his support has facilitated the creation of this non-traditional faculty organization.

The radiology faculty has responded in a very gratifying manner to the challenge of teaching students and residents. We have recently received accreditation for a diagnostic radiology residency program. All members of the radiology faculty participate in the teaching program and are enthusiastic teachers. Within the academic environment the radiology faculty is evolving toward clinical research and scholarly endeavors.

The Liaison Committee for the Medical Education Accreditation Team described the organization of the Department of

Radiology as having a salutary effect on our professional community and was enthusiastic about its development.

The successful organization and operation of our academic department by local physicians have allayed some of the anxieties which inevitably accompany the establishment of a new community based Medical School. Our organization may serve as a model for other physicians confronted with the challenge of developing an academic program within the framework of independent practice.

D. William Sherrick, M.D.
Department of Radiology
Southern Illinois University School of Medicine
P.O. Box 3926
Springfield, Illinois 62708

Vol. 126, No. 4

COMPUTERIZED TOMOGRAPHY (CT) IN ACUTE HEAD TRAUMA*

By JORGE MERINO-DEVILLASANTE, M.D.,† *and* JUAN M. TAVERAS, M.D.
BOSTON, MASSACHUSETTS

ABSTRACT:

The retrospective evaluation of 100 cases of head trauma that were subjected to computerized tomography (CT) leads to the following conclusions: (1) Computerized tomography and plain skull survey, should be the first neuroradiological procedures to perform. (2) Angiography may be carried out after computerized tomography when necessary, but as proved by this series, it will be needed in a relatively small number of cases. These include patients with technically limited CT scans or those in whom the possibility of an associated vascular lesion of the cervical or intracranial vessels is clinically suspected. (3) It is essential to obtain CT scans of the best possible quality. Sedation will be required in many instances, but this is considered worth doing because a normal CT scan, without significant technical limitations, will exclude the presence of lesions requiring prompt surgical intervention. Those patients who require surgery will need general anesthesia under any circumstances. (4) There is generally a direct relationship between the severity of clinical presentation and the CT demonstration of the abnormality responsible for the clinical status. Seventy percent of the patients clinically diagnosed as contusion had positive CT scans, and for all practical purposes, 100 percent of patients having trauma more severe than our Group III (contusion) had abnormal CT scans. Likewise, the number and intensity of tissue abnormalities on CT scans increase proportionately with the severity of the clinical signs and symptoms. (5) It is foreseen that, with the advent of faster computerized tomographic scanners, the usefulness of this method will increase further, owing to a reduction in the total examination time and the lessened requirement for sedation.

WITH the constant increase in high velocity accidents and violence over the past decades, the matter of acute head trauma is one of prime importance in today's medical practice. In his classic textbook dealing with head trauma, Brock states that. "The appalling number of accidents in modern life makes the subject of injury as important as that of any pandemic scourge."

It is our goal to devise methods that would allow us to diagnose readily and with precision the effects of trauma upon the brain and its coverings in order to institute the proper treatment at the earliest possible moment. The acute effects and the chronic sequelae of trauma are often severely disabling and the importance of early therapy cannot be overemphasized. Computerized tomography allows us to make a diagnosis quickly and in a non-invasive manner.

The purpose of this study is to discuss the important role of computerized tomography (CT) in the management of acute head trauma.

PATHOLOGY AND DEFINITIONS

Several pathologic processes occur as a result of trauma to the brain and its coverings:

(1) Edema or brain swelling is of varying intensities, from mild and focal, to severe and diffuse.

(2) Contusion means bruising or crushing without interruption of physical continuity of brain cortex. It is a pathological term,

* From the Departments of Radiology, Massachusetts General Hospital and Harvard Medical School, Boston, Massachusetts.
† Present Address: Institute of Neurology, Mexico City, Mexico.

used widely in clinical practice. Contusion is produced by a sudden blow to the head. Bruises or hemorrhagic areas are macroscopically visible and are the result of disruption of small vessels with extravasation of blood insufficient to produce a frank hematoma. These bruises (or lacerations) can be of variable intensity and the clinical presentations range from mild to severe, and are characterized by focal neurological findings, depending on the site of injury, such as aphasia, monoparesis, hemiplegia, etc. Contusion is one of the lesions typically produced by the *coup-contracoup* type of injury in which the malleable brain adopts a swirling motion due to the acute change in momentum of the head. It is thus crushed against different bony prominences, such as the wings of the sphenoid bones, the petrous ridges, the rough orbital surfaces and the frontal and occipital bones.

(3) Hematomas in different compartments of the brain and its coverings may occur as follows: (a) Intracerebral hematoma. This can be considered one step beyond contusion. (b) Intraventricular hematoma. This was thought to be the least common location of intracranial hematomas, but prior to the advent of computerized tomography the diagnosis could not be made except *via* surgical intervention or autopsy. (c) Epidural hematomas. These result from laceration of a meningeal artery (or are occasionally secondary to venous bleeding). Epidural hematomas are most commonly located in the lower convexity of the skull or in the temporal fossa. Epidural hematomas usually occur within hours, but may take two to three weeks to develop in some cases; they are more common in the second and third decades of life. (d) Acute subdural hematomas. As a rule they develop more slowly, are almost always the result of venous bleeding owing to rupture of the bridging veins of the brain, and occur anywhere over the brain surface, except the occipital region which is unusual as a primary location. Although occurring at any age, they are more common in the sixth to the eighth decades of life. It is postulated that the slight shrinkage of the brain occurring with age permits greater excursion of the free floating organ during sudden deceleration, thus tearing the bridging veins going from the brain cortex to the dural sinuses. (e) Chronic subdural hematomas. Here a traumatic etiology is less clear. It may follow a trivial head injury occurring weeks or months previously. (f) Cortical and subcortical hematomas. These may represent an intermediate stage between contusion and frank intracerebral hematoma. (g) Delayed traumatic intracerebral hematoma. This occurs days or a few weeks after trauma.

(4) Post-traumatic atrophy is the result of the injury and may be focal or generalized producing ventricular dilatation. The focal loss of brain mass leads to localized enlargement of the ventricles and subarachnoid spaces.

(5) Obstructive hydrocephalus may be the result of arachnoid adhesions resulting from subarachnoid bleeding;[5] but the latter may also lead to interference with absorption of cerebrospinal fluid over the hemispheres, and subsequent hydrocephalus.

Concussion is a clinical term and does not imply the presence of any specific lesion in the brain although some cases classified originally as concussion may later develop a mass lesion, most commonly a subdural hematoma.

MATERIAL AND METHOD

One hundred consecutive cases of head trauma of varying degrees were studied by computerized tomography in an 18 month period. The CT scans were obtained from four hours to 31 days after trauma. As the usefulness of the procedure became clearer the studies were carried out earlier, six to 96 hours following the injury. Thirty-six patients had surgery prior to computerized tomography. Twenty patients had sequential scans. During the last six months, emergency coverage was provided 24 hours a day, and more patients were examined soon after the accident.

Table I

CT IN ACUTE HEAD TRAUMA

Group 1	5 patients
Group 2	12 patients
Group 3	24 patients
Group 4	14 patients
Group 5	35 patients
Group 6	10 patients

A correlation between the severity of the trauma based on the clinical status and the findings at computerized tomography was undertaken. Six groups were encountered (Table 1) based on the degree and duration of alteration in consciousness using the grading proposed by Plum and Posner,[8] *e.g.*, alert wakefulness, lethargy, obtundation, stupor, and coma. Abnormal posturing and pupillary reactions were also used.

The abnormalities visualized at computerized tomography correspond to the five types of pathologic change described above.

With the exception of mild focal edema, the first three groups of primary abnormalities, edema, contusion and laceration, and hematomas, are almost always accompanied by a mass effect such as dislocation of the midline structures, compression of the ventricular system, and effacement of sulci and subarachnoid spaces by the swollen tissues.

(1) *Edema.* Edema (Fig. 1) is seen by computerized tomography as an area with an average density lower than that of the surrounding normal tissue.[1–3,7] The severity of the edema was classified as follows: Mild focal edema may produce only slight compression of the closest ventricular structure but no midline dislocation is recognizable. Moderate edema may be unilateral or bilateral, but the secondary mass effect is more obvious as represented by compression of the ventricular system and dislocation of the midline structures. Severe edema is a diffuse low absorption lesion which can be unilateral or bilateral. If unilateral, the compression upon the ventricular system and the midline dislocation is very pronounced, and if generalized, it may be indistinguishable from normal brain. In these cases edema may be recognized only because the lateral ventricles are abnor-

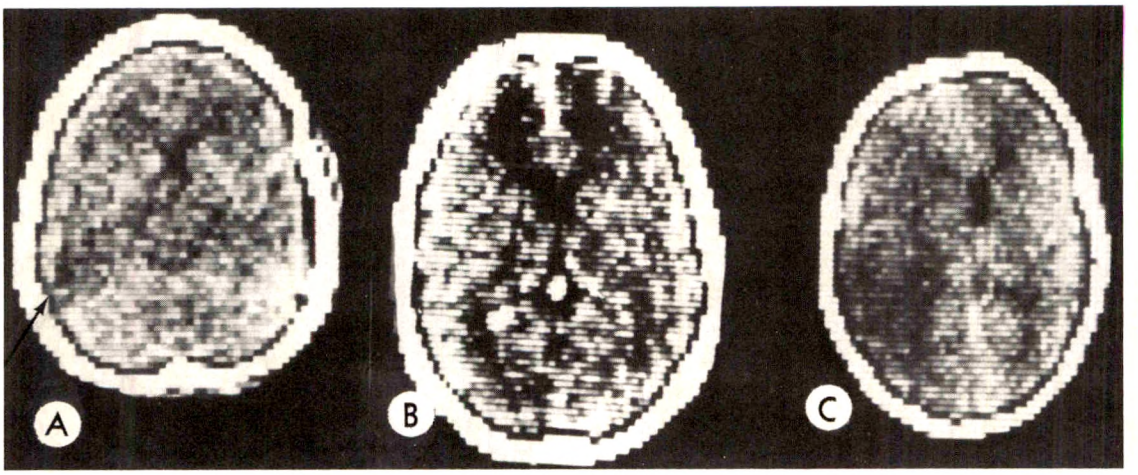


Fig. 1. Post-traumatic edema. (*A*) Mild focal edema. There is a low absorption area in the left posterior temporal region (arrow). (*B*) Moderate edema. Areas of low absorption are seen in both frontal regions with compression of both frontal horns (picture taken with a window setting of 11 EMI units). Patient had an occipital fracture and was initially alert, later became drowsy. No focal signs. The *coup-contracoup* mechanism is clearly responsible for the abnormality shown by CT. (*C*) Severe edema. There is a generalized diffuse low absorption lesion in the left hemisphere with a midline dislocation and distortion of the left frontal horn. Low absorption is also seen in the right frontal and posterior temporal regions. Patient in deep coma after a car accident.

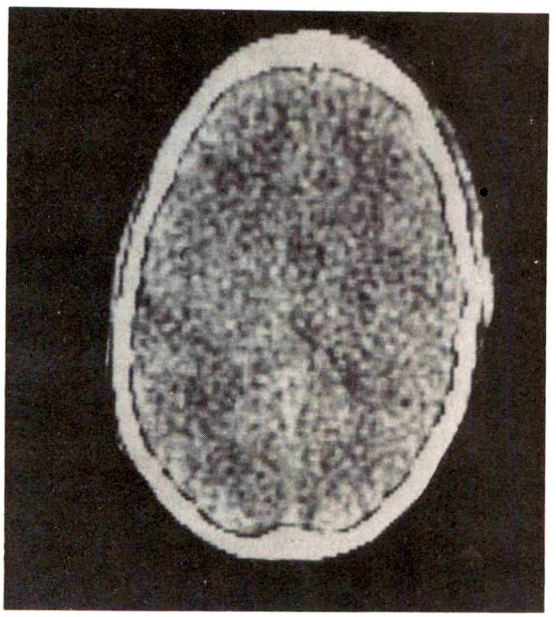


Fig. 2. Severe diffuse generalized edema. A 17 year old male in auto accident, immediately comatose, fixed pupils, and decerebrate posturing. CT scan 48 hours after trauma shows a diffuse heterogeneous picture with scattered areas of diminished absorption and complete obliteration of the ventricular system.

mally small, for the patient's age (Fig. 2), and in subsequent scans return to normal size. Although it has not been proved, it seems probable that generalized edema cannot be demonstrated because it involves the entire brain thus presenting a uniform density.

(2) *Contusion and laceration.* Contusion is seen at computerized tomography as a heterogeneous area with an average density higher than that of surrounding normal tissue. The higher absorption value is due to extravasated blood in swollen brain substance, lending an inhomogeneous appearance to the lesion (Fig. 3; and 8*A*). Contusion is by definition a focal lesion although more than one area of contusion may be present. The contracoup mechanism is probably responsible for the majority of these lesions. Laceration as such is not definable by computerized tomography and it is included with contusion.

(3) *Hematomas.* The hematomas can be further subdivided as follows:

(a) *Cortical and subcortical hematomas.* This lesion probably represents a higher stage of severity of cerebral injury beyond contusion and in this case the average density of the lesion is higher than that of surrounding normal tissues, but is homogeneous as opposed to contusion. These lesions are in the cortical region and differentiation between subpial, cortical or subcortical hemorrhage cannot be made by computerized tomography, but they are clearly distinguishable from the extracerebral and the frank intracerebral hematomas (Fig. 4; and 5). The cortical and subcortical hematomas are usually surrounded by a halo of edema (low absorption) on their medial aspect (Fig. 13).

(b) *Intracerebral hematoma.* These are more centrally located and are always surrounded by a circumferential halo of low absorption representing edema (Fig. 6). The absorption values of the intracerebral

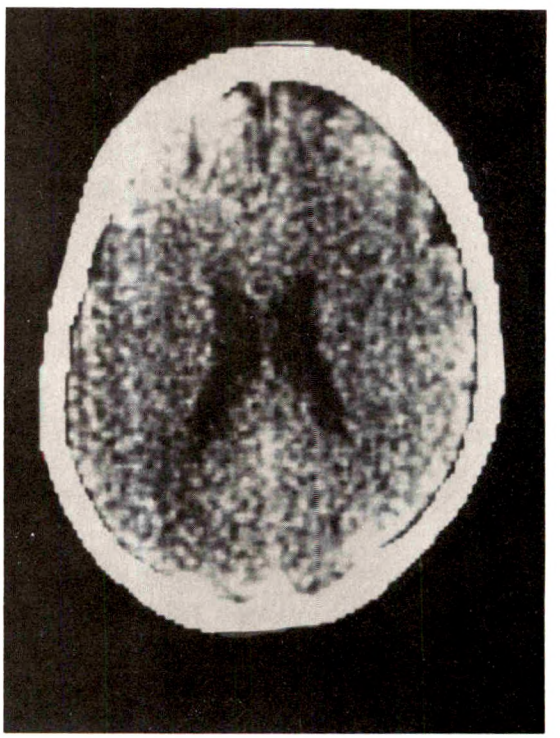


Fig. 3. Contusion. A 63 year old male who struck his head against a beam. Diplopia, confusion, and bloody cerebrospinal fluid. CT shows a poorly circumscribed heterogeneous area of high absorption values in the left frontal region.

hematomas generally range from a high in the 40s to a low limit in the 20s with 80×80 matrix[2] (high in the 60s to a low limit in the low 20s with the new 160×160 matrix). All intracerebral hematomas were associated with a definable mass effect. As mentioned above, older individuals were observed to develop intracerebral hematomas following apparently less severe trauma than younger individuals. In general they were more patchy and more superficially placed than the usual hypertensive intracerebral hematoma.[9]

The entity known as *delayed traumatic intracerebral hematoma*[4,6] was observed in two of our patients, in one of them twelve days and, in the other, two days after the traumatic episode. Both were young individuals (30 and 18 years respectively) (Fig. 7; and 8).

(c) *Epidural Hematoma.* Epidural hematomas are lesions with significantly high absorption values, ranging from the low 20s to the high 60s or low 70s when the 160×160 matrix is used. The higher upper values are probably related to the "computer overshoot" present under the skull bone. This is a band, about the same thickness as the bone, which, according to Gado (1975) measures an average of seven EMI numbers. Generally, epidural hematomas present a biconvex or lenticular shape and are, as it would be expected from their anatomical location, much more focal in nature than the subdural hematomas since their extension is limited by the dural attachments. In our series, they were always accompanied by a well manifested secondary mass effect and in some cases a band of edema was present in its inner or medial aspect (Fig. 9). Of six cases of epidural hematoma, five had an associated skull fracture crossing a meningeal groove; the age distribution is wide-spread.

(d) *Subdural hematoma.* This can be acute or chronic. The acute subdural hematoma is also a lesion with distinctly higher absorption values than normal brain. It may be located over the convexity, against the falx in the interhemispheric fissure, or in the floor of the anterior, middle, or posterior cranial fossa. When located in the floor of the skull it is difficult to diagnose by computerized tomography because of its location against the bone (Fig. 10, *A* and *B*). When located in the convexities they tend to adopt a convex-concave lens configuration resembling a "half moon." The absorption values were similar to those observed in epidural hematomas and as a rule cerebral edema was not present adjacent to the subdural hematoma. The mass effect was always clearly observed and in some instances it was such as to produce bending of the falx (Fig. 10). As previously reported[2] early in our experience, three subdural hematomas were recognized as lesions, but were thought to be intracerebral tumors. With experience, all of the subsequent subdural hematomas were identified and recognition has been facilitated by the new high resolution 160×160 matrix. In

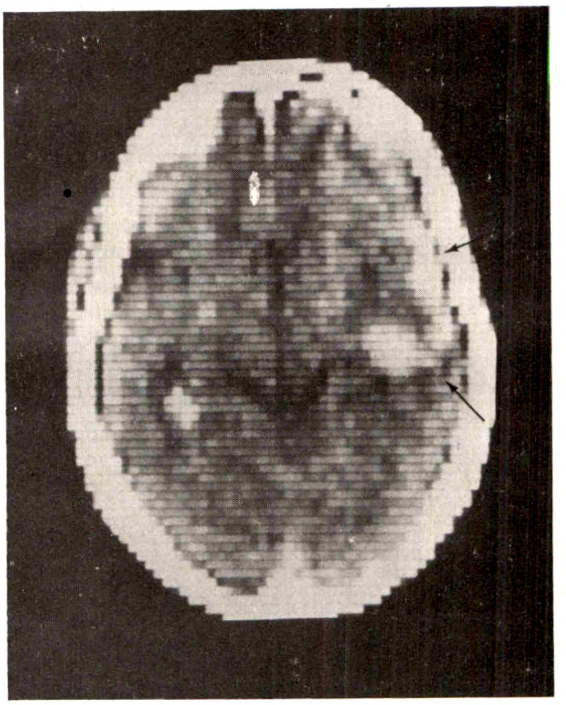


Fig. 4. Subcortical and intracerebral hematoma. A 70 year old male fell and became drowsy and disoriented; spinal puncture revealed xanthochromic fluid. Angiography showed a right temporal intracerebral mass. CT shows a right temporal hematoma with subcortical extension (arrows).

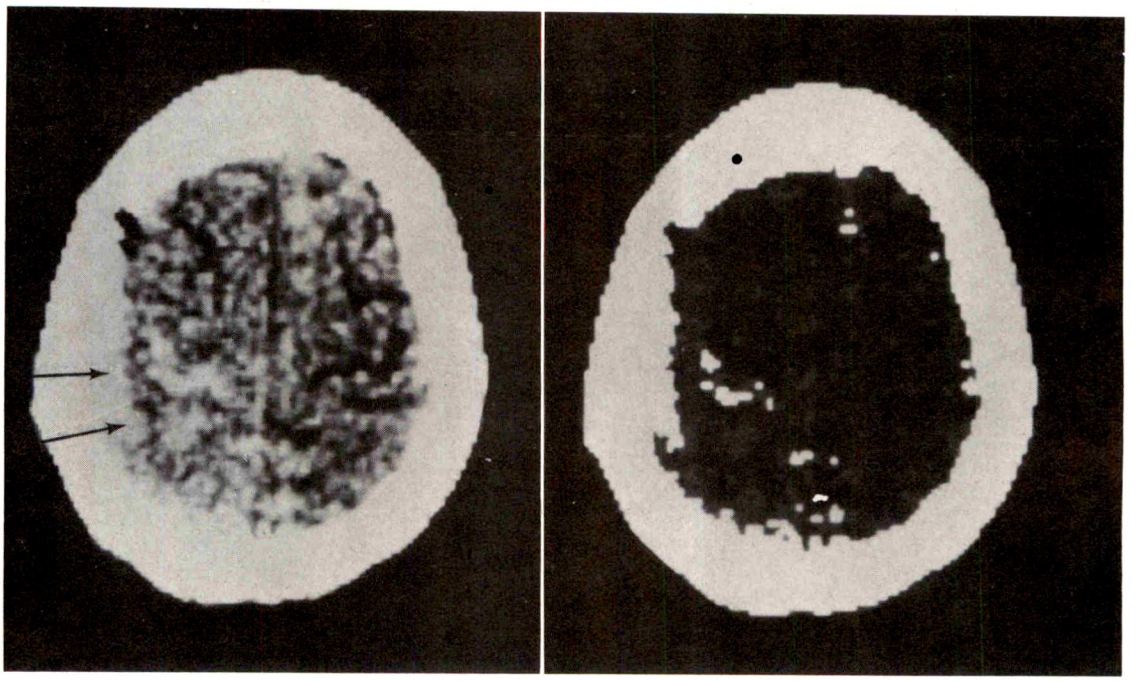
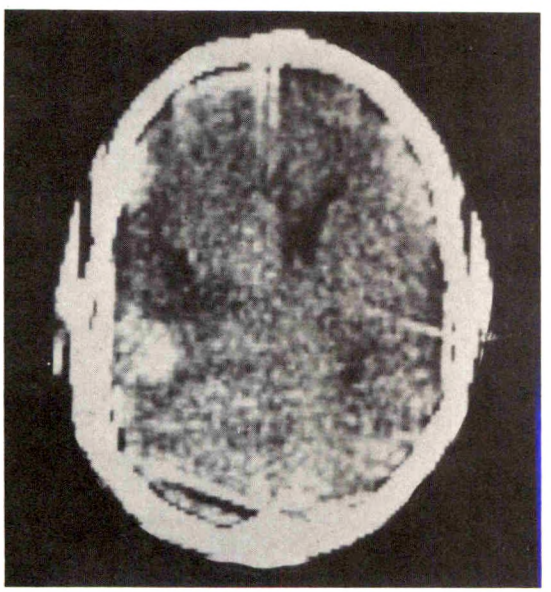


Fig. 5. Subpial hemorrhage. A 66 year old male who struck his head two days prior to admission to the hospital and developed slurred speech and mild right hemiparesis. CT of the high convexity area shows an area of high absorption in a gyrus (arrows), probably a subpial hemorrhage. The picture on the right was taken with a window level setting of 28 and brings out only the higher density areas. More than one gyrus may be involved.

the past twelve months, there have been no false negatives, providing a good quality CT scan was obtained. Sixteen acute and six chronic hematomas were present in our series.



The chronic subdural hematomas and hygromas have had the same configuration as the acute subdural hematomas or may assume a biconvex appearance with greater flattening of the subjacent brain. Chronic subdural hematomas have an average density lower than the surrounding brain tissue. The lesser absorption of these lesions is explained by breakdown and removal of red cell elements and increased fluid contents resulting from osmosis.

In one case of chronic subdural hematoma, gravitation of denser elements in-

Fig. 6. Intracerebral hematoma. A 28 year old male jumped from a second story balcony four days previously. Immediate removal of left subdural hematoma. Six hours after operation, coma and right hemiparesis. CT shows a left posterior temporal hematoma surrounded by a diffuse area of low attenuation (edema). There is marked compression of the left frontal horn and dislocation of the midline to the right.

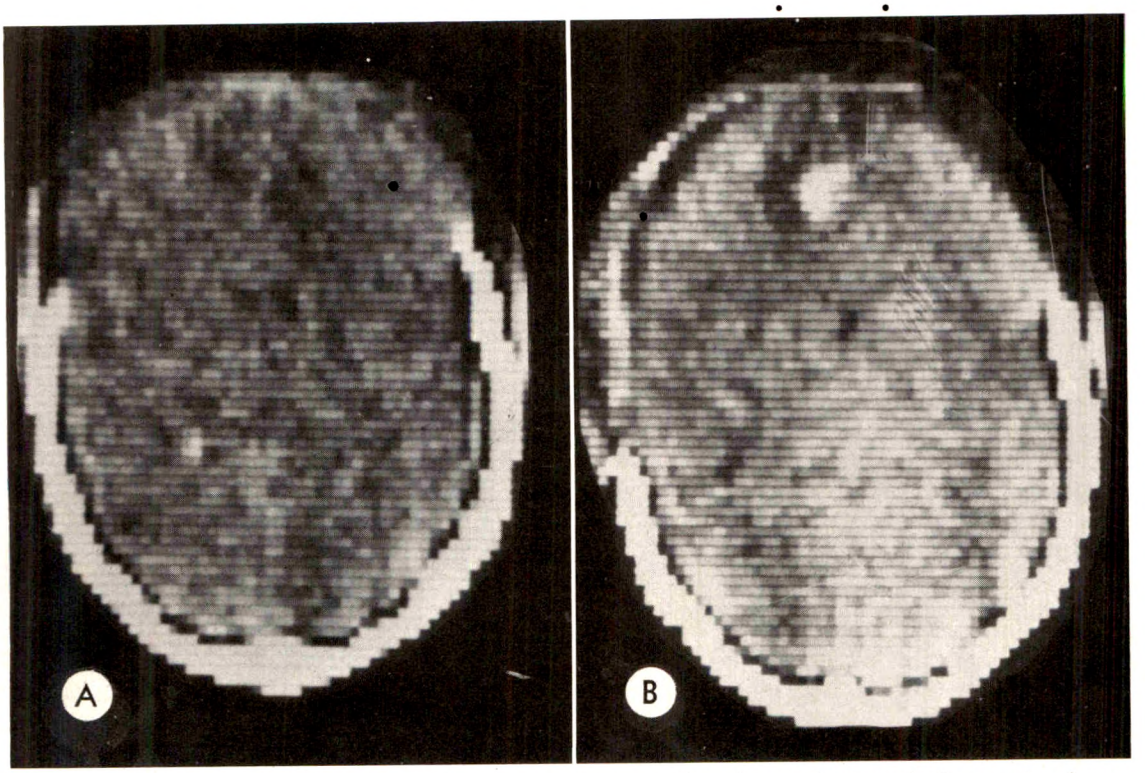


Fig. 7. Delayed intracerebral hematoma. A 30 year old male survivor from a plane crash. Operated on immediately because of depressed fracture of frontal bone; a frontal subdural hematoma was also removed. Patient in deep coma and decerebrate with fixed pupils. (*A*) CT three days post-trauma shows extensive and generalized edema with the ventricles almost completely obliterated and both frontal horns displaced posteriorly. (*B*) Twelve days post-trauma, a CT was repeated because of bulging of the flap. An intracerebral hematoma was readily seen in the midline, frontal region. The falx may be displaced to the left because of the extensive bilateral frontal craniectomy.

feriorly with low absorption supernatant fluid, and a fluid level between the two zones was clearly apparent. This may have represented acute hemorrhage into a chronic subdural hematoma or perhaps a phase in the evolution of a subdural hematoma (Fig. 11).

(e) *Intraventricular hematoma.* Intraventricular hematomas are clearly identified by computerized tomography because the high density lesion adopts the configuration of the ventricle forming a so-called "ventricular cast" (Fig. 12). Three cases are included in this series; two were closely related to an adjacent intracerebral hematoma; in one case it was the only abnormality visualized. It has been postulated that pure intraventricular hematomas following trauma are rare and that they may be related to unsuspected arteriovenous malformations in the ventricular walls which rupture following trauma. However, intraventricular bleeding could not be diagnosed except by ventricular puncture prior to the advent of computerized tomography and they probably are more common than previously suspected.

(f) *Subarachnoid hemorrhage.* Subarachnoid hemorrhage or hematomas were observed in two older patients; both also had extensive acute subdural and intracerebral hematomas (Fig. 13). The hematoma adopted the configuration of the cisternal spaces occupied by the blood.

(4) *Obstructive hydrocephalus.* Post-traumatic obstructive hydrocephalus is observed quite clearly by computerized tomography. Four patients in our series developed this complication, one of them as early as ten days after the traumatic epi-

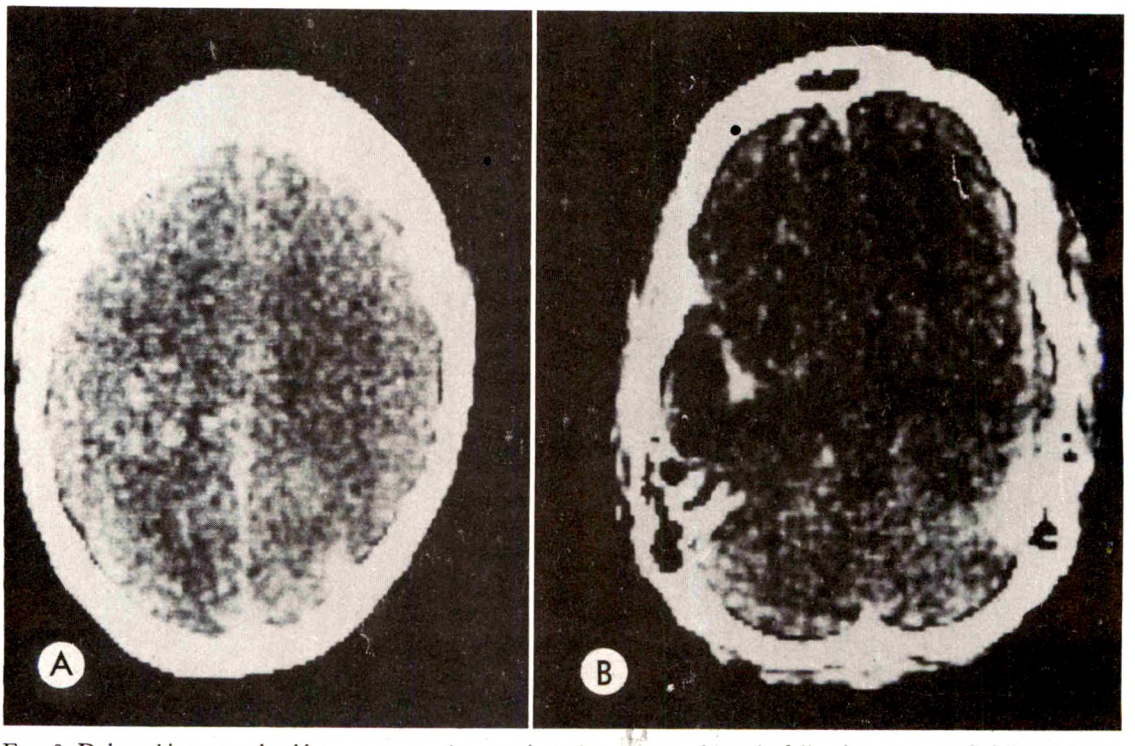


Fig. 8. Delayed intracerebral hematoma and contusion. An 18 year old male following an automobile accident became comatose with decerebrate posturing. (*A*) CT ten hours post-trauma showed a heterogeneous high absorption area in the left frontoparietal region interpreted as contusion with a slight midline shift. Patient's condition worsened and CT scan was repeated at 48 hours. (*B*) A left intratemporal hematoma was seen in addition to generalized swelling shown in a section 2.5 cm lower than (*A*). The area of contusion remained unchanged.

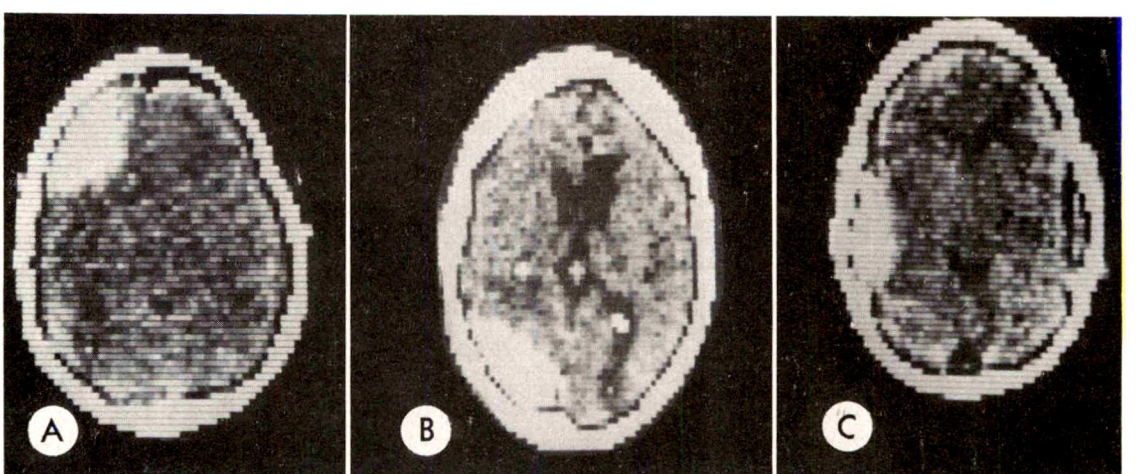


Fig. 9. (*A–C*) Epidural hematoma. Three examples in different locations: The hematomas are focal and limited by the attachments of the dura to the skull which gives them a characteristic biconvex appearance. Patients were 10, 43, and 31 years old respectively.

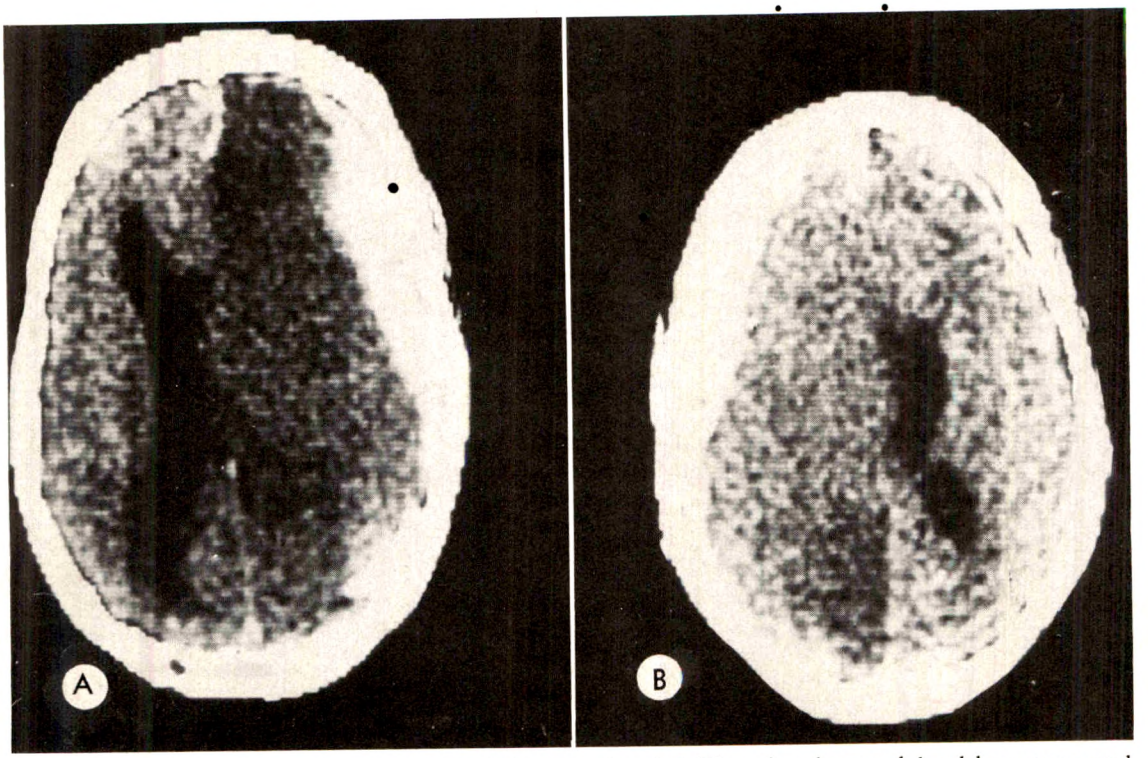


Fig. 10. Subdural hematomas, two characteristic examples. (*A*) There is a large subdural hematoma and severe diminished absorption of the right hemisphere with a midline shift, marked compression of the left lateral ventricle and bending of the falx anteriorly. Patient fell on occiput and was comatose on admission. He remained deeply comatose after removal of large epidural and subdural hematomas upon arrival to the hospital. (*B*) Large left subdural hematoma with pronounced shift of the midline to the right and low absorption in the left occipital region. Patient jumped from a bridge and was admitted to the emergency ward in deep coma, with fixed pupils and decerebrate posture. CT was done six hours after trauma.

sode (Fig. 14). There are no features that distinguish post-traumatic obstructive communicating hydrocephalus from other types. The CT characteristic features of hydrocephalus have been extensively described by others[1–3,7] and will not be further elaborated here.

(5) *Post-traumatic atrophy*. The changes of cerebral atrophy or loss of brain tissue are seen by computerized tomography as ventricular enlargement or as focal areas with abosrption values lower than that of normal brain, and only slightly higher than cerebrospinal fluid. Atrophic changes secondary to trauma cannot be distinguished from those associated with other conditions such as cerebral infarction. A discussion of post-traumatic atrophic changes is beyond the scope of this paper which deals primarily with the acute or subacute phases of head trauma.

Analysis of Clinical Material

Review of the medical records permitted the separation of the 100 cases of head trauma into six groups (Table 1).

In Group 1 the trauma to the head was considered as minimal. Confusion was present as the only clinical finding. In Group 2, patients had very brief periods of loss of consciousness, in the order of two to five minutes generally. No skull fracture was identified. At the time of CT scanning the patients had usually returned to normal except for headache and variable amnesia, in some cases. These patients were clinically diagnosed as having a concussion. Patients in Groups 3 and 4 had focal neurological findings in addition to alteration of the state of consciousness ranging from minutes to hours, with slow steady improvement passing from lethargy or obtundation to confusion and to alertness. In Group 3, pa-

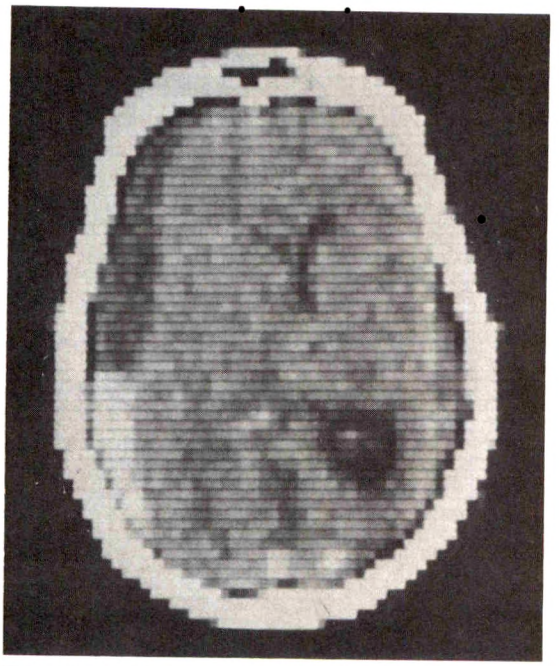


Fig. 11. Acute hemorrhage into a chronic subdural hematoma. A 77 year old female who was struck in the head two days prior to admission and became stuporous. CT shows a blood fluid level probably indicating acute bleeding into a chronic subdural hematoma, or a phase in the evolution of a chronic subdural hematoma.

tients were essentially neurologically intact after 24 hours, whereas in Group 4 the clinical picture lasted up to three or four days. The patients in these two groups were also diagnosed clinically as having a contusion.

Groups 5 and 6 were cases of severe head trauma; the categorization was made on the basis of the depth and duration of coma, the presence and duration of abnormal posturing, and of abnormal pupillary reactions. Patients in Group 5 were in critical condition and those who survived the injury were left with severe and permanent disability. These patients had prolonged coma for several weeks, deepening at the beginning and always with abnormal posturing for long intervals. Most patients in Group 6 had emergency surgery upon arrival in the hospital usually before computerized tomography; most of them died.

As can be seen, classification into six groups of clinical severity presents some problems including the lack of a very precise characterization of each group. It was designed mainly to determine if the clinical

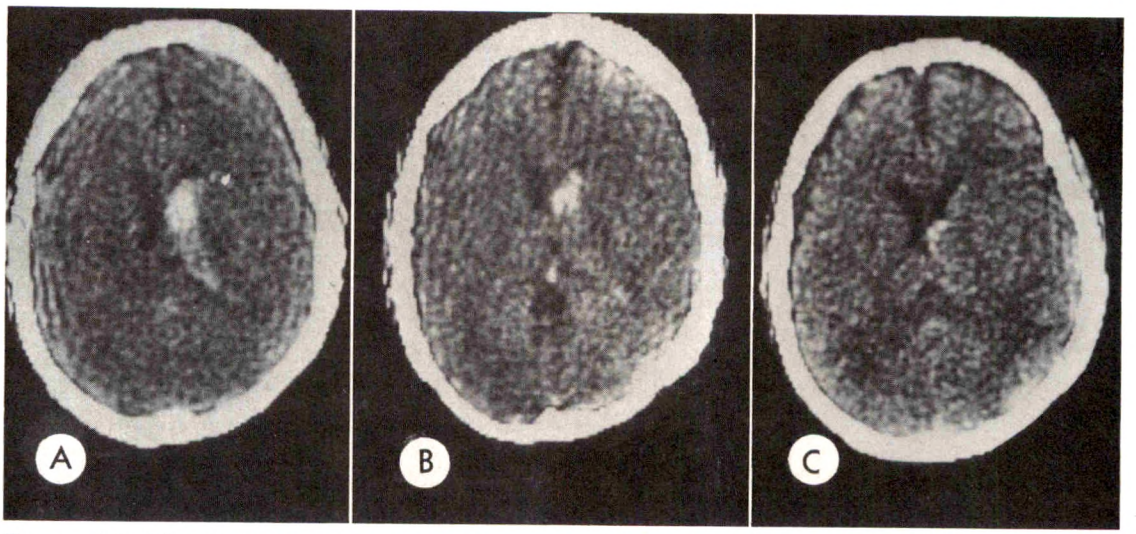


Fig. 12. (*A–C*) Intraventricular hematoma. Three serial CT scans were obtained at 2, 8, and 24 hours after trauma. The patient was in an automobile accident and was comatose with left hemiparesis. At two hours, (*A*) a hematoma is seen within the right lateral ventricle and no mass effect. At eight hours, (*B*) the hematoma had been partially "washed out" and the ventricles have decreased in size indicating diffuse swelling. At 24 hours, (*C*) there is only a small residue of the intraventricular hematoma, the ventricles are larger than in the first CT scan and there is a modest midline shift from right to left. The patient's condition did not change during the period of observation.

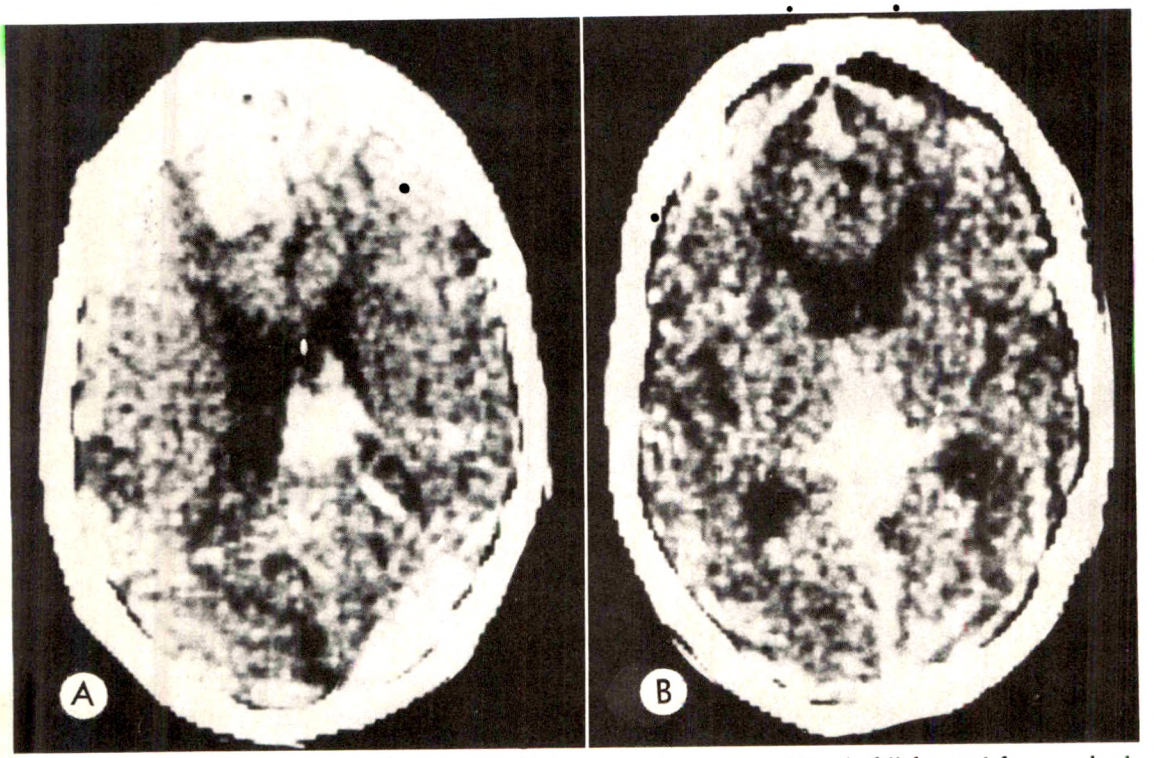


Fig. 13. Subarachnoid bleeding and intracerebral hematoma. An 80 year old male fell forward from a wheelchair and developed coma, a dilated right pupil, and a left Babinski response. Subarachnoid bleeding is seen in the quadrigeminal cistern. There is also a left frontal intracerebral hematoma (*A*); and a left frontotemporal subdural hematoma (*B*), and a hematoma against the falx in the right occipital region. An irregular area of diminished absorption (edema) in the left occipital region is present. The patient recovered.

severity of head trauma had a direct relationship to the variety of CT abnormalities identified.

RESULTS

Correlation between the severity of clinical signs and symptoms and the incidence of positive or negative CT scans is presented in tabular form in Figure 15. It can be observed that as the severity of clinical presentation progresses, the likelihood of having an abnormal CT scan increases pro-

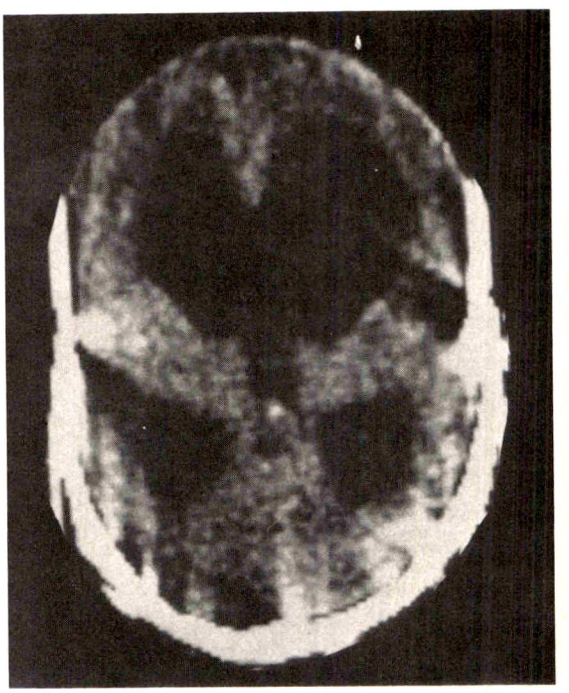


Fig. 14. Post-traumatic obstructive hydrocephalus. Severe obstructive hydrocephalus was present 2 1/2 months after trauma. An extensive craniectomy defect is seen in both frontal areas. The patient had been shunted but the shunt tube had to be removed one month prior to CT because of infection.

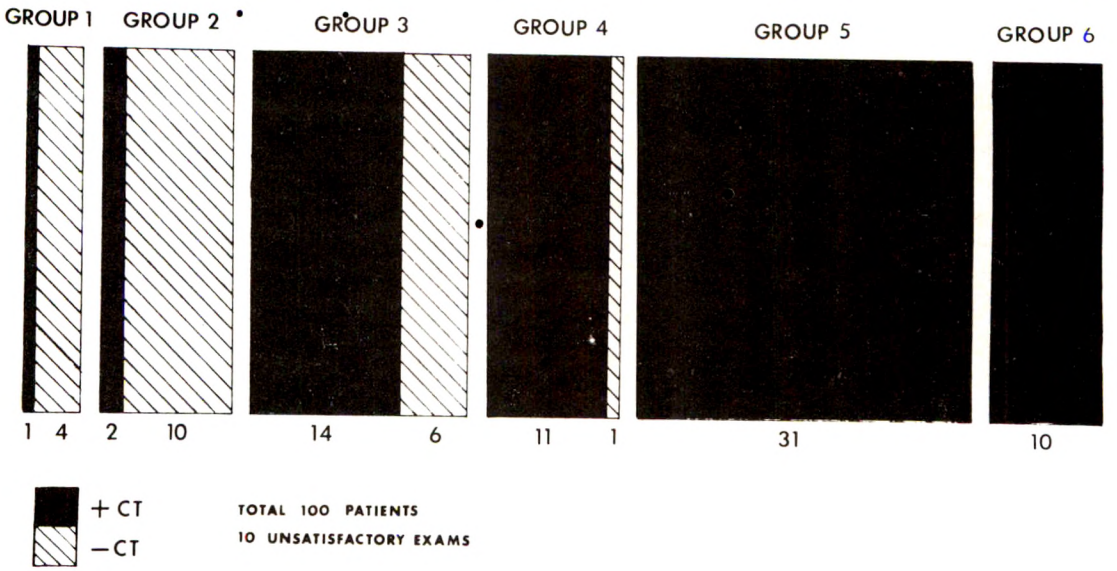


Fig. 15. CT in trauma. Incidence of positive and negative findings according to increasing severity of clinical manifestations.

portionately. In Group 3, usually diagnosed as cerebral contusion on clinical grounds, 14 of 20 cases (70 percent) had an abnormal CT scan and exhibited unilateral abnormalities to account for the focal neurological findings, such as edema of various degrees, contusion, or localized hematomas. In six cases the CT scan was entirely normal. This is felt to be a reflection of the limitation of CT scanning which was unable to detect an abnormality even in the presence of lateralizing clinical findings. In Groups 1 and 2, the vast majority of patients had normal CT scans although three patients were seen (one in Group 1, two in Group 2) with mild focal edema which did not produce lateralizing clinical findings. In Groups 5 and 6, 100 percent of cases were abnormal. In Group 4 the one patient that did not show an abnormality on computerized tomography was in the postoperative period after total removal of a small epidural hematoma. Therefore one could expect to demonstrate abnormalities in every patient in Groups 4, 5, and 6.

The correlation between the severity of clinical presentation and the number and intensity of abnormalities visualized at computerized tomography showed a linear relationship and again one can expect a larger number of lesions and more severe abnormalities as the severity of clinical presentation increases (Fig. 16).

The CT findings were classified as:

Minor
  Local area of edema.
Moderate
  (a) Edema, up to a third of a hemisphere, possibly with slight midline shift.
  (b) Local area of contusion.
Major
  (a) Severe unilateral edema (more than half of a hemisphere).
  (b) Hemorrhages in any location.
  (c) Pronounced midline dislocation.

Ten computerized tomograms were technically unsatisfactory due to motion and no diagnostic information could be obtained. In these cases angiography was carried out.

In several patients when the first pair of scans was of poor technical quality, proper sedation was extremely helpful in obtaining repeat CT scans of good quality. This made other diagnostic procedures unnecessary and either surgical or medical treatment

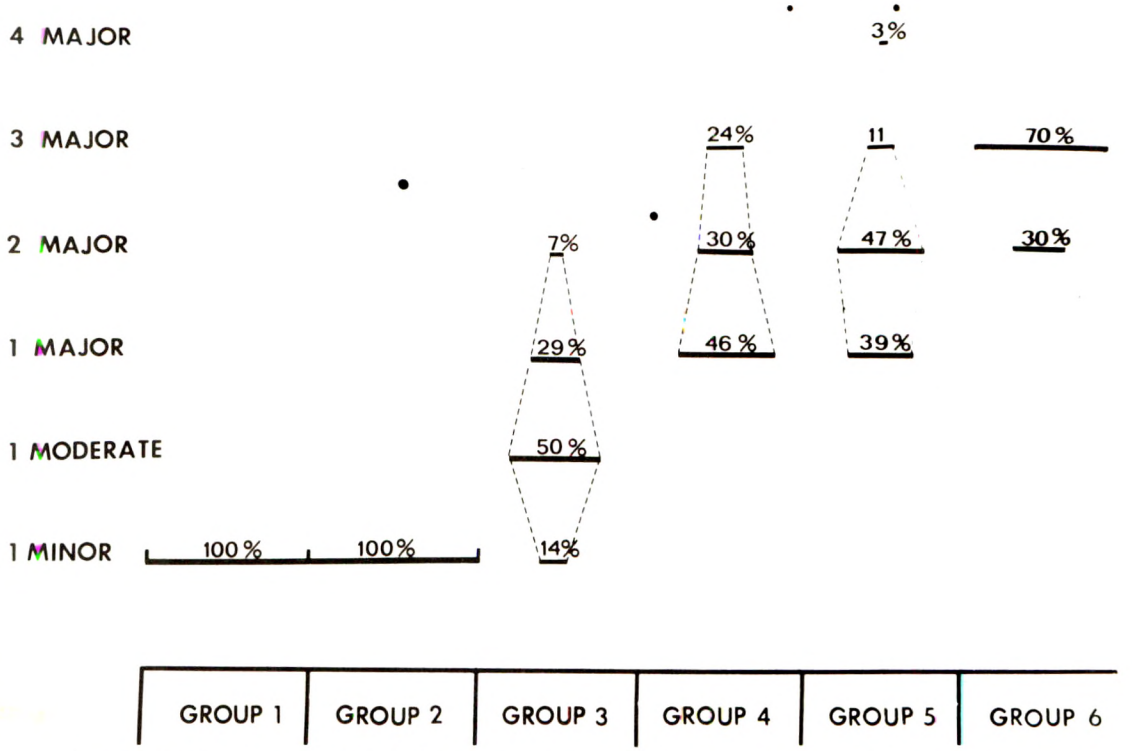


FIG. 16. Relation of severity of clinical manifestations to number and severity of CT findings.

could be instituted on the basis of the CT. At present the new short-acting barbiturates (*e.g.*, Brevital*) are employed in those patients in whom the alteration of the state of consciousness and, specifically, restlessness or agitation would make computerized tomography unlikely to yield satisfactory results. The low risk of administering sedation is fully compensated by the ability to make the pertinent observations necessary for patient management.

DISCUSSION

Computerized tomography has provided a most significant new approach to diagnostic evaluation of the patient with trauma to the brain and its coverings. Providing that a CT scan of good quality is obtained, it is possible to arrive at a diagnosis, and, in the vast majority of cases, other neuroradiological diagnostic procedures will not be necessary, excepting the plain film survey.

* Eli Lilly and Company.

In good quality CT scans the different tissue abnormalities produced by trauma to the brain and its coverings are easily observed including occasionally the subtle changes of mild focal edema. These changes can be subdivided in relation to their average absorption values as follows:

1. Lesions with average absorption value lower than that of normal brain tissue:
   (a) Edema of various degrees, (b) Chronic subdural hematoma and hygroma, (c) Post-traumatic atrophic changes, and (d) Obstructive hydrocephalus.
2. Lesions with average absorption value similar to normal brain or indistinguishable from surrounding brain:
   (a) Generalized diffuse edema
3. Lesions with average absorption greater than normal brain tissue:
   (a) Contusion and laceration
   (b) Hematomas (cortical, subcortical, intracerebral, intraventricular, epidural, acute subdural, fresh hemor-

rhage into a chronic subdural collection, subarachnoid)

With the possible exception of mild focal edema, the significant difference in absorption values in all the other lesions, especially those containing extravasated blood, is obvious, and in this series were accompanied by a secondary mass effect, also easily recognizable.

As has been stressed several times in this presentation good immobilization of the patient is necessary to obtain a good quality CT scan because motion causes deterioration of the image with resulting loss of diagnostic information. The newly developed Patient Movement Control System (PMC) produced by EMI, Ltd., is helpful in eliminating some of the artifacts produced by movement, but not all, and especially so when motion is marked. In addition, the PMC system requires a longer scanning time (6 1/2 minutes and 225° arc of scan instead of the routine 4 minutes and 50 seconds—180° scan), which in head trauma may further complicate the problem associated with motion. Up to the present time no useful fixation device suitable for the agitated patient has been developed, and sedation is, therefore, required.

Sequential CT scans are very helpful in the follow-up of the post-traumatic patient because they permit evaluation of the tissue changes in relation to time. Important observations on the natural evolution of edema can be made, and immediate postoperative CT scans are of value to ascertain the results of surgery. Computerized tomography can be repeated as necessary due to the non-invasive nature of the procedure and the low dose of radiation involved.

The authors have observed the development of edema 48 hours after trauma in several patients having initially unremarkable CT scans. In one patient, shown in Figure 12, with an intraventricular hematoma of moderate size at four hours, the hematoma had been partially "washed out" at twelve hours, associated with decrease in size of the ventricular system indicative of diffuse swelling. By 24 hours, the intraventricular hematoma was only faintly visualized, but edema had progressed on one side as shown by midline dislocation (Fig. 12). It is anticipated that sequential scanning of these patients will yield many more observations regarding the natural evolution of the tissue changes induced by trauma.

Juan M. Taveras, M.D.
Department of Radiology
Massachusetts General Hospital
Boston, Massachusetts 02114

ADDENDUM:

Since this report was submitted, several cases of bilateral subdural hematomas have been encountered where the diagnosis was not made on CT scans.

REFERENCES

1. Ambrose, J. Computerized x-ray scanning of brain. *J. Neurosurg.*, 1974, *40*, 679–695.
2. Ambrose, J. Computerized transverse axial scanning (tomography): Part 2. Clinical application. *Brit. J. Radiol.*, 1973, *46*, 1023–1047.
3. Baker, H. L., Campbell, J. K., Houser, D. W., Reese, D. F., Sheedy, P. K., Holman, C. B., and Kurland, R. L. Computer assisted tomography of head. *Mayo Clin. Proc. Staff Meet.*, 1974, *49*, 17–27.
4. Baratham, G., and Dennyson, W. G. Delayed traumatic intracerebral hemorrhage. *J. Neurol., Neurosurg. & Psych.*, 1972, *35*, 698–706.
5. Foltz, E. L., and Ward, A. A. Communicating hydrocephalus from subarachnoid bleeding. *J. Neurosurg.*, 1956, *13*, 546–566.
6. Morin, M. A., and Pitts, F. W. Delayed apoplexy following head injury (Traumatische Spat-Apoplexie). *J. Neurosurg.*, 1970, *33*, 542–547.
7. New, P. F. J., Scott, W. R., Schnur, J. A., Davis, K. R., and Taveras, J. M. Computerized axial tomography with EMI scanner. *Radiology*, 1974, *110*, 109–123.
8. Plum, E., and Posner, J. Diagnosis of Stupor and Coma. Contemporary Neurology Series, F. A. Davis, Co., Philadelphia, 1960.
9. Scott, W. R., New, P. F. J., Davis, K. R., and Schnur, J. A. Computerized axial tomography of intracerebral and intraventricular hemorrhage. *Radiology*, 1974, *112*, 73–80.

VOL. 126, No. 4

INDIVIDUALIZED COMPUTER TOMOGRAPHY OF THE SKULL WITH THE EMI SCANNER USING THE 160 × 160 MATRIX*

By STEVEN H. CORNELL, M.D., JACOB J. MUSALLAM, M.D., CHING L. CHIU, M.D., *and* JAMES H. CHRISTIE, M.D.
IOWA CITY, IOWA

ABSTRACT:

The individualized approach to the performance of computerized tomography of the skull is described. With the use of the 160×160 matrix it is possible to look at the initial scans almost immediately after their completion. If necessary, unsatisfactory scans can be repeated, the position of the head can be changed and artifacts due to motion can be minimized or eliminated. Lesions can be revealed or enhanced with intravenously injected contrast material if desired. The individualized approach has eliminated the need to recall patients and has improved the diagnostic capability of the method.

THE computer programming of the EMI scanner was changed by the manufacturer so that 160×160 absorption coefficients are obtained instead of the original 80×80. This modification was made at our hospital in October, 1974 and the resolution of the images has been greatly improved. In addition the time between completion of the scanning procedure and viewing the results on the cathode ray tube has been reduced from approximately 20 minutes to under 30 seconds. It is therefore possible to view the scans while the patient is still present and obtain more sections if desired. It is our current practice to make routine scans at four levels (eight slices) with the roentgen-ray beam angled 15–20 degrees to the orbitomeatal line. While the patient is still on the table, the clinical records are examined and the EMI scans are viewed. In many cases the initial set of scans is judged adequate and nothing further is done. Because of problems in positioning or motion, some of the sections may be unsatisfactory and can be repeated immediately, with intravenous sedation if necessary. If contrast material is injected, a decision is made as to which levels should be repeated since it is generally not necessary to repeat the entire study.

This individualized approach has been extremely helpful and has eliminated the need to recall patients. Abnormalities which were initially seen poorly or not at all have been demonstrated by these modifications.

TECHNICAL PROBLEMS

Insufficient number of sections: Occasionally the patient is positioned in the machine so that the base of the skull or the top of the head is not included on the first set of scans. Additional sections are obtained in these cases.

Improper positioning: The head may be tilted from side to side, resulting in a scan of poor quality with artifactitious densities, especially close to the base. This can be remedied by repeating the scan with the head straight (Fig. 1).

Occasionally a lesion can be shown to better advantage by raising or lowering the chin, thereby changing the angle of the beam. Good demonstration of the posterior fossa requires the head to be flexed, a difficult position to maintain for some patients.

Artifacts: Dense streaks tangential to the side of the head are frequently present and

* Presented at the Seventy-sixth Annual Meeting of the American Roentgen Ray Society, Atlanta, Georgia, September 30–October 3, 1975.
From the Department of Radiology, University of Iowa Hospitals and Clinics, Iowa City, Iowa.

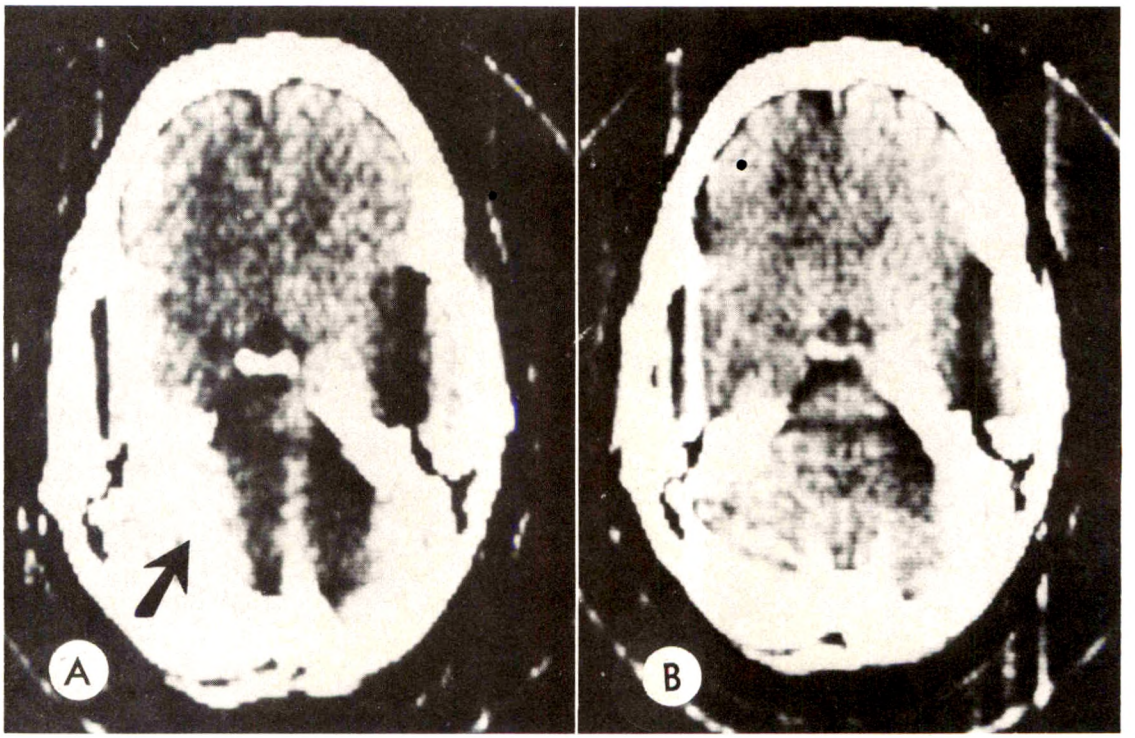


Fig. 1. Correction of head position. (*A*) The head is tilted and an area of increased density is present posteriorly (arrow). This could be misinterpreted as a mass but actually represents the higher floor of the left posterior fossa. (*B*) The posterior fossa looks normal and symmetrical after correction of the head tilt.

may present a problem in the evaluation of patients with possible extracerebral fluid collections. In this situation the head is purposely rotated to one side so that the streaks are projected at a different angle to the skull (Fig. 2). Other artifacts which present problems can sometimes be eliminated merely by repeating the unsatisfactory section.

Motion: Any movement of the head seriously impairs the quality of the scan. This can be partially overcome with the "patient motion control" modification, a recent addition to the EMI scanner. The roentgenographic tube is rotated about the head 225 degrees instead of 180 degrees and more absorption values are analyzed, thereby "smoothing out" the image (Fig. 3). The "patient motion control" device is used only in selected cases as it adds one and one-half minutes to each pair of sections.

Various head holding devices have been developed. We routinely use the Neurological Institute headholder* which stabilizes the chin and the sides of the face.

Some patients, particularly infants and children, require sedation and we have found that diazepam is quite satisfactory for this purpose (Fig. 4). The dose is individualized but 10 mg intravenously is usually adequate for the average adult.

CONTRAST ENHANCEMENT

When the initial set of scans is diagnostic no contrast material is injected. This is usually the case in intracerebral hemorrhage, diffuse cerebral atrophy, hydrocephalus in infants and some adults, and in patients who are being followed to see changes in ventricular size. In patients with psychiatric problems, generalized seizures, chronic headaches, or head injury, no contrast material is injected if the initial

* H and I Instrumentation, Teaneck, New Jersey.

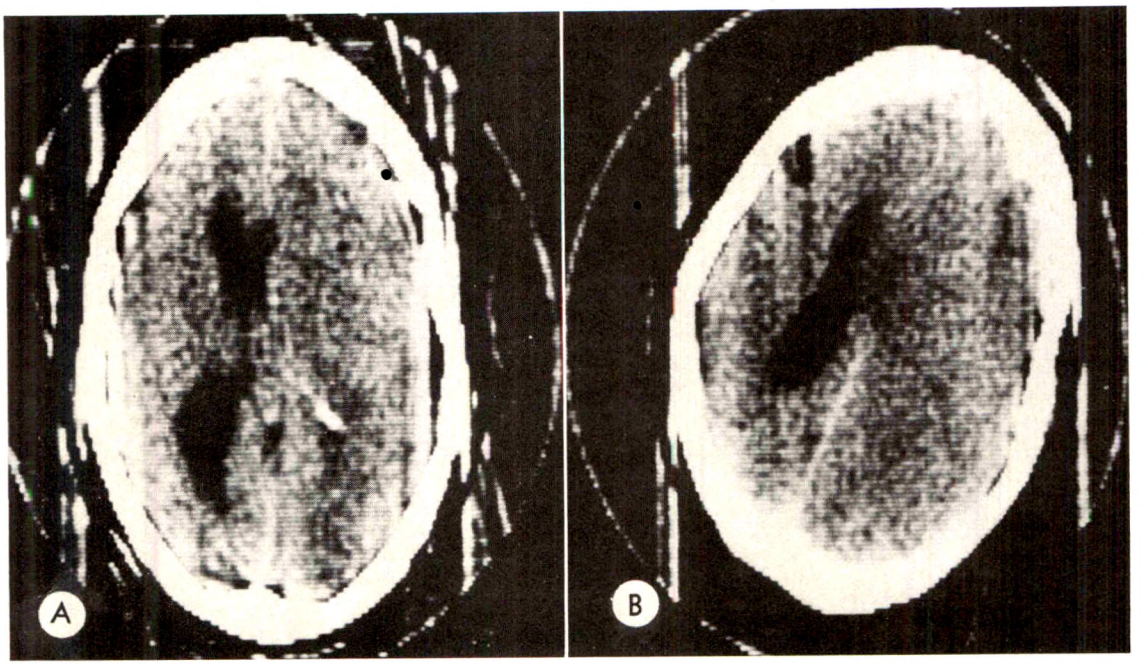


Fig. 2. Purposeful rotation of the head. (*A*) Vertical streaks are projected inside the skull in this patient with a proved right subdural hematoma. The ventricles are displaced to the left and the right lateral ventricle is compressed. (*B*) The head has been turned to the right and the vertical streaks no longer project inside the cranium. The subdural hematoma in this case has the same density as adjacent brain and is therefore not visible.

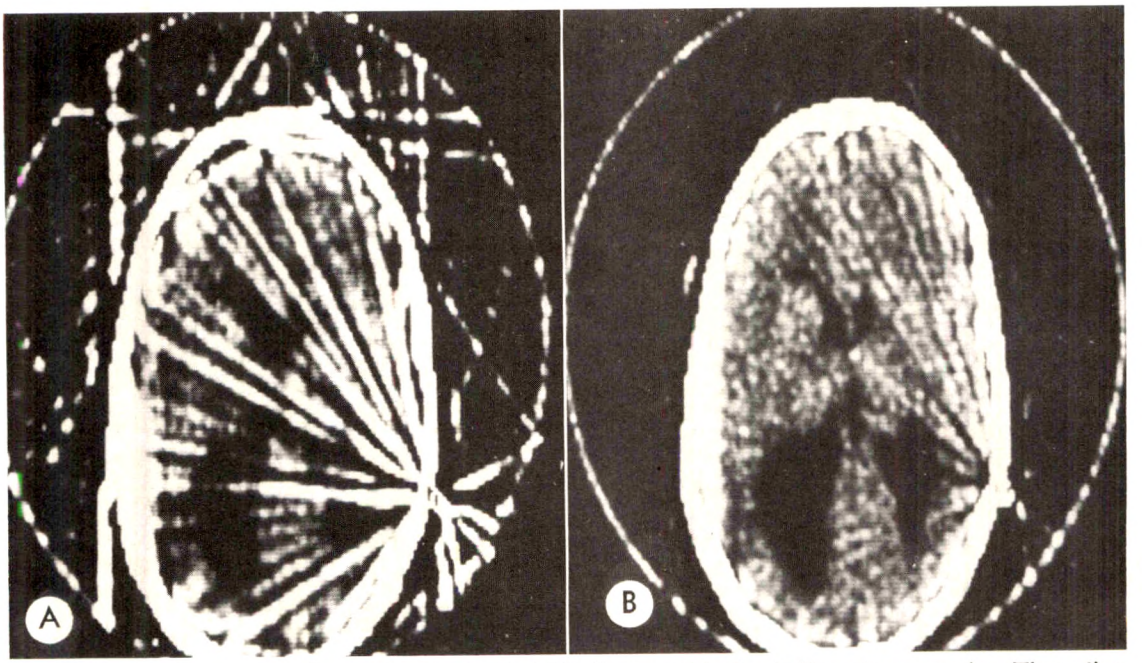


Fig. 3. Use of the patient motion control device. (*A*) The lines outside the skull are due to motion. The radiating streaks inside the skull are produced by a metallic shunt valve in this patient with question of shunt failure. (*B*) With the patient motion control device most of the artifacts have been eliminated. Dilated posterior horns are now well seen.

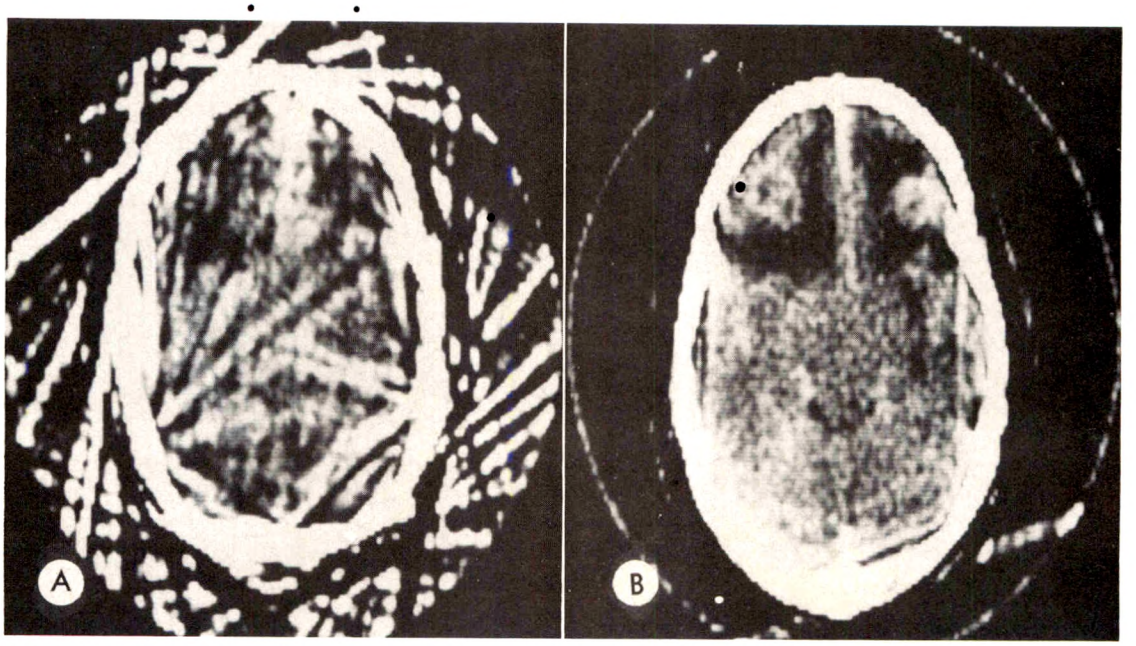


Fig. 4. Use of sedation and intravenous contrast material. (*A*) The scan is totally unsatisfactory because of patient movement. (*B*) Following intravenous injection of 10 mg diazepam and 50 ml 76 percent Renografin, an abnormal spherical density surrounded by an area of lucency is visible in each frontal lobe. These proved to be abscesses surrounded by edema.

examination is completely normal.

We inject 50 ml of 76 percent Renografin intravenously in the average adult and repeat the scans immediately at selected levels on patients with the following problems: (1) Suspicion of primary or metastatic neoplasm. Occasionally these lesions will be shown only after injection of contrast material (Fig. 5). Even when a mass is seen on the plain scans the contrast enhanced examination may show it much better. The solid and cystic components of a tumor can be differentiated, and this may help the surgeon in deciding where to biopsy the lesion. (2) Suspicion of brain abscess. The wall of an abscess may be shown dramatically after contrast material injection (Fig. 6). (3) Differentiation between infarction and tumor. With the amount of contrast material we are using, infarctions usually do not opacify. Some tumors do not light up either and therefore failure to opacify is not useful in the differentiation of these conditions. (4) Suspicion of intracranial aneurysm or vascular malformation. With the equipment in current use only quite large aneurysms (one centimeter in diameter or larger) are demonstrable. Vascular malformations are seen much better after injection of contrast material (Fig. 7). Table 1 summarizes our experience with injection of contrast material since the introduction of the new matrix in October 1974, through August 1975. During this period 1,482 examinations were done and contrast-enhancement was used in 407 instances.

It is noteworthy that of 117 neoplasms, 58 (50 percent) were seen better after injection of contrast material. In many of these cases there was suspicion of abnormality on the initial sections but the lesion was shown much better with contrast enhancement. In 13 cases (eleven percent) the tumor was seen only after contrast material injection. This group consisted of three acoustic neuromas, three gliomas, two meningiomas, and five cases of cerebral metastases. All aneurysms and vascular malformations were seen better with contrast enhancement and this was also true in four cases of cerebral abscess. However

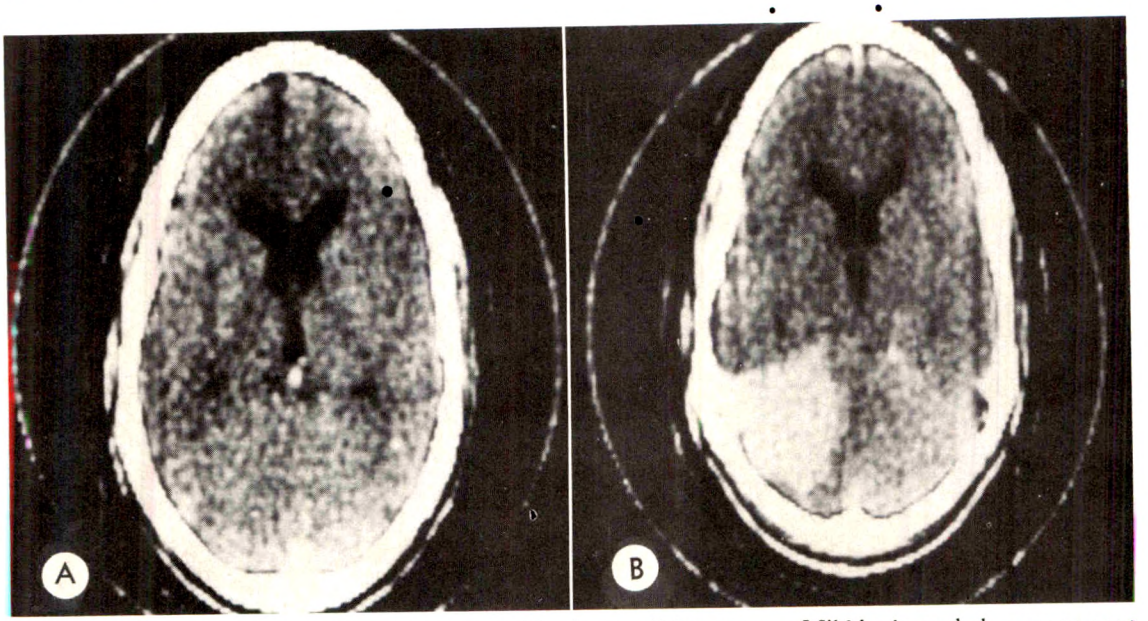


Fig. 5. Use of contrast material in neoplasm. (*A*) No abnormalities are seen. Mild hydrocephalus was present on other sections. (*B*) After intravenous injection of 50 ml 76 percent Renografin, an abnormal density becomes evident in the left posterior fossa. This proved to be a cerebellar astrocytoma.

contrast material was not injected in all cases of abscess.

Although the number of cases studied with and without contrast enhancement since the new matrix was begun is not extremely large it is clear that contrast material is most useful in demonstrating suspected neoplasms, abscesses and vascular lesions.

Some workers use larger volumes of con-

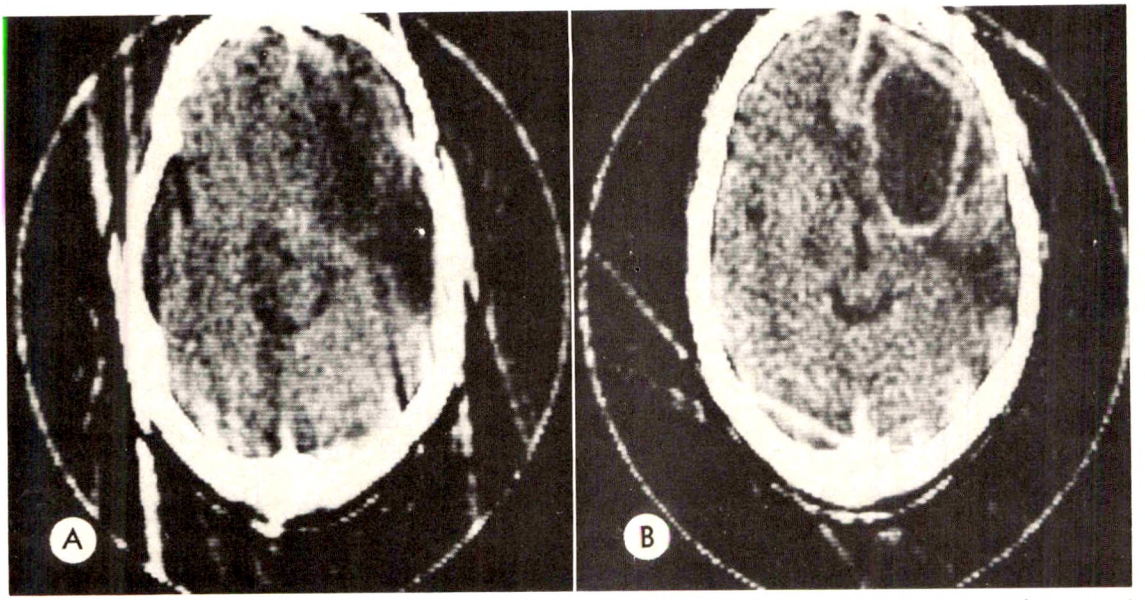


Fig. 6. Use of contrast material in suspected brain abscess. (*A*) There is a poorly defined area of decreased density in the right frontal lobe, probably due to edema. (*B*) A large abscess with a well defined wall becomes evident after intravenous injection of contrast material.

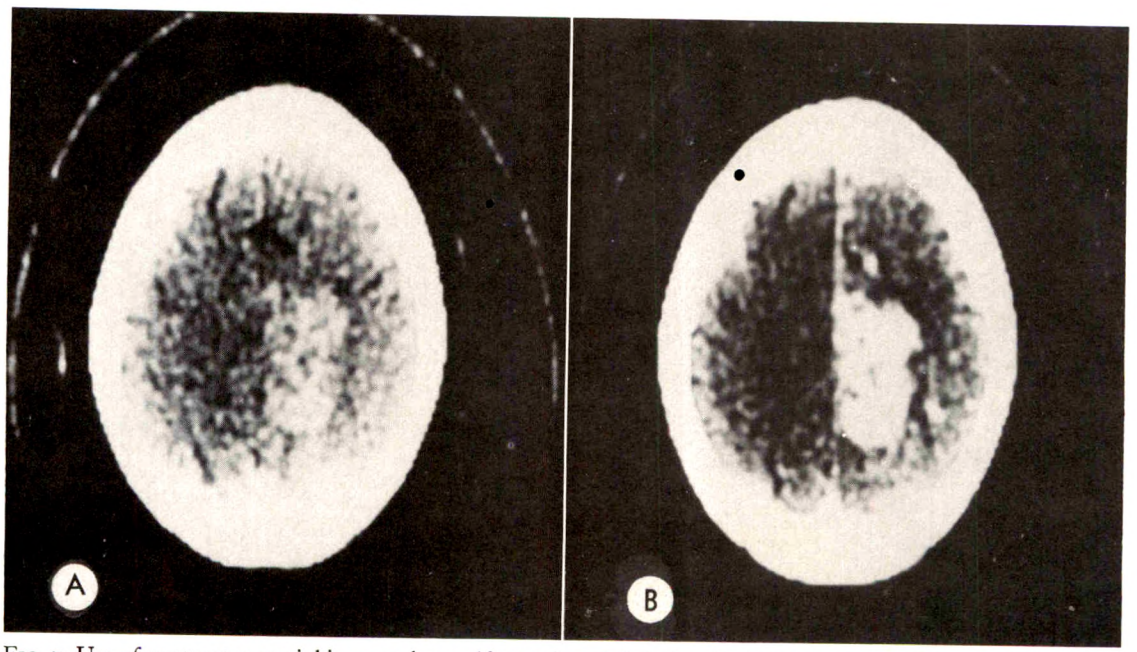


Fig. 7. Use of contrast material in vascular malformation. (*A*) A sizeable but faint area of abnormal density is visible in the right hemisphere. (*B*) After intravenous injection of contrast material there is much better visualization of the lesion and its irregular nature can be appreciated. This proved to be a large arteriovenous malformation at angiography.

trast material either undiluted or by the drip infusion method.[4] Because of time limitations we have not used drip infusion as it takes considerably longer than a simple injection. It is possible that we have missed some lesions which would have been shown with larger volumes of contrast medium but we are not aware of such a case to date. Therefore it is our opinion that 50 ml of 76 percent Renografin, which contains 18.5 grams of organic iodine, is an adequate dose of contrast material for the average adult patient. Obviously any contrast material with an equivalent amount of organic

Table I

ANALYSIS OF 407 CASES INJECTED WITH 50 ML 76 PERCENT RENOGRAFIN

	Total	Tumor*	Vascular Malformation	Abscess	Aneurysm	Negative Examination	Infarction*	Atrophy	Hydrocephalus	Diagnosis Uncertain	Porencephaly	Cerebral Hemorrhage	Subdural Hematoma	Cerebral Edema	Cerebral Calcification
No contrast enhancement	323	46	—	—	—	177	27	20	15	21	4	6	4	2	1
Lesion seen better after contrast medium	69	58	6	4	1	—	—	—	—	—	—	—	—	—	—
Lesion seen only after contrast medium	15	13	2	—	—	—	—	—	—	—	—	—	—	—	—

* Proved or highly probable.

iodine should be satisfactory.

Steven H. Cornell, M.D.
Department of Radiology
University of Iowa Hospitals and Clinics
Iowa City, Iowa 52242

ADDENDUM:

Since this article was submitted, the amount of 76 percent Renografin injected in adults has been adjusted according to weight as follows: up to 120 lbs, 50 ml; 120–170 lbs, 75 ml; 170–220 lbs, 100 ml; over 220 lbs, 125 ml.

REFERENCES

1. Baker, H. L., Jr., Campbell, J. K., Houser, O. W., and Reese, D. F. Early experience with EMI scanner for study of brain. *Radiology*, 1975, *116*, 327–333.
2. Cornell, S. H., Christie, J. H., Chiu, C. L., and Lyon, L. W. Computerized axial tomography of cerebral ventricles and subarachnoid spaces. Am. J. Roentgenol., Rad. Therapy & Nuclear Med., 1975, *124*, 186–194.
3. Davis, D. O., and Pressman, B. D. Computerized tomography of brain. *Radiol. Clin. North America*, 1974, *12*, 297–313.
4. Kramer, R. A., Janetos, G. P., and Perlstein, G. Approach to contrast enhancement in computed tomography of brain. *Radiology*, 1975, *116*, 641–647.
5. New, P. F. J., Scott, W. R., Schnur, J. A., Davis, K. R., and Taveras, J. M. Computerized axial tomography with EMI scanner. *Radiology*, 1974, *110*, 109–123.
6. New P. F. J., Scott, W. R., Schnur, J. A., Davis, K. R., Taveras, J. M., and Hochberg, M. D. Computed tomography with EMI scanner in diagnosis of primary and metastatic intracranial neoplasms. *Radiology*, 1975, *114*, 75–87.
7. Paxton, R., and Ambrose, J. EMI scanner: brief review of first 650 patients. *Brit. J. Radiol.*, 1974, *47*, 530–565.
8. Pressman, B. D., Kirkwood, J. R., and Davis, D. O. Computerized transverse tomography of vascular lesions of brain. Part I: arteriovenous malformations. Am. J. Roentgenol., Rad. Therapy & Nuclear Med., 1975, *124*, 208–214.
9. Pressman, B. D., Gilbert, G. E., and Davis, D. O. Computerized transverse tomography of vascular lesions of brain. Part II: aneurysms. Am. J. Roentgenol., Rad. Therapy & Nuclear Med., 1975, *124*, 215–219.

COMPUTED TOMOGRAPHY OF THE NORMAL AND INFARCTED MYOCARDIUM*

By DOUGLASS F. ADAMS,† SAMUEL J. HESSEL,‡ PHILIP F. JUDY,†
JAY A. STEIN,§ *and* HERBERT L. ABRAMS†
BOSTON AND CAMBRIDGE, MASSACHUSETTS

ABSTRACT:

After intravenous administration of contrast agent, *in vitro* cardiac scanning showed a significant difference between the attenuation coefficients of the intracavitary blood pool and the myocardial wall, permitting clear delineation of the ventricular cavity. A substantial alteration in hematocrit permitted similar visualization of the intracavitary blood pool–myocardial wall interface. The attenuation coefficient of infarcted myocardium differed sufficiently from that of normal myocardium to render computed tomographic distinction feasible. In three hour old infarctions, the differences between normal and ischemic or infarcted tissue were enhanced by prior administration of contrast agent. These differences in attenuation coefficient indicate that a properly gated CT scanner could be utilized as a noninvasive approach to evaluating suspected or known myocardial infarction and other aspects of cardiac structure and function both in man and in experimental animals.

THE development and clinical introduction of computed tomography (CT)[1,2] have provided a unique opportunity for the study of natural and pathologic processes in various organs during life. Since its initial application to the brain,[1,3] the technology has advanced to a point where whole body CT scanning is now feasible.[4,5] The potential of the method for detecting and delineating intra-abdominal and intrathoracic abnormalities is now under investigation.[4,6–8] Little emphasis has been placed on CT scanning of the heart, perhaps because of the rapidity of cardiac motion and the clear evidence that motion blurring degrades computed tomographic images. Nevertheless the possibility of delineating the blood–myocardial wall interface and the presence of infarcted muscle seemed worthy of investigation in postmortem hearts. Our preliminary experience with *in vitro* scanning supported the feasibility of this approach.[17]

MATERIAL AND METHOD

Four normal mongrel dogs weighing 14–35 kg were sacrificed immediately after intravenous administration of 5,000 units of aqueous heparin. A fifth dog was made acutely anemic by withdrawal of approximately 300 cm^3 of blood and administration of 600 cm^3 of dextran. After equilibration for 30 min, the hematocrit dropped from 49 to 26. He was then sacrificed. An additional animal received 1 cm^3/kg of meglumine diatrizoate and sodium diatrizoate 37% iodine (Renografin-76, Squibb, Princeton, N.J.) five minutes prior to death.

Myocardial infarctions were created in four anesthetized dogs by embolization of a radiopaque polyethylene plug into the left anterior descending coronary artery under fluoroscopic control.[9] Two days later, the animals were sacrificed immediately following the intravenous administration of 5,000 units of aqueous heparin. Two other animals had their hearts exposed and occlusive sutures placed around the proximal left anterior descending coronary artery. Three hours after occlusion, 1 ml/kg of Renografin-76 and 5,000 units of aqueous heparin were administered intravenously. After two minutes the animals were sacrificed.

The hearts of all twelve dogs were excised after ligation of the vena cavae, hilar pulmonary arteries and veins, and aorta. Specimens were shaken and placed in a horizontally oriented

* This work was supported in part by U.S. Public Health Service grants GM18674, HL11668, and HL05832.
† Department of Radiology, Harvard Medical School, Peter Bent Brigham Hospital, Boston, Massachusetts.
‡ James Picker Foundation Fellow in Academic Radiology.
§ American Science and Engineering, Inc., Cambridge, Massachusetts.

divided plastic container. The posterior aspect of the heart was lying on the plastic divider. The heart was in the horizontal plane, while the x-ray beam rotated in a vertical plane, perpendicular to the long axis of the specimen. The base of the heart was in the deeper portion of the container and the apex toward the cover. Two silk sutures attached the heart to the edge of the plastic divider to prevent change in its orientation. The container was then filled with 0.9% NaCl and fitted snugly into the head cap of the EMI CT head scanner (EMI Medical, Inc., Northbrook, Ill.) The hearts were scanned within one hour of sacrifice at 120 or 140 kVp. Slice thicknesses were 8 mm or 13 mm.

RESULTS

Blood–Myocardial Wall Interface

Scans of representative areas of the myocardial wall in normal hearts had uniform EMI values of 26.0 ± 0.6 EMI units (mean ± SEM), where 1 EMI unit corresponds to approximately a 0.2% difference in x-ray attenuation coefficient compared to water.[10] In these animals the intracavitary blood pool values were 26.2 ± 1.0 EMI units. There was no consistent delineation of the blood–myocardial wall interface (Fig. 1). When the hearts were allowed to stand for a protracted interval, the red blood cells settled to the dependent portion of the ventricular cavity, which became denser than the myocardial wall. The plasma in the upper portion of the cavity was less dense than the myocardium, having an EMI value of 12.7 ± 0.3 EMI units.

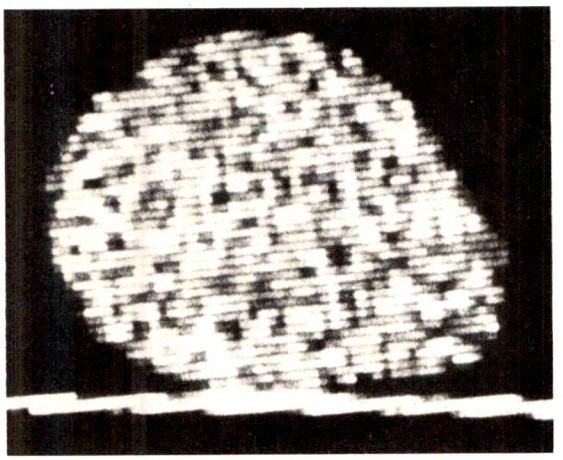


Fig. 1. Section at ventricular level of normal heart with no contrast agent given showing uniform absorption. EMI values of myocardium and blood were 26.0 ± 0.6 and 26.2 ± 1.0 EMI units, respectively.

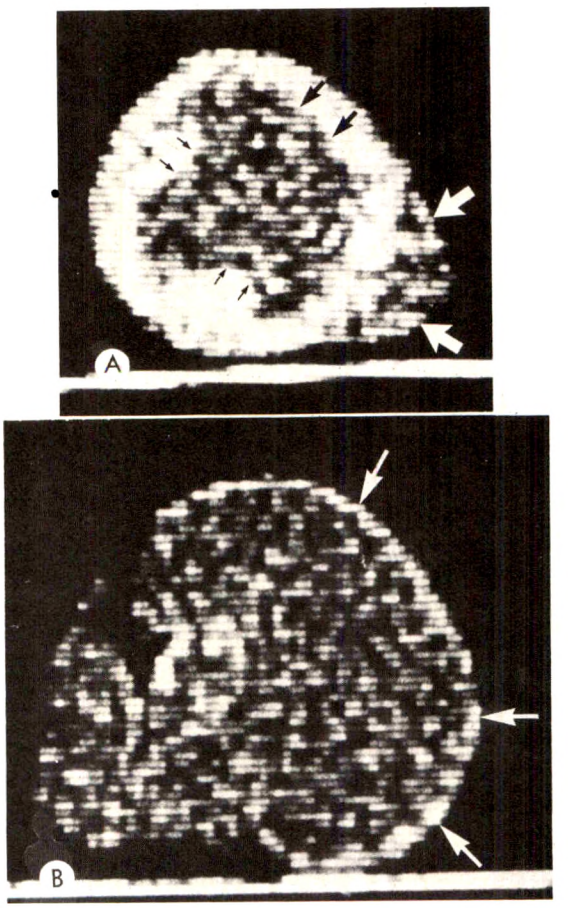


Fig. 2. (*A*) CT scan of normal heart near left ventricular apex of an acutely anemic dog. Note blood–myocardial wall interface (large closed arrows) and details of papillary muscles (small closed arrows). Only a small portion of right ventricle is visible at this level (open arrows). (*B*) CT scan through right ventricle and atrial structures. Note thin right ventricular wall (arrows).

The acutely anemic dog showed the blood–myocardial wall interface clearly (Fig. 2). The wall had an attenuation coefficient of 27.1 ± 1.0 EMI units, while the attenuation coefficient of the intracavitary blood pool was 21.4 ± 1.0 EMI units.

Administration of contrast agent prior to sacrifice resulted in an intracavitary blood pool attenuation coefficient of 43 ± 1 EMI units, compared to a myocardial attenuation coefficient of 33 ± 1 EMI units, with

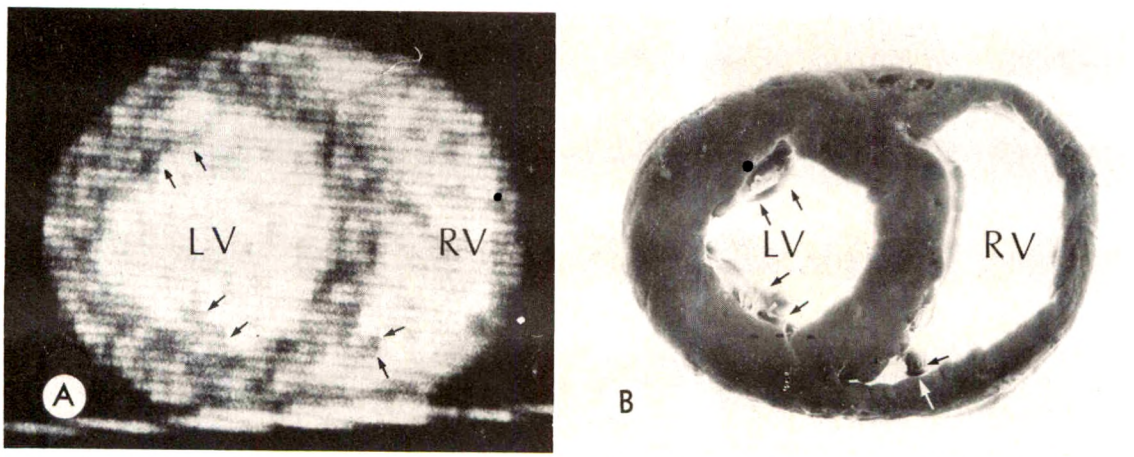


FIG. 3. (*A*) CT scan of normal heart at level of left ventricle (LV) and right ventricle (RV) after injection of one cm^3/kg of Renografin-76 five minutes prior to sacrifice of the animal. Myocardial wall values $= 33 \pm 1$ EMI units; ventricular cavity blood pool values $= 43 \pm 1$ EMI units. (*B*) Slice of myocardial tissue taken at same level. Note trabecular and papillary muscle details (arrows) on both scan and specimen.

clear delineation of the blood–myocardial wall interface (Fig. 3). This difference of ten EMI units corresponds to about a 2% difference in attenuation coefficients between the intracavitary blood pool and myocardial wall. Despite the measurable difference in attenuation coefficient, high quality, low kilovoltage standard roentgenograms taken immediately after scanning failed to demonstrate any detectable difference in roentgenographic density between the myocardial wall and the intracavitary blood.

Myocardial Infarction

The four animals with two day old polyethylene plug–induced myocardial infarctions showed three different scan patterns. In two animals the site of histologically confirmed infarction displayed attenuation coefficients 1% lower than in the surrounding normal myocardium (*i.e.*, infarction $= 21.7 \pm 1.2$ EMI units; normal myocardium $= 26.8 \pm 1.0$ EMI units) (Fig. 4). In a third animal the attenuation coefficient of the infarcted tissue was 1% greater than that of the surrounding normal myocardium (infarction $= 30.8 \pm 1.7$ EMI units; normal myocardium $= 25.7 \pm 1.4$ EMI units) (Fig. 5). By using multiple overlapping scans of known thickness, the localization and extent of infarction could be assessed in these animals. The fourth animal, whose histologic sections showed only a small subendocardial infarction, had no change (to within $\pm 0.2\%$) in attenuation coefficient in the affected area.

The infarctions with a reduced attenuation coefficient were grossly edematous. The infarction with an increased attenuation coefficient was in the retraction stage

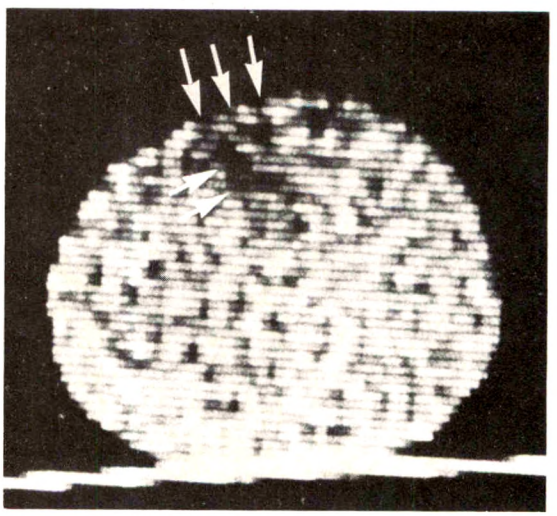


FIG. 4. CT scan two days postinfarction showing rim of tissue extending into region of interventricular septum (arrows) with attenuation coefficients 5.1 EMI units less than in surrounding normal myocardium. Distribution of infarcted tissue was confirmed on sectioned specimen.

of infarction, with gross thinning of the wall readily apparent both on inspection of the specimen and on the CT scan.

Each of the two animals with infarctions induced by ligation of the left anterior descending coronary artery (LAD) and subsequent administration of contrast material showed a large area distal to the LAD occlusion of decreased attenuation coefficient relative to the normal contrast-containing muscle in the same heart (Fig. 6). The infarction EMI value was 30.1 ± 2.8 EMI units, while the normal muscle EMI value was 41.0 ± 1.2 EMI units. The intracavitary blood value was 65.0 ± 1.0 EMI units. These differences account for the clarity of the blood–myocardial wall interface (Fig. 6).

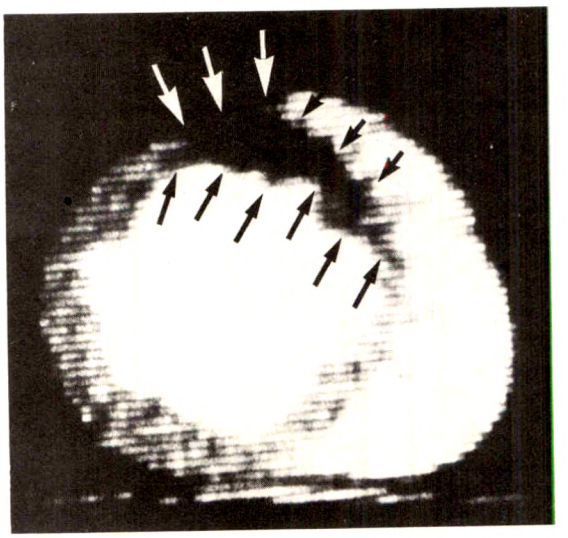


Fig. 6. CT scan three hours after left anterior descending coronary artery occlusion and two minutes after one ml/kg of Renografin-76 was given intravenously. Note area of decreased EMI value (delimited by arrows) in anterior and septal myocardial walls with decreased perfusion due to left anterior descending coronary artery occlusion. Cavity–myocardial wall interface is also well seen.

DISCUSSION

Current methods of delineating the cardiac chambers generally employ intracardiac catheterization and the rapid delivery of an iodinated contrast agent recorded serially on cine or large film. Noninvasive methods, such as radionuclide imaging and echocardiography, have significant limitations of resolution and extent of visualization.

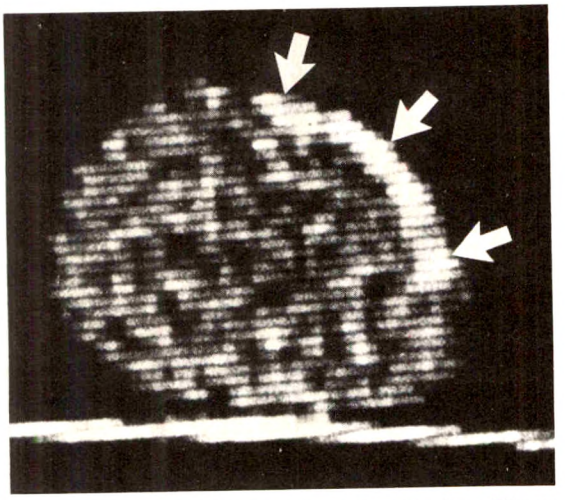


Fig. 5. CT scan with heart in right anterior oblique orientation two days postinfarction showing thinned rim of tissue with attenuation coefficients 5.1 EMI units higher than in normal myocardium along anterior left ventricular wall (arrows). Region of infarction was confirmed on sectioned specimen.

Since CT scanning can record and display absorption coefficients with a precision of 0.5%, small differences in tissue density can be detected.[11] If such differences between the intracavitary blood pool and myocardial wall were normally present, the cardiac chambers could readily be visualized. Our initial experiments with normal dog hearts demonstrated no such difference in density (Fig. 1).

Visualization of the blood–myocardial wall interface with settling of the red cells, as noted above, was anticipated because of the known variations in attenuation coefficient of blood with different hematocrit levels.[6] This finding led us to investigate the acutely anemic dog. The presence of a clear interface (Fig. 2) suggests that anemia or polycythemia in man may provide a sufficient blood–myocardial wall density difference to permit the visualization of the cardiac chambers.

The introduction of an intravenous contrast agent effected prolonged and clear de-

lineation of the blood–myocardial wall interface (Fig. 3). This was true not only in normal dogs but also in those with acute left anterior descending coronary artery occlusion in which the contrast material was given primarily to define the region of myocardium with reduced perfusion (Fig. 6). Thus computed cardiac tomography may represent a useful low-risk method of evaluating myocardial wall structure and function in man.

The accurate detection and sizing of acute myocardial infarction would not only permit early confirmation in questionable cases but also aid in evaluating interventions (pharmacologic or mechanical) designed to limit the volume of infarcted myocardium. Present radionuclide techniques[12,13] are limited both by resolution capacity and heterogeneous isotopic uptake. Because myocardial tissue undergoes profound changes in ionic composition and water content with infarction,[14] the application of CT scanning to detect changes in tissue density seemed appropriate. The demonstrated differences in attenuation coefficients between normal and infarcted myocardium were probably related to the known shifts in intracellular ions and size of the intercellular fluid compartment in infarcted hearts (Fig. 4; and 5). In a fundamental sense, CT scanning of infarcted myocardium represents a novel approach to the study of tissue death *in vivo*.

The spectrum of attenuation coefficient changes (including lower values with edematous areas of infarction, higher values within retracted infarctions, and no detectable change when only a small subendocardial infarction is present) may provide a clinically useful approach to detecting and sizing transmural infarctions. The level and direction of change in attenuation coefficient is probably related to the stages of infarction depicted on pathologic examination. This may prove helpful in dating acute infarctions.

The administration of contrast material prior to scanning increases the density difference between normal and infarcted myocardium and also permits visualization of the blood–myocardium interface (Fig. 6). The use of a contrast agent may simultaneously increase the sensitivity and utility of scanning in acute infarction and permit evaluation of alterations in wall motion. In addition to the obvious clinical applications of this approach, it affords a new and potentially valuable noninvasive method for the sequential *in vivo* study of experimental models of ischemia and infarction.

Requirements for In Vivo *Application*

For clinical applications, a CT scanner capable of measuring and displaying differences of about 1% in attenuation coefficients of heart muscle and intracavitary blood *in vivo* is required. A spatial resolution comparable to that of the EMI scanner is desirable, in which the full width at half maximum of the line spread function is 1.5 mm.[15] To achieve these characteristics for cardiac scanning, precise gating to the dynamic events of the cardiac cycle and acquisition of a series of images corresponding to different phases of the cycle may be required.

Data from this preliminary study suggest that an ideal scanner for *in vivo* study would have the following immediate applications: (1) detection, sizing, and dating of acute myocardial infarctions; (2) evaluation of the effectiveness of mechanical and pharmacologic interventions designed to limit infarction size;[16] (3) evaluation of regional ventricular wall motion and thickness in acute and chronic myocardial ischemia; (4) assessment of ventricular function through measurement of ventricular volumes, ejection fractions, and other physiologic parameters; and (5) the *in vivo* study of experimental tissue ischemia and necrosis and their characteristic alterations in attenuation coefficient.

Douglass F. Adams
Department of Radiology
Harvard Medical School
25 Shattuck Street
Boston, Massachusetts 02115

REFERENCES

1. Ambrose, J. Computerized transverse axial scanning (tomography). II. Clinical application. *Br. J. Radiol.*, 1973, *46*, 1023–1047.
2. Hounsfield, G. N. Computerized transverse axial scanning (tomography) I. Description of system. *Br. J. Radiol.*, 1973, *46*, 1016–1022.
3. New, P. F. J., Scott, W. R., Schnur, J. A., Davis, K. R., and Taveras, J. M. Computerized axial tomography with the EMI scanner. *Radiology*, 1974, *110*, 109–123.
4. Alfidi, R. J., Haaga, J., Meaney, T. F., MacIntyre, W. J., Gonzalez, L., Tarar, R., Zelch, M. G., Boller, M., Cook, S. A., and Jelden, G. Computed tomography of the thorax and abdomen; a preliminary report. *Radiology*, 1975, *117*, 257–264.
5. Schellinger, D., Di Chiro, G., Axelbaum, S. P., Twigg, H. L., and Ledley, R. S. Early clinical experience with the ACTA scanner. *Radiology*, 1975, *114*, 257–261.
6. Alfidi, R. J., MacIntyre, W. J., Meany, T. F., Chernak, E. S., Janciki, P., Tarar, R., and Levin, H. Experimental studies to determine application of CAT scanning to the human body. Am. J. Roentgenol, Rad. Therapy & Nuclear Med., 1975, *124*, 199–207.
7. Philips, R. L., and Stephens, D. H. Computed tomography of liver specimens. *Radiology*, 1975, *115*, 43–46.
8. Pickering, R. S., Hattery, R. R., Hartman G. W., and Holley, K. E. Computed tomography of the excised kidney. *Radiology*, 1974, *113*, 643–647.
9. Holman, B. L., Dewanjee, M. K., Idoine, J., Fliegel, C. P., Davis, M. A., Treves, S., and Eldh, P. Detection and localization of experimental myocardial infarction with ^{99m}Tc-tetracycline. *J. Nucl. Med.*, 1973, *14*, 595–599.
10. McCullough, E. C., Baker, H. L., Jr., Houser, O. W., and Reese, D. F. An evaluation of the quantitative and radiation features of a scanning x-ray transverse axial tomograph: the EMI scanner. *Radiology*, 1974, *111*, 709–715.
11. Ambrose, J. Computerized x-ray scanning of the brain. *J. Neurosurg.*, 1974, *40*, 679–695.
12. Bonte, F. J., Parkey, R. W., Graham, K. D., Moore, J., and Stokely, E. M. A new method for radionuclide imaging of myocardial infarcts. *Radiology*, 1974, *110*, 473–474.
13. Holman, B. L., Lesch, M., Zweiman, F. G., Temte, J., Lown, B., and Gorlin, R. Detection and sizing of acute myocardial infarcts with ^{99m}Tc (Sn) tetracycline. *N. Engl. J. Med.*, 1974, *291*, 159–163.
14. Lie, J. T., Pairolero, P. C., Holley, K. E., McCall, J. T., Thompson, H. K., Jr., and Titus, J. L. Time course and zonal variations of ischemia-induced myocardial cationic electrolyte derangements. *Circulation*, 1975, *51*, 860–866.
15. Judy, P. F. The line spread function and modulation transfer function of a computed tomographic scanner. *Med. Physics*. In press, 1976.
16. Braunwald, E., and Maroko, P. R. Reduction of infarct size: idea whose time for testing has come. *Circulation*, 1974, *50*, 206–209.
17. Adams, D. F., Hessel, S. J., Judy, P., Stein, J. A., and Abrams, H. L. Differing attenuation coefficients in normal and infarcted myocardium. *Science*, 1976. In press.

THE VALUE OF REPEAT CEREBRAL ARTERIOGRAPHY IN THE EVALUATION OF TRAUMA*

By EUGENE J. McDONALD, Jr., M.D.,† DAVID P. WINESTOCK, M.D.,† *and* JULIAN T. HOFF, M.D.‡
SAN FRANCISCO, CALIFORNIA

ABSTRACT:

In most patients with head or neck trauma, a single angiogram is sufficient to guide therapy. For those who improve slowly or not at all, however, this is not an adequate basis for diagnosis. Angiography should be repeated after an interval of time to exclude development of a surgically correctable lesion, such as pseudoaneurysm or intracerebral or extracerebral fluid collection.

THE role of cerebral angiography in the evaluation of trauma to the head and neck has received wide attention. Its value in accurately diagnosing most cases of vascular injury, intracerebral hematoma, and subdural or epidural fluid is accepted.[8]

Approximately 500 cerebral angiograms are obtained each year at our hospital. Many of these are obtained to assess the sequelae of trauma. We have been impressed by the nature of cranial trauma and by the value of repeat cerebral angiography in patients whose clinical condition does not improve satisfactorily. We describe six cases which illustrate how repeat angiography can often disclose abnormalities that are not seen on the initial study.

REPORT OF CASES

Case I. A 56 year old man was brought to our hospital on July 26, 1973, after falling from a roof. He was comatose but without focal neurologic abnormalities. Skull roentgenograms showed bilateral occipital fractures with diastasis of the lambdoid sutures. A cerebral angiogram obtained on the day of admission demonstrated an extracerebral space in the left parietal area. A subdural hematoma was evacuated at craniotomy.

Because the patient failed to improve, cerebral angiography was repeated on August 3, 1973. Severe spasm of many intracranial vessels was seen (Fig. 1, *A* and *B*). The patient was treated conservatively and eventually completely recovered.

Case II. A 30 year old man was brought to the hospital on May 19, 1974, the victim of an automobile accident. He had decerebrate posturing and a large right frontoparietal skull fracture. Multiple burr holes were made to drain a left subdural hematoma. A cerebral angiogram obtained six hours after this procedure demonstrated reaccumulation of the subdural hematoma and severe vascular spasm (Fig. 2*A*). Craniotomy was performed to drain the hematoma.

Return of function was very slow. After one month the patient had a few purposeful movements with his left arm but could not obey commands. A carotid angiogram obtained on June 18, 1974, showed resolution of the vascular spasm and a 2 mm aneurysm of the distal branch of the left middle cerebral artery (Fig. 2*B*). The patient was discharged to a chronic care hospital and fully recovered within three months.

Case III. A 44 year old man was brought to the hospital on February 16, 1974, after being stabbed in the right temporal area with a screwdriver. Within four hours he became lethargic and developed left hemiparesis. A cerebral angiogram demonstrated moderate right temporal swelling and a normal posterior fossa (Fig. 3*A*). Shortly after the angiogram a right temporal craniectomy was performed with débridement of the stab wound.

* From the Departments of Radiology† and Neurological Surgery,‡ University of California School of Medicine and San Francisco General Hospital, San Francisco, California.
Supported in part by National Institutes of Health Trauma Center Program Project Grant GM 18470 from the National Institute of General Medical Sciences.

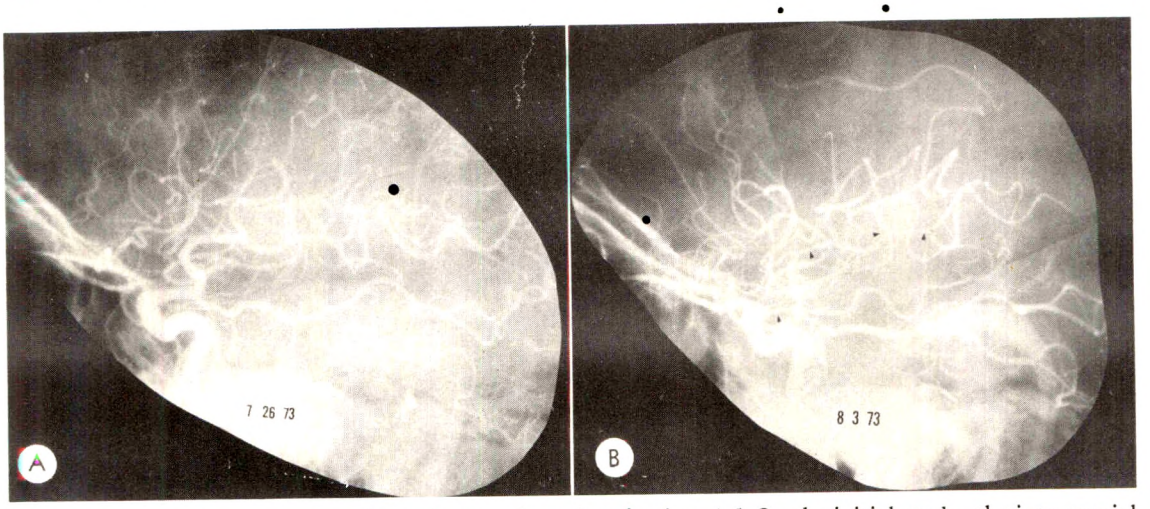


Fig. 1. Case I. Left common carotid angiogram, lateral projection. (*A*) On the initial study, the intracranial arteries are normal in caliber. A small amount of contrast medium has extravasated from the external carotid vessels in the region of the parieto-occipital fractures. (*B*) Eight days after injury, there is severe spasm of the internal carotid artery and of numerous branches of the middle cerebral artery (arrows).

Because the patient failed to improve, cerebral angiography was repeated on March 6, 1974; it demonstrated an aneurysm of the right superior cerebellar artery (Fig. 3*B*). The location of the aneurysm defined precisely the depth of the penetration injury. Conservative therapy was administered. After many months mentation was normal, but dense hemiparesis was still present.

Case IV. A 20 year old man was admitted to the hospital on September 1, 1974, after falling through a plate glass window. He sustained multiple lacerations of the left side of his neck but was otherwise completely normal on physical examination. On plain roentgenograms of the neck, a 2 cm foreign body was observed at the level of C_1 (Fig. 4). A left vertebral angiogram obtained at the same time confirmed the presence of the foreign body and demonstrated mural irregularity in the distal portion of the vertebal artery (Fig. 5*A*). Posterior fossa craniotomy was then performed with exploration confined to the intradural portion of the vertebral artery.

Because no foreign body nor vascular damage

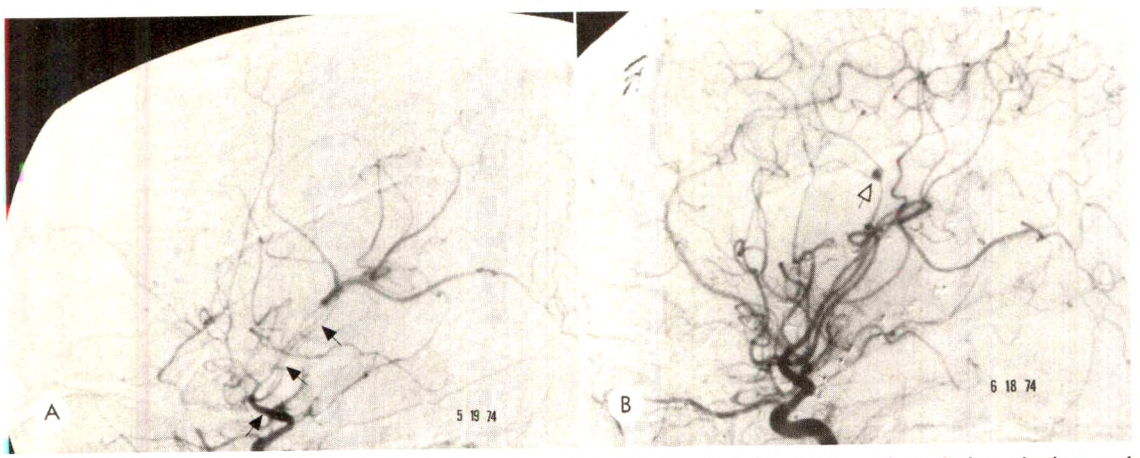


Fig. 2. Case II. Left common carotid angiogram, lateral projection. (*A*) On the day of admission, the internal carotid artery and proximal branches of the middle cerebral artery are severely narrowed (black arrows). (*B*) One month after injury, the spasm has resolved and an aneurysm (open arrow) of a distal branch of the middle cerebral artery has appeared.

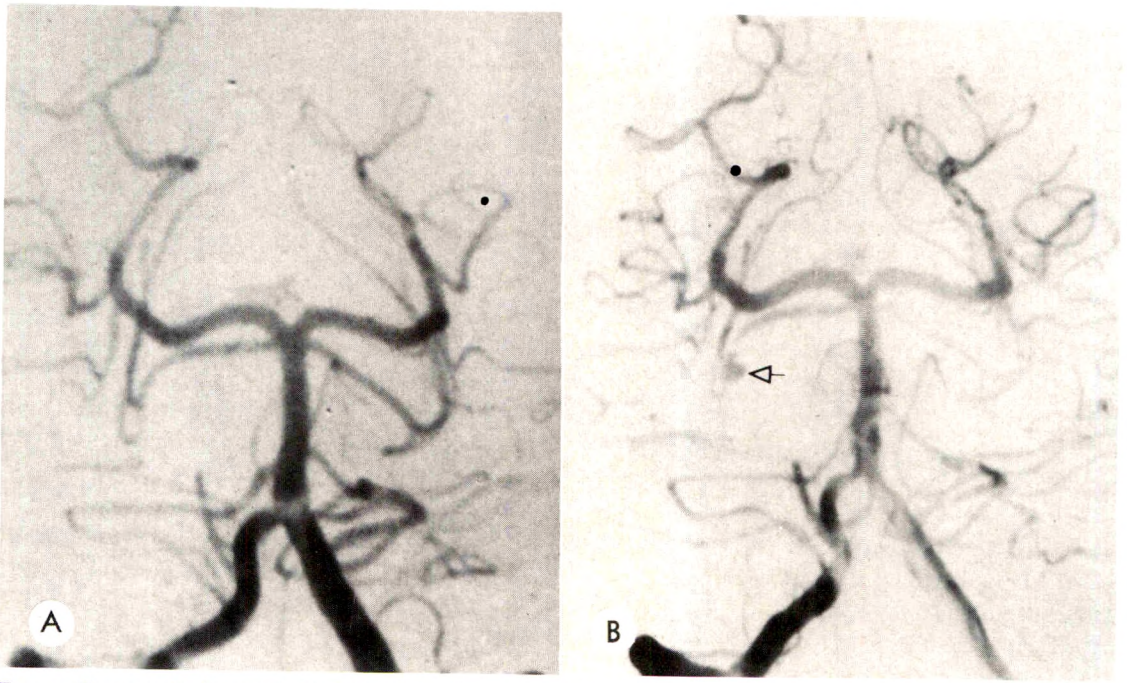


Fig. 3. Case III. Left vertebral angiogram, frontal projection. (*A*) On February 16, 1974, there was no abnormality of the right superior cerebellar artery. (*B*) On March 6, 1974, an aneurysm of the right superior cerebellar artery (open arrow) was seen.

was found at surgery, cerebral angiography was repeated on September 17, 1974. At this time, a 2 cm aneurysm of the left vertebral artery was seen at the site of the previously noted mural irregularity, anterior and medial to the foreign body (Fig. 5*B*). At surgical exploration the aneurysm of the extradural portion of the vertebral artery was trapped and the foreign body removed.

Case V. A 52 year old alcoholic was brought to the hospital on January 6, 1974. He had been found comatose on the street. Skull roentgenograms, obtained on the same day, showed extensive, bilateral skull fractures that were not present on a skull series obtained two days before. Cerebral angiography revealed a large subdural hematoma, which was subsequently drained at right parietal craniotomy (Fig. 6*A*).

Because his neurologic status did not change, angiography was repeated 16 days after injury. A small residual right temporoparietal extracerebral space was noted. In addition a right temporal mass had developed (Fig. 6, *B* and *C*). At reoperation, a small subdural hematoma and a large intratemporal hematoma were evacuated. The patient rapidly improved and was discharged to a convalescent facility.

Case VI. A 60 year old man was brought to the hospital on December 4, 1972, after undergoing a severe beating. He was comatose and had a skull fracture with diastasis of the right sagittal suture. Cerebral angiography demonstrated a small, left, parietal extracerebral space (Fig. 7*A*). The patient was treated conservatively.

The patient's clinical improvement was minimal. Angiography on December 19, 1972, demonstrated a large extracerebral space in the left parietal area with shift of midline structures (Fig. 7*B*). A subdural hygroma was found at surgery and drained. The patient improved after operation.

DISCUSSION

Arterial narrowing or spasm has been found to occur after severe trauma.[3,6,7,9,10] The precise cause is unclear, but contributing factors include increased intracranial pressure, subarachnoid hemorrhage, vascular stretching, and sympathetic discharge at the time of impact.[3] In two of our pa-

tients intracerebral spasm developed after the initial, negative, angiographic studies, and in another patient it was present initially then spontaneously resolved. While there is presently no effective treatment for arterial spasm, its angiographic demonstration is helpful because the resulting cerebral ischemia can explain a patient's failure to improve.[12]

Trauma to an artery can cause intimal disruption or partial transection with formation of a pseudoaneurysm.[2,9] The mechanism of injury may be blunt trauma, a perforating wound, or hyperextension (*i.e.*, of cervical segments of carotid or vertebral arteries).[1,4,11] The correct diagnosis of such injuries is important because the intimal tear may lead to subintimal dissection, complete obstruction, and profuse bleeding of the pseudoaneurysm.[4,5] In both cases surgery is usually required.

In three of our patients pseudoaneurysms were demonstrated as a delayed result of

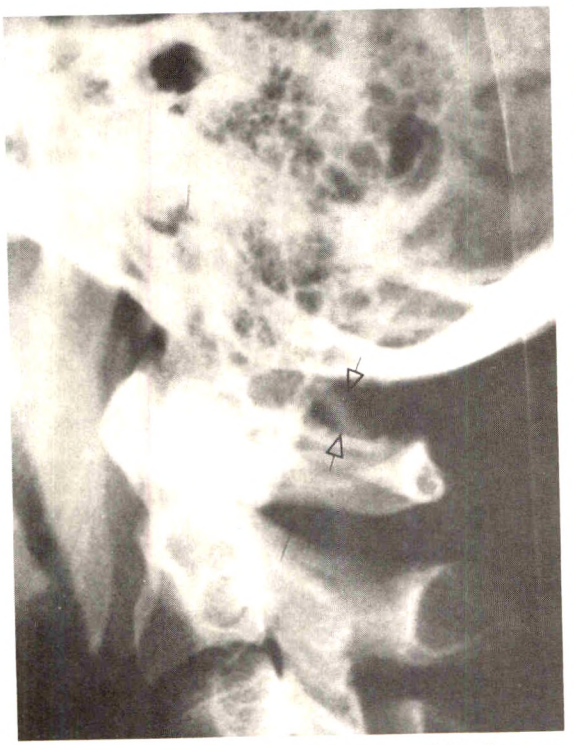


Fig. 4. Case iv. Plain roentgenogram of C_1–C_2 area, lateral projection. Arrows locate the foreign body.

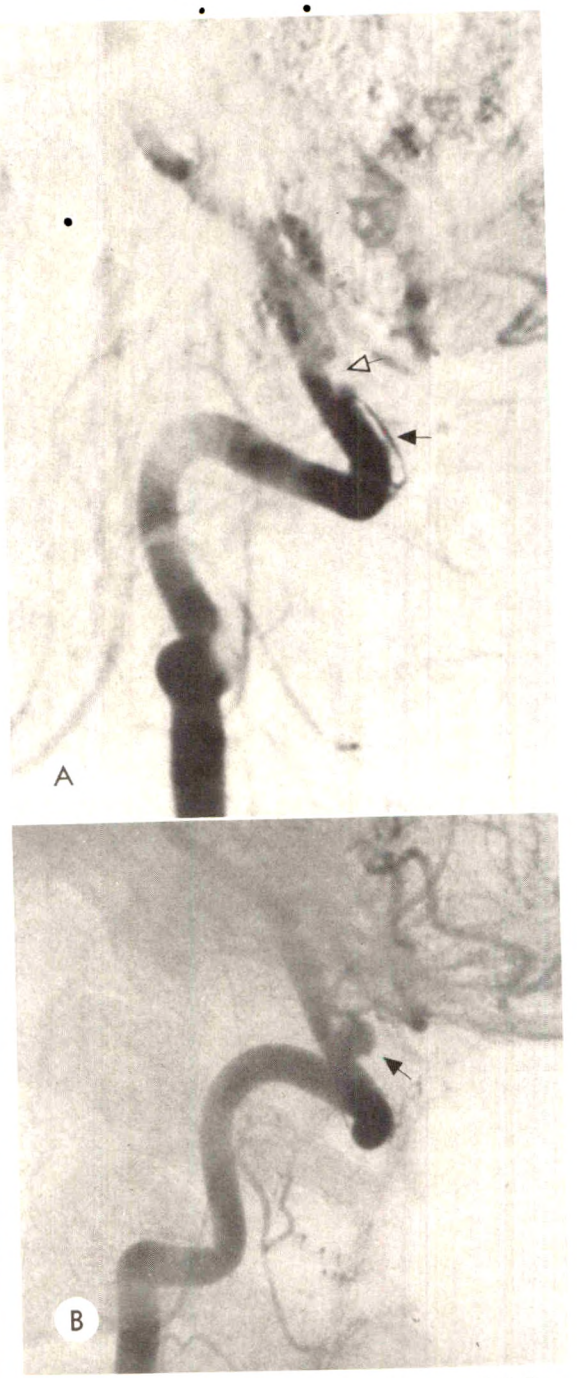


Fig. 5. Case iv. Left vertebral angiogram. (*A*) Lateral projection on day of admission. The foreign body (closed arrow) has been redrawn from nonsubtracted films. Note the irregular appearance of the vertebral artery (open arrow) superior to the foreign body. (*B*) Lateral projection, 16 days after injury. (The foreign body has not been drawn on these subtraction films.) Note the large, irregular aneurysm of the left vertebral artery (arrow).

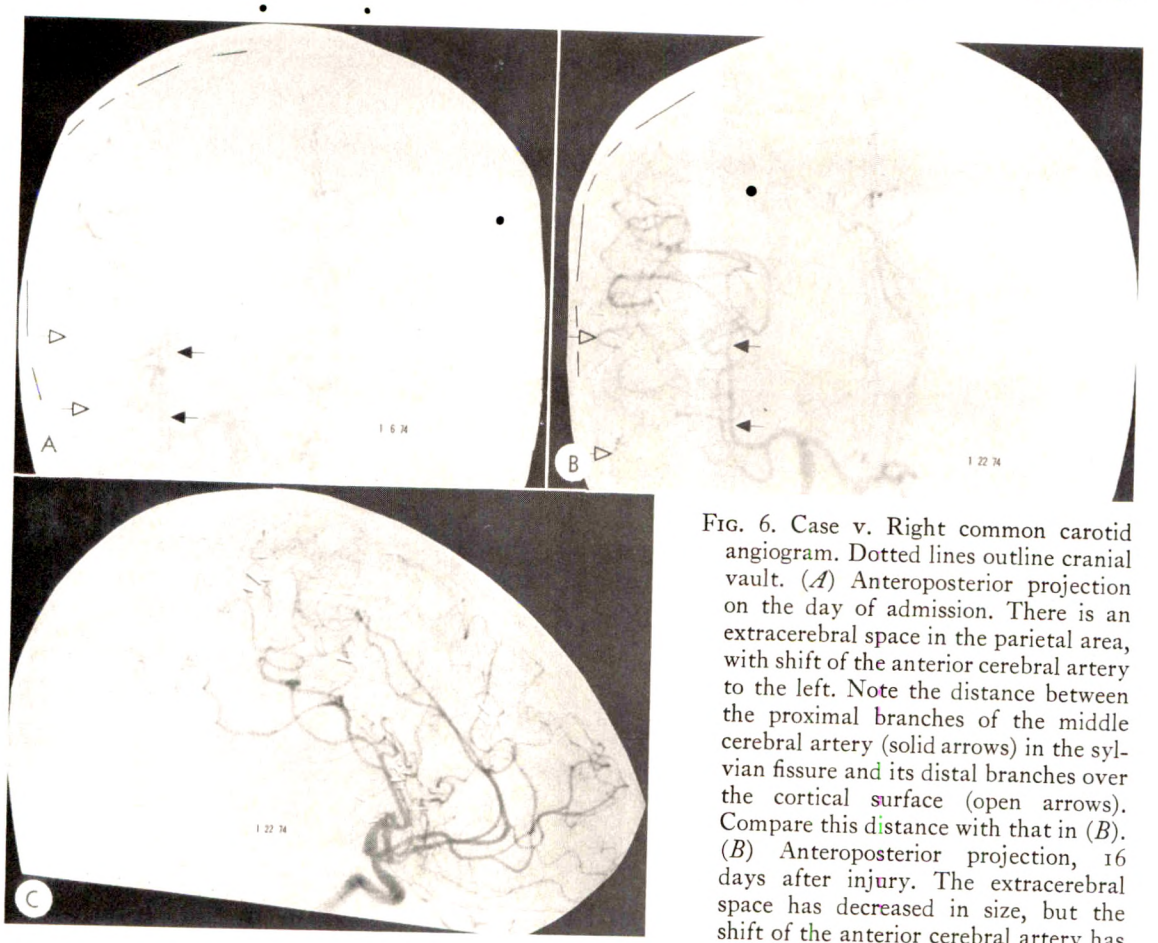


FIG. 6. Case v. Right common carotid angiogram. Dotted lines outline cranial vault. (*A*) Anteroposterior projection on the day of admission. There is an extracerebral space in the parietal area, with shift of the anterior cerebral artery to the left. Note the distance between the proximal branches of the middle cerebral artery (solid arrows) in the sylvian fissure and its distal branches over the cortical surface (open arrows). Compare this distance with that in (*B*). (*B*) Anteroposterior projection, 16 days after injury. The extracerebral space has decreased in size, but the shift of the anterior cerebral artery has increased. The distance between the genu of the middle cerebral artery and its distal branches has increased, indicating an intratemporal mass. (*C*) Lateral projection, 16 days after trauma. The vessels of the sylvian triangle are elevated and draped over the intratemporal mass.

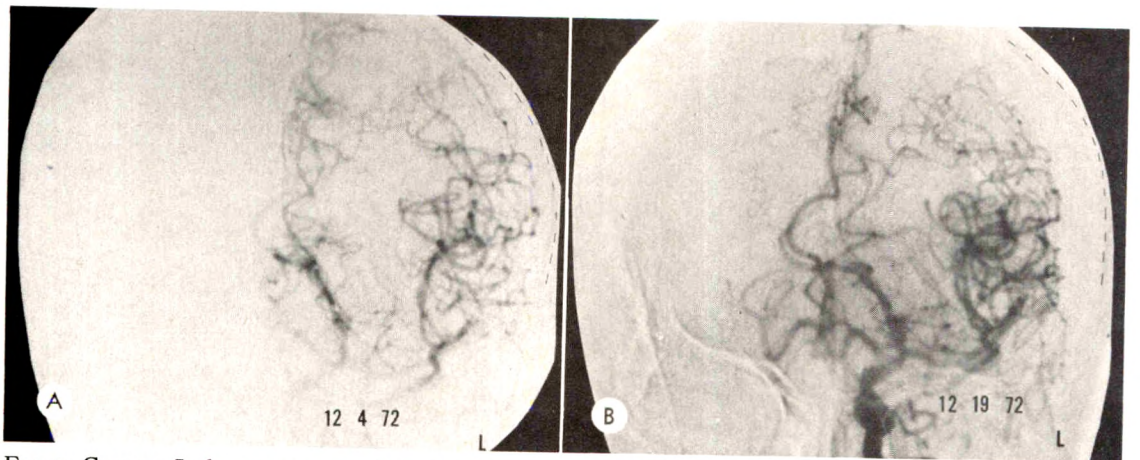


FIG. 7. Case vi. Left common carotid angiogram, anteroposterior projection. (*A*) On the day of admission, a small extracerebral space is seen. (Dotted lines outline the cranial vault.) (Reprinted, with permission, from Winestock *et al.*[13]) (*B*) Fifteen days after trauma, the extracerebral space is increased, and there is now an increased shift of the anterior cerebral artery. (Reprinted, with permission, from Winestock *et al.*[13])

trauma. In one, the aneurysm was preceded by a demonstrated intimal tear. If the aneurysm was accessible, repair was attempted.

Intracerebral hematoma, extracerebral hematoma, and hygroma are well known sequelae of trauma.[8] They may develop or enlarge many days after injury and cause deterioration in the clinical condition of the patient. The subdural hygroma in one of our patients (Case VI) and the intracerebral hematoma in another (Case V) were first apparent on repeat angiograms. These patients improved after appropriate surgery.

David P. Winestock, M.D.
Department of Radiology, 380-M
University of California
San Francisco, California 94143

REFERENCES

1. Acosta, C., Williams, P. E., Jr., and Clark, K. Traumatic aneurysms of cerebral vessels. *J. Neurosurg.*, 1972, *36*, 531–536.
2. Bergeron, R. T., and Rumbaugh, C. L. Non space-occupying sequelae of head trauma. *Radiol. Clin. North America*, 1974, *12*, 315–331.
3. Ekelund, L., Nilsson, B., and Pontén, U. Carotid angiography after experimental head injury in rat. *Neuroradiol.*, 1974, *7*, 209–214.
4. Gurdjian, E. S., Hardy, W. G., Lindner, D. W. and Thomas, L. M. Closed cervical cranial trauma associated with involvement of carotid and vertebral arteries. *J. Neurosurg.*, 1963, *20*, 418–427.
5. Hare, R. R., and Gaspar, M. R. Intimal flap. *A.M.A. Arch. Surg.*, 1971, *102*. 552–555.
6. Kobrine, A. I., and Kempe, L. C. Studies in head injury. *Surgical Neurol.*, 1973, *1*, 34–42.
7. Leeds, N. E., Reid, N. D., and Rosen, L. M. Angiographic changes in cerebral contusions and intracerebral hematomas. *Acta radiol.* (Diag.), 1966, *5*, 320–327.
8. Lofstrom, J. E. Injuries of cranial vault and brain. *Radiol. Clin. North America*, 1966, *4*, 323–340.
9. Love, L. Arterial trauma. *Seminars in Roentgenol.*, 1970, *5*, 267–283.
10. Slaney, G., and Ashton, F. Arterial injuries and their management. *Postgrad. Med.*, 1971, *47*, 257–269.
11. Sullivan, H. G., Vines, F. S., and Becker, D. P. Sequelae of indirect internal carotid injury. *Radiology*, 1973, *109*, 91–98.
12. Wilkins, R. H. Attempts at treatment of intracranial arterial spasm in animals and human beings. *Surgical Neurol.*, 1973, *1*, 148–159.
13. Winestock, D. P., Spetzler, R. F., and Hoff, J. T. Acute post-traumatic subdural hygroma: natural course with angiographic documentation. *Radiology*, 1975, *115*, 373–375.

CAUDAL DISLOCATION OF THE PONS IN THE ADULT ARNOLD-CHIARI MALFORMATION: AN ANGIOGRAPHIC EVALUATION*

By MEREDITH WEINSTEIN, M.D.,† *and* THOMAS H. NEWTON, M.D.
SAN FRANCISCO, CALIFORNIA

ABSTRACT:

The position of the pons, determined angiographically, can be related to the clivus and sella. In adult patients with the Chiari malformation, a caudal dislocation of the pons is frequently associated with the well known anomalously low position of the cerebellar tonsils. This finding may aid in the angiographic diagnosis of the Chiari malformation.

THE Chiari malformation in adults often presents a diagnostic challenge because of its varied presentation.[1,8] The angiographic features of caudal dislocation of the cerebellar tonsils, noted in this condition, have been well described in the past.[5–7,9,11] The following study was undertaken to determine whether the Chiari malformation in adults is also associated with caudal dislocation of the pons, and whether this anomalous position could be diagnosed angiographically.

MATERIAL AND METHOD

The position of the pons is accurately delineated by the anterior pontomesencephalic vein. To determine if the pons was displaced caudally it was necessary to establish the normal variability of the position of the pons. The use of Twining's line as a landmark proved to be unsatisfactory because of the variability in the position of the torcular Herophili and the size of the posterior fossa in patients with the Chiari malformation. The clivus and the floor of the sella were, therefore, selected as reference points. A line (Line A) was drawn connecting the posterior clinoid processes and the anterior aspect of the foramen magnum (Fig. 1). A second line (Line B) was then drawn tangent to the floor of the sella turcica and perpendicular to Line A. The distance from Line B to the most cephalad portion of the pons as outlined by the anterior pontomesencephalic vein (Point C) was measured (Fig. 1). The position of the pons, as determined by vertebral angiography, was evaluated in 150 patients with no posterior fossa pathology and in 14 adult patients with Chiari malformation.

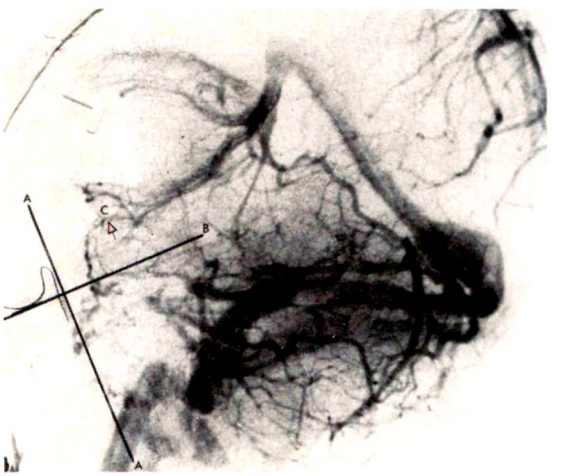


FIG. 1. Normal relationship of anterior pontomesencephalic vein to floor of sella turcica. Line A connects the posterior clinoid processes with the anterior margin of the foramen magnum. Line B is drawn perpendicular to Line A and tangent to the floor of the sella. Point C (arrow) indicates the most cephalad portion of the pons as defined by the anterior pontomesencephalic vein. In this normal adult patient it measured 18.0 mm above Line B (2:1 magnification).

* From the Department of Radiology, University of California Medical Center, San Francisco, California.
Supported by grant NS 2615-02 from the National Institutes of Health, United States Public Health Service.
† Academic Trainee in Diagnostic Radiology and current staff Radiologist, Cleveland Clinic, Cleveland, Ohio.

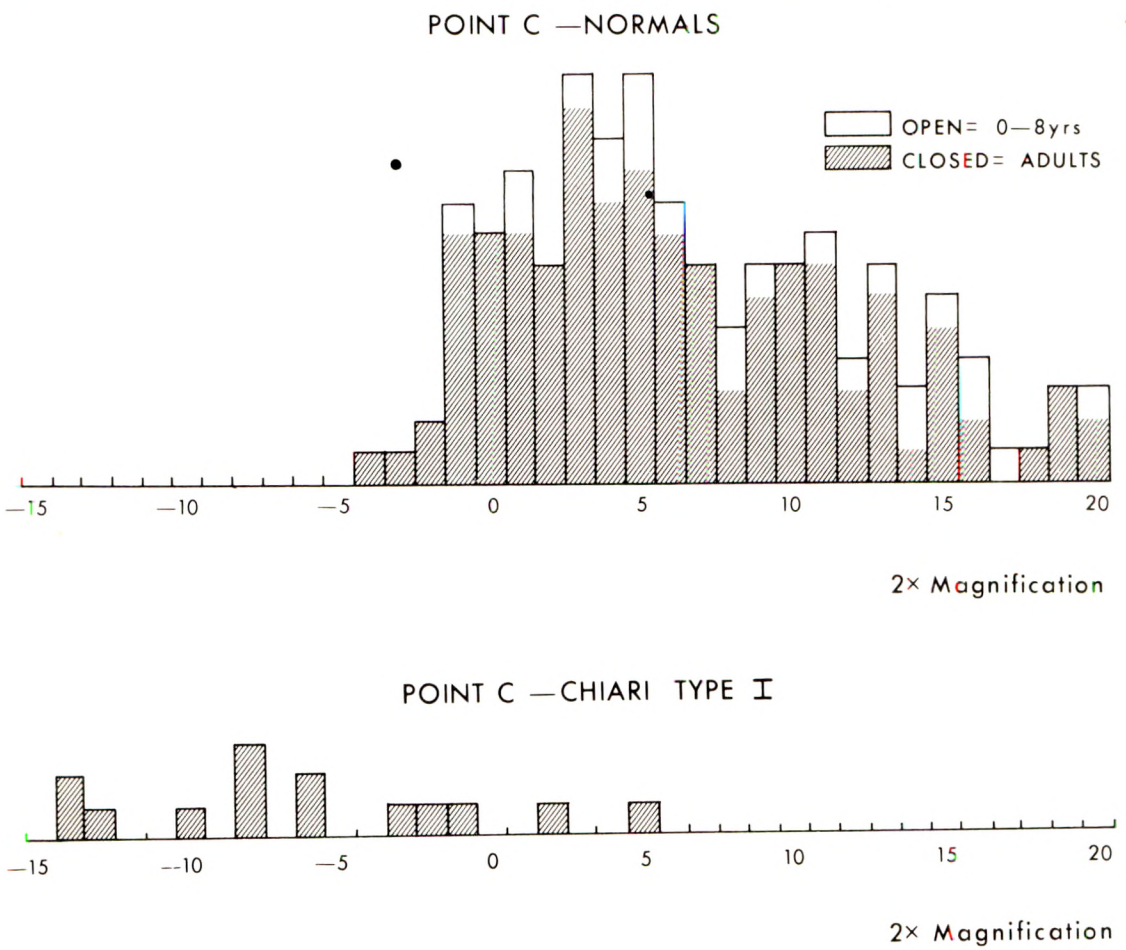


Fig. 2. Histogram to show position of superior aspect of pons (Point C) in 150 normal patients and in 14 adults with Chiari malformation. The position of Line B (see text) is here indicated by zero. Positive numbers indicate position of pons above Line B and negative numbers below Line B.

RESULTS

The position of the superior aspect of the pons (Point C) ranged from 4.0 mm below Line B to 20 mm above Line B, in the normal group of patients using 2:1 magnification angiography (Fig. 2). The mean height of the pons in children was significantly greater than that in adults. In neither the normal children nor the normal adults did the superior aspect of the pons (Point C) have a position more than 4 mm below Line B.

In 9 of 14 adult patients with Chiari malformations, the rostral aspect of the pons (Point C) measured more than 5 mm below the reference Line B (Fig. 2; and 3). In the remaining five patients, the location of the pons appeared to be within the range of normal, although in three of the patients the pons measured from 1–3 mm below reference Line B. The size of the ventricles was either normal or slightly enlarged in eleven patients in whom ventricular size could be determined by air studies or carotid angiography.

DISCUSSION

In 1891 and 1895 Chiari[2,3] described a group of patients with malformations of the posterior fossa in whom portions of the cerebellum and brain stem were below the foramen magnum. Chiari subdivided these

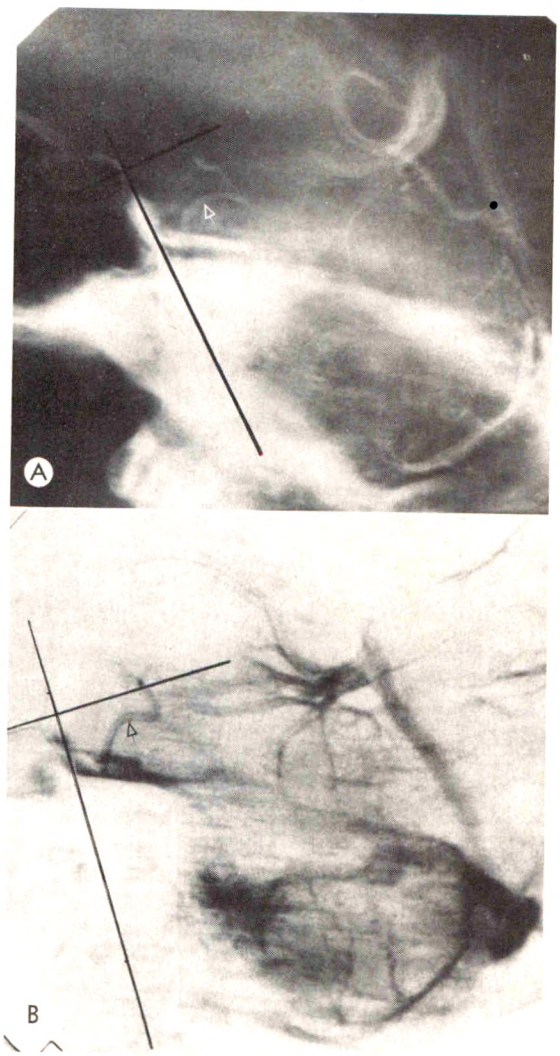


Fig. 3. Chiari malformation. Lateral vertebral angiotomograms, venous phase, in two patients (2:1 magnification). (*A*) The superior aspect of the pons (Point C-arrow) is 14 mm below Line B. (*B*) The superior aspect of the pons (arrow) lies 8 mm below Line B.

malformations into four types; of these, only Type I and II are pertinent to our discussion. The Type I deformity usually affects older children or adults in whom the elongated cerebellar tonsils extend into the upper cervical canal to a variable degree. Abnormalities of the foramen magnum and cervical spine including basilar impression, Klippel-Feil deformity, and hydromyelia are frequently associated anomalies.[4,10] The Type II deformity is seen in infants with hydrocephalus and meningocele or myelomeningocele. In these patients the deformity of the medulla oblongata and cerebellum is more pronounced. Marked downward extension of the cerebellar tonsils and inferior displacement of the fourth ventricle through the foramen magnum as well as caudal displacement of the medulla and pons are usually noted. The infrequent postmortem diagnosis of minor caudal displacement of the pons in Chiari malformations in adults is believed to be related to the lack of precise criteria for the relationship of the pons to bony landmarks and the inability of the pathologist to define accurately the position of the pons.

Our studies indicate that in adult patients with Chiari malformation not only are the cerebellar tonsils dislocated caudally but the pons is also often similarly affected.

Thomas H. Newton, M.D.
Department of Radiology
University of California
Medical Center
San Francisco, California 94143

REFERENCES

1. Appleby, A., Foster, J. B., Hankinson, J., and Hudgson, P. Diagnosis and management of Chiari anomalies in adult life. *Brain*, 1968, *91*, 131–140.
2. Chiari, H. Ueber Veränderungen des Kleinhirns in Folge von Hydrocephalie des Grosshirns. *Deutsche med Wchnschr.*, 1891, *17*, 1172–1175.
3. Chiari, H. Ueber Veränderungen des Kleinhirns, des Pons und der Medulla oblongata in Folge von congenitaler Hydrocephalie des Grosshirns. *Denkschr Akad. Wiss. Math.*, 1895, *63*, 71–116.
4. Davies, H. W. Radiological changes associated with Arnold-Chiari malformations. *Radiology*, 1967, *40*, 262–269.
5. Gabrielsen, T. O., Joachim, F., Seeger, F., and Amundsen, P. Some new angiographic observations in patients with Chiari Type I and II malformations. *Radiology*, 1975, *115*, 627–634.
6. Greitz, T., and Sjögren, S. E. Posterior inferior cerebellar artery. *Acta radiol.* (Diag.), 1963,

1, 284–297.

7. Margolis, M. T., and Newton, T. H. Angiographic sign of cerebellar tonsillar herniation. *Neuroradiol.*, 1971, *2*, 3–8.
8. Norton, T., and Paul, R. P. Arnold-Chiari deformity in elderly patients: diagnosis and treatment. *Neurochirugia*, 1972, *15*, 159–166.
9. Occleshaw, J. V. Posterior inferior cerebellar arteries: some quantitative observations in posterior cranial fossa tumors and Arnold-Chiari malformation. *Clin. Radiol.*, 1970, *21*, 1–9.
10. Spillane, J. D., Pallis, C., and Jones, A. M. Developmental abnormalities in region of foramen magnum. *Brain*, 1957, *80*, 11–48.
11. Wolpert, S. M. Vascular studies of congenital anomalies. Chapter 87. In: Radiology of the Skull and Brain. Edited by T. H. Newton, and D. G. Potts. C. V. Mosby Company, St. Louis, 1974.

ANGIOGRAPHIC MANIFESTATIONS OF BILATERAL WILMS' TUMOR*

By BARRY T. KATZEN, M.D.,† *and* MELVIN MARKOWITZ, M.D.‡
NEW YORK, NEW YORK

ABSTRACT:

Two cases of bilateral Wilms' tumor are presented with discussion of angiographic features. Emphasis is placed on selective angiography in addition to inferior vena cavography for complete evaluation. Because of the incidence of bilateral disease, and the highly vascular nature of the tumor, selective angiography of the contralateral side should be considered in the initial evaluation of unilateral Wilms' tumor. Evaluation of the interface between tumor and normal parenchyma is extremely important in bilateral disease, in anticipation of partial nephrectomy.

WILMS' tumor is one of the most common intra-abdominal tumors of childhood. Incidence has been estimated at 0.4 to 1 per 10,000 live births.[10] In a recent reported review of 1,746 cases, 4.4 percent were noted to be bilateral.[10] Only 65 percent of cases of bilateral Wilms' tumors initially present as masses in both kidneys. Thirty-five percent develop evidence of a second mass within three weeks to ten years,[1] the majority within one year. Although some success in treating bilateral disease has been reported, diagnosis of bilaterality decreases the likelihood of cure, and significantly changes therapy.[1,2,10]

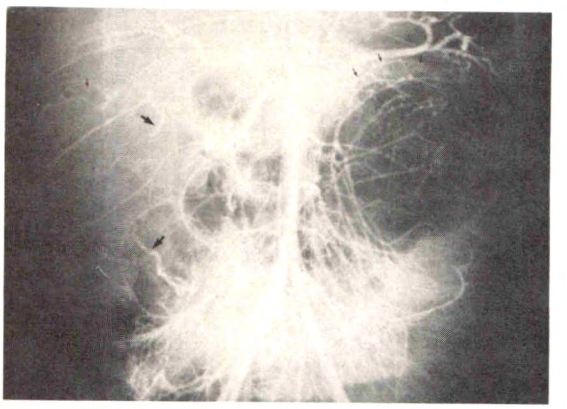


FIG. 2. Late arterial phase of aortogram. Note filling of tumor vessels (arrows) in the periphery of the mass associated with marked stretching (smaller arrows).

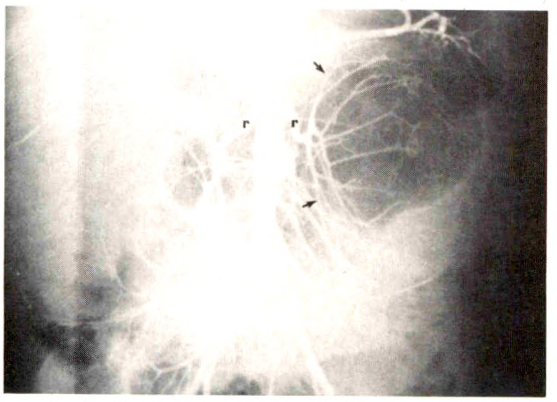


FIG. 1. Arterial phase of aortogram. Note the marked stretching of intrarenal vessels, most notably on the left (arrows).

Therefore, accurate diagnosis of the presence of bilateral disease and the definition of tumor limits are significantly related to therapy.

Angiography has been widely used for evaluation of renal tumors in adults, and more recently has been utilized in Wilms' tumors.[6–9] Important information provided by angiography includes: a) diagnosis of tumor; b) definition of anatomical limits and tumor extention; c) patency of renal veins and inferior vena cava; d) evaluation of residual normal parenchyma in anticipation of partial nephrectomy; e) evaluation

* From the Division of Cardiovascular Radiology, St. Vincent's Hospital and Medical Center of New York, New York, New York.
† Clinical Assistant Professor of Radiology, Cornell University Medical Center.
‡ Resident in Radiology.

of contralateral side in cases of suspected unilateral Wilms' tumor; and f) evaluation of possible metastases or direct extension into the liver.

The authors' experience with two cases of bilateral Wilms' tumor is presented to elucidate the angiographic manifestations and emphasize the pre-therapy importance of such examination.

REPORT OF CASES

Case I. P.L. was a two year and seven month old Black girl who presented in July, 1969 complaining of generalized abdominal pain after unspecified trauma at home. Physical examination revealed diffuse abdominal tenderness and rigidity. Bilateral abdominal masses extending into both flanks were palpated. Blood pressure was 140/110, hemoglobin, 10.4 gm, hematocrit 36 percent, white blood cell count, 7,600 with normal differential. Urinalysis showed 3–4 white blood cells, and 30–35 red blood cells per high power field. While in the hospital, the masses were noted to increase in size. Intravenous pyelography, nephrotomography, and abdominal aortography were performed. Surgical exploration revealed bilateral huge renal masses with the right one firmly attached to the inferior surface of the liver. The patient was subsequently treated with Actinomycin D and radiation therapy. A gradual down hill course followed including disseminated metastases. The patient expired in January, 1970. Autopsy revealed bilateral Wilms' tumors with considerable extension into the liver substance. Bilateral pleural and parenchymal metastases were noted. The inferior vena cava was free of involvement.

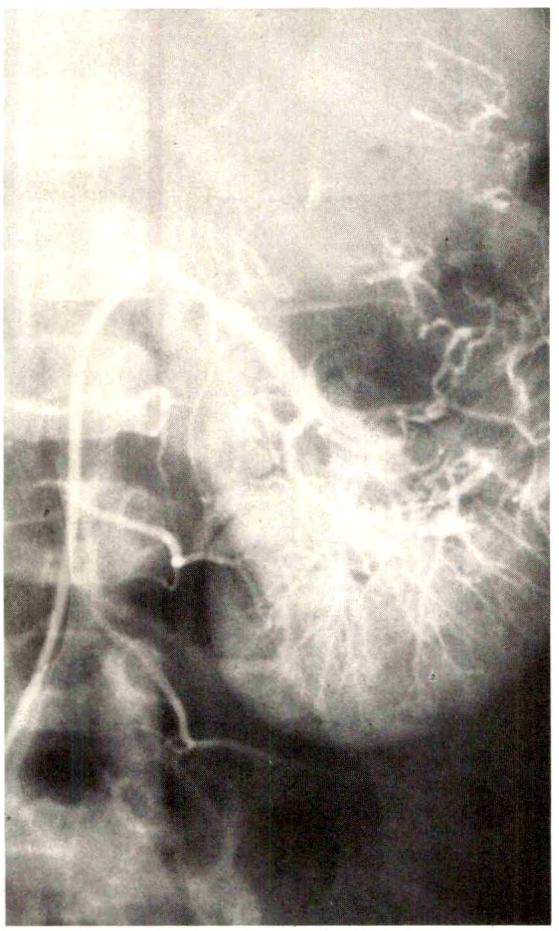


Fig. 3. Left renal arteriogram. Note abnormal vessels distributed in the periphery of the mass.



Fig. 4. Left renal arteriogram, late nephrographic phase. Note size and central distribution of abnormal vessels.

Case II. C.N. is a two year old white boy who was referred to St. Vincent's Hospital in De-

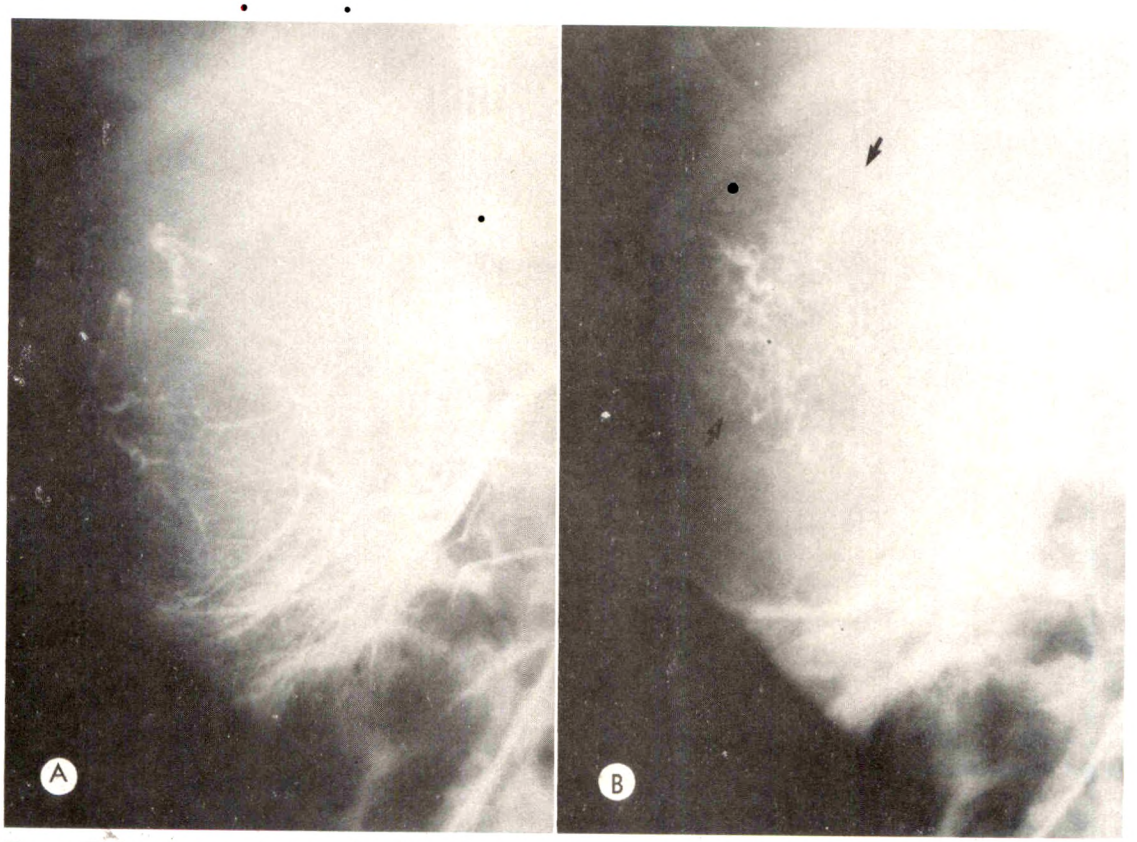


Fig. 5. Right renal arteriogram. (*A*) Arterial phase (three seconds) demonstrates filling of tumor vessels in the periphery of the mass. (*B*) Late nephrographic phase, central collection of tumor vessels with "avascular" surrounding zone (reverse "donut").

cember, 1974 because of a left abdominal mass noted on routine physical examination.

The mass was firm, nontender, extending into the left flank and not moving with respiration. A smaller, nontender right upper quadrant mass was palpated and could not be differentiated from liver. Urinalysis showed 5–8 red blood cells per high power field. Hemoglobin was 12.0 gm. Intravenous pyelography performed at the time of admission revealed bilateral upper pole masses with marked distortion and displacement of the calyces. A chest roentgenogram and a survey for metastasis were negative. Aortography, selective renal and celiac angiography, and inferior vena cavography were performed, without difficulty. Surgical exploration revealed bilateral renal masses which histologically were Wilms' tumor. A right total nephrectomy and left subtotal nephrectomy were performed. The right kidney was entirely involved while the left resected specimen was free of tumor at the margins. The liver was free of tumor.

The patient is presently undergoing chemo- and radiation therapy.

DISCUSSION

The first patient, under general anesthesia, had abdominal aortography *via* a right transfemoral arterial puncture, Seldinger technique. Marked displacement of intrarenal vessels is demonstrated (Fig. 1) and minimal, but definite, tumor vascularity is demonstrated on later films (Fig. 2). However, optimal detail of normal renal parenchyma was not demonstrated.

The second case demonstrates the added information provided by selective angiography. Recently, Lang[6] and others,[1,3,9] described angiographic features of unilateral Wilms' tumor, although most studies are based on nonselective angiography.[3,7] Although aortic displacement is common in cases of unilateral tumors[6,7,8] it was not

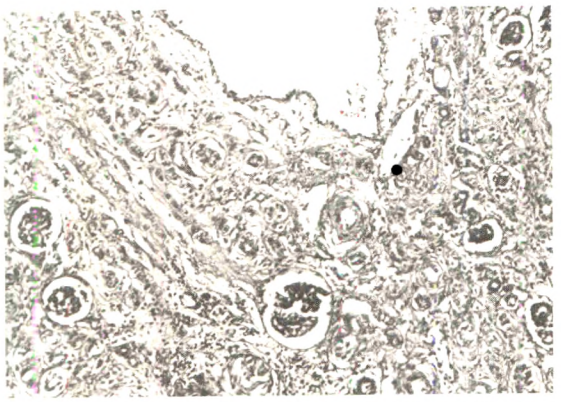


Fig. 6. Photomicrograph (75×) of the kidney—tumor interface demonstrates normal glomeruli on the right with gradual transition to tumor on the left. Note the primitive attempt at glomerulus formation on the left in addition to abnormal vessel above.

noted in the authors' experience of bilateral disease. On selective renal artery injection, malignant vasculature was most prominent in the late arterial-early capillary phase (Fig. 3), with persistent visualization into the late nephrographic phase (Fig. 4). Neoplastic vessels were large, but varied in size. In contradistinction to earlier description,[6] the authors noted early filling of the peripheral part of the tumor, followed by late and persistent filling of the more vascular central portion (Fig. 5, *A* and *B*). This configuration is suggestive of a "reverse donut" in that the central portion demonstrates wild neoplastic vasculature with a rather avascular peripheral rim on late films. The tumor is characteristic in its relative lack of tumor "stain."

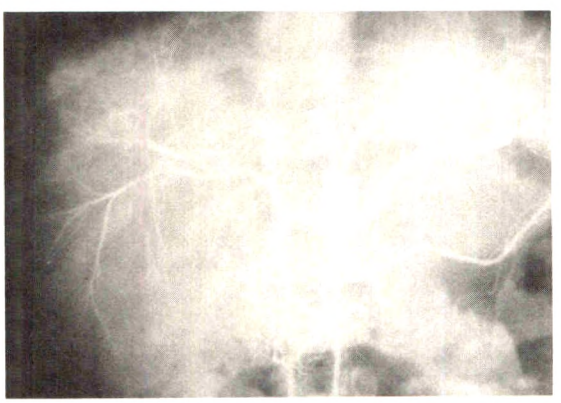


Fig. 7. Celiac angiogram reveals stretching of right lobar arteries, caused by anterior displacement by the renal mass. No evidence of tumor vasculature is noted.

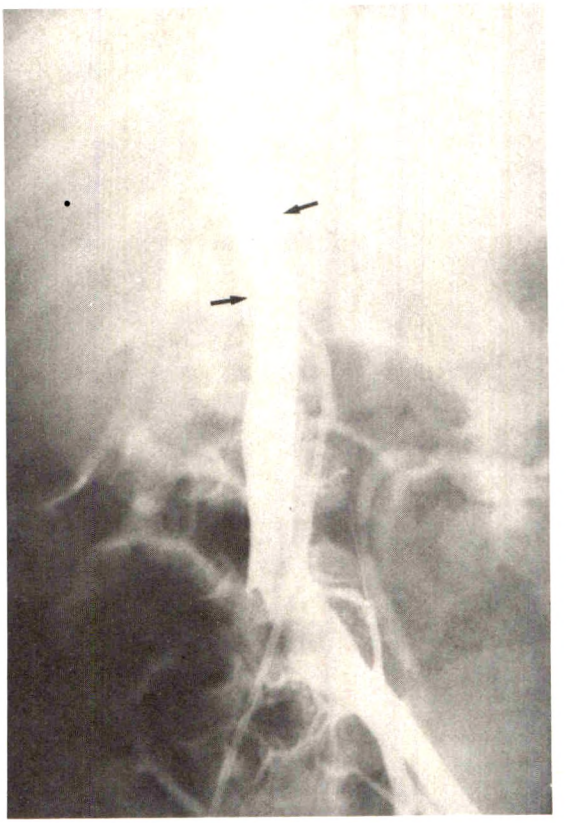


Fig. 8. Inferior vena cavogram reveals no deviation nor occlusion, with good flow from the renal veins (arrows).

As mentioned, of extreme importance is the evaluation of the interface between tumor and normal parenchyma, especially if partial nephrectomy is anticipated. Histologically, Wilms' tumor is characteristically infiltrating (Fig. 6), and this is demonstrated in the ill-defined interface and irregular parenchymal stain in the right lower pole (Fig. 5). These findings suggest involvement of the lower pole which was confirmed at surgery. Selective celiac arteriography demonstrates stretching of intrahepatic vessels secondary to anterior displacement by the renal mass (Fig. 7). No evidence of tumor vessels within the

liver is noted. Inferior vena cavography demonstrated good flow from the renal veins and normal inferior vena cava (Fig. 8).

Involvement of the liver was present in the first case; however, selective angiography was not available.

The question of whether this disease represents a metastatic process or separate primary neoplasms is beyond the scope of this report; however, it should be noted that in neither case was metastatic disease present at the time of initial diagnosis.

Barry T. Katzen, M.D.
Division of Cardiovascular Radiology
St. Vincent's Hospital and Medical
Center of New York
153 West 11th Street
New York, New York 10011

REFERENCES

1. Clark, R. E., Moss, A. A., DeLorimier, A. A., and Palubinskas, A. J. Arteriography of Wilms' tumor. Am. J. Roentgenol., Rad. Therapy & Nuclear Med., 1971, *113*, 476–490.
2. DeLorimier, A. A., Belzer, F. O., Kountz, S. I., and Kushner, J. A. Simultaneous bilateral nephrectomy and renal allotransplantation for bilateral Wilms' tumor. *Surgery*, 1968, *64*, 850–855.
3. Farah, J., and Lofstrom, J. E. Angiography of Wilms' tumor. *Radiology*, 1968, *90*, 775–777.
4. Folin, J. Angiography in Wilms' tumor. *Acta radiol.*, 1969, *8*, 201–308.
5. Hidai, H., Fukuoka, H., and Murayana, T. Arteriography of Wilm's tumor. *J. Urol.*, 1973, *110*, 347–351.
6. Lang, E. K. Contributions of arteriography in assessment of renal lesions encountered in neonatal period and infancy. *Radiology*, 1974, *110*, 429–438.
7. McDonald, P., and Hiller, H. G. Angiography in abdominal tumours in childhood with particular reference to neuroblastoma and Wilms' tumor. *Clin. Radiol.*, 1968, *19*, 1–18.
8. Meng, C., and Elkin, M. Angiographic manifestations of Wilms' tumor. Am. J. Roentgenol., Rad. Therapy & Nuclear Med., 1969, *105*, 95–104.
9. Moes, C. A. F., and Burrington, J. D. Use of aortography in diagnosis of abdominal masses in children. *Radiology*, 1971, *98*, 59–67.
10. Ragab, A. H., Vietti, T. J., Crist, W., Perez, C., and McAllister, W. Bilateral Wilms' tumor. *Cancer*, 1972, *30*, 983–988.

Vol. 126, No. 4

THE ABDOMINAL ANGIOGRAPHIC SPECTRUM OF TUBEROUS SCLEROSIS*

By WILLIAM R. COMPTON, M.D.,† PATRICK D. LESTER, M.D.,†‡
MYO M. KYAW, M.D.,† *and* JACK A. MADSEN, M.D.‡§
SALT LAKE CITY, UTAH

ABSTRACT:

Tuberous sclerosis can present with a variety of clinical, roentgenographic and pathological manifestations. Although we are not advocating abdominal angiography in every patient with tuberous sclerosis, the clinical diagnosis may be difficult in certain cases, particularly in the young patient, and abdominal visceral angiography may lead to the correct diagnosis. In two of our patients, infants ten months of age, the diagnosis of tuberous sclerosis was not made until abdominal angiography had been performed.

The most common changes are seen in the kidney where angiographic demonstration of hamartomas, arterial aneurysms, and multiple small cysts in the renal parenchyma are noted. Renal microcysts have not been previously described angiographically although they have been noted in pathological specimens and represent an important feature of the disorder spectrum.

In addition, vascular hamartomatous lesions may be demonstrated angiographically in other abdominal organs such as the adrenal gland and liver.

TUBEROUS sclerosis classically consists of seizures, mental retardation, and adenoma sebaceum while hamartomatous lesions of multiple organs are the prime roentgenographic features. The abdominal manifestations of tuberous sclerosis are most frequently related to hamartomas of the kidneys which are usually evaluated by intravenous pyelography. We have observed the expected angiographic appearance, but have also seen other changes which appear unique to this disorder. It is the purpose of this paper to present the abdominal angiographic spectrum of tuberous sclerosis which can be useful in the diagnosis.

MATERIAL

From a larger group of patients at the Utah State Training School suspected of having tuberous sclerosis, eight were selected on the basis of clinical features consistent with this disorder (all patients were approved through the Committee on Human Experimentation and studied with parental-guardian permission). Two patients, both infants, were not classified clinically until later, following roentgenographic evaluation.

Abdominal angiography was performed for evaluation of the visceral manifestations of this disorder in all patients, and consisted of selective celiac, superior mesenteric, and bilateral renal angiography. Patient ages ranged from 10 months to 34 years, and there were five females and three males.

RESULTS (TABLE I)

All eight patients had renal angiographic abnormalities. The expected renal hamartomas were seen in all five of the older patients, however, renal artery aneurysms or multiple small renal parenchymal cysts, or both, were also seen. Each of these lesions, when present, could be seen in both kidneys. Two of the eight patients had only multiple hamartomas, three showed only small renal cysts, one had both multiple hamartomas and cysts, another showed

* From the Department of Radiology,† Pediatrics,‡ and Neurology,§ University of Utah Medical Center, Salt Lake City, Utah.

Table I

Case	Age	Sex	Renal			Adrenal	Hepatic	Spleen	Bowel
			Hamartomas	Aneurysms	Cysts	Hamartomas			
1	11 yr.	F	o	o	+	o	+	o	o
2	10 mo.	F	o	o	+	o	+	o	o
3	21 yr.	F	+	o	+	o	o	o	o
4	29 yr.	M	+	o	o	+	+	o	o
5	24 yr.	F	+	+	o	o	+	o	o
6	34 yr.	M	+	o	o	+	o	o	o
7	10 mo.	F	o	o	+	o	+	o	o
8	20 yr.	M	+	+	+	o	o	o	o

multiple hamartomas and renal artery aneurysms, and one patient had kidneys demonstrating all three findings.

Adrenal angiography demonstrated hamartomatous lesions in two of the eight patients. Each patient with adrenal tumor also demonstrated renal hamartomas. While this represents 40 percent of the patients with renal hamartomas (2/5), the other three patients were children, who may yet develop the more characteristic hamartomatous tumors.

Celiac angiography demonstrated hamartomas in the hepatic parenchyma in five patients. These lesions were multiple in all of the patients and ranged in size from 0.3 cm to 6 cm. Only two of the five patients with hepatic hamartomas had renal hamartomas while the other three had only renal microcysts. No definite splenic lesions were seen.

Superior mesenteric artery angiography for evaluation of bowel hamartomas was unremarkable.

DISCUSSION

Tuberous sclerosis was first described as a clinical entity by Bourneville in 1880 and is an autosomal dominant disease with variable expression affecting multiple organs. Although the classical clinical triad of convulsive disorder, mental retardation, and adenoma sebaceum is well known, the spectrum may be quite varied. In a series of 71 patients studied at the Mayo Clinic[7] only 62 percent were mentally retarded. All the mentally retarded patients had a clinical history of seizures, but only 69 percent of the patients with normal intelligence had convulsions. In addition, adenoma sebaceum was present in 83 percent of the patients, usually developing in the second to third year of life.

The hallmark of its pathological involvement is hamartomas. In the eye, retinal tumors, or phakomas, are found in 53 percent of patients.[77] In the brain, intracranial calcifications representing calcified tumor nodules are found in 48–63 percent of patients.[7] These calcifications do not correlate with mental ability, and are found most commonly in the central brain in the paraventricular regions. Pneumoencephalography may demonstrate brain atrophy, dilated ventricles, or subependymal tumor nodules in the ventricular walls.[8]

The bones may demonstrate patchy areas of osteosclerosis in the skull, vertebral

column, and pelvis which can simulate osteoblastic metastases. Additional findings include small phalangeal cysts and a wavy periosteal thickening which may be found about the shafts of the long bones and phalanges.[19]

Spontaneous pneumothorax, cor pulmonale, or interstitial-type infiltrates secondary to small cysts and adenomas reflect the intrathoracic involvement frequently seen. Cardiac tumors, especially rhabdomyomas, may be seen.[19]

KIDNEY

The most frequent abdominal manifestation of tuberous sclerosis is multiple renal hamartomas which have been reported in 60–80 percent of patients.[7,14] Clinically, the patients may have vague urinary tract or abdominal symptoms. Occasionally, the tumors present as asymptomatic abdominal masses.[1] If hemorrhage occurs, patients may have gross hematuria or acute abdominal pain.[4]

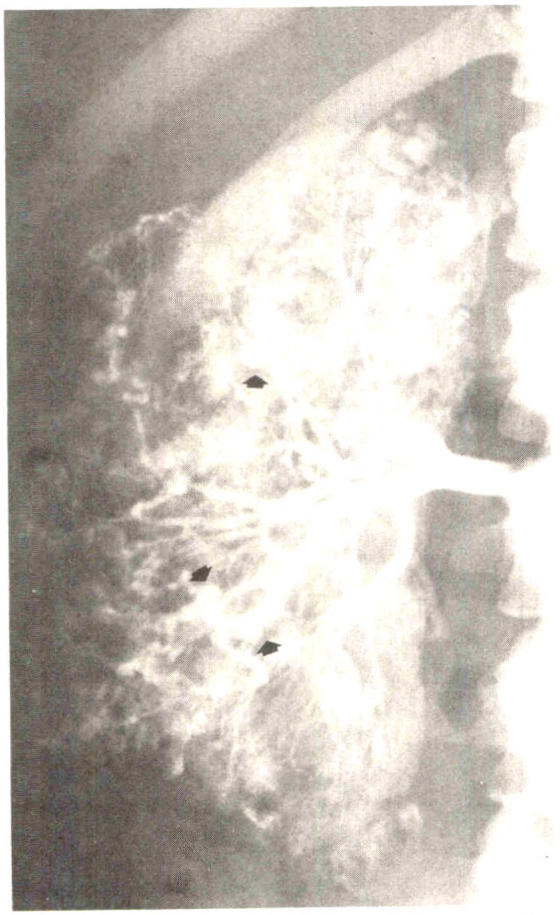


FIG. 1. Case V. A 24 year old female demonstrating the typical angiographic features of multiple hamartomas and renal artery aneurysms (arrows) involving the entire kidney.

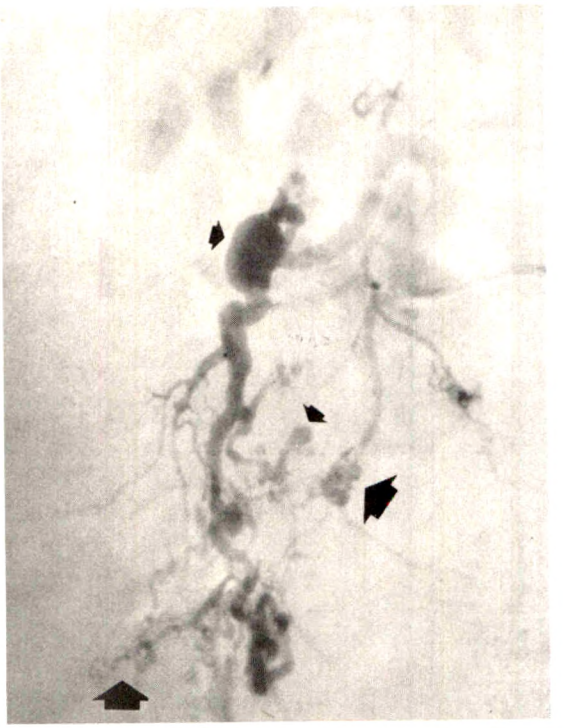


FIG. 2. Case VIII. Subtraction technique in a selective lower pole renal angiogram demonstrating arterial aneurysms (small arrows) and multiple hamartomas (large arrows).

The hamartomas are mixed mesodermal tumors composed of fat, smooth muscle, and blood vessels in varying proportions, therefore the alternative term "angiomyolipomas" has been used. In almost all cases, these lesions are benign; extension into a renal vein or metastasis is rare. Such extension may even represent multiple hamartomatosis.[19] In one of our patients, large hamartomas tremendously increased in size for no apparent reason. There was no basic change in the appearance of the individual lesions and no metastases have occurred.

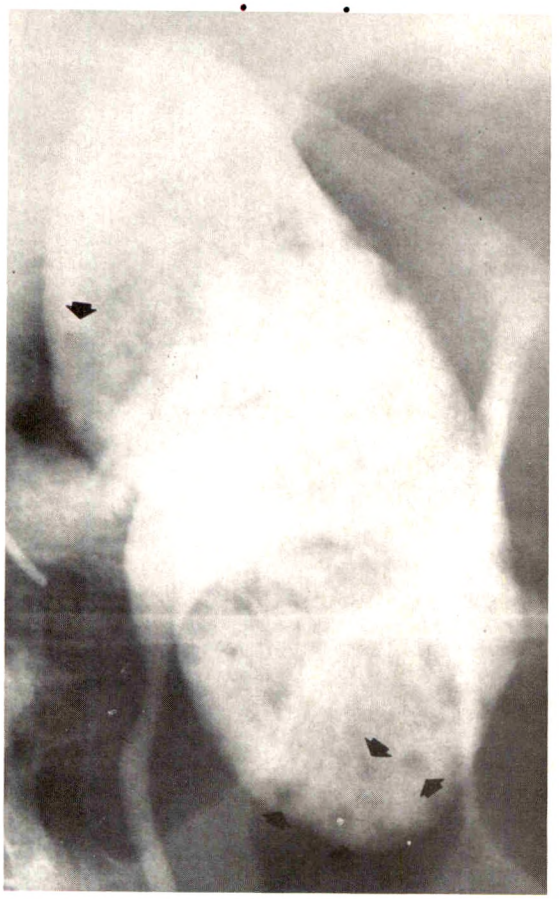


Fig. 3. Case I. Magnification view of a left renal angiogram in the capillary phase demonstrating multiple small round radiolucencies in the renal parenchyma characteristic of renal microcysts (arrows).

The intravenous pyelogram, when positive, will demonstrate multiple mass lesions displacing calyceal structures as seen in polycystic kidney disease. Occasionally, the hamartomas will be radiolucent because of a high fat content, making differentiation from cysts possible.[1,10] It is usually impossible, however, to distinguish these two entities on the pyelogram alone, and correlation with other clinical findings, as well as angiography, is usually necessary. Only three of our five patients with hamartomas had lesions large enough to be seen on intravenous pyelography.

Although solitary renal hamartomas (which are generally not associated with tuberous sclerosis) may have some angiographic features which may simulate renal carcinoma, the multiple lesions in tuberous sclerosis patients usually do not present a diagnostic problem (Fig. 1; and 2). The lesions often show a "whorled" type of arterial appearance with a rather well defined circumferential peripheral arterial network. Multiple aneurysms or aneurysmal dilatations of the interlobar and interlobular arteries is another feature.[2,19] Arteriovenous puddling of contrast material may be seen; however, early arteriovenous shunting does not seem to occur. Attempts to evaluate the lesions with intra-arterial epinephrine shows a similar lack of response as with renal carcinoma because of a deficiency in the smooth muscle lining in the arteries.[2,3,16] This lack of epinephrine response was con-

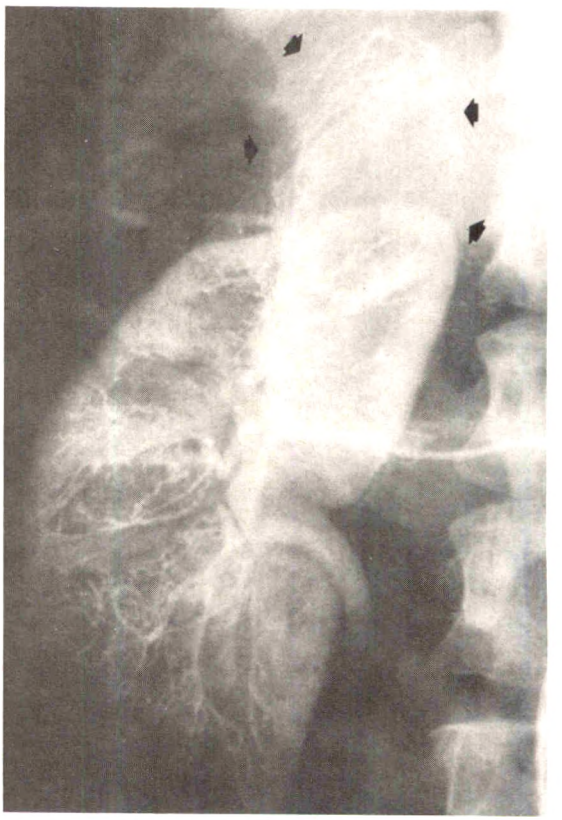


Fig. 4. Case IV. Adrenal gland hamartoma. Note the intact renal cortex of the upper pole indicating adrenal origin of the tumor. This patient also had renal and hepatic hamartomas.

firmed in some of our patients.

The finding of small renal cysts has not previously been described as an angiographic manifestation of tuberous sclerosis. Pathologic evaluation of the kidneys in patients with tuberous sclerosis, however, has shown multiple renal cortical cysts.[9,12,15,17] It is debated whether the cysts represent anomalies of development or whether they are of obstructive origin. Several authors have described patients with combined polycystic disease and the multiple renal hamartomas of tuberous sclerosis.[5,6] We feel that the demonstration of multiple cysts in these patients is merely a part of the spectrum of this disease. Five of our eight patients demonstrated round cortical radiolucencies ranging from 0.1 cm to 1 cm in size (Fig. 3). In three of these patients, the only renal manifestation was renal microcysts, but hepatic hamartomas were also seen.

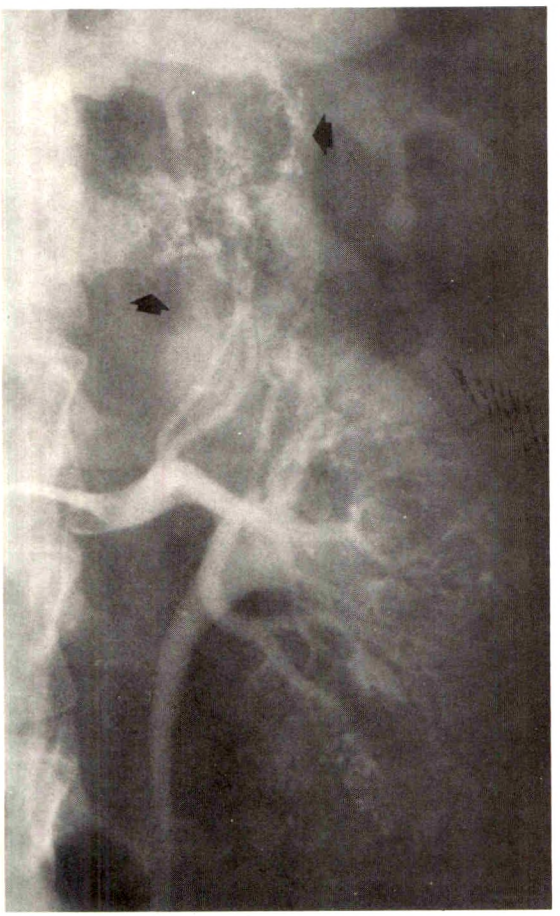


Fig. 5. Case VI. Adrenal gland hamartoma with angiographic features similar to those of the more common renal hamartomas. The adrenal arteries originating from the renal artery are enlarged as they supply this tumor.

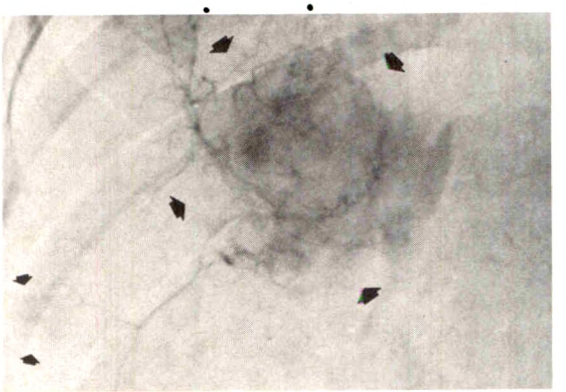


Fig. 6. Case V. Subtraction technique in the late arterial phase of a hepatic angiogram demonstrating two separate and well-defined hamartomas in the hepatic parenchyma (arrows). The larger tumor is 6 cm in diameter and has features similar to its renal counterpart.

The renal angiographic manifestations of tuberous sclerosis consisting of multiple hamartomas with the features described, multiple renal arterial aneurysms, small renal cortical cysts, or some combination of these, are seen in all our patients. At least one of these lesions must be present for us to consider the diagnosis. It may be that the typical hamartomas become more pronounced, and therefore easier to detect, as age progresses.

ADRENAL GLAND

Adrenal gland hamartomas have not been described angiographically in patients with tuberous sclerosis, and have only rarely been described pathologically.[13,17] Two of our eight patients demonstrated adrenal angiomyolipomas with the same angiographic criteria for diagnosis as their renal counterparts (Fig. 4; and 5). It may be difficult to distinguish between upper renal pole tumors and those arising from the adrenal gland. Both tumors were sup-

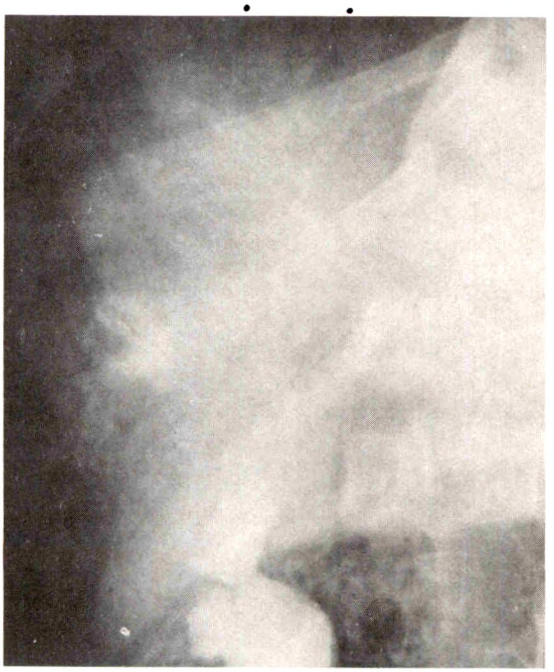


FIG. 7. Case 1. Magnified view of the liver in a selective hepatic capillary phase demonstrating another hepatic hamartoma.

plied primarily by the adrenal arteries.

LIVER

Hepatic hamartomas have also been described pathologically in patients with tuberous sclerosis.[15,18,19] Specific angiographic demonstration of angiomyolipomas of the liver has not been described in tuberous sclerosis, although following angiography, hepatic involvement was suggested in one report.[19] In our series, five of eight patients demonstrated vascular tumors of the liver with celiac angiography (Fig. 6; and 7). The characteristics of these liver lesions were similar in some respects to those of the renal hamartomas, although aneurysms were not identified.

MISCELLANEOUS

Rarely, additional visceral involvement with hamartomas in tuberous sclerosis has been reported in specimens including the spleen and pancreas.[15,18] Angiographic demonstration of these lesions has not been described. In our series none of the patients showed spleen, bowel or pancreatic lesions, but one might anticipate that the usually smaller lesions would be more difficult to detect, especially in the bowel.

Patrick D. Lester, M.D.
Department of Radiology
University of Utah Medical Center
Salt Lake City, Utah 84132

We appreciate the cooperation of the staff, patients, and parents of the Utah State Training School in this evaluation and study.

REFERENCES

1. Anderson, D., and Tannen, R. L. Tuberous sclerosis and chronic renal failure: potential confusion with polycystic kidney disease. *Am. J. Med.*, 1969, *47*, 163–168.
2. Becker, J. A., Kinkhabwalla, M., Pollack, H., and Bosniak, M. Angiomyolipoma (hamartoma) of kidney: angiographic review. *Acta radiol.* (Diag.), 1973, *14*, 561–568.
3. Brendler, H., Maguire, J. W., and Mitty, H. A. Angiographic characteristics of renal hamartoma. *Brit. J. Urol.*, 1971, *43*, 674–678.
4. Clark, R. E., and Palubinskas, A. J. Angiographic spectrum of renal hamartoma. Am. J. Roentgenol., Rad. Therapy & Nuclear Med., 1972, *114*, 715–721.
5. Inglis, K. Neurilemmoblastosis. *Am. J. Clin. Path.*, 1950, *26*, 521–550.
6. Klapproth, H. J., Pontasse, E. F., and Hazard, J. B. Renal angiomyolipomas: report of four cases. *A.M.A. Arch. Path.*, 1959, *67*, 400–411.
7. Lagos, J. C., and Gomez, M. R. Tuberous sclerosis: reappraisal of clinical entity. *Mayo Clin. Proc. Staff Meet.*, 1967, *42*, 26–49.
8. Lagos, J. C., Holman, C. B., and Gomez, M. R. Tuberous sclerosis: neuroroentgenologic observations. Am. J. Roentgenol., Rad. Therapy & Nuclear Med., 1968, *104*, 171–176.
9. LeBrun, H. I., Kellett, H. S., and Macalister, C. L. O. Renal hamartoma. *Brit. J. Urol.*, 1955, *27*, 394–407.
10. McCullough, D. L., Scott, R., Jr., and Seybold, H. M. Renal angiomyolipoma (hamartoma): review of literature and report of seven cases. *J. Urol.*, 1971, *105*, 32–44.
11. Milledge, R. D., Gerald, B. E., and Carte, W. J. Pulmonary manifestations of tuberous sclerosis. Am. J. Roentgenol., Rad. Therapy & Nuclear Med., 1966, *98*, 734–738.
12. Moolter, S. E. Hamartial nature of tuberous sclerosis complex and its bearing on tumor

problem. *Arch. Int. Med.*, 1942, *69*, 589–623.
13. Murphy, E. S., Fujii, Y., Yasuda, A., and Sasabe, S. Tuberous sclerosis complex. *A.M.A. Arch. Path.*, 1958, *65*, 166–173.
14. Olurin, E. O., Ajayi, O. O., and Osunkoya, B. O. Tuberous sclerosis: report of two renal presentations. *Brit. J. Urol.*, 1971, *43*, 432–438.
15. Perou, M. L., and Gray, P. T. Mesenchymal hamartomas of kidney. *J. Urol.*, 1960, *83*, 240–261.
16. Silbiger, M. L., and Peterson, C. C. Renal angiomyolipoma: distinctive angiographic characteristics. *J. Urol.*, 1971, *106*, 363–365.
17. Simopoulous, A. P., and Breslow, A. Tuberous sclerosis in newborn. *A.M.A. Am. J. Dis. Child.*, 1966, *111*, 313–316.
18. Van Heerden, J. A., Longo, M. F., Cardoza, F., and Farrow, G. M. Abdominal mass in patient with tuberous sclerosis. *A.M.A. Arch. Surg.*, 1967, *95*, 317–319.
19. Viamonte, M., Jr., Ravel, R. Politano, V., and Bridges, B. Angiographic findings in patient with tuberous sclerosis. Am. J. Roentgenol., Rad. Therapy & Nuclear Med., 1966, *98*, 723–733.

THE COMPLICATION RATE OF CATHETER ANGIOGRAPHY BY DIRECT PUNCTURE THROUGH AORTO-FEMORAL BYPASS GRAFTS*

By RONALD L. EISENBERG, M.D., RICHARD L. MANI, M.D., *and* EUGENE J. McDONALD, Jr., M.D.
SAN FRANCISCO, CALIFORNIA

ABSTRACT:

A search of the literature revealed no documentation of the complication rate associated with percutaneous catheterization of aorto-femoral bypass grafts in the arteriographic evaluation of graft patency. The authors compared the complication rates of 29 consecutive arteriograms performed through grafts (Group I) with 40 arteriograms performed on non-graft patients (Group II). Neither group had any significant complications, indicating the safety of percutaneous catheterization of the graft site.

CATHETER angiography is employed with increasing frequency in the evaluation of the patency of aorto-femoral bypass grafts in patients with peripheral vascular occlusive disease. To avoid direct puncture of the graft it has been traditional for the vascular surgeon to request that the angiographer use the axillary or translumbar approach. Fear of direct graft puncture has been based on the following potential hazards:[2] (1) Uncontrollable bleeding and hematoma formation because of the non-vascular nature of the punctured graft. (2) Disruption of the anastomotic suture line and consequent false aneurysm formation. (3) Infection of the graft site necessitating surgical intervention. (4) Disruption of the pseudo-intima with possible thrombogenesis.

A search of the literature, however, has revealed no documentation of the complication rate associated with direct puncture of aorto-femoral grafts.

Over the last several years, the authors, with the agreement of the vascular surgeons, have employed catheter angiography by percutaneous puncture of the aorto-femoral graft on a routine basis.

The purpose of this communication is: (1) to review our case material over a three year period; (2) to document the complication rate associated with catheter angiography by direct puncture of aorto-femoral grafts; and (3) to compare this complication rate with femoral catheter angiography in non-graft patients.

MATERIAL AND METHOD

Our method for percutaneous puncture of aorto-femoral bypass grafts follows the conventional Seldinger technique. We employ a No. 6 French dilator prior to the insertion of a straight No. 6 French (0.082 in. O.D.) catheter with five side holes. Direct pressure is applied to the puncture site for 15 minutes after the catheter is withdrawn. Patients are returned to the ward with the following post-angiographic orders:

1. Check vital signs, groin, and peripheral pulses every 15 minutes ×4, every 30 minutes ×2, every hour ×2, then resume routine check of vital signs.
2. Bed rest for eight hours with punctured extremity extended.

The case material was divided into two groups. Group I (Graft Group) consisted of 29 femoral arteriograms performed between January, 1972 and August, 1975 on

* From the Department of Radiology, University of California Medical Center and the Veterans Administration Hospital, San Francisco, California.

20 patients by direct puncture of the aorto-femoral bypass graft. Twelve patients were studied once, seven were studied twice, and one patient had three separate examinations. The average age of these patients was 62 years with a range of 50 to 77 years. All were male and had a history of surgery for claudication. Group II (Control Group) consisted of 40 consecutive aorto-femoral arteriograms performed during the same period on 40 patients by direct puncture through non-grafted femoral arteries. The average age was 65 years with a range of 47 to 94 years. All the patients were male and had a history of claudication and some significant degree of peripheral vascular occlusive disease.

The method of analysis for possible complications was as follows:

1. Complete review of patients' medical charts.
2. Review of all arteriograms.
3. Interview with attending vascular surgeons.
4. Review of arteriographic technicians' records.

Complications were defined as (a) hematoma; (b) bleeding; (c) thromboembolic phenomena (*e.g.*, diminished pulse, cold leg); (d) infection; and (e) false aneurysms. Any of these complications may have required surgical or medical consultation, unanticipated therapy, or additional hospitalization.

RESULTS

Analysis of Group I and Group II demonstrated no evidence of complications as defined by the above criteria. In addition, no systemic complications, *i.e.*, alteration of blood pressure, heart rate or rhythm, were noted.

Uncontrolled bleeding, hematoma, and thromboembolism are possible short-term hazards of percutaneous punctures of aorto-femoral bypass grafts. Our study revealed no evidence of these complications. Post-angiographic infection and false aneurysms are complications requiring a longer period of follow-up. Eight patients in our series had repeat examinations from 6 to 30 months after the original angiogram (Fig. 1). In no case was there any evidence of long term complications (Tables I and II).

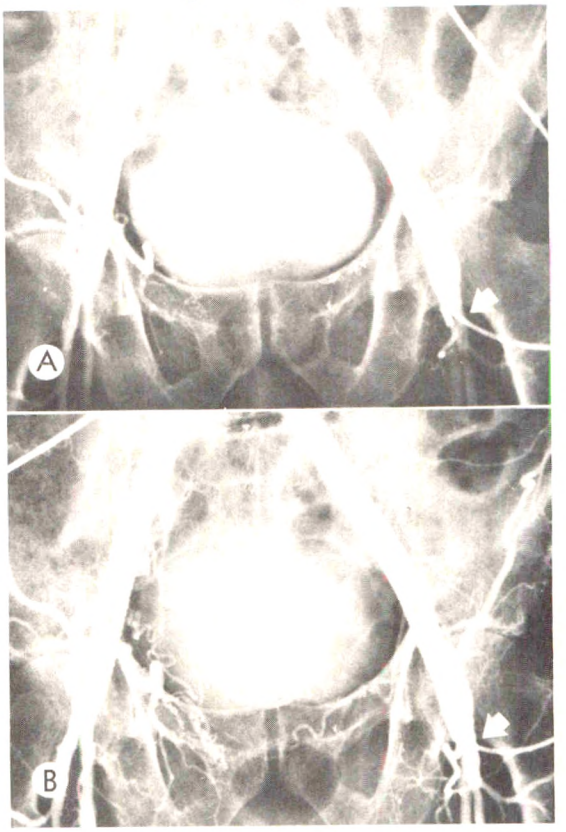


Fig. 1. (*A* and *B*) Anteroposterior projections of consecutive arteriograms (*A*, 3/16/74; *B*, 10/25/74) performed on the same patient by percutaneous catheterization of left limb of aorto-femoral graft (arrow). No evidence of thromboembolism or false aneurysm is seen on follow-up study (*B*).

Table I

EVALUATION OF LONG-TERM COMPLICATIONS (INFECTION, FALSE ANEURYSM, THROMBOEMBOLISM)

Follow-Up Time (in months)	Number of Arteriograms	Complications
0–6	9	0
7–12	11	0
13–18	5	0
19–24	1	0
25–30	1	0
31–36	2	0

TABLE II

ANALYSIS OF PATIENTS WITH REPEAT ANGIOGRAMS

Time Interval between Angiograms (in months)	Number of Patients	Complications
0–6	1	0
7–12	4*	0
13–18	4*	0
19–24	0	0
25–30	2	0

* Includes one patient with 3 examinations (January, 1974, November, 1974, June, 1975).

DISCUSSION

The radiologist is faced with an increasing demand for the angiographic evaluation of patients with aorto-femoral bypass grafts. The traditional approach has been through the axillary route to avoid direct puncture of the graft site because of concern for possible post-angiographic complications. Abrams[1] advises, "In patients with aortic thrombosis or a previous aortic bifurcation graft, the left axillary artery approach to the abdominal aorta is employed" and adds "a prior aorto-iliac or aorto-femoral bypass graft, however, is usually avoided as a catheterization route, despite a strong femoral pulse. . . ."

In our experience, the axillary approach is a much more cumbersome and difficult procedure than the direct femoral route. The axillary puncture requires greater skill, hemostasis is more difficult to achieve, and selective catheterization of aortic branches, when required, is more difficult. The utilization of percutaneous puncture of the aorto-femoral graft increases the speed and ease of the procedure.

A review of our case material demonstrated no evidence of short-term local or systemic complications in 29 direct percutaneous punctures through grafts, and no long-term complications in nine patients evaluated with repeated studies.

These results, therefore, strongly suggest that catheter angiography through percutaneous puncture of an aorto-femoral bypass graft is not only a safe procedure, but the procedure of choice in the evaluation of graft patency.

Ronald L. Eisenberg, M.D.
Department of Radiology
Veterans Administration Hospital
4150 Clement Street
San Francisco, California 94121

REFERENCES

1. Abrams, H. L. Angiography. Little, Brown & Company, Boston, Mass., 1971, 1223–1225.
2. Goldstone, J. Personal communication.

Vol. 126, No. 4

SYSTEMIC ARTERIAL SUPPLY TO NORMAL BASILAR SEGMENTS OF THE LEFT LOWER LOBE*

By DONALD R. KIRKS, M.D.,†‡ PETER E. KANE, M.D.,† EDWARD A. FREE, M.D.,§ *and* HOOSHANG TAYBI, M.D.†

OAKLAND, CALIFORNIA

SYSTEMIC arterial supply to normal pulmonary parenchyma is a rare congenital abnormality with characteristic roentgenological features. Two cases of this lung anomaly are presented.

REPORT OF CASES

CASE I. D.T. was the product of a normal gestation. A heart murmur was first noted at six months of age, but no further investigations were performed. At six years of age, a heart murmur was again detected, during a routine school physical, and he was referred to Children's Hospital Medical Center for further evaluation.

Physical examination revealed an asymptomatic male. The temperature, pulse, respiratory rate, and blood pressure were normal. There were a precordial thrill and a prominent left ventricular impulse. A grade 4/6 continuous heart murmur was best heard beneath the left clavicle but also radiated to the cardiac apex, axilla, and posterior chest. The remainder of the physical examination was normal.

An electrocardiogram demonstrated left ventricular hypertrophy and left atrial enlargement. A chest roentgenogram showed cardiac enlargement and a retrocardiac density which obliterated a portion of the descending thoracic aorta (Fig. 1*A*). Cardiac catheterization revealed slight elevations of the pulmonary wedge and left ventricular end diastolic pressures. The oxygen saturation values in the left ventricle and aorta were normal. There was normal pulmonary arterial supply to the entire right lung, left upper lobe, and superior segment of the left lower lobe. There were no pulmonary arteries to the basilar segments of the left lower lobe (Fig. 1*B*). A large systemic artery from the descending thoracic aorta supplied the basilar segments of the left lower lobe (Fig. 1*C*). There was a capillary phase in these segments with rapid filling of the inferior pulmonary vein (Fig. 1, *D* and *E*) which drained into the left atrium (Fig. 1*F*).

Bronchoscopy immediately prior to thoracotomy showed all major bronchi of the left lung to be in their normal location. Through a left thoracotomy, the large, tortuous vessel off the descending thoracic aorta was readily identified and ligated at its origin. Pulmonary arterial supply to the superior segment of the left lower lobe was identified and a left lower lobectomy performed.

Pathologically, the large artery was elastic-walled. The parenchyma, major bronchi, minor bronchi, and bronchioles of the resected lower lobe were normal.

CASE II. H.R. was the product of a normal gestation with a normal mental and physical development. A heart murmur was heard at one week of age. At 17 months of age, she was admitted to Children's Hospital Medical Center because of recurrent urinary tract infections.

Physical examination showed an asymptomatic well-developed female. The temperature, pulse, respiratory rate, and blood pressure were normal. There was a grade 2/6 systolic ejection murmur along the left lower sternal border as well as a bruit at the left lung base posteriorly. The remainder of the physical examination was normal.

The plain film of an intravenous pyelogram revealed a retrocardiac density which partially obliterated the descending thoracic aorta. This abnormality was confirmed by a chest roentgenogram (Fig. 2*A*). The pulmonary artery pressure, aortic pressure, and descending aortic oxygen saturation were normal. Cine angiocardiography demonstrated normal pulmonary arterial supply to the entire right lung, left upper lobe, and superior segment of the left lower lobe. There were no pulmonary arteries to the basilar segments of the left lower lobe. A large systemic artery arising from the descending thoracic aorta supplied the basilar segments of the left lower lobe (Fig. 2*B*). There was a capillary phase in these basilar segments

* From the Departments of Radiology† and Surgery,§ Children's Hospital Medical Center, Oakland, California.

‡ Present Address: Department of Radiology, Children's Medical Center, The University of Texas Health Science Center, Dallas, Texas.

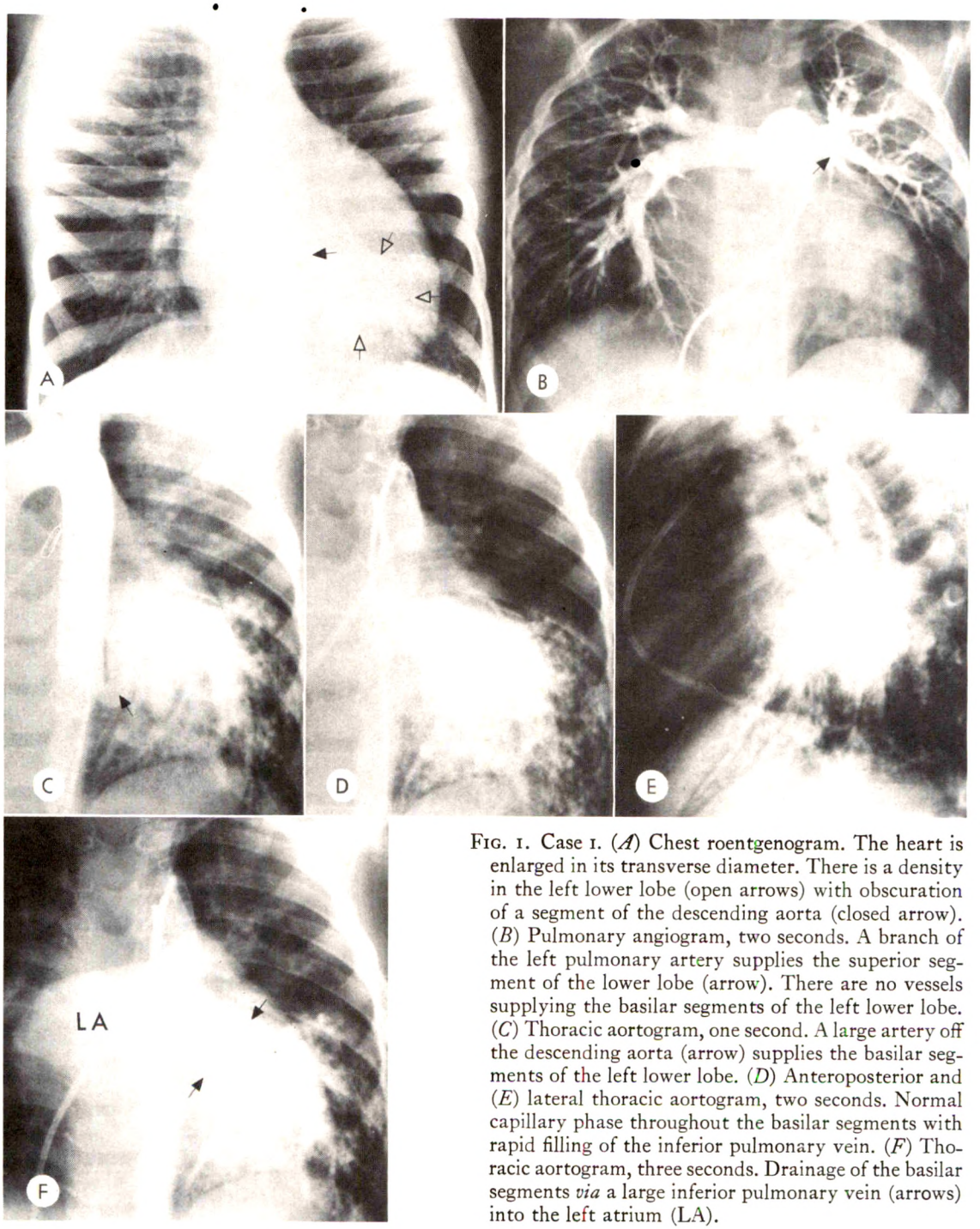


Fig. 1. Case 1. (*A*) Chest roentgenogram. The heart is enlarged in its transverse diameter. There is a density in the left lower lobe (open arrows) with obscuration of a segment of the descending aorta (closed arrow). (*B*) Pulmonary angiogram, two seconds. A branch of the left pulmonary artery supplies the superior segment of the lower lobe (arrow). There are no vessels supplying the basilar segments of the left lower lobe. (*C*) Thoracic aortogram, one second. A large artery off the descending aorta (arrow) supplies the basilar segments of the left lower lobe. (*D*) Anteroposterior and (*E*) lateral thoracic aortogram, two seconds. Normal capillary phase throughout the basilar segments with rapid filling of the inferior pulmonary vein. (*F*) Thoracic aortogram, three seconds. Drainage of the basilar segments *via* a large inferior pulmonary vein (arrows) into the left atrium (LA).

(Fig. 2*C*) with venous drainage (Fig. 2*D*) into the left atrium.

At thoracotomy, a vessel one centimeter in diameter off the descending aorta led into the basilar segments of the left lower lobe. A branch of the left pulmonary artery supplied the superior segment of the left lower lobe. A vein two centimeters in diameter drained from the basilar segments of the left lower lobe into the left atrium. A left lower lobectomy was performed.

Pathologically, there was neither gross nor

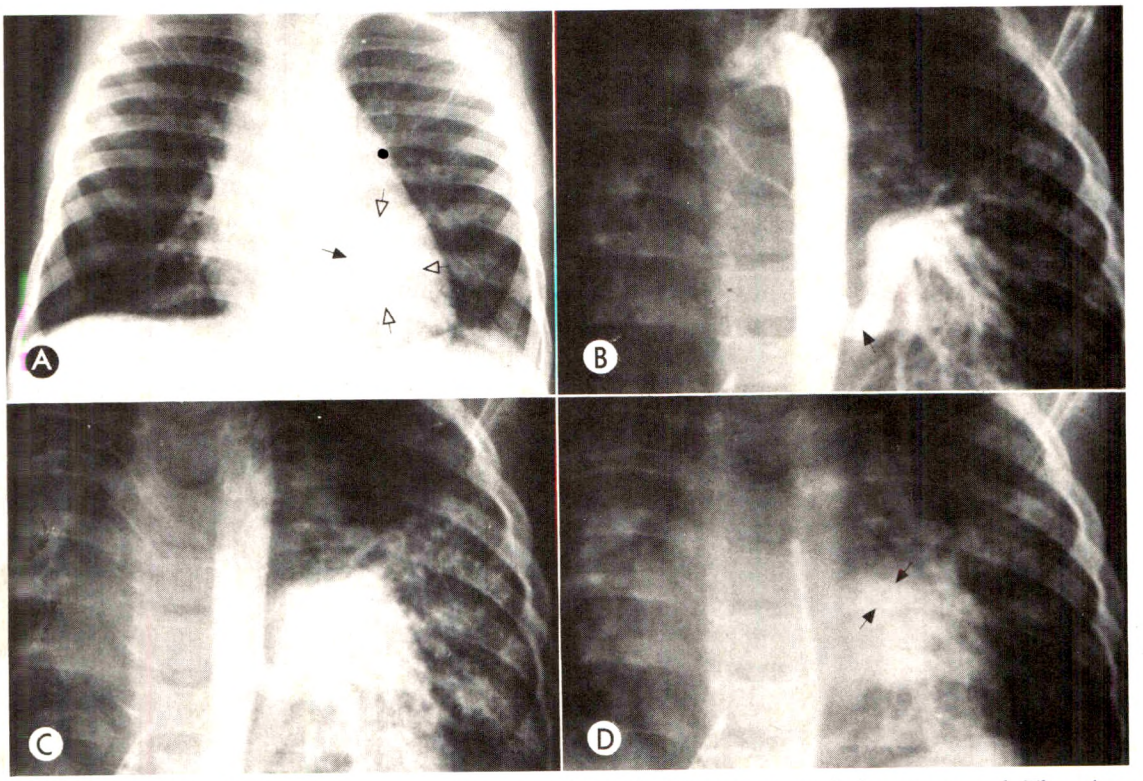


Fig. 2. Case 11. (*A*) Chest roentgenogram. The heart size and pulmonary vascularity are normal. There is a vague density in the left lower lobe (open arrows) with obliteration of the descending aorta (closed arrow). (*B*) Thoracic aortogram, one second. Large systemic artery (arrow) supplies the left lower lobe. (*C*) Thoracic aortogram, three seconds. Normal capillary phase of the basilar segments of the left lower lobe. (*D*) Thoracic aortogram, 6 seconds. Normal venous drainage from the inferior pulmonary vein (arrows) into the left atrium.

microscopic evidence of contiguity between the large systemic artery and vein of the basilar segments. This thick-walled artery had multiple well-defined elastic laminae within its media. The major bronchi, minor bronchi, and bronchioles were normal. There was no evidence of inflammation, sequestration, or dysplastic change within the pulmonary parenchyma.

DISCUSSION

Systemic arterial supply to normal lung is a rare congenital abnormality of pulmonary blood supply.[3,4,6,8,10,12,13] The arterial supply of a normal segment of pulmonary parenchyma is provided by an aberrant vessel that arises from the aorta.

The lungs first appear during the third week of embryonic life as ventral outgrowths of the foregut. By 30 days, a visceral vascular plexus has appeared around the branching primary lung buds.[1] This plexus is fed by "pulmonary" channels from the sixth aortic arches as well as "systemic" channels from the paired dorsal aortas.[2,8] Normally, the channels from the sixth aortic arches as well as the vascular plexus differentiate into the definitive pulmonary arteries, while the systemic channels involute to form the minute bronchial arteries. Although the etiology of a systemic arterial supply to normal lung is unknown, the most likely theory is that one of the systemic arteries retains its original embryonic connection between aorta and pulmonary parenchyma.[8]

Patients with systemic arterial supply to normal lung may be totally asymptomatic. Eventually, left ventricular enlargement and congestive heart failure secondary to the left-to-left shunt may develop.[13] There

TABLE I

SPECTRUM OF CONGENITAL PULMONARY ABNORMALITIES WITH SYSTEMIC ARTERIAL SUPPLY

Congenital Abnormality	Abnormal Bronchial Distribution	Abnormal Pulmonary Artery Distribution	Systemic Artery
Normal	−	−	−
Accessory Arterial Supply to Lung by Systemic Vessel[3,4,10,12]	−	−	+
Only Arterial Supply to Lung by Systemic Vessel (These Two Cases)[8]	−	+	+
Sequestration[7,9,11,14]	+	+	+

are usually no associated pulmonary symptoms.

The roentgenology of this abnormality is demonstrated by these two reported cases. The abnormal vascular supply in the involved segment of lung produces a soft-tissue density with striate margins. The basilar segments of the left lower lobe are most commonly involved,[8] and there is neither associated mass effect nor cystic change of the pulmonary parenchyma. The aorta may be obliterated at the origin of the systemic vessel. There may be associated cardiac enlargement. Bronchoscopy and bronchography demonstrate normal major and minor bronchial anatomy. Aortography and pulmonary angiography show a large systemic artery supplying the only blood flow to the involved segments of lung. Although this aberrant vessel may originate from one of several aortic branches or from the aorta below the diaphragm, it usually arises from the aorta just above the diaphragm.[13] The aortogram shows a normal "parenchymagram" without direct communication between the systemic artery and a pulmonary vein. Drainage of the involved segments is usually *via* the inferior pulmonary vein into the left atrium.

It should be stressed that not all pulmonary lesions with systemic arterial supply are sequestrations. Other congenital causes are arteriovenous fistula,[5] pulmonary artery aplasia,[13] and systemic arterial supply to normal lung.[13] Acquired causes of systemic arterial supply to lung include pulmonary suppuration,[13] pleurectomy,[13] and iatrogenic anastomosis.[10] Pulmonary sequestration is a congenital abnormality characterized by non-functioning, usually cystic lung tissue, which has no normal connection with either the bronchial tree or pulmonary arteries.[4,7,9,11] The absence of mass effect, normal bronchial distribution, and normal parenchyma in the involved segments of lung exclude a diagnosis of sequestration in these two reported cases.

Despite these differences, systemic arterial supply to normal pulmonary parenchyma is probably closely related to sequestration.[4] These patients fit into a spectrum of congenital pulmonary abnormalities (Table 1). The aberrant systemic artery may provide either the only arterial supply to lung as in these reported cases,[8] or may provide arterial supply to lung in addition to normal pulmonary arterial supply.[3,4,10,12] In addition, all of these congenital lesions with an aberrant systemic artery to lung may develop rapid left-to-left shunting.[4,14] This is particularly well illustrated by Case 1. However, the segmental involvement and neither angiographic nor pathologic evidence of direct arteriovenous communication exclude a diagnosis of congenital arteriovenous fistula.[5]

Complete roentgenologic evaluation is critical in planning definitive surgical therapy. The anomalous systemic vessel may simply be ligated if there is associated normal pulmonary artery supply to the involved segment of lung.[3,4] Associated sequestration in the involved pulmonary pa-

renchyma requires complete removal to prevent recurrent infection.[4] Finally, if the involved parenchyma is normal and the only blood supply to the lung segment is *via* the systemic artery, it may be possible to transfer the origin of the anomalous vessel to the pulmonary artery.[8] The anomalous vessel is divided at its origin, the defect in the aorta is closed, and the proximal end of the systemic vessel is sutured to the inferior side of the pulmonary artery. This surgical method requires that the procedure is technically feasible, the involved segment of pulmonary parenchyma is normal, and the anomalous vessel can function physiologically as a pulmonary artery.[8]

SUMMARY

Two cases of sole arterial supply to normal basilar segments of the left lower lobe *via* an aberrant systemic vessel are described. A spectrum of congenital pulmonary abnormalities with systemic arterial supply to the lung is presented. Complete roentgenologic evaluation is necessary prior to definitive surgery.

Hooshang Taybi, M.D.
Department of Radiology
Children's Hospital Medical Center
51st and Grove Streets
Oakland, California 94609

REFERENCES

1. Boyden, E. A. Developmental anomalies of lungs. *Am. J. Surg.*, 1955, *89*, 79–89.
2. Boyden, E. A. Bronchogenic cysts and theory of intralobular sequestration: new embryologic data. *J. Thoracic Surg.*, 1958, *35*, 604–616.
3. Campbell, D. C., Jr., Murney, J. A., and Dominy, D. E. Systemic arterial blood supply to normal lung. *J.A.M.A.*, 1962, *182*, 497–499.
4. Currarino, G., Willis, K., and Miller, W. Congenital fistula between aberrant systemic artery and pulmonary vein without sequestration: report of three cases. *J. Pediat.*, 1975, *87*, 554–557.
5. Dines, D. E., Arms, R. A., Bernatz, P. E., and Gomes, M. R. Pulmonary arteriovenous fistulas. *Mayo Clin. Proc. Staff Meet.*, 1974, *49*, 460–465.
6. Ellis, K., Seaman, W. B., Griffiths, S. P., Berdon, W. E., and Baker, D. H. Some congenital anomalies of pulmonary arteries. *Seminars in Roentgenol.*, 1967, *2*, 325–341.
7. Felson, B. Many faces of pulmonary sequestration. *Seminars in Roentgenol.*, 1972, *7*, 3–16.
8. Hessel, E. A., II, Boyden, E. A., Stamm, S. J., and Sauvage, L. R. High systemic origin of sole artery to basal segments of left lung: findings, surgical treatment, and embryologic interpretation. *Surgery*, 1970, *67*, 624–632.
9. Sane, S. M., and Girdany, B. R. Cysts and neoplasms in infant lung. *Seminars in Roentgenol.*, 1972, *7*, 122–148.
10. Scott, L. P., III, and Perry, L. W. Systemic artery-pulmonary vein fistulas: congenital and acquired left-to-left shunt. *Am. J. Cardiol.*, 1969, *23*, 872–876.
11. Takahashi, M., Ohno, M., Mihara, K., Matsuura, K., and Sumiyoshi, A. Intralobar pulmonary sequestration with special emphasis on bronchial communication. *Radiology*, 1975, *114*, 543–549.
12. Varma, K. K., and Clarke, C. P. Congenital systemic-to-pulmonary arteriovenous fistula: report of a case. *Australian & New Zealand J. Surg.*, 1971, *40*, 360–362.
13. Viamonte, M., Jr. Intrathoracic extracardiac shunts. *Seminars in Roentgenol.*, 1967, *2*, 342–367.
14. White, J. J., Donahoo, J. S., Ostrow, P. T., Murphy, J., and Haller, J. A., Jr. Cardiovascular and respiratory manifestations of pulmonary sequestration in childhood. *Ann. Thoracic Surg.*, 1974, *18*, 286–294.

IATROGENIC EMBOLIZATION OF THE SUPERIOR MESENTERIC ARTERY: ARTERIOGRAPHIC OBSERVATIONS AND CLINICAL IMPLICATIONS*

By ADAM LANDE, M.D., *and* MORTON A. MEYERS, M.D.†
NEW YORK, NEW YORK

ABSTRACT:

Following sudden occlusion of the superior mesenteric artery, there is a characteristic and predictable pattern of blood flow through the instantaneously activated collateral channels. On the left, the first patent jejunal or ileal branch utilizes the central tier of the mesenteric arcades to revascularize the distal trunk of the occluded superior mesenteric artery. On the right, the anastomotic connection between the middle colic, right colic, and ileocolic arteries provides an efficient collateral pathway. These two collateral channels supplement each other and the distal trunk of the occluded superior mesenteric artery is usually rapidly reconstituted.

Superior mesenteric artery embolization is frequently an asymptomatic event. There appears to be a variable tolerance of cardiac and non-cardiac patients to the effect of superior mesenteric embolization. Non-cardiac patients may tolerate embolization of the superior mesenteric artery quite well. Cardiac patients frequently respond with an ischemic crisis. The site of embolization is another determining factor. An embolus below the origin of the middle colic artery provides an incomparably more favorable hemodynamic situation than an embolus proximal to the origin of this vessel.

The excellent tolerance of our group of patients to superior mesenteric embolization appears to be closely related to these two main factors.

INTESTINAL ischemia and infarction may be occlusive or non-occlusive in nature. Non-occlusive forms of intestinal gangrene usually occur in patients with heart disease and a failing myocardium. Severe splanchnic vasoconstriction may lead to irreversible damage in the superior mesenteric territory.[6,7,11,14,15] Non-occlusive bowel infarction may also occur in patients with severe hemorrhage and shock.[6,7,14,15] Spontaneous intestinal ischemia may follow thrombosis of the superior mesenteric artery.[14,15] Thrombotic occlusions generally develop in the first few centimeters close to the origin where atherosclerotic deposits are common in elderly individuals.[5]

This report is concerned with a detailed analysis of ten cases of iatrogenic embolization of the superior mesenteric artery which occurred in the course of selective catheterization of this vessel. Review of the literature provides surprisingly little information regarding the immediate arteriographic alterations and clinical manifestations following embolization of the superior mesenteric artery distal to its middle colic branch. This type of study provides a unique opportunity to determine the immediate circulatory changes following acute occlusion of the superior mesenteric artery and its major branches. It also places the clinical aspects of this syndrome into a new perspective.

MATERIAL AND METHOD

In the six years between 1968 and 1974, 780 selective superior mesenteric arterial catheterizations were performed at the

* From the Department of Radiology, New York Medical College, Metropolitan Hospital Center, New York, New York.
† Present Address: Department of Radiology, The New York Hospital-Cornell Medical Center, New York, New York.

Metropolitan Hospital Center of the New York Medical College. The indications for the examinations were quite variable and ranged from acute abdominal trauma to suspected intra-abdominal malignancy.

The standard procedure for selective superior mesenteric artery catheterizations remained unchanged over this period. A thin-walled, gray Kifa catheter (O.D. 2.8 mm–I.D. 1.8 mm) was routinely employed. Although this catheter accepts a 0.053″ guidewire, the tip of the catheter was molded over a 0.035″ guide and 0.035″ guidewires were employed during catheterization. Selective catheterization was routinely preceded by flush aortography. In all ten instances of superior mesenteric artery embolization, the thrombus formed in the tip of the catheter after it was selectively placed in the superior mesenteric artery trunk and the thrombus was propelled into the vessel during subsequent serial arteriography. The formation of the clot could be traced to negligence in flushing the catheter with heparinized saline. Most of the embolizations occurred during initial experiences with selective catheterizations. In the last several years, with introduction of a continuous arterial perfusion pump, the incidence of this complication has been drastically reduced.

RESULTS

A single embolus was present in all instances except one. The clot preserved its integrity and did not disintegrate into smaller fragments. It varied in length from 5 mm to 4 cms, but averaged 2 cms in length. The embolus was always arrested before it reached the small intestinal arcades. Although all thrombi were formed in the tip of the catheter, they were trapped at various levels of the superior mesenteric artery. This apparently was primarily related to the length of the thrombus and the width of the superior mesenteric artery in a given patient. In eight patients the embolus was arrested in the main trunk of the superior mesenteric artery. The larger emboli were retained high in the superior mesenteric artery and accordingly a much larger arterial tree was rendered ischemic. The two largest emboli lodged just below the origin of the middle colic artery. None occluded the origin of the middle colic artery or the superior mesenteric artery above the origin of the middle colic. There was a definite tendency for the clot to migrate along the main trunk of the vessel. When the thrombus was arrested, at least one but usually several small intestinal branches were occluded and eliminated from circulation. The number of intestinal branches occluded depended on the length of the impacted embolus. The ileo-colic artery was embolized on one occasion and an ileal branch in another patient.

ARTERIOGRAPHIC OBSERVATIONS

In all patients, collateral circulation bypassed the acutely occluded segment within several seconds. The small intestinal arcades composed of several tiers of intercommunicating channels serve as a most efficient collateral pathway.

The central tier of arcuate arteries constitutes the preferential collateral route in sudden occlusion of the main trunk of the superior mesenteric artery (Fig. 1; and 3, *A* and *B*). This is related to its comparatively short course and larger cross-sectional diameter.[4] The collateral by-pass bridging the occluded segment originates from the first patent intestinal branch immediately proximal to the obstruction. Rapid opacification of the central arcades proceeds to the first non-occluded jejunal or ileal artery distally which then revascularizes the main trunk of the superior mesenteric artery. In this fashion, the distal aspect of the superior mesenteric artery is virtually immediately reconstituted.

To the right of the superior mesenteric artery, another collateral circuit is immediately activated to by-pass the obstruction. This bridge is composed of the right branch of the middle colic artery and its anastomosis with the right colic and ileo-colic branches (Fig. 1–3).

These two collateral channels supple-

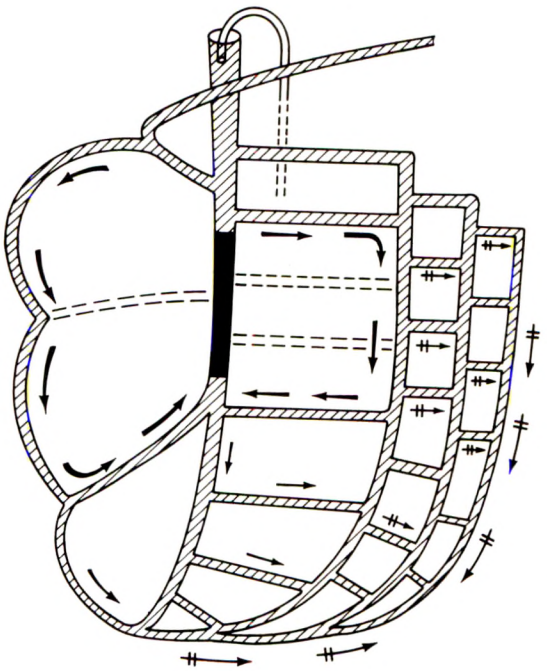


FIG. 1. Schematic illustration of the circulatory conditions in the superior mesenteric artery following embolization of the main trunk. Initially the main collateral pathways are directed towards the distal trunk of the vessel (thick arrows). After revascularization of the central vessels the blood flow is re-routed along the peripheral arcades and into the vasa recta (double-bar arrows).

ment each other and represent a very efficient collateral pathway. The distal stump of the occluded superior mesenteric artery is typically opacified within seconds (Fig. 2–4). The length of the thrombus is thereby precisely delineated by the opacified distal as well as proximal stump of the occluded superior mesenteric artery trunk.

CLINICAL OBSERVATIONS

Seven of the ten patients with iatrogenic embolization of the superior mesenteric artery were totally asymptomatic. In these, the embolus was small in size and located distally in the superior mesenteric artery or its branches. Small intestinal barium examinations performed within 24 hours following the incident demonstrated no abnormality. Stool guaiacs were consistently negative.

Of the three patients who displayed symptoms, two had large emboli impacted just distal to the origin of the middle colic artery (Fig. 3, *A* and *B*) and their clinical manifestations were quite similar. Severe colicky pain developed immediately, persisted for several hours, and required administration of analgesics. Watery diarrhea was guaiac-positive but there was no frank blood in the stool. Following heparinization and administration of broad-spectrum antibiotics, there was rapid resolution of symptoms. Small intestinal series performed in one patient 48 hours following the embolization showed mild edema of mucosal folds but no evidence of thumbprinting. The third patient had an embolic occlusion of the distal aspect of the superior mesenteric artery which, however, was complicated by severe intestinal adhesions developing several months after insertion of a Y-graft prosthesis for a Leriche's syndrome (Fig. 4). Immediately following arteriography, he developed severe colicky pain, and several hours later signs of peritoneal irritation appeared. At laparotomy, extensive small intestinal adhesions were found in the right lower quadrant and were lysed. The entire small intestine showed skip areas of purplish discoloration suggesting imminent gangrene. Because of the diffuse nature of the process, it was elected to re-explore the patient 24 hours later to permit clear demarcation of the gangrenous segments.[8] At re-exploration, the entire small intestine had a normal pink color with complete resolution of the dark patches seen the day before. The patient made an uneventful recovery.

None of the ten patients required embolectomy or small intestinal resection, although one was explored. All had a small intestinal series several weeks following embolization and the examination failed to show any abnormality.

DISCUSSION

The arteriographic alterations as shown in this series of patients provide an unusual opportunity for an *in vivo* demonstration of

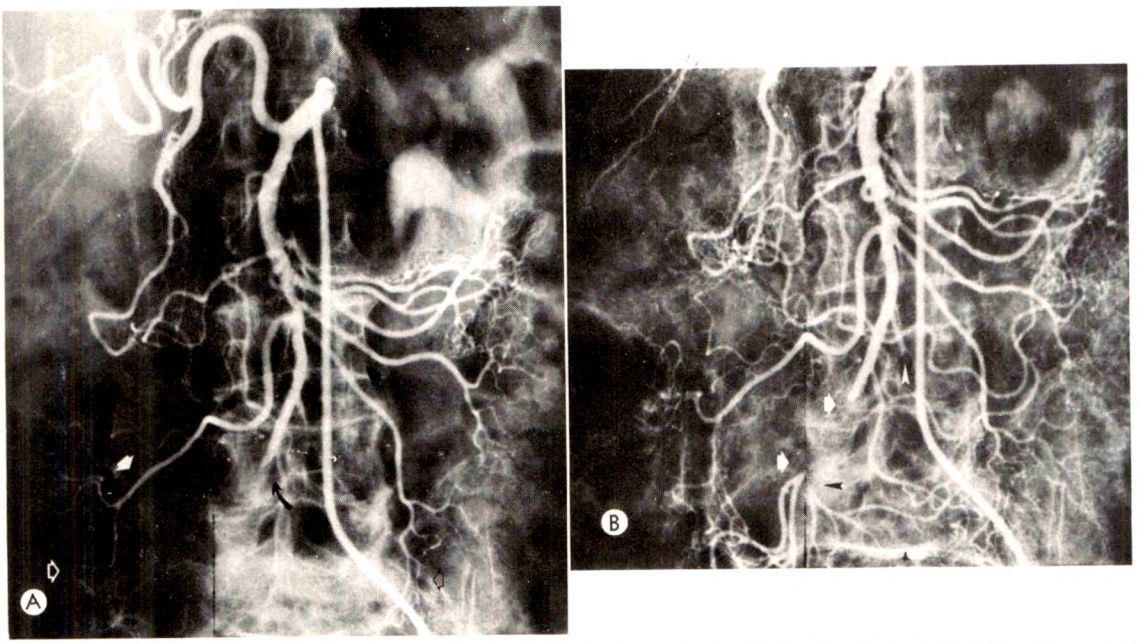


Fig. 2. Selective superior mesenteric arteriogram. (*A*) One second from the start of injection. The main trunk of the superior mesenteric artery is occluded (curved arrow). Two collateral channels are activated. On the left a jejunal branch opacifies the primary arcades (black arrows). On the right the ileocolic artery and its anastomotic connection to the superior mesenteric artery are shown (white arrows). (*B*) Four seconds from the start of injection, the distal trunk of the vessel is reconstituted and the length of the embolus can be now precisely demarcated (broad, white arrows). An occluded ileal branch fails to opacify (black arrowhead). A small embolus occluding another ileal branch is shown (white arrowhead).

the hemodynamic changes following sudden occlusion of the superior mesenteric artery and its branches.

At the very instant of occlusion, total cessation of blood flow and drop in pressure distal to the obstruction attract all collateral channels to this critical central point. Collateral blood flow as seen in our patients was primarily directed toward the occluded distal superior mesenteric artery. However, following reconstitution of the main trunk, the arterial circulation was redirected along the most peripheral small intestinal arcades and into the vasa recta which supply the small intestine (Fig. 1). The low pressure in the venules in the wall of the small intestine now attracts the circulation.

There are only very few illustrations in the literature which depict the local circulatory conditions following superior mesenteric artery embolization distal to its middle colic branch.[1,2,10,15] In all instances, selective arteriography was performed several hours or days following embolization. Analysis of these arteriograms indicates that the contrast material is re-routed predominantly along the most peripheral small intestinal arcades, suggesting that the circulation in the larger vessels and central arcades is relatively sluggish. This is clearly demonstrated in our serial observations by the fact that the contrast material is retained in the distal stump of the occluded superior mesenteric artery for several seconds following rapid initial revascularization.

The practical implication of this observation is apparent. Stagnant flow promotes thrombosis. Formation of secondary thrombosis begins within several hours following embolization, and the distally advancing thrombus may sequentially occlude the orifices of jejunal and ileal arteries.[6,9] This in turn further impairs the efficiency of collateral blood flow. The collateral pathways are overextended and the

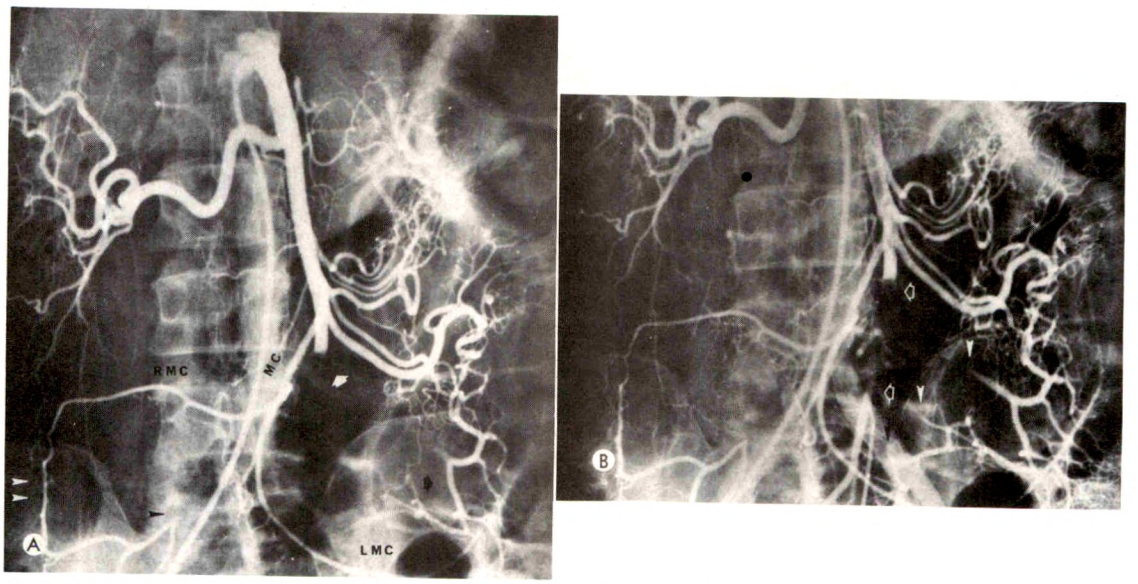


Fig. 3. Selective superior mesenteric arteriogram. (*A*) Occlusion of the main trunk (white arrow) below the origin of the middle colic artery (MC) is shown at one second from the start of injection. The middle colic artery divides into its right (RMC) and left (LMC) branches. An anastomotic channel (white arrowheads) connects the right middle colic artery to ramifications of the occluded ileocolic artery (black arrowhead). Early opacification of the collateral mesenteric arcades (black arrow). (*B*) The distal trunk of the superior mesenteric artery is reconstituted by retrograde collateral flow and the length of the embolus can be demarcated (arrows) within three seconds from the start of injection. There is partial retrograde opacification of the ileal branches from the collateral arcades (arrowheads).

resistance disproportionately rises. Thus, a vicious cycle is established leading to accelerated thrombosis.

The arteriographic appearance of atherosclerotic emboli differs from those described in this paper. Atherosclerotic emboli are usually multiple, vary in size, and are frequently associated with showers of cholesterol microemboli, which may produce a variety of clinical manifestations.[12]

Our experience is at variance with the generally accepted belief that embolization of the main superior mesenteric artery is necessarily a catastrophic event requiring immediate surgical intervention. Small emboli, even if totally occlusive, may be completely asymptomatic, as was demonstrated in seven of our ten patients. Two of the three symptomatic patients with embolization just distal to the middle colic branch recovered on medical therapy and were asymptomatic 24 hours after the acute episode. The third patient had extensive small intestinal adhesions which apparently caused precarious circulation in this segment of the bowel.

Detailed analysis of the experience reported by others and of our series of patients brings out two important differences which apparently influence the clinical behavior: (a) the absence of heart disease; and (b) the relationship of the embolus to the middle colic artery.

The vast majority of patients reported in the literature who required surgery following embolization of the superior mesenteric artery had underlying heart disease, often of a serious degree. Most had atherosclerotic heart disease, some rheumatic heart disease, and others a past or recent myocardial infarction. In contrast, none of our patients had a past history of heart disease and none had cardiac problems at the time of examination.

The heart and particularly the left atrium are the most common sources of spontaneous systemic emboli.[6] Cardiac disease, even well-compensated, appears to exert a pe-

culiar influence upon the splanchnic circulation; a marginal cardiac output renders the superior mesenteric territory very vulnerable to additional insults. This is particularly true in patients on maintenance doses of digitalis which is known to be a potent splanchnic vasoconstrictor.[13] In cardiac patients with borderline splanchnic perfusion, the superior mesenteric circulation seems to react with a reflex vasoconstriction and circulatory embarrassment which are out of proportion to the size of an embolus. Indeed a small embolus may precipitate an ischemic crisis.[2]

In our series of patients, the embolus was always trapped distal to the origin of the middle colic artery. An embolus in this location creates an incomparably more favorable circulatory situation than does an embolus superior to the middle colic artery or a saddle embolus occluding the superior mesenteric and middle colic arteries simultaneously.[11] When the proximal segment of the superior mesenteric artery is occluded, the vessel is revascularized by two tenuous anastomotic connections: one originates in the celiac axis and through the pancreaticoduodenal arcades supplies the superior mesenteric trunk; the second is the well-known Riolan's anastomosis connecting the left colic branch of the inferior mesenteric artery to the left branch of the middle colic artery. This collateral blood supply is capable of maintaining borderline viability of the small intestine and the ascending and transverse colon for several hours.[6] If the obstruction is not removed, however, gangrene invariably ensues. Prompt diagnosis and surgical intervention are of crucial importance.[6,11]

In occlusion of the superior mesenteric artery below the origin of the middle colic, the blood pressure proximal to the obstruction equals the systemic pressure and the efficient collateral circulation assures only a relatively moderate drop in blood pressure distal to the obstruction.

It is for these reasons, we believe, that the majority of successful embolectomies, not requiring simultaneous segmental resection of the small intestine, were performed in patients with an embolus lodged distal to the middle colic artery.[11]

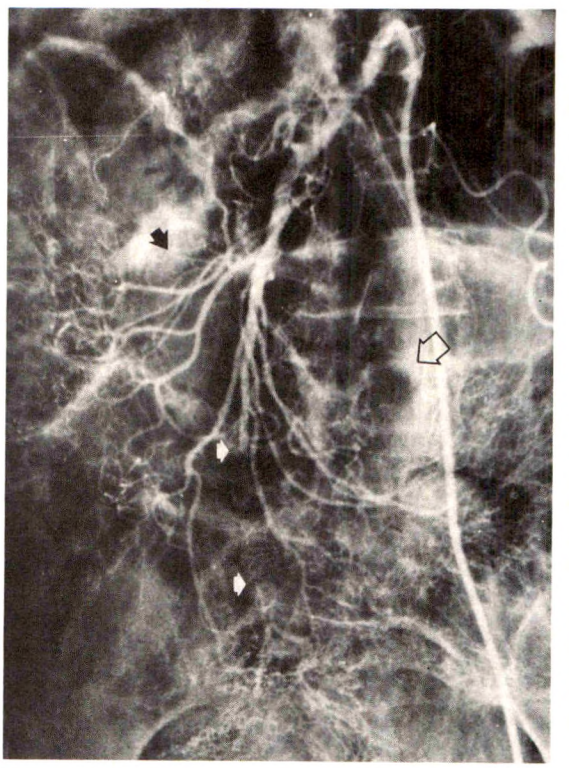


Fig. 4. Selective superior mesenteric arteriogram. Extensive peritoneal adhesions cause deviation of the jejunal vessels to the right (closed black arrow). The ileal branches are retracted caudally and medially (open black arrow). The length of the embolus in the distal superior mesenteric artery is demarcated (white arrows).

Vasoconstriction both proximal and distal to the site of embolization has been noted in several cases of emboli to the superior mesenteric artery.[2,15] However, it was not observed in our patients. This phenomenon is apparently a neural reflex which requires some time to appear. Vasoconstriction of the large and small intestinal arteries is an ominous sign, since it may effectively interfere with the efficiency of collateral blood flow independently of the location of the embolus. Stagnant flow distal to the obstruction in turn promotes development of secondary thrombosis along the distal trunk of the superior mesenteric artery.

In the past, paravertebral and epidural

spinal anesthesia was employed to eliminate the effects of arterial vasoconstriction. Recently, a new technique of intra-arterial infusion of papaverine has been successfully employed. This method appears to be very effective in eliminating the deleterious effect of arterial vasoconstrictions.[14]

Adam Lande, M.D.
Department of Radiology
Metropolitan Hospital
1901 First Avenue
New York, New York 10029

REFERENCES

1. Aakhus, T. Value of angiography in superior mesenteric embolism. *Brit. J. Radiol.*, 1966, *39*, 928–932.
2. Aakhus, T., and Brabrand, G. Angiography in acute superior mesenteric arterial insufficiency. *Acta. radiol.* (Diag.), 1967, *6*, 1–12.
3. Bonakdarpour, A. Angiography of mesenteric arterial occlusion. *Invest. Radiol.*, 1970, *5*, 316–328.
4. Cokkinis, A. J. Mesenteric Vascular Occlusion. Bailliere, Tindall & Cox, London, 1926.
5. Dick, A. P., Graff, R., Gregg, D. M., Peters, N., and Sarner, M. Arteriographic study of mesenteric arterial disease. I: Large vessel changes. *Gut*, 1967, *8*, 206–220.
6. Glotzer, J. D., and Shaw, S. R. Massive bowel infarction: autopsy study assessing potentialities of reconstructive vascular surgery. *New England J. Med.*, 1959, *260*, 162–167.
7. Jackson, B. B. Occlusion of Superior Mesenteric Artery. Monograph, American Lectures in Surgery Series. Charles C Thomas, Springfield, Ill., 1963.
8. Meier, A. L., and Waibel, P. Mesenteric artery occlusion with intestinal gangrene: two stage operative procedure with thrombectomy followed by "second look" to permit resection of irreversibly damaged portion of intestine. *A.M.A. Arch. Surg.*, 1964, *88*, 181–184.
9. Reiner, L., Platt, R., Rodriquez, L. F., and Jiminez, A. F. Injection studies of mesenteric infarction. *Gastroenterology*, 1960, *39*, 747–757.
10. Rösch, J., and Steckel, J. R. Selective angiography of abdominal viscera. (In: "Selective Angiography.") In: Golden's Diagnostic Radiology.) Second edition. Edited by W. N. Hanafee. William & Wilkins, Co., Baltimore, 1972, p. 27.
11. Rutledge, H. R. Superior mesenteric artery embolectomy: review of literature and case report. *Am. J. Surg.*, 1964, *159*, 529–535.
12. Schwartz, S., and Waters, L. Cholesterol embolization. *Radiology*, 1973, *106*, 37–41.
13. Shanbour, L. L., and Jacobson, E. D. Digitalis and mesenteric circulation. *Am. J. Digest. Dis.*, 1972, *17*, 826–828.
14. Siegelman, S. S., Sprayregen, S., and Boley, J. S. Angiographic diagnosis of mesenteric arterial vasoconstriction. *Radiology*, 1974, *112*, 533–542.
15. Wittenberg, J., Athanasoulis, A. C., Shapiro, H. J., and Williams, F. L. Radiological approach to patient with acute extensive bowel ischemia. *Radiology*, 1973, *106*, 13–24.

VOL. 126, NO. 4

PARTIAL MESENTERIC ARTERIAL OCCLUSION WITH SUBSEQUENT ISCHEMIC BOWEL DAMAGE DUE TO PITRESSIN INFUSION*

By CAMERON ROBERTS, M.D., *and* FRANK E. MADDISON, M.D.
MILWAUKEE, WISCONSIN

IN early experimental and clinical experience, Baum, Nusbaum, and Blakemore infused the superior mesenteric artery (SMA) with Pitressin to control variceal bleeding. They found no evidence for ischemic sequelae.[1,5,6] Other authors reported no ischemic complications,[7,8] and such complications remained a theoretical consideration only until 1972, when one case of mesenteric venous thrombosis and jejunal infarction secondary to Pitressin infusion was reported.[9] Also in that year, a case of extensive ischemic damage to the small bowel after Pitressin infusion was reported, but this case was complicated by pre-existing severe atherosclerosis of the mesenteric arteries.[3] Then in 1974, two cases of total thrombosis of the SMA and portal veins in patients who had received Pitressin were reported.[2] However, these diagnoses were made at autopsy. We believe this is the first report of an ante mortem diagnosis of ischemic bowel damage secondary to Pitressin infusion for control of variceal bleeding.

REPORT OF A CASE

A 63 year old white female with a five year history of known chronic active hepatitis was admitted after awakening at home to find a clot of blood in her mouth. The patient denied recent or remote hematemesis, melena, or abdominal pain. Current medications were 2–3 tablets of Anacin daily. She gave no history of excessive alcohol intake.

On examination, the patient was alert and cooperative, in no acute distress. Peripheral arterial pulse was 80/min, blood pressure was 140/90 mm Hg. The abdomen was not tender, with active bowel sounds. The liver was palpable 3 cm below the right costal margin.

The admission hematocrit value was 36 percent, and the prothrombin time was 13.5 sec (control 12 sec).

A nasogastric tube was inserted into the stomach and returned bright red blood. Emergency endoscopy shortly after admission showed large esophageal and gastric varices as well as gastritis. Two of the gastric varices were actively bleeding. Angiography by Seldinger technique using a 7 Fr polyethylene C-shaped catheter for the celiac axis and SMA injections demonstrated splenomegaly and gastric varices. No bleeding site was identified (Fig. 1). Superior mesenteric arterial infusion with 0.2 units/min of Pitressin was initiated. After 20 minutes, a repeat superior mesenteric arteriogram showed marked constriction (Fig. 2). The infusion rate was not, therefore, increased. However, when heavy bleeding persisted despite a Sengstaken-Blakemore tube, the infusion was increased first to 0.3 units/min, then to 0.4 units/min. After Pitressin had been

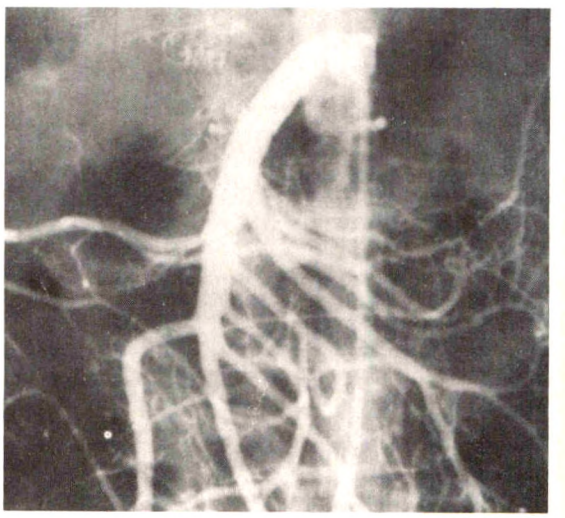


FIG. 1. Initial superior mesenteric arteriogram before vasopressin infusion, demonstrating normal arterial anatomy.

* From the Department of Radiology, The Medical College of Wisconsin, Milwaukee County General Hospital, Milwaukee, Wisconsin.

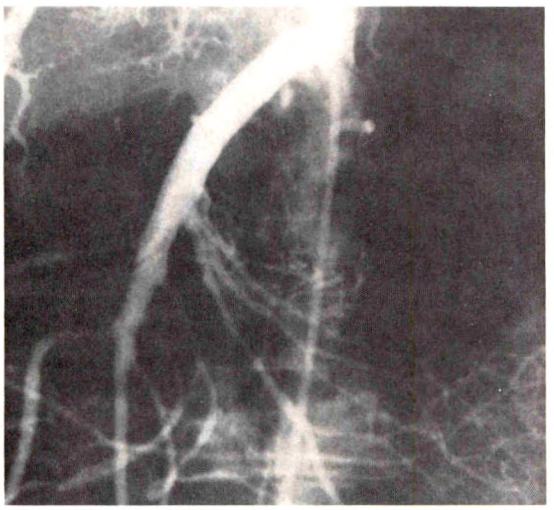


Fig. 2. Repeat superior mesenteric arteriogram after a 20 minute infusion of Pitressin at 0.2 units/min, showing marked constriction of all arterial branches.

administered continuously for 48 hours, the bleeding stopped and vital signs were stable.

The Pitressin infusion was continued at a rate of 0.2 units/min for 32 more hours, after which the catheter was kept open with D_5W. At no time were systemic vasopressors given.

Approximately ten hours after Pitressin infusion had been discontinued, the patient became hypotensive and was found to have a distended, silent abdomen. Because mesenteric infarction was suspected, repeat superior mesenteric arteriography through the infusion catheter was performed twelve hours after Pitressin infusion was discontinued. A thrombus occluding 75 percent of the lumen of the main trunk of the SMA was discovered immediately distal to the tip of the catheter (Fig. 3). In addition, the distal branches of the superior mesenteric artery continued to be significantly constricted. Attempts to aspirate the thrombus failed. After removing the infusion catheter, an aortogram *via* the opposite femoral artery showed no change in the appearance or location of the thrombus. No emboli in the distal superior mesenteric arterial branches or the renal arteries were seen.

Laparotomy revealed no mesenteric arterial pulses. A 0.5×2 cm thrombus was removed from the proximal SMA. Subsequently, peristalsis and arterial pulsations resumed. The proximal jejunum, which had initially appeared severely ischemic, improved markedly in color. Two small areas of the ileum appeared to be necrotic, so 24 hours later repeat laparotomy was performed. The superior mesenteric arterial pulse was strong, and the proximal jejunum was normal. One of the possible ileal infarctions still appeared non-viable and was plicated. Postoperatively the patient developed an adult respiratory distress syndrome. Liver and renal functions gradually deteriorated and the patient died on the 16th day postoperatively. Permission for autopsy was refused.

Comment. No reported incidence of small bowel ischemia following Pitressin infusion has been diagnosed in a living patient. The events documented, if left undiagnosed, might have progressed to total thrombosis of the SMA and portal vein. Berardi[2] reported such an occurrence and suggested that arteriography be done in all patients receiving intra-arterial Pitressin prior to removal of the catheter, or if clinical evidence for bowel ischemia develops. The fact that this condition has not been widely reported implies that it rarely occurs. Nevertheless, the possibility of arterial thrombus formation in patients re-

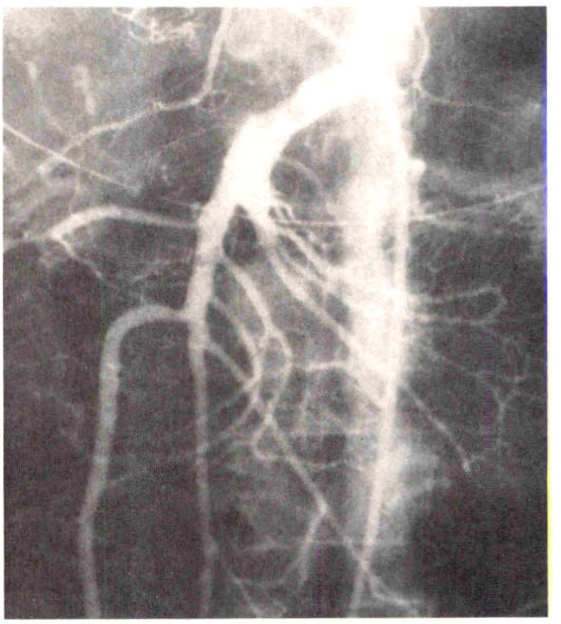


Fig. 3. Superior mesenteric arteriogram after $3\frac{1}{2}$ days of Pitressin infusion, showing thrombus formation in the main trunk of the superior mesenteric artery and constriction of its branches.

ceiving SMA infusion should be investigated, to avoid discharging patients who have unsuspected arterial thrombi that could progress to significant SMA occlusion. Also, the risk of causing ischemic bowel damage must be considered before increasing the rate of Pitressin infusion when bleeding continues.

Cameron Roberts, M.D.
Department of Radiology
The Medical College of Wisconsin
Milwaukee County General Hospital
8700 West Wisconsin Avenue
Milwaukee, Wisconsin 53226

REFERENCES

1. Baum, S., and Nusbaum, M. Control of gastrointestinal hemorrhage by selective mesenteric arterial infusion of vasopressin. *Radiology*, 1971, *98*, 497–505.
2. Berardi, R. S. Vascular complications of superior mesenteric artery infusion with pitressin in treatment of bleeding esophageal varices. *Am. J. Surg.*, 1974, *127*, 757–761.
3. Conn, H. O., Ramsby, G. R., and Storer, E. H. Selective intraarterial vasopressin in treatment of upper gastrointestinal hemorrhage. *Gastroenterology*, 1972, *63*, 634–645.
4. Formanek, G., Frech, R. S., and Amplatz, K. Arterial thrombus formation during clinical percutaneous catheterization. *Circulation*, 1970, *41*, 833–839.
5. Marubbio, A. T., Lombardo, R. P., and Holt, P. R. Control of variceal bleeding by superior mesenteric artery pitressin perfusions: complications and indications. *Am. J. Digest. Dis.*, 1973, *18*, 539–543.
6. Nusbaum, M., Baum, S., and Blakemore, W. S. Clinical experience with diagnosis and management of gastrointestinal hemorrhage by selective mesenteric catheterization. *Ann. Surg.*, 1969, *170*, 506–514.
7. Nusbaum, M., Baum, S., Sakiyalak, P., and Blakemore, W. S. Pharmacologic control of portal hypertension. *Surgery*, 1967, *62*, 299–310.
8. Rösch, J., Dotter, C. T., and Rose, R. W. Selective arterial infusions of vasoconstrictors in acute gastrointestinal bleeding. *Radiology*, 1971, *99*, 27–36.
9. Renert, W. A., Button, K. F., Fuld, S. L., and Casarello, W. J. Mesenteric venous thrombosis and small bowel infarction following infusion of vasopressin into superior mesenteric artery. *Radiology*, 1972, *102*, 299–302.

RADIONUCLIDE IMAGING IN SKELETAL INFLAMMATORY AND ISCHEMIC DISEASE IN CHILDREN*

By MASSOUD MAJD, M.D.,† *and* ROBERT S. FRANKEL, M.D.‡
WASHINGTON, D. C.

ABSTRACT:

Sixty-five children were evaluated for presence of skeletal inflammatory and ischemic disease with bone scans and roentgenograms. Several characteristic scintigraphic patterns were observed. Bone scans were significantly more sensitive than roentgenograms in early diagnosis of osteomyelitis and its differentiation from cellulitis, septic arthritis, and bone infarction.

The child presenting with possible inflammatory bone disease now is benefited by this important refinement in diagnosis. Faced with the difficult dilemma of choosing appropriate therapy in these frustratingly similar problems, the physician can integrate the clinical findings with nuclear imaging to arrive at early appropriate diagnosis and management.

THE early detection of osteomyelitis and its differentiation from cellulitis, bone infarction, or both, is of paramount importance because of significant differences in management of these entities. Acute osteomyelitis is still treated with a minimum of three weeks of high dose intravenous antibiotic therapy, whereas the treatment of cellulitis is significantly less rigorous. Bone infarction in the patients with sickle cell disease may be treated with hydration alone.

The need for early, adequate treatment of osteomyelitis is obvious in order to prevent the sequellae which may result in deformity of the involved limb. Clinical presentation and laboratory findings of osteomyelitis may be quite similar to those of cellulitis or bone infarction. Since roentgenographic changes of acute osteomyelitis do not usually appear until 10–14 days following the onset of symptoms,[5] it is important to have available an alternative means of determining the presence of bone infection in its earliest stage.

Bone scanning is significantly more sensitive than roentgenographic studies in the detection of skeletal lesions in their earliest stages.[2,4,6,7] With the introduction of several phosphate compounds tagged with ^{99m}Tc[1,8,10] and resultant decrease in radiation dose, it is now possible to use skeletal scintigraphy routinely in children in the investigation of suspected inflammatory and ischemic bone lesions.

MATERIAL AND METHOD

Sixty-five children were studied with bone scans because of difficulty in differentiating osteomyelitis from septic arthritis, cellulitis and bone infarction, on the basis of the clinical and roentgenological findings. The patients ranged in age from 8 days to 16 years and all presented with one or more of the following symptoms related to a specific skeletal region: pain, tenderness, local increased heat, erythema, and clinically evident soft tissue edema. In the majority of the patients, roentgenograms of the involved area were obtained at the time of admission and skeletal scintigraphy was performed within the

* Presented at the 22nd Annual Meeting of the Society of Nuclear Medicine, Philadelphia, Pennsylvania, June, 1975.
From the Departments of Radiology, The Children's Hospital National Medical Center and the George Washington University, Washington, D. C.
† Associate Professor of Radiology and of Pediatrics.
‡ Resident in Radiology.

first 24 hours. A few of the patients had more than one bone scan.

The scans were done following the injection of 200 μci/Kg body weight of 99mTc diphosphonate. Studies were performed on a Picker Dyna Camera 2C using a 10,000 parallel hole collimator. In the pelvic area, spine, hands, and feet, a pinhole collimator was frequently used for better detail. Occasionally rectilinear scans were obtained on a 5″ Picker Magna Scanner. Most patients had immediate postinjection (vascular phase) scans of the affected area and contralateral limbs. Two to four hours later, total body scans were obtained, with special attention to the affected area and opposite limb.

For purposes of this retrospective clinical study, all scans and roentgenograms were interpreted independently by one of us without knowledge of clinical or laboratory data.

RESULTS

Osteomyelitis: Twenty-three patients were classified as having osteomyelitis (20 acute and 3 chronic) based on the usual clinical course plus either one or a combination of the following findings: (1) positive bone marrow aspirate; (2) positive blood culture(s); and (3) initial or subsequent compatible roentgenograms of the affected area. Table II summarizes the data in the 20 cases of acute osteomyelitis. Of the 17 Black patients in this group, there was one child with sickle cell (SS) disease and another with sickle cell (SC) disease. The duration of symptoms was from one to seven days. Three patients had chronic forms of osteomyelitis (Table I). Six patients, including the three cases of chronic osteomyelitis initially had abnormal roentgenograms. The remaining 17 patients had normal roentgenograms at the time of the scan, but seven of these subsequently developed roentgenologic changes of osteomyelitis during therapy (Fig. 2). Ten patients did not develop roentgenologic changes, but nine of these had positive bone aspirates, or blood cultures, or both

TABLE I

CLASSIFICATION OF CASES ACCORDING TO DISCHARGE DIAGNOSIS

Osteomyelitis		23
acute	20	
Brodie's abscess	1	
chronic sclerosing osteomyelitis	1	
chronic active suppurative osteomyelitis	1	
Cellulitis		22
Bone Infarct		8
Septic Arthritis		7
Normal		5
Total		65

(Table II). The remaining patient had no other documented evidence of osteomyelitis, but was treated because of the scan findings and a strong clinical suspicion including a persistently elevated erythrocyte sedimentation rate, a finding not usually associated with cellulitis.

All of these children had abnormal scans suggesting the diagnosis of osteomyelitis, although one patient required a follow-up scan one week after the onset of symptoms to make the diagnosis. The typical scan pattern in these patients consisted of increased activity in the soft tissue and bone on the immediate postinjection image, and intensely increased focal uptake in the bone on the delayed scan, with or without increased activity in adjacent soft tissues or joint (Fig. 1; and 3).

Cellulitis: Twenty-two patients were classified as having cellulitis on the basis of subsequent clinical course and failure of laboratory and roentgenologic findings to indicate osteomyelitis. One patient had sickle cell (SC) disease. The duration of the symptoms ranged from two days to one month. *H. influenzae* was cultured from the blood in one patient whose clinical course was not typical of osteomyelitis. Blood cultures in the remaining 21 patients were negative. In this group, the roentgenograms revealed soft tissue swelling in all instances.

All patients had characteristic scan pat-

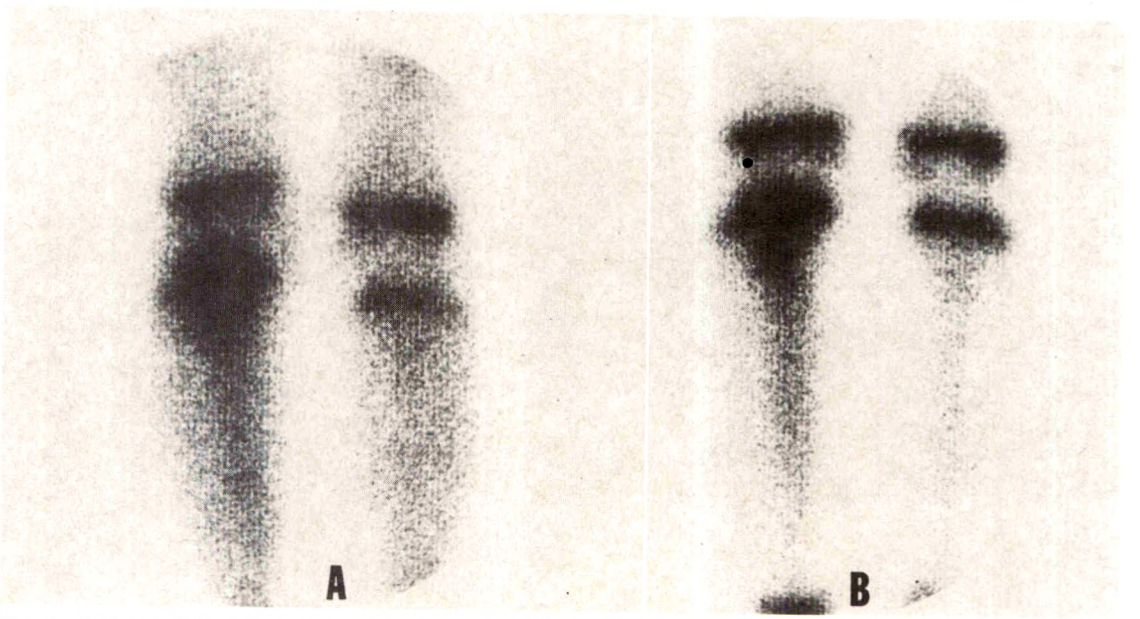


Fig. 1. Osteomyelitis. (*A*) Anterior immediate postinjection image of the legs demonstrating diffuse increased activity on the right with definite increased activity in the right tibia. (*B*) Delayed image of the legs demonstrating increased uptake in the proximal 2/3 of the right tibia.

terns. The immediate postinjection scans showed increased activity diffusely in the soft tissues with no focal increased activity in the bone. Delayed scans were either normal (Fig. 5) or showed slightly increased activity in the soft tissues without focal increased uptake in the bone (Fig. 6).

Bone Infarction in Sickle Cell Disease: Eight patients with sickle cell disease (7 SS and 1 SC), were classified as having bone infarctions on the basis of clinical response to treatment for sickle cell crisis. The duration of symptoms was one to four days. All patients had negative blood cultures. One patient had a bone marrow aspirate, revealing necrotic marrow with a negative culture. The roentgenograms showed non-specific soft tissue swelling in

Table II

X-Ray and Laboratory Findings in 20 Cases of Acute Osteomyelitis with Positive Bone Scans

X-Ray	No. of Cases	Blood Culture	Bone Marrow Aspirate
Initial Abnormal Roentgenogram	3 (1)	+	+
	3 (2)	−	+
Initial Normal Roentgenogram, but Became Abnormal 7–14 Days Later	7 (1)	+	+
	7 (3)	+	−
	7 (2)	−	+
	7 (1)	−	−
Roentgenogram Remained Normal	10 (5)	+	+
	10 (2)	+	−
	10 (2)	−	+
	10 (1)	−	−

five patients. One of these also showed chronic changes of previous infarctions. The roentgenograms were normal in the remaining three.

All patients had abnormal scans. Four of these patients had decreased bone uptake in the symptomatic area (Fig. 7). Two patients showed a non-homogeneous spotty uptake in the involved bone. The other two cases showed a localized area of increased uptake on delayed scans, indistinguishable from osteomyelitis. In these two patients, however, early scans did not show increased activity as described in cases of osteomyelitis.

Septic Arthritis: Seven patients were classified as having septic arthritis on the basis of a positive joint aspirate. None had sickle cell disease. The duration of symptoms was one day to two months. One patient had a positive blood culture for beta hemolytic streptococcus. The remaining six had negative blood cultures. Roentgenograms revealed joint effusion in five patients and were normal in two.

The scans were abnormal in all instances. The pattern was that of increased activity in the joint on both immediate and delayed scans without extension into bone (Fig. 9). One case of septic arthritis in the hip showed decreased activity.

Normal: Five patients who presented primarily with pain were classified as normal on the basis of completely negative clinical and roentgenologic evaluation and early clearing of symptomatology. These all had normal scans.

DISCUSSION

From this experience, several general scintigraphic patterns were observed in the various populations that we studied. As noted before, the typical scan pattern of osteomyelitis was that of increased activity in the soft tissue and bone on the immediate postinjection scan and intensely increased uptake in bone on the delayed scan, the extent of which is probably related to the phase of the disease and the degree of hyperemia. The identification of a definite

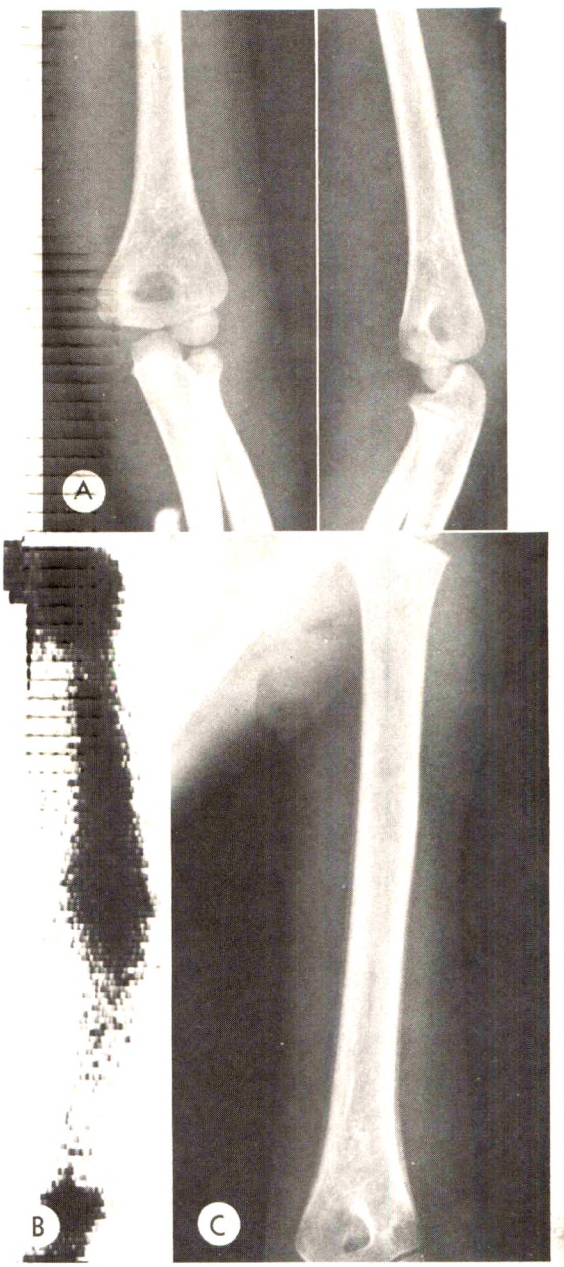
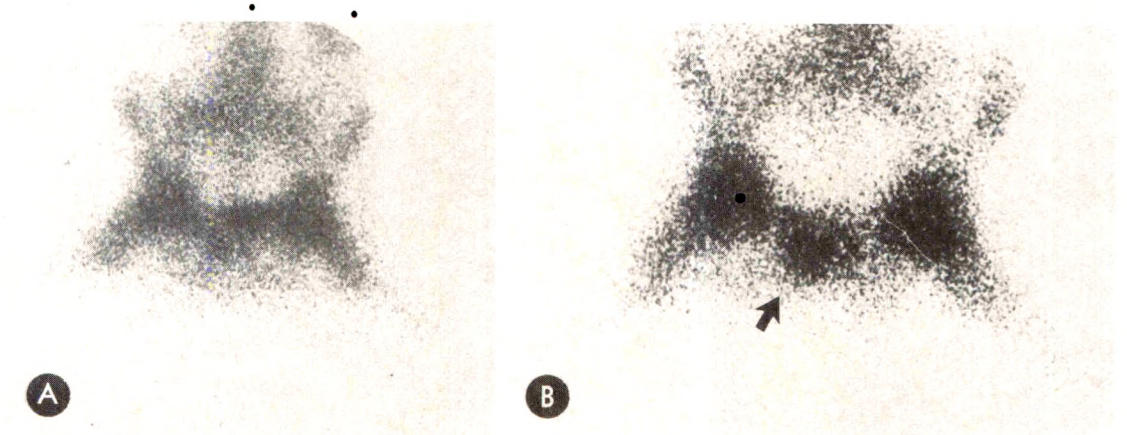


Fig. 2. Osteomyelitis in Sickle Cell Disease. (*A*) Initial roentgenogram of the left arm of this six year old Black girl with known sickle cell (SS) disease and multiple previous crises shows deep soft tissue swelling and evidence of previous infarctions but no definite evidence of acute osteomyelitis. (*B*) Delayed scan performed the same day shows intense homogeneous increased uptake in the entire shaft of the humerus diagnostic of acute osteomyelitis. (*C*) Roentgenogram obtained three weeks later shows periosteal new bone formation involving almost the entire shaft of the humerus. The soft tissues have returned to normal.



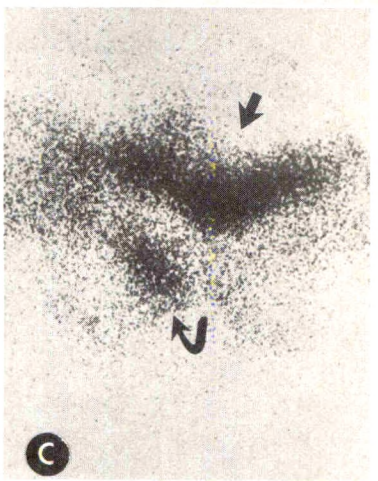
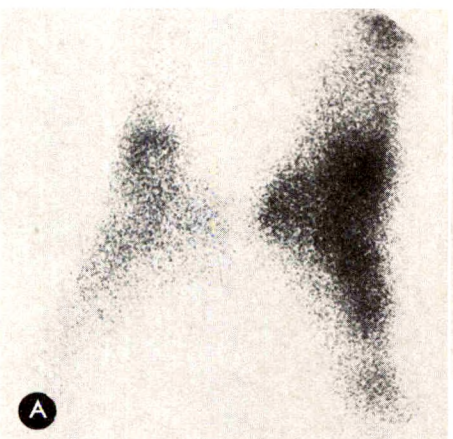


Fig. 3. Osteomyelitis. (*A*) Anterior delayed pelvic image shows no definite abnormal uptake. (*B*) Repeat scan performed one week later, because of persistent symptoms, shows a suggestion of increased uptake (arrow) in the right pubic bone but this could not be definitely differentiated from bladder activity. (*C*) Pinhole collimator view of the area in question, clearly separates bladder activity (straight arrow) from abnormal uptake in the right pubic bone (curved arrow).



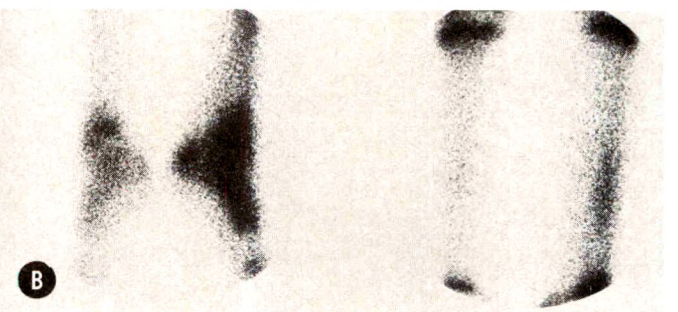


Fig. 4. Osteomyelitis. (*A*) Immediate postinjection lateral scan of a patient with osteomyelitis of the distal metaphysis of the left tibia, shows marked increased activity in the leg, ankle, and foot. (*B*) Delayed scan shows increased uptake in the tibia consistent with osteomyelitis. There is also increased activity in the foot and ankle (extra-lesional uptake). The patient had no clinical nor other evidence of osteomyelitis of the foot.

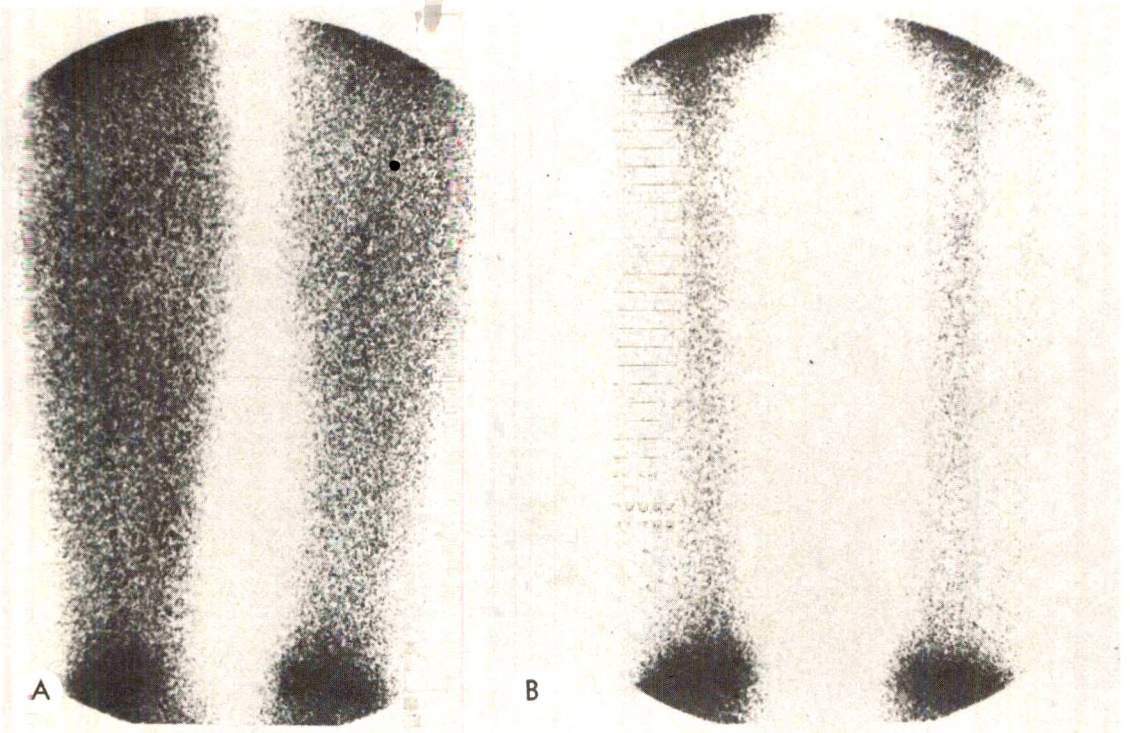


Fig. 5. Cellulitis. (*A*) Immediate postinjection scan of the legs shows increased activity on the right with no localization in bone. (*B*) Delayed scan is normal.

focal area of increased uptake in the bone is an important feature in osteomyelitis and a useful point in its differentiation from cellulitis without osteomyelitis. These findings are similar to those described by others.[2]

Ten of the 20 cases of acute osteomyelitis had initial and subsequent normal roentgenograms of the affected area (Table II). Nine of these had positive bone marrow aspirates or blood cultures or both. This proves that with early and adequate treatment roentgenographic changes of osteomyelitis may not develop.

In some cases of osteomyelitis and cellulitis of the leg there is marked generalized increased activity in the foot which is not localized to any bone. Figure 4 is a good example of this "extended" or "extralesional" uptake in the foot of a ten year old white girl with proved osteomyelitis of the distal metaphysis of the left tibia. There was no initial nor subsequent evidence of osteomyelitis in the foot. This abnormal radionuclide deposition has been reported in a variety of benign and malignant diseases of bone.[9] Its pathogenesis is not clear. Probably it is related to regional hyperemia.

The patient illustrated in Figure 3 emphasizes a technical point. This five year old boy presented with a one day history of fever, pain, and other clinical findings indicative of a disease process in the vicinity of the right hip. The roentgenogram of the pelvis was normal. The bone scan (Fig. 3*A*) was also interpreted as normal. On this basis the patient was not treated. Due to persistence of symptoms, a repeat bone scan was performed after one week (Fig. 3*B*). There was a suggestion of increased uptake in the right pubic bone, but this could not be definitely distinguished from the bladder activity. A pinhole collimator view of the area was then obtained for better detail (Fig. 3*C*). This clearly sepa-



Fig. 6. Cellulitis. Delayed scan of the right arm shows diffusely increased activity not localized to bone.

rates the bladder activity from abnormal bone uptake. The first scan was performed without the use of a pinhole collimator, possibly explaining the false negative result. The pinhole collimator has proved to be extremely valuable in imaging the pelvic bones, spine, hips, and small bones of the hands and feet.

Since completion of this study we have observed a case of acute osteomyelitis of the talus with decreased uptake of the radionuclide. This was associated with septic arthritis of the ankle joint. General poor blood supply to the talus and increased pressure in the joint due to associated septic arthritis may explain the reason for decreased uptake in this case.

In cellulitis, the early postinjection scans showed increased activity diffusely in the soft tissue with no focal increased activity in the bone. Delayed scans were either normal (Fig. 5) or showed slightly increased activity in soft tissues without localization in the bone (Fig. 6). In this group, bone scan proved particularly helpful in the exclusion of osteomyelitis, a

difficult differential diagnosis on the basis of usual clinical and roentgenographic findings. Prolonged high dose intravenous antibiotic therapy was thus avoided. All patients in this group demonstrated complete clinical recovery with the usual therapeutic regimen for cellulitis.

The scan pattern of bone infarction in patients with sickle cell disease appears to depend on the duration of the lesion. In the early stages, probably the first two to three days after an ischemic insult, the scan shows decreased uptake in the affected area. During this time bone blood flow is decreased and reactive hyperemia and new bone formation has not yet begun (Fig. 7). Later, the scan may show a localized area of increased uptake indistinguishable from osteomyelitis (Fig. 8*A*). The use of early postinjection scanning (Fig. 8*B*) may be helpful in differentiating the two entities. In this material the early postinjection scan in patients with bone infarction did not show the typical increased activity seen in osteomyelitis (Fig. 1*A*; and 8*B*).

Although we have not performed Gallium-67 citrate scintigraphy in this group of patients, this technique may be of use in differentiating acute osteomyelitis from acute bone infarction since Gallium-67 citrate probably does not localize in infarction but is avidly concentrated by osteomyelitis.[3]

In septic arthritis the scan pattern is similar to cellulitis. It usually shows increased activity in the joint on both early postinjection and delayed scans without extension into the bone (Fig. 9). One case of septic arthritis of hip in our series showed decreased activity in the area of the joint probably due to decreased blood flow to the area secondary to increased intracapsular pressure. In this particular patient there were no initial nor subsequent evidence of osteomyelitis.

Massoud Majd, M.D.
Children's Hospital NMC
2125 13th Street, Northwest
Washington, D. C. 20009



Fig. 7. Infarction. (*A*) Immediate postinjection scan shows decreased activity in the right proximal tibia (arrow). (*B*) Delayed scan shows decreased uptake in the same location.

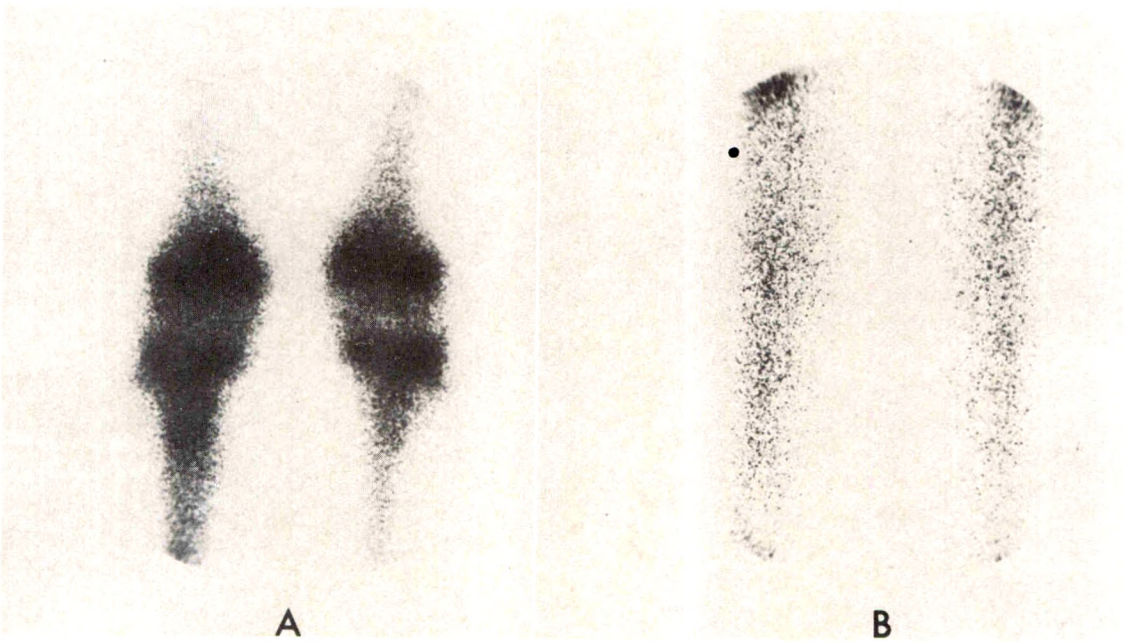


Fig. 8. Infarction. (*A*) Delayed scan shows marked increased uptake in the right proximal tibia, indistinguishable from acute osteomyelitis. (*B*) Immediate postinjection image fails to reveal typical increased activity seen in osteomyelitis.

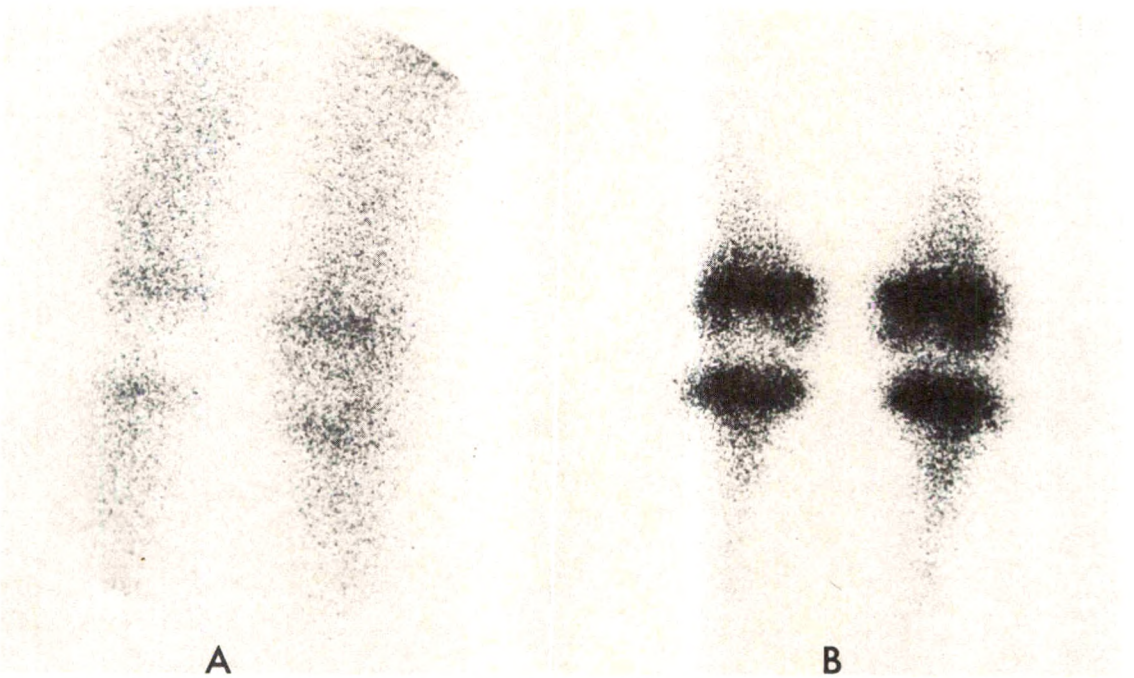


Fig. 9. Septic Arthritis. (*A*) Immediate postinjection scan shows increased activity in the left knee joint. (*B*) Delayed scan shows increased activity localized to the joint on the left with no extension into adjacent bones.

The authors would like to express their appreciation to William J. McSweeney, M.D. for his critical review of this paper and valuable suggestions.

REFERENCES

1. Castronovo, F. P., Jr., and Callahan, R. J. New bone scanning agent: 99mTc labeled 1-hydroxy-ethylidene-1, 1-disodium phosphate. *J. Nuclear Med.*, 1972, *13*, 823–827.
2. Gilday, D. L., and Paul, D. J. Differentiation of osteomyelitis and cellulitis in children using combined blood pool and bone scan. Abstract. *J. Nuclear Med.*, 1974, *15*, 494.
3. Johnston, G. S., and Jones, A. E. Atlas of Gallium-67 Scintigraphy. Plenum Press, New York, 1973.
4. Pendergrass, H. P., Potsaid, M. S., and Castronovo, F. P., Jr. Clinical use of 99mTc-diphosphonate (HEDSPA): new agent for skeletal imaging. *Radiology*, 1973, *197*, 557–562.
5. Sherman, R. S. Nature of radiologic diagnosis in diseases of bone. *Radiol. Clin. North America*, 1970, *8*, 227.
6. Siemsen, J. K., and Waxman, A. D. Early diagnosis of hematogenous osteomyelitis. Abstract. *J. Nuclear Med.*, 1974, *15*, 533.
7. Silberstein, E. B., Saenger, E. L., Tofe, A. J., Alexander, G. W., Jr., and Park, H. M. Imaging of bone metastases with 99mTc-Sn-EHDP (Diphosphonate), 18F and skeletal radiography: comparison of sensitivity. *Radiology*, 1973, *107*, 551–556.
8. Subramanian, G., McAfee, J. G., Bell, E. G., Blair, R. J., O'Mara, R. E., and Ralston, P. H. 99mTc-labeled polyphosphate as skeletal imaging agent. *Radiology*, 1972, *102*, 701–704.
9. Thrall, J. H., Geslien, G. E., Corcoron, R. J., and Johnson, M. C. Abnormal radionuclide deposition patterns adjacent to focal skeletal lesions. *Radiology*, 1975, *115*, 659–663.
10. Weber, D. A., Keyes, J. W., Jr., Benedetto, W. J., and Wilson, G. A. Tc99m pyrophosphate for diagnostic bone imaging. *Radiology*, 1974, *113*, 131–137.

"DOUGHNUT" SIGN IN BRAIN SCANNING*

By YAVUZ A. TARCAN, M.D.,† WILLIAM FAJMAN, M.D.,‡
JOSEPH MARC, M.D.,§ *and* DAVID BERG, D.O.‖
ATLANTA, GEORGIA

ABSTRACT:

The significance of the "doughnut" sign at present is relegated to characterizing the morphology of a lesion. The use of the "doughnut" sign in differential diagnosis should not be attempted except in specific clinical contexts, and never excluding other evidence. The "doughnut" sign in scanning together with other studies such as angiography and computerized axial tomography gives additional characterizing data in the neuroradiologic evaluation of a patient.

THE "doughnut" sign in brain scanning was first described in 1968 by Gottschalk *et al.*[13] using high resolution apparatus and Technetium 99m. In his series, eight cases of 80 (ten percent) showed a central area of diminished radioactivity. There were four glioblastomas, one cystic astrocytoma, two abscesses, and one metastasis. O'Mara *et al.*[24] reported a second series of patients shortly thereafter, in which they observed the "doughnut" sign in seven of 237 positive brain scans (2.9 percent). The pathologic conditions showing the "doughnut" sign included one abscess, three metastases, one meningioma, one intracerebral hematoma, and one cerebrovascular occlusion. Since these early studies, the "doughnut" sign has been reported in other lesions including subdural hematomas,[16] an acoustic neuroma,[20] and even a cephalohematoma,[4] establishing further the nonspecificity of this sign.

Our experience with the "doughnut" sign consists of 27 cases collected since 1970 in more than 300 positive brain scans (nine percent), consisting of three abscesses, four infarctions, eight tumors, four skull metastases, two subdural hematomas, and six metastatic lesions to the brain (Table 1). A review of the "doughnut" sign is presented and correlated with angiography, pathology, and in some cases computerized axial tomography (CAT) in an attempt to re-evaluate its significance in the neuroradiologic evaluation of a patient.

INFLAMMATORY DISEASE

The "doughnut" sign has been reported most frequently in the literature in association with inflammatory disease.[7,11,12,27–30,33] The rate of detection of abscess is high. In a

TABLE I

THE INCIDENCE OF "DOUGHNUT" SIGN IN POSITIVE BRAIN SCANS

	Gott-schalk	O'Mara	Tarcan *et al.*
"Doughnut" Sign per Positive Brain Scan	8.80 10%	7/237 2.9%	27/301 9%
Glioblastoma	50%	—	20%
Astrocytoma	12.5%	—	10%
Meningioma	—	14.3%	10%
Cerebral Metastases	12.5%	43%	22%
Cerebral Abscess	25%	14.3%	10%
Cerebral Infarction	—	14.3%	10%
Cerebral Hemorrhage	—	14.3%	—
Subdural Hematoma	—	—	7.5%
Skull Lesions	—	—	10%

* Presented at the Seventy-sixth Annual Meeting of the American Roentgen Ray Society, Atlanta, Georgia, September 30–October 3, 1975.

From the Department of Radiology, Division of Nuclear Medicine, Emory University School of Medicine, Atlanta, Georgia.
† Director of Nuclear Medicine, Emory University—Grady Memorial Hospital.
‡ Senior Resident in Radiology and Nuclear Medicine.
§ Director Neuroradiology of Grady Memorial Hospital—Emory University.
‖ Fellow in Neurovascular Radiology.

review of the literature Suwanwela and associates[30] found 180 reported cases of abscess of which 163 had positive brain scans. The same author cites 15 subdural abscesses, all of which had positive brain scans. Although the detectability of abscess is high, observation of the "doughnut" sign is apparently uncommon, reportedly observed in no cases[18] to five of 16 cases.[29] Although the "doughnut" sign is nonspecific, some authors[7,29] state that within the context of inflammatory disease a "doughnut" sign is pathognomonic of abscess. Moreover, if a "doughnut" sign appears on sequential scans of a lesion, the lesion is progressing. Conversely, loss of the "doughnut" sign in sequential scans indicates response to therapy.

When inflammatory disease is known to be present the differential diagnosis must include herpes encephalitis and focal cerebritis. Both of these lesions are known to take up the radionuclide, but are noted to have more irregular margins than an abscess and will not demonstrate the "doughnut" sign.[29] A well marginated lesion with homogeneous radioactivity may be an abscess, but one with a "doughnut" sign is most assuredly an abscess.[29]

Epidural and subdural abscesses have exhibited almost uniformly positive brain scans. The "doughnut" sign has not been previously reported in epidural abscess, but we have observed it in one case (Fig. 1*A*).

Cerebral angiography is also often nonspecific for cerebral abscess. Areas of abscess may present as lucent areas in the late arterial and capillary phases (Fig. 1*B*). A hypervascular rim or crescent may be present and is highly suggestive, but is observed in less than 20 percent of cases.[28] The lesion may present only as a mass. In lesions larger than 1 cm the brain scan is almost always densely positive, may be more localizing, and at times is positive before the angiogram shows any abnormality.[28] The computerized axial tomogram may show an abscess as an area of diminished density[2] (Fig. 2, *A–C*).

The pathologically demonstrable capsule of the abscess with its surrounding neovascularity[6] would explain the localization of both radioactivity and angiographic contrast medium. It has been demonstrated that the ratio of isotope in the capsular region to that of the encapsulated liquid is approximately six to one.[30] Subdural abscess

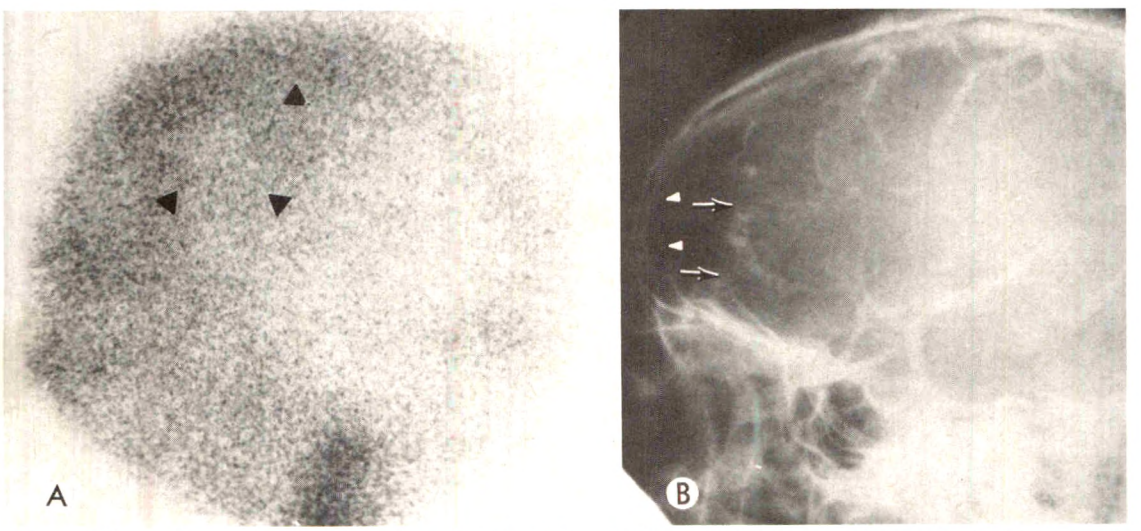


Fig. 1. This twelve year old boy presented with scalp cellulitis and frontal headache. The brain scan (*A*) showed a "doughnut" sign in the left frontal lobe (arrows). An angiogram (*B*) showed displacement of cortical veins from the skull table (arrows) and an air fluid level (arrowheads). Epidural abscess was confirmed at surgery.

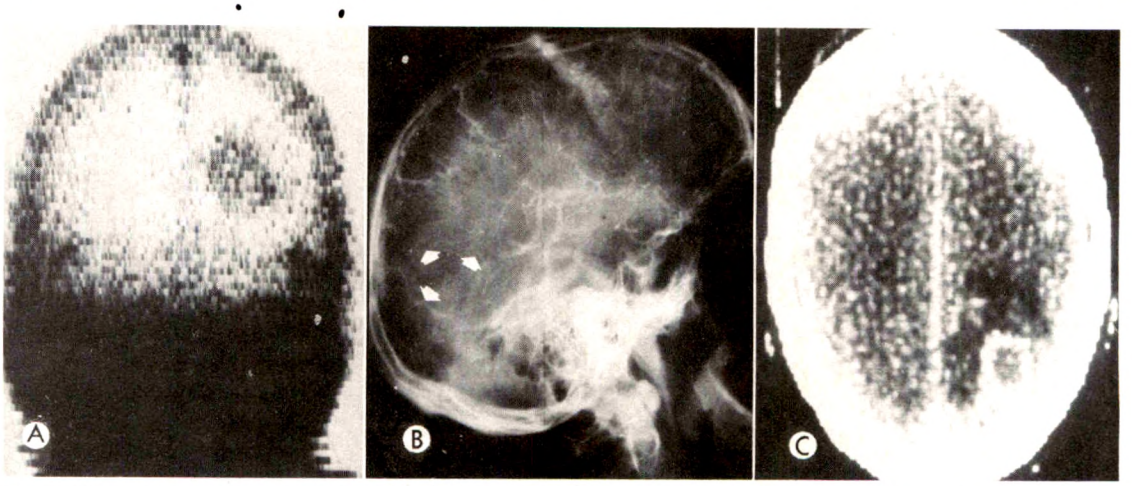


Fig. 2. This 46 year old diabetic developed headache and subsequent seizures. Physical examination revealed a stiff neck, left homonymous hemianopsia, decreased left corneal reflex, but no papilledema. The brain scan (*A*) revealed a right occipital "doughnut" sign. Angiography (*B*) showed a relatively avascular mass with the suggestion of a "vascular" blush (short arrows) in the right occipital lobe. The CAT scan (*C*) showed the lesion to be of diminished absorption surrounded by a ring of increased absorption. An abscess was surgically drained.

showed similar findings. This accounts for the "doughnut" appearance.

NEOPLASM

The "doughnut" sign has been described in multiple different tumors, both primary and metastatic. Glioblastomas,[13] cystic astrocytomas,[13] meningiomas,[24] and an acoustic neuroma[20] have been previously reported. A variety of metastatic lesions has been noted to demonstrate the "doughnut" sign.[13,24]

Meningiomas usually show very dense homogeneous concentration of radioactivity. The majority show rapid uptake of radioactivity early in the cerebral isotope angiogram indicating their vascularity. Early static as well as three to four hour delayed scans show dense uptake. We have observed the "doughnut" sign in three cases (Fig. 3, *A–C*). The meaning of this sign in meningioma is not clear since areas of hemorrhage or necrosis are not a consistent finding in meningiomas pathologically.[22]

Angiographically, meningiomas typically have a dual arterial supply (external and internal carotid), uniform caliber vessels, and persistent dense stain. If selective carotid injections are performed it may show areas of lucency due to washout by the nonopacified vessels.[23]

The pathophysiology of meningiomas including encapsulation, edema in the surrounding brain, bony reaction, or invasion, all could explain the uptake of radioisotope. The appearance of the "doughnut" sign may be the result of preferential uptake in any of these areas or could possibly be the result of timing differences between the dual arterial circulation (Fig. 4, *A* and *B*).

In astrocytomas a pattern of slowly increasing uptake throughout the cerebral radioisotope angiogram is usually seen. The well differentiated astrocytomas typically show low radioactivity. In astrocytomas the "doughnut" sign may be prominent and is attributable to a cystic component.

The more malignant Grade IV astrocytomas (glioblastomas) may show a similar pattern, but usually with greater radioactivity. The "doughnut" sign may be observed in this lesion, also, apparently more commonly than in the less malignant astrocytomas (Table 1). The degree of radioactivity and the frequency of the "dough-

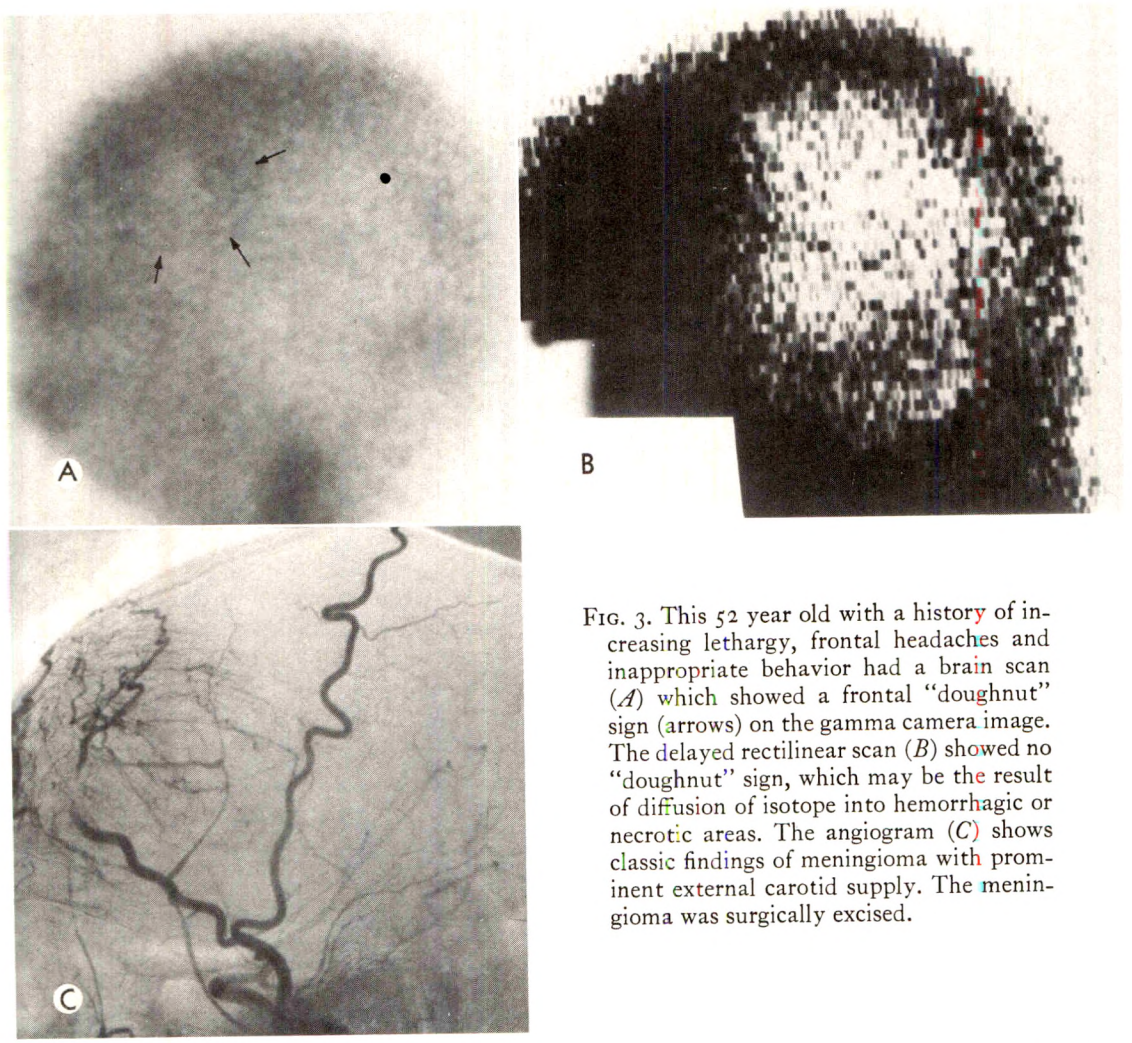


Fig. 3. This 52 year old with a history of increasing lethargy, frontal headaches and inappropriate behavior had a brain scan (*A*) which showed a frontal "doughnut" sign (arrows) on the gamma camera image. The delayed rectilinear scan (*B*) showed no "doughnut" sign, which may be the result of diffusion of isotope into hemorrhagic or necrotic areas. The angiogram (*C*) shows classic findings of meningioma with prominent external carotid supply. The meningioma was surgically excised.

nut" sign, thus appear to increase with increasing malignancy of these tumors (Fig. 5, *A* and *B*). Most authors state that these tumors become more homogeneous over time, suggesting diffusion of isotope into cystic areas (Fig. 6, *A* and *B*).

Angiographically, the more benign astrocytomas typically present as avascular masses. The more malignant types all may both stain and show relatively stain free areas (Fig. 6*C*). Neovascularity with "tumor" vessels is classically observed. Early draining veins are common.

The computerized axial tomogram may show the tumor as one or more areas of decreased density surrounded by areas of increased density (Fig. 7, *A–C*).

Clear fluid filled cysts, observed pathologically, apparently result in the "doughnut" sign in astrocytomas. The Grade IV astrocytomas exhibit areas of necrosis, hemorrhage and cyst formation[22] which would explain the "doughnut" sign in these tumors.

Metastases defy any strict classification in respect to pattern in cerebral radioisotope angiography.[14] The majority behave like astrocytomas. On static scans, metastases may appear as single or multiple areas of increased radioactivity. The "doughnut" sign has been reported in metastases from carcinoma of the breast and lung.[13,24] We have observed the "doughnut" sign in a case of malignant melanoma (Fig. 8, *A*

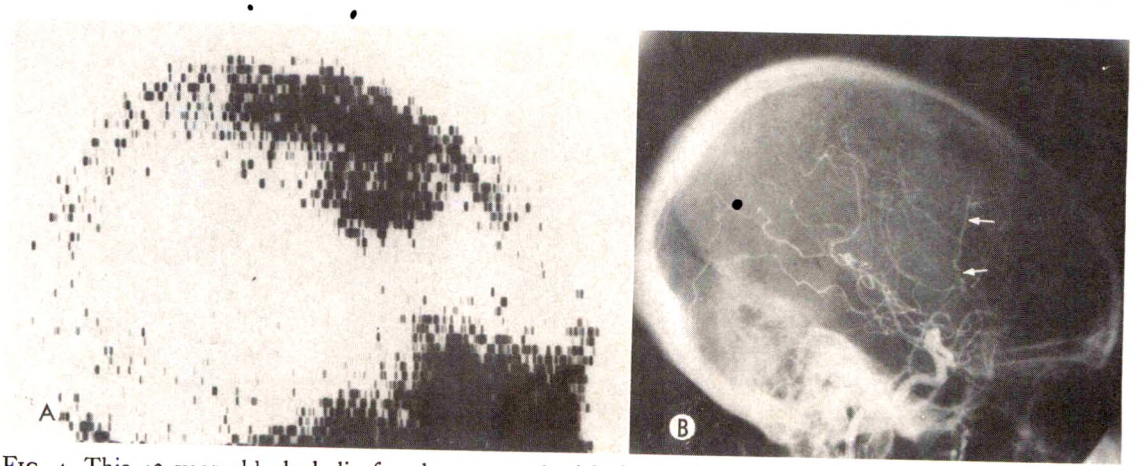


FIG. 4. This 42 year old alcoholic female presented with focal seizures involving the right face. Physical examination showed a central facial weakness on the right and perseveration aphasia. The brain scan (*A*) revealed a left frontoparietal "doughnut" sign. The angiogram (*B*) showed (arrows) classical findings of meningioma. The middle meningeal artery supply appears to enter in the region of the clear area on the scan, suggesting circulatory differences as the cause of the "doughnut" sign in this case.

and *B*) and in metastatic medulloblastoma (Fig. 9*A*). The "doughnut" sign is probably due to necrosis in metastatic lesions. Melanoma, however, may cause bleeding around the metastasis[32] and the scan may reflect this intracerebral hemorrhage, at times, rather than the tumor itself.

The angiographic appearance of metastases is also variable: tumor vessels, a peripheral blush, or meningeal vessels all may be demonstrable in varying degrees.

The computerized axial tomogram may show the metastasis as an area of increased density or a cystic area (Fig. 9*B*).

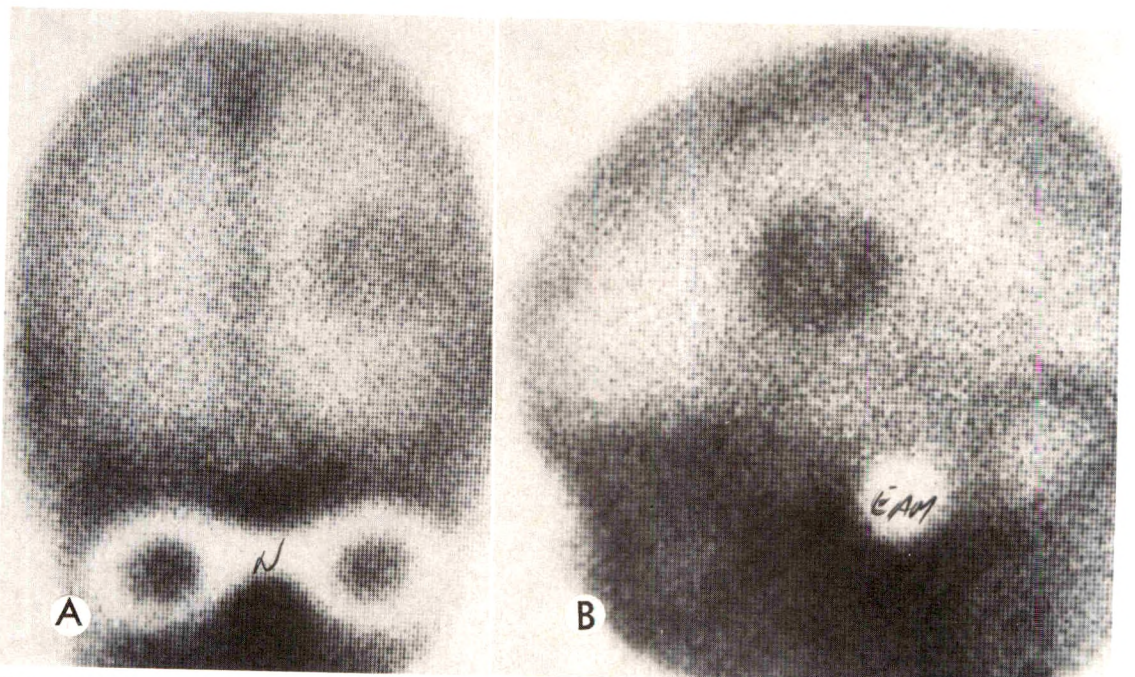


FIG. 5. This 66 year old male was admitted with a history of right hemiparesis and aphasia thought to be secondary to a cerebral vascular accident. The brain scans (*A* and *B*) showed a "doughnut" sign in the left parietal region. Angiography showed only an avascular mass. Glioblastoma multiforme was proved by biopsy.

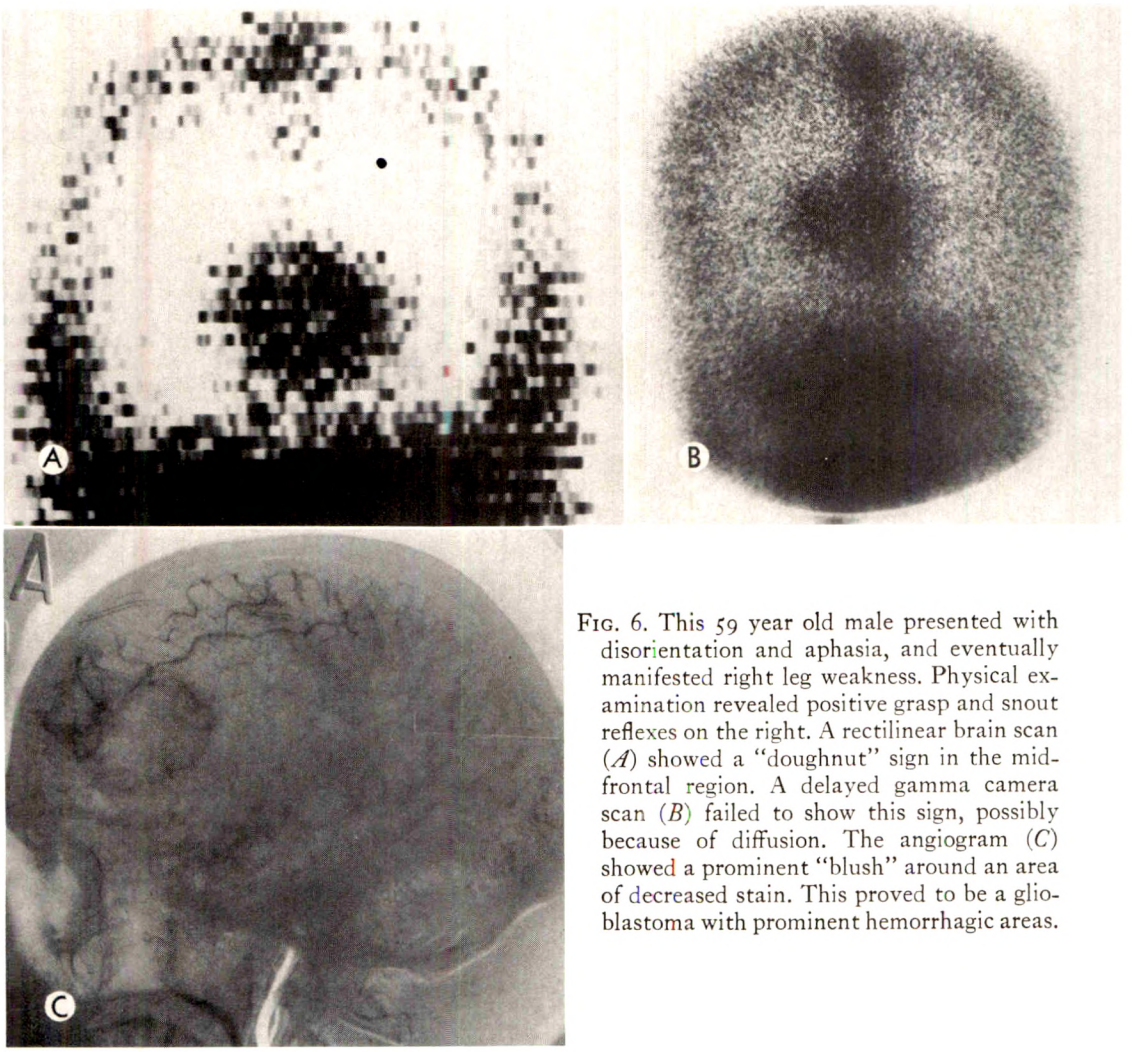


Fig. 6. This 59 year old male presented with disorientation and aphasia, and eventually manifested right leg weakness. Physical examination revealed positive grasp and snout reflexes on the right. A rectilinear brain scan (*A*) showed a "doughnut" sign in the midfrontal region. A delayed gamma camera scan (*B*) failed to show this sign, possibly because of diffusion. The angiogram (*C*) showed a prominent "blush" around an area of decreased stain. This proved to be a glioblastoma with prominent hemorrhagic areas.

CEREBRAL INFARCTION

Cerebral infarction has exhibited the "doughnut" sign on brain scan.[24] We have seen this in four cases. Ancillary findings such as decreased flow to the area on cerebral radioisotope angiography are important in diagnosis. The timing of examination after clinical symptoms appear is important, since up to 75 percent of infarctions show uptake of radioactivity after the first week. The distribution of radioactivity may be a wedge shaped pattern in the distribution of a particular vessel, but atypical configurations occur[15] including the "doughnut" sign (Fig. 10, *A* and *B*).

Angiographically, a decreased staining during the parenchymal phase or an increased stain (luxury perfusion) may be observed.[23] We have not seen an angiographic "doughnut" sign in cerebral infarction.

The pathologic findings of phagocytic cells surrounding an area of softening and necrosis, seen after seven days,[22] would explain the "doughnut" appearance on the scan.

INTRA- AND EXTRACEREBRAL BLEEDING

The "doughnut" sign has been reported in intracerebral hematoma,[24] but we have not observed it in this lesion.

Subdural hematomas are known to give

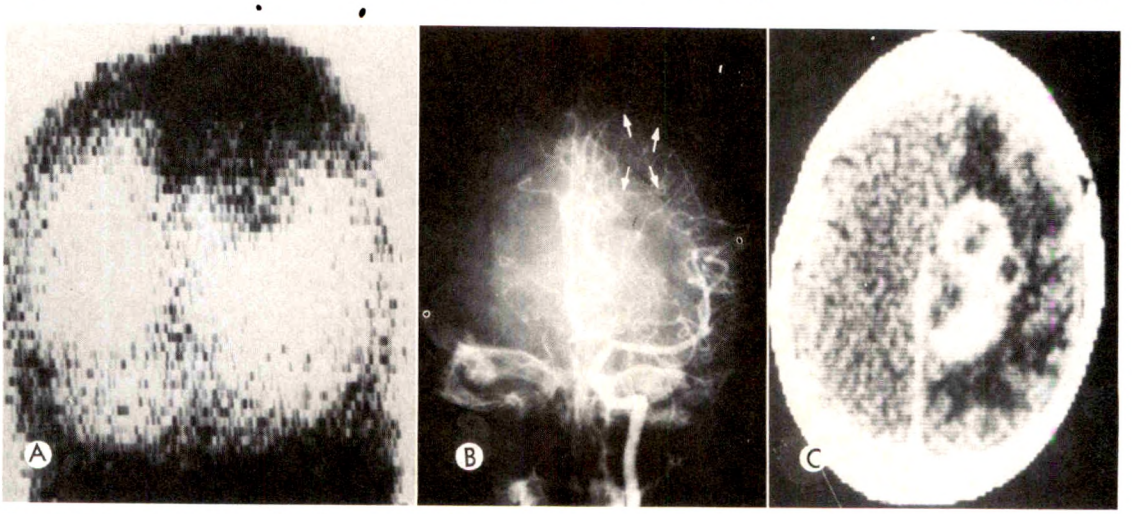


Fig. 7. This twelve year old with previously excised cystic astrocytoma returned after three years with recurrent symptoms. The brain scan (*A*) revealed a "doughnut" sign all but obscured by the skull flap activity on the right. The angiogram (*B*) showed only an avascular mass, (arrows) but the CAT scan (*C*) revealed the true cystic nature of this recurrent cystic astrocytoma.

a variable appearance on the brain scan, most commonly a crescentic or lentiform appearance. The "doughnut" sign has been reported in two cases[16] and has been observed by us.

Angiographic diagnosis is made by observing separation of superficial cerebral arteries and veins from the inner table of the skull.

Pathologically, a subdural hematoma consists of a collection of blood which eventually organizes and becomes surrounded by a "membrane" of varying thickness.[22] Conflicting evidence exists as to whether the uptake of radionuclide is within the fluid collection or its "membrane."[16,34] In the two cases reported previously, the increased radioactivity on the brain scan

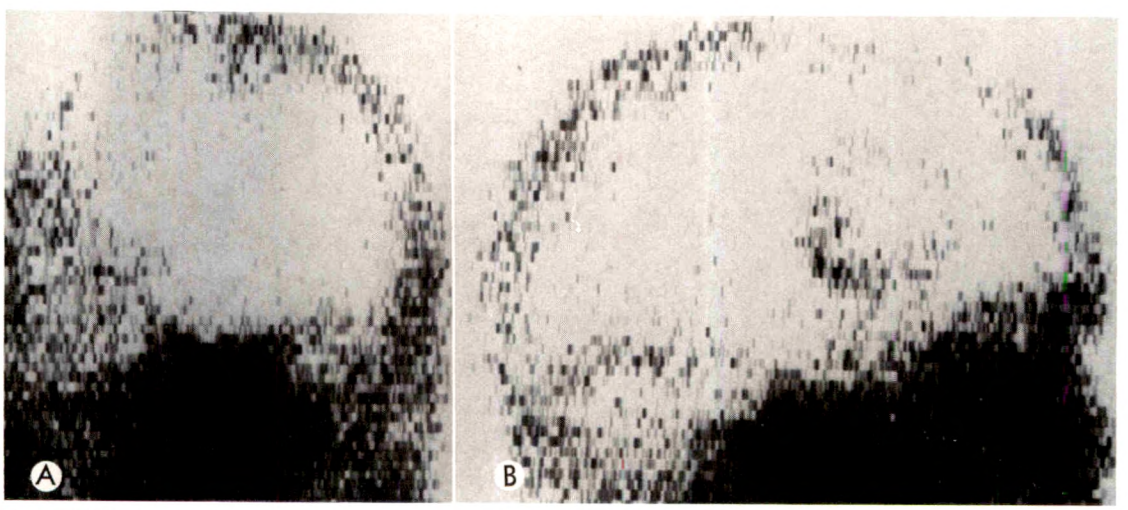


Fig. 8. This 42 year old male with known malignant melanoma presented with headache and signs of increased intracranial pressure. The brain scans (*A* and *B*) showed a "doughnut" sign in the right frontal region. An angiogram confirmed the finding and melanoma metastases were diagnosed.

corresponded to the thick membrane around the hematomas. If this is representative, then the "doughnut" sign in subdural hematoma is indicative of chronicity.

CRANIAL AND EXTRACRANIAL LESIONS

It is well known that Technetium 99m will localize in both benign and malignant lesions of the skull, such as fibrous dysplasia, Paget's disease, inflammatory lesions, and metastases.[19] We have observed the "doughnut" sign in metastases to the calvarium. Differentiation from an intracranial process can usually be made by analyzing the skull film or by repeating the scan with a bone scanning agent.[31] It is of interest that in our cases repeated with technetium polyphosphate, the "doughnut" sign was accentuated (Fig. 11, *A* and *B*; and 12, *A* and *B*).

The increased localization of technetium ion in calvarial lesions is probably due to hyperemia, because of the fact that in the majority of instances radioactivity fades in delayed scans[5] (Fig. 12*C*).

Similarly, uptake of technetium has been observed in lesions of the scalp including hematomas and lacerations. A recent case report demonstrates the "doughnut" sign in a cephalohematoma.[4]

TECHNICAL CONSIDERATIONS

Obviously, the morphology and uptake pattern of many different brain lesions should result in the "doughnut" sign, yet with the technique in routine use it is observed less frequently than expected. We feel this is a function of geometry and resolution of the scanning apparatus. The original description by Gottschalk *et al.*[13] involved high resolution technique. The sign was considered present only when the "clear" area was definitely within and 1/5 the diameter of the area of increased activity. Much of the difficulty in delineating the "doughnut" sign in a particular lesion is probably secondary to scanning geometry. Deep lesions are difficult to detect with the gamma camera, and a "doughnut"

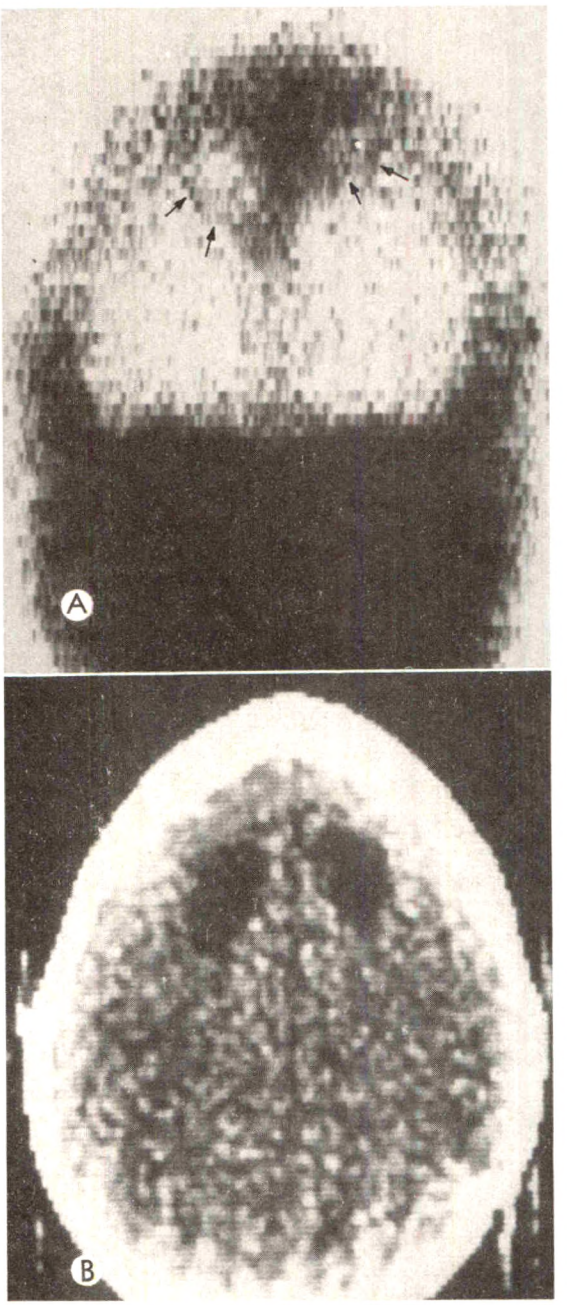


Fig. 9. This ten year old female with known medulloblastoma metastases received cobalt therapy with relief of headaches. The brain scan (*A*) showed bilateral parasagittal "doughnut" sign (arrows) thought to represent necrosis in the lesions secondary to treatment. The CAT scan (*B*) corroborated the scan, revealing cystic areas in the same region.

UNIVERSITY COLLEGE OF MEDICINE LIBRARY

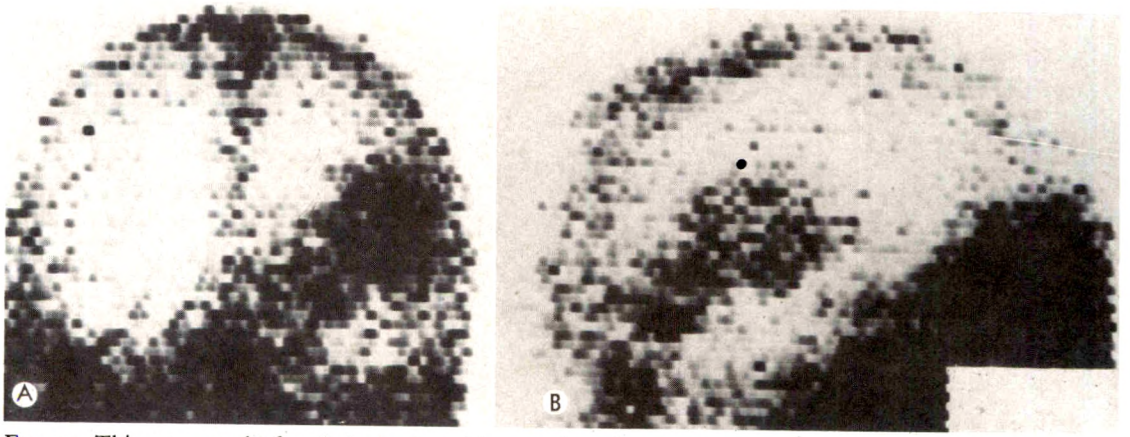
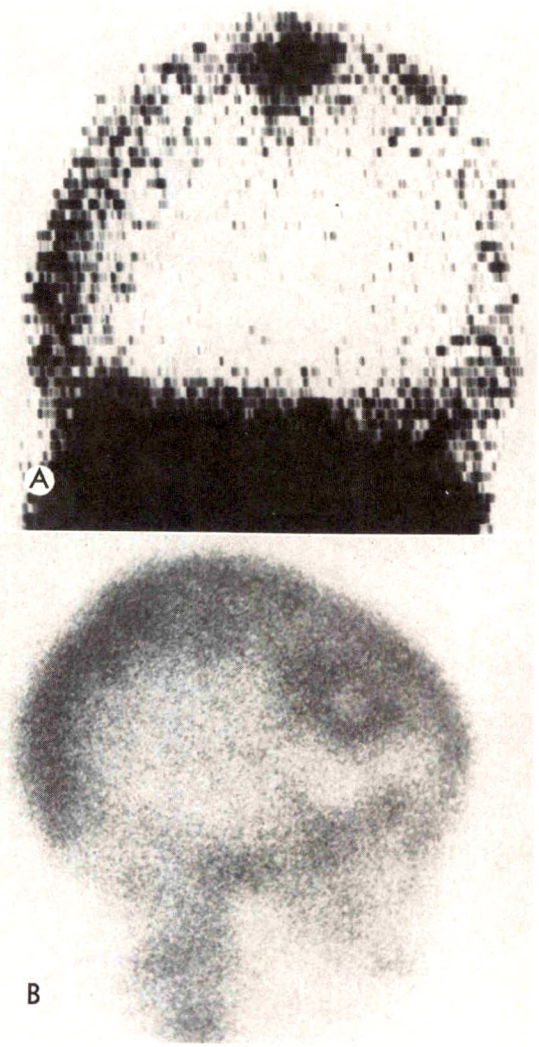


Fig. 10. This 75 year old female had a long history of cerebrovascular disease with multiple "strokes." She entered the hospital with acute symptoms, and a subsequent brain scan showed the classical wedge pattern on anteroposterior view (*A*), but a "doughnut" sign on the lateral view (*B*).



sign, therefore, more difficult to demonstrate. Lesions outside the focal plane of a rectilinear scanner may exhibit a diminished or absent "clear" central area, when scanning in the appropriate plane would demonstrate an obvious "doughnut" sign.

A comparison of the radioisotope brain scan, angiography, and computerized axial tomography shows that angiography has the greatest physical resolution, yet the lesion itself may not be visualized and may be shown only by its displacement of vessels. The complex physical principles of computerized axial tomography, however, enable demonstration of much smaller differences in structure.[17] The radioisotope scan and computerized axial tomography have in common the pictographic presentation of the lesion itself. In our limited experience, internal structure of a lesion demonstrated by brain scan has been cor-

Fig. 11. This 68 year old white female, post mastectomy for carcinoma of the breast, developed syncope. A brain scan (*A*) showed peripheral activity on the right in anteroposterior view which could have been a subdural hematoma, but a Tc polyphosphate bone scan (*B*) showed uptake in that region with a "doughnut" sign, and metastases to the skull were diagnosed.

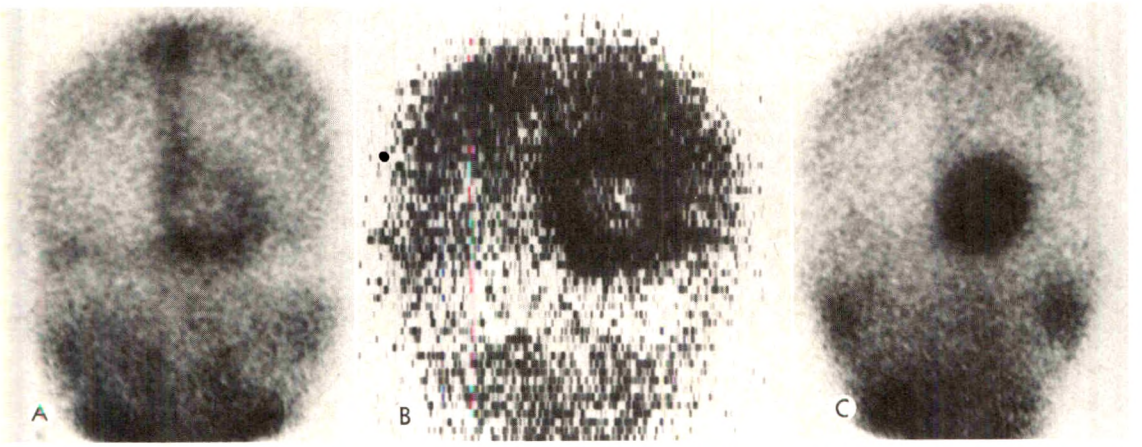


Fig. 12. This 52 year old female presented with a history of weight loss, vomiting and dysphagia. A chest roentgenogram revealed a left upper lobe mass with rib erosion. Brain and bone scans were performed as part of a metastatic evaluation. The brain scan (*A*) showed a left posterior "doughnut" sign which filled in and did not fade as would be expected in superficial lesions on a delayed scan (*C*). The Tc polyphosphate bone scan (*B*), however, showed an accentuated "doughnut" sign, and a skull film confirmed the metastatic skull lesion.

roborated by computerized axial tomography.

Yavuz Tarcan, M.D.
Division of Nuclear Medicine
Emory University School of Medicine
80 Butler Street, Southeast
Atlanta, Georgia 30303

REFERENCES

1. Alker, G. J., Leslie, E. V., and Bakay, L. Differential diagnosis of abnormal brain scan. *Acta radiol.* (Diag.), 1972, *13*, 627–633.
2. Ambrose, J. Computerized transverse axial scanning (tomography): Part 2, clinical application. *Brit. J. Radiol.*, 1973, *46*, 1023–1047.
3. Bawallius, M., Larsson, A., Skoldborn, H., and Wickbom, I. Brain scanning and conventional neuroradiologic methods in intracranial tumours. *Acta radiol.* (Diag.), 1972 *13*, 634–642.
4. Beauchamp, J. M., Belanger, M. A., and Neitzschman, H. R. Unusual cause of "doughnut" sign in brain scanning. *J. Nuclear Med.*, 1975, *16*, 432–433.
5. Bernstein, J., and Hoffer, P. B. Use of delayed brain scan in differentiating calvarial from cerebral lesions. *J. Nuclear Med.*, 1974, *15*, 681–684.
6. Blackwood, W., McMenemey, W. H., Meyer, A., Norman, R. M., and Russell, D. S. Greenfield's Neuropathology. Williams & Wilkins Company, Baltimore, 1963.
7. Crocker, E. F., McLaughlin, A. F., Morris, J. G., Benn, R., McLeon, J. G., and Allsop J. L. Technetium brain scanning in diagnosis and management of cerebral abscess. *Am. J. Med.*, 1974, *56*, 192–201.
8. Cronqvist, S., Efsing, H. O., and Hughes, R. Brain scanning in differential diagnosis of supratentorial tumours. *Acta radiol.* (Diag.), 1972, *13*, 678–692.
9. Cronqvist, S., and Muller, R. Brain scanning in cerebrovascular lesions. *Acta radiol.* (Diag.), 1972, *13*, 659–671.
10. Deland, F. H. Scanning in cerebral vascular disease. *Seminars in Nuclear Med.*, 1971, *1*, 31–40.
11. Edeling, C.-H. ^{99m}Tc-pertechnetate brain scintigraphy in children. *Acta paediat. scandinav.*, 1974, *63*, 193–200.
12. Gilday, D. L. Various radionuclide patterns of cerebral inflammation in infants and children. Am. J. Roentgenol., Rad. Therapy & Nuclear Med., 1974, *120*, 247–253.
13. Gottschalk, A., Abatie, J. D., Petasnick, J. P., Polcyn, R. E., Beck, R. N., and Charleston, D. B. Comparison between sensitivity and resolution based on clinical evaluation with ACRH brain scanner. In: Symposium on Medical Radioisotope Scintigraphy, Salzburg, Austria, 1968.
14. Handa, J., Handa, H., Hamamoto, K., Torizukea, K., and Kousaka, T. Sequential brain imaging as aid in understanding disease etiology. *Seminars in Nuclear Med.*, 1971, *1*, 56–69.
15. Hawes, D. R., and Mishkin, F. S. Brain scans

in watershed infarction and laminar cortical necrosis. *Radiology*, 1972, *103*, 131–134.
16. Holloway, W., El Gammal, T., and Pool, W. H. Doughnut sign in subdural hematomas. *J. Nuclear Med.*, 1971, *13*, 630–632.
17. Hounsfield, G. N. Computerized transverse axial scanning (tomography): Part I, description of system. *Brit. J. Radiol.*, 1973, *41*, 1016–1022.
18. Jordan, C. E., James, A. E., and Hodges, F. J. Comparison of cerebral angiogram and brain radionuclide image in brain abscess. *Radiology*, 1972, *104*, 327–331.
19. Kieffer, S. A., and Loken, M. K. Positive "brain" scans in fibrous dysplasia and other lesions of skull. Am. J. Roentgenol., Rad. Therapy & Nuclear Med., 1969, *106*, 731–738.
20. Kuhl, D. E., and Sanders, T. P. Characterizing brain lesions with use of transverse section scanning. *Radiology*, 1971, *98*, 317–328.
21. Leeds, N. E., and Goldberg, H. I. Angiographic manifestations in cerebral inflammatory disease. *Radiology*, 1971, *98*, 595–604.
22. Minckler, J. Pathology of the Nervous System. McGraw-Hill, New York, 1971.
23. Newton, T. H., and Potts, D. G. Radiology of the Skull and Brain. Volume 4. C. V. Mosby Company, St. Louis, 1971.
24. O'Mara, R. E., McAfee, J. G., and Chodos, R. B. "Doughnut" sign in cerebral radioisotope images. *Radiology*, 1969, *92*, 581–586.
25. O'Mara, R., and Mozley, J. M. Current status of brain scanning. *Seminars in Nuclear Med.*, 1971, *1*, 7–30.
26. Rockett, J. F., Freedman, B. I., and Kaplan, E. S. Significance of "Doughnut" sign. *J. Nuclear Med.*, 1972, *13*, 777–778.
27. Samuels, L. D. There's more than cancer on brain! *Clin. pediat.*, 1973, *12*, 701–706.
28. Segall, H. D., Rumbaugh, C. L., Bergeron, R. T., Teal, J. S., and Gwinn, J. L. Brain and meningeal infections in children. *Neuroradiology*, 1973, *6*, 8–16.
29. Sutherland, J. B., Hill, N., Banerjee, A. K., and Gilday, D. L. Brain scanning and brain abscesses. *J. A. Canad. Radiologists*, 1972, *23*, 176–181.
30. Suwanwela, Ch., Poshyachinda, V., and Poshyachinda, M. Brain scanning in diagnosis of intracranial abscess. *Acta neurochir.*, 1971, *26*, 165–175.
31. Tow, D. E. Differentiation of brain and bone tumors with combined radionuclide technique *Seminars in Nuclear Med.*, 1971, *1*, 85–89.
32. Wolpert, S. M., Zimmer, A., Schechter, M. M., and Zingesser, L. H. Neuroradiology of melanomas of nervous system. Am. J. Roentgenol., Rad. Therapy & Nuclear Med., 1967, *101*, 178–187.
33. Yalaz, K., and Treves, S. Brain scanning and cerebral radioisotope angiography (CRA) in children. *Pediatrics*, 1974, *54*, 696–703.
34. Zingesser, L. H. Scanning in diseases of subdural space. *Seminars in Nuclear Med.*, 1971, *1*, 41–47.

VOL. 126, No. 4

ULTRASONIC EVALUATION OF THE UNILATERAL NONVISUALIZED KIDNEY*

By JOHN P. MARANGOLA, M.D.,† PATRICK J. BRYAN, F.R.C.R.,
and FARHAD AZIMI, M.D.†
SYRACUSE, NEW YORK

ABSTRACT:

There are several techniques for evaluating the nonvisualized kidney. Nephrotomography may be helpful in those patients who have some remaining renal function. Radionuclide renal flow and imaging studies are more sensitive than nephrotomography in detecting hydronephrosis, the most common cause of unilateral renal nonvisualization, but also require some renal function to be of diagnostic value.

Diagnostic ultrasound, since it is independent of renal function, is an even more sensitive indicator of urinary obstruction, detecting those cases where no functioning renal parenchyma is present. This non-invasive technique can accurately guide percutaneous puncture of the collecting system, permitting antegrade localization of the obstructing lesion.

When ultrasonography demonstrates a solid mass in the renal fossa, angiography is recommended for definitive diagnosis. When no kidney is identified renal venography may be useful in differentiating between a small nonfunctioning kidney and renal agenesis.

UNILATERAL nonvisualization of a kidney on intravenous urography is a not infrequent diagnostic problem in an average radiology department. Accurate knowledge of the etiology is of vital importance since certain lesions require rapid intervention. Retrograde pyelography, nephrotomography,[5] arteriography,[21,22] selective renal venography,[1,16] and radionuclide studies[7] can often determine the etiology of the unilateral nonvisualized kidney.

Ultrasonography, a simple non-invasive procedure, has become an important aid in the evaluation of the urinary system.[2,4,10,12,13,17,23,25,29] It is particularly valuable in the diagnosis of hydronephrosis,[9,26] the most common cause of unilateral nonfunction.[27]

The purpose of this communication is to present our experience with B-mode ultrasound scanning in 27 patients with unilateral non-excretion on intravenous urography.

METHOD

A bi-stable modified Picker Laminagraph with a 2 megaHertz (mHz) focussed transducer was used for most of the examinations. The gray scale images were obtained on Unirad and Rohe units using 2.25 mHz focussed transducers.

With the patient in the prone position, the retroperitoneal area is scanned in longitudinal and transverse planes at 1 cm intervals. Oblique scans are performed when they better demonstrate the pathology. Mineral oil is used as the acoustic coupling agent. The images are permanently recorded on 70 mm or Polaroid film.

If the kidney is not identified in the renal fossa, the patient is rescanned in the supine position. The pelvis is examined with a distended urinary bladder to exclude an ectopic kidney.

REPORT OF CASES

CASE 1. This newborn male was found to have

* Presented at the Seventy-sixth Annual Meeting of the American Roentgen Ray Society, Atlanta, Georgia, September 30–October 3, 1975.
From the Department of Radiology, State University of New York, Upstate Medical Center, Syracuse, New York.
† Present Address: St. Joseph's Hospital Health Center, Department of Radiology, Syracuse, New York.

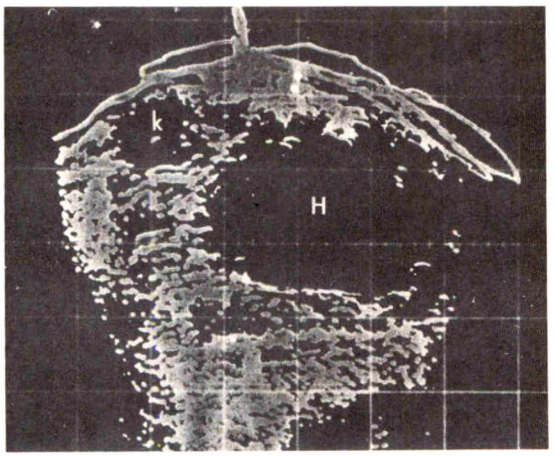


FIG. 1. Case 1. Congenital hydronephrosis (H) of the right kidney seen as a large echo free mass. k = normal left kidney. (Courtesy of *Urology*, January 1975, Vol. V, Page 18)

a right flank mass. An intravenous urogram showed a normal left kidney and no excretion on the right side. Ultrasonography demonstrated a large echo free mass in the right flank extending across the midline (Fig. 1). A diagnosis of congenital hydronephrosis was made and confirmed at surgery.

Comment. The ultrasound findings in this case enabled a precise diagnosis to be made, and surgery was performed without the need for further diagnostic work-up.

CASE V. This 24 year old female was admitted because of fever and back pain. Urine cultures grew *Klebsiella*. An intravenous urogram revealed no excretion on the left side.

Ultrasonography showed hydronephrosis of the left kidney (Fig. 2). This diagnosis was confirmed by radionuclide studies (Fig. 3) and retrograde pyelography. A left nephrectomy was performed and the pathologic specimen showed severe hydronephrosis secondary to ureteropelvic junction obstruction.

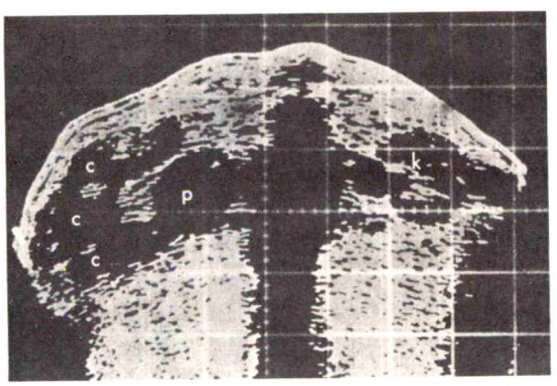


FIG. 2. Case v. Hydronephrosis of the left kidney showing greatly dilated renal pelvis (p) and calyces (c). k = normal right kidney.

Comment. Although the diagnosis of hydronephrosis was established by ultrasound, in the adult patient antegrade or retrograde pyelography is necessary to determine the site and often the cause of obstruction.

CASE VII. This 56 year old female with recurrent adenocarcinoma of the sigmoid colon was found on intravenous urography to have a hydronephrotic left kidney and no excretion on the right side.

Ultrasonography demonstrated bilateral hydronephrosis with the right collecting system being more dilated than the left (Fig. 4). The study also suggested that the hydronephrosis of the right kidney was of recent onset without much loss of renal parenchyma. There was no further work-up nor treatment since the patient had already received maximum dosage of radiation therapy and chemotherapy.

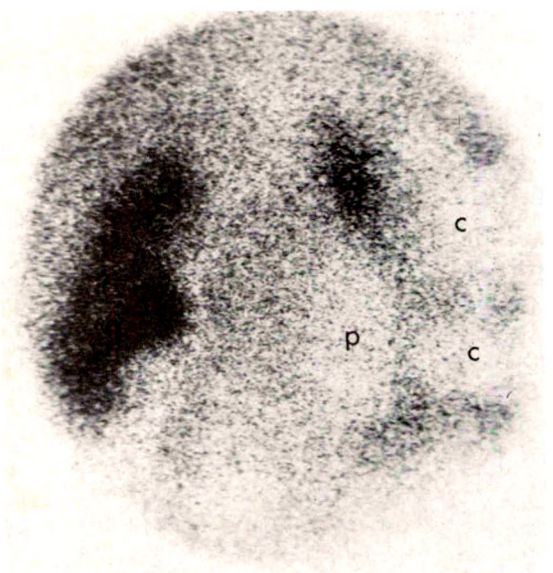


FIG. 3. Case v. Renal imaging with 99m Tc glucoheptonate demonstrating areas of decreased activity in the hugely dilated renal pelvis (p) and calyces (c). A small amount of functioning renal parenchyma is present. The right kidney is normal.

Case IX. This 23 year old male entered the hospital because of acute urinary retention. Intravenous urography revealed enlargement of the right kidney and no excretion on the left side. In addition, there was a filling defect at the base of the bladder. Urinalysis was normal and urine culture grew no bacteria. Ultrasonography showed a large but normal appearing right kidney and a small hydronephrotic left kidney (Fig. 5). At cystoscopy there was a large ureterocele obstructing the left ureter and the bladder neck. The ureterocele was unroofed and pus was drained from the left ureter.

Case X. This 59 year old female was admitted because of a right flank mass, pyuria, and anemia. An intravenous urogram was not performed because of a severe reaction to contrast medium 20 years previously. A radionuclide renal flow and imaging study showed a normal left kidney and no uptake on the right side (Fig. 6).

Ultrasonography demonstrated a 9×9×18 cm echo free mass in the right renal fossa consistent with hydro- or pyonephrosis (Fig. 7). A drainage catheter was inserted into the cystic mass under ultrasonic guidance and thick pus was aspirated. Subsequently the large pyonephrotic kidney was surgically removed. Pathologic examination showed pyonephrosis and a markedly stenotic ureteropelvic junction.

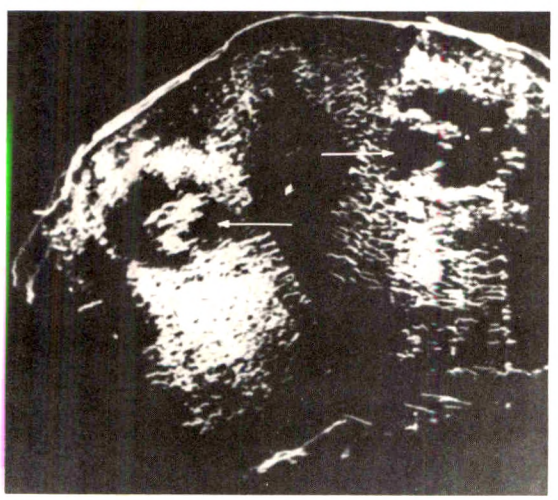


Fig. 4. Case VII. Bilateral hydronephrosis (arrows) in a patient with a nonvisualized right kidney. Note the large amount of remaining renal parenchyma bilaterally indicating recent onset of obstruction.

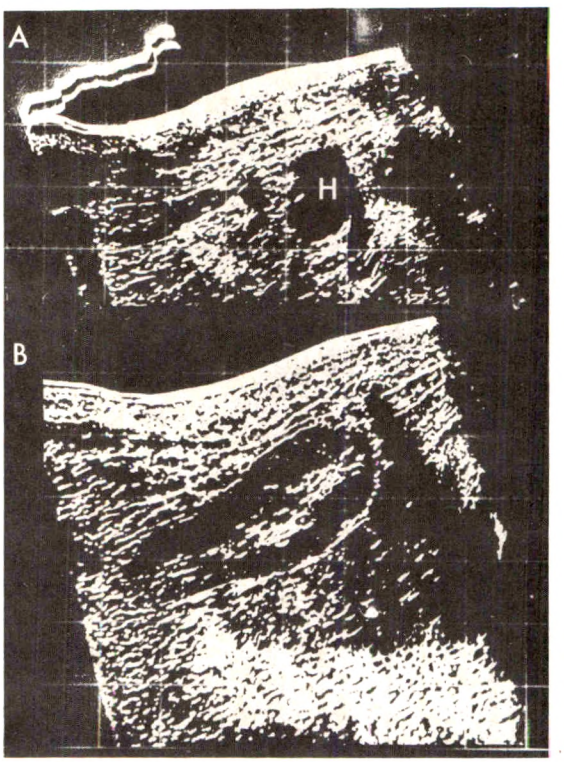


Fig. 5. Case IX. (*A*) Longitudinal scan through small hydronephrotic left kidney (H). (*B*) Longitudinal scan of hypertrophied right kidney.

Comment. Ultrasound established the diagnosis in this case in the absence of an excretory urogram. The radionuclide imaging study was unable to distinguish between hydronephrosis and renal agenesis because of the lack of renal function.

Case XI. This 66 year old male with a history of numerous abdominal surgical procedures was admitted with fever, pain, and a draining left flank sinus. Ten months prior to this admission the patient had undergone a splenectomy for traumatic rupture of the spleen and had subsequently developed a left subphrenic abscess which was surgically drained on two occasions. A previous intravenous urogram had shown enlargement of the right kidney and nonvisualization of the left kidney which was attributed to renal agenesis.

Ultrasonography showed a bilocular cystic mass in the left renal fossa (Fig. 8). The findings were consistent with hydro- or pyonephrosis. Radionuclide renal flow and imaging studies showed no uptake on the left side. A fistulogram through the left flank opening

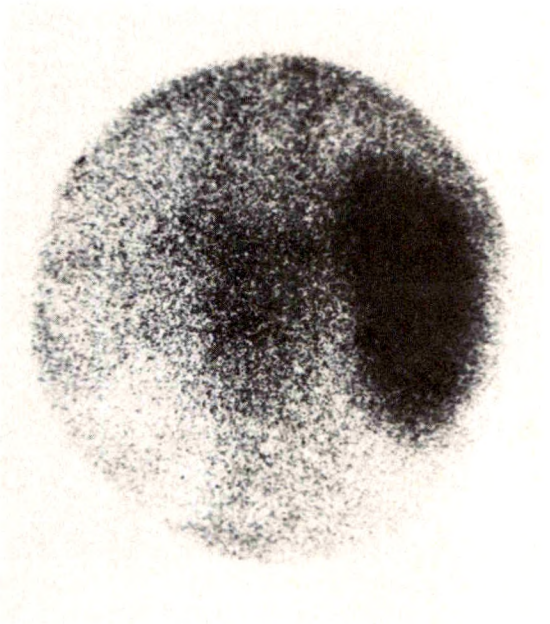


FIG. 6. Case x. The renal imaging study shows a normal left kidney and no visualization on the right side. In this patient, the radionuclide study could not distinguish between hydronephrosis and renal agenesis.

demonstrated a communication with the collecting system of the left kidney (Fig. 9). A large drainage tube was inserted into the pyonephrotic sac under ultrasonic guidance.

Comment. Despite a history of supposed renal agenesis, ultrasound suggested the correct diagnosis of pyonephrosis.

CASE XVII. This three month old male was admitted to the hospital because of a fever of 103° F. A right lower quadrant mass was discovered on physical examination. Intravenous urography demonstrated a normal left kidney and no renal visualization on the right side. Ultrasonography showed a trilocular cystic mass on the right (Fig. 10). This echo pattern was thought to be most consistent with congenital multicystic kidney.

A multicystic mass measuring 5×3.5×2 cm and weighing 40 grams was surgically removed from the right flank. Histologic examination of the specimen confirmed the diagnosis of cystic renal dysplasia.

Comment. This echo pattern in infants can be caused by multicystic kidney or congenital hydronephrosis. Since ultrasound narrowed the diagnostic possibilities to these two entities, surgery could be performed without further investigation.

CASE XX. This 72 year old male presented with hematuria. Excretory urography showed no function on the right side. Ultrasonography demonstrated an enlarged right kidney with a solid echo pattern and distorted internal architecture (Fig. 11). Renal cell carcinoma was suspected and confirmed by open biopsy.

CASE XXI. This newborn female was found to have a mass on the left side of the abdomen approximately 10 cm in diameter. An intravenous urogram showed a normal right kidney and no excretion on the left side.

Ultrasonography showed an enlarged left kidney displaying a complex echo pattern not resembling hydronephrosis (Fig. 12). A left nephrectomy was performed. The kidney was swollen, congested and measured 7×5×5 cm. It contained a hematoma 3 cm in diameter in

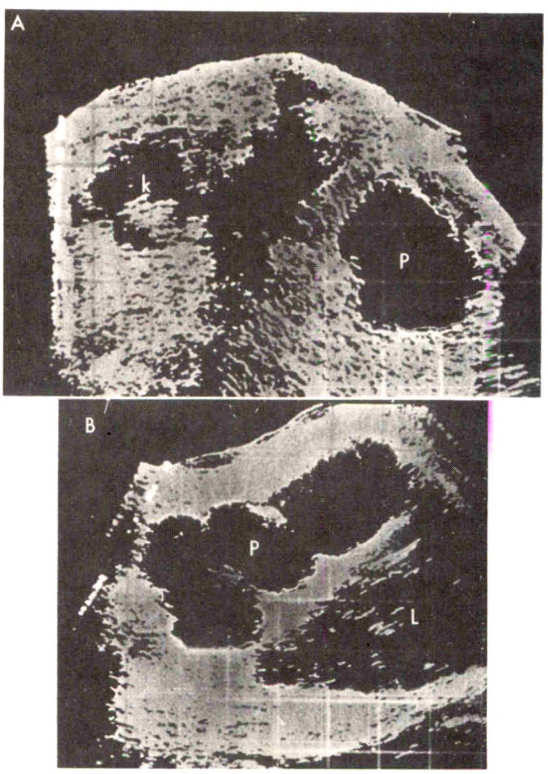


FIG. 7. Case x. Pyonephrosis (P) of right kidney seen as a large cystic mass in the right renal bed on transverse (*A*) and sagittal scans (*B*). There are a few linear echoes from the walls of the dilated calyces. L = liver, k = normal left kidney.

the upper pole. Pathologic examination showed thrombosis of the main renal vein and hemorrhagic necrosis throughout the kidney.

Comment. Ultrasonography did not establish the specific diagnosis in this case but was helpful in excluding congenital hydronephrosis as the cause of nonfunction. The predominantly echo free appearance in this case can be explained by the extensive edema and hemorrhagic necrosis of the kidney.

Case xxii. This 71 year old male was found to have a blood pressure of 250/120 and a pulsatile abdominal mass. Intravenous urography showed a large calcified abdominal aortic aneurysm, a poorly functioning right kidney, and no excretion on the left side (Fig. 13).

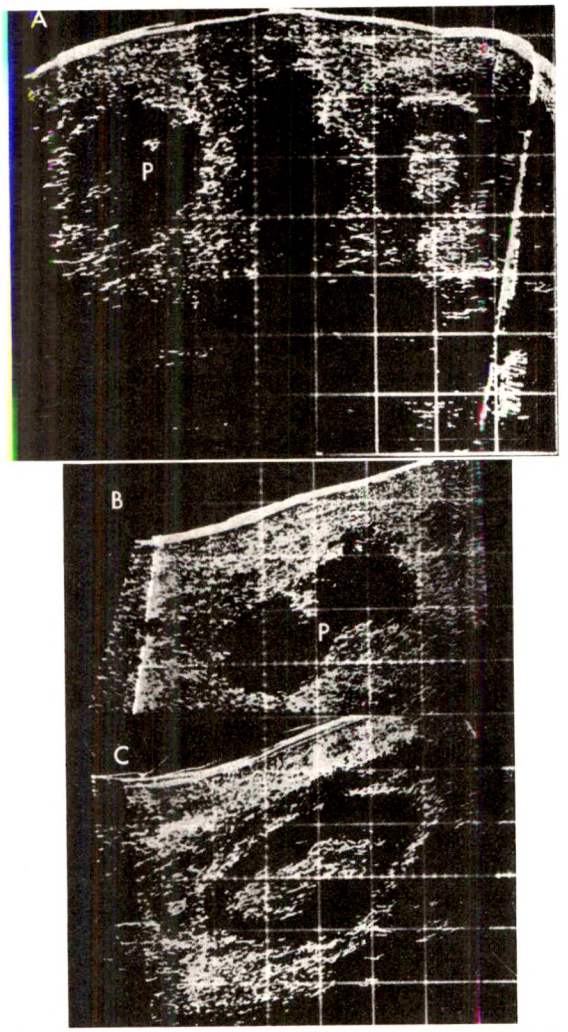


Fig. 8. Case xi. Pyonephrosis. Transverse scan (*A*) shows cystic mass (P) in the left renal fossa which on longitudinal section (*B*) has a reniform shape. Longitudinal scan of the right kidney (*C*) shows compensatory hypertrophy.

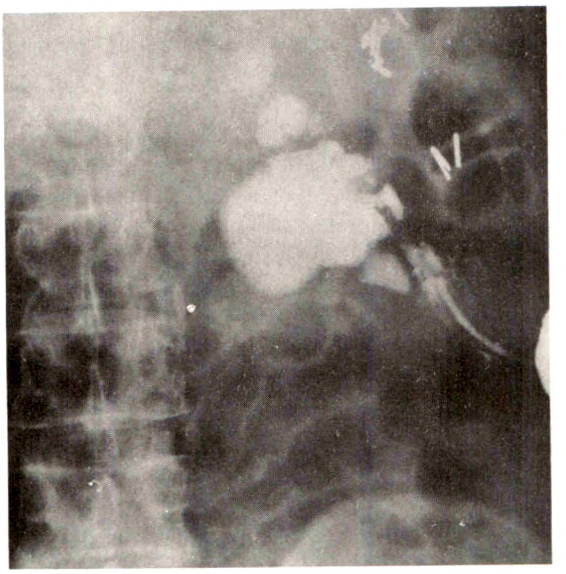


Fig. 9. Case xi. Fistulogram showing dilated collecting system of the left kidney.

Ultrasonography showed the left kidney to be smaller than the right with no hydronephrosis (Fig. 14). Aortography showed complete occlusion of the left renal artery and stenosis of the right renal artery.

Comment. The normal ultrasonic appearance of the collecting system of the left kidney indicated that the lack of function was due to vascular impairment rather than ureteral obstruction by the abdominal aortic aneurysm.

RESULTS

Twenty-seven patients with unilateral renal nonfunction were studied (Table 1). The results are summarized in Table 11. In 20 of the 27 patients, the final diagnosis was proved by nephrectomy, biopsy, or autopsy. In two patients the diagnosis was established by arteriography.

The correct diagnosis was made on ultrasound examination in 17 (77 percent) of the 22 proved cases. In three other patients ultrasound was useful in excluding hydronephrosis and directing further work-up.

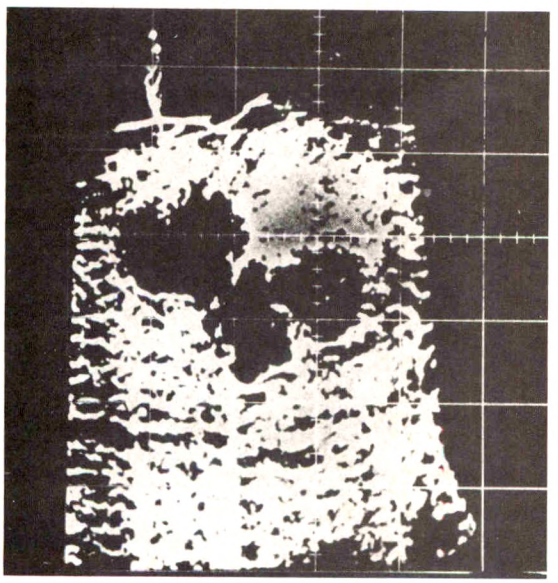


FIG. 10. Case XVII. Multicystic kidney. Longitudinal scan.

Ultrasound was thus diagnostic or helpful in 20 (91 percent) of the 22 proved cases.

There were two diagnostic errors (nine percent). In Case XXIV, the tiny kidney, found at autopsy to weigh only 10 grams, was not identified by ultrasound, and renal agenesis was incorrectly diagnosed. In Case XXVII, a patient with left renal agenesis, the spleen which occupied the renal fossa was erroneously thought to represent a hydronephrotic sac (Fig. 15). The spleen is normally very transonic and can be difficult to differentiate from a fluid filled mass.

All 14 proved cases of obstruction of the collecting system were correctly diagnosed by ultrasound. Obstruction was the most common cause of unilateral nonfunction in this series, comprising 64 percent of the proved cases.

DISCUSSION

There are many causes of unilateral nonvisualization on intravenous urography.[19,28] Ultrasonography is a useful diagnostic modality in evaluating these patients because visualization by this technique depends only on the morphologic and acoustic characteristics of the kidney and is independent of renal function. Using ultrasound, one can determine whether a kidney is present, and if so it can provide information regarding its size, shape, and internal architecture. This information can be used to direct further diagnostic work-up and at times may obviate any further investigation.

Barnett and Morley[2] (1971) and Stuber *et al.*[29] (1972) recommended ultrasonography in the evaluation of unilateral renal nonfunction. Bearman *et al.*[4] (1973) reported its usefulness in four pediatric patients. Hatley and Whitaker[13] (1973) used ultrasound to study eight adult patients with unilateral nonfunction. In four of their eight patients hydronephrosis was found. In 1975, Pitts *et al.*[23] reported a diagnostic

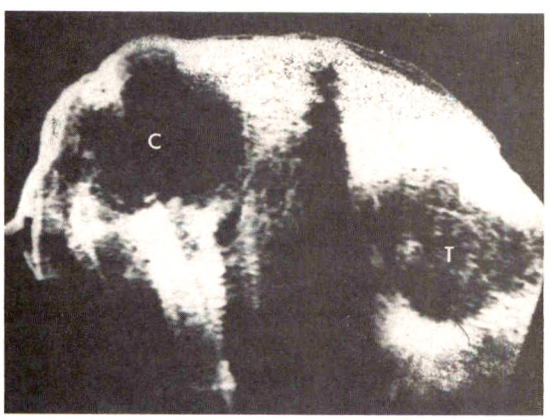


FIG. 11. Case XX. Oblique scan showing a solid mass (renal cell carcinoma) replacing the right kidney. A large simple cyst (C) is seen in the upper pole of the left kidney. T = tumor.

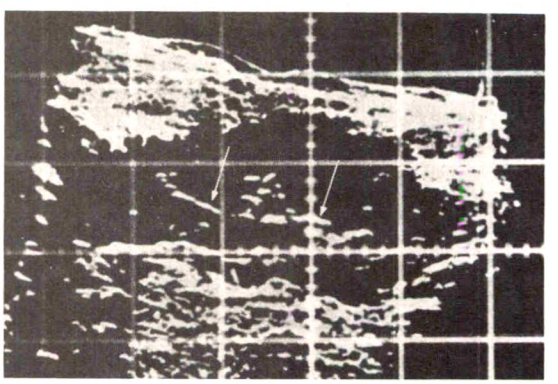


FIG. 12. Case XXI. Renal vein thrombosis. Longitudinal scan showing an enlarged kidney and no dilatation of the collecting system (arrows).

accuracy of 95 percent in 21 adults and 100 percent in nine children with unilateral nonfunction.

Ultrasonography is most helpful when a mass is present in the renal fossa. It can show whether the mass is cystic, solid, or a combination of the two (complex).[12] The state of the collecting system can also be evaluated for hydronephrosis,[9,26] which is the most common cause of a unilateral nonfunctioning kidney.

The differential diagnosis of unilateral nonvisualization can be conveniently subdivided into pediatric and adult age groups. In the child the differential diagnosis includes congenital hydronephrosis secondary to ureteropelvic junction obstruction, multicystic kidney, unilateral renal vein thrombosis, and occasionally Wilms' tumor. Congenital hydronephrosis and multicystic kidney are cystic masses whereas renal vein thrombosis and Wilms' tumor produce solid or complex echo patterns.

Congenital hydronephrosis usually presents as an echo free solitary, fluid filled sac in the renal fossa with little or no identifiable renal parenchyma.[9] Multicystic kidney (unilateral total renal dysplasia) is most often represented by a cystic mass with linear internal echoes from the walls of the individual cysts.[29] Occasionally multicystic kidney can present as a large solitary cystic mass without internal echoes, simulating congenital hydronephrosis.[4] Congenital hydronephrosis and multicystic kidney comprise the vast majority of cases of unilateral renal nonvisualization in childhood, and when their echo patterns are recognized no further work-up is necessary prior to surgery.



Fig. 14. Case xxii. Supine scan showing small kidneys bilaterally with no hydronephrosis. A=abdominal aortic aneurysm. L=liver. rk=right kidney. lk=left kidney.

Renal vein thrombosis and Wilms' tumor are much less common and more difficult to diagnose precisely by ultrasound. They produce a solid or complex echo pattern,[4,12,15,29] and angiography is recommended for definitive diagnosis whenever such a pattern is encountered.

In the adult, the diagnostic possibilities are more varied.[19,28] As in the child, ob-

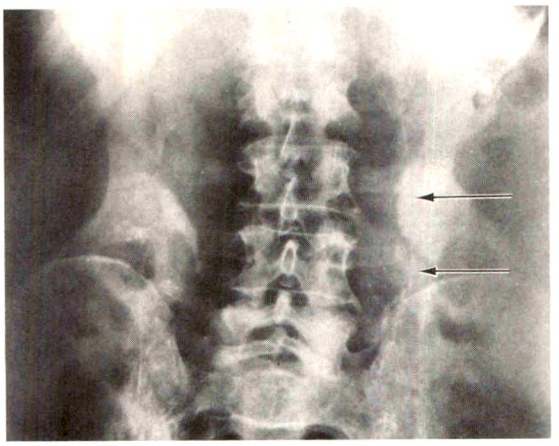


Fig. 13. Case xxii. Intravenous urogram shows aortic aneurysm (arrows) and nonfunctioning left kidney.

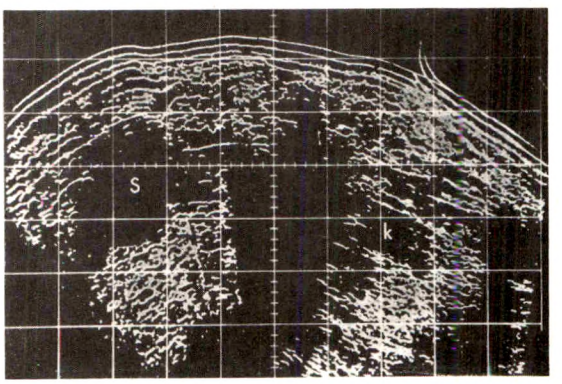


Fig. 15. Case xxvii. Renal agenesis. The transonic spleen (S) occupying the left renal fossa simulates hydronephrosis. k=right kidney.

TABLE I

Case	Sex	Age	Clinical Presentation	Ultrasound Diagnosis	Final Diagnosis
I	M	1 Day	Abdominal mass, fever	Congenital hydronephrosis	Congenital hydronephrosis
II	M	2 Wks	Abdominal mass	Congenital hydronephrosis	Congenital hydronephrosis
III	F	59	Hypertension	Hydronephrosis	Hydronephrosis**
IV	F	59	Hematuria	Hydronephrosis	Hydronephrosis, obstruction by transitional cell carcinoma of bladder drained under ultrasonic guidance
V	F	24	Fever and back pain	Hydro- or pyonephrosis*	Hydronephrosis
VI	M	69	Prostatic hypertrophy	Hydronephrosis	Hydronephrosis
VII	F	56	Carcinoma of colon	Hydronephrosis	Hydronephrosis**
VIII	M	69	Hematuria	Hydronephrosis	Hydronephrosis caused by transitional cell carcinoma of ureter
IX	M	23	Urinary retention	Small hydronephrotic kidney	Small pyonephrotic kidney and ureterocoele
X	F	59	Flank mass and pyuria	Hydro- or pyonephrosis*	Pyonephrosis diagnosed and drained under ultrasonic guidance
XI	M	66	Flank sinus	Hydro- or pyonephrosis*	Pyonephrosis diagnosed and drained under ultrasonic guidance
XII	F	77	Abdominal pain	Hydro- or pyonephrosis*	Pyonephrosis diagnosed and drained under ultrasonic guidance
XIII	F	39	Flank pain	Hydro- or pyonephrosis*	Pyonephrosis
XIV	F	68	Fever and flank mass	Hydro- or pyonephrosis*	Pyonephrosis
XV	M	55	Fever and flank pain	Hydro- or pyonephrosis*	Pyonephrosis
XVI	F	43	Flank pain	Complex echo pattern	Xanthogranulomatous pyelonephritis
XVII	F	3 Mos	Fever and abdominal mass	Multicystic kidney	Multicystic kidney
XVIII	M	45	Epigastric pain	Complex echo pattern	Multicystic kidney with calcified cysts
XIX	M	67	Pain and weight loss	Solid tumor	Renal cell carcinoma
XX	M	72	Hematuria	Solid tumor	Renal cell carcinoma
XXI	F	1 Day	Abdominal mass	Complex echo pattern no hydronephrosis	Renal vein thrombosis
XXII	M	71	Abdominal aneurysm and hypertension	Small kidney no hydronephrosis	Renal artery occlusion
XXIII	M	66	Hypertension	Abdominal aortic aneurysm small kidney	End stage kidney**
XXIV	F	69	Epigastric pain	Renal agenesis	End stage kidney weighing 10 grams
XXV	F	37	Vaginal bleeding	Absent kidney	Renal agenesis**
XXVI	M	6	Undescended testicle	Absent kidney	Renal agenesis**
XXVII	M	57	Hypertension	Hydronephrosis	Renal agenesis (Spleen in left renal fossa)

* Pyonephrosis suggested when obstruction was accompanied by clinical signs of infection.
** No surgical proof.

struction of the collecting system is the most common cause of unilateral nonvisualization, comprising 75 percent of the cases in a study of nephrectomized kidneys,[27] and 64 percent in our series. A solitary echo free mass in the renal fossa signifies long standing hydro- or pyonephrosis. The latter may however contain weak internal echoes depending upon the consistency of the pus. Acute obstruction can also cause unilateral nonvisualization. In these patients, pyelocaliectasis is less severe and a normal amount of renal parenchyma may be present (Fig. 4).

Clinical findings and history are often helpful in distinguishing hydro- from pyonephrosis, but for definitive diagnosis the dilated renal pelvis can be percutaneously punctured under ultrasonic guidance[20] and the aspirated fluid examined and cultured. Contrast agent is then instilled into the cavity under fluoroscopy to outline the hydronephrotic sac, define the site of obstruction, and when possible determine the

etiology. This is important in the adult since the causes of obstruction include calculi, primary and secondary neoplasms of the urinary tract, as well as congenital obstructive lesions.

Ultrasound can play an important role in the management of these patients. In hydronephrosis, percutaneous insertion of drainage tubes under ultrasonic guidance will relieve the obstruction without the necessity for surgical pyelostomy, thus enabling the kidney to recover any function of which it is capable. In pyonephrosis, culture of the aspirate permits appropriate antibiotic therapy. This together with percutaneous drainage allows the patient's condition to improve before elective surgery.

Multicystic kidney in the adult can present as a polycystic mass with an echo pattern similar to that seen in childhood. However, in the only case we have studied, the cysts were not recognized as such because of ultrasonic attenuation by calcification in the cyst walls. In questionable cases, angiography may be necessary for precise diagnosis.[1,21]

Perinephric hematoma and abscess, and subcapsular hematoma[18] can cause nonfunction of a kidney, and are also diagnosable by ultrasound. They present as an echo free area adjacent to and frequently displacing the kidney.

When the echo pattern of a mass in the renal fossa is solid or complex, the differential diagnosis includes renal cell carcinoma, transitional cell carcinoma,[6,8,24] metastases to the kidney, renal artery occlusion, renal vein thrombosis,[4,14] renal trauma,[11] and tumefactive xanthogranulomatous pyelonephritis.[3] In these patients ultrasound can exclude hydronephrosis, thereby obviating the need for retrograde pyelography. Angiography[22] is recommended for definitive diagnosis when a solid or complex echo pattern is encountered.

When a kidney is not identified in the renal fossa on B-scanning, a careful search of the pelvis with the patient in the supine position should be performed to rule out renal ectopia. If no kidney is found, the diagnostic possibilities include agenesis, hypoplasia, and end stage kidney too small to be resolved with our present ultrasound equipment. Angiography,[21] and in particular renal venography,[1,16] may be useful in distinguishing a small kidney from agenesis.

Table II

Diagnosis	Number of Cases
Hydronephrosis	8
Pyonephrosis	7
Agenesis	3
Neoplasia	2
Small end stage kidney	2
Multicystic kidney	2
Renal artery occlusion	1
Renal vein thrombosis	1
Xanthogranulomatous pyelonephritis	1
Total	27

John P. Marangola, M.D.
Department of Radiology
State University of New York
Upstate Medical Center
Syracuse, New York 13210

The authors wish to express their thanks to Mrs. Lori Champlin for her technical assistance and Mrs. Linda Markell for her secretarial assistance.

REFERENCES

1. Athanasoulis, C. A., Brown, B., and Baum, S. Selective renal venography in differentiation between congenitally absent and small contracted kidney. *Radiology*, 1973, *108*, 301–305.
2. Barnett, E., and Morley, P. Ultrasound in investigation of space-occupying lesions of urinary tract. *Brit. J. Radiol.*, 1971, *44*, 733–742.
3. Beachley, M. C., Ranniger, K., and Roth, F. Xanthogranulomatous pyelonephritis. Am. J. Roentgenol., Rad. Therapy & Nuclear Med., 1974, *121*, 500–507.
4. Bearman, S., Sanders, R. C., and Oh, K. S. B-scan ultrasound in evaluation of pediatric abdominal masses. *Radiology*, 1973, *108*, 111–117.
5. Becker, J. A. Nonvisualized kidney: value of

LIBRARY

nephrotomography. *Radiology*, 1967, *89*, 676–681.

6. Becker, J. A. Transitional cell carcinoma of renal pelvis: causes of non-visualization on excretory urography. *J. Urol.*, 1969, *101*, 280–282.
7. Bell, E. G., and Blaufox, M. D. Clinical applications of renal imaging. In: Golden's Diagnostic Radiology Series. Section 20, Chapter 36. To be published.
8. Bogaard, T. P., and Goldstein, A. M. B. Bilateral transitional cell carcinoma of renal pelvis with unilateral nonfunctioning kidney. *J. Urol.*, 1975, *113*, 565–567.
9. Bryan, P. J., and Azimi, F. Ultrasound in diagnosis of congenital hydronephrosis due to obstruction of pelviureteric junction. *Urology*, 1975, *5*, 17–20.
10. Doust, V. L., Doust, B. D., and Redman, H. C. Evaluation of ultrasonic B-mode scanning in diagnosis of renal masses. Am. J. Roentgenol., Rad. Therapy & Nuclear Med., 1973, *117*, 112–118.
11. Elkin, M., Meng, C., and de Paredes, R. G. Correlation of intravenous urography and renal angiography in kidney injury. *Radiology*, 1966, *86*, 496–498.
12. Goldberg, B. B., Capitanio, M. A., and Kirkpatrick, J. A. Ultrasonic evaluation of masses in pediatric patients. Am. J. Roentgenol., Rad. Therapy & Nuclear Med., 1972, *116*, 677–684.
13. Hatley, W., and Whitaker, R. H. How accurate is diagnostic ultrasound in renal disease? *Brit. J. Urol.*, 1973, *45*, 468–473.
14. Hipona, F. A., and Crummy, A. B. Roentgen diagnosis of renal vein thrombosis. Am. J. Roentgenol., Rad. Therapy & Nuclear Med., 1966, *98*, 122–131.
15. Hunig, R., and Kinser, J. Ultrasonic diagnosis of Wilms' tumors. Am. J. Roentgenol., Rad. Therapy & Nuclear Med., 1973, *117*, 119–127.
16. Itzchak, Y., Adar, R., Mozes, M., and Deutsch, V. Renal venography in diagnosis of agenesis and small contracted kidney. *Clin. Radiol.*, 1974, *25*, 379–383.
17. King, D. L. Renal ultrasonography. *Radiology*, 1972, *105*, 633–640.
18. Koehler, P. R., Talner, L. B., Friedenberg, M. J., and Kyaw, M. M. Association of subcapsular hematomas with nonfunctioning kidney. *Radiology*, 1973, *101*, 537–542.
19. Korsower, J. M., and Reeder, M. M. Nonvisualization or nonfunctioning of one kidney on intravenous pyelogram. *J.A.M.A.*, 1975, *232*, 746–747.
20. Leopold, G. R., Talner, L. B., Asher, W. M., Gosink, B. B., and Gittes, R. F. Renal ultrasonography: updated approach to diagnosis of renal cyst. *Radiology*, 1973, *109*, 671–678.
21. Love, L., and Des Rosiers, R. J. Angiography of renal agenesis and dysgenesis. Am. J. Roentgenol., Rad. Therapy & Nuclear Med., 1972, *116*, 137–142.
22. Petasnick, J. P., and Patel, S. K. Angiographic evaluation of nonvisualizing kidney. Am. J. Roentgenol., Rad. Therapy & Nuclear Med., 1973, *119*, 757–766.
23. Pitts, W. R., Kazam, E., Gershowitz, M., and Muecke, E. C. Review of one hundred renal and perinephric sonograms with anatomic diagnoses. *J. Urol.*, 1975, *114*, 21–26.
24. Renert, W. A., Rudin, L. J., and Casarella, W. J. Renal vein thrombosis in carcinoma of renal pelvis. Am. J. Roentgenol., Rad. Therapy & Nuclear Med., 1972, *114*, 735–740.
25. Rose, J. S., Becker, J. A., Staiano, S. J., and Compos, E. B-mode sonographic evaluation of abdominal masses in pediatric patient. Am. J. Roentgenol., Rad. Therapy & Nuclear Med., 1974, *120*, 691–698.
26. Sanders, R. C., and Bearman, S. B-scan ultrasound in diagnosis of hydronephrosis. *Radiology*, 1973, *108*, 375–382.
27. Spjut, H. J., and Nicolai, C. H. Nonvisualizing kidney: pathologic study of eighty-three nephrectomy specimens. *J. Urol.*, 1961, *85*, 115–118.
28. Strandness, D. E. Unilateral nonfunctioning kidney. *A.M.A. Arch. Int. Med.*, 1958, *101*, 611–619.
29. Stuber, J. L., Templeton, A. W., and Bishop, K. Ultrasonic evaluation of kidneys. *Radiology*, 1972, *104*, 139–143.

Vol. 126, No. 4

FACTORS THAT MODIFY THE RADIO-RESPONSE OF CANCER OF THE NASOPHARYNX*

By JOSEPH BOHORQUEZ, M.D., D.M.R.T., F.F.R.†
BROOKLYN, NEW YORK

ABSTRACT:

A study of 152 cases of carcinoma of the nasopharynx was carried out for evaluation of various features of the tumors. Survival is greatest in middle aged patients and poorest in patients under 20 years of age. Patients who presented with lymph node involvement had a better survival rate than those without, and those with undifferentiated tumors survived longer, although tumors in this group metastasized earlier. Those tumors which arose on the postero-superior wall of the nasopharynx were associated with a lower cure rate than those situated elsewhere. Spread to adjacent tissues diminished the cure rate, but the rate fell particularly low if there was spread to bone or to the central nervous system. If no neck lymph nodes were involved, patients with undifferentiated and well-differentiated lesions fared equally well, but if there was involvement of the neck lymph nodes, those with undifferentiated primary lesions obtained a better cure rate. The influence of the type of local spread, the presence of distant metastasis, and survival in relation to the histological and clinical grading of the tumor were also evaluated.

THE biological behavior of a tumor and its relationship to neighboring areas plays a very important role, not only in its management but in the ultimate prognosis. Carcinoma of the nasopharynx, which arises in an area which is a solid bony box, surrounded by vital structures, presents special problems to the radiotherapist. In many instances, these problems are difficult to solve without producing damage to these nearby normal structures. It is, therefore, relevant to have an idea of the importance of those factors which influence on the radio-response of these tumors, and from there to evolve a system of how to treat them.

One hundred and fifty-two cases of squamous cell carcinoma of the nasopharynx seen and treated at the Head and Neck Unit of the Royal Marsden Hospital, London, England from 1933 to 1956 have been analyzed with this scope. All patients had complete physical, roentgenologic and neurologic evaluation as well as histologic confirmation of their disease.

The tumors were graded into well-differentiated, comprising Grades I and II of the Broders Classification, and undifferentiated, comprising Grades III and IV, in agreement with Yeh,[19,24,29] the classical type being called here well-differentiated. All of them were staged according to the International Union Against Cancer Classification outlined in Table I.

TECHNIQUE OF IRRADIATION

In cancer of the nasopharynx a thorough evaluation of the true extent of the tumor is highly rewarding. Since the biological potential of these tumors to invade neighboring areas is rather high the three field technique, two lateral and one nasal, is used in order to tailor the treatment to the individual tumor in the individual patient. In this way, by spreading the dose over three portals I avoid the very troublesome trismus which not only prevents the patient from chewing and swallowing properly, but prevents good follow-up examination. Shielding of both eyes and a dental stent to

* Presented at the Fifty-seventh Annual Meeting of The American Radium Society, Isla Verde, Puerto Rico, May 4–9, 1975.
Downstate Medical Center, State University of New York, Brooklyn, New York.
† Director, Department of Radiotherapy.

TABLE I

INTERNATIONAL UICC STAGING CLASSIFICATION

T1	Tumor limited to one region (one wall)
T2	Tumor limited to two regions (two walls)
T3	Tumor extending beyond nasopharynx without bone invasion
T4	Tumor extending beyond nasopharynx with bone invasion
No	No palpable lymph nodes
N1	Movable homolateral lymph nodes
N2	Movable contralateral or bilateral lymph nodes
N3	Fixed lymph nodes
Mo	No evidence of distant metastasis
M1	Distant metastasis present

push the tongue down out of the anterior field are used when the tumor has not spread to the oropharynx and the latter diminishes the severity of xerostomia. The lower neck is irradiated with the classical anterior and posterior split fields down to the clavicle. When indicated, a boost dose to small areas of the neck is given. Using the moulage technique described by Pierquin an individual applicator is made of lucite to boost the dose to the remaining portion of the tumor in the nasopharynx, loaded in such a way that only the target volume receives the desired dose.

MODIFYING FACTORS

The factors described below were analyzed in an effort to determine (a) their biological potential, (b) their influence in the response to ionizing radiation, (c) their influence on survival, (d) their influence on recurrence, and (e) their influence on radiation damage.

The distribution of cases in each group and the ratio between cases are arbitrarily called, "the established distribution," and "the established ratio," respectively. All results reported here are ratio corrected and the survivals are five years or longer free of disease.

Sex. One hundred and three cases or 67.8 percent were male, and 49 or 32.2 percent were female, a ratio of 2.1:1. There was no statistical difference in survival between the two sexes. The over-all survival for male was 15 percent and female, 16 percent[14,21,26] (Tables II and XII).

Age Group. According to age group the highest survival, 43 percent, was obtained in the 4th decade.[4,14,18,21,23] It is interesting to observe that also in this age group both males and females achieved the highest cure rate, namely 36 percent for the former and 55 percent for the latter. Equally important, the results according to histology are the highest, 33 percent for well-differentiated tumors and 45 percent for undifferentiated tumors. There was no survival in the first two decades,[23] and the survival in the group over 50 dropped to around 18 percent. The reason for these results will be discussed under histological grading. (Table III).

Presenting Symptoms. The highest survival rate, 35 percent, was in the group which presented with lymph node involvement. Undifferentiated tumors had a higher survival, 37 percent, *versus* 25 percent for well-differentiated tumors. Since the ratio

TABLE II

DISTRIBUTION OF CASES ACCORDING TO SEX AND HISTOLOGY

				Ratio
Male	103 (67.8%)	Female	49 (32.2%)	2.1:1
Undifferentiated Tumors	108 (71.1%)	Well Differentiated Tumors	44 (28.9%)	2.5:1
Male/Undifferentiated	74 (48.7%)	Male/Well Differentiated	29 (19.1%)	2.5:1
Female/Undifferentiated	32 (22.4%)	Female/Well Differentiated	15 (9.9%)	2.3:1
Male/Undifferentiated	74 (48.7%)	Female/Undifferentiated	34 (22.4%)	2.1:1
Male/Well Differentiated	29 (19.1%)	Female/Well Differentiated	15 (9.9%)	1.9:1

TABLE III

DISTRIBUTION AND SURVIVAL ACCORDING TO AGE GROUP

Years	10	20	30	40	50	60	70	80
Male/Well Differentiated	—	—	3	—	11	11	4	—
Male/Undifferentiated	3	7	7	14	21	15	6	1
Female/Well Differentiated	—	—	—	3	4	4	4	—
Female/Undifferentiated	1	4	4	6	8	7	4	—
Total Cases	4	11	14	23	44	37	18	1
Percentage Survival	0	0	21	43	16	22	17	0
Male/Survival	0	0	33	36	16	15	20	0
Female/Survival	0	0	0	55	17	36	12	0
Well Differentiated/Survival	0	0	0	33	13	13	25	0
Undifferentiated/Survival	0	0	27	45	17	27	10	0

of undifferentiated to well-differentiated carcinomas in this group is 4.8:1, almost twice the established ratio, it appears that (1) undifferentiated tumors have a higher biological potential to metastasize to the lymph nodes,[4,7,15,16] and (2) the higher cure rate is a function of the histological grading of the tumors which are also probably more radiosensitive and radiocurable.[4] Since male and female survival rates in this group are 36 and 33 percent respectively, sex is not the factor influencing the survival, but the degree of malignancy of the tumor is. The survival for patients presenting with either nasal or oricular symptoms is about the same, around 22 percent. On the other hand, in the group of patients presenting with either bone or central nervous system (CNS) invasion, the survival is very low, around seven percent. The radiosensitivity and radiocurability are so greatly affected with bone or CNS invasion that they are probably the most significant factors in the cure of these patients.[4,7,10,11,16–18] The explanation for this may lie in the fact that once the tumor has invaded bone or the CNS, the radio-response changes either because of changes in the biological nature of the tumor or because the new host tissue reduces the ability of the tumor to respond to ionizing radiation.[4,10] Since these factors are among the major problems that the radiotherapist has to contend with when treating this type of tumor every effort should be made to evaluate them properly when planning the treatment (Table IV).

Initial Site of the Tumor. As seen in Table V the lowest survival rate, 13 percent was in tumors arising primarily in the postero-superior wall.[4] The survival for tumors of both lateral walls and antero-inferior walls is roughly the same, about 29 percent. This difference is statistically significant. The low survival rate for tumors arising in the postero-superior wall remains the same regardless of sex and histology. Therefore, these tumors which were in the majority, accounting for 41 percent of the total, have a tendency towards a greater malignancy. This could be explained on the basis of the anatomical position, since these tumors have a greater tendency to spread upwards to invade the base of the skull and the CNS.[4] It is, therefore, the anatomy[4,10,23] of the nasopharynx that determines and influences both the biological behavior and the survival rate of tumors arising in this area. Equally important in the management is the problem of local recurrence since between 25–50 percent take place in this area.

Time-Delay. The total number of patients was divided into five groups according to delay between the first presenting symptoms and the beginning of treatment.

TABLE IV

DISTRIBUTION AND SURVIVAL ACCORDING TO PRESENTING SYMPTOMS

	1*	2*	3*	4*	5*	6*
Male/Well Differentiated	14	6	2	3	2	2
Male/Undifferentiated	27	19	12	8	2	6
Female/Well Differentiated	4	5	2	1	1	2
Female/Undifferentiated	13	12	7	2	—	—
Total Cases	58	42	23	14	5	10
Percentage Survival	22	19	35	7	0	20
Male/Survival	22	20	36	9	0	0
Female/Survival	23	18	33	0	0	—
Well Differentiated/Survival	6	18	25	25	0	—
Undifferentiated/Survival	30	19	37	0	0	0

* 1—Nasal; 2—Auricular; 3—Lymph node invasion; 4—Bone pain; 5—CNS invasion; 6—Any other symptom.

These five groups had a delay of 3, 6, 9, 12, and more than 12 months. The relationship between tumor extent and time delay is called the "clinical age of a tumor.[4]" It is seen in Table VI that T-1 tumors presented in the first 0–6 months in 82 percent of the cases and the remaining 18 percent between 6 and 12 months. This may reflect more rapidly growing tumors which produce earlier symptoms. Stages II and III tumors have a more or less similar distribution in the groups between 0–6 months, between 6–12 months, and more than 12 months, perhaps reflecting an average growth pattern. On the other hand, Stage IV tumors had a lower incidence in the group 0–6 months, 43 percent; but more important they presented in 28 percent of the cases with more than 12 months of delay, possibly reflecting a slower tumor growth. Relating this time-delay to survival, it is seen in Table VII that the peak survival rate is in the group 6–9 months, 32 percent; the lowest is in the 0–3 months, 10 percent; followed by the group between 3–6 months with 19 percent. In the groups between 9–12 months and more than 12 months the survival is about the same, 26

TABLE V

DISTRIBUTION AND SURVIVAL ACCORDING TO INITIAL SITE

	R.W.*	L.W.*	P.S.W.*	A.I.W.*
Male/Well Differentiated	6	6	15	2
Male/Undifferentiated	23	20	28	3
Female/Well Differentiated	4	3	7	1
Female/Undifferentiated	8	12	13	1
Total Cases	41	41	63	7
Percentage Survival	24	29	13	29
Male/Survival	17	31	14	20
Female/Survival	42	27	10	50
Well Differentiated/Survival	20	0	14	66
Undifferentiated/Survival	26	38	12	0

* R.W.—Right Wall; L.W.—Left Wall; P.S.W.—Postero-Superior Wall; A.I.W.—Antero-Inferior Wall.

TABLE VI

DISTRIBUTION ACCORDING WITH THE RELATION OF TIME DELAY TO TUMOR EXTENT

	0–3	3–6	6–9	9–12	12+
Male/Well Differentiated Carcinoma	8	11	4	5	1
Male/Undifferentiated Carcinoma	23	18	9	10	14
Female/Well Differentiated Carcinoma	5	2	3	1	4
Female/Undifferentiated Carcinoma	3	11	9	6	5
Total Cases	39	42	25	22	24
Percentage Distribution	25.7	27.6	16.4	14.5	15.8
Stage T1 Total	6←—82%←→ 8		←→18%←→3←→ 0%←→ –		
Well Differentiated Carcinoma	1	3	–	1	–
Undifferentiated Carcinoma	5	5	–	2	–
Stage T2 Total	6←—47%←→11		7←→43%←→8←→ 8%←→ 3		
Well Differentiated Carcinoma	1	2	–	2	1
Undifferentiated Carcinoma	5	9	7	6	2
Stage T3 Total	23←—54%←→11		12←→29%←→6←→17%←→11		
Well Differentiated Carcinoma	10	3	6	2	–
Undifferentiated Carcinoma	13	8	6	4	11
Stage T4 Total	4←—43%←→12		6←→29%←→5←→28%←→10		
Well Differentiated Carcinoma	1	5	1	1	4
Undifferentiated Carcinoma	3	7	5	4	6

percent. Therefore I believe that the cases in this series may be considered as being represented by three types of tumors:[4]

(a) Small, highly malignant tumors giving symptoms early and leading to the death of the patient quickly.
(b) Tumors with an average growth pattern giving symptoms later and producing a longer survival.
(c) Tumors having a very slow growth pattern and producing a considerably longer survival.

These growth patterns are not related to the histological type and seem to be an inherent biological characteristic of the primary tumor. Whether this apparently different biological potential influences the radio-response of the primary tumor is unknown,[4,6,10,12,14,15,22] nor whether it has an influence on local recurrence. However, since the patients who died rather quickly usually died from distant metastasis it may well be the case that systemic therapy is indicated in this type of tumor as opposed to those with a slower growth pattern where more concentrated therapy to the primary will be indicated. Since these different behaviors apparently influence survival it would probably mean that we are dealing with different types of tumors, each of them requiring different types of management.[6,9,17,20] Further studies are indicated to ascertain whether this is the case.*

Extent of the Primary Lesion. As seen in Table VIII the highest survival rate, 35 percent, was achieved with T-1 lesions. It dropped slightly to 29 percent for T-2 lesions which may indicate that tumors involving one or two walls of the nasopharynx have a better chance of cure.[4,5,11,17,18,21,28] Once the stage increases to T-3 the survival rate drops significantly to 22 percent. This may indicate that once the tumor spreads outside the nasopharynx into the soft tissues of the neighboring areas it probably changes its radiosensitivity and radiocurability. Furthermore, once a tumor invades bone or the CNS as in T-4 lesions the cure rate is remarkably low, five percent.[4,7,11,13,14,17–19,26,29]

* I ponder, however, whether we should move from the present type of staging classification to what I would call a biological staging classification.[4]

TABLE VII

INFLUENCE OF TIME DELAY ON SURVIVAL

	0–3	3–6	6–9	9–12	12+
Total Cases	39	42	25	22	24
Percentage/Survival	10	19	32	27	25
Well Differentiated Carcinoma	13	13	7	6	5
Percentage/Survival	15	0	28	33	20
Undifferentiated Carcinoma	26	29	18	16	19
Percentage/Survival	8	27	33	25	21

This again emphasizes that once a tumor involves bone or nervous tissue, radiosensitivity and radiocurability are so markedly decreased that this becomes the major factor preventing cure.

Lymph Node Invasion. The influence of the degree of lymph node metastasis is seen in Table IX. The highest survival rate is for N-0 and N-1 tumors, 30 and 27 percent respectively, essentially the same. It drops to 19 percent for N-2 tumors and to 15 percent for N-3 fixed lymph nodes.[4,5,11,13–17,28,29] There was no relationship between the stage of the primary and the incidence of lymph node metastasis, a fact that could also be interpreted as an independent function of the primary tumor.[5,28] However, the undifferentiated tumors produced a higher incidence of nodal metastasis, 76 percent, as compared to the well-differentiated tumors, 59 percent, a factor that indicates a greater biological potential of the undifferentiated tumors to metastasize to the lymph nodes.[4,7,15] Interesting enough, when the neck was negative, both types of tumors had about the same survival, around 30 percent, indicating the value of elective whole-neck irradiation for microscopic disease regardless of histology. But once the lymph nodes were positive, either N-1, -2, or -3, the survival was increasingly superior in the undifferentiated group, again reflecting a higher degree of sensitivity and radio-curability. The degree of lymphatic invasion thus bears a tremendous role on survival which increases with decreasing degree of nodal invasion.[5,7,11,14,17,18] The value of radiation therapy both for cure of nodal disease in the neck and prophylactically for clinically undetected microscopic disease is well beyond doubt and demands complete treatment to all the lymph node drainage stemming from the nasopharynx down to the clavicle regardless of histological type, since both types have a high lymphatic metastatic aggressiveness.[2,3,5,7,10,16–18,26,28] Since undifferentiated tumors respond better to treatment than well-differentiated types the strategy to manage them may vary depending upon their response during the course of treatment. Females seem to score better than males in N-0 and N-1 with 38 and 40 percent respectively for females and 26 and 17 percent for males. However, once we reach more advanced stages, N-2 and N-3, the survival rate is similar for both sexes. It appears that the incidence of females in this group is greater, and despite that the results are better.

Type of Local Spread. As seen in Table X there is a good relationship between survival and area of invasion, the highest, 29 percent, being when the tumor has not spread outside the nasopharynx. Tumors extending inferiorly or anteriorly to the soft tissues of the oropharynx and nose produce slightly lower survival, 23 and 17

TABLE VIII

DISTRIBUTION AND SURVIVAL ACCORDING TO THE EXTENT OF THE PRIMARY

	T1	T2	T3	T4
Male/Undifferentiated	9	20	28	17
Female/Undifferentiated	3	9	14	8
Male/Well Differentiated	5	5	12	7
Female/Well Differentiated	0	1	9	5
Total Cases	17	35	63	37
Percentage Survival	35	29	22	5
Male/Survival	29	28	17	8
Female/Survival	61	33	30	0
Well Differentiated/Survival	0	33	24	0
Undifferentiated/Survival	50	28	21	8

percent, respectively. On the other hand, tumors breaking through the boundaries of the lateral wall into the parapharyngeal fossa have a survival of only eight percent. Equally ominous is the spread superiorly to the base of the skull, either with bone or CNS involvement.[4,7,17,25] This adverse influence on survival demands a review of the strategical management of these tumors with a very accurate and thorough delineation of the real extent of the tumor which frequently excapes us due to their submucosal manner of spreading.[4,7,25]

Distant Metastasis. As seen in Table XI, of the total patient population, five or 3.3 percent presented with distant metastasis when first seen. All were undifferentiated carcinomas indicating a great biological potential to metastasize. The influence of distant metastasis on survival is spectacular, and no patient survived more than six months after diagnosis.[7,11]

Histological Grading. The influence of histological grading was apparent in several instances. According to age group all the tumors in patients below 20 years of age were undifferentiated with a total of 14 percent. From then to the 5th decade the ratio of undifferentiated to well-differentiated carcinomas remains constant. Interestingly enough, from then onward the reverse takes place and the established ratio does not hold any longer. This difference in histological grading is reflected in the results, and the survival rate was lower in the 6th and 7th decades, around 20 percent where the majority were well-differentiated tumors, while the highest survival, 43 percent, was in the 4th decade. The undifferentiated tumors have a higher survival, 45 percent, in this age group than the well-differentiated, 33 percent. No patient below the age of 20 survived,[23] although all of them had undifferentiated tumors. The reason for both this type of distribution and survival is not understood, but it may be that either defense mecha-

TABLE IX

DISTRIBUTION AND SURVIVAL ACCORDING TO LYMPH NODE INVASION

	No	N1	N2	N3
Male/Well Differentiated	11	3	5	10
Male/Undifferentiated	16	3	21	34
Female/Well Differentiated	7	2	1	5
Female/Undifferentiated	9	3	10	12
Total Cases	43	11	37	61
Percentage Survival	30	27	19	15
Male/Survival	26	17	23	14
Female/Survival	38	40	9	18
Well Differentiated/Survival	28	20	0	6
Undifferentiated/Survival	32	33	22	17

TABLE X

DISTRIBUTION AND INFLUENCE OF THE TYPE OF SPREAD ON SURVIVAL

	1*	2*	3*	4*	No Area
Male/Well Differentiated Carcinoma	7	6	7	6	10
Male/Undifferentiated Carcinoma	9	25	14	10	31
Female/Well Differentiated Carcinoma	5	6	5	3	1
Female/Undifferentiated Carcinoma	4	6	10	7	14
Total Cases	25	43	36	26	55
Percentage Distribution	16.4	28.3	23.7	17%	36.2
Percentage/Survival	8	23	17	8%	29
Well/Differentiated Carcinoma	12	12	12	9	11
Percentage/Survival	0	42	8	0	18
Undifferentiated Carcinoma	13	31	24	17	45
Percentage/Survival	15	16	21	12	31

* 1—Superior spread to base of skull; 2—Inferior spread to oropharynx; 3—Anterior spread to nose; 4—Parapharyngeal fossa.

Table XI

DISTRIBUTION AND SURVIVAL ACCORDING TO METASTATIC INVOLVEMENT

	Mo	M1
Male/Well Differentiated Carcinoma	29	—
Male/Undifferentiated Carcinoma	69	5
Female/Well Differentiated Carcinoma	15	—
Female/Undifferentiated Carcinoma	34	—
Total Cases	147	5
Percentage	96.7	3.3
Male	98	5
Percent of Total	95.1	4.9
Female	49	—
Percent of Total	100.0	0.0
Well Differentiated Carcinoma	44	—
Percent of Total	100.0	0.0
Undifferentiated Carcinoma	103	5
Percent of Total	95.4	4.6
Percentage Survival	0%	

nisms, etiological factors, or both, play different roles in different age groups (Table III).

Regarding the presenting symptoms there is a remarkable preponderance of undifferentiated carcinomas, the ratio being 4.8:1, almost twice as many in the group of patients who had lymph nodes in the neck as the first manifestation of the disease reflecting, of course, a higher lymphatic metastatic power. The over-all incidence of patients presenting with lymph nodes in the neck was 15.1 percent and the survival rate in this group was higher, 37 percent in the undifferentiated tumors *versus* 25 percent in the well-differentiated. Equally important, the undifferentiated tumors had a higher survival, 30 percent, than the well-differentiated ones, six percent, in the group presenting with nasal symptoms. On the other hand there was no difference in survival between the two types of tumors in the group of patients presenting with either bone or CNS involvement (Table IV).

In relationship to the time-delay, 52 percent of all tumors presented during the first six months without relation to grading or sex. After the first six months there is an increase in the ratio of females presenting with increased delay.[4] Whether women seek medical advice later than men or that their tumors are slower in growth giving rise to symptoms later cannot be determined from this study (Table VI). The influence of grading on survival according to the time-delay points to a very interesting finding. The lower survival, eight percent, was in the undifferentiated tumors with time-delay of less than three months *versus* 15 percent in the well-differentiated tumors. Both tumors, however, show the lowest survival in this time-delay group. These tumors obviously represent highly malignant neoplasms in general, regardless of histology. The influence of grading is less in the remaining groups where the survival is roughly the same, around 30 percent. This finding indicates perhaps that they are slower growing tumors regardless of their grading and therefore the behavior of the primary is an innate characteristic of the tumor (Table VII).

In relationship to the distribution by extent of the primary there is no significant difference either stage by stage or by sex. One would expect that the proportion of undifferentiated tumors would be greater as the extent of the primary grows bigger as an expression of rapid growth. However, this is not the case. Again it appears that the local behavior of the primary tumor and its growth are innate biological characteristics independent of the grading. The influence of grading on survival according to the extent of the primary shows that undifferentiated carcinomas have the higher survival, 50 percent, of Stage 1 tumors, *versus* 0 percent for well-differentiated carcinomas. From then on, as the stage of the primary increases the survival drops to 28 percent for T-2 and 21 percent for T-3, more or less equal to the well-differentiated

tumors, indicating that the response of the primary is independent of the grading as the local extent increases. No patient with bone or CNS involvement in the well-differentiated group survived five years, but eight percent with undifferentiated tumors survived in that group. Undifferentiated tumors have a higher sensitivity and radiocurability which are functions of the extent of the tumor: the smaller the tumor the higher the probability of local control. The treatment dose should be determined by both the new host-tissue (bone, CNS, cartilage, etc.) and the tumor size (Table VIII).

Regarding the influence of grading on lymph node invasion, the highest incidence of negative lymph nodes was in the well-differentiated group, 40.9 percent *versus* 23.1 percent in the undifferentiated group. Therefore, the reciprocal is also true, that well-differentiated tumors have a lower lymphatic metastatic power. This different behavior remains so when the lymph nodes are positive with either bilateral or fixed lymph nodes, since the incidence of undifferentiated tumors is 28.7 percent for N-2 and 42.6 percent for N-3 *versus* 13.6 percent and 34.1 percent respectively for well-differentiated carcinomas. It seems therefore, that the higher the degree of malignancy of the primary tumor the higher the degree of lymphatic invasion. This apparent difference between the local biological behavior of the primary and its potential to metastasize to the regional lymph nodes cannot be explained from this study. The influence of grading on survival according to lymph node involvement shows that when the neck is negative, N-0, both types of tumors have approximately the same survival around 30 percent. Once the lymph nodes are positive, however, there is a remarkable difference in survival between the two groups. For the undifferentiated tumors the survival for N-1, N-2, N-3 is 33, 22, and 17 percent respectively *versus* 20, 0, and six percent for the well-differentiated group tumors. The treatment of choice for nodal disease is radiation therapy, but well-differentiated tumors may require different management (Table IX). It was found that 3.3 percent of the cases did show distant metastasis when first seen and all of them were undifferentiated tumors in males. One must, therefore, be very cautious when dealing with undifferentiated tumors since besides the treatment to the primary the possibility of systemic therapy either to prevent or delay the appearance of distant metastasis could be entertained (Table XI).

In relation to the direct mode of spread of the primary tumor it is interesting to observe that well-differentiated carcinomas had a higher incidence of spread superiorly to the base of the skull, 27.3 percent, *versus* twelve percent for undifferentiated carcinomas. It seems that well-differentiated tumors have, therefore, a higher tendency to search for bone and CNS invasion while undifferentiated carcinomas have a higher tendency to spread along soft tissues.[4,5,25] This finding should also be seriously considered when treating either type of carcinoma of the nasopharynx. The relationship between grading and survival according to invasion areas shows that undifferentiated carcinomas spreading superiorly to the base of the skull, anteriorly to the nose, and laterally to the parapharyngeal fossa have a higher survival, 15, 21, and twelve percent respectively *versus* 0, eight, and 0 percent for well-differentiated tumors. Once again we encounter the difference in behavior and survival that I have alluded to before. Although undifferentiated tumors respond better when they have spread to the soft tissue of the neighboring areas, when they spread to the oropharynx they have a lower survival, 16 percent *versus* 42 percent for the well-differentiated tumors. The interpretation of these results lies in the fact that undifferentiated carcinomas although more radiosensitive and radio-curable tend to spread submucosally in such an inconspicuous way that they mislead the observer when assessing the true extent of the tumor (Table X).

Relating grade to the over-all five year

survival, it is seen in Table XII that undifferentiated carcinomas have an over-all[4,19] survival of 23 percent *versus* 15 percent for the well-differentiated tumors.

Table XII

OVER-ALL SURVIVAL OF PATIENTS IN YEARS

	5 Years
Male/Well Differentiated Carcinoma	3
Male/Undifferentiated Carcinoma	18
Female/Well Differentiated Carcinoma	4
Female/Undifferentiated Carcinoma	7
Total Cases	32
Percentage Survival	21%
Well Differentiated/Survival	15%
Undifferentiated/Survival	23%

RECURRENCE

Recurrence in the Nasopharynx. Eighty-three percent of all recurrences appeared within three years after initial treatment.[5,11,18] There was no relationship with sex, time-delay, status of the lymph nodes, or with age group as such. Regarding the presenting symptoms, patients presenting with bone or CNS invasion had the highest recurrence rate, 69 percent, as compared with the other groups with around 31 percent.[4,5,7,11,13,14,17,18] Insofar as the site of the primary was concerned, the highest incidence of recurrence, 51 percent, was for tumors arising in the postero-superior wall as opposed to around 18 percent for the other groups.[4] According to extent of the primary, the incidence of recurrence was higher with increasing extent of the primary, from 15 percent for T-1 to 60 percent for T-4.[5,7,11,13] However, this rate of recurrence is not exponential and it seems that it is rather unpredictable. Regarding the type of local spread, the highest incidence, 74 percent, was for those tumors spreading superiorly to the base of the skull followed by the tumors spreading to the parapharyngeal fossa, 42 percent, and then the oropharynx, 36 percent. According to histology, well-differentiated tumors had the highest incidence of recurrence, 68 percent, *versus* 41 percent for undifferentiated tumors in all stages.[5] Regarding the dose in rets, I had the opportunity to compare primary tumor control over a wide dose range (Table XIII). In general the following facts emerged (Fig. 1):

(1) The lower the dose the higher the incidence of local recurrence.
(2) The lower the dose the earlier the recurrence.
(3) Below 1,600 rets, there was no control of the primary.
(4) The NSD did not show good consistency regarding cure since even at very high doses failure[5,11,13,17,18] occurred (Fig. 1), but the general impression is that the higher the stage the higher the dose required in order to achieve cure.

Lymph Node Recurrence. Eighty-seven percent of all lymph node recurrence appeared within the first two years after initial treatment.[5] There was no relationship with sex, site of the primary, or extent of the primary, indicating the independent behavior of both primary and lymph node. There was also no relationship to the type of spread of the primary, the presenting symptoms, time-delay, or age group. Regarding histology, the well-differentiated tumors had a higher incidence of recurrence, 38 percent as opposed to eleven percent for undifferentiated tumors. A very important relationship existed between nodal recurrence and extent of lymphatic invasion at the start of treatment, the incidence of recurrence increasing with increasing initial nodal stage from eleven percent for N-1 to 52 percent for N-3.[5,7,11,14,17,28] Also an important relationship existed between dose and recurrence. Comparing the effect over a broad dose range the following facts emerged (Fig. 2):

(1) The lower the dose the higher the incidence of nodal recurrence.
(2) The lower the dose the earlier the nodal recurrence.

Table XIII

DISTRIBUTION OF CASES ACCORDING TO ENERGY AND TUMOR DOSE (IN RADS)

Energy	2–3,000	3–4,000	4–5,000	5–6,000	6–7,000	Total
HVT*	7	15	38	39	14	113=74%
SVT†	1	0	2	14	22	39=26%

* HVT—High voltage therapy=220 kv, 1.5 mm Cu half-value layer. † SVT—Supervoltage therapy=either Co60 teletherapy or 2 mev roentgen therapy.

(3) Below 1,400 rets, there was no control of nodal disease.
(4) The NSD did show that for N-0 tumors doses between 1,500–1,700 rets are effective for 100 percent control.
(5) The higher the degree of nodal invasion, the higher the dose required to achieve cure.
(6) Well differentiated tumors seem to require higher dose than undifferentiated ones.

Technique of Irradiation. Given the characteristics of this tumor it is understandable that the accuracy of the treatment technique plays a very important role in cure. Failure to assess the true extent of the tumor properly will obviously result in recurrence.[18]

Complications. The complications were related only to the extent of the primary, the extent of nodal disease, and the dose. Regarding the primary tumor the major complications were one case of brain necrosis (Stage IV) treated with over 2,000 rets, and one case of conduction deafness due to fibrosis in the space surrounding the levator palati muscle with partial

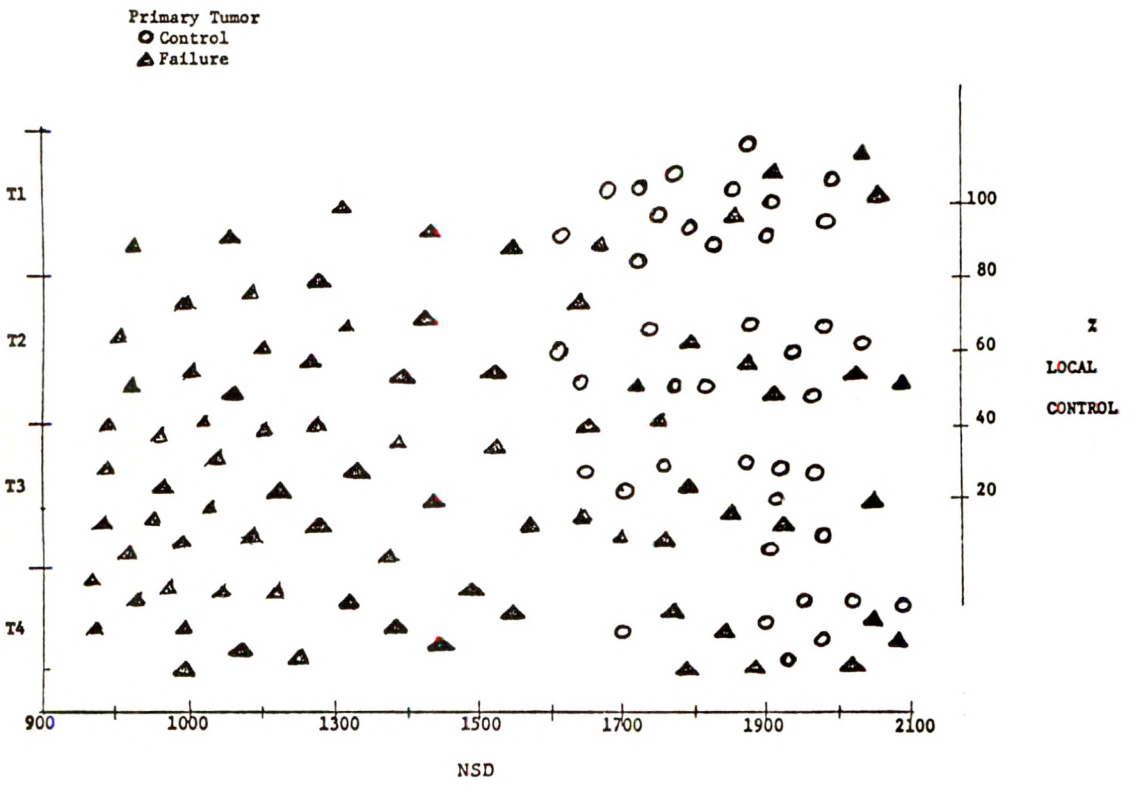


Fig. 1. Probability of local tumor control *versus* NSD.

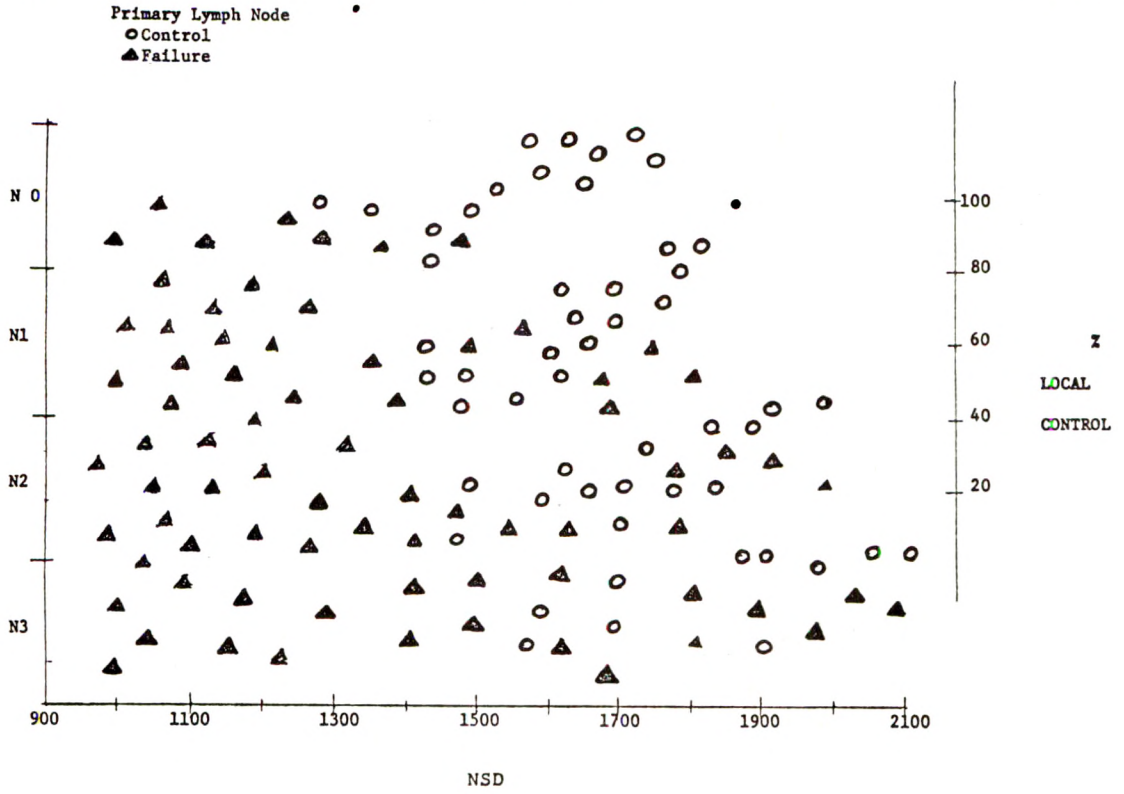


Fig. 2. Probability of local tumor control *versus* NSD.

fixation of the soft palate. Minor complications like xerostomia increased in severity and percentage as the dose increased as did varying degrees of ankylosis of the temporomandibular joints. Since most of these patients (Table XIII) were treated for palliation only and mostly with orthovoltage, the incidence of complications is probably low. Complications in the neck were mostly related to the degree of nodal invasion, the histology of the tumor and the dose. The incidence of complications rose from 0 percent for N-0 to ten percent for N-2 and were mostly in the form of fibrosis in the subcutaneous tissues. In N-3 the incidence rose to 17 percent and was mostly associated with high dosage given in the form of either a boost dose to a smaller area or a permanent or temporary implant. In the majority of these cases the tumor was well-differentiated.

DISCUSSION

Trying to compare the results of different reports is often very difficult since it is not clear in all of them what were the criteria used for staging or for eligibility for radical treatment, so that some element of selection of patients might favorably influence the results.[19] Other inconsistencies are different staging classifications[26] and inclusion of cases treated with both orthovoltage and supervoltage, as in this series.[3,4,9,18]

The five year survival according to stage related to nodal invasion (Table XIV) shows that at one end of the spectrum for T-1 N-0 lesions the survival is 66 percent and at the other end T-4 N-0 the survival is 0. For T-1 N-2 the survival is still good, 60 percent, and for T-4 N-2 is still 0. With similar nodal invasion, the survival is a function of the stage of the primary. Nodal disease is more easily dealt with.[4]

CONCLUSIONS

Survival seems to be higher in adults, and lowest below the age of 20 years. It is also higher in those patients who had

TABLE XIV

>5 YEAR SURVIVAL ACCORDING TO STAGE RELATED TO LYMPH NODE INVASION

Primary \ Node	No	N1	N2	N3	Total
T1	2/3 (66%)	0/0	3/5 (60%)	1/9 (11%)	6/17 (35%)
T2	4/10 (40%)	2/3 (66%)	3/8 (37%)	1/14 (7%)	10/35 (28%)
T3	7/17 (41%)	1/5 (20%)	1/16 (6%)	5/24 (20%)	14/63 (22%)
T4	0/13 (0%)	0/3 (0%)	0/8 (0%)	2/13 (15%)	2/37 (5%)
Total	13/43 (30%)	3/11 (27%)	7/37 (18%)	9/60 (15%)	32/152 (21%)

nodal disease as a presenting symptom. Undifferentiated tumors respond better than well-differentiated ones. Spread to bone or to the central nervous system carries a poor prognosis, as does a primary arising on the postero-superior wall of the nasopharynx. Whole neck irradiation is mandatory. Response of the tumor depends on innate biological characteristics which seem to be independent of grading, either histologic or clinical. Treatment to the primary lesion should be at least 1,600 rets. Tailor the treatment strategy to the biological potential of the individual tumor. The final dose should be determined by the tumor extent, histological grade and the new host-tissue tolerance.

Department of Radiotherapy
Downstate Medical Center
State University of New York
Brooklyn, New York 11203

I am deeply indebted to Dr. Manuel Lederman for letting me analyze this part of his cases. Many thanks to Miss Joan Merton for her valuable help on the Medical Physics part of this paper.

REFERENCES

1. Baclesse, F. Roentgentherapy in Cancer of Hypopharynx. *J.A.M.A.*, 1949, *140*, 525–530.
2. Bagshaw, M. A., and Thompson, R. W. Elective irradiation of neck in patients with primary carcinoma of head and neck. *J.A.M.A.*, 1971, *217*.
3. Berger, D. S., Fletcher, G. H., Lindberg, R. B., and Jesse, R. H., Jr. Elective irradiation of neck lymphatics for squamous cell carcinomas of nasopharynx and oropharynx. Am. J. Roentgenol., Rad. Therapy & Nuclear Med., 1971, *111*.
4. Bohorquez, J. F. Influence of relationship "Local Tumor Extent-Time" upon evolution of tumors of nasopharynx. Am. J. Roentgenol., Rad. Therapy & Nuclear Med., 1969, *105*.
5. Chen, Kuang Y., and Fletcher, G. H. Malignant tumors of nasopharynx. *Radiology*, 1971, *99*, 165–171.
6. Einhorn, N., Henle, G., Henle, W., Klein, G., and Clifford, P. Effect of local radiotherapy on antibody levels against EBV-induced early in capsid antigens (EA and VCA) in patients with certain malignant tumours. *Internat. J. Cancer.*, 1972, *9*, 182–192.
7. Fletcher, G. H., and Million, R. R. Malignant tumors of nasopharynx. Am. J. Roentgenol., Rad. Therapy & Nuclear Med., 1965, *93*, 44–55.
8. Holsti, L. Clinical experience with split-course radiotherapy. *Radiology*, 1969, *92*, 591–596.
9. Lederman, M. Megavoltage advances *vs.* orthovoltage era. *J.A.M.A.*, 1972, *220*.
10. Lederman, M. Cancer of nasopharynx, its natural history and treatment. Charles C Thomas, Publisher, Springfield, Illinois, 1961.
11. Little, J. B., Schulz, M. D., and Wang, C. C. Radiation therapy for cancer of nasopharynx. *A.M.A. Arch. Otolaryng.*, 1963, *77*, 621–624.
12. Loring, M. Malignant tumors of nasopharynx. Am. J. Roentgenol., Rad. Therapy & Nuclear Med., 1965, *93*, 36–43.
13. Matar, J. H., McCarten, A. B. Carcinoma of tonsil and nasopharynx. Am. J. Roentgenol.,

Rad. Therapy & Nuclear Med., 1973, *117*, 517–525.
14. Meyer, J. E., and Wang, C. C. Carcinoma of nasopharynx. *Radiology*, 1971, *100*, 385–388.
15. Million, R. R., Fletcher, G. H., and Jesse, R. H. Evaluation of elective irradiation of neck for squamous-cell carcinoma of nasopharynx, tonsillar fossa, and base of tongue. *Radiology*, 1963, *80*, 973–988.
16. Million, R. R. Management of neck node metastases. *J.A.M.A.*, 1972, *220*, 402–405.
17. Moench, H. C., and Phillips, T. L. Carcinoma of nasopharynx. *Am. J. Surg.*, 1972, *124*, 515–518.
18. Perez, C. A., Ackerman, L. V., Mill, W. B., Ogura, J. H., and Powers, W. E. Cancer of nasopharynx. *Cancer*, 1969, *24*.
19. Peters, L. J. Enigma of nasopharyngeal cancer, selective review incorporating local experience. *Australasian radiology*, 1971, *15*, 123–130.
20. Scanlon, P. W. Split dose radiotherapy. *J.A.M.A.*, 1972, *220*, 400–401.
21. Schnohr, P. Survival rates of nasopharyngeal cancer in California. *Cancer*, 1970, *25*, 1099–1106.
22. Schryver, A., and Epstein, Barr. Virus-associated patterns in cancer of post-nasal space. *Clinical experimental immunology*, 1969, *5*, 443–459.
23. Straka, J. A., and Bluestone, D. C. Nasopharyngeal malignancies in children. *Laryngoscope*, 1972, *82*, 807–816.
24. Svoboda, D. Ultrastructure of nasopharyngeal carcinomas in American and Chinese patients. *Exp. Molec. Path.*, 1965, *4*, 189.
25. Teoh, T. B. Epidermoid carcinoma of nasopharynx among Chinese: study of thirty-one necropsies. *J. Path. Bact.*, 1957, *73*, 451–471.
26. Thompson, R. W., Scotte Doggett, R. L., and Bagshaw, M. A. Ten year experience with linear accelerator irradiation of cancer of nasopharynx. *Radiology*, 1970, *97*, 149–155.
27. Wang, C. Management of locally recurrent carcinoma of nasopharynx. *Radiology*, 1966, *86*, 900–903.
28. Wang, C. C., and Meyer, J. E. Radiotherapeutic management of carcinoma of nasopharynx. *Cancer*, 1971, *28*, 566–570.
29. Yeh, Shu. Histological classification of carcinomas of nasopharynx with critical review to existence of lymphoepitheliomas. *Cancer*, 1962, *15*, 895–920.

VOL. 126, No. 4

DEFINITIVE TREATMENT OF CARCINOMA OF THE RECTUM BY INTRACAVITARY RADIATION THERAPY*

By GWYNN JELDEN, M.D., RANJIT DHALIWAL, M.D., ANTONIO RODRIGUEZ-ANTUNEZ, M.D., EDWARD CHERNAK, B.S., R. TURNBULL, M.D., VICTOR FAZIO, M.D., *and* FRANK WEAKLEY, M.D.
CLEVELAND, OHIO

ABSTRACT:

A combination of external and contact irradiation treatment has been used successfully in treatment of selected patients with carcinoma of the rectum. The advantages include eliminating a permanent colostomy. If the treatment is unsuccessful in controlling the lesion, electrocoagulation and abdominoperineal resection are still available.

THE published results by Jean Papillon[4–6] utilizing intra-cavitary contact radiation therapy in the treatment of early carcinoma of the rectum has provoked considerable controversy. Stimulated by the results in our clinic by Crile and Turbull[1] with local electrocoagulation of early carcinomas of the rectum, we decided to start a trial program utilizing intracavitary irradiation.

In almost all hospitals throughout the world the accepted definitive treatment for carcinoma of the rectum has been primary radical surgery despite the size of the tumor. The primary reason that surgery is the accepted treatment modality is the unknown status of lymph nodes that may contain potential metastatic disease.

However, there is a highly select group of patients who may have small cancers in the range of 3.0 cm, may have medical contraindications for surgery, may be elderly, or may flatly refuse to accept the lifetime inconveniences secondary to a radical surgical procedure.

An alternate method in highly selected small cancers is local intra-cavitary radiation therapy with a Phillips contact unit. Since the status of regional lymph nodes is still unknown we have combined intracavitary local contact therapy with external regional therapy. In a study by Dukes and Bussey[2] in patients with small superficial carcinomas with no local spread clinically, 14.2 percent had positive lymph nodes. In a controlled study Kleigerman *et al.*,[3] using preoperative external radiation therapy, reduced the number of expected positive lymph nodes by one half. Therefore we feel that a combination of radiation therapy modalities is justified.

TECHNIQUE

Our method of delivering external radiation therapy utilizes a 10 mev linear accelerator. We deliver 2,400 rads in three days through two 45° posterior oblique ports using 45° wedges. There is a homogeneous isodose distribution to the rectum and adjacent anatomy. Using the Ellis formula, 2,400 rads in three days is equivalent to 1,632 rets as compared to 1,560 rets for 5,000 rads protracted over five weeks. Clinical regression of tumor bulk has been observed using this method and in several instances over the past few years complete tumor regression has also been observed.

After external therapy, three to four weeks are allowed for tumor regression and improvement of any radiation proctitis before contact therapy is applied. Despite often dramatic reduction in tumor size, we

* Presented at the Seventy-sixth Annual Meeting of the American Roentgen Ray Society, Atlanta, Georgia, September 30–October 3, 1975.
From the Department of Radiation Therapy, Cleveland Clinic, The Clinic Center, Cleveland, Ohio.

feel that the pre-treatment size criterion of 3.0 cm should be strictly adhered to for the combination treatment. No attempt is made to treat larger carcinomas by this program.

Contact therapy is then applied with a Phillips contact unit. The contact unit has an energy of 50 kv, and an output of 1,000 rads/min at 1.0 cm, and the roentgen tube is small enough to fit into a special rectoscope. Approximately 90 percent of the radiation is absorbed within 3.0 cm of tissue. The tumor is evaluated by digital examination to determine consistency and mobility, and by direct observation through a rectoscope. The diameter of the treatment cone is 3.0 cm. After precise localization, the roentgen tube is inserted into the rectoscope. Each treatment delivers a dose of 3,000 to 4,000 rads per treatment. Tumors treated by this method should be in the terminal 10.0 cm of the rectum.

Patients have ordinarily required caudal anesthesia. The treatment can be done with an "in and out" hospital admission. The treatment is repeated in 10 to 14 days following the progressive clinical regression of carcinoma. The total dose required to irradicate a rectal carcinoma is in the range of 8,000 to 15,000 rads.

Corresponding to the finding of Papillon,[4,5] polypoid, well to moderately differentiated carcinomas are the best responding tumors. From our surgical colleagues' view point the primary advantage of local contact radiation therapy over electrocoagulation is that there is less stricture formation. Also there is less muscle destruction, particularly on low lying lesions which cause debilitating pain. The rectal wall after treatment usually demonstrates fibrotic scars which occasionally have telangiectasis that may cause minimal bleeding.

RESULTS

In starting a trial program the problems of patient selection are evident. Over the past one and a half years we have treated a total of nine patients with this technique. We have divided our patients into two groups.

GROUP I. Radiation only. In this group five cases have been treated with radiation only using the combination of external and intra-cavitary therapy. Three of these patients are free of disease ten, eleven, and twelve months after completion of treatment.

Two patients were never free of tumor despite the treatment. Both patients had ulcerative rather than polypoid lesions. One had an abdominoperineal resection and was found to have extension beyond the area of contact therapy. The other patient had electrocoagulation.

GROUP II. Electrocoagulation and Radiation. In this group there are four cases in which electrocoagulation was combined with radiation. Radiation therapy was instituted when local recurrence after electrocoagulation became evident. Three patients are free of disease nine, ten, and twelve months after completion of treatment.

One additional patient failed to have tumor control despite the combination of electrocoagulation and radiation therapy and therefore underwent an abdominoperineal resection.

CONCLUSION

In conclusion, this type of local conservative treatment for small carcinomas of the rectum appears to be a promising means of controlling this disease. We feel that this conservative treatment in no way jeopardizes the life of the patient provided there is close follow-up and good cooperation between colon and rectal surgeons and therapeutic radiologists. At any time if there is evidence of failure by progression of disease radical surgery can be carried out.

We realize that our follow-up time is very short but believe that in a selected group of patients definitive treatment can be offered preventing the lifetime inconveniences of a permanent colostomy.

Gwynn L. Jelden, M.D.
Department of Radiation Therapy
9500 Euclid Avenue
Cleveland, Ohio 44106

REFERENCES

1. Crile, G., and Turnbull, R. Role of electrocoagulation in treatment of carcinoma of rectum. *Surg., Gynec. & Obst.*, 1972, *135*, 391–396.
2. Dukes, C. E., and Bussey, H. J. R. Spread of rectal cancer and its effect on prognosis. *Brit. J. Cancer*, 1958, *12*, 309–320.
3. Kleigerman, M., Urdaneta, N., Knowlton, A., Vidone, R., Hartman, P. U., and Vera, R. Preoperative irradiation of rectosigmoid carcinoma including its regional lymph nodes. Am. J. Roentgenol., Rad. Therapy & Nuclear Med., 1972, *114*, 498–503.
4. Papillon, J. Endocavitary irradiation of early rectal cancers for cure: series of 123 cases. *Proc. Roy. Soc. Med.*, 1973, *66*, 1179–1181.
5. Papillon, J. Endocavitary irradiation in curative treatment of early rectal cancers. *Dis. Colon & Rect.*, 1974, *17*, 172–180.
6. Papillon, J. Resectable rectal cancers: treatment by curative endocavitary irradiation. *J.A.M.A.*, 1975, *231*, 1385–1387.

SERIAL STUDIES OF IMMUNOCOMPETENCE IN HEAD AND NECK CANCER PATIENTS UNDERGOING RADIATION THERAPY*

By STEFANO STEFANI, M.D.,† RONALD KERMAN, Ph.D.,‡ *and* JOSEPH ABBATE, M.D.§
HINES AND CHICAGO, ILLINOIS

ABSTRACT:

Studies of the immunocompetence of patients undergoing radiation therapy were carried out before and after treatment. The immunological evaluation is a valuable prognostic tool for patients with squamous cell carcinomas of the head and neck. The degree of immunoresponsiveness is not related to the stage of the primary tumor, but it definitely correlates with the extent of lymph node involvement. This evaluation may permit identification of those cases for which immunotherapy is indicated.

IMMUNITY may play an important role in the development of human cancers. According to some reports,[10,14,24] patients with lymphoproliferative malignancies have impaired delayed hypersensitivity responses and defects in lymphocyte function as measured by *in vitro* assays. Furthermore, this impairment seems to increase with the progression of the disease. Hersh *et al.*[12] found strong correlation between pre-therapy immunocompetence and prognosis in acute leukemia.

The results of immunologic evaluation of patients with solid tumors are more varied and provide no clear correlation between patient immunity and prognosis. While Eilber and Morton[7] report impaired non-specific immunity in such patients, Catalona *et al.*[4] found that lymphocytes from patients with solid tumors have depressed responses to mitogenic challenge, other studies failed to show any such impairment in similar cases.[19,21]

Delayed hypersensitivity has usually been measured by the patient's response to common microbial skin test antigens and to *de novo* antigens such as dinitrochlorobenzene (DNCB). Recently, evaluation of peripheral blood lymphocytes forming rosettes with sensitized or unsensitized sheep red blood cells (SRBC) has been added.[20,23] These rosette-forming cells (RFC) are thought to represent thymus-derived lymphocytes (T cells) and bone marrow-derived lymphocytes (B cells), and their number has been correlated with host immunocompetence.[25,27]

In the present study, we evaluated the immune competence of patients with head and neck cancers before and at various intervals after radiation therapy. We tested the patients with a battery of five microbial skin-test antigens and DNCB, and determined the total T and B-RFC lymphocytes in their peripheral blood. Correlations were made between the test responses and patient survival.

MATERIAL AND METHOD

PATIENTS

We studied 29 male patients who had been referred to the Therapeutic Radiology Service with confirmed malignancies of head and neck. They ranged in age from

* Presented in part at the Fifty-seventh Annual Meeting of the American Radium Society, Isla Verde, Puerto Rico, May 4–9, 1975.
From the Therapeutic Radiology Service and Radiobiology Research Laboratory, Veterans Administration Hospital, Hines, Illinois, and the Radiotherapy Department, Mount Sinai Medical Center, Chicago, Illinois.
Supported in part by the Veterans Administration Project No. MRIS 8121-08 and The Harry Gleason, Jr., Research Fund.
† Chief, Therapeutic Radiology Service.
‡ Radiobiology Research Laboratory.
§ Staff Physician.

34–70 with a mean of 59 years, and had not undergone any previous therapy. None of them showed evidence of distant metastases at the time of TNM staging (UICC, 1973). The standard protocol called for 1,000 rads/wk over a period of five to seven weeks (mean 6,164 rads) from a Cobalt-60 source to the primary tumor and the regional lymph nodes. Tumors studied were squamous cell carcinomas arising from the following sites: nasopharynx (three), floor of mouth (two), alveolar ridge (two), tonsil (three), tongue (three), larynx (four), hypopharynx (nine), cervical esophagus (two), and metastatic neck lymph node with unknown primary (one).

All patients had immunologic evaluations before and 30, 90, and 180 days after radiation therapy as an integral part of the clinical assessment of their disease.

The control population consisted of 40 healthy adult men between 22 and 58 years. None of them was known to have a disease which would alter their immune responsiveness.

IMMUNOLOGIC EVALUATION

The non-specific general immunocompetence was evaluated by the following methods.

Skin-Test-Antigen Response: The antigens used were: dermatophytin (1:30), dermatophytin-o (1:100) (Hollistersteir), streptokinase-streptodornase (50 units SK) (Lederle), mumps (Eli Lilly) and intermediate-strength tuberculin antigen (Parke, Davis). All were applied by intradermal inoculation in a volume of 0.1 ml through a 27 gauge needle. We observed the reaction at 24 and 48 hours and recorded the average in millimeters of the induration measured at two right angles. Induration greater than 5 mm was considered positive and patients were considered positive responders if they reacted positively to two or more of the five antigens.

DNCB Contact Sensitivity: DNCB reactivity is measured by the spontaneous flare reaction which occurs at the site where the agent had been applied 14 days before.[5] Doses were 2,000 μg to the upper arm and 50 μg to the forearm. A flare at both sites by 14 days is scored 4+, at the 2,000 μg site only, 3+. If neither site develops a flare after 14 days, a challenge of 50 μg is applied to the opposite forearm. A cutaneous hypersensitivity reaction at this new site within 48 hours is scored 2+. An equivocal reaction which requires biopsy for confirmation counts 1+ if the histological features of delayed cutaneous hypersensitivity are present. If no such changes are seen or if no other grossly visible reaction occurs the subject is considered anergic. In practice, reactions at 3+ or 4+ are considered normal; below these values, abnormal or negative to DNCB, without further testing.[3] We adopted this alternative.

Rosette Forming Cell Assays: Freshly drawn venous blood was mixed with heparin (20 units/ml) and layered onto a Ficoll-Hypaque gradient,[1] and peripheral blood lymphocytes (PBL) were separated after centrifugation at 400×g for 40 minutes at room temperature. The PBL separated from the interface were carefully pipetted off, washed three times in Delbecco's phosphate buffered saline (PBS), pH 7.3, and brought to a final concentration of 2×10^6 PBL/ml in PBS.

SRBC were stored at 4°C in Alsevar's solution (1/1) and used within seven to ten days of delivery. They were washed twice and adjusted to a 0.5 percent suspension in PBS.

To measure the total T-RFC population, 0.25 ml (5×10^5) PBL was mixed with 0.25 ml of 0.5 percent unsensitized SRBC and centrifuged at 200×g for five minutes at room temperature and then incubated in an ice-water bath (4–8° C) for 60 minutes. After the cell pellets were gently resuspended, a drop of suspension was placed onto a hemocytometer and the number of rosettes (three or more SRBC surrounding a lymphocyte) was counted. All tests were performed in duplicate and 200 or more lymphocytes were counted to determine the percentage of total T-RFC.[13]

As a test for B-RFC, 5 ml of a five percent solution of washed unsensitized SRBC were incubated for 30 minutes at 37° C with 5 ml of rabbit anti-SRBC sera diluted 1/2,500 in PBS. The cells were washed three times and resuspended in 5 ml of PBS. Five ml of a 1/10 dilution of mouse sera were added and the suspension incubated for 30 minutes in a 37° C water bath. The sensitized SRBC were washed and adjusted to a 0.5 percent final concentration in PBS, containing 0.01 *M* Na HEDTA to inhibit rosette formation by contaminating neutrophils and monocytes.[3,13,15,22]

For the B-RFC assay, 0.25 ml (5×10^5) PBL was mixed with 0.25 ml of 0.5 percent sensitized SRBC, centrifuged at 200×g for two minutes at room temperature and then incubated for 30 minutes in a 37° C water bath. The cell pellets were resuspended by vigorous mixing and the B-RFC were counted as described before. When unsensitized SRBC were tested as controls, no or few rosettes formed.

Absolute numbers of RFC were determined by calculating the corresponding total and differential leukocyte counts. The results are reported as the mean percentage or absolute number/mm³ of RFC ± 1 standard error of the mean. The statistical differences of the groups studied were determined by comparison of the standard error of the difference between means. Individuals counting rosettes were unaware of the source of the sample, the skin test and DNCB results.

RESULTS

The findings of the skin tests are presented in Table I. Seventy-two percent of the patients reacted positively to two or more of the skin-test antigens before radiation therapy and 80 percent responded to at least one of the five agents (data not shown). The percentage of positive skin test responsiveness rose slightly 30 days after the completion of radiation therapy, but a marked decline was seen at 90 and 180 days after treatment. Only 61 percent of our patients responded positively to DNCB before radiation therapy. This responsiveness decreased markedly afterwards.

Table II shows how our patients, classed according to their clinical staging, responded to common skin test antigens and to DNCB before radiation therapy. While the degree of this responsiveness revealed no relationship to the stage of the primary tumor, it definitely correlates with the extent of lymph node involvement.

Figure 1 compares the estimated survival rates, calculated by the Kaplan-Meier formula, of patients with positive and negative responsiveness to microbial antigens before radiation therapy. The difference is statistically significant ($P<0.001$) and

TABLE I

DELAYED HYPERSENSITIVITY RESPONSES IN PATIENTS WITH HEAD AND NECK CANCERS BEFORE AND AFTER RADIATION THERAPY (RT)

Therapy Status	Microbial Antigens		DNCB	
	No. +* / No. Tested	Percent +	No. +* / No. Tested	Percent +
Before RT	21/29	72	14/23	61
30 Days Post-RT	18/22	82	9/21	43
90 Days Post-RT	9/17	53	7/14	50
180 Days Post-RT	9/15	60	6/13	46

* Positive response to 2 or more out of 5 microbial skin test antigens.

TABLE II

PRE-RADIATION THERAPY DELAYED HYPERSENSITIVITY RESPONSE TO COMMON SKIN TEST ANTIGEN AND DNCB ACCORDING TO TNM CLASSIFICATION (UICC—1973)

Staging	Skin Test Response		DNCB Response	
	No. (+)* / No. Tested	Percent	No. (+)* / No. Tested	Percent
T_{1-4}, N_{0-1} M_0	12/12	100	6/8	75
T_{1-4}, N_{2-3} M_0	7/16	44	7/14	50

* Positive response to 2/5 or more skin test antigens.

shows that patients with positive responses have a better survival. As for DNCB, our patients with positive response had a better survival rate but the difference between the two groups was not statistically significant (data not shown).

Table III compares the total T-RFC of controls and patients before and after radiation therapy. The controls had a mean percent of 63.2 and a mean absolute number of 1,745/mm³. For the cancer patients the level was significantly lower before and after therapy by both percent ($P<0.001$) and absolute number ($P<0.001$). The values after therapy were markedly lower than before, both in percent ($P<0.05$) and in absolute number ($P<0.001$).

Table IV compares the B-RFC of controls and patients before and after radiation therapy. The controls had a mean percent of 15.5 and a mean absolute number of 428/mm³. The patients had a significantly lower pre- and post-therapy level by both percent ($P<0.01$) and absolute number ($P<0.001$) than controls. The absolute numbers, but not percentage of B-RFC, decreased ($P<0.01$) after radiation therapy.

Table V shows patient survival as a function of pre-therapy absolute numbers of total T- and B-RFC. Within each of these categories the data are arranged according to their values below or above the median RFC value (874/mm³ for T-RFC and 152/mm³ for B-RFC). For both categories, patients with a total number of RFC above the median showed better survival results. According to the Kaplan-Meier formula, the difference in survival was statistically significant ($P<0.01$) for the B-RFC but not for the T-RFC.

DISCUSSION

Our findings indicate that untreated patients with head and neck cancers are less likely than normals to respond to recall microbial skin test antigens. This agrees with the study by Lundy *et al.*[16] which showed positive responses to these antigens in only 38 percent of patients with squamous cell carcinomas of head and neck. Eilber *et al.*,[8] on the other hand, reported positive responses in 63 percent of their patients, however these authors had in-

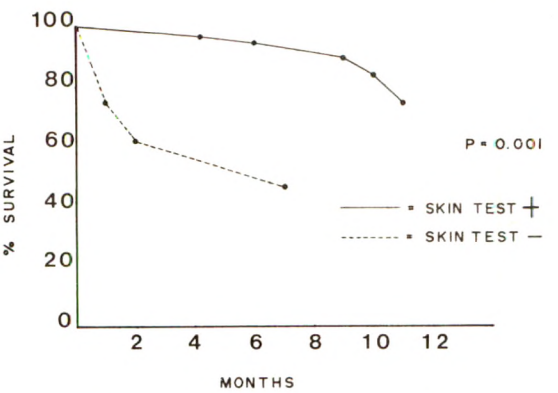


FIG. 1. Estimated survival rate (by the Kaplan-Meier formula) in patients with positive or negative skin test responses to microbial antigen.

TABLE III

TOTAL T-RFC OF HEAD NECK CANCER PATIENTS BEFORE AND AFTER RADIATION THERAPY (RT)

Group	Number	Percent Total T-RFC[a]	P[b]	Absolute No. Total T-RFC/mm³[a]	P[b]
Controls	40	63.2±1.3	——	1,745±34	——
Pre-Radiation Therapy (RT)	29	52.0±2.4[c]	<0.001	888±42[e]	<0.001
30 Days Post-RT	22	42.6±1.9[c,d]	<0.001	419±48[d,e]	<0.001
90 Days Post-RT	17	44.8±2.9[d]	<0.001	503±88[d]	<0.001
180 Days Post-RT	15	46.9±2.5[d]	<0.001	398±75[d]	<0.001

[a] Mean ±1 standard error of the mean.
[b] Significance of 2 sample (unpaired) t-test.
[c] Values differ significantly, P <0.05.
[d] Values not significantly different.
[e] Values differ significantly, P <0.001.

cluded other histologic types of primary malignancies in addition to squamous cell carcinomas.

Only 61 percent of our patients responded positively to DNCB before radiation therapy, whereas 96.5 percent of the normal controls can be sensitized to it by the method used in this study. In the study mentioned above, Eilber *et al.*[8] found positive responses in 56 percent of patients with squamous cell carcinomas of head and neck. If the spread of the disease is indeed associated with lowered responsiveness,[7,9,16] the results are rather disturbing as most head and neck cancers metastasize only to the regional lymph nodes.

Are these reactions related to the TNM stage of the disease? We have found that the response differed significantly with the extent of nodal involvement, but not of the primary tumor. One might further speculate whether the loss or reduction of cytocidal capability of the regional lymph nodes and the subsequent tumor colonization are not an indication (or perhaps the consequence?) of a compromised immune status.

Our results indicate that skin test response to microbial antigens has an excellent prognostic value, patients with pretherapy positive responses having significantly better survival than the other group. On the other hand, we could not detect a statistically significant difference with regard to DNCB response although patients reacting positively to this test did have a better survival. However, in a more extensive study, Eilber and Morton[7] found that patients with positive DNCB response had a much better survival than the others.

TABLE IV

B-RFC OF HEAD AND NECK CANCER PATIENTS BEFORE AND AFTER RADIATION THERAPY

Group	Number	Percent B-RFC[a]	P[b]	Absolute No. B-RFC/mm³[a]	P[b]
Controls	40	15.5±0.80	——	428±22	——
Pre-Radiation Therapy (RT)	29	11.7±0.90[c]	0.01	193±26[d]	0.001
30 days Post-RT	22	12.1±1.30[c]	0.01	124±24[c,d]	0.001
90 days Post-RT	17	12.7±1.70[c]	0.01	144±26[c]	0.001
180 days Post-RT	15	13.6±1.50[c]	0.01	115±23[c]	0.001

[a] Mean ±1 standard error of the mean.
[b] Significance of 2 sample (unpaired) t-test.
[c] Values not significantly different.
[d] Values differ significantly, P <0.01.

Table V

SURVIVAL AS A FUNCTION OF THE ABSOLUTE NUMBER OF TOTAL T-RFC AND B-RFC
(Follow-up: More than 6 and less than 15 months.)

	Total T-RFC*		B-RFC†	
	$<874/mm^3$	$>874/mm^3$	$<152/mm^3$	$>152/mm^3$
Alive free of disease	6	11	5	12
Alive with disease	3	0	2	1
Expired	5	3	7	1

* $874/mm^3$ = median number total T-RFC.
† $152/mm^3$ = median number B-RFC.

The percentage as well as the absolute number of T-RFC was distinctly lower in our patients than in the controls. This lends additional strength to the hypothesis that cancers in the head and neck area are associated with a depressed immunologic profile. While Potvin *et al.*[23] noted a decided drop in both percentage and absolute number of T-RFC in 22 untreated cases of squamous cell carcinoma of the head and neck, we also observed a depression of the absolute number of B-RFC in such cases, a fact that has not been previously reported. Although most other investigators show only the percentages of the total T and B-RFC, we have presented percentages and absolute numbers since we consider both as important.

The post-therapy decline in immune responsiveness we observed might have been due to the normal progression of the malignancy; we attribute it, however, to radiation-induced immunosuppression in view of the relatively short interval between irradiation and the drop in response (30–90 days). Reports on the effect of radiation therapy on the immune response are equivocal: Stjernsward *et al.*[25] and Meyer[17] observed marked and prolonged lymphopenia in their patients after local radiation therapy. Stjernsward *et al.*[25] also noted a decreased lymphocyte response to phytohemagglutinin (PHA), and reduced T-RFC and increased B-RFC following irradiation. Byfield *et al.*[2] reported a similar decrease after radiation therapy. McCredie and associates,[18] however, found an increased proliferative response of lymphocytes to PHA in patients with carcinoma of the breast or the uterine cervix. Other investigators concluded that radiation therapy did not adversely effect immune response to either microbial skin test antigens[6] or DNCB[11] in patients with cancers involving various organs.

Our study confirms that pre-therapy immunocompetence has good prognostic value in patients with malignant disease, as Hersh *et al.*[12] have also found. Patients with positive pre-therapy responses and higher numbers of total T and B-RFC evidently have a better chance for survival. An interesting question to consider is how much immunocompetence is required; for, even though patients with greater than median numbers of total T- and B-RFC showed good prognosis, many of them still had significantly lower values than the controls.

Stefano Stefani, M.D.
Therapeutic Radiology Service
Veterans Administration Hospital
Hines, Illinois 60141

We gratefully acknowledge the excellent technical assistance of Mrs. Barbara Kase and Mr. Erhard Sanders for the reading of the manuscript.

REFERENCES

1. Boyum, A. Separation of leucocytes from blood and bone marrow. *Scandinav. J. Clin. Lab. Invest.*, 1968, (Suppl 21), *97*, 77–89.
2. Byfield, P. E., Stratton, J. A., and Small, R. Lymphocyte response after radiotherapy. *Lancet*, 1974, *1*, 309.

3. Catalona, W. J., and Chretien, P. B. Abnormalities of quantitative dinitrochlorobenzene sensitization in cancer patients-correlation with tumor stage and histology. *Cancer*, 1973, *31*, 353–356.
4. Catalona, W. J., Sample, W. F., and Chretien, P. B. Lymphocyte reactivity in cancer patients: correlation with tumor histology and clinical stage. *Cancer*, 1973, *31*, 65–71.
5. Catalona, W. J., Taylor, P. T., Rabson, A. S. and Chretien, P. B. Method for dinitrochlorobenzene contact sensitization: clinico-pathological study. *New England J. Med.*, 1972, *286*, 399–402.
6. Clement, J. A., and Kramer, S. Immunocompetence in patients with solid tumors undergoing Cobalt-60 irradiation. *Cancer*, 1974, *34*, 193–196.
7. Eilber, F. R., and Morton, D. L. Impaired immunologic reactivity and recurrence following cancer surgery. *Cancer*, 1970, *25*, 362–367.
8. Eilber, F. R., Morton, D. L., and Ketcham, A. S. Immunologic abnormalities in head and neck cancer. *Am. J. Surg.*, 1974, *128*, 534.
9. Eilber, F. R., Nizza, J. A., and Morton, D. L. Sequential evolution of general immune competence in cancer patients: correlation with clinical course. *Cancer*, 1975, *35*, 660.
10. Golub, S. H., O'Connell, T. Y., and Morton, D. L. Correlation of *in vivo* and *in vitro* assays of immunocompetence in cancer patients. *Cancer Research*, 1973, *34*, 1833–1837.
11. Gross, L., Manfredi, O. L., and Protos, A. A. Effect of Cobalt-60 irradiation upon cell-mediated immunity. *Radiology*, 1973, *105*, 653–655.
12. Hersh, E. M., Whitecar, J. P., McCredie, K. B., Bodey, G. P., and Freireich, E. J. Chemotherapy, immunocompetence, immunosuppression, and prognosis in acute leukemia. *New England J. Med.*, 1971, *285*, 1211–1216.
13. Kerman, R., Smith, R., Ezdinli, E., and Stefani, S. Unification and technical aspects of total T, active T and B lymphocyte rosette assays. (Submitted for publication).
14. Lamb, D., Pilney, F., Kelley, J., and Good, R. A. Comparative study of incidence of anergy in patients with carcinoma, leukemia, Hodgkin's disease and other lymphomas. *J. Immunol.*, 1962, *89*, 555–558.
15. Lay, W. H., and Nussenzweig, V. Ca++—dependent binding of antigents-195 antibody complexes to macrophages. *J. Immunol.*, 1969, *102*, 1172–1178.
16. Lundy, J., Wanebo, H., Pinsky, C., Strong, E., and Orhgen, H. Delayed hypersensitivity reactions in patients with squamous cell cancer of head and neck. *Am. J. Surg.*, 1974, *128*, 530.
17. Meyer, K. K. Radiation-induced lymphocyte immune deficiency. *A.M.A. Arch. Surg.*, 1970, *101*, 114–121.
18. McCredie, J. A., Inch, W. R., and Sutterland, R. M. Effect of post-operative radiotherapy on peripheral blood lymphocytes in patients with carcinoma of breast. *Cancer*, 1972, *29*, 349–357.
19. Nelson, H. S. Delayed hypersensitivity in cancer patients: cutaneous and *in vitro* lymphocyte response to specific antigens. *J. Nat. Cancer Inst.*, 1969, *42*, 765–770.
20. Nemoto, T., Han, T., Minowada, J., Angkur, V., Chamberlain, A., and Dao, T. L. Cell-mediated immune status of breast cancer patients: evaluation by skin tests, lymphocyte stimulation, and counts of rosette-forming cells. *J. Nat. Cancer Inst.*, 1974, *53*, 641–645.
21. Paty, D. W., and Bone, G. Responses to P.H.A. in cancer patients. *Lancet*, 1973, *1*, 668–669.
22. Pincus, S., Bianco, C., and Nussenzweig, B. Increased proportion of complement receptor lymphocytes in peripheral blood of patients with chronic lymphocytic leukemia. *Blood*, 1972, *40*, 303–310.
23. Potvin, C., Tarpley, J. L., and Chretien, P. B. Thymus-derived lymphocytes in patients with solid malignancies. *Clin. Immunol. & Immunopathol.*, 1975, *3*, 476–481.
24. Sokal, J. E., and Aungst, C. W. Cellular immune responses and prognosis in malignant lymphoma. *Nat. Cancer Inst. Monogr.*, 1971, *34*, 109–114.
25. Stjernsward, J., Jondal, M., Vanky, F., Wigzell, H., and Sealy, R. Lymphopenia and change in distribution of human B and T lymphocytes in peripheral blood induced by irradiation for mammary carcinoma. *Lancet*, 1972, *1*, 1352–1356.
26. Wybran, J., and Fudenberg, H. H. Thymus-derived rosette-forming cells. *New England J. Med.*, 1973, *288*, 1072–1073.
27. Wybran, J., and Fudenberg, H. H. How clinically useful is T and B cell quantitation? *Ann. Int. Med.*, 1974, *80*, 765–767.

VOL. 126, NO. 4

HEMANGIOPERICYTOMA: REPORT OF THREE CASES REGARDING ROLE OF RADIATION THERAPY*

By HARBANS LAL, M.D., D.M.R.T.,† B. SANYAL, M.D.,† G. C. PANT, M.D., D.M.R.E.,† B. L. RASTOGI, M.D., D.C.P.,‡ N. N. KHANNA, M.S.,§ *and* K. N. UDUPA, M.S., F.R.C.S., F.A.C.S., F.A.M.S.§

VARANASI, INDIA

ABSTRACT:

The experience in treating three patients with hemangiopericytoma is reviewed. One patient was given irradiation alone, and the others were both treated with surgery and irradiation. Our experience reinforces reports of the usefulness of irradiation in treating this neoplasm and its metastases.

HEMANGIOPERICYTOMA was first described by Stout and Murray[8] in 1949. It has been shown to originate from Zimmerman's pericytes associated with the lumen of the blood vessels. Connective tissue silver stain shows these pericytes to be extraluminal, differentiating it from hemangioendothelioma.[7]

Reported cases indicate that the disease occurs in either sex and at all ages, although more commonly in the middle age groups. The clinical presentation varies depending upon the location of tumor, and it cannot be differentiated from other soft tissue neoplasms roentgenographically. The presence of calcification suggests angiosarcoma. Final diagnosis rests with the histopathologic examination.

The treatment of hemangiopericytoma remains controversial, since insufficient data are available from the different modalities adopted. The present cases highlight the role of radiation therapy in this disease.

REPORT OF CASES

CASE 1. S.N., a ten year old boy, came in August, 1972 with a history of progressive swelling over the left scapula of 15 months' duration (Fig. 1; and 2). Swelling started rapidly, increasing in size in two months. On examination the mass measured 15×15 cm in size with a globular shape. It was soft in consistency, non-tender, and the overlying skin was ulcerated and hemorrhagic. There was no lymphadenopathy. Roentgenography revealed a soft tissue mass (Fig. 3). Other investigations were non-contributory. Biopsy revealed malignant hemangiopericytoma (the histology will be described later). The patient was subjected to telecobalt therapy at 60 cm SSD and was

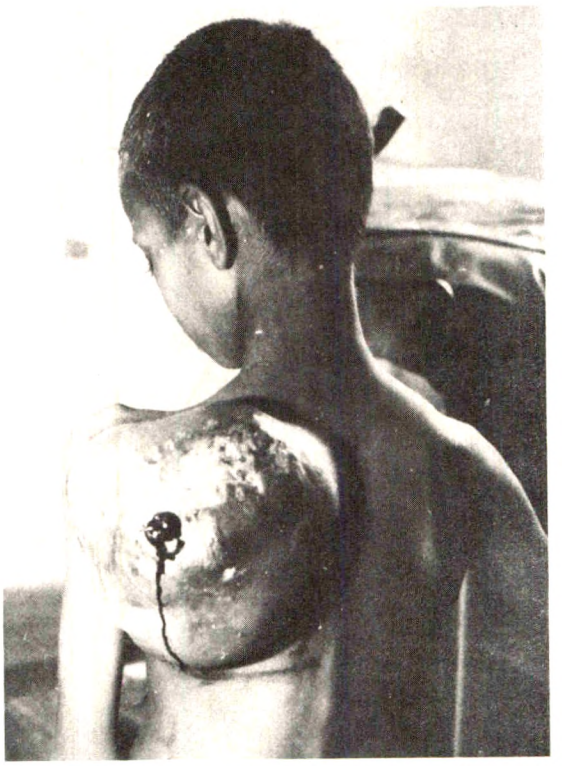


FIG. 1. Growth overlying left scapular region with area of fungation and hemorrhage. Whitish areas are produced by counter irritants applied by the untrained village healer.

* From the Departments of Radiotherapy and Radiation Medicine,† Pathology,‡ and Surgery,§ Institute of Medical Sciences, Banaras Hindu University, Varanasi-221005, India.

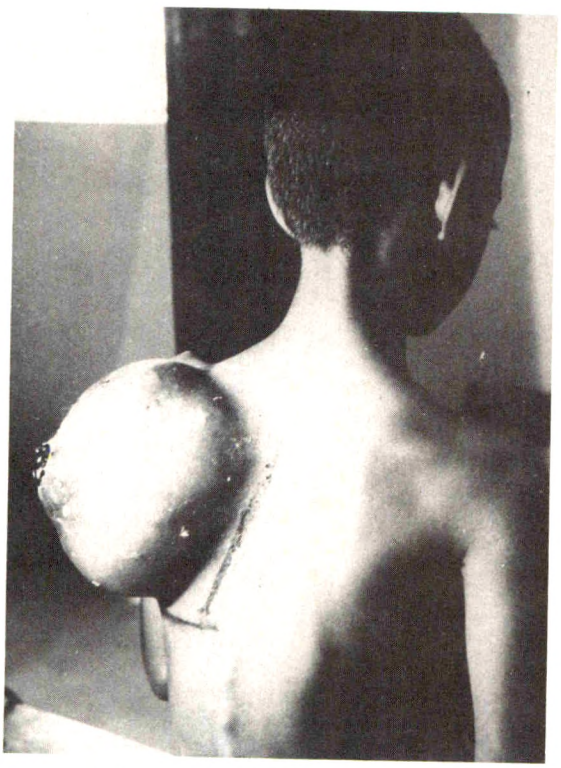


Fig. 2. Lateral view of Figure 1.

treated by two fields: medial and lateral. A tumor dose of 4,500 rads was delivered between September 8 and October 4, 1972. The tumor showed remarkable regression in size at 2,000 rads (Fig. 4–6) and the biopsy was reviewed to confirm the diagnosis. After treatment, a small area which had earlier fungated was given deep therapy at 50 cm SSD and a surface dose of 1,500 rads in five days, after which he was released for regular follow-up.

On January 5, 1974, he complained of pain in the left thigh. Roentgen study did not reveal any bony metastasis. On February 26, 1974, he presented with a lump in the suprapubic region which was hard, fixed, and non-tender. Examination now showed destruction of the pubic bone. He was given telecobalt-60 therapy to the pelvis by two parallel opposing fields and a tumor dose of 4,500 rads was given in four weeks. The lump regressed following treatment. A follow-up intravenous pyelogram performed a month later was normal. Clinically he was normal and his general condition improved. However, he again came to the hospital on June 7, 1974, with pain and swelling in the left clavicle.

A chest roentgenogram showed a large round opacity in the right lung (Fig. 7). The clavicle was irradiated with 1,000 rads in two days and the lung was treated by two parallel opposing fields to a mid-line dose of 3,000 rads between June 10 and June 27, 1974. Follow-up study showed dissolution of chest metastasis (Fig. 8). On August 2, 1974, a tender lump appeared in the right lumbar region and he was put on Cyclophosphamide 50 mgm three times a day.

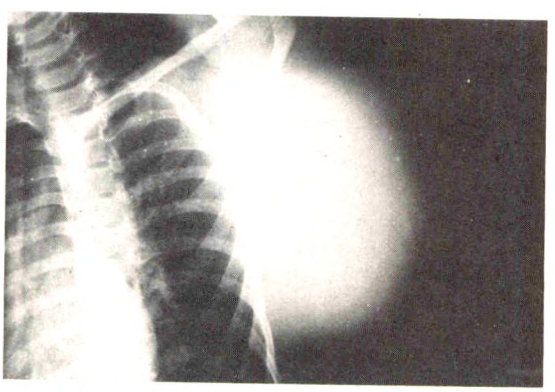


Fig. 3. Soft tissue swelling seen on roentgenogram.

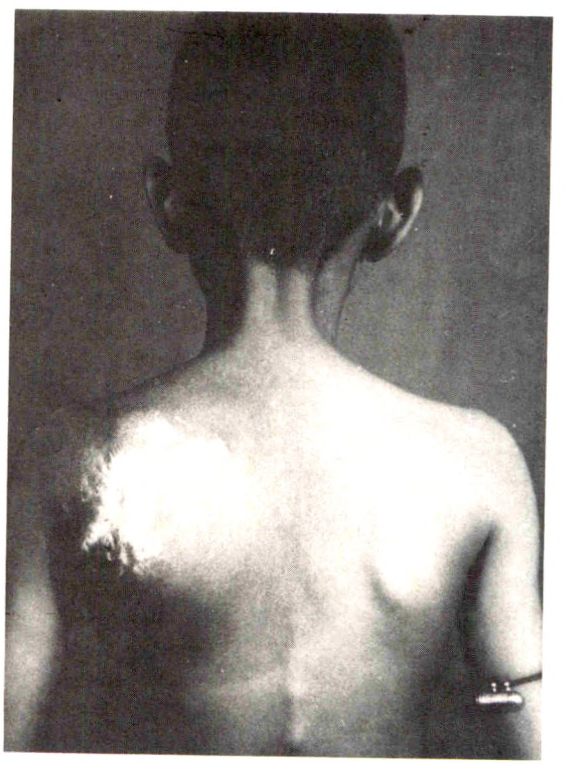


Fig. 4. Post irradiation photographs showing marked regression of tumor.

His condition has been deteriorating since November, 1974.

Case II. N.D., a 26 year old female, presented with a history of pain and a small swelling on the lateral aspect of the left thigh for three years. She was operated elsewhere and excision biopsy was reported as round cell sarcoma. Apparently well for approximately three years following surgery, she reported with a local recurrence of swelling which also was excised on June 29, 1974. She developed two nodules in the left inguinal region four months later. Excision biopsy this time from our hospital was reported as hemangiopericytoma (to be described later). She was put on radiation therapy to the lateral aspect of the left thigh. A dose of 4,000 rads was applied in three weeks time with telecobalt-60. On her last follow-up on May 22, 1975, she did not have any evidence of disease.

Case III. R.B., a 48 year old male, came with a history of progressively increasing swelling in the left axillary region of three years' duration. There was no other symptom.

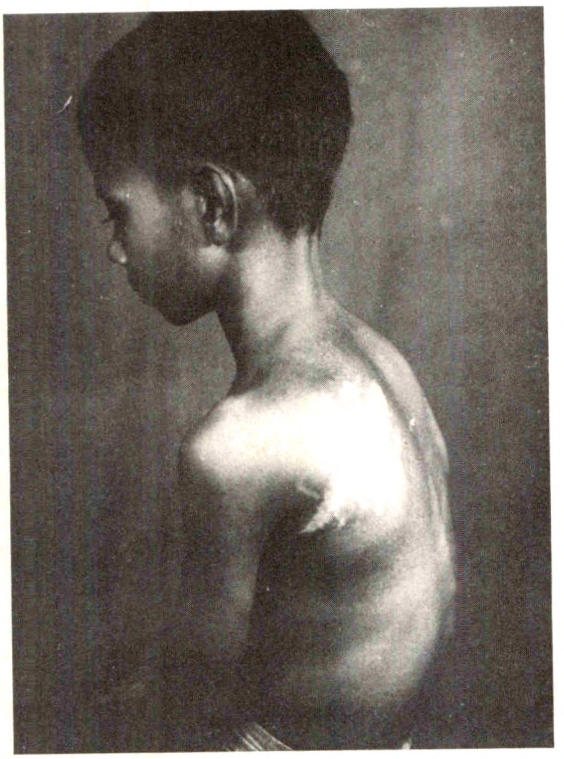


Fig. 5. Post irradiation photograph showing marked regression of tumor.

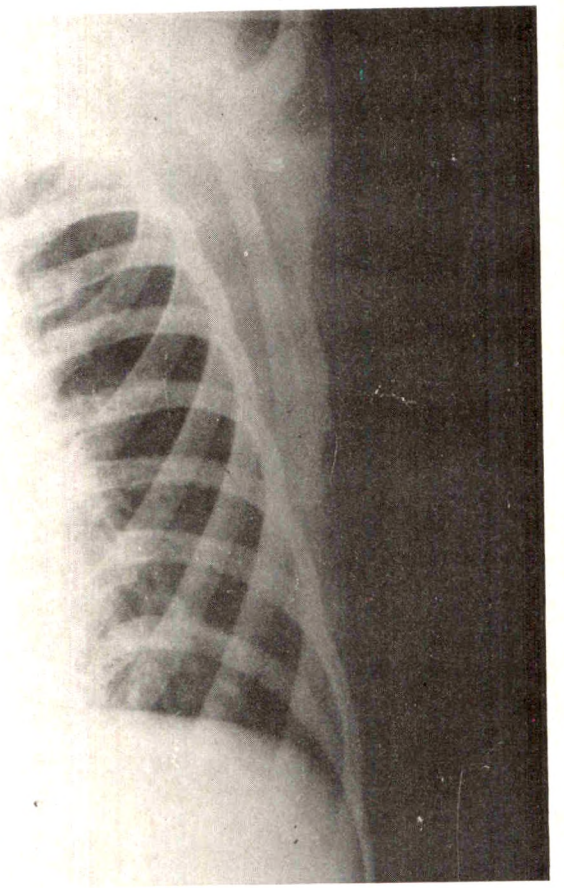


Fig. 6. Post irradiation roentgenogram showing marked regression of tumor.

The mass measured 13×15 cm in size with firm consistency and well defined margins. It moved from side to side.

Excisional biopsy done in May, 1975 was was reported as malignant hemangiopericytoma.

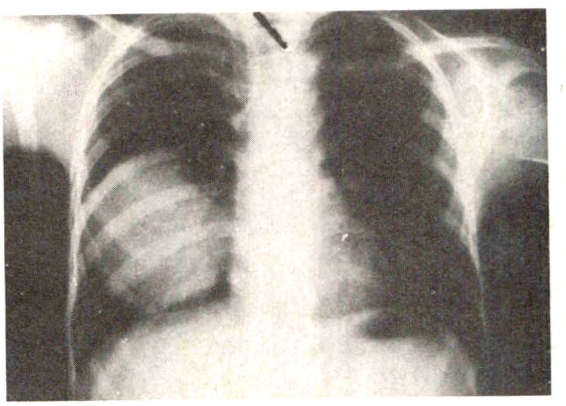


Fig. 7. Metastasis in right lung.

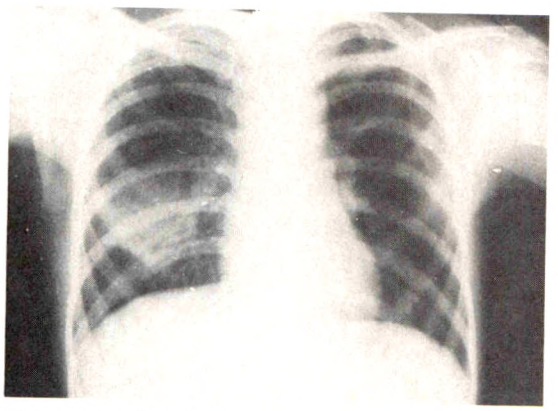


FIG. 8. Post irradiation roentgenogram of Figure 7.

He was given postoperative radiation therapy through a 15×8 cm direct field to the left chest wall, with telecobalt-60 at 60 cm SSD. The surface dose of 4,300 rads was fractionated over 16 days.

The patient has been doing well three months after completion of treatment and is being followed.

MICROSCOPIC PATHOLOGY

Since multiple sections from all the three cases show similar appearances (Fig. 9; and 10), they are described together. The tumor is richly cellular and is composed of non-neoplastic capillaries, the majority of which are small, insignificant, and compressed, visualized better on silver staining. These collapsed and non-collapsed capillaries are surrounded by a sheath of reticulum separating them from the tumor cells. The tumor cells are round, ovoid, or spindle in shape, pale staining, and disposed in whorls or mantles. The cells possess a vesicular nucleus which is large and prominent. Mitotic figures form a prominent feature in all the cases and areas of necrosis are also seen. Morphologically, the diagnosis of hemangioendothelioma, a related tumor, was ruled out by the characteristic reticulin pattern, while that of glomangioma, by the absence of neural elements. Similarly a diagnosis of chemodectoma or vascular leiomyoma was not entertained on histologic and clinical grounds.

DISCUSSION

The role of radiation therapy in hemangiopericytoma is still debatable. There are few reports on its efficacy as an adjunct to surgery or chemotherapy.

O'Brien *et al.*[7] in their series up to 1959 reviewed 24 cases of hemangiopericytoma. They found the tumor to be most common in the 4th decade of life. They did not report any case in children. All their patients were treated by surgery, and in four patients roentgen-ray therapy was given in conjunction with surgery. These cases did not show any beneficial effects of combining these two modalities. Kent[5] observed two cases who were subjected to radiation therapy. He reported favorable initial re-

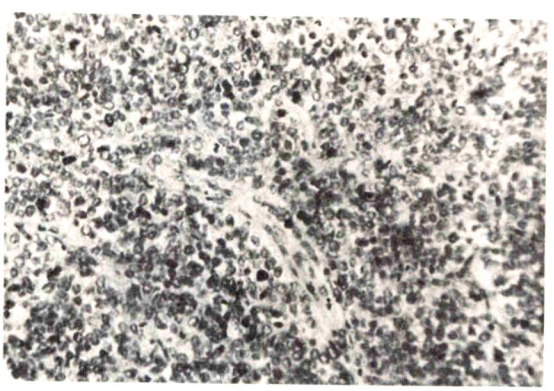


FIG. 9. Low power photomicrograph showing a longitudinally cut vessel in the center, surrounded by monomorphic round tumor cells. Note fair number of tumor cells undergoing mitosis.

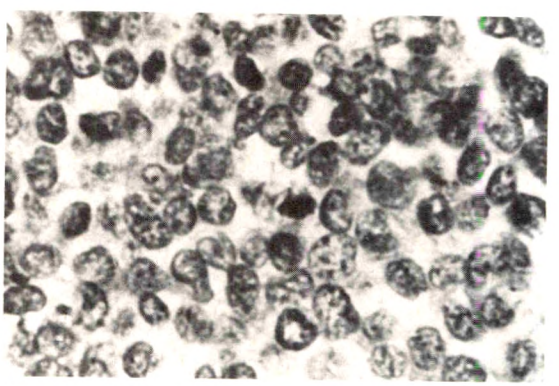


FIG. 10. A higher power view showing the details of morphology of tumor cells. Note mitotic figures.

sponse. Kauffman and Stout[4] in a large series of 307 cases reported only ten percent (31 cases) in the pediatric age group and mentioned the important and efficacious role of radiation therapy in the treatment of this neoplasm in addition to surgery which is the treatment of choice when the disease is localized.

Friedman and Egan[3] are of the opinion that local control of hemangiopericytoma in adults can be obtained with 7,500 to 9,000 rads administered over a period of 30 to 60 days. Mujahed *et al.*[6] reviewed the world literature regarding the treatment of hemangiopericytoma and noted a high percentage of recurrence following surgical removal, whereas radiation therapy offered better results. We concur with the observations of Mujahed *et al.*[6] Case I did not show any local recurrence of disease treated by radiation therapy, though developed metastases which also responded well to radiation treatment. In contrast, Case II showed recurrences at the local site following surgery, also responding well to radiation therapy. It is too early to comment upon Case III, but he has been doing well without any signs of recrudescence of disease.

Though the available data are scanty, from limited experience, it appears that surgery, combined with radiation therapy can give better results. Radiation therapy can be given preoperatively to reduce the size of growth and also reduce bleeding. Chemotherapy does not seem to have any beneficial effects.[1,2,7]

Harbans Lal, M.D., D.M.R.T.
Centre of Radiotherapy and Radiation Medicine
Institute of Medical Sciences
Banaras Hindu University
Varanasi—221005, India

REFERENCES

1. Bogedian, W., and Carpathios, J. Therapy of hemangiopericytoma with pulmonary disease. *Lancet*, 1967, *87*, 213–215.
2. Bredt, A. B., and Serpick, A. A. Metastatic hemangiopericytoma treated with vincristine and actinomycin. *Cancer*, 1959, *24*, 266–269.
3. Friedman, M., and Egan, J. W. Irradiation of hemangiopericytoma of Stout. *Radiology*, 1960, *74*, 721–730.
4. Kauffman, S. L., and Stout, A. P. Hemangiopericytoma in children. *Cancer*, 1960, *13*, 695–710.
5. Kent, K. H. Hemangiopericytoma: report of cases with special reference to roentgen therapy. Am. J. Roentgenol., Rad. Therapy & Nuclear Med., 1957, *77*, 347–356.
6. Mujahed, Z., Vasilas, A., and Evans, J. A. Hemangiopericytoma: report of four cases with review of literature. Am. J. Roentgenol., Rad. Therapy & Nuclear Med., 1959, *82*, 658–666.
7. O'Brien, P., Richard, I., and Basfield, R. D. Hemangiopericytoma. *Cancer*, 1965, *18*, 249–252.
8. Stout, A. P. and Murray, M. M. Hemangiopericytoma: study of twenty-five new cases. *Cancer*, 1949, *2*, 1026–1054.

CONGENITAL ABSENCE OF THE DUCTUS VENOSUS: WITH DIRECT CONNECTION BETWEEN THE UMBILICAL VEIN AND THE DISTAL INFERIOR VENA CAVA*

By JOHN C. LEONIDAS, M.D.,† *and* RICHARD A. FELLOWS, M.D.
KANSAS CITY, MISSOURI

ABSTRACT:

Umbilical vessel catheterization in a neonate with Noonan's syndrome disclosed a unique developmental anomaly of the umbilical vein. There was no evidence of a ductus venosus nor any connection between the vein and the portal hepatic venous system. The umbilical vein instead entered the inferior vena cava directly at the level of the iliac veins. There was a single umbilical artery.

CONGENITAL anomalies of umbilical vessels are quite rare, with the exception of single umbilical artery which occurs in approximately one percent of all deliveries.[2,9] In recent years umbilical vascular catheterization has assumed a very important role in the care of the critically ill newborn infant, and there has been a great interest in the anatomy of these vessels.[1,13] Roentgenographic localization of catheters has served to identify visceral anomalies.[12]

In the case presented here, roentgenographic recognition of abnormal catheter position led to identification of a unique congenital anomaly of the umbilical venous system.

REPORT OF A CASE

CASE 1. A 2,600 gm, 34 week gestation female infant was admitted on the first day of life because of mild respiratory distress. Pregnancy was marked by hyperemesis gravidarum, a weight gain of 11 kg and ankle edema. The mother received, during her pregnancy, ampicillin, propoxyphene hydrochloride (Darvon), and an oral iron preparation. Labor and delivery were uncomplicated.

At birth the infant presented several stigmata of the Turner phenotype. Subsequently a normal female karyotype established the diagnosis of Noonan's syndrome.

On admission a catheter was introduced into what was thought to be one umbilical artery. Anteroposterior and lateral roentgenograms obtained for evaluation of the chest as well as catheter position revealed mild cardiomegaly. The catheter followed the course of the umbilical artery, initially descending toward the pelvis, then ascending anterior to the spine. It terminated, however, anteriorly within the cardiac silhouette, in a position consistent with that of the right atrium (Fig. 1). This course was unexplained. The umbilical stump was examined carefully to resolve the possibility of a vascular anomaly. Three vascular orifices were seen, one of which contained the catheter mentioned above. An additional catheter was introduced into each of the other two orifices and advanced with ease. Roentgenograms were exposed in the anteroposterior and lateral projection (Fig. 2). All three catheters were initially observed to follow the course of the umbilical artery. One remained in a prevertebral position throughout its length, indicating an aortic location, terminating in the thoracic aorta. The third catheter terminated in a position suggesting that it was in an iliac vessel. No catheter followed the normal anterior course of the umbilical vein.[1,3] In the frontal view two catheters were superimposed to the left of the midline. To further clarify these findings, 3 ml of Hypaque 76 percent were injected into the catheter terminating close to the umbilicus and to the left of the midline (Fig. 2, catheter No. 2). Films showed opacification of a normal inferior vena cava (IVC) draining into the right atrium (Fig. 3). They also confirmed that the very first catheter (No. 1, Fig.

* From the Department of Radiology, Children's Mercy Hospital and the University of Missouri School of Medicine, Kansas City, Missouri.
† Present Address: Boston Floating Hospital, Tufts-New England Medical Center, Boston, Massachusetts 02111.

1; and 2) was in the IVC. It was concluded that there was a single umbilical artery and that two umbilical veins joined in the umbilical stalk and then followed a markedly abnormal course draining into the lower part of the IVC.

The patient improved within a few days and was discharged. A cardiac murmur was detected during a clinic visit and was thought to represent mild pulmonary stenosis.

DISCUSSION

Paired umbilical veins appear at the end of the 2nd embryonic week carrying blood from the capillaries of the chorion to the heart.[5] Initially they enter the common cardinal veins which join the sinus venosus. Later on the umbilical veins fuse with the veins of the primitive gut, the omphalomesenteric veins, which drain caudally into the sinus venosus. With the development of the liver in this area, the original umbilical-omphalomesenteric venous anastomosis is converted into a multitude of vessels dispersed among the cell cords of the liver.[11,13] This network has two afferent and

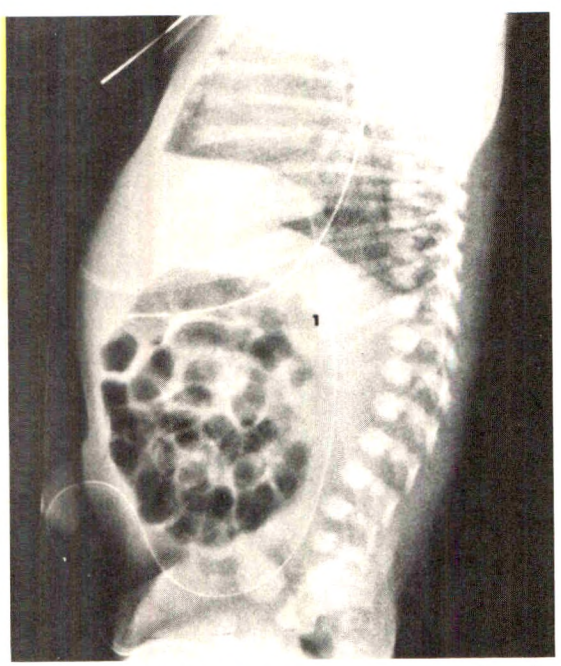


Fig. 1. Initial lateral roentgenogram showing the position of the first catheter (indicated by number 1). Note anterior termination at the level of the junction between the inferior vena cava and right atrium.

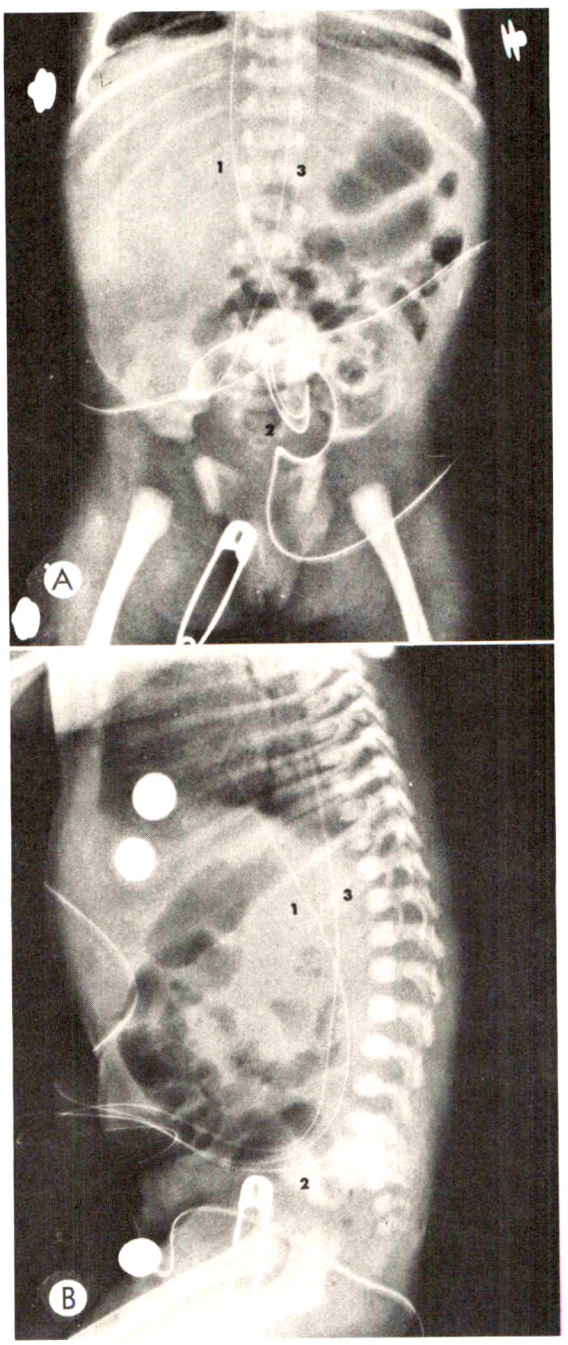


Fig. 2. (*A*) Anteroposterior roentgenogram following catheterization of all umbilical vessels. (*B*) Lateral roentgenogram. Catheter 1 remains unchanged, catheter 2 follows an umbilical arterial course and its termination is uncertain (ileal vessel?), and catheter 3 is obviously an arterial catheter terminating in the thoracic aorta.

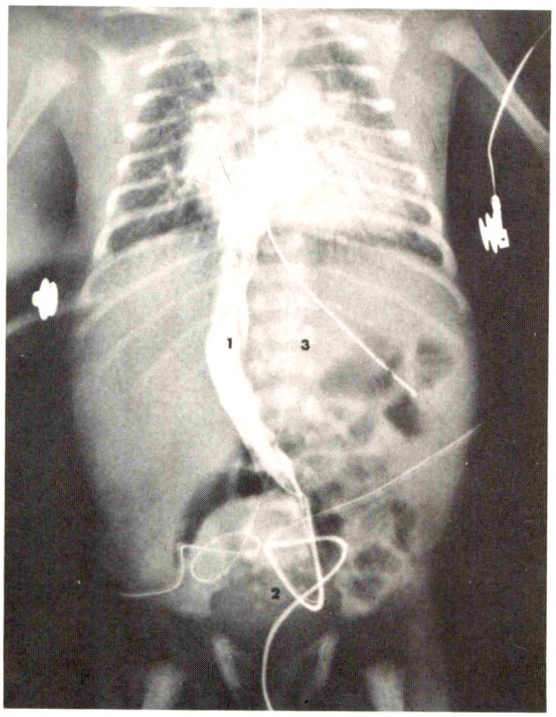


Fig. 3. Injection of contrast material through catheter 2 opacifies the inferior vena cava and the right side of the heart. Catheter 1 is also contained in the inferior vena cava. It is evident that the two umbilical veins join each other in the umbilical stalk and then proceed to directly connect with the inferior vena cava.

two efferent veins called venae advehentes and venae revehentes hepatis respectively.[5] Through the development of larger anastomoses and atrophy of others, a single vena advehens hepatis forms, the precursor of the portal vein. Shift of blood flow along some channels leads to enlargement of these and disappearance of others, with eventual atrophy of the right umbilical vein, as well as atrophy of the most cranial portion of the left umbilical vein. Now blood from the placenta flows exclusively through the proximal left umbilical vein into the portal system and through the latter into the sinus venosus.[5] Further increase of blood return from the placenta creates continuous dilatation of the intrahepatic anastomoses that offer the shortest route; they finally fuse to form the ductus venosus.[5]

After the 3rd embryonic week venous return from the trunk and extremities is carried out through the system of the paired anterior and posterior cardinal veins into the sinus venosus.[5] The former eventually become the superior vena cava (SVC) and its tributaries. The posterior cardinal veins partly disappear and partly fuse with the subcardinal veins, which form between the 5th and 8th week of gestation in close relationship to the developing mesonephros. A second major set of embryonic veins, the supracardinal or lateral sympathetic veins, forms dorsal and medial to the posterior cardinal veins around the 7th week. Cross connection of the posterior cardinal, supracardinal and subcardinal veins forms the IVC,[4] the upper part of which also receives blood from the ductus venosus.

In the case described here, the umbilical veins entered the distal IVC near the iliac veins. This is a unique vascular anomaly and any explanation will have to be speculative. Informal presentation to various groups has not elucidated the question. Professor Lind[6] suggested that through unknown causes of embryonic maldevelopment the umbilical veins in this instance failed to incorporate with the omphalomesenteric venous system. The resulting block to venous return from the placenta led to the opening of new vascular channels through anastomosis to the supracardinal or posterior cardinal components of the IVC. We believe this to be the most reasonable explanation.

In a related case reported by White and colleagues[13] dilated superficial abdominal veins developed in a neonate following failure of the "critical anastomosis" between the omphalomesenteric and umbilical venous systems. In this manner placental venous return was re-routed to the SVC. Monie[8] commented on a case of a stillborn infant whose umbilical vein entered the right atrium directly without passing through the liver. These two cases may suggest persistence of the early developmental connection of the umbilical veins to the common cardinal veins. Multiple con-

genital anomalies[7] and a single umbilical artery[8] seem to be associated findings in these rare abnormalities of the umbilical venous system.

To our knowledge umbilical venous anomalies are not part of Noonan's syndrome, although other cardiovascular malformations are common in this entity.[10]

John C. Leonidas, M.D.
Department of Radiology
Children's Mercy Hospital
24th and Gillham Road
Kansas City, Missouri 64108

The authors gratefully acknowledge the assistance of Dr. Alice C. Yao in reviewing the manuscript.

REFERENCES

1. Baker, D. H., Berdon, W. E., and James, L. S. Proper localization of umbilical artery and venous catheters by lateral roentgenograms. *Pediatrics*, 1969, *43*, 34–39.
2. Benirschke, K. Contribution of pathology laboratory to diagnosis of newborn. *Pediat. Clin. North America*, 1961, *8*, 461–470.
3. Campbell, R. E. Roentgenologic features of umbilical vascular catheterization in newborn. Am. J. Roentgenol., Rad. Therapy & Nuclear Med., 1971, *112*, 68–76.
4. Gray, S. W., and Scandalakis, J. E. Embryology for Surgeons. W. B. Saunders Company, Philadelphia, 1972, pp. 859–876.
5. Kjellberg, S. R., Mannheimer, E., Rudhe, U., and Jonsson, B. Diagnosis of Congenital Heart Disease. Second edition. Year Book Medical Publishers, Inc., Chicago, 1959, pp. 1–12.
6. Lind, J. Personal communication.
7. McMahon, H. E. Congenital absence of ductus venosus. *Lab. Invest.*, 1960, *9*, 127–131.
8. Monie, I. W. Umbilical vein entering right atrium: comments on previously reported human case. *Teratology*, 1971, *4*, 461–464.
9. Monie, I. W. Genesis of single umbilical artery. *Am. J. Obst. & Gynec.*, 1970, *108*, 400–405.
10. Nora, J. J., Nora, A. H., Sinha, A. K., Spangler, R. D., and Lubs, H. A. Ullrich-Noonan syndrome (Turner phenotype). *A.M.A. Am. J. Dis. Child.*, 1974, *127*, 48–55.
11. Patten, B. M. Development of heart. In: Pathology of the Heart. Second edition. Edited by G. E. Gould. Charles C Thomas, Publisher, Springfield, Ill., 1960.
12. Taber, P., Gyepes, M. T., and Lackey, D. A. Malposition of umbilical vascular catheters in diagnosis of congenital diaphragmatic hernia. *Radiology*, 1973, *109*, 413–415.
13. White, J. J., Brenner, H., and Avery, M. E. Umbilical vein collateral circulation: caput medusae in newborn infant. *Pediatrics*, 1969, *43*, 391–395.

ANEURYSMAL BONE CYST OF THE ORBIT WITH UNUSUAL ANGIOGRAPHIC FEATURES*

By A. M. O'GORMAN, M.B., F.R.C.P.(C),† *and* T. H. KIRKHAM, F.R.C.S.‡
MONTREAL, QUEBEC

ABSTRACT:

A 14 month old boy with sudden onset of proptosis of the left eye due to an aneurysmal bone cyst of the orbit is reported. Sequential plain films of the orbital region demonstrated changes ranging from subtle loss of bone definition of the orbital margin to the characteristic appearance of an aneurysmal bone cyst twelve months later. Arteriography at the time of the initial evaluation demonstrated prolonged retention of the contrast medium which we believe represents changes secondary to the number of giant cells present in the tumor rather than the relative vascularity of the lesion. While aneurysmal bone cyst of the orbit is extremely rare, it should be included in the differential diagnosis of proptosis in the pediatric age group.

ANEURYSMAL bone cyst rarely involves the skull bones[2] and fewer than ten patients with proptosis from this cause have been reported.[6,10] Although 80 percent of aneurysmal bone cysts occur before the age of 20 years, they are extremely rare in infants[13] and the youngest reported to date with orbital involvement was a five year old girl.[6] We report here a 14 month old boy with an aneurysmal bone cyst of the orbit, presenting with painless proptosis, in whom the angiographic features differ significantly from previous reports where angiography of the orbital lesion was obtained.[3,10] We wish to emphasize that, even in infancy, aneurysmal bone cyst of the orbit should be considered in the differential diagnosis of proptosis.

REPORT OF A CASE

A 14 month old boy was admitted for investigation of an atypical febrile convulsion in March, 1974. Nothing unusual was found at that time but three weeks later the boy was seen again because of the sudden, dramatic appearence of left proptosis. General physical examination revealed no other abnormalities. The vision, pupillary responses and visual fields were normal as far as could be ascertained in this age group. There was left proptosis of 4 mm and the eye was directed downwards and outwards. All the extraocular movements of the left eye were limited, particularly elevation. Fundus examination was normal and did not reveal evidence of posterior indentation of the globe.

Routine laboratory studies were normal. "B"-mode ultrasound scan of the left orbit suggested a solid, space occupying lesion in the superior medial quadrant of the orbit extending into the retrobulbar space medially, the mass measuring 15×17 mm in size.

Orbital roentgenograms (Fig. 1) in March, 1974 showed loss of definition of the superior medial margin of the left orbit with minimal increase in size of the left orbit. One month later in April, 1974 (Fig. 2), there was definite loss of the lamina papyracea of the left ethmoid sinus and further cortical loss of the left supe-

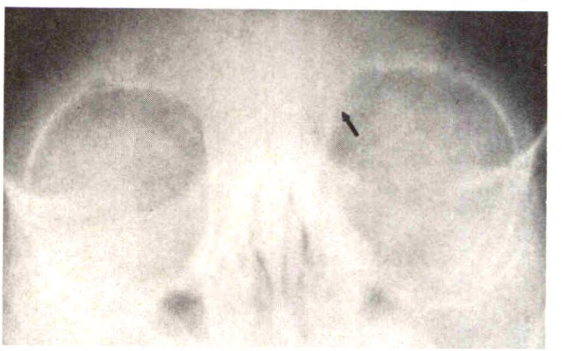


FIG. 1. Waters' projection in March demonstrates loss of definition of the cortical margin at the superior medial aspect of the left orbit (arrow).

* From the Departments of Radiology,† and Ophthalmology,‡ The Montreal Children's Hospital, McGill University, Montreal, Quebec, Canada.

rior medial margin of the orbit. A subsequent common carotid arteriogram demonstrated a well demarcated circular mass lesion measuring approximately 2×2 cm in size with a diffuse increase of opacification located within the bony orbit with its posterior pole located behind the expected site of the choroidal blush of the eye. The ophthalmic artery was normal in caliber but was stretched and displaced inferiorly and laterally (Fig. 3; and 4). No supply from the external carotid artery was detected. There was some early venous filling in the arterial phase and the dense blush persisted into the late venous phase (Fig. 5).

The lesion was totally excised *via* a superomedial approach. A tense, plum colored, mass lesion was encountered lying superomedially in the orbit above the globe and extending behind the globe medially. The lesion appeared well encapsulated. A needle was inserted into the lesion and 2 ml of straw colored fluid, appearing like old blood, was aspirated. No bleeding was encountered and the mass lesion was excised piecemeal. The tissue was extremely friable and jelly-like and no undue bleeding was encountered throughout the procedure.

Histologically there was abundant evidence of hemorrhage with many hemosiderin laden giant cells, fibroblasts, and bone formation within the lesion which was interpreted as being a reaction to a previous hemorrhage. No evidence of any pre-existing vascular malformation was found. The pathological diagnosis was that of aneurysmal bone cyst.

The proptosis and restriction of eye movements did not completely resolve following the surgical procedure and follow-up roentgenograms of the orbit in March, 1975 showed a more characteristic appearance of an aneurysmal bone cyst. At this time there was further expansion of the bone superiorly and laterally with a cystic appearance and a thin sclerotic margin (Fig. 6).

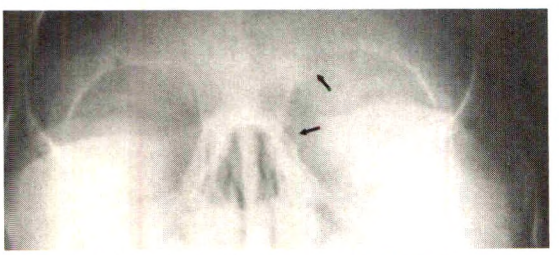


Fig. 2. Waters' projection in April demonstrates further loss of the superior medial cortical margin (upper arrow). There is now also some loss of the left lamina papyracea (lower arrow).



Fig. 3. Lateral view of early arterial phase subtraction film showing inferior displacement of the ophthalmic artery (arrow) and rapid increase in density in the posterior orbital region.

DISCUSSION

The sudden onset of rapid progressive

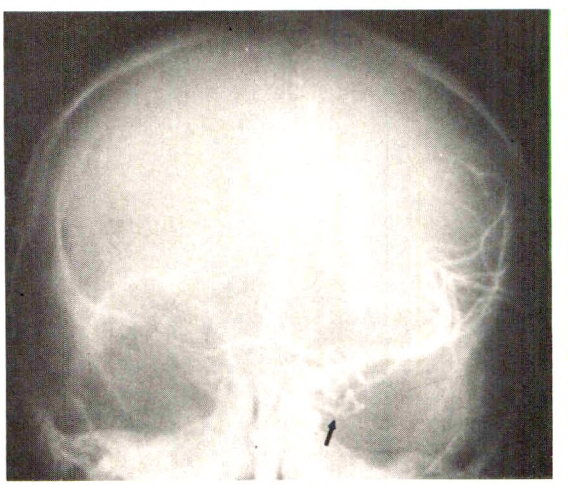


Fig. 4. Anteroposterior view in the early arterial phase demonstrating stretching, with inferior and lateral displacement, of the ophthalmic artery (arrow).

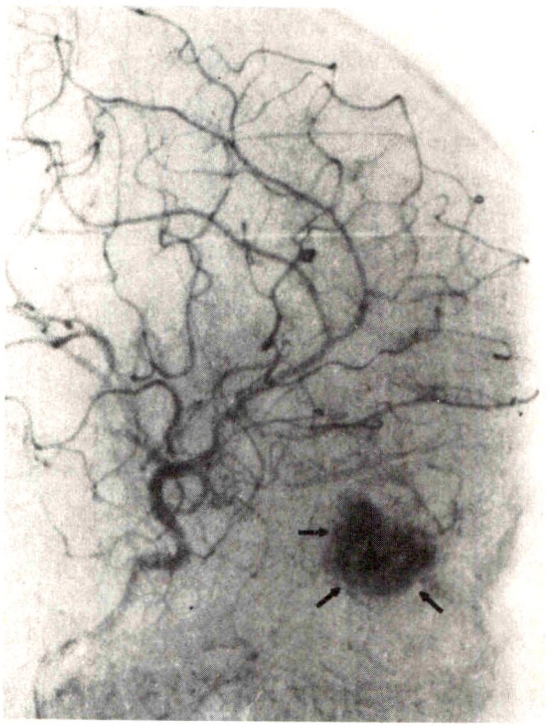


Fig. 5. Lateral view of late arterial phase, with subtraction, showing very marked and well demarcated increase in density outlining the orbital mass lesion (arrows). No branches from the external carotid contribute to the lesion.

proptosis in infancy leads to the suspicion of a malignant orbital tumor such as rhabdomyosarcoma. The extremely rapid development of proptosis in our case of aneurysmal bone cyst was paralleled by that of Fite *et al.*[5] where 8 mm of proptosis was present after eight days. The rapidity of onset could possibly indicate that there had been hemorrhage into a pre-existing lesion such as a hemangioma to produce the sudden expansion in size of the mass, conceivably due to minor unrecognized trauma at the time of the seizure. However, pathologically in our case there was no evidence of any recognizable pre-existing lesion and this was also the experience of a study of 95 cases.[13]

Aneurysmal bone cyst receives its name from its dramatic "blown-out" roentgenographic appearance.[7] This benign tumor is usually found in the ends of long bones but at times in the midshaft. Aneurysmal bone cyst tends to affect older children, adolescents, and young adults, and it is reported that 80 percent of cases occur before the age of 20 years.[10] The characteristic roentgenographic changes are seldom seen when the flat bones of the calvarium are involved.[2] Most commonly the cyst arises within bone, causing an expansion and buckling of the intracranial and especially the orbital surfaces of the frontal bone. In our case, tomography in April, 1974 might have been useful to demonstrate a lateral wall of the bone cyst. The cyst has been shown by tomography to be extra-osseous in type, presenting as a soft tissue tumor adjacent to the bone and eroding to the bone surface.[4,8]

It is well recognized that arteriography is not often rewarding in the differential diagnosis of bone tumors. Arteriography in our patient was undertaken to determine the extent of the lesion and to obtain an indication of its vascularity prior to surgical excision. Common intra-orbital tumors in children include sarcoma, glioma, neuroblastoma, and hemangioma, and mass lesions which may occupy the superomedial quadrant of the orbit include mucocele, sphenoid meningioma, and rhabdomyosarcoma. Juvenile angiofibromas may extend from the nasopharynx or nasal cavity into the orbit. Sarcoma, neuroblastoma, hemangioma, and angiofibroma usually show increased vascular supply with vascular contributions from the ex-



Fig. 6. Waters' projection one year after the initial roentgenogram demonstrates a somewhat "blown-out" lesion with a now well defined thin rim (arrows).

ternal carotid artery.[9] Mucoceles and gliomas of the optic nerve are usually quite avascular. In our case the sharply defined area of contrast medium accumulation, with a regular contour without increased vascular supply but exhibiting a diffuse increase in density during the capillary and venous phase, suggested a benign process. There exists a small group of benign bone neoplasms such as benign giant cell tumor, aneurysmal bone cyst, non-osteogenic fibroma, and the localized destructive lesions of osteitis fibrosis cystica which may have a normal or slight increase in the arterial supply and which show increased ability to retain contrast medium without any other arteriographic criteria of a malignant condition.[11]

Lindbom *et al.*[8] found large arteries leading to aneurysmal bone cysts and Abrams[1] illustrated a case of aneurysmal bone cyst of the dorsal part of the 5th lumbar vertebral body where the arterial phase appeared to be normal and in which the late retention of contrast medium in the well circumscribed opacified lesion was quite similar to our case.

In previously reported cases of aneurysmal bone cyst of the orbit where angiography was performed, the lesion was essentially avascular in contrast to our case. The case of Powell and Glaser[10] showed only elevation of the middle cerebral vessels consistent with a large extracerebral middle fossa lesion which was avascular, and that of Costanini *et al.*[3] showed a large frontal avascular area in both the arterial and venous phase.

The opinion prevails that the opacification is related to the increased number and size of small vessels in the tumor.[11] However, Schobinger and Stoll,[12] comparing the histologic appearance of benign tumors exhibiting prolonged retention of Urokon and Hypaque, suggested that the degree of retention parallels the number of giant cells present rather than the relative vascularity of the lesion. There was no increase in the number or caliber of feeding vessels in our case and therefore, we believe that the increased vascularity and retention of contrast medium were due to the number of giant cells present rather than the relative vascularity of the lesion.

T. H. Kirkham, F.R.C.S.
Department of Ophthalmology
The Montreal Neurological Hospital
3801 University Street
Montreal, Quebec
Canada

REFERENCES

1. Abrams, H. L. Angiography. Volume 2. Second edition. Little, Brown & Co., Boston, 1971, pp. 1304.
2. Caldac, M. A., Malis, L. T., and Anderson, P. J. Aneurysmal parietal bone cyst: case report. *J. Neurosurg.*, 1972, *37*, 237–241.
3. Costanini, F. E., Iraci, G., and Benedetti, A. Aneurysmal bone cyst as intracranial space occupying lesion: case report. *J. Neurosurg.*, 1966, *25*, 205–207.
4. Edeiken, J., and Hodes, P. J. Giant cell tumors versus tumors with giant cells. *Radiol. Clin. North America*, 1963, *1*, 75–100.
5. Fite, J. D., Schwartz, J. F., and Calhoun, F. P. Aneurysmal bone cyst of orbit: clinicopathologic case report. *Tr. Am. Acad. Ophth.*, 1968, *72*, 614–618.
6. Henderson, J. W. Orbital Tumors. W. B. Saunders Company, Philadelphia, 1973, pp. 252.
7. Lichtenstein, L. Aneurysmal bone cyst: pathological entity commonly mistaken for giant cell tumor and occasionally for hemangioma and osteogenic sarcoma. *Cancer*, 1950, *3*, 279–289.
8. Lindbom, A., Soderberg, G., Spjut, H. J., and Sunnqvist, O. Angiography of aneurysmal bone cyst. *Acta. radiol.*, 1961, *55*, 12–16.
9. Newton, T. H., and Potts, D. G. Radiology of skull and brain. In: Angiography. Volume 2. C. V. Mosby Company, St. Louis, 1971, pp. 1371.
10. Powell, J. O., and Glaser, J. S. Aneurysmal bone cyst of orbit. *A.M.A. Arch. Ophth.*, 1975, *93*, 340–342.
11. Schobinger, R., Lin, R. K., and Moss, H. C. Significance of venous phase in arteriographic studies of bone and soft tissue tumors. *Cancer*, 1958, *11*, 315–321.
12. Schobinger, R., and Stoll, H. C. Arteriographic picture of benign bone lesions containing giant cells. *J. Bone & Joint Surg.*, 1957, *39*-A, 953–960.
13. Tillman, B. P., Dahlin, D. C., Lipscomb, P. R., and Stewart, J. R. Aneurysmal bone cyst: analysis of ninety-five cases. *Mayo Clin. Proc. Staff Meet.*, 1968, *43*, 478–495.

VERTEBRAL SARCOIDOSIS*

A CASE REPORT AND REVIEW OF THE LITERATURE

By PHILIP A. BRODEY, M.D.,†‡ STEPHEN PRIPSTEIN, M.D.,†
GERALD STRANGE, M.D.,§ *and* NEVEA D. KOHOUT, M.D.‖
SAN FRANCISCO, CALIFORNIA

THE true incidence of bone involvement in sarcoidosis is unknown. The reported incidence of osseous involvement in systemic sarcoid ranges from five percent to 36 percent.[8,10,11,13] Typically, the lesions involve the small bones of the hands and feet. Lesions involving the skull,[11,12,16,17] long bones,[5,6] large joints[3] and vertebral bodies[1,2,4,7,14,18,19] have been described but are infrequent.

The purpose of this paper is to describe a case of vertebral sarcoidosis. This is the eighth case in the English literature in which vertebral body abnormalities in sarcoid are described and the fifth case in which antemortem diagnosis by biopsy of the vertebral body was made.

REPORT OF A CASE

Case 1. M.H. is a 35 year old, Black, female nurse, admitted to Mt. Zion Hospital for the first time on November 4, 1974. Initial complaints were increasing back pain for the last two months with pain radiating into her right hip and down the posterior aspect of her right leg. Her past medical history was unremarkable.

Physical examination revealed normal straight leg raising bilaterally to 90°, no pain with increased dorsoflexion, and a negative Patrick's sign. There was no muscle fasciculation nor muscle atrophy. The deep tendon reflexes were normal. There was no area of paresthesia or dysesthesia noted. There was no lymphadenopathy nor hepatosplenomegaly. A routine SMA-12 was normal except for persistently elevated serum calcium levels. Renal function was normal as were white blood cell and hemoglobin studies. The sedimentation rate was elevated to 33 mm/hr. A test of compliment fixation to coccidiomycosis was negative, and a skin test for tuberculosis was negative. A urinalysis was normal as was cerebrospinal fluid examination. Roentgen examinations included plain films of the lumbar spine which revealed a destructive lesion involving the antercinferior aspect of the L_3 vertebral body with adjacent sclerosis and with narrowing of the disk space (Fig. 1). Tomograms were obtained showing destruction of the anteroinferior margin of L_3 with adjacent sclerosis and disk space narrowing (Fig. 2). There was no paraspinal mass. A chest examination was normal. A myelogram showed defects compatible only with a herniated disk. An aortogram



Fig. 1. Destructive lesion of the anteroinferior portion of the body of L_3 vertebra with adjacent sclerotic reaction. Disk space at L_3–L_4 is narrowed.

* From the Departments of Radiology,† and Pathology,‖ Mt. Zion Hospital, U.C.S.F. Medical Center, San Francisco, California.
‡ Clinical Instructor, Department of Radiology, U.C.S.F. Medical Center.
§ Attending Orthopedic Surgeon.

TABLE I

REPORTED CASES OF VERTEBRAL SARCOIDOSIS

Author	Type of Lesion	Part of Vertebral Body	Vertebral Body Involved	Disk Space	Paraspinal Mass	Symptoms	Chest X-Ray
Berk and Brower[2]*	Destructive with sclerotic margin	Body and pedicles	L-1 L-5	Normal	None	Present	Lymphadenopathy-parenchymal changes
Goodbar *et al.*[7]*	Destructive with collapse	Body	T-11	Normal	None	Present	Parenchymal changes
Rodman *et al.*[14]*	Destructive	Body	T-11 and T-12	Narrowed	None	Present	Hilar lymphadenopathy and parenchymal change
Zener *et al.*[19]*	Destructive with sclerotic margin (T9), sclerotic (L2)	Body	T-9 L-2	Normal Normal	T spine only	Present	Normal
Present case*	Destructive with sclerotic margin	Body	L-3	Narrowed	None	Present	Normal
Baldwin *et al.*[1]	Destructive with sclerotic margin	Body	T-8	Narrowed	Present	Present	Lymphadenopathy
Bloch *et al.*[4]	Destructive with sclerotic margin	Body	T-11 and T-12	Narrowed	None	Present	Lymphadenopathy
Young and Laman[18]	Sclerotic	Body and pedicles	Cervical through lumbar	Normal	None	None	Lymphadenopathy

* Vertebral body biopsied for diagnosis. Chart includes only cervical through lumbar vertebrae.

in both anteroposterior and cross-table lateral positions was normal as was a bone scan. An open surgical biopsy of L3 included several lymph nodes. The microscopic examination revealed noncaseating granulomatous changes in these lymph nodes. Special stains done on the tissues obtained included stains for acid fast bacilli and fungi. These were negative. Bacteriological cultures were obtained and these also were negative. The pathologic diagnosis was consistent with sarcoidosis.

DISCUSSION

The typical roentgenographic changes of osseous sarcoid involving the small bones of the hands and feet consist of cystic areas or a lace-like, coarsely trabeculated pattern of the medullary portion of the involved bone.[6,15] Recently, osteosclerotic lesions have been reported in sarcoid.[5,9,18] Destructive lesions involving large joints also have recently been described.[3]

Vertebral sarcoidosis is usually a lytic or destructive process with marginal sclerosis

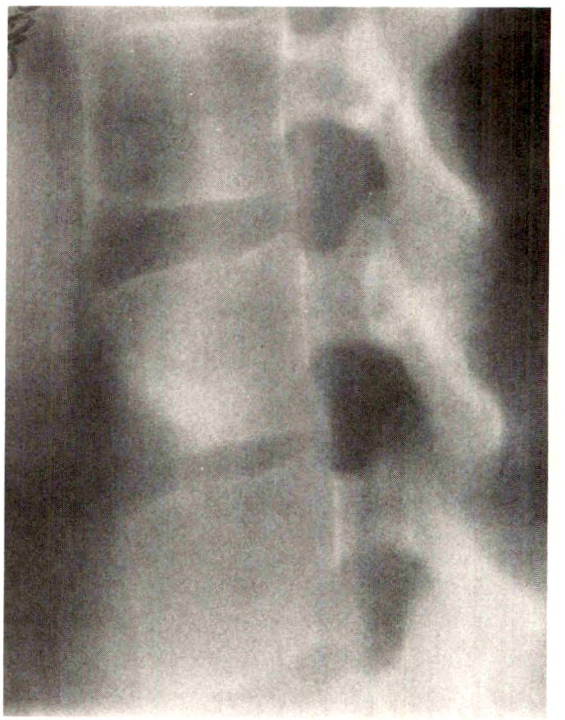


FIG. 2. Tomogram of L3, showing same findings.

that involves one or more vertebral bodies which may or may not be adjacent. The disk space is usually preserved. The destructive form of vertebral sarcoidosis is limited to the thoracic and lumbar spine. In the described osteosclerotic form of vertebral sarcoidosis, cervical spine involvement also occurred. The body of the vertebra is typically involved but the process can extend into the pedicles. A soft tissue mass may be associated with the destructive process. Symptoms are invariably present with the destructive form. Chest abnormalities, including parenchymal changes with or without hilar adenopathy, are not always present, as in this case.

Table 1 gives a review of the literature and the pertinent associated findings.

Differential diagnoses would include tuberculous, fungal, or pyogenic osteomyelitis, Hodgkin's disease, and metastatic carcinoma. Tuberculosis results in destruction of the vertebral body and adjacent disk space leading to collapse and spinal deformity. A soft tissue mass, with or without calcification, may be present. Hodgkin's disease may cause erosion of the anterior margins of the vertebral body. Metastatic disease typically involves the pedicles, spares the disk space, and does not have marginal sclerosis.

Biopsy is necessary to make the definitive diagnosis.

Philip A. Brodey, M.D.
Department of Radiology
Mount Zion Hospital and Medical Center
1600 Divisadero Street
Post Office Box 7921
San Francisco, California 94120

The authors wish to acknowledge the permission of the following physicians: Robert Allen, M.D., William Breall, M.D., Irwin Weinreb, M.D., Michael Grossman, M.D., John O'Brien, M.D. and Michael Finegold, M.D.

REFERENCES

1. Baldwin, D. M., Roberts, J. G., and Croft, H. E. Vertebral sarcoidosis. *J. Bone & Joint Surg.*, 1974, *56*-A, 629–632.
2. Berk, R. N., and Brower, T. D. Vertebral sarcoidosis. *Radiology*, 1964, *82*, 660–663.
3. Bjarnason, D. F., Forrester, D. M., and Swezey, R. L. Destructive arthritis of large joints: rare manifestation of sarcoidosis. *J. Bone & Joint Surg.*, 1973, *55*-A, 618–622.
4. Bloch, S., Movson, I. J., and Seedat, Y. K. Unusual skeletal manifestations in a case of sarcoidosis. *Clin. Radiol.*, 1968, *19*, 226–228.
5. Bonakdarpour, A., Levy, W., and Aegerter, E. E. Osteosclerotic changes in sarcoidosis. Am. J. Roentgenol., Rad. Therapy & Nuclear Med., 1971, *113*, 646–649.
6. Fitzgerald, P., and Meenan, F. O. C. Sarcoidosis of hands. *J. Bone & Joint Surg.*, 1958, *40*-B 256–261.
7. Goodbar, J. E., Gilmer, W. S., Carroll, D. S., and Clark, G. M. Vertebral sarcoidosis. *J.A.M.A.*, 1961, *178*, 1162–1163.
8. Holt, J. F., and Owens, W. I. Osseous lesions of sarcoidosis. *Radiology*, 1949, *51*, 11–30.
9. Lin, S. R., Levy, W., Go, E. B., Lee, I., and Wong, W. K. Unusual osteosclerotic changes in sarcoidosis: simulating osteoblastic metastases. *Radiology*, 1973, *106*, 311–312.
10. Mayock, R. L., Bertrand, P., Morrison, E. C., and Scott, J. H. Manifestations of sarcoidosis: analysis of 145 patients with review of nine series selected from literature. *Am. J. Med.*, 1963, *35*, 67–89.
11. Olsen, T. G. Sarcoidosis of skull. *Radiology*, 1963, *80*, 232–234.
12. Posner, I. Sarcoidosis: case report. *J. Pediat.*, 1942, *20*, 486–495.
13. Ricker, W., and Clark, M. Sarcoidosis: clinicopathologic review of three hundred cases including twenty-two autopsies. *Am. J. Clin. Path.*, 1949, *19*, 725–749.
14. Rodman, T., Funderburk, E. E., Jr., and Myerson, R. M. Sarcoidosis with vertebral involvement. *Ann. Int. Med.*, 1959, *50*, 213–218.
15. Stein, G. L., Israel, H. L., and Jones, M. Roentgenographic study of skeletal lesions in sarcoidosis. *A.M.A. Arch. Int. Med.*, 1956, *97*, 532–536.
16. Teirstein, A. S., Wolf, B. S., and Siltzbach, L. E. Sarcoidosis of skull. *New England J. Med.*, 1961, *265*, 65–68.
17. Turner, O. A., and Weiss, S. R. Sarcoidosis of skull: report of case. Am. J. Roentgenol., Rad. Therapy & Nuclear Med., 1969, *105*, 322–325.
18. Young, D. A., and Laman, M. L. Radiodense skeletal lesions in Boeck's sarcoid. Am. J. Roentgenol., Rad. Therapy & Nuclear Med., 1972, *114*, 538–553.
19. Zener, J. C., Alpert, M., and Klainer, L. M. Vertebral sarcoidosis. *A.M.A. Arch. Int. Med.*, 1963, *111*, 696–702.

Vol. 126, No. 4

EXTRA-ABDOMINAL DESMOID OF THE AXILLARY TAIL MIMICKING BREAST CARCINOMA*

By LESTER KALISHER, M.D., JOHN A. LONG, M.D., *and* ROBERT G. PEYSTER, M.D.
BOSTON, MASSACHUSETTS

ABSTRACT:

A case is reported of an extra-abdominal desmoid tumor presenting as an axillary tail breast mass. This represents the third reported case and the first description of the roentgenographic findings of this entity. That this tumor can be confused with carcinoma of the breast is emphasized.

IN 1832 McFarland described a benign appearing, locally invasive lesion which subsequently was named desmoid tumor (desmos, banding together) by Müller.[8] Since that time numerous reports of extra-abdominal desmoid (EAD) have been described in various anatomic locations. However, in reviewing the world literature, there have been only two reported cases of extra-abdominal desmoid presenting as a breast mass.

A patient referred to the Massachusetts General Hospital was discovered on xeromammography to have an axillary tail mass. Roentgenographically this lesion mimicked an infiltrating ductal carcinoma, yet histologically proved to be a benign, locally invasive desmoid tumor. This case is reported in detail to (a) call attention to the presentation of this tumor as a breast mass; (b) show that the lesion may mimic breast carcinoma roentgenographically, yet appear benign histologically; and (c) provide the first roentgenologic description of this entity.

REPORT OF A CASE

A 50 year old white woman noticed a mass in her left breast three months prior to admission. It was thought to be fibrocystic disease. Nonetheless a xeromammogram was obtained, which showed an ill-defined stellate mass in the upper outer quadrant roentgenographically consistent with an infiltrating ductal carcinoma. The patient was admitted for a biopsy and possible mastectomy. Past history included tonsillectomy and adenoidectomy, and two pregnancies. No family history of breast cancer or desmoid tumor was elicited.

The patient's abnormality was confined to the left breast. A poorly defined subcutaneous mass was felt in the upper outer aspect of the axillary tail near the chest wall. It was not adherent to either the skin or chest wall. It was nontender and firm, measuring 3×5 cm. No axillary lymph nodes were found. Laboratory studies were within normal limits.

The chest roentgenogram was negative. The xeromammogram of the left breast demonstrated an ill-defined, spiculated 2 cm mass with apparent skin retraction located in the upper outer quadrant (Fig. 1; and 2). It was felt to represent an infiltrating ductal carcinoma.

At operation a piece of firm, slightly gritty tan fatty tissue measuring 0.5 cm in diameter was removed. The pathologist suggested on frozen section that the lesion represented a fibroma. Because of the unexpected pathologist's report, the upper outer quadrant was carefully explored, and nothing resembling a discrete neoplasm was found. Two months later, repeat xeromammography was performed, and the lesion was no longer present. The tissue was then sent to the Massachusetts General Hospital for review, and additional sections of the block were cut. The report from the Massachusetts General Hospital showed that the lesion represented an extra-abdominal desmoid with focal muscle invasion (Fig. 3; and 4).

DISCUSSION

In 1832, MacFarlane[5] described two fibrous tumors in the abdominal musculature. Müller[8] is credited with providing the name "desmoid" to this group of tumors, alluding to their band-like or tendon-like

* From the Departments of Radiology, Massachusetts General Hospital and Harvard Medical School, Boston, Massachusetts.

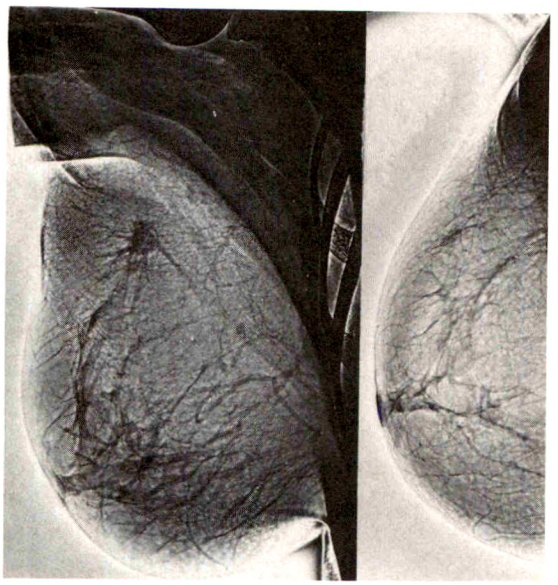


Fig. 1. An irregular spiculated mass can be seen in the axillary tail (upper outer quadrant of the left breast). Note its close relationship to the pectoralis muscle.

appearance. Bennett described three fibrous tumors in extra-abdominal sites in 1849; the description would appear to conform to that of desmoid tumors.[7] Nichols[10] was the first to apply the name desmoid to the tumors occurring in extra-abdominal locations which seemed identical to those arising from the abdominal parietes.

Desmoid tumors are usually oblong and irregular firm masses with their long axis parallel to that of the muscle and fascia from which the tumors arise. They present a trabeculated, rubbery gray to yellowish white cut surface. Microscopically, the tumor consists of fibrous tissue with occasional normal mitotic figures that invade adjacent muscle, often isolating islands of muscle. The engulfed muscle undergoes alterations in morphology, including the formation of muscle giant cells which have been confused with tumor giant cells.[4] It is occasionally difficult to differentiate a desmoid tumor from a mature fibrosarcoma on a histological basis.[9]

The two major theories of etiology of desmoid tumors consider trauma[2,9,14] and hormonal causes.[1,2,9,14] The traumatic theory is most widely accepted, with external trauma, the physiological trauma of labor, and trauma related to previous surgical incisions having been implicated. Heredity has been cited as a possible etiological factor.[11,14] Desmoid tumors have been associated with Gardner's syndrome.[14]

Desmoids usually present as a mass noticed by the patient, occasionally associated with a dull, aching pain.[6,9] If a nerve is entrapped by the tumor, more severe pain can ensue.[9] Desmoids are more frequent in women, with women accounting for from 60 percent to 90 percent of these tumors in several series.[1,3,4,7,9] Patients range in age from 18 months to 72 years, with an average age of about 40 years.[4,6,9,11,14]

Desmoid tumors are rare, representing from 0.013 percent to 0.13 percent of all neoplasms.[13] Those occurring in extra-abdominal sites are less common than those arising from the abdominal wall.[2,3,7,9,11] The literature contains only two reports of an EAD presenting as a breast mass[10,14] with several other desmoids occurring in relation to the pectoralis major muscle.[2,4,6,11] The roentgenographic appearance of an EAD in the breast has not been previously described.

Wide excision is the treatment of choice,

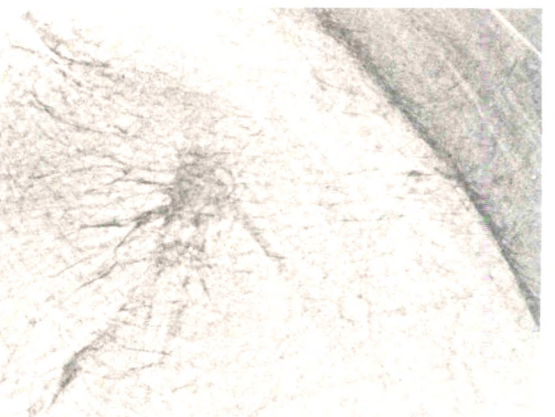


Fig. 2. Close up of Figure 1. Muscle fibers can be seen near the mass. The irregular malignant appearance is better appreciated on this picture.

the extent depending on various factors.[1,2,3,7,9] The role of radiation therapy when complete excision is not feasible is controversial, most authors not including radiation in their treatment.[2,4,10] The efficacy of hormonal therapy is not established.[4,9]

The prognosis for survival with desmoid tumors is excellent, although a few fatal cases due to involvement of vital structures have been reported.[7] It is generally held that these tumors do not undergo sarcomatous degeneration[2,4,9,11] despite two reports to the contrary.[3,12] There are rare reports of spontaneous regression of desmoids.[2,4] The major clinical problem with desmoids is their tendency to recur with frequencies ranging from 11.8 percent to 64.5 percent in several series.[2,4,7,11] Desmoids do not metastasize.[2,3,7,9]

Infiltrating ductal carcinoma, fat necrosis, and scar from previous surgery can present xeromammographic findings identical to an EAD in the axillary tail. The EAD in this report was believed to be a breast carcinoma based on its clinical and roentgenographic presentation. The pathologist's report of fibrous tissue on frozen section was surprising and caused the surgeon to forestall the radical mastectomy that he had planned. The importance of recognizing this conflicting triad of findings in directing the appropriate therapy cannot be overemphasized, and it is hoped that EAD will be considered when such an unexpected report is returned by the pathologist from the biopsy specimen.

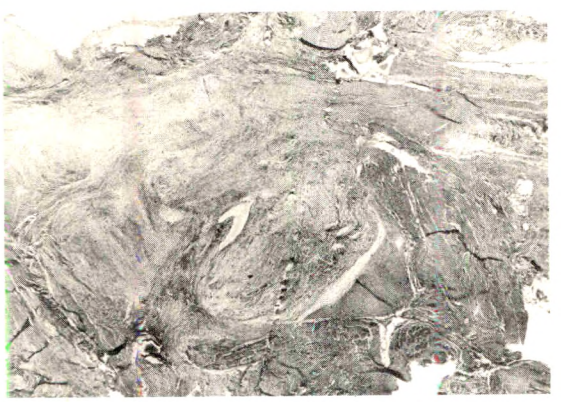


Fig. 3. Low power view of portion of mass, composed of dense, hypocellular fibrous tissue.

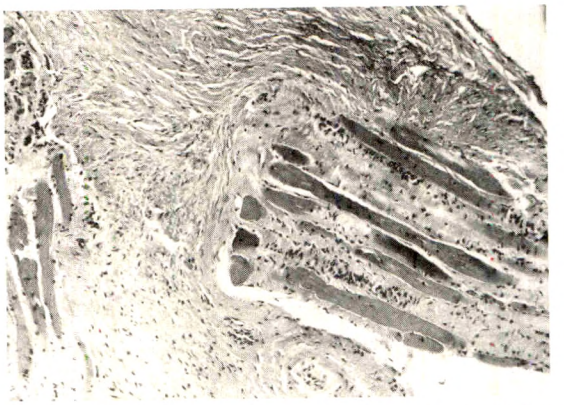


Fig. 4. High power view of lesion. Hypocellular fibrous tissue has dissected between bundles of muscle as well as individual muscle fibers.

Lester Kalisher, M.D.
Department of Radiology
Massachusetts General Hospital
Boston, Massachusetts 02114

REFERENCES

1. Booher, R. J., and Pack, G. T. Desmomas of abdominal wall in children. *Cancer*, 1951, *4*, 1052–1065.
2. Enzinger, F. M., and Shiraki, M. Musculoaponeurotic fibromatosis of shoulder girdle (extra-abdominal desmoid): analysis of 30 cases followed up for ten or more years. *Cancer*, 1967, *20*, 1131–1140.
3. Green, C. C. Desmoid tumor. *Arch. Surg.*, 1945, *50*, 304–306.
4. Hunt, R. T. N., Morgan, H. C., and Ackerman, L. V. Principles in management of extra-abdominal desmoids. *Cancer*, 1960, *13*, 825–836.
5. MacFarlane, J. Clinical reports of surgical practice of Glasgow Royal Infirmary, Glasgow, Scotland. D. Robertson, 1832, pp. 63–66.
6. Mason, J. B. Desmoid tumors. *Ann. Surg.*, 1930, *92*, 444–453.
7. Masson, J. K., and Soule, E. H. Desmoid tumors of head and neck. *Am. J. Surg.*, 1966, *112*, 615–622.
8. Müller, J. Ueber den feinern bau und die formen der krankhaften geschwülste. G. Reimer, Berlin, 1838.

9. MUSGROVE, J. E., and MCDONALD, J. R. Extra-abdominal desmoids; their differential diagnosis and treatment. *Arch. Path.*, 1948, *45*, 513–540.
10. NICHOLS, R. W. Desmoid tumors: report of thirty-one cases. *Arch. Surg.*, 1923, *7*, 227–236.
11. PEARMAN, R. O., and MAYO, C. W. Desmoid tumors: clinical and pathologic study. *Ann. Surg.*, 1942, *115*, 114–125.
12. SOULE, E. W., and SCANLON, P. W. Fibrosarcoma arising in extra-abdominal desmoid tumor: report of case. *Mayo Clin. Proc. Staff Meet.*, 1962, *37*, 443–450.
13. STEINITZ, F. S., and POPPER, H. L. Desmoid tumor of abdominal wall infiltrating splenic flexure of colon. *J.A.M.A.*, 1961, *176*, 610–612.
14. ZAYID, I., and DIHMIS, C. Familial multicentric fibromatosis-desmoids: report of three cases in Jordanian family. *Cancer*, 1969, *24*, 786–795.

AMERICAN ROENTGEN RAY SOCIETY

OFFICERS 1975–76

President: Ted F. Leigh.
President Elect: Seymour F. Ochsner.
1st Vice President: Edward B. Singleton.
2nd Vice President: Sidney W. Nelson.
Secretary: James F. Martin.
Treasurer: Joseph D. Calhoun.
Honorary President: C. L. Sherratt.

COMMITTEES 1975–76

Executive Council: T. F. Leigh, S. F. Ochsner, E. B. Singleton, J. F. Martin, J. D. Calhoun, M. M. Figley, T. Leucutia, H. C. Carlson, R. C. Pfister, R. A. Gagliardi, M. P. Capp, E. Gedgaudas, G. A. Kling, C. B. Holman, W. B. Seaman, E. C. Klatte, J. P. Tampas, J. L. Gwinn, C. E. Bickham, H. L. Friedell, Chairman.

Finance and Budget Committee: J. J. Stein, C. E. Bickham, R. McLelland, J. L. Gwinn, H. C. Carlson, Chairman.

Publication Committee: E. R. Heitzman, J. V. Rogers, K. Ellis, F. F. Ruzicka, Jr., R. A. Gagliardi, Chairman.

Editorial Policy Committee: M. M. Figley, E. F. Lang, L. W. Brady, K. L. Krabbenhoft, R. H. Morgan, E. R. Heitzman, J. V. Rogers, K. Ellis, F. F. Ruzicka, R. A. Gagliardi, Chairman.

Program Committee: T. F. Leigh, J. F. Martin, H. L. Friedell, M. M. Figley, R. A. Gagliardi, R. C. Pfister, E. Gedgaudas, G. A. Kling, M. P. Capp, S. F. Ochsner, Chairman.

Advisory Committee on Education and Research: G. W. Hartman, L. F. Rogers, E. Gedgaudas, A. E. James, M. P. Capp, Chairman.

Scientific Exhibits Committee: B. G. Brogdon, R. J. Alfidi, R. C. Pfister, Chairman.

Instruction Courses: Director, E. Gedgaudas, Associate Director, H. O. Peterson.

Representatives on the American Board of Radiology: R. W. McConnell, J. F. Roach, S. W. Nelson.

Representative on the Board of Chancellors and Council of the American College of Radiology: W. B. Seaman.

ANNUAL MEETING: September 20–24, 1976, Washington, D. C., Washington Hilton Hotel.

SCIENTIFIC PROGRAM: Seymour Ochsner, *President Elect*, Ochsner Clinic, New Orleans, La.

MANAGER ANNUAL MEETING: George A. Kling, Harper Hospital, Detroit, Mich.

MEMBERSHIP: Hymer Friedell, Chairman, Executive Council,
Case Western Reserve University, Cleveland, Ohio 44106.

BUSINESS OFFICE: Keith W. Gundlach, Comptroller, American College of Radiology,
20 North Wacker Drive, Chicago, Illinois 60606.

AMERICAN RADIUM SOCIETY

OFFICERS: 1975–76

President: Felix N. Rutledge.
President Elect: Luther W. Brady.
1st Vice President: Elliott Strong.
2nd Vice President: Alfred Sherman.
Secretary: Richard H. Jesse.
Treasurer: Fred W. George, III.

COMMITTEES 1975–76

Executive Committee: V. A. Marcial, F. N. Rutledge, L. W. Brady, E. Strong, R. H. Jesse, A. I. Sherman, F. George, A. Raventos, Chairman.

Public Relations Committee: W. J. Taylor, R. G. Parker, W. G. Cosbie, J. M. W. Gibson, Chairman.

Publication Committee: K. L. Krabbenhoft, A. F. Schroeder, L. W. Brady, Chairman.

Scientific Program Committee: L. W. Brady, D. Johnson, A. S. Ketcham, F. N. Rutledge, Chairman.

Janeway Lecture Committee: A. S. Ketcham, S. H. Levitt, L. W. Brady, Chairman.

Local Arrangements Committee: J. M. W. Gibson, Chairman.

Representatives on the American Board of Radiology: J. J. Stein, E. Richard King, R. M. Scott.

Representative on the Board of Chancellors of the American College of Radiology: J. A. del Regato.

Liaison Representative on the National Council on Radiation Protection and Measurements: Lawrence W. Davis.

ANNUAL MEETING: May 9–14, 1976, Vancouver, British Columbia, Bayshore Inn.

SCIENTIFIC PROGRAM: Felix N. Rutledge, *President*, Houston, Texas

LOCAL ARRANGEMENTS: John M. W. Gibson, Vancouver, British Columbia

MEMBERSHIP: Richard H. Jesse, *Secretary*, M. D. Anderson Hospital and Tumor Institute,
Houston, Texas 77025.

BUSINESS OFFICE: Richard H. Jesse, 6723 Bertner Avenue, M.D. Anderson Hospital and Tumor Institute,
Houston, Texas 77025.

EDITORIAL

IS NUCLEAR MEDICINE IN TROUBLE?

PHYSICIANS in the field of nuclear medicine are troubled that many of its recent scientific advances are not being used effectively for patient care. Until recently, the United States was the most progressive country in applying nuclear techniques to clinical medicine, but now this distinction is passing to other countries. Why is this happening?

Nuclear medicine in the United States is succumbing to what Daniel P. Moynihan[1] calls "the sickness of overgovernment." In radiology, it is ironic that the degree of escalation of bureaucratic control is inversely proportional to the radiation dose involved. Radiation therapy with its high exposure levels is relatively free of regulatory supervision, whereas diagnostic radiopharmaceuticals which impose far less exposure are controlled by many agencies. In some states, the number of governing agencies is greatest for *in vitro* procedures which expose the patient to no radiation at all! Similarly, the degree of regulatory concern bears no relation to the quantity of drug administered. The radiologist is relatively free to administer large doses of contrast media for angiography but is restricted in administration of miniscule amounts of radioactive compounds which are not on the "established" list.

Transfer of primary jurisdiction over the use of new radiopharmaceuticals from the Atomic Energy Commission to the Food and Drug Administration has been completed under recent federal law.[2] Nevertheless, the United States Nuclear Regulatory Commission (successor of the AEC) continues to retain some licensing control in "nonagreement states." Thirty-three "agreement states" and New York City have separate regulatory powers over licensing and radiopharmaceutical use. Moreover, many states now require nuclear medicine facilities to become licensed and to submit quarterly reports to their laboratory bureaus, resulting in still further duplication of regulatory control. Still more regulatory legislation is in the formative stage, including state licensing of nuclear technologists and a federal law governing hospital radiopharmaceutical operations.[2] Over a one year period in the state of New York, our radiology department was in communication with 32 separate regulatory bodies, including governmental agencies and other groups governing training programs and accreditation. A disproportionate amount of this paperwork was concerned with diagnostic radiopharmaceuticals.

The future of nuclear medicine in the United States will depend to a great extent on how rigidly the new FDA laws are interpreted. If they are administered overzealously, the development of new radiopharmaceuticals could become prohibitively expensive. A few excellent new agents, already in clinical use in Europe, will probably never become available here because of the excessive costs of new drug applications. Our leadership in the development and application of radioactive agents is being lost to Japan and Europe, as has already occurred in the development of antibiotics and other stable drugs.

The current "regulatory crisis" in nuclear medicine is unrelated to any increase in radiation risk or incidence of adverse reactions. There has been no thalidomide episode for radiopharmaceuticals to justify the bureaucratic escalation. Indeed, the incidence of untoward reactions from radioactive drugs has remained excep-

tionally low.[3] Long-lived radionuclides such as ^{203}Hg and ^{85}Sr, with their attendant high radiation dosage, have been replaced by more effective short-lived agents—in the course of progress, not by bureaucratic intervention.

The current situation in nuclear medicine exhibits the classical signs[4] of bureaucratic pollution which, like chemical pollution, begins slowly but increases insidiously and eventually endangers its subjects. Because of public concern about radioactivity and the potential risk of real overexposure to radiation, some degree of governmental regulation is essential; however, the number of regulations has escalated to the point where the public will not benefit by further unbridled expansion.

Satisfactory standards for all phases of medical care can never be achieved through regulatory agencies alone. Recently, we have experienced uncontrolled growth of bureaucratic costs together with severe cutbacks in research and educational grants, particularly in the radiological sciences. Public funds might better be spent restoring support for research and training of personnel rather than for replicating regulatory bodies.

Ponderous state and federal laws governing radioactivity urgently need revision to relieve the current administrative mess. Why can't we have just one regulatory agency at the federal level and just one at the state level? Why can't the existing agencies approve radiopharmaceuticals already known to be safe? How do we get out of the regulatory jungle?

John G. McAfee

State University of New York
Upstate Medical Center
Syracuse, New York 13210

REFERENCES

1. Moynihan, D. P. A diplomat's rhetoric. *Harper's*, *252*, 40, 1976.
2. Department of Health, Education and Welfare, Food and Drug Administration: Radioactive drugs and radioactive biological products. Title 21, Federal Register 40, no. 144, July 25, 1975.
3. Atkins, H. L. Adverse reactions to radiopharmaceuticals, *J. Nucl. Med.*, *13*, 232, 1972.
4. Peter, L. J. *The Peter Prescription*. New York, William Morman & Co., 1972.

NEWS ITEMS

NEW ORLEANS RADIOLOGY SOCIETY

The New Orleans Radiology Society presents the fourth annual Spring Roentgen Conference at the Marriott Hotel, New Orleans, Louisiana, May 6–8, 1976.

The distinguished faculty will present material especially for the radiologists doing general diagnostic radiology. The intent is to provide one and one-half days of concentrated instruction and, for those so inclined a magnificent social program.

The program is co-sponsored by the American College of Radiology and meets the criteria for 12 hours credit in Category 1 for the Physician's Recognition Award of the American Medical Association.

For further information, please contact: Abner M. Landry, M.D., New Orleans Radiology Society, P. O. Box 19024, New Orleans, Louisiana 70179.

ANGIOGRAPHY IN THE ACUTELY ILL PATIENT

A Course in "Angiography in the Acutely Ill Patient" sponsored by the Department of Radiology, St. Vincent's Hospital and Medical Center of New York will be held at the Hotel Commodore, New York, New York, May 12–14, 1976.

Numerous advances have been made in recent years in the field of angiography, both in technique and equipment, and therapeutic applications. Emphasis will be placed on summarizing this information and presenting it so that these techniques may be applied at all levels of radiology practice, but specifically to community hospital radiology practice.

The Guest Faculty will include Chiefs of Cardiovascular Radiology from major New York and European centers of angiography. The importance of "interventional" radiology in the community hospital will be stressed. Demonstration of catheters, techniques, and other specifics will be presented via panel discussion, audience participation and workshops in the angiography suites in the afternoon of May 14. Participation in the workshops will be limited due to space and early registration is suggested.

This course has been approved for 15 hours of Category 1 ACR credit.

For further information, please write to: Barry T. Katzen, M.D., Chief, Cardiovascular Radiology, St. Vincent's Hospital and Medical Center of New York, 153 West 11th Street, New York, New York 10011.

15TH ANNUAL RADIOLOGICAL SYMPOSIUM

The Tel Aviv University School of Medicine, The Municipal Medical Center of Tel Aviv and Jaffa and the Israeli Medical Society announce the 15th Annual Radiological Symposium to be held in a Kibbutz Guest House near Jerusalem and in the Ichilov Hospital in Tel Aviv, Israel, June 9–11, 1976.

The Annual Rigler Lecture will be delivered by Dean Sherman Mellinkoff of the University of California, Los Angeles on the subject of Medical Education. Additional subjects to be presented by a distinguished faculty from Israel and the United States are: Education in Roentgen Diagnosis; Oncological Research and Diagnosis; and Roentgen Pathologic Correlations.

For further information, please contact: Professor S. Schorr, Ichilov Hospital, Tel Aviv, Israel.

SEMINAR IN DIAGNOSTIC ULTRASOUND

The Montreal General Hospital and McGill University will present a Seminar in Diagnostic Ultrasound to be held at the Holiday Inn, Montreal, Quebec, Canada, June 24–26, 1976.

For further information, please contact: The Postgraduate Board, The Montreal

General Hospital, 650 Cedar Avenue, Montreal, Quebec, Canada H3G 1A4.

REFRESHER COURSE IN PHYSICS AND RADIOBIOLOGY

The College of Physicians & Surgeons, Columbia University, New York, will present a refresher course in physics and radiobiology for residents in radiology, May 10–14, 1976.

This course is designed specifically for radiology residents preparing for the boards. Topics include physics of radiodiagnosis, nuclear medicine, and radiation therapy.

For more information, please contact: Jose M. Ferrer, M.D., Associate Dean, Columbia University, College of Physicians & Surgeons, 630 West 168th Street, New York, New York 10032.

ACOUSTICAL IMAGING AND HOLOGRAPHY

The Seventh International Symposium on Acoustical Imaging and Holography will be held in Chicago, Illinois, August 30–September 1, 1976.

This three day symposium will serve as a forum for uniting all aspects of ultrasonic visualization. Papers will be presented on new techniques, theories, devices, applications and practical achievements for producing images by means of ultrasonic energy. Examples of topics covered are pulse echo and continuous wave imaging techniques, acoustic lens systems, shadow imaging, acoustical holography and reconstruction, real time and slow time techniques, computer aided reconstruction, image enhancement and tomography.

This year's symposium will focus on common aspects of imaging systems applicable over a broad frequence range from kilohertz to gigahertz and a broad application range from medicine, non-destructive testing, microscopy, underwater viewing and seismic mapping.

Call for Papers. Abstracts of candidate papers should be in the hands of the chairman prior to the deadline, May 14, 1976. Submit 10 copies, plus the original, 200 word maximum. For details on abstract preparation and further information, please contact the chairman: Dr. Lawrence W. Kessler, Sonoscan, Inc., 752 Foster Avenue, Bensenville, Illinois 60106.

CURRENT CONCEPTS IN RADIATION THERAPY

The Department of Therapeutic Radiology and the Office of Continuing Medical Education of the University of Minnesota Medical School announce the annual Continuation Course in "Current Concepts in Radiation Therapy" to be held in the Mayo Auditorium, May 5–7, 1976.

The course is designed primarily for therapeutic radiologists, general radiologists and residents. As in the past, an outstanding guest faculty has been assembled for the course under the direction of Dr. Seymour H. Levitt, Professor and Head, Department of Therapeutic Radiology. This guest faculty is as follows: Luther W. Brady, M.D., Philadelphia, Pennsylvania; William L. Caldwell, M.D., Madison, Wisconsin; Ronald A. Castellino, M.D., Stanford, California; Luis Delclos, M.D., Houston, Texas; Norah Du V. Tapley, M.D., Houston, Texas; Gilbert H. Fletcher, M.D., Houston, Texas; Leonard L. Gunderson, M.D., Salt Lake City, Utah; David H. Hussey, M.D., Houston, Texas; Carlos A. Perez, M.D., St. Louis, Missouri; Marvin M. Romsdahl, M.D., Houston, Texas; and J. Taylor Wharton, M.D., Houston, Texas. The remainder of the faculty will include members of the teaching staff of the University of Minnesota Medical School.

For further information, please contact: Office of Continuing Medical Education, Nolte Center for Continuing Education, University of Minnesota, Minneapolis, Minnesota 55455.

AMERICAN ASSOCIATION OF PHYSICISTS IN MEDICINE

The American Association of Physicists in Medicine Summer School, "Physics of Clinical Nuclear Medicine" will be held in

Lexington, Kentucky, July 24–29, 1977.

For further information, please contact: Guy H. Simmons, Ph.D., Nuclear Medicine Department, Veterans Administration Hospital, Lexington, Kentucky 40407.

The 19th Annual Meeting will be held in Cincinnati, Ohio, July 31–August 4, 1977.

For further information, please contact: James G. Kereiakes, Ph.D., E555 Medical Sciences Building, University of Cincinnati, Cincinnati, Ohio 45267.

RADIATION PHYSICS AND BIOLOGY

A five day Refresher Course in Radiation Physics and Biology will be given by the Department of Radiology of the New York University Medical Center in the Alumni Hall, Classroom B, May 3–7, 1976.

This course is preparatory for written and oral examinations in Diagnostic Radiology and Nuclear Medicine.

The course is accredited for 30 hours of Category 1.

For further information, please contact: Miss Jean Carpenter, Office of the Recorder, Room 4-44N, LHB, New York University Post Graduate Medical School, 550 First Avenue, New York, New York 10016.

BOOK REVIEWS

Atlas of Hand Radiographs. By Philip Jacobs, T.D., D.M.R.D., F.R.C.P., F.F.R., Consultant Radiologist, Royal Orthopaedic Hospital, Birmingham, Birmingham General Hospital, Birmingham Accident Hospital, and Warwickshire Orthopaedic Hospital for Children; Clinical Lecturer in Radiology, University of Birmingham, England. Cloth. Pp. 246, with 300 illustrations. Price, $24.50. University Park Press, Chamber of Commerce Building, Baltimore, Md. 21202, 1973.

The Hand in Radiologic Diagnosis. By Andrew K. Poznanski, M.D., Professor of Radiology, The University of Michigan; Co-Director of Pediatric Radiology, C. S. Mott Children's Hospital, The University of Michigan; Research Scientist, Center for Human Growth and Development, The University of Michigan, Ann Arbor, Mich. Cloth. Pp. 588, with many illustrations. W. B. Saunders Company, West Washington Square, Philadelphia, Pa. 19105, 1974.

Roentgen Appearance of the Hand in Diffuse Disease. By Howard L. Steinbach, M.D., Chief of Radiology, French Hospital, San Francisco; Clinical Professor of Radiology and Medicine, University of California, San Francisco Medical Center; Clinical Professor of Radiology, Stanford University School of Medicine, Stanford, Calif.; Richard H. Gold, M.D., Associate Professor of Radiological Sciences: Chief, Orthopedic Radiology Section, University of California, Los Angeles Center for the Health Sciences; and Leslie Preger, M.B., Ch.B., F.R.C.R., D. Obst., R.C.O.G., F.F.R.R.C.S. (IREL.), Assistant Chief of Radiology, French Hospital, San Francisco; Associate Clinical Professor of Radiology, University of California, San Francisco Medical Center. Cloth. Pp. 528, with 401 figures. Price, $47.75. Year Book Medical Publishers, Inc., 35 East Wacker Drive, Chicago, Ill. 60601, 1975.

Congenital Deformities of the Hand and Forearm. By H. Kelikian, M.D., Emeritus Professor of Orthopedic Surgery, Northwestern University Medical School; Senior Attending Orthopedic Surgeon, Northwestern Memorial Hospital, Chicago; and Consulting Orthopedic Surgeon, Bethany Methodist, Henrotin and Augustana Hospitals, Chicago, Ill. Cloth. Pp. 1,007, with 620 illustrations. Price, $35.00. W. B. Saunders Company, West Washington Square, Philadelphia, Pa. 19105, 1974.

Here are four excellent volumes, all dealing with the hand, all different, and each well characterized by its title.

The atlas by Dr. Jacobs is purely an atlas, with beautiful, life size reproductions of roentgenograms of the hand and wrist. The text material is limited to the captions, and occasionally includes more than the statement of the diagnosis. The material is well organized, and the 300 illustrations show both common and unusual diseases encountered in the hand, except for trauma.

The volume edited by Dr. Poznanski is written principally by him, with a few contributions from others. It is a much more elaborate undertaking, and covers much more material. Sections made up of several chapters each, cover the normal hand and various techniques of examination; variants and anomalies; congenital abnormalities; and acquired diseases, including trauma, neoplasm, infection, arthritis, hematologic disorders and metabolic problems.

The discussion of each individual disease condition is followed by its short list of references, and the discussions are succinct, thorough, and well written. Scattered throughout are interesting facts from history, geography, anthropology, and similar disciplines—all designed to make this more than a list of diseases, symptoms and roentgen changes. The illustrations are clear, with elaborate legends. There is an excellent index.

Drs. Steinbach, Gold, and Preger point out some of the advantages of studying diffuse diseases by examination of the hand: several types of bone shape and structure are available; exquisite bone detail is possible because of the thin, overlying soft tissues; excellent soft tissue detail in cartilage, tendons and ligaments can be obtained; and low radiation exposure is given to the patient. The authors' emphasis is on diffuse bone disease, and the volume is a storehouse of information. It is divided into an unillustrated text portion and an atlas, so that the roentgen manifestations in the numer-

ous hand illustrations may be readily compared with each other. Leafing through the illustrations thus collected in one section of the book may even solve the problem of an unknown film, and may make reference to the text portion unnecessary because of the generous legends which are supplied.

The text is extensive and gives thorough discussions covering the nature of the disease, its incidence, cause, hereditary pattern, clinical features, pathologic picture, including the laboratory values, roentgen features, and differential diagnosis. Each of more than 100 short chapters is followed by its bibliography.

The index is not complete, but this is compensated for by the organization of the text and the table of contents. The book is divided into nine parts, covering subjects such as arthritis, constitutional disease of known etiology, dysostosis, etc., and each of these parts is divided into sections, with the individual chapters limited, in general, to a discussion of an individual disease.

The beautiful volume by Dr. Kelikian is obviously a labor of love and is a bibliophile's dream. Written by an orthopedic surgeon, it records his work in the surgery of congenital deformities of the hand and forearm, and in addition covers the history and others' treatment as well. It is an encyclopedic treatment of the subject, and covers the classification, etiology, diagnosis, and treatment of anomalies. Each individual deformity is given elaborate consideration from these points of view, although the problems of treatment in general are included in one chapter, and in the consideration of the individual deformities the emphasis is on diagnosis, prognosis, and results. The book is well organized and cross-indexed, to avoid duplication, and it has a wealth of references.

An outstanding feature is the way in which the book is illustrated. There are innumerable photographs, showing hands before and after treatment; there are almost as many roentgenograms and line drawings illustrating the deformities. The author's humane, philosophical attitude shines through on each page. At the end of each chapter there is a summary, an unusual feature, expressing the heart of the matter in a paragraph. This use of a summary indicated the orderly thinking, the assignment of precedence, and the total grasp of the subject possessed by the author.

It is my opinion that the volumes by Poznanski and Steinbach, Gold and Preger should be in the personal library of every radiologist who sees either adults or children for classification of bone diseases. They are complete, well-organized, annotated, and make the information readily available. The atlas by Jacobs is a more specialized book, and would be most important for the beginning or occasional radiologist. The volume by Kelikian is also specialized; for a surgeon or orthopedic surgeon who sees patients with congenital abnormalities, it is a treasure. For the radiologist it is less nearly essential, but should be in libraries, as it is a collection of material for which one might otherwise search in many different sources, and will no doubt become a classic in its field.

E. Frederick Lang, M.D.

Technology and Interpretation of Nuclear Medicine Procedures. By D. Bruce Sodee, M.D., F.A.C.P., F.A.C.G., A.B.N.M., Director, Nuclear Medicine Institute; Director, Nuclear Medicine Department, Hillcrest Hospital, Cleveland Memorial Foundation, Cleveland, Ohio; and Paul J. Early, B.S., President, Nuclear Medicine Associates, Inc., Cleveland, Ohio; with the technical assistance of Ashwin Patel, B.S., R.T. (A.R.R.T.). Second edition. Cloth. Pp. 520, with many illustrations. Price, $26.50. C. V. Mosby Company, 3301 Washington Boulevard, St. Louis, Mo. 63103, 1975.

The book is in its second edition with the first edition appearing in 1972. It is to be correlated with its companion volume, "Textbook of Nuclear Medicine Technology" which is also in its second edition. Both second editions have been updated and revised.

There are 20 outstanding contributors in addition to the authors. The book is divided into two parts: Part I, "Nuclear Science," is concerned with physics, laboratory technique, health physics and nursing. There are 41 chapters with 169 pages. Part II, "Clinical Nuclear Medicine," is concerned with nuclear laboratory procedures, dynamic perfusion/scanning and imaging procedures and special nuclear procedures. There are 22 chapters with 322 pages.

Each test or procedure is well described, giving the purpose, indications, materials needed and patient preparation. Key points, pitfalls and interpretation of results are given at the end of each test or procedure and are very helpful. There are exercises in Part I which are

learning experiences regarding basic principles of nuclear instrumentation, radiochemistry and health physics. Some of the newer procedures that are not classified as routine are not included in the book.

It is a good reference book in that it provides a review of nuclear medicine for those who have become rusty regarding the fundamentals and the reasons for the steps and procedures that are used in the various tests.

The book is understandable and contains much new information.

"Technology and Interpretation of Nuclear Medicine Procedures" is an excellent book for the beginner in nuclear medicine as well as for those who are practicing nuclear medicine.

Charles W. Cooley, M.D.

Radiologic and Other Biophysical Methods in Tumor Diagnosis. A Collection of Papers Presented at the Eighteenth Annual Clinical Conference on Cancer, 1973, at the University of Texas System Cancer Center M. D. Anderson Hospital and Tumor Institute, Houston Texas. Cloth. Pp. 486, with 248 illustrations. Price, $32.50. Year Book Medical Publishers, Inc., 35 E. Wacker Drive, Chicago, Ill. 60601, 1975.

This book is a collection of papers presented in 1973 at a conference devoted to tests used in diagnosis of malignancy. It serves as an excellent introduction to the subject.

The book is essentially divided into two portions. The first is a section describing the physical methods upon which a given diagnostic test is founded; and the second is a discussion of the application of these methods and tests to various forms of abnormality. These two parts are skillfully combined and furnish the reader with the essentials for discussing these topics. Unfortunately, there is no list of references which would permit up-dating the contents in regard to the advances which have occurred between 1973 and the time of publication, 1975.

The book is well packaged and easily read and this is usual with the efforts of Dr. Clark and the University of Texas System Cancer Center. There is a discussion of the advantages and disadvantages of the biophysical techniques and procedures. It is a valuable reference for physicians whose principal interest is cancer, but the book is likewise a reference for the general clinician and should be included in libraries.

Michael D. Henderson, M.D.

MIRD Committee Publications. Pamphlet 10: Radionuclide Decay Schemes and Nuclear Parameters for Use in Radiation-Dose Estimation. Pp. 125. Price, $8.75 with binder, $6.50 without binder. Pamphlet 11: Absorbed Dose per Unit Cumulated Activity for Selected Radionuclides and Organs. Pp. 255. Price, $10.20 with binder, $7.95 without binder. MIRD Committee, 404 Church Avenue, Suite 15, Maryville, Tenn. 37801.

Pamphlet No. 10 presents decay schemes and input and output data, including equilibrium dose constants, for about 120 radionuclides. This is more than double the number covered in MIRD No. 4 and includes nearly every one of interest in nuclear medicine. Unfortunately, Thallium-201 is not included.

Pamphlet No. 11 is concerned with dosimetry. When measurements are made to determine the doses delivered by new radiopharmaceuticals, usually tagged with one of a few dozen radionuclides, on a standard system, namely the human body, it is desirable to simplify the application of the MIRD dose equation by separating anatomical and physical quantities from biological quantities. This separation has been done in MIRD No. 11 and the result is 250 pages of values for "S", the absorbed dose per unit cumulated activity, for combinations of 20 source and 20 target organs and 117 radionuclides. One need only look up the "S's" for the combinations of interest, multiply by the cumulated activities in the source organs and sum over source organs.

The revisions in the Monte Carlo calculations and the organ mass changes in the phantom from MIRD No. 5 are incorporated in the results of this pamphlet.

If one is satisfied with the assumption of uniform radionuclide distribution in organs and the details of the phantom this pamphlet can be a real work saver.

Robert Heck, Ph.D.

BOOKS RECEIVED

"Trauma" and "No-Trauma" of the Cervical Spine. Edited by Kenneth R. Kattan, M.D., Associate Professor of Radiology, University of Cincinnati College of Medicine; Attending Radiologist, Cincinnati General Hospital; Radiologist in Charge, Shriner's Burns Institute; Consultant Radiologist, Veteran's Administration Hospital, Cincinnati and Dayton, Ohio; Consultant in

Nuclear Medicine, The Jewish Hospital, Cincinnati, Ohio. Cloth. Pp. 312, with many illustrations. Price, $24.50. Charles C Thomas, Publisher, 301–327 East Lawrence Avenue, Springfield, Ill. 62717, 1975.

The Pathogenesis of Reflux Nephropathy (Chronic Atrophic Pyelonephritis). By C. John Hodson, F.R.C.P., F.R.C.R., Professor and Chairman of the Department of Radiology, Memorial University of Newfoundland, St. John's, Newfoundland, Canada; Thomas M. J. Maling, M.B., B.Ch., M.C.R.A., F.R.C.R., Department of Radiology, Christchurch General Hospital, Christchurch, New Zealand; Patrick J. McManamon, M.B., B.Ch., L.G.M.C., F.R.C.R., Department of Radiology, The General Hospital, St. John's, Newfoundland, Canada; and Martin G. Lewis, M.B., B.S., M.D., M.R.C.Path., Director, Cancer Research Unit, McGill University, P. O. Box 6070, Montreal, Quebec, Canada. Paper. Pp. 26, with some illustrations. Price, £1.90. British Journal of Radiology Supplement No. 13. British Journal of Radiology, 32 Welbeck Street, London, WIM 7PG, England, 1975.

The Radiologic Clinics of North America. December, 1975. Volume XIII, No. 3. Symposium on B-Scan Ultrasound. Guest Editor, Roger C. Sanders, M.D. Cloth. Pp. 198, with many illustrations. W. B. Saunders Company, West Washington Square, Philadelphia, Pa. 19105, 1975.

SOCIETY PROCEEDINGS

MEETINGS OF RADIOLOGICAL SOCIETIES*

United States of America

American Roentgen Ray Society
Secretary, Dr. James Franklin Martin, 300 S. Hawthorne Rd., Winston-Salem, N. C. 27103. Annual Meeting: Washington Hilton, Washington, D. C., Sept. 20–24, 1976.

American Radium Society
Secretary, Richard H. Jesse, Dept. of Surgery, M. D. Anderson Hosp. and Tumor Institute, Houston, Tex. 77025. Annual Meeting: Bayshore Inn, Vancouver, B. C., Canada, May 9–14, 1976.

Radiological Society of North America
Secretary, Dr. Theodore A. Tristan, Harrisburg, Pennsylvania. Annual Meeting: McCormick Place on the Lake, Chicago, Ill., Nov. 14–19, 1976.

American College of Radiology
Executive Director, William C. Stronach, 20 N. Wacker Drive, Chicago, Ill. 60606. Annual meeting.

Section on Radiology, American Medical Association
Secretary, Dr. Antolin Raventos, Davis, Calif. Annual Meeting.

American Board of Radiology
Secretary, Dr. C. Allen Good. Correspondence should be directed to Kahler East, Rochester, Minn. 55901.
Oral examinations will be held: Marriott Motor Hotel, Chicago, Ill., June 14–19, 1976; Sheraton Biltmore, Atlanta, Ga., Dec. 6–11, 1976.
Written examinations will be held in 14 selected sites on June 26, 1976.
Applications must be received in the Board Office before Sept. 30 of the year preceding the one in which the candidate wishes to be examined.

American Board of Nuclear Medicine, Inc. A Conjoint Board of the American Boards of Internal Medicine, Pathology and Radiology and sponsored by the Society of Nuclear Medicine.
Application forms and further information are available from the American Board of Nuclear Medicine, 305 E. 45th St., New York, N. Y. 10017.

American Association of Physicists in Medicine
Secretary, Dr. Robert G. Waggener, Dept. Radiol., Univ. Tex. Health Sciences Center, San Antonio, Tex. 78284
Annual Meeting: Cincinnati, Ohio, July 31–Aug. 4, 1977.

American Society of Therapeutic Radiologists
Secretary, Dr. Robert W. Edland, 1836 South Ave., La Crosse, Wis., 54601. Annual Meeting:

American Nuclear Society
Program Chairman, Werner K. Kern, IRD, Space Nuclear Systems, F 309, U. S. Atomic Energy Commission, Washington, D.C. 20545.

American Institute of Ultrasound in Medicine
Secretary, John M. Reid, Ph.D., 556 18th Ave., Seattle, Wash. 98122. Annual Meeting.

American Society of Neuroradiology
Secretary, Arthur E. Rosenbaum, University of Pittsburgh, Pittsburgh, Pa. 15261. Annual Meeting: Peachtree Plaza Hotel, Atlanta, Ga., May 18–22, 1976.

Fourteenth International Congress of Radiology
Rio de Janeiro, Brazil, Oct. 23–29, 1977.
President Elect: Prof. Dr. Nicola C. Caminha; *General Secretary:* Dr. Durval Couto. Av. Churchill, 97-50 and-LC-39 20,000 Rio de Janeiro, Brazil.

International Society of Radiology
Hon. Secretary-Treasurer, Prof. W. A. Fuchs, M.D., Department of Diagnostic Radiology, University Hospital, Inselspital, CH-3010 Bern, Switzerland.

Twelfth Inter-American Congress of Radiology
President, Dr. Publio Vargas Pazzos, Casilla 5227, Guayaquil, Ecuador. Meeting in Quito, Ecuador, 1979.

Inter-American College of Radiology
President, Manuel Viamonte, Jr., M.D., Mt. Sinai Medical Center, 4300 Alton Rd., Miami Beach, Fla. 33140.
Secretary, Gaston Morillo, M.D., Jackson Memorial Hosp., 1700 N.W. 10th Ave., Miami, Fla. 33152.
Counselor for the United States, J. A. del Regato, M.D., Univ. of So. Fla. College of Medicine, 13000 No. 30th St., Tampa, Fla. 33612.

Third Congress of the European Association of Radiology
Secretary-General, P.O. Box 14, 79 Lauriston Place, Edinburgh BHI IDB, Scotland.

Second Asian and Oceanian Congress of Radiology
Secretary, Dr. Buenaventura U. V. Angtuaco, Congress Secretariat Headquarters, 2161 Taft Ave., Manila, Philippines. Meeting:

Alabama Chapter of ACR
Secretary-Treasurer, Dr. Lawrence E. Fetterman, 1720 Springhill Ave., Suite 201, Mobile, Ala. 36604. Meets time and place of Alabama State Medical Association.

Alaska Radiological Society, Chapter of ACR
Secretary-Treasurer, Dr. Maurice J. Coyle, 3200 Providence Ave., Anchorage, Alaska 99504.

American Osteopathic College of Radiology
Annual Scientific Meeting: Americana Hotel, Bar Harbor, Fla. Program Administrator: Lawrence J. Jordan, D.O., Suite 21, Ponce American Bldg., 4601 Ponce de Leon Blvd., Coral Gables, Fla. 33146.

American Thermographic Society
Secretary-Treasurer, John Wallace, Ph.D., Dept. Radiol., Thomas Jefferson Univ. Hosp., Philadelphia, Pa. 19107. Annual Meeting.

Arizona Radiological Society, Chapter of ACR
Secretary, Dr. Irwin M. Freundlich, 1501 N. Campbell Ave., Dept. Radiol., Tucson, 85724. Two regular meetings a year. Annual meeting at time and place of State Medical Association and interim meeting six months later.

Ark-La-Tex Radiological Society
Secretary, Dr. Erich K. Lang, 1541 Kings Highway, Shreveport, La. 71130. Meets monthly on fourth Wednesday, 8:00 P.M., Sept. to May.

Arkansas Chapter of ACR
Secretary-Treasurer, Dr. Richard Seibold, Jr., Wadley Hosp., Texarkana, Ark.—Tex. 75501. Meets twice annually, the Spring Meeting being in conjunction with and at the place of the State Medical Association.

Association of University Radiologists
Secretary-Treasurer, Dr. Arch W. Templeton, Univ. of Kansas Med. Center, 39th and Rainbow Blvd., Kansas City, Kansas 66103. Annual Meeting.

Atlanta Radiological Society
Secretary-Treasurer, Dr. James H. Larose, Dept. Nuclear Med., South Fulton Hosp., East Point, Ga. 30344. Meets on four Thursday evenings during the academic year at a time announced in early September of each year, at various Atlanta restaurants.

*** Secretaries of societies are requested to send timely information promptly to the Editor.**

BAVARIAN-AMERICAN RADIOLOGIC SOCIETY
Secretary, LTC. Marco J. DiBiase, M.D., Radiology Service, Heidelberg, 130 Station Hosp., APO N. Y. 09102. Meets quarterly.

BLOCKLEY RADIOLOGICAL SOCIETY
Secretary-Treasurer, Dr. William H. Green, 616 East 24th St., Chester, Pa. 19013.

BLUEGRASS RADIOLOGICAL SOCIETY
Secretary-Treasurer, Dr. James C. King, Jr., 3313 Overbrook Drive, Lexington, Ky. 40502. The Society meets once each month during the school year.

BRONX RADIOLOGICAL SOCIETY, NEW YORK STATE, CHAPTER ACR
Secretary-Treasurer, Dr. Leon J. Corbin, 1369 Rosendale Ave., Bronx, N. Y. 10472. Meets 4 times a year.

BROOKLYN RADIOLOGICAL SOCIETY
Secretary-Treasurer, Dr. Ralph Brancaccio, 7901 4th Ave., Brooklyn, N. Y. 11209. Meets first Thursday of each month, October through June.

BUFFALO RADIOLOGICAL SOCIETY
Secretary, Dr. George J. Alker, Jr., E. J. Meyer Mem. Hosp., Buffalo, N. Y. 14215. Meets second Monday evening each month, October to May inclusive, at University Club.

CALIFORNIA RADIATION THERAPY ASSOCIATION
Secretary-Treasurer, Dr. Duane J. Gillum, Stanford Medical Center, Stanford, Calif. 94304. Meets semiannually in San Francisco and Los Angeles.

CALIFORNIA RADIOLOGICAL SOCIETY, CALIFORNIA CHAPTER OF ACR
Secretary-Treasurer, Dr. John L. Gwinn, 4650 Sunset Blvd., Los Angeles, Calif. 90027.

CATAWBA VALLEY RADIOLOGICAL SOCIETY
Secretary, Dr. Walter Joe Jacumin, P.O. Box 265, Rutherford College, N. C. 28671. Meets the last Thursday of every month, Holiday Inn, Morganton, N. C. at 7:30 P.M.

CENTRAL NEW YORK RADIOLOGICAL SOCIETY
Secretary-Treasurer, Dr. Alfred Brettner, Auburn Mem. Hosp., Auburn, N. Y. 13021. Meets first Monday each month October through May.

CENTRAL OHIO RADIOLOGICAL SOCIETY
Secretary-Treasurer, Dr. Daniel E. Lewis, 309 East State St., Columbus, Ohio 43215. Meets second Thursday in October, November, January, March, and May at Fort Hayes Hotel, Columbus, Ohio.

CENTRAL TEXAS RADIOLOGY SOCIETY
Secretary-Treasurer Dr. E. Jerome Schoolar, Scott and White Clinic, Temple, Tex. 76501. Meets the fourth Monday of each month at Ponderosa Hotel, Temple, Tex. at 7:00 P.M.

CHICAGO RADIOLOGICAL SOCIETY, DIVISION OF THE ILLINOIS RADIOLOGICAL SOCIETY, CHAPTER OF ACR
Secretary-Treasurer, Dr. Harold J. Lasky, 55 E. Washington St., Suite 1735, Chicago, Ill. 60602. Meets third Thursday of each month, October to April, except December, at the Bismark Hotel, Chicago, Ill.

CLEVELAND RADIOLOGICAL SOCIETY
Secretary-Treasurer, Dr. Charles M. Greenwald, 7007 Powers Blvd., X-Ray Dept., Parma, Ohio 44129. Meetings at 7:00 P.M. on fourth Monday of October, November, January, February, March and fifth Monday of April.

COLORADO RADIOLOGICAL SOCIETY, CHAPTER OF ACR
Secretary, Dr. John Pettigrew, Denver, Colo. Meets third Friday of each month at Denver Athletic Club from September through May.

CONNECTICUT VALLEY RADIOLOGIC SOCIETY
Secretary, Dr. Gerald N. LaPierre, 759 Chestnut St., Springfield, Mass. 01107. Meets in April and October.

DALLAS-FORT WORTH RADIOLOGICAL SOCIETY
Secretary-Treasurer, Dr. Robert R. Burns, 1400 Stemmons Ave., Dallas, Tex. 75208. Meets the 3rd Monday of every month at 6:30 P.M., at the Airport Hotel, Arlington, Tex.

DELAWARE CHAPTER OF ACR
Secretary, Dr. Ekkehard S. Schubert, Wilmington Med. Center, P. O. Box 1951, Wilmington, Del. 19899

EAST BAY RADIOLOGICAL SOCIETY
Secretary-Treasurer, Dr. Richard H. Culhane, 4 Vista del Mar, Orinda, Calif. 74563. Meets first Thursday each month, Oct. through May, at University Club, Oakland Calif.

EAST TENNESSEE RADIOLOGICAL SOCIETY
Secretary-Treasurer, Dr. George H. Wood, 205 Medical Arts Bldg., Knoxville, Tenn. 37902. Meets in January and September.

FLORIDA RADIOLOGICAL SOCIETY, CHAPTER OF ACR
Secretary. Dr. Paul J. Popovich, 1350 S. Hickory St., Melbourne, Fla. 32901. Meets twice annually, in the spring with the Annual State Society Meeting and in the fall.

FLORIDA WEST COAST RADIOLOGICAL SOCIETY
Secretary-Treasurer, Dr. Herbert Johnson, Davis Blvd., Tampa, Fla. 33606. Meets on 4th Thursday of the months January, March, May, October, and November.

GEORGIA RADIOLOGICAL SOCIETY, CHAPTER OF ACR
Secretary, Dr. E. P. Rasmussen, Piedmont Prof. Bldg., 35 Collier Rd., N.W., Atlanta, Ga. 30309.

GREATER CINCINNATI RADIOLOGICAL SOCIETY
Secretary-Treasurer, Dr. Owen L. Brown, 2421 Auburn Ave., Cincinnati, Ohio 45219.

GREATER KANSAS CITY RADIOLOGICAL SOCIETY
President-Secretary, Dr. Jay I. Rozen, Suite 216, 6400 Prospect, Kansas City, Mo. 64132. Meets 5 times a year.

GREATER LOUISVILLE RADIOLOGICAL SOCIETY
Secretary-Treasurer, Dr. L. D. LeNeave, 315 E. Broadway, Louisville, Ky. 40202. Meets monthly.

GREATER MIAMI RADIOLOGICAL SOCIETY
Secretary, Dr. David C. Hillman, P. O. Box 610544, North Miami, Fla. 33161. Meets monthly, third Wednesday at 8:00 P.M. at various member hospitals, Miami, Fla.

GREATER ST. LOUIS SOCIETY OF RADIOLOGISTS
Secretary-Treasurer, Dr. Donald Callahan, Northland Med. Bldg., Jennings, Mo. 63136.

HAWAII RADIOLOGICAL SOCIETY, CHAPTER OF ACR
Secretary-Treasurer, Dr. Michael J. McCabe, Straub Clinic and Hosp., Honolulu, Hawaii 96813. Meets third Monday of each month at 7:00 P.M.

HEALTH PHYSICS SOCIETY
Secretary, Russell F. Cowing, P.O. Box 156, E. Weymouth, Mass. 02189. Annual Meeting.

HOUSTON RADIOLOGICAL SOCIETY
Secretary, Dr. Neill B. Longley, 6436 Fannin, Suite 601, Houston, Tex. 77025. Meets fourth Monday of each month, except June, July, August and December, at 6:00 P.M., at 103 Jesse H. Jones Library Building, Texas Medical Center, Houston, Tex. 77025.

IDAHO STATE RADIOLOGICAL SOCIETY, CHAPTER OF ACR
Secretary-Treasurer, Dr. John H. Truksa, 1605 Park Ave., Nampa, Id. 83651. Meets in the spring and fall.

ILLINOIS RADIOLOGICAL SOCIETY, INC., CHAPTER OF ACR
Secretary, Dr. Robert D. Dooley, Hinsdale Med. Center, Hinsdale, Ill. 60521. Meets in the spring and fall.

INDIANA ROENTGEN SOCIETY, INC., CHAPTER OF ACR
Secretary, Dr. John A. Knote, Home Hosp., Lafayette, Ind. 47902.

IOWA RADIOLOGICAL SOCIETY, CHAPTER OF ACR
Secretary-Treasurer, Dr. Dale L. Roberson, 1948 First Ave., NE, Cedar Rapids, Iowa 52402. Luncheon and business meeting during annual session of Iowa State Medical Society. The scientific session is held in the autumn.

KANSAS RADIOLOGICAL SOCIETY, CHAPTER OF ACR
Secretary-Treasurer, Dr. Ralph H. Baehr, 310 Medical Arts Bldg., Topeka, Kan. 66604. Meets in spring with State Medical Society and in winter on call.

KENTUCKY CHAPTER OF ACR
Secretary-Treasurer, Dr. Bernard Sams, St. Joseph In-

firmary, 735 Eastern Parkway, Louisville, Ky. 40217. Meets in April and September.

Kings County Radiological Society
Secretary, Dr. Sidney Hendler, 1880 Ocean Ave., Brooklyn 30, N. Y. Meets Kings County Med. Soc. Bldg. monthly on fourth Thursday, October to May, 8:45 P.M.

Knoxville Radiological Society
Secretary, Dr. Clifford L. Walton, Blount Professional Bldg., Knoxville 20, Tenn. Meetings are held the third Monday of every other month at the University of Tennessee Memorial Research Center and Hospital.

Long Island Radiological Society
Secretary, Dr. Harry L. Stein, North Shore Univ. Hosp., 300 Community Dr., Manhasset, N. Y. 11030.

Los Angeles Radiological Society
Secretary, Dr. Arthur F. Schanche, 333 North Prairie Ave., Inglewood, Calif. 90301. Meets second Wednesday of month in September, November, January, April and June at Los Angeles County Medical Association Building, Los Angeles, Calif. Midwinter Radiological Conference. Century Plaza Hotel, Los Angeles, Calif.

Louisiana Radiological Society, Chapter of ACR
Secretary-Treasurer, Dr. Roger H. Tutton, 1514 Jefferson Hwy., New Orleans, La. 70121.

Louisiana-Texas Gulf Coast Radiological Society
Secretary-Treasurer, Dr. J. Gardiner Bourque, 3155 Stagg Dr., Suite 230, Doctors Bldg., Beaumont, Texas 77701.

Maine Radiological Society, Chapter of ACR
Secretary-Treasurer, Dr. Peter E. Giustra, Dept. Radiology, Penobscot Bay Medical Center, Rockland, Maine 04841. Meets in June, September, December and April.

Maryland Radiological Society, Chapter of ACR
Secretary, Dr. David S. O'Brien, Anne Arundel Hosp., Annapolis, Md. 21401.

Massachusetts Radiological Society, Chapter of ACR
Secretary, Dr. Joseph T. Ferrucci, Jr., Massachusetts Gen. Hosp., Boston, Mass. 02114.

Memphis Roentgen Society
Secretary-Treasurer, Dr. R. Randolph Ramey, Baptist Memorial Hosp., 899 Madison Ave., Memphis, Tenn. 38146. Meets first Monday Oct. through June at the University Club.

Miami Valley Radiological Society
Secretary, Dr. Bert Must, I.B.M. Bldg., Dayton, Ohio. Meets third Thursday of fall, winter and spring months at 7:30 P.M. at Miami Valley Hospital, Dayton, Ohio.

Michigan Radiological Society, Chapter of ACR
Secretary-Treasurer, Dr. Francis P. Shea, Harper Hospital, 3825 Brush St., Detroit, Mich. 48201. Meets monthly, first Thursday, October through May, at David Whitney House, 1010 Antietam, at 6:30 P.M.

Michigan Society of Therapeutic Radiologists
Secretary-Treasurer, Dr. William I. Knapp, St. Mary's Hosp., 830 S. Jefferson, Saginaw, Mich. 48601. Meets bimonthly during the academic year.

Mid-Hudson Radiological Society
Secretary-Treasurer, Dr. William D. Stiehm, 37 Flower Hill Rd., Poughkeepsie, N. Y. 12603. Meets 7:00 P.M., first Wednesday of each month, September to May.

Milwaukee Roentgen Ray Society
Secretary-Treasurer, Dr. Thomas C. Lipscomb, 1004 North Tenth St., Milwaukee, Wis. 53233. Meets monthly on fourth Monday, October through May, at University Club.

Minnesota Radiological Society, Chapter of ACR
Secretary-Treasurer, Dr. Marvin E. Goldberg, Box 292, Mayo Memorial Health Sciences Center, Minneapolis, Minn. 55455.

Mississippi State Radiological Society, Chapter of ACR
Secretary-Treasurer, Dr. Edward L. Gieger, 969 Lakeland Dr., Jackson, Miss. 39216. Meets third Thursday, excluding summer months, at the Primos Northgate Rest., Jackson at 6:30 P.M.

Missouri Radiological Society, Chapter of ACR
Secretary-Treasurer, Dr. Ronald G. Evens, Mallinckrodt Institute of Radiology, 510 S. Kingshighway, St. Louis, Mo. 63110.

Montana Radiological Society, Chapter of ACR
Secretary, Dr. C. H. Agnew, Room 102, Doctors Bldg., Billings, Mont. 59101.

Nebraska Chapter of ACR
Secretary-Treasurer, Dr. Robert Bodmer, Suite 622 Doctors Bdg., Omaha, Neb. 68131. Meets the third Wednesday of the month, Oct. through March, at the Clarkson Hosp., Omaha, Neb. and the fourth Friday of April at the Lincoln Country Club, Lincoln, Neb.

Nevada Radiological Society, Chapter of ACR
Secretary, Dr. Charles F. Veverka, Carson Tahoe Hosp., Carson City, Nev. 89701.

N.E. Society for Radiation Oncology
Secretary, Dr. C. C. Wang, Mass. Gen. Hosp., Boston, Mass. 02114.

New England Roentgen Ray Society
Secretary, Dr. Melvin E. Clouse, 185 Pilgrim Rd., Boston, Mass. 02115. Meets the third Friday of Oct. and Nov., and third Thurs. of each month. Jan. through May, excluding December, at The Longwood Towers, 20 Chapel Street, Brookline, Mass. at 3:00 P.M. Annual Meeting: May 20, 1976.

New Hampshire Roentgen Ray Society, Chapter of ACR
Secretary-Treasurer, Dr. Edward P. Kane, Claremont Gen. Hosp., Claremont, N. H. 03743. Meets four to six times yearly.

New Mexico Society of Radiologists, Chapter of ACR
Secretary, Dr. W. M. Jordan, 1100 Central Ave. S.E., Albuquerque, N. M. 87106. Four meetings annually, three held in Albuquerque, N. M., and one held at time and place of New Mexico State Medical Society annual meeting.

New Orleans Radiological Society, Inc.
Secretary-Treasurer, Dr. Jimmy L. Mains, P.O. Box 446, Gretna, La. 70053. Meets bimonthly at local restaurants selected by the President. Spring Conference.

New York Roentgen Society
Secretary-Treasurer, Dr. Thomas C. Beneventano, 111 East 210th St., Bronx, N. Y. 10467. Meets monthly on the 3rd Monday at the New York Academy of Medicine at 4:30 P.M. Annual Spring Conference, Waldorf-Astoria Hotel, New York, N. Y., April 22–24, 1976. A.M.A. Cat. I credit. Further information may be obtained from Dr. Albert A. Dunn, Roosevelt Hosp., New York, N. Y. 10019.

New York State Chapter of ACR
Secretary-Treasurer, Dr. Albert F. Keegan, 6 Secor Dr., Port Wash., N. Y. 11050.

North American Society of Cardiac Radiology
Secretary-Treasurer, Dr. Erik Carlson, Univ. Calif., San Francisco, Calif. 94143.

North Carolina Chapter of ACR
Secretary-Treasurer, Dr. Ernest B. Spangler, Wesley Long Hosp., Greensboro, N. C. 27402. Meets twice a year. The Spring Meeting is held at the time of the meeting of the North Carolina Medical Society. The Fall Meeting is held in November at the Mid Pines Club, Southern Pines, N. C.

North Dakota Radiological Society, Chapter of ACR
Secretary, Dr. Marshall Landa, P. O. Box 6001, Fargo, N. D. 58102. Meets at time of State Medical Association meeting. Other meetings arranged on call of the President.

North Florida Radiological Society
Secretary, Dr. David F. Bew, University Hospital of

Jacksonville, 655 W. Eighth Street, P.O. Box 2751, Jacksonville, Fla. 32203. Meets quarterly in March, June, September and December.

NORTHEASTERN OKLAHOMA RADIOLOGICAL SOCIETY
Secretary-Treasurer, Dr. Theodore J. Brickner, Jr., 5919 S. Gary Place, Tulsa, Okla. 74110.

NORTHEASTERN NEW YORK RADIOLOGICAL SOCIETY
Secretary, Dr. Donald R. Morton, Dept. of Radiology, St. Clare's Hosp., Schenectady, N. Y. 12304. Meets in Albany area on third Wednesday of October, November, March, April, and May.

NORTHERN CALIFORNIA RADIATION THERAPY ASSOCIATION
Secretary-Treasurer, Dr. John D. Earle, Stanford Medical Center, Stanford, Calif. 94304. Meets quarterly.

NORTHERN CALIFORNIA RADIOLOGICAL SOCIETY
Secretary, Dr. Patrick J. Grinsell, 1207 Fairchild Ct., Woodland, Calif. 95695. Meets on the fourth Monday, Sept. through May at the Mansion Inn, Sacramento, Calif.

NORTHWESTERN NEW YORK RADIOLOGICAL SOCIETY
Secretary, Dr. Barbara E. Chick, Glens Falls Hospital, Glens Falls, N. Y. 12801.

NORTHWESTERN OHIO RADIOLOGICAL SOCIETY
Secretary-Treasurer, Dr. Gerald W. Marsa, 3939 Monroe St., Toledo, Ohio 43606. Meets 3rd Wednesday from September to May excluding Dec. at Academy of Med. of Toledo and Lucas County, 4428 Secor Rd., Toledo, Ohio.

OHIO STATE RADIOLOGICAL SOCIETY, CHAPTER OF ACR
Secretary, Dr. James Farmer, Cleveland, Ohio.

OKLAHOMA STATE RADIOLOGICAL SOCIETY, CHAPTER OF ACR
Secretary, Dr. George H. Ladd, 4616 Denison, Muskogee, Okla. 74401. Meets in January, May and October.

ORANGE COUNTY RADIOLOGICAL SOCIETY
Secretary, Dr. William E. Danko, 2601 E. Chapman, Orange, Calif. 92667. Meets on fourth Tuesday of the month, excluding June, July, August, and December, at Orange County Medical Association Bldg., Orange, Calif.

OREGON STATE RADIOLOGICAL SOCIETY, CHAPTER OF ACR
Secretary-Treasurer, Dr. Ray F. Friedman, 3324 S. W. 44th St., Portland, Ore. 97221. Meets on second Wednesday of month, October through April, at the University Club, Portland, Ore.

ORLEANS PARISH RADIOLOGICAL SOCIETY
Secretary, Dr. Joseph V. Schlosser, Charity Hospital, New Orleans, La. 70113. Meets second Tuesday of each month.

PACIFIC NORTHWEST RADIOLOGICAL SOCIETY
Secretary-Treasurer, Dr. Kenneth D. Moores, 1118 9th Ave., Seattle, Wash. 98101. Annual Meeting: Benson Hotel, Portland, Ore., May 7–9, 1976.

PENNSYLVANIA RADIOLOGICAL SOCIETY, CHAPTER OF ACR
Secretary, Dr. Joseph A. Marasco, Jr., St. Francis General Hosp., Pittsburgh, Pa. 19141.

PHILADELPHIA ROENTGEN RAY SOCIETY
Secretary, Dr. Marvin E. Haskin, 230 N. Broad St., Philadelphia, Pa. 19102. Meets first Thursday of each month at 5 P.M., from October to May in Thompson Hall, College of Physicians.

PITTSBURGH ROENTGEN SOCIETY
Secretary, Dr. Klaus M. Bron, Presbyterian-Univ. Hosp., Pittsburgh 15213. Meets second Wednesday of month, September through May, at the Pittsburgh Athletic Association.

RADIATION RESEARCH SOCIETY
Executive Secretary, Richard J. Burk, Jr., 4211 39th St., N.W., Washington, D. C. 20016. Annual Meeting.

RADIOLOGICAL SOCIETY OF CONNECTICUT, INC., CHAPTER OF ACR
Secretary, Dr. Gerald L. Baker, 85 Jefferson St., Hartford, Conn. 06106. Meets in Oct., Jan., March, and June.

RADIOLOGICAL SOCIETY OF GREATER CINCINNATI
Secretary-Treasurer, Dr. Alvin Nathan, c/o Academy of Medicine, 320 Broadway, Cincinnati, Ohio 45202. Meets first Monday of each month at Cincinnati Academy of Medicine.

RADIOLOGICAL SOCIETY OF NEW JERSEY, CHAPTER OF ACR
Secretary, Dr. Fred M. Palace, 11 Dale Dr., Morristown, N.J. 07960. Monthly meetings in East Orange and Trenton, N.J. Semi-Annual Meeting in Nov.

RADIOLOGICAL SOCIETY OF RHODE ISLAND, CHAPTER OF ACR
Secretary-Treasurer, Dr. Daniel J. Alves, Rhode Island Hosp., Providence, R. I. 02902.

RADIOLOGICAL SOCIETY OF SOUTHERN CALIFORNIA
Secretary-Treasurer, Dr. A. Franklin Turner, LAC-USC Medical Center, Room 3418, 1200 North State St., Los Angeles, Calif. 90033. Meets three times a year, usually October, February and May.

RADIOLOGICAL SOCIETY OF THE STATE OF NEW YORK
Secretary-Treasurer, Dr. John W. Colgan, 273 Hollywood Ave., Rochester, N. Y. 14618.

REDWOOD EMPIRE RADIOLOGICAL SOCIETY
Secretary, Dr. Charles E. Carter, 121 Sotoyome St., Santa Rosa, Calif. 95405. Meets second Monday every other month.

RICHMOND COUNTY RADIOLOGICAL SOCIETY
Secretary, Dr. Frederick S. Vines, 11830 Rothbury Dr., Richmond, Va. 23235. Meets third Thursday of each month at the Aberdeen Barn.

ROCHESTER ROENTGEN RAY SOCIETY, ROCHESTER, N. Y.
Secretary-Treasurer, Dr. Robert J. Bruneau, Rochester General Hosp., Rochester, N. Y. 14621. Quarterly meetings on the call of the President, at the Rochester Academy of Medicine.

ROCKY MOUNTAIN RADIOLOGICAL SOCIETY
Secretary-Treasurer, Dr. Lorenz R. Wurtzebach, 4200 E. Ninth Ave., Denver, Colo. 80220. Annual Meeting: Brown Palace Hotel, Denver, Colo., Aug. 19–21, 1976.

SAN ANTONIO-CIVILIAN MILITARY RADIOLOGICAL SOCIETY
Secretary, Dr. James R. Stewart, Oak Hills Medical Ctr., San Antonio, Tex. 78209. Meets third Wednesday of each month at Fort Sam Houston Officers Club at 6:30 P.M.

SAN DIEGO RADIOLOGICAL SOCIETY
President, Dr. Donald J. Fleischli, 7849 Fay Ave., La Jolla, Calif. 92037. Meets the first Wednesday of each month Sept. through June at the University Club.

SAN FRANCISCO RADIOLOGICAL SOCIETY
Secretary-Treasurer, Dr. Robert L. Koch, 3838 California St., Suite 106, San Francisco, Calif. 94118.

SECTION ON RADIOLOGY, CALIFORNIA MEDICAL ASSOCIATION
Secretary, Dr. William H. Graham, 630 East Santa Clara St., San Jose, Calif.

SECTION ON RADIOLOGY, MEDICAL SOCIETY OF THE DISTRICT OF COLUMBIA
Secretary-Treasurer, Dr. Albert M. Zelna, 21 Masters St., Potomac, Md. 20854. Meets at Medical Society Library, third Wednesday of January, March, May and October at 8:00 P.M.

SECTION OF RADIOLOGY, NATIONAL MEDICAL ASSOCIATION
Secretary, Dr. Ruby Brooks, Dept. Radiol., Veterans Adm. Hosp., P.O. Box 511, Tuskogee, Ala. 36083. Annual Meeting.

SECTION ON RADIOLOGY, SOUTHERN MEDICAL ASSOCIATION
Secretary, Dr. Mario A. Calonje, 1514 Jefferson Highway, New Orleans, La. 70121. Annual Meeting.

SECTION ON RADIOLOGY, TEXAS MEDICAL ASSOCIATION
Secretary, Dr. George F. Crawford, St. Elizabeth Hospital, Beaumont, Tex. Meets annually with the Texas Medical Association.

SOCIETY FOR PEDIATRIC RADIOLOGY
Secretary-Treasurer, Dr. John P. Dorst, 601 N. Broadway, Baltimore, Md. 21205. Annual meeting: Washington Hilton Hotel, Washington, D. C., Sept. 19–20, 1976.

SOCIETY OF GASTRO-INTESTINAL RADIOLOGISTS
Secretary-Treasurer, Dr. John R. Amberg, University Hospital, 225 W. Dickinson St., San Diego, Calif. 92103.

Society of Nuclear Medicine
Secretary, Dr. E. James Potchen, Edward Mallinckrodt Institute of Radiology, 660 S. Euclid Ave., St. Louis, Mo. 63110. *Administrative Officer*, Mrs. Margaret Glos, 211 E. 43rd St., New York, N. Y. 10017. Annual Meeting.

South Bay Radiological Society
Secretary, Dr. Bruce R. Parker, Dept. Radiol., Stanford Univ. Med. Center, Stanford, Calif. 94305. Meets the 2nd Monday of each month at the Santa Clara County Medical Society Bldg., 700 Empey Way, San Jose, Calif.

South Carolina Radiological Society, Chapter of ACR
Secretary, Dr. George W. Brunson, 1406 Gregg St Columbia, S. C. Annual meeting (primarily business) in conjunction with the South Carolina Medical Association meeting in May. Annual fall scientific meeting at time and place designated by the president.

South Coast Radiological Society Chapter of ACR
Secretary-Treasurer, Dr. Richard T. Love, Santa Barbara Med. Clin., 215 Pesetas Lane, Santa Barbara, Calif. 93110. Meets fourth Tuesday of alternate months, Sept., Nov., Jan., March and May.

South Dakota Radiological Society, Chapter of ACR
Secretary, Dr. M. F. Petereit, 2416 S. Phillips, Sioux Falls, S. D. 57105. Meets in spring with State Medical Society and in fall.

Southern California Radiation Therapy Association
Secretary-Treasurer, Dr. Duane J. Gillum, 250 W. Pueblo St., Santa Barbara, Calif. 93105. Meets quarterly.

Southern Radiological Conference
Secretary-Treasurer, Dr. J. W. Maxwell, P.O. Box 2144 Mobile Ala. 36601. Annual Meeting:

Tennessee Radiological Society, Chapter of ACR
Secretary-Treasurer, Dr. Jerry W. Grise, Methodist Hosp., 1265 Union Ave., Memphis, Tenn. 38104. Meets annually at the time and place of the Tennessee State Medical Association meeting.

Texas State Radiological Society, Chapter of ACR
Secretary, Dr. Francis E. O'Neill, 1128 Nix Prof. Bdg., San Antonio, Tex. 78205.

The Fleischner Society
Secretary, Dr. E. Robert Heitzman, State University of New York Upstate Medical Center, Syracuse, N. Y. 13210. Annual Meeting:

Tri-State Radiological Society
Secretary, Dr. Thomas Harmon, St. Mary's Hosp., Evansville, Ind. 47750. Meets bimonthly on the third Wednesday at area Hospitals.

Upper Peninsula Radiological Society
Secretary, Dr. A. Gonty, Menominee, Mich. Meets quarterly.

Utah State Radiological Society, Chapter of ACR
Secretary-Treasurer, D. Michael Edson, Dept. Radiol., Valley West Hosp., 4160 West 3400 South, Granger, Utah 84120. Meets quarterly at Holy Cross Hospital.

Vermont Radiological Society, Chapter of ACR
Secretary, Dr. J. Lorimer Holm, R.R. #3, Barre, Vt. 05641.

Virginia Chapter of ACR
Secretary-Treasurer, Dr. Charles P. Winkler, 3500 Kensington Ave., Suite 2-A, Richmond, Va. 23221.

Washington, D. C., Chapter of ACR
Secretary-Treasurer, Dr. Robert M. Allen, 9312 Convento Terr., Fairfax, Va. 22030.

Washington State Radiological Society, Chapter of ACR
Secretary-Treasurer, Dr. Donald J. Hesch, 3216 N.E. 45th Place, Seattle, Wash. 98105.

West Virginia Radiological Society, Chapter of ACR
Secretary-Treasurer, Dr. Andrew W. Goodwin, II, 200 Med. Arts Bldg., Charleston, W. Va. 25301. Meets concurrently with annual meeting of West Virginia State Medical Society, other meetings arranged by program committee.

Westchester County Radiological Society
Secretary, Dr. Leonard Cutler, 16 Guion Place, New Rochelle, N. Y. 10802. Meets on second Tuesday of October, December, February and May.

Wisconsin Radiological Society, Chapter of ACR
Secretary-Treasurer, Dr. June Unger, Wood VA Hosp., Wood, Wis. 53193. Meets twice a year, May and September.

Wisconsin Society of Therapeutic Radiologists
Secretary, Dr. Alvin Greenberg, Radiother. Ctr., Univ. Hospitals, Madison, Wis. 53706. Meets quarterly.

Wyoming Radiological Society, Chapter of ACR
Secretary, Dr. Ross J. Collie, Box 96, Lander, Wyo. 82520. Meets in fall with State Medical Society and in spring on call of President.

Mexico, Puerto Rico and Central America

Asociación Costarricense de Radiología
Secretary, Dr. Rafael Umaña-Umaña, Apartado 8-5340, San José, Costa Rica.

Asociacón de Radiólogos de Centro America y Panamá. Comprising: Guatemala, El Salvador, Honduras, Nicaragua, Costa Rica and Panamá
Secretary-General, Dr. Francisco Miranbell Solis, Apartado 3352, San José, Costa Rica, Central America. Meets annually in a rotating manner in the six countries.

Sociedad de Radiología de Salvador
Secretary, Dr. Carlos Meijia, 5a Av. Nte. No. 434, San Salvador, Rep. El Salvador.

Sociedad de Radiología de Guatemala
Secretary, Dr. Carlos E. Escobar, 9², Calle A 0–05, Zona 1, Guatemala

Sociedad Mexicana de Radiología, A.C.
Coahuila No. 35, México 7, D.F., México.
Secretary-General, Dr. Jorge Cano Coquí. Meets first Monday of each month.

Sociedad Radiológica Panameña
Secretary, Dr. L. Arrieta Sánchez, Apartado No. 6323, Panamá, R. de P. Meets monthly in a department of radiology of a local hospital chosen at preceding meeting.

Sociedad Radiológica de Puerto Rico
Secretary, Dr. César Rosa, Box 9387, Santurce, Puerto Rico 00908. Meets second Thursday of each month at 8:00 P.M. at the Puerto Rico Medical Association Bldg. in San Juan.

British Commonwealth of Nations

Association of Radiologists of the Province of Quebec
121 Boul. Taschereau, Greenfield Park, P. Q., Canada. Meets four times a year.

British Institute of Radiology
Honorary Secretaries, D. H. Traspnell, M. Cohen, 32 Welbeck St., London, W1M/7PG, England.

Canadian Association of Physicists, Division of Medical and Biological Physics
Honorary Secretary-Treasurer, Dr. R. G. Baker, Ontario Cancer Foundation, Ottawa Civic Clinic, 1053 Carling Ave., Ottawa 3, Ont., Canada.

Canadian Association of Radiologists
Honorary Secretary, Dr. Ross O. Hill, Suite 806, 1440 St. Catherine St. West, Montreal 107, Que., Canada. Annual Meeting:

Edmonton and District Radiological Society
Secretary, Dr. L. A. Koller, Suite 360, Professional Bldg., 10830 Jasper Ave., Edmonton 15, Alberta, Canada. Meets third Thursday of each month October to May, except December, at various Edmonton Hospitals.

Faculty of Radiologists
Honorary Secretary, P. D. Thomson, 28 Portland Pl., London, W1N 4DE.

Montreal Radiological Study Club
Secretary, Dr. W. Paul Butt, Montreal General Hospital, Montreal, Que., Canada. Meets first Tuesday evening, October to April.

Section of Radiology of the Royal Society of Medicine (Confined to Medical Members)
Meets third Friday each month at 8:15 p.m. at the Royal Society of Medicine, 1 Wimpole St., London, W. 1 M8AE, 1 England.

Société Canadienne-Française de Radiologie
Secretary-General, Dr. Hubert Sasseville, Verdun Hospital, Montréal, P. Q., Canada. Meets every third Tuesday from October to April.

The Hospital Physicists' Association
Honorary Secretary, J. B. Massey, B.Sc., Christie Hosp. and Holt Radium Institute, Physics Department, Withington, Manchester M20 9BX, England.

Toronto Radiological Society
Secretary, Dr. George Wortzman, Toronto General Hosp., Toronto 12, Ont., Canada. Meets second Monday of each month, September through May.

The Royal Australasian College of Radiologists
Honorary Secretary, Dr. T. P. Loneragan, 45 Macquarie St., Sydney, N.S.W. 2000, Australia.

South America

Colégio Brasileiro de Radiologia
Secretary-General, Dr. José Marcos Pires de Oliveira, Caixa Postal 5984, São Paulo, Brazil.

Federación Argentina de Sociedades de Radiología
Branches of the Federation are: Sociedad de Radiólogos de la Provincia de Córdoba; Sociedad Argentina de Radiología; Asociación Argentina de Radiología; Sociedad de Radiología, Radioterapéutica y Medicina Nuclear de Rosario; Sociedad de Radiología y Medicina Nuclear del Centro y Sudeste de la Provincia de Buenos Aires (Mar del Plata); Sociedad Salteña de Radiología y Medicina Nuclear; Sociedad de Radiología de Tucumán; Sociedad de Radiologia del Nordeste Argentino; Sociedad de Radiología de La Plata; and Sociedad de Radiología de San Juan.
Secretary-General-Treasurer, Dr. Roberto Habichayn, Av. Colón 637, Córdoba, Argentina.
Congress will be organized by Sociedad de Radiología, Radioterapéutica y Medicina Nuclear de Rosario in 1975.

Sociedad Argentina de Radiología
Secretary-General, Dr. Alba de la Torre, Santa Fé 1171, Buenos Aires, Argentina. Meets first Wednesday evening, April through December.

Sociedad Boliviana de Radiología
Secretary, Dr. Javier Prada Méndez, Casilla 1182, La Paz, Bolivia. Meets monthly. General assembly once every two years.

Sociedade Brasileira de Radiologia
Secretary, Dr. Armando Rocha Amoédo, Caixa Postal 1532, Rio de Janeiro, Brazil. General Assembly meets every two years in December.

Sociedade Brasileira de Radioterapia
Luiz Antonio, 644, São Paulo, Brazil. Meets monthly on second Wednesday at 9:00 p.m. in São Paulo at Av. Brigadeiro Luiz Antonio, 644.

Sociedad Chilena de Radiología
Secretary, Dr. Manuel Neira, Casilla 13426, Santiago, Chile. Meets first Friday of each month at Av. Santa María 1810 at 7:00 p.m.

Sociedad Colombiana de Radiología
Secretary-General, Dr. Gustavo Sánchez Sánchez, Bogotá, Colombia. Meets last Thursday of each month.

Sociedad Ecuatoriana de Radiología
Secretary, Dr. Luis Blum, Casilla 3712, Guayaquil, Ecuador.

Sociedad Paraguaya de Radiología
Secretary, Dr. Hugo Volpe Rios, 15 de Agosto 322, Asunción, Paraguay.

Sociedad Peruana de Radiología
Secretary-General, Dra. Ladis Delpino, Av. General Santa Cruz No. 315, Miraflores, Lima, Perú, Casilla Correo, 2306, Lima, Perú. Meets monthly except during January, February, and March.

Sociedad de Radiología del Atlantico
Secretary, Dr. Raul Fernandez, Calle 40 #41-110, Baranquilla, Colombia. Society meets monthly at the Instituto de Radiología.

Sociedad de Radiología del Nordeste Argentino
Secretary-General, Dr. Francisco J. Velar, Catamarca 561, Corrientes, Argentina.

Sociedad de Radiología de La Plata
Secretary, Dr. Hiram D. Haurigot, Calle 50 No. 374, La Plata, Argentina.

Sociedad de Radiología, Cancerología y Física Médica del Uruguay
Secretary-General, Dr. Manuel Gonzáles Maseda, Av. Agraciada 1464, piso 13, Montevideo, Uruguay.

Sociedade de Radiología de Pernambuco
Secretary, Dr. Manoel Medeiros Instituto de Radiologia da Faculdade de Medicina da Universidade do Recife, Caixa Postal 505, Pernambuco, Brazil.

Sociedad de Roentgenología y Medicina Nuclear de la Provincia de Córdoba
Secretary-General, Dr. Lucas C. Di Rienzo, Ave. Grl. Paz. 151, Córdoba, Argentina.

Sociedad de Radiología, Radioterapéutica y Medicina Nuclear de Rosario
Secretary-General, Dr. Federico Frágola, Santa Fe 1798, Rosario, Argentina.

Sociedad Salteña de Radiología y Medicina Nuclear
Treasurer, Dr. Julio Luis Baldi, Av. Sarmiento 536, Salta, Argentina.

Sociedad Venezolana de Radiología y Medicina Nuclear
Secretary-General, Dr. Salvador Itriago Borgas, Apartado Postal 9213, Candelaria, Caracas, Venezuela. Meets monthly, third Friday at Colegio Médico del Distrito Federal, Caracas.

Continental Europe

Österreichische Röntgen-Gesellschaft
Secretary, Dr. Ernst Kotcher, Wiener Allgemeine Poliklinik Mariannengasse 10, A-1090 Wien, Austria. Meets second Tuesday of each month in Allgemeine Poliklinik.

Société Royale Belge de Radiologie
General Secretary, Dr. Joseph Baeyens, Alost, Belgium. Meets in February, March, May, June, September, October, November and December.

Société Européenne de Radiologie Pédiatrique
Secretary, Dr. J. Corbaton, Clinica Infantil "La Paz," Av. Generalissimo, 117 Madrid 34, Spain. Annual Meeting:
Permanent Secretary, Clément Fauré, Hôpital des Enfants Malades, 149, rue de Sèvres, 75 730, Paris Cadet 15, France.

Société Française de Radiologie Médicale, Médecine Nucléaire et Électrologie, and its branches: Société du Sud-Ouest, du Littoral méditerranéen, du Centre et Lyonnais, du Nord, de l'Ouest, de l'Est, du Massif Central, d'Outre-Mer et d'Étranger.
Parent Society meets third Monday of each month, except during July, August and September, rue de Seine 12, Paris, France.
Secretary-General, Dr. Ch. Proux, 9 rue Daru, Paris 75008, France.

Société Française de Neuroradiologie
Secretary-General, Professeur agr. R. Djindjian 16, rue de l'Université 75, Paris 7e, France. Annual meeting.

Československá Radiologická Společnost
Secretary, Associate Professor Jaromír Kolář, M.D., Sc.D., Radiological Clinic, Praha 2, U nemocnice 2, Czechoslovakia. Meets monthly except during July, August and September. Annual general meeting.

Deutsche Röntgengesellschaft
President, Professor Dr. med. Walter Frommhold, Director of Medizinisches Strahleninstitut der Universität Tübingen, Röntgenweg 11, 7400 Tübingen, Germany.

Faculty of Radiologists of the Royal College of Surgeons in Ireland
Honor. Secretary, Max. J. Ryan, St. Stephen's Green, Dublin 2. Annual Meeting:

Società Italiana di Radiologia Medica e Medicina Nucleare
Administrative Secretary, Prof. E. Conte, Ospedale Mauriziano, 10128 Torino, Italy. Meets annually.

Societas Radiologica Danica
Secretary, Dr. Bent Langenfeldt, Tretommervej 20a, DK. 8240 Risskov, Denmark.

Nederlandse Vereniging voor Radiologie
Secretary, Dr. J. D. Mulder, Dept. of Rad., Akademisch Ziekenhuis, Leiden, Netherlands.

Norsk Forening for Medicinsk Radiologi
General Secretary, Gunnar Stake, Rikshospitalet, Oslo, Norway.

Scandinavian Radiological Society
Secretary-General, Professor C. F. Unnérus, M.D., Hagalung-Tapiola, Havsvindsvägn 5 C., Finland. Annual Meeting.

Sociedad Española de Radiología y Electrología Médicas y de Medicina Nuclear
Secretary-General, Dr. Pilar Gallar Barberá, Villanueva, 11, Madrid 1, España. Meets every other Saturday evening of each month, Oct. to June, inclusive, in Madrid.

Sociedade Portuguesa de Radiologia e Medicina Nuclear
Secretary-General, Dr. Luís Aires de Sousa, Av. Elias Garcia, 123- 1, Esg.-Lisboa i-Portugal.

Svensk Förening för Medicinsk Radiologi
Secretary, Dr. Hanz Ringertz, Röntgendiagnostika Avdelningen, Karolinska Sjukhuset 104 01 Stockholm 60, Sweden.

Schweizerische Vereinigung für Radiologie, Nuklearmedizin und Strahlenbiologie (Association Suisse de Radiologie, Médecine Nucléaire et de Radiobiologie)
Secretary, Dr. med. Gustav Schoch, Bethesdaspital, Gellerstrasse 144, 4000 Basel, Switzerland.

Asia

Bengal Radiological Association
Honorary Secretary, Dr. B. Chatterji, 262 Rash Behari Ave., Calcutta 700019, India. Meets 1st Fri. and 3rd Wed. of every month.

Indian Radiological Association
Honor. Gen. Secretary, Dr. S. P. Aggarwal, 10-B Kasturba Ghandi Marg, New Delhi 11001.

Indonesian Radiological Society
Secretary, Dr. Gani Iljas Sasmitaatmadja, Radiology Dep., Faculty of Medicine, University of Indonesia, Salemba 6, Jakarta, Indonesia.

Iranian Radiological Society
Secretary, Dr. Majid Rooholamini, P.O. Box No. 14–1151, Teheran, Iran. The Society meets on the second Saturday of each month.

Israel Radiological Society
Secretary, Dr. M. A. Lerner, Hesharon Hosp., Petah-Tigva, Israel.

Philippine College of Radiology
Secretary-Treasurer, Dr. Eduardo V. Nievera, Box 1284 Commercial Center, Makati, Rizal D-708, Philippines. Meets every second Thursday of the month.

Radiological Society of Thailand
Secretary, Prof. Rojana Suvansuthi, M.D., Ph.D., Depart. of Rad., Sirizaj Hospital, Faculty of Medicine, Mahidol University, Bangkok 7, Thailand.

Africa

Association of Radiologists of West Africa
Honorary Secretary, C. A. Beetlestone, M.B., B.S., D.M.R.D., Dept. Radiol., University College Hosp., Ibadan, Nigeria.

Radiological Society of South Africa
Secretary, Dr. A. Visser, P. O. Box 8850, Johannesburg, South Africa.

South African International Radiological Congress
Director, Dr. Paul Sneider, P.O. Box 4878, Johannesburg, South Africa.

ABSTRACTS OF RADIOLOGIC LITERATURE

INDEX TO ABSTRACTS

ROENTGEN DIAGNOSIS

Head

Kosowicz, J., and Rzymski, K.: Radiological features of the skull in Klinefelter's syndrome and male hypogonadism 925

Neck and Chest

Dembski, J., and Zeitler, E.: The accuracy of surface kymography following myocardial infarcts, with special reference to cardiac aneurysms 925
Lipton, M. J. *et al.:* Aneurysms of the coronary arteries in the adult: clinical and angiographic features 925
Ramos, L. *et al.:* Radiological characteristics of perforated pulmonary hydatid cysts 926
Delanote, G. J. *et al.:* Pleuropulmonary manifestations of collagen diseases 926
Abadir, R.: Cystosarcoma phyllodes of the breast 927
Reinke, R. T. *et al.:* Pulmonary infarction complicating the use of Swan-Ganz catheters 927
Efsen, F. *et al.:* Arteriographic exposition of the parathyroids 927

Abdomen

Diard, F. *et al.*: Radiologic considerations of primary malignant tumors of the biliary tract: exclusive of tumors of the ampulla of Vater 928
Duscellier, R. *et al.:* Stenosis of the celiac axis: etiologic considerations 928
Swischuk, L. E., and Tyson, K. R.: "Burned-out" pyloric stenosis: an elusive gastic outlet obstruction 929
Julien, P. J. *et al.:* Gastrointestinal complications following renal transplantation 929
Chiles, J. T., and Platz, C. E.: The radiographic manifestations of pseudolymphoma of the stomach 929
Pfister, R. C. *et al.:* Congenital asymmetry (hemihypertrophy) and abdominal disease: radiological features in 9 cases 930
Enayat, U. *et al.:* Diagnostic problems in massive adrenal hemorrhage in the newborn 930

ROENTGEN DIAGNOSIS

Head

Kosowicz, Jerzy, and Rzymski, Kazimierz. Radiological features of the skull in Klinefelter's syndrome and male hypogonadism. *Clin. Radiol.*, July, 1975, *26*, 371–378. (From: The Departments of Endocrinology and Diagnostic Radiology, School of Medicine, Poznań, Poland.)

The skull characteristics were studied in 21 cases of Klinefelter's syndrome ages 12–31 years and in 30 cases of hypogonadotropic eunuchoidism, age 17–48 years. In Klinefelter's syndrome, 17 patients had premature fusion and excessive calcification in the coronal sutures. Fifteen showed shortening of the anterior fossa; 14 had decreased angle of the skull base; twelve had flattening of the temporal regions; and nine had a decreased width of the vault. Also noted in eight patients was a decreased length of the skull, deepening of the posterior fossa and shortening of the mandibular rami.

In contrast, in hypogonadotropic eunuchoidism, the length of the skull and anterior fossa as well as size of the mandibular rami were within the normal range. Only two patients had a reduced angle of the base of the skull. Premature fusion of the coronal sutures was not found. The most striking change was the small sella; in 28 of 30 patients, it was 7–9 mm in length and the area was reduced. The sphenoid sinuses in 24 were enlarged and excessively pneumatized. The bones of the calvarium were thin not exceeding 5 mm (normal 6–8). The mastoid processes were small.

Therefore, in patients with deficient sexual development, the features in the skull may aid in diagnosis.—*Martha Mottram, M.D.*

Neck and Chest

Dembski, J., and Zeitler, E. Sicherheit der Flächenkymographie nach Myokardinfarkt unter besonderer Berücksichtigung der Herzwandaneurysmen. (The accuracy of surface kymography following myocardial infarcts, with special reference to cardiac aneurysms.) *Fortschr. a. d. Geb. d. Röntgenstrahlen u. d. Nuklearmedizin*, July, 1975, *123*, 30–36. (Address: Dr. med. J. Dembski, 5250 Engelskirchen, Aggertalklinik.)

Kymography was carried out in 180 patients who had recently had myocardial infarctions. The studies were carried out in three planes to show the anterior, lateral, and posterior cardiac walls, and the results were compared with the results of coronary angiography and selective cardiography of the left side of the heart.

Kymography performed for the diagnosis of cardiac aneurysms and myocardial scars is accurate in 53 percent of cases. In aneurysms limited to the left ventricle, however, it was possible to show 71 percent by kymographic study. The examination is simple, rapid, and non-invasive.

Of the 180 patients only ten were women; 73 percent of the patients were between the ages of 41 and 55 years.

With the use of kymography to show at least three marginal contours of the left ventricle it is possible to obtain useful information regarding the optimal plane for cardiac injection and it may indicate the presence of myocardial disease and the need for further, invasive study.—*Modified Published English Abstract.*

Lipton, Martin J., Pfeifer, James F., Lopes, Mario G., and Hultgren, Herbert N. Aneurysms of the coronary arteries in the adult: clinical and angiographic features. *Radiology*, Oct., 1975, *117*, 11–18. (Address: Martin J. Lipton, M.D., Veterans Administration Hospital, 3801 Miranda Avenue, Palo Alto, Calif. 94304.)

Bougon in 1912 is usually given credit for first reporting an aneurysm of the coronary artery (ACA) but as early as 1861 Morgagni described a diffuse dilatation of the left coronary artery in a patient with syphilitic aortitis. Several case reports and reviews have subsequently appeared and, in 1963, Daoud (*Am. J. Cardiol.*, 1963 *11;* 228–237) reported the results of a meticulous study involving the dissection of the coronary arteries in 694 consecutive adult autopsies. The incidence of ACA was 1.4 percent (10:694) in that series.

In order to determine the incidence, clinical presentation and angiographic features of ACA the authors have reviewed 1,000 consecutive adult coronary arteriograms. This patient population was comprised primarily of patients being considered for coronary artery-saphenous vein bypass surgery for relief of angina, and also included patients who underwent coronary arteriograms as part of the routine evaluation for valve surgery. All roentgenograms were reviewed retrospectively for ACA. An aneurysm was diagnosed when there was dilatation of 50 percent of the normal coronary artery with either no evidence of a proximal stenotic lesion or when only mild stenosis (less than 50 percent) was present with a disproportionate dilatation beyond it (50 percent greater than the normal lumen). The normal lumen diameter was taken to be that measured at a proximal point along the vessel where no atherosclerotic disease was evident.

Aneurysms of the coronary artery were detected in 1.1 percent (11:1,000) of the patients in this series. The clinical features regarding metabolic and electrocardiographic changes in these eleven patients are presented in tabular form. The angio-

graphic findings showed both saccular and fusiform aneurysms. The aneurysms were localized to one vessel in seven patients and multiple vessels were involved in four. The frequency of vessel involvement was as follows: right coronary artery, left circumflex, and then left anterior descending artery. The left main coronary artery was not affected in this series. Vascular calcification was found in four patients in this series but did not correlate with the occurrence of aneurysm.

The natural history and prognosis of ACA is presently unknown. Thrombosis and thromboembolism may occur, while rupture is usually associated with mycotic aneurysm and periarteritis nodosa. It may well be that atherosclerotic aneurysms do not have the same risks as other varieties. The authors conclude that the role of coronary artery bypass surgery in treatment of ACA has not been determined and, at present, should be reserved for the patient who has a large ACA which presents the threat of rupture, or in the patient who is significantly limited by angina; otherwise the indications for surgery are the same as those for a patient with stable angina due to atherosclerotic coronary artery disease.—*Edward B. Best, M.D.*

Ramos, Luis, Hernandez-Mora, Mariano, Illanas, Mariano, Llorente, Maria Teresa, and Marcos, Justo. Radiological characteristics of perforated pulmonary hydatid cysts. *Radiology*, Sept., 1975, *116*, 539–542. (Address: Luis Ramos, M.D., Servicio de Radiodiagnóstico, Clínica Puerta de Hierro, San Martín de Porres, 4, Madrid-35, Spain.)

The authors describe the roentgenologic findings in spontaneous perforation of hydatid pulmonary cysts. In their series of 239 patients with pulmonary hydatid disease, 56 showed spontaneous perforation. Five ruptured into the pleural space.

Evacuation of the hydatid cyst into the bronchial system may be either total or incomplete. Perforation allows air to enter the hydatid cyst. The entrance of air causes the typical findings which are discussed in the article. The cyst wall is typically thick, 5 mm, with both the inner and outer margins smooth.

Total expulsion or total evacuation of the cyst may be confused with cavitary neoplasm or pulmonary abscess. Typically the smooth thick wall helps to differentiate between the cyst and either abscess or neoplasm. With total evacuation there are no retained membranes or vesicles or fragments of the cyst. Occasionally, surrounding inflammatory change may be present. With total evacuation the diagnosis is somewhat more difficult to make unless the patient recalls expectorating cyst fragments or membranes.

Incomplete evacuation of the hydatid cyst shows a more characteristic roentgenographic pattern. Remnants of the endocyst and membranes remain within the pericyst or adventitia. These fragments give rise to the various roentgenographic signs among which are the "iceberg," "water-lily," "camalote," and "double-arch" signs. Differential diagnosis to consider with incomplete evacuation are pulmonary abscess, cavitary neoplasm with necrotic debris, and pulmonary fungus disease with fungus ball.

A variant of incomplete evacuation occurs when a portion of the adventitia or outer lining of the cyst is also expelled. In this case, a portion of the cyst remains entrapped or incarcerated within the lung. An irregular cavitary lesion with variable thickness walls and entrapped debris results. This particular instance is difficult to tell from primary bronchogenic neoplasm and pulmonary abscess. Differentiation between the etiologies is impossible unless there is a history of expectorated hydatid material—*J. P. Eberts, M.D.*

Delanote, G. J., Heps, S., Baert, A. L., and Dequeker, J. Pleuropulmonary manifestations of collagen diseases. *J. Belge de radiol.*, Sept.–Oct., 1974, *57*, 337–346. (Address: Prof. Dr. A. Baert, Dient van Röntgendiagnostiek, Akadem, Ziekenhuis, 3000 Leuven, Belgium.)

The pleuropulmonary changes of collagen diseases give rather aspecific roentgen signs, but when coupled with clinical history and biochemical studies they can aid significantly in the ultimate diagnosis. The group includes rheumatoid arthritis, scleroderma, dermatomyositis, polymyositis, and pulmonary infiltrations with eosinophilia.

In rheumatoid arthritis the pleuropulmonary manifestations include diffuse interstitial pulmonary fibrosis, pleuritis and pleural effusion, necrobiotic nodules, and Caplan's syndrome. Pleural effusion with diffuse interstitial fibrosis is quite typical of rheumatoid arthritis.

Systemic lupus erythematosis is the collagen disease most frequently associated with pleural effusions, patchy pulmonary infiltrates and pericardial effusions. Fibrosis does not usually develop but there is a progressive loss of lung volume with diaphragmatic elevation.

In scleroderma about 25 percent of patients show a reticular lung pattern and a progressive great loss in lung volume over a period of two to three years. Occasionally an air esophagram is noted in a lateral chest film.

Dermatomyositis and polymyositis only rarely affect the thorax and then give changes identical to other collagen diseases. Aspiration pneumonia can occur secondary to muscle paralysis.

Pulmonary infiltrations associated with eosinophilia are frequently seen in polyarteritis nodosa. They are homogeneous, ill-defined, non-segmental parenchymal consolidations which change in volume

and localization over a period of days or weeks. They can cavitate and result in fibrosis, but they are slower to change than Loeffler's infiltrations. They are often associated with cardiomegaly and pericarditis.

Wegener's granulomatosis can present with multiple nodular opacities within the chest, one third of which undergo cavitation. Often there are atypical bronchopneumonic infiltrations. The authors give differential diagnoses for each of the diseases discussed.—*Arch H. Hall, M.D.*

Abadir, Rushdy. Cystosarcoma phyllodes of the breast. *J. Canad. A. Radiologists*, Sept., 1975, *26*, 192–196. (From: Department of Radiology, Radiotherapy Section, Albert Einstein College of Medicine, Bronx, N. Y.)

Cystosarcoma phyllodes, breast tumors containing both epithelial and mesenchymal elements, generally persue a benign clinical course. Lymph node involvement and distant metastases are rare. Yet in this series of six cases, four were malignant. The behavior of these tumors, whether benign or malignant, was not related to the age of the patient (33 to 65 years), to the size of the tumor (3 to 18 cm), or to the duration of the mass (one month to ten years). Even the histology failed to predict the clinical course.

Two patients' sarcomas were of identical malignant cell type; yet one woman was alive and well 4¼ years after simple mastectomy and full course radiation therapy, the other had a fulminating fatal course with multiple chest wall recurrences, resistant to radiation therapy. This patient's clinical picture was complicated by recurring abdominal wall desmoid tumors, which were radiosensitive. A third patient had a huge posterior mediastinal metastatic mass, the fourth had intramammary lymph node involvement.—*Adele Altman, M.D.*

Reinke, R. T., Higgins, C. B., and Atkin, T. W. Pulmonary infarction complicating the use of Swan-Ganz catheters. *Brit. J. Radiol.*, Nov., 1975, *48*, 885–888. (From: Division of Cardiovascular Radiology, University Hospital, University of California at San Diego, School of Medicine, La Jolla, Calif.)

The Swan-Ganz catheter which is introduced into the antecubital vein has a balloon about its tip which permits its being directed by the flow of blood through the superior vena cava, the right atrium, and into the pulmonary artery. The balloon further permits obtaining a wedge pressure, and after deflation of the balloon the pulmonary arterial pressure is available.

Complications are unusual, but rupture of the balloon, premature ventricular contractions, knotting of the flexible catheter, and perforation of the pulmonary artery have been recorded. Aseptic thrombi apparently occur about the catheter in the superior vena cava.

The authors describe three patients in whom pulmonary infarction had developed distal to the the tip of the catheter. In one of these the apparent cause was excessive length of the catheter coiled in the right atrium, and endothelial damage at the tip of the catheter is postulated as a result of transmitted motion from variation in size of the atrium during cardiac contractions. In the other two cases the infarction resulted from wedging of the Swan-Ganz catheter, and in both the clinician had noted no abnormal pressure tracings. In other recorded cases, likewise, abnormal pressure tracings are unusual and one must not be deterred from the diagnosis by this negative bit of information.

The complications in use of the catheter may be decreased by: (1) advancing the catheter to the wedge position only when it is needed; (2) making certain that the balloon is deflated; (3) the use of heparin in the perfusing solution; and (4) leaving the catheter for not longer than 72 hours at one time.

The roentgenologist is in a position to be the first to discover the presence of complications resulting from the presence of the catheter.—*E. Frederick Lang, M.D.*

Efsen, F., Bruun, E., Lockwood K., and Hasner, E. Arteriographic exposition of the parathyroids. *Brit. J. Surg.*, Feb., 1975, *62*, 96–99. (From: Department of Diagnostic Radiology, Cardiovascular Section and Department of Endocrine Surgery, University Hospital (Rigshospitalet), Copenhagen, Denmark.)

At the present time, angiography appears to be the only method offering a possibility of estimating the volume of the individual parathyroid glands. A series of 52 consecutive patients referred for primary hyperparathyroidism was examined by arteriography. Of these, 13 were not operated on because of lack of evidence for the diagnosis. Exploration in 39 patients was carried out, with the decision based on history, clinical, roentgenologic, and biochemical data. A diagnosis of primary hyperparathyroidism was confirmed surgically in 29 of the patients based on the microscopic examination of the glands.

A total of 98 arteriographic studies was carried out with 70 considered nonselective and with 28 considered selective injections of the inferior thyroid artery. The evaluation of the parathyroid glands was based on stretched or curvilinear arteries suggesting a space-occupying lesion and on parenchymal opacification of the gland itself.

Using the nonselective technique, nine abnormal glands were correctly identified and six were incorrectly called normal. Using the selective technique,

ten glands were accurately called normal and there was no false negative. Selective angiography is superior to the nonselective technique probably because most of the parathyroid glands receive their vascular supply from the inferior thyroid artery. It is apparently unnecessary even to attempt to catheterize the superior thyroid artery.

It is of interest that among 13 patients with normal blood calcium levels there were five with pathologic parathyroid glands. The authors emphasize that the angiographic method requires considerable technical facility and they recommend that the method be restricted to parathyroid centers and principally to patients selected for re-exploration.—*E. Frederick Lang, M.D.*

Abdomen

Diard, F., Tavernier, J., Rabin, A., and Gout, A. Aspects radiologiques des tumeurs malignes primitives des voies bilaires: tumeurs de l'ampoule de Vater exclues. (Radiologic considerations of primary malignant tumors of the biliary tract: exclusive of tumors of the ampulla of Vater.) *J. de radiol., d'électrol. et de méd. nucléaire*, Aug.–Sept., 1974, *55*, 561–568. (Address: Dr. F. Diard, Chaire d'Electroradiologie, Hôpital Saint-André, 1, rue Jean-Burguet, 33075 Bordeaux, France.)

The authors report 30 cases of primary malignant tumors of the biliary tract. There were three cases of tumors of the gallbladder. The diagnosis was made by celiac arteriography in two cases, and by transparietal cholangiography in one case.

Carcinoma of the gallbladder occurs most frequently in the female in the sixth decade. It is often associated with the presence of gallbladder calculi. Direct extension occurs into the local surrounding area, while metastasis is to the liver.

The plain film may reveal the presence of opaque calculi or a calcified gallbladder (porcelain gallbladder). Cholecystography and cholangiography may be performed in the absence of jaundice. However, by means of celiac-mesenteric arteriography, an early and accurate diagnosis can be obtained. Transparietal cholangiography and retrograde cholangiography following catheterization and opacification of the biliary tract are indicated in the presence of jaundice.

There were 27 cases of tumors of the bile ducts, 14 at the hilum, eleven in the common hepatic duct, and two in the common bile duct.

Tumors of the bile ducts occur predominantly in the male, especially in the older age group. Carcinoma of the hepatic duct extends to the liver, carcinoma of the common bile duct extends into the pancreas. Both types metastasize to the liver. The striking clinical finding is jaundice. The liver may be enlarged. The gallbladder is distended and large in carcinoma of the common bile duct. It is empty and nonpalpable in carcinoma of the hepatic duct.

Roentgenologic examination is limited to transparietal cholangiography and retrograde cholangiography following catheterization through the papilla.

Carcinoma involving the hilar portion of the hepatic ducts causes marked dilatation of the intrahepatic ducts. Carcinoma of the common hepatic duct usually causes localized progressive narrowing of a 1–2 cm segment with proximal dilatation. The duct distal to the site of obstruction is of normal caliber.

Carcinoma of the common bile duct, with distal obstruction, causes pronounced proximal dilatation involving the gallbladder, the cystic duct, the common hepatic duct, and the intrahepatic ducts. It may be difficult to differentiate between carcinoma of the common bile duct and carcinoma of the head of the pancreas.

Often the diagnosis of carcinoma of the biliary tract is made late, hence, the poor prognosis of this disease. Only palliative surgery then may be performed.—*William H. Shehadi, M.D.*

Duscellier, R., Gasquet, C., Barfier, J., and Morand, X. Aspects etiologiques des stenoses du tronc coeliaque. (Stensois of the celiac axis: etiologic considerations.) *J. de radiol., d'électrol. et de méd. nucléaire*, Aug.–Sept., 1974, *55*, 569–575. (Address: Dr. C. Gasquet, Service Central de Radiologie, route de limoges, 86021 Poitiers, France.)

The authors stress the importance of routinely obtaining a lateral view of the opacified abdominal aorta, and its branches, during arteriographic studies of the digestive tract. As a result of this technique, the celiac axis was routinely visualized. This led to the discovery of 40 cases of stenosis of the celiac artery in a consecutive series of 100 examinations.

This incidence of 40 percent is relatively high, and the stenotic lesion would have been missed if the lateral view was not routinely obtained.

The 40 patients ranged in age between 17 and 77 years. There were 22 males—average age of 52, and 18 females—average age of 69.

The causes of stenosis are varied. They may be: (1) Intrinsic, invariably due to atheromatous disease, involving a 0.5–1.5 cm segment of the artery. (2) Extrinsic due to compression by: (a) carcinoma of the pancreas; (b) nonmalignant disease of the pancreas (pancreatitis and pseudocyst); (c) other tumorous condition—malignant tumor of the liver, abscess of the liver, splenomegaly; (d) stenosis due to compression of the arcuate ligaments of the diaphragm.

In six cases, the cause of the stenosis could not be determined.

The degree of stenosis varies between 50–70

percent. The degree of prestenotic dilatation as well as the development of collateral circulation are variable.

Two tables and eight figures, illustrating the various types and degrees of stenosis accompany this article.—*William H. Shehadi, M.D.*

Swischuk, Leonard E., and Tyson, Kenneth R. "Burned-out" pyloric stenosis: an elusive gastric outlet obstruction. *Radiology*, Oct., 1975, *117*, 373–379. (Address: Leonard E. Swischuk, M.D., Department of Radiology, University of Texas Medical Branch, Galveston, Texas 77550.)

Classic infantile pyloric stenosis with the onset shortly after birth is usually readily established on the basis of clinical history and roentgenographic examination. The authors present four cases of this condition in which the diagnosis was not established until these infants were somewhat older than the typical case.

These infants presented for the most part with (a) prolonged history of abilious vomiting, often projectile to begin with and usually starting shortly after birth, (b) failure to thrive and gain weight properly, (c) a barely palpable or non-palpable pyloric muscle mass, and (d) an atypical or even deceptively "normal" upper gastrointestinal examination. The authors feel that the diagnosis of "burned-out" pyloric stenosis should be entertained whenever this symptom complex is encountered and when the gastrointestinal examination is atypical or deceptively "normal." It was often helpful to find previous upper gastrointestinal studies which have been interpreted as being equivocal or thought to be normal.

The differential diagnosis should include pylorospasm, and on occasion pylorospasm with peptic ulcer disease. Other rare causes of gastric outlet obstruction such as antral webs, gastric duplication cysts, and congenital stenoses of the stomach should also be considered, but these are extremely rare. A therapeutic trial of medical management with antispasmodic therapy will usually allow differentiation between the two more common conditions of pylorospasm and peptic ulcer disease.

The etiology of "burned-out" pyloric stenosis is not clear but the authors suggest the hypothesis that it may be that as smooth muscle involutes, fibrosis ensues and short segment, fixed, narrowing of the antropyloric canal results, leading to the findings.

The authors recommend that the treatment of this condition should consist first of a short trial of antispasmodic therapy and that if this fails, surgical intervention should then follow with either pyloromyotomy or pyloroplasty performed, depending on the findings at the time of surgery.—*Donald N. Dysart, M.D.*

Julien, Peter J., Goldberg, Henry I., Margulis, Alexander R., and Belzer, Folkert O. Gastrointestinal complications following renal transplantation. *Radiology*, Oct., 1975, *117*, 37–43. (Address: Henry I. Goldberg, M.D., Department of Radiology, M-380, University of California School of Medicine, San Franciso, Calif. 94143.)

Clinical and roentgenographic data for 510 patients who underwent renal transplantation were analyzed. Thirty-three serious gastrointestinal complications developed in 29 patients (six percent). Thirteen of 29 (45 percent) died of these complications. Although the time of onset varied from 12 hours to 30 months, most complications occurred within four months of transplantation, when the greatest incidence of rejection occurred, renal function was depressed and immunosuppressive therapy was at the highest dosage level. Half of the patients had evidence of rejection either immediately before or during the onset of complications; it was also during this period that the clinical diagnosis of gastrointestinal complications was most difficult and roentgenograms became the prime method of diagnosis.

All three patients with bowel infarction died within three weeks of diagnosis. In two patients severe ileus developed immediately after surgery and rapidly progressed to bowel infarction. One patient died following spontaneous perforation of the sigmoid colon. Three of four patients with fistulas, abscesses, or both, died of gram negative sepsis. One of two patients with gangrenous cholecystitis died of gram negative sepsis. One of five patients died with pancreatitis and hyperamylasemia. Seven of nine patients with upper gastrointestinal ulcers had hematemesis. Two of three patients who had upper gastrointestinal series were demonstrated to have ulcers. The other six patients underwent surgery without prior roentgenographic examination. Other complications included small bowel obstruction, massive ileus, diffuse esophagitis and pneumatosis cystoides intestinalis.—*Jon F. Bergstrom, M.D.*

Chiles, John T., and Platz, Charles E. The radiographic manifestations of pseudolymphoma of the stomach. *Radiology*, Sept., 1975, *116*, 551–556. (Address: John T. Chiles, M.D., Department of Radiology, Ohio State University Hospital, Columbus, Ohio 43210.)

Pseudolymphoma of the stomach is a benign proliferation of lymphoreticular tissue which can be mistaken histologically for malignant lymphoma. The authors have reviewed the clinical records and roentgenograms of 18 patients with pseudolymphoma of the stomach. The average age of the patients at the time of diagnosis was 51 years, with ages ranging from 18 to 76. Only five of the patients, however,

were below 40 years of age. There were 14 men and 4 women. Most patients gave a long history of gastrointestinal complaints and some had noted a recent increase in severity. The duration of these symptoms ranged from four months to three years, averaging eleven months.

The roentgenograms of these patients were reviewed and the findings appeared to fall into three relatively distinct groups: tumor masses, enlarged gastric rugae, and benign appearing ulcers.

All of the cases were characterized histologically by a proliferation of lymphoid tissue, usually in an irregular or nodular pattern in relationship to varying amounts of fibrous tissue. Lymphocytes predominated and were mature, and germinal centers were frequently found.

The diagnosis of pseudolymphoma of the stomach is difficult to make preoperatively, in part because of the lack of uniformity of the clinical and laboratory findings. The authors believe the diagnosis of pseudolymphoma may be suggested preoperatively in patients who have malignant appearing or indeterminate ulcers on stomach examinations and repeated negative gastric cytologies and biopies.

The etiology of pseudolymphoma of the stomach remains obscure, however, the authors believe that it is most often a reaction to chronic peptic ulcer disease. Many of their patients had long histories of gastrointestinal complaints, generally with ulcer type symptoms. Morphologically there appears to be a continuum from chronic peptic ulcer with an associated lymphoid hyperplasia to a massive proliferation of lymphoreticular tissue which is designated pseudolymphoma. Roentgenographically, this continuum extends from well defined ulcer to a mass with malignant appearing ulceration. It is unknown why occasional individuals respond to chronic peptic ulceration with formation of a tumor-like proliferation of lymphoid tissue.—*E. Jerome Schoolar, M.D.*

Pfister, Richard C., Weber, Alfred L., Smith, Edward H., Wilkinson, Robert H., and May, Detliff, A. Congenital asymmetry (hemihypertrophy) and abdominal disease: radiological features in 9 cases. *Radiology*, Sept., 1975, *116*, 685–691. (Address: Richard C. Pfister, M.D., Radiology Research Office, Massachusetts General Hospital, Boston, Mass. 02114.)

Nine patients with congenital hemihypertrophy and co-existent abdominal disease are reviewed. Congenital hemihypertrophy or asymmetry is an idiopathic condition which consists of enlargement of part or all of one side of the body. This entity has gained in significance in recent years because of demonstrated association with childhood tumors.

Six of the nine patients in this series had abdominal tumors. Five of these were malignant. The remaining three patients had renal abnormalities, one a medullary sponge kidney and the other two, ectopic kidneys. Of the tumors, one was of the liver, a hepatoblastoma. The remainder were either renal or adrenal. Three were Wilms' tumors, one an adrenal carcinoma, and the other an adrenal adenoma.

The etiology of congenital asymmetry is unknown but the condition has been associated with three major abdominal tumors in children. In other large series of patients, three percent of children with Wilms' tumors had congenital hemihypertrophy, three percent of children with adrenal cortical carcinoma or adenoma also had congenital hemihypertrophy and three percent of children with hepatoblastoma were found to have congenital hemihypertrophy. There is no definite relationship between the laterality of hemihypertrophy and any of the tumors reported. Hemihypertrophy has not been linked with the most common cancers of childhood, leukemia and lymphoma. A number of benign disorders such as hamartomas and congenital defects, especially of the genitourinary tract, have been described with the condition. Congenital asymmetry should not be included with the hypertrophy associated with some vascular malformations or neurogenic disease. Although considered a rare disorder, congenital hemihypertrophy is probably more common than reports would indicate.—*J. M. Stoebner, M.D.*

Enayat, U., Wendler, H., and Hubmer, G. Zur diagnostischen Problematik massiver Nebennierenblutugen Neugeborener. (Diagnostic problems in massive adrenal hemorrhage in the newborn.) *Wien. klin Wochenschrift*, Oct., 1975, *87*, 583–588. (Address: Dr. U. Enayat, Universitäts-Kinderklink, Auenbruggerplatz, A-8036 Graz, Austria.)

Massive adrenal hemorrhage in the newborn frequently presents as an abdominal mass and is difficult to diagnose when this is the sole clinical feature. Surgery is indicated for the diagnosis and treatment of those cases in which a malignant tumor cannot be ruled out with certainty from the appearance of the roentgenograms.

Massive bleeding into the newborn adrenal gland is seen more frequently in the presence of a high birth weight, prematurity, asphyxia or trauma during or after birth, maternal diabetes, infection, bleeding disturbance, and in male infants. Causes of calcification in the region of the adrenal glands in addition to bleeding into the gland include tuberculosis, echinococcosis, and tumors, such as neuroblastoma, nephroblastoma, pheochromocytoma, renal cell carcinoma, adenomas, and ganglioneuroma.

Three patients are presented with detailed descriptions of the clinical and roentgen findings.—*Augmented Published English Abstract.*



Hysterosalpingogram with Salpix Contrast Medium.



24-hour postinjection x-ray of same patient.

now you see it

now you don't

With Salpix as your contrast medium, your gynecologic patient needn't undergo the 24-hour postinjection x-ray usually required with iodized oils. Water-soluble Salpix leaves virtually no irritating radiopaque residue to produce foreign-body reactions, yet it provides the viscosity needed for adequate visualization.

Contraindications: Contraindications to hysterosalpingography include the presence of severe vaginal or cervical infections, existing or recent pelvic infection, marked cervical erosion or endocervicitis, and pregnancy. The procedure is contraindicated during the immediate pre- or post-menstrual phase.

Sensitivity Test: If indicated in the patient's history, an intracutaneous skin test or sublingual absorption observation may be done with 0.1 cc Salpix.

Warning: Not for intravenous use.

CONTRAST MEDIUM

Salpix

TRADEMARK

EACH CC CONTAINS:
sodium acetrizoate 0.53 g and
polyvinylpyrrolidone 0.23 g

Ortho

© ORTHO PHARMACEUTICAL CORPORATION 1970

ORTHO PHARMACEUTICAL CORPORATION • RARITAN, NEW JERSEY 08869

Philips Polytome and

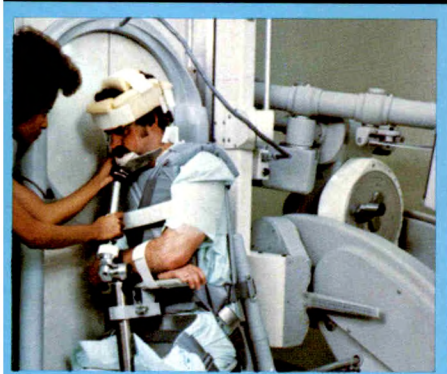
Multi-Directional Tomography for Pneumoencephalography in a fully integrated system.

Now the Polytome—world's most sophisticated tomographic system—has its own snap-on examination chair for pneumo-encephalography. It's never been easier or more efficient to use multi-directional tomography in pneumo studies!

Isocentric patient positioning keeps the patient's head in the fulcrum for all projections. And Polytome and chair are fully synchronized for proper filling of ventricles and temporal horns.

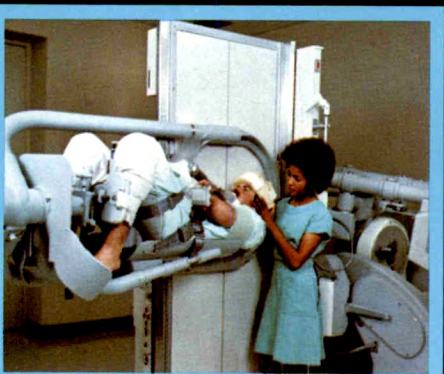
Selected patient positions and visualizations in a common pneumo procedure

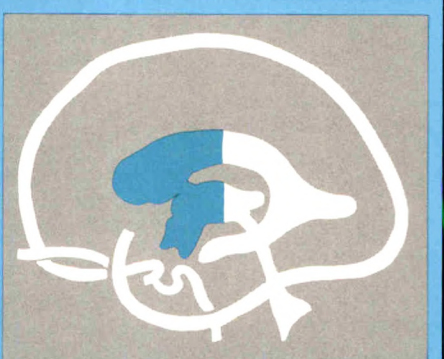
ERECT: LATERAL



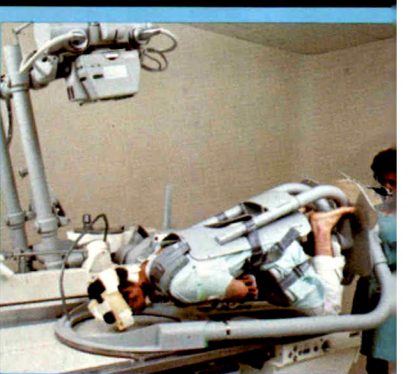


BROW-UP: LATERAL





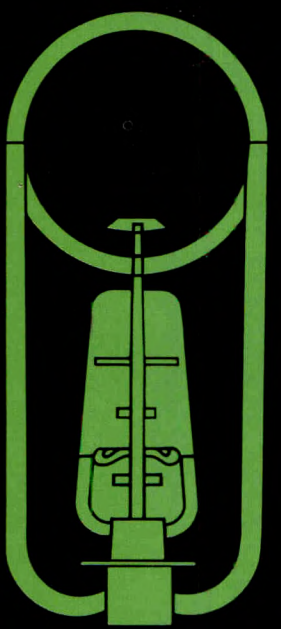
BROW-DOWN: PA





Dedicated Pneumo Chair

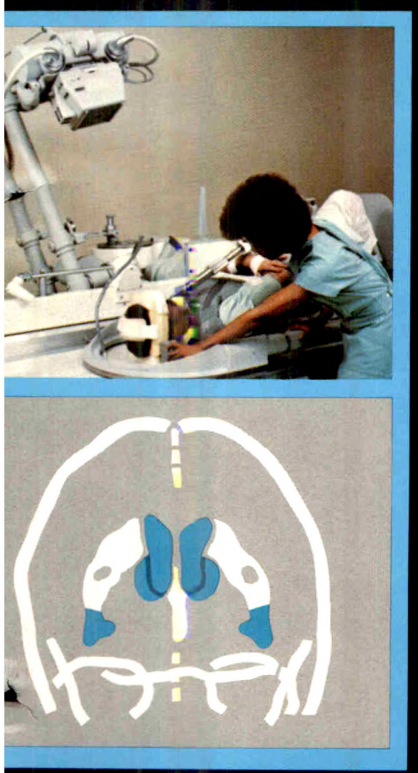
Compact, lightweight, easily and quickly attached, dismounted and stored in the Polytome room, the new chair gives you full use of *all* the Polytome's capabilities: from linear to the famous hypocycloidal blurring motions... layer height adjustment... superb image quality in every exposure... constant enlargement for every layer... optimum visibility of the patient throughout the examination.



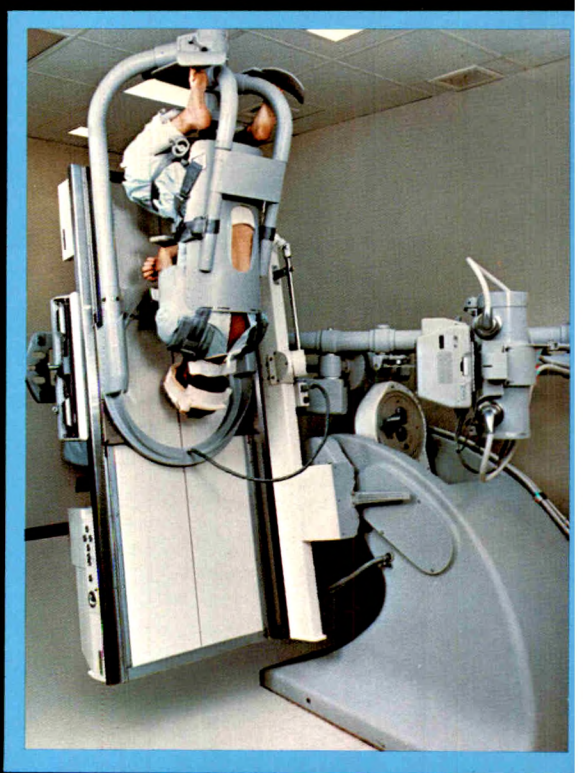
Add a Pneumo Chair to any new or existing Polytome for a dedicated neuroradiological system at a fraction of the cost. Detach the Chair and return the Polytome to its role as top department performer!

Now let *us* "pull up a chair" and show you how it works.

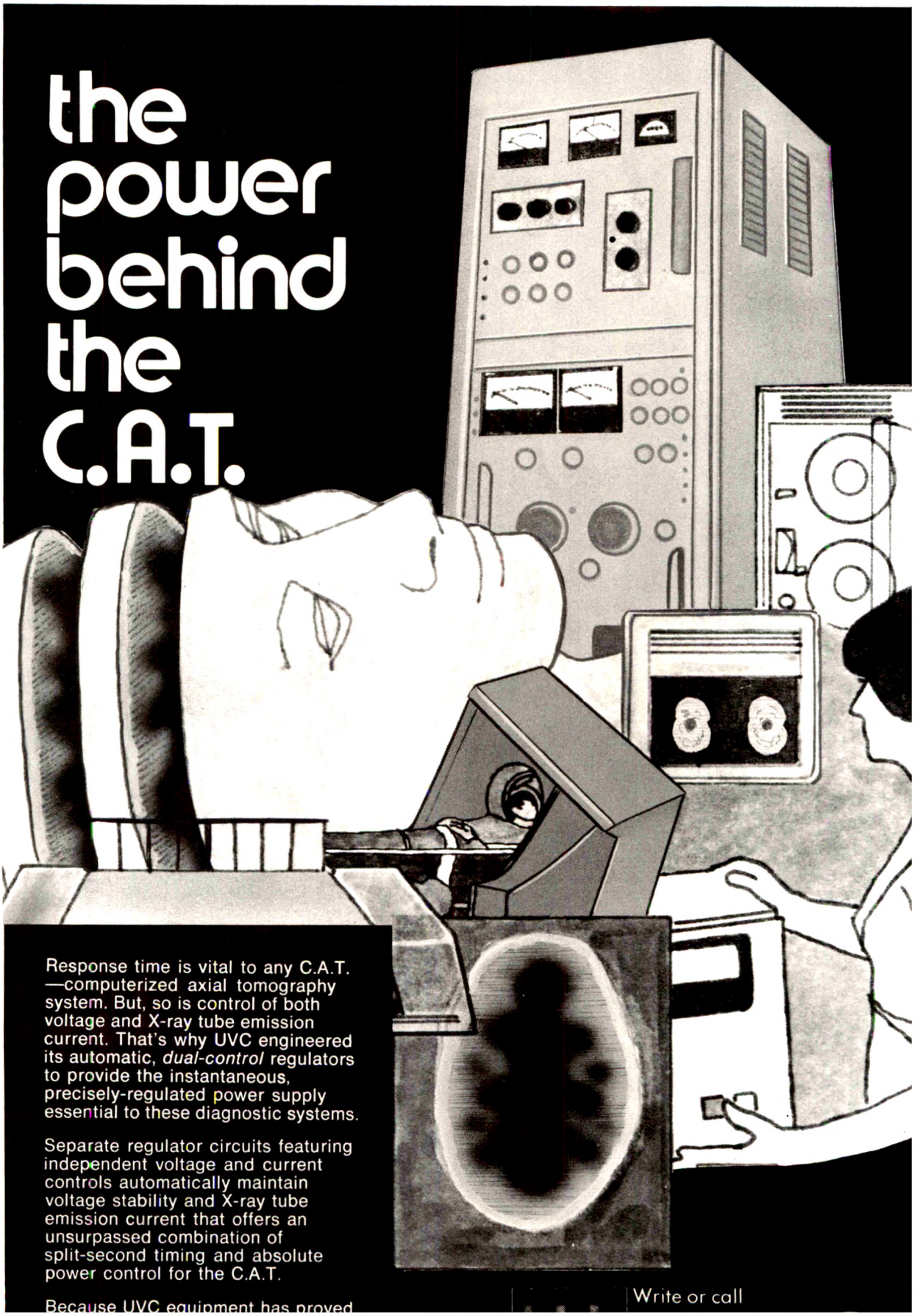
BROW-UP: AP*



A STAGE IN FILLING THE TEMPORAL HORNS



the power behind the C.A.T.



Response time is vital to any C.A.T. —computerized axial tomography system. But, so is control of both voltage and X-ray tube emission current. That's why UVC engineered its automatic, *dual-control* regulators to provide the instantaneous, precisely-regulated power supply essential to these diagnostic systems.

Separate regulator circuits featuring independent voltage and current controls automatically maintain voltage stability and X-ray tube emission current that offers an unsurpassed combination of split-second timing and absolute power control for the C.A.T.

Because UVC equipment has proved

Write or call



When it comes to X-ray Accessories...

(and a **free** Catalog)

Now, you can order **direct from USR,** a world leader in the design and manufacture of X-ray accessories. A new illustrated catalog is just off the press, complete with all the technical information you need to place your order.

- **Halsey Cassettes**
- **Radelin Intensifying Screens and Grid Cassettes**
- **Wafer-Lite Illuminators**
- **Panoramic Illuminators**
- **X-CHEC Protective Aprons**
- **Protective Gloves**
- **Positive Film I.D. Systems**
- **Film Dryers**
- **Darkroom Accessories**

So, when it comes to X-ray accessories, come **direct to USR.** Drop us a line today. Your **free** catalog will come **direct to you.**

come direct to USR

United States Radium Corporation
Medical Products Division
1425-37th Street
Brooklyn, N.Y. 11218

One of the best reasons for cassetteless radiography is about 5'2" tall.

And right next to the 5'2" reason is a 6'8" reason — a stack of 100 conventional cassettes.

One Rapido® film magazine can hold as much film as those 100 cassettes. Which means that a Picker cassetteless system saves a lot of loading time, storage space and tired personnel.

Cassetteless is convenient. But it's also fast, easy and sure. A Picker cassetteless system consisting of Rapido horizontal Bucky, Rap-X™ film transport and Diplomat® automatic processor delivers finished films in 120 seconds.

Push-button control selects one of four film sizes. Total Exposure Automation (TEA) assures consistent film density regardless of type of study. Each study is correctly identified simply by inserting the patient's ID card.

And if you interface Picker's Automatic Chestfilmer with your Rapido system, you have a total cassetteless installation capable of handling up to 70% of an average department's radiographic case load.

But there's one more good reason for Picker cassetteless radiography which your Picker representative will be happy to demonstrate — cassetteless economics.

Cassetteless radiography is an appropriate example of what we mean by the concept of Picker synergy — the complete interfacing of systems and services for improved diagnostic visualization.

Contact your local Picker representative. Or write Picker Corporation, 595 Miner Road, Cleveland, OH 44143.

PICKER®

ONE OF THE C.I.T. COMPANIES


Picker'synergy

UNIVERSITY OF BRITISH COLUMBIA, VANCOUVER B.C., CANADA

GENERAL DIAGNOSTIC RADIOLOGY REFRESHER COURSE
MAY 19, 20, 21, 1976

At the Bayshore Inn (Western International Hotels), Vancouver

PROGRAM

Wednesday, May 19

Morning *Chest*

—Pulmonary Edema .....Robert G. Fraser.
—Diffuse Bilateral Pulmonary Disease in Children .....J. Scott Dunbar.
—Pleuropulmonary Changes in Non-penetrating Thoracic Trauma .....John G. Clement.
—Immunological Diseases of the Thorax ..Robert G. Fraser.
—Cyst and Cyst-like Lesions of the Lung in Children .....J. Scott Dunbar.

Afternoon *Skeletal*

—Iatrogenic Lesions of the Skeleton ....Ronald O. Murray.
—Some Interesting Aspect of Skeletal Trauma .....Harold G. Jacobson.
—Importance of Soft Tissue in Relation to Skeletal Radiology .....Ronald O. Murray.
—The Hand as a Mirror of Local and Systemic Diseases .....Harold G. Jacobson.

Film Reading Session:

Chairman: Harold G. Jacobson
Panelists: J. Scott Dunbar, Robert G. Fraser, Ronald O. Murray.

Thursday, May 20

Practical Techniques in Diagnostic Radiology

Morning

—Gastrointestinal Examination in Infants and Children .....J. Scott Dunbar.
—Non-Operative Removal of Common Duct Stones .....H. Joachim Burhenne.
—Angiographic Techniques in Control of Gastrointestinal Hemorrhage .....Josef Rösch.
—Peritoneography: Normal & Pathological Anatomy .....Morton A. Meyers.
—Genitourinary Examination in Neonates and Infants .....Walter E. Berdon.
—PANEL DISCUSSION.

Afternoon

—Techniques and Advances in Myelography ....Alan J. Fox.
—Percutaneous Biopsy of Lung, Kidney and Bone .....Anthony F. Lalli.
—Chest Radiography .....Robert G. Fraser.
—Equipment and Techniques in Abdominal and Obstetrical Ultrasound .....George R. Leopold.
—PANEL DISCUSSION.

Friday, May 21

Morning *Gastrointestinal Radiology*

—Diagnosis of Gallstones .....H. Joachim Burhenne.
—Seeded Metastases: Pathways and Diagnostic Features .....Morton A. Meyers.
—Abdominal (non-obstetrical) Ultrasonography .....George R. Leopold.
—Angiography of the Liver & Pancreas .....Josef Rösch.
—Anatomy of the Post-Op. Stomach ..H. Joachim Burhenne.
—Intestinal Effects of Pancreatitis .....Morton A. Meyers.

Afternoon *Genitourinary Radiology*

—Controversies on Reflux, Infection and Pyelonephritic Scarring .....Walter E. Berdon.
—Renal Papillary Necrosis .....Anthony F. Lalli.
—Renal & Adrenal Angiography .....Josef Rösch.
—Obstetrical Ultrasonography .....George R. Leopold.
—Obstructive Uropathies .....Walter E. Berdon.
—Calculi and Calcifications of the Urinary Tract .....Anthony F. Lalli.

TUITION FEE

$200. (Canadian) payable when submitting registration form. Fellows and Residents in approved training program $100. (With certification from Chief of Program to accompany registration form), includes Lunches and Coffee Breaks.

ACCREDITATION

The course is approved for 18 hours of credit in Category 1 for the Physicians recognition award of the American Medical Association.

$10 Cancellation Fee for Withdrawals after May 5, 1976

PREREGISTRATION FORM. (please type or print)

Name ..... Telephone .....

Address .....

Type of Practice .....

Date ..... Signature .....

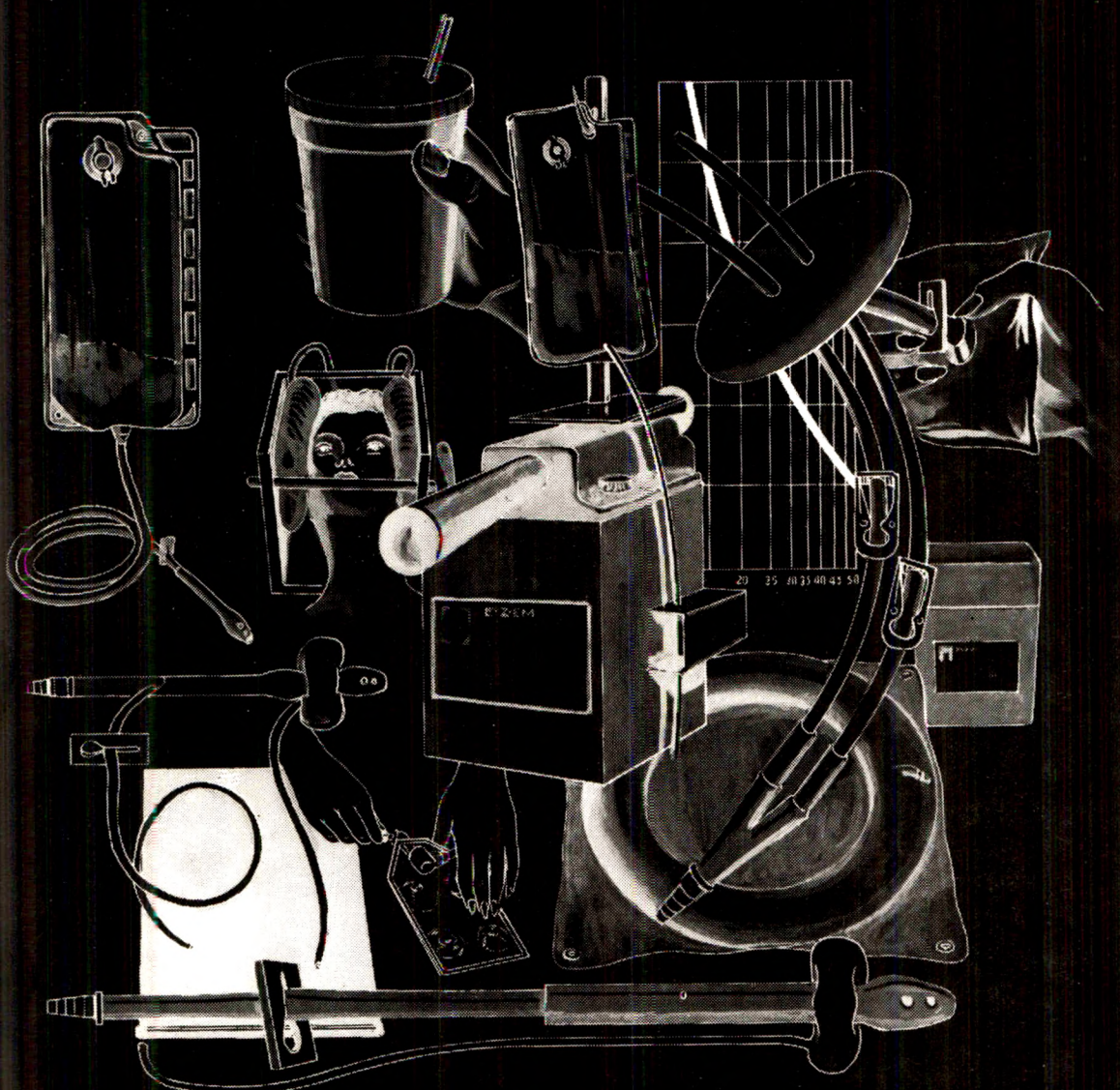
Return with cheque payable to: RADIOLOGY REFRESHER COURSE, C/O D. Gordon Garrow, Department of Diagnostic Radiology, 10th Avenue & Heather St., Vancouver, B.C. V5Z 1M9, Canada.

Accommodation Requested: Single ..... Twin ..... Double .....

Date of Arrival ..... Date of Departure .....

Barium, Barium Systems, and Ancillary Products

...formulated and designed to meet the realistic needs of the Modern Radiology Department



E-Z-EM

System of your choice

111 SWALM STREET

Westbury, N.Y. 11590 (516) 333-8230

International Affiliates: E-Z-EM Rooster B. V., Infirmeriestraat 6-8, Rotterdam 16, Netherlands
E-Z-EM De Mexico, S. A. de C. V., Calz. Azcapotzalco La Villa No 882, Zona Industrial Vallejo, Mexico 16 D. F.

SIEMENS

Optimatic® Generators
Designed-in X-ray serviceability.

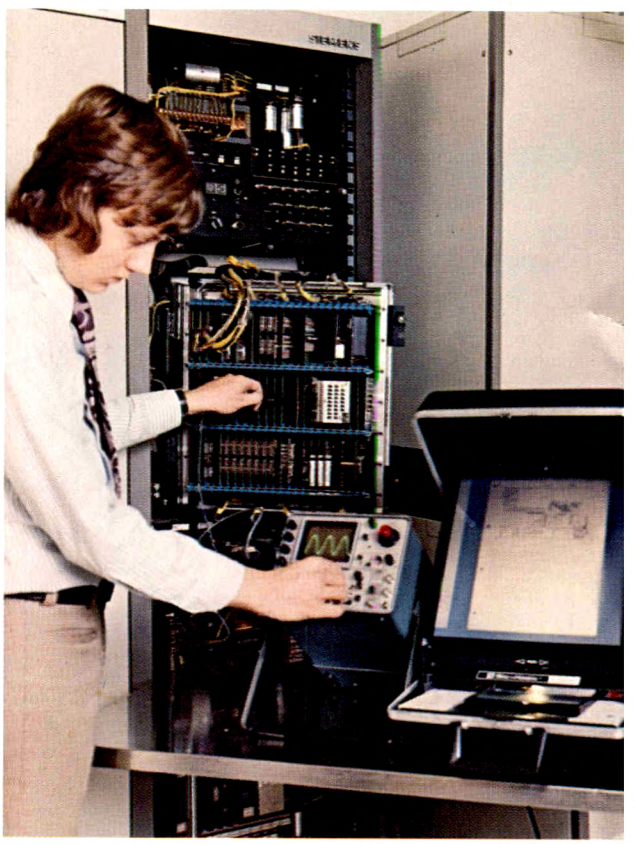
Siemens Optimatic generators are the first X-ray systems with designed-in serviceability. A three-part program helps you get the most from your X-ray equipment and keep it operating.

Siemens Optimatic generators are equipped with an Automatic Fault Finder that tells when your X-ray equipment is functioning normally. It also provides an easy way to discover what is wrong whenever faults occur. In the event of malfunctions, the Automatic Fault Finder, built into the control cabinet, helps pinpoint the problem. No time-consuming and complicated circuit tests and measurements are needed. Repair work can be started immediately.

Finding a fault is one thing. Having the parts to correct it is another. Siemens technicians are equipped with Service Support Kits containing all of the most frequently used parts.

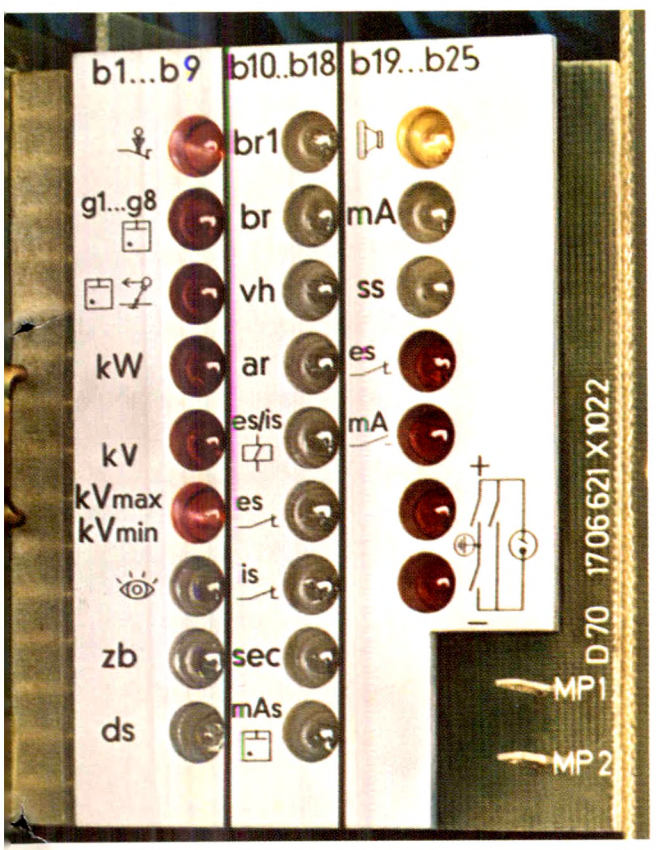
In addition, Siemens service technicians carry complete Microfilm Case Histories of every X-ray system they service. These case histories include circuit diagrams, installation, modification and service records. And they are portable, eliminating the need to check office files for vital information.

Optimatic Generators with designed-in serviceability. Three new service innovations from Siemens. Write for detailed literature.

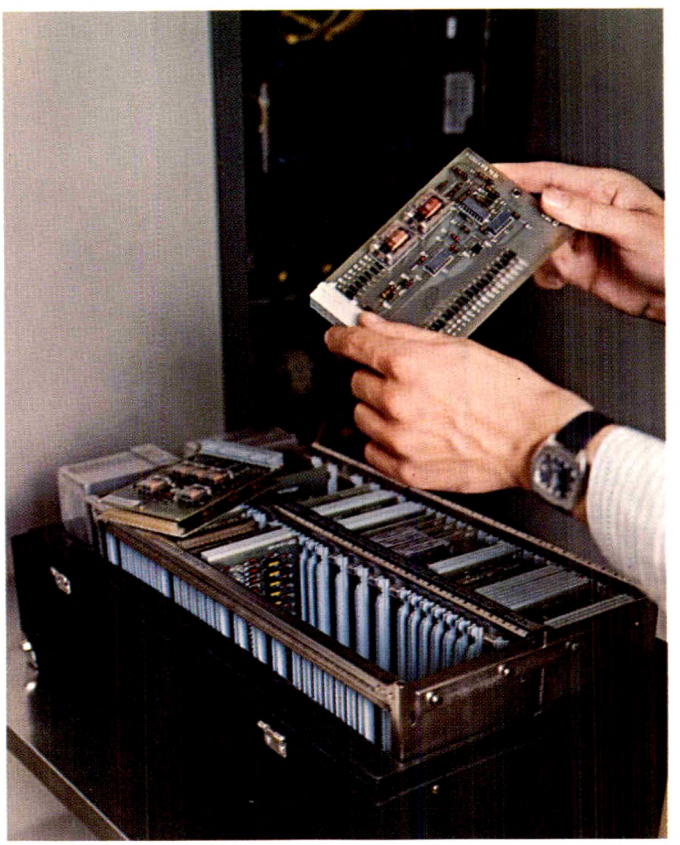


A Microfilm Case History of circuit diagrams for a Siemens X-ray unit.

Siemens Corporation
Medical Systems Division
186 Wood Avenue South, Iselin, New Jersey 08830 (201) 494-1000.
In Canada: Siemens Canada Limited, P.O. Box 7300, Pointe Claire 730-P.Q.



utomatic Fault Finder built into the
entral generator control cabinet.



A typical replacement circuit board in the
Siemens Service Support Kit.



redi-*FLOW*® puts convenience on tap-with four studies from one source.

Now—a presuspended, prehydrated barium preparation that's easy and economical to use in all gastrointestinal radiological studies:

esophageal **upper G.I.** **routine enema** **air contrast enema**

Time-saving redi-Flow is flavored, concentrated, prehydrated, autoclaved, and homogenized.

Ready to use—with simple dilution directions for each type of study (no blender needed).

Produces consistent, uniform coating in all radiological examinations, including excellent readings in post-evacuation films.

Available in individual 16 fl. oz. cans; for added thrift, a plastic top is included to facilitate refrigeration for later use.

All-purpose Suspension redi-Flow (barium sulfate 100% W/V).

Simplifying without compromising



FLOW PHARMACEUTICALS, INC.
Palo Alto, CA. 94303



Now the complete,
flexible ultrasound system:

The RT-400.

For dynamic, two-dimensional,
real-time, high-resolution imaging
(Today and tomorrow.)

For more information, write or call:

Grumman Health Systems
400 Crossways Park Drive
Woodbury, New York 11797
(516/575-3513)

GRUMMAN

The Clinac® 18

Varian Commitment Stands Out

Varian's commitment to radiotherapy has resulted in the powerful Clinac 18, a multi-modality accelerator with 10 MV photons and 6 to 18 MeV electrons. Today the Clinac 18 serves over twenty radiation therapy centers and has become the most widely selected radiotherapy accelerator in its energy range.

But the record shows Varian commitment means even more. It means response . . . our trained field support staff has nearly tripled during the past 2 years. It also means design evolution . . . our engineering team is constantly seeking ways to make refinements, with retrofitability wherever possible.

This is the meaning of Varian commitment. Clinac users have known it for 15 years.

Varian Radiation Division,
611 Hansen Way,
Palo Alto, CA 94303
Phone: 415-493-4000.
World-wide sales and service.

varian





Photographed at Radiation Oncology Center of Sutter Community Hospitals, Sacramento, CA. (right); El Paso Cancer Treatment Center, El Paso, TX. (upper); University of Arizona Medical Center, Tucson, AZ (lower).



CHARLES C THOMAS • PUBLISHER

AN ATLAS OF POLYTOME PNEUMOGRAPHY *by* **Taher El Gammal** *and* **Marshall B. Allen, Jr.**, *both of Medical College of Georgia, Augusta. Assisted by* **Paul Dyken**. This atlas presents a large number of studies which supplement the study of normal anatomy of the cerebrospinal fluid pathways and provide comparison for the identification of abnormal structures. Concentration is on the findings of polytome pneumography but, where possible, correlations are made with angiography, positive contrast ventriculography, and CAT examinations. Relative values of these different examinations are demonstrated. Topics include normal CSF pathways, atrophy, hydrocephalus, intrasellar subarachnoid recess–sellar and suprasellar lesions, and metasellar mass lesions–herniations. *'76, 480 pp. (8 1/2 x 11), 729 il., $39.50*

THE HAND ATLAS *by* **Moulton K. Johnson** *and* **Myles J. Cohen**, *both of UCLA, Los Angeles, California.* This atlas portrays the anatomy of the hand as the surgeon will encounter it in the operating room – layer by layer, beginning with the skin and ending with x-ray studies of the bones. Photographs of dissections of unembalmed specimens are all approximately life-size or larger, resulting in better illustrations. Topics include the distal volar forearm, the palm, thumb, fingers, the radial side of the hand, spaces of the hand and wrist mechanics. *'75, 108 pp. (8 1/2 x 11), 121 il. (8 in color), $22.00*

"TRAUMA" AND "NO-TRAUMA" OF THE CERVICAL SPINE *edited by* **Kenneth R. Kattan**, *Univ. of Cincinnati College of Medicine, Cincinnati, Ohio. (11 Contributors)* This complete volume on the topic of cervical spine trauma includes descriptions and excellent illustrations on the anatomy of the cervical spine and numerous varieties of trauma, their assessment and management. Discussed are the many symptoms attributed to cervical spine trauma as well as diseases which provoke this malfunction. The authors deal not only with trauma, but also with how to differentiate it from other conditions including the normal. *'75, 328 pp., 292 il., $24.50*

ADMINISTRATION OF A RADIOLOGY DEPARTMENT: Hints for Day-to-Day Operation *by* **Murray L. Janower**, *St. Vincent Hospital, Worcester, Massachusetts.* Various systems which can be applied to the radiology department to insure efficient functioning are presented in this book. In addition to a general overall look at a totally functioning diagnostic radiology department, the various subunits in a department are dissected and discussed in detail. All of these discussions are supplemented by a great deal of statistical data. Specific attention has been given to the methods used in handling patients, the establishment of a quality control program, efficient production of radiological reports, methods of film interpretation, and darkroom operations. *'76, 72 pp., 8 il., 7 tables, $7.50*

THE FUNDAMENTALS OF X-RAY AND RADIUM PHYSICS (5th Ed., 4th Ptg.) *by* **Joseph Selman**, *Univ. of Texas, Tyler.* Most of the material in this new, completely revised and updated edition has been rewritten to simplify and clarify further the important physical concepts, although the fundamentals have undergone relatively little revision. Many of the illustrations have also been revised or completely redrawn. New sections have been added on solid state rectification, newer types of mobile apparatus, special tubes for mammography, xeroradiography, and saturable reactor for control of filament current. *'75, 552 pp., 306 il., 16 tables, $12.95*

ELEMENTS OF RADIATION PROTECTION *by* **Ronald V. Scheele** *and* **Jack Wakley**, *both of the Univ. of Virginia School of Medicine, Charlottesville, Virginia.* Information in this textbook includes atomic structure, ionizing radiation, interaction of radiation with matter, sources of radiation exposure, biological manifestation of radiation exposure, permissible dose limits, principles of radiation protection and monitoring devices. Several chapters of the book deal with federal performance standards and Atomic Energy Commission regulations. *'75, 112 pp., 15 il., 10 tables, $7.95, paper*

Orders with remittance sent, on approval, postpaid

301-327 East Lawrence Avenue • Springfield • Illinois • 62717

Ad Council
A Public Service of
This Magazine &
The Advertising Council

Would you hire you?

Of course you would. You work hard.
And you're good at it.
Like most Americans. But, if all of us
did just a little better, we'd
wind up with better products, better
services and even more pride
in the work we do.

America. It only works as well as we do.

The National Commission on Productivity, Washington, D.C.

Hanley Space Saver X-Ray and Medical Record Cabinets are installed in most hospitals in America.

Top quality and low price is the reason.
5 compartment with doors—$199.50
5 compartment less doors—$171.50
Brochure F.O.B. Factory

AMERICA'S LARGEST DISTRIBUTOR OF X-RAY CABINETS

HANLEY MEDICAL EQUIPMENT CO.
5614 South Grand X-Ray Division St. Louis, Mo. 63111

In reply to advertisers
please mention that you saw
their advertisement in

THE
AMERICAN JOURNAL OF
ROENTGENOLOGY

published monthly for
The American
Roentgen Ray Society
by

CHARLES C THOMAS • PUBLISHER
Springfield, Illinois 62717



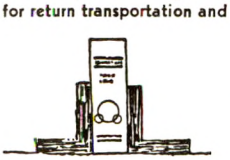
Bind Your Journal Issues Into Valuable Vigilant Volumes

Pertinent information you sometimes desperately need is too often in the Journal issue you cannot find. Single copies have a way of getting lost, misplaced or destroyed. It is better for you to let us permanently bind each journal into semi-annual or annual volumes —then your reference source is always complete, organized and instantly at your service. We call them "Vigilant Volumes"; they so carefully store and provide on instant notice so much knowledge of timely value.

The cost per "Vigilant Volume," by official commission from the journal publishers is but $5.95 per volume, permanently hard bound in washable buckram, gold embossed with period dates, journal name and special insignia—plus your name stamped in gold leaf. "Vigilant Volumes" are handsome library additions too, real conversation pieces. These volumes are bound in the authorized colors.

HOW TO ORDER

Simply ship your journal issues to us via parcel post, together with your name, address, AND REMITTANCE, at $5.95 per volume. Within 45 days after receipt, bound volumes will be shipped to you. Price subject to change without notice. Please remit 50¢ per volume for return transportation and handling.



PUBLISHER'S AUTHORIZED BINDERY SERVICE, Ltd.
(Authorized Binders of All Journals)
4440 W. Roosevelt Rd.
Chicago, Illinois 60624

CGR's Titanos Program. Suddenly, you have the services of five generators-from one generator.

Meeting the generator needs of busy x-ray departments can be a costly-and sometimes unpredictable-necessity.

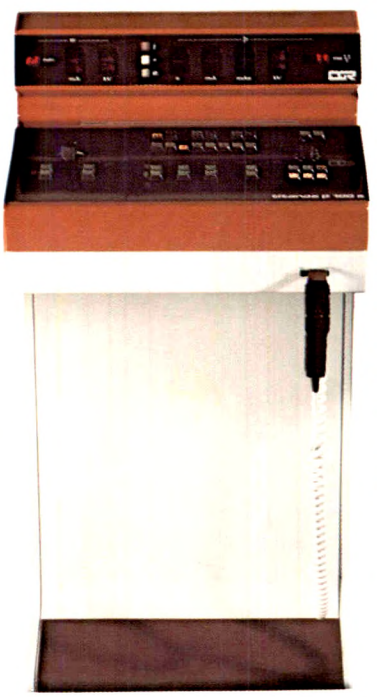


And one requirement is always there-the need for more than one powerful, versatile, three phase generator.

CGR fills this basic need with the new Titanos Program. It offers the significant benefit of a completely modular, remote unit programming system that permits the versatile operation of up to four additional rooms off of one generator.

You start with the Titanos P generator – a three phase, 12 pulse unit available in four power ratings from 50 to 125 kW. Complete with fluoroscopy, anatomical radiography and special technique modules.

From here you expand to one, two, three or four additional remote terminals. Each operating through the master generator – and each acting as a master generator – via a unique time-sharing process. Each capable of operating a specific x-ray system for specific applications. A chest unit. A general radiographic table. A skull system. Or even a sophisticated tomo or remote system.



All told, the basic capacity of one system is 96 programs. The versatility of a three phase generator in five rooms. Increasing your department operations, flexibility and performance – at a significant decrease in cost.

Your CGR representative has all the details.

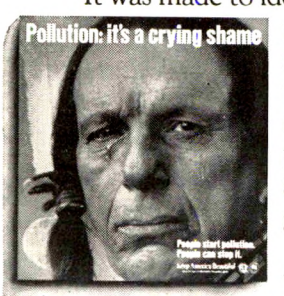
CGR

CGR MEDICAL CORPORATION
2519 Wilkens Avenue
Baltimore, Maryland 21223
(301) 233-2300
CGR CANADA Ltée-Ltd.
500 Boulevard de l'Aéroparc
Lachute, Québec, Canada
(514) 562-8806

We've made our mark.

The symbol you see in the center of this page is the new mark of The Advertising Council.

It was made to identify the public service advertising campaigns provided to scores of worthwhile organizations.

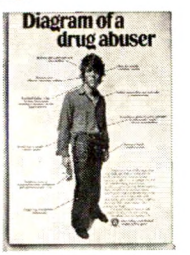


Through these Advertising Council campaigns, the men and women of the American business and communications community are working to make their mark on America's future.

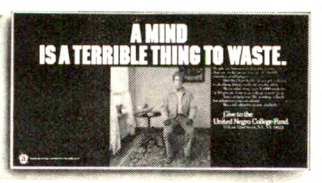




Creative and marketing experts at advertising agencies make their mark. By donating the services it takes to plan and execute these campaigns.



Television/radio networks and local stations, newspapers, business publications, consumer magazines, outdoor and transit media make their mark. By donating the space it takes to run them on the air and in print.



Concerned corporations make their mark. By donating the cash contributions it takes for The Advertising Council to coordinate all these resources and focus them where they are most urgently needed.

In short, every time The Advertising Council stamps its new mark on public service advertising, a lot of people make their mark.

And that mark counts for a lot.



A Public Service of This Magazine & The Advertising Council



Keep it up.

To the thousands of employers who have signed the Statement of Support for the Guard and Reserve, our sincere thanks. To those who haven't, please think it over. It's one of the best investments you can make. And a commitment to your own conscience.

A strong Guard and Reserve is an absolute must for America. Perhaps more so now than at anytime in our history. Today, this vital volunteer force represents almost 30% of our total military personnel needs—at a cost of only 5% of our entire defense budget.

You, as an employer, can help keep the Guard and Reserve trained and ready. This means *all* employers —the large, small, and those in between. Everyone who knows and values the freedom we live in.

Your signature on the Statement of Support is a pledge to back your employees who serve in the Guard and Reserve. It's an assurance that a couple of weeks on military duty won't limit their job opportunities. And for you, it means more productive, more responsible employees. Because in the Guard and Reserve they'll sharpen acquired skills and learn new ones, develop a real sense of leadership, add to their earnings and retirement benefits.

To receive your Statement of Support, or more information, write: EMPLOYER SUPPORT, Arlington, VA 22202.

Ad Council
A Public Service of This Magazine & The Advertising Council

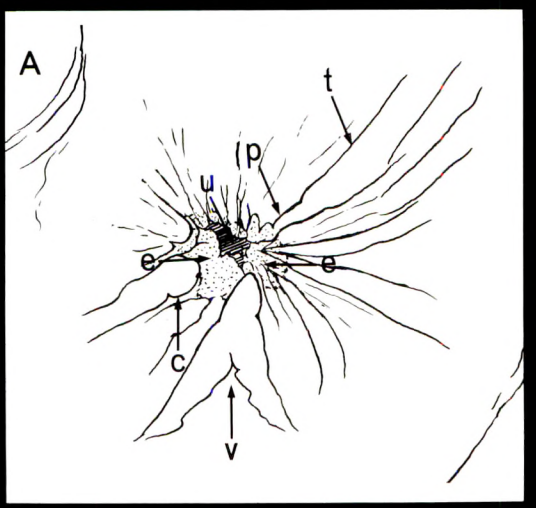
ESGR
EMPLOYER SUPPORT OF
THE GUARD & RESERVE

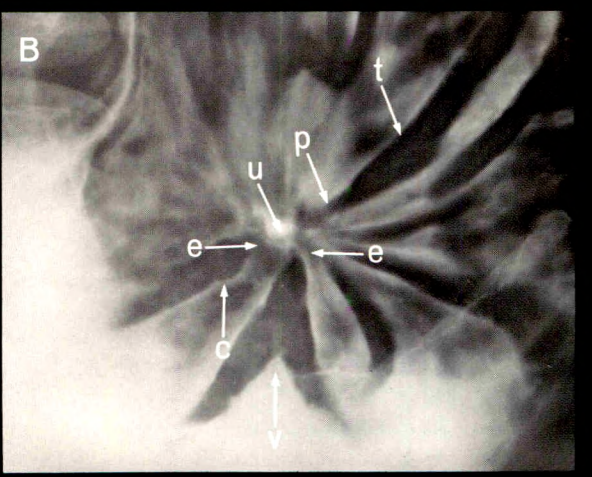
Early Gastric Cancer

To be recognized, this lesion demands radiographic detail of exquisite quality as it involves either gastric mucosa alone or mucosa and submucosa alone. Regardless of size, the lesion usually is curable (Japanese authors). Its hallmarks include the following mucosal abnormalities (coded for reference in illustrations):

Thick fold (t); clubbed fold (c); pointed fold (p); superficial erosion (e); superficial ulcer (u); normal mucosa within erosion (m); normal mucosal fold (n); convergence of abnormal mucosal folds (v).

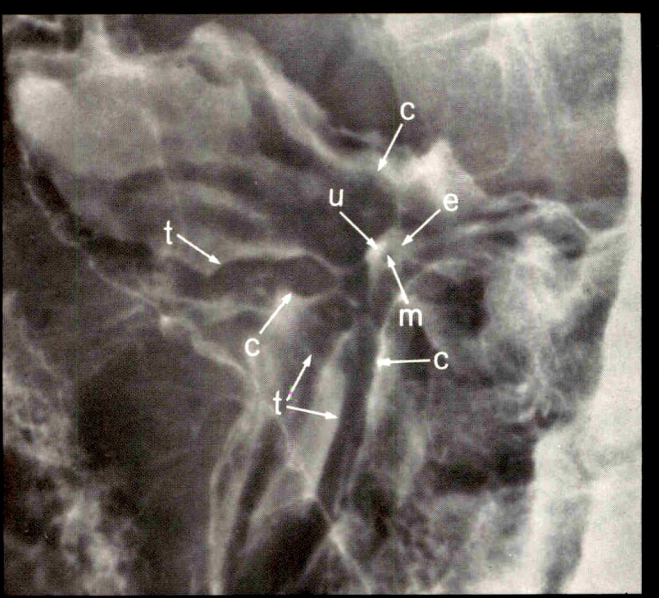
Case I through Case V represent selected radiographic views of mucosal contrast studies of different patients with early gastric cancer.



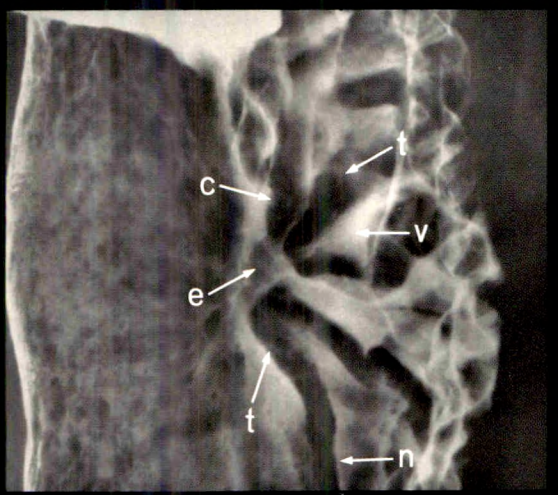


Case I—Early gastric cancer—anterior wall of the body. Figure A is a line drawing of Figure B

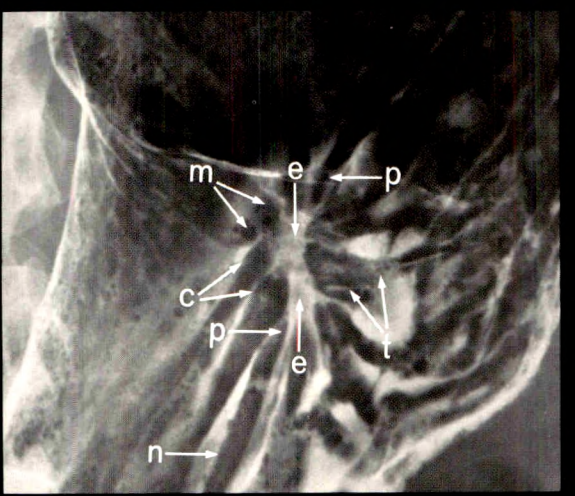
Case II—Early gastric cancer—anterior wall of the antrum.



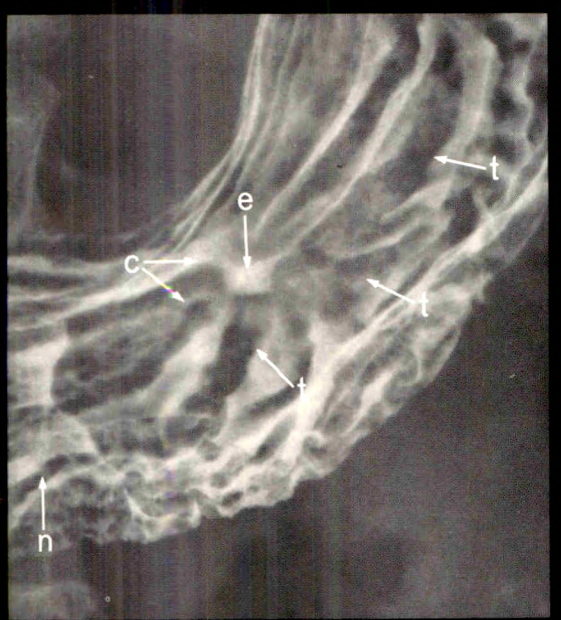
Radiographs and caption material from the American College of Radiology—*An Atlas of Tumor Radiology*—Yearbook Medical Publishers, Inc. Reprints of this and subsequent reports available upon request. Please write Eastman Kodak Company, Dept. 740B, Radiography Markets Division, Rochester, New York 14650.



Case III—Early gastric cancer—posterior wall of the body.



Case IV—Early gastric cancer—anterior wall of the upper portion of the body.



Case V—Early gastric cancer—posterior wall of the body.



Diagnosing disorders like these calls for consistently excellent radiography.

A clearly defined, high-quality image is vital to strengthening and supporting your decisions. And that's the image that sturdy Kodak X-Omatic cassettes help deliver.

As in the cassette pictured here, the curved panel design rolls out air for intimate film/screen contact. The result? A high-quality image characterized by excellent definition and detail.

Kodak offers a choice of x-ray films designed to meet your specific needs. For more information, contact your Kodak Technical Sales Representative or your dealer in Kodak medical x-ray products.

A commitment to quality.

Kodak

Your knowledge... the film of your choice and... HUNT X-RAY CHEMISTRY for maximum information in automatic film processing

With broad years of experience in radiology, you recognize the importance of achieving more readable films.

Hunt Chemistry will increase the diagnostic value of any film you process. Hunt formulas maximize informational content, producing the full range of densities inherent in the films.

For medium to long scale contrast, **Hunt Universal 90 Developer & Replenisher** offers optimum results. If high contrast characteristics are desired, use **Hunt Type 2 Premium 90/90 Developer & Replenisher.**

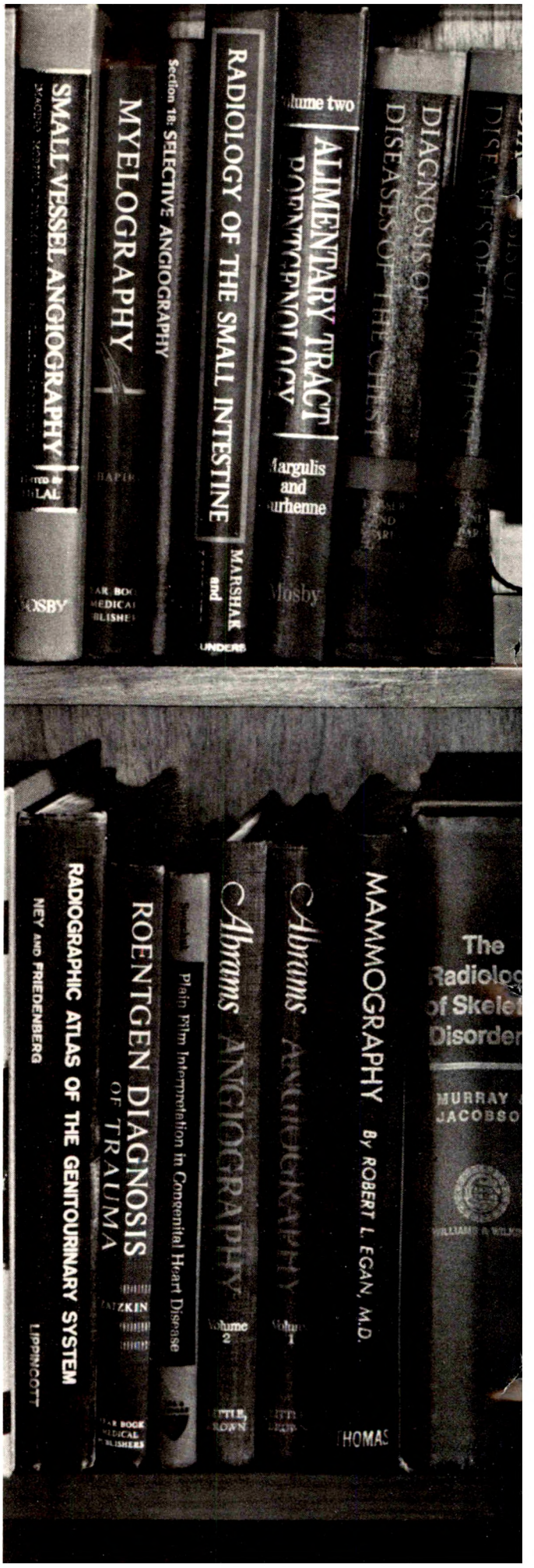
Hunt chemical processing systems are respected for their consistent high quality. These concentrates come to your X-ray department full-strength and in "factory-fresh" containers.

HUNT **The Image Maker**
Photographic Industry Group

Because Hunt markets its products on a direct basis, you can save up to 33% over other major chemical manufacturers' systems.

For more information, call Hunt today.

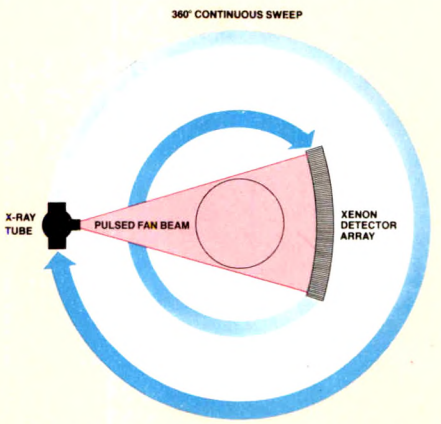
Philip A. Hunt Chemical Corporation, Palisades Park, N.J. 07650
Philip A. Hunt Company (Canada) Ltd., Toronto




KODAK
RP ROYAL X-OMAT
Medical X-ray film
RP/R14
CURIX
GEVAR POLYESTER BASE
RP 2
125 / 8 x 10 in
25539046
2.1977
HR 2000
High Resolution
Medical X-Ray Film
NON-INTERLEAVED
FILMS
8 x 10 INCHES
GAF Corporation
140 West 51 Street
New York, N.Y. 10020
8 x 10 inches
20,3 x 25,4 cm
100 NIF
RAPID R
TYPE S
CRONEX 4 MEDICAL X-RAY FILM
125 SHEETS
FUJI X-RAY FILM
Medical
A TEXT-BOOK OF X-RAY DIAGNOSIS
EDITED BY
S. C. SHANKS
P. KERLEY
THIRD EDITION
ABDOMEN
CHEST
SAUNDERS
JOHN CAFFEY
PEDIATRIC
X-RAY
DIAGNOSIS
5th EDITION
Diagnostic
Neuro-
Radiology
TAVERAS
WOOD
WILLIAMS & WILKINS
YEAR BOOK
HUNT
PREMIUM
90/90
DEVELOPER & REPLENISHER
20 U.S. Gallon Size
PHILIP A. HUNT CHEMICAL CORPORATION
HUNT
UNIVERSAL
90
DEVELOPER & REPLENISHER
20 U.S. Gallon Size
PHILIP A. HUNT CHEMICAL CORPORATION
Palisades Park, New Jersey 07650 • Made in U.S.A.

GE research solves the primary problem of existing total body scanners—motion unsharpness.

GE fast-scan computerized tomography: a whole new generation.



Third generation: GE's continuously rotating pulsed fan beam scanning. 5 to 10 seconds.

First and second generation units aren't fast enough for total body scanning.

First and second generation computerized tomography systems have one major problem: image blurring caused by patient movement during body scans.

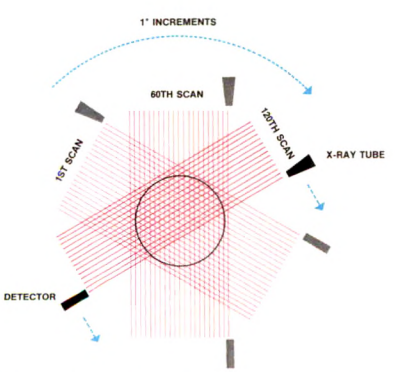
General Electric research has developed a fast-scan technology that is launching a new third generation of computerized tomography (CT) systems. The faster scans provide clear, sharp images.

During body studies, patient movement caused by breathing can result in motion unsharpness.

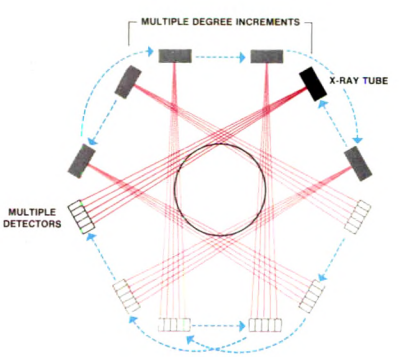
To really tackle this problem, a scan should take less time than a patient can hold his breath comfortably—10 seconds or less. However, existing computerized tomography systems cannot match this speed.

First generation units, using a pencil beam with a 1° incremental rotate-and-translate principle, take 4½ to 5½ minutes to complete a 180° scan.

Second generation systems use multiple pencil beams and more detectors—up to 30. Rotation is in larger angular increments. This configuration takes from 20 seconds to 3½ minutes per scan.



First generation: Pencil beam rectilinear scanning. 4½ to 5½ minutes.



Second generation: Multiple pencil beam rectilinear scanning. 20 seconds to 3½ minutes.

GE develops continuously rotating fan beam technology for fast-scan capability.

In developing an entirely new total body system, GE engineers and scientists abandoned the incremental rotate-and-translate approach of first and second generation units, with their inherent mechanical instability and resultant speed limitations. Instead, GE used a simpler, more stable mechanical approach, in which the tube and detectors rotate smoothly about the body in a continuous 360° scan, without need for translation.

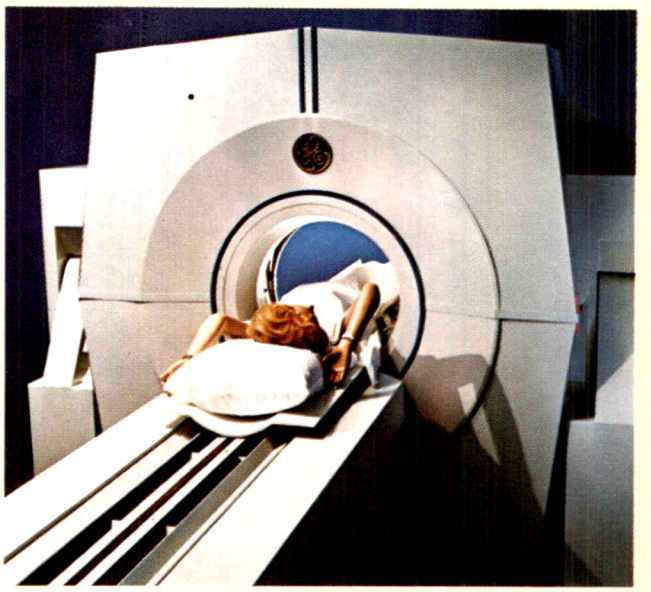
This new third generation technology combines a continuously rotating, pulsed, wide fan x-ray beam with a unique high-pressure xenon detector array of up to 320 stable detectors. Advanced electronics are included to read out the huge volume of data. And GE has successfully conceived and implemented a new computational approach compatible with diverging fan beam geometry.

Third generation fast-scan technology proven on CT/M system.

GE's first application of fast-scan technology utilized computerized tomography's tissue density differentiation capability in the challenging area of breast examinations. This unit, called the CT/M system, is currently being clinically evaluated. Scans are completed in just 10 seconds. Patient handling is minimized. If you are interested in further information about the CT/M system, contact your GE representative or write for Publication 4675.



CT/M System



CT/T System

CT/T system performs body scans in less than 5 seconds.

The CT/T system for total body scanning is moving into the clinical environment. Scan time for the CT/T unit is 4.8 seconds. GE engineers believe this unprecedented scanning speed will provide consistently sharp, clear images for body studies. First production units are scheduled for the last half of 1976. The new CT/T systems represent the culmination of one of General Electric's most extensive research and development programs.

There's a corporate commitment behind GE scanning equipment.

All General Electric scanning systems are backed by the same company that has been serving radiology since the revolutionary Coolidge x-ray tube was introduced 63 years ago. And that kind of corporate dedication to excellence in medical equipment continues today . . . with the development of continuously rotating, pulsed fan beam technology.

As you consider CT scanning equipment, remember GE's continuous commitment to technology, product quality and service. That commitment is an important part of every GE medical system.

Fast-scan CT: backed by GE.

GENERAL ELECTRIC

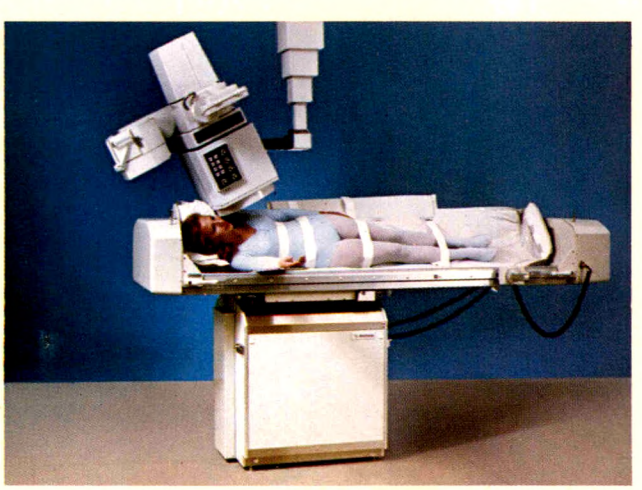
General Electric continues its commitment to the total radiology department.

GE: innovation through technology.

General Electric's extensive CT scanning development program represents only part of a total technological commitment to radiology. As the nation's leading manufacturer of x-ray equipment, GE is pledged to meeting the total needs of radiology departments. A continuing investment in research has resulted in new ideas and product innovations that solve day-to-day departmental problems. Here are some examples:

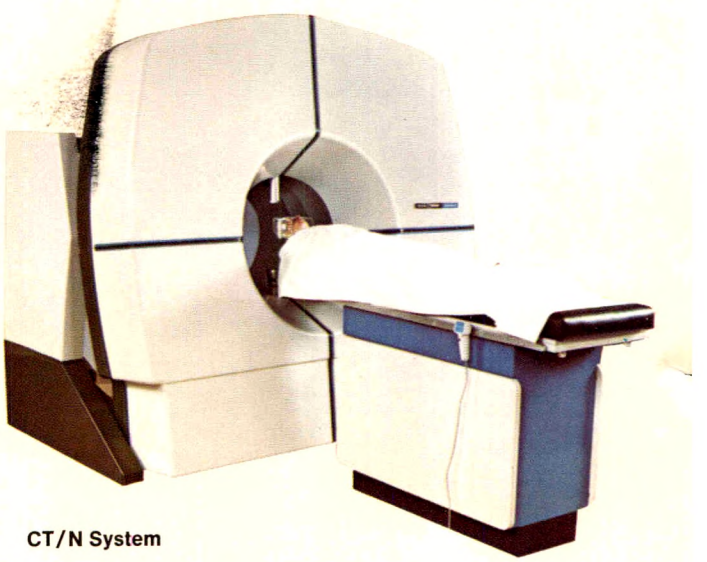
How to give one procedures room the capability of two.

The LAD system adds the capability of a dedicated coronary procedures room to a classical vascular room, permitting all angiographic procedures. Even the axial projection of the left anterior descending coronary artery is obtainable with the LAD system. The unique design features an angulating tube and intensifier with detachable linkage, combined with a rotating patient cradle. Radiation is minimized, with the primary beam shielded by a lead-lined table base. You get Fluoricon® 300 image quality, excellent rigidity and positioning ease. The LAD system: total angiographic capability at minimum cost.



When to use first and second generation CT scanners.

The slower scan times of first and second generation CT systems are acceptable for studies of the head. Here, the anatomy can be immobilized, reducing motion unsharpness.



CT/N System

High quality image performance is provided at a moderate cost. For departments where economics and/or volume indicate a need for this type of scanner, GE offers the CT/N system . . . a dedicated neuro unit. Both first and second generation CT/N systems are available, with scan times of 4½ and 2 minutes, respectively. All CT/N systems feature Individual Patient Discs, which serve as a permanent patient record. These discs store up to eight tomographic scans which can be reconstructed and manipulated at the control console or a viewing unit at any time.



Telegem 90 System

How to get your new R&F room installed in 3 weeks or less.

"Pre-staging" is a new service now being offered by General Electric. *Before* your new pre-staged system leaves our plant, it is completely set up and checked out. All components are assembled, all wiring is checked and all mechanical and electrical functions are tested. We make sure your system is completely operational before it's installed in your department. Pre-staging is available on all GE "preferred" vascular and R&F systems, including Televix™ and Telegem® remote systems. Most pre-staged systems can be fully installed in the hospital in just three weeks or less, from start to finish, minimizing departmental downtime, maximizing patient throughput.

How to give your tube unit solid support.

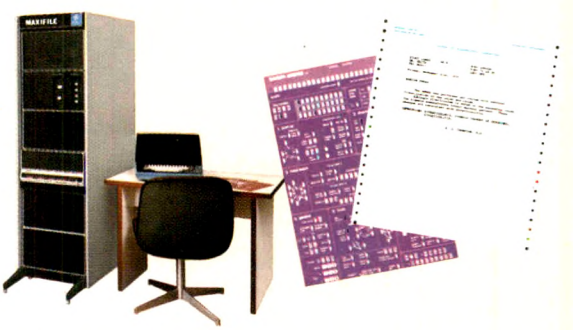
The XT suspension provides exceptional stability for the tube unit and allows remarkably smooth, precise equipment positioning anywhere in the room, with the patient on-table or off. The ease of motion facilitates a broad range of procedures, including cross table studies. A unique cable trim-arm keeps cables orderly and away from the work area.



XT Suspension

How to manage data . . . instantly.

To help radiology departments handle large volumes of data, GE has developed two important systems. Maxifile™ system stores data on hundreds of thousands of patients, and any element of the files can be retrieved in seconds. As patients enter the department, previous records can be instantly retrieved. Films can be quickly located. And lost billing is virtually eliminated. Raport® is a computerized radiographic reporting system. As films are read, the radiologist fills out a mark-sense form. In seconds, the Raport system converts the marks into a complete typed report, ready for



Raport/Maxifile

signature. The combined Raport/Maxfile system gives the radiology department instant data management.

How to get fast, reliable service.



When you select GE, you get a corporate commitment that goes beyond the equipment. We want you to get maximum performance from each system over its full life. That's why GE is committed to supplying the people, the parts and the training necessary to give you fast, dependable service . . . whenever you need it. General Electric Medical Systems, Milwaukee, Toronto, Madrid.

GE: leading the way in x-ray.

GENERAL ELECTRIC

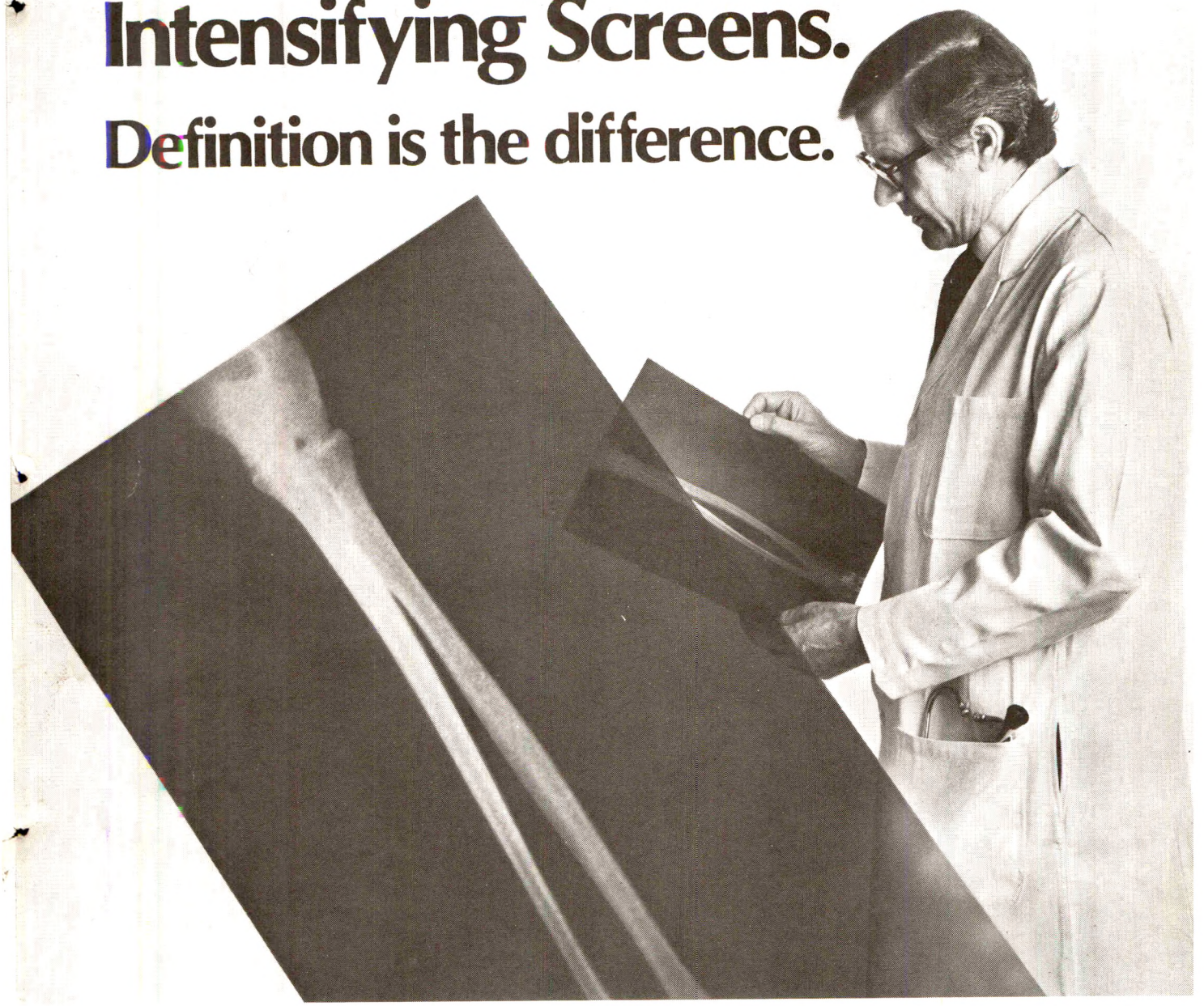
INDEX TO ADVERTISERS

Barnes-Hind Pharmaceuticals ..... xx, xxi
CGR Medical Corporation ..... xliv, xlv
E. I. DuPont de Nemours & Company, Inc. ..... xvi, xvii
Eastman Kodak Company ..... xlviii, xlix
E-Z-EM Company xxxv
Flow Pharmaceuticals xxxviii
General Electric Medical Systems ..... lii, liii, liv, lv
Grumman Health Systems xxxix
Grune & Stratton, Inc. xxii
Hanley Medical Equipment Company xliii
Philip A. Hunt Chemical Corporation ..... l, li
Liebel-Flarsheim Company ..... Cover 2
Machlett Laboratories ii
Donald McElroy, Inc. xviii
Ortho Pharmaceutical Corporation xxvii
Pfizer Medical Systems ..... vii, viii, ix, x, xi
Philips Medical Systems, Inc. (U.S.A.) ..... xxviii, xxix
Picker Corporation ..... xxxii, xxxiii
Purdue-Frederick Company v
Sakura Medical Corporation ..... Cover 3
Searle Radiographics ..... i, vi
Siemans Corporation ..... xxxvi, xxxvii
E. R. Squibb & Sons, Inc. ..... xii, xiii, xxiii, xxiv, xxv, xxvi
Charles C Thomas · Publisher ..... xxi, xlii
Union Carbide ..... xviii, xix
United States Radium Corporation xxxi
Universal Voltronics Corporation xxx
The University of British Columbia xxxiv
Varian Associates ..... xl, xli
Xerox Corporation ..... xiv, xv

We try to present an accurate index. Occasionally this may not be possible because of a last-minute change or an omission.

Sakura X-ray Intensifying Screens.

Definition is the difference.

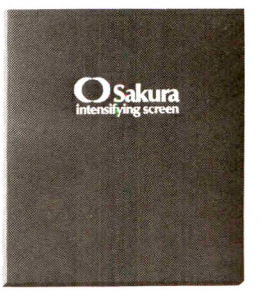


Especially effective in the higher voltage ranges, Sakura X-ray intensifying screens offer higher contrast over a longer life. The advantages are worth considering. Reduced radiation. Minimal loss in resolution. And longer X-ray tube life.

Featuring improved physical and chemical properties, Sakura X-ray screens demonstrate higher surface purity and higher resistance to abrasion. And they are easy to maintain. A plastic coating guards against grime, guaranteeing superior performance after years of continual use.

Sakura X-ray intensifying screens come in popular sizes and are available in three speeds. QD type for excellent contrast without loss of definition. QH type for faster, finer definition. And QS type for fastest, finest definition.

Sakura X-ray intensifying screens. Higher contrast. Longer life. And less expensive than comparable types.



SAKURA

Sakura Medical Corporation
Radiographic Film and Instrumentation
57 Bushes Lane, Elmwood Park, New Jersey 07407
(201) 794-0800

AMERICAN JOURNAL OF ROENTGENOLOGY

VOL. 126 APRIL 1976 NO. 4

DIAGNOSTIC RADIOLOGY

Virus Diseases of Bone. Do They Exist? The Neuhauser Lecture. *Frederic N. Silverman, M.D.* 677

Loss of Colonic Haustration in Progressive Systemic Sclerosis. *William Martel, M.D., Stanley F. Chang, M.D., and Murray R. Abell, M.D.* 704

Roentgen Findings in Aorto-Enteric Fistulae. *George M. Wyatt, M.D., Michael I. Rauchway, M.D., and Harold B. Spitz, M.D.* 714

Multiple Benign Ureteral Fibrous Polyps. *Felix A. Hughes, III, M.D., and Charles S. Davis, Jr., M.D.* 723

Cavitating Lung Nodules and Pneumothorax in Children with Metastatic Wilms' Tumor. *E. George Kassner, M.D., Harold S. Goldman, M.D., and Alberto Elguezabal, M.D.* 728

The Spotted Nephrogram of Renal Scleroderma. *Jeffrey Winograd, M.D., Daniel H. Schimmel, M.D., and Alphonse J. Palubinskas, M.D.* 734

The Role of Emergency Excretory Urography in Evaluation of Blunt, Abdominal Trauma. *Eugene J. McDonald, Jr., M.D., Melvyn Korobkin, M.D., Richard P. Jacobs, M.D., and Hideyo Minagi, M.D.* 739

Arthrography in Total Hip Prosthesis Complications. *Martin I. Gelman, M.D.* 743

The Grooves of the Distal Articular Surface of the Femur—A Normal Variant. *R. Brent Harrison, M.D., Mary Beth Wood, M.D., and Theodore E. Keats, M.D.* 751

Chiba Percutaneous Transhepatic Cholangiography: A Valuable Method for Visualizing the Nondilated Biliary Tract. *Joseph Tabrisky, M.D., Rabbe L. Lindstrom, M.D., Laurence G. Hanelin, M.D., and William F. Pfisterer, M.D.* 755

Organizing a Community Department for Academic Radiology. *D. William Sherrick, M.D., P. F. Mahon, M.D., David B. Lewis, M.D., and Erwin M. Janzen, M.D.* 761

Computerized Tomography (CT) in Acute Head Trauma. *Jorge Merino-deVillasante, M.D., and Juan M. Taveras, M.D.* 765

Individualized Computer Tomography of the Skull with the EMI Scanner Using the 160×160 Matrix. *Steven H. Cornell, M.D., Jacob J. Musallam, M.D., Ching L. Chiu, M.D., and James H. Christie, M.D.* 779

Computed Tomography of the Normal and Infarcted Myocardium. *Douglass F. Adams, Samuel J. Hessel, Philip F. Judy, Jay A. Stein, and Herbert L. Abrams* 786

The Value of Repeat Cerebral Arteriography in the Evaluation of Trauma. *Eugene J. McDonald, Jr., M.D., David P. Winestock, M.D., and Julian T. Hoff, M.D.* 792

Caudal Dislocation of the Pons in the Adult Arnold-Chiari Malformation: An Angiographic Evaluation. *Meredith Weinstein, M.D., and Thomas H. Newton, M.D.* 798

Angiographic Manifestations of Bilateral Wilms' Tumor. *Barry T. Katzen, M.D., and Melvin Markowitz, M.D.* 802

The Abdominal Angiographic Spectrum of Tuberous Sclerosis. *William R. Compton, M.D., Patrick D. Lester, M.D., Myo M. Kyaw, M.D., and Jack A. Madsen, M.D.* 807

The Complication Rate of Catheter Angiography by Direct Puncture Through Aorto-Femoral Bypass Grafts. *Ronald L. Eisenberg, M.D., Richard L. Mani, M.D., and Eugene J. McDonald, Jr., M.D.* 814

Systemic Arterial Supply to Normal Basilar Segments of the Left Lower Lobe. *Donald R. Kirks, M.D., Peter E. Kane, M.D., Edward A. Free, M.D., and Hooshang Taybi, M.D.* 817

Iatrogenic Embolization of the Superior Mesenteric Artery: Arteriographic Observations and Clinical Implications. *Adam Lande, M.D., and Morton A. Meyers, M.D.* 822

Partial Mesenteric Arterial Occlusion with Subsequent Ischemic Bowel Damage Due to Pitressin Infusion. *Cameron Roberts, M.D., and Frank E. Maddison, M.D.* 829

NUCLEAR MEDICINE

Radionuclide Imaging in Skeletal Inflammatory and Ischemic Disease in Children. *Massoud Majd, M.D., and Robert S. Frankel, M.D.* 832

"Doughnut" Sign in Brain Scanning. *Yavuz A. Tarcan, M.D., William Fajman, M.D., Joseph Marc, M.D., and David Berg, D.O.* 842

ULTRASONOGRAPHY

Ultrasonic Evaluation of the Unilateral Nonvisualized Kidney. *John P. Marangola, M.D., Patrick J. Bryan, F.R.C.R., and Farhad Azimi, M.D.* 853

RADIATION ONCOLOGY

Factors that Modify the Radio-Response of Cancer of the Nasopharynx. *Joseph Bohorquez, M.D.* 863

Definitive Treatment of Carcinoma of the Rectum by Intracavitary Radiation Therapy. *Gwynn Jelden, M.D., Ranjit Dhaliwal, M.D., Antonio Rodriguez-Antunez, M.D., Edward Chernak, B.S., R. Turnbull, M.D., Victor Fazio, M.D., and Frank Weakley, M.D.* 877

Serial Studies of Immunocompetence in Head and Neck Cancer Patients Undergoing Radiation Therapy. *Stefano Stefani, M.D., Ronald Kerman, Ph.D., and Joseph Abbate, M.D.* 880

Hemangiopericytoma: Report of Three Cases Regarding Role of Radiation Therapy. *Harbans Lal, M.D., B. Sanyal, M.D., G. C. Pant, M.D., B. L. Rastogi, M.D., N. N. Khanna, M.S., and K. N. Udupa, M.S.* 887

CASE REPORTS

Congenital Absence of the Ductus Venosus: With Direct Connection Between the Umbilical Vein and the Distal Inferior Vena Cava. *John C. Leonidas, M.D., and Richard A. Fellows, M.D.* 892

Aneurysmal Bone Cyst of the Orbit with Unusual Angiographic Features. *A. M. O'Gorman, M.B., and T. H. Kirkham, F.R.C.S.* 896

Vertebral Sarcoidosis: A Case Report and Review of the Literature. *Philip A. Brodey, M.D., Stephen Pripstein, M.D., Gerald Strange, M.D., and Nevea D. Kohout, M.D.* 900

Extra-Abdominal Desmoid of the Axillary Tail Mimicking Breast Carcinoma. *Lester Kalisher, M.D., John A. Long, M.D., and Robert G. Peyster, M.D.* 903

Officers 907

Editorial:

Is Nuclear Medicine in Trouble? John G. McAfee 908

News Items 910

Book Reviews 913

Books Received 915

Society Proceedings 917

Abstracts of Radiologic Literature 924

Acc.
15.11.76

Coming Next Month: International Conference on Bone Mineralization

LIBRARY

AJR

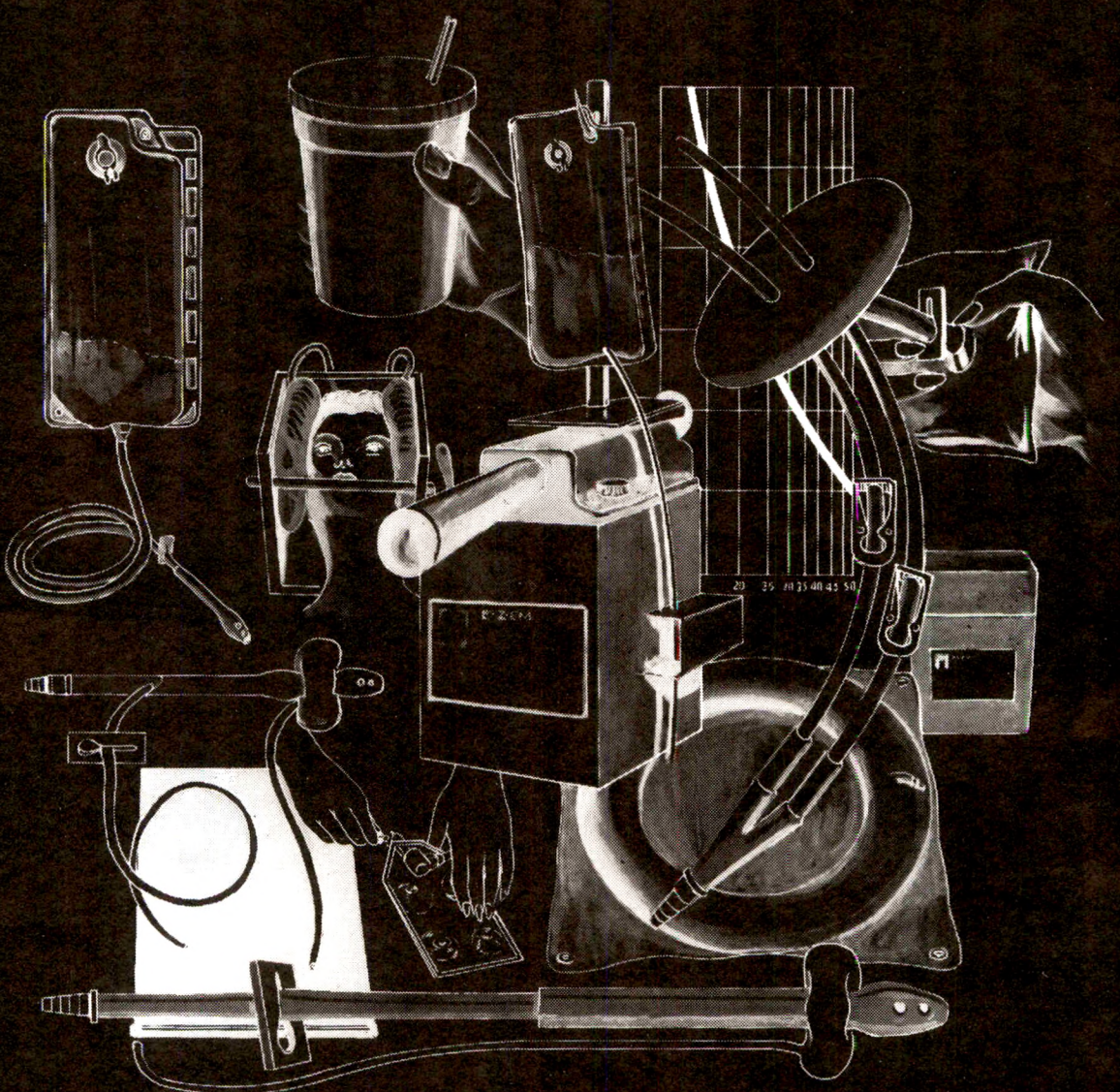
American Journal of Roentgenology

May 1976

UNIVERSITY COLLEGE OF LIBRARY

Barium, Barium Systems, and Ancillary Products

...formulated and designed to meet the realistic needs of the Modern Radiology Department



E-Z-EM

System of your choice

111 SWALM STREET

Westbury, N.Y. 11590 (516) 333-8230

International Affiliates: E-Z-EM Rooster B. V., Infirmeriestraat 6-8, Rotterdam 16, Netherlands
E-Z-EM De Mexico, S. A. de C. V., Calz. Azcapotzalco La Villa No 882, Zona Industrial Vallejo, Mexico 16 D. F.

PERHAPS YOU DON'T REALIZE HOW BADLY YOU NEED THESE MACHINES.

200 & 300
14 x 17" FILM CAPACITY

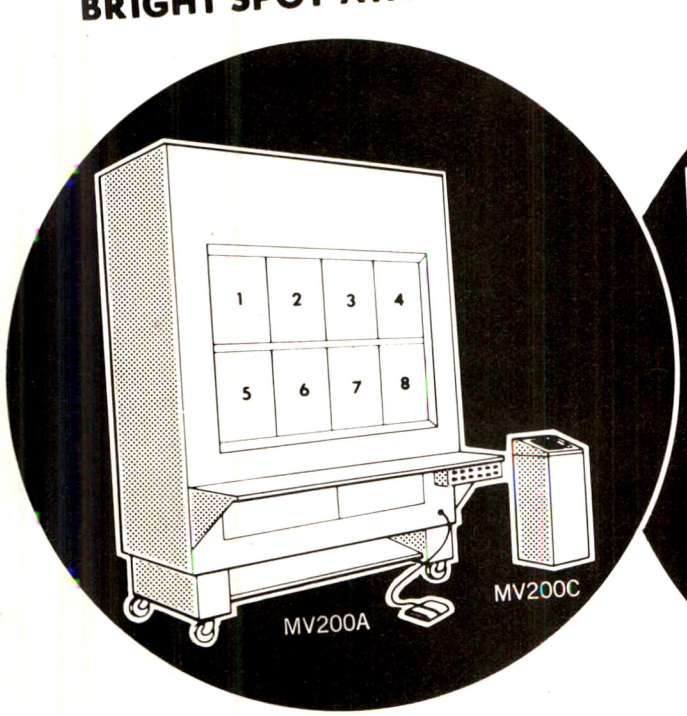
☆ **PUSHBUTTON AUTOMATIC CONTROLLER SELECTOR.**

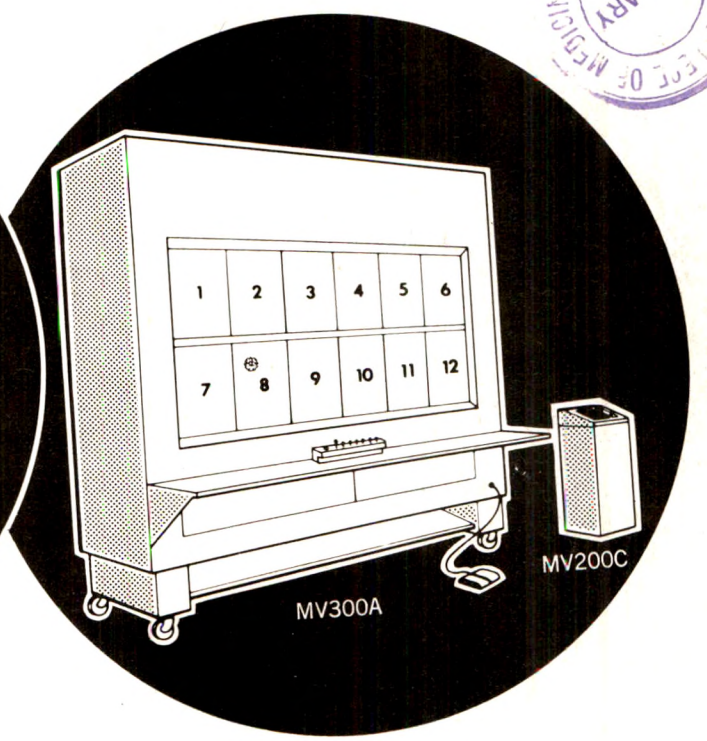
☆ **BUILT-IN FLOATING BRIGHT SPOT AVAILABLE.***

Don't blame us. We've tried and tried to show you how much time and work you can save with the Motorized Viewer.

We are now working on our second thousand installed machines. So we must have something right! Now it's up to you. Think about it.

UNIVERSITY OF ILL. COLLEGE OF MEDICINE LIBRARY





SAVES TIME
Makes Film Reading Easier.

Brochures, Dimensions, Prices and Users' List available on request. Phone or write for complete information.

*FLOATING BRIGHT SPOT

A 3½" diameter Moving Spotlight built into the machine. Completely motorized, the spot can be moved to any point on the viewer to read dense areas. Two speeds in both horizontal and vertical directions permit fast, pinpoint accuracy.

MANUFACTURED BY:

S. & S. X-RAY PRODUCTS INC.

87-93 JAY STREET, BROOKLYN, N.Y. 11201

Telephone: 212-852-6900

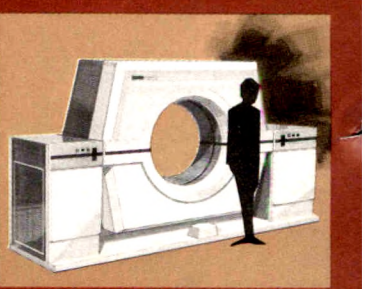
SOME OF THE MANY S. & S. ACCESSORIES SOLD BY YOUR LOCAL X-RAY DEALER

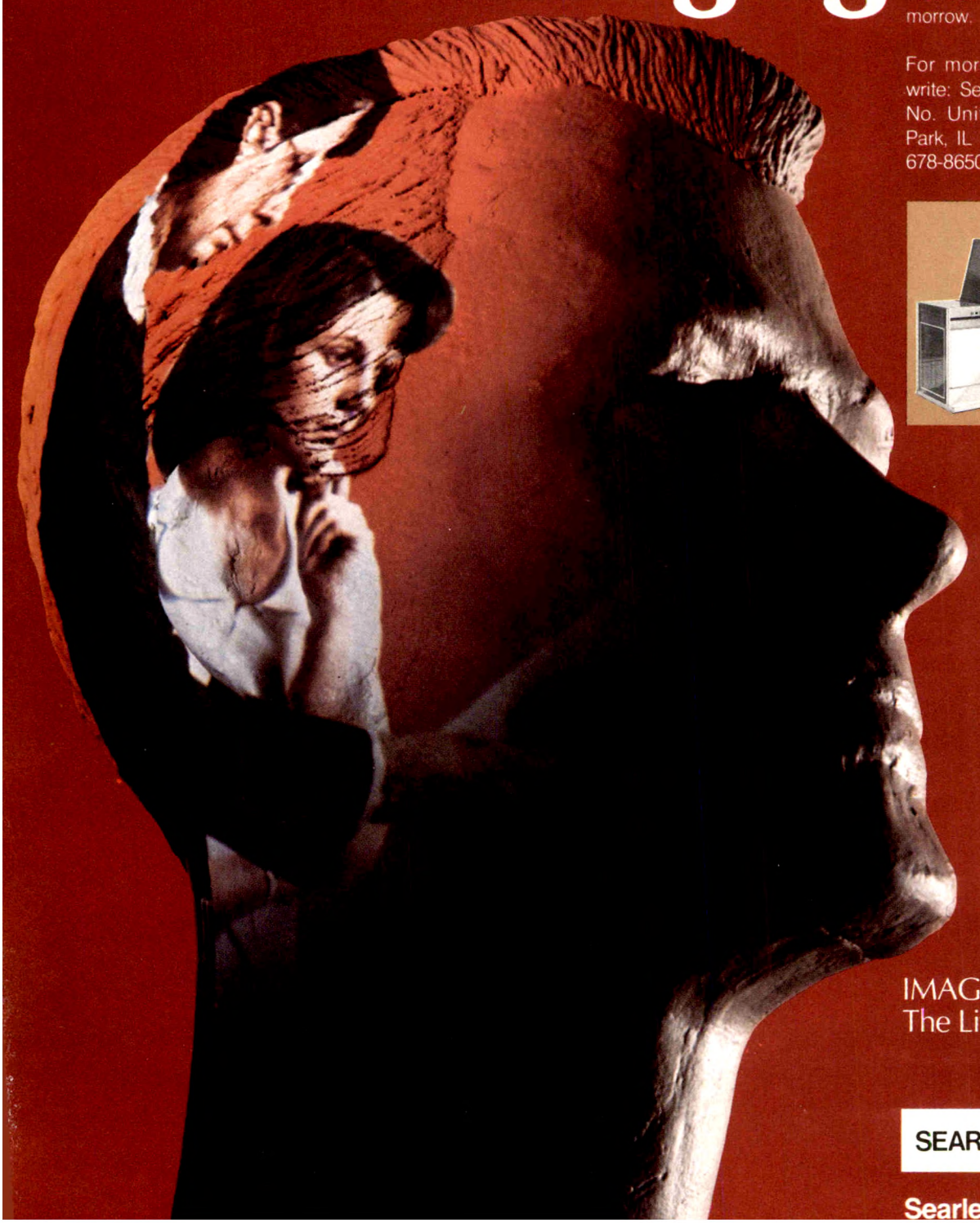
Designed for better CT imaging

Searle will soon introduce a new X-ray CT imager. This highly sophisticated instrument uses advanced mechanical and electronic technology to make CT imaging of the future a practical reality today.

This new system is now being evaluated and will be released for sale when its reliability, speed, and diagnostic superiority have been established. What Searle is developing today, the medical community relies on tomorrow.

For more information, call or write: Searle CT Systems, 4233 No. United Parkway, Schiller Park, IL 60176. Telephone (312) 678-8650.





IMAGING:
The Living Art

SEARLE

Searle CT Systems

AMERICAN JOURNAL OF ROENTGENOLOGY

EDITOR MELVIN M. FIGLEY

ASSISTANT EDITOR ROSALIND H. TROUPIN

ASSOCIATE EDITORS LUTHER W. BRADY
KENNETH L. KRABBENHOFT
E. FREDERICK LANG
RUSSELL H. MORGAN

EDITOR EMERITUS TRAIAN LEUCUTIA

INCLUDING DIAGNOSTIC RADIOLOGY, RADIATION ONCOLOGY, NUCLEAR MEDICINE, ULTRASONOGRAPHY AND RELATED BASIC SCIENCES

CONSULTING EDITORIAL BOARD

KENT ELLIS
E. ROBERT HEITZMAN
DONALD L. KING
JOHN A. KIRKPATRICK, JR.
EUGENE C. KLATTE
JOHN G. McAFEE
THOMAS H. NEWTON
ROBERT G. PARKER
STEWART R. REUTER
WILLIAM B. SEAMAN
ROBERT J. SHALEK
JOHN STORER
MICHEL M. TER-POGOSSIAN
JOSEPH P. WHALEN
DAVID M. WITTEN



OFFICIAL JOURNAL

AMERICAN ROENTGEN RAY SOCIETY

AMERICAN RADIUM SOCIETY



The American Journal of Roentgenology is issued monthly by Charles C Thomas, Publisher, 301–327 East Lawrence Ave., Springfield, Illinois 62717. Correspondence regarding subscriptions, advertisements and other business should be addressed to the Publisher. Annual subscription prices: United States and U. S. Possessions $30.00, Pan America, Canada and others $35.00. Printed by the George Banta Co., Menasha, Wisconsin.

Copyright © 1976 by American Roentgen Ray Society.

Second-class postage paid at Springfield, Illinois and at additional mailing offices. Printed in U.S.A.

GUIDELINES FOR AUTHORS

The AMERICAN JOURNAL OF ROENTGENOLOGY publishes original and timely contributions to the advancement of radiologic diagnosis and treatment. Although the content is predominantly clinical in origin, laboratory investigations are accepted when their relevance to clinical practice is demonstrable. Contributions are reviewed by two outside consultants and are accepted on condition that they are submitted only to this Journal and that they will not be reprinted or translated without consent of the Editor. Statements within an article are the responsibility of the authors and not the Journal or its publisher.

Address all manuscripts and correspondence to the Editor, Dr. Melvin M. Figley, 403 Pacific National Bank Building, 4545 15th Avenue N.E., Seattle, Washington 98105.

Manuscript Form

Manuscripts should be typed double-spaced throughout, including references, tables, and footnotes. Tables, footnotes, and figure legends should be on separate sheets, and a separate title page should be provided. In addition to the original typewritten copy, a duplicate copy complete with figures, tables, and references is required.

Figures should be submitted as 5″×7″ glossy prints, untrimmed and unmounted. Identifying information (author name, figure number, and indication of the top of the figure) should be attached to the back of each figure with a gummed label. Line illustrations and graphs should be drawn in black ink on white background. Labels on all figures should be of professional quality and sufficiently large to be easily read when reduced in size.

References should be cited in the text by number (e.g., [3, 4]). The bibliography should be arranged in the numerical order that references are cited in the text and typed double-spaced throughout. Data for each reference should be arranged according to the uniform style on bibliographic citations adopted by many biomedical journals. Abbreviations for titles of medical periodicals should conform to those published in *Index Medicus*. Examples:

1. Miller RE, Chernish SM, Skulas J, Rosenak BD, Rodda BE: Hypotonic roentgenography with glucagon. *Am J Roentgenol* 121:264–274, 1974
2. Boijsen E: Superior mesenteric angiography, in *Angiography*, edited by Abrams H, Boston, Little, Brown, 1971, pp 1091–1119

Organization

Title page. Titles should be brief and specific. Include full names and addresses of all authors and acknowledgment of grant support when appropriate.

Abstract. A description of the purpose, methods, results, and conclusions of the study is required. It should be informative to a reader who has not read the text of the article.

Key indexing words. Five to 10 words or short phrases should be supplied to enable cross-indexing of the article.

Introduction. Clearly state the purpose of the investigation including necessary background facts.

Materials and methods. Describe the protocol clearly so that an experienced worker can understand what was done. Use standard abbreviations as presented in the *Council of Biology Editors Style Manual*, 3d edition.

Results. Present results in logical sequence.

Discussion. Interpret the results to lend meaning and importance to the observations. If hypotheses and speculation are included, they must be labeled as such. When results differ from those of previous investigators, an attempt should be made to explain the discrepancy.

References. Only include those references which provide adequate background and present fairly any opposing evidence and concepts. Accuracy of reference data is the responsibility of the author.

Legends. Legends should be brief but should provide sufficient description to interpret the figure.

Special Communications

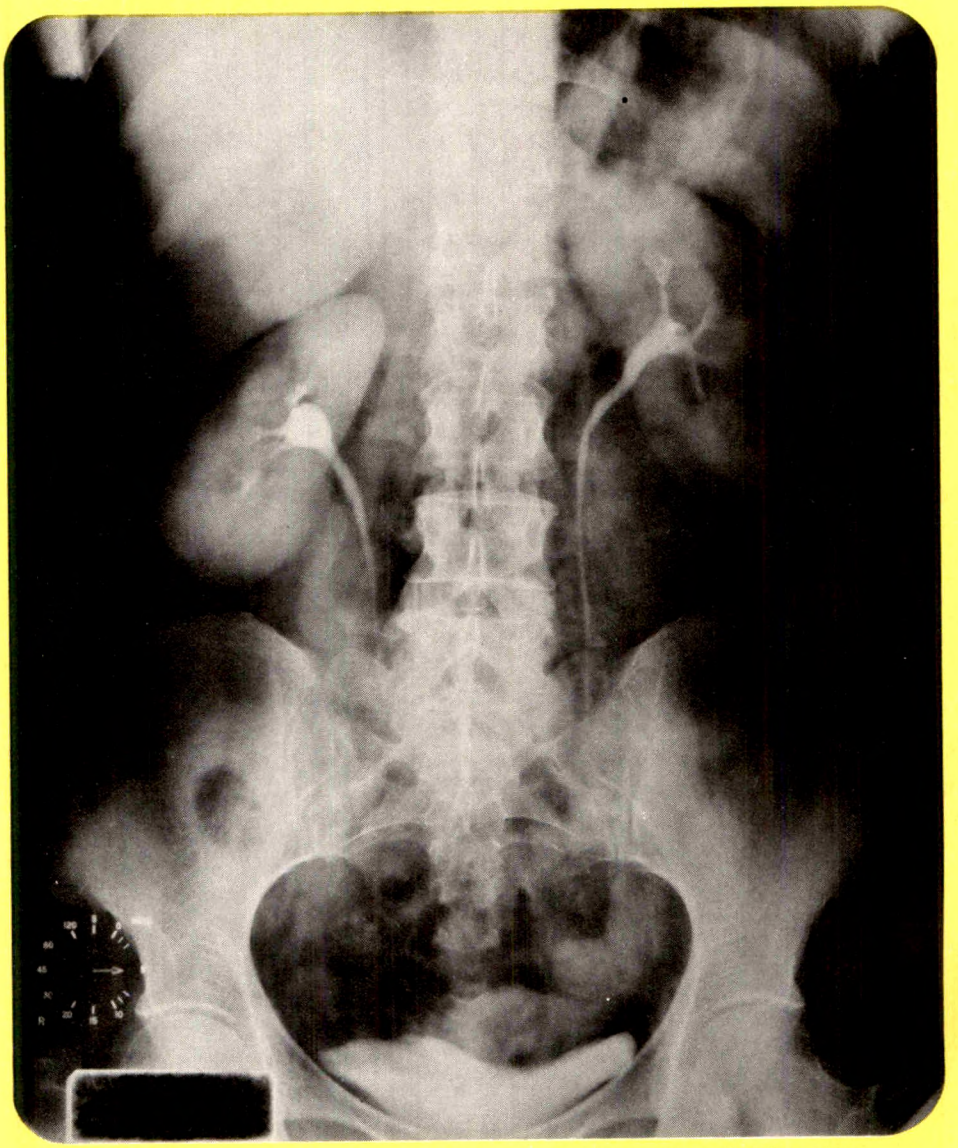
Case Reports. Concise case reports are accepted if they present unusual experiences that are medically important and educational. Clarity and brevity are essential.

Technical notes. Brief descriptions of new techniques or significant modifications of older ones which are directly applicable to clinical practice will be accepted.

Letters to the Editor. Letters should be limited to between 250 and 500 words. Criticism of published articles should be objective and constructive. Letters may also discuss matters of general interest to radiologists.

Proofs and Reprints

Copy-edited manuscripts are sent to the author for checking prior to typesetting. Galley proofs will be sent for correction of typographical errors only. The corrected proof, copy-edited manuscript, and the reprint order should be returned directly to the Editor. If the author fails to return proof by the date specified, it may be necessary to publish without the author's approval.



Excellent visualization in intravenous pyelogram 18 hours after administration of 2½ oz. X-PREP Liquid for preradiographic bowel cleansing. (In the files of the Medical Department of The Purdue Frederick Company.)

To prep the bowel for intravenous pyelography

X-PREP® Liquid

(standardized extract of senna fruit)

One step • One dose • One bottle

☐ X-PREP Liquid is designed specifically for preradiographic bowel cleansing—without enemas, suppositories or overhydration.

☐ A single 2½ oz. oral dose is usually all that is required. No residual oil droplets (such as may occur with castor oil).

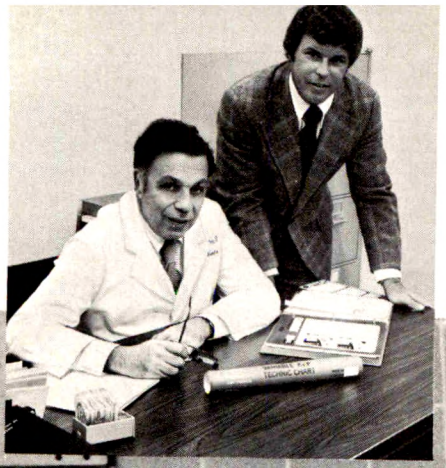
☐ Pleasant taste meets with high patient acceptance. Ease of administration is appreciated by the patient and nursing staff.

Gray Pharmaceutical Co., Affiliate

The Purdue Frederick Company

© COPYRIGHT 1975, GRAY PHARMACEUTICAL CO./ NORWALK, CONN. 06856 A7901 160875

Du Pont consultation saving $12,300 at



Leon Love, M.D., Chairman, Radiology Department, Foster G. McGaw Hospital, Loyola University Medical Center, Maywood, Illinois.
Ted Bauerle, Du Pont Senior Technical Representative.

In May 1974, Ted Bauerle, Du Pont Senior Technical Representative, called in Jack Stevens, a Du Pont Medical X-ray Specialist, to consult with the radiological staff at Loyola.

Jack and Don Falduto, Chief Technologist, conducted a Repeat Analysis of 2,301 discarded films, classifying them by cause for rejection.

Then, based on Du Pont recommendations, the Radiology Department instituted corrective programs to reduce repeats.

After just one year, significant improvements have been made, according to Leon Love, M.D., Chairman of the Department.

A second Repeat Analysis showed only 702 discarded films. Projecting these figures annually, the Department realized a $12,300 savings from the 69% reduction in repeats.

Savings like these are typical of the results which can be achieved when Du Pont works with a Radiology Department to increase efficiency and improve radiographic quality.

In the words of Marianne Troy, R.T., Adminis-

helped reduce repeats 69%, Loyola University Medical Center.



trative Assistant for Radiology, "Du Pont was the catalyst in making us aware of our repeat problems and what corrective action might be taken.

"As a result of our own programs, we now have repeats at a controllable level. Our next goal is to strive for even better performance and radiographic quality."

It's all part of Du Pont's commitment: personal involvement and quality in everything we do and sell to provide reduced operating costs and better patient care.

Personal Involvement: the key to extra quality in radiologic systems.

DU PONT

REG U.S. PAT. & TM. OFF.

We want to make gall bladder studies more convenient.

For you. For your patients.



Oragrafin®
Calcium Granules
Ipodate Calcium for Oral Suspension U.S.P.

Oragrafin®
Sodium Capsules
Ipodate Sodium Capsules U.S.P.

SQUIBB®
contrast media™
the reason is clear™

Oragrafin (Ipodate) conveniences...

Scheduling flexibility

Diagnostically adequate filling of the gallbladder often takes place within 5 hours or less after ingestion of granules, thereby permitting same-day examinations.

In routine overnight procedures, opacification is attained 10 hours after ingestion of capsules.

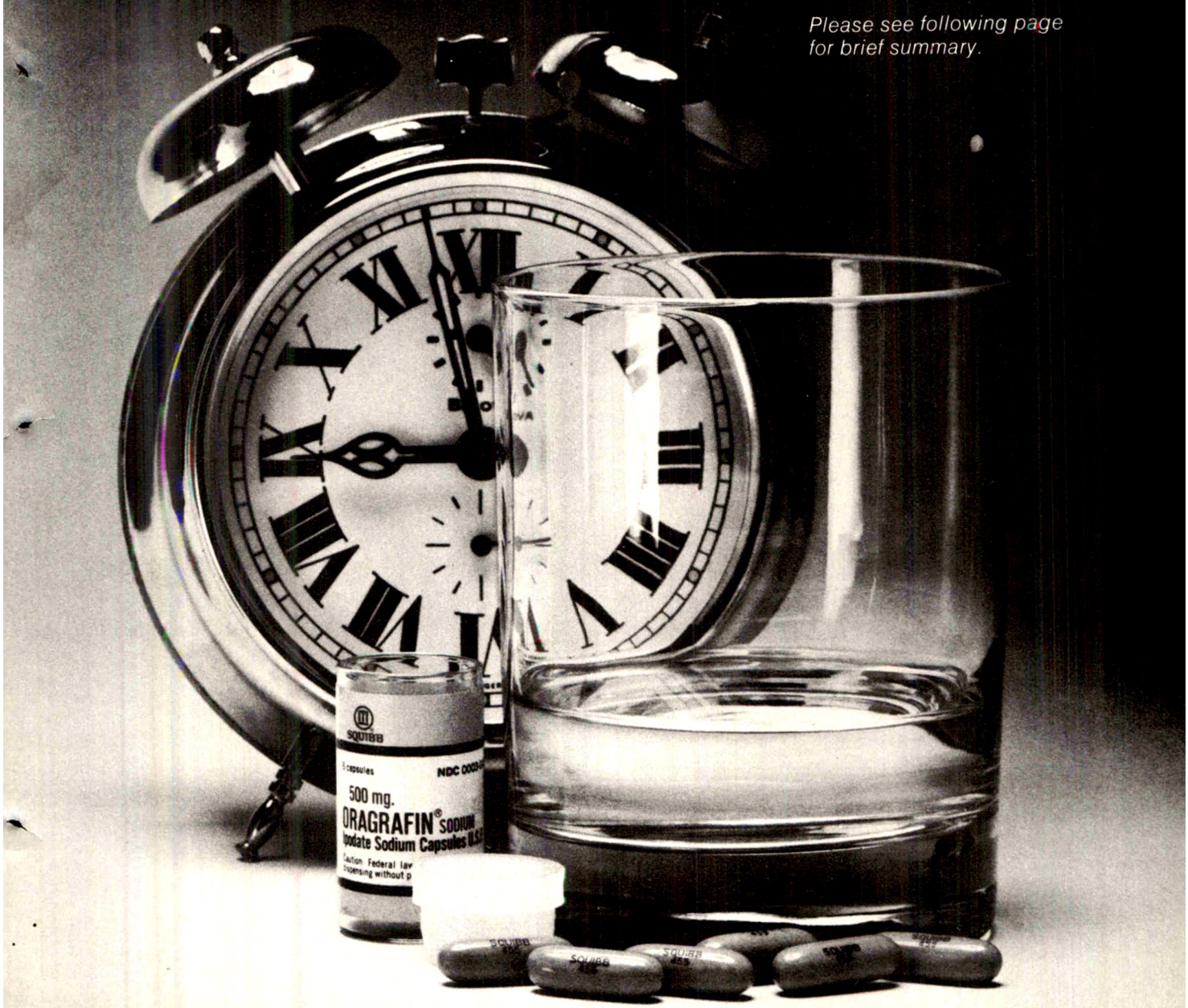
Choice of dose forms

Granules or capsules — Rapid absorption of both calcium salt and sodium salt often permits visualization of even poorly functioning gallbladders.

Prepared or unprepared patients

Both salts have been administered to unprepared patients as well as previously prepared patients, with no significant difference in results.

Please see following page for brief summary.



ORAGRAFIN® CALCIUM GRANULES
Ipodate Calcium for Oral Suspension U.S.P.
ORAGRAFIN® SODIUM CAPSULES
Ipodate Sodium Capsules U.S.P.

CONTRAINDICATIONS: Both preparations are contraindicated in patients who are hypersensitive to ipodate salts.

WARNINGS: A history of sensitivity to iodine *per se* or to other iodinated compounds is not an absolute contraindication to the use of these preparations, but calls for extreme caution in administration.

Usage in Pregnancy: The safety of these preparations for use during pregnancy has not been established; therefore, they should be used in pregnant patients only when, in the judgment of the physician, their use is deemed essential to the welfare of the patient.

PRECAUTIONS: Increasing the dosage above that recommended increases the possibility of hypotension. Anuria may result when these preparations are administered to patients with combined renal and hepatic disease or severe renal impairment. Renal toxicity has been reported in a few patients with liver dysfunction who were given oral cholecystographic agents followed by urographic agents. Administration of urographic agents should therefore be postponed in any patient with a known or suspected hepatic or biliary disorder who has recently taken a cholecystographic contrast agent. Gastrointestinal disorders which interfere with absorption and liver disorders which interfere with excretion may result in nonvisualization of the hepatic and biliary ducts and the gallbladder. Contrast agents may interfere with some chemical determinations made on urine specimens; therefore, urine should be collected before administration of the contrast media or two or more days afterwards. Thyroid function tests, if indicated, should be performed prior to the administration of these preparations since iodine-containing contrast agents may alter the results of these tests.

ADVERSE REACTIONS: Mild and transient nausea, vomiting, or diarrhea sometimes occur; the incidence can be reduced by using the calcium granules and restricting the dosage to 3 g. in persons prone to gastrointestinal reactions. Transient headache, dysuria, or abdominal pains may occur.

Hypersensitivity reactions may include urticaria, serum sickness-like reactions (fever, rash, arthralgia), other skin rashes, and rarely anaphylactoid shock.They are more likely to occur in persons with a history of allergy, asthma, hay fever, or urticaria and in those who are known to be hypersensitive to iodine compounds.

Note Concerning Dosage: A total dose of 6 g. (12 capsules or 2 packets of Granules) per 24-hour period should not be exceeded.

For full information, see Package Insert.

HOW SUPPLIED: Oragrafin Calcium Granules (Ipodate Calcium for Oral Suspension U.S.P.) provide 3 g. ipodate calcium per packet; available in boxes of 25 single-dose foil packets. Oragrafin Sodium Capsules (Ipodate Sodium Capsules U.S.P.) provide 0.5 g. ipodate sodium per capsule; available in boxes of 25 vials (each vial contains 6 capsules), in bottles of 100, and in Unimatic® packages of 100.

the reason is clear™

SQUIBB®

contrast media™

SQUIBB HOSPITAL DIVISION
E. R. Squibb & Sons, Inc.
©1976 E. R. SQUIBB & SONS, INC.

Hanley Space Saver X-Ray and Medical Record Cabinets are installed in most hospitals in America.
Top quality and low price is the reason.
5 compartment with doors—$199.50
5 compartment less doors—$171.50
Brochure F.O.B. Factory
AMERICA'S LARGEST DISTRIBUTOR OF X-RAY CABINETS
HANLEY MEDICAL EQUIPMENT CO.
5614 South Grand X-Ray Division St. Louis, Mo. 63111

In reply to advertisers please mention that you saw their advertisement in

THE AMERICAN JOURNAL OF ROENTGENOLOGY, RADIUM THERAPY AND NUCLEAR MEDICINE

• • •

CHARLES C THOMAS PUBLISHER
Springfield · Illinois

The Department of Radiology of the University of Minnesota will present its Thirty-Ninth Annual Continuing Medical Education Course, September 13-17, 1976.

The two major topical areas will be:

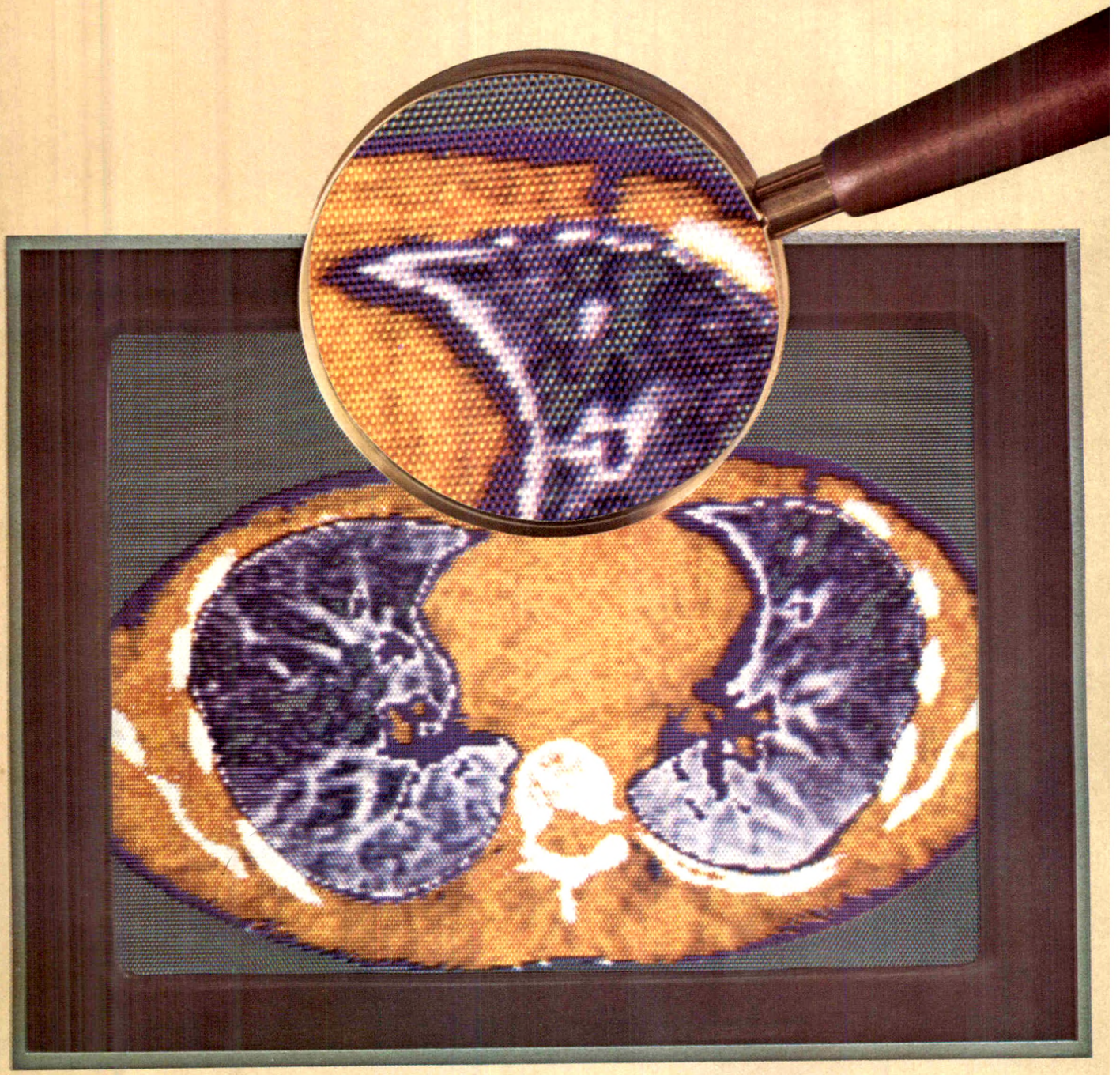
Cardiovascular Radiology—2½ days
Selected Topics in Diagnostic Radiology—2½ days

For further information contact:
Continuing Medical Education
Box 293
Mayo Memorial Building
412 Union Street S.E.
University of Minnesota
Minneapolis, Minnesota 55455

Pfizer Medical Systems, Inc. announces 57,600 reasons why the

ACTA-SCANNER®

provides superior resolution and image clarity in whole body computerized tomographic scanning



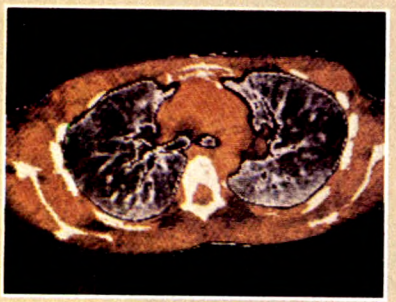
ACTA-SCANNER

WHOLE BODY COMPUTERIZED TOMOGRAPHIC SCANN

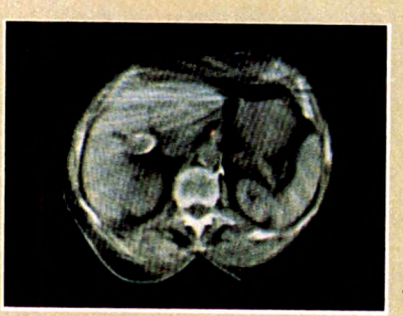
The new matrix improves image quality

Up to 57,600 absorption values are now actually measured for translation into the finished ACTA-scan with the recently developed 320 matrix.

This means a large, high-resolution display (1.5 mm) with greater clarity and true detail—important in extracranial scanning.



Thoracic 320 Scan. (Normal Chest)



Abdominal 320 Scan. "Porcelain" Gallbladder

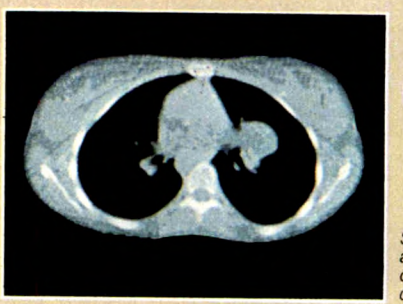
Multiple windows let you see more

With the Pfizer ACTA-Scanner, multiple windows can be imposed upon the image, allowing tissues with great density differences to be viewed at the same time in a single ACTA-scan.

This capability greatly facilitates interpretation of scans in the thoracic and abdominal areas.



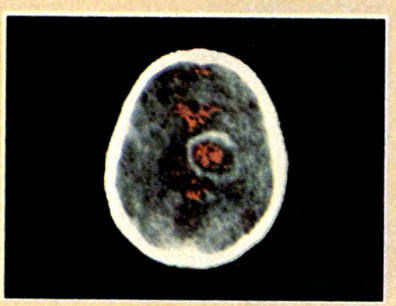
Thoracic scan with multiple windows. Mass in right lung.



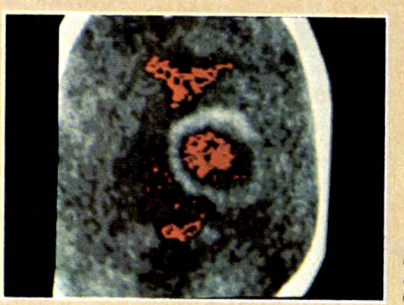
Same area as scanned at left, without imposition of the multiple window capability.

And you can enlarge selected areas

A special cursor—or movable dot—allows the operator of the ACTA-Scanner to enlarge selected areas of interest by a factor of 2 in diameter (4 in area).



Pituitary Adenoma

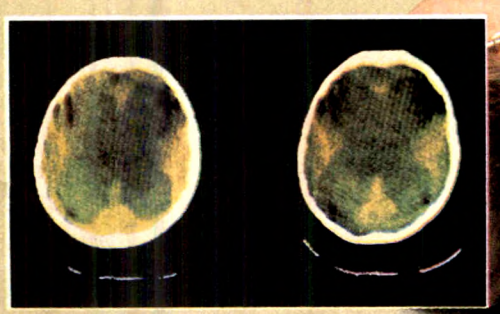


Pituitary Adenoma. Instantaneous enlargement of pathologic area.

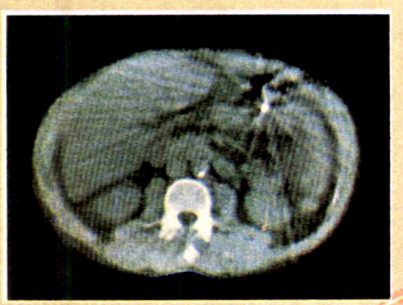
Pathology in virtually any part of the body can be visualized and evaluated.



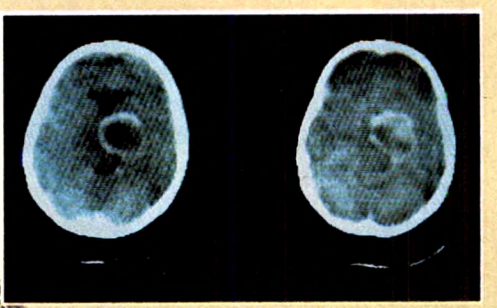
Thoracic 320 Scan.
(Normal Chest)



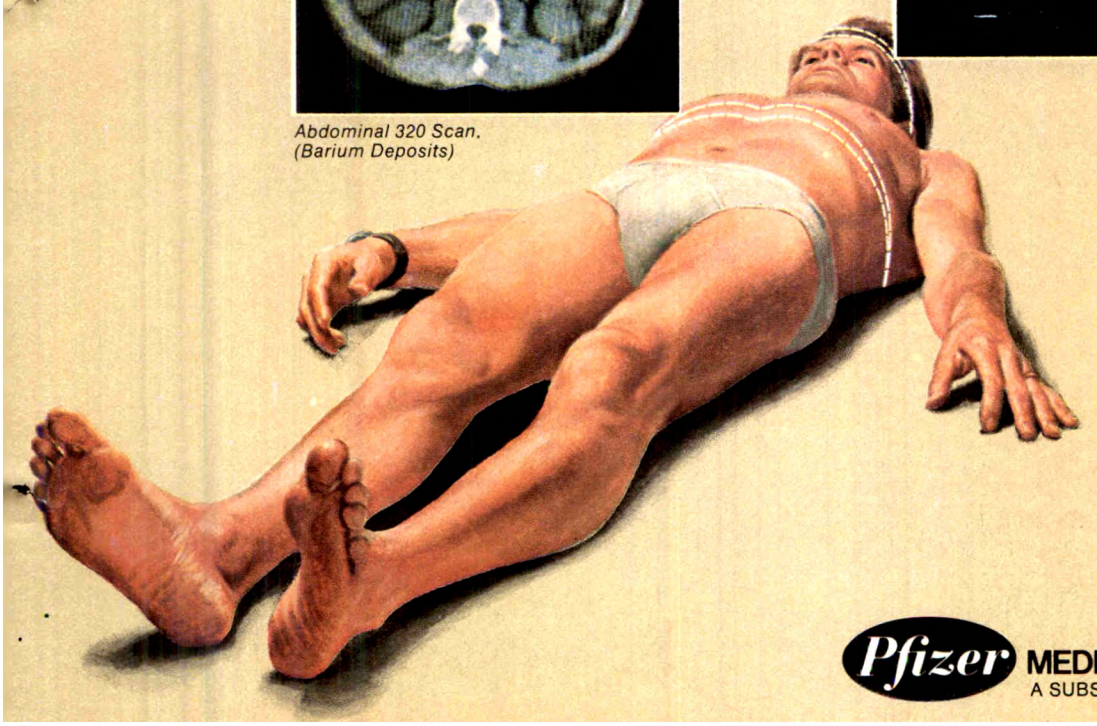
Marked Hydrocephalus



Abdominal 320 Scan.
(Barium Deposits)



Pituitary Adenoma



Pfizer MEDICAL SYSTEMS, INC.
A SUBSIDIARY OF PFIZER INC.

ACTA-SCANNER

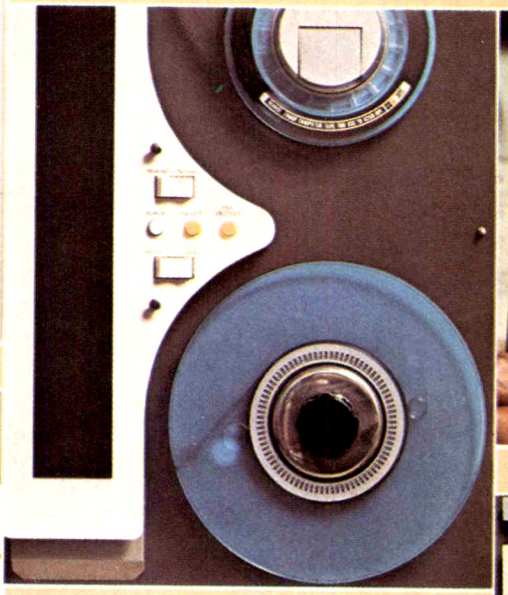
WHOLE BODY COMPUTERIZED TOMOGRAPHIC SCANNE

A revolutionary innovation in diagnostic radiology maintained by an original concept of service...and backed by the full resources of a great medical organization

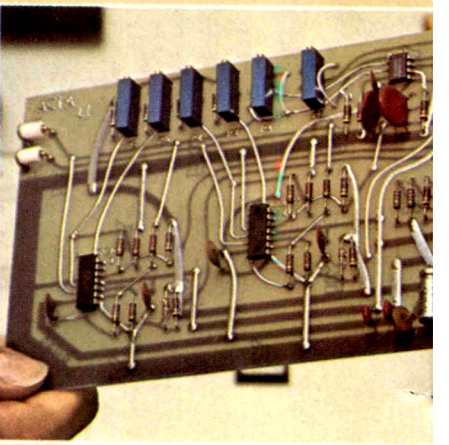
The Pfizer Medical Systems Field Engineer is an integral component of the ACTA-Scanner Service Program.



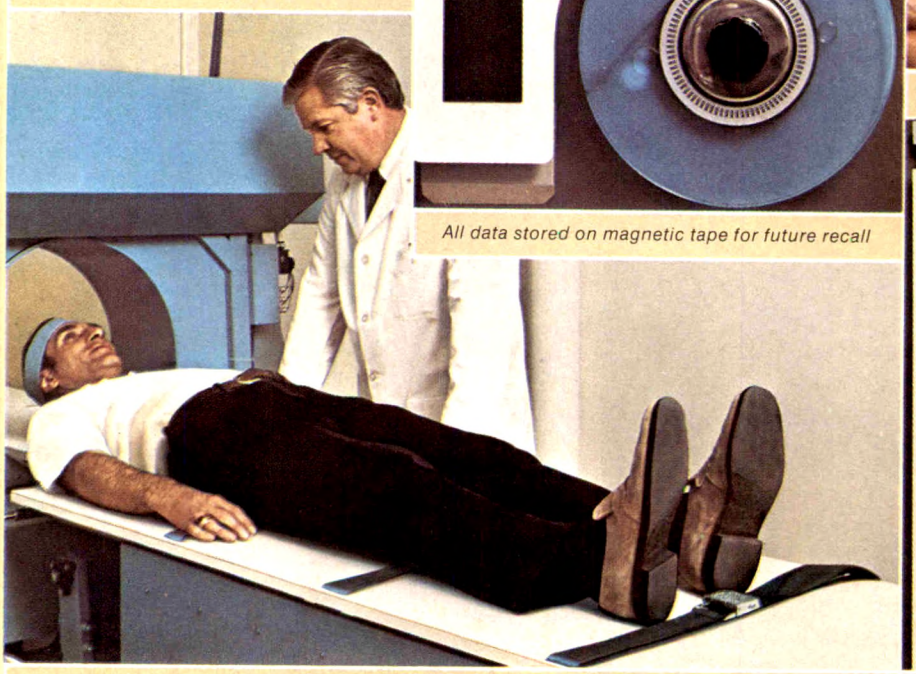
Field engineer readily available



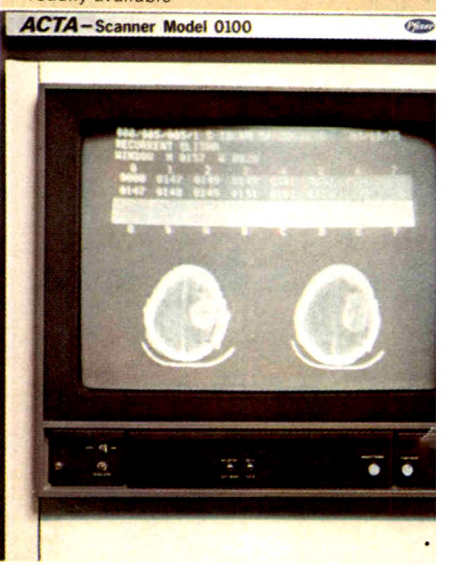
All data stored on magnetic tape for future recall



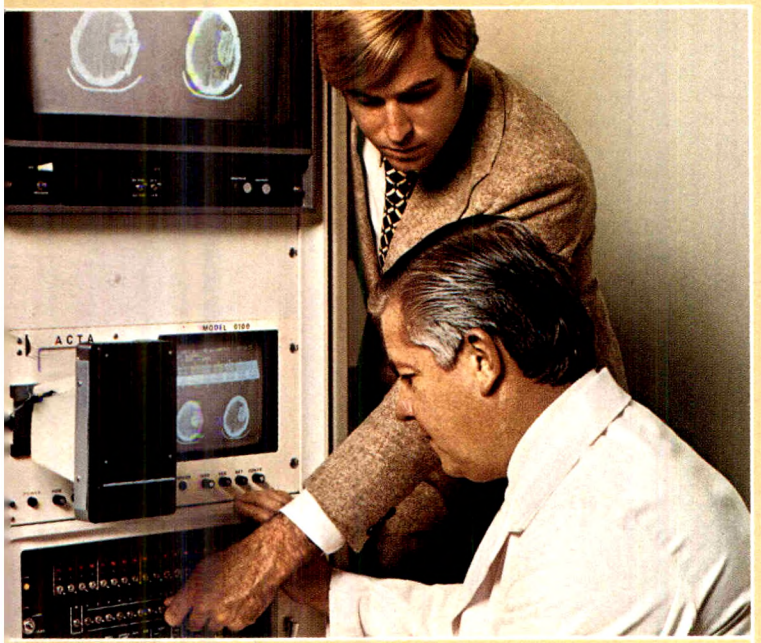
Replacement parts, if needed, are readily available



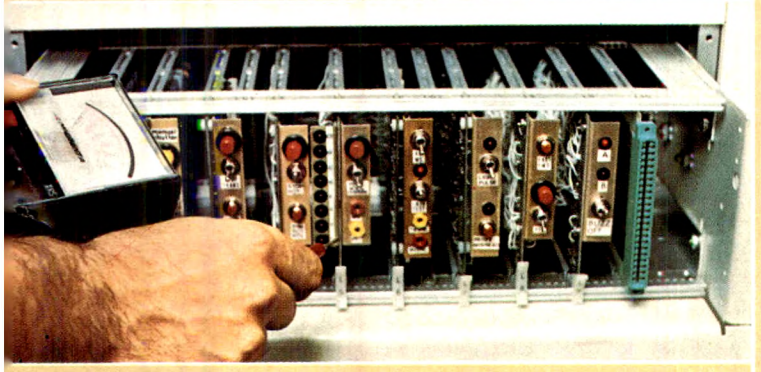
Minimal patient preparation before scan



Instant display following completion of scan



Field engineer provides continued updating on capabilities



Frequent visits by field engineer keep ACTA-Scanner at peak performance

Automation with Representation

A team of highly qualified field engineers is on standby duty to respond to your needs when necessary.

Warranty: No charges for all parts and service support during normal working hours. Any necessary maintenance can be done at night or during nonpeak hours, as requested.

Continuous inspection: Frequent visits, at your convenience, will be made to assure optimum performance.

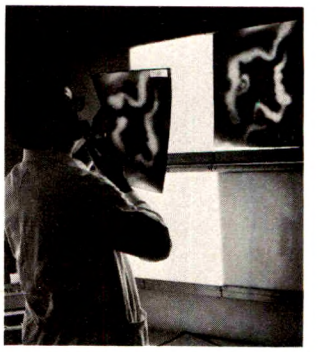
Direct link to research and development: Your representative will keep you apprised of the activities of the Pfizer physicists and x-ray and computer experts who are dedicated to providing ever greater performance and more features on your ACTA-Scanner.

Pfizer MEDICAL SYSTEMS, INC.
A SUBSIDIARY OF PFIZER INC.

Clysodrast®
(BISACODYL TANNEX)

The safe and certain barium additive

Helps you be sure of what you see



Clysodrast is a unique colonic evacuant. It mixes with barium enemas to give radiologists the only form of tannic acid* available for safe, high-resolution barium enema studies. And a growing body of experimental evidence has shown the diagnostic benefits of Clysodrast added to a barium suspension.[1,2,3] This combination provides unmatched mucosal visualization for superior roentgenologic diagnoses.

SAFETY YOU CAN COUNT ON

Only tannic acid really prepares the colon and produces the even, thin-film deposition of barium sulfate that a radiologist needs for maximum clarity. Clysodrast combines tannic acid with the contact laxative bisacodyl, for optimum effectiveness. And Clysodrast comes in accurately measured, 2.5 Gm. packets to avoid the danger of accidental overdose. With Clysodrast, results are consistently safe and uniform, too. No patient has ever suffered hepatic necrosis as a result of Clysodrast being used within the dosage limits indicated in the instructions.[4,5,6] And it has been used in well over 2 million barium enema procedures since 1970 alone, usually with no more side effects than a water enema produces.[7,8]

Clysodrast is recommended for double contrast studies with an appropriate form of barium sulfate, such as Barotrast.® It is also indicated for the preparation of patients for radiologic examinations of the colon, sigmoidoscopy and proctologic examinations, when used as directed.

USE CLYSODRAST, FOR SURE

Clysodrast provides radiologists with the assurance of high resolution barium studies no other product can provide. Find out for yourself how Clysodrast can help you see for sure. Contact your local X-ray supplies dealer.

See summary of prescribing information on adjoining page.

*Bisacodyl tannex

Also see your X-ray supplies dealer for Oratrast,® Barotrast® and Esophotrast.®

INDICATIONS: CLYSODRAST (bisacodyl tannex) may be indicated for the preparation of patients for radiologic examinations of the colon, sigmoidoscopy and proctologic examinations.

CONTRAINDICATIONS: CLYSODRAST is contraindicated in patients under the age of 10 because the possibility of absorption of tannic acid has not been adequately studied in this age group to warrant a conclusion of safety. CLYSODRAST is also contraindicated in cases with known or suspected extensive ulcerative lesions of the colon.

WARNING: Usage in Pregnancy. Safe use of CLYSODRAST has not been established with respect to the adverse effects upon fetal development. Therefore, it should not be used in women of child-bearing potential, particularly during early pregnancy, except where, in the judgment of the physician, the potential benefits outweigh the possible hazards.

PRECAUTIONS: Tannic acid, one of the active ingredients of CLYSODRAST, is hepatotoxic if absorbed in sufficient quantity. Deaths have been reported from hepatic damage due to tannic acid used in barium enema examination. Thus, CLYSODRAST should be used with caution in a regimen where multiple enemas are administered. Certain patients, because of age, debility, or underlying disease, require more gentle preparation than the routine castor oil and CLYSODRAST preparation. It is important that the instructions for preparation and administration be followed in detail, and that the recommended dosages not be exceeded.

ADVERSE REACTIONS: The following adverse reactions have been reported: Cramping, weakness, nausea and fainting.

DOSAGE AND ADMINISTRATION: It is important that the entire medical history and condition of the patient be considered in deciding the dosage regimen. Traumatizing procedures, such as repetition of enemas (with or without CLYSODRAST) should be kept at the minimum necessary to achieve the desired result.

CLEANSING ENEMA: Prepare the cleansing enema by dissolving the contents of one packet (2.5 Gm.) of CLYSODRAST in one liter of lukewarm water and administer.

BARIUM ENEMA: Prepare the barium enema by dissolving the contents of one or not more than two packets (2.5 Gm. or 5.0 Gm.) of CLYSODRAST in one liter of barium suspension. If more than one liter of barium suspension is prepared, it is important that the concentration of CLYSODRAST (bisacodyl tannex) never exceed 0.5 percent (2 packets per liter).

The total dosage of CLYSODRAST for any one complete colonic examination, including the cleansing enema, should not exceed 7.5 Gm. (3 packets). No more than 10 Gm. (4 packets) of CLYSODRAST should be administered to any individual within a 72-hour period.

HOW SUPPLIED: CLYSODRAST is supplied in packets containing 1.5 mg. of 4,4′–(diacetoxydiphenyl)–(pyridyl-2)–methane complexed with 2.5 Gm. of tannic acid, N.F. These packets are supplied in cartons of 25 and 50 packets.

CAUTION: U.S. Federal law prohibits dispensing without prescription.



A Colonic Evacuant

Clysodrast
(bisacodyl tannex)

Barnes-Hind Pharmaceuticals, Inc.
Sunnyvale, California 94086

1. Goldman, L., *Clinical Medicine*, Vol. 28, pg. 28, 1971
2. Hamilton, *American Journal of Roentgenology*, 1946
3. Janower, M. L., *Radiology*, Vol. 85, pg. 887, 1965
4. Burhenne, et al, *American Journal of Roentgenology*, Vol. 96, pg. 510, 1966
5. Lucke, et al, *Canadian Medical Association*, Vol. 89, pg. 1111, 1963
6. McAlister, et al, *Radiology*, Vol. 80, pg. 765, 1963
7. Steinbach, et al, *American Journal of Roentgenology*, Vol. 87, pg. 644, 1962
8. Thomas, *American Journal of Roentgenology*, Vol. 89, pg. 889, 1963

CHARLES C THOMAS • PUBLISHER

LYMPHOPROLIFERATIVE DISEASES *compiled and edited by* **David W. Molander,** *Memorial Hospital for Cancer and Allied Diseases, New York. (23 Contributors)* A compilation of the known facets of lymphosarcoma and related diseases is presented in this text including pathologic anatomy, immune mechanisms, clinical diagnosis and treatment employing irradiation and chemotherapy. The use of isotopes in managing this disease as well as in the diagnosis of occult foci of the disease is examined. The latest methods of treatment and diagnostic methods are detailed with emphasis on infectious and hematopoietic complications. Primary reticulum cell sarcoma of bone and related diseases are dealt with in separate chapters. *'75, 592 pp. (6 3/4 x 9 3/4), 256 il. (9 in color), 45 tables, $39.50*

XERORADIOGRAPHY OF THE BREAST (3rd Ptg.) *by* **John N. Wolfe,** *Hutzel Hospital, Detroit, Michigan. Foreword by* **Wendell G. Scott.** Written for persons working in the field of breast cancer, this text presents a new and significant method for early detection. The mechanics and principles involved in this procedure are clearly defined. Breast anatomy and the normal breast are discussed, providing a thorough understanding necessary to achieve the proper technique and correct interpretation of the xeromammogram. The xeroradiographs are accurately reproduced in their original blue color for consistency of detail. *'75, 194 pp. (8 1/2 x 11), 242 il. (92 in color), $23.50*

A STUDY GUIDE IN NUCLEAR MEDICINE: A Modern Up-to-Date Presentation *compiled and edited by* **Fuad Ashkar, August Miale, Jr.,** *and* **William Smoak,** *all of the Univ. of Miami, Miami, Florida. (22 Contributors)* This book is divided into ten sections covering such topics as basic science, radiopharmaceuticals, radiation biology, protection and dosimetry, therapeutic radionuclides and principles of radiation therapy. Study questions and references to other material in the field are presented at the end of many of the chapters. *'75, 488 pp., 312 il., 44 tables, cloth-$22.75, paper-$17.50*

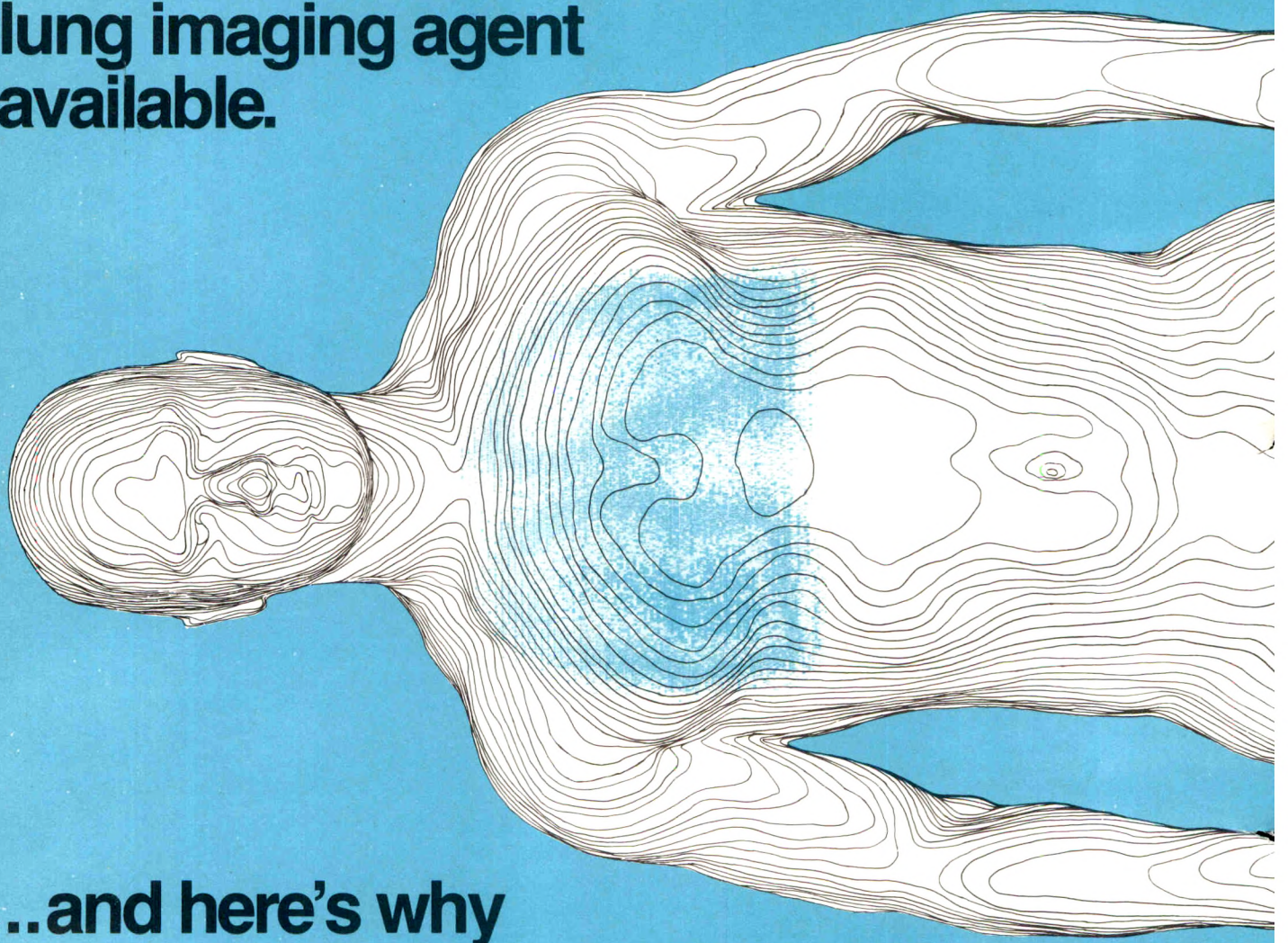
Prepaid orders sent postpaid, on approval

301-327 EAST LAWRENCE
SPRINGFIELD • ILLINOIS • 62717

Macrotec®

Aggregated Albumin (Human)
for labeling with technetium 99m

STILL! the simplest, quickest to prepare lung imaging agent available.



...and here's why

Simple, two-step procedure. Not an ampul, not a frozen material. No waiting, no complicated procedures or specialized equipment required. Just two easy steps and you're ready to assay and inject.

Uniform particle size, excellent labeling efficiency. Particle size meets or exceeds Bureau of Biologics standards; 90% in 5-60 micron range. Excellent labeling efficiency when reconstituted with a compatible technetium 99m.

Won't agglomerate in the vial, loses virtually no labeling for 8 hours (if stored between 2°C. and 8°C.).

Ideal for the busy lab. Recommended amount of 99mTc for reconstitution high enough to allow numerous scans from a single vial.

BASIC STEPS IN PREPARING FOUR TECHNETIUM

Squibb Macrotec® Aggregated Albumin (Human)	**1. Add 1-3 ml. of 99mTc** Maintain shielding at all times.**	**2. Shake vigorously for 10-15 seconds.**
Mallinckrodt TechneScan™ MAA Aggregated Albumin (Human)	**1.** Remove reaction vial from *freezer* and *wait approximately 5 minutes* for contents to come to room temperature.	**2.** Add 99mTc** Maintain shielding at all times.
3M Albumin Microspheres (Human)	**1.** Add 4-10 ml. of 99mTc**	**2.** Shield completely and vigorously shake for 5-15 seconds.
Medi+Physics Lungaggregate™ Reagent Aggregated Albumin (Human)	**1.** Shake *ampul* vigorously to suspend particles.	**2.** Open ampul.

Emphasis added by Squibb to point out certain differences in procedures.

MACROTEC® (Aggregated Albumin [Human])

Macrotec (Aggregated Albumin [Human]) is a sterile, non-pyrogenic, lyophilized preparation of aggregated albumin. Each vial of the preparation contains 0.08 mg. tin as chloride, 1.5 mg. denatured human serum albumin, and 10 mg. Normal Serum Albumin (Human).

INDICATIONS: For use in perfusion lung imaging as an adjunct to other diagnostic procedures.

CONTRAINDICATIONS: At present there are no known contraindications to the use of this product.

WARNINGS: Radiopharmaceuticals should not be administered to patients who are pregnant, or during lactation, unless the benefits to be gained outweigh the potential hazards.

Ideally, examinations using radiopharmaceuticals, especially those elective in nature, of a woman of childbearing capability, should be performed during the first few (approximately 10) days following the onset of menses.

Since ^{99m}Tc is excreted in milk during lactation, formula-feedings should be substituted for breast-feedings.

Radiopharmaceuticals should be used only by physicians who are qualified by specific training in the safe use and handling of radionuclides produced by nuclear reactor or particle accelerator and whose experience and training have been approved by the appropriate government agency authorized to license the use of radionuclides.

Note: Macrotec (Aggregated Albumin [Human]) is not radioactive. However, after ^{99m}Tc is added, adequate shielding of the resultant preparation should be maintained.

PRECAUTIONS: In the use of any radioactive material, care should be taken to insure minimum radiation exposure to the patient consistent with proper patient management, and to insure minimum radiation exposure to occupational workers.

Aseptic technique is essential in the preparation of Technetated (Tc-99m) Aggregated Albumin (Human).

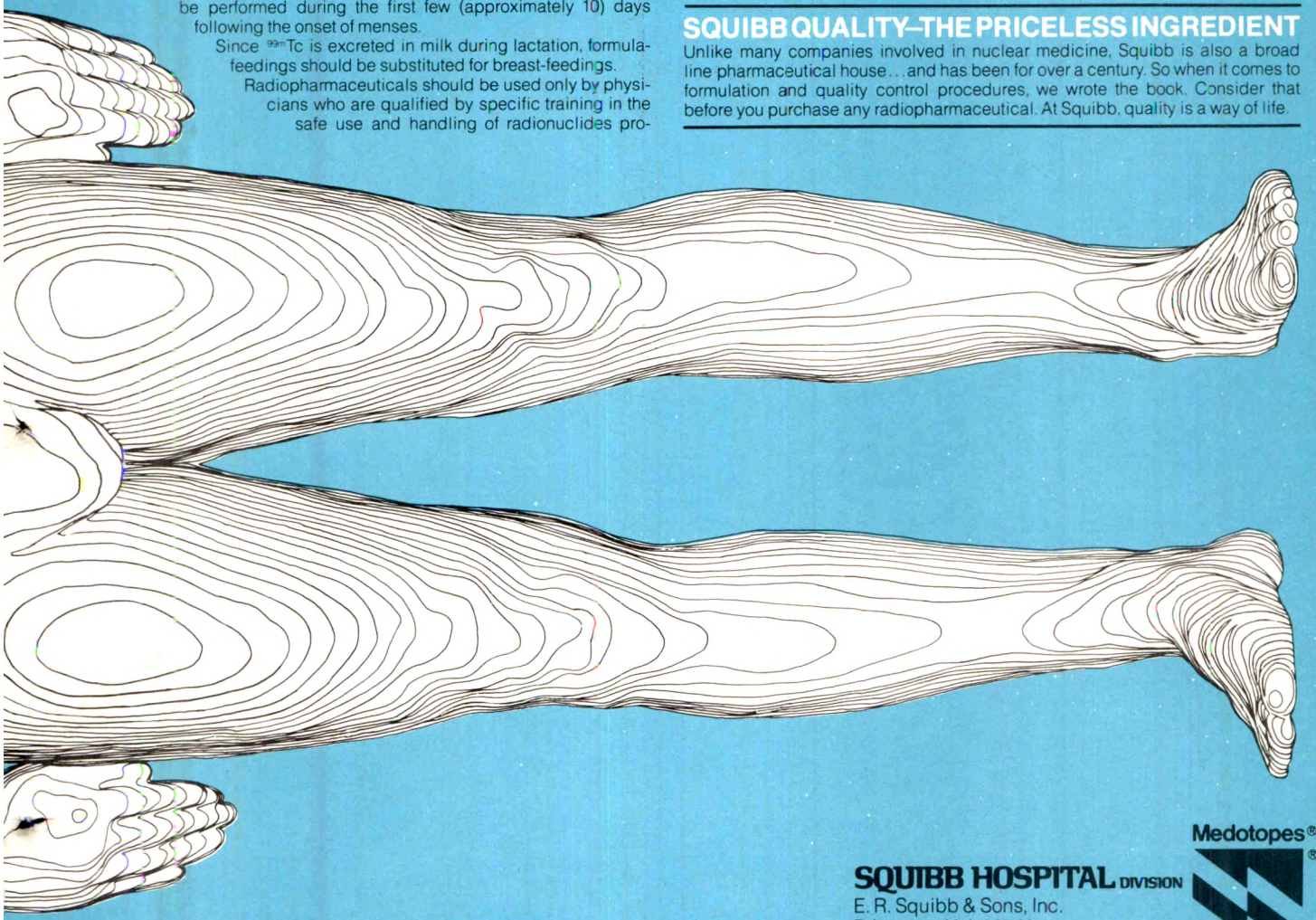
ADVERSE REACTIONS: At present, adverse reactions have not been reported following the administration of this product.

For full prescribing information, consult package insert.

HOW SUPPLIED: In boxes of 5 vials.

SQUIBB QUALITY–THE PRICELESS INGREDIENT

Unlike many companies involved in nuclear medicine, Squibb is also a broad line pharmaceutical house...and has been for over a century. So when it comes to formulation and quality control procedures, we wrote the book. Consider that before you purchase any radiopharmaceutical. At Squibb, quality is a way of life.



Medotopes®

SQUIBB HOSPITAL DIVISION
E. R. Squibb & Sons, Inc.
Princeton, N.J. 08540

©1976 E.R. Squibb & Sons, Inc.

H606-504

99m-LABELED LUNG IMAGING AGENTS*

3. Gently agitate vial for few seconds. **4.** *Allow to stand for 15 minutes* at room temperature. **5.** Visually inspect vial for presence of large aggregates. *If present, do not use.* **6.** *Agitate* to effect homogenous suspension of the aggregated albumin.

**Recommended maximum activity: 60 mCi.

3. Remove vial from shield (with forceps) and place in center of operating *ultrasonic bath* containing 3/4" of water. Bath should be protected by *lead glass or bricks.* *Ultrasound for 5 minutes.*

**Recommended maximum activity: 30 mCi.

3. Withdraw (very slowly) 1.5-2.0 ml. of aggregate from ampul with *syringe.* **4.** Inject (very slowly) syringe contents into *mixing vial.* **5.** Wrap mixing vial in *absorbent paper disc* and place in lead shield. **6.** Add 0.5-2.0 ml. of 99mTc** in saline into shielded mixing vial. Shake vigorously for at least 30 seconds. *Incubate* at room temperature *for 2-5 minutes.* **7.** Shake contents vigorously just before removing aliquot intended for patient use.

**Recommended maximum activity: 25 mCi/ml.

**Recommended maximum activity: 50 mCi.

*Based on manufacturers' product information. **NOTE: See manufacturers' package inserts before the preparation of any of these products.**

The post-graduate course you can carry anywhere.



Conversations in Radiology, Volume 4, is now available for subscription

Like the previous Volumes, Volume 4 consists of 8, one-hour audio cassettes plus appropriate reference materials. Each cassette consists of two, 30-minute programs. All tapes are clearly edited to provide focus on new developments or controversial issues, and, review of pertinent topics in the field of radiology.

A portable reference work.

Conversations in Radiology is more than a seminar, it's a valuable reference library which can be reviewed at the physician's leisure... or, utilized as an adjunct to the teaching process.

Meaningful insights.

Conversations in Radiology, Volume 4, will offer the radiologist and allied specialist continuing updates and insights into important areas of subspecialization. Naturally, all tapes are accompanied by a complete reference bibliography plus occasional illustrations.

Convenient form.

Your subscription to Conversations in Radiology includes eight sequentially issued audio-cassettes, a convenient bookshelf cassette binder, plus, all appropriate reference materials.

Accredited by the AMA and CMA.

The Conversations in Radiology subscription series is acceptable for 8 credit hours in Category 5 for the Physicians' Recognition Award of the American Medical Association. Each Volume is also acceptable for credit in Category II, Formally Constituted Activities, Section "i," toward the California Medical Association's Certificate in Continuing Medical Education.

Annual subscription: $74.

Volume 4 of Conversations in Radiology began in April, 1976. Volumes 2 & 3 are still available at $74 per completed Volume... including binder and reference materials.

8, one-hour conversations with leading authorities.

Participating Editors:

Pediatric Radiology
Walter Berdon, M.D.
Columbia University

Gastrointestinal Radiology
Joseph Ferrucci, Jr., M.D.
Harvard University
Jack Wittenberg, M.D.
Harvard University

Ultrasound
Barry B. Goldberg, M.D.
Temple University

Bone Radiology
William Martel, M.D.
University of Michigan

Neuroradiology
D. Gordon Potts, M.D.
Cornell University
Irvin I. Kricheff, M.D.
New York University

Angiography
Joseph J. Bookstein, M.D.
Univ. of Calif., San Diego
Helen C. Redman, M.D.
Univ. of Calif., San Francisco
Stanford University

Genitourinary Radiology
Lee B. Talner, M.D.
Univ. of Calif., San Diego
Thomas Sherwood, M.B.,
Royal Postgraduate Medical School
University of London

Chest Radiology
Morris Simon, M.D.
Harvard University

Oncologic Radiology
Ronald Castellino, M.D.
Stanford University

Editors:

Ronald C. Ablow, M.D.
Yale University
Alan J. Davidson, M.D.
Univ. of Calif., San Francisco
Stanford University

Conversations in Radiology
170 9th Street, San Francisco, CA 94103

Gentlemen,
Please enter my subscription to Volume 4, Conversations in Radiology. I understand that for $74, I will receive eight, one-hour tape cassettes containing 16 half-hour conversations with leading radiologists... plus, a bookshelf binder and appropriate reference materials.

Name _____

Address _____

City _____ State _____ Zip _____

☐ Bill me ☐ Check enclosed

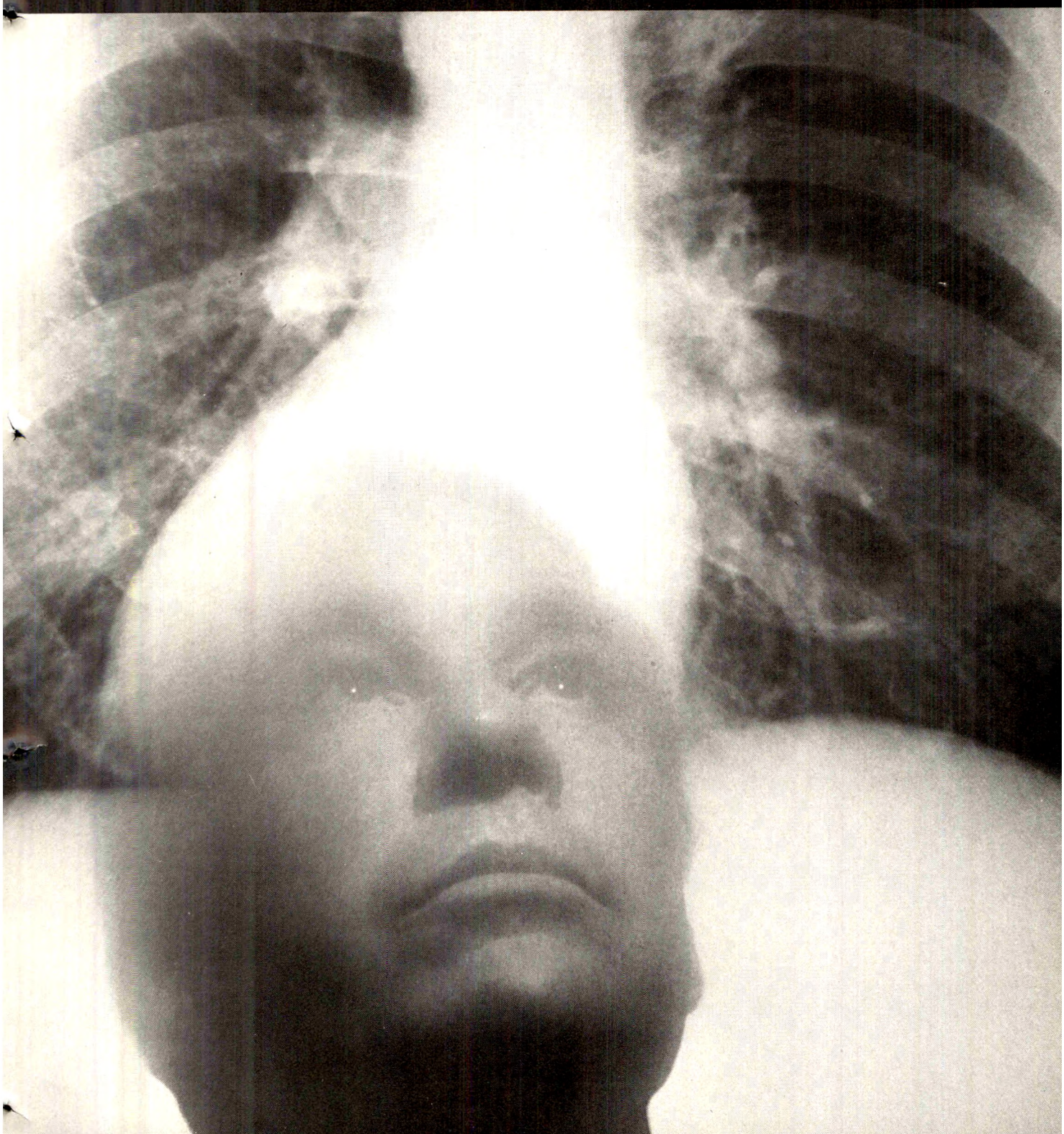
☐ Please send me Volume 3. ☐ Bill me $74. ☐ Check enclosed.

☐ Please send me Volume 2. ☐ Bill me $74. ☐ Check enclosed.

Quality is what Kodak is all about.

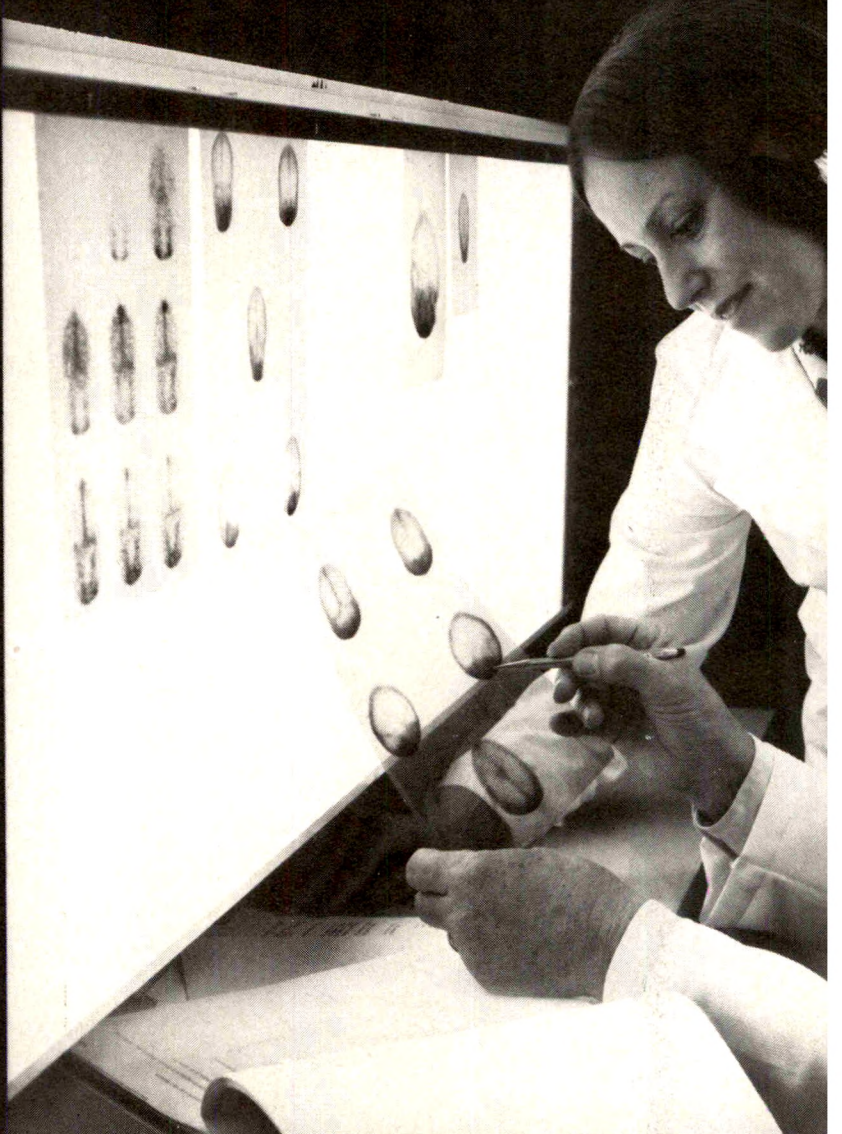
It goes a long way toward providing consistent imaging results. Quality is the heart of our products. The ingredient of our services. The extra advantage of the skilled counsel of our technically experienced representatives who can meet your radiographic requirements.

Quality is the Kodak expertise in imaging technology which can be of value to you because diagnostic decisions can sometimes depend on the quality of the diagnostic image.



When what you want is image quality, consider Kodak quality... where can we help you most?

Your concern is
Ours is meeting you
with Kodak quality.



Focus on KODAK Medical X-ray Films.

To meet your varied imaging requirements, Kodak offers a wide range of quality films. Each is designed to consistently provide well-defined diagnostic information on the viewbox—where quality images count.

Films for general radiography. Whether you need a high-contrast film for maximum detail or a wide-latitude film to record variations in tissue densities, Kodak has them. If speed is your concern, use our high-speed films to shorten exposure time. Each of our films provides good transport reliability in automatic film-handling equipment.

Films for special technics. In addition to general radiographic needs, you may have other areas where you require consistent image quality. Here you also have a choice of Kodak films: for special procedures; for subtraction; for therapy localization; for cinefluorography; for spot film radiography; and for cathode-ray tube imaging—thermography, ultrasonography, computerized axial tomography.

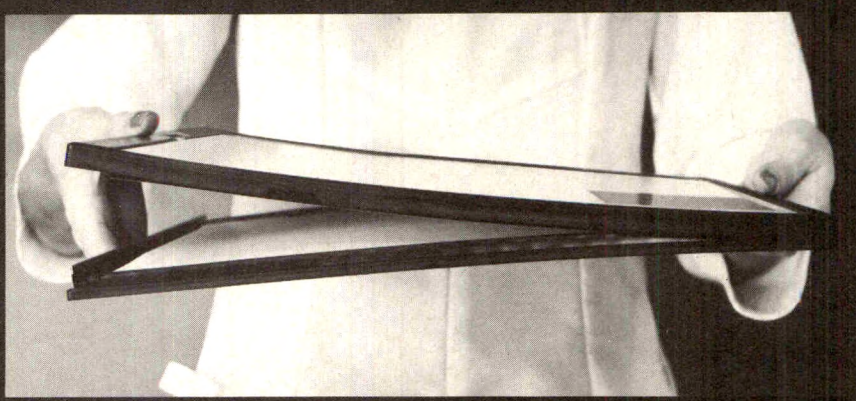
New Advances in Imaging Technology.

Products for mammography. Compared with any current Kodak film and screen combination for mammography, two new products—Kodak Min-R film and Kodak Min-R screen—offer the fastest speed with equal or better image sharpness.

Rare earth imaging products. Research in rare earth phosphors resulted in Kodak Lanex regular screens and Koda ortho G film. They provide highe speed—so you can shorten exposure time, or reduce kilovol age, or decrease milliamperage. All of which can help extend your radiographic technic and equipment capabilities.

making a diagnosis. imaging needs...





Films for nuclear medicine. Kodak offers transparency films for single, multiple, or dynamic imaging. These include Kodak film for nuclear medicine SO-179—ideal for recording images from cathode-ray tube displays. Transparency films resist fading and curling, are easy to store. And they can provide high-quality images through automatic processing in 90 or 150 seconds.

Kodak Efficiency Improvers.

The curved cassette. Kodak X-Omatic cassettes have specially designed, curved covers that force out air when closed, creating an intimate screen/film contact for consistently high image quality. Easy to open and close with one hand. Durable—resists damage, either to the cassette or in the screen/film contact.

The positive patient data keeper. The Kodak X-Omatic identification camera records data on the radiograph itself, in full room light. No lead letters or numbers to fall off, less chances for misidentification. It's an accurate and efficient means of monitoring patient flow.

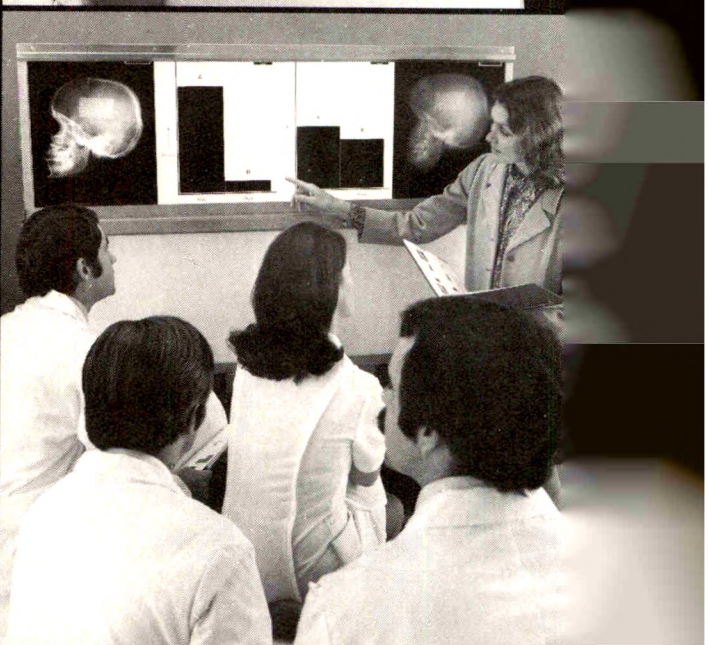
Automatic processing. When patient load requires rapid access to processed radiographs, Kodak has a 90-second automatic processor you can depend on. If you need a compact processor for emergency or satellite areas, Kodak has a 150-second automatic processor that uses unheated water, cuts back on costs. Both deliver consistent quality radiographs.

How do you get all this from Kodak? Turn the page...

Having a Kodak TSR who knows your problems gives you a head start on the answers.







What can you expect from your Kodak Technical Sales Representative? More than the name implies.

Your TSR is a professional consultant—highly trained and technically experienced in imaging technology, with a working background in medical radiography, nuclear imaging, photofluorography, cinefluorography. Here's what the TSR can do:

- Conduct training courses for x-ray department personnel
- Arrange for special courses or group training programs
- Give your staff ready access to comprehensive technical information to help you get the most out of your Kodak films, chemicals, processing equipment
- Provide manuals, product brochures, medical charts, audiovisual presentations, slide lectures, clinical case studies, and a variety of technical publications on radiography

To get the most out of your Kodak products, get the most out of your TSR. Contact your Kodak representative. Or consult your x-ray products dealer. Or write: Eastman Kodak Company, Department 740-B, Rochester, N.Y. 14650.

A commitment to quality.

Kodak



ROBERT M. ZOLLINGER
CANNON LECTURER, 1975

UNIVERSITY OF MICHIGAN LIBRARY

AMERICAN JOURNAL OF ROENTGENOLOGY

VOL. 126 MAY 1976 No. 5

ISLET CELL TUMORS AND THE ALIMENTARY TRACT

FOURTH WALTER B. CANNON LECTURE

ROBERT M. ZOLLINGER[1]

"Cannon did not conceive of humoral control. In his days, secretin was only a pancreatic stimulator and gastrin a discredited mistake"[8].

I am deeply sensible of the great privilege of delivering the Fourth Walter Bradford Cannon Lecture to this distinguished society. Certainly everyone interested in the gastrointestinal tract recognizes the great debt owed to Walter Cannon. The magic name of Cannon has never ceased to electrify the world of medicine, and only this year, three decades after his death, a book entitled "The Life and Contributions of Walter B. Cannon: 1871–1945, His Influence on the Development of Physiology in the 20th Century" was published [21]. Walter Cannon's legacy to gastrointestinal surgery and roentgenology as we know it today is truly amazing. In the words of his friend and colleague, Ralph Barton Perry, "He was a good prospector—he knew how to locate the veins of rich scientific ore. But he also knew how to refine the gold."

I am indebted to your President, Dr. Sidney W. Nelson, for the privilege of discussing certain hormone-producing islet cell tumors of the pancreas and their effects on the gastrointestinal tract. At the turn of the century when Bayliss and Starling [1] discovered secretin and Edkins [12] reported on a substance prepared from gastric antrum, which he called gastrin, Dr. Cannon was making his fundamental contributions on visualization of the gastrointestinal tract. For another 50 or more years, it was not apparent that gastrin or secretin could be produced outside the stomach or duodenum, or that they might be elaborated in excessive amounts by certain endocrine tumors, particularly of the pancreas, thereby producing recognizable clinical syndromes. The development of these syndromes and some current reflections on their diagnosis and treatment will be the subject of this presentation.

The many contributions and personal attributes of Dr. Walter Cannon have been amplified by the previous Cannon lecturers [7, 9, 11]. However, I first recall meeting Dr. Cannon while a surgical intern under the late Harvey Cushing at the Peter Bent Brigham Hospital. He frequently ate

Presented to the Society of Gastrointestinal Radiologists, Hilton Head, South Carolina, September 28, 1975.

This work supported by a grant from The John A. Hartford Foundation, Inc., New York, New York, Grant GM 1539-04 from the National Institutes of Health, and USPHS Grant RR-34.

[1] Regents Professor and Chairman Emeritus, Department of Surgery, Ohio State University College of Medicine, Columbus, Ohio 43210.

lunch at the hospital with such clinical luminaries as Cushing, Christian, Sosman, Homans, Cutler, and Cheever, to name but a few. The staff of the Brigham always felt close to Dr. Cannon, not only for his interest in clinical medicine, but also because of his disability stemming from exposure to the roentgen ray, and his interest in his distinguished son, Bradford, who graduated from Harvard Medical School in 1933.

Though Walter Cannon made many fundamental contributions in numerous fields, including the function of the autonomic nervous system, traumatic shock, and surgical metabolism, physiologists, roentgenologists, and clinicians interested in the problems of the gastrointestinal tract are ever mindful of his basic and enduring discoveries in this field. Truly he was an international scholar and humanist because of his interest in the problems of his fellow scientists worldwide. His name is rightly linked with that of Beaumont, Pavlov, and Roentgen as one of the pioneers in the development of the physiology of the alimentary tract. Indeed your specialty was founded as a result of his pioneer studies in 1897.

We midwesterners are justifiably proud that both Walter Cannon and his medical student associate, Albert Moser, came from our area. Cannon was born in Prairie du Chein, Wisconsin, where William Beaumont carried out so many of his basic experiments on the French trapper, Alexis St. Martin. Moser, although born in Indiana, spent most of his young life in Lima, Ohio. Both migrated to Boston to enter Harvard Medical School, Moser in 1895 and Cannon in 1896. Davenport in his documentary on Moser entitled, "An Eagle Feather: The Short Life of Albert Moser, M.D. A Footnote to the Life of Walter B. Cannon" [9], saliently relates Moser's role in their initial endeavors to visualize the gastrointestinal tract, prior to his demise from tuberculosis at the young age of 33.

These Harvard medical students developed a variety of experiments to challenge the concepts of Kronecker and Meltzer regarding the mechanism of swallowing. Using a primitive roentgen apparatus, and Roentgen's report that the salts of heavy metals are opaque to the "ray," it was possible to study the movements of the esophagus without anesthesia or operative interference. Between January and March of 1897, they used a Canadian goose to demonstrate the movements of a capsule of subnitrate of bismuth down the gander's gullet [5]. In retrospect, it would seem appropriate that the Canadian goose, also known as a "honker," might well occupy a prominent position in this organization's shield or logo.

Besides visualizing the gastrointestinal tract, the early astute experiments of Cannon and Blake [4], as well as Cannon and Murphy [6], explained some of the clinical problems encountered by gastroenterologists and surgeons.

The studies of Cannon and Blake on gastroenterostomy and pyloroplasty, for example, included observations on gastric drainage, the vicious circle phenomenon, anastomotic kinks, disturbances of the digestive processes, and the formation of jejunal ulcerations.

Cannon and Murphy were intrigued by the effect of anesthesia and laparotomy on the activity of the stomach and small intestine [6]. They noted that ether anesthesia resulted in slight gastrointestinal delay, as did laparotomy, followed by exposure to the air or to cold. A far greater paralysis occurred when the intestine was roughly handled, and this tended to last for as long as three hours. Gentleness in the handling of the intestine is a fundamental taught to the young surgeon, but it must be constantly re-emphasized. Cannon and Murphy also studied the problem of end-to-end versus side-to-side types of anastomoses. They pointed out that the lateral anastomosis gives rise to accumulation of food in the chamber formed by the apposed loops which can lead to a series of symptoms now known as the "blind loop" syndrome. They suggested an injury to any

point along the alimentary canal produces a functional blocking effect which saves the injured part from activity until a certain degree of repair has taken place. This phenomenon explains the so-called "gas stoppage" sign which is one of the well known clues to the early diagnosis of acute appendicitis. The patient has the feeling that the intestine should empty, but is unable to relieve this sensation. Cannon also developed the concept of monitoring intestinal peristalsis with the stethoscope. He stated that "a clinician listening to the bowel sounds could reverse his intellectual process and deduce from the sound, the movements of the gut." Yet another significant contribution was the use of barium in intestinal obstruction. They observed that food left the stomach without delay in the presence of mechanical obstruction, while there was usually no movement of the stomach or intestine when a thrombosis or embolism had occurred. This observation has been put into clinical practice by giving barium by mouth in the presence of a suspected small bowel obstruction.

As mentioned earlier, Cannon and Blake were greatly concerned about the systemic effects of gastroenterostomy, since food leaving the stoma was not mixed with the important digestive enzymes of the duodenum. They correctly reasoned that the occurrence of jejunal ulceration after this procedure was the result of the gastric acid not being neutralized by pancreatic juice or bile and recommended that the situation could be overcome by the addition of a Finney type of pyloroplasty.

The distressing situation of dealing with a *primary* ulceration of the jejunum, on the other hand, is altogether a different matter; and during the late summer and fall of 1954 my colleague, the late Dr. Edwin H. Ellison, and I were forced to cope with two such catastrophes. Both patients were women, one 36 and the other 19 years of age; and each had ulcerations beyond the ligament of Treitz associated with an unbelievable outpouring of gastric juice that was rich in hydrochloric acid. So severe were the symptoms and complications that Dr. Ellison and I were constantly seeking each other out for consultation as well as consolation. The subsequent course of these two women is, of course, well known to you. The younger patient finally came to total gastrectomy; and, upon the advice of the late Hilger Jenkins, we looked for and found two small non-insulin-producing tumors on the anterior aspect of the left side of the body of the pancreas. Because of this, the autopsy records of the older patient were re-checked and it was noted that there were several nodules in the central portion of her pancreas. The younger patient has survived and is perfectly well almost 21 years later. She has two healthy daughters, born eight and ten years after the total gastrectomy.

On the basis of these two cases, it was suggested that these "non-functioning" islet cell tumors elaborated a potent gastric secretagogue which caused the stomach to digest itself. A diagnostic triad, later named the Zollinger-Ellison syndrome by Eiseman and Maynard [14], was developed consisting of a fulminating ulcer diathesis, marked gastric hypersecretion, and a non-beta islet cell tumor of the pancreas [37].

It is noteworthy that three years prior to this, two British radiologists, Forty and Barrett [14], had emphasized changes in the third portion of the duodenum associated with islet cell tumors of the pancreas. They reported ulcerations in the third part of the duodenum associated with islet cell tumors in five of 14 patients examined. Indeed, the roentgenologist must be placed among the pioneers in either making or suggesting the diagnosis of an ulcerogenic tumor of the pancreas. Christoforidis and Nelson [7] thoroughly reviewed this subject and found the characteristic findings to include excessive gastric fluid, even after fasting, and the lack of any obstruction; an enlarged, shaggy-appearing duodenum, with or without ulcerations in unusual locations; irregularities of the duodenal wall from edema which may be mistaken for Crohn's disease; and increased small bowel motil-

ity. Postresectional or marginal ulcerations were described as deep, penetrating, and multiple, and located on the mesenteric border of the efferent loop rather than in the usual marginal location. More recently, selective celiac arteriography and radioisotope scanning have been employed but, in general, their value in diagnosis has been minimal.

The finding of an ulceration beyond the ligament of Treitz has long been considered as pathognomonic of an ulcerogenic islet cell tumor. This may be explained as a mechanical effect resulting from the large volumes of gastric acid "jetted" by the thick-walled duodenum against the thinner jejunum which has a smaller blood supply.

Within five years after the ulcerogenic islet cell tumor syndrome was suggested, Gregory et al. [19] proved that these tumors as well as their metastases produced the potent gastric secretagogue, gastrin, in amounts 35 times greater than that found in an equal amount of porcine antrum. This discovery offered a ready explanation for the severity of the symptoms. Since ulcerogenic tumors are so frequently multiple, malignant with metastases, or both, the sources for the potent hormone are multicentric, thus confirming the original recommendation of total gastrectomy as the best treatment for the disease. It should be remembered that in the presence of an ulcerogenic tumor, several liters of gastric juice have been secreted in twelve hours by a gastric remnant *no larger than an orange*. This results from the known trophic effects of hypergastrinemia resulting in a profound hyperplasia of the gastric mucosa which greatly enhances its capacity to secrete hydrochloric acid.

The diagnosis of an ulcerogenic tumor has become more common, more certain, and earlier as a result of the gastrin radioimmunoassay as first developed by McGuigan and Trudeau [22]. Diagnostic serum gastrin levels coupled with positive barium studies and a good clinical history, regardless of the patient's age, have rendered the diagnosis quite accurate. Elevated gastrin levels, however, may also occur in association with pernicious anemia, atrophic gastritis in the absence of antral gastritis [34], renal failure, retained antrum, carcinoma of the body of the stomach, and antral G-cell hyperplasia.

In tandem with positive clinical, laboratory, and roentgen evidence, patients with an ulcerogenic tumor tend to fall into one of five clinical groups. First are those patients who demonstrate only a borderline elevation in the serum gastrin levels. The second group includes those patients who also have hyperparathyroidism. The third, who present all too often, are those patients who have had multiple gastric operations, with either only temporary relief or almost immediate recurrence of the ulcer symptoms. Finally, there are those patients who have the classical ulcerogenic tumor syndrome. They are informed of the possibility of total gastrectomy. More recently it has been suggested that hyperplasia of the antral G-cells may produce a pseudo-ulcerogenic syndrome which can be controlled by vagotomy and antrectomy [16].

Experience has shown that the serum gastrin levels are not always diagnostic even in the presence of a tumor, particularly in those cases of duodenal wall adenomata which occur in approximately ten percent of the reported cases. In such cases, it is advisable to employ the calcium challenge or infusion test, as developed by Passaro et al. [26]. Calcium gluconate (15 mg/kg) given over a four hour period will dramatically elevate the serum gastrin levels if any tumor is present or if undiscovered metastases have been left behind. If the serum calcium levels are elevated, as in cases of hyperparathyroidism, magnesium sulfate (1.6 mg/kg) can be administered over a four hour period [32]. This will mobilize the serum gastrin, though not to the extent seen following the calcium infusion. Secretin, although expensive, may also be used as a challenge test in dosages of one to four clinical units over a period of one hour [18, 31]. One or more of these tests,

when strongly positive preoperatively, will provide the surgeon with the evidence to proceed with a total gastrectomy even when a thorough surgical exploration is negative.

The surgical treatment of an ulcerogenic tumor has changed relatively little since the original report in 1955, although after the abdomen is opened, the surgeon may encounter circumstances which require various surgical decisions. Total gastrectomy, despite a negative exploration, is indicated if the preoperative basal serum gastrin levels are high and the infusion studies resulted in doubling or tripling of the basal values. Under these circumstances, blind resection of the body and tail of the pancreas is unnecessary since it often increases the incidence of complications associated with the procedure. Total gastrectomy is likewise indicated when metastases or multiple tumors are found, regardless of the patient's age. The very young tend to grow and develop normally after total gastrectomy [36]; and the elderly are spared from a potentially fatal hemorrhage or perforation. Lesser procedures to remove small adenomata from the wall of the first portion of the duodenum or solitary tumors from the body of the pancreas or the antrum, in the presence of the as yet insufficiently tested antral G-cell hyperplasia, have met with limited success [17]. In general, however, a distressingly high recurrence rate of at least 50 percent can be anticipated if anything less than total gastrectomy is undertaken [16].

A Roux-en-Y type of esophagojejunostomy has been preferred for reconstructing the gastrointestinal tract, although others favor creating some type of pouch. The ability of the ulcerogenic tumor patient to sustain an ideal weight suggests that persistent hypergastrinemia, due to retained or recurrent tumor, may well stimulate the patient's appetite. It should be noted that recent studies have failed to support the value of pouches in improving postoperative nutrition after total gastrectomy [3]. Years ago, Walter Cannon determined that contractions of the stomach were the source of hunger sensations. However, he did admit that "it seems possible that a substance exists in the blood which acts to excite the hunger mechanism." This could certainly explain the usual hunger sensations invariably experienced by patients after having undergone total gastrectomy.

The follow-up of patients with a proved ulcerogenic tumor should be frequent and extended over a period of many years. These tumors grow very slowly and some have suggested that their growth is inhibited by removal of the target organ, the stomach. Following total gastrectomy, monthly vitamin B-12 injections are required, and the patient's weight trends must be monitored regularly. Better results are ensured if the patient is hospitalized several times during the first year after surgery to review the diet, evaluate the adequacy of the esophagojejunal anastomosis, and determine the extent of tumor progression or regression by four hour calcium infusion studies [29]. In the presence of weight loss and high serum gastrin levels, an arteriogram should be advised.

The roentgenologist's role in these follow-up studies is very important. When the patient loses weight or has difficulty eating, the possibility of stenosis at the esophagojejunal anastomosis must be evaluated. In addition, some patients have developed cholelithiasis, requiring evaluation of the gallbladder by cholecystography. If hypercalcemia is documented, intravenous pyelograms as well as a limited bone survey are indicated to prove or disprove hyperparathyroidism. When either the basal or stimulated follow-up gastrin levels are markedly elevated, an angiogram is advisable to determine if hepatic metastases are present.

Although the fasting gastrin levels may be only moderately elevated (300–400 pg/ml), calcium-, magnesium-, and secretin-stimulated levels will show a modest to marked elevation in patients who have a proved gastrinoma, regardless, in our experience, of the number of years which

have elapsed since the total gastrectomy even up to 21 years. These findings support the concept of multicentric sources of gastrin in the majority of patients and suggest that tumor activity persists despite total gastrectomy. Ulcerogenic tumors appear to progress in approximately one-third of the patients and hepatic metastases may be found unexpectedly by angiography.

Such patients may be given a combination chemotherapy program consisting of Tubercidin, 1.5 mg/kg, mixed with 500 ml of the patient's blood and administered intravenously over a period of four hours. Five-Fluorouracil, 12.5 mg/kg, is given for three days; and after one week the dosage is repeated every other week for a total of six courses. Streptozotocin, 12.5 mg/kg, is given intravenously on the alternate weeks for a total of three courses. After one month, the Tubercidin is once again administered. The total interval between the Tubercidin averages 70 to 80 days. Frequent blood studies and serum gastrin determinations are recorded and the preliminary observations are encouraging [30].

Although present in one of the original patients, diarrhea was not emphasized in the clinical syndrome because we had held to the triad concept as popularized by Whipple [35]. Within two years of the original report, however, Priest and Alexander [27] called attention to a patient with an islet cell tumor of the pancreas and associated peptic ulceration, diarrhea, and hypokalemia. Verner and Morrison [33] later reported additional cases characterized by watery diarrhea and hypokalemia, but with no ulceration. It remained for Murray and colleagues [25] in 1961 to document achlorhydria in such a patient. This syndrome currently has several appelations including pancreatic cholera [24], Verner-Morrison, WDHA [23], and diarrheogenic [38] syndrome. These patients have fulminating watery diarrhea, severe hypokalemia, and usually achlorhydria. Hypercalcemia is present in about two-thirds of the cases, but is often reversed after the pancreatic tumor is removed. Approximately 40 percent of the patients demonstrate hyperglycemia, and cutaneous flushing may also be a complaint [20].

Patients with the diarrheogenic syndrome lose as much as six liters of fluid by stool a day. The hypokalemia is so severe that more than 250 mEq of potassium along with five or six liters of other electrolytes and fluids may be required over a 24 hour period to avoid the serious complication of hypokalemic nephropathy. These tumors may be of such size as to cause displacement of the stomach on barium studies. Of diagnostic significance is the finding of a large gallbladder by cholecystogram. We have verified this observation in three such patients, and analysis of aspirated bile has shown chemical changes consistent with a secretin-like hydrocholeresis [38]. At the time of operation, the small intestine may appear enlarged with evidence of dilution of the barium given by mouth.

A diarrheogenic tumor should be considered when all other causes of severe watery diarrhea have been excluded. The investigation should include an augmented histamine gastric analysis, as well as serum calcium and glucose determinations. If the potassium loss, which is so marked as to produce the signs and symptoms of intestinal obstruction, can be corrected only by vigorous fluid and electrolyte replacement, the possibility of such a tumor must be suspected.

Thorough investigations of three such patients had convinced us that diarrheogenic tumors elaborate secretin or a secretin-like polypeptide which inhibited hydrochloric acid and stimulated the secretion of bile and pancreatic juice along with alterations in the absorption of fluid and electrolytes by the intestine [29, 38]. Recent studies by several investigators, including Bloom et al. [2] and Said and Faloona [19], have presented good evidence that the secretin-like polypeptide is vasoactive intestinal polypeptide (VIP). The development of additional radioimmunoassays may eventually provide that the ten or more hor-

mones and hormone-candidates already identified in the duodenal mucosa may be produced by an islet cell tumor. The clinical symptoms of the diarrheogenic syndrome are completely abolished by tumor excision, unless it is malignant with metastases and cannot be totally resected. Furthermore, the achlorhydria may be replaced with normal or even high acid values during the post-operative period if no tumor remains. Chemotherapy appears to be effective in these cases in controlling the recurrent diarrhea [19].

Islet cell tumors of the pancreas have been proved to have the potential for causing recognizable, often life-threatening clinical and roentgenological syndromes related to the gastrointestinal tract. The accumen and skills of the gastrointestinal radiologist will always be essential in the diagnosis of these syndromes. There is every reason to believe that additional syndromes associated with islet cell tumors will be recognized; and credit will always be given to Walter B. Cannon for teaching us the fascinating challenges of the gastrointestinal tract.

REFERENCES

1. Bayliss WM, Starling EH: Mechanism of pancreatic secretion. *J Physiol* 28:32–51, 1902
2. Bloom SR, Polak JM, Pearse AGE: Vasoactive intestinal peptide and watery diarrhea syndrome. *Lancet* 2:14, 1973
3. Bradley EL III, et al: Metabolic consequences of total gastrectomy. Submitted for publication.
4. Cannon WB, Blake JR: Gastro-enterostomy and pyloroplasty: experimental study by means of roentgen rays. *Ann Surg* 41:686, 1905
5. Cannon WB, Moser A: Movements of food in esophagus. *Am J Physiol* 1:435, 1898
6. Cannon WB, Murphy FT: Movements of stomach and intestines in some surgical conditions. *Ann Surg* 43:512, 1906
7. Christoforidis AJ, Nelson SW: Radiological manifestations of ulcerogenic tumors of pancreas: Zollinger-Ellison syndrome. *JAMA* 198: 5, 1966
8. Davenport HW: Walter B. Cannon's contribution to gastroenterology. *Gastroenterology* 63: 878, 1972
9. Davenport HW: First Walter Bradford Cannon Lecture before Society of Gastrointestinal Radiologists. *Am J Roentgenol* 119:235–240, 1973
10. Davenport HW: Eagle-feather: short life of Albert Moser, MD. Submitted for publication
11. Dunphy JE: Third Walter B. Cannon lecture, 1974. Surgical treatment of gastrointestinal ulcer: past and future. *Am J Roentgenol* 123:229, 1975
12. Edkins JS: Chemical mechanism of gastric secretion. *J Physiol* 34:133, 1906
13. Eiseman B, Maynard RM: Non-insulin producing islet cell adenoma associated with progressive peptic ulceration. *Gastroenterology* 31: 296, 1956
14. Forty F, Barrett GM: Peptic ulcerations of third part of duodenum associated with islet cell tumors of pancreas. *Br J Surg* 40:60, 1952
15. Fox PS, Hofmann JE, DeCosse JJ, Wilson SD: Influence of total gastrectomy on survival in malignant Zollinger-Ellison syndrome. Submitted for publication
16. Friesen SR, Shimke RN, Pearse AGE: Genetic aspects of ZE syndrome: antral gastrin cell hyperplasia. *Ann Surg* 176:370, 1972
17. Gregory RA, Tracy HJ, French JM, et al: Extraction of gastrin-like substance from pancreatic tumor in case of Zollinger-Ellison syndrome. *Lancet* 1:1049, 1960
18. Isenberg JL, Walsh JH, Passaro E Jr, et al: Unusual effects of secretin on serum gastrin, serum calcium and gastric acid secretion in patient with suspected Zollinger-Ellison syndrome. *Gastroenterology* 62:626, 1972
19. Kahn CR, Levy AG, Gardner JE, et al: Pancreatic cholera: beneficial effects of treatment with streptozotocin. *N Engl J Med* 292:941, 1975
20. Kraft AR, Tompkins RK, Zollinger RM: Recognition and management of diarrheal syndrome caused by non-beta islet cell tumors of pancreas. *Am J Surg* 119:163, 1970
21. Mac Brooks C: *The Life and Contributions of Walter Bradford Cannon, 1871–1945*. Albany, University Press, 1975
22. McGuigan JE, Trudeau WL: Immunochemical measurements of elevated levels of gastrin in serum of patients with tumors of Zollinger-Ellison variety. *N Engl J Med* 178:1308, 1968
23. Marks IN, Bank S, Louw JH: Islet cell tumor of pancreas with reversible watery diarrhea and achlorhyria. *Gastroenterology* 50:695, 1967
24. Matsumoto KK, Peter JB, et al: Watery diarrhea and hypokalemia associated with pancreatic islet cell adenoma. *Gastroenterology* 50:321, 1966
25. Murray JS, Paton RR, Pope CE: Pancreatic tumor associated with flushing and diarrhea. *N Engl J Med* 264:436, 1961
26. Passaro E, Basso N, Walsh JH: Calcium challenge in Zollinger-Ellison syndrome. *Surgery* 72:60, 1972
27. Protocol 7230: Central Oncology Group, Madison, Wisconsin. Phase III study.

28. Priest WM, Alexander MK: Islet cell tumor of pancreas with peptic ulceration, diarrhea and hypokalemia. *Lancet* 2:1145, 1957
29. Said SI, Faloona GR: Vasoactive intestinal peptide and watery diarrhea. *N Engl J Med* 393:255, 1975
30. Sanzenbacher LI, Mekhjian HS, King DR, Zollinger RM: Studies on potential role of secretin in islet cell tumor diarrheogenic syndrome. *Ann Surg* 176:394, 1972
31. Thompson J, Reeder DD, Villar HV, et al: Natural history and experience with diagnosis and treatment of Zollinger-Ellison syndrome. *Surg Gynecol Obstet* 140:5, 1975
32. Thompson JC, Feeder DD, Bunchman HH, et al: Effect of secretin on circulating gastrin. *Ann Surg* 176:384, 1972
33. Verner JV, Morrison AB: Islet cell tumor and syndrome of refractory watery diarrhea and hypokalemia. *Am J Med* 25:374, 1958
34. Turnipseed W, Keith LM: Gastrin responses to calcium and secretin infusions in achlorhydric patients. Submitted for publication
35. Whipple AO: Surgical therapy of hyperinsulinism. *J Internat Chir* 3:237, 1938
36. Wilson SD, Schulte WJ, Meade RC: Longevity studies following total gastrectomy: in children with Zollinger-Ellison syndrome. *Arch Surg* 103:108, 1971
37. Zollinger RM, Ellison EH: Primary peptic ulcerations of jejunum associated with islet cell tumors of pancreas. *Ann Surg* 142:709, 1955
38. Zollinger RM, Tompkins RK, American JR, et al: Identification of diarrheogenic hormone associated with non-beta islet cell tumors of pancreas. *Ann Surg* 168:502, 1968

Am J Roentgenol 126:941–951, 1976

ANGIOGRAPHY IN CROHN'S DISEASE REVISITED

FOLKE BRAHME[1,2] AND JAN HILDELL[1]

ABSTRACT:

The diagnostic value of angiography was studied in 116 patients with Crohn's disease. Angiograms showed abnormalities in over 90% of the cases. Many angiographic features were nonspecific; only the "zoning sign" and the presence of paraintestinal mesenteric neovasculature were considered diagnostic. Crohn's colitis could be distinguished from ulcerative colitis in only 30% of the cases. Angiography, as a diagnostic adjunct to barium studies, will reveal the presence of lesions and their extent. This is particularly important in suspected postoperative recurrence of Crohn's disease. Angiography is a potential differential diagnostic aid in doubtful cases of inflammatory and malignant bowel disease.

In spite of the abundance of information available on gastrointestinal abnormalities in Crohn's disease, as seen by conventional radiological studies, the diagnosis remains in doubt in at least 5%–10% of the cases in most series. In addition, the extent of the lesions in the individual patient is frequently difficult to assess; this information is of critical importance whenever surgical treatment is contemplated.

Attempts to explore angiography as an additional diagnostic modality in Crohn's disease were initially reported in 1966 [1, 2]. Subsequent reports have described angiographic features in Crohn's disease in series consisting of 33 patients [3] or less [4–7]. Several of the older reports present conflicting opinions on the usefulness of angiography for differential diagnostic purposes. Herlinger [6] states that angiography can be of positive assistance to separate Crohn's disease of the colon from ulcerative colitis in approximately 85% of cases, whereas Eriksson et al. [5] contend that the method allows no conclusive differential diagnosis. Postoperative angiographic studies, performed to detect recurrence of Crohn's disease, have attracted little interest.

This communication attempts to reevaluate the merits and limitations of angiography in Crohn's disease using a larger series of patients and to define indications for its use.

SUBJECTS AND METHODS

Subjects Studied

A total of 123 angiograms were performed in 116 patients with Crohn's disease; 115 small bowel lesions and 55 colonic lesions were encountered in these patients. (Eighty-three patients were examined at Malmö General Hospital, and 33 patients at the University Hospital of Lund, Sweden). The diagnosis was ascertained by histological examination of surgically excised specimens in 98 patients, by rectal or peroperative biopsy in nine, and by a minimum of two consecutive barium examinations of the large and small bowel, showing characteristic abnormalities, in the remaining nine. The number of pre- and postoperative examinations as well as the distribution of the lesions appear in table 1.

For the purpose of overall evaluation of the results, the angiograms, barium studies, and the excised specimens were examined independently. In addition, angiograms were performed on 24 excised specimens in order to clarify features seen in the in vivo angiograms.

Technique

Conventional percutaneous catheterization technique was used. Superior mesenteric angiography was performed in all 123 studies, supplemented by inferior mesenteric angiography

[1] Department of Diagnostic Radiology, Malmö General Hospital, University of Lund, Malmö, Sweden.
[2] Present address: Radiology Department, Veterans Administration Hospital, San Diego, California 92161.

TABLE 1

DISTRIBUTION OF LESIONS IN 123 EXAMINATIONS

LOCATION	ANGIOGRAPHY		
	Followed by Exploratory Laparotomy, or No Surgery	Followed by Surgery with Excision of Gut	In Suspected Post-operative Recurrence
Duodenum, proximal jejunum	2	...	...
Jejunum, proximal or mid-ileum	6	2	...
Distal ileum	1	24	33
Distal ileum and cecum	1	11	...
Ileum and colon, extensively	7	26	2
Colon (and rectum) only	1	6	1
Total	18	69	36

in 63. The superselective catheterization and magnification technique was used only in a few cases. For superior mesenteric angiography, 20–40 cm^3 of a water-soluble contrast medium in a concentration of 60% or 76% were injected at the rate of 8–10 cm^3/sec; for inferior mesenteric angiography, 10–15 cm^3 were used.

Straight frontal projections were standard, supplemented by oblique views when necessary. Prior to the injection of the contrast medium, the colon was either moderately inflated by air or distended by instillation of saline, as suggested by Lunderquist and Lunderquist [8].

RESULTS

The findings in the arterial, capillary, and venous phases, as well as their relative frequency in affected bowel segments, are described separately below. The frequency of the various angiographic features are given in table 2 as percentages of the 115 small bowel and 55 colonic lesions studied. The angiographic features in normal subjects are referred to only briefly; more complete information on the normal angiographic anatomy of the intestine is available elsewhere [9–13].

Arterial Phase

The *caliber* of the main stem of the superior mesenteric artery varied from 5 to 9 mm (mean, 6.5 mm), that of the ileocolic artery from 3 to 5 mm (mean, 4 mm), and that of the inferior mesenteric artery from 4 to 6 mm (mean, 4.5 mm). All these measurements were within the normal range [12, 13].

The *arteriae rectae longae*, which arise in pairs from the marginal mesenteric artery and encircle the gut in the subserosal layer, were *numerically increased* in 74 of 115 lesions of the small bowel (64%) and in 28 of 55 colonic lesions (51%) (fig. 1). Numerical increase was considered present when the number of arteriae rectae longae exceeded five per centimeter in the small bowel and 0.5 per centimeter in the colon,

TABLE 2

SUMMARY OF ANGIOGRAPHIC CHANGES IN CROHN'S DISEASE

Angiographic Change	Small Bowel Lesions	Colonic Lesions
Arteries:		
Normal	18 (16)	23 (42)
Numerically increased	74 (64)	28 (51)
Tortuous	67 (58)	27 (49)
Nontapering	38 (33)	19 (35)
Branching at right angles	36 (31)	6 (11)
Bowel wall:		
Increased opacification	91 (79)	35 (63)
Thickness	71 (62)	17 (31)
Zoning sign	10 (6)	16 (29)
Veins:		
Normal	9 (8)	4 (7)
Early opacified	101 (88)	44 (80)
Mural veins visible	49 (42)	22 (40)

NOTE.—Numbers in parentheses represent percentage of 115 small bowel lesions or 55 colonic lesions, respectively.

counted along the axis of the gut. Estimations were considered reasonably accurate in bowel segments running parallel to the film; in other areas, estimations were made.

The *arteriae rectae breves*, minor branches of the arteriae rectae longae not seen at angiography in normal subjects, could be clearly identified in most areas of the colon in which the arterial supply was markedly increased, as evidenced by the increased number of arteriae rectae longae. Arteriae rectae breves were difficult to observe in small bowel lesions but could usually be seen on magnification angiograms (fig. 2).

Increased tortuosity of the arteriae rectae was seen in 58% of small bowel lesions and in 49% of colonic lesions. Abnormal tortuosity was only recorded when the vessels followed a markedly irregular course across the wall of a distended segment of the gut or when "terminal coiling" of the arteriae rectae was present. In the small intestine, tortuosity was only considered present if the arteriae rectae had a tight corkscrew appearance (figs. 1 and 3*A*).

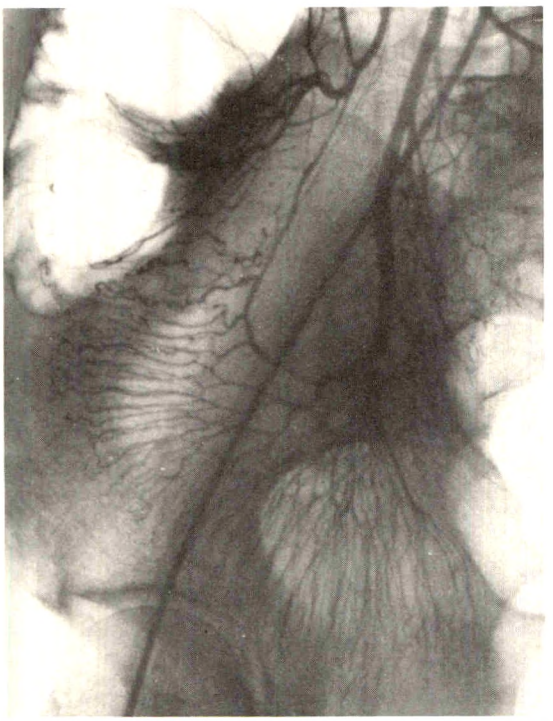


FIG. 1.—Crohn's disease of the distal ileum and right hemicolon. Note wide, tortuous, and numerically increased arteriae rectae of distal ileum.

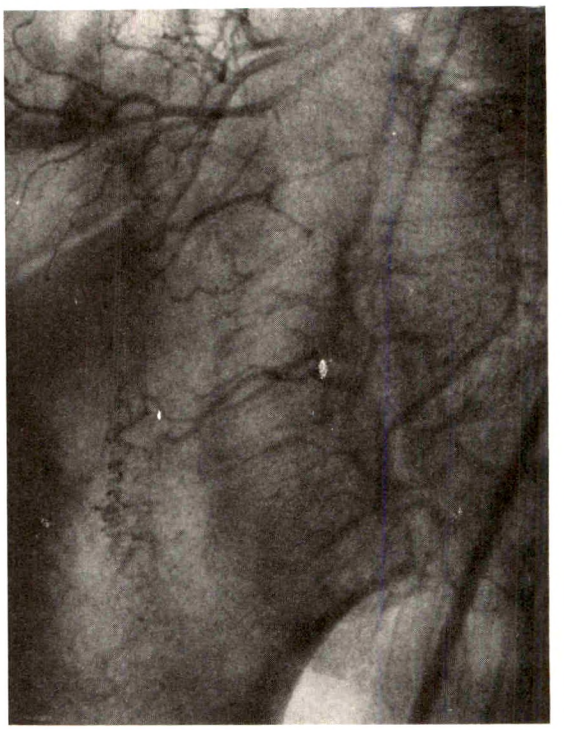


FIG. 2.—Ileocecal Crohn's disease. Magnification angiogram showing arteriae rectae breves (*arrows*) and wide arteriae rectae longae with terminal coiling.

Abrupt tapering [6, 7] refers to the absence of the normal smooth tapering of the arteriae rectae longae. When abrupt tapering (which might more appropriately be termed nontapering) was present, the arteriae rectae longae could be traced with maintained caliber to the antimesenteric border of the gut, where they abruptly broke up into numerous minor branches. This feature was observed in one-third of all lesions (figs. 1, 2, and 3*A*). Wide, nontapering arteriae rectae were occasionally seen to supply localized inflammatory areas with large solitary ulcers in the colon (fig. 4).

Right angle branching [7] refers to the separation of the paired arteriae rectae in right, rather than acute, angles at their origin from the marginal artery and was observed in 31% of small bowel lesions and in 11% of colonic lesions. This abnormality was difficult to assess in jejunal segments, where irregular branching patterns fre-

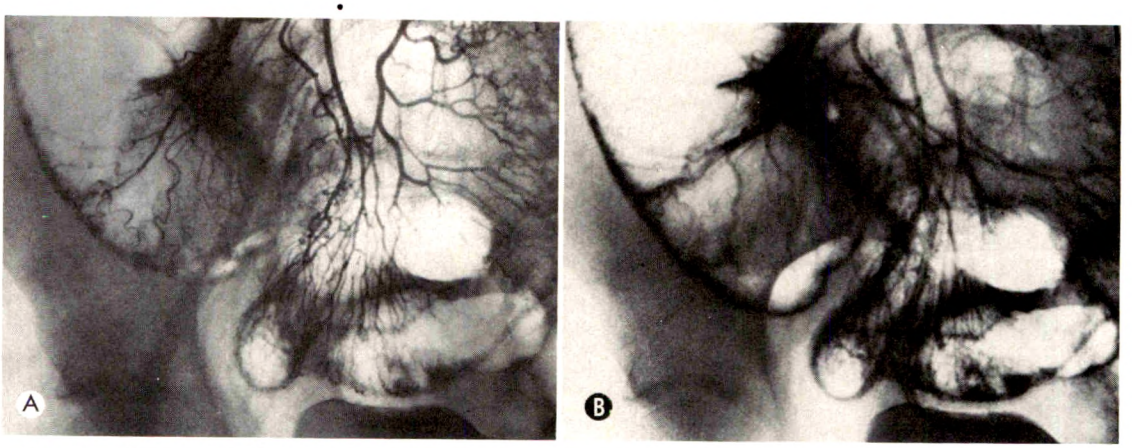


FIG. 3.—Ileocecal Crohn's disease of more than 10 years' duration. *A*, Film at 4 sec; *B*, film at 6 sec. Note wide and tortuous arteriae rectae, dense staining of the bowel wall, premature venous return.

quently occur in normal subjects.

Small irregular tangles of inflammatory neovasculature, corresponding to the "Gefässknäuelchen" described by Dombrowskij and Korb [4], were noted in 10 small bowel lesions and along or adjacent to colonic lesions in nine (fig. 5). In three cases inflammatory neovasculature was observed in the mesentery, several centimeters away from the wall of the gut.

Other arterial changes observed were gross distortion of the course of the marginal artery and the arteriae rectae in areas of strictures, kinking and abnormal course of major mesenteric arteries suggesting mesenteric adhesions, and, in four patients, a "standing wave phenomenon" [14] indicating abnormal flow patterns. Arterial occlusions were not observed, but minor variations in caliber of the marginal artery and the arteriae rectae were present in cases with marked thickening of the mesentery or of the wall of the gut. Reduction of the number of arteriae rectae were seen in two cases, in both of which the lesions were pathologically characterized as "fibrotic and inactive." In some cases, the circulation time through peripheral arteries was prolonged, but premature opacification of the mural veins occurred also in these cases. This phenomenon, previously described by Boijsen and Härtel [11], was recorded with certainty only in the distal part of the ileum.

Capillary Phase

In the normal mesenteric angiogram the wall of the gut appears as a 2–3 mm wide stripe. Opacification usually begins 5–7 sec after the start of the injection and lasts for

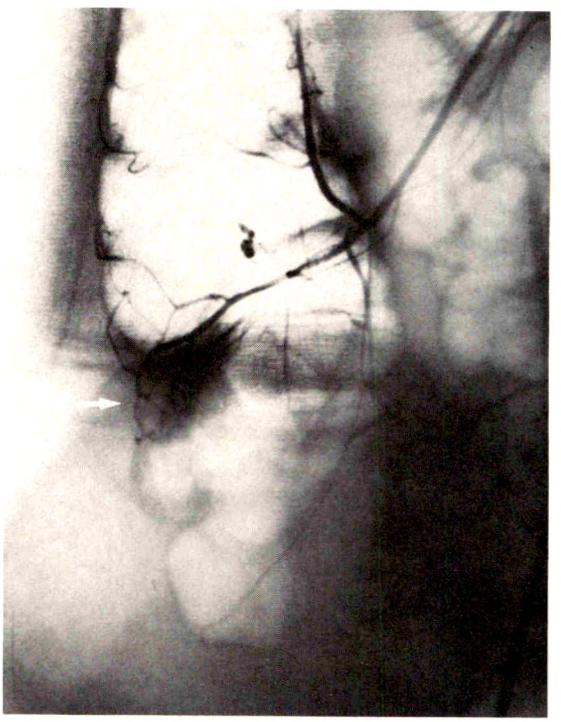


FIG. 4.—Distal ileal Crohn's disease revealed by barium study. Angiography demonstrates additional lesions of the cecum. Note arterial hypervascularity, increased staining, and premature venous return from inflammatory locus in cecum (*arrow*). Excised specimen showed large solitary cecal ulcer.

4–6 sec. In Crohn's disease, clearly *increased opacification* of the intestinal wall was seen in 74% of all small and large bowel lesions (figs. 3*B* and 6). Abnormal thickening of the wall of the gut, exceeding 4 mm, was noted in 62% of small bowel lesions and in 34% of colonic lesions. The thickness of the wall of the gut could only be properly assessed on distended segments. Consequently, the thickness of the wall of the colon could be determined more accurately than that of the small bowel. In four cases, short colonic segments showed a wall thickness exceeding 10 mm.

Herlinger's *zoning sign* [6], referring to the appearance of one densely opacified inner layer and one faintly opacified outer layer of the gut in the angiograms, was noted in 29% of colonic lesions (fig. 6*A*). The phenomenon was less readily identified in small bowel lesions and could only be seen with certainty in 6% of these.

Venous Phase

The mesenteric veins normally become opacified 8–10 sec after injection of contrast medium, and opacification is usually only moderate. Mural veins of the intestinal wall are normally only barely, or not at all visible in angiograms. In Crohn's disease, *premature and dense opacification of mesenteric veins*, occurring after 6 sec or less, was seen in 88% of small bowel lesions and in 80% of colonic lesions (figs. 3*B*, 6, and 7). *Mural intestinal veins* were clearly visible in 41% of all small and large bowel lesions. In most cases there was a distinct time interval between the disappearance of the arteries and the opacification of mural veins, but in some cases mural veins and arteries appeared simultaneously (fig. 6*A*).

Overall Results

Various combinations of the above described vascular changes were recorded in the angiograms. Vascular abnormalities indicating presence of disease were seen in the arterial phase in 78% of the lesions, in the capillary phase in 74%, and in the venous phase in 90%.

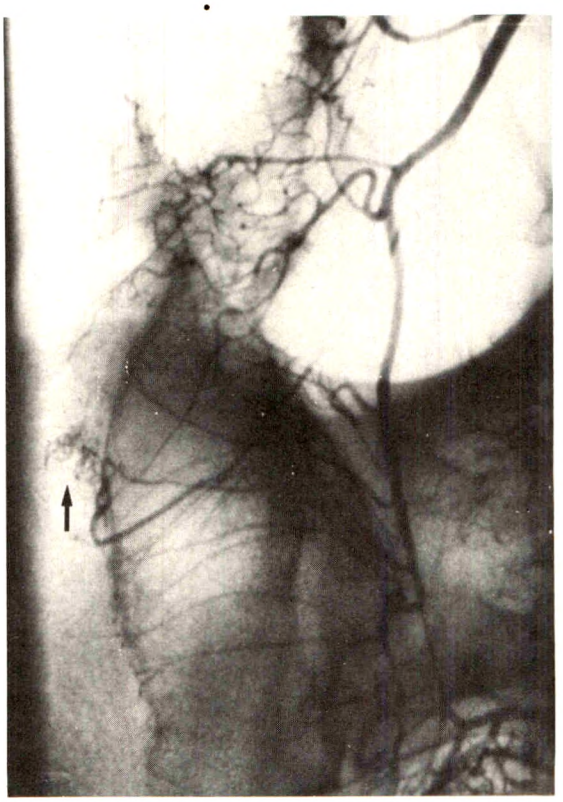


FIG. 5.—Crohn's disease of ileum and right hemicolon. Gefässknäuelchen (*arrow*) adjacent to colonic wall.

Assessment of Extent of Lesions

In 98 patients who underwent operation subsequent to barium studies and angiography, the radiographic findings could be compared to observations on excised specimens. The barium studies showed various types of abnormalities in all 98 patients. The combined observations from barium studies and angiography permitted adequate estimation of the extent of the lesions in 90 of these 98 patients. In 67, the extent of the process was demonstrated with roughly equal accuracy by the two techniques; in 11 the extent was best evaluated by barium studies; and in 12 angiography was best. The extent of small bowel lesions was generally better demonstrated by barium studies, whereas colonic involvement was more accurately determined by angiography (figs. 8*B* and 8*C*).

In the remaining eight patients, considerable discrepancy existed between the pre-

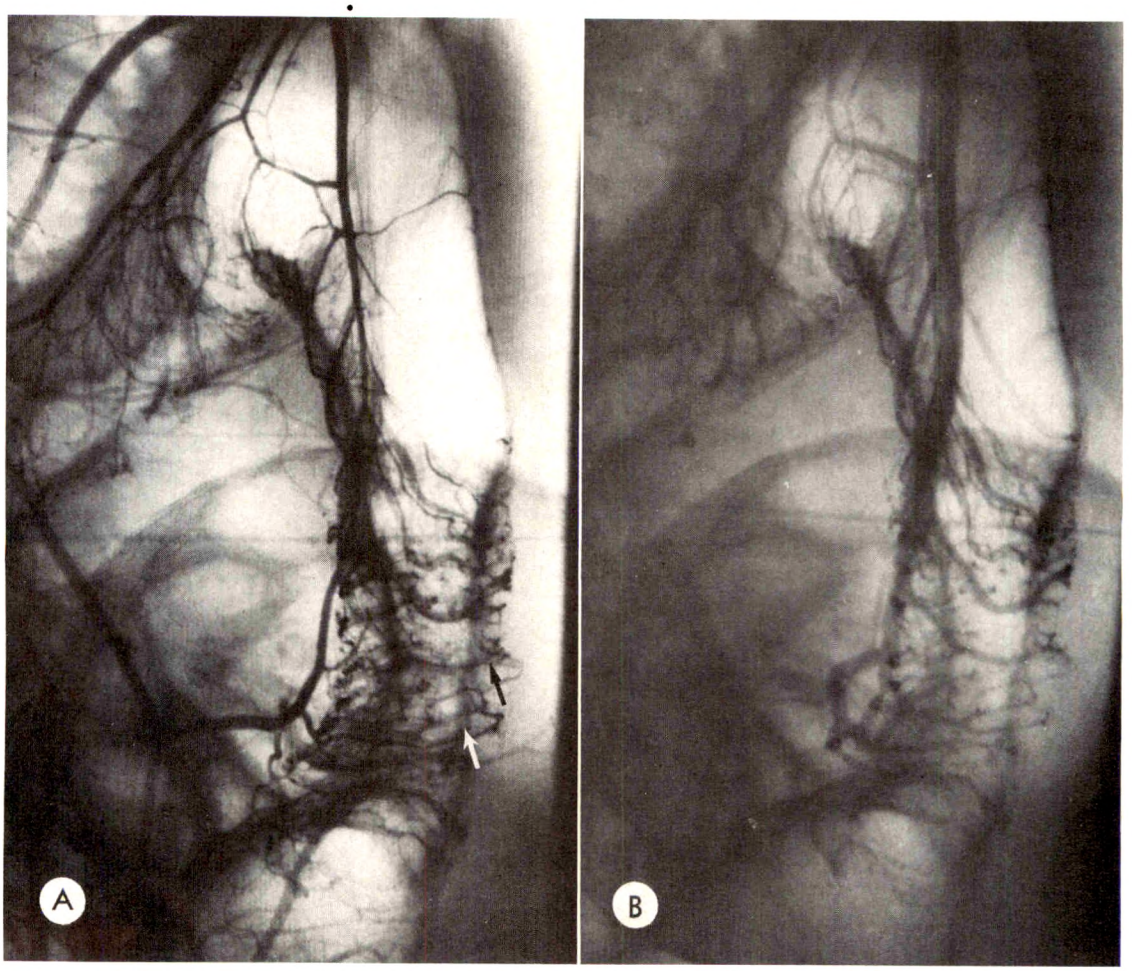


FIG. 6.—Medically managed ileocolic Crohn's disease. *A*, Zoning sign with densely opacified inner zone A (*open arrow*) and faintly opacified outer zone B (*closed arrow*). *B*, Simultaneous demonstration of arteries and veins (film at 4.5 sec).

operative angiograms and barium studies, on the one hand, and operative findings on the other (fig. 8*A*). The disagreement was regarded as considerable when the extent of the process, as seen on specimens, exceeded that observed by radiology by 10 cm or more, or when lesions present in specimens had altogether escaped radiological detection. There was no difference in diagnostic efficiency between angiography and barium studies in these eight patients.

Angiography in Postoperative Recurrence of Lesions

In 36 of the 116 patients, angiography



FIG. 7.—Ileocolic Crohn's disease. Enlarged, densely opacified mural and mesenteric veins (8 sec).

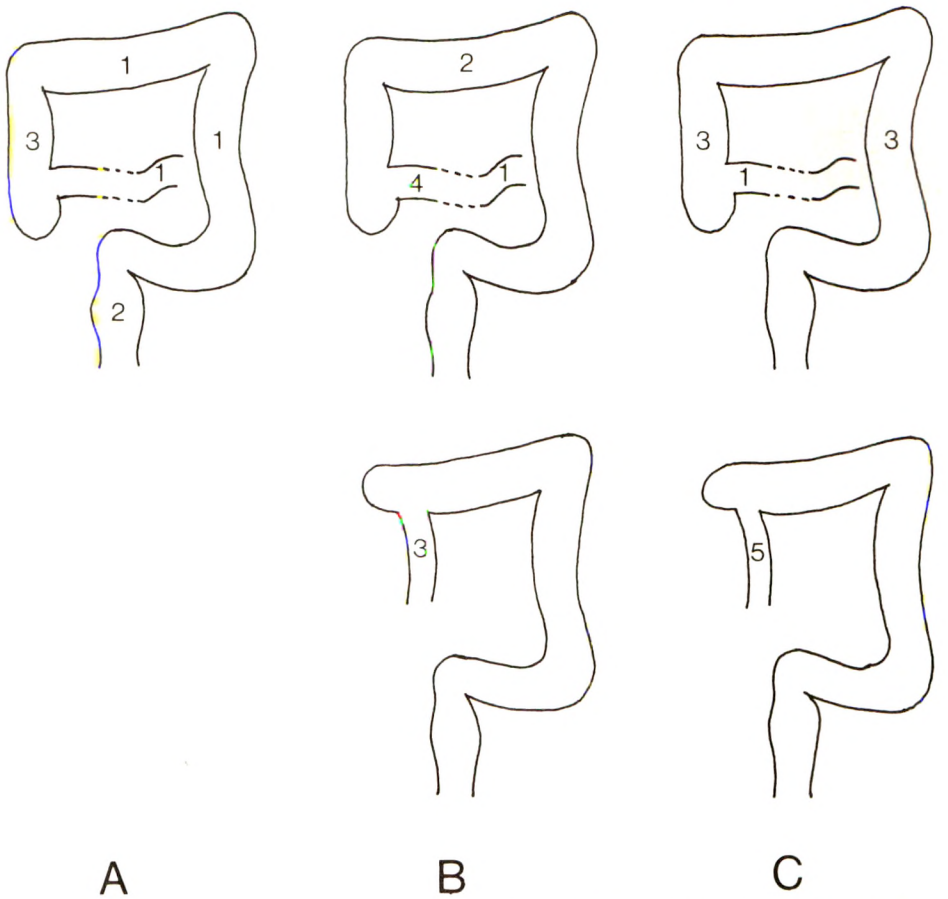


FIG. 8.—Discrepancy between radiological and operative findings. *A*, Location of lesions inadequately shown by preoperative barium and angiographic studies. *B*, Location of lesions shown by barium studies but shown poorly or not at all by angiography. *C*, Location of lesions shown by angiography but shown poorly or not at all by barium studies. Numerals refer to number of lesions in each area.

was performed because of clinical suspicion of postoperatively recurrent Crohn's disease. Barium studies, done prior to the angiograms, had been inconclusive in several of these cases, either because of paucity of findings or because of the presence of confusing features, such as postoperative deformity of the gut or disarray of the mucosal pattern secondary to partial bowel obstruction. Angiography clearly demonstrated abnormalities consistent with active inflammation in 33 of the 36 cases. Increased accumulation of contrast medium in the bowel wall and premature venous drainage were the most frequent indicators of disease. Most of the recurrent lesions were located to the distal segment of the small intestine, immediately proximal to the surgical anastomosis.

Of these 36 patients, 21 underwent laparotomy subsequent to angiography, with resection of gut in 20. The remaining 16 were treated conservatively. In 13 of the 20 patients who underwent resection, the diseased segment was demonstrated equally well by barium studies and angiography. In another three, barium studies showed lesions not seen at angiography. In one of these, the changes in the excised specimen were histologically described as "fibrotic and inactive"; no satisfactory explanation for the discrepancy was obtained in the

other two. In five cases the angiograms clearly demonstrated lesions which were equivocally or not at all shown by barium studies (fig. 8). In none of these operated patients did both angiography and barium studies fail to reveal lesions found at subsequent operation. One additional angiogram was probably falsely positive: at the time of laparotomy the presumably involved segment appeared normal at inspection and palpation, and no resection was performed.

DISCUSSION

Most of the angiographic changes seen in Crohn's disease are readily explained by the gross and microscopic anatomical features of the disease. The changes may be separated in two categories: (1) those caused by the nonspecific inflammatory reaction in the wall of the gut and (2) those produced by the proliferative and desmoid changes characteristic of Crohn's disease. The nonspecific inflammation produces the hypervascularity of the bowel, seen in angiograms as an abundance of wide (nontapering) arteriae rectae, accumulation of contrast medium in the bowel wall, dilated mural veins, and rapid venous return. The inflammatory changes in Crohn's disease may extend to the mesentery, which explains the occasional occurrence of inflammatory neovasculature adjacent to the wall of the gut. The desmoid and proliferative changes refer to the fibrosis, edema, and thickening of the submucosa and muscularis of the gut, all of which are characteristic of Crohn's disease. Similar changes may involve the adjacent mesentery which will then shrink and increase in thickness. This type of alteration will produce angiographic changes which permit a diagnosis of Crohn's disease.

The course of the arteriae rectae, which are normally given off at acute angles from the marginal artery, may be altered secondary to thickening, shrinking, and deformation of the mesentery. This explains the distortion and right angle branching [7] of the vessels.

The zoning sign, originally described by Herlinger [6], is an angiographic expression of intestinal changes known to occur only in Crohn's disease. The gut has a double-layer appearance with an inner densely staining zone A and a relatively avascular outer zone B, peripherally delineated by the occasionally visible serosal fat line. No clear anatomical explanation of this feature was given by Herlinger, but it appears from transverse sections of injected specimens that zone A corresponds to the thickened and hypervascular mucosa and submucosa and zone B to the hyperplastic but sparsely vascularized muscularis (fig. 9). The zoning sign occurred exclusively in patients with Crohn's disease but was clearly discernible only in 15% of all lesions in our series.

The segmental distribution of the lesions which characteristically, but not always, occurs in Crohn's disease may be difficult to discern in angiograms, but local areas of intense inflammatory reaction were usually well demonstrated (fig. 4).

Various combinations of the nonspecific and specific angiographic changes were seen in cases in which both the desmoid-proliferative and the inflammatory components were marked. Whenever one or both components were less pronounced, the angiographic changes were modified accordingly.

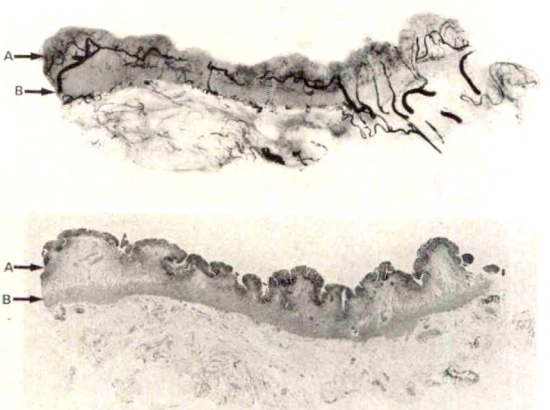


FIG. 9.—Zoning sign in ileal Crohn's disease. Injected specimen (*upper*) and large histologic section (*lower*). Hypervascular and thickened mucosa-submucosa (zone A); sparsely vascularized muscularis (Zone B).

Previous reports on histopathological changes in Crohn's disease have suggested that the pathological changes of the bowel may be caused by or associated with ischemia of the bowel wall [15, 16]. Our findings at in vivo angiography, specimen angiography, and histological studies of excised specimens gave no anatomical support to the concept of ischemia as a causative factor in Crohn's disease [17].

Sources of Error

Erroneous angiographic evaluation of diseased bowel segments as normal may be caused by the following factors. First, in mildly affected segments, vascular changes may be insignificant and only observable at microscopy. Angiograms do not show abnormalities in such areas. Second, there normally is a relative paucity of vasculature in two critical areas of the gut: the terminal 3–5 cm of the distal ileum and the left half of the transverse colon. Moderate inflammatory involvement of these segments may produce only minor vascular alterations (fig. 10).

A falsely positive diagnosis of inflammatory disease may sometimes be suggested by mesenteric angiographic findings in normal subjects. Physiological hyperemia of the bowel is known to be caused by ingestion of foods [18]. Such hyperemia of normal jejunal segments was, in the present series, occasionally seen also in fasting patients. This may tentatively be explained either as a physiological occurrence or as a result of the particular position of the catheter tip. The phenomenon was not associated with other arterial or venous changes. Similarly, wedging of the catheter in the inferior mesenteric artery may result in dense opacification of the bowel wall, suggestive of inflammatory lesions.

Mesenteric angiography, performed a few days after bowel resection for detection of a source of postoperative hemorrhage, revealed marked hyperemia of the bowel wall and rapid arteriovenous transit, probably secondary to the operative trauma to the bowel.

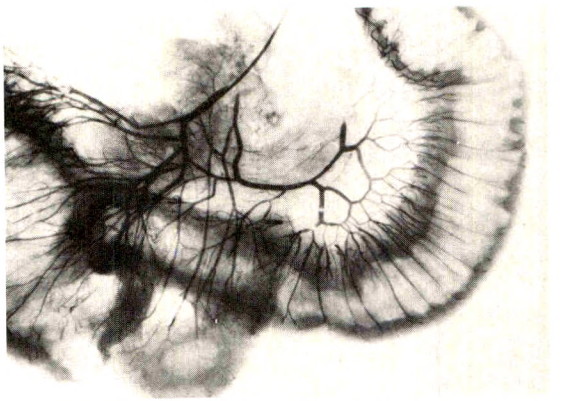


FIG. 10.—Crohn's disease of distal ileum and right hemicolon. Ileal lesions not revealed by angiography. Specimen angiogram showing thickened ileal wall, mildly abnormal arteriae rectae, and paucity of vasculature in the terminal 5 cm of the distal ileum.

Differential Diagnosis

Most of the angiographic changes in Crohn's disease are nonspecific and may be seen in other intestinal diseases as well. In our experience, the only angiographic features unique to Crohn's disease are the zoning sign and the mesenteric Gefässknäuelchen. These distinguishing signs were present in about 30% of the cases of colonic Crohn's disease (table 2). Right angle branching was frequently difficult to evaluate, and thickening of the gut was sometimes seen also in ulcerative colitis. The presence of ileal abnormalities is diagnostically helpful in ileocolic Crohn's disease, but other signs must be resorted to in patients with exclusively colonic involvement. Among eight patients with Crohn's disease confined to the colon, a clearly recognizable zoning sign was present in five, but distinguishing features were absent in three.

The angiographic changes in ulcerative colitis, described by Herlinger [6] and Lunderquist and Lunderquist [8], were largely confirmed in our series of 13 patients with this disease. These changes are nonspecific and do not permit a diagnosis of the disease. Ischemic disease of the colon could angiographically be distinguished

from Crohn's disease only in those cases in which occlusions of larger or smaller arteries were demonstrated.

Neovasculature as well as arteriovenous shunting was frequently observed in carcinoma of the colon, but also here differential diagnostic problems have been reported [1]. Angiography is of diagnostic value in mesenteric carcinomatosis and carcinoid tumors, revealing encasement and obliteration of smaller and larger mesenteric arteries, neovasculature, and, in carcinoid tumors, characteristically radiating vasa recta and mesenteric arcade arteries [1, 19].

Acute terminal ileitis, a segmental enteritis frequently caused by *Yersinia enterocolitica* infection [20], was angiographically indistinguishable from ileal Crohn's disease.

CONCLUSIONS

Angiography provided information on the presence and the location of the lesions in Crohn's disease in more than 90% of the cases. Diagnostic failures were mainly due to paucity of changes in lesions of mild inflammatory activity. Falsely positive diagnoses may be made by angiographers unfamiliar with features in normal angiograms which may mimic inflammatory changes.

The diagnostic value of angiography was limited in unoperated cases of Crohn's disease, but the method did permit assessment of the extent of the lesions, particularly in colonic Crohn's disease. Colitis, caused by Crohn's disease, could be distinguished from ulcerative colitis by angiography in only 30% of the cases. In suspected postoperative recurrence of Crohn's disease, angiography proved to be of definitive clinical value, adding sufficient information to barium studies to influence the treatment of the patients. In ischemic colitis and in malignant conditions of the intestine and the mesentery, angiography regularly demonstrated the presence of lesions; however, their nature could only be diagnosed when distinguishing angiographic signs were present.

Our current experience suggests the following indications for angiography in known or suspected Crohn's disease: (1) preoperatively, to reveal the presence of lesions and to assess the extent of colonic involvement; (2) as an aid in differential diagnosis when other studies have failed to reveal the nature of the lesions; and (3) postoperatively, to distinguish postsurgical alterations of the intestine from recurrent active Crohn's disease.

REFERENCES

1. Boijsen E, Reuter SR: Mesenteric angiography in evaluation of inflammatory and neoplastic disease of the intestine. *Radiology* 87:1037–1042, 1966
2. Brahme F: Mesenteric angiography in regional entero-colitis. *Radiology* 87:1028–1036, 1966
3. Vogeli E: *Die Angiographie bei Dünndarm-und Dickdarmerkrankungen*. Stuttgart, Georg Thieme Verlag, 1974
4. Dombrowskij H, Korb G: The vascular pattern in regional enteritis (morbus Crohn) and its diagnostic significance. *Der Radiologe* 10:17–24, 1970
5. Eriksson U, Fagerberg S, Krause U, Olding L: Angiographic studies in Crohn's disease and ulcerative colitis. *Am J Roentgenol* 110:385–392, 1970
6. Herlinger H: Angiography in Crohn's disease. *Clin Gastroenterol* 1:383–408, 1972
7. Lunderquist A, Lunderquist A, Knutsson H: Angiography in Crohn's disease of the small bowel and colon. *Am J Roentgenol* 101:338–344, 1967
8. Lunderquist A, Lunderquist A: Angiography in ulcerative colitis. *Am J Roentgenol* 99:18–23, 1967
9. Aakhus T: Angiography in acute mechanical obstruction of the small intestine. *Acta Radiol* 306, suppl.: 12–22, 1971
10. Boijsen E: Superior mesenteric angiography, in *Angiography*, edited by Abrams H, Boston, Little, Brown, 1971, pp 1091–1119
11. Boijsen, E, Härtel M: Kontrastmittelpassagezeiten im Versorgungsgebiet der Arteria Mesenterica Superior. *Fortschr Rontgenstr* 118:491–498, 1973
12. Michels NA: *Blood Supply and Anatomy of Upper Abdominal Organs*. Philadelphia, Lippincott, 1955
13. Michels NA, Siddarth P, Kornblith PE, Parke WW: The variant blood supply to the small and large intestine: its importance in regional resections. *J Int Coll Surg* 39:127–170, 1963

14. Theander G: Arteriographic demonstration of stationary arterial waves. *Acta Radiol* 53:417–425, 1968
15. Knutsson H, Lunderquist A, Lunderquist A: Vascular changes in Crohn's disease. *Am J Roentgenol* 103:380–385, 1968
16. Warren S, Sommers SC: Pathology of regional enteritis and ulcerative colitis. *JAMA* 154:189–193, 1954
17. Brahme F, Lindström CG: A comparative radiographic and pathological study of intestinal vaso-architecture in Crohn's disease and ulcerative colitis. *Gut* 11:928–940, 1970
18. Lunderquist A, Lunderquist A, Mommesen N: Angiographic changes during digestion. *Am J Roentgenol* 107:191–197, 1969
19. Boijsen E, Kaude J, Tylén U: Radiologic diagnosis of carcinoid tumors. *Acta Radiol* 15:65–82, 1974
20. Winblad S, Nihlén B, Sternby NH: Yersinia entercolitica in human enteric infections. *Br Med J* 2:1363–1366, 1966

Am J Roentgenol 126:952–956, 1976

HEPATIC ANGIOGRAPHY IN ULCERATIVE COLITIS AND CROHN'S DISEASE

LEIF EKELUND,[1] ANDERS LUNDERQUIST,[1] HANS DENCKER,[2] AND MÅNS ÅKERMAN[3]

ABSTRACT:

Liver angiography was performed in 13 patients with Crohn's disease and three with ulcerative colitis. Of these patients, 13 underwent liver biopsy, and findings were correlated with results of angiography and biochemical tests. Twelve liver biopsies were abnormal, primarily showing fatty infiltration and reactive hepatitis. Thirteen angiographies were abnormal, with widened and tortuous liver arteries being the most common finding. Liver function tests were within normal limits for all but three of the 16 patients, thus correlating poorly with findings of the other tests. These data show that angiography is useful in detecting hepatic abnormality, but evaluation with liver biopsy is necessary to determine the nature of the lesion.

Recently a number of reports concerning hepatobiliary disease associated with ulcerative colitis and Crohn's disease have been published [1–6]. Fatty changes, pericholangitis, hepatic granulomata, amyloidosis, increased fibrosis, and cirrhosis are the most frequently reported lesions. A thorough survey of the hepatic changes in Crohn's disease and ulcerative colitis is given by Perrett et al. [4, 5]. However, to our knowledge no reports on angiographic findings have been published. When patients with Crohn's disease and ulcerative colitis were referred for angiographic evaluation of the extent of the inflammatory lesions, we therefore thought it worthwhile to extend the study to the liver.

MATERIALS AND METHODS

Three patients with ulcerative colitis and 13 with Crohn's disease were examined. Six were males and 10 were females; ages ranged from 16 to 57 years. The diagnosis was verified in all cases by histological examination. The extent and site of the lesions in the 13 patients with Crohn's disease are given in table 1. For the three patients with ulcerative colitis, radiological evidence indicated involvement of the entire colon.

Selective angiography of the celiac axis was performed in all patients, followed by catheterization of the common hepatic artery in four. In another four patients with supplemental arterial supply to the liver from the superior mesenteric artery, this accessory artery was also catheterized. A radiopaque catheter (ID/OD = 1.4/2.2 mm) was used in all examinations, and the contrast medium (Isopaque Coronar, Nyco, Norway) was injected at a rate of 4–12.5 ml/sec, depending on the size of the catheterized artery. In evaluating the angiograms, attention was paid to size of liver and spleen, caliber of common hepatic and splenic artery as well as intrahepatic branches, tortuosity of intrahepatic arteries, density of hepatogram, visualization of veins, and eventual signs of portal hypertension.

A liver biopsy was performed in 13 of the patients. Five patients had a large needle histological biopsy and the other eight a fine needle aspiration biopsy for cytologic analysis.

RESULTS

Hepatic Angiography

The angiographic findings are summarized in table 2. All 13 patients with Crohn's disease had some type of angiographic abnormality. Five had liver enlargement and one had decreased liver size, while three patients had enlarged spleens. In eight patients the diameter of the common hepatic artery was larger than or equal to that of the splenic artery, indicating an increased hepatic flow, and six of these patients also

[1] Department of Diagnostic Radiology, University of Lund, Lund, Sweden.
[2] Department of Surgery, University of Lund, Lund, Sweden.
[3] Department of Pathology, University of Lund, Lund, Sweden.

TABLE 1

EXTENT AND SITE OF LESIONS IN PATIENTS WITH CROHN'S DISEASE

Site	No. Patients
Terminal ileum and caecum	5
Terminal ileum	3
Multiple small intestinal lesions	3
Extensive colonic involvement	2

had widened intrahepatic arteries. Seven patients had increased tortuosity of intrahepatic arteries, while five had nonhomogeneous hepatograms (fig. 1).

In 12 cases the portal and splenic veins appeared normal; in one case these veins were widened. Retrograde flow in the gastroducdenal artery was demonstrated in one case in which widening of the hepatic artery was also present. Stenosis of the celiac artery was found in one case.

Of the patients with ulcerative colitis, one had a normal hepatic angiogram, except for a slight stenosis of the common hepatic artery which could be due to spasm. The second had normal liver size but enlargement of the spleen. Intrahepatic arteries were tortuous and the hepatogram was nonhomogeneous. The hepatic vein was visualized in spite of injection into the

TABLE 2

ANGIOGRAPHIC FINDINGS

Finding	No. Patients
Widening of common hepatic artery	9
Increased tortuosity of intrahepatic arteries	9
Nonhomogenous hepatogram	7
Widening of intrahepatic arteries	7
Hepatomegaly	6
Splenomegaly	5
Visualization of hepatic veins	3
Retrograde flow in gastroduodenal artery	1
Portal hypertension with collateral circulation	1

NOTE.—13 patients have Crohn's disease and three have ulcerative colitis.

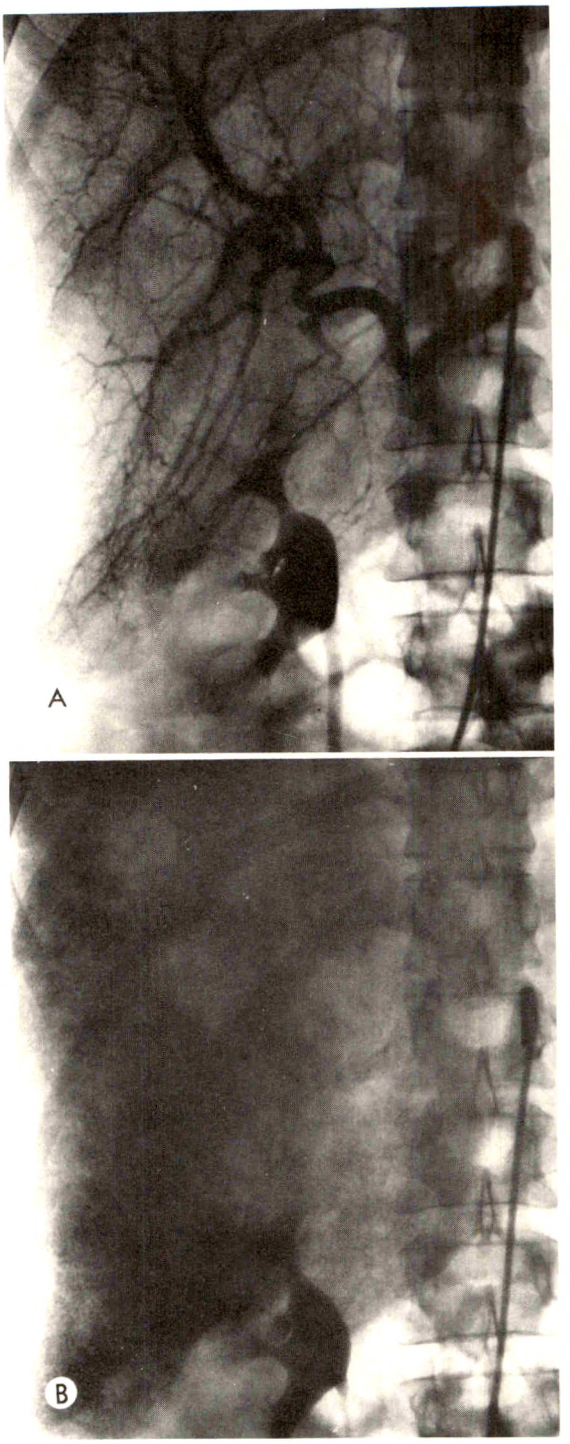


FIG. 1.—Selective common hepatic angiography in 33-year-old woman with Crohn's disease. *A*, Arterial phase; *B*, parenchymal phase. Intrahepatic arteries wide and tortuous; nonhomogeneous hepatogram.

UNIVERSITY COLLEGE LIBRARY

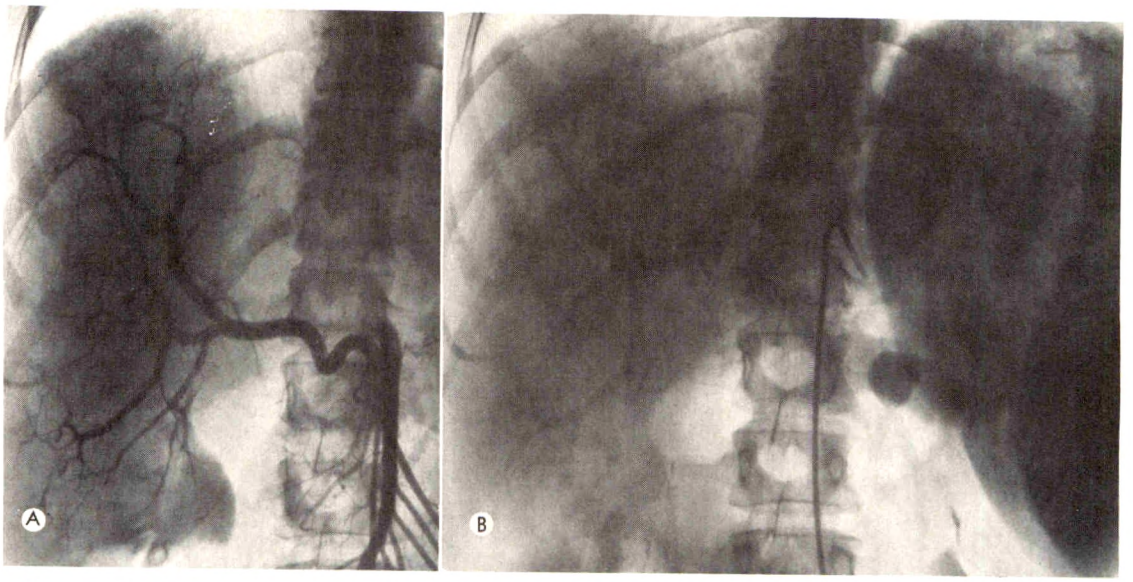


FIG. 2.—Angiography in 32-year-old woman with ulcerative colitis since childhood. *A*, Superior mesenteric angiography showing supplementary artery to enlarged right liver lobe; wide and tortuous intrahepatic arteries. *B*, Celiac angiography, venous phase. Note splenomegaly with collateral circulation over inferior mesenteric vein indicating portal hypertension.

celiac artery in this case. The third patient was a 32-year-old woman who had colitis since she was seven. She developed carcinoma of the transverse colon, and colectomy was performed. At operation portal hypertension was diagnosed, and subsequent angiography demonstrated enlargement of the liver and spleen, widened and tortuous intrahepatic arteries, and signs of portal hypertension (fig. 2).

Liver Function Tests

Liver function studies including serum bilirubin, bromsulftalein retention test (BSP), serum alkaline phosphatase, lactic dehydrogenase (LDH), and serum glutamic oxalacetic transaminase (SGOT) were within normal limits in 13 of the 16 patients. In the other three (two with ulcerative colitis and one with Crohn's disease), all liver function tests were abnormal: serum bilirubin, 1.4–5.5 mg/100 ml; BSP, 20–30%; serum alkaline phosphatase, 30–50 U; LDH, 500–700 U; and SGOT, 100–150 U.

Liver Biopsy

Of the 13 patients who underwent liver biopsy, only one showed a normal liver. In six cases reactive hepatitis with a more or less pronounced fatty infiltration was noted. Five patients had reactive hepatitis without fatty infiltration, and one patient with ulcerative colitis had cirrhosis. Cholangitis or granulomata were not found.

In 10 of 12 patients whose liver biopsies were abnormal, angiography also showed pathological changes (table 3). In one case the biopsy was normal, but angiography showed pathological changes.

DISCUSSION

Eade and Cooke [2] found inflammatory changes of the liver in about 70% of the patients with ulcerative colitis. According to these authors, cirrhosis develops in 2%–3% of cases. Mistilis [3] performed 82 aspiration liver biopsies in 49 patients with ulcerative colitis and found pericholangitis to be the most common change, followed by

TABLE 3

CORRELATION BETWEEN HEPATIC ANGIOGRAPHY, LIVER BIOPSY, AND LIVER FUNCTION TESTS

No. Patients	Angiography		Biopsy			Liver Function Tests	
	+	−	+	−	N.D.	+	−
8	8	...	8	...	...	...	8
2	2	...	2	...	...	2	...
2	2	...	...	...	2	...	2
1	1	...	...	1	...	...	1
1	...	1*	1	...	...	1	...
1	...	1*	1	...	...	...	1
1	...	1	...	...	1	...	1

NOTE.—+ = pathological; − = normal; N.D. = not done.
* Only splenomegaly, otherwise normal.

active chronic hepatitis. Severe fatty liver degeneration was uncommon during life but was the most common postmortem finding. Thorpe et al. [6] described four cases of primary sclerosing cholangitis associated with ulcerative colitis. Similar changes associated with Crohn's disease have been reported as well. Thus Eade et al. [7] found abnormalities in 18 of 20 operative biopsies (90%), with 75% showing more than minor changes. Cirrhosis, amyloidosis, and multiple hepatic granulomata were also found. Perrett et al. [4] studied clinical, hematological, biochemical, bacteriological, histological, and immunological data of 100 patients with Crohn's disease. Of 39 patients who underwent liver biopsy, 19 had pathological specimens, with fatty change and pericholangitis being the most common findings.

The liver changes referred to above can explain the angiographic findings in our patients. All 13 patients with Crohn's disease and two of three with ulcerative colitis had angiographic abnormalities. Increased blood flow with dilated arteries is a common finding in inflammatory lesions. Widening of the common hepatic artery (ratio of the diameters of the common hepatic artery and the splenic artery ≥ 1 [8]) as well as intrahepatic branches, indicating increased blood flow to the liver, may also be present in cases of malignant tumors of the liver [8]. Increased tortuosity of intrahepatic arteries was also a fairly common finding in our material (nine of 16 cases), but the pathologic significance may be uncertain, at least in older age groups [8]. However, 11 of our patients were under the age of 40. Nonhomogeneous hepatograms (seen in seven of our patients) may indicate a scattered distribution of liver changes, which is also reported in histological examinations [2]. This may explain why liver biopsy can fail to demonstrate abnormality. In this study, however, angiographic abnormalities were found at about the same frequency as pathological changes at biopsy. Angiography may thus suggest hepatic abnormality, but further evaluation with liver biopsy is necessary to determine the nature of the lesion.

Regarding the efficiency of laboratory tests, Dyer and Dawson [9] found that 16 of 62 patients (26%) with Crohn's disease had elevated serum level of alkaline phosphatase and 22 of 38 patients (58%) showed impaired excretion of BSP. Eade et al. [7] found a poor correlation between biochemical and histological findings in their patients with Crohn's disease, which is in accordance with our results. In our material only three of 16 patients had abnormal liver function tests.

The genesis of the hepatic changes seen in connection with ulcerative colitis and Crohn's disease is unclear. Portal bacteremia has been found in 24% of patients with ulcerative colitis at the time of colectomy [7], and this may be a triggering factor. One point of theoretical interest is the reported release of bradykinin from inflammatory tissue [10, 11]. This might explain the widening of the hepatic artery and its branches, since bradykinin is known to be a potent vasodilator.

REFERENCES

1. Eade MN, Cooke WT, Williams JA: Liver disease in Crohn's disease. *Scand J Gastroenterol* 6:199–204, 1971
2. Eade MN, Cook WT: Hepatobiliary disease associated with ulcerative colitis. *Postgrad Med* 53:112–118, 1973

3. Mistilis SP: Pericholangitis and ulcerative colitis. *Ann Intern Med* 63:1–16, 1965
4. Perrett AD, Higgins G, Johnston HH, Massarella GR, Truelove SC, Wright R: The liver in Crohn's disease. *Q J Med* 158:187–209, 1971
5. Perrett AD, Higgins G, Johnston HH, Massarella GR, Truelove SC, Wright R: The liver in ulcerative colitis. *Q J Med* 158:211–238, 1971
6. Thorpe MEC, Scheuer PJ, Sherlock S: Primary sclerosering cholangitis in the biliary tract, and ulcerative colitis. *Gut* 8:435–448, 1967
7. Eade MN, Cooke WT, Brooke BN: Liver disease in Crohn's disease. A study of 21 consecutive patients having colectomy. *Ann Intern Med* 74:518–528, 1971
8. Lunderquist A: Arterial segmental supply of the liver. An angiographic study. *Acta Radiol [Suppl]* (Stockh) 272:36, 70, 1967
9. Dyer NH, Dawson AM: The incidence and significance of liver dysfunction in Crohn's disease. *Digestion* 5:317–325, 1972
10. Haverback BJ: Vasoactive substances and the gastrointestinal tract. *Gastroenterology* 53:326–331, 1967
11. Lewis GP: Bradykinin. *Nature* 192:596–599, 1961

Am J Roentgenol 126:957–964, 1976

MEGACYSTIS-MICROCOLON–INTESTINAL HYPOPERISTALSIS SYNDROME: A NEW CAUSE OF INTESTINAL OBSTRUCTION IN THE NEWBORN. REPORT OF RADIOLOGIC FINDINGS IN FIVE NEWBORN GIRLS

W. E. Berdon,[1] D. H. Baker, W. A. Blanc, Britt Gay, T. V. Santulli, and Carmel Donovan

ABSTRACT:

Five newborn girls presented with small intestinal obstruction and microcolon and a giant bladder (megacystis). Organic causes of obstruction were not found, and the gastrointestinal tract failed to function after appropriate diversion. Two died in the postoperative period, two lived several months on central venous hyperalimentation, and one died at 34 months of age following chronic though intermittent hyperalimentation. Pathologic studies showed an abundance of ganglion cells in both dilated and narrowed areas of intestine; the combined small bowel–colon length was one-third of normal in the absence of an evident obstructive or vascular insult. The five patients represent the most severe manifestation of defective intestinal peristalsis in a larger group of distended newborns in whom organic gastrointestinal obstruction is not found. Treatment with central venous hyperalimentation may sustain life, and some patients eventually recover gastrointestinal function. The hypoperistalsis is largely refractory to pharmacologic treatment; its cause is unknown.

INTRODUCTION

Five newborn girls presented with marked abdominal distention and bile vomiting. All were explored for intestinal obstruction; dilated small bowel with a distal microcolon was found in the absence of organic obstruction. The bulk of the abdominal distension was due to a giant bladder (megacystis) in the absence of distal genitourinary obstruction. Those who survived the immediate postoperative period never developed adequate intestinal function, surviving for varying periods of time on hyperalimentation. All had ganglion cells present in both the dilated and narrowed segments of bowel.

CASE REPORTS

Case 1

Patient L. B. was a term female born on August 26, 1961, with massive abdominal distension. There was no history of hydramnios, and she was explored with the preoperative diagnosis of intestinal obstruction. When the abdomen was opened, it was filled with a huge cystic mass rising out of the pelvis. The small intestine was dilated, and the colon was described as a microbowel 4–5 mm in diameter. Organic stenosis was not found; mesenteric fixation of the midgut was lacking, but there was no volvulus. The "cystic mass" was the bladder, which contained 250 cm^3 of urine; the ureters were dilated and tortuous. She died on the first postoperative day following a suprapubic cystostomy and gastrostomy and sigmoid biopsy. The biopsy showed ganglion cells in abundance.

Case 2

C. B., the sibling of case 1, was a term female born on July 24, 1962, and was also noted to have massive abdominal distension in the ab-

Presented at the annual meeting of the Society for Pediatric Radiology, Atlanta, Georgia, October 1975.

[1] Department of Radiology, Babies Hospital, Columbia-Presbyterian Medical Center, New York, New York 10032. Address reprint requests to W. E. Berdon, Department of Radiology, Babies Hospital, 167th Street and Broadway, New York, New York 10032.

sence of a history of hydramnios. Plain films (fig. 1*A*) and a contrast enema (fig. 1*B*) showed a malrotated microcolon and dilated air-filled small bowel loops displaced by a huge abdominal mass of soft tissue. This proved to be the bladder, which contained 370 cm^3 of urine. She also had malfixation of the midgut without volvulus. The dilated small bowel led to a tiny distal ileum and microcolon without organic obstruction. The genitourinary tract showed massive hydronephrosis (fig. 1*C*) and a thick-walled, enlarged bladder in the absence of distal obstruction. She also died in the immediate postoperative period from infection. The autopsy revealed ganglion cells throughout the bowel.

Comment. At the time these two siblings seemed to have a partial expression of the prune belly syndrome, with dilated ureters, giant bladders, and stretched abdominal walls. They did not survive long enough for the problem of intestinal peristalsis to become manifest.

Case 3

J. C. was a term female born on December 30, 1971, with marked abdominal distension; bile vomiting soon developed. She too was explored for intestinal obstruction after preliminary plain films (figs. 2*A* and 2*B*) showed dilated loops of small bowel; however, the bulk of the abdominal distension was not due to these loops. When the abdomen was opened, it was found to be virtually filled by a huge cystic mass. The abdomen was closed and the patient was transferred to Babies Hospital, where a contrast enema showed a displaced microcolon (fig. 2*C*). Repeat laparotomy showed the mass to be the bladder, which contained several hundred cubic centimeters of urine. A suprapubic cystostomy and ileostomy were performed. She too had a dilated small bowel and tiny colon; anomalous fixation of the midgut was present in the absence of volvulus. Examination of the urinary tract showed the bladder to be thick walled and the ureters to be dilated (fig. 2*D*). The patient required continuous intravenous feedings, and finally hyperalimentation had to be instituted. Attempts to feed her through the gastrostomy were never successful, and ileostomy drainage was minimal. Contrast agents were injected into the stomach which showed it to empty into the duodenum and upper jejunum followed by retrograde passage of the contrast into the stomach. When contrast was injected into the ileostomy stoma, it flowed in retrograde fashion to the stomach. The patient survived until May 13, 1972. Ganglion cells were present at autopsy in both the dilated and narrowed segments of bowel.

Comment. This was our first such patient to survive the immediate postoperative period; it became apparent that the gastrointestinal tract was unable to achieve effective peristaltic activity. Repeated operations and revisions of anastomoses were undertaken as well as trials of various peristaltic stimulants. None of these measures resulted in a functioning intestinal tract.

Case 4

N. B. was a term female born on July 19, 1974, with massive abdominal distension (fig. 3*A*). Preoperative radiographic studies showed the presence of a huge bladder as the main source of the mass, with small bowel dilatation and a microcolon as well (fig. 3*B*). Surgical exploration revealed 35 cm of dilated small bowel with a contracted distal small bowel of 20 cm. (Total small bowel length was 55 cm compared to a normal length of 240 cm.) A malfixed midgut and microcolon were also observed. No organic obstruction was found, and volvulus was absent. The bladder was thick walled with tortuous ureters. Suprapubic cystostomy and ileostomy were performed. Ganglion cells were present in the rectal biopsy. The baby was transferred to Babies Hospital for hyperalimentation treatment.

Despite a variety of formulas and peristaltic stimulants, ileostomy drainage was minimal and gastrostomy feedings could not be maintained. Intravenous pyelogram showed return of the upper tracts to normal following bladder drainage (fig. 3*C*). Again, as in case 3, contrast injection into the stomach (fig. 3*D*) showed filling of the duodenum and proximal jejunum; then the contrast material would back up into the stomach. Contrast injected into the ileostomy stoma would pass in retrograde fashion into the stomach. Death finally occurred at 6 months of age.

Case 5

S. D. was a term female born on March 6, 1973, and immediately noted to be distended. She was examined at the Henrietta Eggleston Hospital in Atlanta for suspected ileal atresia. As in the previous cases, the bulk of the abdominal distension was due to a huge bladder

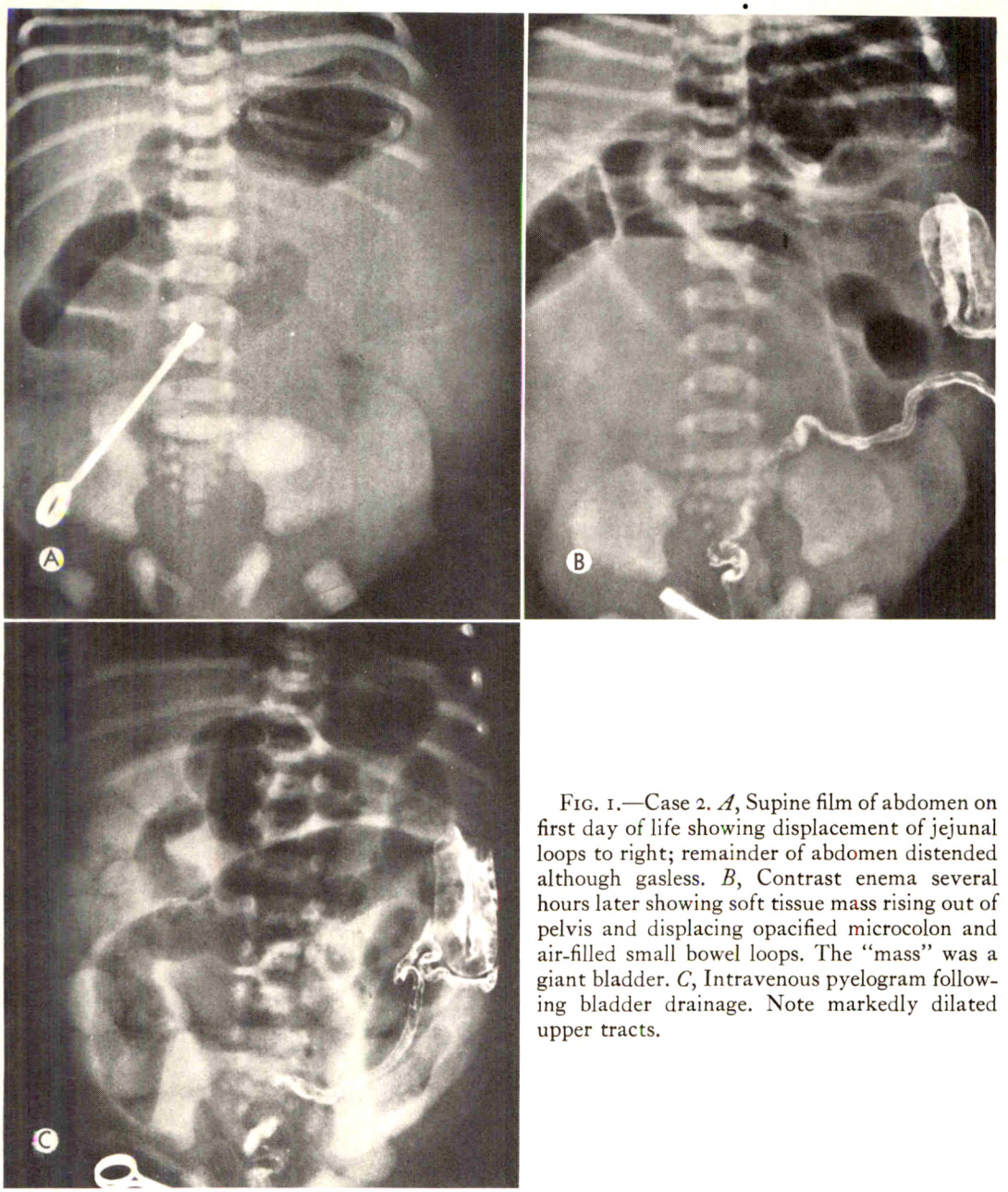


FIG. 1.—Case 2. *A*, Supine film of abdomen on first day of life showing displacement of jejunal loops to right; remainder of abdomen distended although gasless. *B*, Contrast enema several hours later showing soft tissue mass rising out of pelvis and displacing opacified microcolon and air-filled small bowel loops. The "mass" was a giant bladder. *C*, Intravenous pyelogram following bladder drainage. Note markedly dilated upper tracts.

(fig. 4*A*) associated with tortuous ureters. The small bowel was dilated and malfixed, but there was no volvulus and the colon was of a tiny caliber. Ganglion cells were present in the rectal and other biopsies. The intravenous pyelogram (after bladder drainage) showed normal upper tracts (fig. 4*B*). She has been continuously hospitalized, both in Georgia and in Babies Hospital in New York for hyperalimentation treatment, formula changes, and pharmacological trials in an attempt to promote intestinal peristalsis.

She has never achieved a functional gastrointestinal tract for more than a few days at a time. At $2\frac{1}{2}$ years of age she is a bright girl of normal intelligence and rides a bicycle through the hospital corridors while attached to a hyperalimentation pump. Parasympathomimetic agents as well as adrenergic blockade regimens have been tried without success.

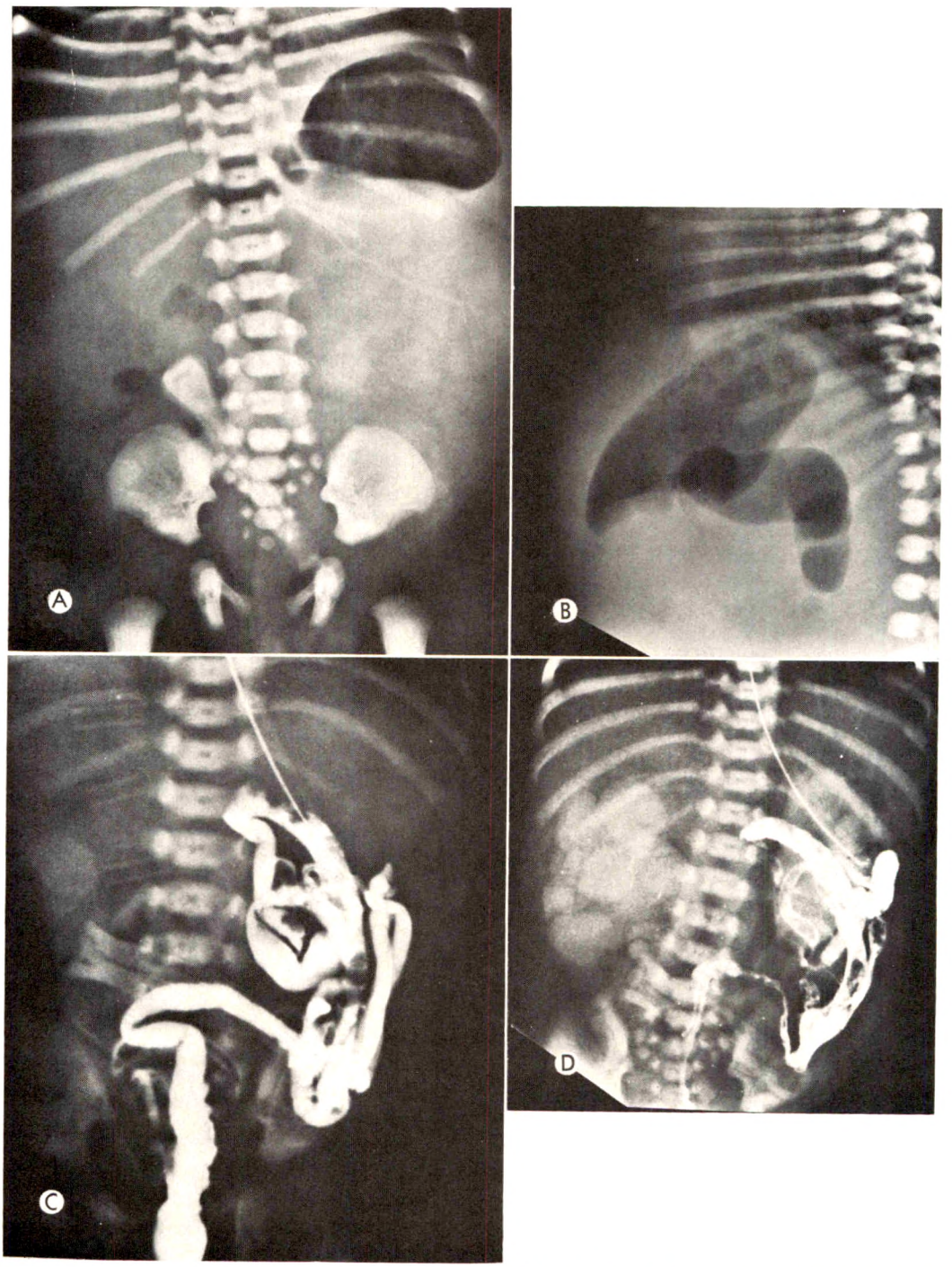


FIG. 2.—Case 3. *A*, Supine film of abdomen on first day of life showing distended gasless abdomen save for stomach. Soft tissue mass indents inferior gastric wall. *B*, Lateral plain film showing cutoff of gas distal to dilated duodenum. *C*, Contrast enema showing malrotation of microcolon. *D*, Intravenous pyelogram following bladder drainage. Note dilated upper tracts.

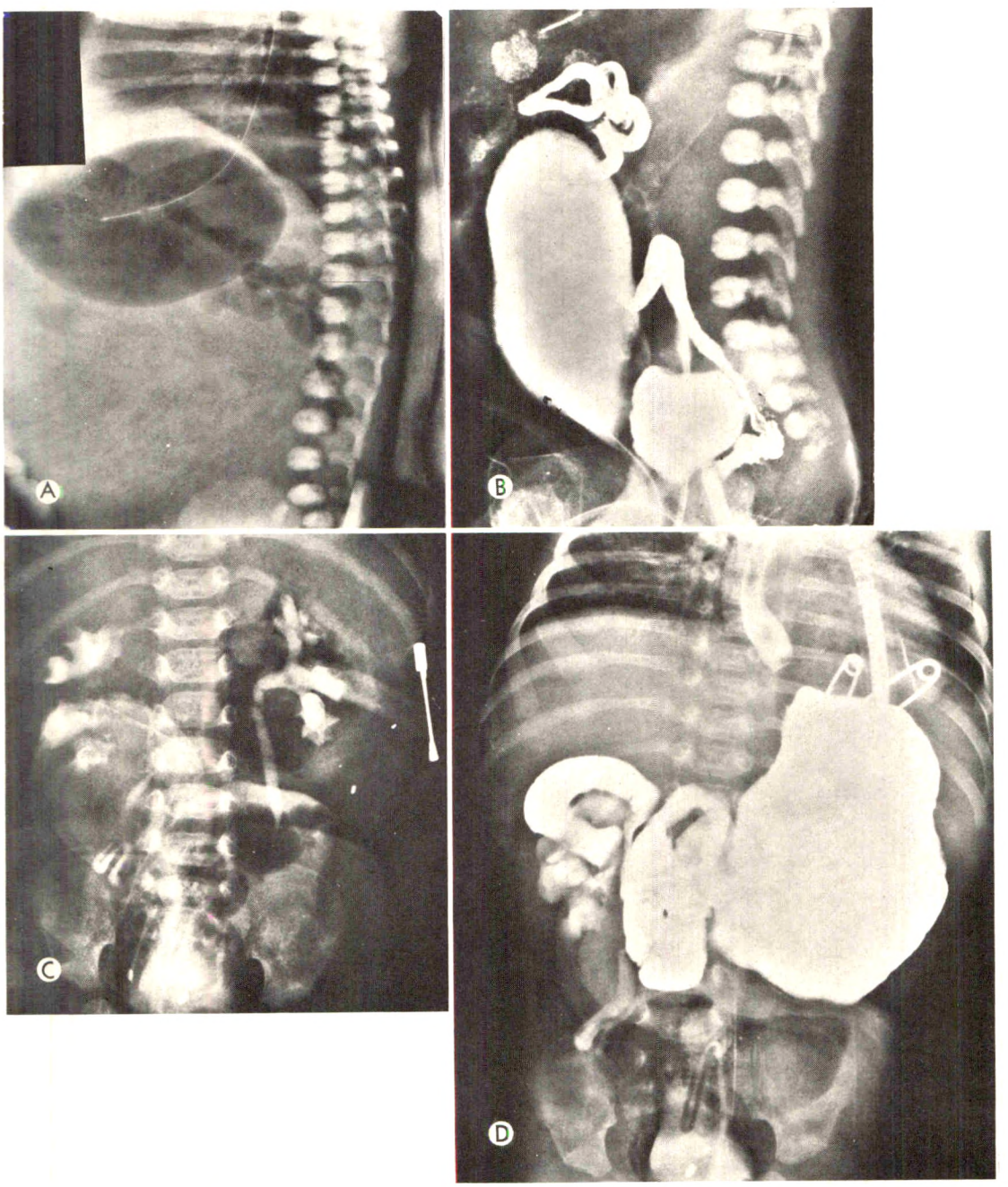


FIG. 3.—Case 4. *A*, Lateral film on first day of life showing stomach and proximal small bowel displaced by soft tissue mass that fills abdomen. *B*, Cystogram showing bladder to rise above umbilicus. Vagina and microcolon also opacified; injections were made separately into each structure. *C*, Intravenous pyelogram after several weeks of bladder drainage. Normal upper tracts. *D*, Upper GI series following contrast injection into gastrostomy showing filling of duodenum and proximal jejunem. They then emptied back into stomach.

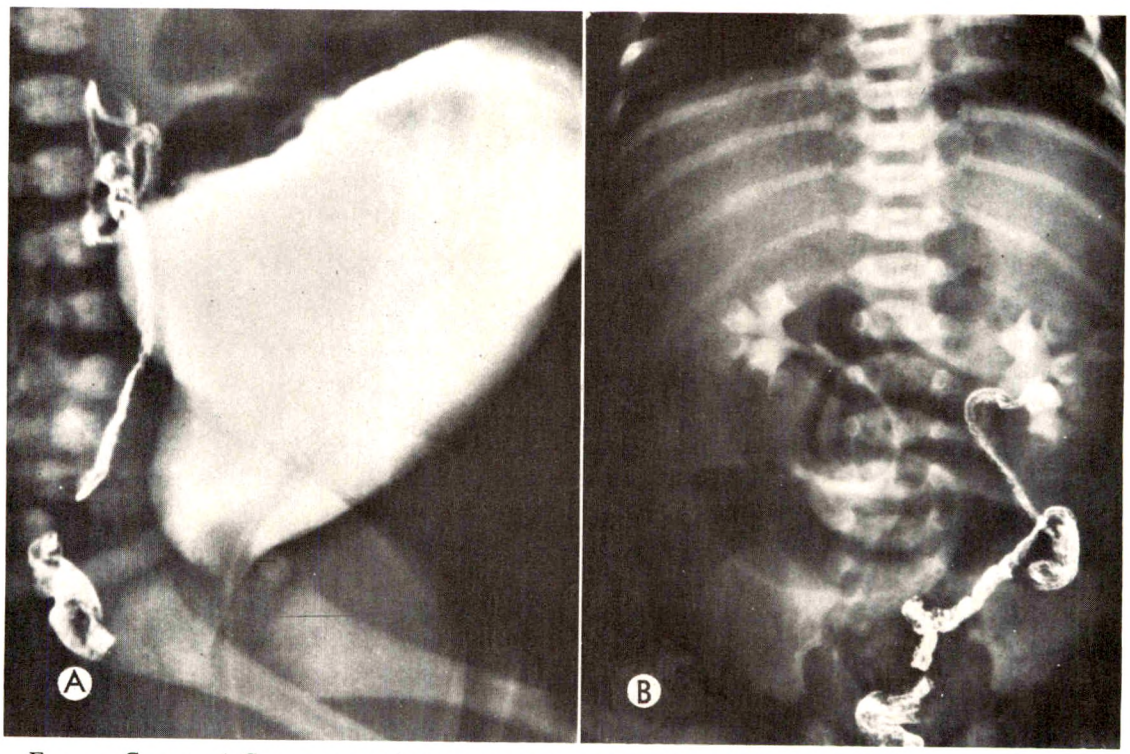


FIG. 4.—Case 5. *A*, Cystogram and contrast enema on first day. Microcolon displaced by huge bladder. *B*, Intravenous pyelogram after bladder drainage. Normal upper tracts; residual contrast persists in colon.

Following submission of this manuscript in the fall of 1975, it was learned that the patient died in Atlanta at approximately 34 months of age; there was no autopsy.

PATHOLOGIC FINDINGS

Either biopsies or autopsies were performed on the five patients in an attempt to determine the cause of their distension and failure of normal peristaltic activity (table 1). All had dramatic shortening of the total intestinal length to one-third of normal. This was in the absence of organic obstruction or signs of a prenatal vascular catastrophe of any type. All had abdominal wall musculature, although in case 1 it was quite thin. All of the patients not only had ganglion cells but seemed to have an excess of both ganglion cells and nerve fibers. The distribution of colon ganglion cells may reflect an artifact of disuse atrophy and empty lumen. The ganglion cells appear mature. This seeming "hyperganglionosis" was focal in some of the pathological sections and widespread at other sites.

Pressure exerted by the huge bladders filled with several hundred cubic centimeters of urine might be expected to interfere with fetal swallowing sufficiently to produce hydramnios. Such was not the case in any of the patients. Neither was there evidence of oligohydramnios. (None of them had the clinical features of low-set ears, club feet, Potter's facies, or hypoplastic lungs which are seen in patients with failure of normal fetal urination.) It is possible that a delicate balance existed in these patients between interference of swallowing

TABLE 1

PATHOLOGICAL FINDINGS

Case No.	Combined Small Bowel—Colon Length at Autopsy (Cm)	Organic Stenosis	Ganglion Cells	Nerve Fibers	Maturity of Ganglion Cells
1.....	N.D.	None	Abundant in colon biopsy	Increased	Normal
2.....	105	None, although terminal ileum narrow	Hyper throughout	Increased	Normal
3.....	110	None	Irregular pattern, focal hyper and focal normal	Increased	Normal
4.....	111	None	Hyper in colon	Increased	Normal
5.....	N.D.	...	Abundant in colon biopsy	Increased	Normal

NOTE.—Average newborn small bowel length = 240 cm; average colon length = 60–90 cm. N.D. = not done.

of amnion (hydramnios) and fetal retention of urine (oligohydramnios) so that pulmonary development was not significantly affected.

DISCUSSION

In recent years with the application of central venous hyperalimentation to newborns with complicated problems of intestinal obstruction, a group of patients have emerged who have become "prisoners" of hyperalimentation, despite seemingly adequate surgery for their intestinal obstruction. Some of the patients (both male and female) present with colon distension and are explored with a preoperative suspicion of Hirschsprung's disease, only to show ganglion cells on their rectal biopsy as well as an absence of an organic site of obstruction. In others there is massive small bowel distension so that the patients are explored with the preoperative diagnosis of ileal atresia. Again, as in our cases, organic obstruction is absent and biopsy shows ganglion cells to be present. Some patients eventually recover gastrointestinal function, while others survive for varying periods of time on hyperalimentation.

Thus, the "megacystis-microcolon" syndrome, as such, is only a part of the major problem of intestinal hypoperistalsis in the absence of aganglionosis. The cause is unknown. Familial incidence was noted in cases 1 and 2. (When this report was presented at the 1975 meeting of the Society for Pediatric Radiology, several members responded that they have seen similar cases.) In its full-blown form it appears to represent a new syndrome of "functional" intestinal obstruction; it has possibly been confused in the past with a form of the prune belly syndrome. Though the bladder is the main source of the abdominal mass, the urinary tract function does return after appropriate urinary diversion; in the gastrointestinal tract, appropriate diversion fails to work.

These patients have the most severe manifestation of intestinal hypoperistalsis among a wider group of newborns [1–4]. The mildest manifestation of hypoperistalsis in newborns is probably among those with the "small left colon" syndrome (i.e., meconium plug syndrome) [2, 3], where one or more enemas usually succeeds in establishing normal intestinal function. The strikingly high incidence of maternal diabetes seen in the "small left colon" syndrome was not noted in any of the patients with the megacystis-microcolon syndrome. None had pathologic or other signs of cystic fibrosis [5].

Biopsies from some premature infants with marked small bowel distension have shown "immature" ganglion cells [3]. These were not present in any of our cases. The abnormality was not in the maturation of the ganglion cells or their absence, but rather in a seeming increase in number of normal-appearing ganglion cells and nerve

fibers. Chemical studies of ganglion cell function have not been performed.

Radiologic Findings and Differential Diagnosis

Calcification was not present in any of the five cases; all showed displacement of stomach and small bowel by the huge bladder that filled the abdomen (figs. 1*A*, 2*A*, 2*B*, and 3*A*). Four of the five patients had contrast enemas since intestinal obstruction was diagnosed from distension and bile vomiting; all showed a displaced microcolon (figs. 1*B*, 2*C*, 3*B*, and 4*B*) [6]. The true genitourinary nature of the mass was revealed only when the bladder was either drained or opacified (figs. 3*B* and 4*A*). Intravenous pyelograms showed varying degrees of hydronephrosis (figs. 1*C* and 2*D*) in part related to the time interval between bladder drainage and the performance of the intravenous pyelogram. Vesicoureteral reflux was absent. The upper tracts of cases 4 and 5 returned to normal despite repeated attacks of urinary tract infection (fig. 3*C* and 4*B*).

The major problem in differential diagnosis was to distinguish these cases from patients with a *prenatal volvulus* where the volvulated loops present as a water density mass, with microcolon distal and dilated stomach and duodenum proximal [5]. (We had previously noted this "pseudocyst" in a report on the gastrointestinal findings in meconium ileus, since more than half of the patients with the prenatal matted volvulus had underlying cystic fibrosis.) None of the five girls in this report had pathologic or familial evidence of cystic fibrosis.

Obviously, more confusion could occur were the giant bladder to be studied as an "abdominal mass." To avoid such confusion, radiologists confronted with plain films, as in our cases, should have such patients catheterized before any contrast studies of either the urinary or intestinal tract are contemplated. The megacystis component of the syndrome will be apparent after bladder drainage, and the microcolon component will be obvious from the contrast enema. Alternatively ultrasonography could be done to delineate the size of the bladder.

The postoperative radiographic studies in these patients consisted of repeated attempts to find the site of obstruction that could account for the failure of the intestinal tract to function. Contrast medium did indeed leave the stomach and fill the dilated duodenum and jejunum, leading to repeated operations in search of adhesions or jejunal stenosis. Only with time did it become apparent that the "obstruction" in these patients was functional.

All of the cases have succumbed, either in the immediate postoperative period or after months or even years of hyperalimentation. Proper treatment of this syndrome will have to await clarification of its cause.

REFERENCES

1. Cremin BJ: Functional intestinal obstruction in premature infants. *Pediatr Radiol* 1:109–112, 1973
2. Davis WS, Allen RP, Favara BE, Slovis TL: Neonatal small left colon syndrome. *Am J Roentgenol* 120:322–329, 1974
3. Le Quesne GW, Reilly BJ: Functional immaturity of the large bowel in the newborn infant. *Radiol Clin North Am* 13:331–342, 1975
4. Sieber, WK, Girdany BR: Functional intestinal obstruction in newborn infants with morphologically normal gastrointestinal tracts. *Surgery* 53: 357–361, 1963
5. Leonidas JC, Berdon WE, Baker DH, Santulli TV: Meconium ileus and its complications. *Am J Roentgenol* 108:598–609, 1970
6. Berdon WE, Baker DH, Santulli TV, Amoury RA, Blanc WA: Microcolon in newborn infants with intestinal obstruction. *Radiology* 90:878–885, 1968

Am J Roentgenol 126:965–969, 1976

MULTIPLE "BULL'S-EYE" LESIONS IN GASTRIC LYMPHOMA

N. Reed Dunnick,[1] George S. Harell, and Bruce R. Parker

ABSTRACT:

Three adolescent patients with multiple gastric target lesions and gastric lymphoma are reported. Each had either histiocytic or poorly differentiated lymphoma. The literature was reviewed to ascertain whether multiple gastric lymphomatous target lesions were confined to adolescent patients or to patients with a particular histologic subtype. Review of 119 cases in the literature did not support either hypothesis.

INTRODUCTION

Multiple "target" or "bull's-eye" lesions of the stomach, consisting of large, centrally located collections of barium within ulcerated masses, are an infrequent roentgenographic finding on upper gastrointestinal barium examinations in patients with lymphoma. Three adolescent patients with multiple gastric bull's-eye lesions caused by non-Hodgkin's lymphoma have been treated at Stanford University Hospital Medical Center. Because all three patients were adolescents, a literature search was performed to determine whether bull's-eye lesions are peculiar to the adolescent age group or to a particular histologic subgroup of non-Hodgkin's lymphoma.

CASE REPORTS

Case 1

A 17-year-old white female with recurrent abdominal pain and vomiting was admitted to Stanford University Hospital in May 1968. An elevated serum amylase suggested pancreatitis, and conservative therapy was employed until June 2, 1968, when she passed a tarry stool. An upper gastrointestinal series demonstrated bull's eye lesions in the stomach (fig. 1). The masses varied in size, as did the ulcers within them. On June 5, 1968, she underwent exploratory laparotomy where tumor was found involving the stomach, pancreas, right ovary, and fallopian tube. The gastric and pelvic tumor masses were removed. Histologic examination revealed undifferentiated Burkitt type lymphoma. The patient was referred to the National Institutes of Health for further evaluation and therapy. Despite an initial response to chemotherapeutic agents including cyclophosphamide, methotrexate, vincristine, and prednisone, the patient expired 8 months after initial diagnosis.

Case 2

A 16-year-old white male was hospitalized in November 1974 with recurrent abdominal pain, vomiting, and guaiac-positive stools. A left cervical node biopsy showed lymphoma. On November 21, 1974, he was transferred to Stanford University Hospital where an upper gastrointestinal and small bowel series demonstrated multiple gastric bull's-eye lesions (figs. 2*A* and 2*B*). The jejunum and ileum contained multiple endoexcentric masses and intraluminal masses, but no bull's-eye lesions were demonstrated (figs. 2*C* and 2*D*). Paraortic lymphadenopathy was demonstrated by lymphography and excretory urography. Barium enema was normal. Repeat biopsy of the left cervical mass revealed undifferentiated non-Hodgkin's lymphoma. After initial therapy with intravenous cyclophosphamide, he returned to the referring institution for further treatment. In March 1975 he developed a local recurrence of tumor in the left neck, and in May 1975 intestinal perforation occurred which was presumed secondary to the intestinal involvement.

Case 3

A 16-year-old white male presented with a 2-month history of fever, cough, night sweats,

[1] All authors: Department of Radiology, Diagnostic Division, Stanford University School of Medicine, Stanford, California 94305. Address reprint requests to G. S. Harell.

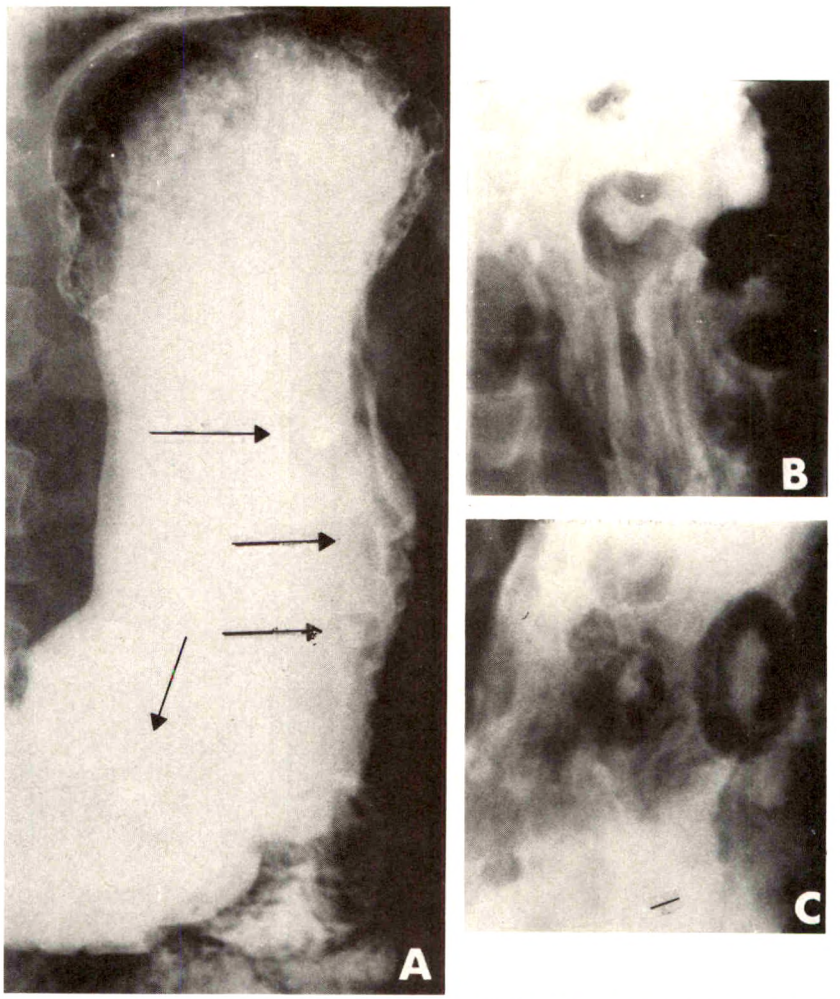


FIG. 1.—Case 1: 17-year-old Caucasian female with undifferentiated gastric lymphoma (Burkitt type). Lymphoma also involved the pancreas, right ovary, and right fallopian tube. *A*, Multiple gastric bull's-eye lesions (*arrows*); *B and C*, detail utilizing compression showing the different size tumor masses and ulcers.

and chest and shoulder pain on August 21, 1972. A chest radiograph showed a large anterior mediastinal mass and a smaller left hilar mass. On September 14, 1972, he was transferred to Stanford University Hospital where a chest radiograph revealed pulmonary as well as mediastinal involvement. Histologic examination of tumor obtained at thoractomy revealed diffuse histiocytic lymphoma. Following an episode of nausea and vomiting, an upper gastrointestinal series disclosed multiple bull's-eye lesions of varying size in the stomach and in the duodenum (fig. 3). A bipedal lymphogram showed enlarged para-aortic lymph nodes consistent with lymphoma. The pulmonary and mediastinal lesions responded to radiation therapy, and chemotherapy was also initiated. His stool guaiacs were negative at discharge on October 10, 1972, after being positive throughout most of the hospitalization. However, progressive pulmonary and intracranial disease resulted in death 5 months after diagnosis. Permission for postmortem examination was denied.

DISCUSSION

The differential diagnosis of multiple bull's-eye lesions in the gastrointestinal tract includes metastatic tumor, especially melanosarcoma and lymphoma, and far less frequently Kaposi's sarcoma, carcinoid tu-

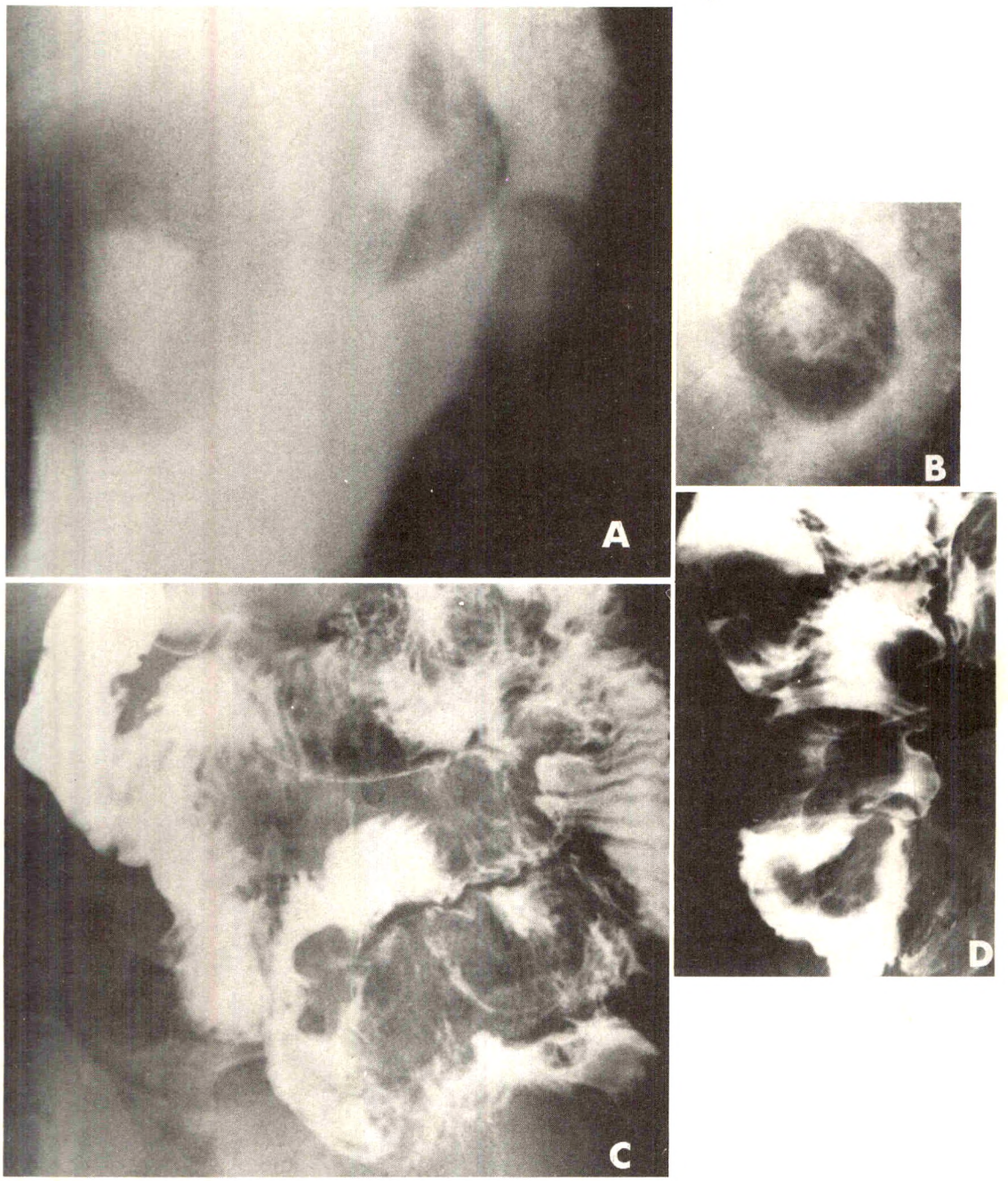


FIG. 2.—Case 2: 16-year-old Caucasian male with diffuse histiocytic lymphoma involving stomach, small bowel, paraaortic lymph nodes, mediastinum, left hilus, and pulmonary parenchyma. *A*, Varying size bull's-eye lesions in distal body; *B*, detail utilizing compression; *C*, small bowel demonstrating intraluminal and endoexocentric masses; *D*, detail. No bull's-eye lesions were seen in the small intestines.

mors, and multiple ulcerated spindle cell tumors [1–5]. Multiple target lesions of the same size limited to one or several segments of the small bowel are reported to suggest lymphoma [1]. In the stomach, the target lesions of lymphoma may vary in size (figs. 1–3). Multiple bull's-eye lesions of the small bowel of varying size are more commonly

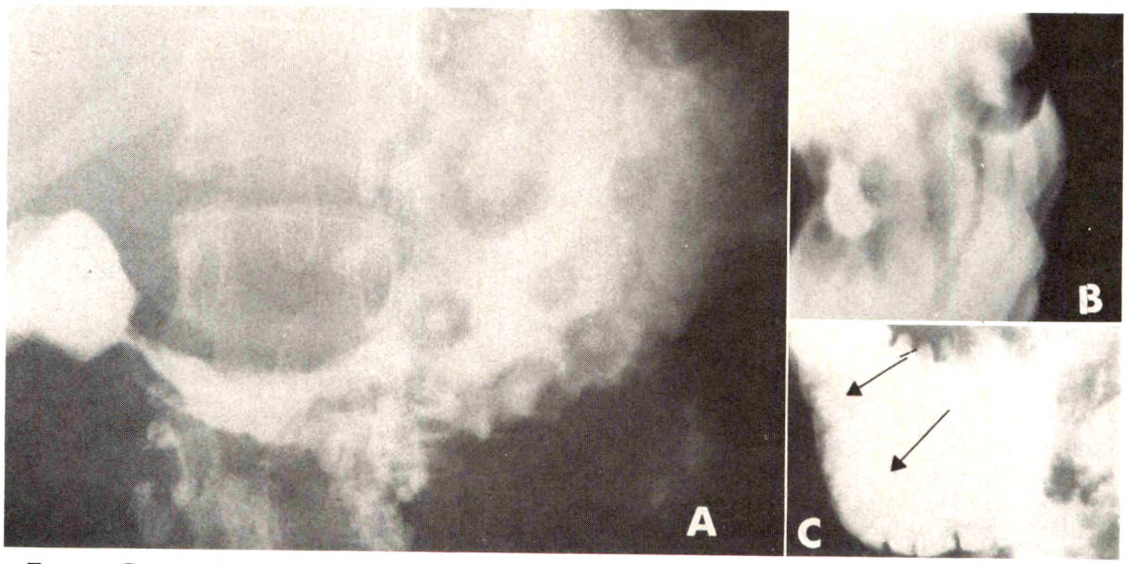


FIG. 3.—Case 3: 16-year-old Caucasian male with stage 4B undifferentiated, non-Hodgkin's lymphoma involving the stomach and small bowel. *A*, Multiple gastric target lesions; most are the same size but one in the high body near the lesser curve is considerably larger. *B*, Detail of two similar size target lesions. *C*, Multiple target lesions of the distal second part of the duodenum (*arrows*).

found in metastatic melanosarcoma [1]. Other causes of bull's-eye lesions are reported to include eosinophilic granuloma, aberrant pancreas, and adenocarcinoma [1]. Our three patients with multiple gastric bull's-eye lesions secondary to lymphoma were adolescents with a poorly differentiated or histiocytic lymphoma (Rappaport classification [6]). Each had abdominal pain, nausea, and vomiting. All had disease at other sites and were stage 4B. Two of the three (cases 2 and 3) had lymphoma involving the small bowel as well as the stomach. Case 2 had multiple small bowel endoexcentric and polypoid intraluminal masses (figs. 2*C* and 2*D*). In case 3, multiple target lesions were present in the duodenum (fig. 3*C*).

A review of 119 cases in the literature of well-documented gastric lymphoma dis-

TABLE 1

OCCURRENCE OF MULTIPLE BULL'S EYE LESIONS

Reference	Classification	Age	Sex
Wang and Peterson [7]	"Hodgkin's disease"	...	...
Fuchs et al. [8]	Lymphosarcoma	22	M
Keller and Hering [9]	Reticulum cell sarcoma*	...	...
	Reticuloblastoma*	...	...
Ohtake et al. [10]	Reticulum cell sarcoma*	35	M
	Reticulum cell sarcoma*	47	M
Present report	Undifferentiated lymphoma, Burkitt type	17	F
	Undifferentiated lymphoma	16	M
	Histiocytic lymphoma	16	M

* Histiocytic lymphoma in Rappaport classification [6].

closed six cases of clearly demonstrated multiple bull's-eye lesions (table 1) [7–10]. Including our three cases, the age range was 16–47 years; five of the patients were male and one female. Using the Rappaport classification [6], the histologic diagnosis in five patients would be considered histiocytic lymphoma. Two patients had poorly differentiated lymphoma, one of which was Burkitt type. The number of cases of multiple lymphomatous gastric bull's-eye lesions is too few for statistical evaluation, and the age distribution of the patients and the histologic subtypes found do not as yet suggest a definite trend toward a particular age group nor a particular subtype of non-Hodgkin's lymphoma.

REFERENCES

1. Cavanagh RC, Buchignani JS, Rulon, DB: Metastatic melanoma of the small intestine. *Radiology* 101:195–200, 1971
2. Dodds WJ, Goldberg, HI, Margulis, AR: Leiomyosarcoma of the small intestine. *Am J Roentgenol* 107:142–149, 1969
3. Marshak RH, Lindner AE: *Radiology of the Small Intestine*. Philadelphia, Saunders, 1970
4. Pomerantz H, Margolin HN: Metastases to the gastrointestinal tract from malignant melanoma. *Am J Roentgenol* 88:112–117, 1972
5. Richey LE, Cooley RN: Kaposi's sarcoma: the radiographic manifestations of involvement of the stomach. *Gastroenterology* 44:195–198, 1973
6. Rappaport H: Tumors of the hematopoietic system, in *Atlas of Tumor Pathology*, sec 3, fasc. 8, Washington, D.C., Government Printing Office, 1966
7. Wang CC, Peterson JA: Malignant lymphoma of the gastrointestinal tract: roentgenographic considerations. *Acta Radiol* 46:523–532, 1956
8. Fuchs H, Heckhausen H, Hartwich G, Sturm G, Fritsch, EV: Rontgendiagnostik der Magenlymphome. *Med Klin* 67:1074–1079, 1972
9. Keller VH, Hering K: Retikuloblastomatosen des Magens. *Fortschr Röntgenstr* 118:16–22, 1973
10. Ohtake H, Matsuoka S, Oikawa M, Suzuki T, Syo T, Toda H, Sugiyama T: The role of diagnostic radiology including lymphography in malignant lymphomas. *Aust Radiol* 16:303–308, 1972

Am J Roentgenol 126:970–973, 1976

VASCULAR IMPRESSIONS OF THE GUT SECONDARY TO CHRONIC VASCULAR OCCLUSIVE DISEASE

LESLIE MENUCK[1] AND MARC COEL[1]

ABSTRACT:

Clinical diagnosis of chronic vascular occlusive disease is difficult since symptoms are often vague. The presence of discrete extrinsic contoural defects along the medial aspect of the descending duodenum or proximal small bowel is a useful diagnostic feature in such patients. Five of eight patients with chronic vascular occlusion who had examination of the upper gastrointestinal tract demonstrated this finding. If presented with this radiographic observation on barium study, visceral arteriography should then be considered.

The clinical diagnosis of chronic vascular occlusive disease involving the gut is difficult since the clinical symptoms and findings are often vague and nonspecific. These patients often will have multiple exams of the upper gastrointestinal tract and small bowel before the diagnosis is finally made by arteriography or at surgery. The presence of contoural defects of the gut from large collateral vessels may be seen on barium study early before irreversible ischemic changes to the bowel occur.

Patients were selected from the Veterans Administration Hospital in San Diego who had visceral arteriograms which demonstrated occlusion of one of the three major visceral vessels. Cases which were felt to be acute were excluded. Of the 12 patients with chronic vascular occlusion, eight had barium studies of the upper gastrointestinal tract. Five of the eight patients demonstrated definite contoural defects related to large collaterals. One study was equivocal and two were normal.

CASE REPORTS

Case 1

A 52-year-old man presented with a several-month history of nonspecific epigastric pain which was partially relieved by food and antacids. A barium exam of the upper gastrointestinal tract demonstrated a small prepyloric ulcer and two small discrete extrinsic impressions on the medial portion of the duodenal sweep. Endoscopy confirmed the prepyloric ulcer and suggested two small extrinsic filling defects along the medial aspect of the proximal descending duodenum and at the junction of the second and third portions of the duodenum. The patient was treated conservatively, but because of persistent discomfort and the clinical question of carcinoma of the pancreas, visceral angiography was performed. Arteriography demonstrated occlusion of the celiac axis with retrograde filling of the celiac axis from the superior mesenteric artery through very large collaterals in the pancreatoduodenal arcade. The discrete filling defects in the medial duodenal sweep were related to the large collateral vessels. The patient refused surgery and was subsequently lost to follow-up (fig. 1).

Case 2

This 48-year-old man had a long history of spastic neurogenic bladder secondary to multiple sclerosis. An excretory urogram was performed which suggested a right renal mass. Renal arteriography was then done and showed a normal kidney. However, there was occlusion of the celiac axis which was filled in a retrograde manner from the superior mesenteric artery via the large collaterals of the pancreatoduodenal arcade. A barium exam of the gastrointestinal tract demonstrated multiple filling defects of the duodenal sweep secondary to these enlarged collateral vessels (fig. 2).

[1] Department of Radiology, University of California at San Diego, and Veterans Administration Hospital, San Diego, California 92161.

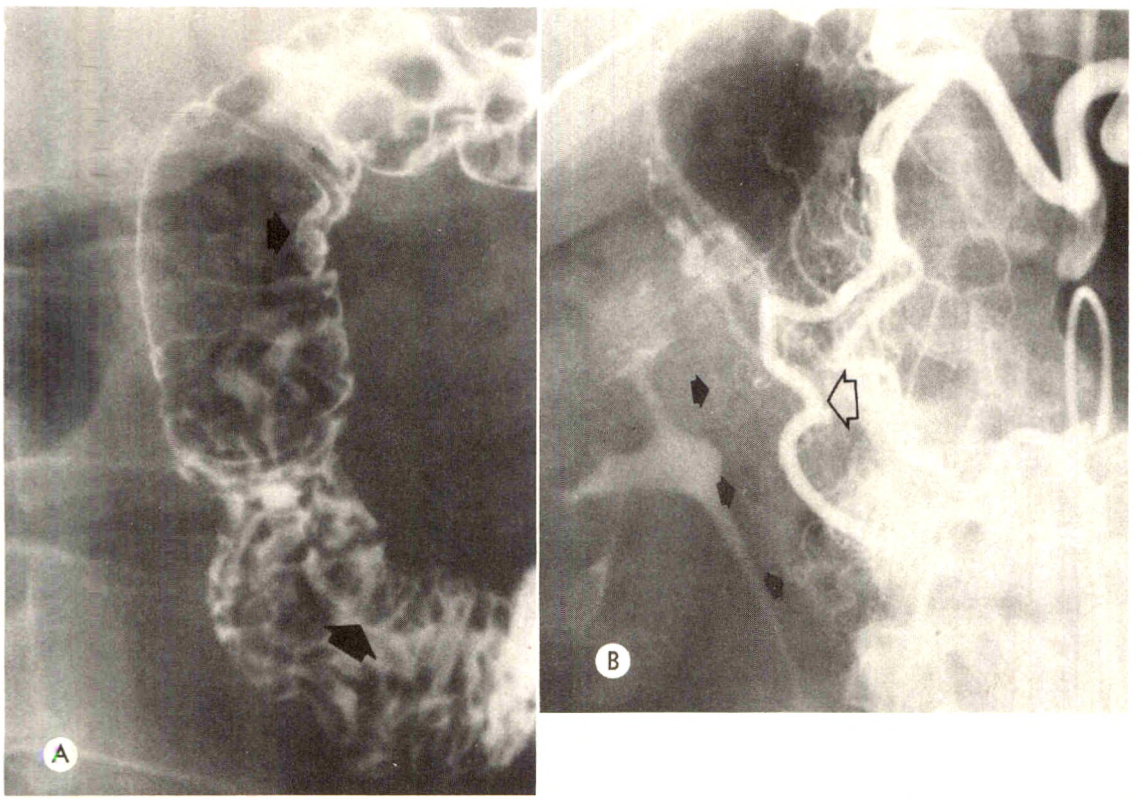


FIG. 1.—*A*, Two extrinsic impressions (*arrows*) on medial aspect of proximal descending duodenum and at junction of second and third portions. *B*, Enlarged pancreatic arcade vessels impressing upon median duodenal border (*open arrow*). Note lateral duodenal margins (*closed arrows*).

Case 3

This 58-year-old man presented with a 3 month history of intermittent dull periumbilical pain and a 15 pound weight loss. An examination of the upper gastrointestinal tract showed an extrinsic deformity to the medial aspect of the descending duodenum. An ultrasound examination of the abdomen was normal. Visceral arteriography was then performed because of the clinical suspicion of pancreatic neoplasm. There was occlusion of the celiac axis with retrograde filling through the enlarged pancreaticoduodenal arcades. The patient was treated conservatively with medical follow-up (fig. 3).

DISCUSSION

The clinical diagnosis of chronic vascular occlusive disease is an extremely difficult one. Most commonly, these patients have a long history of nonspecific vague abdominal pain which is often classified as "of unknown origin." Sometimes their symptoms become more characteristic as in "postprandial angina." Some patients may develop malabsorption secondary to chronic ischemia [1, 2]. With chronic borderline vascular perfusion of the gut, any acute superimposed episode of ischemia (hypotension, hypoxia, arrhythmia, blood loss, emboli, etc.) may further decrease perfusion and lead to irreversible infarction. Most patients who ultimately do develop a significant occlusion have chronic complaints and usually have had a previous upper gastrointestinal series which might have allowed the diagnosis to be made at an earlier time.

Occlusion of the celiac axis or superior

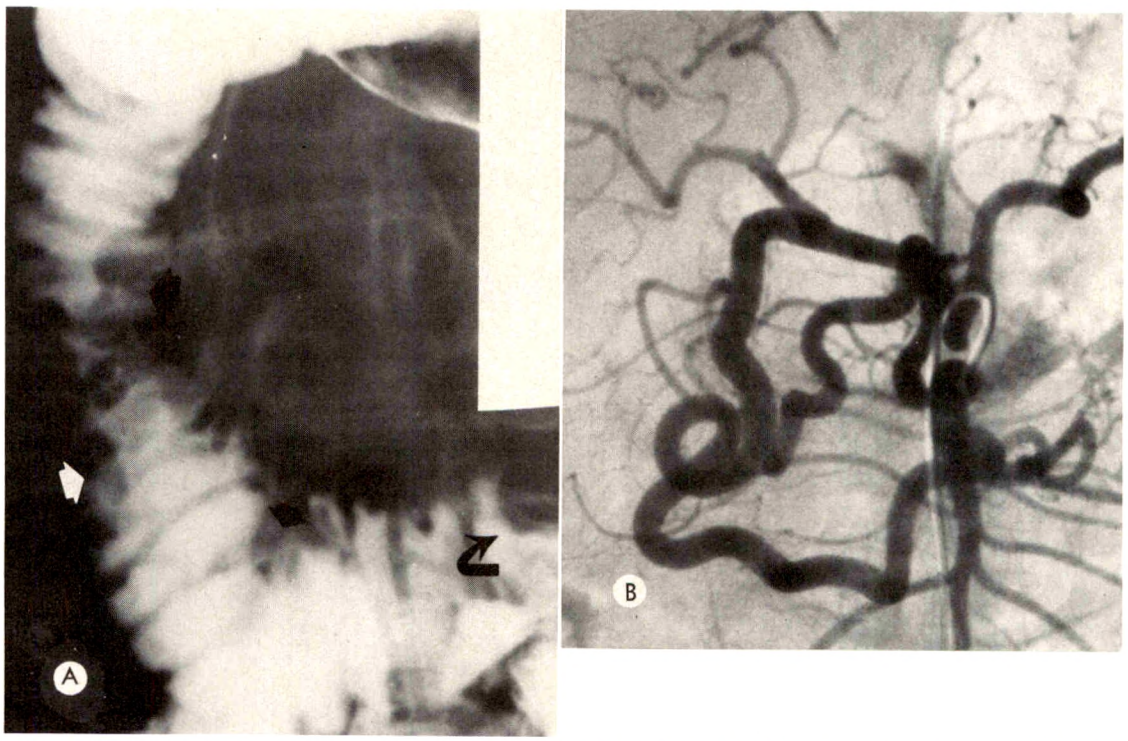


FIG. 2.—*A*, Extrinsic impressions on medial and lateral aspects of descending duodenum and of inner aspect of third portion of duodenum. *B*, Tortuous, enlarged pancreatic arcades fitting contoural defects seen on barium study.

mesenteric artery will lead to a marked increase in flow in the pancreatoduodenal arcade. These collaterals, which are the primary arterial connection between the celiac trunk and superior mesenteric artery, parallel the descending portion of the duodenum [3, 4].

When there is occlusion of both the celiac axis and the superior mesenteric artery, the gut is primarily supplied by a collateral network originating from the inferior mesenteric artery. In this situation, a large left colonic collateral vessel passes around the splenic flexure of the colon to the central anastomotic artery (meandering mesenteric artery) and supplies first the superior mesenteric artery [4, 5] and subsequently the celiac axis (through the pancreatoduodenal arcade).

If the inferior mesenteric artery is occluded, the collateral flow comes primarily from the superior mesenteric artery through the middle colic–left colic anastomosis and from the internal iliac via the hemorrhoidal arterial network.

When all three splanchnic vessels are occluded, the primary collateral flow to the gut is from the internal iliac arteries which first fill the hemorrhoidal network and then, in a retrograde manner, feed the colonic collaterals, the superior mesenteric artery, and the celiac axis.

A barium study of the gastrointestinal tract in patients with chronic occlusive visceral vascular disease will often demonstrate extrinsic contoural defects related to these enlarged collateral vessels [3, 6]. Due to the relationship of the pancreatoduodenal arcade to the duodenum, vascular impressions are a common finding, especially on the medial aspect of the proximal descending duodenum. These impressions,

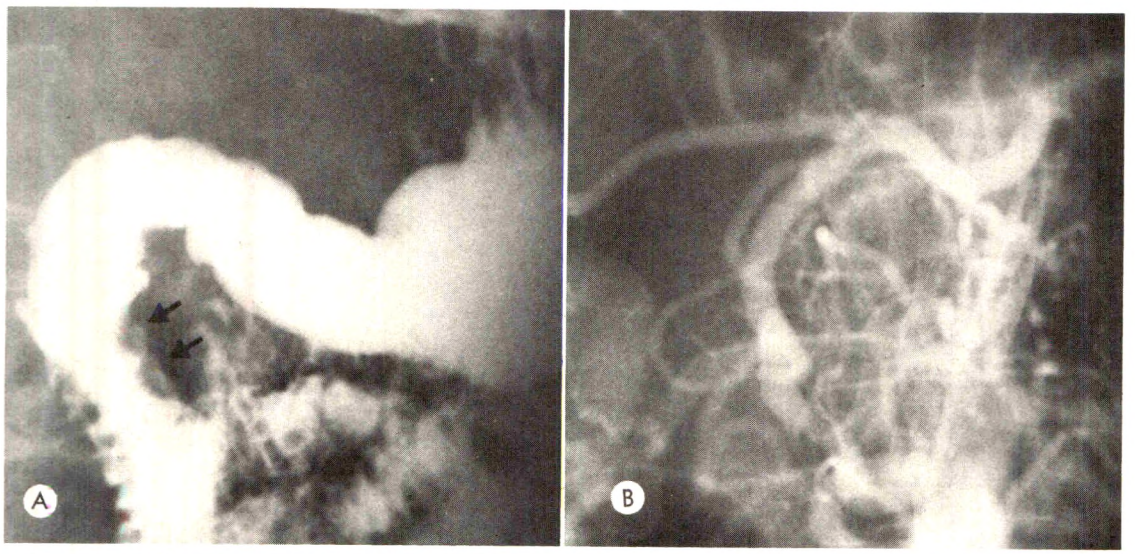


FIG. 3.—*A*, Biconcave extrinsic impressions (*arrows*) on anterior medial aspect of descending duodenum. *B*, Enlarged pancreaticoduodenal arcade filling occluded celiac axis via superior mesenteric artery.

best demonstrated with hypotonic duodenography, are often multiple. The large meandering mesenteric vessels may also produce an extrinsic pressure defect. Its location and course in the left upper quadrant will cause a discrete impression on the adjacent gut which is usually the proximal jejunum. While the location may vary somewhat, the appearance of a well-defined discrete impression should raise the possibility of a large collateral vessel.

When smooth extrinsic defects are found in the small bowel, especially along the medial aspect of the second portion of the duodenum, collateral flow from vascular occlusive disease should enter the differential diagnosis. Arteriography should then be performed for confirmation. Thus, in patients with nonspecific symptomatology, hypotonic duodenography and small bowel examinations may lead to earlier diagnosis and earlier therapy of visceral vascular occlusive disease.

ADDENDUM

Since submitting this paper we have had an additional case in an asymptomatic 58-year-old male.

REFERENCES

1. Ockner RK: Vascular diseases of bowel, in *Gastrointestinal Diseases*, edited by Sleisenger MH, Fordtran JS, Philadelphia, Saunders, 1973, p 1561
2. Williams LF Jr: Chronic intestinal ischemia, in *Vascular Disorders of the Intestines*, edited by Boley JJ, Schwartz SS, Williams LF, New York, Meredith, 1971, p 554
3. Baum S, Stein GN, Baue A: Extrinsic pressure defects on the duodenal loop: mesenteric occlusive disease. *Radiology* 85:866–874, 1965
4. Michaels NA: *Blood Supply and Anatomy of the Upper Abdominal Organs*. Philadelphia, Lippincott, 1955
5. Moscowitz M, Zimmerman H, Felson B: Meandering mesenteric artery of the colon. *Am J Roentgenol* 92:1088–1099, 1964
6. Shimkin PM, Pearson KD: Unusual arterial impression upon the duodenum. *Radiology* 103:295–297, 1972

Am J Roentgenol 126:974–980, 1976

A NEW CONCEPT OF ASCITIC FLUID DISTRIBUTION

ANTHONY V. PROTO,[1] EDWARD J. LANE, AND JOHN P. MARANGOLA

ABSTRACT:

Of 26 patients with ascites examined by B-mode ultrasonography, 14 had scans appropriate for evaluating the presence of fluid within the abdominal cavity. These studies demonstrate localization of fluid anteriorly around the tip of the liver and emphasize the importance of such factors as density relationships and the "pliability" of the anterior abdominal wall in the distribution of ascitic fluid. A review of the literature is presented.

A recent investigation [1] of soft tissue densities has shown that on plain films of the abdomen the lateral liver border is visualized in ascites as a result of a difference in density between the liver and surrounding ascitic fluid. An interesting offshoot of this work was that the larger intraperitoneal organs all were found to have densities greater than that of ascitic fluid, suggesting that organs should sink in ascitic fluid rather than float. In addition, cadaver experimentation demonstrated a different localization of ascitic fluid than had been anticipated. These findings prompted a review of the literature as well as further investigation of the distribution of ascitic fluid.

LITERATURE REVIEW

The literature contains several reports on the path of spread and localization of intraperitoneal fluid. The conclusions drawn from these studies have been based on clinical observations [2, 3] and on cadaver and in vivo studies [4–6].

It is generally agreed that fluids will avail themselves of those naturally occurring intraperitoneal compartments formed by the mesenteric attachments and peritoneal reflections (fig. 1). The peritoneal cavity can be divided into both abdominal and pelvic components, the division between the two being located at the level of the iliac vessels and posterior pelvic brim. Further division of the larger abdominal cavity into supramesocolic and inframesocolic spaces occurs by virtue of the transverse colon and its associated mesocolon. The external paracolic gutters are potential areas of communication between these two spaces. Diagrammatic representations of these compartments have been presented [4–6].

1) *Supramesocolic space.* This extends from the diaphragm to the transverse colon and mesocolon. It is further divided into the right and left subhepatic and subphrenic spaces.

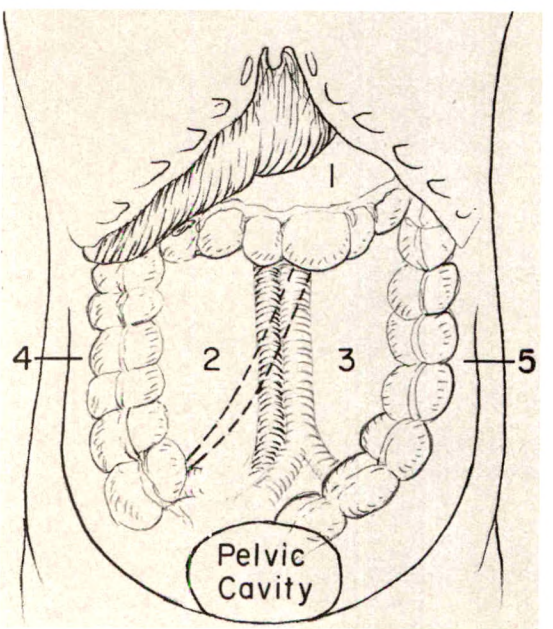


FIG. 1.—Diagram of intraperitoneal compartments. *1*, Supramesocolic space; *2*, right inframesocolic space; *3*, left inframesocolic space; *4*, right paracolic gutter; *5*, left paracolic gutter.

Presented at the annual meeting of the American Roentgen Ray Society, Atlanta, Georgia, October 1975.
[1] Department of Radiology, Upstate Medical Center, Syracuse, New York 13210.

2) *Inframesocolic space.* This extends from the transverse colon and mesocolon to the pelvic brim; it is further divided into a smaller right infracolic and a larger left infracolic space by the obliquely oriented small bowel mesentery as well as the spine, aorta, and inferior vena cava. The left infracolic space is more anatomically contiguous with the pelvis than the right.

3) *Paracolic gutters.* The right paracolic gutter extends from the right lateral abdominal wall to the ascending colon, while the left gutter extends from the descending colon to the left lateral abdominal wall. The right gutter is deeper than the left, and Mitchell [6] mentions that at times the right may have peritoneal folds across it hindering fluid flow (hepatorenal ligament superiorly, cecal fold inferiorly). The left gutter is more shallow than the right and has a fold coursing its superior aspect—the phrenicocolic ligament.

Experimental work with various types of contrast material (barium, iodized poppy seed oil, methyl-glucamine diatrizoate) instilled into the peritoneal cavity has resulted in proposed methods of spread of intraperitoneal fluid. The right paracolic gutter is said to act as an avenue of transport of fluid from the lower to upper abdominal cavity. Yet injection of contrast material in areas about the cecum has resulted in flow either preferentially to the pelvis and then up the right gutter [5] or preferentially to the right gutter with less going to the pelvis [4, 6]. Similarly, some have shown the left infracolic space to be invaded by contrast injection in the cecal area while others have not.

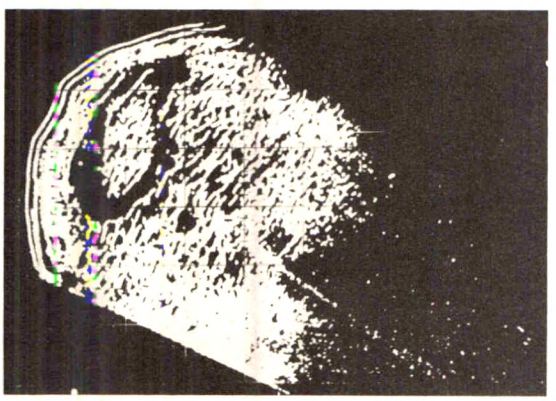


FIG. 2.—Transverse scan 6 cm above umbilicus illustrating fluid around liver tip.

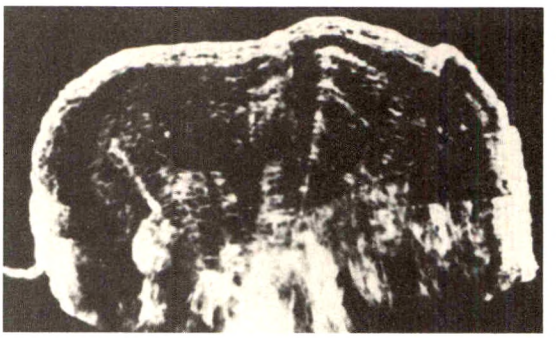


FIG. 3.—Transverse scan 7 cm above umbilicus illustrating fluid lateral to liver.

Injection of contrast material into the right supramesocolic space has also resulted in disagreement as to major pathways of flow. One school of thought maintains that flow preferentially occurs over the transverse colon to the right infracolic space and right paracolic gutter. Some fluid may invade the left infracolic space from the right and then go to the pelvis. Another school maintains that fluid does not go over the transverse colon but rather flows via the right gutter to the pelvis.

In addition to flowing caudally, fluid in the right supramesocolic space will also seek the right subhepatic space. Yet whether flow continues from there to the right subphrenic space is not totally agreed upon. Differing amounts of emphasis have been placed on the effectiveness of the falciform ligament in preventing flow from the right to the left subphrenic space.

Obviously, there is disagreement over the spread of intraperitoneal fluid. While it is convenient to think that fluid flow is determined only by the various peritoneal compartments, there are other factors to be considered.

Intraperitoneal pressure has been studied by several investigators. Keppich (cited in [7]) has shown that the pressure in the upper abdominal area is subatmospheric. Us-

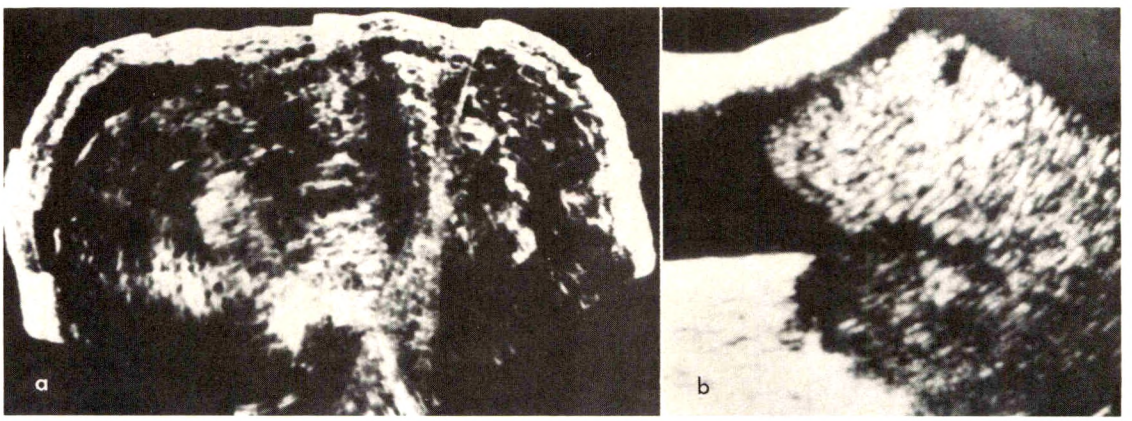


FIG. 4.—*a*, Transverse scan 7 cm above umbilicus illustrating fluid lateral and anterior to the liver. *b*, Longitudinal scan 12 cm to right of midline illustrating fluid around liver tip and anterior to liver.

ing animal experimentation, Overholt [8] also demonstrated a lower pressure in the upper abdomen, the pressure in the abdomen varying with respiration. Drye [9] emphasized the importance of position: the pressure in the lower abdomen of an upright patient is three times as great as in the upper abdomen. A change in patient position will also cause variation in dependence of the abdominal compartments, thus allowing fluid to gravitate to different areas.

Other important factors are: (1) the area from which the peritoneal fluid originates; (2) the rapidity with which the fluid accumulates; (3) the presence or absence of adhesions; (4) the intraperitoneal organs and their ligamentous attachments; (5) anatomic variation among patients; and (6) the amount of fluid present.

There is also some question as to how accurately the experimental data reflect the clinical situation. For example, cadaver studies obliterate the effects of respiration and, to some extent, patient position. In vivo studies have not been performed with amounts of fluid as might be seen in ascites. Similarly, the density of the contrast agents employed to determine spread of peritoneal fluid (approximately 1.30 g/ml) is 27.5% greater than the density of ascitic fluid (1.01–1.03 g/ml).

OUR EXPERIENCE

Of 26 patients with ascites examined by B-mode ultrasonography, 14 had scans appropriate for evaluating the presence of fluid within the abdominal cavity. The pelvis was not included in this study. Some of the 14 had multiple examinations. The causes of ascites included cirrhosis, chronic renal disease, and metastatic disease. While fluid in some patients was identified only around the inferior portion of the right lobe of the liver (liver tip), those with larger

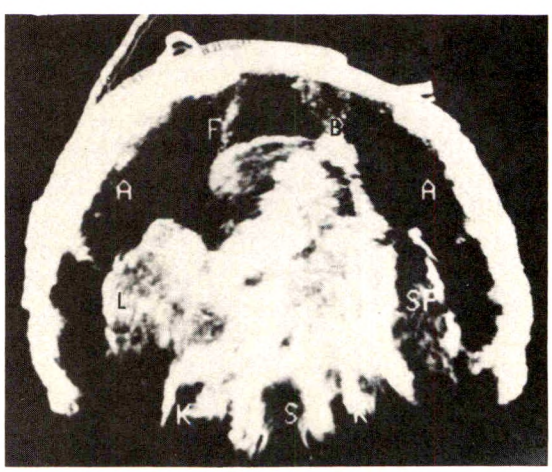


FIG. 5.—Transverse scan 12 cm above umbilicus illustrating massive ascites anterior and lateral to the liver. L = liver; SP = spleen; S = spine; K = kidney; F = falciform ligament; A = ascites; B = bowel.

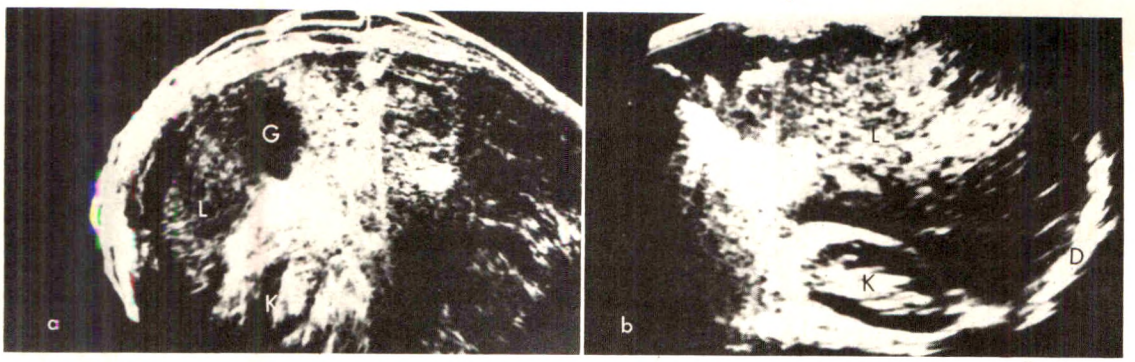


FIG. 6.—Transverse scan 12 cm above umbilicus (*a*) and longitudinal scan 8 cm to right of midline (*b*) illustrating absence of fluid accumulation between liver (L) and kidney (K). G = gallbladder; D = diaphragm.

amounts of fluid demonstrated further accumulation around the liver tip as well as in the right flank and lateral to the liver (figs. 2 and 3). Those with even larger amounts of ascites demonstrated accumulation in all of the aforementioned locations, anterior to the liver and in the left flank, as well as throughout the remainder of the abdominal cavity (figs. 4 and 5). However, none demonstrated the presence of fluid posterior to the liver at the level where the liver contacts the kidney (fig. 6). This was true even with massive ascites (fig. 5). In only one patient was the location of ascites with respect to the spleen noted (fig. 5). Since it is difficult to obtain satisfactory splenic images in a supine patient, the relationship of ascitic fluid to the spleen could not be satisfactorily determined.

Gas-containing loops of bowel were noted to float, while fluid-filled bowel loops sank, displacing the ascitic fluid to just beneath the anterior abdominal wall (figs. 7 and 8*a*). Gas-containing loops also changed position (fig. 8*b*) on scans of the right abdomen with the patient in the left lateral decubitus position (four of 14 cases). In these scans some fluid relocated against the left anterior abdominal wall which was dependent in this position. Perhaps this relocation is attributable to the "pliability" of the abdominal wall, which allows the fluid to collect in a more dependent position than would be expected with a rigid system.

The evaluation of ascites using A-mode ultrasonography has been reported by Goldberg et al [10]. The lowest amount detectable in experiments with five cadavers was 100 ml. We have performed ultrasonic B-mode scanning on a cadaver after the injection of fluid into the abdomen via a catheter inserted just below the umbilicus. A gelatin mixture of average ascitic fluid density (1.015 g/ml) was used. Scans were performed in the supine position. No fluid pattern was recognized at 200 ml, but the next increment used (400 ml) did show fluid located around the tip of the liver. Further increments demonstrated fluid in the right flank and a small amount lateral to the liver at 800 ml, with increased accumulation in these areas as well as anterior to the liver at 1,600 ml (fig. 9). Fluid also localized at the anterior portion of the abdomen over fluid-filled bowel loops.

Since a fluid similar in density to ascitic fluid accumulated around the liver tip which is located anteriorly (fig. 10) and since this fluid localized over bowel as well, it was thought that density differences might also play a role in the localization of ascitic fluid. Thus autopsy specimens of liver, spleen, small bowel, and transverse colon were obtained for density measurement. The density was calculated by dividing a known weight of the specimen in grams by the volume of water it displaced.

Fifteen specimens each were obtained of liver, spleen, and small and large bowel. Table 1 lists the mean and range of density for each organ. The values are in close

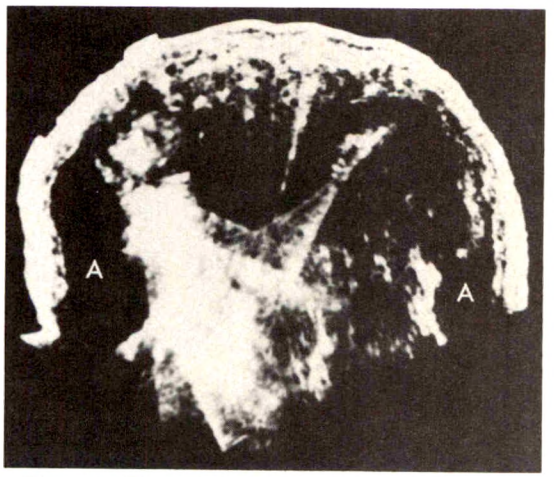


FIG. 7.—Transverse scan 8 cm above umbilicus illustrating floating bowel loops. Note ascites (A) in both flanks.

agreement with those obtained by Rao and Gregg [11] as well as those from another investigation [1] in which liver density was measured. Histologic analyses were as follows: liver—normal, congested, moderately fibrotic; spleen—normal, congested; and small and large bowel—normal.

It can be seen from table 1 that all of the measured intraperitoneal organs had densities greater than that of ascitic fluid. Thus the relative densities of ascitic fluid and the organs it surrounds are probably also a factor to be considered in distribution of peritoneal fluid. For example, gas-containing small bowel loops will float since their weight per unit volume is less than that of ascitic fluid, while fluid-filled loops will not because the opposite is true. Similarly, in both cadaveric and clinical ultrasound examinations, fluid was noted to localize anteriorly in surrounding the tip of the liver.

We also scanned a patient undergoing peritoneal dialysis: 2,000 ml of Dianeal (peritoneal dialysate fluid) were injected via a catheter placed 1 cm below the umbilicus. Scans were performed in the supine position. This study was of particular interest since it was performed on a live patient and the fluid used was of average ascitic fluid density (1.015 g/ml). Results were in accord with both our clinical and cadaver studies. The scans demonstrated fluid localization around the liver tip, lateral and anterior to the liver, and in the flanks. Fluid anterior to bowel loops was also noted.

DISCUSSION

Several studies have been undertaken to elaborate the various abdominal compartments and the distribution of peritoneal

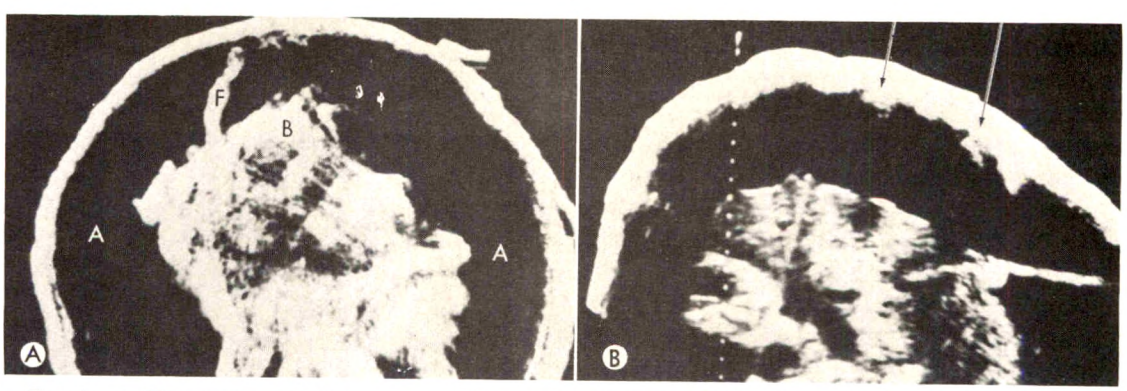


FIG. 8.—*a*, Transverse scan 8 cm above umbilicus illustrating massive ascites with fluid (A) in both flank and nonfloating bowel loops (B). F = falciform ligament. *b*, Transverse scan 8 cm above umbilicius with patient in left lateral decubitus position. Note increased accumulation of fluid in the now dependent left anterior abdominal compartment with stretching of falciform ligament. Also note floating bowel loops (*arrows*).

fluid. While disagreement exists in some areas, large clinical studies have shown inflammatory exudates to be localized in the major pathways elaborated. Yet these pathways may not be entirely applicable to the localization of a less dense ascitic fluid. The contrast media employed have densities approximately 27% greater than that of ascitic fluid. Furthermore, the effects of respiration and, to some extent, patient position are eliminated in cadaver studies.

Many factors appear to affect the spread of intraperitoneal fluid: peritoneal compartments, intraperitoneal pressure, patient position, area from which the fluid originates, rapidity with which fluid accumulates, the presence or absence of adhesions, ligamentous attachments, anatomic variations, and the amount of fluid present. In addition we feel the density of the fluid with respect to other abdominal organs is important: liver, spleen, and small and large bowel have densities greater than that of the average ascitic fluid. Similarly, the pliability of the abdominal wall might also account for ascitic fluid localization.

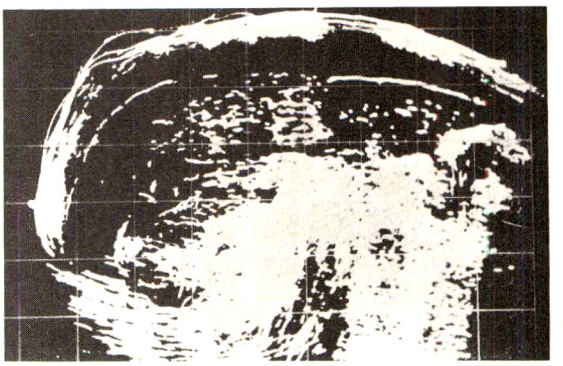


FIG. 9.—Transverse scan of cadaver (1,600 ml fluid) 6 cm below xiphoid with fluid lateral and anterior to liver.

Clinical ultrasound review and cadaver

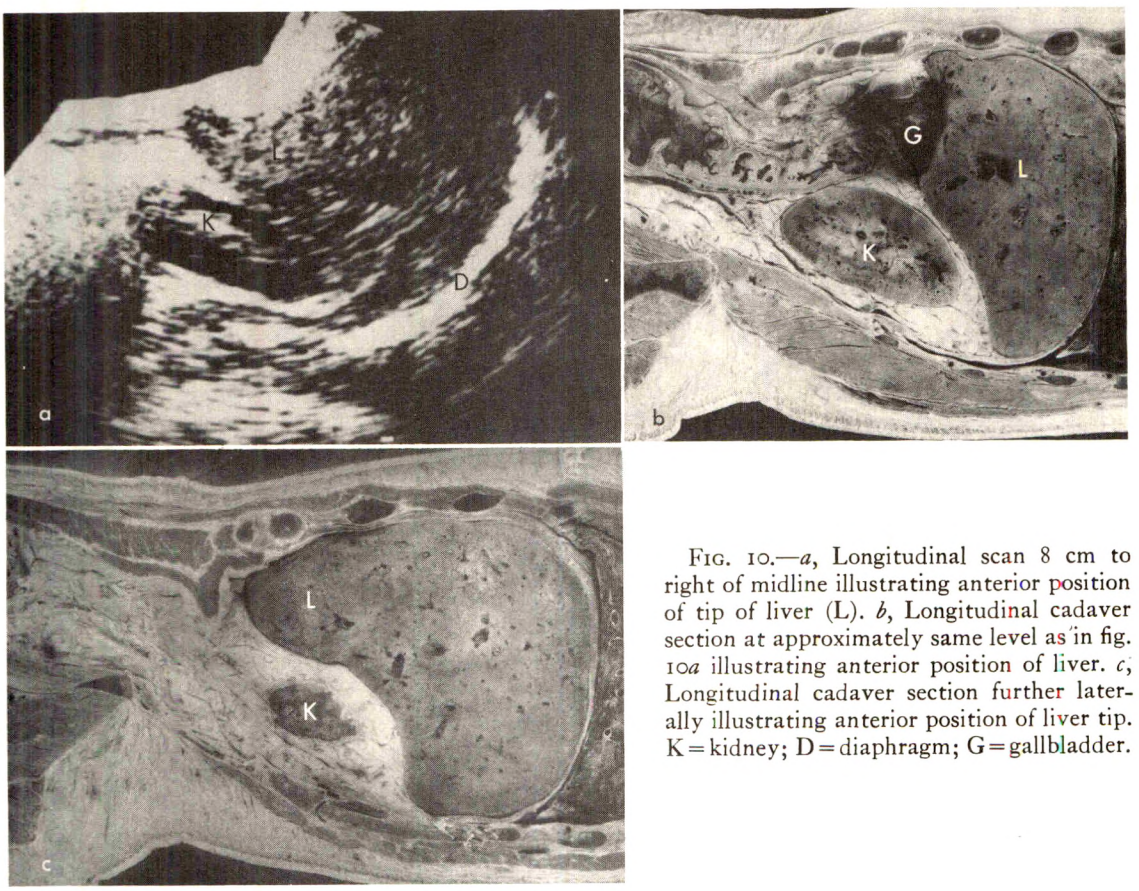


FIG. 10.—*a*, Longitudinal scan 8 cm to right of midline illustrating anterior position of tip of liver (L). *b*, Longitudinal cadaver section at approximately same level as in fig. 10*a* illustrating anterior position of liver. *c*, Longitudinal cadaver section further laterally illustrating anterior position of liver tip. K = kidney; D = diaphragm; G = gallbladder.

TABLE 1

ORGAN DENSITIES

ORGAN	DENSITY (g/ml)	
	Mean	Range
Liver	1.066	1.052–1.082
Spleen	1.066	1.058–1.081
Small bowel	1.054	1.030–1.072
Large bowel	1.051	1.030–1.077

experimentation have shown anterior localization of fluid. Scanning at the time of peritoneal dialysis with a fluid in the density range of ascitic fluid has demonstrated similar findings. While it was hoped that this anterior localization might have resulted in plain film recognition of ascites with lesser amounts than are presently necessary for its recognition, this did not prove to be the case. However, it seems worthwhile to keep in mind this localization when performing ultrasonic evaluation to detect the presence of ascites. Further investigation in this regard is planned as well as further work with ultrasonic monitoring of peritoneal dialysis.

ACKNOWLEDGMENTS

We thank Dr. Patrick J. Bryan and Mrs. Lori Champlin for assistance with the ultrasound portion of the study and Mrs. Diane Pajak for secretarial assistance.

REFERENCES

1. Proto AV, Lane EJ: Visualization of differences in soft tissue densities: the liver in ascites. Submitted for publication
2. Ochsner A, DeBakey M: Subphrenic abscess: collective review and an analysis of 3,608 collected and personal cases. *Int Abstr Surg* 66:426–438, 1938
3. Wettefors J: Subphrenic abscess: a clinical study of 101 cases. *Acta Chir Scand* 117:388–408, 1959
4. Autio V: The spread of intraperitoneal infection: studies with roentgen contrast medium. *Acta Chir Scand [Suppl]* 321:1–31, 1964
5. Meyers MA: The spread and localization of acute intraperitoneal effusions. *Radiology* 95: 547–554, 1970
6. Mitchell GAG: The spread of acute intraperitoneal effusions. *Br J Surg* 28:291–313, 1940
7. Holmes F: Intraperitoneal and intrapleural pressures: an experimental study. *Anaesthesia* 11:69–76, 1956
8. Overholt RH: Intraperitoneal pressure. *Arch Surg* 22:691–703, 1931
9. Drye JC: Intraperitoneal pressure. *Arch Surg* 22:691–703, 1931
10. Goldberg BB, Goodman GA, Clearfield HR: Evaluation of ascites by ultrasound. Radiology 96:15–22, 1970
11. Rao PS, Gregg EC: Attenuation of monoenergetic gamma rays in tissues. *Am J Roentgenol* 123:631–637, 1975

Am J Roentgenol 126:981–984, 1976

GLUCAGON AND BARIUM ENEMA EXAMINATIONS: A CONTROLLED CLINICAL TRIAL

ROGER K. HARNED,[1] CAROL B. STELLING, SUSAN WILLIAMS, AND GERALD L. WOLF[2]

ABSTRACT:

In a double-blind crossover clinical trial, 10 healthy volunteers received placebo and 2 mg glucagon intramuscularly preceding barium enema examination on separate days. In addition, 50 patients were given either placebo or 2 mg glucagon prior to barium enema examination in a double-blind study. The results of 38 variables determined on each study population were similar. When glucagon was given, both the patients and examiners noted significantly less discomfort and more bowel relaxation. There were no significant changes in pulse, blood pressure, or electrocardiogram. Adverse reactions did not occur frequently enough to allow confident comparison of placebo and glucagon. It is concluded that the use of glucagon can provide a more comfortable barium examination with acceptable safety.

INTRODUCTION

The relaxed colon allows for a more comfortable barium examination of better diagnostic quality. For some time the anticholinergics were the drugs of choice for reducing smooth muscle spasm [1, 2]. However, these agents have been associated with adverse effects that may limit routine use [3]. Recently, glucagon has been advocated as a safer pharmacologic adjunct to barium studies of the duodenum [4, 5] and colon [5–7]. The pharmacologic effects of glucagon are not limited to the enteric tract, and present drug regulations require rigid evidence of both safety and efficacy. This study was performed on both volunteers and patients to provide such information, using established techniques for controlled clinical trials.

SUBJECTS AND METHODS

Normal Subjects

Ten healthy adult men participated in the study after informed consent was obtained and documented in writing. A short history and physical examination was performed with special care to detect cardiovascular or endocrine abnormalities. Subjects received 2½ oz of X-prep (Gray Pharmaceutical) on the evenings before examination and were examined the following morning in the fasting state. Either 2 mg glucagon or placebo (diluting solution for glucagon) was administered intramuscularly 10 min prior to barium enema. Neither subjects nor investigators were aware of the content of the injectate. The barium study was then performed using standard procedures, except that barium amounts and times were recorded to provide the parameters listed in table 1. A gonadal shield was used in all cases. Films were obtained during the examination, postevacuation, and 1 hr later. The pulse and blood pressure were recorded before and on completion of the examination. On completion of the exam, the subject and the radiologist independently completed a standard question sheet concerning the ease of the exam and any side effects. The following morning each subject reported the type and severity of any side effects that occurred in the interval.

The subjects returned 7–10 days later for a second identical experience with intramuscular injection of the other agent—either glucagon or placebo. Thus the study was designed in a randomized, double-blind, crossover manner.

Patients

Fifty adult men or women scheduled for regular barium examination consented to participate in a similar study without the cross-

[1] All authors: Department of Radiology, University of Nebraska Medical Center, Omaha, Nebraska 68105.

[2] Recipient of U.S. Public Health Service research career development award no. I KO4 GM 70683-03 from the National Institute of General Medical Sciences.

TABLE 1

VARIABLES MEASURED IN EACH STUDY GROUP

Subject's Report	Radiologist's Report	Cardiovascular Measurements
Discomfort at cecum	Width of sigmoid, middescending, transverse, and midascending colon, cecum, and terminal ileum; length of terminal ileum:	Pulse and blood pressure:
Discomfort at end of examination	Following filling	Before drug
Urge to defecate	Immediately postevacuation	At completion of study
Symptoms of adverse effect	1 hr postevacuation	Electrocardiogram (patients only):
Preference (crossover only)	Height of barium column	Before drug
	Time to reach ileocecal valve	During examination
	Time to fill small bowel	Immediately postevacuation
	Number and severity of contractions on filled colon films	During unusual periods detected by continuous monitor
	Loss of barium on table	
	Subjective estimate of colon and small intestine tonicity	
	Filled colon	
	Immediately postevacuation	
	1 hr postevacuation	
	Preference (crossover only)	

over feature. Since the study population was composed of patients, the monitored parameters were expanded to include a single-lead electrocardiogram. The ECG was recorded prior to drug administration, when the barium enema was started, at the end of examination, and immediately after evacuation. In addition, an audio signal (Health Tech) was continuously monitored throughout the exam, and any unusual cardiac rhythm detected was recorded. The use of auditory monitoring allowed the radiologist to concentrate his visual attention on the fluoroscopic aspects of the study.

Data Analysis

Variables of a continuous nature were evaluated with paired *t* tests. The variables included all measurements. For all questions concerning efficacy, one-tailed *t* tests were used. For cardiovascular parameters where changes in either direction could be important, two-tailed tests were used. Subjective variables were ranked from 0 to 4, where 0=none and 4=severe. The statistical significance of differences in scores between placebo and control groups was determined using a simple unidirectional binomial test [8].

RESULTS AND DISCUSSION

One of the first concerns in a controlled clinical trial is whether the populations studied with active drug or placebo differed even though the assignment was thought to be random. On completion of the study, no significant differences were found in sex, age, weight, height, pulse, or blood pressure between the two groups of patients. Of course the crossover design for the volunteers eliminates this risk (at the cost of a second examination for each subject). The results of virtually all parameters were reassuringly similar in both patients and volunteers.

The subjective results from both subjects and radiologists are easiest to interpret. Both clearly preferred glucagon over placebo (tables 2 and 3). The objective mea-

TABLE 2

SIGNIFICANT DIFFERENCES IN SUBJECT RES PONSES

Subjects	Placebo	Glucagon	*P*
Volunteers:			
Discomfort.....	1.7	0.8	<.05
Preference.....	1.2	1.9	<.05
Patients:			
Discomfort.....	1.3	0.3	<.001

NOTE.—Discomfort score: 0=none, 1=mild, 2=moderate, 3=moderately severe, 4=severe. Preference score: 1=least preferred, 2=most preferred. Values shown are mean scores.

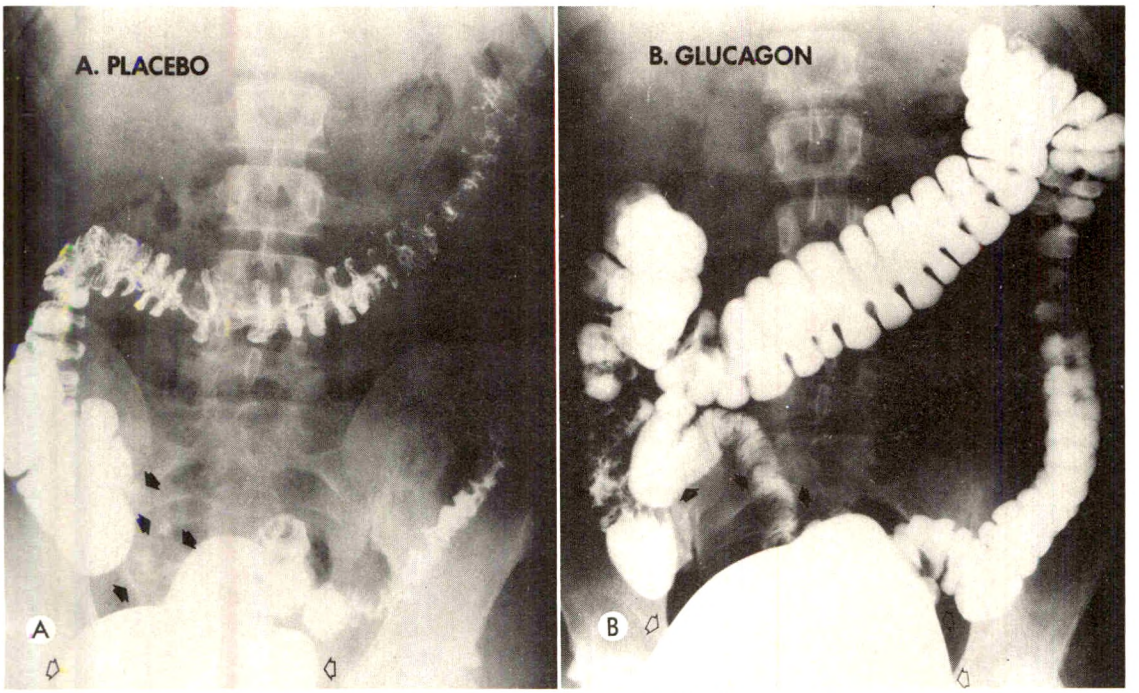


FIG. 1.—Postevacuation studies in same patient. *A*, Most of colon in contracted state with minimal filling of terminal ileum. *B*, More relaxation of colon with increased filling of terminal ileum. Closed arrows = terminal ileum; open arrows = lead shielding of genitalia.

surements were less strikingly different. Despite the profusion of indices measured (table 1), only a few were significantly different. Of course, the subjective estimates concern the whole exam whereas the objective measurements individually assess only small parts of the total response to glucagon. However, there were subtle differences in the appearance of the glucagon-treated colon that were easily detectable by the radiologist after some experience (see fig. 1).

Adverse side effects were assessed, with special attention to the cardiovascular system. Table 4 lists the symptoms and signs reported by the subjects. Although there were clearly more events with glucagon, the difference does not achieve statistical significance. Pulse and blood pressure were

TABLE 3

SIGNIFICANT DIFFERENCES IN RADIOLOGIST RESPONSES

Subjects	Placebo	Glucagon	*P*
Volunteers:			
Preference*.....	0	6	<.05
Patients:			
Overall score.....	3.13	3.88	<.01
Number of spasms	0.56	0.12	<.05
Severity of spasms	0.60	0.20	<.05
Ease of filling cecum.....	3.38	4.52	<.01
Bowel relaxation, 1 hr.....	2.38	2.92	<.05

NOTE.—See table 2 for explanation of scores.
* Four had no preference.

TABLE 4

ADVERSE EFFECTS REPORTED

Symptom	Placebo		Glucagon	
	No. Reports	Total Score*	No. Reports	Total Score*
Nausea.....	1	1	8	11
Vomiting.....	...	...	3	4
Dizziness.....	2	2	...	...
Headache.....	2	2	2	2
Abdominal distress	...	...	1	2
Total.....	5	5	14	19

* Score: 0 = none, 1 = mild, 2 = moderate, 3 = moderately severe, 4 = severe.

TABLE 5

CARDIOVASCULAR MEASUREMENTS BEFORE AND AFTER TEST DRUG

Measurement	Placebo		Glucagon	
	Before	After	Before	After
Pulse:				
Volunteers....	72.6	67.2	72.1	67.6
Patients.....	78.8	73.8	84.6	78.0
Blood Pressure:				
Volunteers:				
Systolic.....	122.4	123.2	120.4	122.0
Diastolic....	81.0	82.4	79.6	80.0
Patients:				
Systolic.....	128.2	127.1	122.3	122.3
Diastolic....	77.8	75.8	76.2	75.9

NOTE.—Electrocardiographic changes occurred in three patients in the placebo group and one in the glucagon group. See text.

not meaningfully altered by glucagon (table 5). ECG changes occurred in only four of the patients. One patient receiving glucagon had an ectopic atrial contraction before the drug was administered. The other three events occurred in the placebo group and were premature ventricular contractions. On two occasions the arrhythmia was observed during the barium enema, and the other occurred prior to administering placebo. The stress of barium enema examination alone can be associated with electrocardiographic changes [9]. Apparently the effects of glucagon on the heart did not enhance the tendency to arrhythmia. In fact, recent papers suggest that glucagon may decrease reentrant types of cardiac arrhythmias [10, 11]. Our results suggest that there is no reason for undue alarm about the induction of serious cardiac irregularities and, in fact, the more comfortable exam with glucagon may even diminish the risk.

The results of this study indicate that after glucagon is given, as compared with placebo, there is definite relaxation of the colon with few serious side effects. Our data confirm previous controlled clinical trials of glucagon in normal volunteers [4] and in patients [6, 7]. The use of glucagon in barium enema examinations is both safe and efficacious providing the contraindications of either are considered. We have no experience on the use of glucagon in the presence of such diseases as granulomatous or ulcerative colitis. However, further investigations may better delineate the contribution of glucagon in providing barium examinations that are more comfortable and of better diagnostic quality.

ACKNOWLEDGMENTS

The authors wish to thank Dr. Bruce Rodda for assistance with the statistical analyses.

REFERENCES

1. Ferruci JT Jr, Benedict KT Jr: Anti-cholinergic-aided study of the gastrointestinal tract. *Radiol Clin North Am* 9:23–29, 1971
2. Gohel VK, Dalinka MK, Mandell GA, Azimi F: Pharmacology of the gastrointestinal tract. *CRC Crit Rev Clin Radiol Nucl Med* 5:69–110, 1974
3. Gelfand DW, Moskovitz M: Massive gastric dilatation complicating hypotonic duodenography: report of three cases. *Radiology* 97:637–639, 1970
4. Miller RE, Chernish SM, Rosenak BD, Rodda BE: Hypotonic duodenography with glucagon. *Radiology* 108:35–42, 1973
5. Miller RE, Chernish SM, Skulas J, Rosenak BD, Rodda BE: Hypotonic roentgenography with glucagon. *Am J Roentgenol* 121:264–274, 1974
6. Gohel VK, Dalinka MK, Coren GS: Hypotonic examination of the colon with glucagon. *Radiology* 115:1–4, 1975
7. Meeroff JC, Jorgens J, Isenburg JI: The effect of glucagon on barium-enema examination. *Radiology* 115:5–7, 1975
8. Snedecor GW: *Statistical Methods*, 5th ed. Ames, Iowa State University Press, 1956
9. Eastwood GL: ECG abnormalities associated with the barium enema. *JAMA* 219:719–721, 1972
10. Nishimura A, Fortner RB, Williams JF Jr: Effect of glucagon on automatacity, threshold for stimulation, and atrioventricular conduction in patients with impaired impulse formation or conduction. *Am Heart J* 84:359–365, 1972
11. Prasad K: Electrophysiologic effects of glucagon on human cardiac muscle. *Clin Pharmacol Ther* 18:22–30, 1975

Am J Roentgenol 126:985–991, 1976

SPONTANEOUS INTERNAL DRAINAGE OF PANCREATIC PSEUDOCYSTS

J. Luther Clements, Jr.,[1] E. L. Bradley, III,[2] and S. Boyd Eaton, Jr.[1]

ABSTRACT:

Six cases are reported in which spontaneous internal drainage between a pancreatic pseudocyst and the alimentary tract became established. In each instance the communication was demonstrated radiologically. The clinical circumstances and radiographic features of these cases are described, and the existing literature pertaining to this phenomenon is reviewed.

Pseudocysts of the pancreas are collections of old blood, pancreatic juice, fat, and partially digested tissue debris which arise in the vicinity of the pancreas as a consequence of pancreatic inflammation. Such a collection is initiated by inflammatory disruption of pancreatic tissue with resulting emission of digestive enzymes and blood into the peripancreatic region, most often the lesser omental sac. The enzymatic and inflammatory action of this material evokes a reactive fibrosis in adjacent tissues. This results in formation of fibrous walls which enclose the fluid collection.

Many aspects of the natural history of pancreatic pseudocysts are incompletely understood. One phenomenon which has received sporadic attention in previous reports is spontaneous decompression via rupture of a cyst into an adjacent hollow viscus. Solitary examples of such naturally occurring internal drainage have been described in several previous publications. It is the purpose of this communication to report six additional cases—all documented by roentgen demonstration of fistulous communication between the cyst and the gastrointestinal tract.

CLINICAL MATERIAL

Representative Case Report

B. W., a 28-year-old black alcoholic, had had several previous chemically documented attacks of acute pancreatitis. He was admitted because of severe epigastric pain with radiation to the back, a sense of abdominal fullness, nausea, vomiting, and anorexia. Physical examination revealed epigastric tenderness and decreased bowel sounds. Laboratory studies showed glycosuria, hyperglycemia, and marked hyperamylasemia. Initially the symptoms remitted and serum amylase values fell, but after a few relatively symptom-free days, the epigastric pain recurred, serum amylase values rose, and a large epigastric mass became palpable. An ultrasonic abdominal examination performed at this time (fig. 1*A*) demonstrated a large left upper quadrant cystic mass. Two days later the patient developed mild hematemesis, and an upper gastrointestinal barium examination revealed communication between the stomach and an irregular cystic space (fig. 1*B*). During the next 2 days the epigastric mass disappeared, and 3 days after the barium study a repeat ultrasonic examination confirmed complete resolution of the mass (fig. 1*C*).

Series Analysis

The six patients in this series ranged from 28 to 64 years of age, and all were alcoholic males (table 1, figs. 1–6). Two had no prior diagnosis of pancreatitis, but episodes of documented pancreatitis had occurred in the others intermittently for from 2 to 17 years. In three patients the pseudocyst had not been suspected before the barium examination which also demonstrated communication between the cavity and the alimentary tract. In the other

Presented at the annual meeting of the American Roentgen Ray Society, Atlanta, Georgia, October 1975.

[1] Department of Radiology, Emory University School of Medicine and Grady Memorial Hospital, 80 Butler Street S.E., Atlanta, Georgia 30303.

[2] Department of Surgery, Emory University School of Medicine and Grady Memorial Hospital, 80 Butler Street S.E., Atlanta, Georgia 30303.

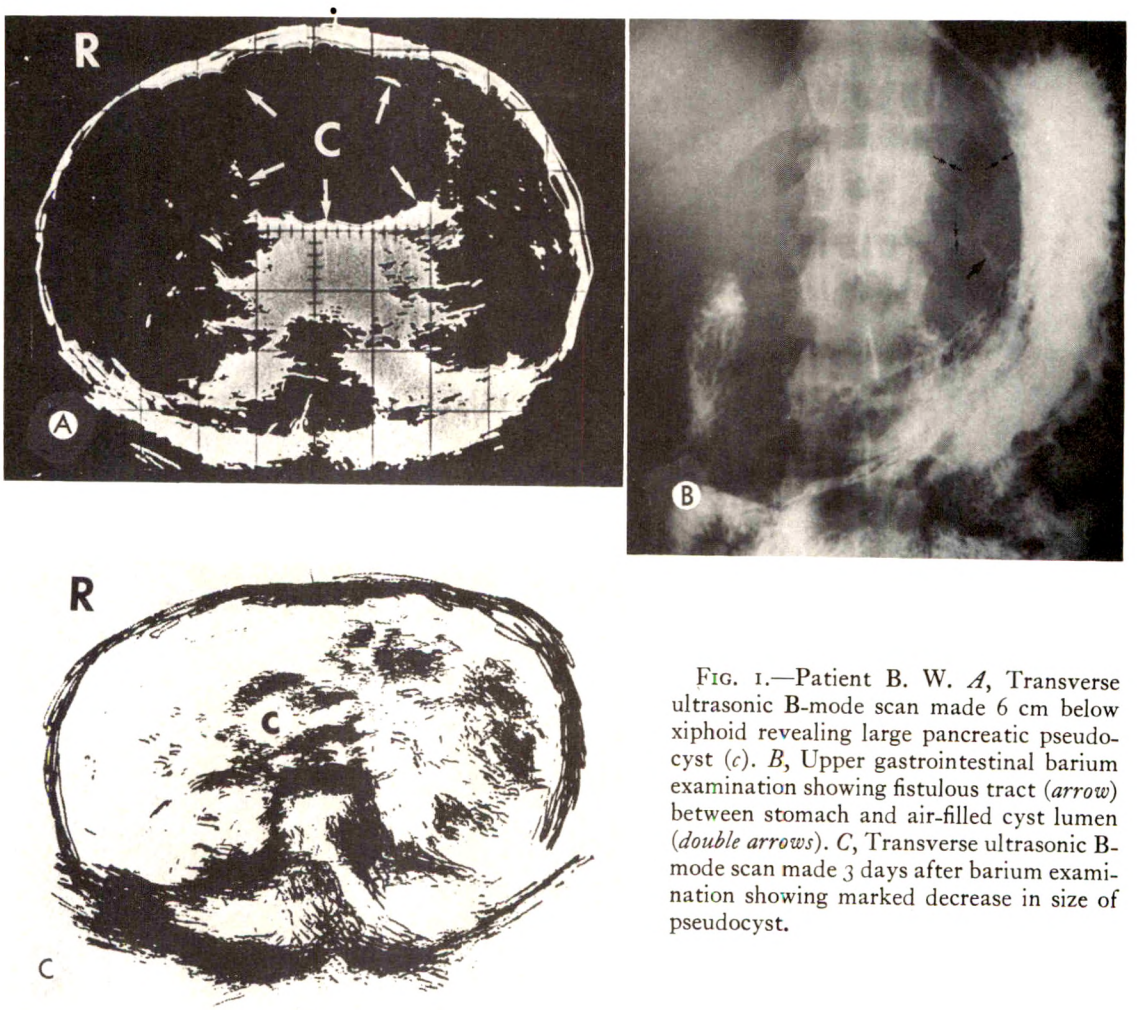
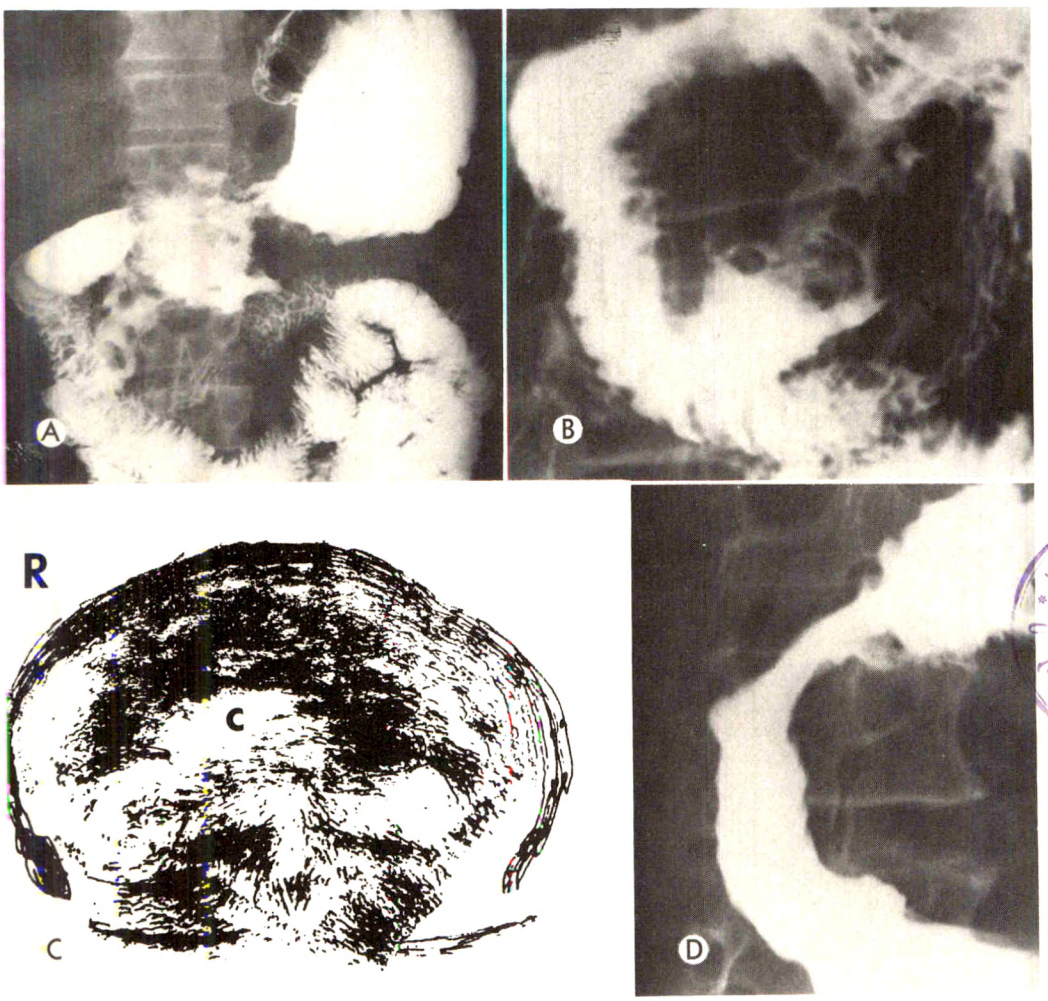


FIG. 1.—Patient B. W. *A*, Transverse ultrasonic B-mode scan made 6 cm below xiphoid revealing large pancreatic pseudocyst (*c*). *B*, Upper gastrointestinal barium examination showing fistulous tract (*arrow*) between stomach and air-filled cyst lumen (*double arrows*). *C*, Transverse ultrasonic B-mode scan made 3 days after barium examination showing marked decrease in size of pseudocyst.

TABLE 1

CLINICAL FEATURES

Patient	Age (Yr)	Sex	Alcoholism	Prior History of Pancreatitis (Yrs)	Days between Detection of Cyst and Spontaneous Drainage	Organ Involved	Effect of Drainage, on Immediate Course	Subsequent Course	Figure No.
B. W.	28	M	+	2	2	Stomach	Rapid improvement	One subsequent episode of pancreatitis	1
E. R.	61	M	+	0	5	Duodenum	Gradual improvement	Recent case; short follow-up	2
G. H. Y.	64	M	+	0	26	Left colon	Continued downhill	Died 36 days after drainage detected	3
E. R. F.	36	M	+	Several	Same	Duodenum	No effect	Continued intermittant pancreatitis; recurrent pseudocyst 8 mo later	4
M. M.	48	M	+	17	Same	Esophagus	Rapid improvement	Remained well for 18 mo; then died secondary to massive GI bleeding	5
C. M.	30	M	+	Several	Same	Duodenum	Gradual improvement	Lost to follow-up	



UNIVERSITY OF MEDICINE LIBRARY

FIG. 2.—Patient E. R. *A and B*, Barium upper gastrointestinal examination showing communication between duodenum and irregular pseudocyst cavity. *C*, Transverse ultrasonic B-mode scan made 10 cm below xiphoid revealing small pancreatic pseudocyst (*c*). *D*, Barium upper gastrointestinal examination made 19 days later showing that fistula has closed.

three a mass was palpable from 2 to 26 days before demonstration of internal drainage. The clinical effect of spontaneous internal decompression was quite variable and ranged from rapid improvement, through no apparent change, to continued downhill progression and death. In the three cases where long-term follow-up is available, alcoholism, cirrhosis, and/or recurrent pancreatic inflammation continued in all. There were three cases of internal communication between the pseudocyst and the duodenum. Solitary instances of communication between the pseudocyst and the esophagus, stomach, and colon occurred.

DISCUSSION

The natural history of pancreatic pseudocysts is incompletely understood: why some cyst walls rupture and others do not is unclear. The delimiting "wall" of an expanding pseudocyst is comprised of those structures (such as the posterior wall of the stomach, the transverse mesocolon, etc.) adjacent to the inflammatory collection. These components become thickened as inflammatory organization and fibrosis continue. Pseudocyst rupture apparently results from tryptic digestion of the wall. In

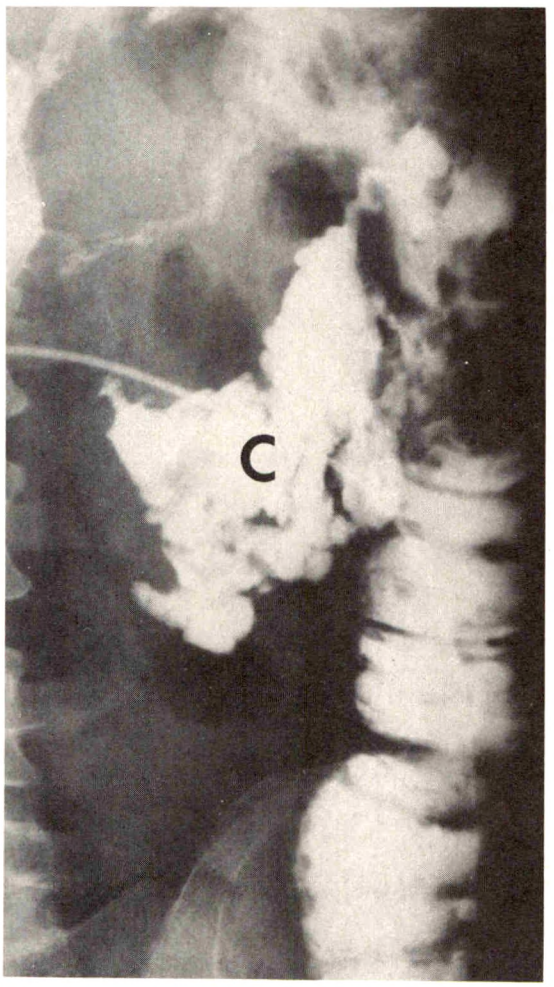


FIG. 3.—Fistulogram made into pseudocyst cavity (*c*) of patient G. H. Y. demonstrating spontaneous communication with splenic flexure of colon.

those cases where erosion into an adjacent hollow viscus occurs, digestion of the visceral wall and pressure necrosis produced by the expanding cyst are additional pathophysiologic factors.

It has been estimated that rupture occurs in something less than 5% of all cases of pancreatic pseudocyst [1]. About half such ruptures empty into the peritoneal cavity. This complication is of extreme severity; in the past more than 70% mortality has resulted [2]. If the diagnosis can be made promptly, however, vigorous operative treatment can save most of these patients [3]. In contrast to the dire potential consequences of free peritoneal rupture, erosion of a pseudocyst into the gastrointestinal tract is often beneficial: temporary or even permanent remission may result (table 1). Nevertheless, mortality from this "complication" is high (about 50%) [1] because many instances are associated with gastrointestinal hemorrhage [4] (as occurred in patients G. H. Y., E. R., and B. W.) and because infection (with conversion of the pseudocyst into an abscess) usually attends spontaneous drainage into the colon [5]. (This exact sequence was observed in patient G. H. Y.)

Radke and Bell [6] have described the entity of gastric intramural pseudocyst documented surgically. They believed that it was certainly possible that a pancreaticogastric fistula might have developed without surgical intervention. We believe that case C. M. (fig. 6) represents intramural dissection of the pseudocyst into the duodenal wall followed by rupture into the duodenal lumen.

While documentation has in some instances been incomplete, an analysis of the literature [1–5, 7–13] reveals 61 previously reported cases in which spontaneous communication between a pseudocyst and the gastrointestinal tract developed (table 2). On at least one occasion communication between a pseudocyst and the stomach has been observed and photographed gastroscopically (fig. 7). Rupture into the colon was most frequent (27 cases), while duodenal (16) and gastric (12) communications

TABLE 2

SPONTANEOUS INTERNAL DRAINAGE OF PANCREATIC PSEUDOCYSTS

Organ Involved	No. Cases Reported*	Present Series	Total
Esophagus	...	1	1
Stomach	12	1	13
Duodenum	16	3	19
Colon	27	1	28
Unspecified	6	...	6

* Data from [1–5, 7–13].

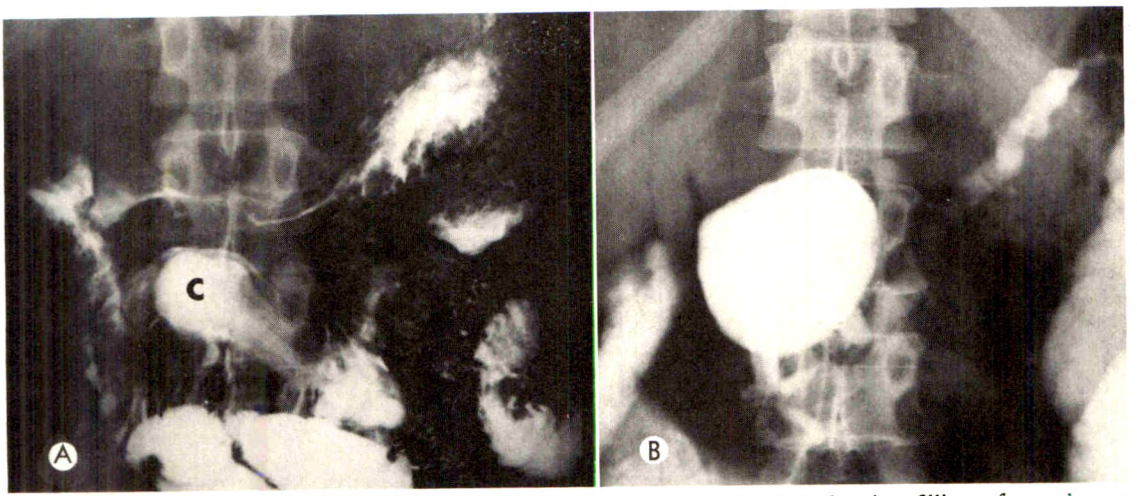


FIG. 4.—Patient E. R. F. *A*, Barium upper gastrointestinal examination showing filling of pseudocyst cavity (*c*) from third portion of duodenum. *B*, Operative pancreatogram 8 months after barium examination demonstrating recurrent pseudocyst.

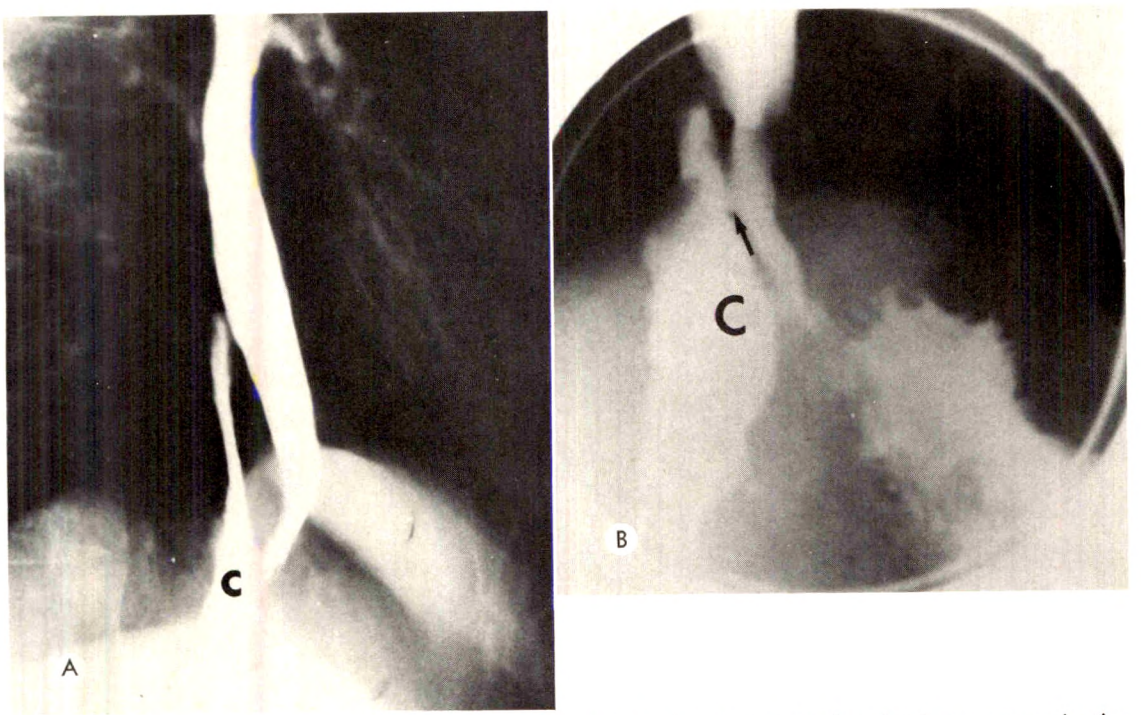


FIG. 5.—*A and B*, Upper gastrointestinal barium examination demonstrating fistulous communication (*arrow*) between lower esophagus and mediastinal pseudocyst (*c*).

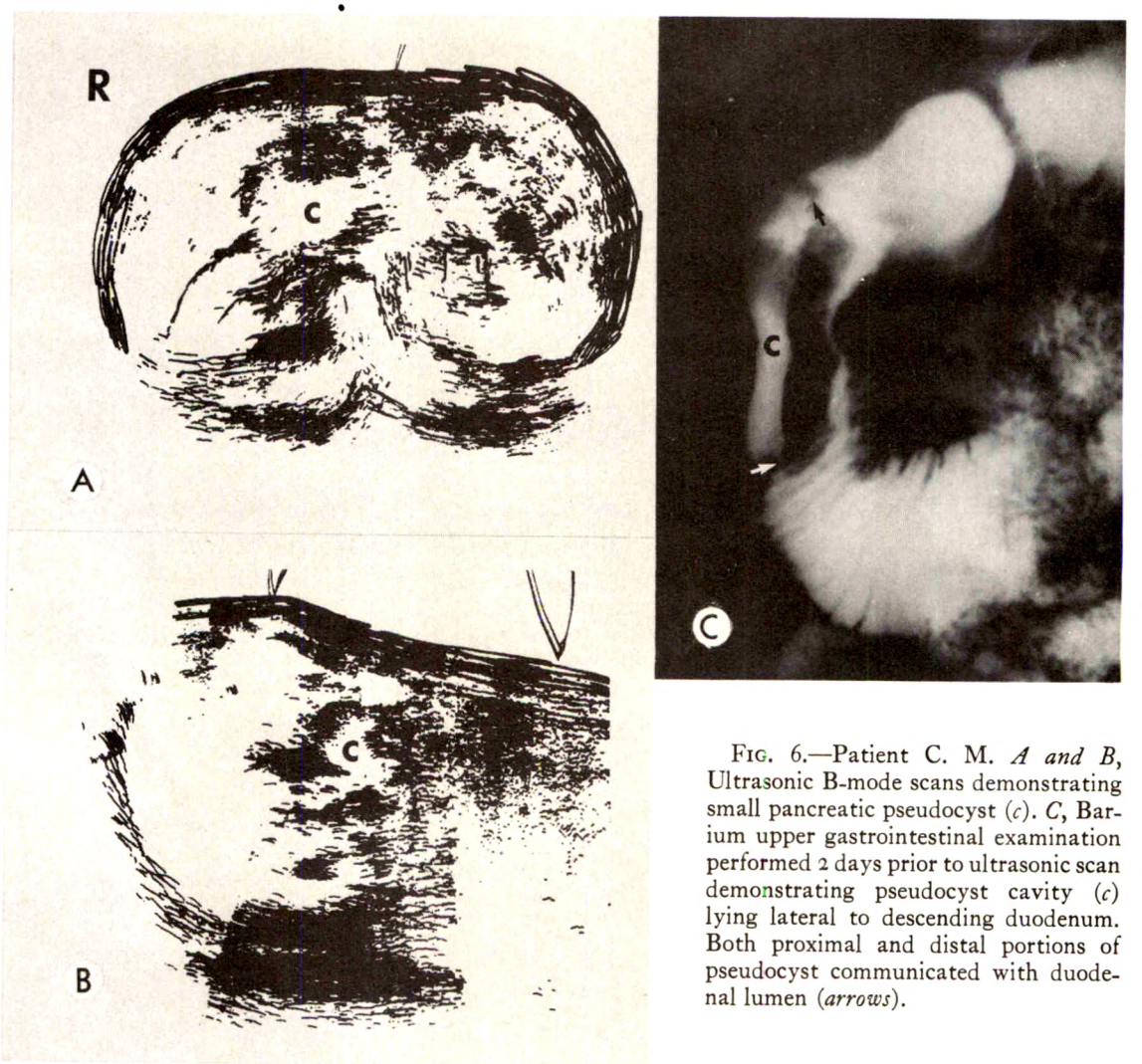
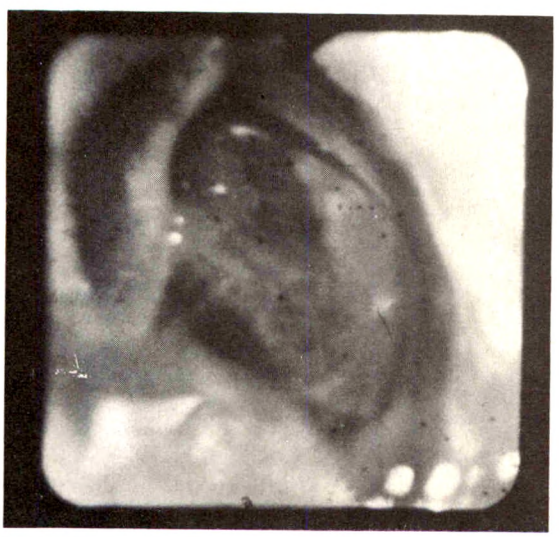


FIG. 6.—Patient C. M. *A and B*, Ultrasonic B-mode scans demonstrating small pancreatic pseudocyst (*c*). *C*, Barium upper gastrointestinal examination performed 2 days prior to ultrasonic scan demonstrating pseudocyst cavity (*c*) lying lateral to descending duodenum. Both proximal and distal portions of pseudocyst communicated with duodenal lumen (*arrows*).



were reported less commonly. To our knowledge communication between a pancreatic pseudocyst and the esophagus has never previously been described.

Since these six cases were observed over a relatively brief period in a single institution, it seems likely that the actual incidence of this phenomenon may be higher than has previously been recognized. Per-

FIG. 7.—Gastroscopic view into pancreatic pseudocyst which spontaneously communicated with stomach. (Courtesy of N. J. Greenberger, University of Kansas Medical Center)

haps the increasingly widespread application of ultrasonography in patients with pancreatic pseudocysts will provide documentation for this supposition.

REFERENCES

1. Hanna WA: Rupture of pancreatic cysts: report of a case and review of the literature. *Br J Surg* 47:495–498, 1960
2. Littmann R, Pochaczevsky R, Richter RM: Spontaneous rupture of a pancreatic pseudocyst into the duodenum. *Arch Surg* 100:76–78, 1970
3. Rosenberg LK, Kahn JA, Walt AJ: Surgical experience with pancreatic pseudocysts. *Am J Surg* 117:11–17, 1969
4. Greenstein A, DeMaio EF, Nabseth DC: Acute hemorrhage associated with pancreatic pseudocysts. *Surgery* 69:56–62, 1971
5. Berne TV, Edmondson HH: Colonic fistulization due to pancreatitis. *Am. J Surg* 111:359–363, 1956
6. Radke HM, Bell JW: Gastric intramural pseudocyst in chronic pancreatitis. *Am J Surg* 111:584–586, 1966
7. Koucky JD, Beck WA, Todd MC: The perforation of pancreatic pseudocysts: a report of six cases. *Surg Gynecol Obstet* 73:113–119, 1941
8. Becker WF, Pratt HS, Ganji H: Pseudocysts of the pancreas. *Surg Gynecol Obstet* 127:744–747, 1968
9. Thomford NR, Jesseph JE: Pseudocyst of the pancreas: a review of fifty cases. *Am J Surg* 118:86–94, 1969
10. Leopold GR, Berk RN, Reinke RT: Echographic-radiological documentation of spontaneous rupture of a pancreatic pseudocyst into the duodenum. *Radiology* 102:699–700, 1972
11. Guyer PB, Amin PH: Radiologic demonstration of spontaneous rupture of pancreatic pseudocysts. *Br J Radiol* 43:342–343, 1970
12. Barnado DE, Grogono JL, Parks AG: Spontaneous rupture of a pancreatic pseudocyst into the colon. *Digestive Dis* 19:1165–1167, 1974
13. Goldin AG, Wald H: Acute pancreatic pseudocysts with spontaneous drainage into descending colon. *J Ky Med Assoc* 63:98–100, 1965

Am J Roentgenol 126:992–1002, 1976

LUMBAR EPIDURAL VENOGRAPHY IN THE DIAGNOSIS OF DISC HERNIATIONS

RAZIEL GERSHATER[1] AND RICHARD C. HOLGATE[2]

ABSTRACT:

Epidural venography is a relatively simple and highly accurate method of diagnosing disc herniations in the lumbar region. Good opacification of the epidural venous plexus can be obtained by selective catheterization of ascending lumbar and/or internal iliac veins. Experience with 227 cases is described. The examination appears to be at least as accurate as myelography at the L4–L5 level and more reliable than myelography in cases of lateral disc herniations at L5–S1. Epidural venography is recommended as the examination of choice in patients with suspected lumbar disc herniation.

INTRODUCTION

The clinical and radiological diagnosis of lumbar disc herniation depends upon the demonstration of nerve root compression. The radiological approach of opacifying the subarachnoid space with oily and, more recently, water-soluble contrast agents, is usually diagnostic. There remains a group of patients with strong clinical evidence of disc herniation and "negative" myelography. In such patients, the nerve root is presumably compressed after it leaves the subarachnoid space, and other methods of investigation must be undertaken. Discography, nerve root injections, and epidurography are, in part, attempts to solve this problem. Epidural venography is a relatively new method of clarifying problematic lumbar disc herniations.

RADIOLOGIC ANATOMY

It has become increasingly evident to angiographers that venous anatomy is much more constant than heretofore appreciated. The rationale of epidural venography is founded on the knowledge that the anterior internal vertebral veins bear a constant relationship to the vertebral bodies and hence the intervertebral discs (fig. 1). The venous drainage of the axial skeleton and its musculature is via a segmental vertebral and paravertebral latticework of veins. Simply viewed, there are four vertical channels with segmental connections. Two of these channels run in the paravertebral gutters, and two (the anterior internal vertebral veins) run within the spinal canal.

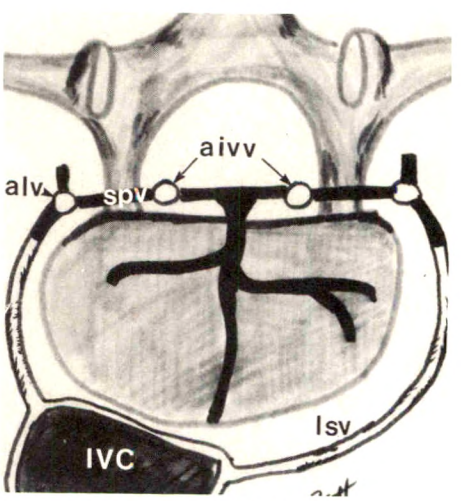


FIG. 1.—Diagram (axial view) showing intimate relationship of anterior internal vertebral veins (aivv) to backs of vertebrae. Four vertical channels are seen end-on as white dots. alv = ascending lumbar vein; spv = suprapedicular communicating vein; lsv = lumbar segmental vein; IVC = inferior vena cava.

[1] Department of Radiology, North York General Hospital, 4001 Leslie Street, Willowdale, Ontario, Canada M2K 1E1.
[2] Department of Radiological Sciences, Mount Sinai Hospital, University of Toronto, Toronto, Ontario.

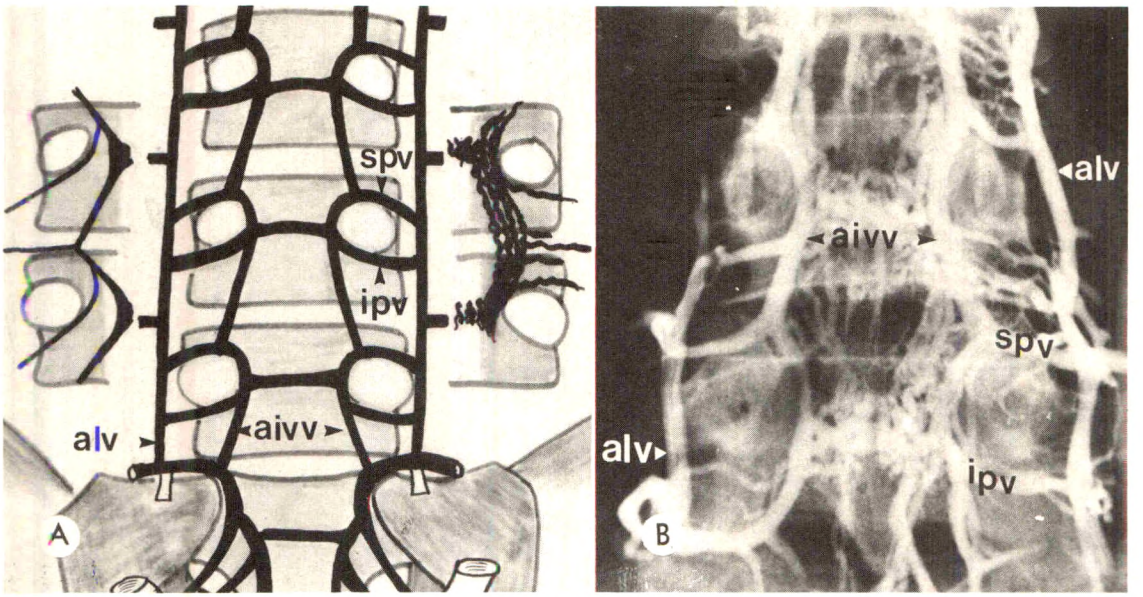


FIG. 2.—Diagrammatic (*A*) and angiographic (*B*) demonstration of epidural venus plexus. Inserts in fig 2A show common variations. alv = ascending lumbar vein; aivv = anterior internal vertebral vein; spv = supra-pedicular vein; ipv = infrapedicular vein.

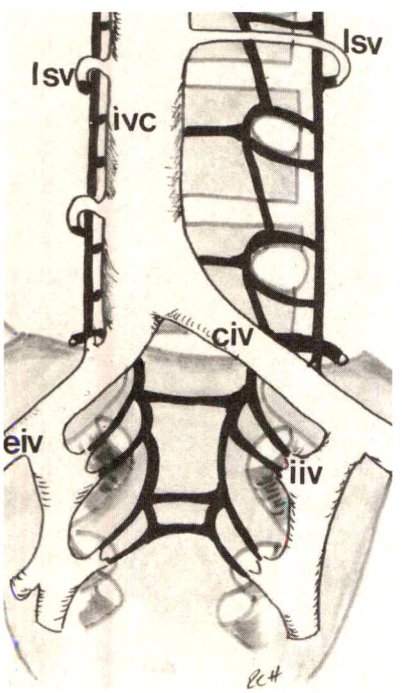


FIG. 3.—Diagram showing prevertebral abdominal veins (*white*) and paravertebral and epidural veins (*black*). ivc = inferior vena cava; eiv = external iliac vein; iiv = internal iliac vein; civ = common iliac vein; lsv = lumbar segmental vein.

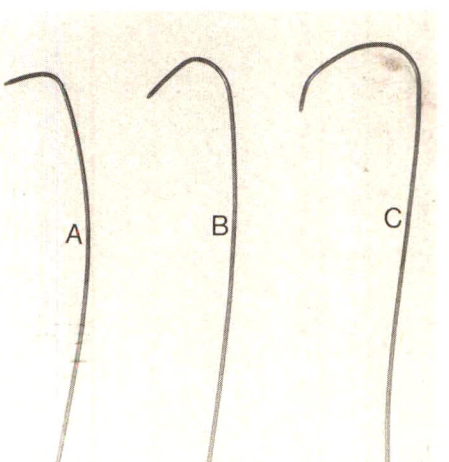


FIG. 4.—Catheters. *A*, Standard shape with 1½ cm curved tip for catheterization of ascending lumbar vein or internal iliac vein. *B* and *C*, Types which may be necessary for catheterization of ipsilateral or contralateral internal iliac veins, respectively.

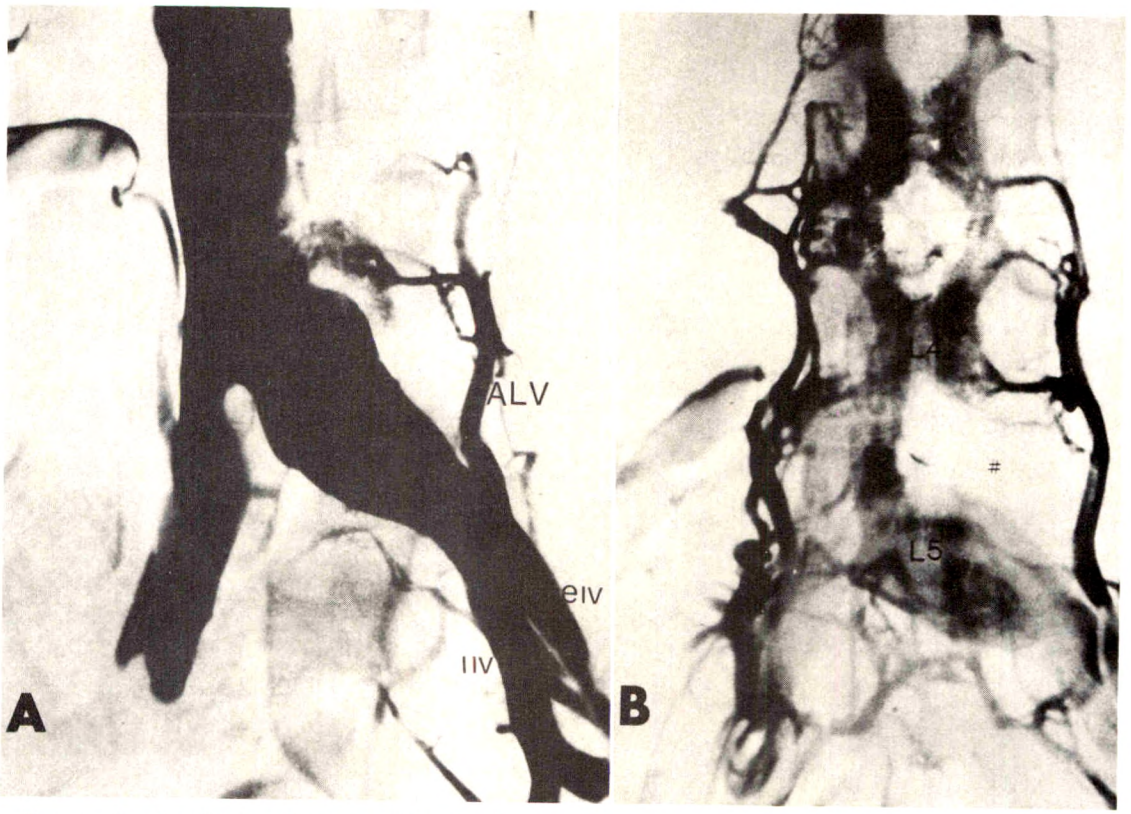


FIG. 5.—L4–L5 disc herniation on left. *A*, Injection of left ascending lumbar vein (ALV) showing reflux of most of contrast material into iliac veins (iiv and eiv) and inferior vena cava. *B*, Injection of right ascending lumbar vein clearly demonstrating occlusion of left anterior internal vertebral vein at L4–L5 (#). In this case, left internal iliac vein injection would probably have provided same information.

Epidural Veins

The anterior internal vertebral veins hug the backs of the vertebral bodies and discs. They are just medial to the pedicles and exhibit a tendency to bulge laterally between vertebrae. Lateral intervertebral branches connect them to the paravertebral channels above and below each pedicle. These branches have been variously named but are perhaps best referred to as suprapedicular and infrapedicular communicating veins. Cross-connections between the anterior internal vertebral veins as they course between the pedicles complete this simplified version of the lattice (figs. 2*A* and 2*B*).

The system of veins within the vertebral canal, the internal vertebral venous plexus, maintains the form described above but is slightly more complex. Venous blood from the vertebral bodies drains into the cross-connections between the anterior internal vertebral veins. The drainage of the less voluminous posterior elements is via a correspondingly smaller chain of longitudinal veins—the posterior internal vertebral veins. The anterior and posterior chains connect around the dural sac producing an envelope of veins that separates the dura and its contents from their osseous and fibrocartilaginous container. The posterior veins are not always filled or identified

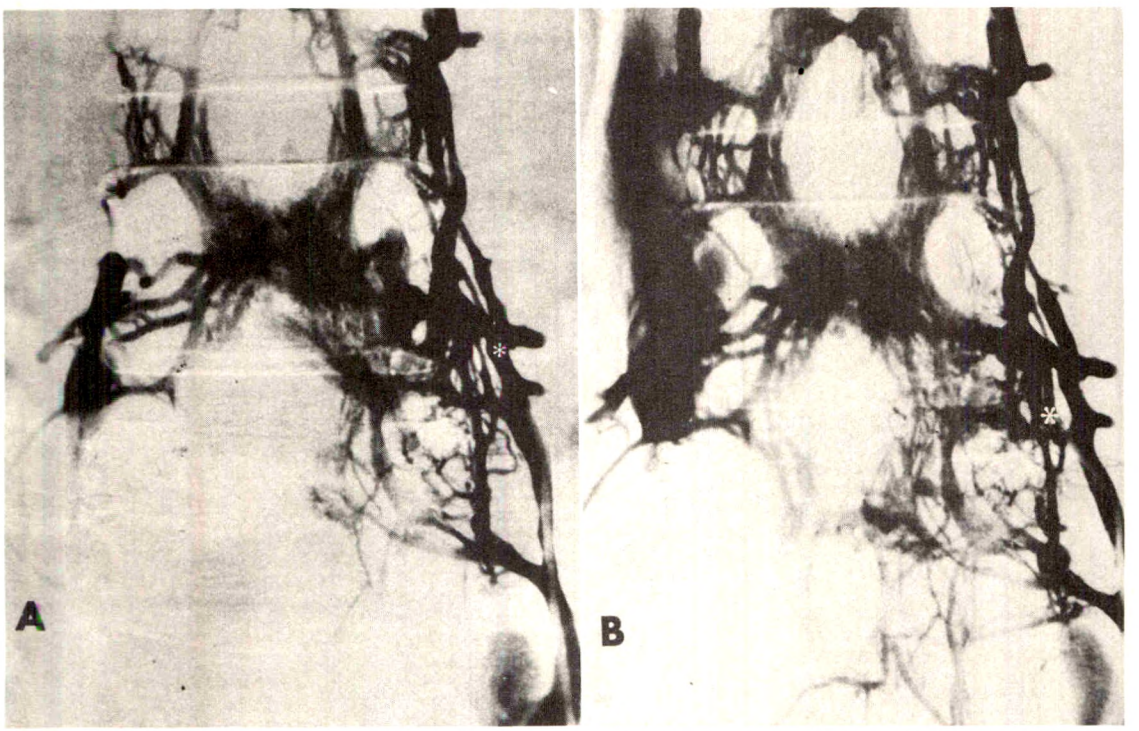


FIG. 6.—Normal case. *A*, Left ascending lumbar vein injection. Catheter tip (*) at L4–L5 level showing normal epidural veins from L3–L4 upward. No conclusions can be drawn about lower levels because of inadequate filling with contrast material. *B*, Catheter withdrawn slightly with tip (*) placed into suprapedicular vein at L4–L5. Injection of contrast there shows lower levels to be within normal limits.

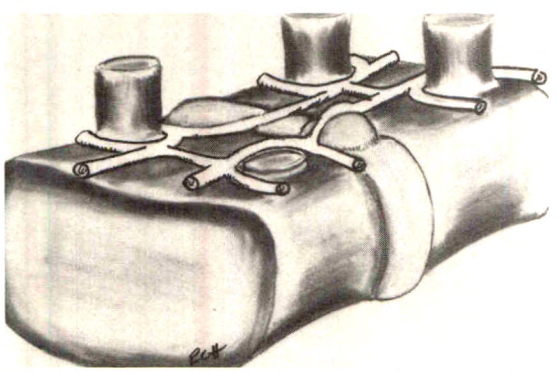


FIG. 7.—Diagrammatic representation of disc herniation. Anterior internal vertebral vein displaced directly backward. Depending on location of bulge, it is easy to visualize medial or lateral displacement. The most common and reliable angiographic finding is nonfilling due to compression.

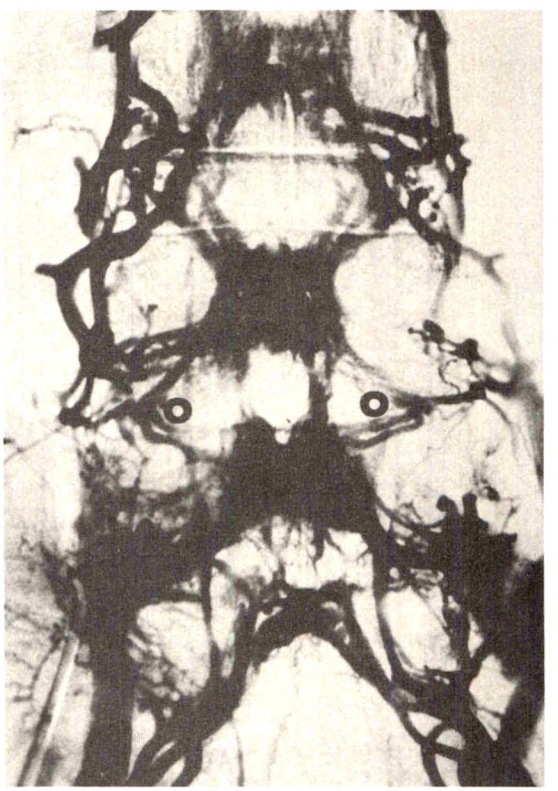


FIG. 8.—L4–L5 disc herniation; right ascending lumbar vein injection. Lateral deviation of anterior internal vertebral veins is demonstrated bilaterally at L4–L5 (*open circles*).

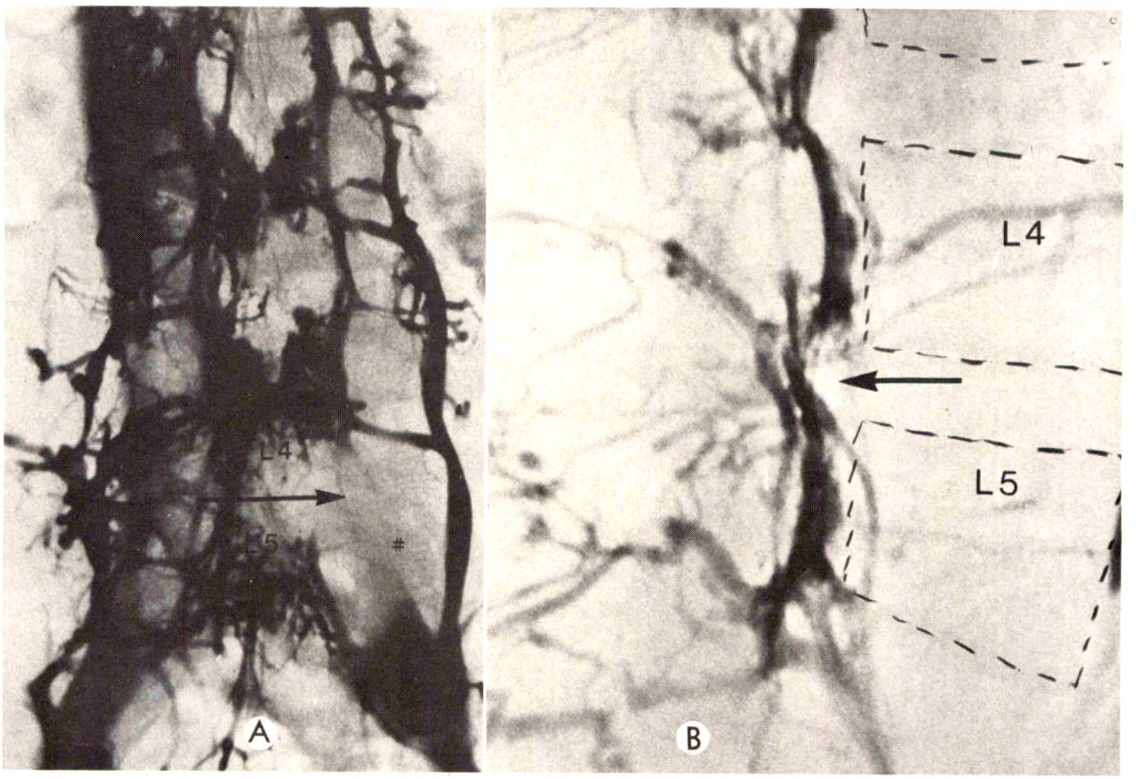


FIG. 9.—Left L4–L5 disc herniation; right ascending lumbar vein injection. *A*, AP view showing obstruction of left anterior internal vertebral vein (*arrow*) and suprapedicular vein (#). Note that all epidural vessels near obstructed veins are well opacified. *B*, Lateral view showing venous displacement at L4–L5 (*arrow*). Veins at L5–S1 level were shown to be normal on injection of internal iliac vein.

during transfemoral venography.

Paravertebral Chain

The longitudinal paravertebral venous channels change their names as they course from clivus to coccyx (e.g., vertebral veins in the neck, azygous and hemiazygous veins in the chest, ascending lumbar veins in the abdomen, and internal iliac veins in the pelvis). The paravertebral system communicates with the caval system in multiple locations. The vertebral veins that run with the vertebral arteries join the subclavian veins just medial to the internal jugular veins. The azygous and hemiazygous veins join the superior vena cava above the right atrium. The ascending lumbar veins, abdominal analogues of the azygous system, connect to the common iliac veins just as they cross the ala of the sacrum. In addition, the ascending lumbar veins connect directly to the inferior vena cava by means of segmental veins which course around the vertebral bodies (figs. 1 and 3). These paravertebral-caval connections allow for ready access via catheters to the epidural venous system.

Variations

For the most part venous anatomy shows variation in number and size rather than presence and absence. The ascending lumbar veins may be rudimentary and difficult to catheterize (see later). The individual

veins of the internal plexus and the communicating peripedicular veins may be represented by single or multiple channels, a multitude of fine veins, or a broad flat sheath. In any one patient there is side-to-side symmetry and level-to-level similarity.

METHOD

The lumbar epidural venous plexus can be opacified by catheterization and injection of contrast material into the ascending lumbar or internal iliac veins. Usually the examination is begun on the symptomatic side, but this is not crucial since there are no valves in the epidural veins and therefore good cross-filling generally occurs. The transfemoral approach is used.

A 35-cm no. 5 French end-hole polyethylene catheter and a straight 0.038-inch diameter guidewire are used. An injection 30–40 cm^3 of Renographin 76 or 60 (Squibb) is made into either the ascending lumbar or internal iliac vein at a flow rate of 5 cm^3/sec. The denser contrast agent is preferred, but it does cause the patient low back pain for about 20 sec. Injection of the less concentrated agent is relatively painless. Eight films are taken over a 12 sec period, preferably with 2:1 direct serial magnification. To decrease reflux into the common iliac veins and inferior vena cava, external abdominal compression and the Valsalva maneuver are used.

The frontal projection contains most of the diagnostic information. Oblique views are rarely of any value. Lateral films can sometimes be useful, particularly in cases of suspected spinal stenosis.

The catheter shapes are shown in figure 4. Catheter A is advanced into the ipsilateral ascending lumbar vein that arises from the superior margin of the common iliac vein, very close to the sacrovertebral angle (fig. 5). Frequently, after the guidewire has been inserted into the common femoral vein, some resistance is felt as it is being advanced towards the inferior vena cava because it has spontaneously entered the ascending lumbar vein. Usually the catheter cannot be advanced more than 1–3 cm into the ascending lumbar vein.

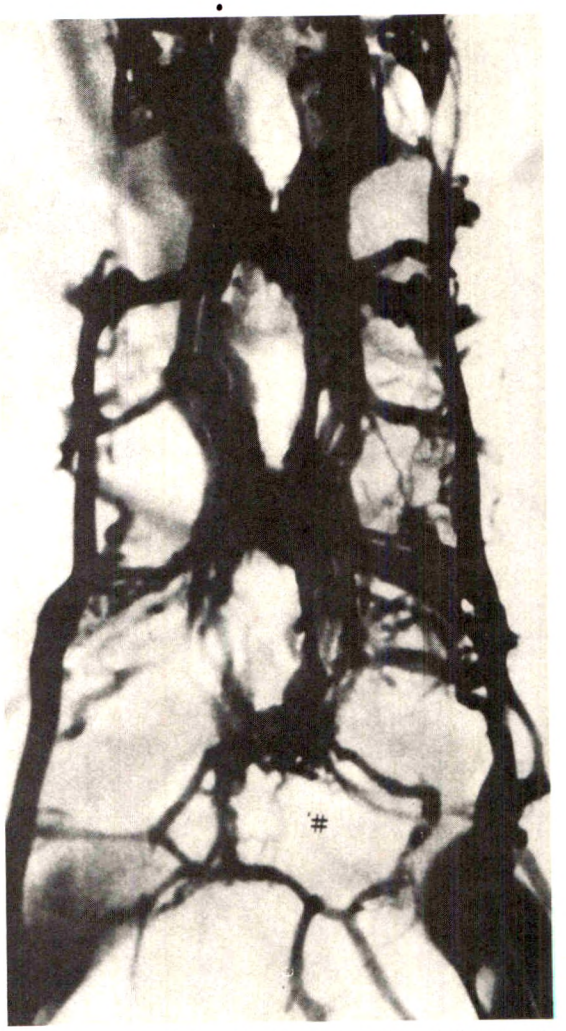


FIG. 10.—Left L5–S1 disc herniation; left ascending lumbar vein injection. Left anterior internal vertebral vein is obstructed at L5–S1 (#). Note that all veins about obstructed vein are well opacified.

If the epidural venous plexus is well opacified on the first ascending lumbar vein injection, the examination is terminated. If there is an unfilled vein, usually an anterior internal vertebral vein, it must be determined whether contrast material has been adequately presented to that vein. In other words, all the epidural veins proximal and distal to the unfilled vein must be well opacified. If this prerequisite is not satisfied, further contrast injections are necessary (fig. 6). This occurs most frequently at the L5–S1 level, where cross-

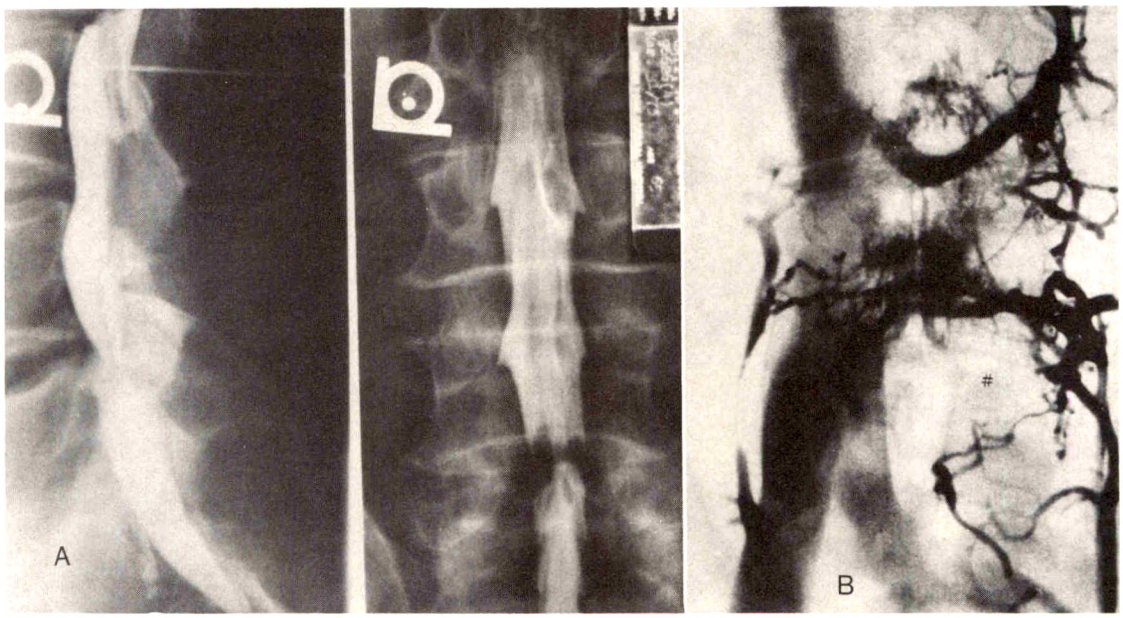


FIG. 11.—L4–L5 central disc herniation. *A*, Myelogram. *B*, Venogram (left ascending lumbar vein injection) showing obstruction of all epidural veins at L4–L5 (#). Enlarged connecting veins have opened up between epidural plexus and extravertebral veins. An internal iliac vein injection was necessary to show that L5–S1 level was normal.

filling of the anterior internal vertebral veins is not as reliable as at the higher levels. The ipsilateral internal iliac vein should then be catheterized (fig. 5). Usually the original catheter can be used for this second vessel, but it is sometimes necessary to switch to another shape (fig. 4, *B*).

In the unusual event that opacification is still unsatisfactory, the contralateral internal iliac vein should be catheterized, again with the original catheter, or, if necessary, after changing to another (fig. 4, *C*). After the catheter has been passed over to the opposite common iliac vein, it tends to naturally enter the internal iliac vein as it is advanced. Often it is possible to manipulate the catheter tip medially from the internal iliac vein into one of the sacral segmental veins. Injection of these leads to particularly good opacification of the epidural plexus.

Assuming the examination goes smoothly and only one or two film series are required, the entire procedure takes only about 20 min. Even if multiple injections are needed, the examination can be completed in about 45 min. Most of our venograms are done on an outpatient basis, which is a distinct advantage over myelography. The patients accept the procedure very well, and for many of them it is less traumatic emotionally than having a myelogram.

Complications

The potential complications of epidural venography are the same as for any femoral vein catheterization and intravenous injection of iodinated contrast material. In 227 cases, only one minor complication occurred—some haemorrhage into the soft tissues around the puncture site in the groin.

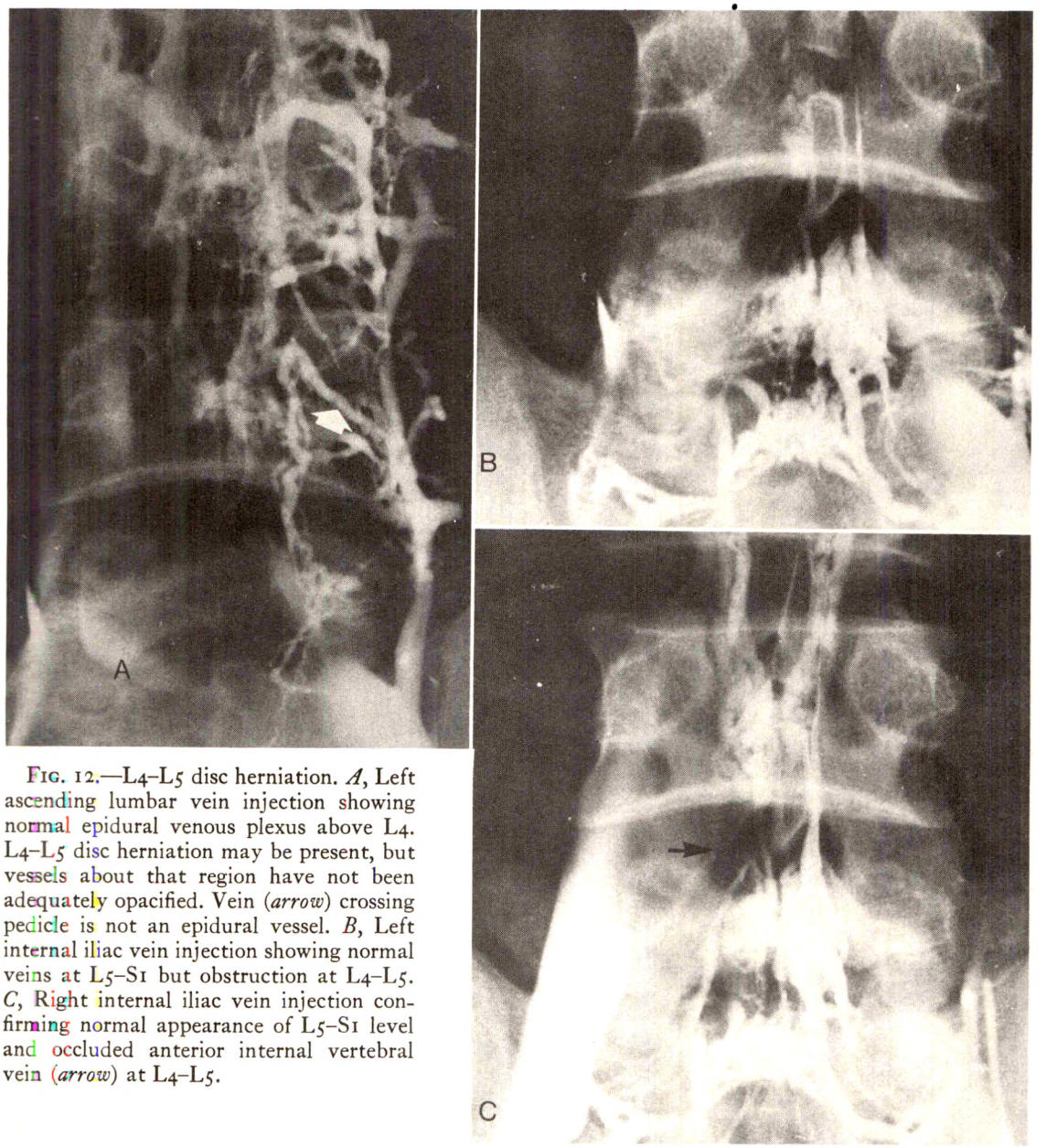


FIG. 12.—L4–L5 disc herniation. *A*, Left ascending lumbar vein injection showing normal epidural venous plexus above L4. L4–L5 disc herniation may be present, but vessels about that region have not been adequately opacified. Vein (*arrow*) crossing pedicle is not an epidural vessel. *B*, Left internal iliac vein injection showing normal veins at L5–S1 but obstruction at L4–L5. *C*, Right internal iliac vein injection confirming normal appearance of L5–S1 level and occluded anterior internal vertebral vein (*arrow*) at L4–L5.

FINDINGS

The venographic signs of lumbar disc herniation are produced when the herniating disc gradually compresses, thins, displaces, and finally obstructs the adjacent veins. This is particularly true of the anterior internal vertebral veins which lie immediately adjacent to the intervertebral discs. The positive findings have been well described by Gargano et al. [2]. Briefly, the two most important signs are:

1. Abnormal curvature of an anterior internal vertebral vein (figs. 7 and 8). The vein is usually bowed laterally on the anteroposterior view of the venogram, being displaced posterolaterally by the herniated disc. However, the direction of the displacement varies and may be medial, depending upon the direction of the disc herniation.

2. Unilateral or bilateral occlusion of the anterior internal vertebral vein as it

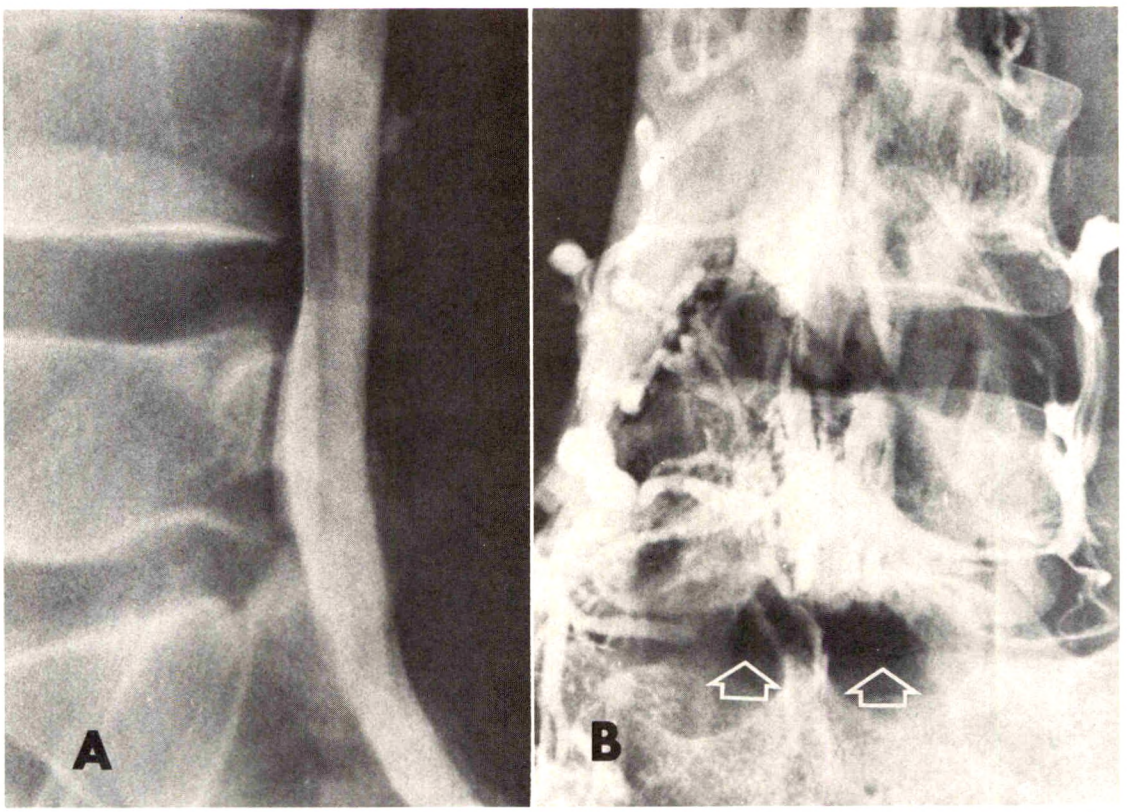


FIG. 13.—L5–S1 disc herniation. *A*, Normal myelogram. *B*, Venogram (right ascending lumbar vein injection) showing blocked epidural veins at L5–S1 (*arrow*). Internal iliac vein injection produced similar picture. Lateral disc herniations at L5–S1 can be particularly difficult to demonstrate with myelography [1] and, at this level, epidural venography appears to be the more reliable investigation. We have examined a number of such cases.

crosses the disc interspace (figs. 5, and 9–14). Suprapedicular vein occlusion often occurs as well but is a secondary feature and taken alone, is of questionable significance. Sometimes complete block of both anterior internal vertebral veins will prevent filling of the epidural plexus above the level of the herniation (fig. 11). Note that if a vein crosses a pedicle on the AP view, it cannot be an epidural vein (fig. 12).

Supplementary findings are localized dilatation of epidural and extravertebral veins and opening of collateral channels around the obstructed veins (fig. 11).

The pattern of the epidural venous plexus varies considerably among patients, but in each individual it is remarkably symmetrical on the two sides; any localized asymmetry should raise suspicion of an abnormality. It should be emphasized again that a vein should not be judged occluded unless all the veins about the unopacified segment are well filled with contrast material (fig. 6). In patients who have had discotomies or laminectomies, the epidural veins are usually occluded at the levels of the previous surgery. In one case of an L4–S1 spinal fusion, many small epidural veins had developed all along the fusion.

Several examples of epidural venograms (figs. 5, 6, and 8–14) are presented to illustrate the significant diagnostic features and

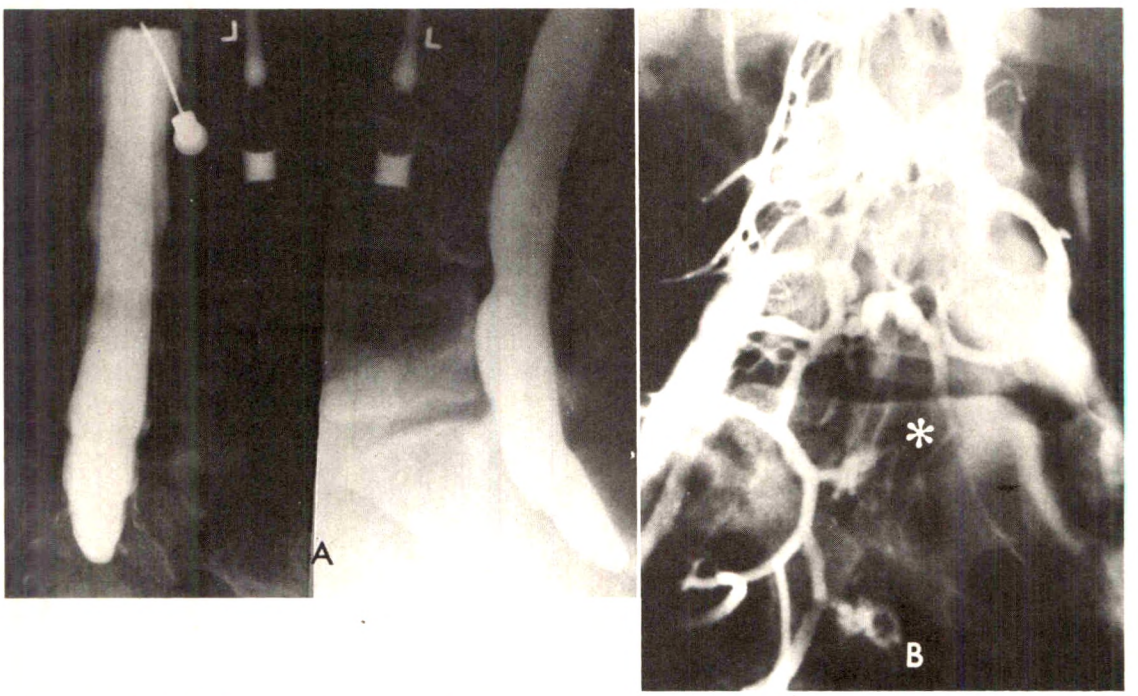


FIG. 14.—Left L5–S1 disc herniation. *A*, Myelogram showing anterior defect at L4–L5 and possible flattening of contrast column at L5–S1 on lateral view. *B*, Venogram (right ascending lumbar vein injection) showing incomplete filling of left anterior internal vertebral vein at L5–S1 (*); L4–L5 level appears normal. At surgery, a left disc herniation was found at L5–S1 and osteophytes with normal disc at L4–L5.

to show the sequence of injections used. All positive examples have been confirmed at surgery.

DISCUSSION

We have so far studied 227 patients. Complications such as contrast reactions, pulmonary emboli and thrombophlebitis, although considered inevitable, have not yet occurred. A statistical analysis of our material is not presented, but our experience regarding reliability is similar to that of others [2–4]. The selective catheterization method is clearly superior to the transosseous approach [5, 6].

The usefulness of epidural venography is well established in patients with a good clinical picture of herniated disc and a nondiagnostic myelogram (e.g., negative, insensitive, inadequate, or equivocal). Patients accept and tolerate the procedure well and do not harbor the usual fears held for myelography. Another very important advantage of venography is its usefulness in the diagnosis of extreme lateral disc herniations. In these cases, myelography is usually negative [1], whereas the venogram is diagnostic. Because of accuracy, reliability, low complication rate, and ease of performance, venography is recommended as an alternative rather than an adjunct to myelography. These features, along with the notable absence of postprocedure headache, have led us to perform the examination on outpatients.

In two-thirds of the 227 patients studied, myelography was considered unnecessary. A total of 170 examinations were done on an outpatient basis; patients were observed and kept at rest for 2 hr after the procedure. Of the 227 cases, 152 were positive for disc herniation, 60 of the venograms were nor-

mal, and eight were inadequate. Five extradural and two intradural neoplasms were found and produced changes sufficiently different from disc disease to prompt myelography. There has been one false positive among the 130 surgically explored cases. We await, as all investigators must, the return of the false negative cases.

ACKNOWLEDGMENTS

We thank the orthopaedic surgeons and neurologists at our hospitals for their support and cooperation. Also, thanks to Bella Chang Fong and Elizabeth Hughes for their assistance, and to Rita Hosking and Christine Bobkowski for typing this manuscript.

REFERENCES

1. Abdullah AF, Ditto EW III, Byrd BB, Williams R: Extreme-lateral lumbar disc herniations. Clinical diagnosis and special problems of diagnosis. *J Neurosurg* 41:229–234, 1974
2. Gargano FP, Meyer JD, Sheldon JJ: Transfemoral ascending lumbar catheterization of the epidural veins in lumbar disc disease. *Radiology* 111:329–336, 1974
3. Miller M, Handel S, Coan J: Lumbar epidural venography experience in over 75 cases. Paper presented at the annual meeting of the American Society of Neuroradiology, Vancouver, B.C., June 1975
4. Schobinger RA, Krueger EG, Sobel GL: Comparison of intraosseous vertebral venography and Pantopaque myelography in the diagnosis of surgical conditions of the lumbar spine and nerve roots. *Radiology* 77:376–397, 1961
5. Finney LA, Gargano FP, Buermann A: Intraosseous vertebral venography in the diagnosis of lumbar disc disease. *Am J Roentgenol* 92:1282–1292, 1964
6. Schobinger RA, Krueger EG: Intraosseous epidural venography in the diagnosis of surgical diseases of the lumbar spine. *Acta Radiol* 1:763–776, 1963

Am J Roentgenol 126:1003–1009, 1976

TRANSFEMORAL LUMBAR EPIDURAL VENOGRAPHY

MARK H. MILLER,[1] STANLEY F. HANDEL, AND JOHN D. COAN

ABSTRACT:

Lumbar epidural venography performed in 107 patients with normal or nondiagnostic myelograms resulted in correct preoperative diagnosis in 25 of 27 patients (92%) with herniated disc disease and three of six patients (50%) with nerve root compression without associated disc herniation. Compression or occlusion of an epidural and/or radicular vein at the disc level is the most significant venographic abnormality. Potentially confusing venographic findings such as flow defects, extravertebral veins mimicking epidural veins, and occlusion of radicular veins by the catheter must be recognized to prevent false diagnoses. Lumbar epidural venography is valuable for the diagnoses of herniated lumbar discs not demonstrated by myelography.

Angiographic visualization of the epidural veins was first reported in 1954 when accidental wedging of a catheter took place during infant heart catheterization [1]. Subsequently, disc disease was investigated by intraosseous injection of contrast into the lumbar spinous processes [2–5] and by contrast injection into the iliac or lower extremity veins [6, 7]. These techniques have not achieved widespread use because of limitations involving pain as well as inconstant opacification. Selective catheterization of the ascending lumbar vein improves filling of the epidural venous plexus. This technical advancement permitted excellent results in the diagnosis of lumbar disc disease [8–10]. In this report we relate our experience with transfemoral lumbar epidural venography in 105 patients, 38 of whom underwent surgical exploration.

MATERIALS AND METHODS

After medicating the patient, both inguinal regions are prepared for femoral vein puncture. The left femoral vein is punctured initially, and a no. 5 French polyethylene catheter is introduced under fluoroscopic control into the left ascending lumbar vein by Seldinger technique (fig. 1). The left ascending lumbar vein has proven easier to locate and enter than the right one. Alternatively, injection of the left or right internal iliac vein or small sacral branches of common iliac vein will also opacify the epidural venous plexus, but generally to a lesser degree than when an ascending lumbar vein is used.

Following selective venous catheterization, tight abdominal compression and the Valsalva maneuver are employed during contrast injection. Approximately 35–40 cm^3 ov 76% iodide contrast are injected at the rate of 2–9 cm^3/sec. One film per second is obtained for 10 sec in the frontal projection. If a second projection is needed, a lateral-oblique series using the horizontal x-ray tube is employed, since this view avoids superimposition of ascending lumbar veins and anterior epidural veins. A true lateral view may also be obtained.

RADIOGRAPHIC INTERPRETATION

The entire lumbar venous plexus can be opacified by injection of the ascending lumbar vein since the system is valveless. Each ascending lumbar vein usually arises from the common iliac vein between the vertebral column and the sacroiliac joint. Radicular veins bridge the ascending lumbar vein to the epidural veins within the spinal canal. We have observed that at least two radicular veins lie within the neural foramen of the lumbar spine and that the inferior radicular vein relates most closely to the posterolateral aspect of the intervertebral disc (fig. 2). Within the

[1] All authors: Department of Diagnostic Radiology, University of Texas Medical School at Houston, Hermann Hospital, Houston, Texas 77025.

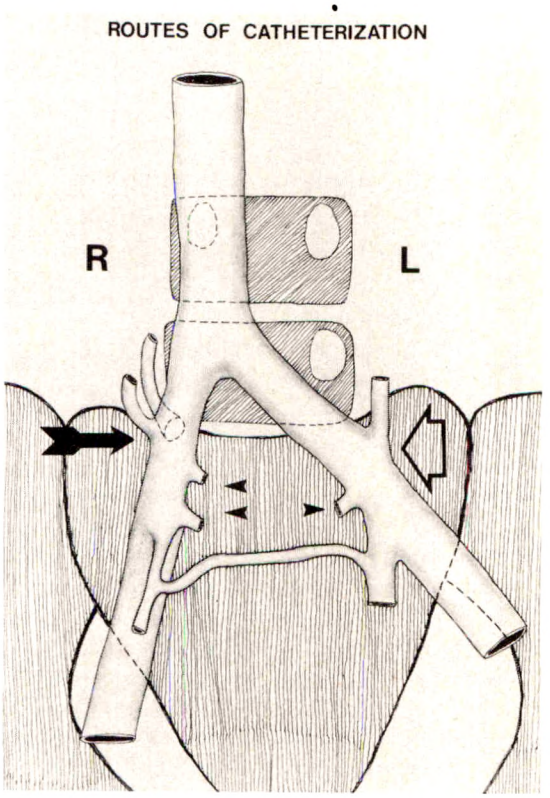


FIG. 1.—Routes of venous catheterization. Left ascending lumbar vein (*open arrow*) is usually readily accessible for catheterization. Alternative veins include left and right sacral veins (*arrowheads*) and right ascending lumbar vein (*closed arrow*).

spinal canal the most important veins are the anterior epidural longitudinal veins outlining the width of the spinal canal on the frontal projection (fig. 2). Occasionally the two separate chains are replaced by a broad sheath of veins (fig. 3). The lateral-oblique projection reveals the intimate relationship of the anterior epidural veins to the posterior aspects of the vertebral bodies and discs at all lumbar levels, including L5–S1 (fig. 4). A herniating disc must transverse this epidural space containing the epidural veins before impinging on the caudal sac.

RESULTS

Diagnostic opacification of the epidural and radicular veins occurred in 100 of 107 attempted examinations (93%). Failure to obtain adequate examinations resulted from poor filling of the veins in four patients and inability to find a suitable vein in three patients. Retroperitoneal extravasation of contrast from the ascending lumbar vein occurred in four patients with no significant clinical sequelae in three. The fourth patient experienced diarrhea and abdominal cramps but subsequently did well. Because of the potential danger of retroperitoneal bleeding, patients are not heparinized.

Compression or occlusion of epidural and radicular veins are the most important signs of intervertebral disc disease. The entire epidural chain (fig. 5) or only a por-

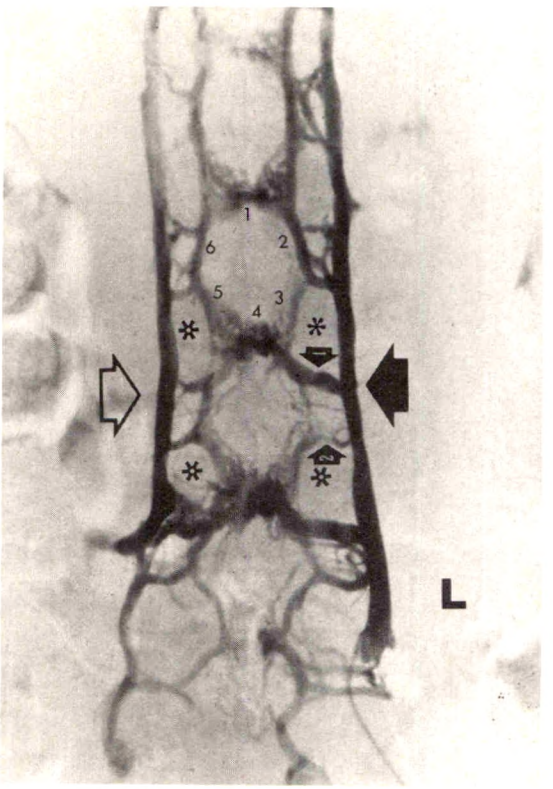


FIG. 2.—Normal frontal epidural venogram. Injection of left ascending lumbar vein (*closed arrow*) opacifies two radicular veins in each neural foramen (*vertical arrows*), and the anterior epidural veins simulate a "stack of hexagons." Struts 3 and 5 cross disc space. Each pedicle (*asterisk*) is outlined by a venous monocle. Cross-filling opacifies right ascending lumbar vein (*open arrow*).

tion of the chain (fig. 6) may be occluded on the side of disc herniation. Displacement of a vein by a bulging intervertebral disc without compression is not considered evidence of a herniated disc.

The interpretation of the venogram was proven correct in 33 of the 38 patients who underwent surgical exploration, for an accuracy rate of 87%. In this operated group, abnormal venograms were present in 25 patients with herniated discs, three with nerve root entrapment without disc herniation, one with intraspinal neurilemmoma, and one with discitis and osteomyelitis. Three patients had a normal venogram and a negative back exploration.

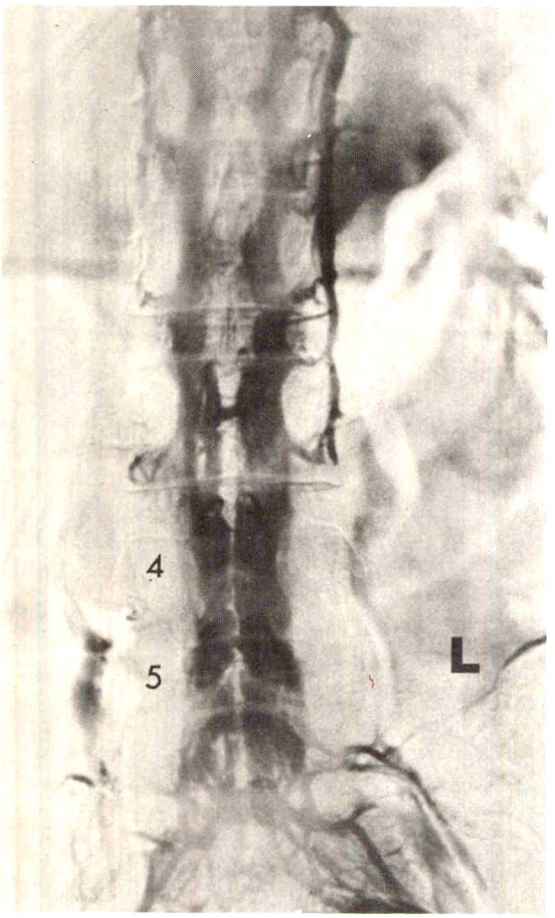


FIG. 3.—Normal frontal epidural venogram. Broad sheaths of anterior epidural veins replace more common form of two longitudinal chains. Radicular veins at L4–L5 and L5–S1 do not fill.

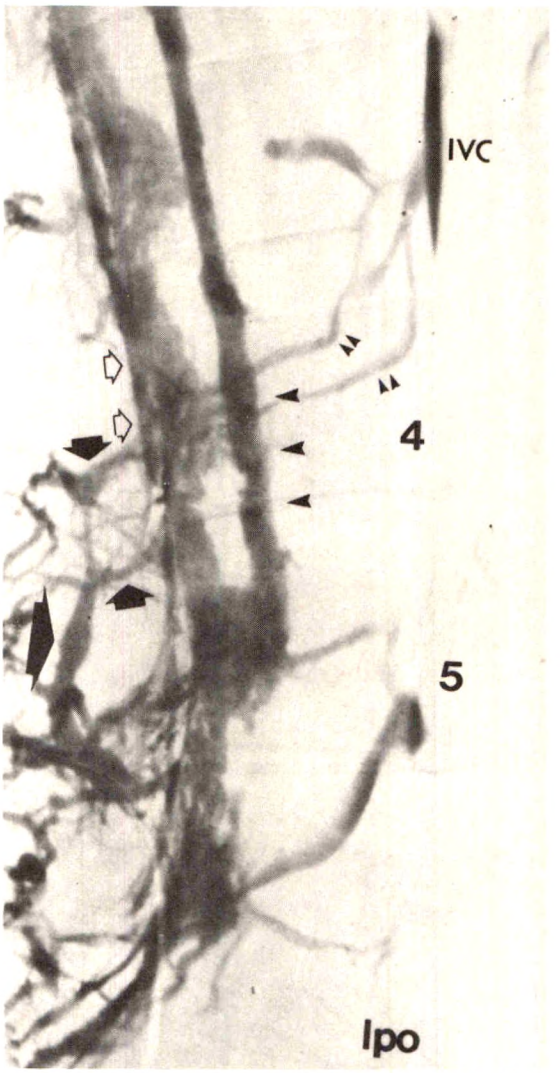


FIG. 4.—Normal lateral-oblique venogram. Left ascending lumbar vein injection (*large arrow*) opacifies two radicular veins (*vertical arrows*), left anterior epidural chain (*open arrows*), and right anterior epidural chain (*three arrowheads*). Extravertebral lumbar veins (*paired arrowheads*) connect left ascending lumbar vein to inferior vena cava (IVC).

There were no false positive diagnoses in the operated group; an abnormal venogram was associated with definite pathology in all cases. Five false negative venograms occurred with two herniated discs and three nerve root entrapments found at surgery. Thus the venogram detected 25 of 27 disc herniations (92%) but proved less effective in other conditions causing

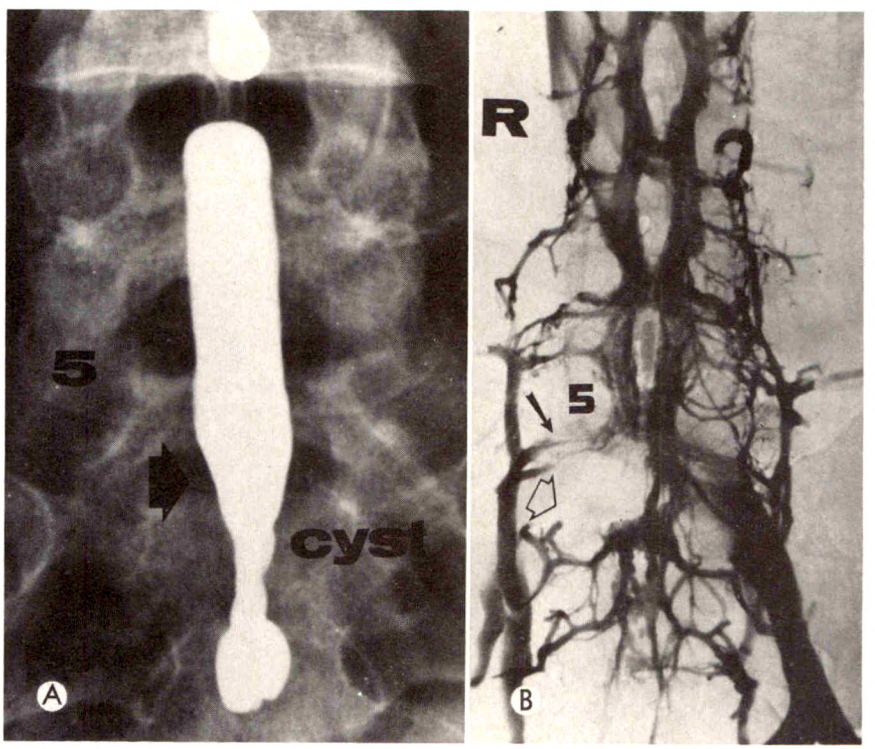


FIG. 5.—*A*, Myelogram demonstrating slight straightening of L5–S1 portion of caudal sac on right (*arrow*). Spinal arachnoid cyst is present in sacrum. *B*, Epidural venogram of same patient showing occlusion of inferior radicular vein at L5–S1 on right (*open arrow*). Entire right anterior epidural chain at same level is occluded. Opacification of two superior radicular veins is present (*closed arrow*). At surgery, a large herniated disc was present at L5–S1 on right.

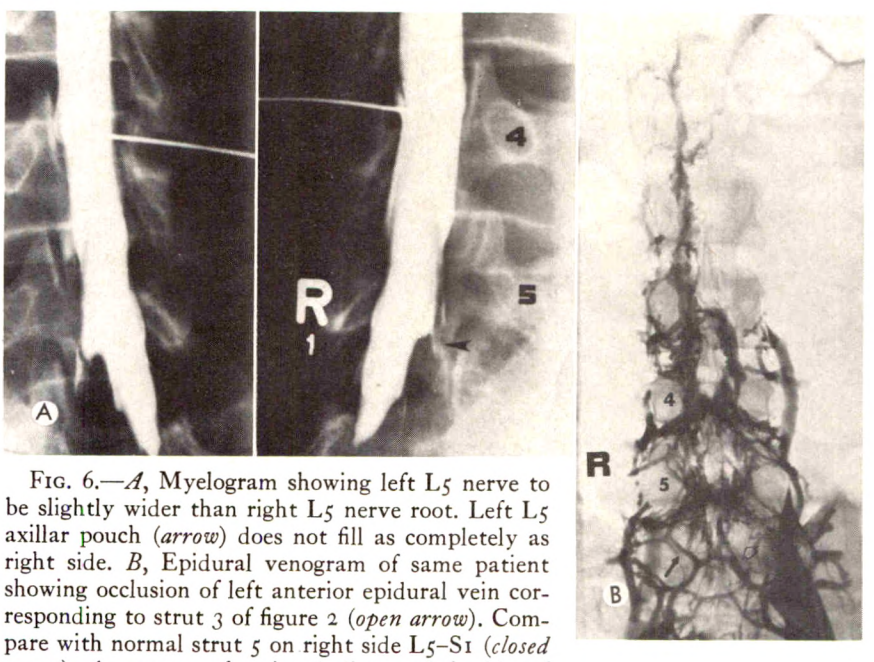


FIG. 6.—*A*, Myelogram showing left L5 nerve to be slightly wider than right L5 nerve root. Left L5 axillar pouch (*arrow*) does not fill as completely as right side. *B*, Epidural venogram of same patient showing occlusion of left anterior epidural vein corresponding to strut 3 of figure 2 (*open arrow*). Compare with normal strut 5 on right side L5–S1 (*closed arrow*). At surgery, herniated disc on left side of L5–S1 was identified.

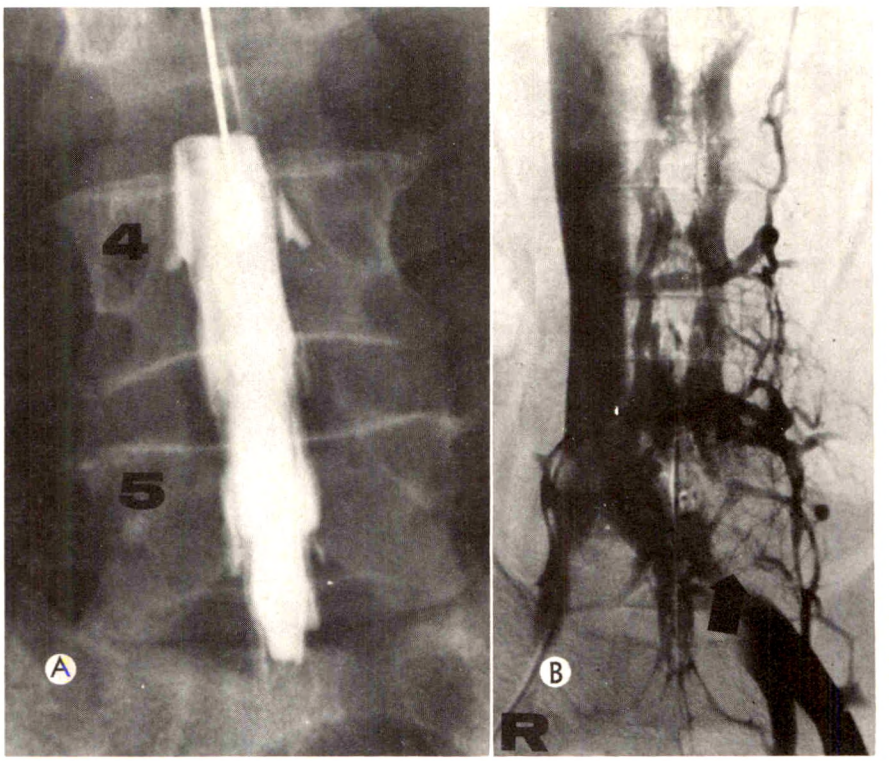


FIG. 7.—*A*, Myelogram showing no definite deformity of caudal sac. Enlarged nerve roots are present on right side at L4–L5 and L5–S1 levels. *B*, Epidural venogram of same patient showing compression of inferior radicular veins at L4–L5 on left (*arrow*). At surgery, lumbar spinal stenosis without disc herniation was present.

nerve root entrapment, detecting only three of six preoperatively (table 1).

DISCUSSION

Lumbar epidural venography compares favorably to positive contrast myelography, in which equivocal results may occur in up to 25% of studies [11] and in which a wide epidural space of L5–S1 can obscure underlying disc herniation in approximately 20% of patients [4]. Our overall accuracy rate of 87% is comparable to Gargano's reported 91% accuracy in 32 operated patients [10]. Better filling of the epidural and radicular veins by contrast injection into the ascending lumbar vein probably accounts for the improvement over the 78% accuracy rate reported in Vogelsang's series of 99 patients studied by intraosseous venography [5].

Nerve root entrapment without disc protrusion may result from narrowing of the disc space and associated narrowing of the neural foramen, spondylolysis, bony encroachment by pedicle or facets, previous spinal fusions, lumbar stenosis, and infrequently by spur formation [12]. We ob-

TABLE 1

ACCURACY OF LUMBAR VENOGRAPHY IN 38 SURGICALLY VERIFIED CASES

Cases	No.	%
Correctly diagnosed	33	87
Incorrectly diagnosed negative:		
Herniated disc at operation	2	...
Nerve root entrapment:		
With spondylolysis	1	...
Without spondylolysis	2	...
Total	5	13
Incorrectly diagnosed positive	0	0

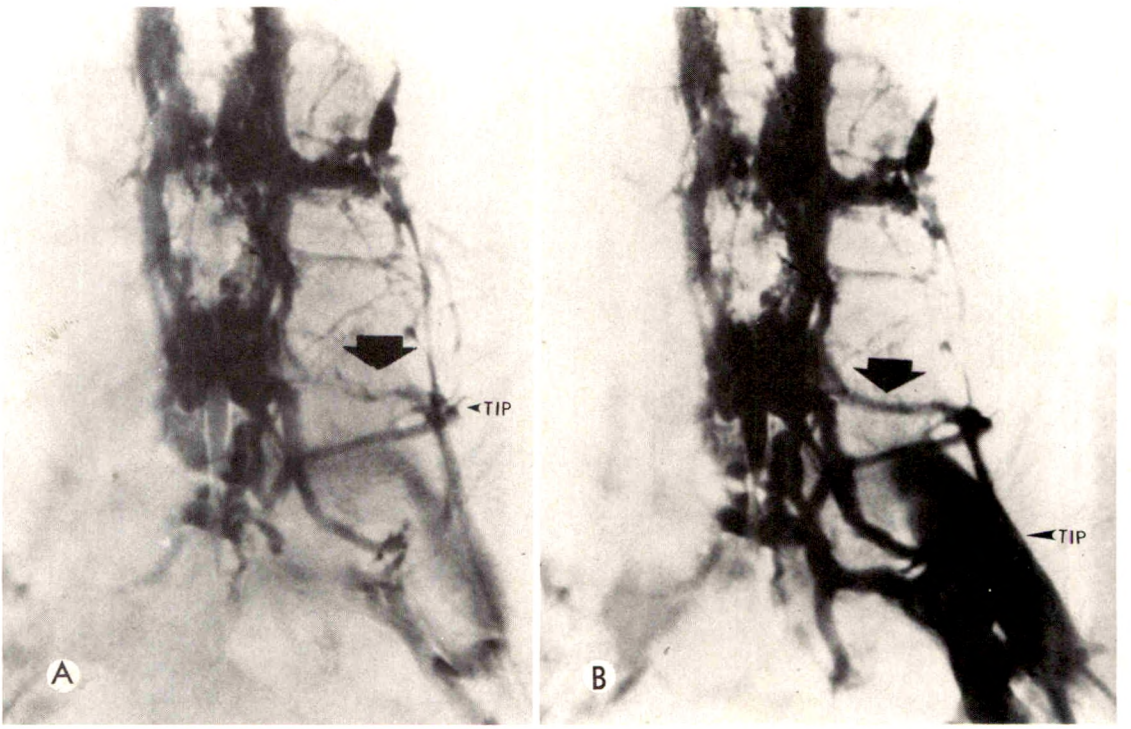


FIG. 8.—*A*, Epidural venogram showing apparent compression of superior radicular vein at L5–S1 on left (*arrow*). Catheter tip is at level of radicular vein. *B*, Venogram of same patient after catheter tip lowered below radicular vein. Note normal opacification of vein.

served occlusion of the inferior radicular vein and associated epidural vein in three patients without disc disease who had narrowing of the neural foramen noted at surgery (fig. 7). The venographic findings of occlusion of radicular and epidural veins are indistinguishable from findings associated with disc herniation.

Interpretation of lumbar venograms requires an awareness of the situations that can cause confusion. Epidural veins are generally occluded in an area of previous surgery, but the nonoperated sites may be evaluated. In order to have absolute confidence in diagnosing venous obstruction, we require adequate filling of the veins surrounding the area of venous occlusion to exclude flow defects. The catheter can obstruct radicular veins branching from the ascending lumbar vein, resulting in incomplete opacification (fig. 8). Radicular venous occlusion can be overlooked if one does not methodically check for the presence of two radicular veins per neural foramen. Since extravertebral veins can mimic intraspinal veins on the frontal projection, it may be necessary to obtain a lateral projection. As in myelography, careful clinical localization of disease remains important in the interpretation of venograms.

Lumbar epidural venography has proved to be a most useful method for evaluation of lumbar disc disease. This procedure may be performed on outpatients and inpatients. We have also examined two achondroplasts by this method, since myelography can be very difficult to perform in this situation. In general, however, we prefer to perform epidural venography only on those patients whose myelogram is nondiagnostic.

REFERENCES

1. Lind J, Wegelius C: Discussion, in *Medicinsk Riksstamma*, 1954
2. Finney LA, Gargano FP, Buermann A: Intraosseous vertebral venography in the diagnosis of lumbar disk disease. *Am J Roentgenol* 92:1282–1292, 1964
3. Fischgold H, Adam H, Ecoiffier J, Pieguet J:

Opacification des plexus rachidiens et des veines azygos par voie osseuse. *J Radiol Electrol Med Nucl* 33:37, 1952

4. Schobinger RA, Krueger EG: Intraosseous epidural venography in the diagnosis of surgical diseases of the lumbar spine. *Acta Radiol* 1:763–776, 1963
5. Vogelsang H: *Intraosseous Spinal Venography*. Baltimore, Williams and Wilkins, 1970
6. Nathan MH, Blum L: Evaluation of vertebral venography. *Am J Roentgenol* 83:1027–1033, 1960
7. Perey O, Lind J, Wegelius C: Phlebography of the intervertebral plexus. *Acta Orthop Scand* 25:228–233, 1956
8. Bucheler E, Janson R: Combined catheter venography of the lumbar venous system and the inferior vena cava. *Br J Radiol* 46:655–661, 1973
9. LePage JR: Transfemoral ascending lumbar catheterization of the epidural veins. *Radiology* 111:337–339, 1974
10. Gargano FP, Meyer JJ: Transfemoral ascending lumbar catheterization of the epidural veins in lumbar disk disease. *Radiology* 111:329–336, 1974
11. Scoville WB, Moretz WH, Hawkins WD: Discrepancies in myelography: statistical survey of 200 operative cases undergoing pantopaque myelography. *Surg Gynecol Obstet* 86:559–564, 1948

Am J Roentgenol 126:1010–1016, 1976

EPIDURAL VENOGRAPHY: DIAGNOSIS OF HERNIATED LUMBAR INTERVERTEBRAL DISC AND OTHER DISEASE OF THE EPIDURAL SPACE

GEORGE F. DRASIN,[1,2] RICHARD H. DAFFNER,[1] ROBERT F. SEXTON,[3] AND WILLIAM C. CHEATHAM[1]

ABSTRACT:

Epidural venography is a simple and safe procedure for the diagnosis of herniated intervertebral disc and other disease of the epidural space. It is especially useful in symptomatic patients with normal or equivocal myelographic findings. The accuracy rate of positive venograms is 88.2% in this series of 58 patients. Five illustrative cases are presented.

The false negative rate of myelography in diagnosing herniated intervertebral discs has been estimated at approximately 15% [1–7]. Scoville operated on 200 consecutive cases for clinical reasons alone and found disc herniation in 13% of patients who had

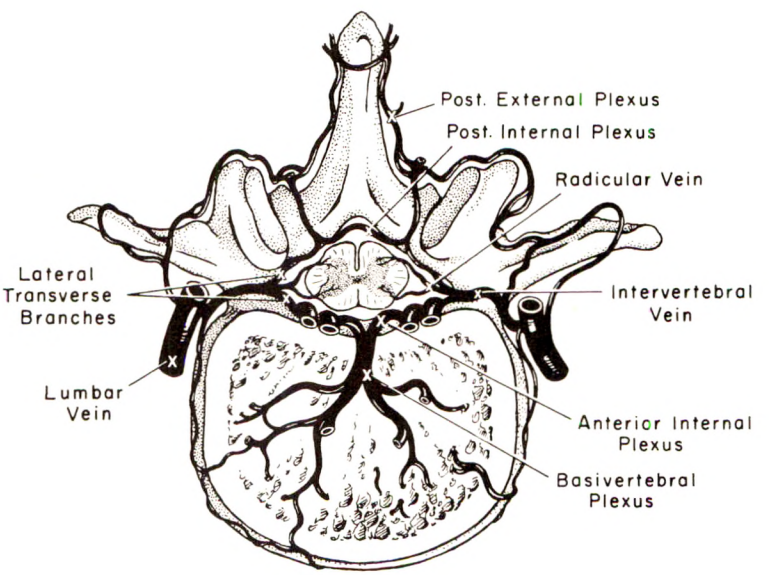


FIG. 1.—Transverse schematic drawing of vertebral venous system.

Presented at the annual meeting of the American Roentgen Ray Society, Atlanta, Georgia, October 1975.

[1] Department of Radiology, University of Louisville School of Medicine, Louisville General Hospital, and S. S. Mary and Elizabeth Hospital, Louisville, Kentucky 40215.

[2] Present address: Department of Radiology, Jewish Hospital, 217 East Chestnut Street, Louisville, Kentucky 40202.

[3] Department of Neurosurgery, University of Louisville School of Medicine, Louisville, Kentucky 40201.

normal myelograms [7]. In a similar study, Ford [3] discovered 27 positive discs at surgery in 39 patients with normal myelograms. Another 10 cases had positive myelograms at L4–L5 and negative findings at L5–S1 with surgery revealing herniated disc material at L5–S1. False negative rates will vary according to clinicians' indications for myelography and can only be ascertained if all patients are surgically explored.

The major source of error in myelography lies in the inability of the Pantopaque column to cover all areas where herniated discs or other lesions may be. The thecal column may be narrow, leaving a large unexamined space between the dura and the inner margins of the spinal canal. Laterally herniated discs are especially difficult to discover, possibly compressing a nerve root but causing no impression on the Pantopaque column. Another hazardous area is the L5–S1 level. The spinal canal becomes larger while the thecal column narrows, leaving a wide epidural space. At other times, the thecal column does not descend to L5–S1, making that level impossible to investigage by myelography (e.g., figs. 5 and 7). Almost all false negative myelograms reported have been at L5–S1 [1–6, 8].

Opacification of the epidural plexus was first performed in an attempt to discover cerebral metastases [9, 10]. It has subsequently been found to be an accurate and sensitive method of investigating the epidural space when myelograms are normal but there is continued suspicion of disc or other epidural disease [6, 11]. While the first studies were performed by the transosseous route [6, 8, 10–15], the transfemoral method is now accepted as the technique of choice [16, 17].

SUBJECTS AND METHODS

Epidural venography was performed on 58 patients. They were chosen for this procedure because of their clinical status after normal or equivocal myelograms. Many other patients with a normal myelogram had no further evaluation. For one patient with a grossly positive myelogram, the venogram was done to outline the tumor extent.

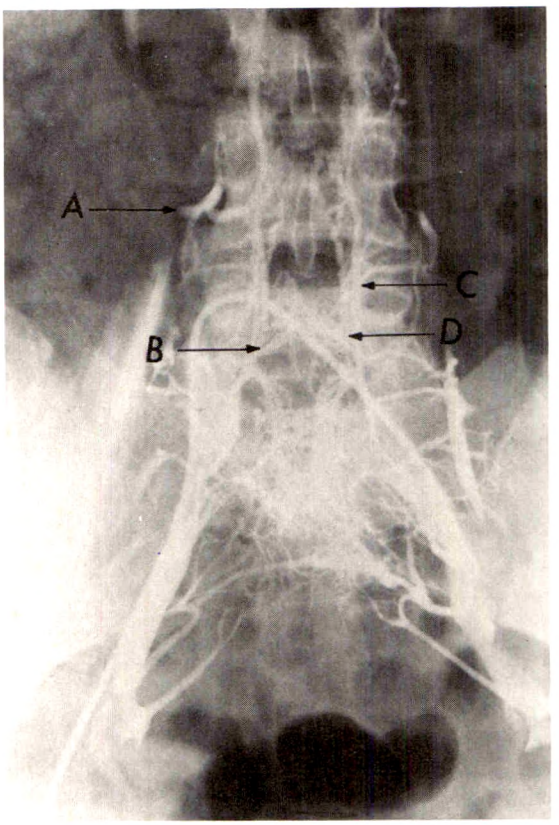


FIG. 2.—Normal epidural venogram. *A*, Ascending lumbar vein draining intervertebral vein; *B*, radicular vein; *C*, anterior intravertebral vein; *D*, posterior intravertebral vein.

A comprehensive discussion of the radiographic anatomy of the epidural space has been presented by Gargano et al. [16]. The method of examination has been elucidated by LePage [17]. We would only add that catheterization of the ascending lumbar veins has not always been possible in our experience, but catheterizing small sacral branches of the hypogastric veins has been uniformly successful in opacifying the epidural plexus and has been performed without difficulty or morbidity. Figure 1 shows a cross-sectional diagram of the spinal canal and its veins. Normal vein anatomy is shown in figure 2.

RESULTS

Of the 58 venograms performed, 16 were positive and demonstrated 17 lesions. At

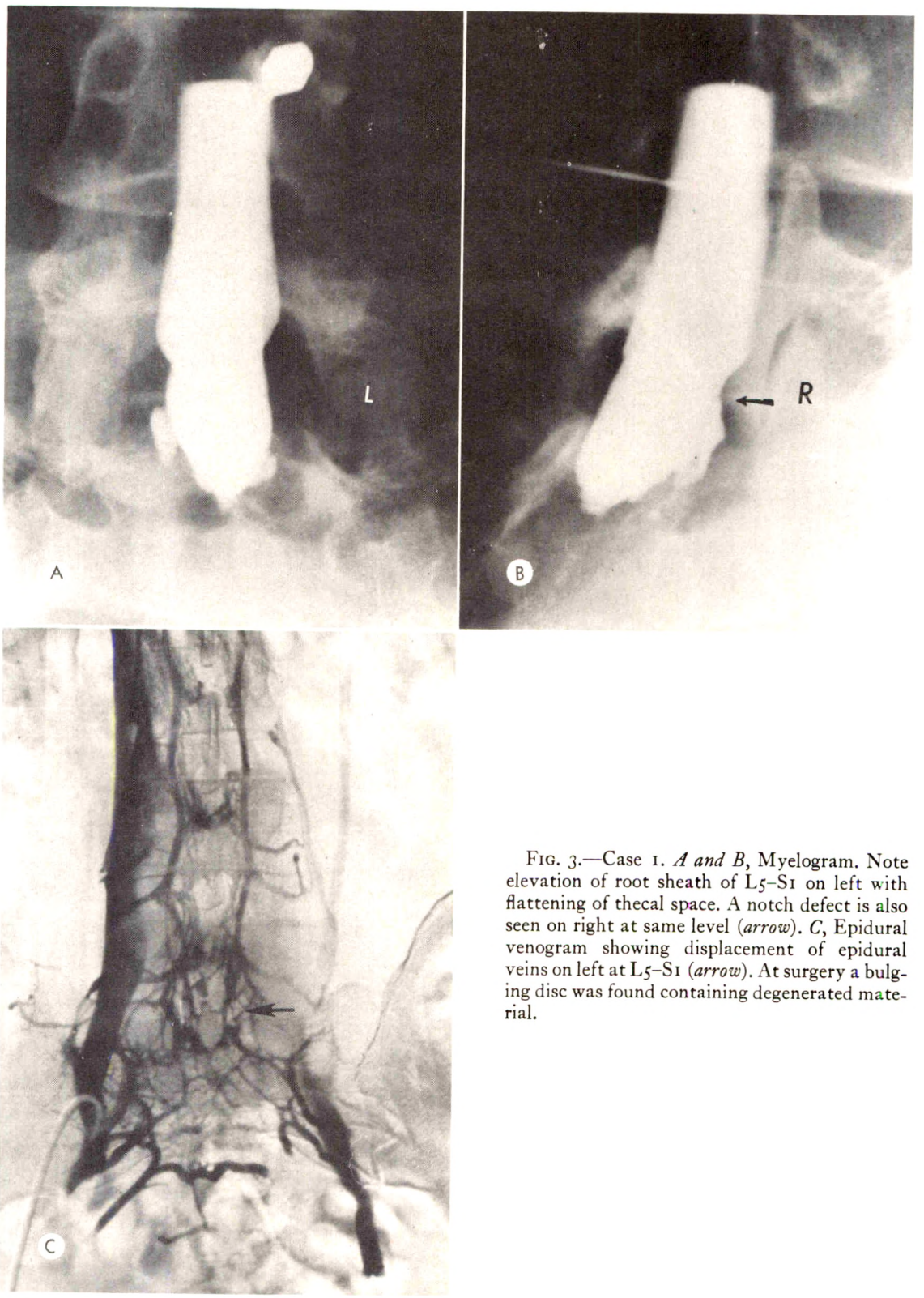


FIG. 3.—Case 1. *A and B*, Myelogram. Note elevation of root sheath of L5–S1 on left with flattening of thecal space. A notch defect is also seen on right at same level (*arrow*). *C*, Epidural venogram showing displacement of epidural veins on left at L5–S1 (*arrow*). At surgery a bulging disc was found containing degenerated material.

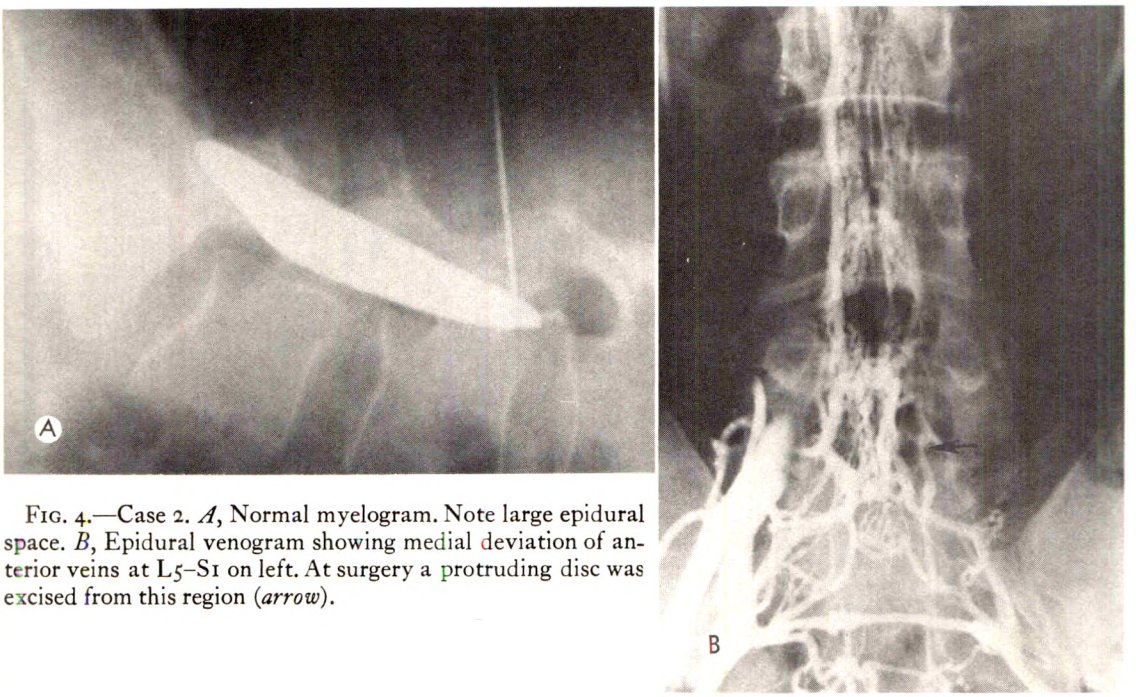


FIG. 4.—Case 2. *A*, Normal myelogram. Note large epidural space. *B*, Epidural venogram showing medial deviation of anterior veins at L5–S1 on left. At surgery a protruding disc was excised from this region (*arrow*).

surgery 15 lesions were found, for an accuracy rate of 88.2%. Of that group, eight patients had previously normal myelograms. Two other patients had surgery after normal epidural venograms. No abnormality was found in one; the second had a mild disc herniation ventrally which had been demonstrated on myelography.

CASE REPORTS

Case 1

E. T., a 36-year-old female, complained of a 2-month history of back pain which radiated into her left leg and ankle. Straight leg raising was positive at 45° on the right, but no pathological reflexes could be elicited. A myelogram showed elevation of the L5–S1 nerve root sheath on the left with flattening of the thecal space (fig. 3*A*). A notch defect was also seen on the right at the same level (fig. 3*B*). An epidural venogram (fig. 3*C*) showed displacement of the epidural veins on the left at L5–S1. At surgery the patient was found to have a bulging annulus fibrosus from which degenerated disc material was removed.

Case 2

J. B., a 26-year-old man, developed sudden onset of low back pain which radiated into the left leg 2 weeks prior to admission. On physical examination, weakness was noted of the extensor hallicis longus on the left. Although his myelogram was considered normal, a large epidural space was present (fig. 4*A*). An epidural venogram demonstrated deviation of the anterior veins at L5–S1 on the left (fig. 4*B*). At surgery a protruding disc was excised from the L5–S1 region.

Comment. This case emphasizes the value of epidural venography when a wide epidural space is present.

Case 3

P. Y., a 48-year-old woman, complained of a 3-day history of severe low back pain radiating into the left leg. On physical examination, straight leg raising was positive at 15° on the left. There was decreased strength of the dorsiflexors on the left, and the ankle jerk on the left was also weakened. A lumbar myelogram was originally considered normal, but in retrospect mild asymmetry is noted at L4–L5 on the left (fig. 5*A*). The epidural venogram showed

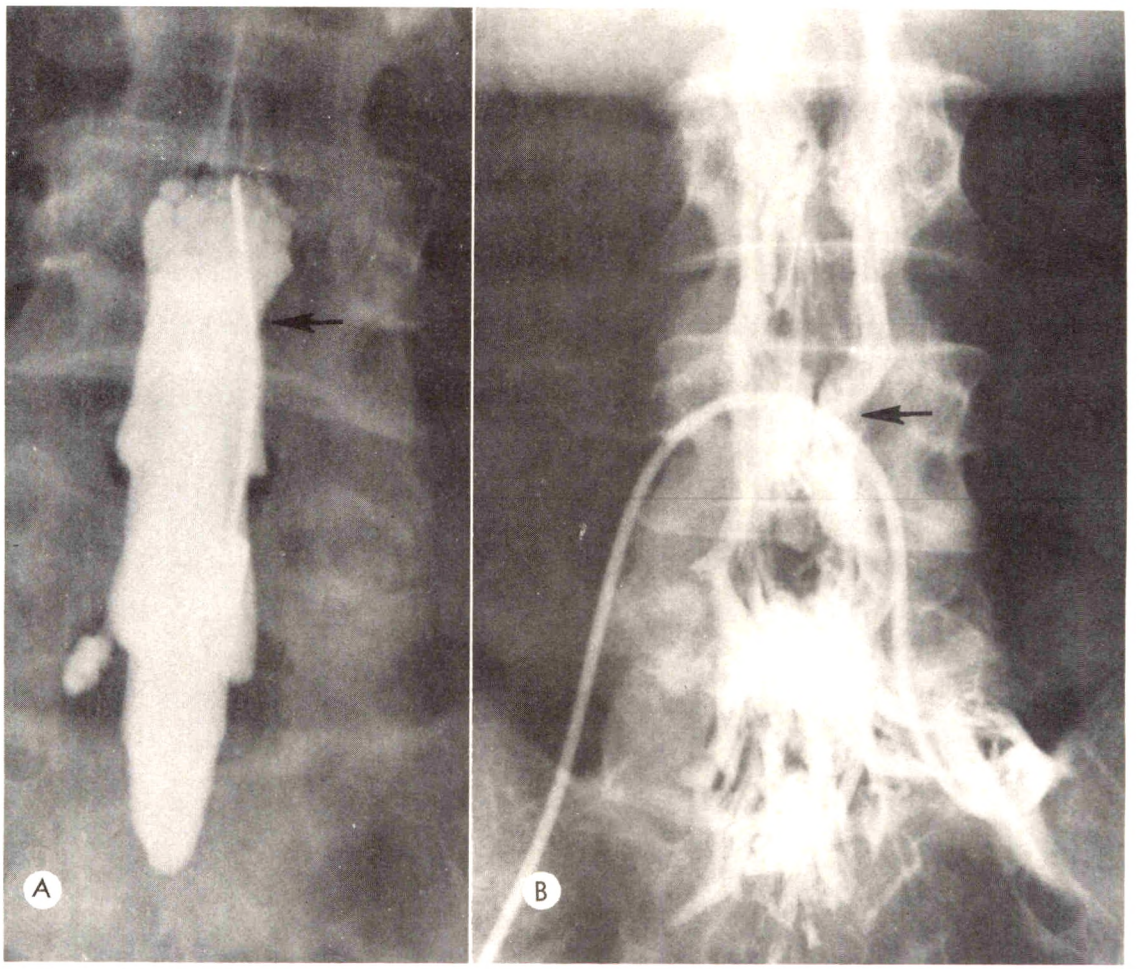


FIG. 5.—Case 3. *A*, Lumbar myelogram showing mild asymmetry at L4–L5 on left. *B*, Epidural venogram showing medial deviation of anterior veins at L4–L5 on left (*arrow*). At surgery a bulging disc was encountered at L4–L5 on left.

a marked deviation of the anterior veins at L4–L5 on the left (fig. 5*B*). At surgery a bulging disc was encountered at L4–L5 on the left associated with an epidural hematoma along the body of L4.

Case 4

E. S., a 40-year-old woman, complained of lumbar back pain for several years. The pain extended into her right posterolateral thigh, calf, and heel with occasional mild numbness. Physical examination demonstrated decreased ankle jerk reflexes bilaterally. Plain films of the lumbosacral spine showed spondylolysis of L5 on the left with sclerosis of the L5–S1 joint facet on the right. The myelogram was interpreted as being normal. Epidural venogram demonstrated angular deviation of the posterior veins on the right at the midbody of L5 (fig. 6). Subsequent injections adequately visualized the anterior and left-sided veins which were normal. At surgery the nerve root was found to be compressed by a medially buckled and hypertrophied joint facet.

Case 5

W. H., a 32-year-old woman, developed gradual onset of lumbosacral backache over a 1-year period. Straight leg raising was positive bilaterally at 30°. Pathologic reflexes could not be elicited, but minimal S1 dermatome hypalgesia was found on the left. The lumbar myelogram demonstrated a large intradural defect at L5 (fig. 7*A*). Epidural venogram showed virtual absence of both anterior and posterior veins at the same level of the myelographic defect (fig. 7B). A single vein on the left was thinned and displaced laterally in a curvilinear

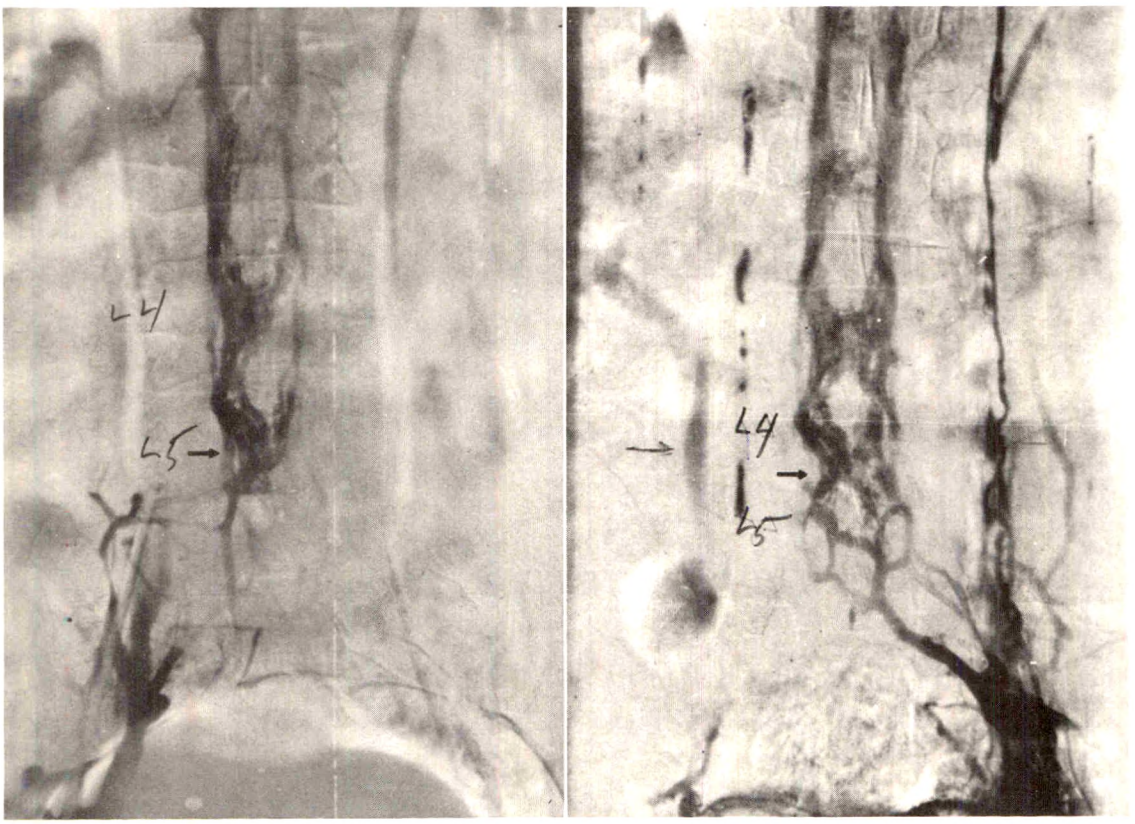


FIG. 6.—Case 4. Epidural venogram showing medial deviation of posterior veins on right at midbody of L5 (*arrows*). At surgery there was nerve root compression by narrowed neural foramen and buckling of facet.

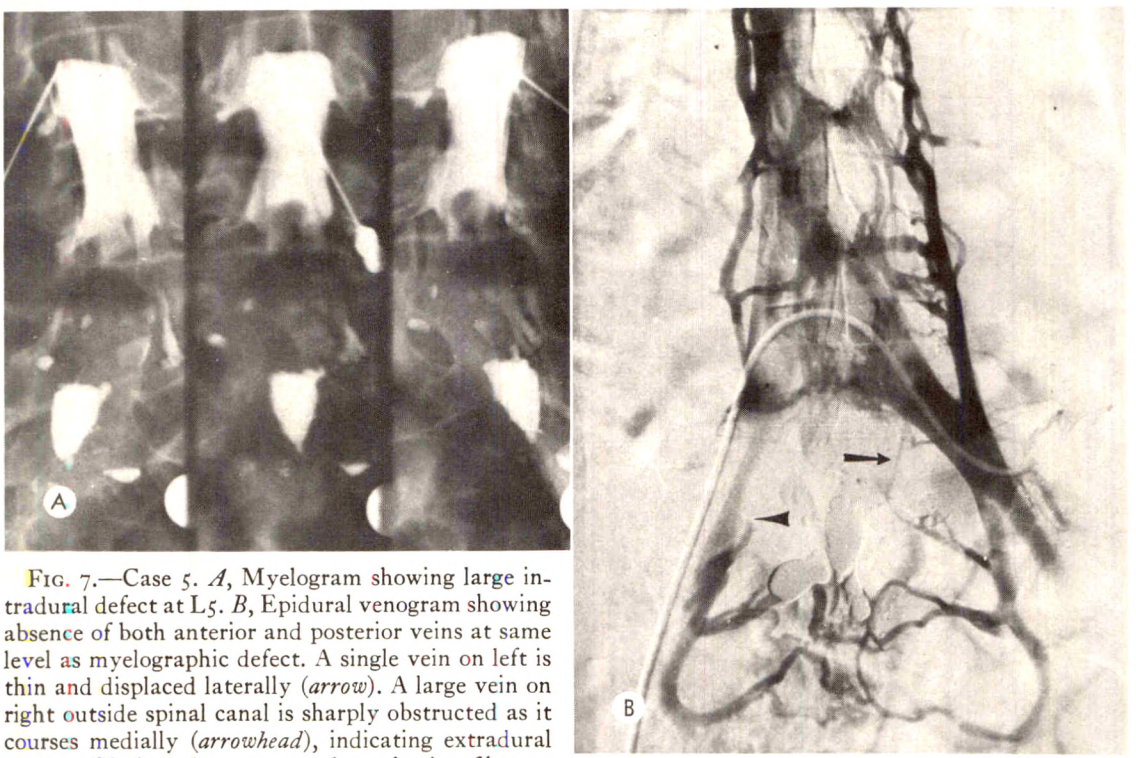


FIG. 7.—Case 5. *A*, Myelogram showing large intradural defect at L5. *B*, Epidural venogram showing absence of both anterior and posterior veins at same level as myelographic defect. A single vein on left is thin and displaced laterally (*arrow*). A large vein on right outside spinal canal is sharply obstructed as it courses medially (*arrowhead*), indicating extradural extent of lesion. At surgery a large benign fibroma was encountered, approximately 25% extradural.

configuration. A large vein on the right outside the spinal canal was sharply obstructed as it coursed medially. It was felt that this vein had encountered tumor as it approached or entered the spinal canal, indicating that there was a significant extradural component to the mass. At surgery a large benign fibroma was removed. Approximately 25% was extradural. No malignant cells were found.

Comment. Although this was not a case of intervertebral disc disease, it was included to demonstrate the value of epidural venography in outlining the extent of a lesion. In this case the extradural component was not suspected by myelography alone but was clearly shown on the venogram.

ACKNOWLEDGMENTS

We thank Barbara Moss, Shirley Gentry, and Pamela Napier for technical assistance.

REFERENCES

1. Arbuckle RK, Sheldon CH, Pudenz RH: Pantopaque myelography: correlation of roentgenologic and neurologic findings. *Radiology* 45:356–369, 1945
2. Begg AC, Falconer MA, McGeorge M: Myelography in lumbar intervertebral disk lesions: correlation with operative findings. *Br J Surg* 34: 141–157, 1946
3. Ford LT, Key JA: Evaluation of myelography in diagnosis of intervertebral-disc lesions in low back. *J Bone Joint Surg* 32A:257–266, 306, 1950
4. Leader SA, Rassell MJ: Value of Pantopaque myelography in diagnosis of herniation of nucleus pulposus in lumbosacral spine. *Am J Roentgenol* 69:231–241, 1953
5. Maltby GL, Pendergrass RC: Pantopaque myelography: diagnostic errors and review of cases. *Radiology* 47:35–46, 1946
6. Schobinger RA, Krueger EG, Sobel GL: Comparison of intraosseous vertebral venography and Pantopaque myelography in diagnosis of surgical conditions of lumbar spine and nerve roots. *Radiology* 77:376–397, 1961
7. Scoville WB, Moretz WH, Hankins WD: Discrepancies in myelography: statistical survey of 200 operative cases undergoing Pantopaque myelography. *Surg Gynecol Obstet* 86:559–564, 1948
8. Schobinger RA, Krueger EG: Intraosseous epidural venography in the diagnosis of surgical diseases of the lumbar spine. *Acta Radiol* 1:763–776, 1963
9. Anderson RK: Diodrast studies of vertebral and cranial systems to show their probable role in cerebral metastases. *J Neurosurg* 8:411–422, 1951
10. Helander CG, Lindbom A: Sacrolumbar venography. *Acta Radiol* 44:410–416, 1955
11. Schobinger RA: *Intra-osseous Venography*. New York, Grune & Stratton, 1960
12. Finney LA, Gargano FP, Buermann A: Intraosseous vertebral venography in diagnosis of lumbar disc disease. *Am J Roentgenol* 92:1282–1292, 1964
13. Isherwood I: Spinal intra-osseous venography. *Clin Radiol* 13:73–82, 1962
14. Lessman FP, Schobinger R, Lasser EC: Intraosseous venography in skeletal and soft tissue abnormalities. *Acta Radiol* 44:397–409, 1955
15. Nathan MH, Blum L: Evaluation of vertebral venography. *Am J Roentgenol* 83:1027–1033, 1960
16. Gargano FP, Meyer JD, Shelton JJ: Transfemoral ascending lumbar catheterization of epidural veins in lumbar disc disease. *Radiology* 111:329–336, 1974
17. LePage JR: Transfemoral ascending lumbar catheterization of epidural veins. *Radiology* 111: 337–339, 1974

Am J Roentgenol 126:1017–1018, 1976

THE CARDIAC PACEMAKER: A DIFFERENT TWIST

CHARLES J. TEGTMEYER[1] AND JOSEPH MICHAEL DEIGNAN[2]

ABSTRACT:

A new complication of transvenous pacing is described. Twists developing in an endocardial lead indicate that the pulse generator pocket is too large. Pacemaker failure because of electrode dislodgement or lead fracture will ensue.

The implantation of transvenous pacemakers to stimulate the heart is a well-established procedure of great benefit. However, once a pacemaker has been installed, the physician's attention is directed not only to the patient's illness but also to the unique complications of cardiac pacemakers. The electrode complications of displacement, malposition, fracture, perforation, and migration have been documented [1]. Electrode dislodgement caused by the patient twisting the pulse generator and winding the electrode around the generator has been described as the "pacemaker twiddler's syndrome" [2, 3].

The following case illustrates a fractured lead caused by the twisting of the pulse generator in its subcutaneous pocket. The case is unique because a roentgenogram obtained 13 days after insertion predicted early pacemaker failure.

CASE REPORT

R. F., a 66-year-old female, was readmitted to the hospital because of pacemaker failure. The pacemaker had been inserted 7 months previously for control of sinus bradycardia and congestive heart failure. A transvenous electrode was inserted through the internal jugular vein, and a Medtronic model 5942 pulse generator was implanted in a subcutaneous pocket beneath the right breast. A chest roentgenogram obtained following insertion of the pacemaker demonstrated good position of the transvenous lead (fig. 1). A repeat roentgenogram obtained 13 days after insertion showed twisting of the ascending portion of the pacemaker lead (fig. 2); however, this was not noted at the time. Postoperatively the patient did well for 7 months until she awoke on the day of admission with precordial pain, a feeling of pressure in her chest, and a rapid heart rate.

Physical examination revealed an obese woman with large pendulous breasts and bradycardia. The EKG demonstrated atrial fibrillation and an absence of the pacemaker artifact. A radiograph of the chest revealed a fracture of the transvenous lead in its ascending portion just above the pulse generator (fig. 3). On close questioning, the patient stated that she had occasionally felt the pacemaker turn over in the pouch when she rolled over in bed. The patient denied twiddling with the generator.

At surgery the subcutaneous pocket was found to have enlarged sufficiently to permit free rotation of the pulse generator within the

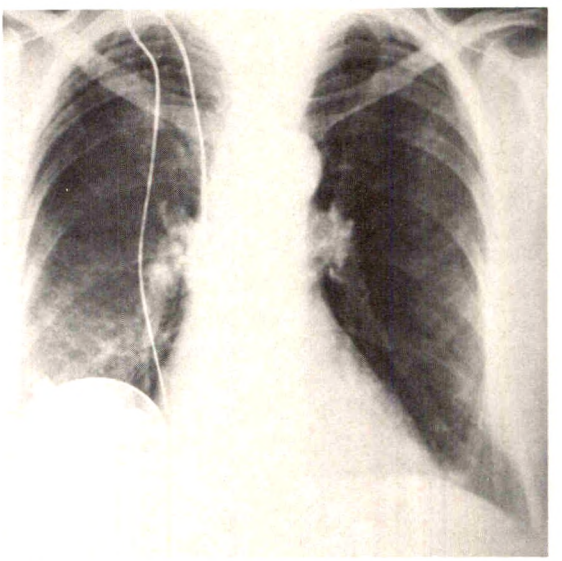


FIG. 1.—Postimplantation frontal chest roentgenogram demonstrating normal transvenous lead in good position.

[1] Department of Radiology, University of Virginia School of Medicine, Charlottesville, Virginia 22901.
[2] Department of Surgery, Winchester Memorial Hospital, Winchester, Virginia 22601.

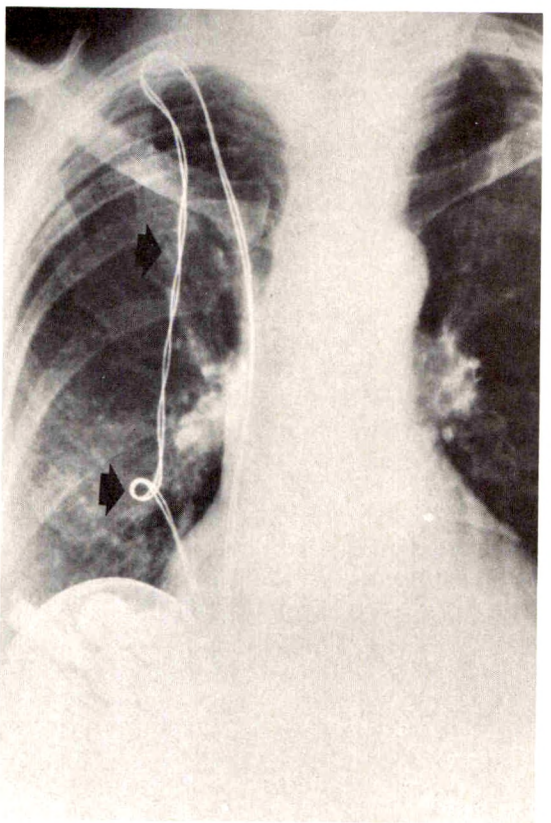


FIG. 2.—Follow-up frontal chest radiograph taken 13 days later showing twisted endocardial lead (*arrows*). Electrode tip remains in good position.

pocket. A new transvenous lead was inserted through the internal jugular vein, and a new pocket for the pulse generator was developed deep to the pectoral muscles.

DISCUSSION

The "pacemaker twiddler's syndrome" has been well documented [2, 3]. Displacement of the transvenous lead results from traction on the lead produced by rotating the pulse generator within a capacious pocket [2, 3]. Rotation can occur spontaneously, as in our case, or as a result of the patient twiddling with the generator. Dislodgement of the endocardial electrode is caused either by the windlass mechanism (the electrode is reeled onto the pulse generator) or by twisting the electrode wire.

The electrode was not dislodged in our case. The twisting of the wire imposed additional strain on the electrode, resulting in lead fracture. The roentgenogram (fig. 2) obtained 13 days after insertion of the lead demonstrated the twists in the endocardial lead. Unfortunately, the significance of the twisted lead was overlooked and the lead subsequently fractured.

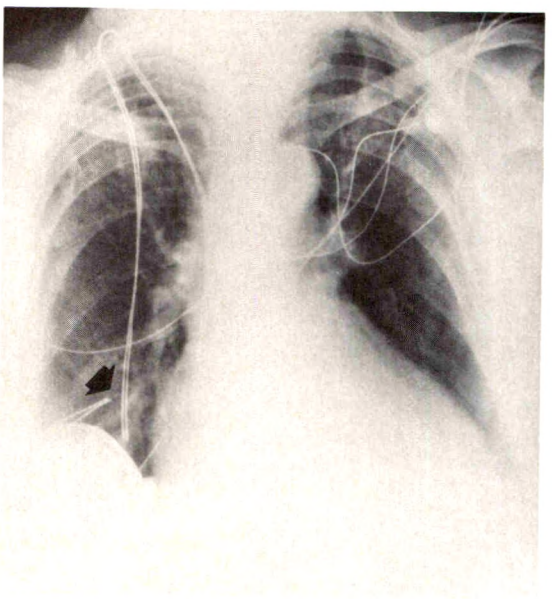


FIG. 3.—Frontal roentgenogram obtained 7 months later revealing fractured transvenous lead (*arrow*). Uncoiled lead indicates that tension had been placed on it.

Twists in a lead indicate that the generator pocket is too large. The pulse generator is rotating in a capacious pocket either spontaneously or because the patient is twiddling with the generator. This will eventually result in pacemaker failure because of electrode dislodgement or lead fracture. This potentially lethal but correctable complication of cardiac pacing can be prevented if detected. It is important to recognize that a twisted transvenous electrode is abnormal, even when the tip of the electrode remains in the right ventricular apex.

REFERENCES

1. Tegtmeyer CJ: The roentgenology of cardiac pacemakers. *Contemp Surg* 1:79–88, 1972.
2. Bayliss CE, Beanlands DS, Baird RJ: The pacemaker-twiddler's syndrome: a new complication of implantable transvenous pacemakers. *Can Med Assoc J* 99:371–373, 1968
3. Meyer JA, Fruehan TC, Delmonico JE: The pacemaker twiddler's syndrome: a further note. *J Thorac Cardiovasc Surg* 67:903–907, 1974

Am J Roentgenol 126:1019–1022, 1976

ILIOCAVAL THROMBI IN PULMONARY THROMBOEMBOLIC DISEASE

JEFFREY C. RUDIKOFF,[1] PETER R. CLAPP, AND ERNEST J. FERRIS

ABSTRACT:

Rational management of patients with pulmonary thromboembolic disease should include assessment of the risk of additional emboli. Other authors have shown that the possibility of fatal pulmonary embolism is higher when the iliofemoral system contains thrombus, and it is recommended that vena caval interruption rather than simple anticoagulation is indicated. Additional factors governing the therapeutic choice should include the magnitude of the original embolic occlusion as well as the presence of antecedent cardiopulmonary disease. In these instances large thrombi in the iliocaval system should be regarded as potentially life threatening.

A sequence of angiography beginning with right iliac and vena caval opacification, proceeding to pulmonary arteriography, and terminating with retrograde left iliac vein study provided information needed to individualize the therapeutic approach. Several case reports illustrate the spectrum of abnormalities and their therapeutic implications.

The diagnosis of pulmonary thromboembolic disease can be made with certainty only by pulmonary angiography. Frequently a presumptive diagnosis is established by relying upon a number of clinical and laboratory modalities including chest roentgenograms, perfusion-inhalation scans, blood gases, and clinical symptomatology. In recent years, emphasis has been on determining the site of origin of potential emboli, using techniques such as isotopic phlebography [1], ultrasound [2], ascending phlebography [3], and retrograde phlebography [4]. In this paper we attempt to formulate a more rational approach for the prevention of future thromboembolic episodes by appropriate choice of the therapeutic modalities available—anticoagulation, femoral vein ligation, inferior vena cava interruption, or Mobin-Uddin umbrella.

MATERIALS AND METHODS

For approximately 5 years pulmonary angiograms were performed on virtually all patients with an appropriate history and a positive perfusion lung scan. Approximately 85% of all patients fulfilling these criteria were studied. Nearly all studies were done within 24 hr of onset of symptoms.

A catheter was placed in the right femoral vein using the Seldinger approach. The right iliac vein and the inferior vena cava were studied. If these were free of thrombi, a pulmonary angiogram was performed. This was subsequently followed by a retrograde left iliac vein study prior to terminating the procedure. If the inferior vena cava was filled with thrombus, the pulmonary angiogram was performed via the upper extremity or jugular vein.

RESULTS

Pulmonary angiograms were performed on 226 patients suspected of having pulmonary thromboembolic disease; 137 were found to have occlusions in the pulmonary arterial system. Fifteen of the 137 had a thrombus in the iliocaval system, for a frequency of 11%. The frequency of iliocaval thrombi among the total group studied was 6.5%.

CASE REPORTS

Case 1

N. B. (no. 474970) was a 21-year-old female who had been on oral contraceptives for 3

Presented at the annual meeting of the American Roentgen Ray Society, Atlanta, Georgia, October 1975.

[1] All authors: Department of Radiology, University Hospital, Boston University School of Medicine, Boston, Massachusetts 02118.

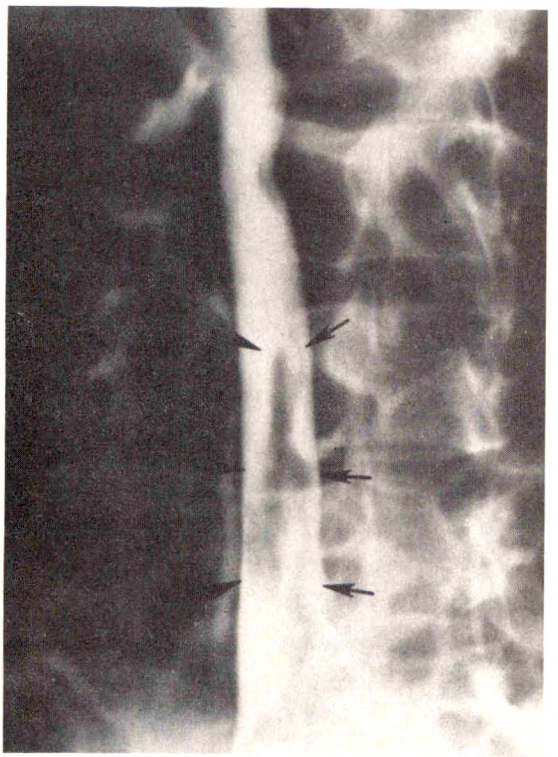


FIG. 1.—Case 1. Large lobulated thrombus (*arrows*) in distal portion of inferior vena cava.

months. Six days prior to admission she experienced sudden onset of left parasternal pleuritic chest pain. The next day she was seen at an outside hospital where she had a lung scan (results not known) and a left thoracentesis (clear fluid). The day prior to admission she developed left thigh pain and heparin therapy was begun.

She was admitted to University Hospital and underwent an emergency pulmonary angiogram. Her left main pulmonary artery was almost completely occluded, and there were multiple intravascular defects in the right lower lobe. The inferior vena cavagram showed a large thrombus filling the distal inferior vena cava and the left common iliac vein (fig. 1).

Comment. Since the amount of pulmonary arterial occlusion was greater than 50% and the thrombus in the inferior vena cava was quite large, an immediate inferior vena cava plication was performed.

Case 2

C. D. (no. 510027) was a 17-year-old female who was seen 1 day earlier at an outside hospital because of sudden onset of shortness of breath and chest pain. She had been on oral contraceptives for 5 months. Results of a perfusion lung scan performed at that hospital were consistent with massive pulmonary embolus. Immediately following admission, a pulmonary angiogram was performed. Pulmonary artery pressure was 21/12 mm of mercury, and there was nearly complete occlusion of the right main pulmonary artery. In addition there were filling defects in the smaller vessels of the left lower lobe. The inferior vena cava was clear, but a small thrombus was seen in the left iliac vein (fig. 2).

Comment. Since the thrombus in the left iliac vein was small, this patient was treated with heparin.

Case 3

M. O. (no. 437216) was a 59-year-old female who had been seen many times because of multiple endocrine adenomas. She also had diabetes mellitus and an old myocardial infarct. Six weeks after pituitary surgery, she was found lying in bed diaphoretic and cold with a blood pressure of 80/20 mm of mercury. Perfusion lung scan findings were consistent with pulmonary emboli. Emergency pulmonary angiography was performed. The pulmonary artery pressure was 58/28 mm of mercury; mean right atrial pressure was 20 mm of mercury. There was nearly complete occlusion of the right main pulmonary artery (fig. 3*A*). In addition, smaller filling defects in the more distal branches of the left lower lobe pulmonary artery were noted. The inferior vena cava was normal but there was a large thrombus in the right common iliac vein (fig. 3*B*).

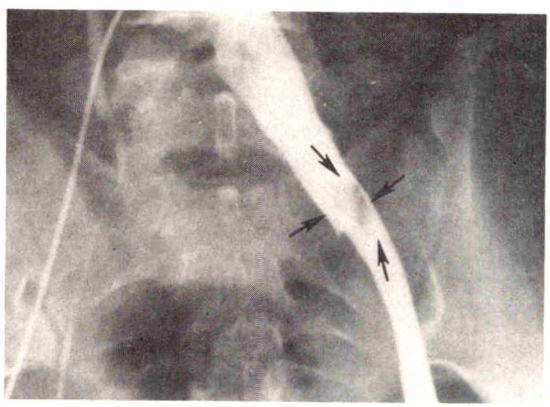


FIG. 2.—Case 2. Small thrombus (*arrows*) in left iliac vein.

Comment. Since the patient had a large thrombus in the right iliac vein as well as extensive pulmonary arterial occlusion and elevated right-side pressures, it was decided to perform an immediate inferior vena cava plication.

Case 4

L. J. (no. 489260) was a 55-year-old hypertensive male who sustained a head injury in an auto accident 2 months earlier. Since the accident he had been quadrapalegic. While in the hospital he was noted to have episodes of transient tachycardia. The patient's left leg was slightly swollen, although he was not thought to have phlebitis. His condition remained relatively unchanged for approximately 10 days. At that time a perfusion lung scan was performed which revealed findings consistent with pulmonary emboli. A pulmonary angiogram did not demonstrate any intraluminal filling defects, although there was "pruning" of lower lobe vessels consistent with old emboli. Examination of the inferior vena cava and iliac system revealed extensive thrombosis of the left iliac vein extending into the inferior vena cava (fig. 4).

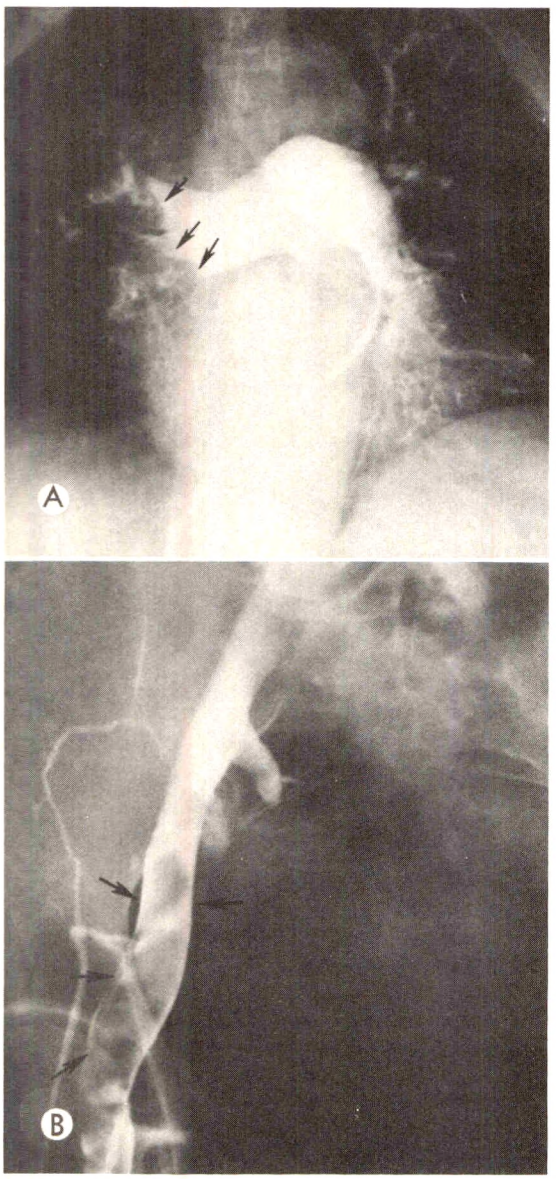


FIG. 3.—Case 3. *A*, Thrombus (*arrows*) which nearly completely occludes right main pulmonary artery. *B*, Large thrombus (*arrows*) in right external iliac vein.

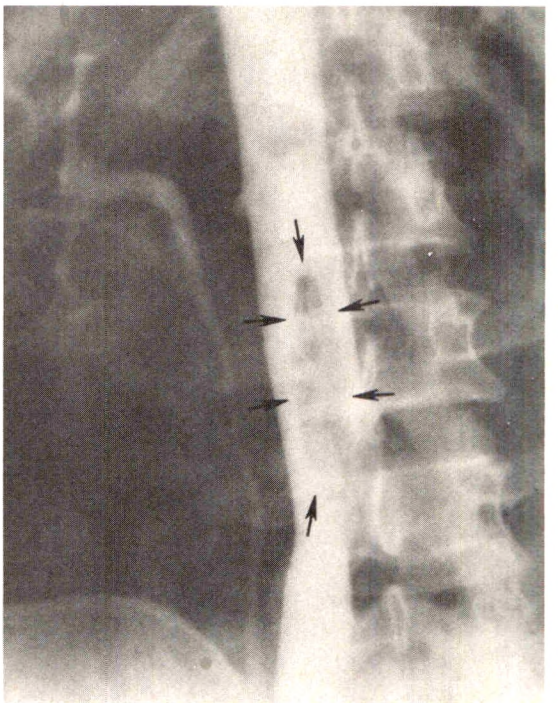


FIG. 4.—Case 4. Large thrombus (*arrows*) in distal inferior vena cava which also involved left internal iliac vein.

Comment. Because the patient had extensive thrombosis of the iliac and proximal inferior vena cava and because his bedridden condition made him prone to venous stasis, it was decided to perform an inferior vena cava plication.

DISCUSSION

The incidence of iliocaval thrombosis associated with pulmonary embolic disease is

difficult to assess because of the inherent problems in diagnosis of pulmonary thromboembolic disease. Of 226 patients in this study suspected of having pulmonary thromboembolic disease, nearly all of whom were studied within 24 hr of onset of symptoms, 137 were shown to have occlusions in the pulmonary arterial system. It is possible that some of the patients with negative angiograms did indeed have pulmonary emboli; however, the number is probably small. Of the 137 patients with positive pulmonary angiograms, 15 had a thrombus in the iliocaval system. This 11% incidence compares favorably with an autopsy series which showed a 12% incidence of iliocaval thrombus in pathologically proven pulmonary emboli [5].

It is logical to assume that in some patients, iliocaval thrombus may be a source of future emboli. It has already been shown by Gibbs [6] in an autopsy series that the incidence of pulmonary embolism is higher in patients with inferior vena cava and iliac thrombosis compared to patients with thrombus found more distally in the legs. It has further been shown on a clinical level by Mavor and Galloway [7] that the incidence of fatal pulmonary embolism is higher when the iliofemoral system contains thrombus. As yet, however, no prospective study has randomized patients with iliocaval thrombus into a heparin-treated group and a vena cava–interruption group. It is for this reason that we have adopted the policy of individualizing each case.

In patients with severe pulmonary arterial embolic occlusion, emphysema, or cardiac disease, the presence of large thrombi in the iliocaval system represents a potentially life-threatening hazard. For these patients we recommend inferior vena cava surgery or placement of a Mobin-Uddin umbrella. This recommendation has also been made for patients who are chronically bedridden or who have an underlying thrombogenic condition such as a malignant tumor. In younger patients with less severe cardiovascular disease and smaller iliocaval thrombi, we feel heparin therapy is adequate. Until the danger of iliocaval thrombus has been adequately evaluated statistically, we recommend individualizing each case along the lines described.

REFERENCES

1. Henkin RE, Quinn JL: Nuclear medicine techniques in diagnosis of deep vein thrombosis. *Surg Clin North Am* 54:57–67, 1974
2. Yao JS, Bergan JJ: Application of ultrasound to arterial and venous diagnosis. *Surg Clin North Am* 54:23–38, 1974
3. Editorial: Prevention of pulmonary embolism. *Br Med J* 2:1–2, 1973
4. Dow JD: Retrograde phlebography in major pulmonary embolism. *Lancet* 2:407–409, 1973
5. Cohn R, Walsh J: Incidence and anatomical site of origin of pulmonary emboli. *Stanford Med Bull* 4:97–99, 1946
6. Gibbs NM: Venous thrombosis of lower limbs with particular reference to bed rest. *Br J Surg* 45:209–236, 1957
7. Mavor GE, Galloway JMD: Ileofemoral venous thrombosis: pathological considerations and surgical management. *Br J Surg* 56:45–59, 1969

Am J Roentgenol 126:1023–1027, 1976

VENOGRAPHY IN PENETRATING INJURIES OF THE EXTREMITIES

AMIL JAMES GERLOCK, JR.,[1] ERWIN R. THAL,[2] AND WILLIAM H. SNYDER, III[2]

ABSTRACT:

Of 30 consecutive cases of penetrating injuries to the extremities studied both by arteriography and venography, five were found to have significant venous injuries. Three of these cases are presented to show the value of venography in detecting inadequate venous collateral circulation, intraluminal thrombus, and venous obstruction. It is suggested that preoperative venography will compliment arteriography, aid in the diagnosis of venous injuries, demonstrate variable venous anatomy, and outline other venous pathology outside of the area of trauma.

INTRODUCTION

Arteriography of the acutely injured extremity is a well-established diagnostic study used by trauma surgeons. Unfortunately, unless an arteriovenous fistula is present, no information is gained regarding the venous side of the circulation.

Gaspar and Treiman [1], in their evaluation of civilian extremity injuries, reported that 22.4% of the 228 patients with arterial injuries had associated venous injuries. The superficial femoral vein was most frequently injured, although injuries of the brachial, axillary, and popliteal veins occurred as well.

Many surgeons now favor repair of major venous injuries, thereby creating a need for preoperative venography. Venography of the acutely injured extremity will provide information about the variable anatomy of the veins, localize the site and type of injury, and demonstrate other venous pathology such as intraluminal clots.

MATERIALS AND METHODS

To evaluate the use of venography in the acutely injured extremity, 30 consecutive cases were examined, both by arteriography and venography. These x-rays were obtained in the emergency room prior to surgical exploration.

The venograms were performed by injecting 60–100 cc of Renografin 76 through a needle into a vein on the hand, wrist, or foot. Tourniquets were used around the ankle in all cases of lower extremity trauma to insure filling of the deep venous system, since these patients could not be placed in an upright position. Radiographs of venous filling of the veins in the region of the injury were obtained with portable x-ray equipment in the emergency room. The results of venography were correlated with the findings at surgical exploration.

RESULTS

Five positive venograms were identified in the group of 30 patients studied. The veins injured and associated arterial injuries are recorded in table 1. Three cases are presented, each illustrating specific information which can be derived from preoperative venography.

CASE REPORTS

Case 1

A 24-year-old male sustained a deep laceration of the antecubital fossa. Upon arrival in the emergency room, both the radial and ulnar pulses were absent. The arteriogram showed complete obstruction of the brachial artery at the level of the distal humerus (fig. 1). Collateral blood flow to the distal brachial, interosseous, ulnar, and radial arteries was present through the superficial ulnar collateral artery and middle collateral branch of the profunda

Presented at the annual meeting of the American Roentgen Ray Society, Atlanta, Georgia, October 1975.

[1] Department of Radiology, University of Texas Health Science Center, Southwestern Medical School, Dallas, Texas 75235. Address reprint requests to A. J. Gerlock.

[2] Department of Surgery, University of Texas Health Science Center, Southwestern Medical School, Dallas, Texas 75235.

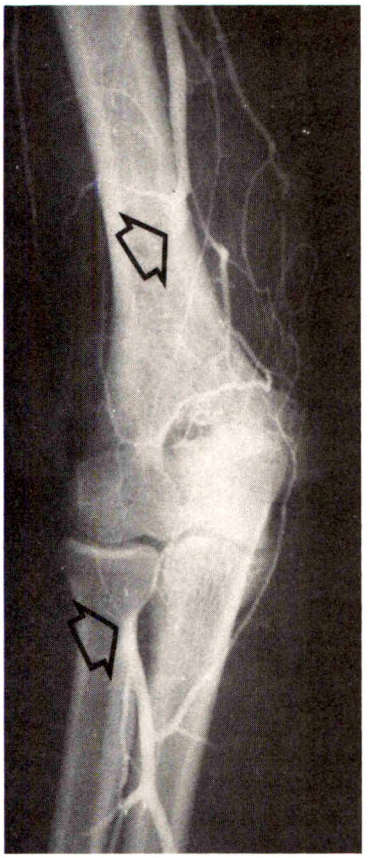


FIG. 1.—Arteriogram showing obstruction of brachial artery (*arrows*) with collateral blood flow around elbow to radial, ulnar, and interosseous arteries.

artery. The venogram showed complete obstruction of the major trunks of the basilic vein and occlusion of one of the cephalic veins (fig. 2).

Surgical exploration revealed that the brachial artery was lacerated and obstructed at the level demonstrated by arteriography. Both of the major trunks of the cephalic and basilic veins were completely severed. The brachial artery was repaired by an end-to-end anastomosis. Based on the appearance of only a few patent superficial veins on the venogram, the basilic vein was also repaired by an end-to-end anastomosis. A follow-up venogram, done 72 hr after surgical repair of the basilic vein, showed the anastomotic site to be patent. The peripheral pulses in the radial and ulnar artery remained palpable postoperatively. Examination of the extremity 4 months later showed no evidence of venous insufficiency or pulse deficit.

Case 2

A 22-year-old male received a gunshot wound to the thigh, sustaining a comminuted fracture of the femur. Physical examination revealed the peripheral pulses to be present. Arteriography of the extremity was normal, while venography demonstrated partial obstruction of the popliteal vein and complete obstruction of the superficial femoral vein in the area of the fracture. Obstruction of the common femoral vein was also present proximal to the site of the gunshot wound, and collateral venous flow could be seen in the inguinal and groin region (fig. 3). Surgical exploration of the vessels showed the arteries to be intact, while the superficial femoral vein was found to be lacerated. A thrombus was removed from the common femoral vein at the site of obstruction seen on the venogram. The lacerated superficial femoral vein was repaired, and the patient showed no evidence of venous insufficiency 1 year after injury.

Case 3

A 20-year-old male received a gunshot wound to the popliteal region. Examination of the extremity revealed complete absence of pulses in the foot. Arteriography showed complete obstruction of the popliteal artery (fig. 4*A*), while venography showed almost complete occlusion of the popliteal vein with extension of a large intraluminal thrombus from the area of the injury to the superficial femoral vein (fig. 4*B*).

Findings at surgical exploration consisted of an occluded distal popliteal artery secondary

TABLE 1

VENOUS AND ARTERIAL INJURIES IN PATIENTS WITH POSITIVE VENOGRAMS

Case No.	Venous Injury	Arterial Injury
1.....	Obs. basilic and branches of cephalic	Obs. brachial
2.....	Obs. common femoral, superficial femoral, and popliteal	None
3.....	Obs. popliteal with thrombus	Obs. popliteal
4.....	Obs. brachial	Pseudoaneurysm, brachial
5.....	Obs. brachial	Obs. brachial

NOTE.—Obs = obstructed.

to a primary injury to the anterior tibial artery just distal to the trifurcation. The popliteal vein likewise was injured with massive bleeding. A saphenous vein interposition graft was inserted between the distal popliteal artery and anterior tibial artery, restoring the pulse to the lower extremity.

DISCUSSION

Arteriography of the acutely injured extremity is now a well-established diagnostic radiologic procedure. The site and extent of the arterial injury can be quickly evaluated by this procedure and the appropriate surgical repair undertaken. Arterial vascular techniques continue to improve, with the emphasis focused primarily on arterial repair rather than ligation. This has resulted in a markedly decreased amputation rate from 49% of peripheral arterial injuries during World War II [2] to 14% in 1960 [3]. The surgical approach of repair rather than ligation is now being applied with increasing frequency to venous injuries as well. Hopefully this will reduce the amputation rate even further.

The repair of injured veins has been stimulated by the accumulation of laboratory and clinical data demonstrating the adverse circulatory hemodynamics of venous ligation. In a study by Barcia et al. [4], total venous occlusion of the canine hind limb resulted in a considerable decrease of femoral arterial flow. From this study it was concluded that venous obstruction caused venous hypertension and venostasis, which in turn caused increased resistance to the in-flow of arterial blood. These authors proposed that the resultant arterial low-flow state may increase the tendency for arterial thrombosis. The low-flow state may also cause tissue death from poor perfusion, even in the presence of a patent arterial system.

Further studies by Hobson and associates [5] have shown an initial reduction of 50%–75% in the femoral arterial blood flow in the canine hind limb with ligation of the femoral vein. This is accompanied by a sharp increase in femoral venous pressure as well as an increase in peripheral resistance. Within 72 hr of femoral venous ligation, these measurements returned to normal preligation pressure. This suggests the need for immediate adequate venous circulation in the first 72 hr following arterial repair in order to prevent arterial occlusion.

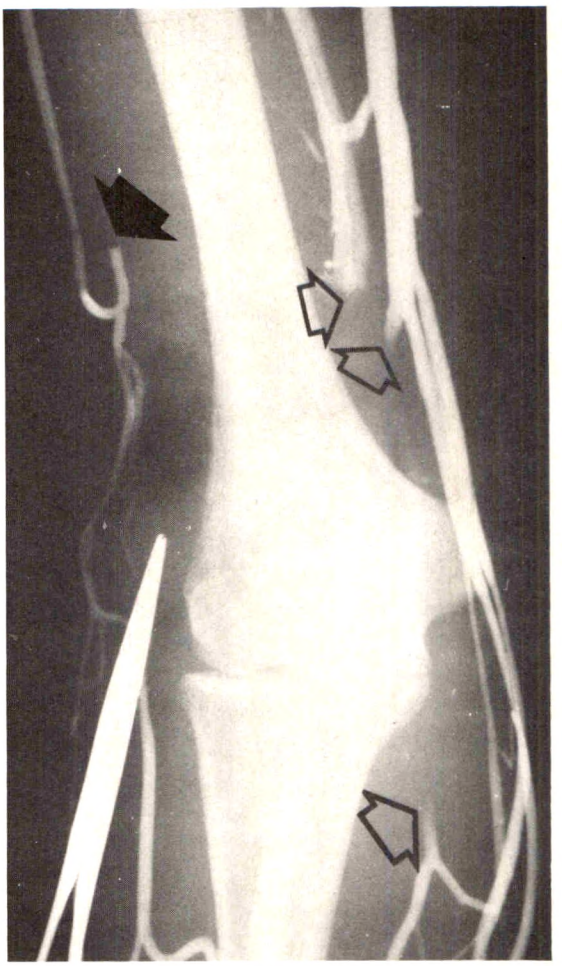


FIG. 2.—Venogram showing complete obstruction of major trunks of basilic vein (*open arrows*) and occlusion of a cephalic vein (*closed arrow*).

Numerous clinical impressions from the Korean conflict [6–8] and Vietnam [9, 10] indicate that venostasis alone may jeopardize an extremity even when distal pulses and arterial patency have been restored. Rich et al. [11] reviewed 125 popliteal artery injuries which ultimately required amputation. Concomitant venous injury was present in 80%. Popliteal vein ligation was performed in 82 patients, while repair was undertaken in 16 cases. With popliteal vein

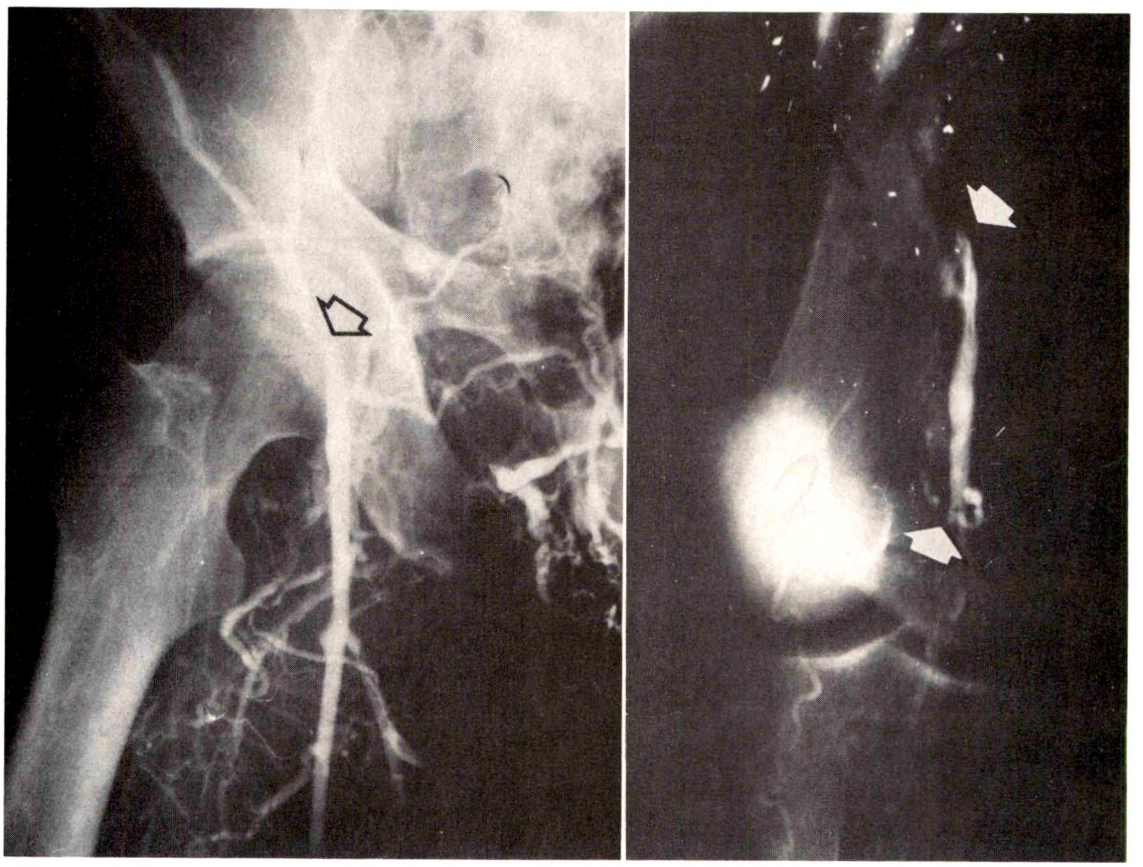


FIG. 3.—Venogram showing obstruction of common femoral vein (*open arrow*). Collateral venous flow around areas of obstruction can be seen in inguinal and groin regions. Complete obstruction of superficial femoral vein and partial obstruction of popliteal vein is also present (*closed arrows*).

ligation, it was reported that severe postoperative edema and acute venous insufficiency frequently contributed to the ultimate need for amputation. It is particularly important to emphasize that 19 of the arterial repairs remained patent following amputation for massive venous insufficiency, as proved by arteriography or dissection. This further supports the concept that venous insufficiency alone in the injured extremity can result in nonviability of the extremity and lead to amputation.

These laboratory and clinical studies emphasize the importance of a patent venous system in managing vascular trauma. Preoperative venography can serve as a useful adjunctive study for the clinician. Venous injuries are easy to diagnose by virtue of either obstruction or extravasation. External compression of the venous system by hematoma or soft tissue swelling is frequently seen.

Venography outlines the venous anatomy for the surgeon. Since collateral circulation seems to play an important role in maintaining patency of the arterial system and preventing venous stasis, this information is important. Should a rich collateral circulation pattern be present, the surgeon may elect to ligate the injured vein rather than spend additional time in attempting a venous repair. This is especially helpful in the critical patient when time is an important factor. However, if collateral circulation does not appear adequate on preoperative venography, then venous repair is likely indicated when major systems are involved.

Occasionally, venography may demonstrate intraluminal clots in the venous sys-

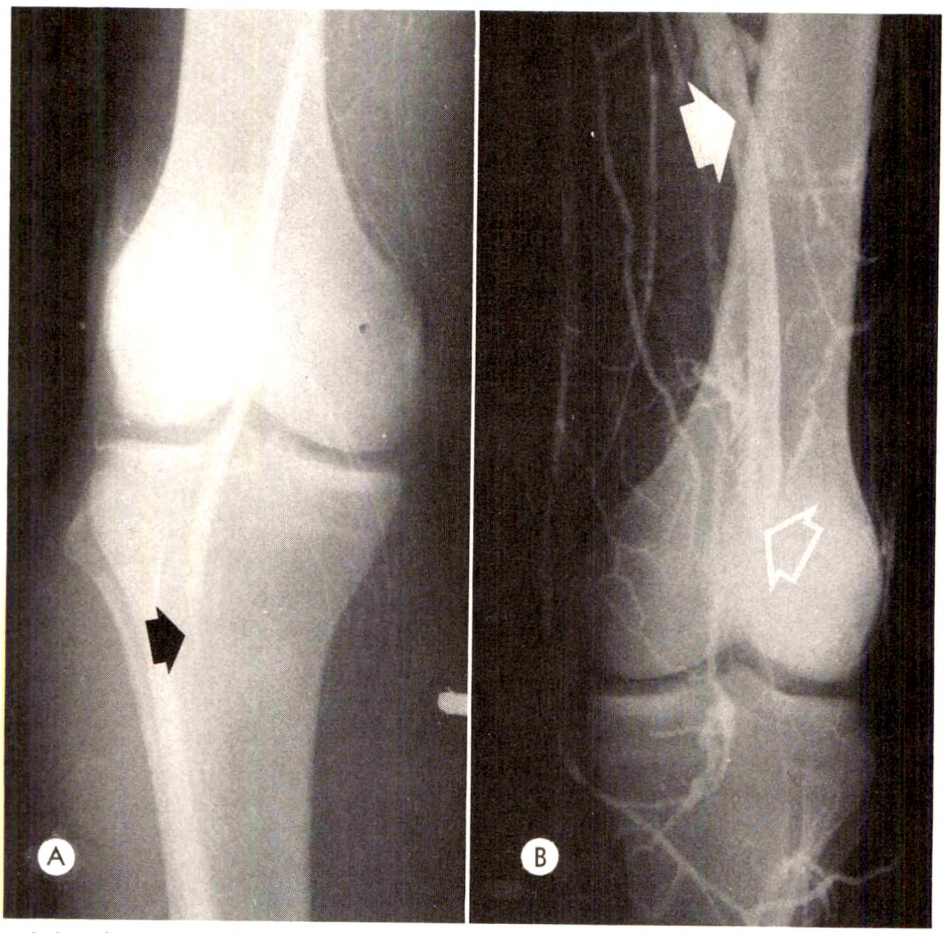


FIG. 4.—*A*, Arteriogram showing obstruction of popliteal artery secondary to penetrating trauma of knee (*arrow*). *B*, Venogram showing partial occlusion of popliteal vein (*open arrow*). A large thrombus is present within superficial femoral vein (*closed arrow*).

tem, either at or distant to the site of injury, that are not evident clinically. These clots may occur in the absence of venous injuries per se.

REFERENCES

1. Gaspar MR, Treiman RL: The management of injuries to major veins. *Am J Surg* 100:171–175, 1960
2. DeBakey ME, Simeone F: Battle injuries of the arteries in World War II; an analysis of 2,471 cases. *Ann Surg* 123:534–579, 1946
3. Morris GC Jr, Beall AC Jr, Roof WR, DeBakey ME: Surgical experience with 220 arterial injuries in civilian practice, Houston, Texas. *Am J Surg* 99:775–781, 1960
4. Barcia PJ, Nelson TG, Whelan TJ: Importance of venous occlusion in arterial repair failure: an experimental study. *Ann Surg* 175:223–227, 1972
5. Hobson RW II, Howard EW, Wright CB, Collins GJ, Rich NM: Hemodynamics of canine femoral venous ligation: significance in combined arterial and venous injuries. *Surgery* 73:824–829, 1973
6. Hughes CW: Acute vascular trauma in Korean casualties. *Surg Gynecol Obstet* 99:91–100, 1954
7. Hughes CW: Arterial repair during the Korean War. *Ann Surg* 147:555–561, 1958
8. Spencer FC, Grewe RV: The management of arterial injuries in battle casualties. *Ann Surg* 141:304–309, 1955
9. Rich NM, Baugh JH, Hughes CW: Popliteal artery injuries in Vietnam. *Am J Surg* 118:531–534, 1969
10. Rich NM, Hughes CW, Baugh JH: Management of venous injuries. *Ann Surg* 171:724–730, 1970
11. Rich NM, Hobson RW, Wright CB, Fedde CW: Repair of lower extremity venous trauma: a more aggressive approach required. *J Trauma* 14:639–649, 1974

Am J Roentgenol 126:1028–1032, 1976

SELECTIVE ARTERIAL EMBOLIZATION FOR CONTROL OF HEMORRHAGE IN PELVIC MALIGNANCY: FEMORAL AND BRACHIAL CATHETER APPROACHES

FRANKLIN J. MILLER, JR.,[1] RODRIGUE MORTEL,[2] WILLIAM J. MANN,[2] AND ANTOINE E. JAHSHAN[2]

ABSTRACT:

Selective transcatheter embolization with Gelfoam pledgets was used to control intractable pelvic hemorrhage in two patients with gynecologic malignancy. There were no complications or sequelae associated with the procedure, and no further bleeding occurred. This method requires only Seldinger catheterization techniques under local anesthesia and should be considered in patients whose medical condition precludes major surgery or in whom operative ligation cannot be performed.

External pelvic hemorrhage is a very distressing complication in obstetrics and gynecology. Whether occurring post partum, after gynecologic surgery, or secondary to genital malignancy or its therapy, this complication can be life threatening and is unresponsive to usual conservative measures. In these situations, internal iliac artery ligation has been successfully employed. No immediate mortality has been reported to be associated with this procedure [1, 2]. However, technical difficulties such as injury to the external iliac vein, vessel encasement with tumor, or extensive tissue necrosis may be encountered.

The purpose of this paper is to report an alternate means of controlling recurrent pelvic hemorrhage by selective arterial embolization with absorbable gelatin sponge (Gelfoam®, Upjohn Co., Kalamazoo, Mich.). Two cases are presented to illustrate the method.

CASE REPORTS

Case 1

A 31-year-old woman, G2P2002, first presented in June 1974 with vaginal bleeding. A stage IIIB epidermoid carcinoma of the cervix was diagnosed. She was treated with a combination of megavoltage external radiation delivering 5,940 rads homogeneously to the whole pelvis and intracavitary cesium using a Fletcher-Suit applicator deliverying 2,880 rads to point A. Following therapy, a large vesicovaginal fistula was noted, and barium enema also revealed a tight radiation stricture of the sigmoid colon. An ileal conduit and transverse colostomy were constructed. In January 1975 the patient developed vaginal hemorrhage, was admitted in shock to an outlying hospital where she was "massively transfused," and was subsequently transferred to our hospital. Hemorrhage and shock recurred in the hospital but were successfully controlled by 2,000 cm^3 of whole blood replacement and vaginal packing of a 2-cm hole in the anterior vaginal wall where bleeding was evident. The vaginal pack was removed 24 hr later, the patient remained stable, and she was discharged 1 week later.

Vaginal hemorrhage recurred the day of discharge, and she was again admitted in hemorrhagic shock. Transfusion of five units of blood and vaginal packing left in place 48 hr brought the bleeding under control. Shortly after the pack was removed, two more units of blood were transfused and the packing reinserted for control of another episode of vaginal hemorrhage. Ligation of the hypogastric artery was considered, but at laparotomy a large necrotic cavity was found occupying the entire left side

[1] Department of Radiology, Milton S. Hershey Medical Center, Pennsylvania State University College of Medicine, Hershey, Pennsylvania 17033. Address reprint requests to F. J. Miller, Jr.

[2] Division of Gynecologic Oncology, Department of Obstetrics and Gynecology, Milton S. Hershey Medical Center, Pennsylvania State University College of Medicine, Hershey, Pennsylvania 17033.

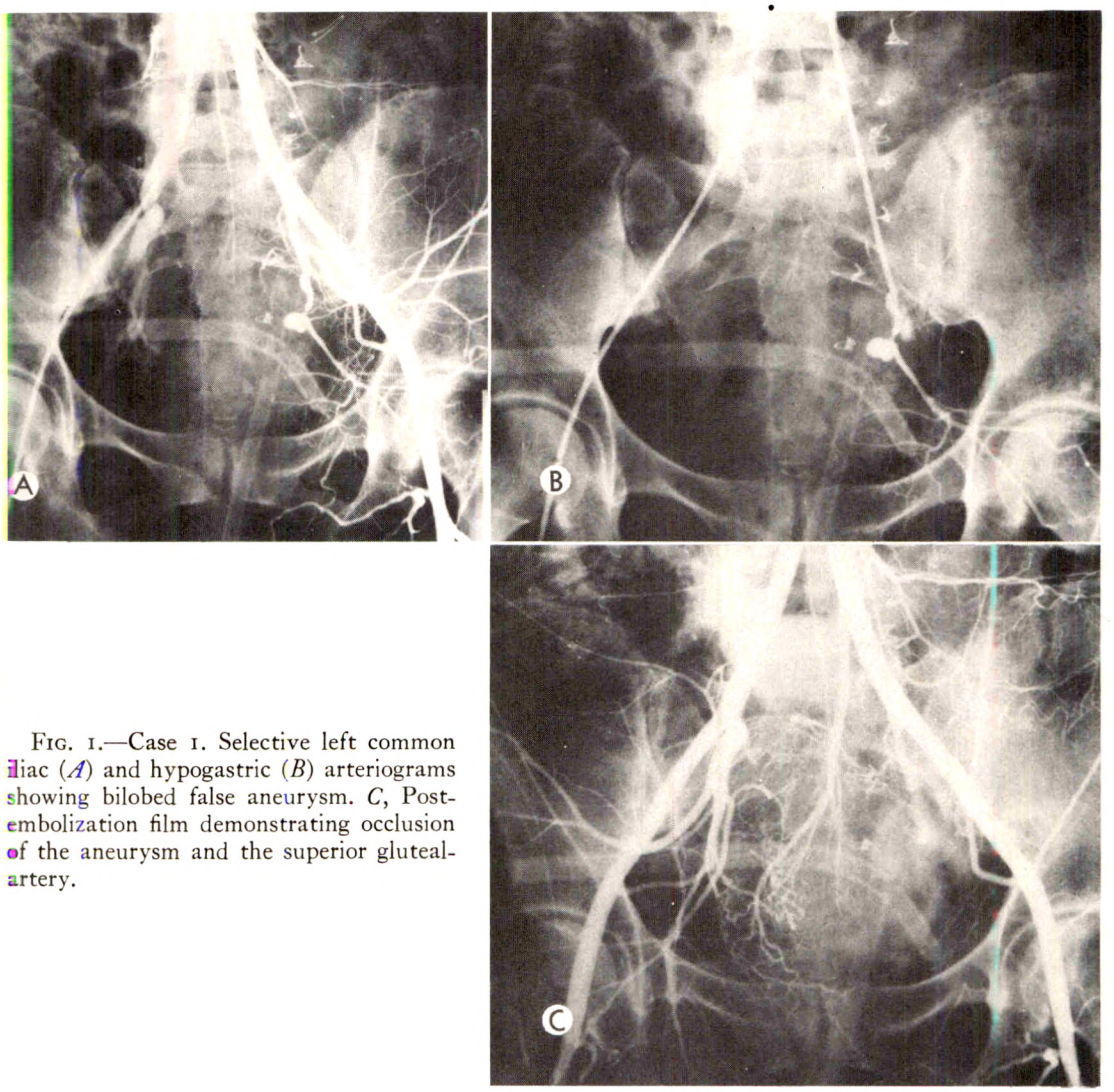


FIG. 1.—Case 1. Selective left common iliac (*A*) and hypogastric (*B*) arteriograms showing bilobed false aneurysm. *C*, Post-embolization film demonstrating occlusion of the aneurysm and the superior gluteal-artery.

of the pelvis. Even after debridement, irrigation, and drainage, the marked distortion of the pelvic anatomy prevented identification and ligation of the left hypogastric artery.

Profuse vaginal hemorrhage recurred on the third postoperative day, and an emergency femoral arteriogram revealed a bilobed aneurysm of the left hypogastric artery (figs. 1*A* and 1*B*). Gelfoam® embolization of the artery was performed without complication (fig. 1*C*). The patient stabilized, there were no further bleeding episodes, and she was discharged. No further bleeding occurred; the patient expired of pneumonia 4 months later in a nursing home.

Case 2

A 55-year-old woman, G2P2002, had a total abdominal hysterectomy and bilateral salpingo-oophorectomy in 1970 for "pelvic relaxation." Histologic examination of the surgical specimen revealed invasive epidermoid carcinoma of the cervix. She subsequently received a course of external orthovoltage irradiation followed by an intracavitary radium insertion. In December 1971, biopsy of the vaginal vault lesion was reported to show recurrent epidermoid carcinoma; the patient underwent an anterior exenteration with construction of an ileal conduit in February 1972. Metastatic epidermoid carcinoma was discovered histologically in the parametrium. The postoperative course was complicated by wound infection and dehiscence, but the patient recovered and was discharged 4 weeks later. A diverting colostomy was con-

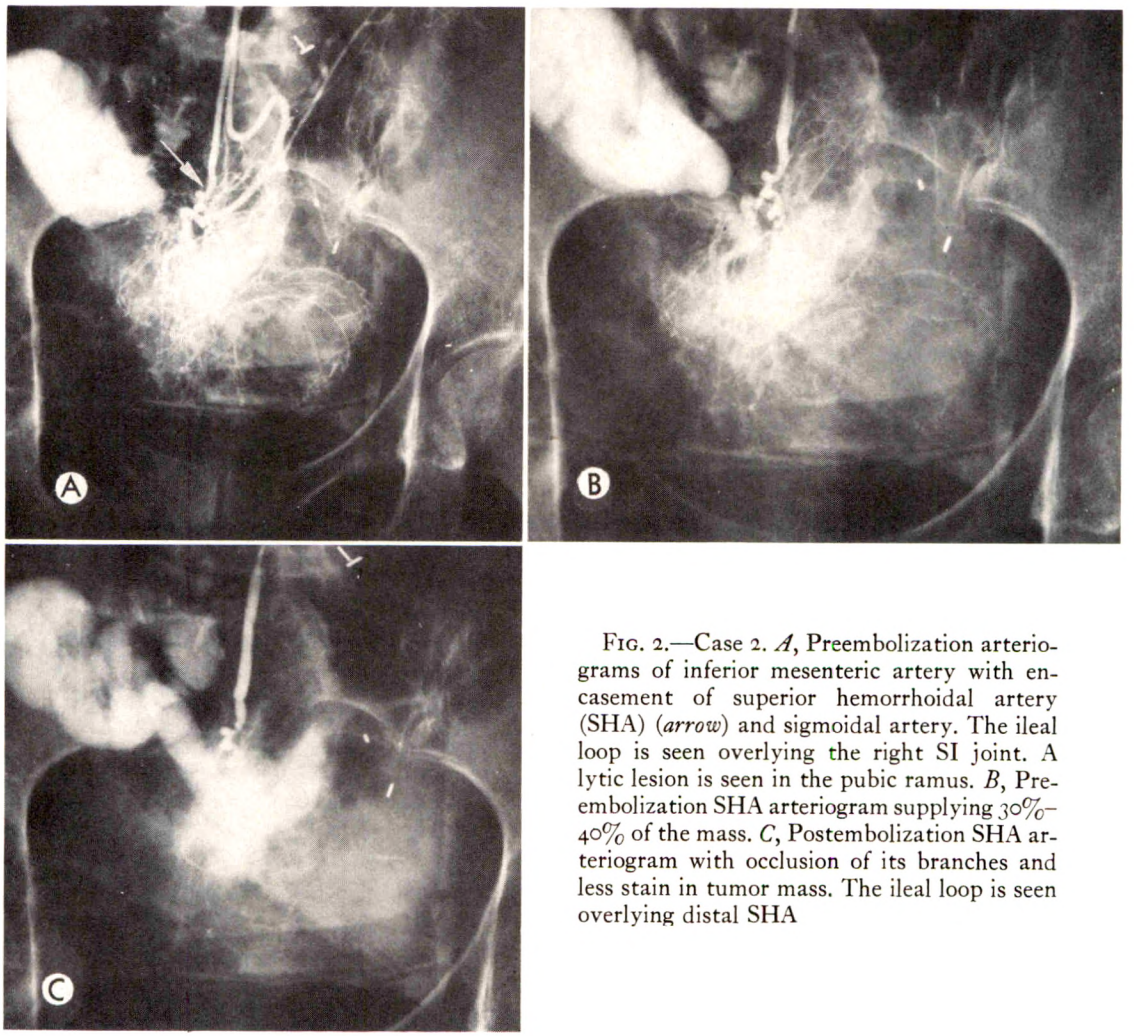


FIG. 2.—Case 2. *A*, Preembolization arteriograms of inferior mesenteric artery with encasement of superior hemorrhoidal artery (SHA) (*arrow*) and sigmoidal artery. The ileal loop is seen overlying the right SI joint. A lytic lesion is seen in the pubic ramus. *B*, Preembolization SHA arteriogram supplying 30%–40% of the mass. *C*, Postembolization SHA arteriogram with occlusion of its branches and less stain in tumor mass. The ileal loop is seen overlying distal SHA

structed in April 1974 because of local tumor occluding the rectum.

Six months later, in November 1974, she developed rectal bleeding and profound anemia. Over a 1-month interval, eight units of blood were transfused. The bleeding continued, became more prominent, and required hospitalization in February 1975. Examination disclosed a large necrotic cavity anterior to the sacrum, a hard nodular mass surrounding the rectum, and painful lymphedema of the right lower extremity. Colonoscopy failed to reveal the exact bleeding site but demonstrated that it originated from the area of the tumor mass. Radiographs of the pelvis revealed metastatic disease in the right acetabulum. The rectal bleeding persisted, and the patient required seven units of blood over 35 days to raise her hematocrit to 32%. One week later profuse rectal hemorrhage recurred requiring two units of blood. Arteriography was performed (figs. 2*A* and 2*B*), and the superior hemorrhoidal branch of the inferior mesenteric artery was embolized with Gelfoam® (fig. 2*C*). The patient maintained a stable hematocrit, and no further bleeding occurred. She died of carcinomatosis 5 months later.

METHOD

For case 1, catheterization was performed with a 6.7 French polyethylene catheter using the Seldinger technique via the right femoral artery. A bilobed false aneurysm of the left hypogastric artery was detected which was selectively occluded using Gelfoam®. The duration of the procedure was approximately 60 min.

Case 2 was studied in a similar fashion, with pelvic and abdominal arteriograms revealing tumor-encased colonic vessels. Selective arteriography of the inferior mesenteric artery revealed that the tumor was supplied by the sigmoid branch of the left colic artery and the superior hemorrhoidal branch of the inferior mesenteric artery. Because selective embolization from the femoral artery approach could not be safely accomplished, a left brachial artery approach was used to catheterize the branches of the inferior mesenteric artery. The percutaneous brachial puncture is made high on the brachial artery, and small catheters (4 or 5 French) must be used. The brachial vessel is entered two-thirds of the distance from the head of the humerus to the antecubital fossa. Using a 265 cm guide wire simplifies the catheterization, especially if an exchange is needed. The guide wire itself is used to engage the inferior mesenteric artery from above, and a straight end-hole catheter is advanced over the wire. The procedure was performed within 90 min.

In both patients, Gelfoam® emboli were prepared and aspirated into a 5-cm^3 plastic syringe, filled with contrast media, and the emboli were then hand injected under fluoroscopy. Gelfoam® shavings were used initially, followed by 2–3 mm pledgets to occlude the larger feeding vessels. Two arteriograms were performed during the embolization in each patient to monitor the area of embolization.

DISCUSSION

Recurrent bleeding from pelvic vessels in gynecologic patients can usually be controlled with hypogastric artery ligation with reported low morbidity [1–3]. Selective transcatheter arterial embolization represents an alternate method of treating pelvic hemorrhage with low morbidity, using local anesthesia and avoiding the risks of a major operative procedure [4–7]. In addition, catheterization can be performed when technical difficulties preclude surgical management. The transcatheter embolization technique has been of proven value in areas such as the gastrointestinal tract [8–10] and the head and neck [11–13].

Arteriography via the femoral route for embolization of the contralateral internal iliac vessels can be accomplished with standard selective catheters. Once the artery is properly engaged, Gelfoam® particles can be easily injected through catheters under fluoroscopy.

If the femoral approach does not allow safe engagement of a pelvic or mesenteric vessel, the brachial artery approach using small catheters can be substituted. Wirtanen has used the latter technique on 332 patients who had primary and metastatic tumors to the liver [14]. These catheters have been left in place for as long as 4 months with minimal morbidity. We have treated two cancer patients via brachial catheters for 6 months without any sequelae. Brachial artery catheterization seems reasonable when the femoral route is not technically feasible and avoids the axillary approach which has the added risk of brachial plexus injury. The duration of the procedure could easily be prolonged in large tumors, and therefore the brachial approach would again be preferable, in our opinion, to the axillary.

Successful catheter control of pelvic hemorrhage secondary to trauma has been reported by Paster et al. [6] and Ring et al. [7]. In Ring's series, embolization was carried out with autologous blood clot in eight cases, and in a ninth patient a Fogarty balloon was used for thrombosis. More recently, Gelfoam® is used [8, 12, 15] because it is easily manageable, effective, and probably longer lasting than blood clot. Other agents including silicone rubber [16] and isobutyl 2-cyanoacrylate [17] have been used clinically and experimentally, although both are technically difficult to use.

Case 1 represents an example of a patient in whom surgical ligation of the hypogastric artery was attempted but not possible because of a marked anatomic distortion secondary to a large necrotic cavity in the pelvis. Hypogastric artery embolization was easily and safely carried out when hemorrhage occurred.

Our second patient was a poor operative risk because of debilitation secondary to widespread metastatic disease and compli-

cations of previous therapy. Although actual extravasation of contrast was not seen, arteriography demonstrated recurrent cancer supplied by the superior hemorrhoidal branch of the left colic artery. The superior hemorrhoidal artery appeared to be entirely involved by the cancerous mass, and because it could be safely catheterized and was separated from the branches of the left colic artery by a distance of 4 cm, it was embolized. No attempt was made to engage the sigmoid branch of the left colic artery, despite the fact that it comprised 60%–70% of the blood supply of tumor, because of its tortuous course and the associated increased risk of occluding it entirely. Even though a transverse colostomy was present, occlusion of the marginal artery of Drummond could lead to ischemia, infarction, and perforation of the descending colon. Collaterals from the sigmoidal vessels anastomose to the superior hemorrhoidal artery in 95% of patients [18] allow occlusion of this artery with relative safety. The smallest vessels that are occluded by Gelfoam® are approximately 100–150 μm in diameter [9]. Therefore, the capillary bed which is left intact can be supplied by collateral circulation, but the arterial pulsation is markedly reduced [3, 19].

REFERENCES

1. Shafiroff BG, Grillo EB, Baron H: Bilateral ligation of the hypogastric arteries. *Am J Surg* 98: 34–40, 1959
2. Siegel P, Mengert WF: Internal iliac artery ligation in obstetrics and gynecology. *JAMA* 178: 1059–1062, 1961
3. Binder GS, Mitchell GA: The control of intractable pelvic hemorrhage by ligation of the hypogastric artery. *South Med J* 53:837–843, 1960
4. Goldstein HM, Meddlin H, Ben-Manachem Y, Wallace S: Transcatheter arterial embolization in the management of bleeding in the cancer patient. *Radiology* 115:603–608, 1975
5. Margolies MN, Ring EJ, Waltman AC, Kerr WS, Baum S: Arteriography in the management of hemorrhage from pelvic fractures. *N Engl J Med* 287:317–321, 1972
6. Paster SB, Van Houten FX, Adams DF: Percutaneous balloon catheterization: a technique for the control of arterial hemorrhage caused by pelvic trauma. *JAMA* 230:573–575, 1974
7. Ring EG, Athanasoulis C, Waltman AC, Margolies MN, Baum S: Arteriographic management of hemorrhage following pelvic fracture. *Radiology* 109:65–70, 1973
8. Bookstein JJ, Chlosta EM, Foley D, Walter JF: Transcatheter hemostasis of gastrointestinal bleeding using modified autogenous clot. *Radiology* 113:277–285, 1974
9. Manelfe C, Guiraud B, David J, Eymeri JC, Tremoulet M, Espagno J, Rasiol A, Geraud J: Embolisation par catheterisme des meningiomes intracraniens. *Rev Neurol* (Paris) 128:339–351, 1973
10. White RI, Giargiana FA, Bell W: Bleeding duodenal ulcer control. Selective arterial embolization with autologous blood clot. *JAMA* 229: 546–548, 1974
11. Adams DM: Transantral internal maxillary artery ligation in prolonged or severe posterior epistaxis. *J La State Med Soc* 1251:389–391, 1973
12. Djindjian R, Cophignon J, Theron JX, Merland JJ, Houdart R: Embolization by super-selective arteriography from the femoral route in neuroradiology. Review of 60 cases. I. Technique, indications and complications. *Neuroradiology* 6: 20–26, 1973
13. Miller FJ, Entzminger LB, Coleman LL, Conner GH, Weidner WA: Successful catheter embolization of a false aneurysm of internal maxillary artery. *Arch Otolaryngol* 101–8, 517–519, August 1975
14. Wirtanen GW: A new angiographic technique in the diagnosis of liver tumor. *Radiology* 108:51–54, 1973
15. Carey LS, Grace DM: The brisk bleed: control by arterial catheterization and Gelfoam plug. *J Can Assoc Radiol* 25:113–115, 1974
16. Doppman JL, Zapol W, Pierce J: Transcatheter embolization with a silicone rubber preparation: experimental observations. *Invest Radiol* 6:304, 1971
17. Dotter CT, Goldman ML, Rösch J: Instant selective arterial occlusion with isobutyl 2-cyanoacrylate. *Radiology* 114:227–230, 1975
18. Reuter SR, Redman HC: *Gastrointestinal Angiography*. Philadelphia, Saunders, 1972
19. Burchell RC: Physiology of internal iliac artery ligation. *J Obstet Gynaecol Br Commonw* 75:642–651, 1968

Am J Roentgenol 126:1033–1034, 1976

PERIPHERAL EMBOLIZATION COMPLICATING BILATERAL RENAL INFARCTION WITH GELFOAM

JEFFREY WOODSIDE,[1] HANS SCHWARZ,[2] AND PETER BERGREEN[1]

ABSTRACT:

Selective arterial embolization is a technique with wide therapeutic applicability. However, regardless of the nature of the embolic particles, reflux into the aorta with peripheral embolization is a serious potential complication. A case is described in which this complication occurred. We recommend that all such embolizations be performed with a balloon catheter occluding the target artery.

Selective arterial embolization has been gaining favor as a nonoperative technique for the treatment of cerebral arteriovenous malformations [1], gastrointestinal and pelvic hemorrhage [2], postbiopsy renal arteriovenous fistulas [3], delivering radioactive infarct particles to tumors, [4], infarcting renal tumors prior to nephrectomy [5, 6], and infarcting kidneys for malignant hypertension [7]. No complications of these procedures in humans have been reported, but we recently encountered a serious complication of Gelfoam infarction for malignant hypertension in a dialysis patient.

CASE REPORT

A 40-year-old black woman was undergoing center dialysis for malignant hypertension and chronic renal failure. Because of poor control on antihypertensives and high peripheral plasma renin levels, she was referred for bilateral nephrectomy. Because she had had recent pulmonary emboli and her general medical condition was poor, bilateral nephrectomy was considered too dangerous. After a detailed informed consent was obtained, it was elected to perform percutaneous transfemoral bilateral renal infarction.

Using the inguinal approach and standard Seldinger technique, a no. 6.7 French-Cook pigtail catheter was introduced and an abdominal aortogram performed. Early films from this examination demonstrated renal arteries of normal caliber. Subsequent films showed persistence of a large amount of contrast material within the renal arterial system indicative of markedly slowed renal blood flow. Selective renal artery catheterizations were next performed using a no. 7 French-Cook catheter, and the kidneys were infarcted with a suspension of shredded Gelfoam in normal saline to which several cubic centimeters of Renografin 76 were added. Infarction was accomplished under fluoroscopic control with repeated small injections of the above mixture. A small amount of back flow into the aorta was seen on a single injection toward the completion of infarction of the left kidney. The patient denied any back or lower extremity pain while in the x-ray department, and her peripheral pulses remained unchanged. Postinfarction selective renal arteriograms under fluoroscopic monitoring failed to reveal any evidence of significant blood flow to either of the infarcted kidneys.

On the evening of the infaraction, she complained of pain in her left foot, but no physical findings were present until the third postinfarction day when areas of dry gangrene appeared and gradually involved the entire left forefoot and several toes on the right foot. Dry gangrene progressed (fig. 1) requiring midfoot amputation 6 weeks later. The response of her hypertension and renin levels to infarction are the subject of a future report, but management of her hypertension has been significantly improved.

DISCUSSION

Many substances have been used for arterial embolization: autologous clot, mus-

[1] Division of Urology, Department of Surgery, University of New Mexico School of Medicine, Albuquerque, New Mexico 87131.
[2] Department of Radiology, University of New Mexico School of Medicine, Albuquerque, New Mexico 87131.

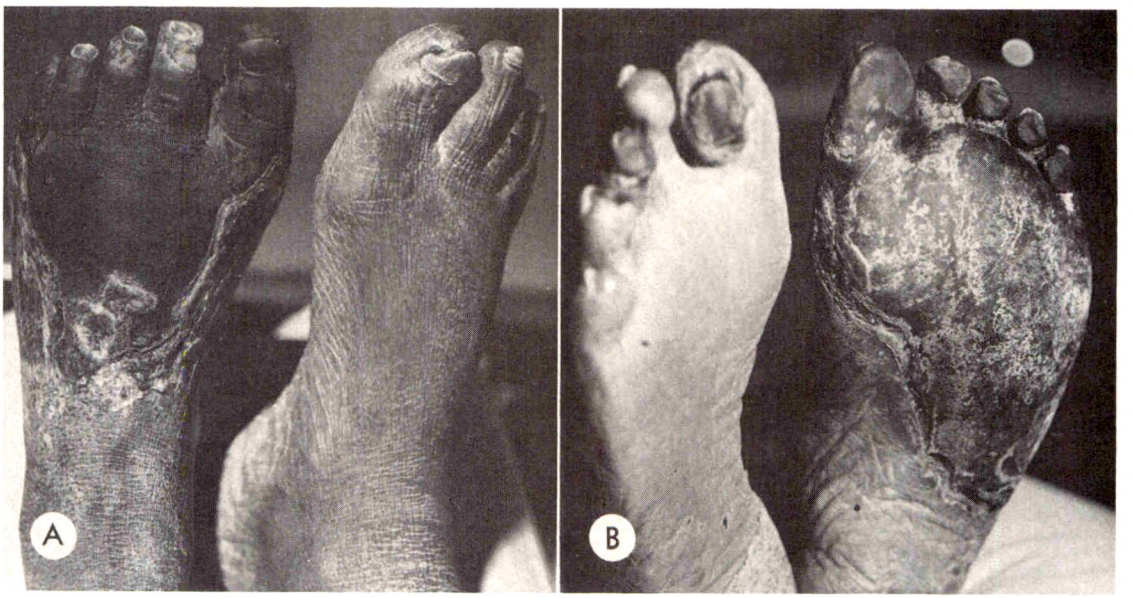


FIG. 1.—*A and B*, Views of feet demonstrating dry gangrene of distal half of left foot 6 weeks after embolization.

cle, fat, lead shot, Sephadex G-50, plastic pellets, barium, and silicone. At our institution, we have successfully used Gelfoam to infarct renal adenocarcinomas prior to nephrectomy without complications in eight patients. We chose Gelfoam because it is easily cut to the particle size desired, is readily suspended in saline for injection, and should promote thrombosis within the renal arterial tree.

A serious complication of arterial embolization that has not been reported in humans is the reflux of the particles into the aorta and subsequent peripheral embolization. Lalli et al [8], while infarcting dog kidneys with Sephadex G-50, noted reflux and embolization of lumbar arteries with resultant spinal cord infarction. They were able to prevent this by using a balloon catheter to occlude the renal artery during injection.

A relatively low renal blood flow and the injection of a larger than usual amount of Gelfoam to attempt a more total renal infarction may have contributed to this serious complication in our patient. However, we feel that it could have been prevented if a balloon catheter had been used. Consequently, we recommend that all such embolizations be performed with a balloon catheter occluding the target artery.

REFERENCES

1. Robles C, Carrasco-Zanini J: Treatment of cerebral arteriovenous malformations by muscle embolization. *J. Neurosurg* 29:603–608, 1968
2. Rosch J, Dotter CT, Brown MJ: Selective arterial embolization. *Radiology* 102:303–306, 1972
3. Boodstein JJ, Goldstein HM: Successful management of postbiopsy arteriovenous fistula with selective arterial embolization. *Radiology* 109: 535–536, 1973
4. Lang EG: Supraselective arterial catheterization as a vehicle for deliver of radioactive infarct particles to tumors. *Radiology* 98:391–399, 1971
5. Almgard LE, Fernstrom I, Haverling M, Ljungqvist A: Treatment of renal adenocarcinoma by embolic occlusion of the renal circulation. *Br J Urol* 45:474–479, 1973
6. Goldstein HM, Medellin H, Beydown TM, Wallace S, Ben-Menachem Y, Bracken RB, Johnson DE: Transcatheter embolization of renal cell carcinoma. *Am J Roentgenol* 123:557–562, 1975
7. Goldin AR, Naude JH, Thatcher GN: Therapeutic percutaneous renal infarction. *Br J Urol* 46:133–135, 1974
8. Lalli AF, Bookstein JJ, Lapides J: Experimental renal infarctions in dogs. *Invest Urol* 8:516–520, 1971

Am J Roentgenol 126:1035–1038, 1976

CROSSED RENAL ECTOPIA: ANGIOGRAPHIC FINDINGS IN SIX CASES

ZALMAN J. RUBINSTEIN,[1] MARJORIE HERTZ, NAZIM SHAHIN, AND VICTOR DEUTSCH

ABSTRACT:

Angiographic findings in six patients with crossed renal ectopia are reported. Crossed fused ectopia was present in four cases, and the remaining two had single crossed ectopic kidneys. All kidneys, including the nonectopic ones, had an anomalous blood supply. No constant arterial pattern was discernible, and renal arteries were found to arise from the aorta both above and below the normal level as well as from the iliac arteries. It is suggested that angiography be undertaken in all cases when surgery is contemplated.

INTRODUCTION

In a recent report [1], the clinical and radiological features of 22 cases of crossed renal ectopia were described. Five of these were studied angiographically, and the purpose of this paper is to describe the findings in these patients. Subsequently another patient was found to have single crossed renal ectopia, thus making a total of six patients for whom angiographic studies were available.

MATERIALS AND METHODS

Arteriography was performed via the femoral artery using the Seldinger technique. Films of the upper abdomen and the pelvis were obtained after contrast injection into the upper and lower abdominal aorta, respectively.

RESULTS

No constant pattern of arterial supply could be discerned in the six cases studied. The two patients with single crossed renal ectopia both had a single renal artery which originated from the common iliac artery (fig. 1). Three renal arteries were present in each of two additional patients (fig. 2), while the remaining two patients had two renal arteries each (fig. 3). Therefore a total of 12 renal arteries supplying 10 kidneys in the six patients were demonstrated; their sites of origin varied considerably. The common iliac artery gave rise to four of these 12 arteries, while another four were given off from the distal aorta at the L3–L4 levels. A high aortic origin was noted at the D12 level in a further three vessels (fig. 4). The remaining twelfth artery arose from the expected level of L1, but even this origin was not completely normal since the artery was seen to come off the anterior surface of the aorta.

In one instance an artery arising from the aorta crossed from one side to another. The artery originated from the right side of the aorta and crossed over to supply the ectopically situated kidney on the left (fig. 2). This was also the only instance in which the inferior adrenal artery was seen to arise from a renal artery. It came off the right-sided renal artery before the latter crossed to the left and supplied the right adrenal gland which was normally situated.

DISCUSSION

The anomaly of crossed renal ectopia is a rare condition in which both kidneys are found to lie on the same side of the body, while their ureters have normally situated entrances into the bladder. Single crossed renal ectopia is even more uncommon, with only 15 cases reported in the literature. In this latter form of anomaly only one kidney is present which derives its blood supply from one side of the body while the ureter enters the opposite side of the bladder.

[1] All authors: Department of Diagnostic Radiology, Chaim Sheba Medical Center, Tel Hashomer, and Tel Aviv University Medical School, Tel Aviv, Israel.

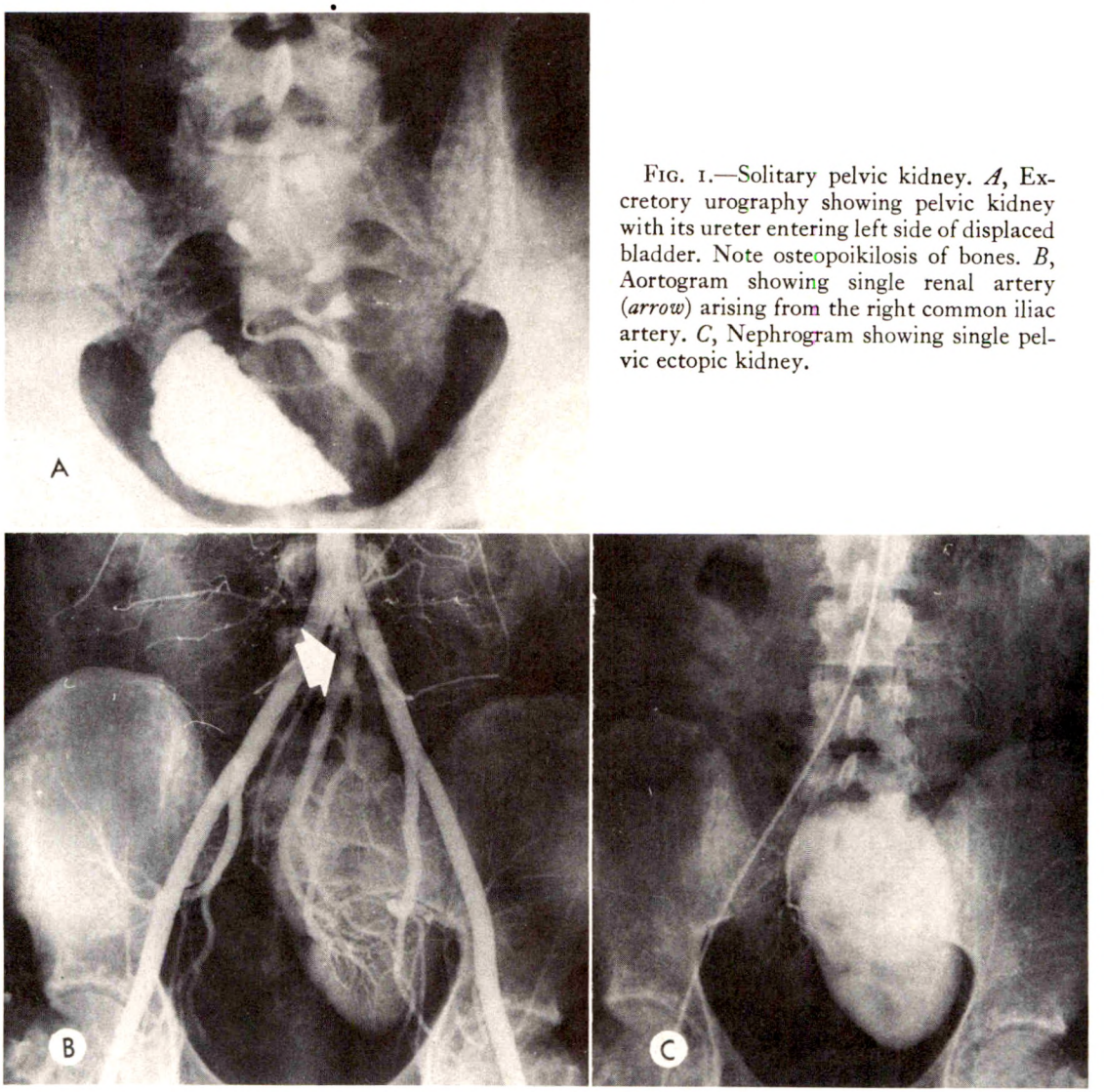


FIG. 1.—Solitary pelvic kidney. *A*, Excretory urography showing pelvic kidney with its ureter entering left side of displaced bladder. Note osteopoikilosis of bones. *B*, Aortogram showing single renal artery (*arrow*) arising from the right common iliac artery. *C*, Nephrogram showing single pelvic ectopic kidney.

That renal ectopia, a developmental anomaly, should be associated with a varying blood supply to these abnormally situated kidneys is not surprising. However, documentation of this variable blood supply has usually been by means of surgical and pathological description. To our knowledge only five cases of crossed renal ectopia have been reported in which the pattern of vascularization was demonstrated by angiography. The three cases described by Olsson and Whorley [2] had branches arising from various levels of the abdominal aorta in addition to others from the iliac vessels. In two of these cases the ectopic kidney was simultaneously supplied by branches from both the left and right iliac arteries. Tannenbaum et al. [3] mention two further cases in which renal arteries arising from the iliac vessels were demonstrated by angiography.

The diagnosis of crossed renal ectopia is usually made by means of excretory urography. It is frequently an incidental finding or is found during the course of investigation of an abdominal "mass," urinary infection, hypertension, or suspected calculous disease. Pelvic angiography should be

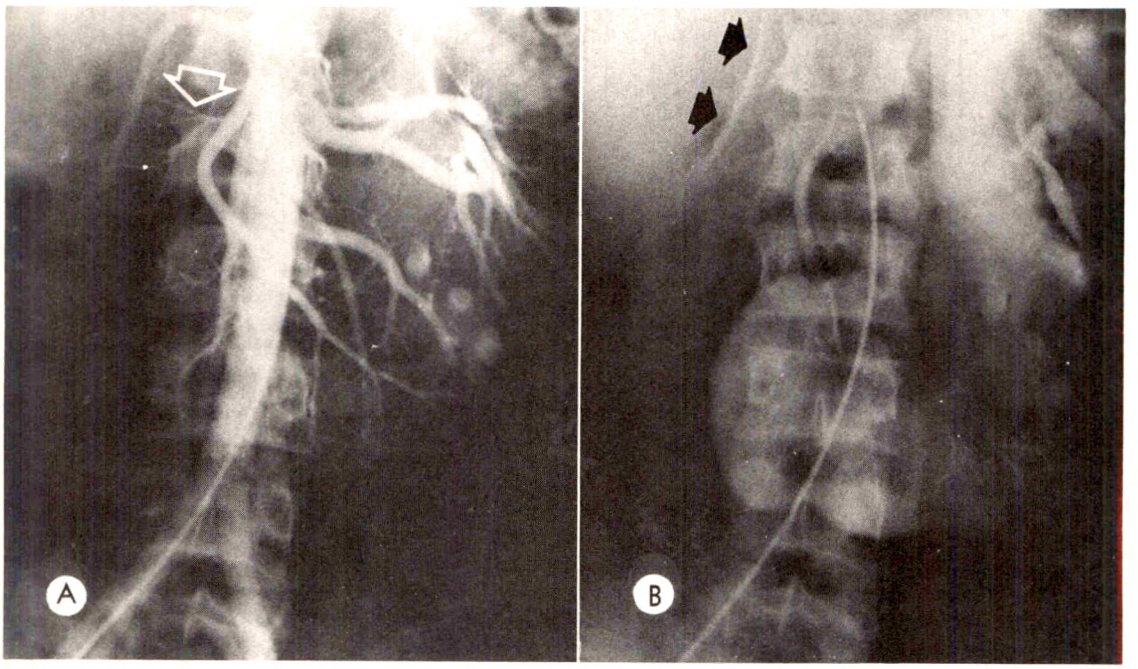


FIG. 2.—Left crossed ectopic kidney, fused. *A*, Arterial phase showing multiple renal arteries. Note right inferior adrenal artery (*arrow*) coming off right renal artery before latter crosses midline. *B*, Nephrogram showing fused kidneys. Note normally situated right adrenal gland (*arrows*).

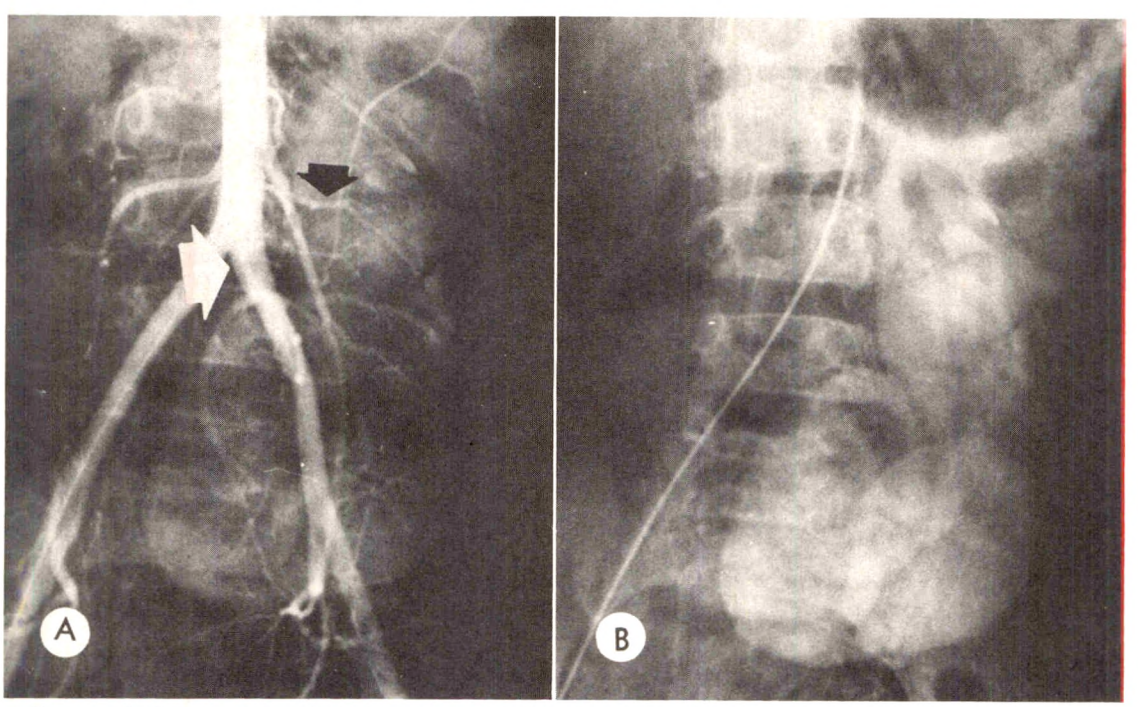


FIG. 3.—Left crossed ectopic kidney, fused. *A*, Renal arteries arising from aortic bifurcation and anterior aorta at level of L2 (*arrows*). *B*, Nephrographic phase.

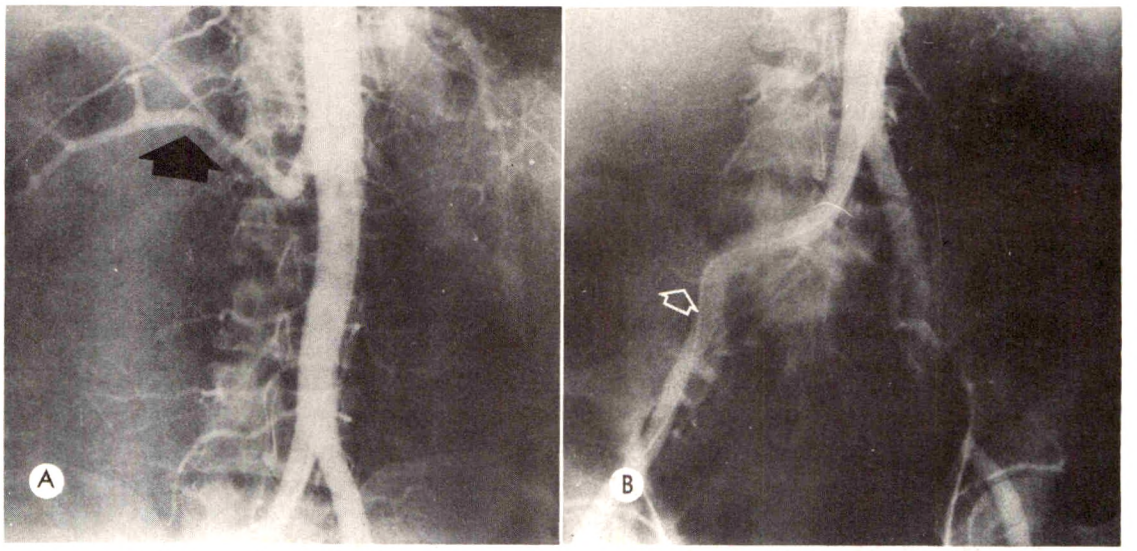


FIG. 4.—Right crossed ectopic kidney, fused. *A*, Aortogram showing high aortic origin (D12 level) of dilated and markedly stretched renal artery (*arrow*). *B*, Pelvic arteriogram showing small atrophic renal artery (*arrow*) arising from right iliac artery and supplying lower hydronephrotic kidney.

performed in patients with a unilateral nonfunctioning kidney on pyelography whose subsequent abdominal angiography fails to show either the kidney or the renal artery.

The diagnosis of crossed ectopic kidney by excretory urography is not in itself an indication for either angiography or surgery. However, whenever the diagnosis is uncertain or complications necessitate surgery, angiography becomes essential. In addition to defining the pathology it also delineates the exact vascular anatomy, which is of crucial importance to the surgeon, especially when the kidneys are fused.

With the obviously disturbed embryological development in these cases, it is understandable that the ectopic kidney is supplied by vessels originating from varying sites. However, it is of interest to note that in all four cases of crossed fused renal ectopia, the arteries to the nonectopic kidney also had abnormal origins from the aorta.

REFERENCES

1. Hertz M, Rubinstein ZJ, Shahin N, Melzer M: Crossed renal ectopia: clinical and radiological findings in 22 cases. Submitted for publication
2. Olsson O, Whorley M: Vascular abnormalities in gross anomalies of kidneys. *Acta Radiol* [*Diagn*] (Stockh) 2:240–432, 1964
3. Tannenbaum B, Silverman N, Weinberg SR: Solitary crossed renal ectopia. *Arch Surg* 101:616–618, 1970

Am J Roentgenol 126:1039–1045, 1976

ANGIOGRAPHICALLY INDUCED RENAL FAILURE AND ITS RADIOGRAPHIC DETECTION

ROBERT A. OLDER,[1] JOSEPH P. MILLER, DONALD C. JACKSON, IRWIN S. JOHNSRUDE, AND WILLIAM M. THOMPSON

ABSTRACT:

Decreased renal function following arteriography is much more common than is currently realized. Steps to detect this failure are necessary, especially in high risk patients, so that stressful situations such as surgery can be avoided. A recently performed prospective random study of 100 patients undergoing angiography demonstrated a 10% incidence of renal failure. Those patients most at risk had preexisting renal disease as indicated by an elevated serum creatinine and/or cardiovascular disease severe enough to require digoxin, diuretics, or nitroglycerin. No cases of renal failure occurred in the absence of one or both of these processes. The likelihood of postangiographic renal failure was unrelated to the quantity of contrast as measured either by total volume or per kilogram body weight.

INTRODUCTION

Toxicity of intravenous contrast media has been a matter of concern since the technique was first used. In the 1950s and early 1960s the serious and frequent complication of renal failure secondary to administration of angiographic contrast media was recognized and documented by prospective studies [1–6]. With the introduction of newer and safer contrast media, the incidence of renal failure diminished and was no longer considered a major problem [7–12]. Although renal toxicity has been demonstrated with the newer media both clinically and experimentally [13–15], studies indicate that current contrast is safe (table 1). Recently Port et al. [20] reported eight cases of renal failure secondary to arteriography. This was not a high incidence considering that 7,400 studies were performed over a period of 6 years. This was a retrospective study, however, and the authors suggested that there may have been a considerably higher incidence than detected.

Two recent cases of renal failure were detected in rapid succession in our hospital. Both occurred immediately postangiography, and both were initially uncovered in our radiology department on the basis of a persistent 24-hr nephrogram. Stimulated by these observations, a prospective study on 100 randomly chosen patients was undertaken to determine the incidence of renal failure after angiography. This paper reports the results of this study.

MATERIALS AND METHODS

A 24-hr postangiogram abdominal film was used as the initial method of detection of renal failure. A persistent nephrogram indicates poor excretion of the contrast and has been shown to be associated with renal failure [22] (fig. 1). The film of the abdomen was obtained on 100 random patients undergoing various types of arteriography. The contrast media used were salts of diatrizoates or iothalamates in concentrations and amounts within generally accepted levels. A 24-hr film was reviewed by one of us. When a persistent nephrogram was observed, serum creatinines were obtained for three consecutive days. Creatinines were not routinely obtained in patients without a positive nephrogram. A preangiographic creatinine level greater than 1.2 mg/100 ml was used as the criterion for preexisting renal disease. Deterioration in renal function subsequent to an angiogram was considered to have occurred if

Presented at the annual meeting of the American Roentgen Ray Society, Atlanta, Georgia, October 1975.
W. M. Thompson is a James Picker Foundation Scholar.
[1] All authors: Department of Radiology, Duke University Medical Center, Durham, North Carolina 27710.

TABLE 1

RENAL FAILURE DUE TO CONTRAST MEDIA

REFERENCE	YEAR	CONTRAST	TYPE OF STUDY	NO. STUDIED	RENAL COMPROMISE	
					No.	%
Miller et al. [6]	1953	Diiodinated	Translumbar	250	4	1.6
Idbohrn [4]	1955	Diiodinated	Abdomen	186	10	5.3
McAfee [5]	1956	Diiodinated	Abdomen	13,207	39	0.3
Edling and Helander [2]	1957	Diiodinated	Abdomen	302	7	2.1
Bartley et al. [16]	1969	Triiodinated	Abdominal-renal	26	0	0*
Metys et al. [17]	1971	Triiodinated	Abdomen	110	0	0*
Reiss et al. [18]	1972	Triiodinated	Abdominal-renal	2,710	8	0.29
Doust and Redman [19]	1972	Triiodinated	Abdominal-peripheral	71	2	2.8
Port et al. [20]	1974	Triiodinated	Various	7,400	8	0.1
Brewster et al. [21]	1975	Triiodinated	Abdomen	190	1	0.5

* Prospective study.

the serum creatinine level changed by at least 20% or 0.3 mg/100 ml.

RESULTS

Of the 100 patients initially in the study, 10 were eliminated because of insufficient data. Of the remaining 90, 17 had a positive nephrogram at 24 hr. Nine of the 17 showed a significant change in renal function, indicating a 10% incidence of renal failure. Table 2 and figures 2 and 3 show the change in serum creatinine levels in these nine patients. One patient was oliguric for 24 hr but due to laboratory error, renal function studies were not obtained until the failure had been resolved. The incidence of failure detected was considerably higher than has been reported with current contrast media [16–21].

Additional Data

During the 4 months of the prospective study, five patients not included in our random selection also developed clinically documented renal failure following angiography (table 2 and fig. 4). Of this combined group of 14 patients, 10 had renal failure of sufficient magnitude to be life threatening, especially if they were to be subjected to further stress.

The amount of contrast media used and the type of angiographic study performed in this combined group of patients are summarized in table 3. Possible predisposing factors are listed in table 4.

CASE REPORTS

Case 1

B. D. (patient no. 14) had an aortofemoral arteriogram for evaluation of peripheral vascular disease. The patient was being treated with digoxin for congestive heart failure. Renal function was within normal limits with a serum creatinine level of 1 mg/100 ml prior to the angiogram. During angiography, the patient received 100 cm^3 of Renografin 60 and 100 cm^3 of Renografin 76 (2.0 cm^3/kg body weight). The morning following angiography, the patient's serum creatinine level was 3.0 mg/100 ml, but this result was not available prior to surgery. Immediately following surgery the

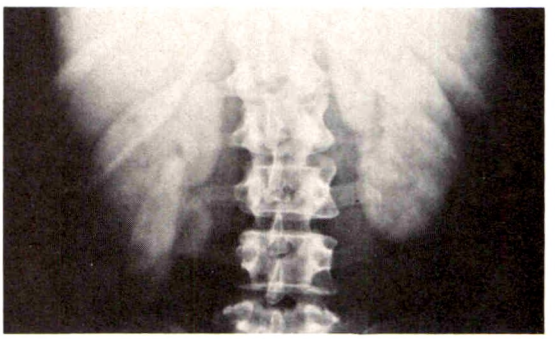


FIG. 1.—Persistent nephrogram 24 hr after arteriography. Contrast in gallbladder is from catheterization; patient did not have gallbladder study.

TABLE 2

CHANGES IN RENAL FUNCTION AFTER ANGIOGRAPHY

PATIENT NO.	INCREASE IN SERUM CREATININE	
	Mg/100 ml	%
Primary study:		
1	2.1	95
2	2.5	109
3	0.5	21
4	1.0	67
5	0.6	60
6	0.5	20
7	0.3	30
8	2.1	140
9*	...	...
Additional cases:		
10	1.4	93
11	3.3	220
12	5.8	252
13	3.0	230
14	2.0	200

* Oliguric but insufficient laboratory data.

patient developed severe renal failure (creatinine = 6.5 mg/100 ml) which returned to normal on the ninth postoperative day.

Comment. It is important to detect changes in renal failure following arteriography so that stressful situations which may lead to further renal failure and even death may be avoided. Surgery is the most common form of such stress. It is not at all unusual to have angiography performed the day prior to surgery without reevaluation of the patient's renal status between the two events. The complication of significant renal failure may have been avoided if the laboratory results had been known prior to the operation.

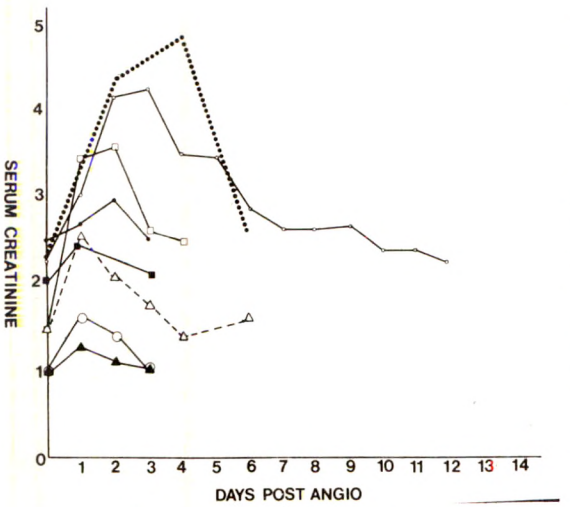


FIG. 2.—Serum creatinine levels (mg/100 ml) in eight patients with postangiographic renal failure.

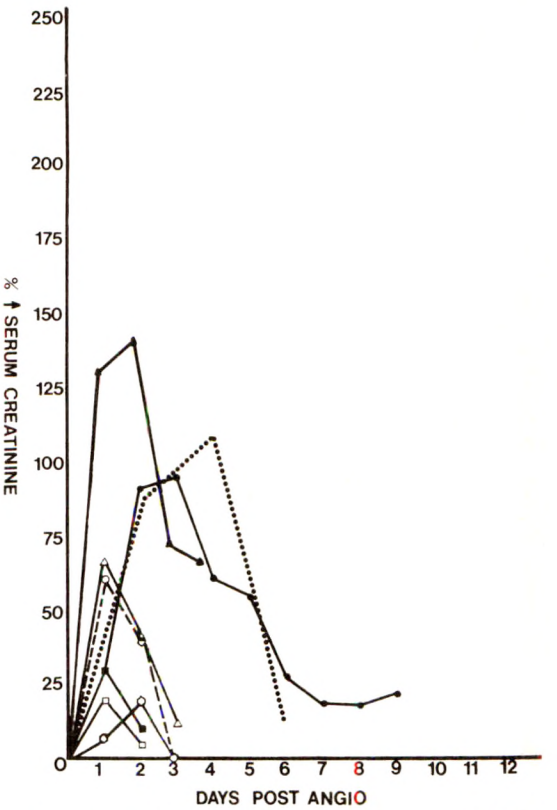


FIG. 3.—Percentage change in serum creatinine levels in eight patients with postangiographic renal failure.

Case 2

E. B. (patient no. 8) was evaluated angiographically for brachiocephalic, renal vascular, and aortofemoral occulsive disease. She had mild renal insufficiency (serum creatinine of 1.5 mg/100 ml) at the time of the study. She received 340 cm^3 of Renografin 76 and 40 cm^3 of Renografin 60 (4.3 cm^3/kg body weight). Following arteriography, renal failure was detected on the basis of the 24-hr abdominal film. Renal function studies showed a 140% elevation of serum creatinine to 3.6 mg/100 ml. These renal abnormalities cleared with diuretics and fluids in approximately 4–5 days. Since the surgery was not an emergency, she was discharged and returned 6 weeks later for an

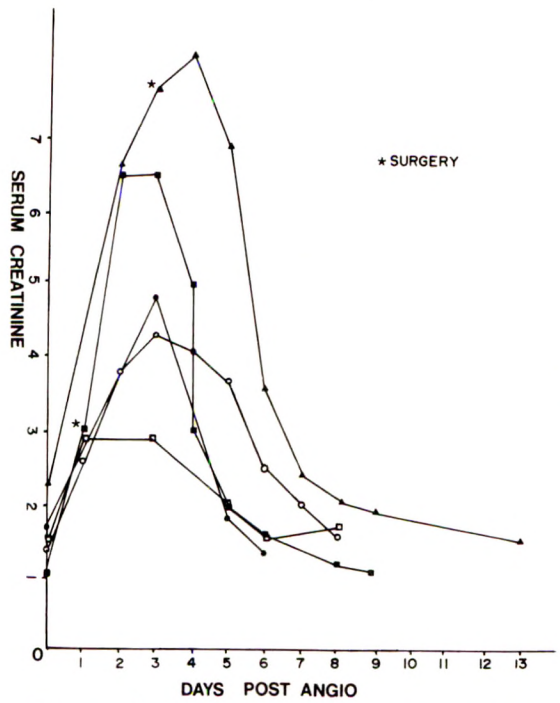


FIG. 4.—Serum creatinine levels (mg/100 ml) in five patients not included in primary study.

elective procedure. Her creatinine at this time was still elevated (2.2 mg/100 ml). Following aortofemoral bypass surgery, she developed further renal deterioration with the creatinine rising to 2.9 mg/100 ml. However, this returned promptly to her previous level.

Comment. In this patient, knowledge of the renal failure prior to surgery allowed the elective operation to be delayed and may have prevented more severe renal damage from occurring after surgery.

DISCUSSION

The pathogenesis of renal failure following contrast injection has received considerable attention. Several mechanisms have been postulated: precipitation of Tamm-Horsfall proteins [22, 23]; increased blood viscosity due to aggregation and clumping of red cells [24–27]; direct toxic effect on the renal tubules [7, 28, 29]; allergic reactions including antibodies to sodium iothalamate [30, 31]; uricosuric effect [32]; and anoxia due either to replacement of oxygenated blood by contrast or to a shift of the oxyhemaglobin curve to the left [33]. Osmotic nephrosis has been detected after contrast studies, but the relationship of this histologic entity to clinical renal failure is not certain [34]. The importance of each of the above in renal failure due to contrast media is uncertain.

Prior to angiography, those patients who are most likely to develop renal compromise as the result of the procedure should be identified. Our study indicates that the patient most at risk is hypertensive, has preexisting renal disease as evidenced by elevated serum creatinine, has some form of cardiovascular disease severe enough to require digoxin, diuretics, or nitroglycerin, and may be in congestive heart failure (table 4). In our series, no patient had multiple myeloma, and only one had hyperuricemia. The role of diabetes mellitus may be significant, since four of the 14 patients had this disease.

Ten of the 14 patients who developed renal failure had preexisting renal disease (table 4). This has prompted us to obtain serum creatinines prior to all angiographic procedures. The clinical review of systems was most often negative with regard to preexisting renal disease and is not by itself a

TABLE 3

ANGIOGRAPHIC DETAILS IN PATIENTS WITH RENAL FAILURE

PATIENT No.	AMOUNT OF CONTRAST: Cm^3/kg Body Weight	AMOUNT OF CONTRAST: Total (cm^3)	TYPE OF ANGIOGRAPHIC STUDY*
1.....	2.0	170	Multiple
2.....	3.6	200	Multiple
3.....	1.9	166	Multiple
4.....	2.7	178	Multiple
5.....	4.6	256	Arch
6.....	3.1	225	Multiple
7.....	1.9	140	Aortofemoral
8.....	4.3	380	Multiple
9.....	3.8	240	Multiple
10.....	4.1	410	Multiple
11.....	2.7	190	Arch
12.....	5.0	270	Multiple
13.....	1.4	85	Heart Catheterization
14.....	2.8	200	Aortofemoral

*Multiple = flush aortogram and at least one selective injection.

TABLE 4

CLINICAL DETAILS IN PATIENTS WITH RENAL FAILURE

Patient No.	Primary Diagnosis	Preexisting Renal Disease	Congestive Heart Failure	High Blood Pressure	Cardiovascular Medication
1.....	Nephrotic syndrome	+	+	+	Digoxin, diuretics
2.....	ASCVD	+	+	+	Lanoxin, diuretics
3.....	Renovascular hypertension	+	...	+	Antihypertensives, Inderal
4.....	Hypernephroma	+	...	...	None
5.....	ASCVD, mitral regurgitation	...	...	...	Digoxin, Persantine
6.....	Aortic aneurysm	+	...	+	Digoxin, antihypertensives
7.....	ASCVD	...	...	+	Inderal, nitrogylcerine
8.....	ASCVD, rheumatic heart disease	+	+	+	Diuretics, antihypertensives
9.....	ASCVD	...	...	...	Digoxin, nitroglycerine
10.....	left hydronephrosis, CAD	+	...	+	Nitroglycerine
11.....	ASCVD	+	...	...	Digoxin, diuretics
12.....	Bilateral hydronephrosis	+	...	+	None
13.....	Endocarditis, mitral and aortic regurgitation	+	+	+	Digoxin, diuretics
14.....	ASCVD	...	+	+	Digoxin

sufficient technique for screening.

Cardiovascular disease was present in 12 of the 14 patients who developed renal failure (table 4). Of these 12 patients, nine had arteriosclerotic vascular disease manifested by transient cerebral ischemic attacks, angina, or claudication. One patient had severe rheumatic heart disease with two prosthetic valves, one had severe renal vascular hypertension, and one had nephrotic syndrome complicated by congestive heart failure. While only five of these 12 patients had congestive heart failure, all 12 had cardiovascular disease significant enough to require digoxin, diuretics, or nitroglycerin.

The generally accepted upper limits of dose tolerance for contrast media in an angiographic study vary up to a total of 5 cm^3/kg body weight during the entire procedure. In our series (table 3), renal failure developed in patients who received as little as 1.4 cm^3/kg (85 cm^3 total) during a cardiac catheterization. Although as much as 5 cm^3/kg was given in one patient, the average dose in patients entering into renal failure was 3 cm^3/kg.) No correlation was seen between the amount of contrast (either total or per kilogram body weight) and the severity or likelihood of developing renal failure.

No single angiographic procedure predisposed the patient to postangiographic renal failure. Two of the patients had aortofemoral arteriograms, one had cardiac catheterization, three had arch arteriograms, and nine had multiple injections, including at least one selective renal injection in six. One of the 14 patients had an obvious allergic reaction to the contrast media, developing a mild urticaria which responded promptly to parenteral Benadryl. In no case was sustained hypotension documented during any of the angiographic procedures.

Patients are often fasted after midnight while in the hospital. Specific clear liquid breakfast orders are routine prior to angiography in our department. No doubt many patients were inadvertently fasted for variable periods prior to angiography, and we are unable to comment upon the significance of dehydration in contributing to renal failure.

Several patients had other contrast studies (intravenous pyelography, cardiac catheterization, etc.) the day before or after angiography. In light of our findings, this

added insult to the kidneys could only be detrimental and may under some circumstances have been the deciding factor as to whether the patient developed renal failure. Several days should elapse between contrast studies if the patient's condition permits. When delay is not possible, the patient should be carefully monitored for renal failure for several days.

The importance of the positive nephrogram should be considered: 53% of our patients who showed contrast media lying within the renal parenchyma on the 24-hr films had documented renal failure. Chart review of the majority of cases without a positive nephrogram, and in whom routine laboratory studies were not obtained, revealed no instances of clinical renal failure. Sufficient laboratory data was available for 30% of these patients to exclude subclinical renal failure.

We are currently performing a larger study which includes a renal profile both before and after arteriography in all patients studied rather than just those with a positive nephrogram. This will give a broader appreciation of the full scope of the problem of renal failure as it relates to angiography. The profile includes a KUB using identical geometry and radiographic factors before and after angiography. This should provide a better baseline for more accurate determination of a positive nephrogram. The role of the KUB as a sensitive tool in the investigation of postangiographic renal failure will thus be more accurately evaluated.

REFERENCES

1. Alwall N, Johnsson S, Tornberg A, Werko L: Acute renal failure following angiography: especially the risk of repeated examination revealed by eight cases (two deaths). *Acta Chir Scand* 109:11, 1955
2. Edling NPG, Helander CG: On renal damage due to aortography and its detection by renal tests: with reports of five cases of severe renal damage. *Acta Radiol* 47:473–480, 1957
3. Fry WJ: Acute renal failure and death following aortography: report of case. *Univ Michigan Med Bull* 20:201–207, 1954
4. Idbohrn H: Tolerance to contrast media in renal angiography. *Acta Radiol* 45:141, 1956
5. McAfee JG: Survey of complications of abdominal aortography. *Radiology* 68:825–838, 1957
6. Miller GM, Wylie EJ, Hinman F Jr: Renal complications from aortography. *Surgery* 35:885–896, 1954
7. Davidson AJ, Abrams HL, Stamey TA: Renal extraction of PAH in man following abdominal aortography. *Radiology* 85:1043–1046, 1965
8. Davidson AJ, Becker J, Rothfield N, Unger G, Ploch, DR: Evaluation of effect of high-dose urography on previously impaired renal and hepatic function in man. . *Radiology* 97:249–254, 1970
9. Grainger RG: Renal toxicity of radiological contrast media. *Br Med Bull* 28:191–195, 1972
10. McEvoy J, McGeown MG, Kumar R: Renal failure after radiological contrast media. *Br Med J* 4:717–718, 1970
11. Walsh PC, Gittes RF, Lecky JW: Aortography in experimental renal failure: evaluation of contrast media toxicity. *Radiology* 97:33–37, 1970
12. Wollowick HE, Foster JH, Snyder HE, Younger, R, Killen DA: Effect of abdominal aortography on proximal renal tubule function. *J Surg Res* 6:346–353, 1966
13. Gruskin AB, Oetliker OH, Wolfish NM, Gootman NL, Bernstein J, Edelmann CM Jr: Effects of angiography on renal function and histology in infants and piglets. *J Pediatr* 76:41–48, 1970
14. Rhea WG Jr, O'Neill JA Jr, Killen DA, Foster JH: Toxic reactions incident to aortography: the hazard of repeat injection. *Circulation* 2, suppl. 29:161, 1964
15. Rhea WG Jr, Killen DA, Foster JH: Relative nephrotoxicity of Hypaque and Angioconray. *Surgery* 57:554, 1965
16. Bartley O, Bentsson U, Cederbom G: Renal function before and after urography and angiography with large doses of contrast media. *Acta Radiol* [*Diagn*] (Stockh) 8:9–16, 1969
17. Metys R, Horynch A, Burianova B, Jirka J: Influence of tri-iodinated contrast media on renal function. *Nephron* 8:559, 1971
18. Reiss MD, Bookstein JJ, Bleifer KH: Radiology aspects of renovascular hypertension. *JAMA* 221:375–378, 1972
19. Doust BD, Redman HC: Myth of 1 ml/kg in angiography: study to determine relationship of contrast medium dosage to complications. *Radiology* 104:557–560, 1972
20. Port W, Wagoner R, Fulton R: Acute renal failure after angiography. *Am J Roentgenol* 121:544–550, 1974
21. Brewster DC, Retana A, Waltman AC, Darling RC: Angiography in the management of aneurysms of the abdominal aorta; its value and safety. *N Engl J Med* 292:822–825, 1975
22. Berdon WE, Schwartz RH, Becker J, Baker DH: Tamm-Horsfall proteinuria; its relation-

ship to prolonged nephrogram in infants and children and to renal failure following intravenous urography in adults with multiple myeloma. *Radiology* 92:714–722, 1969

23. Perillie PE, Conn HO: Acute renal failure after intravenous pyelography in plasma cell myeloma. *JAMA* 167:2186–2189, 1958
24. Dean RE, Andrew JH, Read RC: Red cell factor in renal damage from angiographic media: perfusion studies of in situ canine kidney with cellular and acellular perfusates. *JAMA* 187:27–31, 1964
25. Derrick JR, Brown RW, Livanec G, Bond TP, Guest MM: Experimental effects of selective arteriography on microcirculation. *Am J Surg* 116:712–714, 1968
26. Pillay WKG, Robbins PC, Schwartz FD, Kark RM: Acute renal failure following intravenous urography in patients with long-standing diabetes mellitus and azotemia. *Radiology* 95:633–636, 1970
27. Stark FR, Coburn JW: Renal failure following methylglucamine diatrizoate (Renografin) aortography: report of case with unilateral renal artery stenosis. *J Urol* 96:848–851, 1966
28. Sorby WA, Hoy RJ: Renal arteriography and renal function: short-term effect of aortography, selective renal arteriography, adrenalin suppression and renal venography on PAH extraction ratio. *Australas Radiol* 12:252–255, 1968
29. Talner LB, Davidson AJ: Effect of contrast media on renal extraction of PAH. *Invest Radiol* 3:301–309, 1968
30. Borra S, Hawkins D, Duguid W, Kaye M: Acute renal failure and nephrotic syndrome after angiocardiography with meglumine diatrizoate. *N Engl J Med* 284:592–593, 1971
31. Kleinknecht D, Deloux J, Homberg JC: Acute renal failure after intravenous urography: detection of antibodies against contrast media. *Clin Nephrol* 2:116–119, 1974
32. Postlehwaite AE, Kelley WN: Uricosuric effect of radiocontrast agents: study in man of four commonly used preparations. *Ann Intern Med* 74:845–852, 1971
33. Rosenthal A, Litwin SB, Laver MB: Effects of contrast media used in angiocardiography on henoglobin-oxygen equilibrium. *Invest Radiol* 8:191–198, 1973
34. Moreau J, Droz D, Sabto J, Junjers P, Kleinknecht D, Hinglais N, Michel J: Osmotic nephrosis induced by water-soluble tri-iodinated contrast media in man. *Radiology* 115:329–336, 1975

Am J Roentgenol 126:1046–1052, 1976

ARTHROGRAPHIC EVALUATION OF INJURIES OF THE FIRST METACARPOPHALANGEAL JOINT: GAMEKEEPER'S THUMB

DONALD RESNICK[1] AND LARRY A. DANZIG[2]

ABSTRACT:

The radiographic evaluation of gamekeeper's thumb is described in an experimental study in nine cadaveric hands. After the application of radial stress at the metacarpophalangeal joint in the extended and abducted thumbs in an attempt to create defects in the ulnar collateral ligament, initial and stress radiography and arthrography were employed. In four cadavers a fracture of the proximal phalanx was noted; stress radiography revealed variability in joint stability. Arthrography outlined ulnar extravasation in six of the nine cadavers; surgical confirmation of a capsular tear was obtained following careful dissection in each of these six cadavers. It would appear that plain films, stress radiography, and arthrography complement each other in the diagnosis of gamekeeper's thumb.

Ligamentous injuries along the ulnar aspect of the metacarpophalangeal joint of the thumb have received considerable attention [1–3]. Initially described as an occupational hazard in English gamewardens who destroyed rabbits by twisting their necks, thus sustaining repeated stresses about this articulation (fig. 1*A*), the condition became known as gamekeeper's thumb [4]. More recently, similar injuries have been noted in skiers (fig. 1*B*) [5]. In either case this is a significant condition resulting in instability of pinch. It is our purpose to outline the radiographic evaluation of gamekeeper's thumb from observations made on a group of cadavers, emphasizing arthrographic abnormalities.

MATERIALS AND METHODS

Fresh nonembalmed hand specimens in nine cadavers were utilized in the investigation. In each case radial stress at the metacarpophalangeal joint was applied in the extended and abducted thumb. Plain films and stress radiographs were then obtained. Arthrography of the first metacarpophalangeal joint was accomplished using 1–1½ cm^3 of contrast material (Renografin 60, Squibb). Injection was made into the joint from a dorsoradial approach with fluoroscopic monitoring. Careful surgical dissection of the ligamentous apparatus on the ulnar aspect of the articulation was performed by one of us (L. Danzig) in the nine cadavers without knowledge of the radiographic findings.

ANATOMIC AND PATHOLOGIC CONSIDERATIONS

The metacarpophalangeal joint of the thumb is a diarthrodial articulation with a loose joint capsule. It derives its stability from surrounding collateral, accessory collateral, and palmar ligaments as well as intrinsic muscles (fig. 2) [6]. The collateral ligaments course from the dorsoulnar and radial aspects of the metacarpal head in a volar direction, attaching to the lateral tubercle of the proximal phalanx. The accessory collateral ligaments originate adjacent to the collateral ligaments and attach to the volar plate.

There have been conflicting opinions regarding the site of injury in gamekeeper's thumb. Kaplan [7] believes that capsular tearing in the dorsal expansion between the tendons of the extensor pollicis longus and

This work was supported in part by Veterans Administration grant no. 7406.

[1] Department of Radiology, University Hospital, University of California at San Diego, and Veterans Administration Hospital, San Diego, California 92161.

[2] Department of Orthopedic Surgery, University Hospital, University of California at San Diego, and Veterans Administration Hospital, San Diego, California 92161.

the adductor pollicis is the initial abnormality. It is generally held, however, that the most frequently damaged structure is the ulnar collateral ligament [4, 8]. This ligament may be avulsed from its distal phalangeal attachment or, more rarely, its proximal metacarpal attachment. A small piece of bone may accompany the avulsion [6, 8, 9]. Usually, the dorsoulnar capsule tears in conjunction with defects in the ulnar collateral and accessory collateral ligaments and volar plate [2, 6], although the capsule is occasionally intact [9]. Articular cartilage injury may be an associated abnormality [2, 6] leading to significant arthrosis.

Stener [3], in an evaluation of 40 patients, described a characteristic displacement of the ruptured ulnar collateral ligament (fig. 3). During surgical observation, he noted that the ulnar expansion of the dorsal aponeurosis was interspersed between the ruptured end of the ligament and its site of attachment to the phalanx. He postulated that in time the torn end of the ligament could pass beyond the proximal edge of the adductor aponeurosis.

RESULTS

Initial radiographs were negative in five of the nine cadavers (table 1). In the remaining four, fractures of variable size originating from the ulnar aspect of the proximal phalanx were evident. The fragments remained near their site of detachment or were displaced slightly proximally; rotation of the piece of bone occurred in two cadavers (fig. 4*A*).

X-rays taken during radial stress were obtained in seven of the nine cadaveric hands. Separation at the ulnar aspect of the joint between the metacarpal and proximal phalanx varied from 2 mm (two cadavers) to 7 mm (one cadaver). In the two hands with the greatest separation (6 mm and 7 mm), fractures of the proximal phalanx were present (fig. 4*B*).

Arthrography was performed in all nine specimens; normal findings were noted in three (figs. 5*A* and 5*B*). Extravasations of



FIG. 1.—*A*, Classic mechanism of injury. To kill a wounded rabbit, gamekeeper extends rabbit's neck and applies traction. Although a strong pull in direction of arrow would normally exert pressure only in cleft between first and second fingers, a loose grip produced strain along ulnar aspect of thumb (*curved arrow*) stretching ulnar collateral ligament. *B*, Modern mechanism of injury. Incorrect implantation of ski pole produces abduction and extension of thumb (*arrow*) as momentum carries skier downhill. This creates stress on ulnar aspect of first metacarpophalangeal joint with injury to ulnar collateral ligament.

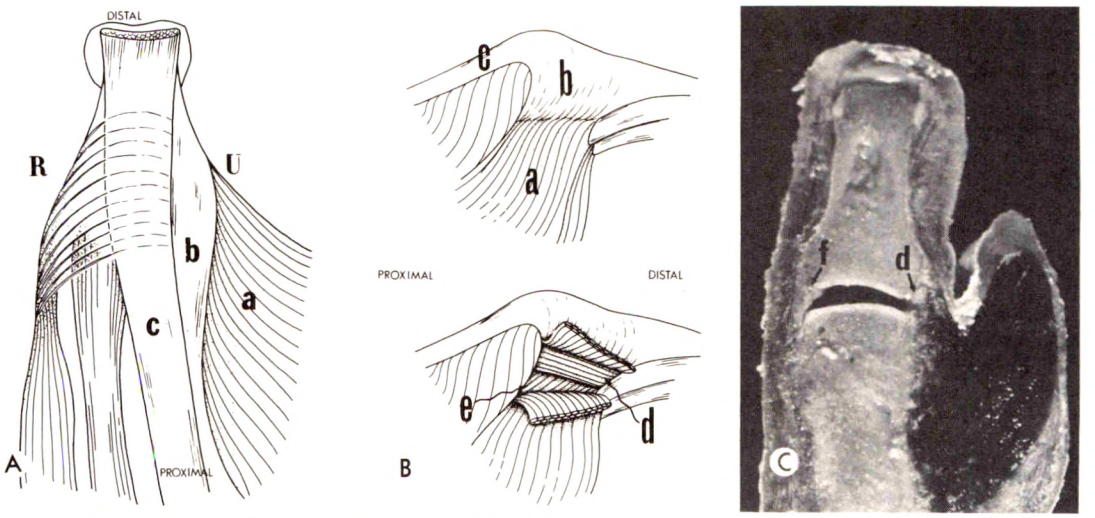


FIG. 2.—Anatomy of ligaments of metacarpophalangeal joint of thumb. *A*, Dorsal aspect showing radial (*R*) and ulnar (*U*) sides of metacarpophalangeal joint. Tendon of extensor pollicis longis (*c*) passes over metacarpophalangeal joint running from proximal to distal aspect of digit. Adductor pollicis muscle (*a*) inserts in part on the proximal phalanx, some of its fibers fusing with a portion of the dorsal aponeurosis, termed the adductor aponeurosis (*b*). *B*, Ulnar aspect showing adductor pollicis (*a*), adductor aponeurosis (*b*), and tendon of the extensor pollicis longus (*c*). In lower drawing the adductor pollicis has been incised and opened exposing ulnar collateral (*d*) and accessory collateral (*e*) ligaments. *C*, Coronal section of first metacarpophalangeal joint. Note position of ulnar (*d*) and radial (*f*) collateral ligaments.

variable size occurred along the ulnar aspect of the joint in the other six cadavers: in cadavers 1 and 3 a fanlike pattern of extravasation occurred opposite the joint (fig. 6*A*); in cadavers 1, 6, and 8 the extravasated dye flowed distally along the phalanx (fig. 6*B*), and in cadavers 5, 7, and 8 the extraarticular dye flowed in a proximal direction along the metacarpal (figs. 6*C* and 6*D*). In two cadavers (nos. 1 and 3) radial extravasation also occurred at the site of needle puncture (fig. 6*A*).

Dissection demonstrated abnormalities in six of the cadavers; in three, no defects in the ligamentous apparatus or capsule could be seen (fig. 5*B*). In cadavers 1, 3, 6, and 7, capsular tears were associated with avulsed phalangeal fragments (fig. 6*D*); the ulnar collateral ligaments were attached to the displaced bone and were not torn. In

TABLE 1

ANALYSIS OF THUMBS

Cadaver No.	Plain Films	Stress Films*	Arthrograms	Dissections
1.....	Fracture of proximal phalanx	N.D.	+	+
2.....	...	4	−	−
3.....	Fracture of proximal phalanx	N.D.	+	+
4.....	...	4	−	−
5.....	...	5	+	+
6.....	Fracture of proximal phalanx	6	+	+
7.....	Fracture of proximal phalanx	7	+	+
8.....	...	2	+	+
9.....	...	2	−	−

* Numbers represent measurement (mm) of widest separation of metacarpal and proximal phalanx at metacarpophalangeal joint. N.D. = not done.

one (cadaver 8), defects of the ulnar collateral ligament and capsule near the base of the proximal phalanx were apparent. In another case (cadaver 5) the avulsion of the ulnar collateral ligament occurred at its metacarpal attachment in association with a capsular tear. In no instance was interposition of the dorsal aponeurosis between the torn ligament and its phalangeal attachment noted.

DISCUSSION

Gamekeeper's thumb is a significant injury resulting in attenuation and/or disruption of the ligamentous apparatus along the ulnar aspect of the first digit. The problem may be difficult to diagnose clinically [5, 10], although pain, swelling, tenderness, edema, and pinch instability may be important symptoms and signs. X-ray evaluation includes plain film and stress radiography as well as arthrography.

Initial radiographs (positive in four of our cadavers) may disclose avulsed fragments from the base of the proximal phalanx [3, 6, 9]. The fractured piece of

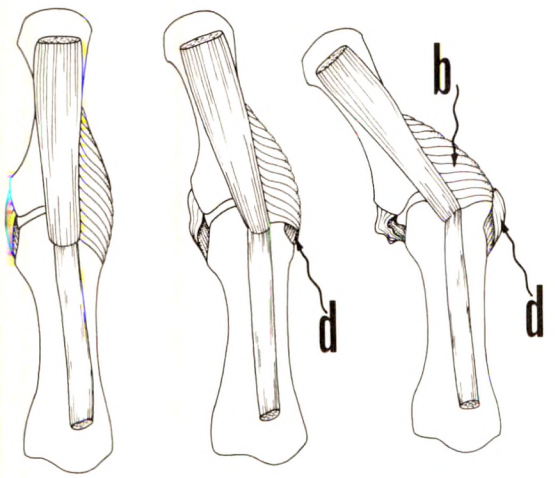
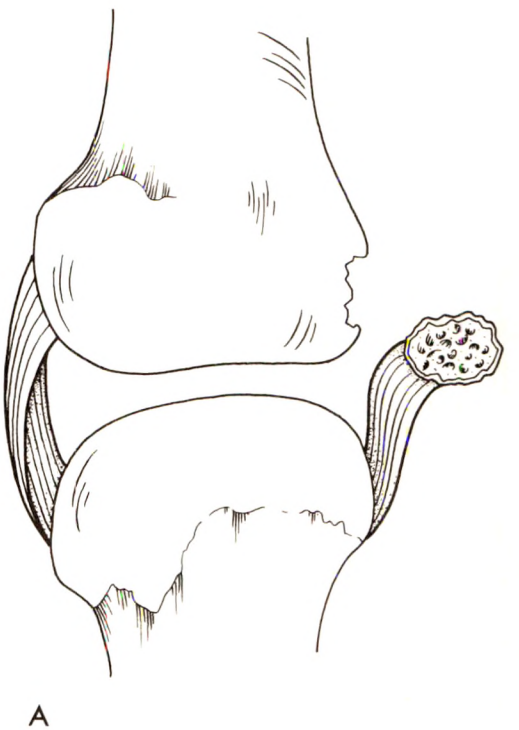


FIG. 3.—Dorsal aspect of first metacarpophalangeal joint following rupture of ulnar collateral ligament. With time, torn ligament (*d*) can protrude from proximal edge of adductor aponeurosis (*b*), the latter preventing its return. (Modified with permission from Stener B: Displacement of the ruptured ulnar collateral ligament of the metacarpo-phalangeal joint of the thumb. A clinical and anatomical study. *J Bone Joint Surg* 44B:869–879, 1962)



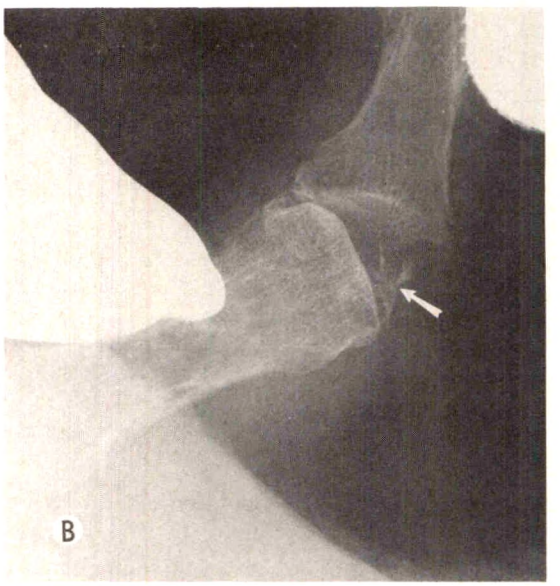


FIG. 4.—*A*, Small fragment of bone detached by ulnar collateral ligament from ulnar aspect of proximal phalanx. *B*, Stress radiograph of cadaver 7 showing avulsed fragment of bone from ulnar aspect of proximal phalanx (*arrow*). Wide separation of phalanx and metacarpal is apparent.

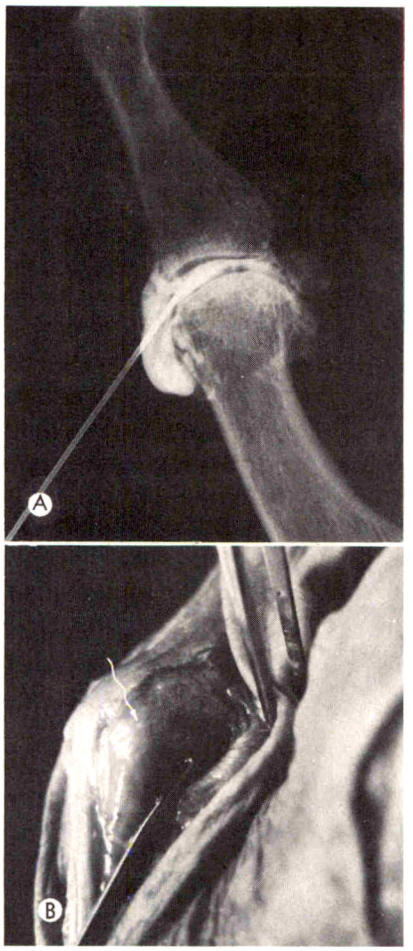


FIG. 5.—Normal arthrogram of cadaver 4. *A*, Contrast outlines distended first metacarpophalangeal joint with no evidence of extravasation. *B*, Surgical dissection of ulnar aspect of joint revealing intact ulnar collateral ligament. Overlying soft tissues have been retracted to expose ulnar side of metacarpal head and proximal phalanx. Ulnar collateral ligament (*arrow*) is not disrupted.

bone may be displaced proximally and rotated from 45° to 90° [3]. In addition, ossific flecks or exostoses may be noted [6].

Since the initial films are frequently negative, stress x-rays may be necessary to evaluate joint stability [2, 4, 6–11]. Adequate anesthesia and comparison films of the opposite side are required. Radial subluxation with widening of the ulnar aspect of the joint is noted although some variability exists in the normal stability of the first MCP joint [6]. In our series, radiographs in radial stress were obtained in seven cases, and comparison views were not available. Although the three cadavers with the widest separation between metacarpal and phalanx (5, 6, and 7 mm) had ligament tears on direct observation, one additional cadaver with a 2-mm separation had abnormality of the ligamentous apparatus and two cadavers, each with 4-mm separations, did not. Thus the degree of separation at the joint space in the normal and abnormal thumb is somewhat variable, and stress radiographs may be inconclusive.

Linscheid [10] employed arthrography in the evaluation of the injured first metacarpophalangeal joint and treated conservatively those patients who failed to demonstrate a definite capsular tear. He suggested that the folded position of the ulnar collateral ligament as described by Stener [3] could be visualized. Arthrography was obtained in all nine cadavers in our series and revealed capsular leaks on the ulnar aspect of the first MCP joint in six. In each of these cases surgical dissection confirmed the presence of a defect in the capsule. Arthrography is safe and easy, requiring only local skin anesthesia.

From our results, it appears that initial and stress radiography and arthrography may complement one another in the diagnosis of gamekeeper's thumb. Displacement of an avulsed bony fragment and/or abnormal mobility indicate joint instability and may obviate the need for arthrography. In addition, arthrography may be negative if the ulnar collateral ligament is injured but the capsule is intact. In patients whose initial and stress films are negative or equivocal, arthrography will accurately outline the capsular tear.

REFERENCES

1. Moberg E, Stener B: Injuries to the ligaments of the thumb and fingers. Diagnosis, treatment and prognosis. *Acta Chir Scand* 106:166–186, 1954
2. Neviaser RJ, Wilson JN, Lievans A: Rupture of the ulnar collateral ligament of the thumb (gamekeeper's thumb). Correction by dynamic repair. *J Bone Joint Surg* 53A:1357–1364, 1971

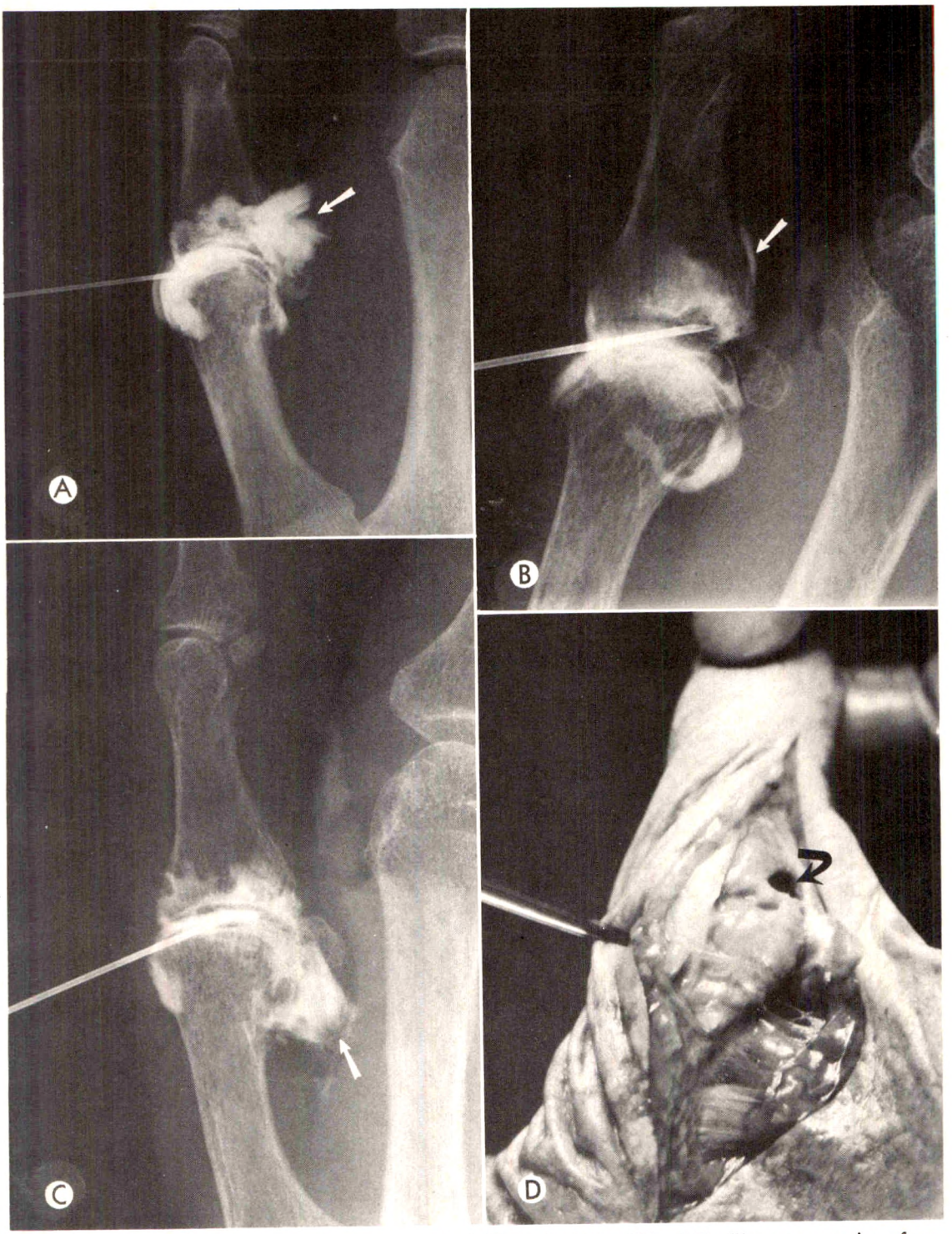


FIG. 6.—Abnormal arthograms of cadavers 3 (*A*), 6 (*B*), and 7 (*C and D*). *A*, Fanlike extravasation of contrast material on ulnar aspect of joint (*arrow*). Note radial extravasation at needle site. *B*, Extravasated dye flowing distally along ulnar aspect of proximal phalanx (*arrow*). *C*, Extraarticular dye flowing proximally along ulnar aspect of first metacarpal (*arrow*). *D*, Dissection showing space (*arrow*) between avulsed fragment and its origin on proximal phalanx.

3. Stener B: Displacement of the ruptured ulnar collateral ligament of the metacarpophalangeal joint of the thumb: a clinical and anatomical study. *J Bone Joint Surg* 44B:869–879, 1962
4. Campbell CS: Gamekeeper's thumb. *J Bone Joint Surg* 37B:148–149, 1955
5. Schultz RJ, Fox JM: Gamekeeper's thumb. Result of skiing injuries. *NY State J Med* 73:2329–2331, 1973
6. Frank WE, Dobyns J: Surgical pathology of the collateral ligamentous injuries of the thumb. *Clin Orthop* 83:102–114, 1972
7. Kaplan EB: Lateral subluxation of the metacarpophalangeal joint of the thumb: experimental study. *Bull Hosp Joint Dis* 21:200–205, 1960
8. Ahmad I, DePalma AF: Treatment of gamekeeper's thumb by a new operation. *Clin Orthop* 103:167–169, 1974
9. Coonrad RW, Goldner JL: A study of the pathological findings and treatment in soft tissue injury of the thumb metacarpophalangeal joint. With a clinical study of the normal range of motion in 1,000 thumbs and a study of post-mortem findings of ligamentous structures in relation to function. *J Bone Joint Surg* 50A:439–451, 1968
10. Linscheid RL: Arthrography of the metacarpophalangeal joint. *Clin Orthop* 103:91, 1974
11. Alldred AJ: Rupture of the collateral ligament of the metacarpophalangeal joint of the thumb. *J Bone Joint Surg* 37B:443–445, 1955

Am J Roentgenol 126:1053–1058, 1976

ISOLATED FRACTURE OF THE MEDIAL PORTION OF THE LATERAL MASS OF THE ATLAS: A PREVIOUSLY UNDESCRIBED ENTITY

E. Gail Barker, Jr.,[1] Jerome Krumpelman, and John M. Long

ABSTRACT:

Four cases of fracture of the medial aspect of the lateral mass of the atlas are presented. Unlike most cases of atlantal fracture, definite history of a blow to the vertex could not be established. While the exact mechanism of injury is unknown, it is postulated that the bone fragment is produced by a combination of stretching the ligamentum transversarium and pressure on the lateral mass due to contraction of the neck muscles. All four patients were neurologically intact and complained of pain in the distribution of the greater occipital nerve. It is suggested that this fracture might be identified more often in patients with similar histories and complaints by use of laminagraphy, since part or all of the atlas is frequently obscured on routine open mouth roentgenograms of the upper cervical spine.

During the past year four cases of fracture of the lateral mass of the atlas were encountered. In three of them no other associated abnormality of the cervical spine or skull could be demonstrated. This small series is being reported for several reasons: (1) a reference describing the radiographic diagnosis of this fracture as an isolated entity could not be found; (2) the fracture may be incurred by mechanisms other than those usually associated with atlantal fractures; (3) routine cervical spine films may appear normal, with laminagraphy required for demonstration of the fracture; and (4) rather than being extremely rare, this fracture may occasionally prove to be the cause of persistent pain in the suboccipital region following a variety of head and neck injuries including those of the whiplash type.

CASE REPORTS

Case 1

A 27-year-old male was seen in the emergency room complaining of pain and numbness behind his left ear which had been present since he fell and struck the back of his head 8½ months previously. Rotation of his head to either side produced pain in the suboccipital region, and he was tender to palpation in this area bilaterally. Neurological examination was otherwise normal. Cervical spine roentgenograms demonstrated a Jefferson fracture of the atlas with lateral displacement of both lateral masses (fig. 1*A*). Laminagraphy was performed which demonstrated, in addition to the bursting fracture of Jefferson, a fragment of bone which originated from the medial aspect of the left lateral mass (fig. 1*B*).

Case 2

A 34-year-old male who had been involved in an automobile accident 12 hr earlier came to the emergency room complaining of pain in the left upper portion of his neck which radiated into the suboccipital area. He was vague regarding details of the accident but did not recall sustaining a blow to the vertex. Neurological examination revealed no sensory or motor loss. Deep tendon reflexes were normal. Cervical spine roentgenograms were obtained: the lateral view was normal, but the frontal open mouth view revealed a vertical fracture through the midportion of the left lateral mass of the atlas with no significant displacement of the fracture fragment (fig. 2*A*). No associated injuries were found. Laminagraphic examination confirmed the plain film roentgenographic findings (fig. 2*B*).

Presented at the annual meeting of the American Roentgen Ray Society, Atlanta, Georgia, October 1975.
[1] All authors: Department of Diagnostic Radiology, University of Kentucky Medical Center, Lexington, Kentucky 40506.

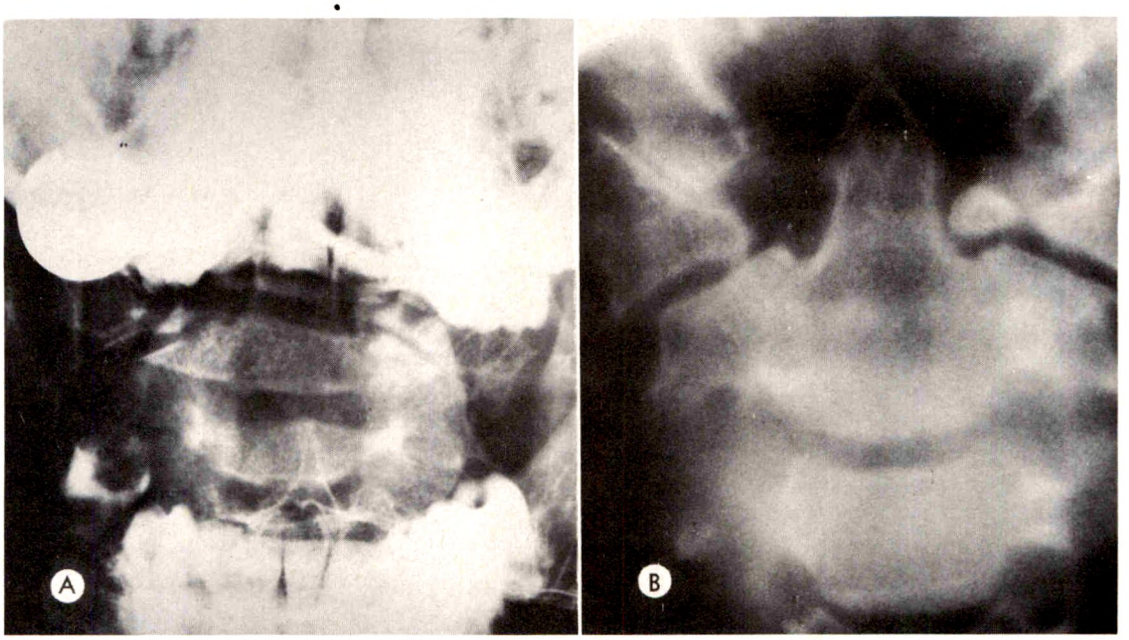


FIG. 1.—Case 1. *A*, Open mouth view showing lateral displacement of lateral masses of C1. *B*, Laminagraphy demonstrating fracture of medial portion of left lateral mass in addition to bursting fracture.

Case 3

A 25-year-old female was driving her automobile while wearing a shoulder harness. She had come to a full stop at an intersection, when she was struck from the rear by another vehicle. She experienced a violent whiplash type of motion but denied striking her head on any object in the automobile. Subsequent physical examination did not reveal any bruises or lacerations about the head or neck. After the accident, she had severe pain and tenderness in the suboccipital region, greater on the right than on the left. The pain radiated into the right jaw. On initial physical examination she

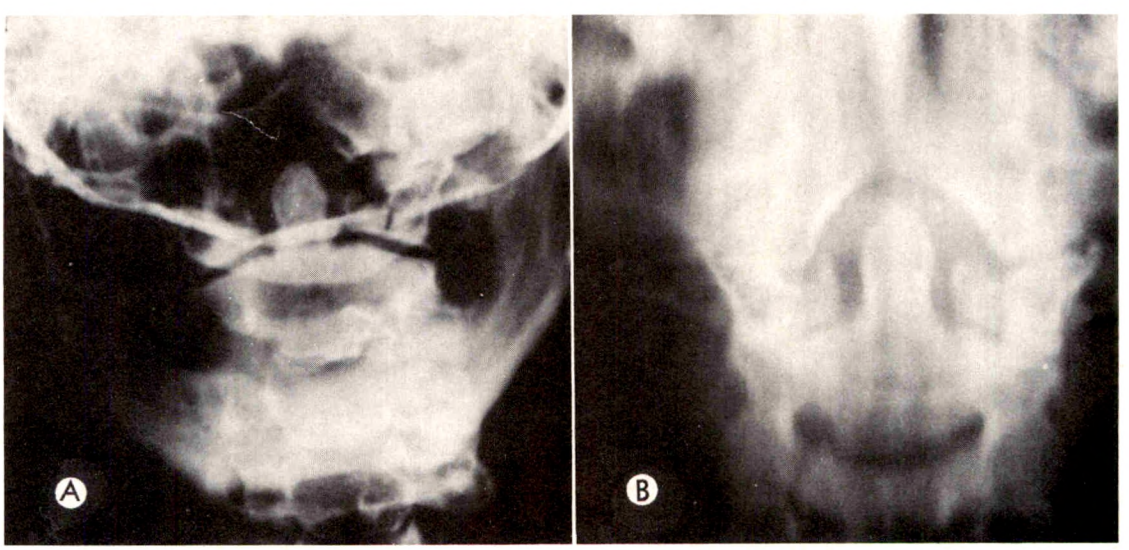


FIG. 2.—Case 2. *A*, Open mouth view showing vertical fracture through midportion of left lateral mass of atlas without significant displacement of fracture fragment. *B*, Laminagraphy demonstrating fracture in more detail.

was unable to extend her neck fully. Full left and right lateral rotation was possible but was extremely painful beyond 30°. No motor weakness or sensory deficit was demonstrable, and deep tendon reflexes were normal. Routine cervical spine roentgenograms were normal (figs. 3*A* and 3*B*). Because of the persistent severe suboccipital pain, laminagraphy was performed which revealed a vertical linear fracture of the medial aspect of the lateral mass of the atlas on the right side (fig. 3*C*). This patient is the only one in which prolonged follow-up has been possible. One year after the injury she was still symptomatic with pain in the right suboccipital region and considerable muscle spasm. She denied significant lessening of the pain since the time of injury. The follow-up laminagraphic examination of the cervical spine showed the fracture line still to be present, but sclerosis was beginning to appear along the borders and the fracture line had lost sharpness (fig. 3*D*).

Case 4

A somewhat confused 58-year-old male was seen in the emergency room for evaluation of tinnitus, dizziness, and pain in the postauricular area bilaterally. He was a poor historian but thought that he might have fallen recently. Roentgenograms of the cervical spine demonstrated a possible fracture of the medial aspect of the left lateral mass of the atlas (fig. 4*A*). Laminagraphy showed that there was a small chip fracture of the superiomedial aspect of the left lateral mass (fig. 4*B*). The patient was lost to follow-up after his initial emergency room visit.

DISCUSSION

Fractures involving the atlas are relatively rare because of the well-protected anatomical location of this vertebral body. Atlantal fractures are reported to comprise from 2% to 13% of all fractures of the cervical spine and about 1.3% of fractures of the entire spinal column [1]. In our experience the incidence has been toward the lower end of the cited range. Most fractures of the atlas are the result of a fall or blow to the head by a semicompressible object, the point of impact generally being in the region of the vertex. The most commonly seen fracture of the atlas involves one or both posterior arches, the fracture line passing close to or through the groove of the vertebral artery. Also relatively common is the bursting fracture of Jefferson in which bilateral fractures of the anterior and posterior arches allow the lateral masses to be displaced laterally. Fractures of the anterior arch alone are less common and may be vertical or horizontal in orientation. The horizontal fracture is extremely rare [1–3].

Atlantal fractures are commonly seen in association with other injuries of the cervical spine and skull, especially fractures of the odontoid or the body and arches of the axis; these additional injuries are frequently the determinants of the patient's clinical course.

Plaut [4], in his exhaustive review of atlantal fractures, states that the three mechanisms of fracture of the atlas are (1) an atlantal squeeze due to fixation of the head and spine by contracting musculature; (2) a leverlike action on the posterior arch; and (3) pressure of the odontoid against the anterior arch. It is not clear which of the above mechanisms, if any, were involved in production of the isolated fractures seen in three of our patients. It is possible that sudden muscular contraction and flexion were both important contributors. The laminagraphic studies show that the fracture fragments originated from or lateral to the tubercle to which the ligamentum transversarium attaches. It may be that in these cases acute flexion of the neck resulted in the bone fragments being avulsed by the ligamentum transversarium as it stretched across the posterior surface of the odontoid. This type of motion usually produces a fracture of the odontoid with forward dislocation and, on rare occasions, results in rupture of the ligamentum transversarium. It is difficult to imagine this type of force alone producing a fragment as large as that seen in case 2 without any other associated bony injury. In this latter instance, at least, one is led to postulate the additional factor of a sudden increase in pressure on the lateral mass in a vertical

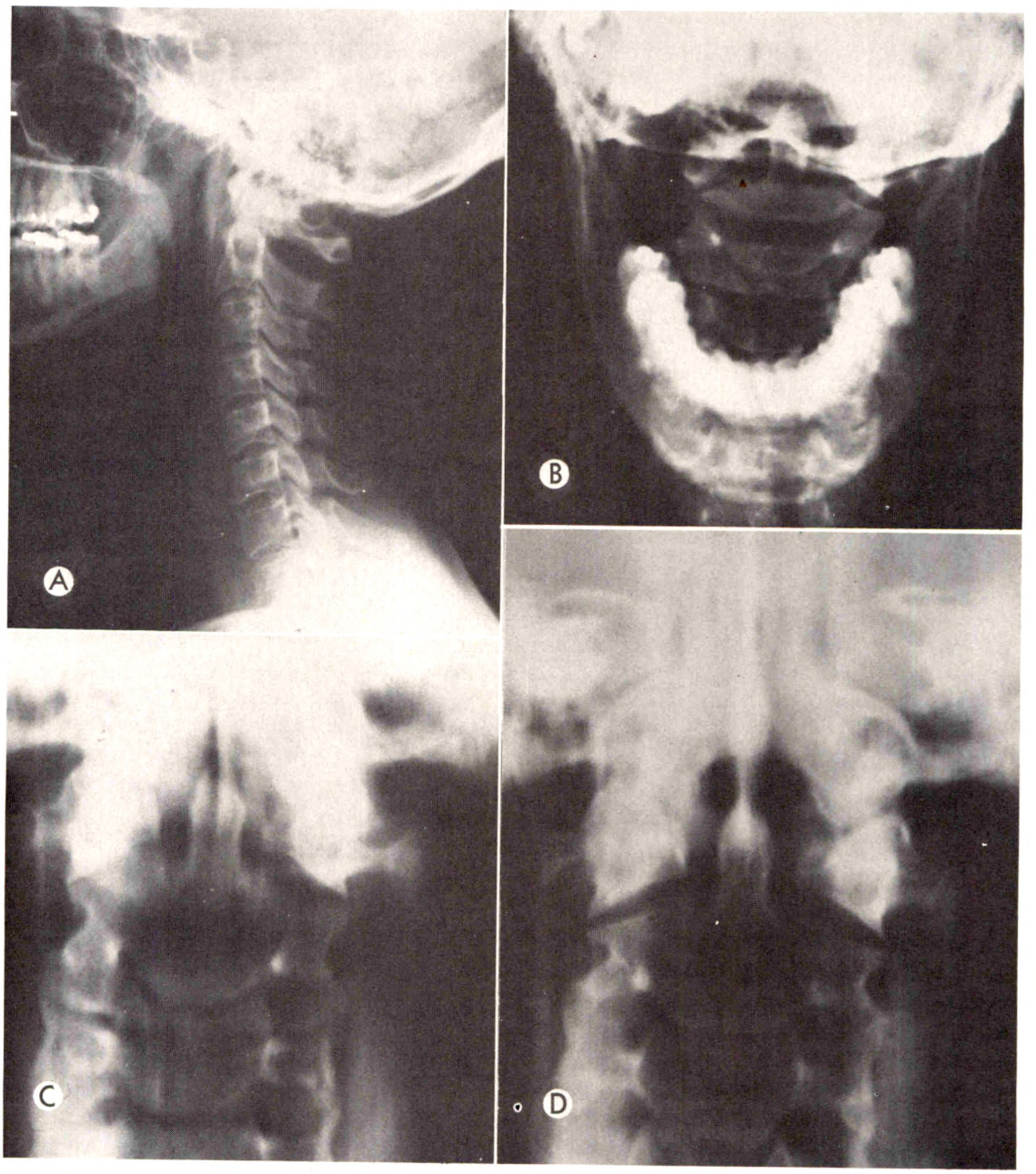


FIG. 3.—Case 3. Routine lateral view (*A*) and open mouth view (*B*) are normal. *C*, Laminagraphy revealing vertical fracture of medial aspect of right lateral mass of atlas. *D*, Follow-up laminagraphic examination 1 year after injury showing fracture line still to be visible but less sharp and with slight sclerosis present in bone adjacent to fracture.

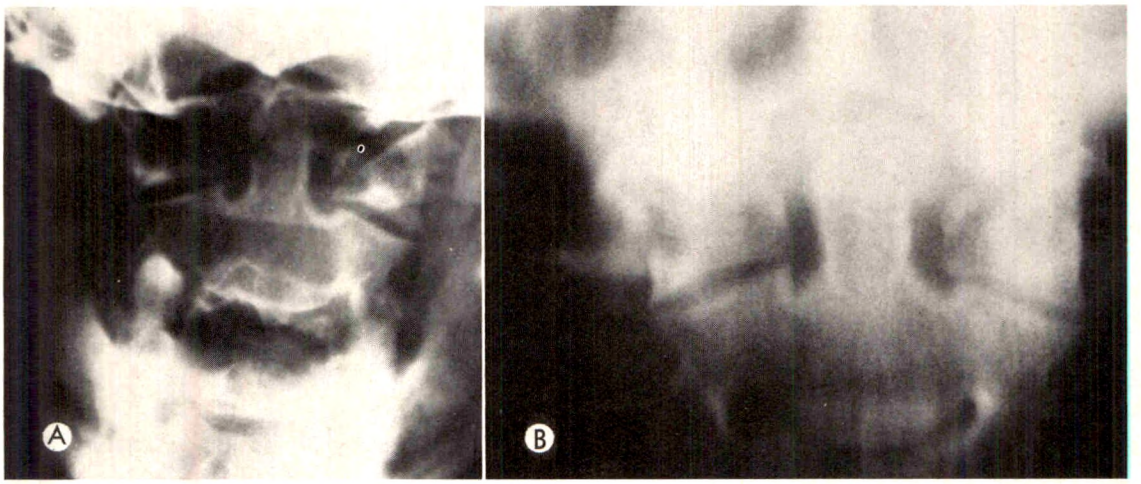


FIG. 4.—Case 4. *A*, Routine open mouth view showing what appears to be fracture of superiomedial aspect of left lateral mass of atlas. *B*, Laminagraphy confirming presence of small chip fracture.

direction due to muscular contraction.

A frequent complaint in atlantal fractures, especially those involving the posterior arch near the groove of the vertebral artery, is pain in the distribution of the greater occipital nerve whose ganglion lies just below the posterior arch of the atlas. All four of our patients had symptoms of pain referable to the distribution of this nerve without associated sensory or motor deficit.

A literature search has failed to reveal any reproduction of a roentgenogram of an isolated fracture of the lateral mass of the atlas. Plaut [4] tabulated 40 reported cases of fractures of the atlas alone and 59 cases of fractures of the atlas in association with fractures elsewhere in the cervical spine or skull. In the first group there were four fractures involving the lateral mass. Three of these occurred in association with other fractures of the atlas. The only case stated to solely involve the lateral mass was one reported by Ludloff in 1906. This case was first tabulated by Jefferson [5] in 1919 in his original paper describing the bursting fracture of the atlas. Jefferson stated that he was aware of the case only by means of an abstract of the original article in the German literature. We also were unable to locate the original report of this case and thus cannot state how the fracture was diagnosed, although the diagnosis must have been clinical since the patient was reported to have survived his injury. Braakman and Penning [2] allude to the occasional occurrence of a small bone chip being torn from the medial side of the lateral mass by the transverse atlantal ligament, citing Von Torklus and Gehle [6]. Review of this reference, however, failed to reveal specific mention of this injury, and Von Torklus and Gehle do not mention it in their book [3]. The only illustration of this type of fracture which could be found was in a report by Sicard et al. [7] in which an avulsion of the medial portion of the lateral mass was seen in association with a complex bursting fracture of the atlas.

Despite failure to locate illustrations or specific reports of this fracture as an isolated entity, it is felt that rather than being rare, its occurrence may be overlooked. Without tabulating statistical incidence, review of a number of routine cervical spine examinations revealed that either the cephalad portion or the entirety of the lateral masses of the atlas were obscured by overlying bone structures on the open mouth view(s) in a large number of instances. Clear visualization of the lateral masses of the atlas, especially its superior aspect, is necessary for diagnosis of this



FIG. 5.—Laminagraphic view of atlas demonstrating asymmetric but normal notches in medial portions of superior articular masses.

fracture. It is conceivable that the fracture could be obscured by soft tissue densities alone when the fragment is small, even if the atlas is free of overlying bone structures.

The fracture was visible only on the frontal open mouth projections in our cases. (Submentovertex views were not obtained in the initial evaluations.) The other routine views were negative. Thus for a patient with neck or head trauma of any type who has pain in the distribution of the greater occipital nerve and negative routine cervical spine roentgenograms, laminagraphy should be performed to detect possible fracture of the medial portion of the lateral mass.

The other more common injury which may present with similar complaints and negative cervical spine roentgenograms, and which must be excluded, is a nondisplaced odontoid fracture. Such cases may have rather unremarkable symptoms, but they are not always so specifically localized to the distribution of the greater occipital nerve.

The normal notchlike defect of variable depth which is seen frequently in the medial portion of the superior articular mass of the atlas should not be confused with a fracture (fig. 5). This defect is formed on its medial aspect by the margin of the medial tubercle of the lateral mass and laterally by the most concave portion of the superior articular facet [8].

Treatment of this fracture is not well defined. As with most fractures of flat bones, healing is slow (e.g., case 3). Cervical collars, analgesics, and muscle relaxants have been used with variable results in those cases which were followed. The symptoms produced by the fracture, as in some cases of odontoid fracture, do not always prompt the patient to seek immediate medical treatment (e.g., case 1).

REFERENCES

1. Sherk HH, Nicholson JT: Fractures of the atlas. *J Bone Joint Surg* 52A:1017–1024, 1970
2. Braakman R, Penning L: *Injuries of the Cervical Spine*. Amsterdam, Excerpta Medica, 1971
3. Von Torklus D, Gehle W: *The Upper Cervical Spine*. New York, Grune & Stratton, 1972
4. Plaut HF: Fractures of the atlas resulting from automobile accidents. *Am J Roentgenol* 40:867–890, 1938
5. Jefferson G: Fracture of the atlas vertebra. *Br J Surg* 7:407–412, 1919–1920
6. Von Torklus D, Gehle W: Neue Perspektiven der Entwicklungsstorungen der oberen Halswirtelsaule. *Z Orthop* 106:78–84, 1969
7. Sicard A, Picard J, Martin H: Les fractures isolées de l'atlas. *J Fr Med Chir Thorac* 75:521–538, 1958
8. Meghrouni V, Jacobson G: The pseudonotch of the atlas. *Radiology* 72:260–262, 1959

Am J Roentgenol 126:1059–1062, 1976

CONCOMITANT DISLOCATION AND INTRA-ARTICULAR FOREIGN BODY: A RARE COMPLICATION OF THE CHARNLEY TOTAL HIP ARTHROPLASTY

ROBERT E. CAMPBELL[1] AND JAMES P. MARVEL, JR.[2]

ABSTRACT:

In the Charnley total hip arthroplasty, periarticular foreign bodies represent potential foci for intraarticular migration at the time of hip dislocation. This complication, although very rare, should be verified radiographically to prevent unsuccessful attempts at closed reduction. Although intraarticular radiopaque foreign bodies should be identified on plain radiographs of the hip, intraarticular radiolucent foreign bodies require positive-contrast arthrography for identification. Two illustrative cases are presented.

Dislocation with concomitant migration of an intraarticular foreign body is an extremely rare complication of the Charnley total hip arthroplasty. The intraarticular foreign body, consisting of either a fragment of acrylic bone cement (polymethylmethacrylate), a piece of fractured wire suture, or a focus of heterotopic bone, acts as a block to closed reduction, a maneuver generally successful in simple total hip dislocation. To our knowledge, this complication of the Charnley procedure has not been reported previously. Thus the purpose of this paper is to alert both radiologists and orthopedists about it by presenting two illustrative cases. Correct radiological evaluation of this complication will prevent unsuccessful, perhaps repeated, attempts at closed reduction of the dislocated hip.

CASE REPORTS

Case 1

O. M., an 85-year-old white female, had a left Charnley low friction total hip replacement in July 1973 for noninfectious complications following internal fixation of a previously comminuted intertrochanteric fracture. She did well postoperatively and was walking without pain until October 1974 when her hip "gave way" after a rapid squatting maneuver. Her dislocated femoral prosthesis could not be reduced by the usual closed method, and at surgery an unsuspected intraarticular fragment of acrylic bone cement was discovered and removed. In retrospect, the intraarticular foreign body was evident on the immediate preoperative roentgenograms of the hip (fig. 1*A*) and had migrated into the joint space from the periarticular soft tissues about the prosthetic femoral neck (fig. 1*B*). At present the patient is again walking well without pain.

Case 2

E. H., a 72-year-old white female, had bilateral Charnley low friction total hip replacements, the right in December 1972 and the left in July 1973, with dramatic relief of constant excruciating pain from severe degenerative joint disease. One month following the left hip procedure, the wire sutures surrounding the osteotomized femoral greater trochanter were intact; however, the trochanter itself had migrated slightly superiorly. The patient, who lived alone despite senility, was then lost to follow-up until June 1975 when a daughter found her in bed unable to move her left hip. At that time, frontal and cross-table lateral radiographs revealed the dislocated left hip, fractured wire sutures about the superiorly displaced, ununited greater trochanter, and the intraarticular fragment of wire suture (fig. 2). The patient was unable to give a history of trauma to the hip. Subsequently the intraarticular fragment of wire suture was surgically removed, and

[1] Department of Radiology, Pennsylvania Hospital, 8th and Spruce Streets, Philadelphia, Pennsylvania 19107.
[2] Division of Orthopedic Surgery, Pennsylvania Hospital, 8th and Spruce Streets, Philadelphia, Pennsylvania 19107.

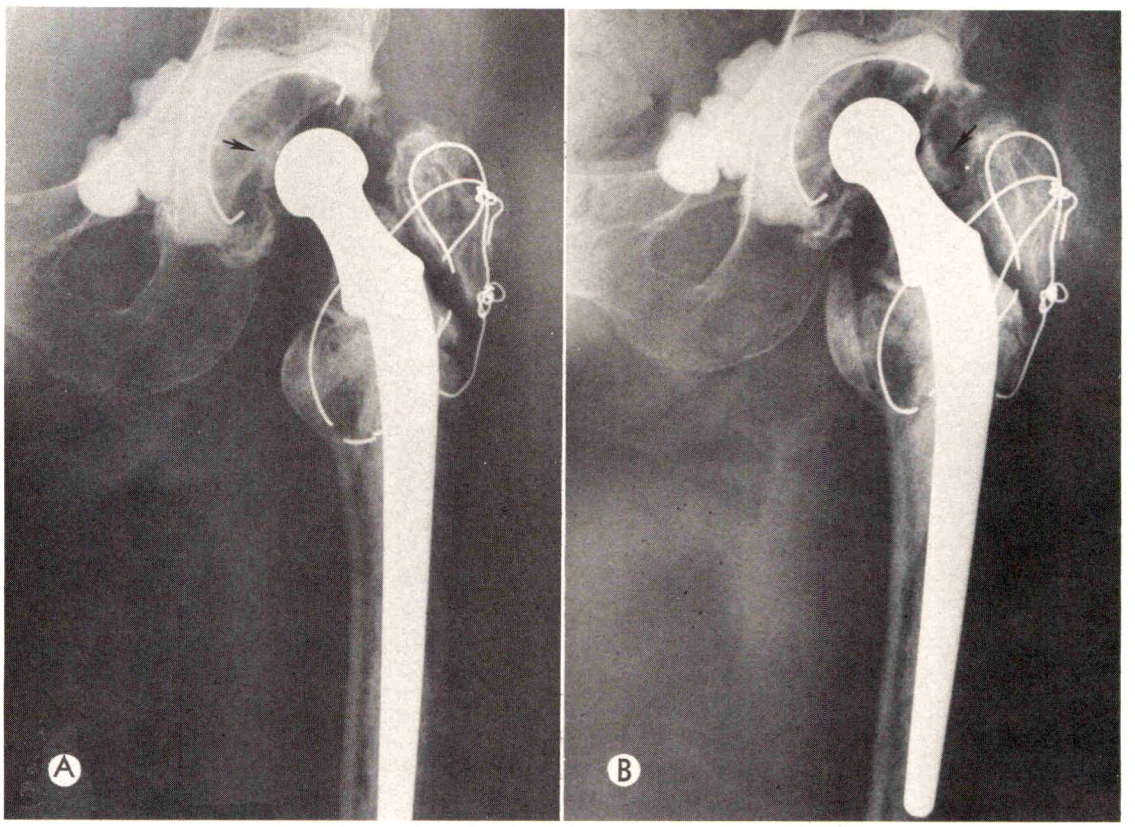


FIG. 1.—Case 1. *A*, Preoperative roentgenogram of hip showing intraarticular fragment of polymethylmethacrylate (*arrow*). *B*, Periarticular position of fragment of polymethylmethacrylate (*arrow*) 2 weeks before dislocation of hip.

the greater trochanter was reattached to the femur by additional heavy wire sutures. To date the patient has not redislocated her left hip.

DISCUSSION

During the past 2 decades total hip replacements have enabled thousands of previously incapacitated individuals to walk without pain. Today the Charnley procedure is the most popular and successful of the total hip arthroplasties.

Basically, all total hip arthroplasties include replacement of both the diseased acetabulum and femoral head by prosthetic components which vary in design, size, and composition. The small head of the metallic femoral prosthesis, the high molecular weight polyethylene acetabular prosthesis, the acrylic bone cement used to anchor both prostheses to surrounding bone, and the greater trochanter osteotomized and subsequently reattached to the femur by multiple crossed heavy 18-gauge wire sutures are distinctive features of the Charnley total hip replacement.

Early critics of the Charnley procedure predicted frequent dislocations because of the 22-mm diameter "smaller than life" head of the metallic femoral prosthesis. In reality, dislocation is rare [1–3]. Two recent large series of Charnley hip procedures from the Mayo Clinic [2] and the University of Southern California Medical Center [4] report a dislocation rate of 3% and 4.2%, respectively. Dislocation of the femoral prosthesis occurs in the immediate postoperative period secondary either to forced adduction of the hip prior to formation of a fibrous pseudocapsule or to operative geometric malposition of the acetabu-

lar or femoral prostheses. At a later date, dislocation is secondary to unusual, forceful hip maneuvers or direct trauma to the hip. Although not mentioned in previous reports, periarticular fragments of acrylic bone cement or fractured wire sutures may migrate intraarticularly during hip dislocation.

Prosthetic fixation has been enhanced by the perfection and utilization of polymethylmethacrylate, which serves as a filler between both prosthetic devices and bone [5]. Loosening of the prostheses remains a potential complication in the metal-to-metal press-fit procedures which do not use bone cement for fixation. During the surgical procedure, polymethylmethacrylate may be deposited inadvertently in the periarticular soft tissues where it ordinarily remains asymptomatic unless it migrates intraarticularly. In its natural state polymethylmethacrylate is radiolucent, but it can be rendered radiopaque by impregnation with barium sulfate. Positive-contrast arthrography is required to outline an intraarticular fragment of radiolucent polymethylmethacrylate, and this procedure should be undertaken when the cause of persistent dislocation is not evident radiographically following attempted closed reduction.

In case 1, several unsuccessful attempts at closed reduction of the dislocated hip were undertaken before open surgery revealed the previously unsuspected intraarticular fragment of acrylic bone cement, polymethylmethacrylate. In retrospect, the fragment of polymethylmethacrylate was obvious intraarticularly on the original radiographs at the time of dislocation (fig. 1*A*) and on prior radiographs in the periarticular soft tissues near the femoral neck (fig. 1*B*). The intraarticular polymethylmethacrylate was not overlooked by both the radiologist and orthopedist because it was obscure, but rather because neither physician was familiar with this possibility.

In the Charnley operation the femoral greater trochanter, with its attached muscles, is osteotomized and reflected away from the operative site to afford the orthopedist a better approach to the diseased acetabulum. At the completion of the total hip replacement, the greater trochanter is reattached and stabilized to the femur by multiple crossed heavy wire sutures. Under recurring stress the wire sutures may fracture and even fragment. Generally these fractured or fragmented wire sutures do not produce symptoms unless they migrate into the greater trochanteric bursa, producing a painful bursitis. However, these wire fragments are potential foreign body foci for both intraarticular and intravascular migration. In case 2 the intraarticular piece of metal wire was identified radiographically before closed reduction was attempted.

Theoretically, periarticular heterotopic

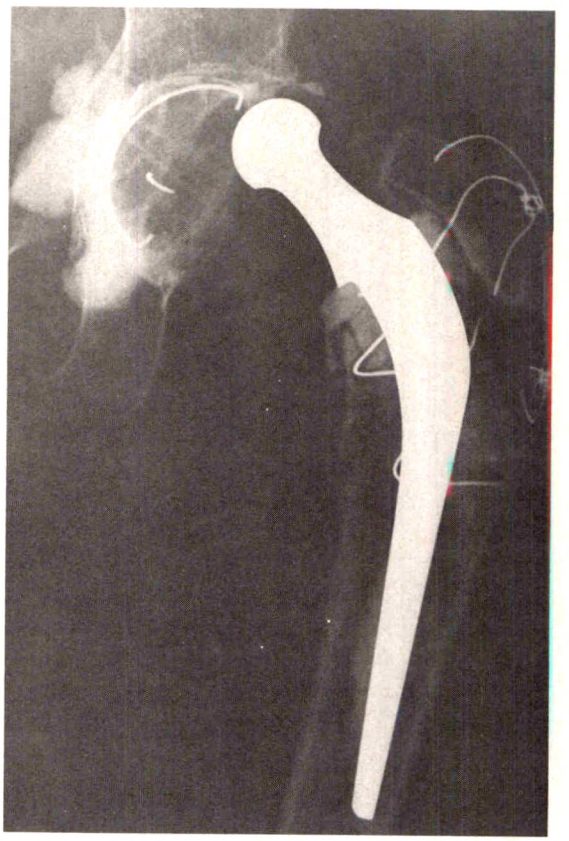


FIG. 2.—Case 2. Intraarticular location of fragment of broken wire suture obvious on both the frontal and cross-table lateral (not shown) projections.

bone represents another potential foreign body for intraarticular migration with dislocation of the hip. However, the authors have not witnessed this complication. Heterotopic bone is common about the operative site but is usually asymptomatic unless it is massive and limits motion of the hip. It develops more frequently in reoperated [6] and infected hips.

REFERENCES

1. Amstutz HC: Complications of total hip replacement. *Clin Orthop* 72:123–137, 1970
2. Coventry MB, Beckenbaugh RD, Nolan DR, Ilstrup DM: 2,012 total hip arthroplasties: a study of postoperative course and early complications. *J Bone and Joint Surg* [*Am*] 56A:273–284, 1974
3. Lazansky MG: Complications in total hip replacement with Charnley technic. *Clin Orthop* 72:40–45, 1970
4. Pepper HW, Noonan CD: Radiographic evaluation of total hip arthroplasty. *Radiology* 108:23–29, 1973
5. Charnley J: *Acrylic Cement in Orthopaedic Surgery*. Edinburgh, E. & S. Livingstone, 1970
6. Beaubout JW: Radiology of total hip arthroplasty. *Radiol Clin North Am* 13:3–19, 1975

Am. J Roentgenol 126:1063–1067, 1976

EMBRYOGENESIS OF THE HUMAN OCCIPITAL BONE

ROBERT SHAPIRO[1] AND FRANKLIN ROBINSON[2]

ABSTRACT:

From an original study of fetal specimens, the embryogenesis of the human occipital bone is described. The occipital bone in man is derived from cartilage, except for the interparietal segment which has a membranous origin. Normally there is no midline cerebellar fissure or synchondrosis.

An understanding of the embryological development of the occipital bone is essential for an appreciation of craniovertebral anomalies and occipital fractures. The literature contains inconsistencies with respect to the nomenclature and ossification of the various components of the occipital bone, which add to the confusion [1–8]. The following report is based upon our own studies and attempts to clarify the inconsistencies.

MATERIALS AND METHODS

A total of 125 skulls were collected from fetuses between 8 and 40 weeks of gestation. These skulls were prepared in the dry state and radiographed in standard projections. In addition, a group of 30 cleared, alizirin-stained fetal skulls of varying age prepared according to the classical Spalteholtz technique were investigated. Multiple coronal and midline sagittal sections of representative decalcified fetal skulls were embedded in paraffin and celloidin. Ages were 8, 10, 12, 18, 20, 30, and 40 weeks as assessed by crown-rump measurement. These were studied grossly and microscopically.

EMBRYOLOGY

The occipital bone is formed from the union of four primary cartilaginous centers laid down in the chondrocranium around the foramen magnum and from a fifth membranous element (fig. 1). Thus the occipital bone has a dual origin from cartilage and membrane. The four cartilaginous components are the basioccipital anterior to the foramen magnum, the lateral or exoccipitals on each side of the foramen magnum, and the supraoccipital posterior to the foramen magnum (i.e., the inferior squama below the mendosal suture). The membranous component gives rise to the

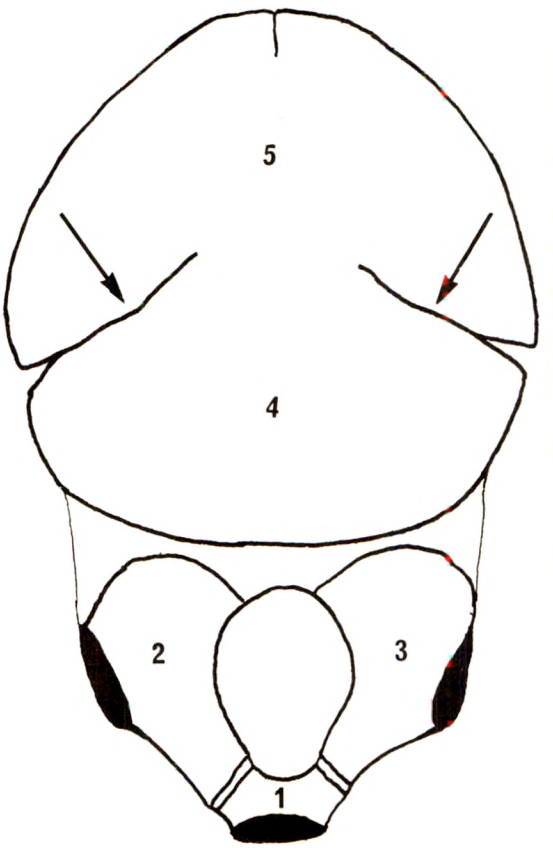


FIG. 1.—Diagram of ossification of occipital bone. Basioccipital (*1*), paired exoccipitals (*2 and 3*), and supraoccipital (*4*) derived from cartilage; interparietal (*5*) derived from membrane. Arrows point to mendosal sutures which separate interparietal from supraoccipital segment.

[1] Department of Radiology, Hospital of St. Raphael, Yale University School of Medicine, New Haven, Connecticut 06511.
[2] Department of Neurosurgery, Hospital of St. Raphael, Yale University School of Medicine, New Haven, Connecticut 06511.

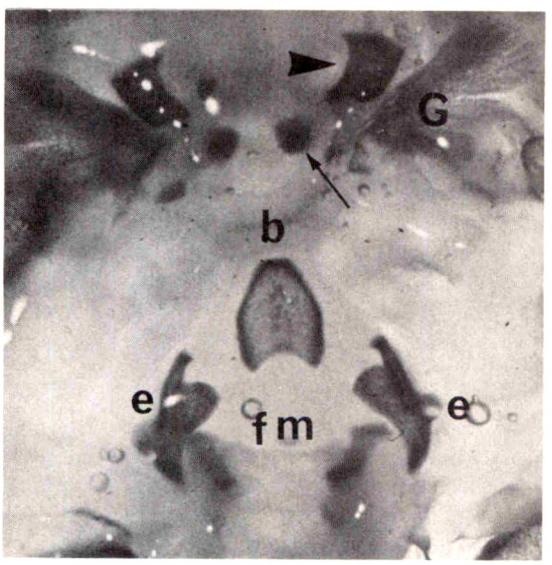


FIG. 2.—Photograph of base of 14-week-old fetal skull prepared by Spalteholtz technique. Basioccipital (b) and paired lateral exoccipital centers (e) surround foramen magnum (fm). Note also ossification of greater (G) and lesser (*arrowhead*) sphenoidal wings and postsphenoid centers (*arrow*) anterior to basioccipital bone.

interparietal bone (i.e., the superior squama above the mendosal suture).

At 9 weeks of gestation, a single median ossification center is present in the cartilaginous basiocciput ventral to the notochord and in each lateral occipital cartilage around the hypoglossal canal (fig. 2). In all the specimens, the supraoccipital segment also ossified from a single focus in the tectum synoticum (i.e., that portion of the chondrocranial roof connecting the auditory bullae). Coronal sections at this fetal stage demonstrate ossification in the membranous interparietal segment as well (figs. 3 and 4).

By 12 weeks of gestation, the interparietal and supraoccipital segments have fused in the midline but remain separated laterally by the mendosal sutures (fig. 5). Ossification in the supraoccipital segment is more advanced than in the interparietal. At 14 weeks there is further union of the interparietal and supraoccipital segments, and the mendosal sutures are reduced to narrow slits. In some specimens, a linear vertical strip of unossified membrane is present in the midline along the superior margin of the interparietal segment. This may ossify later or persist at full term. Similar unossified strips may occur elsewhere in the membranous interparietal segment. These can be mistaken for fractures in the neonatal period.

In a few specimens (four in our series), there may be a midline cleft in the inferior margin of the supraoccipital bone (fig. 6).

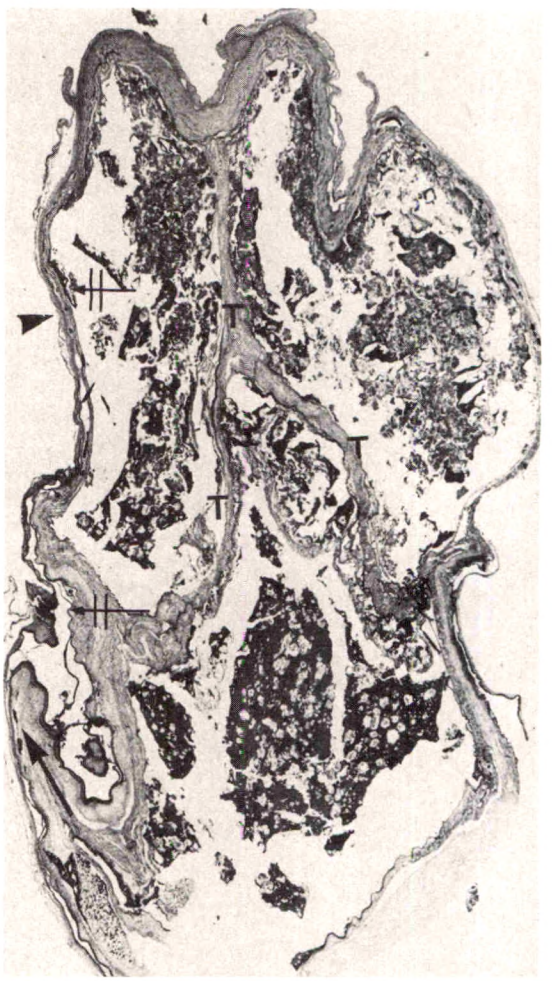


FIG. 3.—Low power coronal section of 10-week-old human fetal cranium embedded in paraffin and stained with H and E. Foci of ossification (*arrowhead*) are seen in membranous portion of occipital bone above level of tentorium (T) as well as in chondral portion of occipital bone below tentorium (*arrow*). Crosshatched arrows outline area shown in high power section (fig. 4).

Such clefts may persist or subsequently fill in with bone. Less commonly (two specimens), a small central bony projection is present on the inferior aspect of the supraoccipital segment (i.e., Kerckring's bone; figs. 7–9). Rarely, the latter may be detached and lie in a rather broad midline cleft. One or more accessory ossicles may be found in the innominate synchondrosis between the supraoccipital and exoccipital segments (fig. 10). According to Caffey [9], these ossicles usually fuse with the supraoccipital bone by the end of the first year of life.

Ossification of the basioccipital segment proceeds laterally into the ventral portion of each condyle. Simultaneously, ossification of the lateral occipitals advances into the dorsal portion of the occipital condyles (fig. 11). At birth, the basioccipital and lateral occipital bones are separated on each side by a prominent synchondrosis.

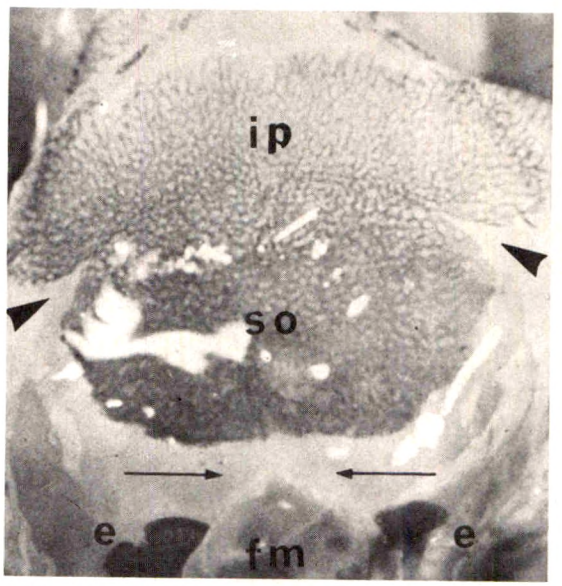


FIG. 5.—Photograph of posterior aspect of fetal skull of 12 weeks gestation (Spalteholtz preparation). ip = interparietal segment; so = supraoccipital segment; e = exoccipitals; fm = foramen magnum; arrowheads = mendosal sutures; arrows = innominate synchondrosis.

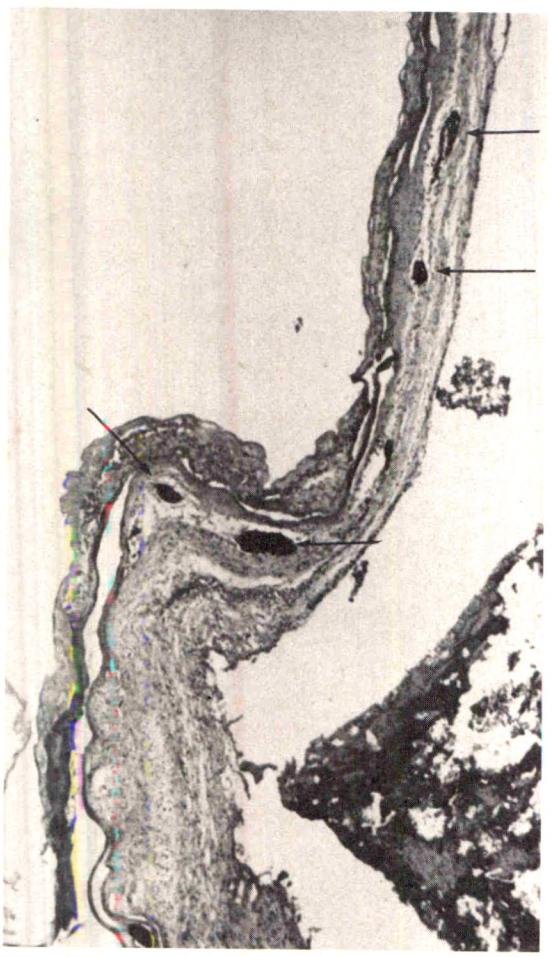


FIG. 4.—High power view of ossification (*arrows*) in membranous portion of occipital bone above tentorium (see fig. 3).

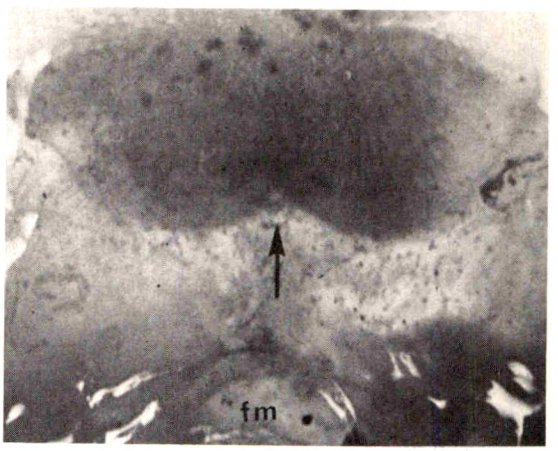


FIG. 6.—Photograph of posterior aspect of fetal skull of 4 months gestation (Spalteholtz preparation). Arrow points to cleft in midportion of inferior margin of supraoccipital segment. fm = foramen magnum.

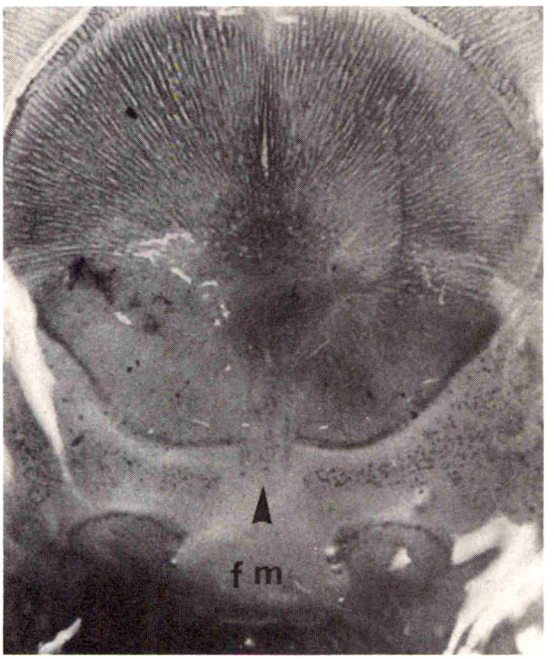


FIG. 7.—Kerckring's bone (*arrowhead*) projecting from inferior margin of supraoccipital segment in 15-week-old fetus. Note exoccipital centers on either side of foramen magnum (fm).

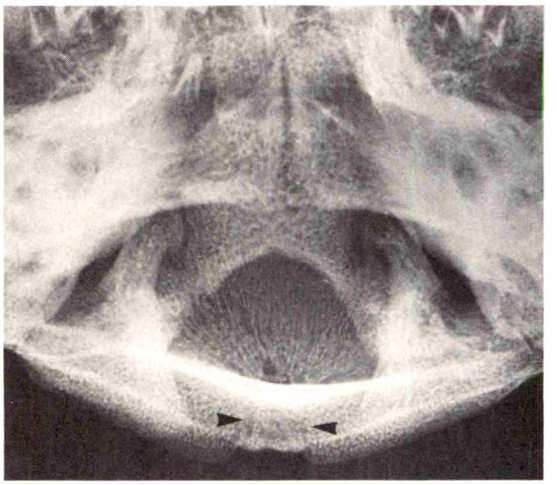
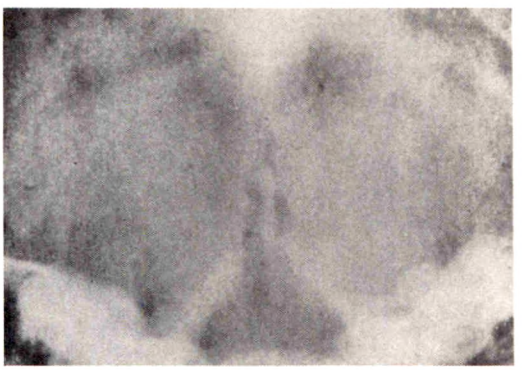


FIG. 8.—Exaggerated Waters view of skull of full-term stillborn infant demonstrating Kerckring's bone (*arrowheads*) almost completely fused to supraoccipital segment.

Obliteration of these synchondroses normally occurs at 2–4 years of age. The lateral occipitals are separated from the supraoccipital segment by the prominent innominate synchondrosis; bony fusion of these segments also takes place between 2 and 4 years of age. There is an additional synchondrosis between the basiocciput and the basisphenoid (sphenooccipital synchondrosis). According to Melsen [10], ossification between the sphenoid and occipital bones begins at 12–13 years of age in girls and 14–15 years in boys. Complete closure of the synchondrosis does not occur until 16–20 years of age. Occasionally the sphenooccipital synchondrosis persists into adult life.

At birth (fig. 12), the interparietal and supraoccipital segments are fused, except laterally where they are separated by the mendosal sutures. Complete obliteration of the mendosal sutures usually occurs by the end of the second year. Rarely, one or both



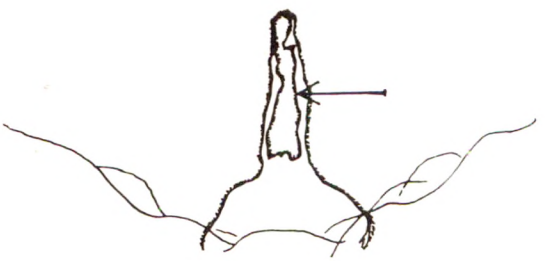


FIG. 9.—Radiograph (*left*) and diagram (*right*) of adult skull in the Towne projection showing ununited Kerckring's bone. (Reprinted with permission from Shapiro R, Janzen A: *The Normal Skull.* New York, Harper & Row, 1960)

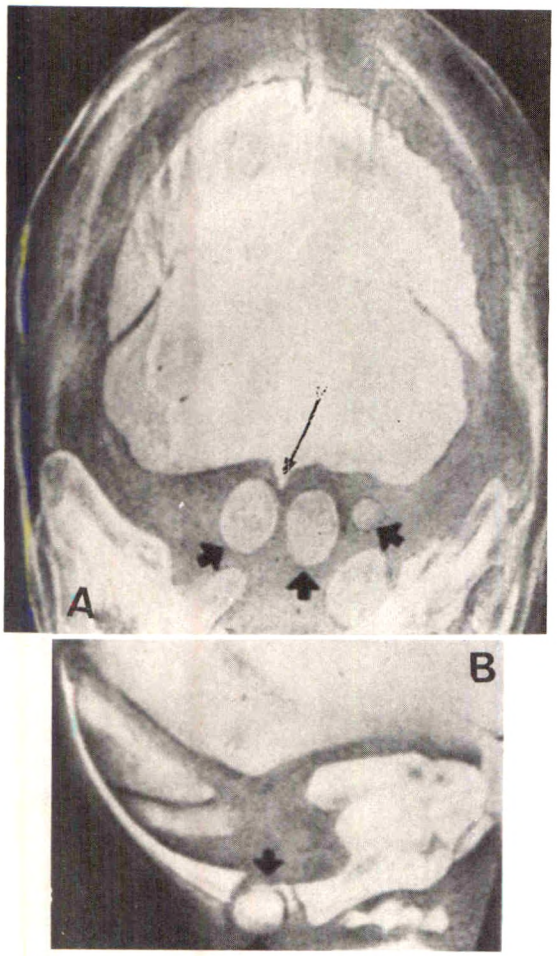


FIG. 10.—Anteroposterior Towne (*A*) and lateral (*B*) views of newborn fetal skull with three ossicles (*arrowheads*) in innominate synchondrosis. Note presence of Kerckring's process (*arrow*). (Reprinted with permission from Caffey J: *Pediatric X-Ray Diagnosis*, 6th ed. Chicago, Year Book Medical Publishers, 1972).

mendosal sutures may remain open in adult life. Should this happen, the patent suture, particularly if unilateral, may be mistaken for a fracture. Since the supraoccipital segment (inferior squama) ossifies from a single bone center, there is no normal midline suture or synchondrosis, despite contrary statements in the literature [11, 12]. Therefore, a linear midline radiolucency within the supraoccipital segment of the occipital bone must be considered to be a fracture [2, 13] (fig. 13). A persistent metopic suture superimposed on the occipital bone in the Towne projection may be recognized by its projection beyond the occipital bone onto the foramen magnum.

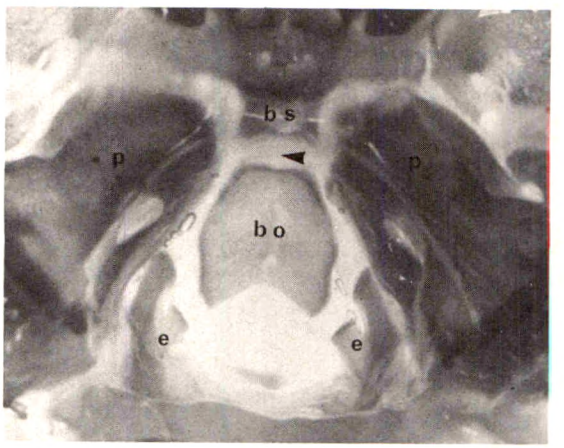


FIG. 11.—Photograph of base of 22-week-old fetal skull (Spalteholtz preparation). Basisphenoid (bs) separated from basioccipital (bo) by sphenooccipital synchondrosis (*arrowhead*). p = petrous bones; e = exoccipital bones.

ACKNOWLEDGMENTS

We are deeply grateful to Dr. Melvin L. Moss, Columbia University, and the late

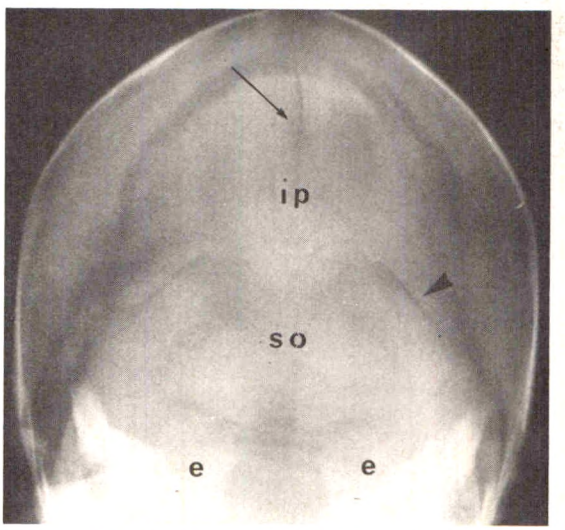


FIG. 12.—Towne projection of skull of newborn full term infant. Arrow points to midline unossified membranous strip in interparietal segment (ip). The latter is separated by mendosal suture (*arrowhead*) from supraoccipital segment (so). e = paired exoccipital segments on either side of foramen magnum.

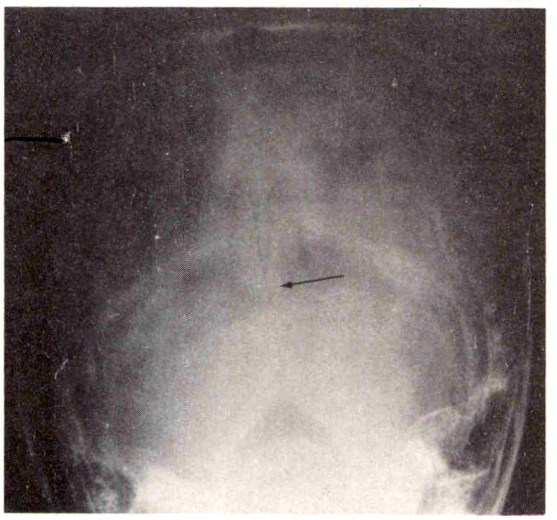


FIG. 13.—Midline vertical fracture (*arrow*) involving both interparietal and supraoccipital segments.

Dr. Bertram S. Kraus, University of Pittsburgh, for the generous loan of human embryos prepared by the Spalteholtz technique; to Dr. E. Leon Kier for the loan of several prepared fetal skulls; and to Dr. John Ostrom for making available mammalian skulls from the Peabody Museum collection. We are also grateful to Drs. Keszler, Lohman, Mansourian, and Weisfenung for various translations from German and French, to Ovidio Gallo for the photographs, and to Miss Angela Brunetti for typing the manuscript.

REFERENCES

1. Augier M: Quelques problèmes relatifs au développement du crâne. I. Voute occipitale chez l'homme et d'autres mammifères. *Arch Anat Histol Embryol* (Strasb) 13:33–66, 1931
2. Franken EA Jr: The midline occipital fissure; diagnosis of fracture versus anatomic variants. *Radiology* 93:1043–1046, 1969
3. Hadley LA: *Anatomico-Roentgenographic Studies of the Spine*. Springfield, Ill., Thomas, 1964
4. Kier EL: Fetal skull, in *Radiology of the Skull and Brain*, vol. 1, book 1, edited by Newton TH, Potts DG, Saint Louis, Mosby, 1971, pp 99–117
5. Lacoste A: Sur le développement de l'écaille occipitale étudiée comparativement chez le mouton et chez l'homme. *Arch Anat Histol Embryol* (Strasb) 12:1–47, 1930
6. LeDouble AF: *Traite des variations des os du crâne de l'homme*. Paris, Vigot Freres, 1903
7. Matthes E: Neuere Arbeiten über das Primordialcranium der Säugetiere. II. Teil. Arbeiten über einzelne Regionen des Cranium. *Ergeb Anat Entwicklungsgesch* 24:117–243, 1923
8. Parker WK, Bettany GI: *The Morphology of the Skull*. London, McMillan, 1877
9. Caffey J: On the accessory ossicles of the supraoccipital bone. *Am J Roentgenol* 70:401–412, 1953
10. Melsen B: The cranial base. *Acta Odontol Scand* 32, suppl. 62, 1974
11. Caffey J: *Pediatric X-Ray Diagnosis*, 6th ed. Chicago, Year Book Medical Publishers, 1972
12. Koehler A, Zimmer EA: *Borderlands of the Normal and Early Pathologic in Skeletal Roentgenology*, 11th ed. New York, Grune & Stratton, 1968
13. Allen WE III, Kier EL, Rothman SLG: Pitfalls in the evaluation of skull trauma: a review. *Radiol Clin North Am* 11:479–503, 1974

Am J Roentgenol 126:1069–1076, 1976

FILM SCREENING BY PHYSICIAN ASSISTANTS IN DIAGNOSTIC RADIOLOGY

E. Gail Barker, Jr.,[1] H. D. Rosenbaum, Albert C. Selke, Jr., Del Henderson, and Jack H. Hildner

ABSTRACT:

Data are presented which indicate that specially selected ART students can be trained to evaluate radiographs as to the presence or absence of significant pathology with an accuracy equivalent to that of experienced staff radiologists. The methods employed in this training program—namely, stressing perceptual recognition of normal and abnormal findings—may be beneficial in the early months of training of diagnostic radiology residents to hasten achievement of an acceptable perceptual performance. Test films, used in this study as an evaluation technique, may also be useful to assess residents' progress.

Over the past few years our department has developed a training program for physician assistants in diagnostic radiology. The major objective of this project was to train specially selected radiologic technologists to perform a number of duties beyond the usual scope, including some previously discharged only by physician radiologists. These students have been designated advanced radiologic technologists (ART) but presently are considered to be more accurately called diagnostic radiology assistants or, better yet, physician assistants in diagnostic radiology. A major aspect of their instruction centers on how to screen a wide variety of routine radiographs to determine whether they are positive or negative for significant pathology. Image recognition has been emphasized. A second objective has been to determine the level of accuracy that can be achieved by ART students in this type of screening. To be a successful program, it was felt essential that the students achieve an accuracy at least approximating that of staff radiologists. Consequently it was necessary to precisely quantitate their performance. The third objective is to determine whether the services performed by ART personnel are of significant benefit to the radiologist. In theory, it should be possible for the radiologist to direct more time to patients with significant abnormalities, to consultation with clinicians, and to other activities requiring more sophisticated knowledge. Evaluation of this objective is underway and will be reported elsewhere [1].

METHOD

Accuracy was quantitated by use of the signal detection theory and decision matrices as applied by Lusted [2] to similar problems. Tests consisted of carefully selected sets of radiographs of from 25 to 100 cases, each set with approximately equal numbers of normal and abnormal studies. Many cases had only one radiograph, but others required two or more films. No clinical information was provided.

The examinations were administered to staff radiologists, radiology residents, medical students, and radiologic technologists in our department and elsewhere* to establish norms to which the performance of ART students could be compared. All followed our examination

This investigation was supported by U.S. Public Health Service research grants RM 00048-02A2 and HS-00567 from the Bureau of Health Services Research and Evaluation, Health Resources Administration, Department of Health. Education, and Welfare (formerly National Center for Health Services Research and Development, Health Services and Mental Health Administration).

[1] All authors: Department of Diagnostic Radiology, University of Kentucky Medical Center, Lexington, Kentucky 40506. Address reprint requests to H. D. Rosenbaum.

* Two sets of test films containing a total of 180 cases were sent to the following radiology departments: University of California, San Francisco (M. Jones); Rush-Presbyterian–St. Luke's Medical Center, Chicago (F. Alcorn); McMaster University, Hamilton, Ontario (P. Cockshott); and New York Medical College, New York City (N. Avnet).

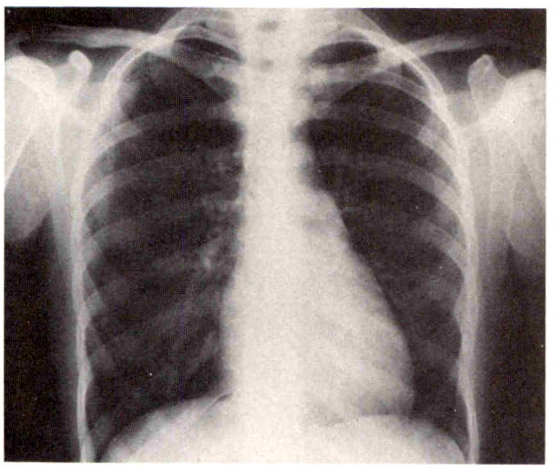


FIG. 1.—Fibrous dysplasia of posterior portion of right third rib and proximal portion of left humerus.

methods as closely as possible. Comparison of the performances of staff radiologists and residents from other institutions with our results showed substantially no differences. In addition, the first class of ART students spent an entire week at the University of California for evaluation by M. Jones.

The test film sets included routine examinations of the head and neck, chest, abdomen, and extremities (e.g., figs. 1–4). Some of the sets contained contrast examinations of the alimentary and genitourinary tracts. No angiograms were included. Each test set included a number of films which were clearly positive or negative as well as a relatively large number of cases containing subtle abnormalities or multiple abnormalities. Only in this respect were the test sets thought to differ from representative studies seen in a general radiology department of moderate size. Figures 1–3 are examples of the more difficult positive films. They were included to detect superficial or improper analysis of the films. Subsequent statistical analysis showed these cases to be highly discriminative. For example, each case illustrated in figures 1–3 had a discrimination power of .46.

The examination was administered by placing the films on a multiviewer where the examinee read each case individually. No time limit was imposed; however, the subjects were told to proceed as if they were reading the films in a work situation and to indicate the amount of time spent on each examination. Examinees were asked to designate each case as positive or negative for significant pathology. Because some cases contained more than one positive finding, each of varying significance, the film reader was also required to indicate the most significant finding which led to the positive designation. Thus it was possible for a person to correctly identify an examination as positive but be graded as having misread the case if the most significant lesion was not identified. (An example of this type of error is to designate a film positive because of an old fractured rib but miss a soft apical pulmonary infiltrate.) All abnormalities other than the one designated as the correct answer were of relatively minor significance.

Some of the test sets were administered to ART students twice to assess their progress. These individuals were not informed of the correct answers until after the final examination. Also, months elapsed between the two examinations to minimize the effect of memory.

Scores were evaluated in terms of the rates of false-positive and false-negative responses. Among false-positive responses were negative radiographs incorrectly identified as abnormal or insignificant findings selected as reasons for positive designations. Thus false-positive responses are a measure of inefficiency, since the labors of the physician radiologist are not lessened by the prior review. False-negative

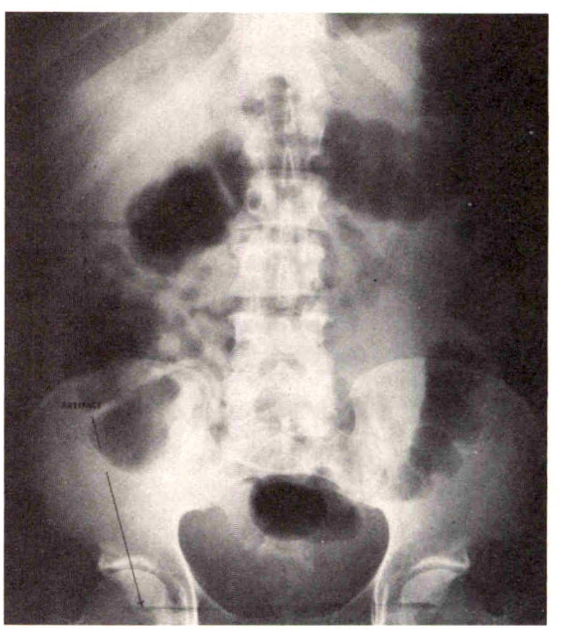


FIG. 2.—Normal abdomen, mongoloid pelvis. Bony changes were frequently overlooked. Arrows indicate artifacts.

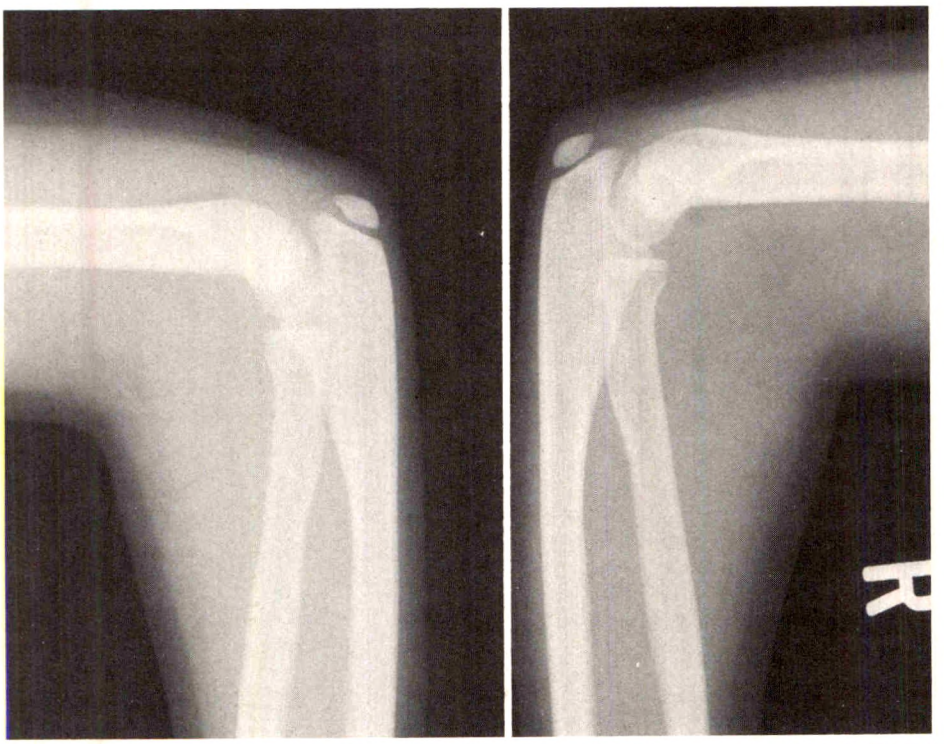


FIG. 3.—Positive fat pad sign on left; minimal slipping of the distal left humeral epiphysis. Ventral fat pad on right often incorrectly diagnosed as positive finding.

responses include positive radiographs which were incorrectly identified as negative. These errors represent a serious risk since patients may leave the medical care environment under the false impression that no disease exists. While a somewhat increased false-positive rate by ART students could be tolerated, a false-negative rate significantly higher than that of a well-trained physician radiologist is unacceptable.

False-positive and false-negative percentages were calculated as follows:

$$\text{False-positive \%} = \frac{\text{No. false-positive responses}}{\text{Total no. negative examinations in set}} \times 100.$$

$$\text{False-negative \%} = \frac{\text{No. false-negative responses}}{\text{Total no. positive examinations in set}} \times 100.$$

The performance of the ART students was evaluated by comparing their scores with those of staff radiologists and residents in radiology. Because the scores of the other groups tested were so low, they were dropped from the study. The months of training of each ART class at the time of examination was an additional parameter considered.

RESULTS

Figure 5 shows an arbitrarily selected ideal performance and the usual or expected performance of experienced radiologists on an examination of this type [3–5]. *It is important to note that an average of the false-positive and false-negative percentages must be used in comparing these results with usual methods of recording error rates since both the false-positive and false-negative rate could reach 100%.*

Table 1 compares the mean scores of our staff radiologists and residents on com-

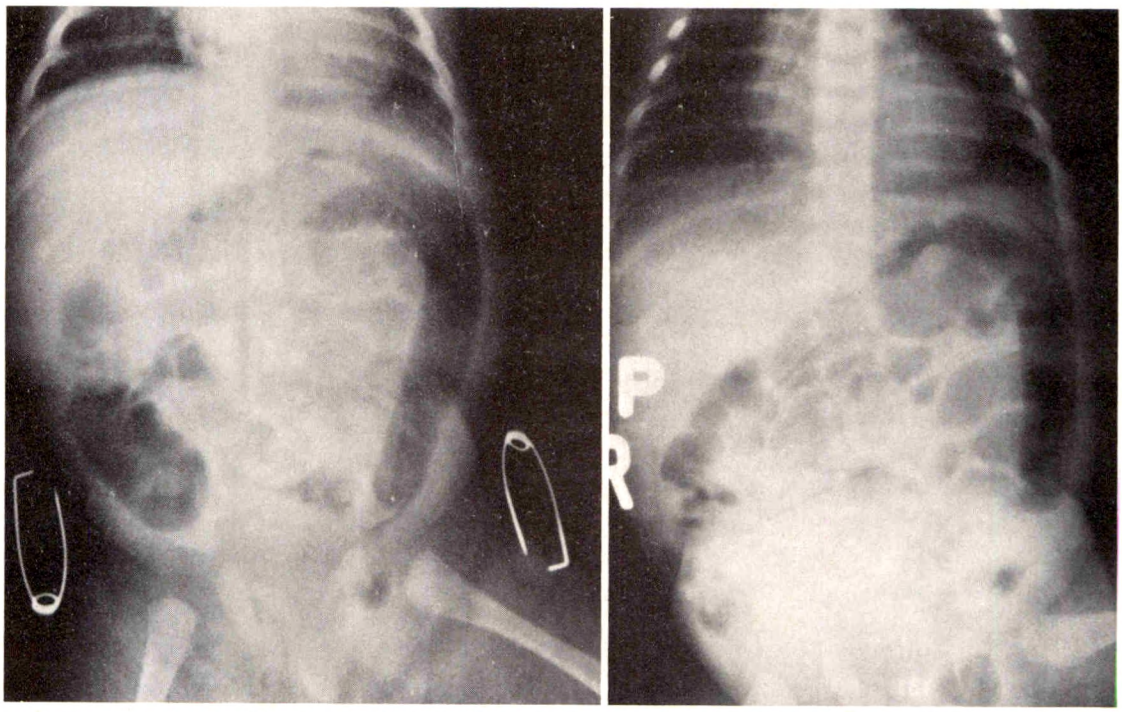


FIG. 4.—Left inguinal hernia. Pathology of this type was missed relatively infrequently (discrimination power .19).

posite tests 1 and 2 with scores of the first two classes of ART students. After 9 months of training, the first ART class scored higher on composite test 1 than either the staff or resident physicians. Only the latter difference was statistically significant ($t=3.32$, df$=15$, $P<.01$). This ART class also had the highest score on composite test 2 after 12 months of training. Again, only the residents had significantly lower scores ($t=3.80$, df$=15$, $P<.01$).

The second ART class scored much lower than either the staff ($t=-5.44$, df$=9$, $P<.001$) or the residents ($t=3.90$, df$=15$, $P<.01$) on composite test 2 during the first month of their training. The same differences were observed on composite test 1 during the second month of the program ($t=-5.24$, df$=9$, $P<.001$; $t=-3.44$, df$=15$, $P<.01$, respectively). By the end of the ninth month of training they achieved a slightly higher score than the staff and a significantly higher score than the residents on composite test 1 ($t=3.60$, df$=15$, $P<.01$). On composite test 2, they scored slightly lower than the staff but significantly higher than the residents ($t=3.26$, df$=15$, $P<.01$).

Figure 6 shows the percentages of false-positive and false-negative readings by the second ART class on composite test 1 after 2 and 9 months of training. The remarkable improvement is obvious. Figure 7 shows the performance of staff radiologists, radiology residents, and the first class of ART students on composite test 2 after 12 months of training.

The test sets were analyzed statistically and found to be highly reliable: Kuder-Richardson coefficients ranged from .61 to .81. The cases in the test sets were examined

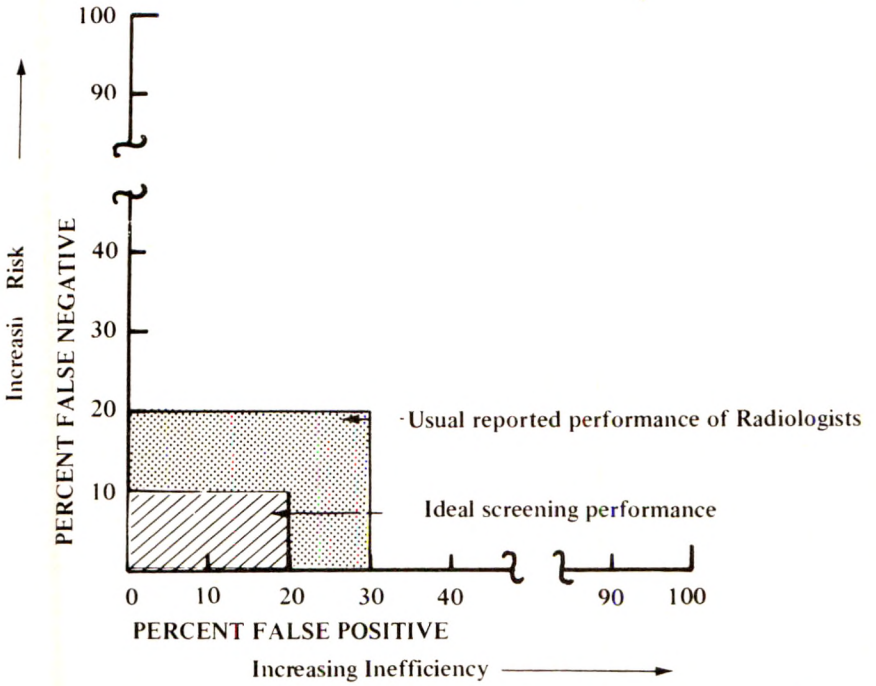


FIG. 5.—Expected performance of experienced radiologists in screening radiographs for presence or absence of pathology [3–5]. Ideal performance was arbitrarily selected. Maximum total error is 200% (i.e., all negative films read as positive and all positive films read as negative).

individually. Of a total of 393 cases, 228 had an average discrimination power of .30. The remaining films did not adequately discriminate between high and low performers (e.g., fig. 4). Additional analyses have been performed [6].

Five smaller sets of test films were administered to both groups of ART students as well as to our residents and staff radiologists. On these tests, both classes of ART students performed equally well by their ninth month of training. All tests, whether administered by us or at the participating institutions listed above, produced similar data. In general, both classes of ART students reached their maximum proficiency in film screening by 9 months. By this time they demonstrated greater perceptual proficiency in sorting films into positive and negative categories than the radiology residents and were approximately equal in accuracy to staff radiologists.

DISCUSSION

Earlier studies on the perceptual aspects of radiology have demonstrated that experienced radiologists often fail to identify all the significant pathology depicted on radiographs and that their error rates are relatively constant [3–5]. For example, Garland [3, 4] found that radiologists disagreed with each other about 30% of the time and disagreed with themselves ap-

TABLE 1

MEAN SCORES (CORRECT RESPONSES) ON COMPOSITE TESTS 1 AND 2

Group (No.)	Composite Test 1 (100 Cases)	Composite Test 2 (80 Cases)
Staff (5)	85.6	62.6
Residents (11)	76.4	53.6
ART class 1 (6):		
9- mo training	87.5	...
12-mo training	...	63.5
ART class 2 (6):		
1-mo training	...	42.5
2-mo training	64.5	...
9-mo training	86.0	61.0

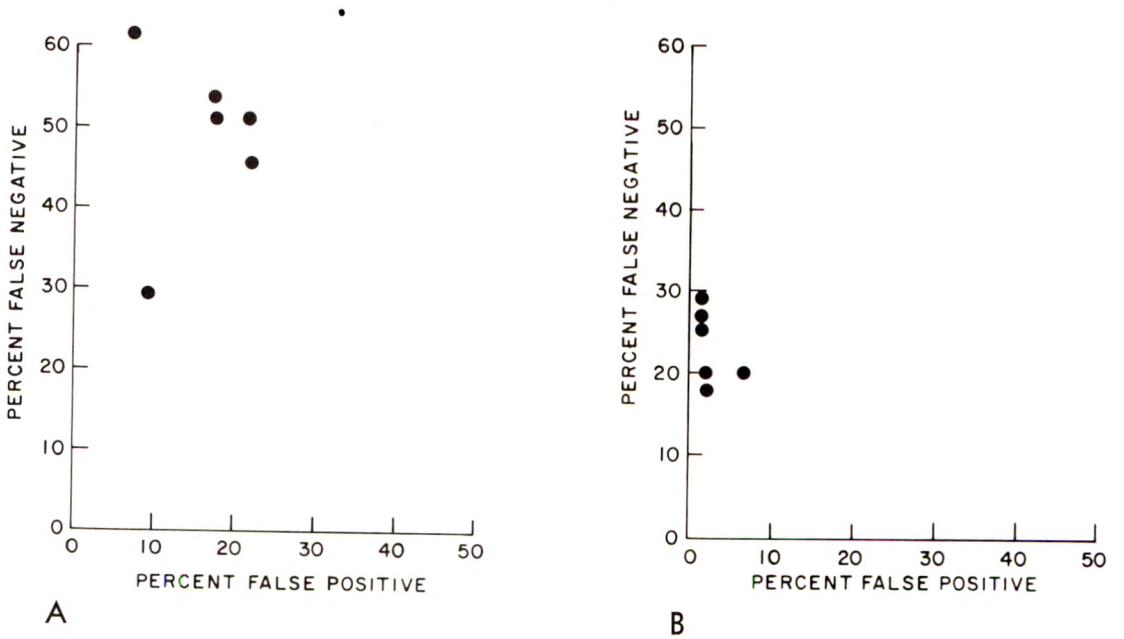


FIG. 6.—Performance of second class of ART students on composite test 1 after 2 months (*A*) and 9 months (*B*) of training. Test included 45 positive and 55 negative films.

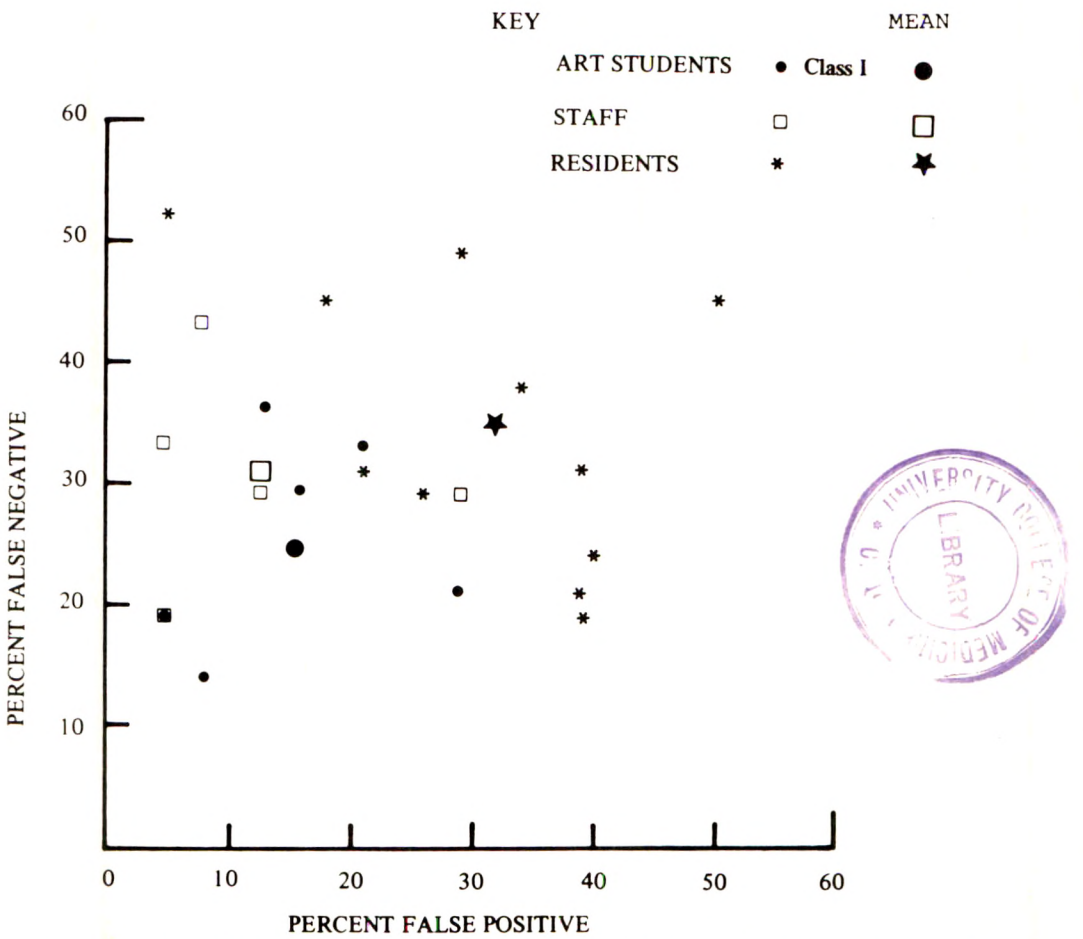
proximately 15% of the time. In a study involving a large number of chest films screened by experienced readers for the presence of inflammatory disease, Yerushalmy [5] recorded a false-negative observer rate of about 25%. The error rate of the staff radiologists on these examinations approximates that observed by Yerushalmy.

Several factors account for the relatively high rate of observer errors encountered on our sets of test films. First, the test films included a high proportion of difficult cases. It is recognized that such radiographs do not represent a typical daily work load. Nevertheless, since films of this type are the ones most frequently misinterpreted, every effort should be directed toward identification of the significant information they reveal. Second, the examinations were lengthy and fatiguing. To minimize the effects of fatigue, shorter tests with fewer highly discriminative films [6] are now being used.

The poor performance by radiology residents warrants comment. Their relative lack of enthusiasm compared to the ART students in taking these examinations no doubt affected their scores. In some instances they approached the tests with a measure of disinterest and may well have read the radiographs too rapidly. The level of interest, enthusiasm, and effort was a less significant factor for staff members, although it still may have had an effect.

In contrast, ART students were highly motivated to perform at their best. They were a highly intelligent, cooperative, and unusually industrious group with abundant previous experience. There is no thought that an "average" radiologic technologist could be trained so rapidly to this level of competence. Nevertheless, we believe we have assembled strong evidence that properly selected and adequately instructed ART students can assess films for the presence or absence of significant pathology with an error rate equivalent to that of experienced radiologists.

The instruction of the ART students was directed toward teaching them how to look at films, how to assess normalcy, and how to recognize the changes that indicate abnormality. The emphasis of the didactic material was on perceptual aspects. Repetition and reinforcement were frequently used to emphasize important abnormalities,



UNIVERSITY OF MEDICINE & DENTISTRY LIBRARY

FIG. 7.—Comparison of performance of first class of ART students on composite test 2 after 12 months of training with that of staff radiologists and residents.

especially the more subtle ones. Much time was spent discussing normal variations and structural changes expected at various ages. Specific abnormalities to search for and frequently missed lesions, especially in trauma, were emphasized. Minimal time was spent on specific diagnoses. Diagnosis and differential diagnosis entered the instructional sessions only as secondary considerations. *The main emphasis was to teach the ART student to identify those films that should be brought to the attention of the physician radiologist.*

These data in no way suggest that radiology residents possess less knowledge or perceptual ability than ART students. They indicate only that on these examinations the ART students exhibited a better perceptual performance. Preconceptions from previous medical training may have led the residents, perhaps even subconsciously, to abort their search for subtle abnormalities more quickly than the ART students who lack such extensive physiological and pathological knowledge. It could be that an expectation of normality gleaned from previous experience or from an overall benign appearance of a radiograph may in part explain the less satisfactory perceptual performance of the residents. The ART students were not affected by these considerations.

These data should be verified by similar studies elsewhere. If our results are corroborated, perhaps a change in the method used to instruct radiology residents in the

early months of their training would be beneficial and result in more rapid achievement of acceptable proficiency. Such a change would include stronger emphasis on image recognition in early training than has occurred in the past. However, many important questions remain which need objective evaluation. For example, Should there be a delay in providing detailed pathogenic explanations of abnormal shadows until appropriate perceptual proficiency is demonstrated? and Will the residents knowledge of diseases make this approach more difficult?

ACKNOWLEDGMENT

We thank Dr. John V. Haley for performing some of the statistical analyses.

REFERENCES

1. Kiernan B, Rosenbaum HD: The impact of a physician assistant in diagnostic radiology on the delivery of diagnostic radiologic clinical services. Submitted for publication
2. Lusted LB: *Introduction to Medical Decision Making*. Springfield, Ill., Thomas, 1968
3. Garland HL: On the scientific evaluation of diagnostic procedures. *Radiology* 52:309–328, 1949
4. Garland HL: Studies on the accuracy of diagnostic procedures. *Am J Roentgenol* 82:25–38, 1959
5. Yerushalmy J: The statistical assessment of the variabiliity in observer perception and the description of roentgenographic pulmonary shadows. *Radiol Clin North Am* 7: 381–392, 1969
6. Haley JV, Kiernan B: Evaluation of physician assistants in diagnostic radiology. Submitted for publication

Am J Roentgenol 126:1077–1081, 1976

^{99m}Tc-DIPHOSPHONATE UPTAKE IN NEUROBLASTOMA

WILLIAM MCCARTNEY,[1] MARTIN L. NUSYNOWITZ,[1] BERNHARD E. F. REIMANN,[2] JERRY PRATHER,[1] AND BRUCE MAZAT[1]

ABSTRACT:

Marked uptake of ^{99m}Tc-diphosphonate was noted in an extraadrenal neuroblastoma. Calcification was not demonstrable on radiographic or light microscopic examination, nor was crystalline material identified on electron microscopic examination; capillaries in the lesion appeared to be intact. Similar uptake of phosphate radiopharmaceuticals by a variety of lesions has been reported, and possible mechanisms for this phenomenon are discussed.

Increasing numbers of cases of extraosseous deposition of activity by the currently used phosphate bone-scanning agents (^{99m}Tc-diphosphonate, ^{99m}Tc-pyrophosphate, and ^{99m}Tc-polyphosphate) have been reported in the literature. We have recently demonstrated marked uptake of ^{99m}Tc-diphosphonate in an extraadrenal neuroblastoma and studied possible mechanisms for its localization in this lesion.

CASE REPORT

A nine-year-old white girl was admitted to the hospital for evaluation of an incidentally discovered abdominal mass. The patient had no gastrointestinal or urologic symptoms, no trauma, and had never noticed the presence of the mass. She was well developed and well nourished, weighing 62 lbs. The single pertinent physical finding was a firm, nontender, nonmoveable 8×8 cm mass located in the right lower quadrant. The admission hematocrit was 39% and the white blood cell count was 8,100/mm^3; the differential count was normal. There was an elevated sedimentation rate of 50 mm/hr. Serum chemistry determination revealed normal calcium, phosphorus, glucose, BUN, total protein, and albumin values. The alkaline phosphatase, LDH, and SGOT values were 123, 330, and 48 IU, respectively, all within normal limits. Urinalysis was normal. Urinary vanillylmandelic acid excretion was 7.8 mg/24 hr (normal = 1.0–7.1). An excretory urogram (fig. 1) revealed a mass in the right lower quadrant which extended into the pelvis and caused deviation of the right ureter anteriorly and medially. There was minimal urinary obstruction on the right; the left kidney and collecting system were entirely normal. Inferior vena cavagram and barium enema studies demonstrated extrinsic compression of surrounding structures by the retroperitoneal mass, without evidence of invasion. Liver scan was normal. Bone images (fig. 2) were obtained with a Searle Radiographic Pho Gamma HP camera 3 hr after intravenous administration of 10 mCi of ^{99m}Tc-diphosphonate. These revealed normal osseous structures; however, the right lower quadrant mass showed marked accumulation of the ^{99m}Tc-diphosphonate.

Surgical exploration revealed a large right lower quadrant retroperitoneal mass with several adjacent enlarged lymph nodes. The pathologic diagnosis was neuroblastoma. No gross or microscopic evidence of tissue calcification was noted. Electron microscopic studies of the tumor tissue showed a uniform cell population characterized by circular to oval configuration of the cells, relatively large nuclei, frequent mitotic figures, and nuclear sequestration (fig. 3). Examination of capillaries traversing the tumor tissue revealed no abnormalities. Electron diffraction studies with special attention to mitochondria did not show any evidence of inorganic crystalline structures.

DISCUSSION

Many different types of nonosseous lesions may demonstrate significant accumulation of the currently used ^{99m}Tc-phos-

[1] Nuclear Medicine–Endocrine Service, William Beaumont Army Medical Center, El Paso, Texas 79920. Address reprint requests to Editorial Assistant, Medical Research and Development Services, William Beaumont Army Medical Center, El Paso, Texas 79920.
[2] Pathology Department, William Beaumont Army Medical Center, El Paso, Texas 79920.

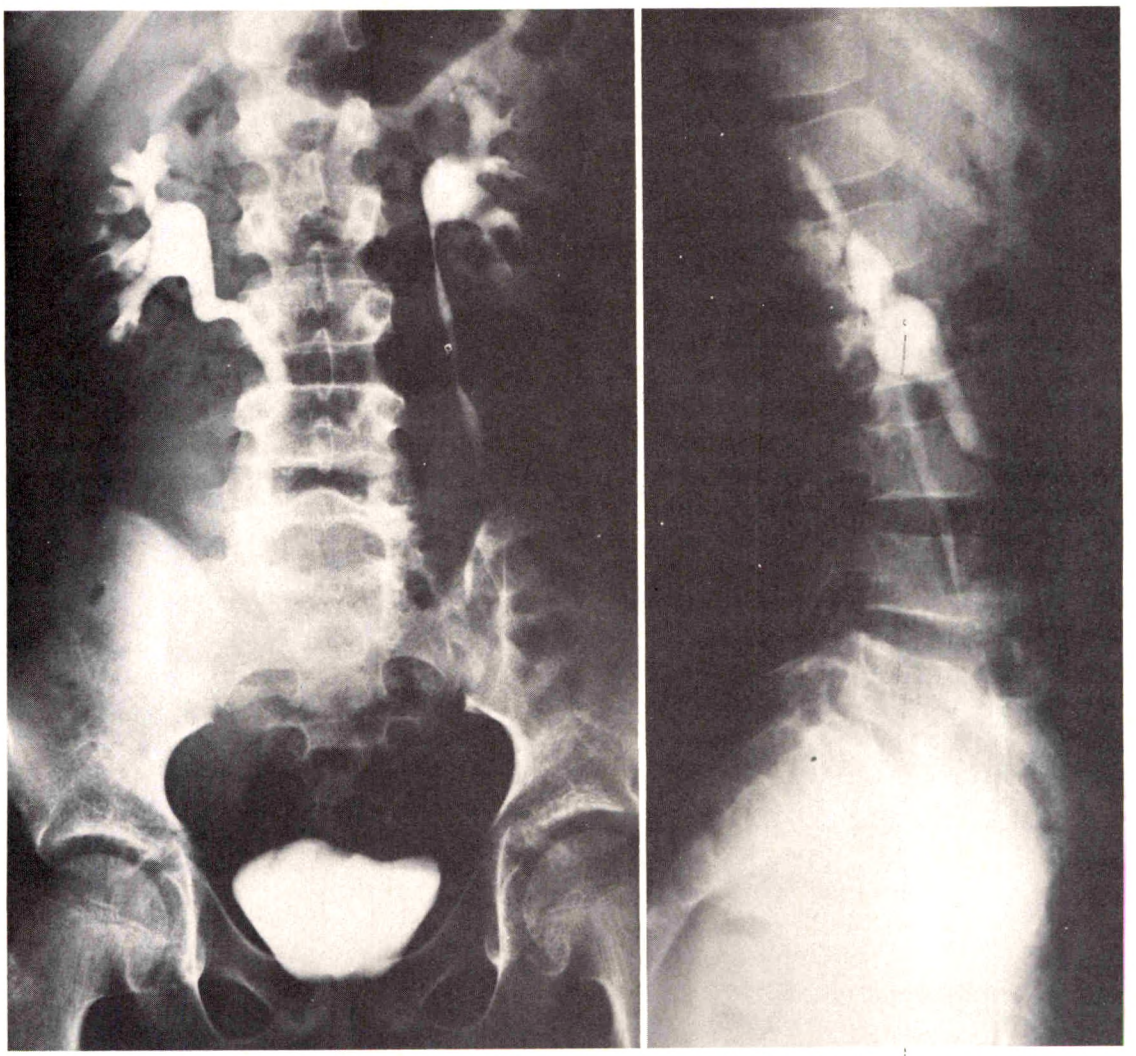


FIG. 1.—AP (*left*) and lateral (*right*) views of the abdomen obtained during intravenous pyelography. Large mass in the right lower quadrant displaces the right ureter medially and anteriorly.

phate bone-scanning radiopharmaceuticals. The various lesions associated with this soft tissue deposition of radionuclide activity include breast carcinoma [1–5], malignant lymphoma [4, 6, 7], lung carcinoma [4], melanoma [7], embryonal cell carcinoma [4], adenocarcinoma of the rectum [8], various primary brain tumors [2, 4, 9, 10], cerebral infarction [9–11], myocardial infarction or contusion [12–15], soft tissue abscess and inflammation [2, 14], neurofibroma [16], and one case of adrenal neuroblastoma [17]. Most of the soft tissue lesions involved apparently contain no significant calcification using conventional light microscopy.

The mechanism for the accumulation of phosphate radiopharmaceuticals in soft tissue lesions has not been well explained. While increased blood flow may be a factor in at least some of these lesions, it would not account for the dramatic accumulation seen in many instances. Also militating against this mechanism is the fact that no thermographic abnormalities were seen in patients with breast malignancies who showed increased uptake of bone-scanning agents [18]. Alteration of capillary perme-

ability associated with neovascularity, allowing "leakage" of the radiopharmaceutical into the soft tissue lesions, has been suggested as another possible mechanism.

Another plausible hypothesis is that high concentrations of phosphatase enzyme systems are present in those lesions which bind the Tc-labeled phosphate agents [2, 19]. In support of this mechanism, Zimmer et al. [19] have shown that high concentrations of acid phosphatase were present in both normal and pathologic breast tissue which showed increased uptake of the ^{99m}Tc-diphosphonate; they suggest that acid phosphatase binding of these phosphate bone scan agents may be responsible for their soft tissue concentration. To test this hypothesis, they studied the effect of diphosphonate in varying concentrations on the activity of acid phosphatase in vitro. Inhibition of acid phosphatase activity was noted with a diphosphonate concentration of 1 μmol/liter; no other enzyme system tested was appreciably inhibited at this concentration of diphosphonate. Such data give strong support to the hypothesis of enzyme receptor binding by diphosphonate.

The work of D'Agostino et al. [20] with cardiac muscle necrosis offers another explanation as to the soft tissue activity seen with phosphate bone scan agents. Their electron microscopic observations of mitochondrial binding of calcium ions within a crystalline structure, thought to be similar to hydroxyapatite, led Bonte and Parkey [13] to utilize ^{99m}Tc-polyphosphate in imaging myocardial infarcts.

However, electron microscopic examination and diffraction studies of the tissues from our patient failed to reveal inorganic crystalline structures in the tissue, including the mitochondria. Special attention was also directed to the capillaries traversing the tumor tissue, but no abnormalities were found; they exhibited the usual narrow endothelial cells lining a basement membrane of particularly high electron opacity. No breaks in the capillary wall were observed. Thus, no evidence was found to support the concept of defects of integrity in the capillary wall as a mechanism accounting for "leakage."

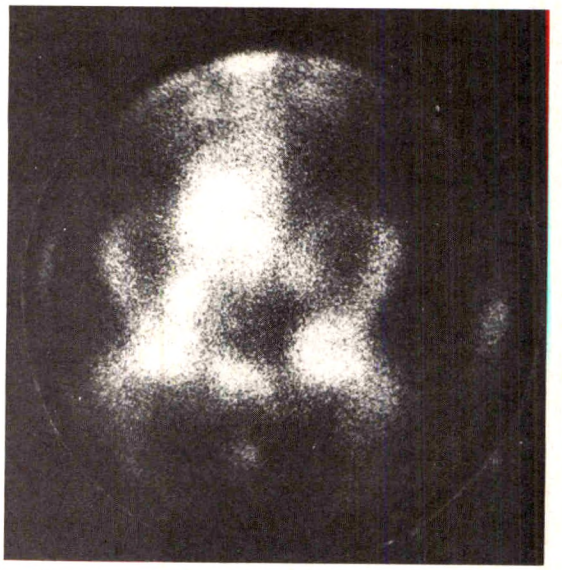


FIG. 2.—Anterior view of the lower abdomen and pelvis showing large right lower quadrant mass with marked uptake of ^{99m}Tc-diphosphonate.

In the only other reported case of a neuroblastoma demonstrating uptake of a ^{99m}Tc-phosphate bone-scanning radiopharmaceutical, the tumor was located in the adrenal gland and had extensive diffuse calcification [17]. Such calcifications are less common in extraadrenal neuroblastomas [21]. Thus it is not surprising that no gross or microscopic calcifications were noted in the case described in this report. The observation of an extraadrenal neuroblastoma concentrating ^{99m}Tc-diphosphonate, even though no calcification was present, tends to support the concept that enzymatic binding may be responsible for accumulation of phosphate bone-scanning agents in at least some types of soft tissue lesions.

The marked increase in the number of reports of unusual soft tissue accumulation of the phosphate radiopharmaceuticals suggests that a greater clinical utilization of these agents should be explored. When performing bone scans in evaluation of possible metastatic disease, the soft tissues should be examined most carefully to delineate any possible areas of increased activity.

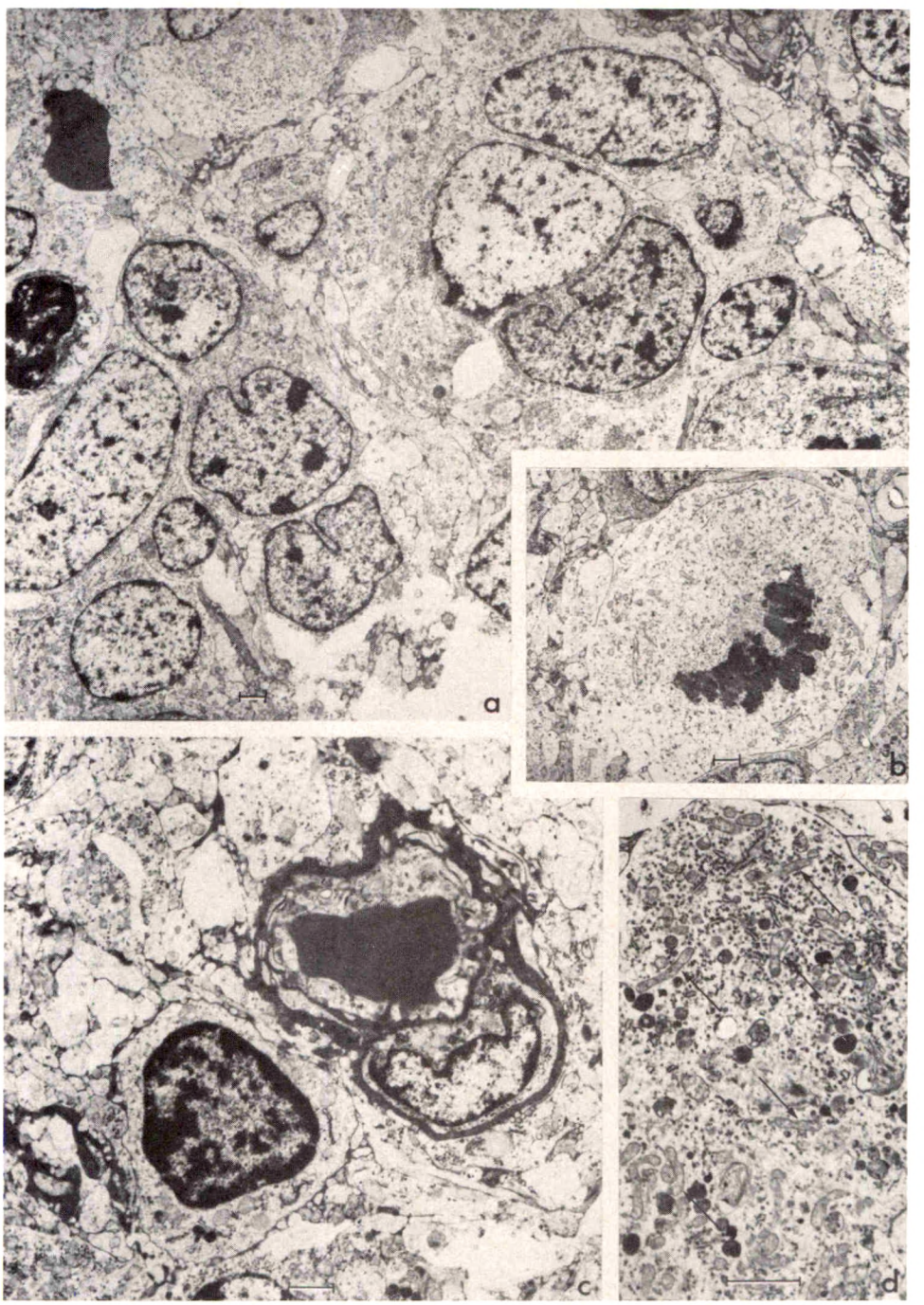


FIG. 3.—Electron micrograph of the neuroblastoma. *a*, Overall appearance of tumor cells; *b*, mitotic figure; *c*, capillary with electron dense basement membrane; *d*, cytoplasm of tumor cell with empty mitochondria (*arrow*). Bars represent 1 μm.

ACKNOWLEDGMENTS

The contributions of Mr. Wayne B. Gysland for electron microscopic studies and Peggy Casteel for editorial assistance are gratefully acknowledged.

REFEKENCES

1. Berg GR, Kalisher L, Osmond JD, Pendergrass HP, Potsaid MS: ^{99m}Tc-diphosphonate concentration in primary breast carcinoma. *Radiology* 109:393–394, 1973
2. Chaudhuri TK, Chaudhuri TK, Gulesserian H, Christie JH, Tonami N: Extraosseous noncalcified soft-tissue uptake of ^{99m}Tc-polyphosphate. *J Nucl Med* 15:1054–1056, 1974
3. Friedman BH, Siegel ME, Wagner HN: Breast uptake of ^{99m}Tc HEDSPA (diphosphonate): an indicator of breast carcinoma. *J Nucl Med* 15: 491–492, 1974
4. Matsui K, Yamada H, Chiba K, Ho M: Visualization of soft tissue malignancies by using ^{99m}Tc-polyphosphate, pyrophosphate and diphosphonate (^{99m}Tc-P). *J Nucl Med* 14:632–633, 1973
5. Serafini AN, Raskin MM, Zand LC, Watson DD: Radionuclide breast scanning in carcinoma of the breast. *J Nucl Med* 15:1149–1152, 1974
6. Richards AG: Metastatic calcification detected through scanning with ^{99m}Tc-polyphosphate. *J Nucl Med* 15:1057–1060, 1974
7. Thrall JH, Ghaed N, Pinsky SM, Grove RB, Johnson MC: Pitfalls in the use of ^{99m}Tc-polyphosphate for bone scanning. *J Nucl Med* 14: 460–461, 1973
8. Chaudhuri TK, Chaudhuri TK, Christie JH: Tumor uptake of ^{99m}Tc-polyphosphate: its similarity with ^{87m}Sr-citrate and dissimilarity with ^{67}Ga-citrate. *J Nucl Med* 15:458–459, 1974
9. Fischer KC, Pendergrass HP, McKusick KA, Potsaid MS: Increased brain scan specificity by the use of ^{99m}Tc-diphosphonate. *J Nucl Med* 15: 490, 1974
10. Wenzel WW, Heasty RG: Uptake of ^{99m}Tc stannous polyphosphate in an area of cerebral infarction. *J Nucl Med* 15:207–209, 1974
11. Grames GM, Jansen C: The abnormal bone scan in cerebral infarction. *J Nucl Med* 14:941–943, 1973
12. Bonte FJ, Parkey RW, Graham KD, Moore J, Stokely EM: A new method for radionuclide imaging of myocardial infarcts. *Radiology* 110: 473–474, 1974
13. Bonte FJ, Parkey RW: A new method for imaging myocardial infarcts. *J Nucl Med* 15:479, 1974
14. Go RT, Chiu CL, Doty DB, Cheng H, Christie J: Radionuclide imaging of experimental myocardial contusion. *J Nucl Med* 15:1174–1175, 1974
15. Parkey RW, Bonte FJ, Meyer SL, Willerson JT, Atkins JM, Curry GC: Detection of acute myocardial infarction in humans using ^{99m}Tc stannous pyrophosphate (PYP). *J Nucl Med* 15:521, 1974
16. Nolan NG: Intense uptake of ^{99m}Tc diphosphonate by extra-osseous neurofibroma. *J Nucl Med* 15:1207–1208, 1974
17. Fitzer PM: ^{99m}Tc polyphosphate concentration in a neuroblastoma. *J Nucl Med* 15:904–906, 1974
18. Bautovich G, Genant HK, Hoffer PB, Harper PV, Lathrop K: In vivo studies of the effects of tissue inflammation in the uptake of bone seeking radionuclides. *J Nucl Med* 15:476, 1974
19. Zimmer AM, Isitman AT, Schmitt GH, Holmes RA: Enzymatic inhibition by diphosphonate: a proposed mechanism of tissue uptake. *J Nucl Med* 15:546, 1974
20. D'Agostino AN, Chiga M: Mitochondrial mineralization in human myocardium. *Am J Clin Pathol* 53:820–824, 1970
21. Young LW, Rubin P, Hanson RE: The extra-adrenal neuroblastoma: high radiocurability and diagnostic accuracy. *Am J Roentgenol* 108:75–91, 1970

Am J Roentgenol 126:1082–1087, 1976

ADJUVANT CHEMOIMMUNOTHERAPY IN ADVANCED LESIONS OF THE HEAD AND NECK

FREDERICK R. EILBER[1] AND DONALD L. MORTON[1]

ABSTRACT:

Growth of malignant tumors of the head and neck has been associated with progressive impairment of immunologic activity. Successful control of disease has been shown to reverse this defect. Preliminary results of a nonrandomized trial reduced recurrence of head and neck cancer for a median time of 11.5 months in eight of 10 patients who received chemoimmunotherapy adjuvant to surgical resection or radiation treatment. The number of patients in the series was small and the follow-up time too short to determine the length of effectiveness for this treatment. Based on these results, a new protocol has been initiated to randomize patients with advanced T_3 and T_4 lesions into groups for comparison of adjuvant chemotherapy alone with adjuvant chemoimmunotherapy.

INTRODUCTION

The concept of host resistance as an important factor in both the inception and progression of head and neck malignancy has been proposed for many years. It originates from observations of the unpredictable clinical course for patients with tumors in these anatomic locations. Whereas some patients have a rapid recurrence of disease despite apparently adequate treatment for early tumors, other patients demonstrate a relatively slow progression of disease despite far-advanced malignancies.

Growth of malignant tumors of the head and neck has been associated with progressive impairment of immunologic reactivity [1]. Anergy has been observed in patients prior to the development of cachexia and malnutrition, even without widespread visceral and bone marrow involvement. The immunologic impairment noted in cancer patients was not a defect that preceded the development of malignancy because it could be reversed if successful control of disease was achieved [2–4]. Optimistically, then, it might be possible to augment the immunologic reactivity of the cancer patient. However, additional reports have shown that the therapeutic modalities used to treat neoplasms of the head and neck are themselves immunosuppressive. The suppressive effects of surgery [5] and chemotherapy [6] appear to be of relatively short duration; the immunosuppressive effects of radiotherapy [7, 8] may or may not be more prolonged [9–11]. Thus it would seem that if immunologic reactivity could be maintained during treatment, a greater therapeutic benefit might be achieved.

While immunotherapy for treatment of malignancies in laboratory animals as well as for malignant melanoma in man has been shown to be effective its use is limited. In laboratory animals it was of benefit when the tumor burden was in a ratio of approximately 10^7–10^8 cells [12]; larger amounts of tumor rarely responded to immunologic manipulation. These same principles seem to be applicable in man. A therapeutic effect was generally achieved in patients with subclinical disease [13] whereas for more advanced disease, results were not nearly as impressive [14]. If immunotherapy is applied to the treatment of patients with tumors of the head and neck,

These investigations were supported by grants from the U.S. Public Health Service (CA 12582) and from Surgical Services, Sepulveda Veterans Administration Hospital.

[1] Division of Oncology, Department of Surgery, UCLA Center for the Health Sciences, Los Angeles, California 90024, and Surgical Services, Sepulveda Veterans Administration Hospital, Sepulveda, California 91343. Address reprint requests to the Division of Oncology.

it cannot be used as a primary treatment modality but rather as an adjuvant to the existing therapeutic modalities of surgery, radiation, and chemotherapy.

Preliminary reports from Donaldson [15, 16] have shown that a greater therapeutic response was achieved in head and neck patients when BCG, a nonspecific immune stimulant, was combined with chemotherapy (methotrexate) than when chemotherapy alone was used.

This paper describes a phase I pilot study designed to determine the effect of BCG immunotherapy in combination with methotrexate. This regimen was evaluated in patients with recurrent malignant disease of the head and neck and in patients with advanced lesions who had an 80% chance of recurrence with standard modes of therapy.

SUBJECTS AND METHODS

The 20 patients investigated were evaluated either in the Department of Surgery, Division of Oncology, UCLA School of Medicine, or the Sepulveda Veterans Administration Hospital, Sepulveda, California. They ranged in age from 29 to 73 years. All had advanced T_3 or T_4 squamous cell neoplasms of the head and neck region and had no history of prior malignancies or evidence of widespread tumor before administration of chemoimmunotherapy. Patients were clinically evaluated by complete physical examination, chest x-ray, and liver, brain, and bone scan prior to entering the study. Histologic confirmation of squamous cell carcinoma was obtained in every case.

The experimental nature of the procedures was explained to each patient prior to entering the study and a signed consent was obtained. Patients were divided into three categories: those who had failed on all previous therapy and had established disease (table 1); and those who did not have clinically evident disease but who were treated prophylactically for subclinical disease following radiation therapy (table 2) or surgery and radiation therapy (table 3).

The chemotherapeutic drug methotrexate (50 mg/m^2) was administered once a week for 1 month and every other week thereafter for the duration of the study. Immunotherapy was accomplished with BCG Tice strain from Chicago Research, administered by the Tine technique to the axillae and both groins every week for 3 months and then every other week for the duration of the study. Follow-up examination was performed each month.

A complete response to chemotherapy was defined as the disappearance of all visible disease and no evidence of new disease for a period of 2 months. A partial response was defined as 50% reduction in established disease and no new lesions. While surgical procedures differed for each patient, they basically included en bloc resection of the primary tumor and regional lymph nodes. X-ray treatment was given using cobalt 60 teletherapy at a dosage of 5,000–6,000 rads over 5–6 weeks.

Immunologic evaluations of delayed cutaneous hypersensitivity were performed with topically applied dinitrochlorobenzene (DNCB) and a battery of recall antigens. Reactions were recorded after 48 hr. Serial DNCB skin testing was performed at monthly intervals [3]. A hypersensitivity score was assigned to each test, and a score of 3 or greater was considered positive [17].

RESULTS

Table 1 shows the results of chemoimmunotherapy in six patients with established recurrent disease. A complete response to chemoimmunotherapy was obtained in only one patient, no. 1. This patient had reexcision of the primary tumor, maxillary antrum, and orbit 4 months after initiation of chemoimmunotherapy and has been free of disease 6 months following this surgery. Microscopic residual disease was present in the operative specimen. Patients 2 and 3 have maintained a 50% reduction in tumor size for 4 and 5 months, respectively. Both patients have clinically evident residual disease but have not developed new lesions. The remaining three patients did not have any measurable decrease in tumor size, and all expired.

Simultaneously, we began a nonrandomized prospective study of the BCG-methotrexate combination as adjuvant treatment to radiation or surgery. Table 2 shows the results of treatment with adjuvant chemoimmunotherapy for stage T_3 and T_4

TABLE 1

CHEMOIMMUNOTHERAPY IN PATIENTS WITH ESTABLISHED RECURRENT DISEASE

Patient No.	Age (Yr)	Location of Primary Tumor	Malignant Neck Nodes	Date of Operation	X-ray Therapy	Date of Recurrence	Chemoimmuno-therapy	Response (%)	Follow-up (Mo)
1.....	56	Antrum and intra-cranial	—	10/'74	PreOp 8/'73	4/'74	Mtx, BCG	100	6
2.....	73	Temporal bone	4/12	12/'74	PostOp 12/'74	1/'75*	Mtx, BCG	50	4
3.....	54	Retromolar	10/15	8/'74	PostOp 9/'74	10/'74*	Mtx, BCG	50	5
4.....	62	Larynx	4/10	8/'74	PostOp 9/'74	12/'74	Mtx, BCG	0	3
5.....	61	Tonsil	+	...	8/'73	12/'73	Mtx, BCG	0	3
6.....	54	Tongue base	+	...	8/'73	10/'73	Mtx, BCG	0	2

* During x-ray therapy.

squamous cell carcinoma of the head and neck in which radiation therapy was the primary modality. Of the four patients treated thus far, three are free of recurrent disease after a median of 6 months. One patient had rapid recurrence despite radiation and chemoimmunotherapy and expired within 4 months of onset of treatment. Although the follow-up time is relatively short for these patients, their clinical response has been dramatic.

A series of 10 patients was treated with adjuvant chemoimmunotherapy following surgical excision of all gross tumor plus radiation therapy (table 3). Eight of the 10 (80%) are alive and free of recurrent disease after a median of 11.5 months. All patients had postoperative radiation therapy to the tumor bed and the regional lymphatics except for patients 4 and 5, who were operated on after radiation therapy failure.

Toxicity

For six of the 14 patients (40%) treated with adjuvant chemoimmunotherapy, it was necessary to decrease the scheduled dosage of methotrexate. The major toxic effect was hematopoetic, manifested by white cell counts lower than 2,000. The delay in treatment was never more than 1 week. No incidence of renal toxicity, sepsis, or permanent bone marrow toxicity was observed. Oral ulceration was observed in

TABLE 2

CHEMOIMMUNOTHERAPY AS ADJUVANT TREATMENT TO RADIATION THERAPY

Patient No.	Age (Yr)	Location of Primary Tumor	Malignant Neck Nodes	X-Ray Therapy (Rad)	Chemoimmuno-therapy	Status	Follow-up (Mo)
1.....	68	Retromolar	+	5,000	Mtx, BCG	N.E.D.	4
2.....	48	Tongue base	+	5,000	Mtx, BCG	N.E.D.	8
3.....	47	Tongue base	—	5,000	Mtx, BCG	N.E.D.	6
4.....	65	Larynx	—	5,000	Mtx, BCG	Expired (recurrence)	4

NOTE.—None of these patients were treated surgically.

TABLE 3

CHEMOIMMUNOTHERAPY AS ADJUVANT TREATMENT TO SURGERY AND RADIATION THERAPY

Patient No.	Age (Yr)	Location of Primary Tumor	Malignant Neck Nodes	Date of Operation	X-ray Therapy	Chemoimmuno-therapy	Status	Follow-up (Mo)
1.....	62	Larynx	2/10	1/'74	PostOp	Mtx, BCG	N.E.D.	14
2.....	52	Epiglottis	4/10	1/'74	PostOp	Mtx, BCG	N.E.D.	16
3.....	72	Pyriform sinus	3/10	9/'74	PostOp	Mtx, BCG	N.E.D.	6
4.....	48	Tongue base	2/12	7/'73	PreOp failure	Mtx, BCG	N.E.D.	24
5.....	65	Tongue base	2/15	8/'74	PreOp failure	Mtx, BCG	N.E.D.	8
6.....	53	Tongue anterior	2/16	10/'74*	PostOp	Mtx, BCG	Recurrence (alive)	4
7.....	73	Buccal mucosa	4/20	10/'73	PostOp	Mtx, BCG	N.E.D.	15
8.....	66	Postpharynx	5/20	3/'74	PostOp	Mtx, BCG	Recurrence (expired)	12
9.....	62	Retromolar	3/10	10/'74	PostOp	Mtx, BCG	N.E.D.	6
10.....	29	Retromolar	3/12	7/'74	PostOp	Mtx, BCG	N.E.D.	8

NOTE.—Eight of 10 have no evident disease after a median of 11.5 months.
* Resected nodes.

20% of the patients. None of the patients developed systemic BCG infection, although two patients developed moderately severe pruritus at the site of the BCG injection, resulting in discontinuance of BCG for 2 weeks.

Immunologic Evaluation

On initial evaluation, 16 of 20 (80%) of the patients were nonresponsive to DNCB (fig. 1). Following definitive surgery and during chemotherapy, 12 of the 16 (75%) converted to positive and remain free of disease. Of the four who did not become responsive to DNCB, three developed recurrent disease within 3 months. The four patients who were DNCB positive on initial evaluation have remained positive and free of recurrence. All patients treated with BCG converted to a positive PPD skin test during the study.

DISCUSSION

The treatment of patients with advanced T_3 or T_4 lesions of the head and neck continues to present a very difficult therapeutic problem. Although surgery and postoperative radiotherapy have greatly improved local control of the tumors, the overall results indicate an eventual failure in more than 80% of the patients [18]. Thus it is imperative that some form of systemically active adjuvant therapy be administered to prolong their survival. Preliminary results from Donaldson [15, 16] together with the present results of treatment in the six patients with established disease show that methotrexate is an active agent in squamous cell carcinoma of the head and neck. However, in

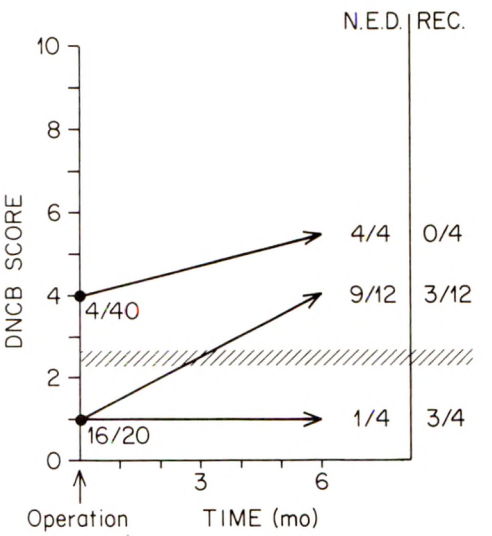


FIG. 1.—Sequential DNCB reactivity in patients with head and neck neoplasms.

our opinion, the BCG-methotrexate combination appears to have limited value for this type of patient. Only one of six patients achieved a complete response, and that had to be followed by further surgical intervention. Thus it appears unlikely that complete tumor destruction was ever achieved.

The results of chemoimmunotherapy as adjuvant to surgery or irradiation were much more impressive. Since, statistically, 80% of these patients would develop recurrent disease, residual subclinical disease was very likely present at the completion of surgery and/or radiation therapy. The favorable results reported here must be tempered by the fact that this was not a randomized trial nor did it include consecutive patients; also, the duration of the study was relatively short. However, the results are encouraging since the clinical course of patients with advanced tumors of the head and neck is relatively constant. The median time to recurrence in several series is approximately 8 months. A much longer follow-up time is obviously required before the actual outcome for these patients can be determined. However, it does appear that the procedure of chemoimmunotherapy is well tolerated with acceptable toxicity and that it decreases the recurrence rate, at least based on the short-term follow-up of these patients. Whether the disease will eventually recur remains to be seen.

In addition, the question remains of whether BCG immunotherapy contributed to the chemotherapeutic regimen. On the basis of these limited data, the answer is uncertain. Although the nonspecific reactivity to DNCB was maintained in four patients and even reversed from negative to positive in 12 patients, it is not clear whether BCG was responsible. Consequently we have begun a prospective trial that will randomize patients with advanced T_3 and T_4 lesions into adjuvant chemotherapy alone versus chemoimmunotherapy.

Hopefully a combination of presently available treatment modalities—surgery, radiation therapy, chemotherapy, and immunotherapy—will result in a more successful means for disease control in a greater percentage of these patients.

REFERENCES

1. Eilber FR, Morton DL, Ketcham AS: Correlation of immunologic reactivity and clinical course in patients with solid neoplasms of the head and neck in *Neoplasia of the Head and Neck*, Proceedings 17th Annual Clinical Conference on Cancer, M. D. Anderson Hospital and Tumor Institute, Chicago, Year Book Medical Publishers, 1974, pp. 211–219
2. Young RC, Corder MP, Haynes HA, *et. al.*: Delayed hypersensitivity in Hodgkin's disease—a study of 103 untreated patients. *Am J Med* 52:63–72, 1972
3. Eilber FR, Nizze JA, Morton DL: Sequential evaluation of general immune competence in cancer patients: correlation with clinical course. *Cancer* 35:660–665, 1975
4. Eilber FR, Morton DL, Ketcham AS: Immunologic abnormalities in head and neck cancer. *Am J Surg* 128:534–538, 1974
5. Roth JA, Eilber FR, Morton DL: Effect of surgery on in vitro lymphocyte function. *Surg Forum* 25:102–104, 1974
6. Hersh EM: Modification of host defense mechanisms, in *Cancer Medicine*, edited by Holland JF, Frei E, Philadelphia, Lea & Febiger, 1973, pp 681–699
7. Cosimi AB, Brunstetter FH, Kemmerer WT, Miller BN: Cellular immune competence of breast cancer patients receiving radiotherapy. *Arch Surg* 107:531–535, 1973
8. Thomas JW, Coy P, Lewis HS, Yuen A: Effect of therapeutic irradiation on lymphocyte transformation in lung cancer. *Cancer* 27:1046–1050, 1971
9. Ghossein NA, Bosworth JL, Bases RE: The effect of radical radiotherapy on delayed hypersensitivity and the inflammatory response. *Cancer* 35:1616–1620, 1975
10. Clement JA, Kramer S: Immunocompetence in patients with solid tumors undergoing cobalt 60 irradiation. *Cancer* 34:193–196, 1974
11. Gross L, Manfredi OL, Protos A: Effect of cobalt 60 irradiation upon cell-mediated immunity. *Radiology* 106:653–655, 1973
12. Morton DL: Cancer immunotherapy: an overview. *Semin Oncology* 1:297–310, 1974
13. Morton DL, Eilber FR, Holmes EC, Hunt JS, Ketcham AS, Silverstein MJ, Sparks FC: BCG

immunotherapy of melanoma: summary of seven year experience. *Ann Surg* 180:635–643, 1974

14. Gutterman JU, Mavligit G, Gottleib JA: Chemoimmunotherapy of disseminated malignant melanoma with dimethyl triazeno imidazole carboxomide (DTIC) and *Bacillus Calmette-Guerin*. *N Engl J Med* 291:592–597, 1974
15. Donaldson RC: Methotrexate plus *Bacillus Calmette-Guerin* (BCG) and isoniazid in the treatment of cancer of the head and neck. *Am J Surg* 124:527–534, 1972
16. Donaldson RC: Chemoimmunotherapy for cancer of the head and neck. *Am J Surg* 126:507–512, 1973
17. Bleumink E, Nater JP, Koops HS, Tite TH: A standard method for DNCB sensitization testing in patients with neoplasms. *Cancer* 33:911–915, 1974
18. Jesse RH, Lindberg RD: Efficacy of combining radiation therapy with surgical procedures in patients with cervical metastasis from squamous cancer of the oropharynx and hypopharynx. *Cancer* 35:1163–1166, 1975

Am J Roentgenol 126:1088–1093, 1976

IMMUNOTHERAPY OF MALIGNANCIES: CURRENT STATUS

FREDERICK R. EILBER,[1] E. CARMACK HOLMES, DONALD L. MORTON, KENNETH P. RAMMING, AND FRANK C. SPARKS

The importance of host resistance against neoplastic cells has been espoused for a long time. Observations of spontaneous regression of tumors and long disease-free intervals in patients otherwise expected to have rapid recurrences have provided credence for this theory [1]. For the immune system to selectively destroy malignant cells, the tumor must contain antigens that are unique and distinct from those on normal cells. Otherwise there would be no stimulus for the immune system to mount response against.

Numerous reports document in vitro evidence for the presence of tumor-associated antigens on malignant cells [2–9]. These antigens have been identified by several different immunologic techniques and were shown to be immunogenic in patients because the in vitro reactions were demonstrated in sera from tumor-bearing patients. Therefore, it would appear that there is an in vivo immunologic response against these antigens.

The clinical question posed as a result of these studies is whether this immune activity could be augmented to achieve a therapeutic destruction of tumor cells.

EXPERIENCE WITH IMMUNOTHERAPY

In Animals

Experiments in animal tumor systems have shown that there are several nonspecific immunostimulating agents that can be used successfully both for immunoprophylaxis and for immunotherapy: BCG [10, 11], MER [12], and *C. parvum* [13–15]. If administered prior to tumor challenge, each of these was effective in preventing the growth of a transplanted tumor in animal systems. They also were effective in destroying growing tumors if directly injected into intracutaneous lesions [16, 17]. Finally, a systemic immunotherapeutic effect was achieved when these immunostimulants were administered at the same time or a limited number of days after tumor cell transplant [17, 18]. The evidence for an immunologic phenomenon comes from the observation that these agents were not effective in the immunosuppressed host [11]. However, it must be emphasized that the presently available methods of immunoprophylaxis and immunotherapy have a finite therapeutic effectiveness. Most investigators believe that the limit is 10^7 or 10^8 tumor cells [19, 20]. In immunoprophylaxis, immunity can be overcome by increasing the dosage of challenging tumor cells, and in the therapy situation either by increasing the dosage or delaying the onset of immunotherapy following cell challenge [18].

In Man

The original trials of immunotherapy for human malignancies consisted of administration by local injection of nonspecific immunologic adjuvants in patients who had disseminated disease. The first report by Morton et al [21] described results in patients treated by direct injection of BCG for intracutaneous and subcutaneous deposits of metastatic malignant melanoma. A recent report [22] summarized further results and showed that approximately 95% of the directly injected intracutaneous lesions regressed, indicating that BCG had

These investigations were supported by U.S. Public Health Service grants CA12582 and contract NIH0732001 CB43852 and Surgical Services, Sepulveda Veterans Administration Hospital.

[1] All authors: Division of Oncology, Department of Surgery, UCLA Center for the Health Sciences, Los Angeles, California 90024, and Surgical Services, Sepulveda Veterans Administration Hospital, Sepulveda, California 91343. Address reprint requests to Division of Oncology.

a remarkable local effect. This effect appeared to be an immunologic one because it did not occur in patients who did not have a positive reaction to the PPD skin test or who could not demonstrate a nonspecific immunologic reaction to DNCB. A systemic reactivity was suggested by the observation that approximately 20% of the patients had regression of noninjected lesions. These results have been confirmed by several other investigators [23–25] and appear to be a reproducible phenomenon.

However, the results in patients who had direct injection of subcutaneous nodules were not nearly as good. In this group only about 10% of lesions regressed or were controlled. More important, there was no regression of noninjected lesions [22]. This response could be related to poor infiltration of the tumor as well as to the large bulk of tumor cells present at the time of immunologic therapy.

The phenomenon of regression of directly injected intracutaneous lesions is not peculiar to malignant melanoma. There have been several reports of excellent control of chest wall recurrent carcinoma of the breast [26] and of multiple basal cell carcinomas [27]. Thus it appears that BCG and other nonspecific immunostimulants are effective when injected directly into intracutaneous tumors even in patients with disseminated disease.

SYSTEMIC EFFECT OF IMMUNOLOGIC STIMULANTS

Since BCG appeared to be locally effective for disseminated disease, the next question concerned whether it might be active as a systemic adjuvant following surgical resection for widespread disease. In 1971, a pilot study was begun at UCLA to determine the feasibility of such treatment for malignant melanoma.

Forty-four patients with disseminated melanoma underwent surgical resection of all gross tumor. At 3–6 weeks after the resection, weekly immunizations were begun with BCG (Tice strain) for 3 months followed by biweekly intervals for 1 year

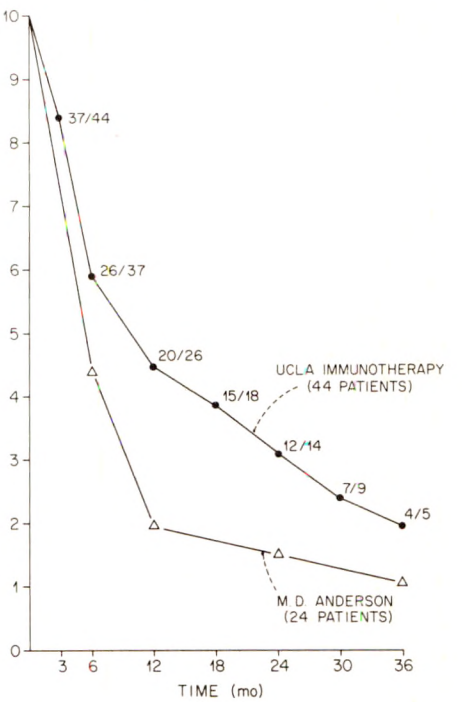


FIG. 1.—Recurrence rate in patients with stage III melanoma. Vertical axis = cumulative percentage of patients free of disease; horizontal axis = time from operative procedure.

[22]. Results showed a difference at all points of analysis in both recurrence (fig. 1) and survival (fig. 2) for patients treated with surgical resection and adjuvant immunotherapy compared to patients treated by surgery alone. However, these results were not statistically significant. Therefore, although some clinical improvement was observed, it was minimal.

A recent report from M.D. Anderson Hospital [28] indicated a slight improvement in survival for patients with disseminated malignant melanoma who were treated with chemotherapy and adjuvant BCG immunotherapy. In a similar chemotherapy trial, Israel [29, 30] reported dramatically improved response to chemotherapy in patients with oat cell carcinoma of the lung treated with *C. parvum* immunotherapy. While the reason for these results is unclear, Israel has hypothesized that immunotherapy decreased marrow toxicity

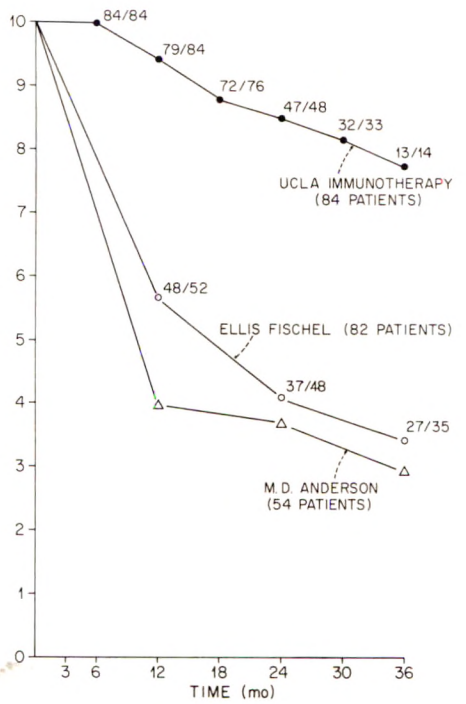


FIG. 2.—Survival rate of patients with stage II melanoma. Vertical axis = cumulative percentage of patients alive; horizontal axis = time following operative procedure.

so that an increased amount of chemotherapy could be administered.

ADJUVANT IMMUNOTHERAPY IN MORE LOCALIZED DISEASE

As a result of the animal studies and the pilot immunotherapy experience in human malignant disease, investigators concluded that although immunotherapy could be administered with relatively minimal toxicity [31], it had limited therapeutic potential for treatment of disseminated malignancy when combined with surgical therapy. Therefore, they reasoned that a greater therapeutic benefit might be realized if adjuvant immunotherapy were administered in a more favorable clinical situation, that is, in patients with a smaller amount of residual subclinical disease.

Thus another pilot study was designed using adjuvant immunotherapy in patients with malignant melanoma metastatic to regional lymph nodes. Since this group of patients had an 80% chance of developing recurrent disseminated disease within 2 years of surgery, it was assumed that subclinical residual disease was present following surgery [32]. A total of 118 patients with pathologically proven metastasis to regional nodes were studied: 34 were treated by lymphadenectomy alone and 84 with the identical surgical procedures plus adjuvant immunotherapy. Again, Tice strain BCG was administered intradermally every week for 3 months and biweekly thereafter.

The results of this trial showed a decreased recurrence rate (fig. 3) and an improved survival (fig. 4) in patients treated with adjuvant immunotherapy compared to a nonrandomized control group treated by surgery alone. Statistical analysis showed no differences in response in the two groups using the criteria of age, sex, number of nodes involved, or anatomic location of the primary tumor. However,

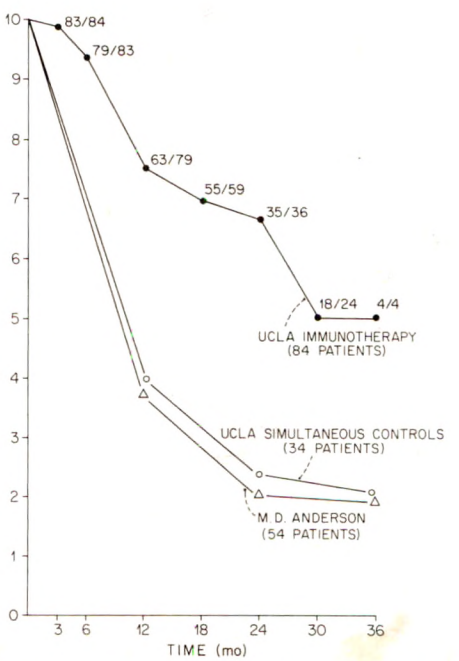


FIG. 3.—Recurrence rate in patients with stage II melanoma according to number of regional nodes involved. Vertical axis = cumulative percentage of patients free of disease; horizontal axis = time following operative procedure.

when time to recurrence was analyzed (up to 30 months), a statistical difference was observed between the control and treatment group at all points of analysis. Whereas half of the control group had recurrent disease at 6 months, half of the treatment group have still not had a recurrence. A therapeutic effect was demonstrated even in patients who had a recurrence. When nonrecurrent patients were excluded, 50% of the control patients' disease recurred by 4 months, whereas the 50% recurrence interval was prolonged to 11 months in the group treated with adjuvant immunotherapy.

Further segregation of these stage II melanoma patients according to the number of regional nodes involved indicated the importance of the amount of residual tumor burden. Although a statistical improvement was observed in patients treated with adjuvant immunotherapy, regardless of the number of involved nodes, the most favorable group had only one node involved. While 85% of these patients are free of disease, only 35% of patients with five or more nodes involved are free of disease. There was no correlation between recurrence and the number of involved nodes in the group treated with surgery alone, which emphasizes the high incidence of subclinical residual disease even in patients with metastasis to only one regional lymph node.

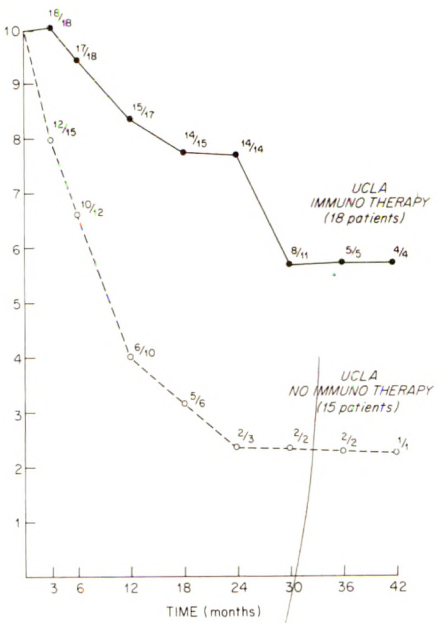


FIG. 5.—Recurrence rate in patients with stage I and II soft tissue sarcomas. Horizontal axis = time to recurrence; vertical axis = cumulative percentage of patients free of disease by life table analysis.

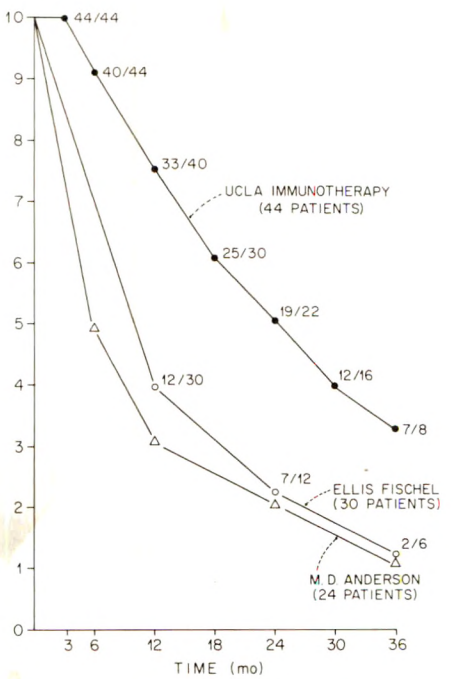


FIG. 4.—Survival rate of patients with stage III melanoma. Vertical axis = cumulative percentage of patients alive; horizontal axis = time from operative procedure.

The systemic effectiveness of nontumor-specific adjuvant immunotherapy for other histologic types of malignancy has also been demonstrated. Of patients with localized soft tissue sarcoma treated by surgery alone, 80% developed recurrent disseminated disease within 2 years of operation (fig. 5). However, analysis of patients with soft tissue tumors treated by surgery and adjuvant BCG immunotherapy showed 60% free of disease at 2 years. Again, the group of patients with the least number of failures were those with stage I or primary tumors.

SUMMARY

The results of various in vitro analyses indicate there is an active immune response against antigens associated with human malignancies. This immune response apparently can be augmented by nonspecific immunologic stimulants such as BCG. These agents are effective for destroying tumor when injected locally into intracutaneous disease but are not as effective for subcutaneous disease. Preliminary clinical trials indicated that immune stimulants are effective when administered systemically. The effect is only minimal for disseminated disease, but the therapeutic benefit is clearly augmented for patients with a minimal residual tumor burden, such as those patients with metastases to regional lymph nodes. Thus immunotherapy is a systemically active mode of therapy. Its toxicity is minimal, and it appears to be effective in a wide spectrum of the disease. However, immunotherapy is not effective for a large residual tumor burden; consequently it must be used in combination with other modes of treatment such as irradiation therapy or chemotherapy.

Early experiences with BCG immunotherapy for malignant melanoma and *C. parvum* for oat cell carcinoma are encouraging. It is remarkable that a nonspecific immunologic stimulant does, in fact, have this effect. Immunotherapy experiments in animals suggest that in order to achieve maximal benefit, BCG must have close contact with tumor cells or must be combined with a tumor-associated antigen. If these principles are true for man, it would seem that improvements for nonspecific immunotherapy in human neoplasms would be further augmented if a tumor-related antigen could be extracted from human tumors and combined with a nonspecific immunologic stimulant.

REFERENCES

1. Everson TC, Cole WH: *Spontaneous Regression of Cancer*. Philadelphia, Saunders, 1966
2. Morton DL, Malmgren RA: Human osteosarcomas: immunologic evidence suggesting an associated infectious agent. *Science* 162:1279–1281, 1968
3. Lewis MG, Ikonopisov RL, Nairn RC, Phillips TM, Fairley GH, Bodenham DC, Alexander P: Tumor-specific antibodies in human malignant melanoma and their relationship to the extent of the disease. *Br Med J* 1:547–562, 1969
4. Morton DL, Eilber FR, Malmgren RA: Immunologic factors in malignant melanomas, skeletal and soft tissue sarcomas of man. *Oncology* 1:242–255, 1970
5. Hellstrom I, Sjogren HO, Warner G, Hellstrom KE: Blocking of cell-mediated tumor immunity by sera from patients with growing neoplasms. *Int J Cancer* 7:226–237, 1971
6. Priori ES, Wilbur JH, Dmochowski L: Immunofluorescence tests on sera of patients with osteosarcoma. *J Natl Cancer Inst* 46:1299–1308, 1971
7. Wood WC, Morton DL: Microcytotoxicity tests: detection of antibody in sarcoma patients cytotoxic to human sarcoma cells. *Science* 170:1318–1320, 1970
8. Cohen AM, Ketcham AS, Morton DL: Tumor-specific cellular cytotoxicity to human sarcomas: evidence for a cell-mediated host immune response to a common sarcoma cell-surface antigen. *J Natl Cancer Inst* 50:585–589, 1973
9. Marsh B, Flynn L, Enneking W: Immunologic aspects of osteosarcoma and their application to therapy. *J Bone Joint Surg [Am]* 54A:1367–1397, 1972
10. Brispen R: BCG vaccine in perspective. *Semin Oncology* 1:311–317, 1974
11. Bast RC, Zbar B, Borsos T, Rapp HJ: BCG and cancer. *N Eng J Med* 290:1413–1420, 1458–1470, 1974
12. Weiss DW: Nonspecific stimulation and modulation of the immune response and of states of resistance by the MER fraction of tubercle bacilli. *Natl Cancer Inst Monogr* 35:157–171, 1972
13. Scott MT: *Corynebacterium parvum* as an immunotherapeutic anti-cancer agent. *Semin Oncology* 1:367–378, 1974
14. Howard TG, Christie GH, Scott MT: Biologic effects of *Corynebacterium parvum*. IV. Adjuvant and inhibition activities on "B" lymphocytes. *Cell Immunol* 7:290–301, 1973
15. Milas L, Hunter N, Withers HR: Combination of local irradiation with systemic application of anaerobic *Corynebacteria* in therapy of a murine fibrosarcoma. *Cancer Res* 35:1274–1277, 1975
16. Zbar B, Tanaka T: Immunotherapy of cancer: regression of tumors after intralesional injection of living *Mycobacterium bovis*. *Science* 172:271–273, 1971
17. Kronman BS, Wepsic HT, Churchill WH, Zbar B, Borsos T, Rapp HJ: Immunotherapy of cancer: an experimental model in syngeneic guinea pigs. *Science* 168:257–259, 1970
18. Eilber FR, Holmes EC, Morton DL: Immuno-

therapy experiments with a methylcholanthrene-induced guinea pig liposarcoma. *J Natl Cancer Inst* 46:803–808, 1971
19. Morton DL: Immunotherapy of cancer: present status and future potential. *Cancer* 30:1647–1655, 1972
20. Baldwin RW, Pimm MV: BCG immunotherapy. *Br J Cancer* 27:48–54, 1973
21. Morton DL, Eilber FR, Malmgren RA, Wood WC: Immunological factors which influence response to immunotherapy in malignant melanoma. *Surgery* 68:158, 1970
22. Morton DL, Eilber FR, Holmes EC, Hunt JS, Ketcham AS, Silverstein MJ, Sparks FC: BCG immunotherapy of malignant melanoma: summary of a seven-year experience. *Ann Surg* 180: 635–643, 1974
23. Nathanson L: Regression of intradermal malignant melanoma after intralesional injection of BCG. *Cancer Chemother Rep* 56:659–665, 1972
24. Nathanson L: Use of BCG in the treatment of human neoplasms: a review. *Semin Oncology* 1: 337–350, 1974
25. Pinsky C, Hisschant G, Oettgen H: Treatment of malignant melanoma by intralesional injections of BCG. *Proc Am Assoc Cancer Res* 13:21, 1972
26. Rosenberg E, Powell R: Active tumor immunotherapy with BCG. *South Med J* 66:1359–1363, 1973
27. Klein E: Immunotherapeutic approaches to the management of neoplasms. *Natl Cancer Inst Monogr* 35:379–402, 1972
28. Gutterman JU, Mavligit G, Gottlieb J, Burgess MA, McBride CE, Einhorn L, Freireich EJ, Hersh EM: Chemo-immunotherapy of disseminated malignant melanoma with dimethyl triazeno imidazole carboxamide (DTIC) and *Bacillus Calmette-Guerin* (BCG). *N Eng J Med* 291: 592–597, 1974
29. Israel L: Preliminary results of non-specific immunotherapy for lung cancer. *Cancer Chemother Rep* 4, suppl.:283–286, 1973
30. Israel L, Edelstein R: Non-specific immunostimulation with *Corynebacterium parvum* in human cancer, in *Proceedings 26th Annual M. D. Anderson Symposium on Fundamental Cancer Research*, Chicago, Year Book Medical Publishers, 1973
31. Sparks FC, Silverstein MJ, Hunt JS, Haskell CM, Pilch YH, Morton DL: Complications of BCG immunotherapy in patients with cancer. *N Eng J Med* 289:827–830, 1973
32. Gutterman JU: Active immunotherapy with BCG for recurrent malignant melanoma. *Lancet* 1:1208, 1973

AMERICAN ROENTGEN RAY SOCIETY

OFFICERS 1975–76

President: Ted F. Leigh.
President Elect: Seymour F. Ochsner.
1st Vice President: Edward B. Singleton.
2nd Vice President: Sidney W. Nelson.
Secretary: James F. Martin.
Treasurer: Joseph D. Calhoun.
Honorary President: C. L. Sherratt.

COMMITTEES 1975–76

Executive Council: T. F. Leigh, S. F. Ochsner, E. B. Singleton, J. F. Martin, J. D. Calhoun, M. M. Figley, T. Leucutia, H. C. Carlson, R. C. Pfister, R. A. Gagliardi, M. P. Capp, E. Gedgaudas, G. A. Kling, C. B. Holman, W. B. Seaman, E. C. Klatte, J. P. Tampas, J. L. Gwinn, C. E. Bickham, H. L. Friedell, Chairman.

Finance and Budget Committee: J. J. Stein, C. E. Bickham, R. McLelland, J. L. Gwinn, H. C. Carlson, Chairman.

Publication Committee: E. R. Heitzman, J. V. Rogers, K. Ellis, F. F. Ruzicka, Jr., R. A. Gagliardi, Chairman.

Editorial Policy Committee: M. M. Figley, E. F. Lang, L. W. Brady, K. L. Krabbenhoft, R. H. Morgan, E. R. Heitzman, J. V. Rogers, K. Ellis, F. F. Ruzicka, R. A. Gagliardi, Chairman.

Program Committee: T. F. Leigh, J. F. Martin, H. L. Friedell, M. M. Figley, R. A. Gagliardi, R. C. Pfister, E. Gedgaudas, G. A. Kling, M. P. Capp, S. F. Ochsner, Chairman.

Advisory Committee on Education and Research: G. W. Hartman, L. F. Rogers, E. Gedgaudas, A. E. James, M. P. Capp, Chairman.

Scientific Exhibits Committee: B. G. Brogdon, R. J. Alfidi, R. C. Pfister, Chairman.

Instruction Courses: Director, E. Gedgaudas, Associate Director, H. O. Peterson.

Representatives on the American Board of Radiology: R. W. McConnell, J. F. Roach, S. W. Nelson.

Representative on the Board of Chancellors and Council of the American College of Radiology: W. B. Seaman.

ANNUAL MEETING: September 20–24, 1976, Washington, D. C., Washington Hilton Hotel.

SCIENTIFIC PROGRAM: Seymour Ochsner, *President Elect*, Ochsner Clinic, New Orleans, La.

MANAGER ANNUAL MEETING: George A. Kling, Harper Hospital, Detroit, Mich.

MEMBERSHIP: Hymer Friedell, Chairman, Executive Council,
Case Western Reserve University, Cleveland, Ohio 44106.

BUSINESS OFFICE: Keith W. Gundlach, Comptroller, American College of Radiology,
20 North Wacker Drive, Chicago, Illinois 60606.

AMERICAN RADIUM SOCIETY

OFFICERS: 1975–76

President: Felix N. Rutledge.
President Elect: Luther W. Brady.
1st Vice President: Elliott Strong.
2nd Vice President: Alfred Sherman.
Secretary: Richard H. Jesse.
Treasurer: Fred W. George, III.

COMMITTEES 1975–76

Executive Committee: V. A. Marcial, F. N. Rutledge, L. W. Brady, E. Strong, R. H. Jesse, A. I. Sherman, F. George, A. Raventos, Chairman.

Public Relations Committee: W. J. Taylor, R. G. Parker, W. G. Cosbie, J. M. W. Gibson, Chairman.

Publication Committee: K. L. Krabbenhoft, A. F. Schroeder, L. W. Brady, Chairman.

Scientific Program Committee: L. W. Brady, D. Johnson, A. S. Ketcham, F. N. Rutledge, Chairman.

Janeway Lecture Committee: A. S. Ketcham, S. H. Levitt, L. W. Brady, Chairman.

Local Arrangements Committee: J. M. W. Gibson, Chairman.

Representatives on the American Board of Radiology: J. J. Stein, E. Richard King, R. M. Scott.

Representative on the Board of Chancellors of the American College of Radiology: J. A. del Regato.

Liaison Representative on the National Council on Radiation Protection and Measurements: Lawrence W. Davis.

ANNUAL MEETING: May 9–14, 1976, Vancouver, British Columbia, Bayshore Inn.

SCIENTIFIC PROGRAM: Felix N. Rutledge, *President*, Houston, Texas

LOCAL ARRANGEMENTS: John M. W. Gibson, Vancouver, British Columbia

MEMBERSHIP: Richard H. Jesse, *Secretary*, M. D. Anderson Hospital and Tumor Institute,
Houston, Texas 77025.

BUSINESS OFFICE: Richard H. Jesse, 6723 Bertner Avenue, M.D. Anderson Hospital and Tumor Institute,
Houston, Texas 77025.

EDITORIAL

CT AND THE PLANNERS

Radiologists considering the acquisition of computed tomography (CT) units for hospital installation have learned the necessity for obtaining approval from a designated planning organization. These organizations derive their authority from various local, state, or federal laws. The federal legislation concerning health planning is found in the Social Security Act, section 1122, the purpose of which is to assure that federal funds are not used to support unnecessary capital expenditures for health care facilities. Under this section, each state must have a designated planning agency to review all capital proposals and submit recommendations to the secretary of the Department of Health, Education, and Welfare. The law further authorizes the secretary to withhold reimbursement from institutions that fail to file the required Statement of Need for services provided patients sponsored under Maternal and Child Health legislation and Medicare programs of the Social Security Act. The criteria which the designated planning agency uses in evaluating proposals include (1) the current or projected community need for health services, (2) the prospect of adequate staffing and operation, (3) economic feasibility, and (4) cost containment through productivity.

Unlike the authors of the legislation, many in the medical profession believe that cost control as a primary goal is inappropriate. However, the law exists, and short of unlikely legislation to alter it, we must live within its framework.

For most radiologists, the impact of this legislation was minimal until the arrival of CT scanners because the federal law concerns itself with capital expenditures over $100,000. But as CT prices are well in excess of this figure, approval of planning bodies is a requirement for acquisition of this equipment in the hospital setting.

There are a number of reasons why planning agencies are concerned about CT. The substantial capitalization cost for the equipment will be reflected in the growing cost of health care for this nation, now approximately 7% of the gross national product. In addition to capitalization expense, the individual fees for CT which have been established thus far will result in a significant increase in annual medical care costs. The planners are understandably seeking evidence of cost effectiveness of CT in eliminating other diagnostic studies or reducing hospitalization expense. They are also concerned that present units will be outmoded quickly, requiring replacement or expensive modification.

In many communities, planning organizations have been able to develop workable criteria and guidelines for acquisition of CT brain scanners but have discovered that similar criteria and guidelines for whole-body CT are very elusive. In some areas the restrictive conditions being imposed by health planners on hospital acquisition have paradoxically resulted in the rapid expansion of CT installations in private offices.

There are significant dangers to the radiologic community, the public, the industrial complex, and, indeed, to the entire medical community in misguided actions—or inaction—by the planners. These dangers include:

1. An invitation to legislate planning authority over the nonhospital practice of medicine. Currently, the only leverage which planners have is to influence the Blues and Medicare to refuse reimburse-

ment for potentially covered patients in the private office; but it has not escaped their attention that this situation could be altered by extending their authority to equipment purchases in the nonhospital environment.

2. Further invasion of medical practice by government. At least one planning organization has suggested that equipment acquisition should be restricted until the diagnostic value and potential of the equipment are better known. Moreover, it suggests planners should concern themselves with setting priorities by type of patient, disease entity, and physician specialty in use of the equipment.

3. Review of radiologic research by planning organizations. If the radiological community is unable to scientifically justify the efficacy of CT, particularly in the whole-body area, it has occurred to some planners that they might fill this void. A recent draft of criteria and guidelines from one planning agency contained provisions for whole-body scanning, including development of hypotheses, research design, statistical procedures to be used, and willingness of the applicant to release test results to the planning agency. It also proposed the requirement for performance of comparative analyses between CT and traditional diagnostic procedures, with the planning body assuming authority to review the medical research.

4. A potentially inferior level of patient care. With newer generations of CT scanners purported to be more efficaceous clinically, some radiologists consider themselves prudent in waiting to evaluate the emergence of newer generations of scanners. Yet while their investigation is underway, other, less conservative hospitals in the community may receive the necessary certification of need and potentially deny acquisition of future, improved units in that community.

5. Reduction in research and development funds by industry. The enthusiasm of industry to continue funding development may be dampened by market restriction as the planning organizations and the federal government overreact to the current intensity of purchase efforts. The general enthusiasm for CT by the medical profession has fostered fierce competition among the commercial companies, with several announcing great claims for the future in order to gain their share of the market. Whereas competition could cause a reduction in the cost of CT units, market restriction will produce the opposite result, since manufacturers will be forced to amortize their very high development costs over a smaller number of units.

There is a compelling need, then, for the medical profession to actively engage in seeking ways to prevent these dangers from being translated into devastating laws and regulations that will affect not only the radiological community but potentially all of medicine. I presume to offer a few suggestions which, considering the alternatives, are worthy of thought, modification, and attempted implementation, depending on the specific community setting.

Drastic reduction in fees for CT are imperative. Most of us who purchased the initial CT units established fees which, judged in retrospect, seem entirely too high. We were concerned about amortization of our very expensive equipment and the maintenance of financial credibility with our hospital boards. At the time, we had no concept of the number of patients who might be studied and the impact of large patient volume on lower individual costs to patients. And we correctly expected additional expenses (e.g., higher matrices, archival magnetic tape systems, remote viewers, and, more recently, redesign of early units).

Despite these concerns, experience has proven that CT, at least of the head, is an exceedingly profitable undertaking. The result, almost unprecedented in the history of radiology, is that corporations and partnerships for profit are springing up around the country, commonly composed of neurologists, neurosurgeons, perhaps radiologists, and other interested investors,

for the purchase and operation of CT units in outpatient settings. These arrangements have significant advantages to the investor who can expect substantial depreciation to reduce taxable income and gain a significant return on investment. One is tempted to make analogies between these situations and those of doctors owning drugstores or engaging in fee splitting with the referring physician. This level of profit has not gone unnoticed by commercial manufacturers who can calculate the large profits and are at least tempted, if not persuaded, to price their equipment, accessories, and modifications at a level where they will share in the "retail" profit.

In my opinion, the only remedy to correct these temptations and put CT in proper perspective in the health care area is a realistic reappraisal of fees. This seems especially important in the initial phase of body scanning where the medical efficacy of CT has yet to be established. Lower fees might also dampen the enthusiasm of those who wish to enter the field primarily for economic reasons.

A second possible solution is the development of community coordination of procurement so that all authorized units would not be of the same vintage. A "sequential certification" procedure might be invoked which would authorize purchase of a succession of CT units staggered over 2–3 years. Under this mechanism, radiologists in hospitals could obtain authorization for purchase which then could be implemented at a later date, allowing them opportunity to appraise and investigate newer generations of units without being penalized.

A third approach is the radiation center concept in which there would be multiinstitutional capital investment and interhospital staff participation in the operation of a centralized CT unit or units. There are a number of obvious disadvantages of this concept. Aside from hurt of personal pride of a particular institution that would not have sole propriety, a primary medical reason against the centralized concept would be the inability of some patients to be transported to the facility because of their medical condition. However, it should not be difficult to justify location of a satellite unit in a particular hospital if it has a sufficient number of seriously ill patients requiring CT. This might be the equivalent of the several types of radiation therapy centers we know today, some primarily designed for definitive therapy and others for palliation, each requiring different physical equipment and personnel support.

The alternative to such suggestions is to leave things alone and take a chance that local, state, and federal planners will be omniscient and make the proper decisions for us. In doing so, the risk is that patients, individual radiologists, hospitals, the industrial community—indeed the entire free medical enterprise system—might be denied the full potential of this magnificent technical achievement. Radiologists must take initiatives both locally and nationally to assure that wisdom, including personal fee restraint, prevails as this exciting new era in medicine takes shape.

THOMAS F. MEANEY
Cleveland Clinic
Cleveland, Ohio 44106

Editor's Note: The Journal would welcome responses to this and other statements and will initiate a Letters to the Editor section if there is sufficient interest.

NEWS ITEMS

DIAGNOSTIC ULTRASOUND IN GASTROENTEROLOGY AND UROLOGY

A symposium on Diagnostic Ultrasound in Gastroenterology and Urology is slated for September 9–10 at Johns Hopkins Hospital, Baltimore.

Sponsored by the radiology, gastroenterology, and urology departments at Johns Hopkins, the program is designed for the practicing ultrasonographer, gastroenterologist, and urologist. In-depth coverage of applications of diagnostic ultrasound will be provided. The fee is $150, $100 for residents and technicians.

For additional information, write to Dr. Janet B. Hardy, Department of Continuing Education, Room 17, Johns Hopkins University School of Medicine, 720 Rutland Avenue, Baltimore, Maryland 21205.

PARTICLES AND RADIATION THERAPY CONFERENCE

Recent developments in the use of neutrons and charged particles in cancer therapy will be the subject of an international conference. Entitled "Particles and Radiation Therapy (Part II), the conference will be held September 15–17, 1976 at the University of California, Berkeley.

The conference is sponsored by the American College of Radiology and funded by the National Cancer Institute Division of Cancer Research Resources and Centers. Category I continuing education credit is available. Registration fee is $100, and attendance is limited to 400.

Clinicians, biologists, physicists, and nuclear engineers will discuss the advantages and problems involved in the clinical applications of pions, protons and heavy ions, and neutrons. The agenda also will cover other aspects of particle use, including diagnosis and economic factors.

For additional information, contact Dr. William E. Powers, Chairman, Part 2 Conference, American College of Radiology, 130 South 9th Street, Philadelphia, Pennsylvania 19107.

GASTROINTESTINAL RADIOLOGY

A 3-day postgraduate course in gastrointestinal radiology sponsored by the Society of Gastrointestinal Radiologists will be held in Bermuda on September 16–19. The course will be offered in conjunction with the society's 1976 meeting at the Princess Hamilton Hotel. Registration fee is $175.

For more information, contact Dr. Sidney Nelson, 4615 139th Street SE, Bellevue, Washington 98006.

CANCER RESEARCH AND CLINICAL INVESTIGATION

A National Conference on Cancer Research and Clinical Investigation sponsored by the American Cancer Society and the National Cancer Institute will be held September 20–22 at the Chase-Park Plaza Hotel in St. Louis. (Previously the conference location had been announced as Atlanta, Georgia.)

Purpose of the conference is to present important developments in basic cancer research and to demonstrate the relationship of that work to clinical investigation. Sessions are open to all members and students of the medical and dental professions. The conference meets the criteria for credit by the American Medical Association, the American Academy of Family Physicians, and the American Osteopathic Association.

Additional information is available from Dr. Sidney L. Arje, American Cancer Society, 777 Third Avenue, New York, New York 10017.

RADIATION-ASSOCIATED THYROID CANCER

A conference and workshop on radiation-associated thyroid cancer is scheduled for September 30 and October 1, 1976, at the

Center for Continuing Education of the University of Chicago. The purpose is to analyze available data on the association between x-ray and cancer; to analyze the biologic significance of the tumors; to discuss patient finding, diagnosis, treatment; and to offer recommended approaches to the problem.

Among topics to be discussed are: clinical staging and pathological classification of thyroid neoplasms; clinical course of radiation-associated cancers; incidence of tumors with and without radiation; pathology of radiated thyroids; relation of radiation dose to incidence; publicity, screening programs, costs; thyroid scans, blood tests, and biopsy; criteria for surgery and type of surgery; thyroid suppression; and other radiation hazards.

Individuals who have critical data or analyses related to any of the topic areas are invited to submit presentations, providing titles and a paragraph summary.

A U.S. Public Health Service grant will provide limited funds for travel awards to U.S. or foreign participants who could not otherwise attend.

For more information contact Dr. Leslie J. DeGroot, Thyroid Study Unit, Department of Medicine, University of Chicago, 950 East 59th Street, Chicago, Illinois 60637.



SOCIETY PROCEEDINGS

MEETINGS OF RADIOLOGICAL SOCIETIES*

United States of America

American Roentgen Ray Society
Secretary, Dr. James Franklin Martin, 300 S. Hawthorne Rd., Winston-Salem, N. C. 27103. Annual Meeting: Washington Hilton, Washington, D. C., Sept. 20–24, 1976.

American Radium Society
Secretary, Richard H. Jesse, Dept. of Surgery, M. D. Anderson Hosp. and Tumor Institute, Houston, Tex. 77025.

Radiological Society of North America
Secretary, Dr. Theodore A. Tristan, Harrisburg, Pennsylvania.

American College of Radiology
Executive Director, William C. Stronach, 20 N. Wacker Drive, Chicago, Ill. 60606.

Section on Radiology, American Medical Association
Secretary, Dr. Antolin Raventos, Davis, Calif.

American Board of Radiology
Secretary, Dr. C. Allen Good. Correspondence should be directed to Kahler East, Rochester, Minn. 55901.
Oral examinations will be held: Marriott Motor Hotel, Chicago, Ill., June 14–19, 1976; Sheraton Biltmore, Atlanta, Ga., Dec. 6–11, 1976.
Written examinations will be held in 14 selected sites on June 26, 1976.
Applications must be received in the Board Office before Sept. 30 of the year preceding the one in which the candidate wishes to be examined.

American Board of Nuclear Medicine, Inc. A Conjoint Board of the American Boards of Internal Medicine, Pathology and Radiology and sponsored by the Society of Nuclear Medicine.
Application forms and further information are available from the American Board of Nuclear Medicine, 305 E. 45th St., New York, N. Y. 10017.

American Association of Physicists in Medicine
Secretary, Dr. Robert G. Waggener, Dept. Radiol., Univ. Tex. Health Sciences Center, San Antonio, Tex. 78284
Annual Meeting: Cincinnati, Ohio, July 31–Aug. 4, 1977.

American Society of Therapeutic Radiologists
Secretary, Dr. Robert W. Edland, 1836 South Ave., La Crosse, Wis., 54601. Annual Meeting:

American Nuclear Society
Program Chairman, Werner K. Kern, IRD, Space Nuclear Systems, F 309, U. S. Atomic Energy Commission, Washington, D.C. 20545.

American Institute of Ultrasound in Medicine
Secretary, John M. Reid, Ph.D., 556 18th Ave., Seattle, Wash. 98122. Annual Meeting.

American Society of Neuroradiology
Secretary, Arthur E. Rosenbaum, University of Pittsburgh, Pittsburgh, Pa. 15261.

Fourteenth International Congress of Radiology
Rio de Janeiro, Brazil, Oct. 23–29, 1977.
President Elect: Prof. Dr. Nicola C. Caminha; *General Secretary:* Dr. Durval Couto. Av. Churchill, 97-50 and-LC-39 20,000 Rio de Janeiro, Brazil.

International Society of Radiology
Hon. Secretary-Treasurer, Prof. W. A. Fuchs, M.D., Department of Diagnostic Radiology, University Hospital, Inselspital, CH-3010 Bern, Switzerland.

Twelfth Inter-American Congress of Radiology
President, Dr. Publio Vargas Pazzos, Casilla 5227, Guayaquil, Ecuador. Meeting in Quito, Ecuador, 1979.

Inter-American College of Radiology
President, Manuel Viamonte, Jr., M.D., Mt. Sinai Medical Center, 4300 Alton Rd., Miami Beach, Fla. 33140.
Secretary, Gaston Morillo, M.D., Jackson Memorial Hosp., 1700 N.W. 10th Ave., Miami, Fla. 33152.
Counselor for the United States, J. A. del Regato, M.D., Univ. of So. Fla. College of Medicine, 13000 No. 30th St., Tampa, Fla. 33612.

Third Congress of the European Association of Radiology
Secretary-General, P.O. Box 14, 79 Lauriston Place, Edinburgh BHI IDB, Scotland.

Second Asian and Oceanian Congress of Radiology
Secretary, Dr. Buenaventura U. V. Angtuaco, Congress Secretariat Headquarters, 2161 Taft Ave., Manila, Philippines. Meeting:

Alabama Chapter of ACR
Secretary-Treasurer, Dr. Lawrence E. Fetterman, 1720 Springhill Ave., Suite 201, Mobile, Ala. 36604. Meets time and place of Alabama State Medical Association.

Alaska Radiological Society, Chapter of ACR
Secretary-Treasurer, Dr. Maurice J. Coyle, 3200 Providence Ave., Anchorage, Alaska 99504.

American Osteopathic College of Radiology
Annual Scientific Meeting: Americana Hotel, Bar Harbor, Fla. Program Administrator: Lawrence J. Jordan, D.O., Suite 21, Ponce American Bldg., 4601 Ponce de Leon Blvd., Coral Gables, Fla. 33146.

American Thermographic Society
Secretary-Treasurer, John Wallace, Ph.D., Dept. Radiol., Thomas Jefferson Univ. Hosp., Philadelphia, Pa. 19107. Annual Meeting.

Arizona Radiological Society, Chapter of ACR
Secretary, Dr. Irwin M. Freundlich, 1501 N. Campbell Ave., Dept. Radiol., Tucson, 85724. Two regular meetings a year. Annual meeting at time and place of State Medical Association and interim meeting six months later.

Ark-La-Tex Radiological Society
Secretary, Dr. Erich K. Lang, 1541 Kings Highway, Shreveport, La. 71130. Meets monthly on fourth Wednesday, 8:00 P.M., Sept. to May.

Arkansas Chapter of ACR
Secretary-Treasurer, Dr. Richard Seibold, Jr., Wadley Hosp., Texarkana, Ark.—Tex. 75501. Meets twice annually, the Spring Meeting being in conjunction with and at the place of the State Medical Association.

Association of University Radiologists
Secretary-Treasurer, Dr. Arch W. Templeton, Univ. of Kansas Med. Center, 39th and Rainbow Blvd., Kansas City, Kansas 66103. Annual Meeting.

Atlanta Radiological Society
Secretary-Treasurer, Dr. James H. Larose, Dept. Nuclear Med., South Fulton Hosp., East Point, Ga. 30344. Meets on four Thursday evenings during the academic year at a time announced in early September of each year, at various Atlanta restaurants.

*** Secretaries of societies are requested to send timely information promptly to the Editor.**

BAVARIAN-AMERICAN RADIOLOGIC SOCIETY
Secretary, LTC. Marco J. DiBiase, M.D., Radiology Service, Heidelberg, 130 Station Hosp., APO N. Y. 09102. Meets quarterly.

BLOCKLEY RADIOLOGICAL SOCIETY
Secretary-Treasurer, Dr. William H. Green, 616 East 24th St., Chester, Pa. 19013.

BLUEGRASS RADIOLOGICAL SOCIETY
Secretary-Treasurer, Dr. James C. King, Jr., 3313 Overbrook Drive, Lexington, Ky. 40502. The Society meets once each month during the school year.

BRONX RADIOLOGICAL SOCIETY, NEW YORK STATE, CHAPTER ACR
Secretary-Treasurer, Dr. Leon J. Corbin, 1369 Rosendale Ave., Bronx, N. Y. 10472. Meets 4 times a year.

BROOKLYN RADIOLOGICAL SOCIETY
Secretary-Treasurer, Dr. Ralph Brancaccio, 7901 4th Ave., Brooklyn, N. Y. 11209. Meets first Thursday of each month, October through June.

BUFFALO RADIOLOGICAL SOCIETY
Secretary, Dr. George J. Alker, Jr., E. J. Meyer Mem. Hosp., Buffalo, N. Y. 14215. Meets second Monday evening each month, October to May inclusive, at University Club.

CALIFORNIA RADIATION THERAPY ASSOCIATION
Secretary-Treasurer, Dr. Duane J. Gillum, Stanford Medical Center, Stanford, Calif. 94304. Meets semiannually in San Francisco and Los Angeles.

CALIFORNIA RADIOLOGICAL SOCIETY, CALIFORNIA CHAPTER OF ACR
Secretary-Treasurer, Dr. John L. Gwinn, 4650 Sunset Blvd., Los Angeles, Calif. 90027.

CATAWBA VALLEY RADIOLOGICAL SOCIETY
Secretary, Dr. Walter Joe Jacumin, P.O. Box 265, Rutherford College, N. C. 28671. Meets the last Thursday of every month, Holiday Inn, Morganton, N. C. at 7:30 P.M.

CENTRAL NEW YORK RADIOLOGICAL SOCIETY
Secretary-Treasurer, Dr. Alfred Brettner, Auburn Mem. Hosp., Auburn, N. Y. 13021. Meets first Monday each month October through May.

CENTRAL OHIO RADIOLOGICAL SOCIETY
Secretary-Treasurer, Dr. Daniel E. Lewis, 309 East State St., Columbus, Ohio 43215. Meets second Thursday in October, November, January, March, and May at Fort Hayes Hotel, Columbus, Ohio.

CENTRAL TEXAS RADIOLOGY SOCIETY
Secretary-Treasurer Dr. E. Jerome Schoolar, Scott and White Clinic, Temple, Tex. 76501. Meets the fourth Monday of each month at Ponderosa Hotel, Temple, Tex. at 7:00 P.M.

CHICAGO RADIOLOGICAL SOCIETY, DIVISION OF THE ILLINOIS RADIOLOGICAL SOCIETY, CHAPTER OF ACR
Secretary-Treasurer, Dr. Harold J. Lasky, 55 E. Washington St., Suite 1735, Chicago, Ill. 60602. Meets third Thursday of each month, October to April, except December, at the Bismark Hotel, Chicago, Ill.

CLEVELAND RADIOLOGICAL SOCIETY
Secretary-Treasurer, Dr. Charles M. Greenwald, 7007 Powers Blvd., X-Ray Dept., Parma, Ohio 44129. Meetings at 7:00 P.M. on fourth Monday of October, November, January, February, March and fifth Monday of April.

COLORADO RADIOLOGICAL SOCIETY, CHAPTER OF ACR
Secretary, Dr. John Pettigrew, Denver, Colo. Meets third Friday of each month at Denver Athletic Club from September through May.

CONNECTICUT VALLEY RADIOLOGIC SOCIETY
Secretary, Dr. Gerald N. LaPierre, 759 Chestnut St., Springfield, Mass. 01107. Meets in April and October.

DALLAS-FORT WORTH RADIOLOGICAL SOCIETY
Secretary-Treasurer, Dr. Robert R. Burns, 1400 Stemmons Ave., Dallas, Tex. 75208. Meets the 3rd Monday of every month at 6:30 P.M., at the Airport Hotel, Arlington, Tex.

DELAWARE CHAPTER OF ACR
Secretary, Dr. Ekkehard S. Schubert, Wilmington Med. Center, P. O. Box 1951, Wilmington, Del. 19899.

EAST BAY RADIOLOGICAL SOCIETY
Secretary-Treasurer, Dr. Richard H. Culhane, 4 Vista del Mar, Orinda, Calif. 74563. Meets first Thursday each month, Oct. through May, at University Club, Oakland Calif.

EAST TENNESSEE RADIOLOGICAL SOCIETY
Secretary-Treasurer, Dr. George H. Wood, 205 Medical Arts Bldg., Knoxville, Tenn. 37902. Meets in January and September.

FLORIDA RADIOLOGICAL SOCIETY, CHAPTER OF ACR
Secretary. Dr. Paul J. Popovich, 1350 S. Hickory St., Melbourne, Fla. 32901. Meets twice annually, in the spring with the Annual State Society Meeting and in the fall.

FLORIDA WEST COAST RADIOLOGICAL SOCIETY
Secretary-Treasurer, Dr. Herbert Johnson, Davis Blvd., Tampa, Fla. 33606. Meets on 4th Thursday of the months January, March, May, October, and November.

GEORGIA RADIOLOGICAL SOCIETY, CHAPTER OF ACR
Secretary, Dr. E. P. Rasmussen, Piedmont Prof. Bldg., 35 Collier Rd., N.W., Atlanta, Ga. 30309.

GREATER CINCINNATI RADIOLOGICAL SOCIETY
Secretary-Treasurer, Dr. Owen L. Brown, 2421 Auburn Ave., Cincinnati, Ohio 45219.

GREATER KANSAS CITY RADIOLOGICAL SOCIETY
President-Secretary, Dr. Jay I. Rozen, Suite 216, 6400 Prospect, Kansas City, Mo. 64132. Meets 5 times a year.

GREATER LOUISVILLE RADIOLOGICAL SOCIETY
Secretary-Treasurer, Dr. L. D. LeNeave, 315 E. Broadway, Louisville, Ky. 40202. Meets monthly.

GREATER MIAMI RADIOLOGICAL SOCIETY
Secretary, Dr. David C. Hillman, P. O. Box 610544, North Miami, Fla. 33161. Meets monthly, third Wednesday at 8:00 P.M. at various member hospitals, Miami, Fla.

GREATER ST. LOUIS SOCIETY OF RADIOLOGISTS
Secretary-Treasurer, Dr. Donald Callahan, Northland Med. Bldg., Jennings, Mo. 63136.

HAWAII RADIOLOGICAL SOCIETY, CHAPTER OF ACR
Secretary-Treasurer, Dr. Michael J. McCabe, Straub Clinic and Hosp., Honolulu, Hawaii 96813. Meets third Monday of each month at 7:00 P.M.

HEALTH PHYSICS SOCIETY
Secretary, Russell F. Cowing, P.O. Box 156, E. Weymouth, Mass. 02189. Annual Meeting.

HOUSTON RADIOLOGICAL SOCIETY
Secretary, Dr. Neill B. Longley, 6436 Fannin, Suite 601, Houston, Tex. 77025. Meets fourth Monday of each month, except June, July, August and December, at 6:00 P.M., at 103 Jesse H. Jones Library Building, Texas Medical Center, Houston, Tex. 77025.

IDAHO STATE RADIOLOGICAL SOCIETY, CHAPTER OF ACR
Secretary-Treasurer, Dr. John H. Truksa, 1605 Park Ave., Nampa, Id. 83651. Meets in the spring and fall.

ILLINOIS RADIOLOGICAL SOCIETY, INC., CHAPTER OF ACR
Secretary, Dr. Robert D. Dooley, Hinsdale Med. Center, Hinsdale, Ill. 60521. Meets in the spring and fall.

INDIANA ROENTGEN SOCIETY, INC., CHAPTER OF ACR
Secretary, Dr. John A. Knote, Home Hosp., Lafayette, Ind. 47902.

IOWA RADIOLOGICAL SOCIETY, CHAPTER OF ACR
Secretary-Treasurer, Dr. Dale L. Roberson, 1948 First Ave., NE, Cedar Rapids, Iowa 52402. Luncheon and business meeting during annual session of Iowa State Medical Society. The scientific session is held in the autumn.

KANSAS RADIOLOGICAL SOCIETY, CHAPTER OF ACR
Secretary-Treasurer, Dr. Ralph H. Baehr, 310 Medical Arts Bldg., Topeka, Kan. 66604. Meets in spring with State Medical Society and in winter on call.

KENTUCKY CHAPTER OF ACR
Secretary-Treasurer, Dr. Bernard Sams, St. Joseph In-

firmary, 735 Eastern Parkway, Louisville, Ky. 40217. Meets in April and September.

KINGS COUNTY RADIOLOGICAL SOCIETY
Secretary, Dr. Sidney Hendler, 1880 Ocean Ave., Brooklyn 30, N. Y. Meets Kings County Med. Soc. Bldg. monthly on fourth Thursday, October to May, 8:45 P.M.

KNOXVILLE RADIOLOGICAL SOCIETY
Secretary, Dr. Clifford L. Walton, Blount Professional Bldg., Knoxville 20, Tenn. Meetings are held the third Monday of every other month at the University of Tennessee Memorial Research Center and Hospital.

LONG ISLAND RADIOLOGICAL SOCIETY
Secretary, Dr. Harry L. Stein, North Shore Univ. Hosp., 300 Community Dr., Manhasset, N. Y. 11030.

LOS ANGELES RADIOLOGICAL SOCIETY
Secretary, Dr. Arthur F. Schanche, 333 North Prairie Ave., Inglewood, Calif. 90301. Meets second Wednesday of month in September, November, January, April and June at Los Angeles County Medical Association Building, Los Angeles, Calif. Midwinter Radiological Conference. Century Plaza Hotel, Los Angeles, Calif.

LOUISIANA RADIOLOGICAL SOCIETY, CHAPTER OF ACR
Secretary-Treasurer, Dr. Roger H. Tutton, 1514 Jefferson Hwy., New Orleans, La. 70121.

LOUISIANA-TEXAS GULF COAST RADIOLOGICAL SOCIETY
Secretary-Treasurer, Dr. J. Gardiner Bourque, 3155 Stagg Dr., Suite 230, Doctors Bldg., Beaumont, Texas 77701.

MAINE RADIOLOGICAL SOCIETY, CHAPTER OF ACR
Secretary-Treasurer, Dr. Peter E. Giustra, Dept. Radiology, Penobscot Bay Medical Center, Rockland, Maine 04841. Meets in June, September, December and April.

MARYLAND RADIOLOGICAL SOCIETY, CHAPTER OF ACR
Secretary, Dr. David S. O'Brien, Anne Arundel Hosp., Annapolis, Md. 21401.

MASSACHUSETTS RADIOLOGICAL SOCIETY, CHAPTER OF ACR
Secretary, Dr. Joseph T. Ferrucci, Jr., Massachusetts Gen. Hosp., Boston, Mass. 02114.

MEMPHIS ROENTGEN SOCIETY
Secretary-Treasurer, Dr. R. Randolph Ramey, Baptist Memorial Hosp., 899 Madison Ave., Memphis, Tenn. 38146. Meets first Monday Oct. through June at the University Club.

MIAMI VALLEY RADIOLOGICAL SOCIETY
Secretary, Dr. Bert Must, I.B.M. Bldg., Dayton, Ohio. Meets third Thursday of fall, winter and spring months at 7:30 P.M. at Miami Valley Hospital, Dayton, Ohio.

MICHIGAN RADIOLOGICAL SOCIETY, CHAPTER OF ACR
Secretary-Treasurer, Dr. Francis P. Shea, Harper Hospital, 3825 Brush St., Detroit, Mich. 48201. Meets monthly, first Thursday, October through May, at David Whitney House, 1010 Antietam, at 6:30 P.M.

MICHIGAN SOCIETY OF THERAPEUTIC RADIOLOGISTS
Secretary-Treasurer, Dr. William I. Knapp, St. Mary's Hosp., 830 S. Jefferson, Saginaw, Mich. 48601. Meets bimonthly during the academic year.

MID-HUDSON RADIOLOGICAL SOCIETY
Secretary-Treasurer, Dr. William D. Stiehm, 37 Flower Hill Rd., Poughkeepsie, N. Y. 12603. Meets 7:00 P.M., first Wednesday of each month, September to May.

MILWAUKEE ROENTGEN RAY SOCIETY
Secretary-Treasurer, Dr. Thomas C. Lipscomb, 1004 North Tenth St., Milwaukee, Wis. 53233. Meets monthly on fourth Monday, October through May, at University Club.

MINNESOTA RADIOLOGICAL SOCIETY, CHAPTER OF ACR
Secretary-Treasurer, Dr. Marvin E. Goldberg, Box 292, Mayo Memorial Health Sciences Center, Minneapolis, Minn. 55455.

MISSISSIPPI STATE RADIOLOGICAL SOCIETY, CHAPTER OF ACR
Secretary-Treasurer, Dr. Edward L. Gieger, 969 Lakeland Dr., Jackson, Miss. 39216. Meets third Thursday, excluding summer months, at the Primos Northgate Rest., Jackson at 6:30 P.M.

MISSOURI RADIOLOGICAL SOCIETY, CHAPTER OF ACR
Secretary-Treasurer, Dr. Ronald G. Evens, Mallinckrodt Institute of Radiology, 510 S. Kingshighway, St. Louis, Mo. 63110.

MONTANA RADIOLOGICAL SOCIETY, CHAPTER OF ACR
Secretary, Dr. C. H. Agnew, Room 102, Doctors Bldg., Billings, Mont. 59101.

NEBRASKA CHAPTER OF ACR
Secretary-Treasurer, Dr. Robert Bodmer, Suite 622 Doctors Bdg., Omaha, Neb. 68131. Meets the third Wednesday of the month, Oct. through March, at the Clarkson Hosp., Omaha, Neb. and the fourth Friday of April at the Lincoln Country Club, Lincoln, Neb.

NEVADA RADIOLOGICAL SOCIETY, CHAPTER OF ACR
Secretary, Dr. Charles F. Veverka, Carson Tahoe Hosp., Carson City, Nev. 89701.

N.E. SOCIETY FOR RADIATION ONCOLOGY
Secretary, Dr. C. C. Wang, Mass. Gen. Hosp., Boston, Mass. 02114.

NEW ENGLAND ROENTGEN RAY SOCIETY
Secretary, Dr. Melvin E. Clouse, 185 Pilgrim Rd., Boston, Mass. 02115. Meets the third Friday of Oct. and Nov., and third Thurs. of each month. Jan. through May, excluding December, at The Longwood Towers, 20 Chapel Street, Brookline, Mass. at 3:00 P.M.

NEW HAMPSHIRE ROENTGEN RAY SOCIETY, CHAPTER OF ACR
Secretary-Treasurer, Dr. Edward P. Kane, Claremont Gen. Hosp., Claremont, N. H. 03743. Meets four to six times yearly.

NEW MEXICO SOCIETY OF RADIOLOGISTS, CHAPTER OF ACR
Secretary, Dr. W. M. Jordan, 1100 Central Ave. S.E., Albuquerque, N. M. 87106. Four meetings annually, three held in Albuquerque, N. M., and one held at time and place of New Mexico State Medical Society annual meeting.

NEW ORLEANS RADIOLOGICAL SOCIETY, INC.
Secretary-Treasurer, Dr. Jimmy L. Mains, P.O. Box 446, Gretna, La. 70053. Meets bimonthly at local restaurants selected by the President. Spring Conference.

NEW YORK ROENTGEN SOCIETY
Secretary-Treasurer, Dr. Thomas C. Beneventano, 111 East 210th St., Bronx, N. Y. 10467. Meets monthly on the 3rd Monday at the New York Academy of Medicine at 4:30 P.M. Annual Spring Conference, Waldorf-Astoria Hotel, New York, N. Y., April 22–24, 1976. A.M.A. Cat. I credit. Further information may be obtained from Dr. Albert A. Dunn, Roosevelt Hosp., New York, N. Y. 10019.

NEW YORK STATE CHAPTER OF ACR
Secretary-Treasurer, Dr. Albert F. Keegan, 6 Secor Dr., Port Wash., N. Y. 11050.

NORTH AMERICAN SOCIETY OF CARDIAC RADIOLOGY
Secretary-Treasurer, Dr. Erik Carlson, Univ. Calif., San Francisco, Calif. 94143.

NORTH CAROLINA CHAPTER OF ACR
Secretary-Treasurer, Dr. Ernest B. Spangler, Wesley Long Hosp., Greensboro, N. C. 27402. Meets twice a year. The Spring Meeting is held at the time of the meeting of the North Carolina Medical Society. The Fall Meeting is held in November at the Mid Pines Club, Southern Pines, N. C.

NORTH DAKOTA RADIOLOGICAL SOCIETY, CHAPTER OF ACR
Secretary, Dr. Marshall Landa, P. O. Box 6001, Fargo, N. D. 58102. Meets at time of State Medical Association meeting. Other meetings arranged on call of the President.

NORTH FLORIDA RADIOLOGICAL SOCIETY
Secretary, Dr. David F. Bew, University Hospital of

Jacksonville, 655 W. Eighth Street, P.O. Box 2751, Jacksonville, Fla. 32203. Meets quarterly in March, June, September and December.

NORTHEASTERN OKLAHOMA RADIOLOGICAL SOCIETY
Secretary-Treasurer, Dr. Theodore J. Brickner, Jr., 5919 S. Gary Place, Tulsa, Okla. 74110.

NORTHEASTERN NEW YORK RADIOLOGICAL SOCIETY
Secretary, Dr. Donald R. Morton, Dept. of Radiology, St. Clare's Hosp., Schenectady, N. Y. 12304. Meets in Albany area on third Wednesday of October, November, March, April, and May.

NORTHERN CALIFORNIA RADIATION THERAPY ASSOCIATION
Secretary-Treasurer, Dr. John D. Earle, Stanford Medical Center, Stanford, Calif. 94304. Meets quarterly.

NORTHERN CALIFORNIA RADIOLOGICAL SOCIETY
Secretary, Dr. Patrick J. Grinsell, 1207 Fairchild Ct., Woodland, Calif. 95695. Meets on the fourth Monday, Sept. through May at the Mansion Inn, Sacramento, Calif.

NORTHWESTERN NEW YORK RADIOLOGICAL SOCIETY
Secretary, Dr. Barbara E. Chick, Glens Falls Hospital, Glens Falls, N. Y. 12801.

NORTHWESTERN OHIO RADIOLOGICAL SOCIETY
Secretary-Treasurer, Dr. Gerald W. Marsa, 3939 Monroe St., Toledo, Ohio 43606. Meets 3rd Wednesday from September to May excluding Dec. at Academy of Med. of Toledo and Lucas County, 4428 Secor Rd., Toledo, Ohio.

OHIO STATE RADIOLOGICAL SOCIETY, CHAPTER OF ACR
Secretary, Dr. James Farmer, Cleveland, Ohio.

OKLAHOMA STATE RADIOLOGICAL SOCIETY, CHAPTER OF ACR
Secretary, Dr. George H. Ladd, 4616 Denison, Muskogee, Okla. 74401. Meets in January, May and October.

ORANGE COUNTY RADIOLOGICAL SOCIETY
Secretary, Dr. William E. Danko, 2601 E. Chapman, Orange, Calif. 92667. Meets on fourth Tuesday of the month, excluding June, July, August, and December, at Orange County Medical Association Bldg., Orange, Calif.

OREGON STATE RADIOLOGICAL SOCIETY, CHAPTER OF ACR
Secretary-Treasurer, Dr. Ray F. Friedman, 3324 S. W. 44th St., Portland, Ore. 97221. Meets on second Wednesday of month, October through April, at the University Club, Portland, Ore.

ORLEANS PARISH RADIOLOGICAL SOCIETY
Secretary, Dr. Joseph V. Schlosser, Charity Hospital, New Orleans, La. 70113. Meets second Tuesday of each month.

PACIFIC NORTHWEST RADIOLOGICAL SOCIETY
Secretary-Treasurer, Dr. Kenneth D. Moores, 1118 9th Ave., Seattle, Wash. 98101.

PENNSYLVANIA RADIOLOGICAL SOCIETY, CHAPTER OF ACR
Secretary, Dr. Joseph A. Marasco, Jr., St. Francis General Hosp., Pittsburgh, Pa. 19141.

PHILADELPHIA ROENTGEN RAY SOCIETY
Secretary, Dr. Marvin E. Haskin, 230 N. Broad St., Philadelphia, Pa. 19102. Meets first Thursday of each month at 5 P.M., from October to May in Thompson Hall, College of Physicians.

PITTSBURGH ROENTGEN SOCIETY
Secretary, Dr. Klaus M. Bron, Presbyterian-Univ. Hosp., Pittsburgh 15213. Meets second Wednesday of month, September through May, at the Pittsburgh Athletic Association.

RADIATION RESEARCH SOCIETY
Executive Secretary, Richard J. Burk, Jr., 4211 39th St., N.W., Washington, D. C. 20016. Annual Meeting.

RADIOLOGICAL SOCIETY OF CONNECTICUT, INC., CHAPTER OF ACR
Secretary, Dr. Gerald L. Baker, 85 Jefferson St., Hartford, Conn. 06106. Meets in Oct., Jan., March, and June.

RADIOLOGICAL SOCIETY OF GREATER CINCINNATI
Secretary-Treasurer, Dr. Alvin Nathan, c/o Academy of Medicine, 320 Broadway, Cincinnati, Ohio 45202. Meets first Monday of each month at Cincinnati Academy of Medicine.

RADIOLOGICAL SOCIETY OF NEW JERSEY, CHAPTER OF ACR
Secretary, Dr. Fred M. Palace, 11 Dale Dr., Morristown, N.J. 07960. Monthly meetings in East Orange and Trenton, N.J. Semi-Annual Meeting in Nov.

RADIOLOGICAL SOCIETY OF RHODE ISLAND, CHAPTER OF ACR
Secretary-Treasurer, Dr. Daniel J. Alves, Rhode Island Hosp., Providence, R. I. 02902.

RADIOLOGICAL SOCIETY OF SOUTHERN CALIFORNIA
Secretary-Treasurer, Dr. A. Franklin Turner, LAC-USC Medical Center, Room 3418, 1200 North State St., Los Angeles, Calif. 90033. Meets three times a year, usually October, February and May.

RADIOLOGICAL SOCIETY OF THE STATE OF NEW YORK
Secretary-Treasurer, Dr. John W. Colgan, 273 Hollywood Ave., Rochester, N. Y. 14618.

REDWOOD EMPIRE RADIOLOGICAL SOCIETY
Secretary, Dr. Charles E. Carter, 121 Sotoyome St., Santa Rosa, Calif. 95405. Meets second Monday every other month.

RICHMOND COUNTY RADIOLOGICAL SOCIETY
Secretary, Dr. Frederick S. Vines, 11830 Rothbury Dr., Richmond, Va. 23235. Meets third Thursday of each month at the Aberdeen Barn.

ROCHESTER ROENTGEN RAY SOCIETY, ROCHESTER, N. Y.
Secretary-Treasurer, Dr. Robert J. Bruneau, Rochester General Hosp., Rochester, N. Y. 14621. Quarterly meetings on the call of the President, at the Rochester Academy of Medicine.

ROCKY MOUNTAIN RADIOLOGICAL SOCIETY
Secretary-Treasurer, Dr. Lorenz R. Wurtzebach, 4200 E. Ninth Ave., Denver, Colo. 80220. Annual Meeting: Brown Palace Hotel, Denver, Colo., Aug. 19–21, 1976.

SAN ANTONIO-CIVILIAN MILITARY RADIOLOGICAL SOCIETY
Secretary, Dr. James R. Stewart, Oak Hills Medical Ctr., San Antonio, Tex. 78209. Meets third Wednesday of each month at Fort Sam Houston Officers Club at 6:30 P.M.

SAN DIEGO RADIOLOGICAL SOCIETY
President, Dr. Donald J. Fleischli, 7849 Fay Ave., La Jolla, Calif. 92037. Meets the first Wednesday of each month Sept. through June at the University Club.

SAN FRANCISCO RADIOLOGICAL SOCIETY
Secretary-Treasurer, Dr. Robert L. Koch, 3838 California St., Suite 106, San Francisco, Calif. 94118.

SECTION ON RADIOLOGY, CALIFORNIA MEDICAL ASSOCIATION
Secretary, Dr. William H. Graham, 630 East Santa Clara St., San Jose, Calif.

SECTION ON RADIOLOGY, MEDICAL SOCIETY OF THE DISTRICT OF COLUMBIA
Secretary-Treasurer, Dr. Albert M. Zelna, 21 Masters St., Potomac, Md. 20854. Meets at Medical Society Library, third Wednesday of January, March, May and October at 8:00 P.M.

SECTION OF RADIOLOGY, NATIONAL MEDICAL ASSOCIATION
Secretary, Dr. Ruby Brooks, Dept. Radiol., Veterans Adm. Hosp., P.O. Box 511, Tuskogee, Ala. 36083. Annual Meeting.

SECTION ON RADIOLOGY, SOUTHERN MEDICAL ASSOCIATION
Secretary, Dr. Mario A. Calonje, 1514 Jefferson Highway, New Orleans, La. 70121. Annual Meeting.

SECTION ON RADIOLOGY, TEXAS MEDICAL ASSOCIATION
Secretary, Dr. George F. Crawford, St. Elizabeth Hospital, Beaumont, Tex. Meets annually with the Texas Medical Association.

SOCIETY FOR PEDIATRIC RADIOLOGY
Secretary-Treasurer, Dr. John P. Dorst, 601 N. Broadway, Baltimore, Md. 21205. Annual meeting: Washington Hilton Hotel, Washington, D. C., Sept. 19–20, 1976.

SOCIETY OF GASTRO-INTESTINAL RADIOLOGISTS
Secretary-Treasurer, Dr. John R. Amberg, University Hospital, 225 W. Dickinson St., San Diego, Calif. 92103.

SOCIETY OF NUCLEAR MEDICINE
Secretary, Dr. E. James Potchen, Edward Mallinckrodt Institute of Radiology, 660 S. Euclid Ave., St. Louis, Mo. 63110. *Administrative Officer*, Mrs. Margaret Glos, 211 E. 43rd St., New York, N. Y. 10017. Annual Meeting.

SOUTH BAY RADIOLOGICAL SOCIETY
Secretary, Dr. Bruce R. Parker, Dept. Radiol., Stanford Univ. Med. Center, Stanford, Calif. 94305. Meets the 2nd Monday of each month at the Santa Clara County Medical Society Bldg., 700 Empey Way, San Jose, Calif

SOUTH CAROLINA RADIOLOGICAL SOCIETY, CHAPTER OF ACR
Secretary, Dr. George W. Brunson, 1406 Gregg St Columbia, S. C. Annual meeting (primarily business) in conjunction with the South Carolina Medical Association meeting in May. Annual fall scientific meeting at time and place designated by the president.

SOUTH COAST RADIOLOGICAL SOCIETY CHAPTER OF ACR
Secretary-Treasurer, Dr. Richard T. Love, Santa Barbara Med. Clin., 215 Pesetas Lane, Santa Barbara, Calif. 93110. Meets fourth Tuesday of alternate months, Sept., Nov., Jan., March and May.

SOUTH DAKOTA RADIOLOGICAL SOCIETY, CHAPTER OF ACR
Secretary, Dr. M. F. Petereit, 2416 S. Phillips, Sioux Falls, S. D. 57105. Meets in spring with State Medical Society and in fall.

SOUTHERN CALIFORNIA RADIATION THERAPY ASSOCIATION
Secretary-Treasurer, Dr. Duane J. Gillum, 250 W. Pueblo St., Santa Barbara, Calif. 93105. Meets quarterly.

SOUTHERN RADIOLOGICAL CONFERENCE
Secretary-Treasurer, Dr. J. W. Maxwell, P.O. Box 2144 Mobile Ala. 36601. Annual Meeting:

TENNESSEE RADIOLOGICAL SOCIETY, CHAPTER OF ACR
Secretary-Treasurer, Dr. Jerry W. Grise, Methodist Hosp., 1265 Union Ave., Memphis, Tenn. 38104. Meets annually at the time and place of the Tennessee State Medical Association meeting.

TEXAS STATE RADIOLOGICAL SOCIETY, CHAPTER OF ACR
Secretary, Dr. Francis E. O'Neill, 1128 Nix Prof. Bdg., San Antonio, Tex. 78205.

THE FLEISCHNER SOCIETY
Secretary, Dr. E. Robert Heitzman, State University of New York Upstate Medical Center, Syracuse, N. Y. 13210. Annual Meeting:

TRI-STATE RADIOLOGICAL SOCIETY
Secretary, Dr. Thomas Harmon, St. Mary's Hosp., Evansville, Ind. 47750. Meets bimonthly on the third Wednesday at area Hospitals.

UPPER PENINSULA RADIOLOGICAL SOCIETY
Secretary, Dr. A. Gonty, Menominee, Mich. Meets quarterly.

UTAH STATE RADIOLOGICAL SOCIETY, CHAPTER OF ACR
Secretary-Treasurer, D. Michael Edson, Dept. Radiol., Valley West Hosp., 4160 West 3400 South, Granger, Utah 84120. Meets quarterly at Holy Cross Hospital.

VERMONT RADIOLOGICAL SOCIETY, CHAPTER OF ACR
Secretary, Dr. J. Lorimer Holm, R.R. #3, Barre, Vt. 05641.

VIRGINIA CHAPTER OF ACR
Secretary-Treasurer, Dr. Charles P. Winkler, 3500 Kensington Ave., Suite 2-A, Richmond, Va. 23221.

WASHINGTON, D. C., CHAPTER OF ACR
Secretary-Treasurer, Dr. Robert M. Allen, 9312 Convento Terr., Fairfax, Va. 22030.

WASHINGTON STATE RADIOLOGICAL SOCIETY, CHAPTER OF ACR
Secretary-Treasurer, Dr. Donald J. Hesch, 3216 N.E. 45th Place, Seattle, Wash. 98105.

WEST VIRGINIA RADIOLOGICAL SOCIETY, CHAPTER OF ACR
Secretary-Treasurer, Dr. Andrew W. Goodwin, II, 200 Med. Arts Bldg., Charleston, W. Va. 25301. Meets concurrently with annual meeting of West Virginia State Medical Society, other meetings arranged by program committee.

WESTCHESTER COUNTY RADIOLOGICAL SOCIETY
Secretary, Dr. Leonard Cutler, 16 Guion Place, New Rochelle, N. Y. 10802. Meets on second Tuesday of October, December, February and May.

WISCONSIN RADIOLOGICAL SOCIETY, CHAPTER OF ACR
Secretary-Treasurer, Dr. June Unger, Wood VA Hosp., Wood, Wis. 53193. Meets twice a year, May and September.

WISCONSIN SOCIETY OF THERAPEUTIC RADIOLOGISTS
Secretary, Dr. Alvin Greenberg, Radiother. Ctr., Univ. Hospitals, Madison, Wis. 53706. Meets quarterly.

WYOMING RADIOLOGICAL SOCIETY, CHAPTER OF ACR
Secretary, Dr. Ross J. Collie, Box 96, Lander, Wyo. 82520. Meets in fall with State Medical Society and in spring on call of President.

MEXICO, PUERTO RICO AND CENTRAL AMERICA

ASOCIACIÓN COSTARRICENSE DE RADIOLOGÍA
Secretary, Dr. Rafael Umaña-Umaña, Apartado 8-5340, San José, Costa Rica.

ASOCIACÓN DE RADIÓLOGOS DE CENTRO AMERICA Y PANAMÁ. Comprising: Guatemala, El Salvador, Honduras, Nicaragua, Costa Rica and Panamá
Secretary-General, Dr. Francisco Miranbell Solis, Apartado 3352, San José, Costa Rica, Central America. Meets annually in a rotating manner in the six countries.

SOCIEDAD DE RADIOLOGÍA DE SALVADOR
Secretary, Dr. Carlos Meijia, 5a Av. Nte. No. 434, San Salvador, Rep. El Salvador.

SOCIEDAD DE RADIOLOGÍA DE GUATEMALA
Secretary, Dr. Carlos E. Escobar, 9², Calle A 0–05, Zona 1, Guatemala

SOCIEDAD MEXICANA DE RADIOLOGÍA, A.C.
Coahuila No. 35, México 7, D.F., México.
Secretary-General, Dr. Jorge Cano Coquí. Meets first Monday of each month.

SOCIEDAD RADIOLÓGICA PANAMEÑA
Secretary, Dr. L. Arrieta Sánchez, Apartado No. 6323, Panamá, R. de P. Meets monthly in a department of radiology of a local hospital chosen at preceding meeting.

SOCIEDAD RADIOLÓGICA DE PUERTO RICO
Secretary, Dr. César Rosa, Box 9387, Santurce, Puerto Rico 00908. Meets second Thursday of each month at 8:00 P.M. at the Puerto Rico Medical Association Bldg. in San Juan.

BRITISH COMMONWEALTH OF NATIONS

ASSOCIATION OF RADIOLOGISTS OF THE PROVINCE OF QUEBEC
121 Boul. Taschereau, Greenfield Park, P. Q., Canada. Meets four times a year.

BRITISH INSTITUTE OF RADIOLOGY
Honorary Secretaries, D. H. Traspnell, M. Cohen, 32 Welbeck St., London, W1M/7PG, England.

CANADIAN ASSOCIATION OF PHYSICISTS, DIVISION OF MEDICAL AND BIOLOGICAL PHYSICS
Honorary Secretary-Treasurer, Dr. R. G. Baker, Ontario Cancer Foundation, Ottawa Civic Clinic, 1053 Carling Ave., Ottawa 3, Ont., Canada.

CANADIAN ASSOCIATION OF RADIOLOGISTS
Honorary Secretary, Dr. Ross O. Hill, Suite 806, 1440 St. Catherine St. West, Montreal 107, Que., Canada. Annual Meeting:

EDMONTON AND DISTRICT RADIOLOGICAL SOCIETY
Secretary, Dr. L. A. Koller, Suite 360, Professional Bldg., 10830 Jasper Ave., Edmonton 15, Alberta, Canada. Meets third Thursday of each month October to May, except December, at various Edmonton Hospitals.

FACULTY OF RADIOLOGISTS
Honorary Secretary, P. D. Thomson, 28 Portland Pl., London, W1N 4DE.

MONTREAL RADIOLOGICAL STUDY CLUB
Secretary, Dr. W. Paul Butt, Montreal General Hospital, Montreal, Que., Canada. Meets first Tuesday evening, October to April.

SECTION OF RADIOLOGY OF THE ROYAL SOCIETY OF MEDICINE (CONFINED TO MEDICAL MEMBERS)
Meets third Friday each month at 8:15 P.M. at the Royal Society of Medicine, 1 Wimpole St., London, W. 1 M8AE, 1 England.

SOCIÉTÉ CANADIENNE-FRANÇAISE DE RADIOLOGIE
Secretary-General, Dr. Hubert Sasseville, Verdun Hospital, Montréal, P. Q., Canada. Meets every third Tuesday from October to April.

THE HOSPITAL PHYSICISTS' ASSOCIATION
Honorary Secretary, J. B. Massey, B.Sc., Christie Hosp. and Holt Radium Institute, Physics Department, Withington, Manchester M20 9BX, England.

TORONTO RADIOLOGICAL SOCIETY
Secretary, Dr. George Wortzman, Toronto General Hosp., Toronto 12, Ont., Canada. Meets second Monday of each month, September through May.

THE ROYAL AUSTRALASIAN COLLEGE OF RADIOLOGISTS
Honorary Secretary, Dr. T. P. Loneragan, 45 Macquarie St., Sydney, N.S.W. 2000, Australia.

SOUTH AMERICA

COLÉGIO BRASILEIRO DE RADIOLOGIA
Secretary-General, Dr. José Marcos Pires de Oliveira, Caixa Postal 5984, São Paulo, Brazil.

FEDERACIÓN ARGENTINA DE SOCIEDADES DE RADIOLOGÍA
Branches of the Federation are: Sociedad de Radiólogos de la Provincia de Córdoba; Sociedad Argentina de Radiología; Asociación Argentina de Radiología; Sociedad de Radiología, Radioterapéutica y Medicina Nuclear de Rosario; Sociedad de Radiología y Medicina Nuclear del Centro y Sudeste de la Provincia de Buenos Aires (Mar del Plata); Sociedad Salteña de Radiología y Medicina Nuclear; Sociedad de Radiología de Tucumán; Sociedad de Radiologia del Nordeste Argentino; Sociedad de Radiología de La Plata; and Sociedad de Radiología de San Juan.
Secretary-General-Treasurer, Dr. Roberto Habichayn, Av. Colón 637, Córdoba, Argentina.
Congress will be organized by Sociedad de Radiología, Radioterapéutica y Medicina Nuclear de Rosario in 1975.

SOCIEDAD ARGENTINA DE RADIOLOGÍA
Secretary-General, Dr. Alba de la Torre, Santa Fé 1171, Buenos Aires, Argentina. Meets first Wednesday evening, April through December.

SOCIEDAD BOLIVIANA DE RADIOLOGÍA
Secretary, Dr. Javier Prada Méndez, Casilla 1182, La Paz, Bolivia. Meets monthly. General assembly once every two years.

SOCIEDADE BRASILEIRA DE RADIOLOGIA
Secretary, Dr. Armando Rocha Amoédo, Caixa Postal 1532, Rio de Janeiro, Brazil. General Assembly meets every two years in December.

SOCIEDADE BRASILEIRA DE RADIOTERAPIA
Luiz Antonio, 644, São Paulo, Brazil. Meets monthly on second Wednesday at 9:00 P.M. in São Paulo at Av. Brigadeiro Luiz Antonio, 644.

SOCIEDAD CHILENA DE RADIOLOGÍA
Secretary, Dr. Manuel Neira, Casilla 13426, Santiago, Chile. Meets first Friday of each month at Av. Santa María 1810 at 7:00 P.M.

SOCIEDAD COLOMBIANA DE RADIOLOGÍA
Secretary-General, Dr. Gustavo Sánchez Sánchez, Bogotá, Colombia. Meets last Thursday of each month.

SOCIEDAD ECUATORIANA DE RADIOLOGÍA
Secretary, Dr. Luis Blum, Casilla 3712, Guayaquil, Ecuador.

SOCIEDAD PARAGUAYA DE RADIOLOGÍA
Secretary, Dr. Hugo Volpe Rios, 15 de Agosto 322, Asunción, Paraguay.

SOCIEDAD PERUANA DE RADIOLOGÍA
Secretary-General, Dra. Ladis Delpino, Av. General Santa Cruz No. 315, Miraflores, Lima, Perú, Casilla Correo, 2306, Lima, Perú. Meets monthly except during January, February, and March.

SOCIEDAD DE RADIOLOGÍA DEL ATLANTICO
Secretary, Dr. Raul Fernandez, Calle 40 #41-110, Baranquilla, Colombia. Society meets monthly at the Instituto de Radiología.

SOCIEDAD DE RADIOLOGÍA DEL NORDESTE ARGENTINO
Secretary-General, Dr. Francisco J. Velar, Catamarca 561, Corrientes, Argentina.

SOCIEDAD DE RADIOLOGÍA DE LA PLATA
Secretary, Dr. Hiram D. Haurigot, Calle 50 No. 374, La Plata, Argentina.

SOCIEDAD DE RADIOLOGÍA, CANCEROLOGÍA Y FÍSICA MÉDICA DEL URUGUAY
Secretary-General, Dr. Manuel Gonzáles Maseda, Av. Agraciada 1464, piso 13, Montevideo, Uruguay.

SOCIEDADE DE RADIOLOGÍA DE PERNAMBUCO
Secretary, Dr. Manoel Medeiros Instituto de Radiologia da Faculdade de Medicina da Universidade do Recife, Caixa Postal 505, Pernambuco, Brazil.

SOCIEDAD DE ROENTGENOLOGÍA Y MEDICINA NUCLEAR DE LA PROVINCIA DE CÓRDOBA
Secretary-General, Dr. Lucas C. Di Rienzo, Ave. Grl. Paz. 151, Córdoba, Argentina.

SOCIEDAD DE RADIOLOGÍA, RADIOTERAPÉUTICA Y MEDICINA NUCLEAR DE ROSARIO
Secretary-General, Dr. Federico Frágola, Santa Fe 1798, Rosario, Argentina.

SOCIEDAD SALTEÑA DE RADIOLOGÍA Y MEDICINA NUCLEAR
Treasurer, Dr. Julio Luis Baldi, Av. Sarmiento 536, Salta, Argentina.

SOCIEDAD VENEZOLANA DE RADIOLOGÍA Y MEDICINA NUCLEAR
Secretary-General, Dr. Salvador Itriago Borgas, Apartado Postal 9213, Candelaria, Caracas, Venezuela. Meets monthly, third Friday at Colegio Médico del Distrito Federal, Caracas.

CONTINENTAL EUROPE

ÖSTERREICHISCHE RÖNTGEN-GESELLSCHAFT
Secretary, Dr. Ernst Kotcher, Wiener Allgemeine Poliklinik Mariannengasse 10, A-1090 Wien, Austria. Meets second Tuesday of each month in Allgemeine Poliklinik.

SOCIÉTÉ ROYALE BELGE DE RADIOLOGIE
General Secretary, Dr. Joseph Baeyens, Alost, Belgium. Meets in February, March, May, June, September, October, November and December.

SOCIÉTÉ EUROPÉENNE DE RADIOLOGIE PÉDIATRIQUE
Secretary, Dr. J. Corbaton, Clinica Infantil "La Paz," Av. Generalissimo, 117 Madrid 34, Spain. Annual Meeting:
Permanent Secretary, Clément Fauré, Hôpital des Enfants Malades, 149, rue de Sèvres, 75 730, Paris Cadet 15, France.

SOCIÉTÉ FRANÇAISE DE RADIOLOGIE MÉDICALE, MÉDECINE NUCLÉAIRE ET ÉLECTROLOGIE, and its branches: SOCIÉTÉ DU SUD-OUEST, DU LITTORAL MÉDITERRANÉEN, DU CENTRE ET LYONNAIS, DU NORD, DE L'OUEST, DE L'EST, DU MASSIF CENTRAL, D'OUTRE-MER ET D'ÉTRANGER.
Parent Society meets third Monday of each month, except during July, August and September, rue de Seine 12, Paris, France.
Secretary-General, Dr. Ch. Proux, 9 rue Daru, Paris 75008, France.

SOCIÉTÉ FRANÇAISE DE NEURORADIOLOGIE
Secretary-General, Professeur agr. R. Djindjian 16, rue de l'Université 75, Paris 7e, France. Annual meeting.

Československá Radiologická Společnost
Secretary, Associate Professor Jaromír Kolář, M.D., Sc.D., Radiological Clinic, Praha 2, U nemocnice 2, Czechoslovakia. Meets monthly except during July, August and September. Annual general meeting.

Deutsche Röntgengesellschaft
President, Professor Dr. med. Walter Frommhold, Director of Medizinisches Strahleninstitut der Universität Tübingen, Röntgenweg 11, 7400 Tübingen, Germany.

Faculty of Radiologists of the Royal College of Surgeons in Ireland
Honor. Secretary, Max. J. Ryan, St. Stephen's Green, Dublin 2. Annual Meeting:

Società Italiana di Radiologia Medica e Medicina Nucleare
Administrative Secretary, Prof. E. Conte, Ospedale Mauriziano, 10128 Torino, Italy. Meets annually.

Societas Radiologica Danica
Secretary, Dr. Bent Langenfeldt, Tretommervej 20a, DK. 8240 Risskov, Denmark.

Nederlandse Vereniging voor Radiologie
Secretary, Dr. J. D. Mulder, Dept. of Rad., Akademisch Ziekenhuis, Leiden, Netherlands.

Norsk Forening for Medicinsk Radiologi
General Secretary, Gunnar Stake, Rikshospitalet, Oslo, Norway.

Scandinavian Radiological Society
Secretary-General, Professor C. F. Unnérus, M.D., Hagalung-Tapiola, Havsvindsvägn 5 C., Finland. Annual Meeting.

Sociedad Española de Radiología y Electrología Médicas y de Medicina Nuclear
Secretary-General, Dr. Pilar Gallar Barberá, Villanueva, 11, Madrid 1, España. Meets every other Saturday evening of each month, Oct. to June, inclusive, in Madrid.

Sociedade Portuguesa de Radiologia e Medicina Nuclear
Secretary-General, Dr. Luís Aires de Sousa, Av. Elias Garcia, 123- 1, Esg.-Lisboa i-Portugal.

Svensk Förening för Medicinsk Radiologi
Secretary, Dr. Hanz Ringertz, Röntgendiagnostika Avdelningen, Karolinska Sjukhuset 104 01 Stockholm 60, Sweden.

Schweizerische Vereinigung für Radiologie, Nuklearmedizin und Strahlenbiologie (Association Suisse de Radiologie, Médecine Nucléaire et de Radiobiologie)
Secretary, Dr. med. Gustav Schoch, Bethesdaspital, Gellerstrasse 144, 4000 Basel, Switzerland.

Asia

Bengal Radiological Association
Honorary Secretary, Dr. B. Chatterji, 262 Rash Behari Ave., Calcutta 700019, India. Meets 1st Fri. and 3rd Wed. of every month.

Indian Radiological Association
Honor. Gen. Secretary, Dr. S. P. Aggarwa', 10-B Kasturba Ghandi Marg, New Delhi 110001.

Indonesian Radiological Society
Secretary, Dr. Gani Iljas Sasmitaatmadja, Radiology Dep., Faculty of Medicine, University of Indonesia, Salemba 6, Jakarta, Indonesia.

Iranian Radiological Society
Secretary, Dr. Majid Rooholamini, P.O. Box No. 14–1151, Teheran, Iran. The Society meets on the second Saturday of each month.

Israel Radiological Society
Secretary, Dr. M. A. Lerner, Hesharon Hosp., Petah-Tigva, Israel.

Philippine College of Radiology
Secretary-Treasurer, Dr. Eduardo V. Nievera, Box 1284 Commercial Center, Makati, Rizal D-708, Philippines. Meets every second Thursday of the month.

Radiological Society of Thailand
Secretary, Prof. Rojana Suvansuthi, M.D., Ph.D., Depart. of Rad., Sirizaj Hospital, Faculty of Medicine, Mahidol University, Bangkok 7, Thailand.

Africa

Association of Radiologists of West Africa
Honorary Secretary, C. A. Beetlestone, M.B., B.S., D.M.R.D., Dept. Radiol., University College Hosp., Ibadan, Nigeria.

Radiological Society of South Africa
Secretary, Dr. A. Visser, P. O. Box 8850, Johannesburg, South Africa.

South African International Radiological Congress
Director, Dr. Paul Sneider, P.O. Box 4878, Johannesburg, South Africa.

ABSTRACTS OF RADIOLOGIC LITERATURE

INDEX TO ABSTRACTS

ROENTGEN DIAGNOSIS

Abdomen

Escobar-Prieto, A. *et al.:* Infusion tomography of the gallbladder 1108

Wyatt, A. P.: Prolonged symptomatic and radiological remission of colonic gas cysts after oxygen therapy 1108

Kim, D. K. *et al.:* Tumors of the liver as demonstrated by angiography, scan and laparotomy 1108

Gierson, E. D. *et al.:* Caecal rupture due to colonic ileus 1109

Vandendris, M., and Gerard, A.: Primary malignant tumors of the biliary tract 1109

Gynecology and Obstetrics

Schabel, S. I. *et al.:* Radiographic manifestations of malignant mixed uterine tumors 1109

Schulman, A., and Herlinger, H.: Urinary tract dilatation in pregnancy 1110

Genitourinary System

Jouve, P. *et al.:* Observations on 45 cases of urethral valves in children 1110

Pollack, H. M. *et al.:* Hernias of the ureter: an anatomic-roentgenographic study 1110

Ben-Menachem, Y. *et al.:* Angiography of renal metastases 1111

Cremin, B. J.: The "spinnaker sail" appearance of the posterior urethral valve in infants 1111

Hug, I., and Mihatsch, J. M.: Primary oxalosis: report of a case with radiologic-pathologic-anatomical correlation and review of the literature 1111

Wagenknecht, L. V., and Wehling, H.: The value of roentgen diagnostic methods in retroperitoneal fibrosis 1112

Skeletal System

Schneider, K. *et al.:* Eosinophilic granuloma (histiocytosis-X) with lung and bone manifestations 1112

Loeffler, R. K. *et al.:* Limitations of bone scanning in clinical oncology 1113

Tomeno, B., and Forest, M.: Occurrence and nature of bone tumors: 25 years experience in an orthopedic service 1113

Davidson, J. K.: Radiology of aseptic necrosis of bone 1113

Lateur, L., and Baert, A.: Radiological features in Reiter's disease 1114

Galasko, C. S. B.: The significance of occult skeletal metastases, detected by skeletal scintigraphy, in patients with otherwise apparently "early" mammary carcinoma 1114

ROENTGEN DIAGNOSIS

Abdomen

Escobar-Prieto, Adolfo, Barrera, Arnoldo, Cabrera, Vera L., Cohen, Jaime, and Leal, Pedro, Jr. Infusion tomography of the gallbladder. *Surg., Gynec. & Obst.*, Sept., 1975, *141*, 340–346. (From: The Departments of Radiology, Medicine and Surgery, Hospital Clínica del Parque, Chihuahua, Mexico.)

Contrast enhancement of the wall of the gallbladder in total-body opacification was a useful method of evaluating the gallbladder in certain disease processes. It has been found particularly useful in the following conditions: (1) immediate evaluation of pain in the right upper quadrant; (2) obstructive jaundice; (3) nonvisualization on oral and intravenous cholangiography; and (4) recurrent symptomatology of extrahepatic biliary tract disease with normal or impaired cholangiography.

The wall of the normal gallbladder was seldom opacified, and, when visualized, was 1 mm or less in thickness (Rabushka, S.E. *et al.*, *Radiology*, 1973, *109*, p. 549). The gallbladder was abnormal or pathologic when the wall was clearly opacified, and measured more than 1 mm in thickness at any point. The increased thickness of the wall was due to altered permeability, increased vascularity, and extravasated contrast material into the interstitial spaces.

Forty-three of 45 patients studied for suspected biliary tract disease had an abnormally thick gallbladder wall. Chololithiasis and/or cholecystitis was found at surgery in 37 of these cases. Four persons refused surgery, but had clinical evidence of cholecystitis, chololithiasis, or advanced neoplasm of the extrahepatic biliary tract. Cirrhosis of the liver was confirmed by biopsy in two patients who died in hepatic coma. There was one false positive and one false negative result.

The examination was usually done without preparation. Tomograms of the gallbladder area were made in the prone position, beginning at 4 or 5 cm from the table top and increasing the distance by 2 cm for each film, for a total of four or five films. Two ml per Kg of body weight of a low sodium, water soluble, 50 to 65 percent iodized urographic medium was diluted with an equal volume of five percent dextrose in water, and infused in ten to 15 minutes. Tomogram studies were repeated immediately after the infusion. The gallbladder remained opacified for 30 to 45 minutes following the intravenous infusion.—*Paul M. Dassel, M.D.*

Wyatt, A. P. Prolonged symptomatic and radiological remission of colonic gas cysts after oxygen therapy. *Brit. J. Surg.*, Oct., 1975, *62*, 837–839. (From: The Brook Hospital, London, England.)

Oxygen therapy was an effective treatment for symptomatic primary pneumatosis cystoides intestinalis. The cysts shrank or disappeared, and symptoms subsided following inhalation of oxygen.

The colonic gas cysts were associated with the following complaints in patients treated by oxygen breathing: diarrhea, excessive flatus, abdominal pain, mucus and occasionally blood in the stool, and mild incontinence. There were one male and five female patients, all of whom had either coexisting cardiac or pulmonary disease.

Humidified oxygen at eight liters/minute was delivered to a mask with an inflatable rim. This concentration resulted in an inspired oxygen of 70–75 percent, and PaO_2 levels in excess of 300 mm Hg. Therapy was given for a minimum of 16 hours a day, and continued for 48 hours after complete disappearance of all cysts. Daily roentgenograms of the abdomen and chest were made to monitor cyst size, and to exclude atelectasis related to oxygen therapy.

The pneumocysts disappeared in each case between the fourth and seventh days. Symptomatic relief was dramatic and was associated with decreasing size of the cysts. In two cases the cysts reappeared at one and one and one-half years.—*Paul M. Dassel, M.D.*

Kim, Dong K., McSweeney, James, Yeh, Samuel D. J., and Fortner, Joseph G. Tumors of the liver as demonstrated by angiography, scan and laparotomy. *Surg., Gynec. & Obst.*, Sept., 1975, *141*, 409–410. (From: The Departments of Surgery, Diagnostic Radiology and Nuclear Medicine, Memorial Sloan-Kettering Cancer Center, New York, N. Y.)

The accuracy of detection and localization of tumors of the liver by angiography and scan was analyzed in 118 patients. Primary or metastatic hepatic tumors were found at laparotomy in 91 percent of the cases. Primary hepatomas and metastatic carcinoma of the colon accounted for 65 percent of these tumors. Benign lesions were found in nine percent of the patients.

Angiography through the celiac and superior mesenteric arteries, and ^{99m}Tc sulfur colloid liver scan were done preoperatively in each case.

Neoplasms were detected by angiography in 93 percent of the cases and by scan in 87 percent, for a combined accuracy of 97 percent. Localization of the tumor by angiography was correct in 75 percent, and by scan in 62 percent of these patients. The common error in both angiography and scan was to localize lesions to the right lobe. However, 11 of 39 resectable tumors were considered nonresectable in preoperative studies.

Angiography and scan are the best available means of diagnosing hepatic tumors, but resectability of a lesion can be determined only at laparotomy.—*Paul M. Dassel, M.D.*

GIERSON, EUGENE D., STORM, F. KRISTIAN, SHAW, WILLIAM, and COYNE, SUSAN K. Caecal rupture due to colonic ileus. *Brit. J. Surg.*, May, 1975, *62*, 383–386. (From: UCLA Medical Centre, Los Angeles, and Department of Surgery, Sepulveda Veterans Administration Hospital, Sepulveda, Calif.)

Cecal rupture due to paralytic ileus of the colon is an unusual complication of pseudo-obstruction of the colon (Ogilvie's syndrome). A total of 18 cases has been found in the literature including the three presented here.

The patients are usually over 55 years of age and in each there was associated major illness, trauma, or recent surgery. Preoperative roentgenograms are not reliable for determining the presence of perforation, and free intraperitoneal air was absent in one-half the cases. The cecal diameter was always nine centimeters or larger and ranged in the reported cases up to 20 centimeters. The over-all mortality is 43 percent and because of this, prevention of perforation is important.

The authors suggest that if the cecum measures nine centimeters or more there is danger of perforation and they describe a simple, safe, "blow-hole" cecostomy for decompensation.—*E. Frederick Lang, M.D.*

VANDENDRIS, M., and GERARD, A. Les tumeurs malignes primitives des voies biliaires. (Primary malignant tumors of the biliary tract.) *Acta gastro-enterol. belg.*, May–June, 1975, *38*, 196–206.) (Address: A. Gerard, Service de Chirurgie, Institut Bordet, Rue Héger Bordet 1, B-1000 Bruxelles, Belgium.)

A total of 55 patients with primary malignant neoplasm of the biliary tract was seen in the 13 years between 1960–1973. Thirty-six of these had tumors of the gallbladder and 19 had tumors of the principal bile ducts.

The commonest single complaint among patients with gallbladder tumors was general malaise. Other common complaints were abdominal pain, jaundice, disturbed gastrointestinal motility, fever, and a palpable mass. Almost one-third of the total was inoperable at the time of discovery, seven of the 36 were subjected to radical resection, and only one survived for longer than five years.

Of the 19 patients with neoplasm of the biliary ducts, the presenting sign was jaundice in ten. More than one-half of the patients had one or more of the following: jaundice, general malaise, abdominal pain, pruritis, and anemia. Only two were subjected to radical resection and both died within six months.

The prognosis of these lesions is so poor because treatment is delayed as a result of late diagnosis. The absence of definitive symptoms until the disease is well advanced delays the diagnosis. It is apparent that radical surgery is not the complete answer. The authors suggest prophylactic cholecystectomy in the presence of cholelithiasis, and after a neoplasm is discovered, a combination of palliative surgery, radiation therapy, and chemotherapy.—*E. Frederick Lang, M.D.*

GYNECOLOGY AND OBSTETRICS

SCHABEL, STEPHEN I., BURGENER, FRANCIS A., REYNOLDS, JONATHAN, and GEPHARDT, GORDON. Radiographic manifestations of malignant mixed uterine tumors. *J. Canad. A. Radiologists*, Sept., 1975, *26*, 176–183. (From: The Departments of Radiology and Pathology, The University of Rochester School of Medicine and Dentistry, Strong Memorial Hospital, Rochester, N. Y.)

Malignant mixed uterine tumors contain both carcinomatous and sarcomatous elements. The stroma of carcino-sarcomas or mixed homologous tumors contain analogues of normal uterine tissue, while mixed mesenchymal tumors or mixed heterologous tumors contain stromal elements not normally found in the uterus, such as liposarcoma, chondrosarcoma or rhabdomyosarcoma. These aggressive tumors metastasize widely: five year survival is less than 20 percent. The metastases may contain any or all of the stromal elements found in the original tumor.

Case histories, surgical and autopsy pathological findings of 14 patients were reviewed in conjunction with their roentgenographic examinations. All patients were post-menopausal, and presented with uterine bleeding. Two had previous pelvic irradiation for cancer of the cervix and one for metrorrhagia. One patient had received prolonged diathermy treatment for pelvic inflammatory disease.

Roentgenograms of the pelvis were available in ten patients—eight had centrally located soft tissue masses, varying in size from 7×7 to 20×25 cm, consistent with the diagnosis of uterine enlargement. Five showed fine, punctate calcifications, localized to a small area within the mass. Five intravenous urograms were reviewed, two showed obstructive ureteropathy. The pelvic mass extended inferiorly and posteriorly to the bladder in one, suggesting local spread of tumor, confirmed at surgery.

Initial chest roentgenograms were normal. In twelve patients, pulmonary metastases were apparent within a year. The pattern varied from "cannon ball," nodular hematogenous dissemination, lymphangitic spread with pleural effusions, and hilar lymphadenopathy. Cavitary necrotic lesions and calcified nodules due to osteogenic sarcomatous components were confirmed at autopsy. The postmortem examinations also showed widely disseminated disease, involving liver, lymph nodes, kidneys, adrenals, bone, brain, etc.

The authors suggest that the roentgenographic

demonstration of new, faint, punctate calcifications in an enlarging uterus, associated with post-menopausal uterine bleeding, should raise the suspicion of mixed uterine tumors.—*Adele Altman, M.D.*

SCHULMAN, A., and HERLINGER, H. Urinary tract dilatation in pregnancy. *Brit. J. Radiol.*, Aug., 1975, *48*, 638–645. (From: Department of Radiology, Leeds (St. James's) University Hospital, Leeds 9, England.)

When contrast studies were carried out on pregnant women for bleeding or suspected placenta previa and when additional information was desired about fetal number, attitude, maturity, and normality, a single survey study, 20 minutes after the aortic injection, was made to include the uterus and the entire urinary tract. Over a period of several years (ultrasound has replaced many of these studies), films were obtained in many patients in whom there was no indication of previous or subsequent urinary tract disease except for short episodes of infection. Films of 220 of these patients were evaluated independently by each of two radiologists who, at the time of viewing of the films, knew nothing about the patients. The degree and localization of dilatation of the upper urinary tract were assessed and later this information was correlated with the mother's gravidity and with fetal maturity.

The study suggests that dilatation of the upper urinary tract is uncommon or mild before 21 weeks and that it appears abruptly shortly after this. Between then and delivery, little or no change in the incidence and severity of dilatation on either side occurs. In the latter half of pregnancy about three-quarters of the cases showed dilatation on the right side of moderate degree, and about one-third showed dilatation on the left side of somewhat lesser degree. Severe dilatation occurred infrequently (4.5 percent) on the right and was rare (1 percent) on the left.

In 10 percent of the patients, the left side was dilated more than the right and in 86 percent, the right side was dilated more than the left.

Dilatation of the ureter below the pelvic brim was never seen. In the latter half of pregnancy, 9 percent of the right ureters and 22 percent of the left ureters were displaced away from the midline, presumably by the enlarging uterus. Multigravid and primagravid women showed no difference in the incidence or severity of urinary tract dilatation after 20 weeks. The figures showed no evidence to suggest that urinary infection, in the present pregnancy or at any time in the past, produces a greater tendency to dilatation or more severe dilatation after midterm. —*E. Frederick Lang, M.D.*

GENITOURINARY SYSTEM

JOUVE, P., MONFORT, G., MORISSON-LACOMBE, G., DALMAS, J., and LECAQUE, G. A propos de 45 observations de valves urétrales de l'enfant. (Observations on 45 cases of urethral valves in children.) *J. de radiol., d'électrol. et de méd. nucléaire*, Aug.–Sept., 1974, *55*, 549–553. (Address: Pr. P. Jouve, Service central de Radiologie, C.H.U. Nord de Marseille, boulevard Pierre-Dramard, 13326 Marseille, Cedex 3, France.)

The authors stress the relative frequency of congenital urethral valves in children. They found that 45 cases in a series 1,800 uropathies were due to congenital malformation.

The urethral valves are congenital mucosal folds located at the posterior urethra, or at the verumontanum. The valves may be: (1) two leaves, separated, but the medial walls are in contact, but not fused, or they may be fused; (2) single leaflet unilaterally placed. These may be directed upwards to the bladder or downwards to the urethra; (3) a horizontal membrane forming a diaphragm, with a central opening.

The clinical findings include disturbed micturition, urinary tract infection, albuminuria, hematuria, renal and vesical lithiasis.

In the series reviewed, there were ten patients under six months of age of whom two were less than one month old.

The degree of involvement of the urinary tract is divided into four Stages:

I. The valve is roentgenologically demonstrated. This is the only finding, confirmed endoscopically.

II. The same as I, but with proximal involvement of the urinary tract. These changse are reversible after treatment of the valve.

III and IV. The pathological findings are the same, except that there is no renal insufficiency in Stage III.

The findings include: poor general condition of the patient, renal insufficiency (not in Stage III), pathological changes in the posterior urethra, bladder dilation and trabeculation, dilated ureters and renal pelves, pyelonephritis, vesico-ureteral reflux.

Excretion urography adequately demonstrates the changes in the kidneys, ureters, and bladder. Voiding cystourethrography is essential for demonstrating the valves and the condition of the urethra. —*William H. Shehadi, M.D.*

POLLACK, HOWARD M., POPKY, GEORGE L., and BLUMBERG, MYRON L. Hernias of the ureter: an anatomic-roentgenographic study. *Radiology*, Nov., 1975, *117*, 275–281. (Address: Howard M. Pollack, M.D., Department of Radiology, Episcopal Hospital, Philadelphia, Penn. 19125.)

Four new cases of herniation of the ureter are added to the previously recorded 120 cases. A breakdown of the reported sites of ureteral herniation is given with the most common sites being inguinal and femoral. Ureteroinguinal hernias are further sepa-

rated into paraperitoneal and extraperitoneal varieties. Since the ureteral hernia may be reduced on a supine film, the roentgenographic finding of a redundant loop of pelvic ureter which has been given the name of "curlicue ureter" should prompt further evaluation. This evaluation should include upright and appropriate oblique filming according to orientation of the redundant segment. The films should include the external genitalia. Recognition of the "curlicue ureter" and subsequent roentgenographic confirmation of the ureteral hernia could aid in avoiding inadvertent injury to the ureter during hernia repair.—*R. F. Kuhnhein, M.D.*

BEN-MENACHEM, YORAM, MARCOS, JULIO, WALLACE, SIDNEY, and MEDELLIN, HECTOR. Angiography of renal metastases. *Brit. J. Radiol.*, Dec., 1974, *47*, 869–874. (Address: Yoram Ben-Menachem, M.D., Hermann Hospital, 1203 Ross Sterling, Houston, Texas 77025.)

Renal metastases are commonly encountered at autopsy when clinical diagnosis of such metastases has not been made. Thirteen patients were studied by angiography for various reasons, such as pain or hematuria and the diagnosis of metastasis was made.

Seven of these patients had squamous cell carcinoma, of which five originated in the lung, and one each in the larynx and uterine cervix. In these seven patients, the angiogram disclosed encasement, amputation, and displacement due to the mass. In only a few cases was there slight hypervascularity in the periphery of the lesion, and this may have been inflammatory in tissues surrounding the metastasis. In six of the seven, renal involvement was bilateral.

One patient had an anaplastic carcinoma of the lung, and the renal involvement was bilateral and characterized by hypervascularity.

In five patients, the metastasis was from a renal cell carcinoma in the opposite kidney, and in two of these the primary and the metastasis were discovered simultaneously. This presentation naturally gives rise to the suggestion that there were simultaneous bilateral primary carcinomas. This question remains open. In some of these patients, the examination showed a large tumor in one kidney and at least two small lesions in the opposite kidney, somewhat more suggestive of metastasis. In one of the five, the metastasis exhibited arterial encasement and amputation, but in the other four, there were multiple irregular tumor vessels with an intense tumor blush.

Thus, in most cases close correlation was found between the histology of the tumor and the vascular pattern of its metastases. In six of the seven patients with metastasis from lung primary lesions, five had bilateral renal metastasis.

The principal value of the examination appears to be in patients with metastases who are bleeding significantly and in whom arrest of the bleeding by infarcting the tumor is possible. In a patient with a primary renal tumor on one side and a single metastasis on the other side, surgical removal of the primary is probably contraindicated.—*E. Frederick Lang, M.D.*

CREMIN, B. J. The "spinnaker sail" appearance of the posterior urethral valve in infants. *J. Canad. A. Radiologists*, Sept., 1975, *26*, 188–191. (From: Groote Schuur Hospital and Red Cross Children's Hospital, University of Cape Town, South Africa.)

Any male neonate presenting with a distended bladder or urinary ascites should be suspected of having posterior urethral valves, which are an exaggeration of the normal ridges of mucous membrane that extend downward and laterally, almost surrounding the urethra a little above the membranous region (Type 1). The author believes this to be the only true obstructing valve.

Fifty cases, seen between 1967 and 1973 were reviewed; 30 were under six months of age. Abdominal distention and vomiting were common presenting symptoms in infants. Other symptoms included failure to thrive, difficulties in micturition, ascites, renal masses and pneumothorax. Vesico-ureteral reflux was common early in life, less frequent in later childhood.

The preferred diagnostic approach includes preliminary intravenous urogram and determination of serum electrolytes. Voiding cystourethrography is the definitive examination. The bladder may be trabeculated; the prostatic urethra is dilated. In lateral projection, the valve has a ballooning spinnaker appearance. (*Webster*: spinnaker—a large triangular baggy headsail used on some racing yachts when running before the wind.) In severe neonatal cases, the "sail" balloons distally causing further obstruction of the urethra which emerges from a tiny aperture situated dorsally and proximally.

In young infants, the valve is a sail-like structure consisting of a single fold rather than the commonly accepted "pair of sails." This concept is important if ablation using an insulated diathermy hook is contemplated.

Posterior urethral valves are the most common cause of neonatal urinary ascites and resulted in 67 percent mortality during the first three years of this study. Mortality rates have been improved significantly in recent years by early recognition of the lesion, correction of electrolyte imbalance, and performing initial drainage ureterostomies in poor risk cases.—*Adele Altman, M.D.*

HUG, I., and MIHATSCH, J. M. Die primäre oxalosis: Fallmitteilung mit radiologisch-pathologisch-anatomischer Korrelation und Literaturübersicht. (Primary oxalosis: report of a case with radiologic-pathologic-anatomi-

cal correlation and review of the literature.) *Fortschr. a. d. Geb. d. Röntgenstrahlen u. d. Nuklearmedizin*, Aug., 1975, *123*, 154–162. (Address: Dr. med. Iso Hug, Universitätsinstitut für Medizinische Radiologie, Kantonsspital, CH-4004 Basel, Switzerland.)

A 20 year old woman with no familial history of kidney disease was found to have primary oxalosis. The first indication of abnormality was recurrent syncope. This was found to be due to total heart block, and subsequent examination of other structures showed a fully developed uremia, a nonfunctioning left kidney, and an extensively damaged right kidney. She was supported by periodic dialysis.

In the following three years while this was being carried out, she developed depression, generalized skeletal pain, with immobilization and irreversible contractures in the left hand, the skin became indurated and discolored, crystals became visible in the perimacular region in the eyes, and she died suddenly apparently because of disturbance in cardiac rhythm.

Roentgen findings included severe calcinosis. The right kidney was contracted and very dense. There was diffuse skeletal dystrophy with high-grade secondary hyperparathyroidism and diffuse arteriosclerosis, subcutaneous calcification, and periarticular calcification.

The patient was subjected to autopsy.

Excellent illustrations show the skeleton in a relatively normal state and subsequently after the full development of secondary hyperparathyroidism. —*E. Frederick Lang, M.D.*

WAGENKNECHT, L. V., and WEHLING, H. Wertigkeit röntgendiagnostischer Verfahren bei retroperitonealer Fibrose. (The value of roentgen diagnostic methods in retroperitoneal fibrosis.) *München-med. Wchnschr.*, Nov., 1975, *117*, 1835–1838. (Address: Priv.-Doz. Dr. med. L. V. Wagenknecht, Urologische Klinik und Poliklinik, der Universitätskliniken Hamburg-Eppendorf, D-2000 Hamburg 20, Martinistrasse 52, Germany.)

The cause of primary retroperitoneal fibrosis is still unknown. Its occurrence in some patients who have used methysergide is known, but a large number remains idiopathic. The relationship of the lesion with the iliac vessels has led to the suggestion of vascular disease as a possible basis; other suggestions have included autoimmune disease, lymphatic obstruction, local inflammatory changes, and systemic diseases. The authors have observed a total of 48 patients. They present detailed descriptions of two, one with idiopathic retroperitoneal fibrosis, and the other following treatment with methysergide for ten years because of migraine.

The most satisfactory method for making the diagnosis is intravenous urography. Plain film studies of the abdomen occasionally show nonspecific changes in the psoas muscles. Medial displacement and compression of the ureters are typical early signs well shown by urography. In 98 percent of patients the disease is unilateral at first, and in 70 percent it later becomes bilateral. In 75 percent the involved ureteral segments are in the region of fourth and fifth lumbar vertebrae. Examination in the lateral view and during respiration adds further information in these individuals.

Contrast study of the inferior vena cava is the second most important roentgenologic method of investigation. In about 42 percent of patients, the inferior vena cava is compromised, and in more than half of these the iliac veins as well. The lateral view of the contrast study of the vena cava is likewise important as the vessel is displaced anteriorly. Although thrombosis and thrombophlebitis occur relatively frequently, almost never is there embolization because the narrowing of the vena cava prevents this.

Lymphangiography and arteriography are of value and are particularly valuable in determining the downward extent of involvement which may not be shown in studies of the urinary tract.—*E. Frederick Lang, M.D.*

SKELETAL SYSTEM

SCHNEIDER, K., ERD, W., LOBENWEIN, E., PENNER, E., and WILLVONSEDER. Eosinophiles Granulom (Histiozytosis-X) mit pulmonaler und ossärer Manifestation. (Eosinophilic granuloma (histiocytosis-X) with lung and bone manifestations.) *Wien. klin. Wchnschr.*, Aug., 1975, *15*, 486–488. (Address: Dr. K. Schneider, Medizinische Universitätsklinik, Garnisongasse 13, A-1090 Wien, Austria.)

A 26 year old man presented with a spontaneous fracture of the neck of the right femur through an osteolytic lesion. A chest roentgenogram demonstrated an appearance suggesting interstitial pulmonary fibrosis. Tuberculosis and wide-spread malignancy were considered, but were excluded by appropriate investigation.

Isotope studies with strontium showed what might have been a second lesion in the humerus, but there was no roentgen change to indicate this. There were calcified hilar lymph nodes, and the skin test was positive for tuberculosis. He was therefore put on anti-tuberculous treatment before the operation.

At the time of surgery on the femoral fracture, material for microscopic investigation was obtained and a clear differentiation between eosinophilic granuloma and hyperparathyroidism could not be established histologically. Clinical and biochemical evidence of disturbance in calcium metabolism was

not present, however. A lung biopsy was carried out and this established the diagnosis of esoinophilic granuloma. The combination of pulmonary and skeletal change due to eosinophilic granuloma is rare.—*Modified Published English Abstract.*

LOEFFLER, R. KENNETH, DISIMONE, ROBERT N., and HOWLAND, WILLARD J. Limitations of bone scanning in clinical oncology. *J.A.M.A.*, Dec., 1975, *234*, 1228–1232. (Address: R. Kenneth Loeffler, M.D., NEORAD, Radiation Oncology Associates, 430 Lake Avenue, N.E., Massillon, Ohio 44646.)

One hundred patients with cancer were assessed by complete bone scans and roentgenologic surveys. In seven patients, the scans with technetium-99m labeled phosphate compounds were completely normal, but roentgenograms showed definite abnormalities consistent with metastatic disease. Primary lesions of these seven include breast in three, kidney in two, endometrium in one, follicular carcinoma of the thyroid in one. Since the bone scan is specific for neoplastic disease involving the bone, an abnormal bone scan in the absence of definitive changes on roentgenograms or other indications of generalized neoplasia is not sufficient indication to assume that the patient has metastases, particularly if such assumption results in failure to offer potentially curative therapy. However, the bone scan may be very helpful in indicating areas from which biopsy specimens could be obtained. The study emphasizes the need to obtain bone surveys in patients where a normal bone scan occurs in the presence of significant symptoms.—*H. William Strauss, M.D.*

TOMENO, B., and FOREST, M. Fréquence et nature des tumeurs osseuses: 25 ans d'expérience en service orthopédique. (Occurrence and nature of bone tumors: 25 years experience in an orthopedic service.) *Presse méd.*, Sept., 1975, *31*, 2243–2244. (Address: Dr. B. Tomeno, Clinique chirurgicale orthopédique et réparatrice, Service B, Pavillon Ollier, Hôpital Cochin, 27, rue du Faubourg-Saint-Jacques, F 75674, Paris Cedex 14, France.)

A total of 1,329 benign and malignant tumors of bone were encountered in a 25 year period among 63, 798 patients hospitalized in a hospital devoted to orthopedics and rehabilitation. Fifty-five percent of the lesions were benign. Of 516 (45 percent) tumors which were malignant, 320 (62 percent) were primary, 163 (32 percent) were metastatic, and 33 (6 percent) could not be classified either primary or secondary. Of the metastases, 30 percent were from breast, 15 percent from the kidney, 8 percent each from the digestive tract and the lung, 6 percent from the prostate and 5 percent form the thyroid.

Several aphoristic generalizations are offered. The most common bone tumor is metastasis. Beyond 50 years, osseous lesions suggesting tumors should be considered myeloma or metastasis until proved otherwise. The most frequent primary malignant tumors are, in order; osteosarcoma, in the adolescent; chondrosarcoma, between the ages of 30 and 45 years; and reticulum cell sarcoma, including Ewing's tumor. The three most frequent benign tumors are exostosis, giant cell tumor, and osteoid osteoma. The lesions which most frequently undergo malignant degeneration are giant cell tumors, exostosis, (particularly if multiple), chondromas, adamantinomas, and chordomas.—*Augmented Published English Abstract.*

DAVIDSON, J. K. Radiology of aseptic necrosis of bone. *J. belge de radiol.*, May–June, 1975, *58*, 189–204. (Address: Department of Diagnostic Radiology, Western Infirmary, Glasgow, G11 6NT, Scotland.)

Aseptic necrosis of bone, also termed osteonecrosis, infarction, or avascular necrosis is commonly associated with trauma. It can be related to other conditions such as prolonged steroid therapy, the hemoglobinopathies, and dysbaric disease. The bone becomes nonviable due to loss of blood supply.

The actual necrosis can occur within six to twelve hours after arterial occlusion, but the earliest roentgenographic sign of an absolute increase in bone density may not be present for six months following trauma. This increase in density is secondary to revascularization of the necrotic bone with the laying down of new bone on the dead trabeculae. The articular cartilage can remain healthy for a considerable time, but it finally may undergo a structural failure and collapse into the underlying necrotic bone. This results in a step formation or sequestration of the previously smooth joint surface. A radiolucent crescent sign may appear in the subcortical area indicating a fracture through the necrotic bone.

The most common sites include the femoral head, the talus, the humerus, and the carpal navicular bones. In femoral neck fractures it is extremely difficult to predict if necrosis of the head will occur. This cannot be ascertained even at surgery, and appropriate follow-up roentgenograms are of extreme importance.

Severe talar injuries produce a very high incidence of aseptic necrosis, but simple dislocations show an incidence of only 28 percent. About 10 to 15 percent of carpal navicular fractures result in osteonecrosis. This is seen only after immobilization for four ro six weeks and osteoporosis has developed in surrounding bones.

Dysbaric osteonecrosis, Caisson disease, most commonly affects the distal femoral shaft and never involves the knee joint surface. Spontaneous osteone-

crosis is often associated with steroid or immunosuppressive therapy, and alcoholism. Lesions are multiple and bilateral.—*Arch H. Hall, M.D.*

LATEUR, L., and BAERT, AL. Radiological features in Reiter's disease. *J. belge de radiol.*, May–June, 1975, *58*, 205–211. (Address: Prof. A. Baert, Dienst Röntgendiagnostiek, Universitaire Kliniken St.-Rafaël, Capucijnenvoer 35, 3000 Leuven, Belgium.)

The clinical triad of conjunctivitis, urethritis, and arthritis was first described by Reiter some 60 years ago. The conjunctivitis may be subclinical and of short duration but it can lead to chronic iritis. The urethritis is abacterial in type with some exceptions. The arthritis affects one or more joints with asymmetrical distribution usually involving the lower limbs or the sacroiliac joints. Fifty percent of cases become chronic but are seldom incapacitating such as in rheumatoid arthritis. A fourth symptom may develop: painless mucocutaneous lesions which are indistinguishable from psoriasis.

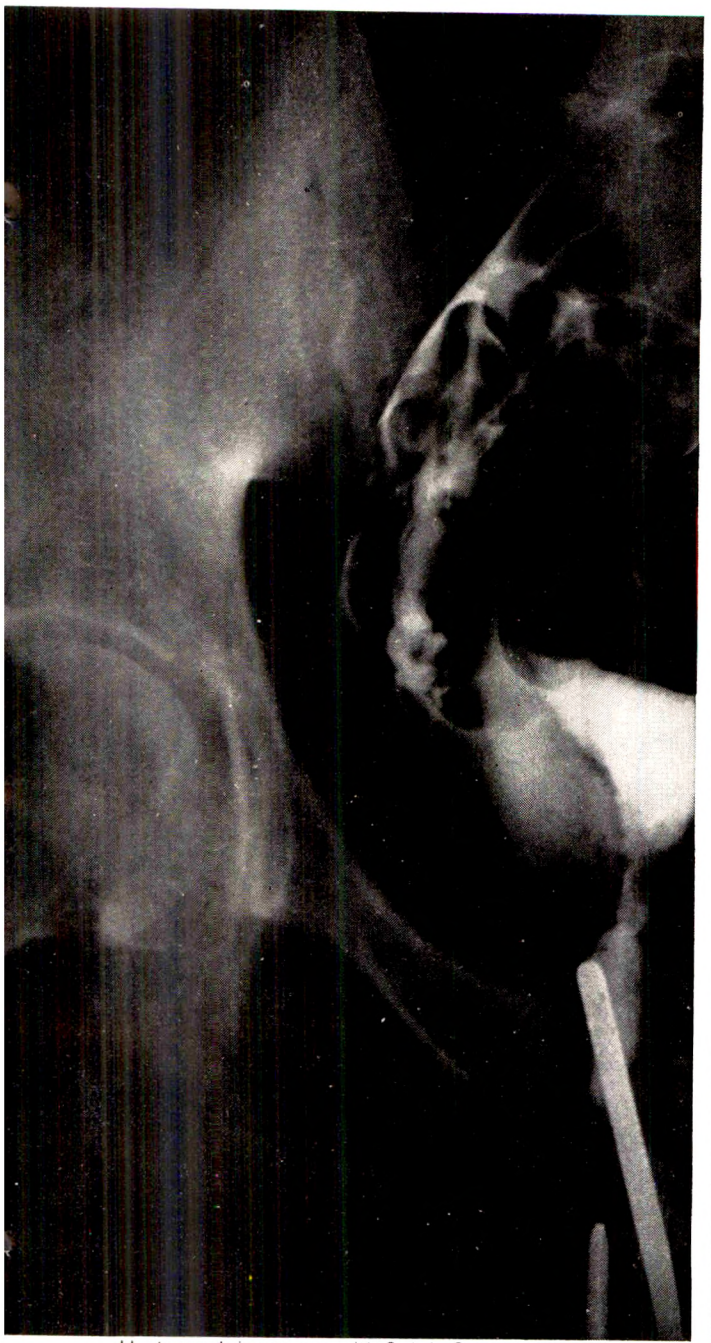
The roentgenological features are derived from the synovitis and fibrositis. The features often cannot be differentiated from ankylosing spondylitis, psoriatic arthritis, or rheumatoid arthritis. Initially they include perarticular soft tissue swelling, periarticular demineralization, and periosteal ossification. Joint space narrowing develops after one month.

In the chronic stage Reiter's disease closely simulates advanced rheumatoid arthritis with marked joint space narrowing leading to ankylosis, articular cortical erosions, and luxations, but the lesions are asymmetrical and do not affect the upper extremities. More than half the cases involve dorsal calcaneal spurs and erosions as well as unilateral sacroiliac disease. In the spine there may be one or more large unilateral cowhorn shaped osteophytes. Bony proliferation at the inferior margins of the descending ischial rami is common.—*Arch H. Hall, M.D.*

GALASKO, C. S. B. The significance of occult skeletal metastases, detected by skeletal scintigraphy, in patients with otherwise apparently "early" mammary carcinoma. *Brit. J. Surg.*, Sept., 1975, *62*, 694–696. (From: Department of Surgery, Royal Postgraduate Medical School, London, England.)

Occult skeletal metastases have been found on scans in about 25 percent of patients with "early mammary carcinoma." The significance of these occult lesions was evaluated by following 60 consecutive patients with early mammary carcinoma who had a skeletal scintigram with fluorine-18 when they first presented. All patients had been followed for a period of five years. Following initial evaluation, all patients had a mastectomy, either simple or radical, followed by a course of radiation therapy to the local lymph nodes. Twelve of the 50 patients had abnormal scans. All twelve subsequently developed disseminated cancer and nine died of their carcinoma. Two are alive at five years with disseminated disease. Of the 38 patients with negative scintigrams, ten have subsequently developed disseminated disease and eight have died from their cancer. Two are presently alive with disseminated disease, and 25 are alive with no evidence of recurrence (three patients died of intercurrent disease).

The results of this study suggest that there may be three stages of mammary carcinoma: (1) early, where there is no clinical roentgenographic or scintigraphic evidence of disseminated disease; (2) early advanced disease where occult skeletal metastases are seen on scintigraphy but there are no clinical or roentgenographic evidence of disseminated disease; and (3) advanced disease, when metastases are obvious on clinical or roentgenographic examination. Clinical trials should evaluate each group separately. The interesting group would appear to be those with occult skeletal metastases, since recent evidence suggest that chemotherapy is most effective when tumor deposits are very small. It is possible that these patients should be treated by some form of therapy as well as local excision when they first present.—*H. William Strauss, M.D.*



Hysterosalpingogram with Salpix Contrast Medium.



24-hour postinjection x-ray of same patient.

now you see it

now you don't

With Salpix as your contrast medium, your gynecologic patient needn't undergo the 24-hour postinjection x-ray usually required with iodized oils. Water-soluble Salpix leaves virtually no irritating radiopaque residue to produce foreign-body reactions, yet it provides the viscosity needed for adequate visualization.

Contraindications: Contraindications to hysterosalpingography include the presence of severe vaginal or cervical infections, existing or recent pelvic infection, marked cervical erosion or endocervicitis, and pregnancy. The procedure is contraindicated during the immediate pre- or post-menstrual phase.

Sensitivity Test: If indicated in the patient's history, an intracutaneous skin test or sublingual absorption observation may be done with 0.1 cc Salpix.

Warning: Not for intravenous use.

© ORTHO PHARMACEUTICAL CORPORATION 1970

CONTRAST MEDIUM

Salpix

TRADEMARK

EACH CC CONTAINS:

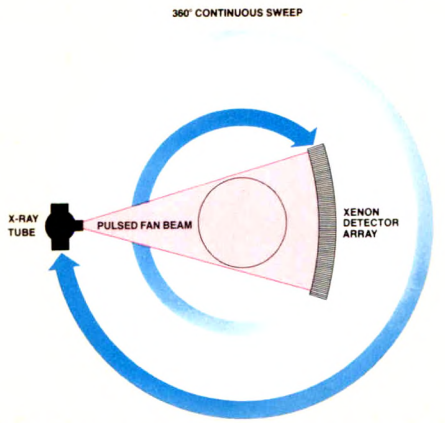
sodium acetrizoate 0.53 g and
polyvinylpyrrolidone 0.23 g

Ortho

ORTHO PHARMACEUTICAL CORPORATION • RARITAN, NEW JERSEY 08869

GE research solves the primary problem of existing total body scanners—motion unsharpness.

GE fast-scan computerized tomography: a whole new generation.



Third generation: GE's continuously rotating pulsed fan beam scanning. 5 to 10 seconds.

First and second generation units aren't fast enough for total body scanning.

First and second generation computerized tomography systems have one major problem: image blurring caused by patient movement during body scans.

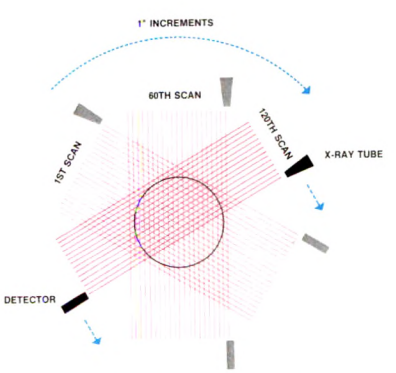
General Electric research has developed a fast-scan technology that is launching a new third generation of computerized tomography (CT) systems. The faster scans provide clear, sharp images.

During body studies, patient movement caused by breathing can result in motion unsharpness.

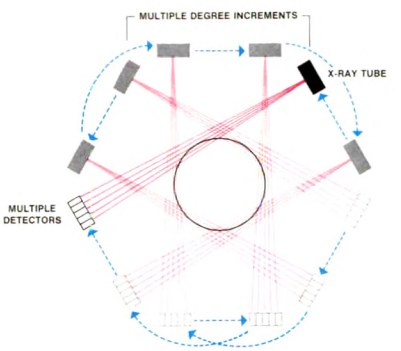
To really tackle this problem, a scan should tal less time than a patient can hold his breath comfortably—10 seconds or less. However, existing computerized tomography systems cannot match this speed.

First generation units, using a pencil beam witl 1° incremental rotate-and-translate principle, take 4½ to 5½ minutes to complete a 180° sca

Second generation systems use multiple penci beams and more detectors—up to 30. Rotation in larger angular increments. This configuratic takes from 20 seconds to 3½ minutes per scar



First generation: Pencil beam rectilinear scanning. 4½ to 5½ minutes.



Second generation: Multiple pencil beam rectilinear scanning. 20 seconds to 3½ minutes.

GE develops continuously rotating fan beam technology for fast-scan capability.

In developing an entirely new total body system, GE engineers and scientists abandoned the incremental rotate-and-translate approach of first and second generation units, with their inherent mechanical instability and resultant speed limitations. Instead, GE used a simpler, more stable mechanical approach, in which the tube and detectors rotate smoothly about the body in a continuous 360° scan, without need for translation.

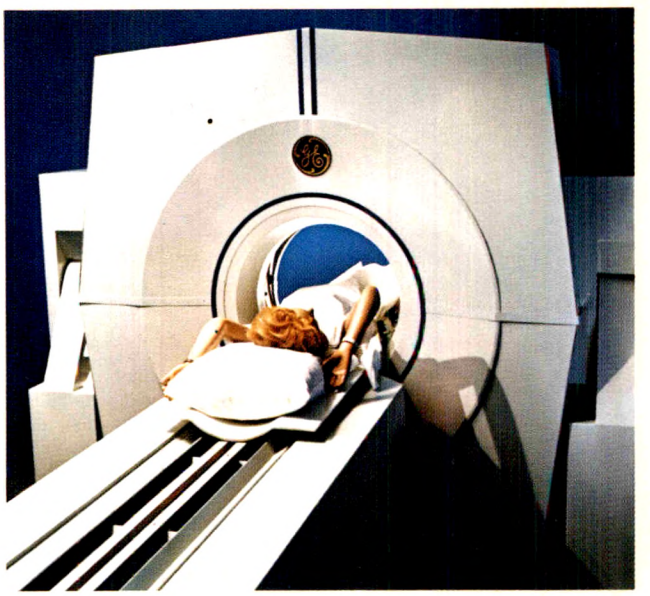
This new third generation technology combines a continuously rotating, pulsed, wide fan x-ray beam with a unique high-pressure xenon detector array of up to 320 stable detectors. Advanced electronics are included to read out the huge volume of data. And GE has successfully conceived and implemented a new computational approach compatible with diverging fan beam geometry.

Third generation fast-scan technology proven on CT/M system.

GE's first application of fast-scan technology utilized computerized tomography's tissue density differentiation capability in the challenging area of breast examinations. This unit, called the CT/M system, is currently being clinically evaluated. Scans are completed in just 10 seconds. Patient handling is minimized. If you are interested in further information about the CT/M system, contact your GE representative or write for Publication 4675.



CT/M System



CT/T System

CT/T system performs body scans in less than 5 seconds.

The CT/T system for total body scanning is moving into the clinical environment. Scan time for the CT/T unit is 4.8 seconds. GE engineers believe this unprecedented scanning speed will provide consistently sharp, clear images for body studies. First production units are scheduled for the last half of 1976. The new CT/T systems represent the culmination of one of General Electric's most extensive research and development programs.

There's a corporate commitment behind GE scanning equipment.

All General Electric scanning systems are backed by the same company that has been serving radiology since the revolutionary Coolidge x-ray tube was introduced 63 years ago. And that kind of corporate dedication to excellence in medical equipment continues today . . . with the development of continuously rotating, pulsed fan beam technology.

As you consider CT scanning equipment, remember GE's continuous commitment to technology, product quality and service. That commitment is an important part of every GE medical system.

Fast-scan CT: backed by GE.

GENERAL ELECTRIC

Improving productivity is important to radiology departments. GE equipment can help make it happen.

GE: committed to helping x-ray departments do more.

The prime concern of any radiology department is serving patients. And the more efficient that service, the more everyone benefits. That's why GE is committed to providing systems that help your x-ray department make optimum use of time, space, resources and personnel. Here are some examples:

MMX system...optimum capability and efficiency for breast exams, with minimum patient apprehension.

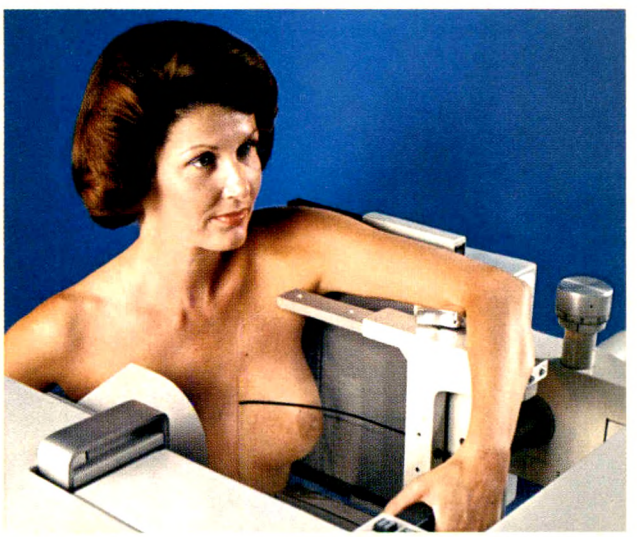
This dedicated, self-contained system offers a wide variety of tube angulations and compression positions for virtually any breast projection. Today, in hundreds of hospitals, MMX™ is delivering high quality images of the entire area of interest, using xeroradiography or mammography, including new fast screen/low dose film procedures. The technologist can perform exams quickly and confidently, assured of minimum retakes.

Patient confidence is also increased, because the patient can maintain visual contact with the technologist throughout the exam.

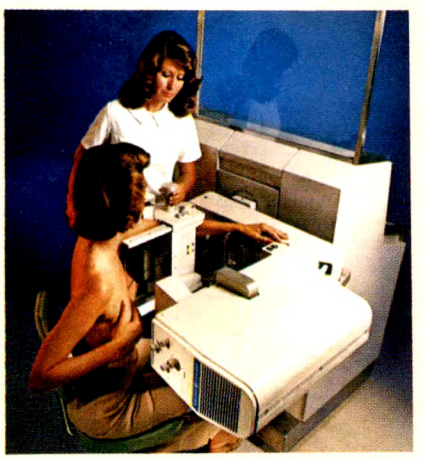
Quantamat™ automatic exposure control provides correct exposure, regardless of breast size or firmness. This control assures consistent image density from one exam to the next. Resulting image quality is excellent, from craniocaudad views to axillary and mediolateral.

With this specialized system, any radiology room can become a dedicated breast examination area. Since no wall, ceiling or floor supports are needed, installation is fast and inexpensive. If department layout changes at a later date, the MMX system can be easily moved to a different room.

If seeing is believing, here's your opportunity to do so. Now, the ease and versatility of positioning and operating the MMX system are demonstrated in a new desk-top motion picture and related application guide. Featured are positioning directions, suggested technics, a critique of actual films and more. Ask your GE medical systems representative to arrange for a showing and a supply of application guides for your department.



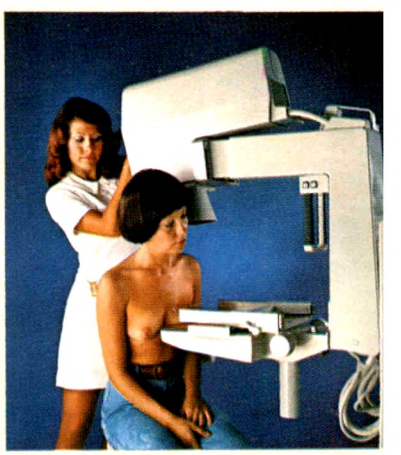
Axillary view



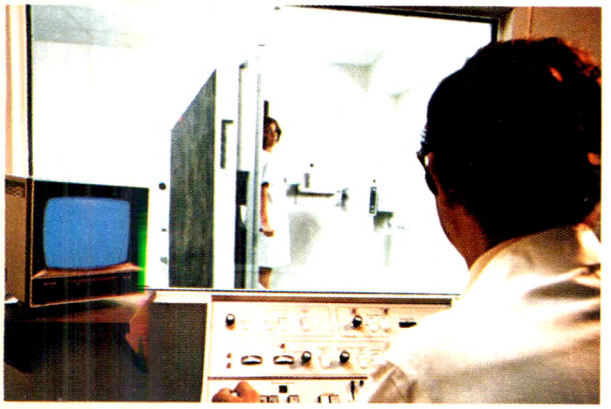
Mediolateral view



Supine mediolateral view



Craniocaudad view (with tube unit angulated)

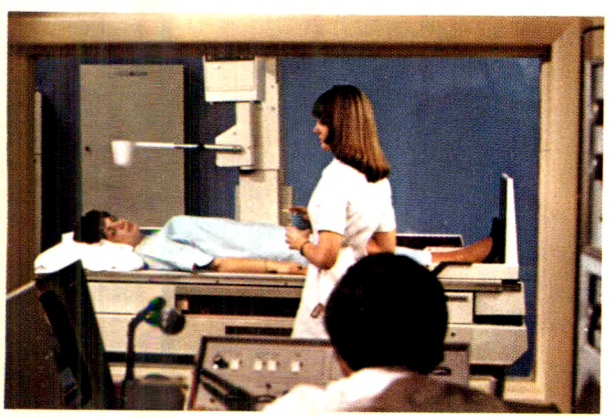


Televix remote control system...technic versatility provides more image information; improves patient flow.

Versatile, proven performance makes the Televix™ system the logical alternative to classical approaches. Any tableside R&F procedure can be handled by Televix remote control, with some very real advantages.

Maximum image information—plus better image quality—result from the system's optimized geometry (43-inch SID). And, there's greater convenience because of integrated multi-procedural capability...immediate changeover between fluoroscopy, Bucky radiography and true linear tomography. This significantly improves patient flow and, in many hospitals, results in operational cost savings up to 25%. In addition, there's reduced radiation exposure to the radiologist, because of total remote control. And, fewer retakes, less total time per examination means less exposure to patients too...the result of sharp fluoro images and immediate recording of precisely what has been viewed, as well as Quantamat™ automatic exposure control that provides the desired density in every image.

Televix system smoothly handles the full range of morning GI studies, including longitudinal oblique angle fluoroscopy in any scanning position, with 105 mm photospotting that can record up to 10 images per second, plus Bucky radiography. Then, in the afternoon, Televix takes on the department's high volume of radiographic and tomographic procedures.

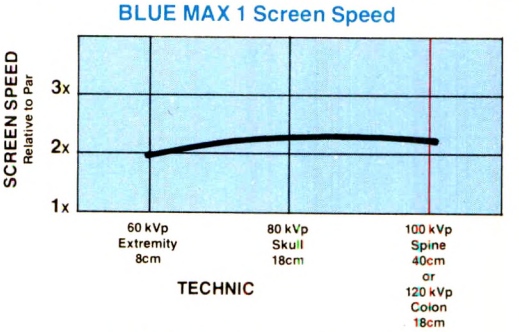


Blue Max screens... precise image quality and reduced radiation without drastic changes in equipment or technic.

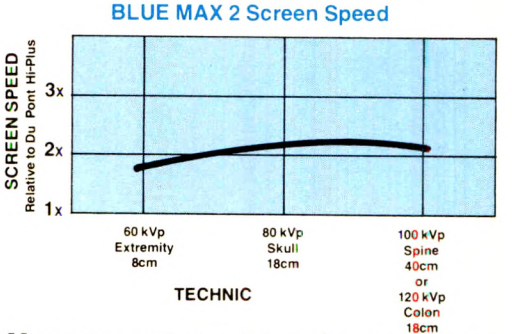


GE Blue Max™ screens provide maximum image quality and diagnostic data at much lower radiation levels than standard screens. Blue Max 1 and 2 intensifying screens feature GE-developed lanthanum oxybromide phosphors which absorb twice the x-rays, compared to standard calcium tungstate screens. Thus, Blue Max screens deliver the same image quality at half the mAs. This allows shorter exposure times, reducing motion unsharpness. Standard cassettes and any blue-sensitive film can be used. Blue Max screens are blue-emitting, so they require no unusual darkroom lighting or special processing techniques.

BLUE MAX 1 Screen Speed



BLUE MAX 2 Screen Speed



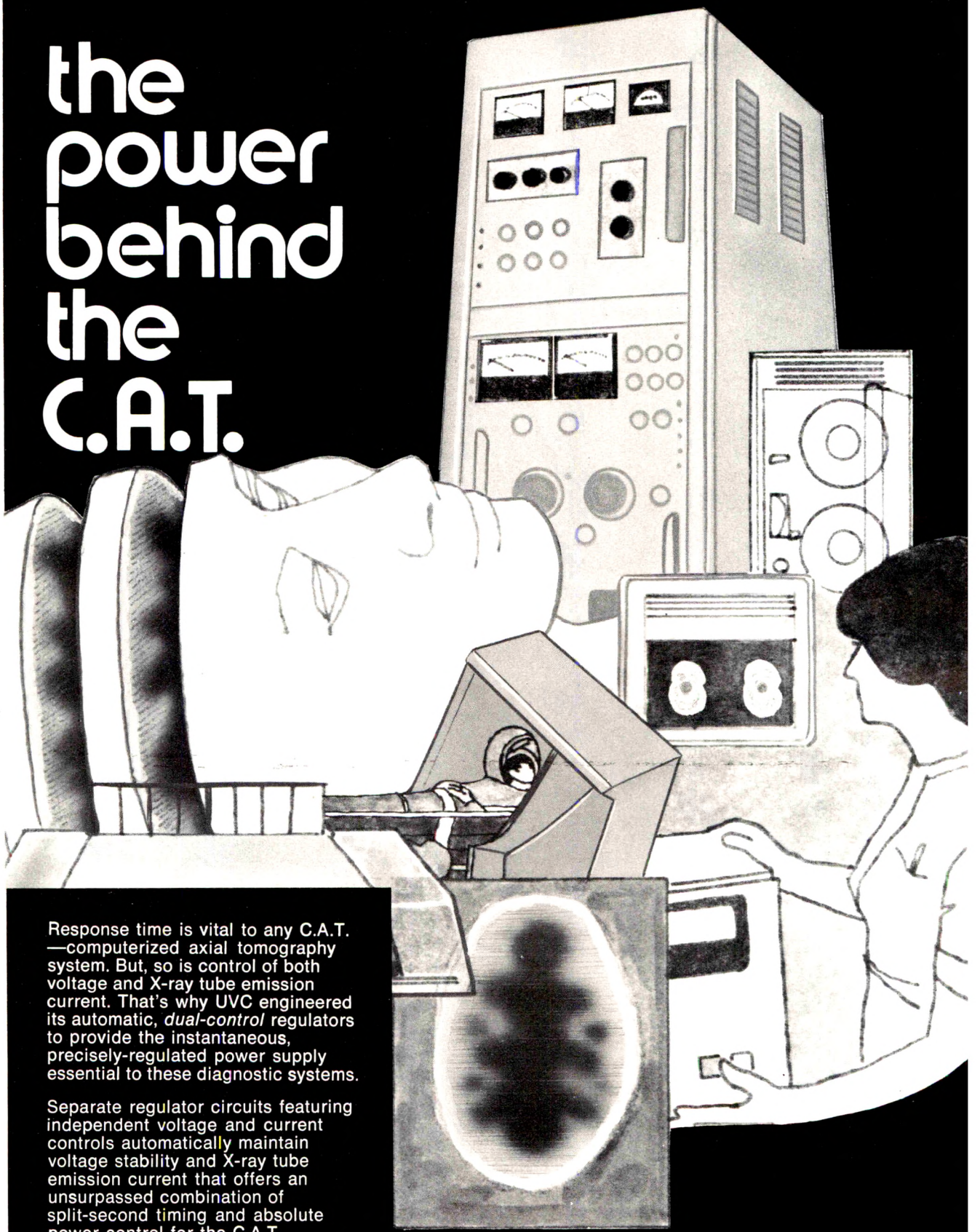
Blue Max screens' consistent 2x speed over the diagnostic kVp range makes modification of technic charts simple.

General Electric has many other time-saving, cost saving systems to improve radiology productivity. Find out how these systems can help your x-ray department do more. Talk to your GE representati
General Electric Medical Systems
Milwaukee, Toronto, Madrid

GE: leading the way in x-ray.

GENERAL ELECTRIC

the power behind the C.A.T.



Response time is vital to any C.A.T. —computerized axial tomography system. But, so is control of both voltage and X-ray tube emission current. That's why UVC engineered its automatic, *dual-control* regulators to provide the instantaneous, precisely-regulated power supply essential to these diagnostic systems.

Separate regulator circuits featuring independent voltage and current controls automatically maintain voltage stability and X-ray tube emission current that offers an unsurpassed combination of split-second timing and absolute power control for the C.A.T.

Because UVC equipment has proved so constant, safe, and sure in repeated clinical use, it is now the first choice of most C.A.T. systems. Insist on UVC-equipped C.A.T.s . . . *more power to you.*

Write or call

UNIVERSAL VOLTRONICS CORPORATION

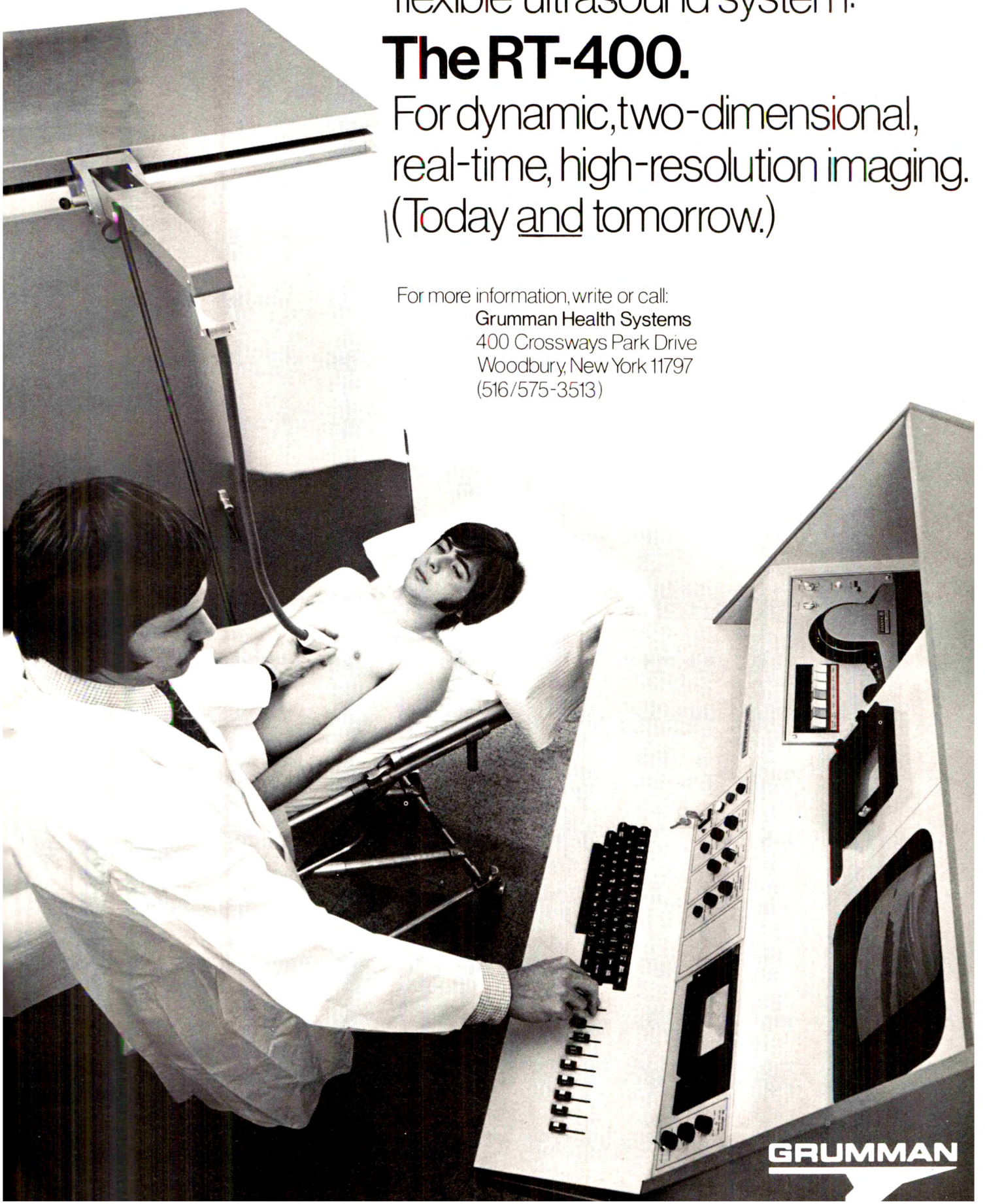
27 Radio Circle Drive, Mount Kisco, N.Y. 10549
(914) 241-1300

Now the complete,
flexible ultrasound system:

The RT-400.

For dynamic, two-dimensional,
real-time, high-resolution imaging.
(Today and tomorrow.)

For more information, write or call:
Grumman Health Systems
400 Crossways Park Drive
Woodbury, New York 11797
(516/575-3513)



Synerview™ produces images of startling worth.



Computed Tomography is here now and it works. From the array of today's CATs will emerge the systems of tomorrow.

Today, the fine detail apparent in Computed Tomography images has generated a great deal of interest and excitement in the field of diagnostic visualization.

It takes no great insight to predict that this is only the beginning. In the not-distant future today's CT imaging systems may appear almost primitive.

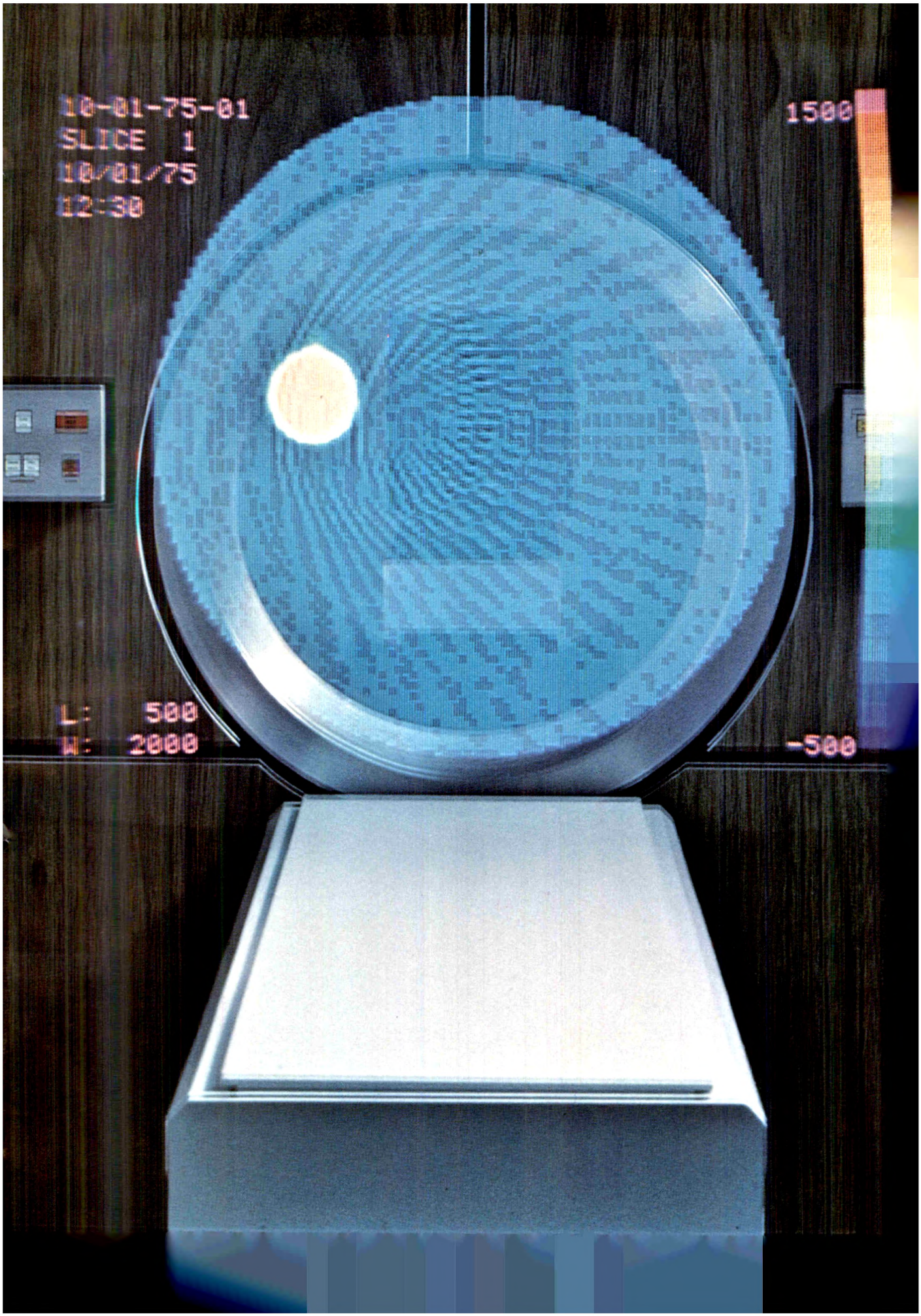
The developmental thrust behind Synerview has been painstakingly thorough to circumvent "generation" obsolescence. The concept of Computed Tomography is unquestionably viable. But at this early stage of its development, implementation is still open to a great deal of speculation.

The fact is that some of today's designs will not be able to live up to tomorrow's standards. After time and experience have taken the measure of today's systems, a few will remain.

One of them will be Synerview.

Discuss Synerview with your Picker representative. Or write Picker Corporation, 595 Miner Road, Cleveland, OH 44143.

PICKER®
ONE OF THE C.I.T. COMPANIES


10-01-75-01
SLICE 1
10/01/75
12:30
1500
L: 500
W: 2000
-500

lea & febiger

WASHINGTON SQUARE
PHILADELPHIA, PA. 19106

THE SPINE:

A Radiological Text and Atlas, 4th ed.

This exceptionally complete book considers the vertebral column as a system and is, through this unique approach, reviewed in full relationship to osseous disease, diseases of the central nervous system, metabolic and nutritional disturbances, effects of trauma, degenerative and neoplastic conditions. Classical changes, as well as variations and similarities with pathologic states are cited through hundreds of unretouched roentgenograms which describe fully the most pertinent areas of radiologic interest.

By BERNARD S. EPSTEIN, M.D., University of Texas Health Science Center at San Antonio. *856 pp. (7 x 10), illus., 1976, Ready Now.*

FUNDAMENTALS OF VASCULAR RADIOLOGY

In-depth description of angiographic and catheterization technics for vascular radiology is provided in this book. Each chapter begins with a discussion of the indications and contraindications for angiography of a particular organ system. Specialized radiographic equipment, including equipment necessary for pressure recordings and cardiac output measurements, and indications for pressure measurements during angiographic procedures are thoroughly described.

By ROBERT I. WHITE, JR., M.D., Johns Hopkins University School of Medicine, Baltimore, Maryland. *151 pp. (7 x 10), illus., 1976, $13.00.*

M-MODE ECHOCARDIOGRAPHIC TECHNIQUES AND PATTERN RECOGNITION

Emphasis is placed on how to find and record useful echocardiographic motion, technically satisfactory for interpretation. Definitive data derived from cardiac catheterization and surgery support the echocardiographic interpretations.

By SONIA CHANG, B.S., Emory University School of Medicine, Atlanta, Georgia. *160 pp., 137 illus., paperback, 1976, $7.00.*

INTRODUCTORY PHYSICS OF NUCLEAR MEDICINE

A concise, readable presentation of fundamentals of physics necessary in understanding various nuclear medicine procedures. Examples and problems from routine practice are given. Discussed are radioactivity, production of radionuclides and radiopharmaceuticals, and interaction and detection of radiation.

By RAMESH CHANDRA, Ph.D., New York University Medical School, New York, New York. *185 pp., 68 illus., 1976, Ready June.*

BASIC RADIATION BIOLOGY, 2nd ed.

This book uses straightforward style and simple tables, charts and diagrams to present the general principles and important techniques of radiation biology.

By DONALD J. PIZZARELLO, Ph.D., New York University Medical Center, New York; and RICHARD L. WITCOFSKI, Ph.D., The Bowman Gray School of Medicine of Wake Forest University, Winston-Salem, North Carolina. *143 pp. (7 x 10), 42 illus., 1975, $11.75.*

Order any book from your bookstore or directly from Lea & Febiger on 14 day approval.

ILMENITE

High density aggregate for Hospital X-Ray shielding. Canadian Ilmenite ore offers a widely accepted source of shielding against X-Rays and other medical sources of radiation.

Recent Ilmenite applications at:

General Hospital—Montreal
Civic Hospital—Ottawa
Princess Margaret Hospital—Toronto
Queen's Cancer Clinic—Kingston
M.D. Anderson Hospital—Houston
Allegheny Hospital—Pittsburgh
Rhode Island Hospital—Providence
Memorial Hospital—Newfoundland
Massachusetts General Hospital—Boston
St. Josephs Hospital—Houston

Also used for nuclear shielding with poured-in-place concrete, high density block applications, weighting and counter-weighting, ballasting, and as a component in mixed media filtration beds.

Write for brochure and technical data:

NUCLEAR SHIELDING SUPPLIES & SERVICE OF CANADA LIMITED

2545 Delorimier Avenue
Longueuil, Quebec, Canada
(514) 677-6333 • Telex 05-25448

United States Offices:

NUCLEAR SHIELDING SUPPLIES AND SERVICE, INC.

4328 East Tradewinds Avenue
Lauderdale-by-the-Sea
Florida 33308
(305) 776-4482 • Telex 514-527

NUCLEAR SHIELDING SUPPLIES AND SERVICE, INC.

3130 Southwest Freeway
Suite #204
Houston, Texas 77006
(713) 526-6461 • Telex 76-2047

Philips Polytome an

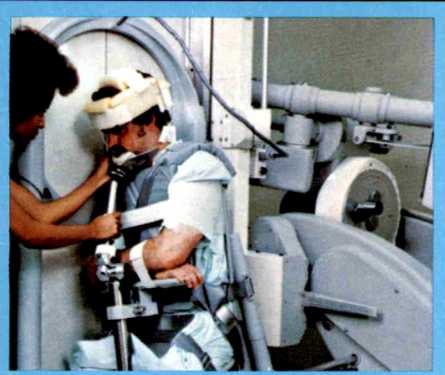
Multi-Directional Tomography for Pneumoencephalography n a fully integrated system.

Now the Polytome – world's mo sophisticated tomographic system – has its own snap-on examination chair for pneumo-encephalography. It's never bee easier or more efficient to use multi-directional tomography in pneumo studies!

Isocentric patient positioning keeps the patient's head in the fulcrum for all projections. And Polytome and chair are fully syn chronized for proper filling of ventricles and temporal horns.

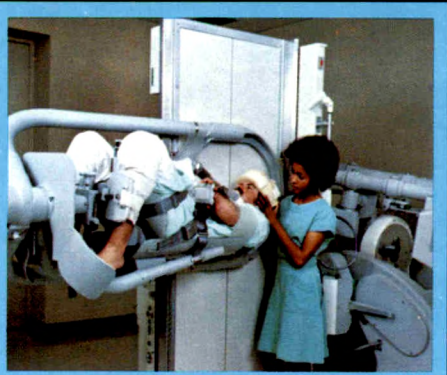
Selected patient positions and visualizations in a common pneumo procedure

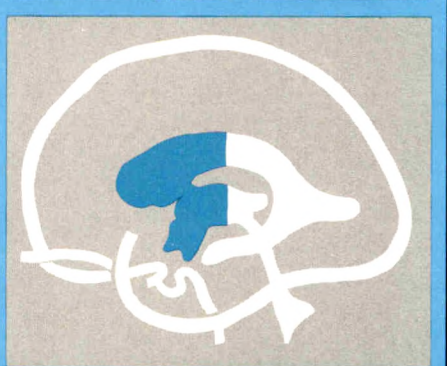
ERECT: LATERAL



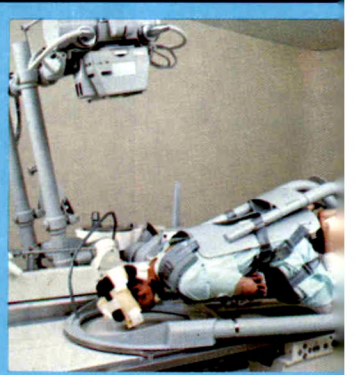


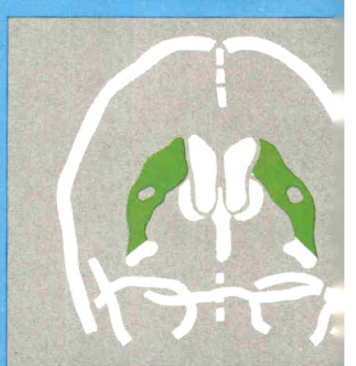
BROW-UP: LATERAL





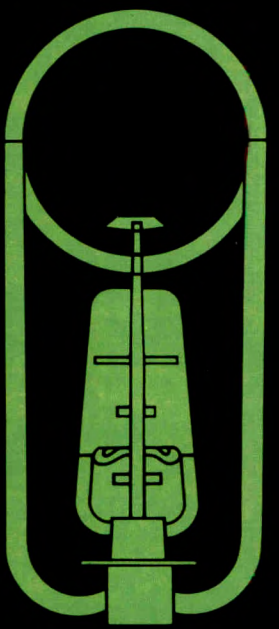
BROW-DOWN: PA





edicated Pneumo Chair

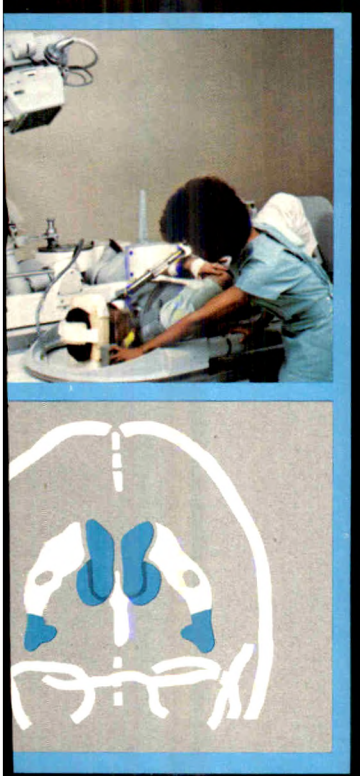
mpact, lightweight, easily and ickly attached, dismounted and ored in the Polytome room, the w chair gives you full use of *all* e Polytome's capabilities: from ear to the famous hypocycloidal urring motions... layer height justment... superb image qual- in every exposure... constant largement for every layer... timum visibility of the patient roughout the examination.



Add a Pneumo Chair to any new or existing Polytome for a dedicated neuroradiological system at a fraction of the cost. Detach the Chair and return the Polytome to its role as top department performer!

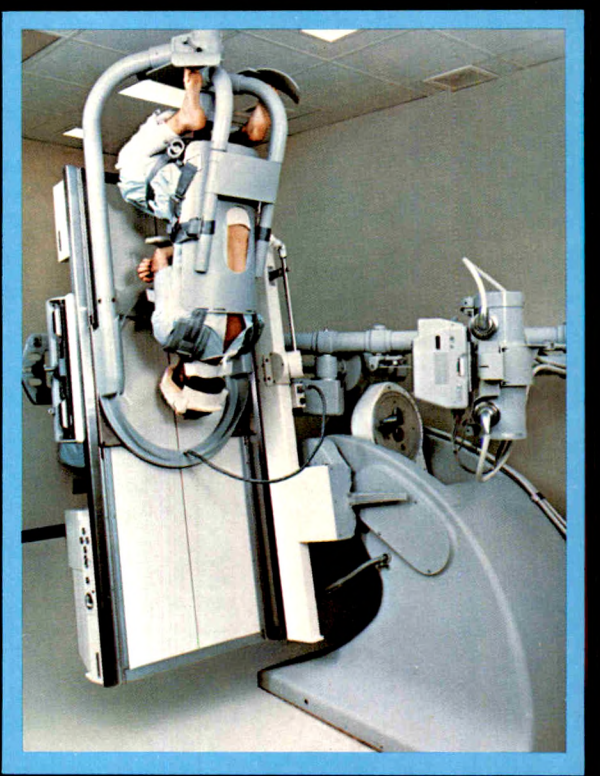
Now let *us* "pull up a chair" and show you how it works.

BROW-UP: AP*



*After sequential filling of temporal horns

A STAGE IN FILLING THE TEMPORAL HORNS



For additional information, contact your Philips representative. Or, call or write:

PHILIPS MEDICAL SYSTEMS, INC.
710 Bridgeport Avenue, Shelton, Conn. 06484

CHARLES C THOMAS • PUBLISHER

PANORAMIC DENTAL RADIOGRAPHY *by* **Lincoln R. Manson-Hing,** *Univ. of Alabama, Birmingham.* Comprehensive material on the subject of panoramic radiography is presented with a great number of illustrations and a minimum of text. The basic technical systems underlying the operating of the various machines are presented in a manner whereby diagnostically meaningful variations between radiographs made by different machines can be easily understood. This volume is unique in featuring the history of pantomography, the basic radiographic systems used, the variety of machines available, and radiographic anatomy and artifacts. *'76, 196 pp. (8 1/2 x 11), 296 il., 6 tables, $32.50*

CORONARY ANGIOGRAPHY (2nd Ptg.) *by* **Harold A. Baltaxe,** *Cornell Medical College, New York;* **Kurt Amplatz,** *Univ. of Minnesota, Minneapolis; and* **David C. Levin,** *Cornell Medical College, New York.* The gross and radiographic anatomy of the coronary artery tree is described in this book which deals with the description of diverse pathologic processes involving the coronary artery tree. The scope of the book is not restricted to atherosclerotic coronary artery disease, but also deals with congenital anomalies. A section in this book describes equipment and different techniques of catheterization. The chapter on complications gives a listing of problems encountered and their order of frequency. *'76, 256 pp., 173 il., $22.50*

ADMINISTRATION OF A RADIOLOGY DEPARTMENT: Hints for Day-to-Day Operation *by* **Murray L. Janower,** *St. Vincent Hospital, Worcester, Massachusetts.* To demonstrate that the application of common sense and sound business management principles to a radiology department will result in a marked improvement in its day-to-day operation is the purpose of this volume. Specific attention has been given to the methods used in handling patients, functions of the technologists, the establishment of a quality control program, efficient production of radiological reports, methods of film interpretation, darkroom operations, and functions of a file room. *'76, 72 pp., 8 il., 7 tables, $7.50*

THE RENAL UPTAKE OF RADIOACTIVE MERCURY ($^{197}HgCl_2$): Method for Testing the Functional Value of Each Kidney, Technique-Results- and Clinical Application in Urology and Nephrology *edited by* **Claude Raynaud,** *Service Hospitalier Frederic Joliot, Orsay, France. Foreword by* **Pierre Royer.** *(41 Contributors)* Several techniques of uptake measurement are described along with simplified systems of external counting, scanners or gamma cameras. Normal values of Hg renal uptake as well as the results obtained in patients are outlined. The test described is easy to use, accurate and can be repeated with the same patient. *'76, 248 pp., 110 il., 47 tables, $22.75*

ARTHROGRAPHY OF THE SHOULDER: The Diagnosis and Management of the Lesions Visualized *by* **Julius S. Neviaser,** *George Washington Univ. Medical School, Washington, D. C.* The author of this book emphasizes the minute points of technique, illustrates normal arthrograms, and describes anatomical variations of a normal shoulder joint. Chapters present clinical and arthrographic findings with explanatory roentgenographic illustrations. Outlines of conservative and operative treatment principles are also presented. Case studies highlight specific problems in which a definite diagnosis has been made by use of arthrography. *'75, 288 pp., 265 il., $22.50*

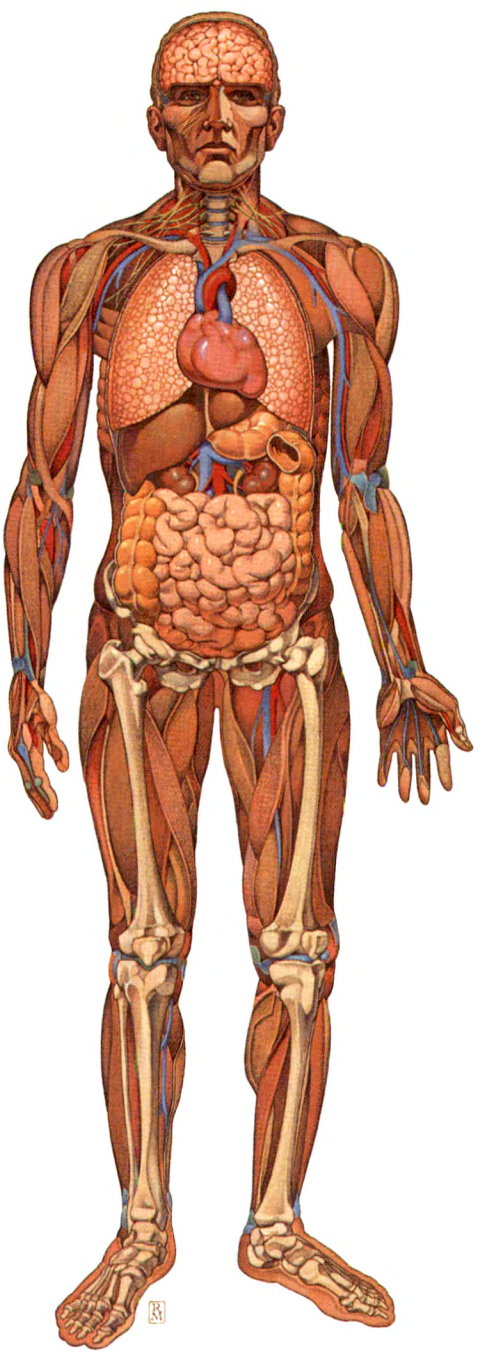
INDICATIONS AND ALTERNATIVES IN X-RAY DIAGNOSIS: A Guide to the Effective Employment of Roentgenologic Studies in the Solution of Diagnostic Problems (2nd Ed.) *by* **Melvyn H. Schreiber,** *Univ. of Texas Medical Branch, Galveston.* Various kinds of roentgenologic examinations available for the unravelling of diagnostic problems are examined in this book. Emphasis is on providing the reader with a thorough background in the uses to which the ordinary and special x-ray studies may be put, with alternatives emphasized when the indicated examination cannot be performed or when more than one kind of examination is available for the solution of a specific problem. *'74, 192 pp., 98 il., $11.50, paper*

Orders with remittance sent, on approval, postpaid

301-327 East Lawrence Avenue • Springfield • Illinois • 62717

Consider our total human resources.

X-Ray
Ultrasound
Nuclear
Computed Tomography
Clinical Laboratory
Accessories
Therapy



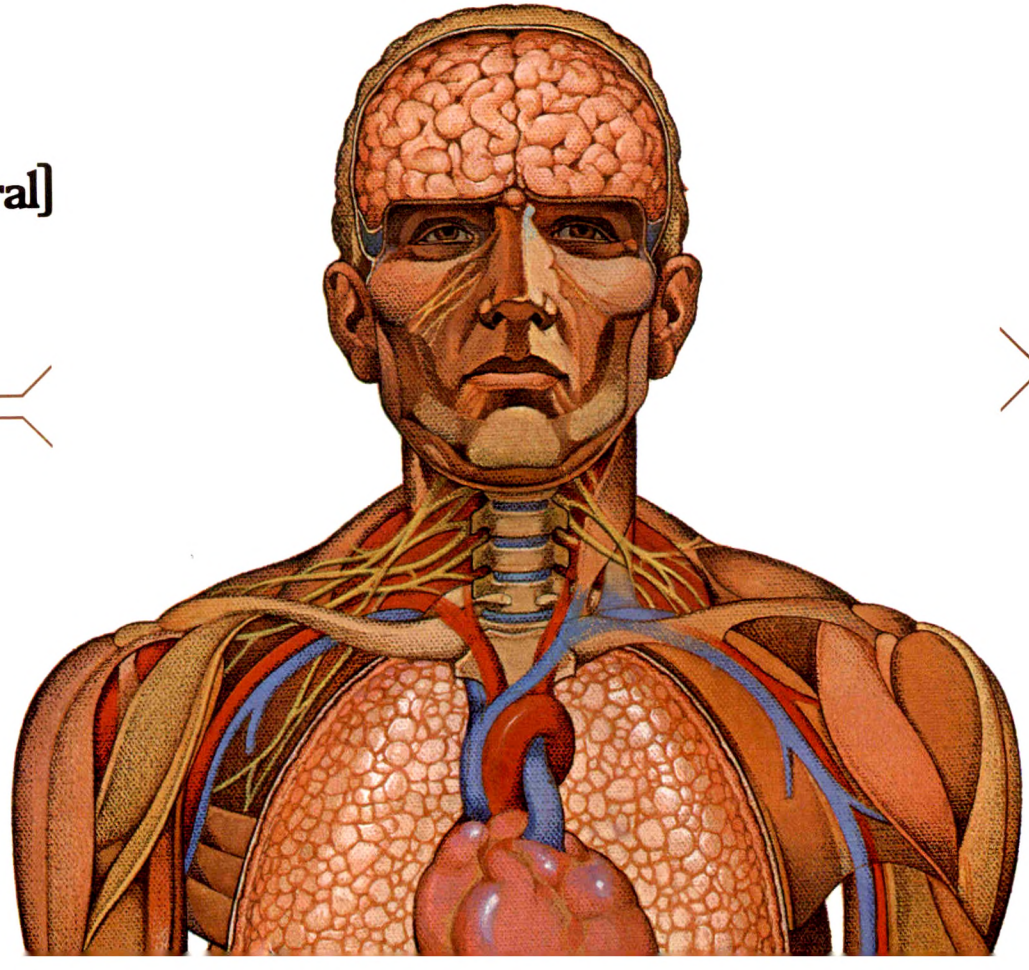
PICKER®

Types of Applications

Space occupying and atrophic lesions
Hematoma
RCVF
Vascular Lesions
Cerebral Angiography
Drug Abuse

Picker Systems

X-Ray
Ultrasound
Nuclear
Computed Tomography
Clinical Laboratory
Accessories



scular [Cardio & General]

Types of Applications

Circulatory Disease
Cardiac Deficiency Studies
Hematoma
General Malfunction

Picker Systems

X-Ray
Ultrasound
Nuclear
Clinical Laboratory
Therapy
Accessories

Lungs

Types of Applications

Ventilation & Perfusion
Lesions
Respiratory Diseases

Picker Systems

Nuclear
X-Ray
Computed Tomography
Accessories
Therapy

"How many people do you know who have been cured of cancer?"

Almost everybody knows someone who has died of cancer. But the fact is about two million living Americans have been cured. Not only cured but leading active, normal lives. Another fact is millions more could be.

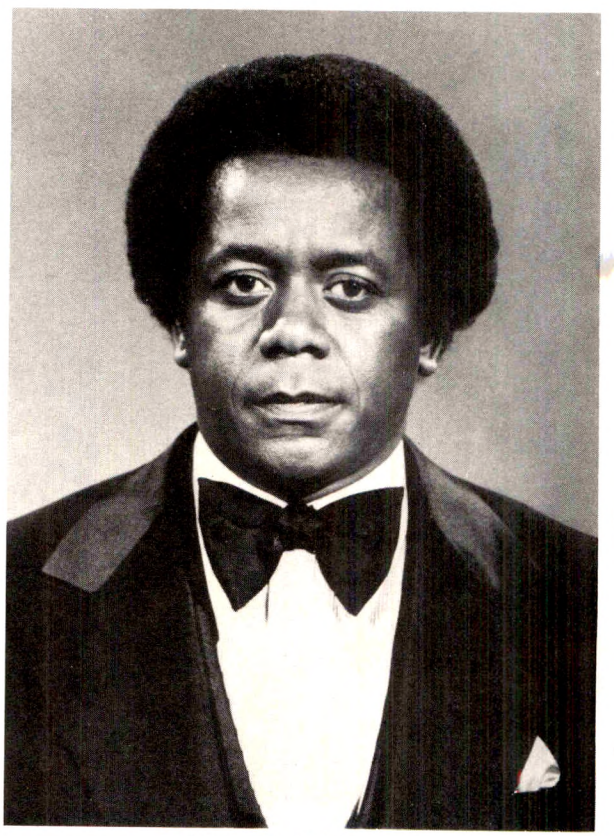
By getting to the doctor in time.

By availing themselves of the most effective methods of treatment today.

By advances made through cancer research. Research made possible with the help of the American Cancer Society.

However, there's much more to be done. To help save more people, the American Cancer Society needs more money. So, please, give. We want to wipe out cancer in your lifetime.

American Cancer Society



Flip Wilson,
National Crusade Chairman

This space contributed by the publisher as a public service

The Clinac® 18

Varian Commitment Stands Out

Varian's commitment to radiotherapy has resulted in the powerful Clinac 18, a multi-modality accelerator with 10 MV photons and 6 to 18 MeV electrons. Today the Clinac 18 serves over twenty radiation therapy centers and has become the most widely selected radiotherapy accelerator in its energy range.

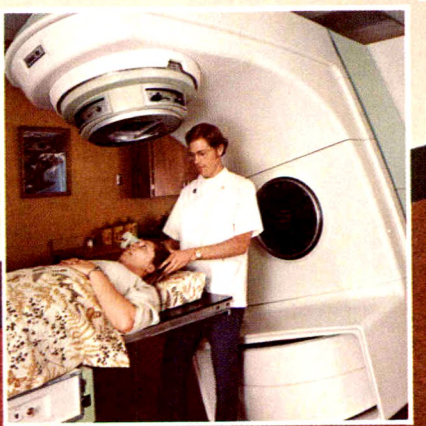
But the record shows Varian commitment means even more. It means response . . . our trained field support staff has nearly tripled during the past 2 years. It also means design evolution . . . our engineering team is constantly seeking ways to make refinements, with retrofitability wherever possible.

This is the meaning of Varian commitment. Clinac users have known it for 15 years.

Varian Radiation Division,
611 Hansen Way,
Palo Alto, CA 94303
Phone: 415-493-4000.
World-wide sales and service.

varian

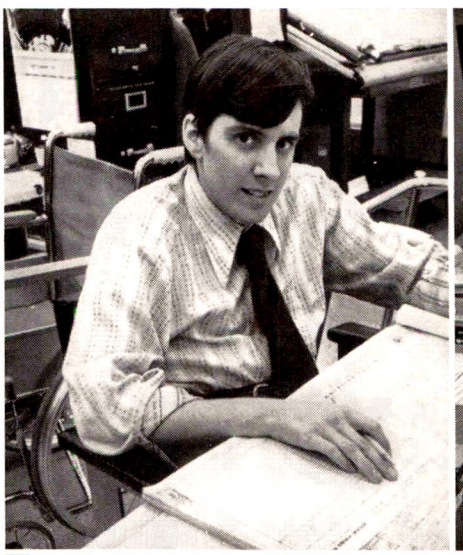
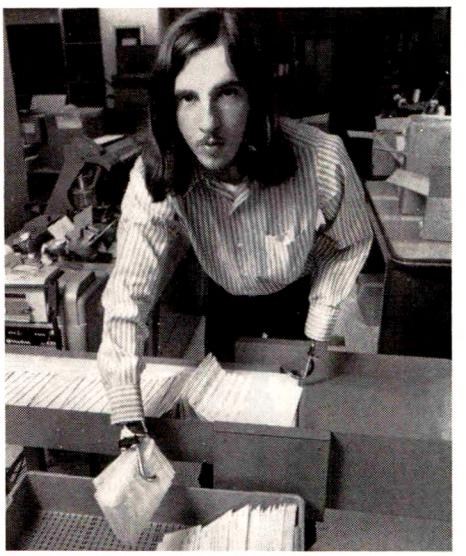


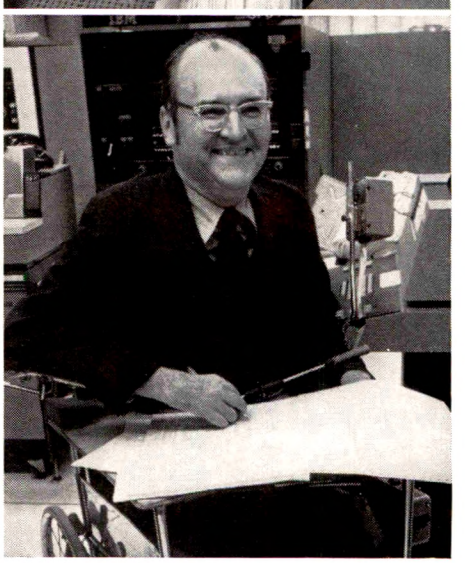


Photographed at Radiation Oncology Center of Sutter Community Hospitals, Sacramento, CA. (right); El Paso Cancer Treatment Center, El Paso, TX. (upper); University of Arizona Medical Center, Tucson, AZ (lower).



If these six people don't impress you, maybe the companies who hired them will.

These people aren't actors. They are real people doing real jobs for real companies.

Take Joseph Minikovsky, for example (top left), an electronic maintenance engineer. He has learned to use one hand the way most people in his field have to use two. As quickly, as efficiently, as accurately. He's a crackerjack technician and the National Broadcasting Company knows it. Yes, he works for NBC.

Robert Thompson (top center) is a mechanical engineer. At Syska & Hennessy in New York.

Frank Gaal (top right), a machine operator for Con Edison.

James Withers (bottom left), an administrative assistant with Control Data Corporation.

Mildred Hudson (bottom center), a coding and terminations clerk for Standard Security Life Insurance.

And Thomas Clancy (bottom right) is one of the best computer programmers New York University ever had.

They're all working. At jobs they enjoy. For companies who are very grateful to have them.

You see, despite their obvious disabilities, these people are skilled, hard-working men and women. And traits like that are hard to come by these days. (Ms. Hudson's supervisor told us she was one of only three people in their company who made it to work during a heavy snowstorm.)

It takes a lot of determination and many months of rehabilitation to get where these people are.

But it takes very little more than a letter to find people like them and hire them.

The Director of Vocational Rehabilitation in your state has a file of skilled, trained, rehabilitated people in every field. Ready, willing and able to work.

Write to him, next time you have an opening. His office is in your state capital.

And join the impressive ranks of Con Edison. And NBC. And Syska & Hennessy. And Control Data. And Standard Security Life. And NYU.

Write the Director of Vocational Rehabilitation in your State Capital.

The U.S. Department of Health, Education, and Welfare.

A Public Service of This Magazine & The Advertising Council

Ad Council

Double up, America.









Two can ride cheaper than one.

When people drive to work alone, they spend twice as much money on commuting as they should.

That's too much.

They can cut it in half. They can take a friend.

Not only will that daily commute cost less (and be a lot more pleasant), but when people carpool, they cut pollution, congestion and gasoline usage.

And companies benefit directly, because, obviously, fewer cars will make less demand on the parking spaces in the company lot. And some companies have attributed an increase in punctuality to the fact that more and more of their employees were carpooling.

Help the people in your company carpool. Texas Instruments in Dallas did it. 3M Company in St. Paul did it. Prudential Insurance Company of America in Boston did it.

Do it.

For your "Double up Kit," write to Double up, U.S. Department of Transportation, P.O. Box 1813, Washington, D.C. 20013. It outlines how companies can help organize carpools.

Let's double up. We'll all get where we're going. Faster and cheaper.

Ad Council

A Public Service of This Magazine & The Advertising Council

CARPOOLING CAMPAIGN (ENERGY CONSERVATION)
BUSINESS PRESS AD NO. EC-2211-75--7″ x 10″ (110 Screen)
Volunteer Agency: APCL&K, Inc., Volunteer Coordinator: John P. Kelley, The Goodyear Tire & Rubber Company

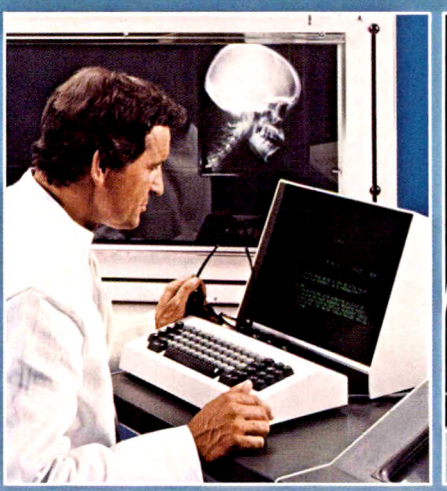
BP-375

Presenting SIREP
For computerized radiological reporting.

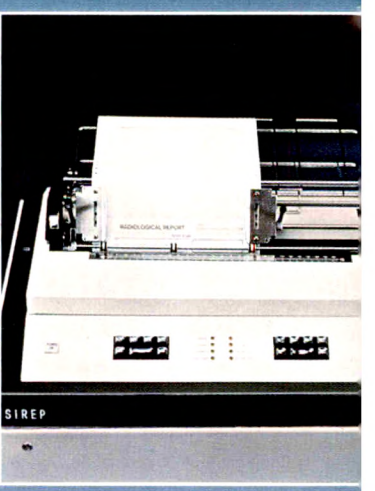




The Terminal
Reports are easily composed at The Terminal which has access to over 6500 anatomical, pathological and descriptive terms and illustrations.



The Keyboard/Display
All entries appear here for review. Corrections, cancellations or insertions can be made at any time before final printout.



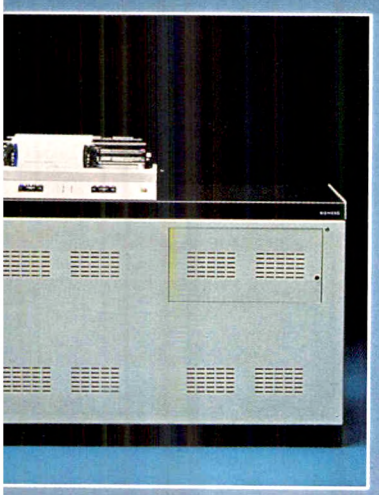
The Printer
After completing all entries, the radiologist activates The Printer and the report is printed quickly and accurately.



SIREP makes radiological reporting easier, while allowing data to reach the referring physician sooner. In addition to real savings in time and labor, SIREP serves as the basis for an improved system of information processing and communication. The result is a more efficient radiology department.

SIREP offers the speed, flexibility and depth of a conventionally dictated report. Clinical findings are entered with the touch of a finger—multi-copy finished reports are printed in seconds. The content is precise, abbreviated and free of clerical errors. The many advantages of SIREP are applicable to any size hospital, clinic or private practice.

Investigate the Siemens SIREP and ask about convenient lease financing arrangements. For detailed information, a comprehensive brochure is available from your Siemens representative, or you may write to Siemens Corporation, Iselin, New Jersey 08830.



ontrol Unit

rocessor-controlled for
and accuracy, this computer
rates the functions of a
data processing system.

SIEMENS



Yes... you're a candidate for Heart Attack

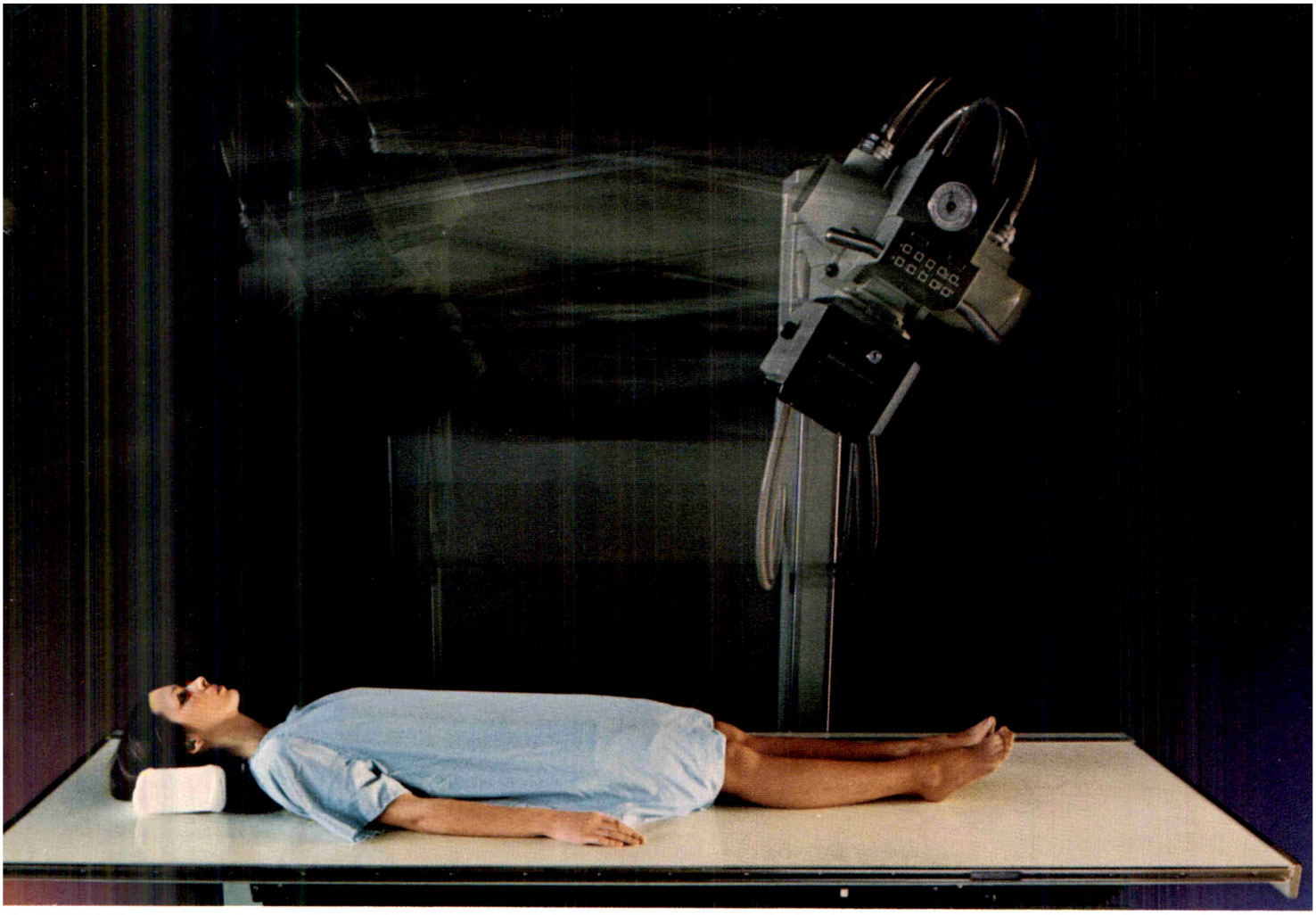
You can reduce your risk by

- Not smoking cigarettes,
- Eating foods low in animal fats and cholesterol,
- Reducing if overweight,
- Exercising regularly, moderately,
- Controlling high blood pressure,
- Seeing your doctor regularly,

and by supporting your Heart Association's programs of research, education and community service.

GIVE... so more will live **HEART FUND**

Contributed by the Publisher



Tomolex™ has replaced the fulcrum bar with touch-button control.

Every radiographic or tomographic setup with the Tomolex is assisted by touch button. Engage tomography, then return to radiography in seconds by touching a button. Quickly position the x-ray tubehead into the vertical mode and touch another button for erect radiography.

Tomolex simplifies the mechanics of setup so you can concentrate on better patient management.

And Tomolex helps you achieve unsurpassed film quality with the universal grid-free Bucky, incomparable film geometry, sinusoidal tomographic drive and a list of options including automatic exposure control.

The flat top and tuck away tableside control panel make patient transfer easy. The extra-wide top contributes to a patient's sense of security and simplifies cross-table radiography.

For ease, speed and quality results, Tomolex with four-way float top is the ultimate radiographic/linear tomographic system available today. It is another example of Picker'synergy — the complete interfacing of systems and services for ever better diagnostic visualization.

Talk to your Picker representative, or contact Picker Corporation, 595 Miner Road, Cleveland,OH 44143.

Picker'synergy

PICKER®
ONE OF THE C.I.T. COMPANIES

Can we just forget the one million veterans who will need a job this year?



It's only natural to want to forget war once it's over. To want to pack away all those bitter memories. But what about the people who served their country? Can we pack them away like toy soldiers? Forget them till they're needed again? And can we tell the disabled they're no longer of any use to us?

If you're someone with jobs to give, can you forget the jobs our veterans did for us? Can you let these good, capable people languish on the welfare rolls? What a waste of your tax dollars. And their lives.

These are responsible men and women. With experience, skills and maturity. Even the disabled can do a job well.

The way to get this country working is to get people working. So if you have a job to give, call the National Alliance of Businessmen.

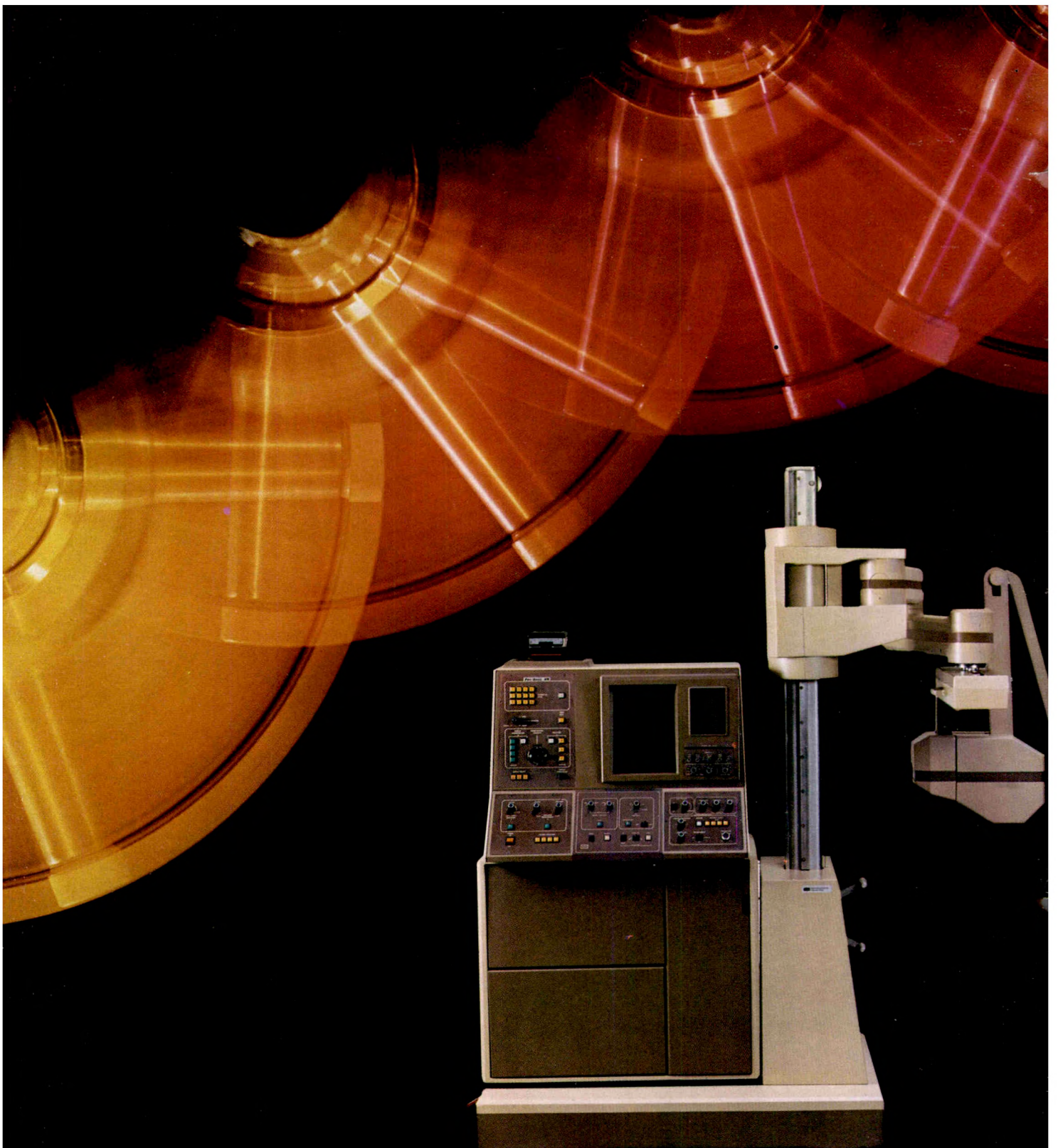
Help America work.

The National Alliance of Businessmen

Ad Council A Public Service of This Publication & The Advert sing Council

Searle Announces A New Concept in Diagnostic Ultrasound:

PHO/SONIC™-SM



The Most Important Development in Sonic Imaging Since Grey-Scale



PHO/SONIC™-SM

A compact B-scanner with TM capability

- Outstanding image quality with high resolution, good grey scale and wide acoustic dynamic range.
- Consistent results due to ease of operation, precise mechanical construction and unique automatic functions.
- Improved scan conversion system for fast, single-pass scans.
- Novel TV format displays patient and exam data below the active image area, automatically updated throughout the examination.

. . . And many more exciting new features we would like to present to you.

Before making any purchase decision, contact:

SEARLE

Searle Ultrasound

Division of Searle Radiographics Inc.
2270 Martin Avenue
Santa Clara, California 95050
(408) 984-2900

NATIONWIDE SERVICE

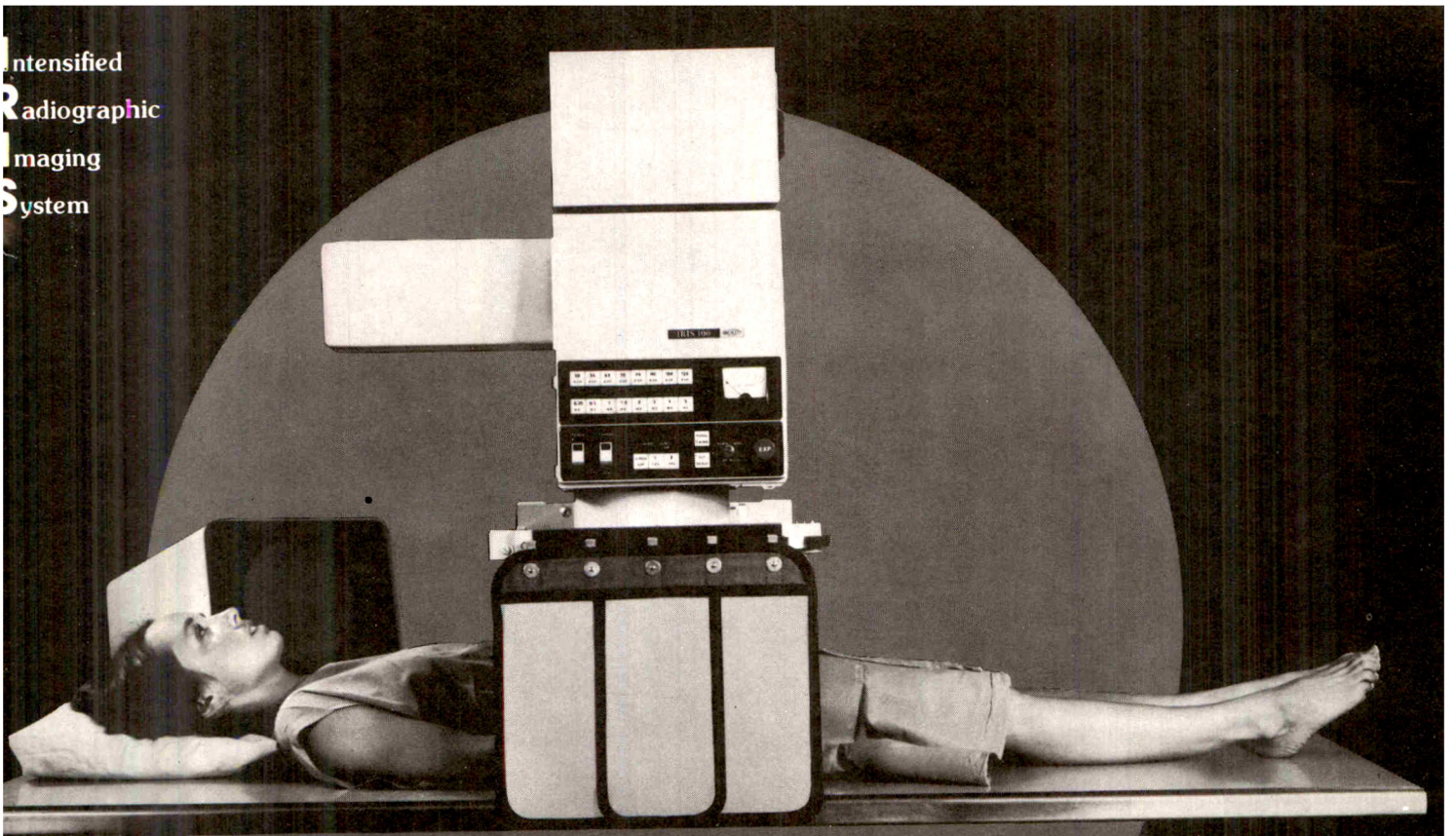
A Smart Ultrasound Machine

INDEX TO ADVERTISERS

Barnes-Hind Pharmaceuticals ..... xvi, xvii
Conversations in Radiology xx
E. I. DuPont de Nemours & Company, Inc. ..... vi, vii
Eastman Kodak Company ..... xxi, xxii, xxiii, xxiv
E-Z-EM Company ..... Cover 2
General Electric Medical Systems ..... xxvi, xxvii, xxviii, xxix
Grumman Health Systems xxxi
Hanley Medical Equipment Company x
Lea & Febiger xxxiv
Machlett Laboratories ..... Cover 3
Nuclear Shielding Supplies and Service xxxv
Ortho Pharmaceuticals Corporation xxv
Pfizer Medical Systems ..... xi, xii, xiii, xiv, xv
Philips Medical Systems, Inc. ..... xxxvi, xxxvii
Picker Corporation ..... xxxii, xxxiii, xxxix, xl, xli, xlii, xliii, xliv, liii
The Purdue-Frederick Company v
Searle Radiographics ..... ii, lv, lvi, lvii
Siemens Corporation ..... l, li
E. R. Squibb & Sons, Inc. ..... viii, ix, x, xviii, xix
S & S X-Ray i
Charles C Thomas · Publisher ..... xvii, xxxviii
Universal Voltronics Corporation xxx
University of Minnesota x
Varian Associates ..... xlvi, xlvii

We try to present an accurate index. Occasionally this may not be possible because of a last-minute change or an omission.

Intensified
Radiographic
Imaging
System



IRIS 100 adds television fluoroscopy and 100mm spotfilming to your present x-ray room.

Machlett's IRIS 100 system is a sound investment — both for the diagnostician and for the hospital — because it provides the most modern television fluoroscopy/spotfilming capabilities without the need for buying a whole new x-ray room. By improving the radiologist's productivity, moreover, IRIS 100 enables him to apply his much needed skills to a greater patient load.

While its cost is attractive, the real reasons for selecting IRIS 100 for your x-ray room are far more important:

Image Sharpness Machlett's Cesium Iodide Image Intensifier tube with its three focusing grids assures bright, sharp images both on film and on the television screen.

Short F-R-F Time Machlett's "sliding mirror" image distributor lets you quietly shift from fluoroscopy to spot radiography and back to fluoroscopy in *less than one second*.

Rapid Filming The Old Delft "Anodica" camera takes 100mm films singly or sequentially at 1-per-second or 2-per-second rates. Exposures are short enough to freeze peristaltic motion. Phototiming assures uniform film densities.

Human-Engineered Controls Controls are conveniently placed and designed for operation with gloved hands. Warning lights and interlocks eliminate such human errors as exposure without film.

Positive Patient ID The 100mm camera will not operate without the patient identification card in place. Film is identified at the time it is exposed.

For the whole story on IRIS 100, contact your x-ray equipment dealer or

MACHLETT

Machlett Laboratories, Incorporated

1063 Hope Street
Stamford, Connecticut 06907
(203) 348-7511

A Raytheon Company

American Journal of Roentgenology

Vol. 126 May 1976 No. 5

DIAGNOSTIC RADIOLOGY

Cannon Lecture: Islet Cell Tumors and the Alimentary Tract. *R. M. Zollinger* 933

Angiography in Crohn's Disease Revisited. *F. Brahme and J. Hildell* 941

Hepatic Angiography in Ulcerative Colitis and Crohn's Disease. *L. Ekelund, A. Lunderquist, H. Dencker, and M. Åkerman* 952

Megacystis-Microcolon–Intestinal Hypoperistalsis Syndrome: A New Cause of Intestinal Obstruction in the Newborn. Report of Radiologic Findings in Five Newborn Girls. *W. E. Berdon, D. H. Baker, W. A. Blanc, B. Gay, T. V. Santulli, and C. Donovan* 957

Multiple "Bull's-eye" Lesions in Gastric Lymphoma. *N. R. Dunnick, G. S. Harell, and B. R. Parker* 965

Vascular Impressions of the Gut Secondary to Chronic Vascular Occlusive Disease. *L. Menuck and M. Coel* 970

A New Concept of Ascitic Fluid Distribution. *A. V. Proto, E. J. Lane, and J. P. Marangola* 974

Glucagon and Barium Enema Examinations: A Controlled Clinical Trial. *R. K. Harned, C. B. Stelling, S. Williams, and G. L. Wolf* 981

Spontaneous Internal Drainage of Pancreatic Pseudocysts. *J. L. Clements, Jr., E. L. Bradley, III, and S. B. Eaton, Jr.* 985

Lumbar Epidural Venography in the Diagnosis of Disc Herniations. *R. Gershater and R. C. Holgate* 992

Transfemoral Lumbar Epidural Venography. *M. H. Miller, S. F. Handel, and J. D. Coan* 1003

Epidural Venography: Diagnosis of Herniated Lumbar Intervertebral Disc and Other Disease of the Epidural Space. *G. F. Drasin, R. H. Daffner, R. F. Sexton, and W. C. Cheatham* 1010

The Cardiac Pacemaker: A Different Twist. *C. J. Tegtmeyer and J. M. Deignan* 1017

Iliocaval Thrombi in Pulmonary Thromboembolic Disease. *J. C. Rudikoff, P. R. Clapp, and E. J. Ferris* 1019

Venography in Penetrating Injuries of the Extremities. *A. J. Gerlock, Jr., E. R. Thal, and W. H. Snyder, III* 1023

Selective Arterial Embolization for Control of Hemorrhage in Pelvic Malignancy: Femoral and Brachial Catheter Approaches. *F. J. Miller, Jr., R. Mortel, W. J. Mann, and A. E. Jahshan* 1028

Peripheral Embolization Complicating Bilateral Renal Infarction with Gelfoam. *J. Woodside, H. Schwarz, and P. Bergreen* 1033

Crossed Renal Ectopia: Angiographic Findings in Six Cases. *Z. J. Rubinstein, M. Hertz, N. Shahin, and V. Deutsch* 1035

Angiographically Induced Renal Failure and Its Radiographic Detection. *R. A. Older, J. P. Miller, D. C. Jackson, I. S. Johnsrude, and W. M. Thompson* 1039

Arthrographic Evaluation of Injuries of the First Metacarpophalangeal Joint: Gamekeeper's Thumb. *D. Resnick and L. A. Danzig* 1046

Isolated Fracture of the Medial Portion of the Lateral Mass of the Atlas: A Previously Undescribed Entity. *E. G. Barker, Jr., J. Krumpelman, and J. M. Long* 1053

Concomitant Dislocation and Intraarticular Foreign Body: A Rare Complication of the Charnley Total Hip Arthroplasty. *R. E. Campbell and J. P. Marvel, Jr.* 1059

Embryogenesis of the Human Occipital Bone. *R. Shapiro and F. Robinson* 1063

Film Screening by Physician Assistants in Diagnostic Radiology. *E. G. Barker, Jr., H. D. Rosenbaum, A. C. Selke, Jr., D. Henderson, and J. H. Hildner* 1069

NUCLEAR MEDICINE

^{99m}Tc-Diphosphonate Uptake in Neuroblastoma. *W. McCartney, M. L. Nusynowitz, B. E. F. Reimann, J. Prather, and B. Mazat* 1077

RADIATION ONCOLOGY

Adjuvant Chemoimmunotherapy in Advanced Lesions of the Head and Neck. *F. R. Eilber and D. L. Morton* 1082

Immunotherapy of Malignancies: Current Status. *F. R. Eilber, E. C. Holmes, D. L. Morton, K. P. Ramming, and F. C. Sparks* 1088

Editorial: CT and the Planners. *T. F. Meaney* 1095

News Items 1098

Society Proceedings 1100

Abstracts of Radiologic Literature 1107

Rec.
15.11.76

Coming in July: Special Issue on
Computed Tomography

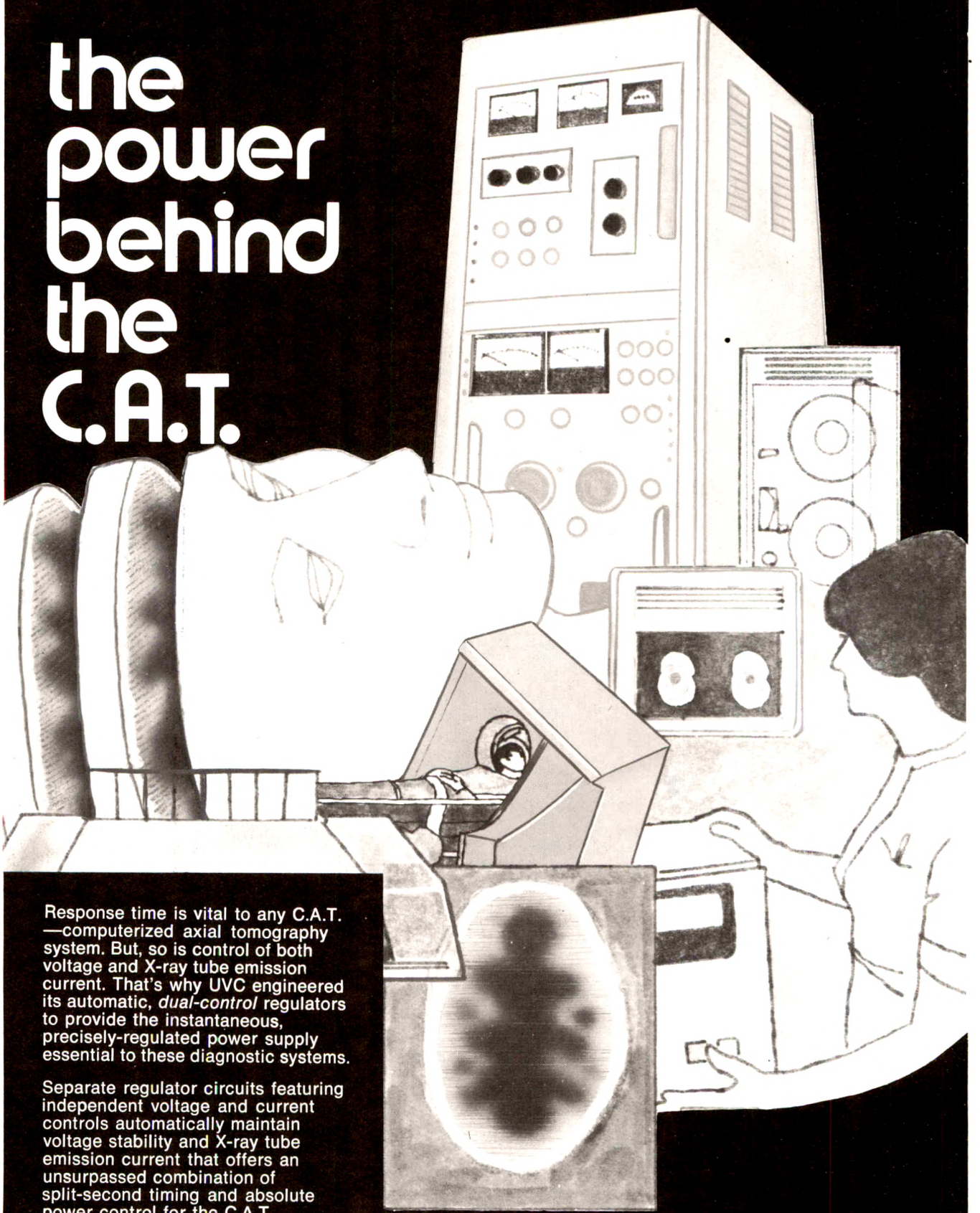


AJR

American
Journal of
Roentgenology

June 1976

the power behind the C.A.T.



Response time is vital to any C.A.T. —computerized axial tomography system. But, so is control of both voltage and X-ray tube emission current. That's why UVC engineered its automatic, *dual-control* regulators to provide the instantaneous, precisely-regulated power supply essential to these diagnostic systems.

Separate regulator circuits featuring independent voltage and current controls automatically maintain voltage stability and X-ray tube emission current that offers an unsurpassed combination of split-second timing and absolute power control for the C.A.T.

Because UVC equipment has proved so constant, safe, and sure in repeated clinical use, it is now the first choice of most C.A.T. systems. Insist on UVC-equipped C.A.T.s . . . *more power to you!*

Write or call

UNIVERSAL VOLTRONICS CORPORATION

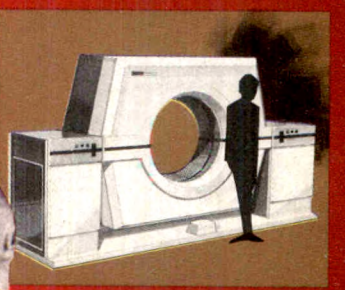
27 Radio Circle Drive, Mount Kisco, N.Y. 10549
(914) 241-1300

Designed for better CT imaging

Searle will soon introduce a new X-ray CT imager. This highly sophisticated instrument uses advanced mechanical and electronic technology to make CT imaging of the future a practical reality today.

This new system is now being evaluated and will be released for sale when its reliability, speed, and diagnostic superiority have been established. What Searle is developing today, the medical community relies on tomorrow.

For more information, call or write: Searle CT Systems, 4233 No. United Parkway, Schiller Park, IL 60176. Telephone (312) 678-8650.





IMAGING:
The Living Art

SEARLE

Searle CT Systems

One if by land...two if by sea.

This was a very important message in the history of our country. Liebel-Flarsheim also has an important message and it has many of the same characteristics as that earlier message . . .

- It's short
- It's considered revolutionary by many
- If missed, it could be very costly
- If received, it could help you form a more perfect union

Liebel-Flarsheim is proud to be the only Company that manufactures, within the USA, both an Angiographic Injector (the Viamonte/ Hobbs Angiomat 3000) and a variable speed Film Changer (the Franklin F-200) for your angiographic needs.

Through this expanded manufacturing capability Liebel-Flarsheim offers you . . .

- Proven performance
- Design compatibility
- Single source supply
- Coordinated field support

Check the many features offered by these two units and form a more perfect union of your angiographic equipment by specifying Liebel-Flarsheim.

VIAMONTE/HOBBS ANGIOMAT 3000 INJECTOR

- Disposable syringe
- Modern functional design
- Solid state circuitry
- Modular design to meet all your requirements
- Table mounting of syringe power head

FRANKLIN VARIABLE SPEED FILM CHANGER F-200

- Daylight loading of 65 exposure frames
- Ideal format for neurological and selected vessel studies
- Compact — easy to position and store
- Solid state program selector



For more information on both of these products, call your local x-ray dealer or write direct.

LIEBEL-FLARSHEIM
SYBRON CORPORATION
111 East Amity, Cincinnati, Ohio 45215 U. S. A.

AMERICAN JOURNAL OF ROENTGENOLOGY

EDITOR MELVIN M. FIGLEY

ASSISTANT EDITOR ROSALIND H. TROUPIN

ASSOCIATE EDITORS LUTHER W. BRADY
KENNETH L. KRABBENHOFT
E. FREDERICK LANG
RUSSELL H. MORGAN

EDITOR EMERITUS TRAIAN LEUCUTIA

INCLUDING DIAGNOSTIC RADIOLOGY, RADIATION ONCOLOGY, NUCLEAR MEDICINE, ULTRASONOGRAPHY AND RELATED BASIC SCIENCES

CONSULTING EDITORIAL BOARD

KENT ELLIS
E. ROBERT HEITZMAN
DONALD L. KING
JOHN A. KIRKPATRICK, JR.
EUGENE C. KLATTE
JOHN G. McAFEE
THOMAS H. NEWTON
ROBERT G. PARKER
STEWART R. REUTER
WILLIAM B. SEAMAN
ROBERT J. SHALEK
JOHN STORER
MICHEL M. TER-POGOSSIAN
JOSEPH P. WHALEN
DAVID M. WITTEN





OFFICIAL JOURNAL

AMERICAN ROENTGEN RAY SOCIETY

AMERICAN RADIUM SOCIETY



The American Journal of Roentgenology is issued monthly by Charles C Thomas, Publisher, 301–327 East Lawrence Ave., Springfield, Illinois 62717. Correspondence regarding subscriptions, advertisements and other business should be addressed to the Publisher. Annual subscription prices: United States and U. S. Possessions $30.00, Pan America, Canada and others $35.00. Printed by the George Banta Co., Menasha, Wisconsin.

Copyright © 1976 by American Roentgen Ray Society.

Second-class postage paid at Springfield, Illinois and at additional mailing offices. Printed in U.S.A.

GUIDELINES FOR AUTHORS

The AMERICAN JOURNAL OF ROENTGENOLOGY publishes original and timely contributions to the advancement of radiologic diagnosis and treatment. Although the content is predominantly clinical in origin, laboratory investigations are accepted when their relevance to clinical practice is demonstrable. Contributions are reviewed by two outside consultants and are accepted on condition that they are submitted only to this Journal and that they will not be reprinted or translated without consent of the Editor. Statements within an article are the responsibility of the authors and not the Journal or its publisher.

Address all manuscripts and correspondence to the Editor, Dr. Melvin M. Figley, 403 Pacific National Bank Building, 4545 15th Avenue N.E., Seattle, Washington 98105.

Manuscript Form

Manuscripts should be typed double-spaced throughout, including references, tables, and footnotes. Tables, footnotes, and figure legends should be on separate sheets, and a separate title page should be provided. In addition to the original typewritten copy, a duplicate copy complete with figures, tables, and references is required.

Figures should be submitted as 5″×7″ glossy prints, untrimmed and unmounted. Identifying information (author name, figure number, and indication of the top of the figure) should be attached to the back of each figure with a gummed label. Line illustrations and graphs should be drawn in black ink on white background. Labels on all figures should be of professional quality and sufficiently large to be easily read when reduced in size.

References should be cited in the text by number (e.g., [3, 4]). The bibliography should be arranged in the numerical order that references are cited in the text and typed double-spaced throughout. Data for each reference should be arranged according to the uniform style on bibliographic citations adopted by many biomedical journals. Abbreviations for titles of medical periodicals should conform to those published in *Index Medicus*. Examples:

1. Miller RE, Chernish SM, Skulas J, Rosenak BD, Rodda BE: Hypotonic roentgenography with glucagon. *Am J Roentgenol* 121:264–274, 1974
2. Boijsen E: Superior mesenteric angiography, in *Angiography*, edited by Abrams H, Boston, Little, Brown, 1971, pp 1091–1119

Organization

Title page. Titles should be brief and specific. Include full names and addresses of all authors and acknowledgment of grant support when appropriate.

Abstract. A description of the purpose, methods, results, and conclusions of the study is required. It should be informative to a reader who has not read the text of the article.

Key indexing words. Five to 10 words or short phrases should be supplied to enable cross-indexing of the article.

Introduction. Clearly state the purpose of the investigation including necessary background facts.

Materials and methods. Describe the protocol clearly so that an experienced worker can understand what was done. Use standard abbreviations as presented in the *Council of Biology Editors Style Manual*, 3d edition.

Results. Present results in logical sequence.

Discussion. Interpret the results to lend meaning and importance to the observations. If hypotheses and speculation are included, they must be labeled as such. When results differ from those of previous investigators, an attempt should be made to explain the discrepancy.

References. Only include those references which provide adequate background and present fairly any opposing evidence and concepts. Accuracy of reference data is the responsibility of the author.

Legends. Legends should be brief but should provide sufficient description to interpret the figure.

Special Communications

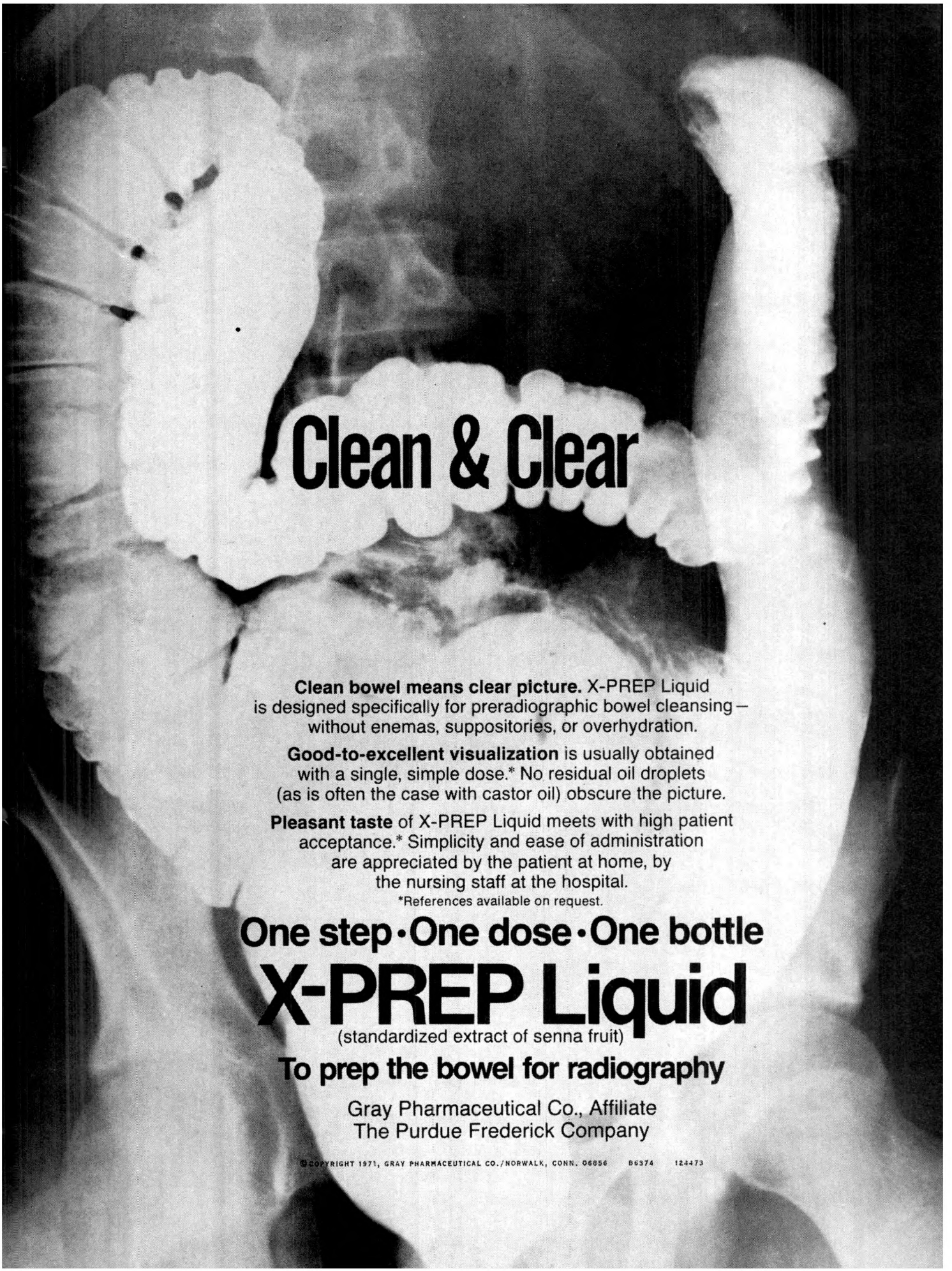
Case Reports. Concise case reports are accepted if they present unusual experiences that are medically important and educational. Clarity and brevity are essential.

Technical notes. Brief descriptions of new techniques or significant modifications of older ones which are directly applicable to clinical practice will be accepted.

Letters to the Editor. Letters should be limited to between 250 and 500 words. Criticism of published articles should be objective and constructive. Letters may also discuss matters of general interest to radiologists.

Proofs and Reprints

Copy-edited manuscripts are sent to the author for checking prior to typesetting. Galley proofs will be sent for correction of typographical errors only. The corrected proof, copy-edited manuscript, and the reprint order should be returned directly to the Editor. If the author fails to return proof by the date specified, it may be necessary to publish without the author's approval.


Clean & Clear
Clean bowel means clear picture. X-PREP Liquid is designed specifically for preradiographic bowel cleansing – without enemas, suppositories, or overhydration.
Good-to-excellent visualization is usually obtained with a single, simple dose.* No residual oil droplets (as is often the case with castor oil) obscure the picture.
Pleasant taste of X-PREP Liquid meets with high patient acceptance.* Simplicity and ease of administration are appreciated by the patient at home, by the nursing staff at the hospital.
*References available on request.
One step • One dose • One bottle
X-PREP Liquid
(standardized extract of senna fruit)
To prep the bowel for radiography
Gray Pharmaceutical Co., Affiliate
The Purdue Frederick Company
©COPYRIGHT 1971, GRAY PHARMACEUTICAL CO./NORWALK, CONN. 06856 B6374 124473



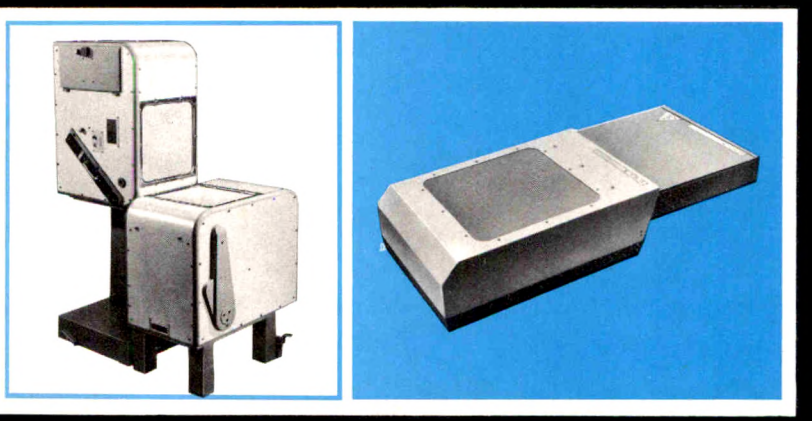
the beauty of the naked film sheet

in SCHONANDER CUTFILM CHANGERS is that...

- it has the lowest possible inertia — therefore it can be accelerated and decelerated fast in the machine to give adequate exposure times at all exposure rates, and the changer does not cause disturbing vibrations when it runs;
- it gives excellent detail without vacuum procedures;
- the handling is so simple: just load the unexposed films in the loading bin and pick up the exposed films in the receiver;
- it allows you to take any number of single films without wasting any film;
- it allows preliminary evaluation of the examination without delay by having just a few films processed immediately;
- it allows alternate exposures in biplane operation — for a minimum of scatter — without any film waste;
- unlike rollfilm (cut or uncut) it is initially flat, so it runs smoothly through the processor;
- the viewing and filing is so convenient.

SCHONANDER FILMCHANGERS for naked sheetfilm are

CONVENIENT
ECONOMICAL
DEPENDABLE



AOT-R max. 6 exp./sec.
Universal filmchanger for all angiographic examinations

PUCK max. 3 exp./sec.
Punch card controlled filmchanger with see-through options; also useful to replace cassettes in conventional radiography

ELEMA-SCHONANDER

ELEMA-SCHONANDER, INC.

699 LIVELY BOULEVARD ▪ ELK GROVE VILLAGE, ILL. 60007 ▪ (312) 593-6770

This poster on your x-ray room wall can save you money



(Actual size 17" x 22".)

It's free from Machlett!

MACHLETT
Machlett Laboratories, Incorporated
1063 Hope Street
Stamford, Connecticut 06907
(203) 348-7511
A Raytheon Company

WHAT'S NOW SQUIBB?

On the current nuclear medicine scene



MINITEC® (Technetium 99m) Generator

The Technetium 99m Generator using fission product molybdenum to produce technetium 99m. MINITEC is unlike any generator you've ever used—made small to make sense.

Designed for easy handling

- MINITEC has its own handle for easy lifting, easy carrying and reduced hand exposure
- Weighs only 24½ lbs., less than 5" in diameter, under 8½" high

Designed for easy elution

- Sets up in seconds
- Elutes in only 3 minutes after eluent vial has emptied

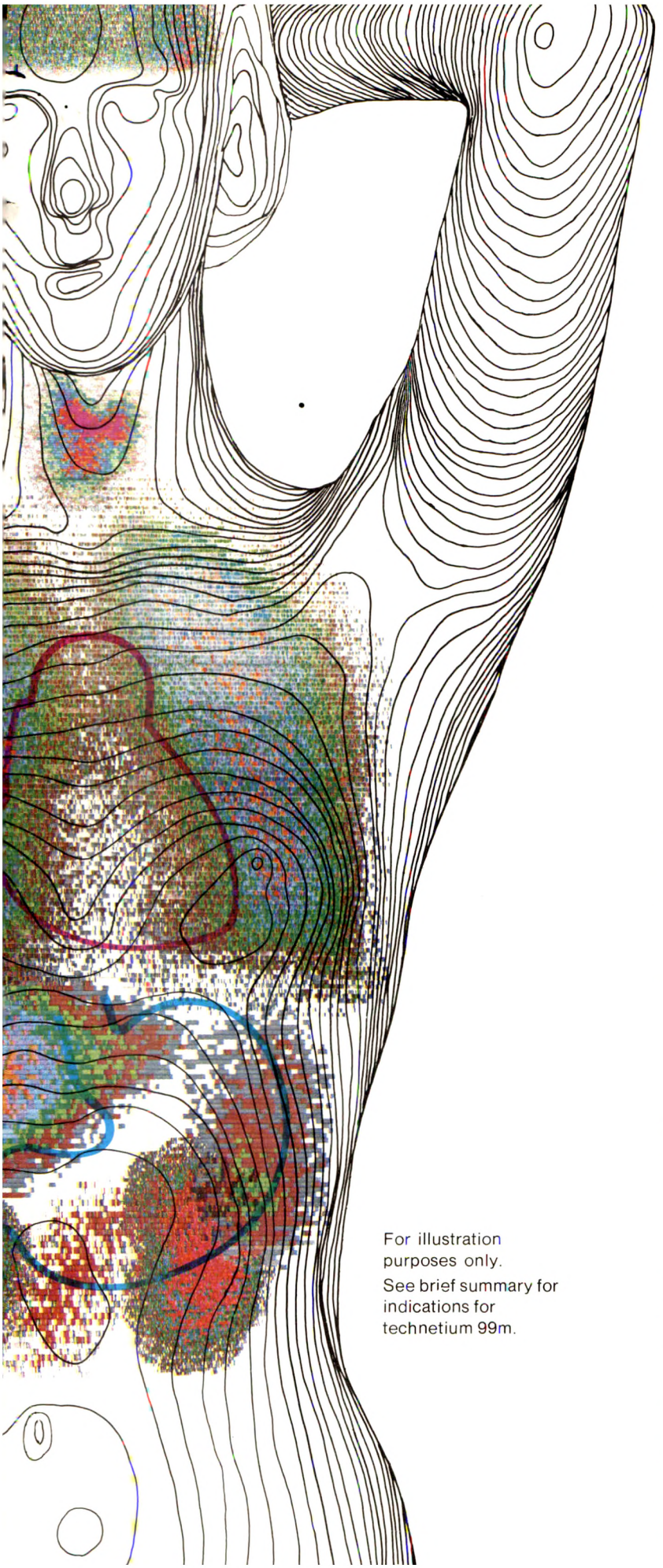
Designed for safety

- No exposed tubing when eluting
- 1⅝" lead surrounds the MINITEC column
- 1½" of extra lead protection from MAXI-SHIELD™. Base, cap and interlocking half rings easily assembled on site . . . only the cap is removed for elution. (You get MAXI-SHIELD free with your first MINITEC Generator purchase.)

Designed for convenience

- MINITEC Generator is available in 50,100, 200, 300, 400 and 500 mCi potencies. Delivery on Monday AM (precalibrated through Thursday) and Wednesday (precalibrated through Monday) provides maximum versatility to satisfy technetium requirements of your lab's work load.

© 1975 E. R. Squibb & Sons, Inc. H605-021



For illustration purposes only.

See brief summary for indications for technetium 99m.

Minitec®
(Technetium 99m)
Generator

Minitec® (Technetium 99m) Generator provides a means of obtaining a sterile, non-pyrogenic supply of technetium 99m (^{99m}Tc) as sodium pertechnetate ^{99m}Tc.

Indications: Sodium pertechnetate ^{99m}Tc is indicated for brain imaging, thyroid imaging, salivary gland imaging, blood pool imaging, and placenta localization.

Contraindications: At present, there are no known contraindications to the use of sodium pertechnetate ^{99m}Tc.

Warnings: Radiopharmaceuticals should be used only by physicians who are qualified by specific training in the safe use and safe handling of radionuclides, produced by nuclear reactor or cyclotron, and whose experience and training have been approved by the appropriate federal or state agency authorized to license the use of radionuclides.

This radiopharmaceutical should not be administered to women who are pregnant or who may become pregnant or during lactation unless the information to be obtained outweighs the possible potential risks from the radiation exposure involved. Ideally, examinations using radiopharmaceuticals, especially those elective in nature, of a woman of childbearing capability should be performed during the first few (approximately 10) days following the onset of menses.

Since radioactive pertechnetate is secreted in milk during lactation, formula-feedings should be substituted for breast-feedings.

Important: Since material obtained from the generator may be intended for intravenous administration, aseptic technique must be strictly observed in all handling. Only the eluent provided should be used to elute the generator. Do not administer material eluted from the generator if there is any evidence of foreign matter.

Precautions: As in the use of any other radioactive material, care should be taken to insure minimum radiation exposure to the patient consistent with proper patient management and to insure minimum radiation exposure to occupational workers.

At the time of administration, the solution should be crystal clear.

Adverse Reactions: At present, adverse reactions have not been reported following the use of sodium pertechnetate ^{99m}Tc.

For complete prescribing information, consult package insert.

How Supplied: Minitec (Technetium 99m) Generator is available in potencies of 50, 100, 200, 300, 400, and 500 mCi. Supplied with the generator are vials of eluent containing 5 ml. of a sterile, non-pyrogenic solution of 0.9% sodium chloride in water for injection. Also supplied is suitable equipment for eluting, collecting, and assaying the technetium 99m.

Medotopes®

SQUIBB HOSPITAL DIVISION
E. R Squibb & Sons, Inc.
Princeton, N.J. 08540

SILVER
IS OUR ONLY BUSINESS
(and has been since 1937)

IF YOU PROCESS . . .
X-RAY FILM

OUR TOTAL SILVER RECOVERY SERVICE

MEANS MONEY TO YOUR DEPARTMENT.

We Purchase

* Outdated or damaged unexposed x-ray film
* Exposed x-ray film
* Silver chip, flake and sludge

Write or call for full information

CALL TOLL FREE
(800) 323-4503
Ill residents call (312) 473-4800

McELROY
INTEGRITY LEADERSHIP
INC.

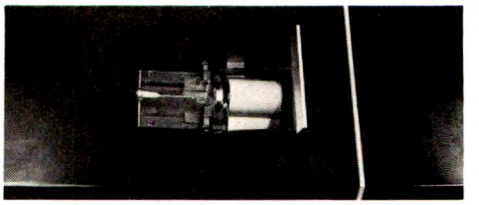
A subsidiary of AgMet, Inc.
2730 Commonwealth
North Chicago, Illinois 60064

CardioChem™
Automated ^{99m}Tc Unit-Dose Delivery System

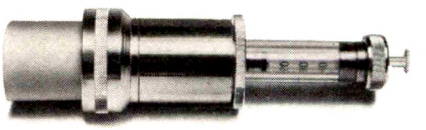
Systematically safer.



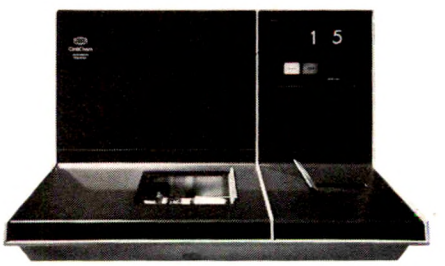
Organ-specific agents for optimum imaging of brain, kidney, bone and lung, and for glomerular filtration rate studies, are provided in kits containing 10 unit-dose vials. Each kit is single step, requiring only addition of technetium to produce the scanning agent.



Preselected amount of ^{99m}Tc activity is automatically dispensed into vial, then diluted with saline to 1.3 ml. Entire dispense/dilute cycle is automatic and shielded, and is completed within 75 seconds.



Unit-dose vial is entered only once for technetium delivery, once for agent withdrawal. Shielded syringe assembly automatically centers disposable syringe with vial. A 1.0-ml patient injection is reproducibly withdrawn into syringe.



Dispenser fully automates isotope measurement, reagent transfer and dose calibration. Eliminates time-consuming manual steps, computations and potential radiation exposure.

UNION CARBIDE

Delivering the future in imaging agents:

The CINTICHEM System, a total unit-dose ^{99m}Tc delivery system...

- ☐ Simplifies radionuclide delivery
- ☐ Improves dosage accuracy and reproducibility
- ☐ Reduces radiation burden
- ☐ Permits precise, contaminant-free administration of agents
- ☐ Reduces labor and cost per test
- ☐ Simplifies record keeping and calculations

The CINTICHEM System includes: an automated technetium dispenser, a high-yield molybdenum 99/technetium 99m generator, organ-specific kits and a unique unit-dose shielded syringe assembly. All integrated for the preparation of sterile, pyrogen-free radiodiagnostic agents—precisely, reliably and with greatly reduced radiation burden to the user.

The CINTICHEM Dispenser automatically delivers a preselected amount of ^{99m}Tc activity (TcO_4^- in saline) into a single-use unit-dose vial. Vial contents are transferred to a disposable syringe via a shielded syringe assembly that permits reproducible withdrawal of a 1.0-ml patient dose.

The CINTICHEM Generator is an optimized, advanced-technology ^{99m}Tc generator. It offers exceptionally high yields and is available in 500-, 1,000-, 1,500- and 2,000-mCi sizes. (Sodium pertechnetate ^{99m}Tc in isotonic saline.)

A series of organ-specific CINTICHEM Agents incorporates optimum current formulations for organ specificity. Each kit contains 10 unit-dose vials. (Kits containing five multidose vials are also available.) Each kit is single step. Requires only the addition of technetium to produce the imaging agent. And the CINTICHEM Dispenser performs this step automatically.

Kits currently available include: DTPA (diethylene triamine pentaacetic acid [calcium trisodium salt]). For brain and kidney imaging, and glomerular filtration rate (GFR) studies. Unit dose contains 3.3 mg $CaNa_3$ DTPA, 0.17 mg $SnCl_2$-$2H_20$, pH adjusted to 4 with HCl. HEDSPA (1-hydroxy-ethylidene-1,1 disodium phosphonate). For bone imaging. Unit dose contains 0.75 mg HEDSPA, 0.08 mg stannous ion as tartrate, pH adjusted to 4 with HCl. MAA (macroaggregated albumin). For lung perfusion studies. Unit dose contains 0.11 mg MAA ($0.3\text{-}1.3 \times 10^6$ particles), 0.09 mg stannous tartrate, isotonic saline. HCl and NaOH may be present for pH adjustment. Additional radiopharmaceuticals will also be offered.

Let us send detailed data on the CINTICHEM System. Simply return the coupon and we'll come back with a glimpse into the future.

CintiChem™
Systematically safer.

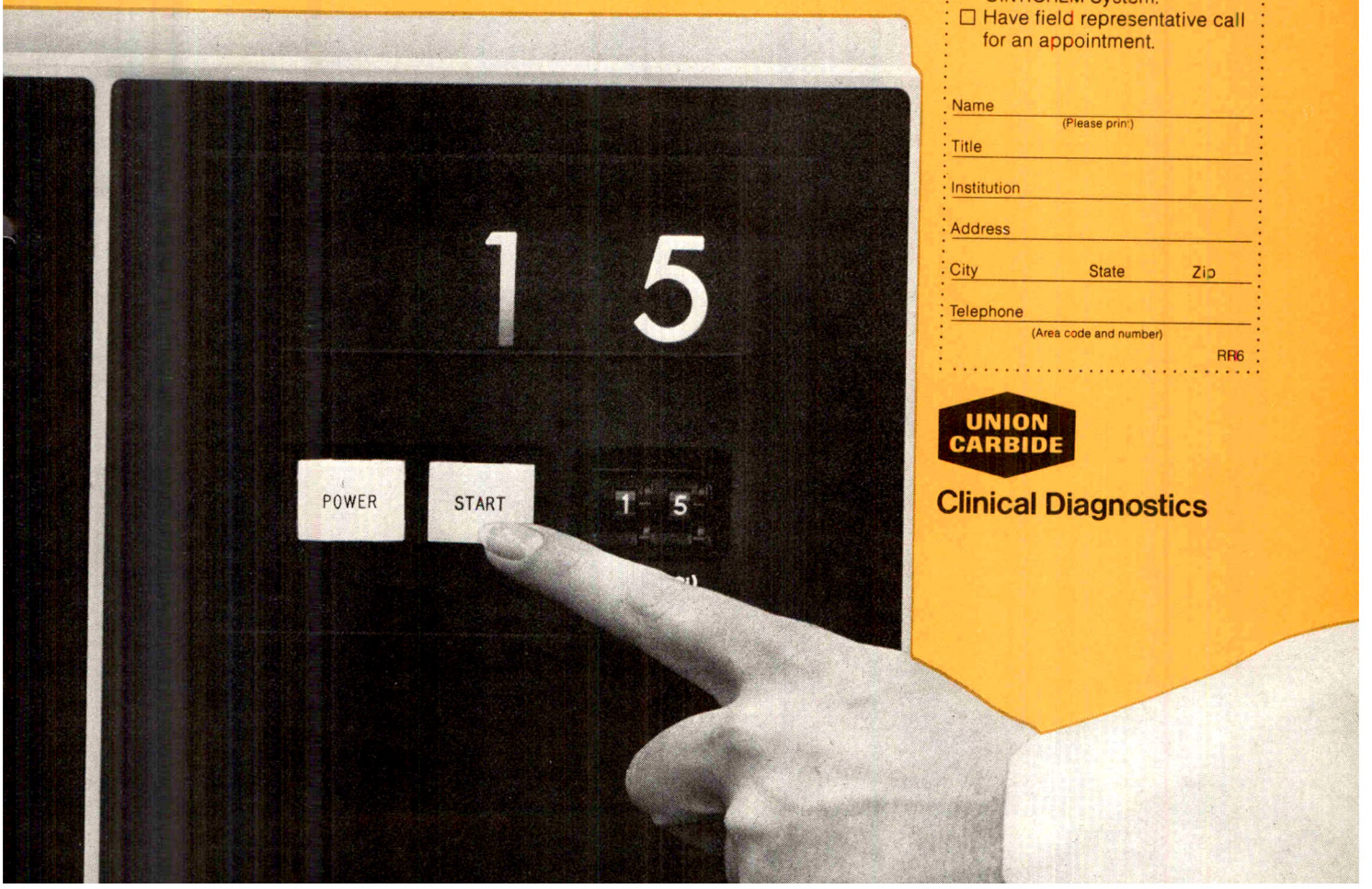
Union Carbide Corporation
Clinical Diagnostics
401 Theodore Fremd Avenue
Rye, New York 10580

- ☐ Send brochure on the CINTICHEM System.
- ☐ Have field representative call for an appointment.

Name _____
(Please print)
Title _____
Institution _____
Address _____
City _____ State _____ Zip _____
Telephone _____
(Area code and number)
RR6

UNION CARBIDE
Clinical Diagnostics

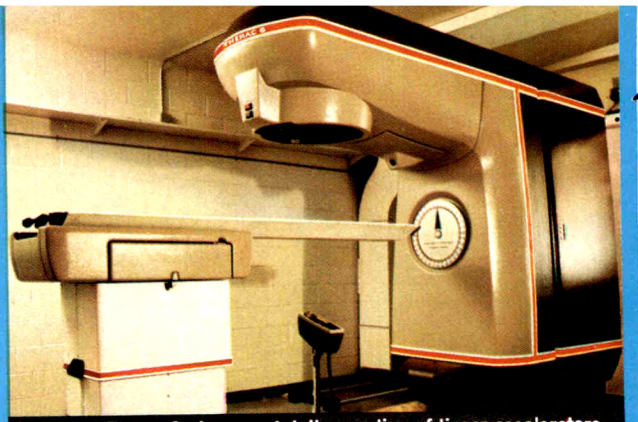
Unit-dose.



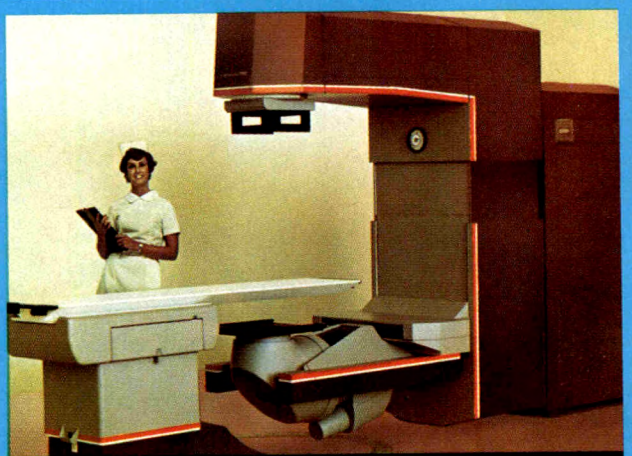
Yes-

Cobalt 60 is still an important part of AECL's business

— But there is MUCH MORE!



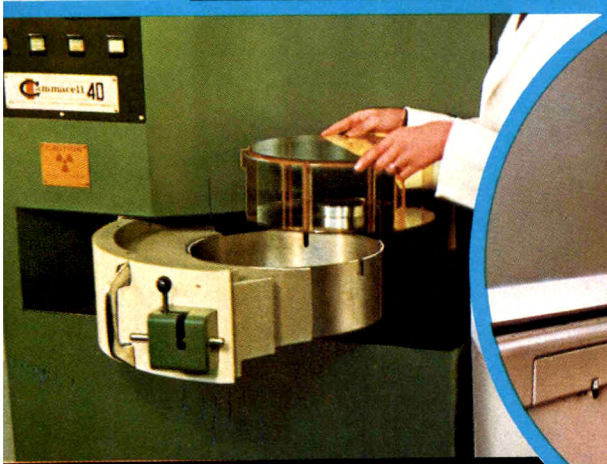
Like the Therac Series — a totally new line of linear accelerators with energy output from 6 to 40 MeV.



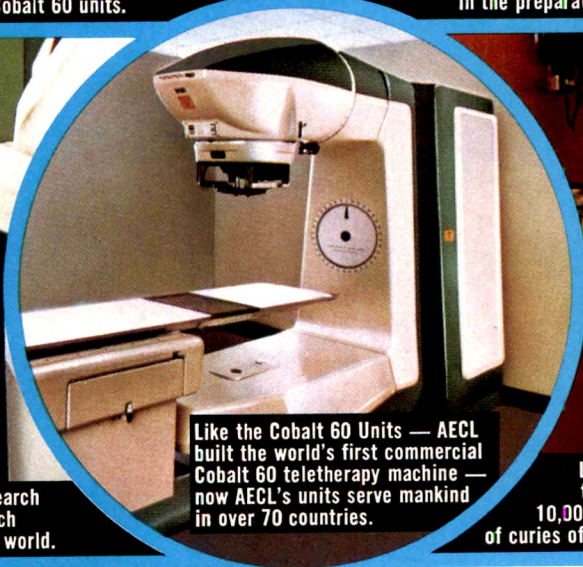
Like the Therasim 750 Universal Simulator — AECL pioneered the design of therapy simulators for use with all makes of accelerators, betatrons and Cobalt 60 units.



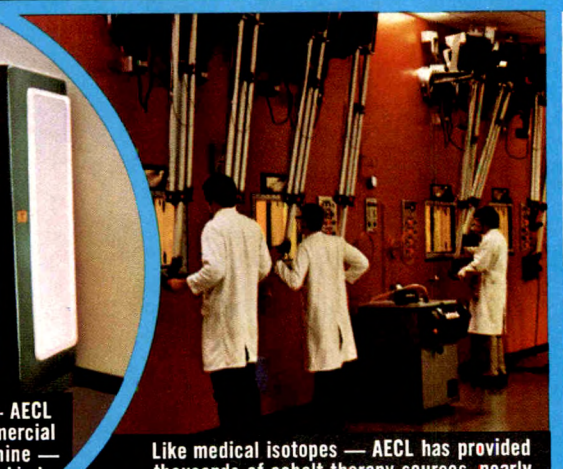
Like the T.P. 11 treatment planning system — a sophisticated blend of computerization and electronics which adds a new dimension in the preparation of reliable therapy treatment planning.



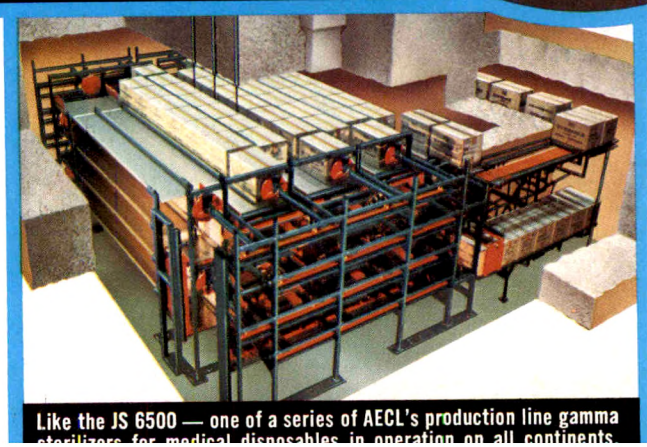
Like the Gammacell 40 Biological Research Irradiator — Hundreds of AECL research irradiators are in daily use around the world.



Like the Cobalt 60 Units — AECL built the world's first commercial Cobalt 60 teletherapy machine — now AECL's units serve mankind in over 70 countries.



Like medical isotopes — AECL has provided thousands of cobalt therapy sources, nearly 10,000,000 curies of medical cobalt and millions of curies of isotopes for diagnostic and treatment use.



Like the JS 6500 — one of a series of AECL's production line gamma sterilizers for medical disposables in operation on all continents.

Atomic Energy of Canada Limited Commercial Products

P.O. Box 6300, Ottawa, Canada.
K2A 3W3. Tel. 613/592-2790

Total Dedication to Medical Treatment and Research

IMAGING:
The Living Art



...are entering a remarkable era of diagnostic advancement. Instead of being limited to a single imaging method, you will take advantage of many techniques, choosing them to meet your specific diagnostic criteria and the condition of your patient.

Searle is helping shape this era of advancement. Over the past decade, guided by your needs, we have developed sophisticated nuclear imaging instruments to a high degree of performance. Now, the knowledge gained during that time is being applied to the creation of instrumentation in the fields of ultrasound and CT scanning.

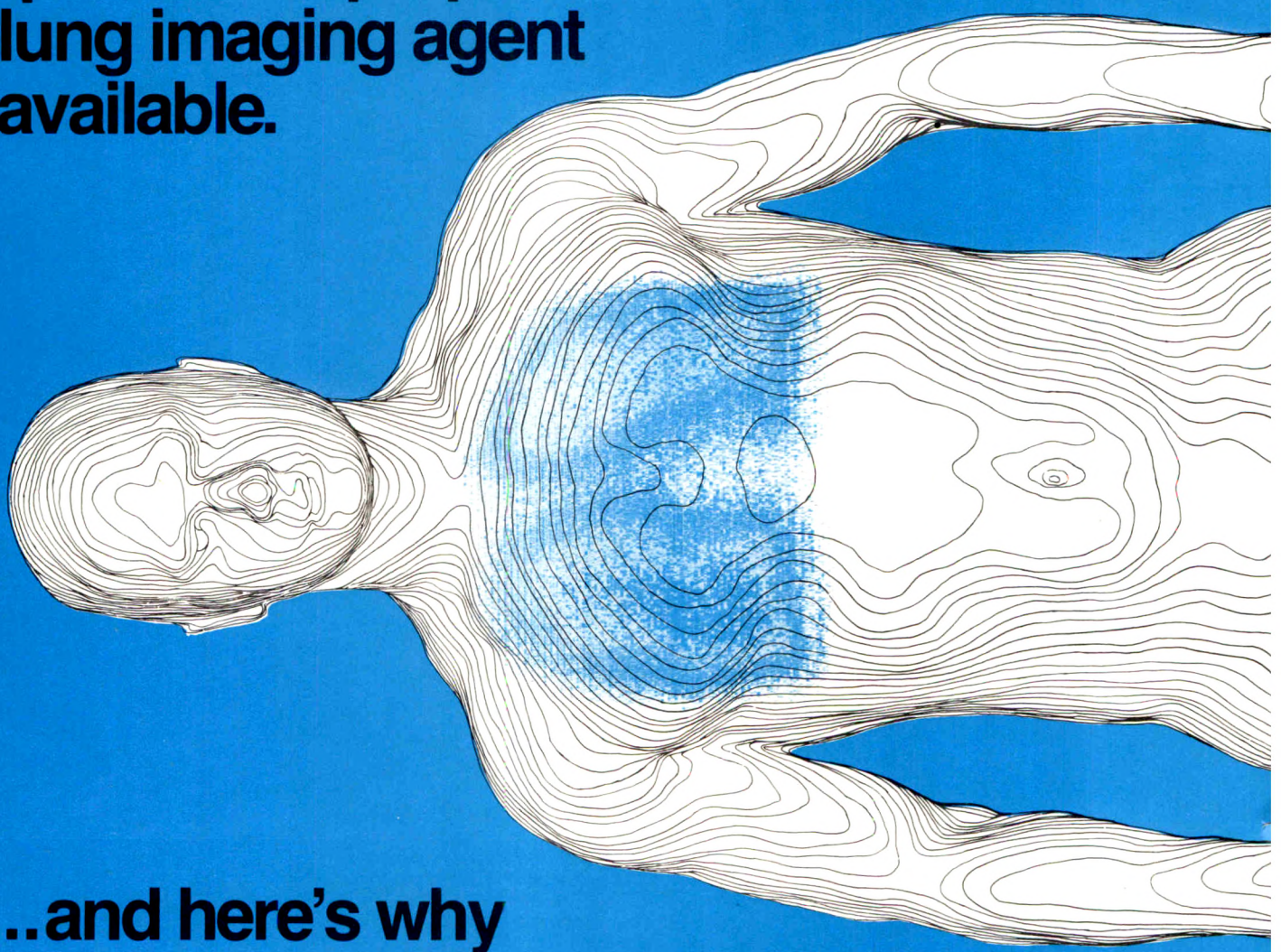
What Searle developed yesterday in nuclear imaging, the medical community relies on today. And *today* we are planning significant advances in ultrasonic, CT, and nuclear imaging. Tomorrow is in view.

SEARLE

Searle Radiographics Inc.

Macrotec®
Aggregated Albumin (Human)
for labeling with technetium 99m

STILL! the simplest, quickest to prepare lung imaging agent available.



...and here's why

Simple, two-step procedure. Not an ampul, not a frozen material. No waiting, no complicated procedures or specialized equipment required. Just two easy steps and you're ready to assay and inject.

Uniform particle size, excellent labeling efficiency. Particle size meets or exceeds Bureau of Biologics standards; 90% in 5-60 micron range. Excellent labeling efficiency when reconstituted with a compatible technetium 99m.

Won't agglomerate in the vial, loses virtually no labeling for 8 hours (if stored between 2°C. and 8°C.).

Ideal for the busy lab. Recommended amount of 99mTc for reconstitution high enough to allow

BASIC STEPS IN PREPARING FOUR TECHNETIUM

Squibb Macrotec® Aggregated Albumin (Human)	**1. Add 1-3 ml. of 99mTc*.* Maintain shielding at all times.**	**2. Shake vigorously for 10-15 seconds.**
Mallinckrodt TechneScan™ MAA Aggregated Albumin (Human)	**1.** Remove reaction vial from *freezer* and *wait approximately 5 minutes* for contents to come to room temperature.	**2.** Add 99mTc*.* Maintain shielding at all times.
3M Albumin Microspheres (Human)	**1.** Add 4-10 ml. of 99mTc*.*	**2.** Shield completely and vigorously shake for 5-15 seconds.
Medi+Physics Lungaggregate™ Reagent Aggregated Albumin (Human)	**1.** Shake *ampul* vigorously to suspend particles.	**2.** Open ampul.

MACROTEC® (Aggregated Albumin [Human])

Macrotec (Aggregated Albumin [Human]) is a sterile, non-pyrogenic, lyophilized preparation of aggregated albumin. Each vial of the preparation contains 0.08 mg. tin as chloride, 1.5 mg. denatured human serum albumin, and 10 mg. Normal Serum Albumin (Human).

INDICATIONS: For use in perfusion lung imaging as an adjunct to other diagnostic procedures.

CONTRAINDICATIONS: At present there are no known contraindications to the use of this product.

WARNINGS: Radiopharmaceuticals should not be administered to patients who are pregnant, or during lactation, unless the benefits to be gained outweigh the potential hazards.

Ideally, examinations using radiopharmaceuticals, especially those elective in nature, of a woman of childbearing capability, should be performed during the first few (approximately 10) days following the onset of menses.

Since ^{99m}Tc is excreted in milk during lactation, formula-feedings should be substituted for breast-feedings.

Radiopharmaceuticals should be used only by physicians who are qualified by specific training in the safe use and handling of radionuclides produced by nuclear reactor or particle accelerator and whose experience and training have been approved by the appropriate government agency authorized to license the use of radionuclides.

Note: Macrotec (Aggregated Albumin [Human]) is not radioactive. However, after ^{99m}Tc is added, adequate shielding of the resultant preparation should be maintained.

PRECAUTIONS: In the use of any radioactive material, care should be taken to insure minimum radiation exposure to the patient consistent with proper patient management, and to insure minimum radiation exposure to occupational workers.

Aseptic technique is essential in the preparation of Technetated [Tc-99m] Aggregated Albumin (Human).

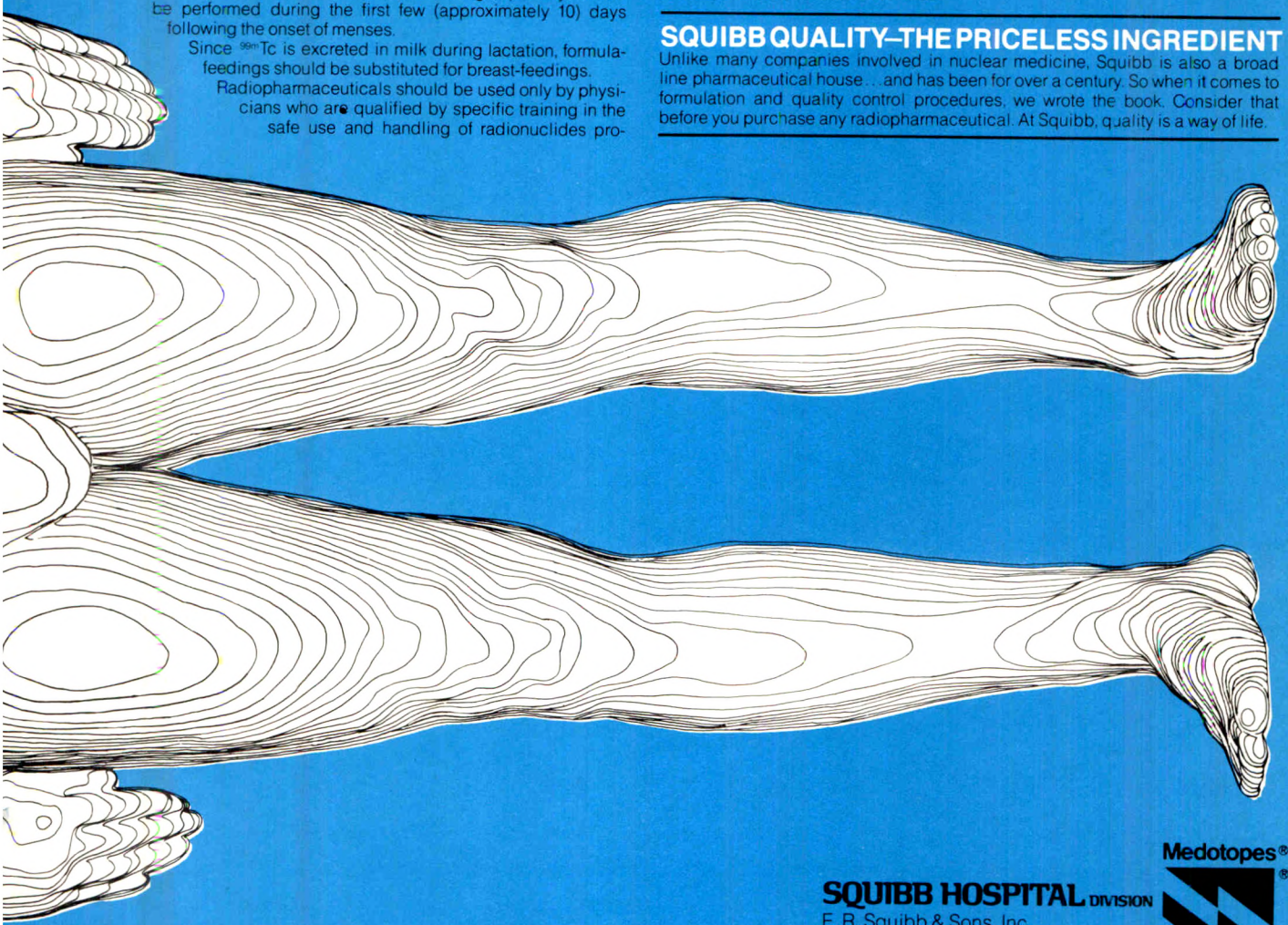
ADVERSE REACTIONS: At present, adverse reactions have not been reported following the administration of this product.

For full prescribing information, consult package insert.

HOW SUPPLIED: In boxes of 5 vials.

SQUIBB QUALITY—THE PRICELESS INGREDIENT

Unlike many companies involved in nuclear medicine, Squibb is also a broad line pharmaceutical house... and has been for over a century. So when it comes to formulation and quality control procedures, we wrote the book. Consider that before you purchase any radiopharmaceutical. At Squibb, quality is a way of life.



Medotopes®

SQUIBB HOSPITAL DIVISION
E. R. Squibb & Sons, Inc.
Princeton, N.J. 08540

©1976 E.R. Squibb & Sons, Inc.

H606-504

99m-LABELED LUNG IMAGING AGENTS*

3. Gently agitate vial for few seconds.

4. *Allow to stand for 15 minutes* at room temperature.

5. Visually inspect vial for presence of large aggregates. *If present, do not use.*

6. *Agitate* to effect homogenous suspension of the aggregated albumin.

**Recommended maximum activity: 60 mCi.

3. Remove vial from shield (with forceps) and place in center of operating *ultrasonic bath* containing 3/4" of water. Bath should be protected by *lead glass or bricks.*
Ultrasound for 5 minutes.

**Recommended maximum activity: 30 mCi.

3. Withdraw (very slowly) 1.5-2.0 ml. of aggregate from ampul with *syringe.*

4. Inject (very slowly) syringe contents into *mixing vial.*

5. Wrap mixing vial in *absorbent paper disc* and place in lead shield.

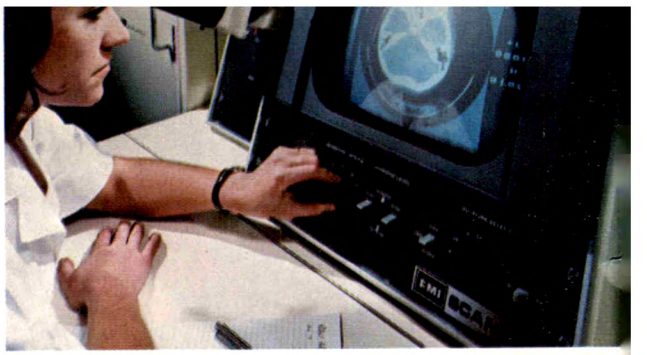
6. Add 0.5-2.0 ml. of 99mTc** in saline into shielded mixing vial. Shake vigorously for at least 30 seconds. *Incubate* at room temperature *for 2-5 minutes.*

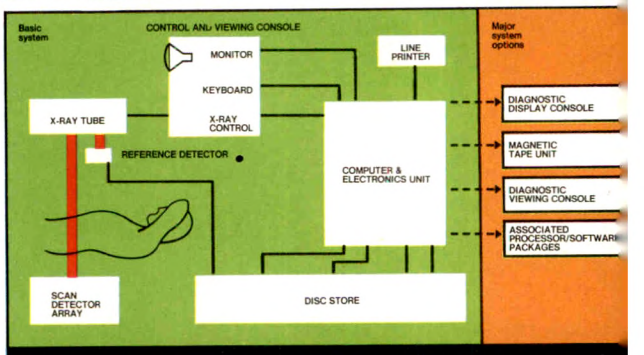
7. Shake contents vigorously just before removing aliquot intended for patient use.

**Recommended maximum activity: 25 mCi/ml.

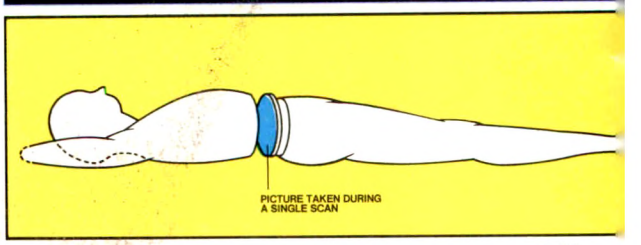
**Recommended maximum activity: 50 mCi.







The EMI-Scanner CT5005 can resolve picture elements as small as 0.75 mm x 0.75 mm.



6-216

The EMI CT5005 head and body scanner provides

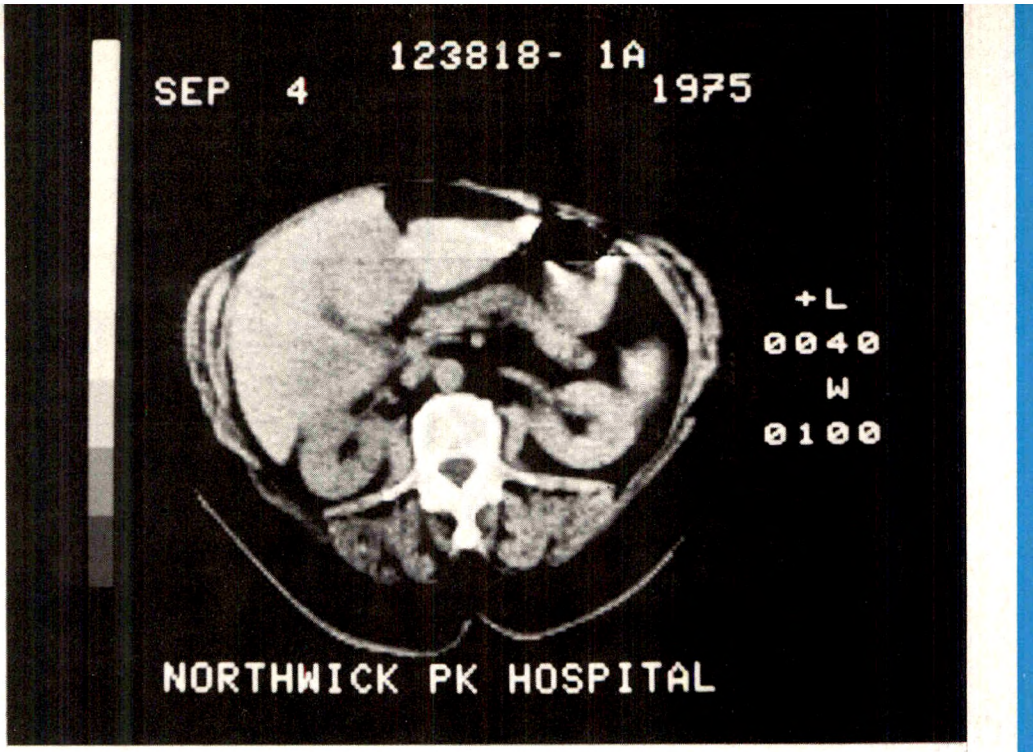
CT Scans, cranium to calcaneus

Like its companion system—the EMI CT1010 Neuro C.T. Scanner—our new EMI-Scanner CT5005 Advanced General Diagnostic C.T. System is based on fully proven technology that has established EMI as the unrivaled world leader in computerized tomographic scanning. This new head and body scanning system combines the capability for exceptional resolution, definition and accuracy in the pictures produced, a very fast scanning cycle, unusually powerful computing capability and other advanced features that contribute to ease-of-operation and efficient patient handling. The CT5005 General Diagnostic System can be tailored by selection of the appropriate choice of peripherals and software packages to meet specific clinical needs. Obviously, for the radiologist and referring physician alike, the quality of the scan picture itself is the final proof of any CT system's performance. The EMI-Scanner System has met this test in hundreds of institutions. It is the world's only fully proven scanner system. For information, call us or write.

EMI

First in CT system engineering

EMI MEDICAL INC



Scan taken through the 1st lumbar vertebra. Note the liver, spleen, kidneys, aorta, superior mesenteric artery, stomach, pancreas, inferior vena cava, and right renal vein.

6-217

Superior diagnostic information in every EMI-SCAN:

A bright window at L1

The picture you see above is a reproduction of an EMI-SCAN. The EMI-Scanner CT5005 Advanced General Diagnostic C.T. System (cranium and body scanner) results in pictures composed of more than 300,000 X-ray readings. The CT5005 differentiates between tissue densities that can vary by as little as one unit in 2000. In addition to resolving picture elements 0.75 mm x 0.75 mm in area, the EMI-Scanner CT5005 high-resolution option provides a special clinician's Diagnostic Viewing Console that enables any section of the total scan picture to be enlarged four times. This special viewing facility may be operated completely independently of the in-use status of the main installation—either at the scanner site or a remote location. Additional diagnostic display and data processing options are provided to meet specific clinical needs. The EMI-Scanner is unexcelled in accuracy, resolution, and clinical versatility. It is unrivaled in clinical acceptance and use, worldwide. There is no brighter diagnostic window. For more information, call us or write.

EMI

First in CT imaging, worldwide

EMI MEDICAL INC

3605 Woodhead Drive, Northbrook, Illinois 60062 Telephone: (312) 564-2000

We want to make gall bladder studies more convenient.

For you. For your patients.



Oragrafin®
Calcium Granules
Ipodate Calcium for Oral Suspension U.S.P.

Oragrafin®
Sodium Capsules
Ipodate Sodium Capsules U.S.P.

SQUIBB®
contrast media™
the reason is clear™

Oragrafin (Ipodate) conveniences...

Scheduling flexibility

Diagnostically adequate filling of the gallbladder often takes place within 5 hours or less after ingestion of granules, thereby permitting same-day examinations.

In routine overnight procedures, opacification is attained 10 hours after ingestion of capsules.

Choice of dose forms

Granules or capsules – Rapid absorption of both calcium salt and sodium salt often permits visualization of even poorly functioning gallbladders.

Prepared or unprepared patients

Both salts have been administered to unprepared patients as well as previously prepared patients, with no significant difference in results.

Please see following page for brief summary.



ORAGRAFIN® CALCIUM GRANULES
Ipodate Calcium for Oral Suspension U.S.P.
ORAGRAFIN® SODIUM CAPSULES
Ipodate Sodium Capsules U.S.P.

CONTRAINDICATIONS: Both preparations are contraindicated in patients who are hypersensitive to ipodate salts.

WARNINGS: A history of sensitivity to iodine *per se* or to other iodinated compounds is not an absolute contraindication to the use of these preparations, but calls for extreme caution in administration.

Usage in Pregnancy: The safety of these preparations for use during pregnancy has not been established; therefore, they should be used in pregnant patients only when, in the judgment of the physician, their use is deemed essential to the welfare of the patient.

PRECAUTIONS: Increasing the dosage above that recommended increases the possibility of hypotension. Anuria may result when these preparations are administered to patients with combined renal and hepatic disease or severe renal impairment. Renal toxicity has been reported in a few patients with liver dysfunction who were given oral cholecystographic agents followed by urographic agents. Administration of urographic agents should therefore be postponed in any patient with a known or suspected hepatic or biliary disorder who has recently taken a cholecystographic contrast agent. Gastrointestinal disorders which interfere with absorption and liver disorders which interfere with excretion may result in nonvisualization of the hepatic and biliary ducts and the gallbladder. Contrast agents may interfere with some chemical determinations made on urine specimens; therefore, urine should be collected before administration of the contrast media or two or more days afterwards. Thyroid function tests, if indicated, should be performed prior to the administration of these preparations since iodine-containing contrast agents may alter the results of these tests.

ADVERSE REACTIONS: Mild and transient nausea, vomiting, or diarrhea sometimes occur; the incidence can be reduced by using the calcium granules and restricting the dosage to 3 g. in persons prone to gastrointestinal reactions. Transient headache, dysuria, or abdominal pains may occur.

Hypersensitivity reactions may include urticaria, serum sickness-like reactions (fever, rash, arthralgia), other skin rashes, and rarely anaphylactoid shock.They are more likely to occur in persons with a history of allergy, asthma, hay fever, or urticaria and in those who are known to be hypersensitive to iodine compounds.

Note Concerning Dosage: A total dose of 6 g. (12 capsules or 2 packets of Granules) per 24-hour period should not be exceeded.

For full information, see Package Insert.

HOW SUPPLIED: Oragrafin Calcium Granules (Ipodate Calcium for Oral Suspension U.S.P.) provide 3 g. ipodate calcium per packet; available in boxes of 25 single-dose foil packets. Oragrafin Sodium Capsules (Ipodate Sodium Capsules U.S.P.) provide 0.5 g. ipodate sodium per capsule; available in boxes of 25 vials (each vial contains 6 capsules), in bottles of 100, and in Unimatic® packages of 100.

the reason is clear™

SQUIBB®
contrast media

SQUIBB HOSPITAL DIVISION
E. R. Squibb & Sons, Inc.
©1976 E. R. SQUIBB & SONS, INC. H636-5011

CHARLES C THOMAS • PUBLISHER

THE RENAL UPTAKE OF RADIOACTIVE MERCURY ($^{197}HgCl_2$): Method for Testing the Functional Value of Each Kidney, Technique–Results– and Clinical Application in Urology and Nephrology *edited by* **Claude Raynaud,** *Service Hospitalier Frederic Joliot, Orsay, France. Foreword by* **Pierre Royer.** *(41 Contributors)* Several techniques of uptake measurement are described in the first chapters of this text along with simplified systems of external counting, scanners or gamma cameras, and specific problems associated with the deep position of the kidney or Hg metabolism. The remainder of the book discusses the normal values of Hg renal uptake as well as the results obtained in patients. *'76, 248 pp., 110 il., 47 tables, $22.75*

THE HAND ATLAS *by* **Moulton K. Johnson** *and* **Myles J. Cohen,** *both of UCLA, Los Angeles, California.* This atlas portrays the anatomy of the hand as the surgeon will encounter it in the operating room – layer by layer, beginning with the skin and ending with x-ray studies of the bones. Photographs of dissections of unembalmed specimens are all approximately life-size or larger, resulting in better illustrations. Topics include the distal volar forearm, the palm, thumb, fingers, the radial side of the hand, spaces of the hand and wrist mechanics. *'75, 108 pp. (8 1/2 x 11), 121 il. (8 in color), $22.00*

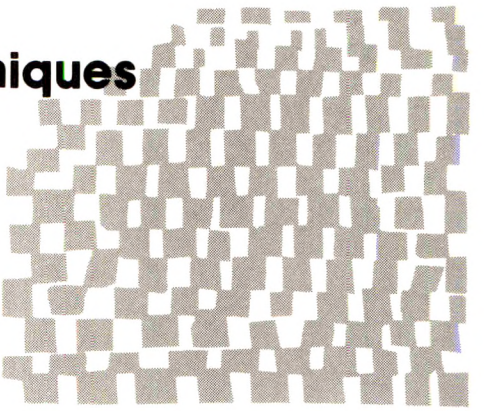
RADIONUCLIDE SCANNING IN CYANOTIC HEART DISEASE *by* **Gary F. Gates,** *UCLA, Los Angeles.* A new, unique application of nuclear medicine in the clinical management of children with cyanotic congenital heart disease is described in this monograph. The procedure is fully described and steps used in performing the examination are thoroughly outlined. Possible pitfalls and sources of error are also discussed. The calculation of results does not require sophisticated mathematics or complicated computer analysis. Accuracy is assured by correlation with surgery or cardiac catheterization. Although this procedure has usefulness in many pediatric cardiopulmonary disorders, its application to the surgical patient is unique. *'74, 114 pp., 88 il., 5 tables, $15.00*

Prepaid orders sent postpaid, on approval

301-327 EAST LAWRENCE
SPRINGFIELD • ILLINOIS • 62717

MOSBY
TIMES MIRROR

How You Can Incorporate the Latest Ultrasonic Techniques into Your Practice....



carefully explained in a new reference from Mosby

A New Book!

CARDIAC ULTRASOUND

This superb new book offers you a complete discussion of cardiac ultrasound, from basic physical principles to specific applications of the newest techniques. Internationally-recognized authorities discuss recording methods, structure identification, specific heart valves, chamber and great vessel size, pericardial effusion, congenital heart disease, and much more. You'll find precise information on acquisition and interpretation of patient examination data and on factors affecting the accuracy of measurements. An enlightening section describes new and emerging techniques, including methods for two-dimensional cardiac imaging: ECG gated B-scanning, multi-element arrays, acoustic holography, computer based reconstruction, and more.

Edited by Raymond Gramiak, M.D. and Robert C. Waag, Ph.D.; with 18 contributors. November, 1975. 308 pages plus FM I-XIV, 7" x 10", 465 illustrations. Price, $36.50.

Also of interest . . .

A New Book!

RADIOTHERAPY IN MODERN CLINICAL PRACTICE

This new volume examines the most recent advances in the treatment of malignant disease by irradiation. Dr. H. F. Hope-Stone and 10 contributors provide you with detailed information on the principles and practice of radiotherapy. The authors discuss methods and degree of radiation; diagnostic and therapeutic usage; protection of patient and operator; and patient positioning.

By Dr. H. F. Hope-Stone, L.R.C.P., M.R.C.S., M.B.B.S., D.M.R.T., F.F.R. April, 1976. 368 pages plus FM I-X, 6" × 9", 139 illustrations. Price, $24.50.

MOSBY
TIMES MIRROR

THE C V MOSBY COMPANY
11830 WESTLINE INDUSTRIAL DRIVE
ST LOUIS MISSOURI 63141

Clysodrast®
(BISACODYL TANNEX)

The safe and certain barium additive

Helps you be sure of what you see



Clysodrast is a unique colonic evacuant. It mixes with barium enemas to give radiologists the only form of tannic acid* available for safe, high-resolution barium enema studies. And a growing body of experimental evidence has shown the diagnostic benefits of Clysodrast added to a barium suspension.[1,2,3] This combination provides unmatched mucosal visualization for superior roentgenologic diagnoses.

SAFETY YOU CAN COUNT ON

Only tannic acid really prepares the colon and produces the even, thin-film deposition of barium sulfate that a radiologist needs for maximum clarity. Clysodrast combines tannic acid with the contact laxative bisacodyl, for optimum effectiveness. And Clysodrast comes in accurately measured, 2.5 Gm. packets to avoid the danger of accidental overdose. With Clysodrast, results are consistently safe and uniform, too. No patient has ever suffered hepatic necrosis as a result of Clysodrast being used within the dosage limits indicated in the instructions.[4,5,6] And it has been used in well over 2 million barium enema procedures since 1970 alone, usually with no more side effects than a water enema produces.[7,8]

Clysodrast is recommended for double contrast studies with an appropriate form of barium sulfate, such as Barotrast.® It is also indicated for the preparation of patients for radiologic examinations of the colon, sigmoidoscopy and proctologic examinations, when used as directed.

USE CLYSODRAST, FOR SURE

Clysodrast provides radiologists with the assurance of high resolution barium studies no other product can provide. Find out for yourself how Clysodrast can help you see for sure. Contact your local X-ray supplies dealer.

See summary of prescribing information on adjoining page.

*Bisacodyl tannex

Also see your X-ray supplies dealer for Oratrast,® Barotrast® and Esophotrast.®

INDICATIONS: CLYSODRAST (bisacodyl tannex) may be indicated for the preparation of patients for radiologic examinations of the colon, sigmoidoscopy and proctologic examinations.

CONTRAINDICATIONS: CLYSODRAST is contraindicated in patients under the age of 10 because the possibility of absorption of tannic acid has not been adequately studied in this age group to warrant a conclusion of safety. CLYSODRAST is also contraindicated in cases with known or suspected extensive ulcerative lesions of the colon.

WARNING: Usage in Pregnancy. Safe use of CLYSODRAST has not been established with respect to the adverse effects upon fetal development. Therefore, it should not be used in women of child-bearing potential, particularly during early pregnancy, except where, in the judgment of the physician, the potential benefits outweigh the possible hazards.

PRECAUTIONS: Tannic acid, one of the active ingredients of CLYSODRAST, is hepatotoxic if absorbed in sufficient quantity. Deaths have been reported from hepatic damage due to tannic acid used in barium enema examination. Thus, CLYSODRAST should be used with caution in a regimen where multiple enemas are administered. Certain patients, because of age, debility, or underlying disease, require more gentle preparation than the routine castor oil and CLYSODRAST preparation. It is important that the instructions for preparation and administration be followed in detail, and that the recommended dosages not be exceeded.

ADVERSE REACTIONS: The following adverse reactions have been reported: Cramping, weakness, nausea and fainting.

DOSAGE AND ADMINISTRATION: It is important that the entire medical history and condition of the patient be considered in deciding the dosage regimen. Traumatizing procedures, such as repetition of enemas (with or without CLYSODRAST) should be kept at the minimum necessary to achieve the desired result.

CLEANSING ENEMA: Prepare the cleansing enema by dissolving the contents of one packet (2.5 Gm.) of CLYSODRAST in one liter of lukewarm water and administer.

BARIUM ENEMA: Prepare the barium enema by dissolving the contents of one or not more than two packets (2.5 Gm. or 5.0 Gm.) of CLYSODRAST in one liter of barium suspension. If more than one liter of barium suspension is prepared, it is important that the concentration of CLYSODRAST (bisacodyl tannex) never exceed 0.5 percent (2 packets per liter).

The total dosage of CLYSODRAST for any one complete colonic examination, including the cleansing enema, should not exceed 7.5 Gm. (3 packets). No more than 10 Gm. (4 packets) of CLYSODRAST should be administered to any individual within a 72-hour period.

HOW SUPPLIED: CLYSODRAST is supplied in packets containing 1.5 mg. of 4,4′-(diacetoxydiphenyl)-(pyridyl-2)-methane complexed with 2.5 Gm. of tannic acid, N.F. These packets are supplied in cartons of 25 and 50 packets.

CAUTION: U.S. Federal law prohibits dispensing without prescription.



A Colonic Evacuant

Clysodrast®
(bisacodyl tannex)

Barnes-Hind Pharmaceuticals, Inc.
Sunnyvale, California 94086

1. Goldman, L., *Clinical Medicine*, Vol. 28, pg. 28, 1971
2. Hamilton, *American Journal of Roentgenology*, 1946
3. Janower, M. L., *Radiology*, Vol. 85, pg. 887, 1965
4. Burhenne, et al, *American Journal of Roentgenology*, Vol. 96, pg. 510, 1966
5. Lucke, et al, *Canadian Medical Association*, Vol. 89, pg. 1111, 1963
6. McAlister, et al, *Radiology*, Vol. 80, pg. 765, 1963
7. Steinbach, et al, *American Journal of Roentgenology*, Vol. 87, pg. 644, 1962
8. Thomas, *American Journal of Roentgenology*, Vol. 89, pg. 889, 1963

Hanley Space Saver X-Ray and Medical Record Cabinets are installed in most hospitals in America.

Top quality and low price is the reason.
5 compartment with doors—$199.50
5 compartment less doors—$171.50
Brochure F.O.B. Factory

AMERICA'S LARGEST DISTRIBUTOR OF X-RAY CABINETS

HANLEY MEDICAL EQUIPMENT CO.
5614 South Grand X-Ray Division St. Louis, Mo. 63111

In reply to advertisers please mention that you saw their advertisement in

THE AMERICAN JOURNAL OF ROENTGENOLOGY, RADIUM THERAPY AND NUCLEAR MEDICINE

• • •

CHARLES C THOMAS PUBLISHER
Springfield · Illinois

The Department of Radiology of the University of Minnesota will present its Thirty-Ninth Annual Continuing Medical Education Course, September 13-17, 1976.

The two major topical areas will be:

Cardiovascular Radiology—2½ days

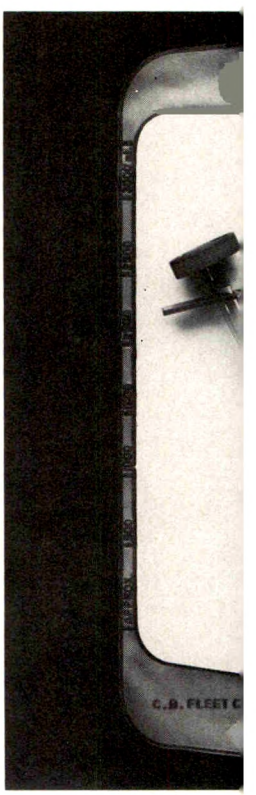
Selected Topics in Diagnostic Radiology—2½ days

For further information contact:
Continuing Medical Education
Box 293
Mayo Memorial Building
412 Union Street S.E.
University of Minnesota
Minneapolis, Minnesota 55455

From start to finish, Fleet systematizes

For cleaner colons, clearer x-rays, and fewer retakes





For preparation,
Fleet Barium Enema Prep Kits assure thorough, reliable colon cleansing by utilizing a combination of diet, hydration, and evacuation.

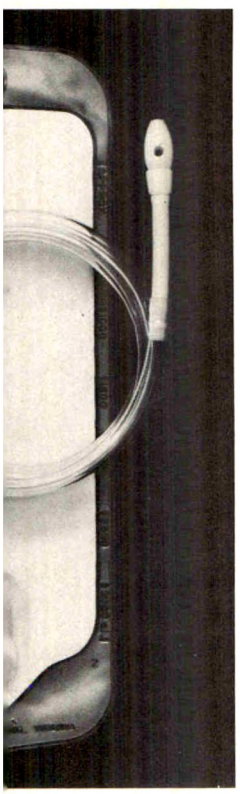
- Available in two convenient forms with suppository or enema as final step.
- Offering an effective and balanced method of prepping.
- Meeting all criteria for colon preparation as recommended by the American College of Radiology Ad Hoc Committee on Detection of Cancer of the Colon.
- With easy-to-follow instructions.
- With 3 convenient time schedules to fit better into your schedule and your patient's routine.

For the examinatio
Fleet Barobag offers greater visibility because it contains Ultrasperse® with a combination of barium sulfate USP (98%) and selected suspensing and dispersing agents (2%) for "instantized" mixability.

- With excellent suspension stability—up to 2 hours.
- With rapid, free-flow emptying.

barium enema exams...

3. Fleet presents a unique ee-part system of products t can help you give quality barium enema exams. It includes Fleet® Barium Enema Prep Kits for colon preparation, Fleet® Barobag for the actual barium enema examination, and Fleet® Phospho-Soda for aftercare.





kproof with screw sures for conven- ce.
n angled spout) for easier filling handling.
ilable with either 12 6 oz. Ultrasperse® rium sulfate USP).
o available with ntion catheter.

For aftercare,
Fleet Phospho-Soda is gentle and most effective for cleansing the colon of barium and for preventing fecal impaction.

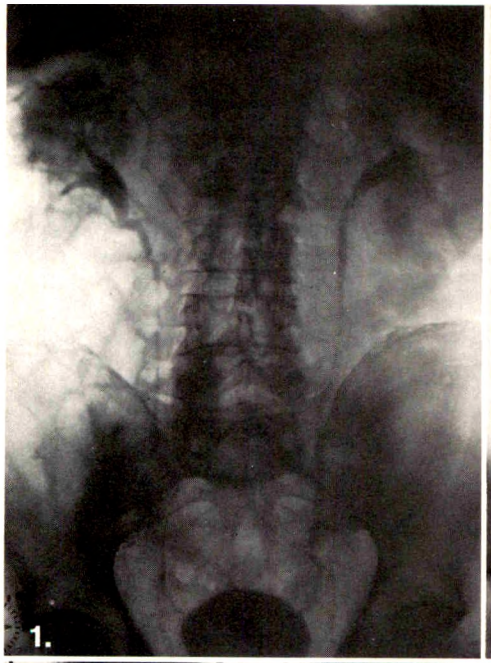
- Works in an hour or overnight, according to dosage, for convenience and flexibility in scheduling.
- Usually produces soft, formed stool with no unusual side effects.
- Promotes natural peristalsis to assure thorough action.
- Buffered for gentleness.
- Easy-to-take.
- Safe for use by patients of all ages, as indicated.

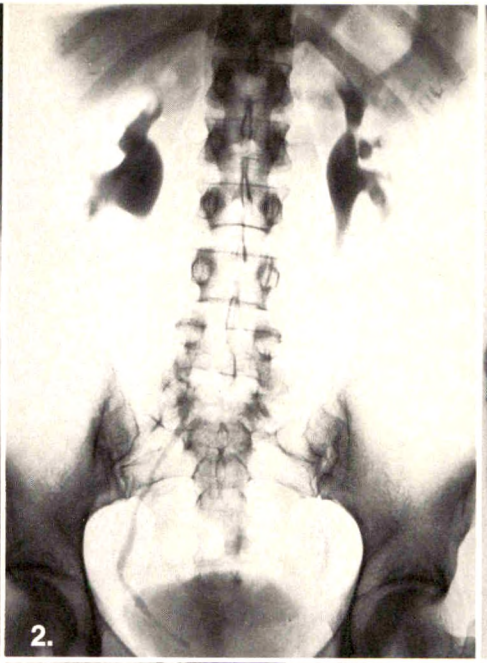
In the final note to *Detection of Colon Lesions* by the American College of Radiology Ad Hoc Committee on Detection of Cancer of the Colon, R. E. Miller states: "Almost every recommendation made is part of urging *quality control* by the radiologist in all aspects of his colon examination."

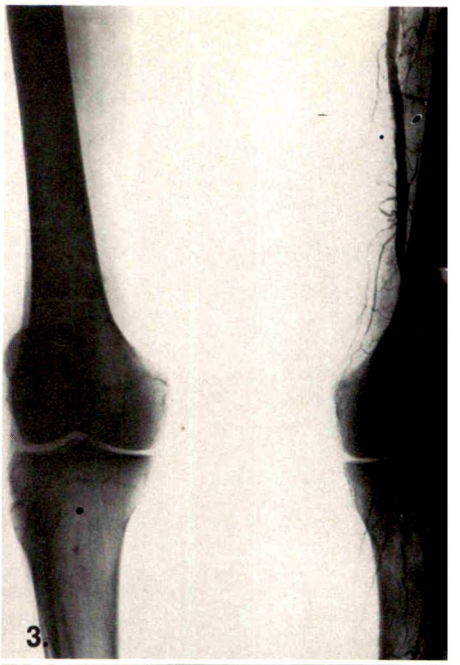
Fleet's new system of products will answer almost every need you'll encounter in barium enema examinations—from start to finish.

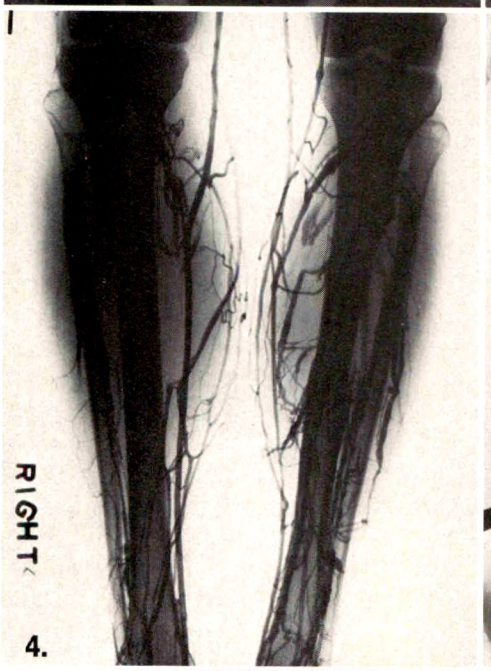
In barium enema exams, quality controls results. And Fleet controls quality.

Fleet pharmaceuticals
C.B. FLEET CO., INC.
Lynchburg, Va. 24505

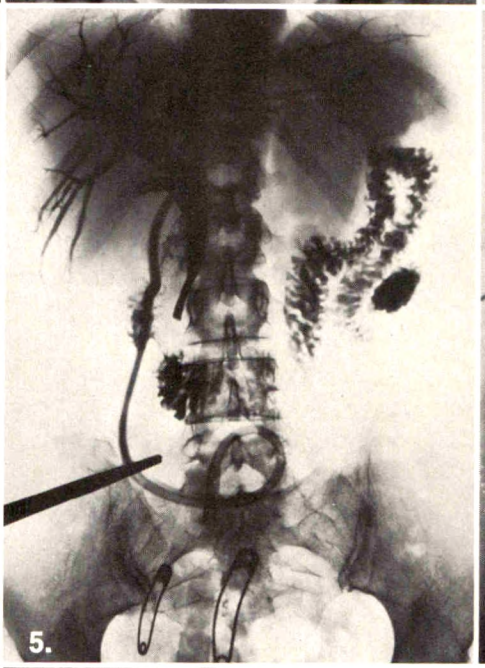

1.


2.


3.



4.


5.


6.


7.


8.


9.

The many applications* of Renografin®-60

Diatrizoate Meglumine and Diatrizoate Sodium Injection U.S.P.

COLLEGE OF RADIOLOGY LIBRARY

Count them:

1. Drip infusion pyelography
2. Excretion urography (direct I.V.)
3. Peripheral arteriography
4. Venography
5. Cholangiography—operative, T-tube†, and percutaneous transhepatic
6. Splenoportography
7. Arthrography
8. Discography
9. Cerebral angiography

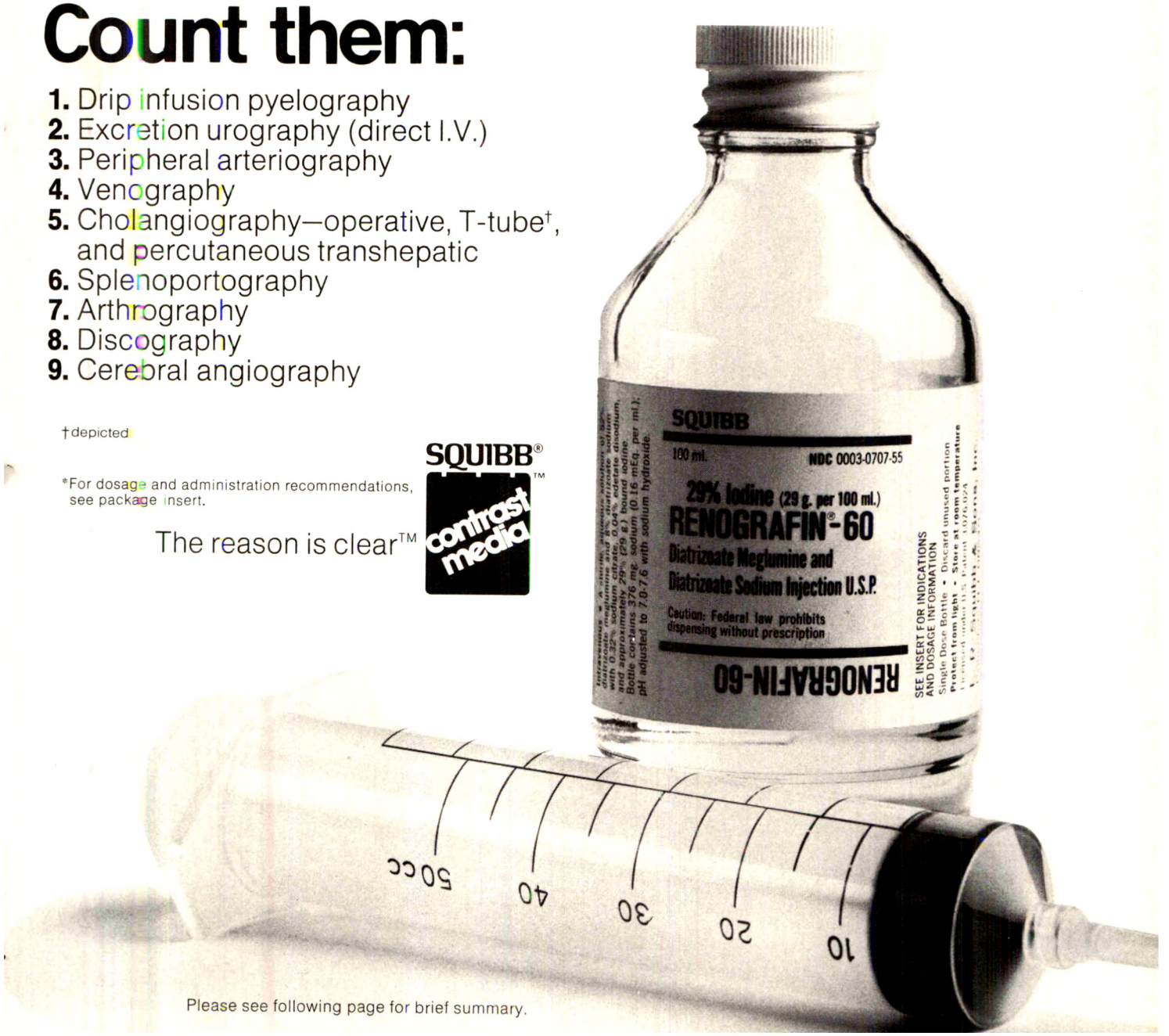
†depicted

*For dosage and administration recommendations, see package insert.

SQUIBB®

contrast media™

The reason is clear™



Please see following page for brief summary.

RENOGRAFIN®-60
Diatrizoate Meglumine and Diatrizoate Sodium Injection U.S.P.

CONTRAINDICATIONS: Contraindicated in persons hypersensitive to salts of diatrizoic acid. **Urography** is contraindicated in patients with anuria. A prothrombin time below 50% and evidence of coagulation defects are contraindications to **percutaneous transhepatic cholangiography** and **splenoportography.** When splenectomy is contraindicated, **splenoportography** should not be performed since complications of the procedure make splenectomy necessary at times. Significant thrombocytopenia and any condition which may increase the possibility of splenic rupture are contraindications to **splenoportography. Arthrography** is contraindicated if infection is present in or near the joint. **Discography** is contraindicated if there is infection or open injury near the region to be examined.

WARNINGS: A definite risk exists with the use of contrast agents in excretion urography in patients with multiple myeloma. There has been anuria with progressive uremia, renal failure and death. This risk of the procedure in these patients is not a contraindication; however, partial dehydration in preparation for study is not recommended since it may predispose for precipitation of myeloma protein in renal tubules. No therapy, including dialysis, has been successful in reversing this effect. Myeloma should be considered in persons over 40 before undertaking urographic procedures.

In cases of known or suspected pheochromocytoma, if the physician feels that the possible benefits outweigh the considered risks, radiopaque materials should be administered with extreme caution; however, an absolute minimum of material should be injected, the blood pressure should be assessed throughout the procedure, and measures for treating a hypertensive crisis should be available.

Contrast media may promote sickling in homozygous individuals when injected I.V. or intra-arterially. Although a history of sensitivity to iodine *per se* or to other contrast media is not an absolute contraindication, administration of diatrizoate requires extreme caution in such cases. Perform thyroid function tests prior to administration of this preparation since iodine-containing contrast agents may alter the test results. Avoid accidental introduction of this preparation into the subarachnoid space since even small amounts may produce convulsions and possible fatal reactions.

Perform **cerebral angiography** with special caution in extreme age, poor clinical condition, advanced arteriosclerosis, severe arterial hypertension, cardiac decompensation, recent cerebral embolism, or thrombosis. Perform **urography** with extreme caution in persons with severe concomitant hepatic and renal disease.

Usage in Pregnancy: This preparation should be used in pregnant patients only when the physician deems its use essential to the welfare of the patient since safe use during pregnancy has not been established.

PRECAUTIONS: Diagnostic procedures involving use of contrast agents should be performed under the direction of personnel with prerequisite training and a thorough knowledge of the particular procedure. Appropriate facilities should be available for coping with situations which may arise as a result of the procedure and for emergency treatment of severe reactions to the contrast agent itself; competent personnel and emergency facilities should be available for at least 30 to 60 minutes after I.V. administration since delayed reactions have been known to occur. These severe life-threatening reactions suggest hypersensitivity to the contrast agent. A personal or family history of asthma or allergy or a history of a previous reaction to a contrast agent warrants special attention and may predict more accurately than pretesting the likelihood of a reaction although not the type nor severity of the reaction in the individual. The value of any pretest is questionable. The pretest most performed is the slow I.V. injection of 0.5-1.0 ml. of the preparation prior to injection of the full dose; however, the absence of a reaction to the test dose does not preclude the possibility of reaction to the full diagnostic dose. Should the test dose produce an untoward response, the necessity for continuing the examination should be carefully re-evaluated; if deemed essential, examination should proceed with all possible caution. In rare instances, reaction to the test dose may be extremely severe; therefore, close observation and facilities for emergency treatment appear indicated.

Renal toxicity has been reported in a few patients with liver dysfunction who were given oral cholecystographic agents followed by urographic agents; therefore, if known or suspected hepatic or biliary disorder exists, administration of Diatrizoate Meglumine and Diatrizoate Sodium Injection U.S.P. should be postponed following the ingestion of cholecystographic agents. Exercise caution with use of contrast media in severely debilitated patients and in those with marked hypertension. When percutaneous techniques are used, bear in mind the possibility of thrombosis. Consider the functional ability of the kidneys before injecting Diatrizoate Meglumine and Diatrizoate Sodium Injection U.S.P. Contrast agents may interfere with some chemical determinations made on urine specimens; therefore, collect urine before or two or more days after administration of the contrast medium.

In **peripheral arteriography,** hypotension or moderate decreases in blood pressure seem to occur frequently with intra-arterial (brachial) injections; this is transient and usually requires no treatment; monitor blood pressure during the immediate 10 minutes after injection. In **excretion urography,** adequate visualization may be difficult or impossible in uremic patients or others with severely impaired renal function (see Contraindications). Consider the increased osmotic load associated with drip infusion pyelography in presence of congestive heart failure. The diuretic effect of drip infusion pyelography may hinder assessment of residual urine in the bladder. Do not exceed recommended rate (40 ml./min.) of infusion. In **operative and T-tube cholangiography,** inject the contrast agent slowly to prevent extravasation into peritoneal cavity and to minimize reflux flow into pancreatic duct which may result in pancreatic irritation. In **percutaneous transhepatic cholangiography,** aspirate as much of the contrast agent as possible on completion of successful films to reduce possibility of bile leakage and consequent peritonitis. For 24 hours after the procedure carefully and constantly monitor all patients for signs of internal hemorrhage or bile leakage; if these complications are recognized immediately, remedial measures can be instituted promptly with minimal increase in morbidity. Percutaneous transhepatic cholangiography should be reserved for jaundiced patients who are not good candidates for surgery when requisite information has not been obtained with ordinary studies since the procedure is not without risks; attempt the procedure only when competent surgical intervention can be obtained promptly if needed. In **splenoportography,** manipulations which will prolong the time the needle is in the spleen should be avoided since this may contribute to postpuncture bleeding and subcapsular extravasation of the contrast agent. Following splenoportography, closely observe the patient for 24 hours for signs of internal bleeding; patient should lie on his left side for several hours. Leakage of up to 300 ml. of blood from the spleen is apparently not uncommon; fatal hemorrhage has occurred rarely. Blood transfusions and, rarely, splenectomy may be required. In **discography,** postpone the procedure if an infection (including U.R.I. in cervical discography) or open injury is present near the region to be examined to minimize possible introduction of infection. Disk infection has occurred after discography; therefore, care should be taken to preclude contamination and resultant disk infection. Contamination may be introduced into the disk if care is not taken to avoid puncturing the esophagus during cervical discography. If the needle becomes barbed by contact with bone (the two-needle technique helps reduce this hazard), rupture of the disk may occur; this is highly unlikely if the procedure is performed carefully.

ADVERSE REACTIONS: Nausea, vomiting, flushing, or a generalized feeling of warmth are the reactions seen most frequently with intravascular injection. Symptoms which may occur are chills, fever, sweating, headache, dizziness, pallor, weakness, severe retching and choking, wheezing, a rise or fall in blood pressure, facial or conjunctival petechiae, urticaria, pruritus, rash, and other eruptions, edema, cramps, tremors, itching, sneezing, lacrimation, etc. Antihistaminic agents may be of benefit; rarely, such reactions may be severe enough to require discontinuation of dosage. Severe reactions which may require emergency measures (see Precautions) are a possibility and include cardiovascular reaction characterized by peripheral vasodilatation with hypotension and reflex tachycardia, dyspnea, agitation, confusion, and cyanosis progressing to unconsciousness. An allergic-like reaction ranging from rhinitis or angioneurotic edema to laryngeal or bronchial spasm or anaphylactoid shock may occur. Temporary renal shutdown or other nephropathy may occur. Temporary neurologic effects of varying severity have occurred in a few instances particularly in cerebral angiography. There have been a few reports of a burning or stinging sensation or numbness, of venospasm or venous pain, and of partial collapse of the injected vein. Neutropenia or thrombophlebitis may occur.

Adverse reactions as a consequence of **excretion urography** have included cardiac arrest, ventricular fibrillation, anaphylaxis with severe asthmatic reaction, and flushing due to generalized vasodilation. **Cerebral angiography** has caused temporary neurologic complications such as induction of seizures (particularly in patients with convulsive disorders), confusional states or drowsiness, transient paresis, coma, temporary disturbances in vision, or seventh nerve weakness. During **peripheral arteriography,** hemorrhage from puncture site, thrombosis of the vessel, and brachial plexus palsy (following axillary artery injection) have occurred. Complications (in an estimated 4 to 6% of cases) of **percutaneous transhepatic cholangiography** include bile leakage (more likely in presence of complete obstruction due to carcinoma) and biliary peritonitis, gallbladder perforation, internal bleeding, gram-negative bacterial septicemia, and tension pneumothorax from inadvertent puncture of diaphragm and lung. During **splenoportography,** intraperitoneal extravasation of the medium may cause transient diaphragmatic irritation or mild to moderate transient pain which may sometimes be referred to the shoulder, periumbilical region, or other areas; accidental pneumothorax (because of proximity of pleural cavity) may occur. **Arthrography** may induce joint pain or increase existing pain (usually immediate and transient but may be delayed or prolonged up to 24 hours) particularly with large doses and extravasation of medium into soft tissue surrounding the joint. Lipid-like histiocytes have been found in tissue removed following arthrography. The technique of **discography** may be painful particularly when disk pathology exists; pain on injection may also be related to volume of the dose; the nature of the disk pathology or extravasation of the medium may cause referred pain.

Bear in mind the possibility of thrombosis or of other complications due to mechanical trauma when any percutaneous technique is used.

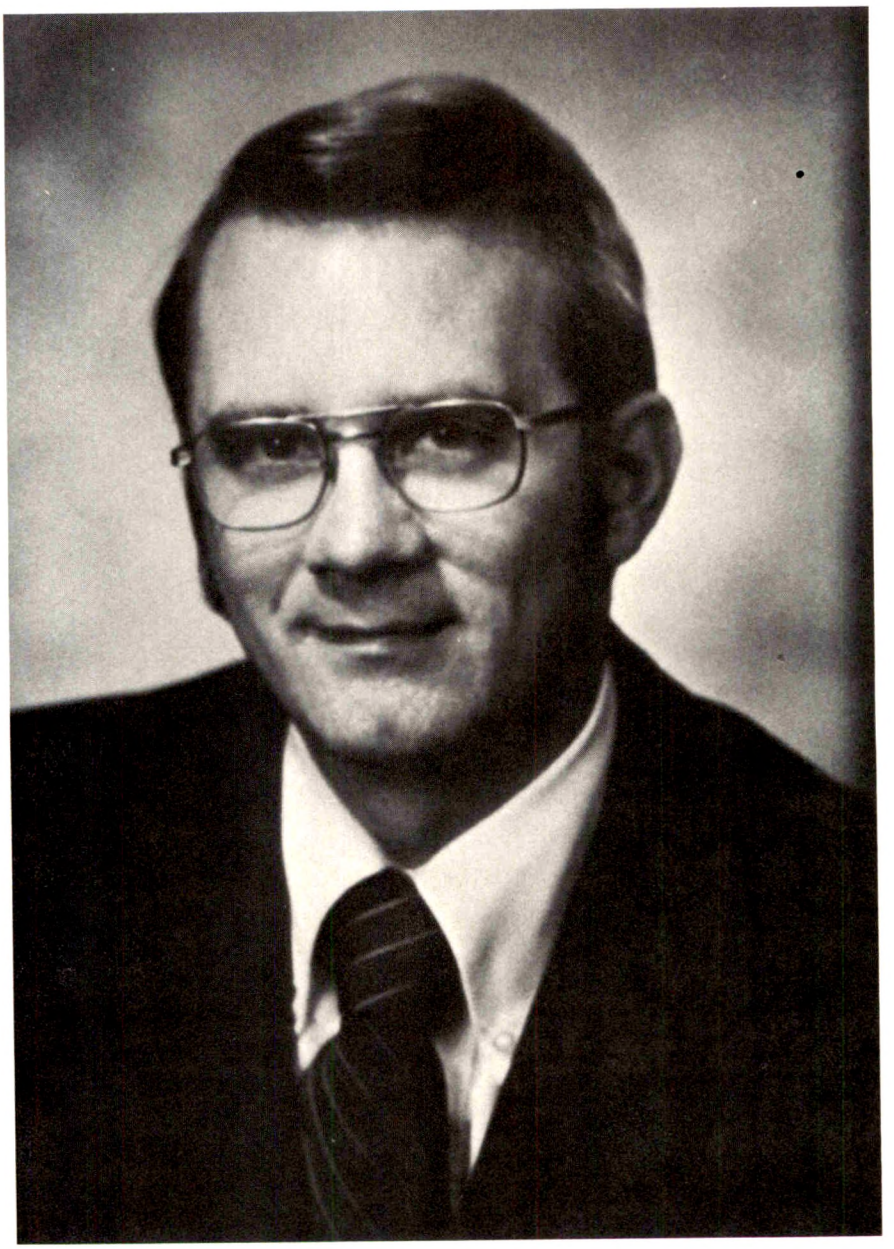
For full information, consult package insert.

HOW SUPPLIED: Renografin-60 (Diatrizoate Meglumine and Diatrizoate Sodium Injection U.S.P.) is a sterile aqueous solution providing 52% diatrizoate meglumine and 8% diatrizoate sodium; the solution contains approximately 29% (288 mg./ml.) bound iodine, 0.32% sodium citrate (buffer), 0.04% edetate disodium (sequestering agent); *the solution contains approximately 3.76 mg. (0.16 mEq.) sodium per ml.* Available in 10, 30, and 50 ml. single-dose vials and in 100 ml. single-dose bottles.

SQUIBB®
contrast media™

SQUIBB HOSPITAL DIVISION
E. R. Squibb & Sons, Inc.

© 1976 E. R. SQUIBB & SONS, INC. H526-501



RONALD G. EVENS
HICKEY LECTURER, 1976

AMERICAN JOURNAL OF ROENTGENOLOGY

VOL. 126 JUNE 1976 No. 6

NEW FRONTIER FOR RADIOLOGY: COMPUTED TOMOGRAPHY

40th ANNUAL PRESTON M. HICKEY MEMORIAL LECTURE

RONALD G. EVENS[1]

ABSTRACT:

The basic principles of computed tomography (CT) and their application are discussed. The impact of this method on neuroradiologic diagnosis is reviewed, including economic considerations and the effect on nuclear medicine and other diagnostic procedures. The initial experiences of the Mallinckrodt Institute with whole body scanning are illustrated, and future possibilities for CT are predicted.

The Hickey lecture series was established to honor the memory of a distinguished pioneer in the specialty of radiology and one of the best loved teachers in its history. Preston M. Hickey was born and educated in Michigan, graduating from the Detroit College of Medicine and Surgery (the present Wayne State College of Medicine) in 1892, 3½ years before Röentgen's discovery. Initially he specialized in diseases of the nose, throat, and chest and also lectured in pathology. He began his work in roentgenology in 1899 and became professor of roentgenology at the Detroit College of Medicine and Surgery in 1909, continuing in this position untill 1922. He served in the United States Army during the World War I as chief of the x-ray division. During the war he made many contacts with European radiologists, thus becoming a spokesman for radiology throughout the world.

In 1922, he was appointed professor of roentgenology at the Universityof Michigan and planned the new department. Hickey did much to establish radiology as an academic discipline, initiating lectures in roentgenology for freshman medical students and encouraging faculty to present and publish thier observations. For a time he served as acting dean of the medical school.

In 1906 he established and was first editor of the *American Quarterly of Roentgenology*, forerunner of this journal. He helped found the American Roentgen Ray Society and served as its president. He delivered the Caldwell Lecture in 1928, received the gold medal of the Radiological Society of North America, and served as a member of the National Research Council.

In 1904, Hickey contributed a paper to the transactions of the American Roentgen Ray Society entitled "The Interpretation of Radiographs of the Chest." His concluding remarks were, "The marked improvement in radiographic technique has resulted in adding a diagnostic measure of great value to our armamentarium of al-

Presented at the annual meeting of the Wayne County Medical Society, the Wayne State University College of Medicine, and the Michigan Radiological Society, Detroit, March 4, 1976.

[1] Department of Radiology, Washington University School of Medicine, and Mallinckrodt Institute of Radiology, 510 South Kingshighway, St. Louis, Missouri 63110.

ready tried methods. This means of thoracic exploration, while already developed enough so as to be of considerable diagnostic value, is destined through future study and experiment to yield conclusions which will be still more valuable." Perhaps Hickey's remarks about the chest radiograph in 1904 will prove true for computed tomography in 1976.

BEGINNING OF THE NEW FRONTIER

Until recently, radiologists have been limited to two-dimensional images which superimpose important organs. Radiographic tomography (moving the tube and film in a variety of patterns in order to "blur" structures outside a specific plane of interest) was useful to limit the problem of overlapping structures in certain areas of the body, but the "blurring" added to the problem of density resolution.

The specialty of radiology has recently been changed by the dramatic introduction of computed tomography (CT) [1]. The system consists of a scanning unit (containing an x-ray tube and two accurately aligned radiation crystal detectors), an x-ray generator and controls, a computer with a magnetic disc and printer, and a viewing unit consisting of a cathode-ray tube. The following description pertains to head scanning equipment available in 1975.

The x-ray tube and detectors are mounted opposite each other and the detectors receive and record the intensity of the x-ray beam as it passes through the head. The x-ray beam is collimated so that a 13 or 8 mm "slice" of the head is evaluated. The detector system moves in a linear fashion across the head and takes multiple readings. The frame then rotates 1°, the linear path is repeated, and this sequence is repeated through an arc of 180°. With each linear movement, 240 measurements of x-ray intensity are recorded by each detector. After 180°, 43,200 measurements are obtained which are continuously fed to the system's computer. The computer rapidly calculates 25,600 attenuation values within each slice, and the data create a picture of the contents within the slice on a matrix composed of 160×160 pixels. Pixel is a relatively new word, a contraction of the words "picture element." It refers to the number of elements in an electronic image, in this case, the cathode-ray tube. Each point on the matrix accurately depicts the attenuation value of the tissue at that site in the slice under examination and each pixel has a volume of 1.5×1.5×13 (or 8) mm. The attenuation values are printed as well as displayed in shades of gray by the cathode-ray tube.

Each measurement from a detector forms one of a series of 43,200 simultaneous equations in which 25,600 variables exist. If there are more equations than variables, the unique value of each volume element in the matrix can be solved.

The first generation of CT units required a scanning time of about 5 min and several minutes for computer calculation. To allow more accurate measurement, a water bag was placed over the scanned area to minimize differences of attenuation. This system accurately measured the attenuation coefficients of biologic materials with a precision of 0.5%, although in actual clinical use this precision is approximately 1% or 5 EMI units [2, 3]. Spatial resolution has been measured as low as 3 mm. The first published clinical material [4] demonstrated the ability of head scanners to image small areas of calcification, clotted blood, edematous brain, cerebrospinal fluid, fat-containing objects, small amounts of iodinated contrast agents.

By 1975, at least two other manufacturers announced CT equipment for use in the head and body [5, 6]. This equipment was similar to Hounsfield's [1], and, although not requiring a water bag, the scanning time remained at several minutes. Second generation systems have scanning time of less than 20 sec; the matrix capability is now 320×320 pixels.

CT OF THE HEAD

Several medical centers have utilized CT in neuroradiology for more than 3 years.

As of January 1976, approximately 140 units are in operation throughout the world (primarily in the United States), and hundreds of examinations have been reported [7–12].

The cranium can usually be evaluated with eight slices (four scans) and the appearance of normal tissue is well documented. The bony calvarium appears white on the cathode-ray tube display, brain tissues are displayed as various shades of gray, and cerebrospinal fluid appears as a black density. Physiologic areas of calcification (pineal gland and the glomus of the choroid plexus), (fig. 1) serve as useful landmarks. Initially it was suggested that the cerebral cortex could be distinguished from underlying white matter, but it has recently been shown that this observation was an artifact of the computer program and its reconstruction capabilities [13]. The ventricular system, sylvian fissures, and the basal cisterns are easily recognized and the diagnostic criteria learned from pneumoencephalography are valid with CT, without the need of injected air.

The presence of calvarial lesions, deformity, or volume change of the ventricles as well as variations in the parenchymal density of the brain allow a wide variety of diagnostic observations. A rapidly growing literature describes CT findings in primary and secondary tumors, cerebral vascular accidents, subdural and epidural hematomas, and degenerative neurologic processes.

Dilitation of the cerebrospinal fluid spaces is easily discernible and, if due to an obstructive process, the level and pathologic cause for the block may be detected. If the enlarged ventricles are due to a decrease in parenchymal volume, enlargement of the subarachnoid sulci and basal cisterns can permit the diagnosis of cerebral atrophy (fig. 2).

Primary and secondary tumors are detected by changes in cerebral density and their mass effect on the ventricular system (fig. 3). The density changes are of mixed patterns with increased density related to areas of hemorrhage or calcification, while areas of low density are probably related to areas of necrosis and edema. Many tumors (both primary and metastatic) are often "enhanced" by iodinated contrast agents so that areas of the tumor significantly increase in density after the intravenous injection. This observation is noted in many tumors (e.g. glioblastoma multiforme, meningioma, and metastatic lesions) and in arteriovenous malformations. The "enhancement" is partially due to increased vascularity and has recently been shown to relate to a breakdown in the blood-brain barrier [14].

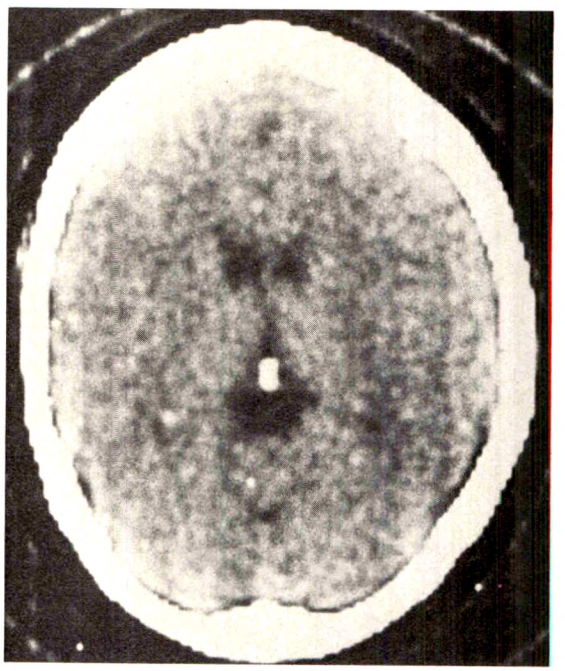


FIG. 1.—CT scan of normal head. Calvarium and midline pineal are displayed as white density, cerebral cortex as shades of gray, and ventricles and subarachnoid space (cerebrospinal fluid) as black density.

The findings with cerebral infarction vary with the time after the onset of clinical symptoms and are observed in approximately half of the patients with a clinical stroke. In the first few days after the ictus, a region of low density is noted (fig. 4). A midline shift is often absent and, when observed, the amount of displacement is proportional to the size of the infarct—a useful finding to differentiate

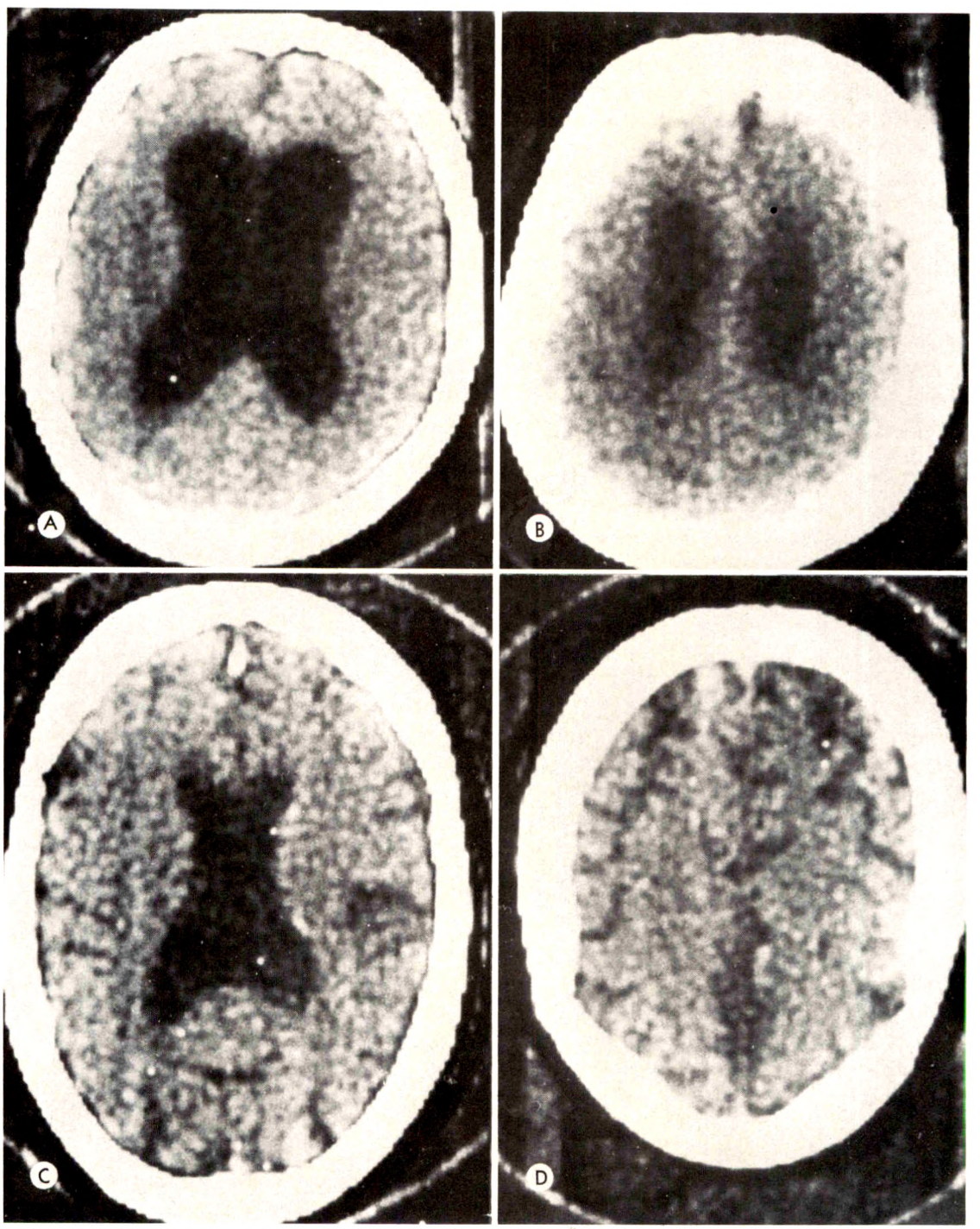


FIG. 2.—Differentiation of hydrocephalus and cerebral atrophy. *A* and *B*, Normal subarachnoid space and moderately dilated ventricles in communicating hydrocephalus. *C* and *D*, Enlarged subarachnoid space and mildly dilated ventricles in cerebral atrophy.

regions of low density in areas of infarction from mass lesions. After about 10 days, a well-defined area of low density is commonly seen, and after 1 month the area of infarction may be cystic. This is not a consistent finding, and some regions of infarction appear normal after 1 month.

Intracerebral hematomas are visualized as areas of high attenuation density (fig. 5). The etiology of the bleeding may be inferred from the position and clinical presentation. Epidural and subdural hematomas are recognized by their mass effect on the ventricular system and midline structures, as well as changes in density from the normal. Fluid collections with low blood content have a low density absorption (fig. 6*A*), and collections of clotted blood are clearly differentiated by their high density values. Unfortunately, many chronic subdural hematomas lie in an intermediate range and can be difficult to differentiate from underlying brain.

Experience of our center and others point to a diagnostic accuracy of 95%. This is undoubtedly related to the sensitivity of CT as well as the skill of neuroradiologists. The false positive and false negative cases are nearly equally divided in most series.

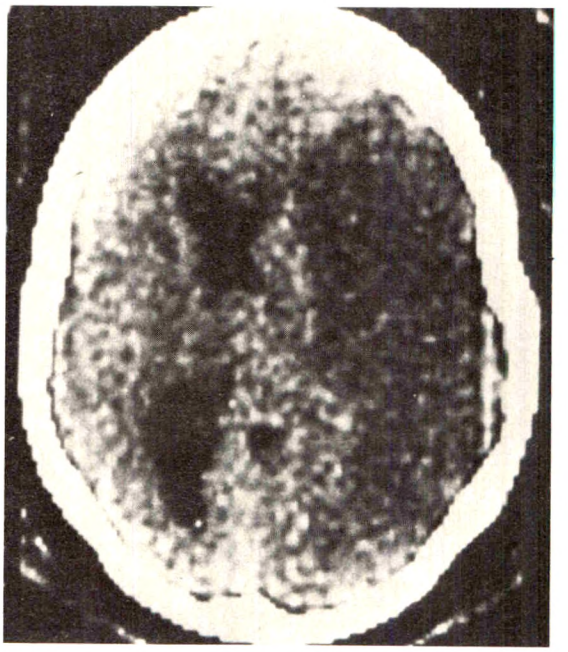


FIG. 4.—Acute right middle cerebral infarct. Edematous right cerebral cortex has low attenuation coefficient 24 hr after onset of symptoms. Midline slightly shifted to left.

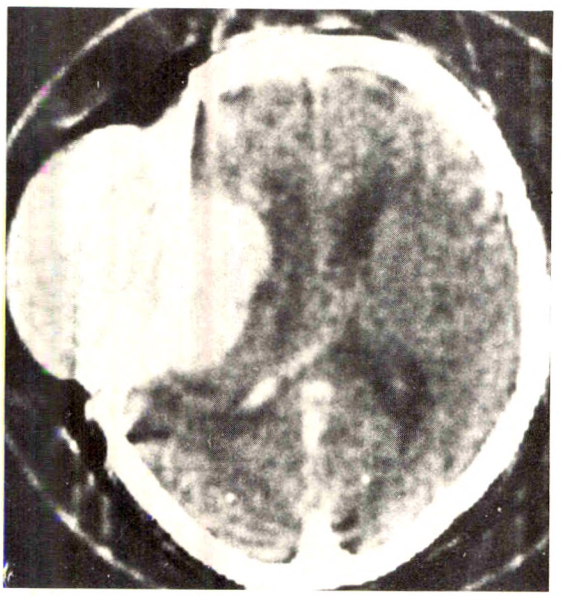


FIG. 3.—Recurrent meningioma after contrast enhancement. Large tumor has intra- and extracranial component and marked increase in density after intravenous injection of contrast. Note surrounding cerebral edema (low density) and distortion of ventricular system.

The rapid clinical acceptance of head CT is not only related to its high accuracy, but also to its significant effect on the management of many patients. Four examples follow.

1. A common neurologic presentation in the elderly is dementia, which requires the differentiation of patients with communicating hydrocephalus, noncommunicating hydrocephalus, and cerebral atrophy. CT helps distinguish patients with cerebral atrophy from individuals with hydrocephalus without resorting to air studies (fig. 2). Radionuclide cisternography is then performed on the hydrocephalic patients in order to distinguish communicating isotopic patterns [15]. In certain patients with "classical" communicating hydrocephalus by CT and radionuclide cis-

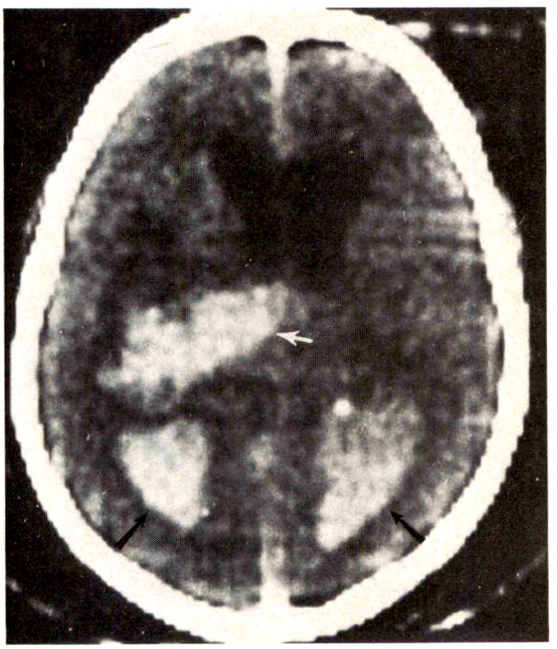


FIG. 5.—Intercerebral hematoma in patient with left thalamic hemorrhagic infarct. Hematoma shown as area of increased density (*white arrow*) with surrounding cerebral edema. Blood has also collected in ventricular system (*black arrows*).

ternography, cerebrospinal fluid shunt surgery may be performed without the need of air studies.

2. Certain categories of patients with a clinical "stroke" are treated with anticoagulation. This treatment has a definite morbidity in patients with a hemorrhagic stroke. CT accurately detects intracerebral hemorrhage even when the spinal fluid examination shows no blood (fig. 5), so that the patient's treatment can be appropriately directed.

3. The diagnosis of pseudotumor cerebri (benign intracranial hypertension) was previously made with difficulty and often required air studies and arteriography. The typical clinical presentation is an obese female with significant papilledema but without focal signs. Evaluation can now be completed with CT alone. The demonstration of a nondisplaced and normal sized ventricular system and a normal cerebral cortex strongly suggests this diagnosis, and the patient can be treated with diuretic therapy and/or multiple lumbar punctures.

4. A common pediatric neurologic presentation is the infant or child with an enlarging head. CT differentiates hydrocephalus from extracerebral fluid collection (fig. 6). Patients with fluid collections can be treated immediately without air or contrast studies.

Since the introduction of this technique at the Mallinckrodt Institute, air studies have diminished by 66%, cerebroangiographic procedures by 34%, and radionuclide brain scans by 29%. Similar patterns of utilization have been reported at the Mayo Clinic [16]. One study [17] estimates a possible savings of greater than $2,000,000 per year per CT unit. These predictions were based on savings in hospital days and diagnostic procedures; the estimated savings were validated by statistics in pneumoencephalography but not with angiography. Data on hospital admissions were not reported.

I am currently surveying all CT users to determine actual costs [18]. The equipment is complex, sophisticated, and expensive to purchase and operate, so that this study will undoubtedly demonstrate an added cost to neuroradiologic diagnosis. The additional cost will be partially offset by decreases in other examinations, but the decrease in costs will not parallel the reduction in air or contrast studies. Pneumoencephalography, cerebral angiography, and radionuclide brain scans remain necessary in certain patients, and the space and equipment (and to some degree personnel) must be maintained. The high fixed costs [19] of these procedures will continue while examinations and revenues decrease; thus air and angiographic studies will become an even greater financial burden to radiology departments.

Calculations of cost must also consider the "mix" of patients studied because an increasing ratio of normal to abnormal diagnoses will affect the dollar cost or calculated "savings." Published studies indicate a diagnosis of normal in 10%–40% of CT examinations, while radionuclide brain

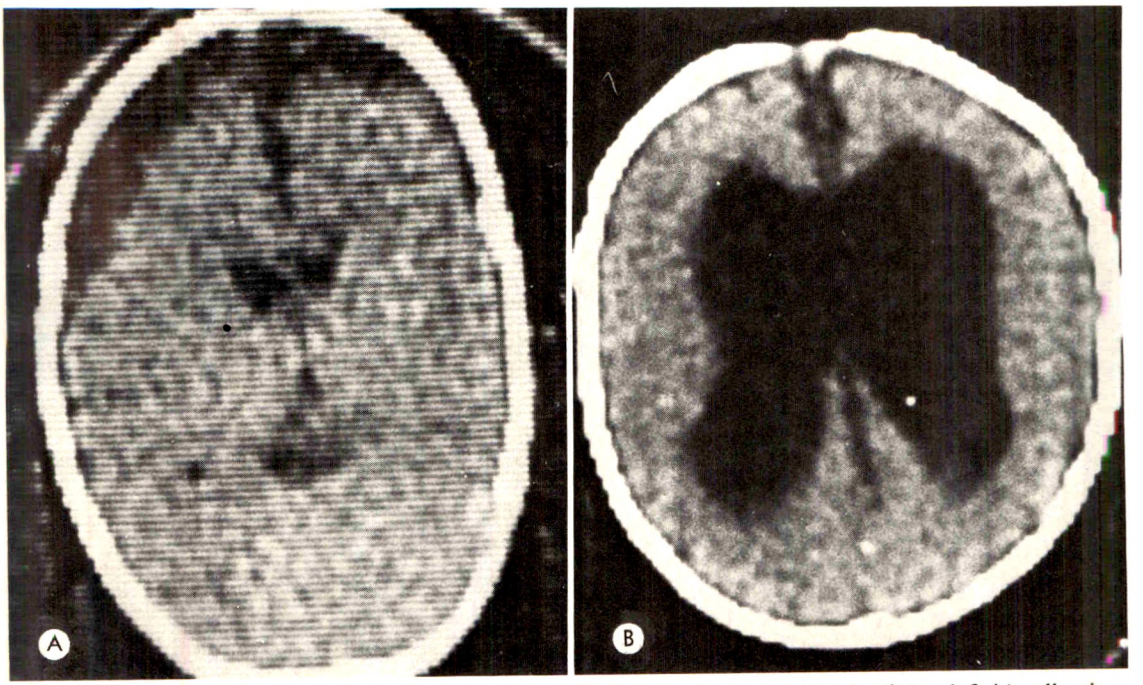


FIG. 6.—Computed tomography in infants with enlarging heads. *A*, Bilateral subdural fluid collections (hygromas) seen as regions of low density between calvarium and cerebral cortex in infant with enlarging head. *B*, CT findings in child with aqueductal stenosis and hydrocephalus.

scans are normal in approximately 90% of cases. If CT replaces the nuclide study as a "screening test," the percentage of normal results will undoubtedly increase and have a definite effect on the analysis of cost effectiveness. Further discussion of cost effectiveness must be postponed for additional data. *However, CT has proved to be an effective examination which has markedly improved diagnostic capabilities and reduced pain and hazard to many patients.*

CT has made a substantial impact on the specialty of nuclear medicine because the radionuclide brain scan previously composed approximately 50% of all nuclide imaging studies in many medical centers. CT is somewhat better than radionuclide imaging in the detection of significant abnormalities [20]; however, the major reason for its replacement of brain scans has been the ability to detect intracerebral hemorrhage, abnormalities of the ventricular system, and to provide more definitive information about pathologic lesions. Radionuclide studies will continue to play a role in the evaluation of communicating hydrocephalus and mass lesions located near bony density (calvarium, base of the skull, and posterior fossa). I also believe it will play a role as a screening test in patients with a low probability for significant abnormality (e.g., minimal neurologic symptoms without focal neurologic signs) where a readily available and relatively inexpensive test is required.

BODY CT

By 1975, body scanning capabilities were possible on at least two types of equipment (the ACTA and Delta scanners [5, 6]. An overlying water bag was not required and all portions of the body could be placed between the x-ray beam and the crystal detectors. Respiratory motion was a problem since the scanning time was 2 min or more. In this same year, a second generation CT unit was developed capable of completing the scan in less than 20 sec and producing dramatically clear images of the abdomen and thorax. One of the

first units was installed in the Mallinckrodt Institute of Radiology in October 1975, and we have recently reported our experience with the first 100 patients [21].

The basic principles remain the same, but the x-ray source is a fan beam mounted diametrically opposite an array of 30 highly sensitive sodium iodide crystal detectors. The x-ray beam and detectors traverse the region being scanned in a linear fashion. More than 18,000 individual readings of x-ray intensity are recorded with each linear path. The scanning frame is then indexed by 10°, another linear traverse is made, and this process continues for 180°, all in less than 20 sec.

The patient reclines on an adjustable couch extending through a circular opening in the scanning gantry and is positioned so that any portion of the body can be studied. The computer calculates the x-ray attenuation values for 80,000 volume elements within each slice and reproduces the data as a 320×320 matrix array. Currently available computer programs can adjust to dramatic changes in attentuation.

Our initial studies were performed on a highly selected patient population. The examination was not utilized as a screening procedure nor were uncooperative patients selected. All individuals were normal volunteers or patients with a well-defined clinical problem. We have now examined more than 300 individuals with emphasis on the abdomen and chest, and a few patients with abnormalities of the extremities and head and neck. Slightly more than 90% of our patients are able to suspend respiration for 20 sec. There is significant degradation of the image with respiratory motion.

CT easily delineates many normal structures, including the aorta, iliac arteries, superior mesenteric artery, renal arteries, pulmonary arteries through several branches, and vena cava. The normal spleen, liver, and gallbladder are of homogeneous density. The pancreas is seen in nearly every patient and is recognized by a characteristic size, shape, and its anterior relationship to the superior mesenteric artery (fig. 7). The kidneys and other retroperitoneal organs are clearly visualized because of the surrounding retroperitoneal fat with a relatively low absorption coefficient. The bladder and retroperitoneal rectosigmoid are delineated and usually can be distinguished from the prostate, seminal vesicles (fig. 8), or uterus.

In the thorax, lung parenchyma, pulmonary vascularity, major bronchi, and the mediastinum are defined by their differing attenuation coefficients and surrounding structures. Intracardiac anatomy is not demonstrated, undoubtedly due to cardiac motion. Tomographic sections of body structures include a very detailed trabecular pattern, and sections through joint articulations demonstrate the synovial space (fig. 8).

Many organs have an increased absorption density following the intravenous injection of water soluble iodinated contrast media. Contrast in the renal collecting system can be detected for as long as 48 hr after injection.

Although our experience with body CT is limited, significant pathologic observations have already been observed. Since dilated biliary ducts are easily recognized (fig. 9), this method may be the most specific noninvasive test to differentiate ob-

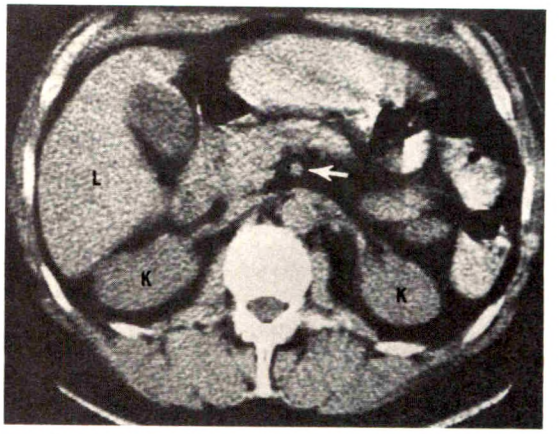


FIG. 7.—Normal upper abdominal anatomy. Pancreas is above superior mesenteric artery (*arrow*). Liver (L) has homogeneous density with lower density gallbladder to right. Aorta and renal arteries are visualized. K = kidneys.

structive from nonobstructive jaundice. Liver metastases are recognized as distinct areas of lower absorption density than normal liver; we have seen metastases as small as 1 cm in diameter. Fatty infiltration of the liver is detected by its uniformly low attenuation coefficient, and primary hepatic tumors and liver abscesses have also been identified. Splenomegaly and intrasplenic lesions (tumors, metastases, or infarcts) have been detected.

Pancreatic abnormalities are detected by alterations in the normal pancreatic size, shape, and density. We have correctly diagnosed 27 of 30 patients with pancreatic carcinoma (fig. 10). One false negative was an emaciated patient who lacked the normal fat planes in the retroperitoneum. In the other two false negative studies, enlarged hepatic biliary ducts were seen but the obstructing pancreatic carcinoma was not detected. Pseudocysts of the pancreas have a characteristic presentation and can be differentiated from carcinoma. We have studied a variety of abdominal masses (fig. 11), and CT delineates their size, consistency (solid versus cystic), attenuation coefficient (fat, muscle, or calcium), and relationship to other organs and structures.

Mass lesions of the kidney produce a change in the normal renal architecture, whereas benign renal cysts present as sharply demarcated regions of water density that do not increase in density after contrast injection. Malignant renal lesions are of similar density to the kidney and have a slight increase (but less than the normal kidney) in density after contrast injection. CT visualizes levels of iodine concentration in the renal collecting system which are completely undetectable by standard radiography, but we have not quantitated this increased sensitivity at this time.

Hilar and pulmonary mass lesions are well defined by the large difference in attenuation coefficient between the mass

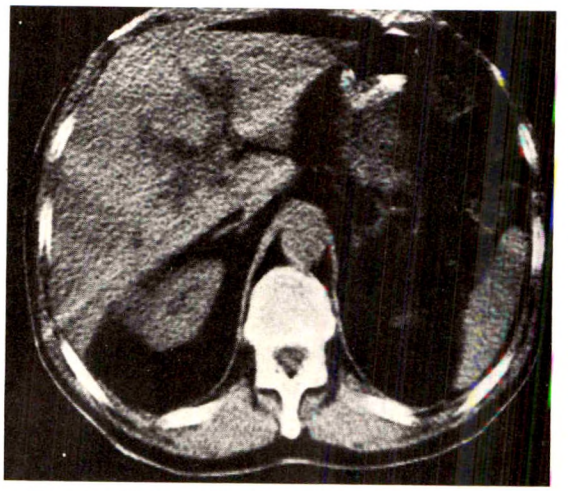


FIG. 9.—Obstructive jaundice. Dilated biliary ducts seen as regions of low density within liver.

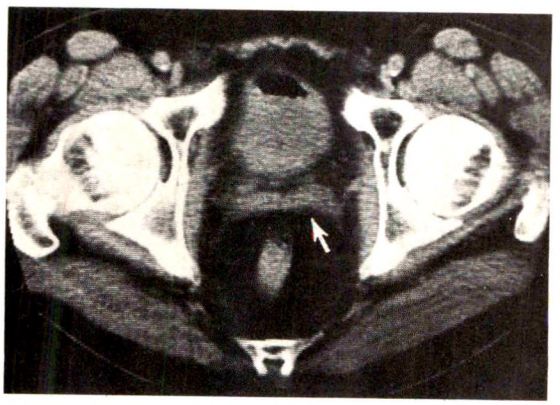


FIG. 8.—Normal male lower abdominal anatomy. Seminal vesicles (*arrow*) between bladder (above) and rectosigmoid (below). Note synovial space between acetabulum and femoral head. Air (black density) present in bladder from recent cystoscopy.

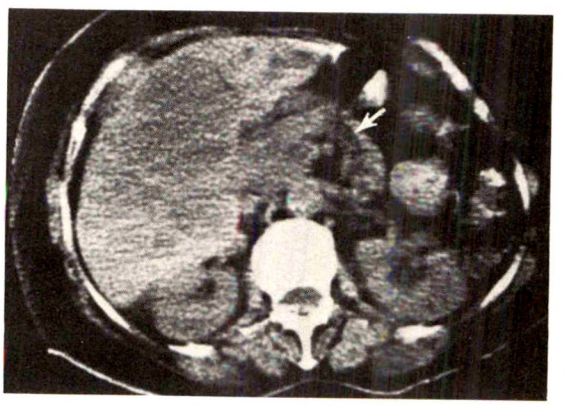


FIG. 10.—Carcinoma of pancreas. Head of pancreas enlarged and central pancreatic duct (*arrow*) dilated. Multiple liver metastases seen as areas of decreased density from normal liver.

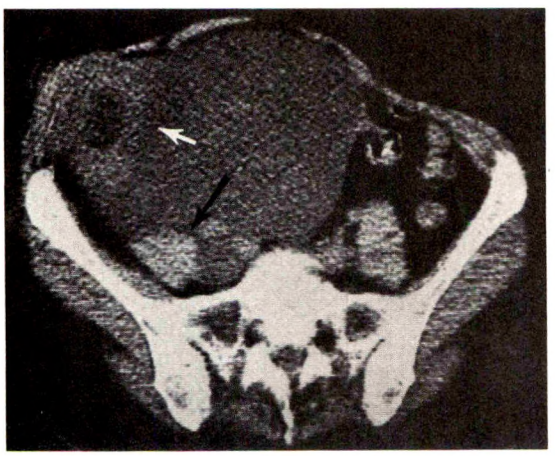


FIG. 11.—Large lower abdominal mass several days after renal transplant shown to be lymphocele. Fluid collection appears as homogeneous density with lower attenuation coefficient than functioning transplanted kidney (*white arrow*) after intravenous contrast injection. Renal concentration of contrast could not be detected by standard radiography. Note mass effect on psoas muscle (*black arrow*).

and surrounding lung (fig. 12), and we can describe their relationship to the major bronchi and mediastinum. Calcifications within benign pulmonary granulomas have been detected that could not be observed by standard techniques. Certain mediastinal masses (e.g. pericardial fat pad, and aortic aneurysms) have very characteristic patterns by CT (fig. 13). Our experience in patients with abnormalities of the extremities and head and neck is limited at this time, although a variety of anatomical structures have been defined. The body scanner obtains excellent studies of the cranial vault that are certainly comparable and perhaps superior to examinations from current head units.

While I am convinced that whole body CT will be of great significance to diagnostic radiology and to the welfare of patients, its impact will not be as dramatic as for the head due to several reasons.

1. A variety of excellent, well-tested, and noninvasive radiographic techniques are currently available for the thorax, abdomen, and extremities. These include the chest film, upper gastrointestinal examination, barium enema, and plain films of the abdomen and extremities.

2. Nuclear medicine and ultrasound as well as percutaneous biopsy provide additional diagnostic tests for the thorax and abdomen.

3. The thorax and abdomen lack the symmetry of the head.

4. Important anatomical areas cannot

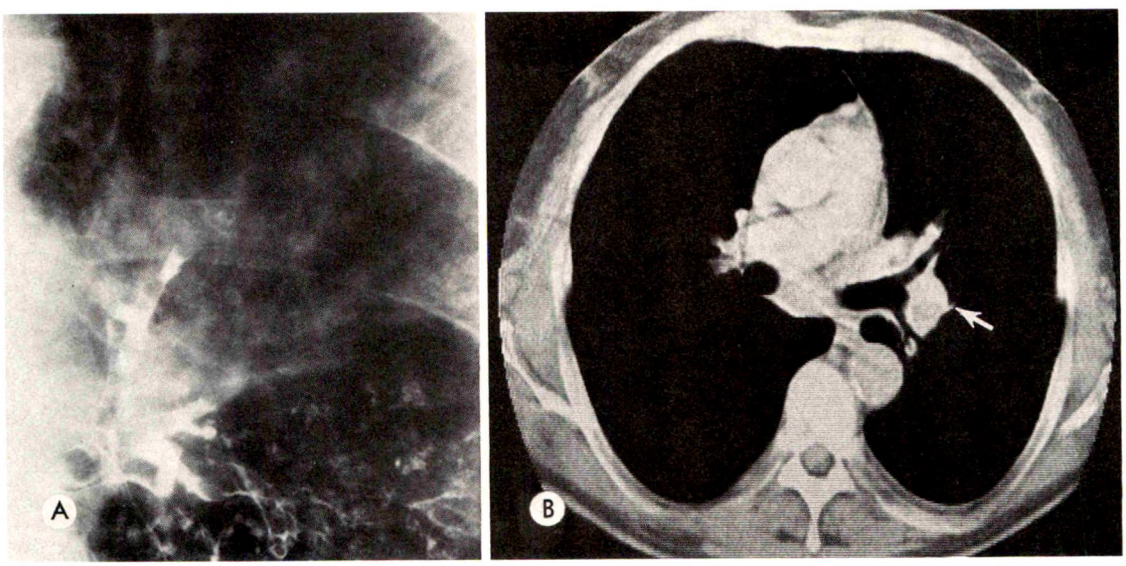


FIG. 12.—Carcinoma of lung. Enlarged pulmonary hilum (*A*) studied by CT (*B*). Water density irregular mass (*arrow*) has narrowed posterior segmental upper lobe bronchus. Analysis of mass by narrow window widths demonstrated no calcification. Pathologic diagnosis was squamous cell carcinoma.

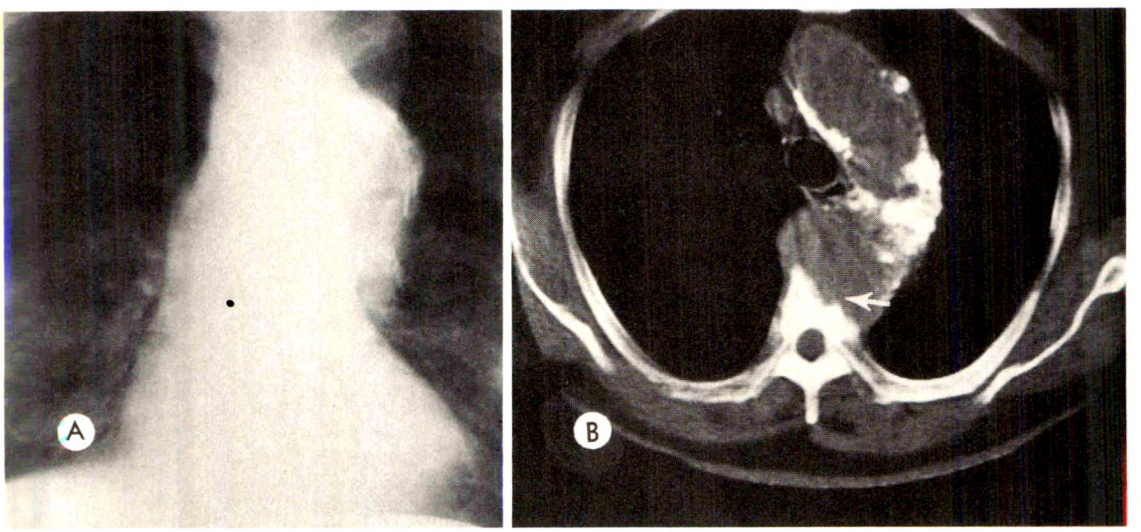


FIG. 13.—Aortic aneurysm. *A*, Chest radiograph demonstrating multilobulated mediastinal mass with calcifications typical for aortic aneurysm. *B*, CT scan showing markedly enlarged aortic arch with large amounts of calcification and erosion of thoracic vertebral body (*arrow*).

be evaluated by second generation CT, including the heart and gastrointestinal tract.

THE FUTURE OF CT

Godfrey Hounsfield's invention is a fundamental development that will surely be expanded and improved. The general principle of transaxial reconstructive tomography has already been applied to the reconstruction of radionuclide distributions in the brain and body [22–24]. Ter-Pogossian and co-workers at the Mallinckrodt Institute have developed a system to image the radionuclide distribution of positron-emitting isotopes in a cross-sectional slice of an object by external detection. The system is called PETT (positron emission transverse tomography) and has already been utilized in physiologic studies of the cerebral cortex, myocardium, lung, and abdominal viscera. Information is collected by performing a series of rectilinear scans at a number of discrete angles about the cross-section of interest. The system consists of 48 scintillation detectors placed in a hexagonal array of six banks with eight detectors each. The minimum time for total data collection is 2 min, and an image is reconstructed in a matrix of 100×100 pixels and displayed on a television monitor. A variety of radioactive compounds can measure several physiologic parameters and we are quite optimistic regarding future clinical uses—especially with studies of the heart and brain (fig. 14). The principles of CT should also be applicable to other energy modalities, including ultrasound.

Several centers are evaluating methods to improve radiation therapy treatment planning and dosimetry by CT, and our Division of Radiation Oncology is actively developing interface systems for clinical trials.

Further improvements in CT equipment seem to be on the horizon. As scanning time is reduced, the examination becomes available to the uncooperative or pediatric patient. Evaluation of cardiac anatomy may be possible by coordinating information collection with the cardiac cycle.

A major improvement will be the ability to obtain thinner "slices" so that small and important anatomical structures can be resolved, particularly when they traverse the plane of study in a diagonal fashion or when they are adjacent to other structures. Thinner slices may also allow the computer to reconstruct images in a variety of

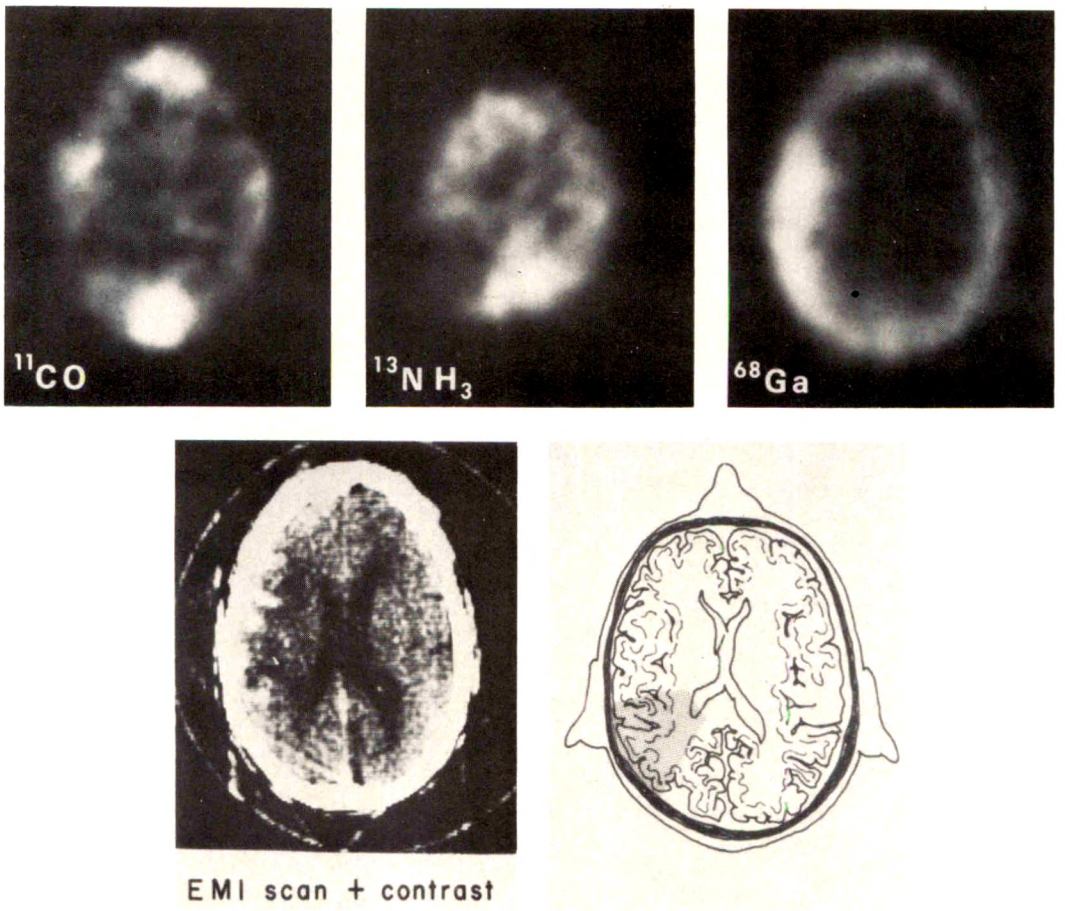


FIG. 14.—Isotope distribution studies in patient with cerebral infarct. *Lower right*, area of infarct; *lower left*, EMI scan; *upper images*, distribution of labeled compounds in same cross-sectional area of brain as EMI scan. Upper left image is distribution of ^{11}CO-tagged red blood cells and represents cerebral blood volume. Upper center image is distribution of ^{13}N-ammonia and relates to blood perfusion, while upper right image depicts distribution of ^{68}Ga (probably area of abnormal blood-brain barrier). Note different regions of abnormality defined by three labeled substances.

planes and angles [25].

Improvements in equipment, computers, and programming will be coordinated by an expanding scientific understanding in this relatively new area of image reconstruction. Continued progress seems assured. The future holds a promise of faster scanning time, rapid computer reconstruction, improved spatial and density, resolution, and application to other areas of the body (heart, gastrointestinal tract, spinal canal).

ACKNOWLEDGMENTS

I would like to gratefully acknowledge the many members of the Mallinckrodt Institute who have been involved with the development and use of CT. In particular, Drs. Edward Coleman, Mokhtar Gado, Stuart Sagel, Robert Stanley, and Michel Ter-Pogossian have provided valuable advice and counsel.

REFERENCES

1. Hounsfield GN: Computerized transverse axial scanning (tomography). I. Description of system. *Br J Radiol* 46:1016–1022, 1973
2. Phelps ME, Hoffman EJ, Ter-Pogossian MM: Attenuation coefficients of various body tissues, fluids, and lesions at photon energies of 18 to 136 keV. *Radiology* 117:573–583, 1975
3. McCullough EC, Baker HL Jr, Houser OW,

Reese DF: An evaluation of the quantitative and radiation features of a scanning x-ray transverse axial tomograph: the EMI scanner. *Radiology* 111:709–715, 1974

4. Ambrose J: Computerized transverse axial scanning (tomography). II. Clinical application. *Br J Radiol* 46:1023–1047, 1973
5. Alfidi RJ, Haaga J, Meaney TF, MacIntyre WJ, Gonzalez L, Tarar R, Zelch MG, Boller M, Cook SA, Jelden G: Computed tomography of the thorax and abdomen; a preliminary report. *Radiology* 117:257–264, 1975
6. Twigg HL, Axelbaum SP, Schellinger D: Computerized body tomography with the ACTA scanner. *JAMA* 234:314–317, 1975
7. Paxton R, Ambrose J: The EMI scanner: a brief review of the first 650 patients. *Br J Radiol* 47: 530–565, 1974
8. Davis DO, Pressman BD: Computerized tomography of the brain. *Radiol Clin North Am* 12: 297–313, 1974
9. New PFJ, Scott WR, Schnur JA, Davis KR, Taveras JM: Computerized axial tomography with the EMI scanner. *Radiology* 110:109–123, 1974
10. Alderson PO, Mikhael M, Coleman RE, Gado M: Optimal utilization of computerized cranial tomography and radionuclide brain imaging. *Neurology*. In press, 1976
11. Baker HL Jr, Campbell JK, Houser OW, Reese DF: Early experience with the EMI scanner for study of the brain. *Radiology* 116:327–333, 1975
12. Baker HL Jr, Houser OW, Campbell JK, Reese DF, Holman CB: Computerized tomography of the head. *JAMA* 233:1304–1308, 1975
13. Gado M, Phelps M: The peripheral zone of increased density in cranial computed tomography. *Radiology* 117:71–74, 1975
14. Gado MH, Phelps ME, Coleman RE: An extravascular component of contrast enhancement in cranial computed tomography. *Radiology* 117: 595–597, 1975
15. Gado MH, Coleman RE, Lee KS, Mikhael MA, Alderson PO, Archer CR: Correlation between computerized tomography and radionuclide cisternography in dementia. *Neurology*. In press, 1976
16. Baker HL Jr: The impact of computed tomography on neuroradiologic practice. *Radiology* 116:637–640, 1975
17. Wortzman G, Holgate RC, Morgan PP: Cranial computed tomography: an evaluation of cost effectiveness. *Radiology* 117:75–77, 1975
18. Evens RG, Jost RG: Economic analysis of computed tomography radiologic units. *Am J Roentgenol*. In press, 1976
19. Evens RG: Cost accounting in radiology and nuclear medicine. *CRC Crit Rev Clin Radiol Nucl Med* 6:67–79, 1975
20. Gado M, Coleman RE, Alderson PO: Clinical comparison of radionuclide brain imaging and computerized transmission tomography of the brain. I., in *Noninvasive Brain Imaging: Computed Tomography and Radionuclides*, edited by DeBlanc HJ Jr, Sorenson JA, New York, Society of Nuclear Medicine, 1975, pp 147–172
21. Sagel SS, Stanley RJ, Evens RG: Early clinical experience with motionless whole body computerized tomography. *Radiology*. In press, 1976
22. Kuhl DE, Edwards RQ: The Mark III scanner: a compact device for multiple-view and section scanning of the brain. *Radiology* 96:563–570, 1970
23. Phelps ME, Hoffman EJ, Mullani NA, Ter-Pogossian MM: Application of annihilation coincidence detection to transaxial reconstruction tomography. *J Nucl Med* 16:210–224, 1975
24. Ter-Pogossian ME, Phelps ME, Hoffman EJ, Mullani NA: A positron-emission transaxial tomograph for nuclear imaging (PETT). *Radiology* 114:89–98, 1975
25. Glenn WV Jr, Johnston RJ, Morton PE, Dwyer SJ: Image generation and display techniques for CT scan data. Thin transverse and reconstructed coronal and sagittal planes. *Invest Radiol* 10:403–416, 1975



Am J Roentgenol 126:1130–1139, 1976

BREAST PATTERNS AS AN INDEX OF RISK FOR DEVELOPING BREAST CANCER

JOHN N. WOLFE[1]

ABSTRACT:

The radiographic appearance of the breast parenchyma provides a method of predicting who will develop a breast cancer. This paper describes a retrospective study of 7,214 patients. On the basis of the radiographic appearance of the breast parenchyma, patients were placed into one of four groups of risk for developing carcinoma of the breast. Follow-up studies revealed a stepwise progression in the incidence of developing carcinoma of the breast at least 6 months after the radiographic examination. In one of the two substudies, there was a 37 times greater incidence for those at highest risk compared to the low risk group. The classifications presented are thought to be of value in the everyday practice of mammography as well as in planning screening programs.

The parenchymal patterns of the breast, as depicted radiographically, provide significant clues as to who will develop breast cancer. Groups can be isolated with as much as a 37 times greater incidence of the disease. This has two implications: (1) in certain groups cancer detection must be stressed and, in some cases, anticipatory therapy recommended; and (2) large groups of women can be identified who should have routine radiographic screening examinations.

This communication describes the criteria for classification, the projected incidence of carcinoma for the various classification groups, comparison of projected incidence to that of the general population, and utilization of the classification.

BACKGROUND

After noting variation in the radiographic appearance of the breast parenchyma, a study was done to categorize the appearance of the normal breast [1]. The parenchyma was recognized as having basically three components: fat, densities corresponding to connective and epithelial tissues, and what was termed prominent ducts. It was noted that with aging, the connective and epithelial tissues regressed with a corresponding increase in observations of the prominent duct pattern. The premise that the prominent duct pattern was an evolutionary change associated with aging was probably incorrect. Further studies have shown that the prominent ducts are present from a very early age (at least the twenties), becoming visible with the regression of overshadowing connective and epithelial tissue density (J. N. Wolfe, unpublished data).

An important observation was an association of the prominent duct pattern with the presence of a breast carcinoma, the history of having a breast carcinoma, and in women who were considered at risk for the disease by virtue of age and nulliparity. It was reasoned that this association might be utilized to identify a group of women who would be at risk for developing breast cancer some time in the future [2, 3]. As will be seen, this premise was correct, but dysplasia with or without an element of prominent duct pattern was found to be an even more important indicator of risk.

CRITERIA FOR CLASSIFICATION

The classification is based on the relative amounts of fat, epithelial and connective tissue densities, and prominent ducts ob-

Presented at the annual meeting of the American Roentgen Ray Society, Atlanta, Georgia, October 1975.
[1] Hutzel Hospital, 432 East Hancock Avenue, Detroit, Michigan 48201.

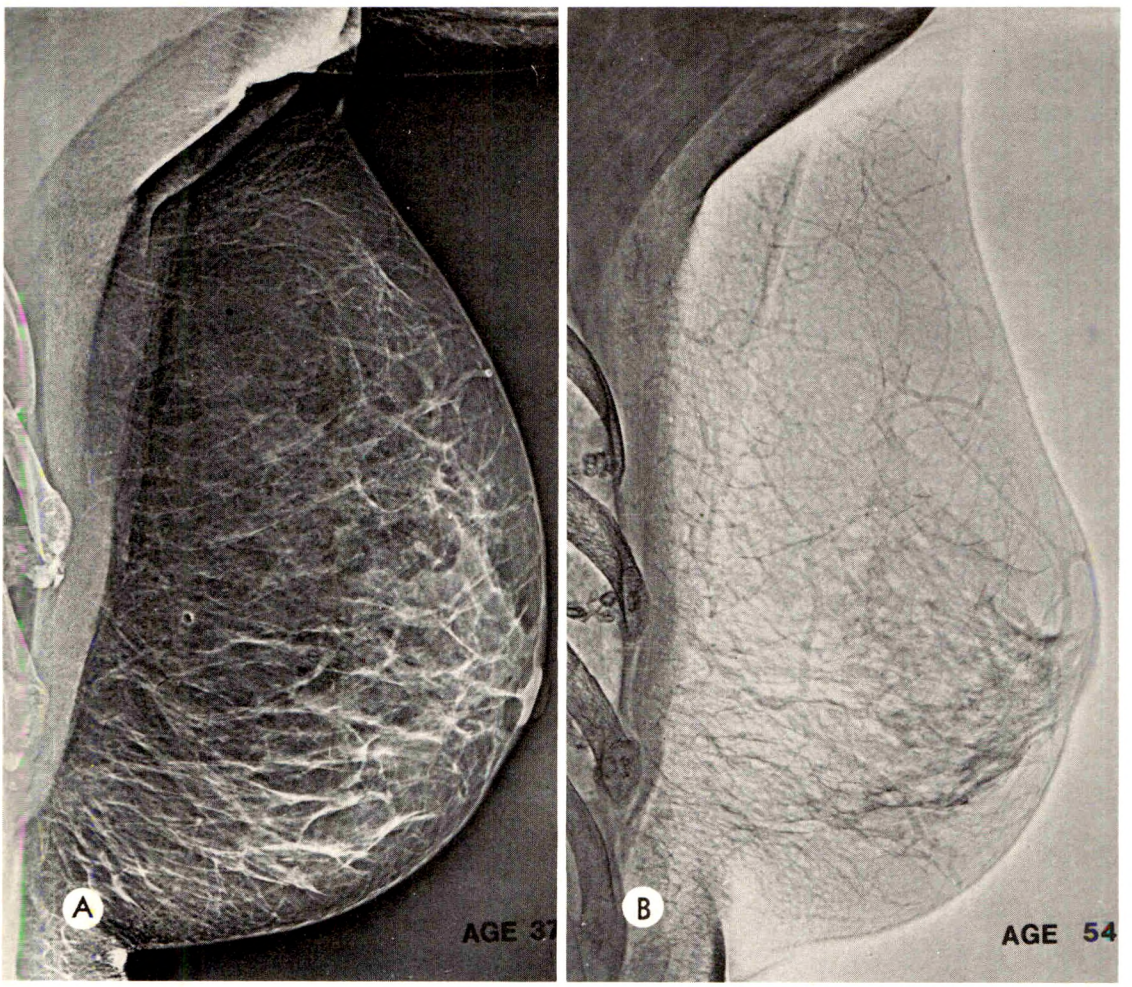


FIG. 1.—*A*, N1 breast. Lateral projection showing trabeculated appearance; no palpable abnormalities. *B*, P1 breast. Lateral projection showing some prominent ducts in subareolar area; breast otherwise composed of fat.

served on the mammogram. The epithelial and connective tissue densities correspond roughly to what the pathologist usually identifies as benign disease of the breast, such as adenosis or fibrocystic disease. I prefer the term mammary dysplasia for these densities. They are evidenced as densities over that of fat and usually do not have clearly definable margins. The changes are typically bilateral and symmetrical. The prominent duct pattern corresponds to a periductal collagenosis histologically and has in the past been considered by some writers as an aging process. The classification is as follows:

N1, *lowest risk*. Parenchyma composed primarily of fat with at most small amounts of "dysplasia." No ducts visible.

P1, *low risk*. Parenchyma chiefly fat with prominent ducts in anterior portion up to one-fourth of volume of breast. Also, may be a thin band of ducts extending into a quadrant.

P2, *high risk*. Severe involvement with prominent duct pattern occupying more than one-fourth of volume of breast.

DY, *highest risk*. Severe involvement with "dysplasia." Often obscures an underlying prominent duct pattern.

The N1 breast is considered essentially "normal." The appearance varies somewhat with the age of the patient. In the young

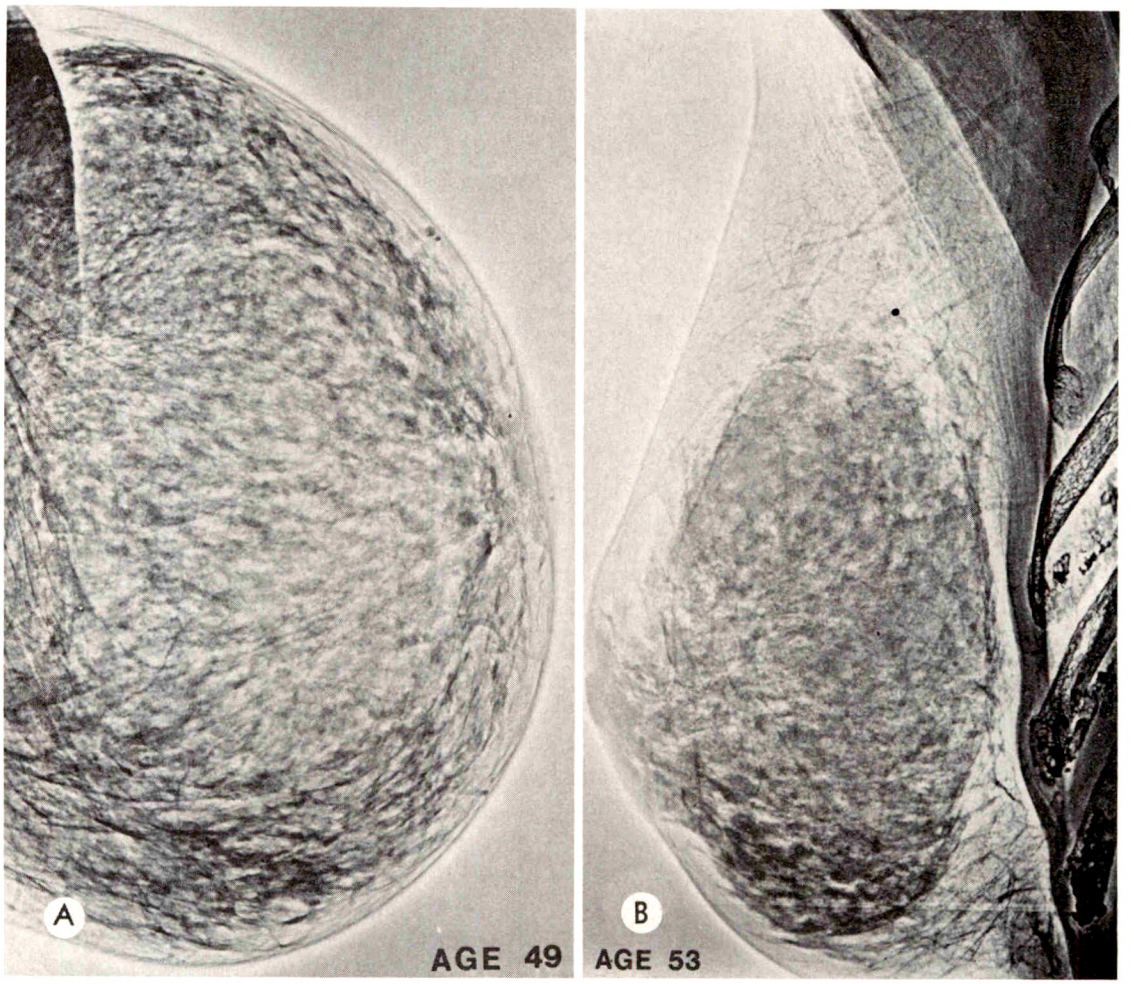


FIG. 2.—*A*, P2 breast. Caudal projection showing severe involvement with prominent duct pattern. *B*, P2 breast. Lateral projection showing severe involvement with prominent duct pattern.

woman, there can be some densities over and above that of fat, but a prominent feature will be islands of fat seen as oval and round areas of relative radiolucency. Ideally it is a breast composed almost solely of fat or one which has a so-called trabeculated appearance (fig. 1*A*).

The breast classified as P1 is composed chiefly of fat, but cordlike structures or a beaded appearance corresponding to prominent ducts are visible in the subareolar area, occupying less than one-fourth of the breast volume. A variation on the subareolar location can be a thin band of ductlike structures extending into one of the quadrants, typically the upper axillary one (fig. 1*B*).

The P2 breast indicates severe involvement of the breast (more than one-fourth of the volume) with a prominent duct pattern. In its severest form, it occupies all of the parenchyma (fig. 2).

The DY breast has a great deal of increase in density over and above that of fat but without the prominent duct pattern as the dominant feature. In its severest form, the parenchyma will appear rather homogeneous (fig. 3).

A proposed fifth group (QDY) is discussed later. This classification is useful in women below the age of 40 because of the strong tendency of the DY group to change at that age.

The histopathology of the groups is as

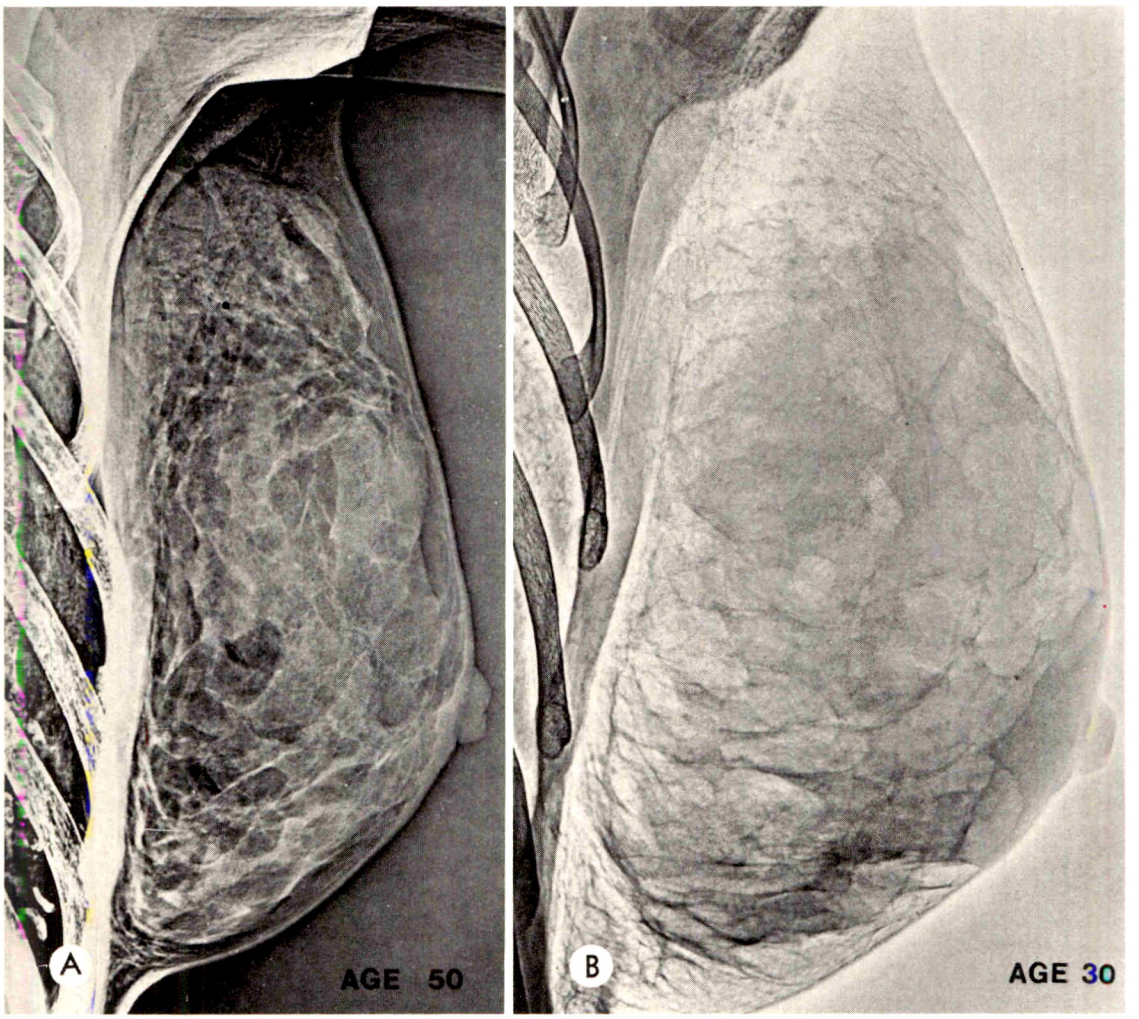


FIG. 3.—*A*, DY breast. Lateral projection showing severe involvement with mammary dysplasia as evidenced by plaquelike areas of increased density. *B*, DY breast. Lateral projection has dense radiographic appearance due to severe mammary dysplasia. (The DY category in the young woman may change dramatically at about age 40 or 50 but usually reverts only to P2.)

expected. The N1 type is composed mainly of fat, usually with normal lobules and ducts. There may be very minimal mammary dysplasia (fig. 4*A*). The chief feature of the P1 and P2 types is connective tissue hyperplasia surrounding the ducts. There are usually some additional elements of mammary dysplasia (fig. 4*B*). The DY group presents the histologic characteristics of severe mammary dysplasia with a great deal of desmoplasia. The pathologist usually identifies at least adenosis and microcyst formation. In some instances, there are epithelial changes ranging from hyperplasia to atypia (fig. 5).

SUBJECTS AND METHODS

Only women 30 years of age or older with an initial radiographic report negative for carcinoma were included. In addition, none of the women included had a history of breast cancer. To be considered a "positive case," breast cancer had to be proven histologically at least 6 months after the radiographic examination. Finally, no information was available to the classifier other than knowledge that the patient was at least 30 years of age.

Two retrospective studies were done. In the first study (termed study 1), all mammograms

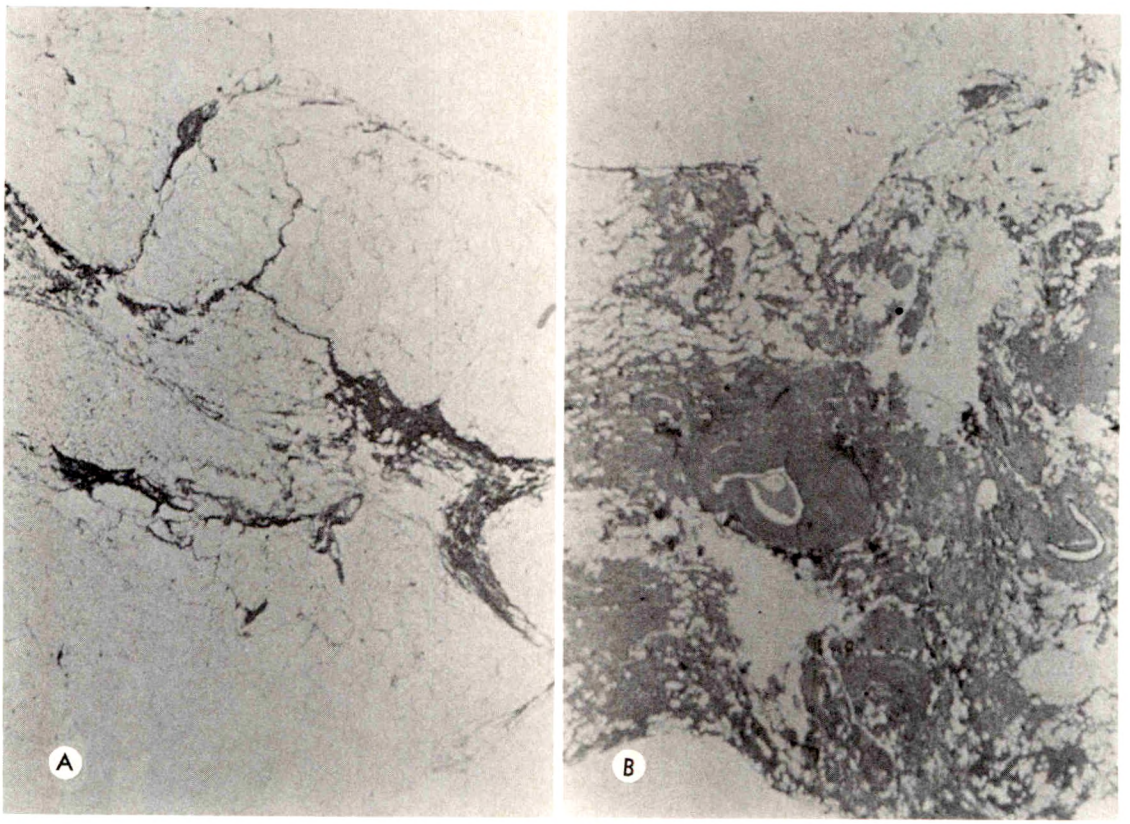


FIG. 4.—*A*, Histologic appearance of N1 breast parenchyma; breast composed mainly of fat. *B*, Histologic appearance of P1 breast. Ducts are undilated, have irregular lumens, and are encircled by deposition of collagenous tissue.

made at Hutzel Hospital on women 30 years of age or more from January 1967 to January 1972 were classified. Study 2 did the same for the period between January 1972 and January 1973.

The case finding procedure differed between the two studies. In study 1, alphabetized lists of patients by classification were furnished to the Tumor Registry of the Michigan Cancer Foundation. An independent search was then made to identify those women who developed a breast cancer. Supplemental case finding was carried out by searching the files of Hutzel Hospital, since because of the geographic limitations of the registry it was estimated to cover significantly less than 100% of the study population. The average time of follow-up was estimated at 3 years. This was selected because of the known time lag between histologic proof of the development of a breast cancer and incorporation of the record into the tumor registry.

For study 2, a questionnaire was mailed to each patient asking for the necessary information to determine if and when she had breast cancer and where it was proven. Responses were obtained from 75%. The vast majority of the nonresponders were patients who had moved and left no forwarding address. The failure to obtain responses in 25% of the study population is not considered a deterrent for two reasons: the cross section of responders versus nonresponders by classification did not differ, and, in addition, the results of study 2 paralleled those of study 1.

Criteria for classification were deliberately varied in the two studies. An attempt was made in study 2 to capture within a larger population a greater number of the developing cancers. This was successful, as will be seen in the results. The other alternative was to select criteria to give smaller numbers of cancers in significantly smaller populations.

RESULTS

The results demonstrate the ability to identify groups of women at significantly

higher risk for developing breast cancer. Study 1 (table 1) shows a stepwise increase in incidence of breast cancer according to classification: 0.14%, 0.52%, 1.96%, and 5.22% for N1, P1, P2, and DY, respectively. The DY group had a 37 times greater incidence than N1. The data show basically two groups at significant risk (P2+DY, incidence of 2.65%) and two groups at relatively low risk (N1+P1, incidence of 0.28%). In this study, 82.14% of the cancers were noted in 33% of the study population (P2+DY).

Study 2 (table 2) shows a similar pattern of incidence for the N1, P1, P2, and DY groups: 0.17%, 0.00%, 1.2%, and 3.6%, respectively. The disparity between DY and N1 groups is present in study 2 but is not as great as in the first analysis (21:1 compared to 37:1). Under the criteria of study 2 (greater numbers of patients placed in the P2 and DY groups), 95% of the developing breast cancers were noted in 46.8% of the population (P2+DY).

For the majority of cases in study 1, the interval between the radiographic examination and histologic proof of the cancer was not available. The Tumor Registry of the Michigan Cancer Foundation would not furnish the information because of confidentiality rules. It was known that the interval was at least 6 months. The intervals for study 2 were as follows: average —2 years, 6 months; extremes—3 years, 5 months and 6 months (N1); and median—2 years, 8 months.

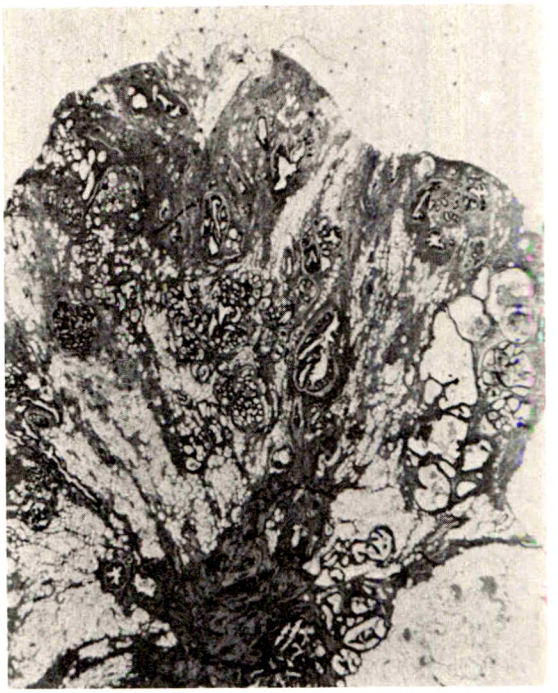


FIG. 5.—Histologic appearance of DY breast; breast involved severely with mammary dysplasia.

Age Distribution

Several observations can be made regarding the age distribution of the combined study population (table 3). First, 15% of the cancers developed in women between the ages of 30 and 39. Second, 85.5% of the cancers occurred in 36.6% of the combined study population (groups P2+DY).

A more important observation concerns the change in role of the P2 and DY classi-

TABLE 1

Study 1: 1967–1971

Class	Cases		Carcinomas		Incidence (%)
	No.	%	No.	%	
N1	2,190	41.4	3	5.36	0.14
P1	1,355	26.0	7	12.5	0.52
N1 and P1	3,545	67.4	10	17.86	0.28
P2	1,375	26.0	27	48.21	1.96
DY	364	7.0	19	33.93	5.22
P2 and DY	1,739	33.0	46	82.14	2.65
Total	5,284	100.4	56	100.00	1.06

TABLE 2

Study 2: 1972

Class	Cases		Carcinomas		Incidence (%)
	No.	%	No.	%	
N1	561	29.1	1	5.0	0.17
P1	465	24.1	0	0.0	0.0
N1 and P1	1,026	53.2	1	5.0	.09
P2	573	29.7	7	35.0	1.2
DY	331	17.1	12	60.0	3.6
P2 and DY	904	46.8	19	95.0	2.1
Total	1,930	100.0	20	100.0	1.04

TABLE 3

CARCINOMAS BY AGE AND CLASS

AGE	N1		P1		P2		DY		TOTAL	
	No.	%	No.	%	No.	%	No.	%	No.	%
30–39	1	9.1	1	9.1	4	36.4	5	45.4	11	100.0
40–49	1	2.9	4	11.4	12	34.3	18	51.4	35	100.0
50–59	1	4.2	1	4.2	14	58.3	8	33.3	24	100.0
60+	1	16.6	1	16.6	4	66.6	0	0.0	6	99.8
Total	4	5.3	7	9.2	34	44.7	31	40.8	76	100.0

NOTE.—Data from combined studies 1 and 2.

fications. The DY group accounts for 50% of the cancers which occurred under the age of 50 years. After that age it accounts for only 8%. Conversely, the P2 classifisation assumes paramount importance after the age of 50 accounting for 60% of the cancers compared to only 34.8% of those discovered before age 50. Table 4 presents a breakdown of the frequency of occurrence of the various groups considered against age.

There is a significant diminution in the number of women in the DY classification with increasing age: 22.4% in the 30–39 age group compared to 4.9% in women 60 years of age or more. Conversely, the number of women in the P2 group increases significantly: 16.7% in the 30–39 age group compared to 36% of the women aged 60 and more. Studies involving serial breast examinations over a long period of time explain these changing incidences (J. N. Wolfe, unpublished data). The dysplasias disappear with aging, and this occurs significantly during the 40–49 year interval. With the disappearance, the breasts are very often noted to be involved with a prominent duct pattern, frequently to a severe degree (P2). A lesser number of the DY group revert to P1, and a few will change to N1. The prominent duct pattern is not thought to be an evolutionary change but rather a pattern that has always been present but masked by the overshadowing densities of mammary dysplasia.

Because of the change that occurs in the DY group with aging, a fifth group, QDY, should be employed for those women below age 40–45 whose degree of dysplasia is not severe. Studies show that their breasts may change dramatically at about the time of the menopause and revert to a lesser class of risk. If the dysplasia is very severe in the young woman, with large areas of homogeneous density, then the chances of that type of breast changing significantly

TABLE 4

RISK CLASSIFICATION BY AGE

AGE	N1		P1		P2		DY		TOTAL	
	No.	%	No.	%	No.	%	No.	%	No.	%
30–39	216	44.1	82	16.7	82	16.7	110	22.4	490	99.9
40–49	189	23.9	159	20.1	258	32.6	186	23.5	792	100.1
50–59	103	24.4	144	33.9	152	35.9	24	5.6	423	99.8
60+	53	23.6	80	35.6	81	36.0	11	4.9	225	100.1
Total	561	29.1	465	24.1	573	29.7	331	17.7	1,930	100.0

are far more remote and the DY classification may be utilized despite the young age (fig. 3*B*).

A similar but less dramatic change occurs between the N1 and P1 groups. The N1 group includes breasts with minimal degrees of mammary dysplasia, often located in the subareolar area. When this recedes as the patient grows older, minor involvement of the breast with a prominent duct pattern is frequently revealed. The N1 group constitutes 44.1% of the 30–39 age group but only 23.6% of the women aged 60 or more. Conversely, P1 changes from 16.7% in the young age group to 35.6% in those aged 60 or more. However, the N1 group does not become P2 or DY. Similarly, P2 does not become N1, P1, or DY.

The smaller number of patients in the N1 category at the older age levels is influenced greatly by the fact that this study does not encompass a cross section of the population. Rather the figures are from a symptomatic population referred, for the most part, for palpable breast disease. A group which more closely resembles a cross section of the general population reveals only a 15% decrease in the N1 group over the years compared to the 30% drop noted here [4].

Projected Risk

Figures for projected risk can be calculated for the lifetime of the entire study population, but more significant data are derived from analysis of certain age groups and classifications. For example, the projected risk for the DY group in the 40–59 age group is as high as 464 breast carcinomas per 1,000 women. This can be compared to the risk in other groups and in the general population.

For the study group, the average time for effective follow-up is considered 3 years. However, the effectiveness of follow-up was significantly less than 100% (estimated at 75%). The incidence in the general population is taken as 6.6% for lifetime risk. The study also indicates that 15% of the breast cancers developed before the age of 40, and that fact is used in some of the computations.

TABLE 5
PROJECTED RISK

	N1	P1	P2	DY	Total
	No. Studied				
Study 1....	2,190	1,355	1,375	364	5,284
Study 2....	561	465	573	331	1,930
Total....	1,751	1,820	1,948	695	7,214
	Incidence (%)				
Study 1....	0.14	0.52	1.96	5.22	1.06
Study 2....	0.17	0.0	1.2	3.6	1.04
Total....	0.145	0.385	1.745	4.460	1.053
	Rate per 1,000 in 3 Years				
Study 1....	1.4	5.2	19.6	52.2	10.6
Study 2....	1.7	0	12.0	36.0	10.4
Total....	1.45	3.85	17.45	44.6	10.5

A summary of the risk observed in the two studies and their combination can be seen in table 5. The similarity of incidence (1.06% and 1.04%) is evident. The rate per 1,000 women over a 3-year period reveals a ratio of 31:1 for DY compared to N1. A more significant comparison is the projected risk over remaining lifetime for the DY and N1 groups. Table 6 presents these data for the 40–59 age group, since this is the peak period for breast cancer in the DY classification. The average age of the DY group was 46 years, the average time of follow-up considered 3 years, and the anticipated life span 70 years. The projected risk for the DY group is very high: 464/1,000 and 432/1,000, respectively, and 448/1,000 for the two studies combined. This figure must be tempered with the knowledge that follow-up information is probably about 75% inclusive. For the N1 group, the projected risk was low: 19/1,000 and 25/1,000, respectively, and 20/1,000 for the two studies combined. The ratio to DY was 1:22. Average age of the N1 group was 48.

TABLE 6

PROJECTED RISK FOR GROUPS DY AND N1

Group	No. Studied	Average Age	No. Cancers	Incidence/3 Yr (%)	Projected Risk to Age 70 (per 1,000)
DY:					
Study 1....	242	46	14	5.8	464
Study 2....	221	46	12	5.4	432
Total....	463	46	26	5.6	448
N1:					
Study 1....	1,138	48	3	0.26	19
Study 2....	292	48	1	0.34	25
Total....	1,430	48	4	0.28	20

NOTE.—Data for the 40–59 age group.

The N1+P1 combination is broadly considered as low risk, whereas DY+P2 is high risk. A comparison between them reveals similar significant differences of projected risk over expected life span but slightly less dramatic (1:6) than that observed in the comparison between DY and N1 alone (table 7).

The figures for the general population can be derived as follows. Assuming 15% of the cancers occur before the age of 40 and assuming the lifetime risk for all women is 6.6%, the projected lifetime risk for the general population is 66/1,000. For the general population above the age of 40, the risk is 56/1,000. Table 8 summarizes projected lifetime risks for the 40–59 age group in the various categories.

Table 9 shows the projected risk for the DY group by age. The numbers in some instances are small, but in general there is fair agreement between the two studies. A detailed comparison with the N1 group is unnecessary since the total expected inci-

TABLE 7

PROJECTED RISK FOR GROUPS P2 AND DY AND GROUPS N1 AND P1

Group	No. Studied	Average Age	No. Cancers	Incidence/3 Yr (%)	Projected Risk to Age 70 (per 1,000)
P2 and DY:					
Study 1....	1,411	50	39	2.76	184
Study 2....	712	49	17	2.39	159
Total....	2,123	50	56	2.64	176
N1 and P1:					
Study 1....	1,019	49	6	0.59	41
Study 2....	595	49	1	0.16	30
Total....	1,614	49	7	0.43	30

NOTE.—Data for the 40–50 age agroup.

TABLE 8

PROJECTED LIFETIME RISKS FOR 40–59 AGE GROUP

Group	Projected Risk for Remainder of Lifetime (per 1,000)
N1	20
General population	56
DY	448
N1+P1	30
P2+DY	176

TABLE 9

PROJECTED RISK FOR DY GROUP BY AGE

Age	No. Studied	No. Cancers	Incidence/3 Yr (%)	Projected Risk for Remainder of Lifetime (per 1,000)
30–39:				
Study 1..	120	5	4.17	490
Study 2..	100	0	0	0
Total..	330	5	1.5	175
40–49:				
Study 1..	204	9	4.4	367
Study 2..	186	9	4.8	400
Total..	390	18	4.6	383
50–59:				
Study 1..	25	25	20	1,000
Study 2..	24	24	12.5	625
Total..	49	49	16.3	815

dence of cancer in the N1 group for these ages is only 10/1,000 women.

CONCLUSION

Two retrospective studies have demonstrated the ability to isolate from the general population those women who are most likely to develop breast cancer. These women have a prominent duct pattern or mammary dysplasia with or without elements of a prominent duct pattern. The former is important no matter what age, whereas the latter, although important in women between 30 and 39, becomes extremely significant after that age.

The identification of two factors, prominent duct pattern and mammary dysplasia, which have some age specificity suggests perhaps the existence of "two types" of breasts prone to cancer. It seems unlikely that these two types of breasts "degenerate" into cancer; rather, it is possible that the stimulus for the development of cancer also produces the prominent duct pattern and acts to prevent the normal regression of mammary dysplasia.

While the correlation of these risk factors with other items of risk such as nulliparity, age, and family history is incomplete, it does not appear to follow precisely. That is, some women in the low risk groups are nulliparous or have a family history of breast cancer, and others in the high risk groups are multiparous, young, and have no family history of breast cancer.

The classifications presented have two applications. First, the symptomatic woman in a high risk group should be watched very carefully for the development of breast cancer. This should include proper instruction in breast self-examination, routine physical examination, and mammography. Subcutaneous mastectomy may be the treatment of choice in some. For instance, a small breasted 50-year-old woman with a firm classification of DY might be well treated by this procedure. Her projected chances of developing breast cancer are nearly one in two. Pathologists must develop methods to determine whether these women have breast cancers at the time of subcutaneous mastectomy; the usual specimen examination is insufficient.

The other broad application should be in routine screening programs. The task of examining the entire female population for breast cancer on a regular basis is formidable. It would be much better if a decision were made as to whether detection of 75% of the cancers in 20%–25% of the population is sufficient or whether figures such as 95% in 45% of the population or even 50% of the cancers in 10% of the population are sufficient. These distributions are thought to be attainable by the proper selection of criteria.

REFERENCES

1. Wolfe JN: A study of breast parenchyma by mammography in the normal woman and those with benign and malignant disease. *Radiology* 89:210–215, 1967
2. Wolfe JN: Mammography: ducts as a sole indicator of breast carcinoma. *Radiology* 89:206–210, 1967
3. Wolfe JN: The prominent duct pattern as an indicator of cancer risk. *Oncology* 23:149–158, 1969
4. Wolfe JN: Risk for breast cancer development determined by mammographic parenchymal pattern. *Cancer*. In press, 1976

Am J Roentgenol 126:1140–1146, 1976

RADIOGRAPHIC VISUALIZATION OF LEFT VENTRICULAR ANEURYSMS ON LATERAL CHEST FILM

RICHARD D. KITTREDGE,[1] BENJAMIN GAMBOA,[2] AND HARVEY G. KEMP[2]

ABSTRACT:

The diagnosis of left ventricular aneurysm on routine chest examination can be elusive. Six cases are presented which illustrate a radiographic sign not previously emphasized: a soft tissue border seen retrosternally or superiorly on lateral chest film produced by the wall of the aneurysm silhouetting against the midline cardiac shadow. This sign is not always present since it is dependent on the direction of projection of the aneurysm. However, when observed, it should suggest the proper diagnosis.

As the precise radiographic visualization of the left ventricle by cardiac catheterization becomes routine in evaluation of coronary artery occlusive disease, so the elusive left ventricular aneurysm diagnosis by routine chest x-ray becomes painfully obvious [1, 2]. We have defined left ventricular aneurysm as a permanent abnormal blood-filled dilatation of the left ventricular chamber resulting from disease of the wall. This follows directly from the Greek word *aneurysma* (to dilate). In all our cine studies the aneurysm does not contribute to muscular contraction during systole; therefore, it does not empty and is clearly seen to pool contrast material. It may or may not demonstrate paradoxical activity [3], but it is clearly discrete and saclike in con-

TABLE 1

PATIENT DATA

Case No.	Age (Yr)	MI	CHF	Electrocardiogram	Hemodynamic Data
1	57	2	Mild	Anteroseptal infarction, left atrial enlargement, possible left ventricular aneurysm	Biventricular failure, LVEDP 21 mm Hg, cardiac index slightly reduced
2	56	1	Mild	Diaphragmatic and anteroseptal infarction	LVEDP 19 mm Hg, normal right heart pressure, cardiac index normal
3	44	1	Moderate	Anterolateral infarction, possible left ventricular aneurysm	Moderate left ventricular failure, LVEDP 18 mm Hg, cardiac index reduced
4	68	1	Moderate	Extensive anterior infarction, possible left ventricular aneurysm	Left ventricular failure, LVEDP 24 mm Hg, slightly reduced cardiac index
5	44	1	Moderate	Anterolateral infarction, possible left ventricular aneurysm	Left ventricular failure, LVEDP 29 mm Hg
6	53	1	Absent	Old diaphragmatic infarction, anterolateral infarction, possible left ventricular aneurysm	Left heart pressure slightly elevated, LVEDP 14 mm Hg, cardiac index low

NOTE.—All subjects were male and all had angina.

[1] Department of Radiology, St. Luke's Hospital Center, College of Physicians and Surgeons, Columbia University, 114th Street and Amsterdam Avenue, New York, New York 10025. Address reprint requests to R. Kittredge at St. Luke's Hospital.

[2] Department of Cardiology, College of Physicians and Suregons Columbia University, and St. Luke's Hospital Center, New York, New York 10025.

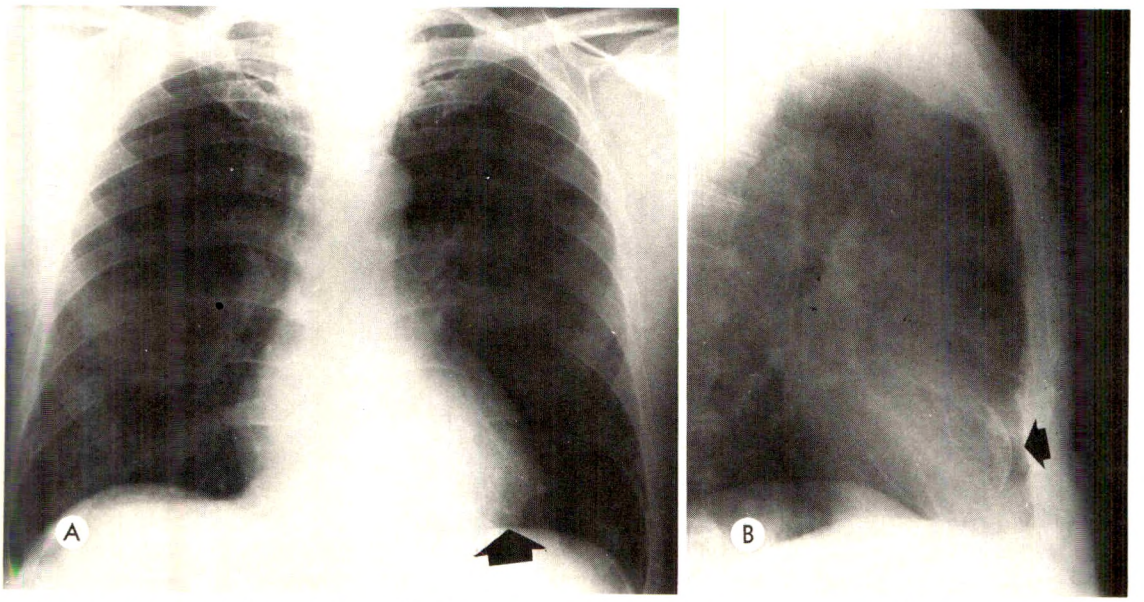


FIG. 1.—Case 1. *A*, Frontal chest film showing normal cardiac contour except for slight cardiac fullness. Note faint calcification of left ventricular border laterally (*arrow*). *B*, Lateral chest film showing anterior crescent shaped calcification of left ventricular aneurysm projected in retrosternal position (*arrow*). It is in fact in outer anterior left hemithorax.

figuration and is easily distinguished from akinetic segments of heart wall by its characteristic shape, the pooling and stagnation of blood, and the complete loss of normal heart muscle activity.

Chest x-rays often do not suggest ventricular wall abnormalities, even when as much as 50% of the left ventricle chamber is aneurysmal [1]. Irregularity of cardiac contour is often absent. Calcification of myocardium is uncommon. An enlarged heart is often seen with left ventricular aneurysm but is so common without aneurysm that it becomes insignificant as a radiographic finding.

A radiographic sign of left ventricular aneurysm not previously reported is a soft tissue margin seen retrosternally or superiorly on lateral chest film. This is produced by the border of an aneurysm silhouetting against the midline cardiac shadow. The localized bulge of the aneurysm loses continuity with the normal line of the left ventricular wall silhouette, especially if the aneurysm involves the anterolateral or superior portions of the left ventricle and is therefore seen as an additional superimposed border. This report demonstrates the above described sign in its most obvious and more subtle forms. Two calcified aneurysms are included as visual aids so

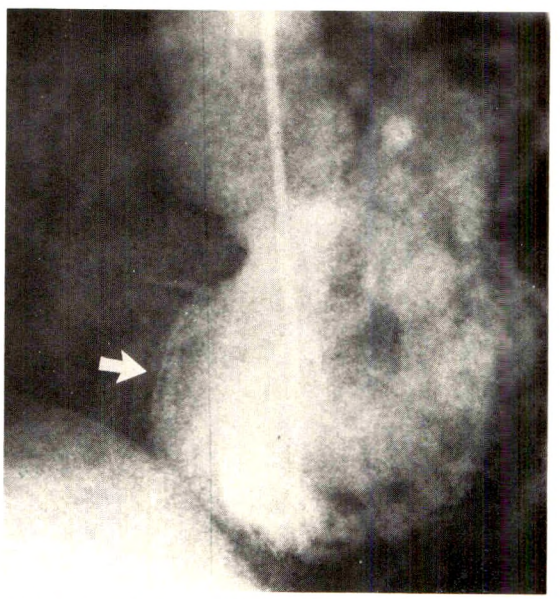


FIG. 2.—Case 1, left ventricular cine angiography in left anterior oblique projection showing ventricular diastole. Peripheral calcification again seen anterior and lateral in aneurysmal wall (*arrow*).

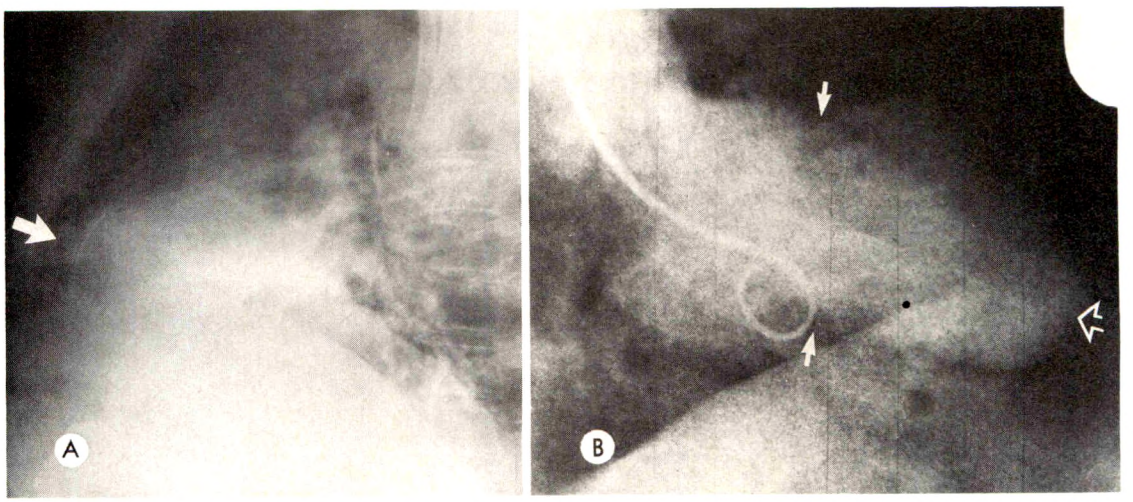


FIG. 3.—Case 2. *A*, Lateral projection showing clearly defined calcific rim (*arrow*) involving left ventricular border laterally and anteriorly. This projects retrosternally just posterior to anterior border of midline cardiac shadow but is in fact in outer anterior left hemithorax. *B*, Left ventricular cine angiography in right anterior oblique projection showing large ventricular aneurysm involving distal half of ventricle (*arrows*). Calcific rim seen at apex of aneurysm (*open arrow*).

that the noncalcified aneurysm border seen only as a linear soft tissue border will be better appreciated.

DEMONSTRATION OF SIGN

All six cases presented had aneurysms with clearly identifiable borders. A summary of patient data is shown in table 1.

Calcified Aneurysms

Cases 1 and 2 show faint calcifications in frontal projection and anteriorly placed

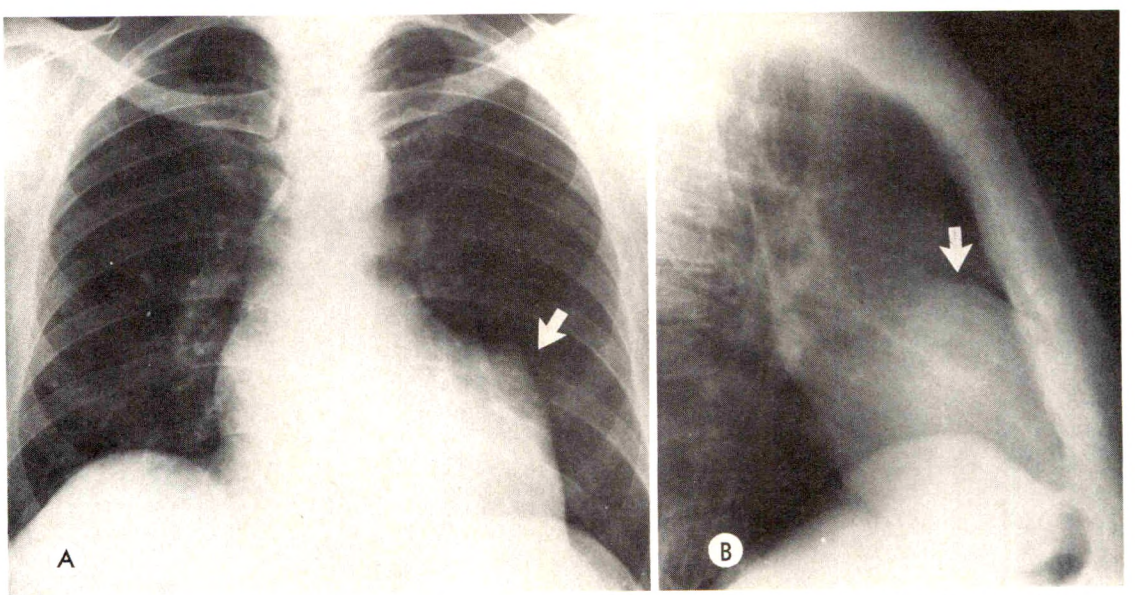


FIG. 4.—Case 3. *A*, Frontal chest film showing irregular left ventricular contour with bulge superior laterally strongly suggesting aneurysm formation (*arrow*). *B*, Lateral chest film showing superior anterior density (*arrow*) representing anterior superior margin of left ventricular aneurysm in left hemithorax silhouetting against midline cardiac shadow.

crescent-shaped calcification on lateral chest film (figs. 1 and 3*A*). This calcium was in the anterolateral and apical walls of the left ventricular aneurysms proven on angiography (figs. 2 and 3*B*). These two cases demonstrate the position that a calcified anterolateral border of an aneurysm can assume on lateral chest film. Although considerably to the left of midline, they project quite far anteriorly in a retrosternal position against the midline cardiac shadow.

Uncalcified Aneurysms

Cases 3 and 4 show prominent aneurysms bulging laterally and superiorly (figs. 4–6). These are the most obvious examples of aneurysm silhouetting against the midline cardiac shadow. The silhouetting phenomenon occurs as the aneurysm loses its smooth, continuous border with the ventricular wall due to localized bulging superiorly. This localized bulge surrounded by lung in the left hemithorax develops a clearly discernable border as it projects on lateral film against the midline cardiac shadow.

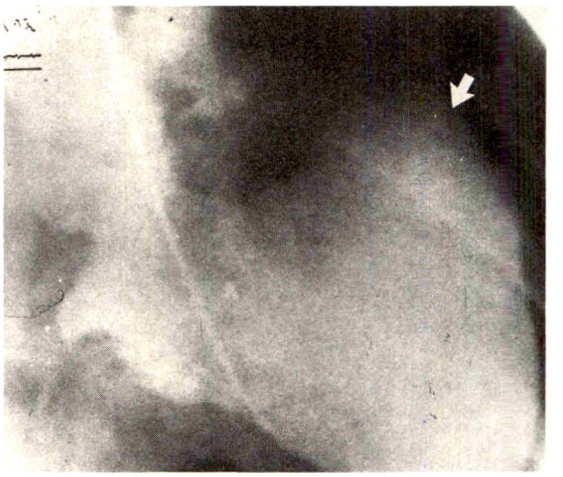


FIG. 5.—Case 3, left ventricular cine angiography in right anterior oblique projection showing large ventricular aneurysm involving distal half of left ventricle. Bulging superior border of aneurysm causes silhouette as seen on lateral projection (*arrow*). Ventricle is in late systole.

Cases 5 and 6 demonstrate the more subtle manifestations of the sign. The

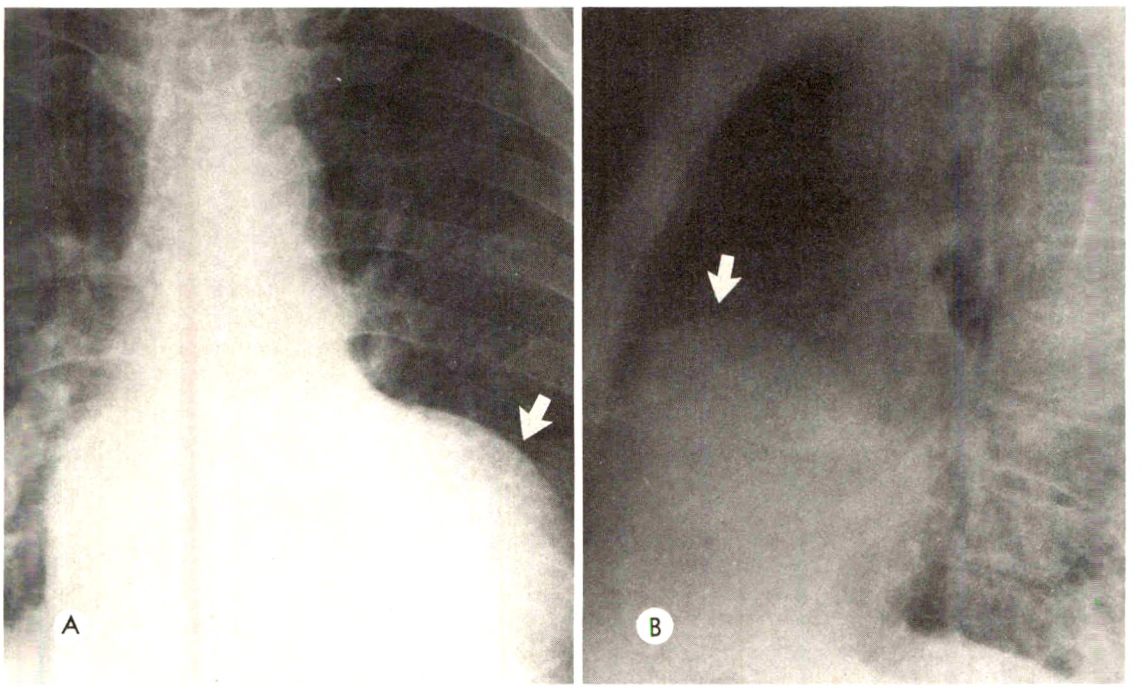


FIG. 6.—Case 4. *A*, Frontal chest film showing large cardiac contour with prominent left ventricular border extending to lateral chest wall. *B*, Lateral chest film showing superior anterior density (*arrow*) indicating superior lateral border of left ventricular aneurysm.

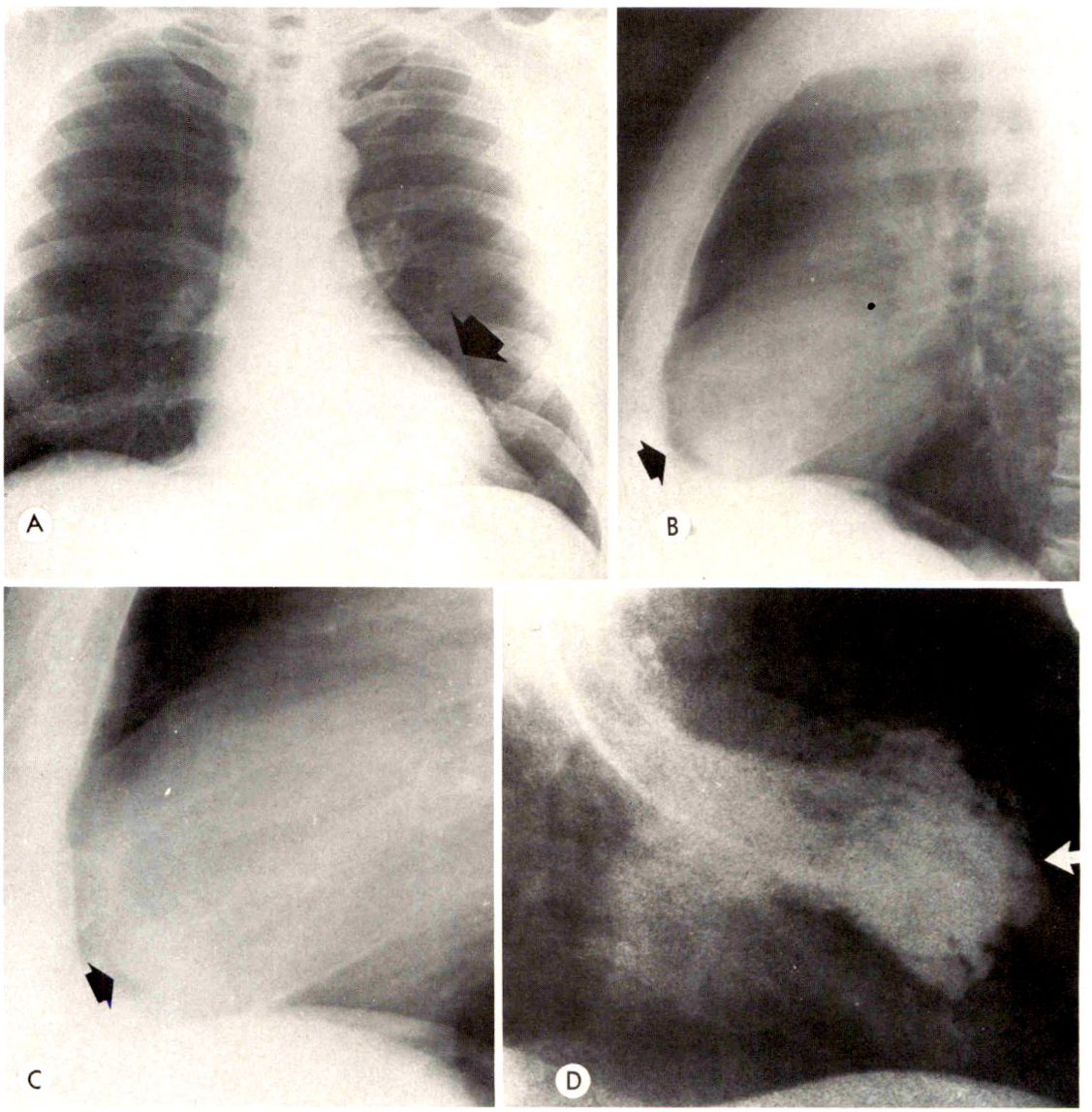


FIG. 7.—Case 5. *A*, Frontal chest film showing normal cardiac contour except for slight bulging along left ventricular border (*arrow*) easily minimized in routine chest interpretation. *B*, Lateral film showing density silhouette approximately 1 cm from inner sternal margin (*arrow*) representing anterior lateral margin of ventricular aneurysm in left hemithorax surrounded by lung and silhouetting against midline cardiac shadow. *C*, Enlarged view of lateral projection showing to better advantage profile of aneurysm (*arrow*). *D*, left ventricular cine angiography in right anterior oblique projection in late systole demonstrating large left ventricular aneurysm involving distal half of left ventricle and apex (*arrow*). Irregularity along lateral margin suggests clot formation.

aneurysm bulges laterally and anteriorly in the left hemithorax. As the aneurysm loses its smooth, continuous line with the left ventricular wall, it develops a discernible border which silhouettes against the midline cardiac shadow on lateral chest film in a retrosternal position (figs. 7 and 8). The position is similar to that of the calcification of the first two aneurysms described.

DISCUSSION

The cases presented demonstrate specific

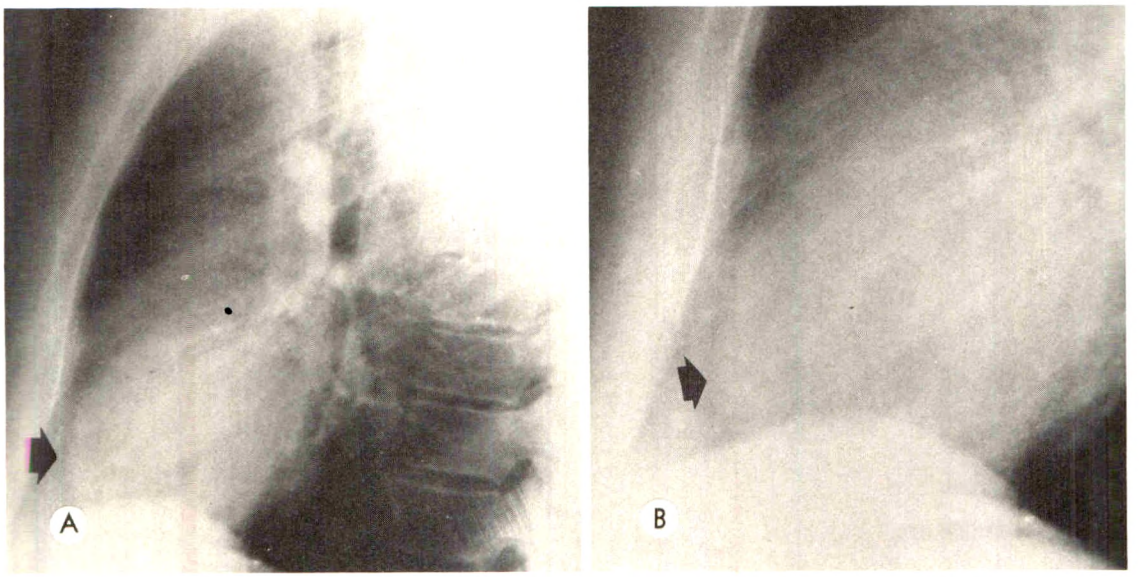


FIG. 8.—Case 6. *A*, Lateral chest film showing density silhouette approximately 1 cm from inner sternal margin (*arrow*) representing anterior lateral margin of left ventricular aneurysm in left hemithorax projecting against the midline cardiac shadow. Frontal chest film showed fairly normal cardiac contour. *B*, Enlarged view of inner sternal margin on lateral film showing to better advantage density silhouette (*arrow*) representing anterior lateral margin of left ventricular aneurysm.

types of aneurysm formation of the left ventricle. The less prominent the aneurysm, the less will be the loss of continuous left ventricular border and consequently the more difficult it will be to see an additional border silhouetting on the lateral chest film.

However, the sign depends more upon the shape of the aneurysm and its direction of protrusion than its actual size. An aneurysm of the anterolateral wall that bulges anteriorly and somewhat laterally will more likely develop a radiologically visualized border projecting retrosternally in position on lateral chest film than a diaphragmatic aneurysm which would have a tendency to project downward and blend with the diaphragmatic shadow. The anterolateral bulge can be well documented during coronary arteriography with the typical bowing forward of the left anterior descending artery, if patent, as it traverses the interventricular groove. Similarly, an aneurysm of the lateral free wall of the left ventricle bulging superiorly will rapidly develop a radiographically visualized border as it projects against the base of the heart.

The characteristic of an aneurysm to produce irregularity and a bulgelike protrusion of the cardiac contour has long been described as one of the classic findings on frontal chest film. The contour abnormality silhouettes against the lung and is clearly discernable. However, on lateral chest film the aneurysm margin is not as easily seen since it must be viewed overlying soft tissue rather than lung.

The frequency of this sign in angiographically proven aneurysms depends entirely on the direction of aneurysm formation. The aneurysms that involve the apex only and protrude laterally only or downward toward the diaphragm will not produce borders seen on lateral film. However, if the direction of the protrusion is anterior, anterolateral, or superior, it is our experience that at least 50% of the cases will show an abnormal border on lateral chest film.

Clinical correlation (table 1) was significant in that patients showed moderate

and two patients showed mild evidence of congestive heart failure; (only one patient was relatively free of failure). Significant angina was present in all patients.

REFERENCES

1. Kittredge RD, Cameron A: Abnormalities of left ventricular wall motion and aneurysm formation. *Am J Roentgenol* 116:110–124, 1972
2. Shanks SC, Kerley P: *A Textbook of X-Ray Diagnosis*, vol 2, 4th ed. Philadelphia, Saunders, 1972
3. Kurtzman RS, Lofstrom JE: Detection and evaluation of myocardial infarction by image amplification and cinefluorography. *Radiology* 81:57–64,1963

Am J Roentgenol 126:1147–1154, 1976

THE CHEST X-RAY IN ACUTE LEFT VENTRICULAR POWER FAILURE: AN AID TO DETERMINING PROGNOSIS OF PATIENTS SUPPORTED BY INTRAAORTIC BALLOON PUMPING

PHILIP N. CASCADE,[1] ADRIAN KANTROWITZ,[2] WALDEMAR J. WAJSZCZUK[3] AND MELVYN RUBENFIRE[3]

ABSTRACT:

Serial chest x-rays were used as a means of evaluating the hemodynamic status of 43 patients in acute left ventricular power failure (LVPF) complicating acute myocardial infarction who were assisted with balloon pumping. The following findings were reported:

1. In patients with acute myocardial infarction, prediction of the hemodynamic status on the basis of chest x-rays is less reliable when severe LVPF is present as a complication.

2. The incidence and severity of roentgenographic findings of congestive heart failure and pulmonary edema are increased in patients with severe LVPF compared to patients with uncomplicated myocardial infarction.

3. Improvement in the roentgenographic degree of heart failure with positive clinical and hemodynamic responses to 24 hr or less of balloon pumping is an indication that patients in severe acute LVPF may survive. Patients with deteriorating or unchanging chest x-ray findings have an extremely poor prognosis. These patients should be evaluated by cardiac catheterization and coronary arteriography to determine the appropriateness of emergency surgical correction.

Chest roentgenograms have been used in assessing hemodynamic status and in following sequential cardiovascular changes of patients with acute myocardial infarction [1–9]. Serial chest roentgenograms have been used as one means of evaluating the hemodynamic status of patients in acute left ventricular power failure (LVPF) [10] complicating acute myocardial infarction who require support by intraaortic balloon pumping [11–13]. This study was designed to demonstrate the spectrum of chest x-ray findings in these patients and to determine whether serial chest x-ray changes can be used as a guide to prognosis.

SUBJECTS AND METHODS

From 1971 to 1974, 43 patients in acute LVPF complicating acute myocardial infarction were assisted by balloon pumping. Physiologic findings in all cases fit the following criteria: central aortic systolic pressure below 90 mm Hg or, in previously hypertensive patients, no more than 75% of the prior level; urine output less than 30 ml/hr; rales in the lungs; usually an S_3 gallop and sinus tachycardia; and arterial hypoxemia. In all cases the cardiac index before pumping was less than 2 liters/min per square meter and the arteriovenous oxygen differential was greater than 6 vol/100 ml. The patients were usually obtunded, had cold clammy skin and cyanosis, and often required mechanical respiratory assistance. The average age of the patients was 57.5 years; 35 were males and eight were females. Of the 43, 32 had histories of hypertension and diabetes, with or without arteriosclerotic heart disease. In 16 patients LVPF developed within 12 hr of admission to the hospital; the remaining patients had delayed onset of LVPF.

Presented at the annual meeting of the American Roentgen Ray Society, Atlanta, Georgia, October 1975.
This work was supported in part by U.S. Public Health Service grant HL 13737.
[1] Department of Radiology, Sinai Hospital of Detroit, 6767 West Outer Drive, Detroit, Michigan 48235. Address reprint requests to P. N. Cascade.
[2] Department of Cardiovascular/Thoracic Surgery, Sinai Hospital of Detroit, Detroit, Michigan 48235.
[3] Department of Medicine, Sinai Hospital of Detroit, Detroit, Michigan 48235.

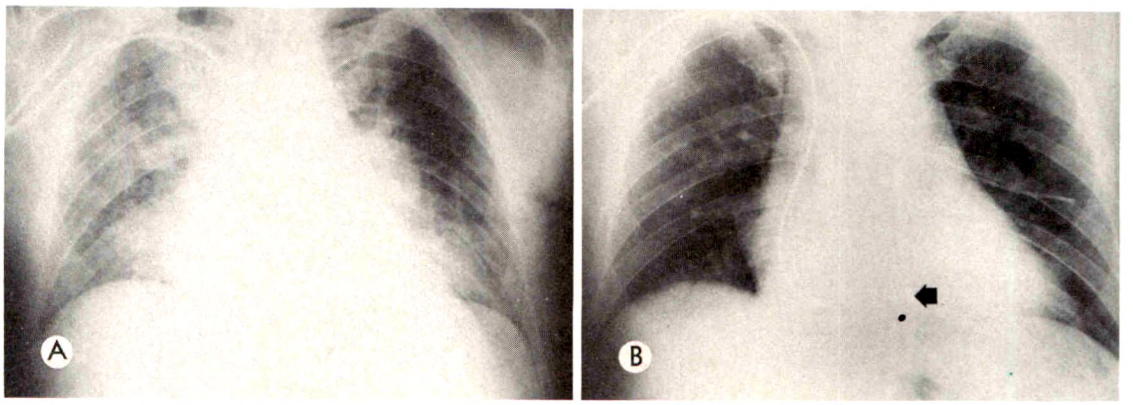


FIG. 1.—*A*, AP portable chest roentgenogram obtained immediately following insertion of intraaortic balloon pump demonstrating presence of interstitial and alveolar pulmonary edema. *B*, Marked improvement 24 hr later in degree of heart failure. Balloon pump remains in position (*arrow*) within descending thoracic aorta.

All patients were treated with combinations of drugs such as digitalis preparations, diruretics, antiarrhythmic agents, and vasoactive substances. The duration of balloon pumping ranged from 2 hr to 61 days; 65% of the patients were assisted for periods of 3 days or less.

Portable chest x-rays were taken at the onset of LVPF, following insertion of the balloon pump, and at 12–24 hr intervals during the acute phase of the illness. Subsequent films were made at longer intervals. For initial exposures, the patients were erect or semierect; follow-up films were made with the patient sitting, semierect, or supine depending on the degree of restriction of patient mobility. Exposure factors varied from 5 to 20 mA and from 65 to 85 kVp. The tube-film distance for upright films was 72 inches. Films of supine patients were taken at the maximum obtainable distance (approximately 50 inches). Each film was examined to detect radiographic evidence of heart failure.

The severity of heart failure was categorized as pulmonary venous hypertension without edema, interstitial pulmonary edema, or alveolar pulmonary edema. These categories were defined on the basis of the appearance of the pulmonary vasculature and the presence or absence of pulmonary parenchymal changes. When a film included radiographic signs of more than one of the categories, it was assigned to the most severe group.

1. *Pulmonary venous hypertension.* A change in the normal distribution of blood flow to the lungs as reflected by increased caliber of the upper lobe vessels. Supporting this diagnosis were accompanying cardiomegaly, pleural effusions, or distension of the azygous vein.

2. *Interstitial pulmonary edema.* The radiographic presence of Kerley A, B, and C lines, diffuse haziness in the lung bases and in the perihilar regions, perivascular fluid (demonstrated as blurring of the margins of the pulmonary vessels or "cuffing"), and peribronchial edema (manifested as thickening of the bronchial walls).

3. *Alveolar pulmonary edema.* The appearance of "fluffy" pulmonary infiltrates.

Serial films of each patient were compared with the initial film in order to determine improvement (fig. 1), lack of change, or deterioration (fig. 2) of the hemodynamic status. These assessments were then correlated with the patient's clinical course. The factors considered included clinical outcome (survival or death), temporal relationship of infarction and onset of circulatory collapse, and interval from diagnosis of LVPF to initiation of balloon pumping. The radiographic changes in response to the pumping were also correlated with clinical and hemodynamic changes in each patient. The hemodynamic response to balloon pumping was considered positive when the systolic brachial artery pressure was stabilized, mean pulmonary capillary wedge and pulmonary artery pressures were substantially reduced, and the cardiac output increased. The clinical response was considered positive when mentation had improved, skin color had returned to normal with cessation of diaphoresis, vasopressor dosage could be progressively reduced, and weaning of the patient from the balloon pump could be started

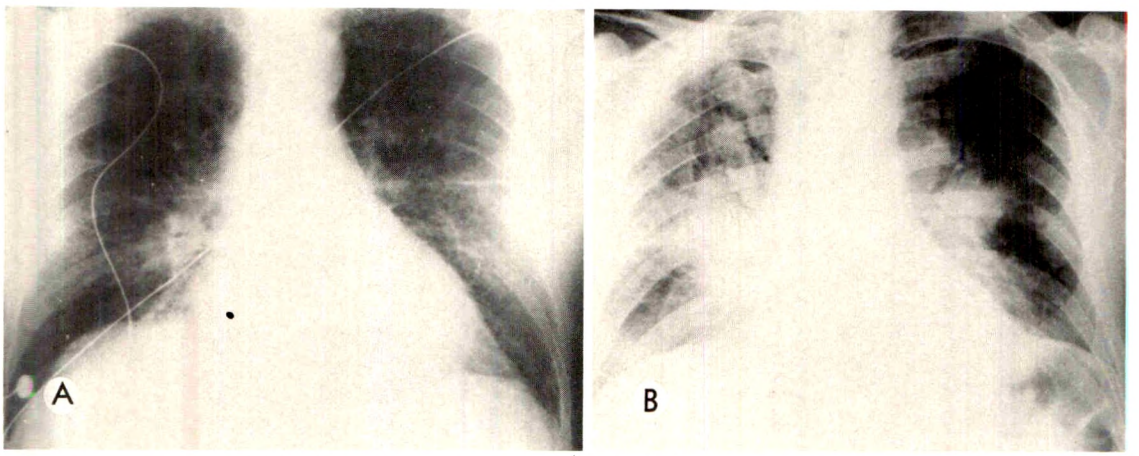


FIG. 2.—*A*, AP portable chest roentgenogram obtained before insertion of intraaortic balloon pump demonstrating loss of margination of lung roots indicating interstitial pulmonary edema. *B*, Roentgenogram after 24 hr of balloon pumping demonstrating increased interstitial pulmonary edema and infiltrates of alveolar pulmonary edema.

within the first 24 hr.

RESULTS

Of the 43 patients studied, 15 presented radiographic findings of alveolar pulmonary edema, 19 of interstitial pulmonary edema, and nine of pulmonary venous hypertension without edema. No correlations were found between initial chest x-ray appearance and factors such as age, presence or absence of previous myocardial infarction or hypertension, delay in onset of LVPF, or delay in initiating intraaortic balloon pumping following the diagnosis of LVPF (table 1). No significant differences were found ($P = .05$) in initial baseline hemodynamic measurements for patients in any of the three roentgenographic grades of heart failure (table 2).

The survival data were analyzed from several clinical standpoints. In all, 12 patients survived for an overall rate of 28%. Three of eight patients (37%) who had emergency cardiac surgery in an attempt to reverse LVPF survived, whereas nine of 35 (25.7%) who had balloon pumping without surgery survived. The survival ratio of patients with immediate onset of LVPF (less than 24 hr following clinical signs and symptoms of acute myocardial infarction) was higher than for those with delayed onset, and the survival ratio was also higher

TABLE 1

RELATIONSHIP OF INITIAL RADIOGRAPHIC APPEARANCE OF CHEST AND HISTORY

HISTORY	INITIAL CHEST X-RAY FINDING		
	Pulmonary Venous Hypertension	Interstitial Pulmonary Edema	Alveolar Pulmonary Edema
No. patients	9	19	15
Average age (range)	58.0 (34–73)	58.0 (41–77)	56.5 (34–69)
Previous myocardial infarction	2 (22)	5 (26)	6 (40)
Hypertension	4 (44)	5 (26)	6 (40)
LVPF:			
Immediate onset	2 (22)	9 (47)	5 (33)
Delayed onset	7 (78)	10 (53)	10 (67)

NOTE.—Numbers in parentheses are percentages.

TABLE 2

RELATIONSHIP OF INITIAL CHEST X-RAY FINDING AND HEMODYNAMIC MEASUREMENTS

Initial X-ray Finding	$\bar{X}$	SD	Range	Coefficient of Variation (%)
	Systolic Brachial Artery Pressure			
Pulmonary venous hypertension	76.67	15.61	45	20.36
Interstitial pulmonary edema	64.42	32.29*	104*	50.12
Alveolar pulmonary edema	75.85	25.62*	102*	33.78
Combined	70.73	27.39*	104*	38.72
	Pulmonary Capillary Wedge Pressure			
Pulmonary venous hypertension	27.60	8.91	19	32.26
Interstitial pulmonary edema	25.36	8.76	28	34.52
Alveolar pulmonary edema	27.78	8.96	27	32.24
Combined	26.68	8.56	28	32.09
	Pulmonary Artery Pressure			
Pulmonary venous hypertension	33.22	10.50	28	31.60
Interstitial venous hypertension	30.61	9.29	44	30.34
Alveolar pulmonary edema	33.42	7.76	22	23.23
Combined	32.08	9.01	44	28.08

NOTE.—Values shown are bedside hemodynamic measurements at onset of LVPF (mm Hg).
* Values large because measurements contained values of zero.

when balloon pumping was started immediately. However, the differences in survival in these groups could not be shown to be statistically significant.

There was no significant difference ($P > .05$) in survival among patients in the three roentgenographic levels of heart failure as determined on the initial chest x-ray examination (table 3).

Serial changes in the x-ray appearance of pulmonary vessels and parenchymal infiltrates were correlated with survival (table 4). Patients whose outcome was influenced by cardiac surgery were excluded from this evaluation. Among patients whose chest x-rays improved within 24 hr of initiation of balloon pumping, the survival rate was 63.6%. This survival figure was significantly higher than the 8% rate among patients with unchanging x-rays ($P < .001$) or the 10% survival rate in those patients who demonstrated roentgenographic deterioration in the first 24 hr ($P = .005$). Two patients did not survive long enough for a follow-up chest x-ray.

All nine patients who survived without surgical intervention sustained rapid hemodynamic and clinical improvement after initiation of balloon pumping, although only seven improved radiographically. In the two patients who did not have immediate chest x-ray improvement, the radiographic findings improved after 48 hr of circulatory assistance. Of the 24 patients who did not have surgery and died but survived long enough for follow-up films, only four had rapid x-ray improvement. Onset of LVPF was delayed in all four, and in three initiation of balloon pumping was also delayed. These three patients improved roentgenographically in the first 24 hr but either deteriorated or did not manifest further improvement on subsequent films and remained in alveolar or interstitial pulmo-

nary edema until death. In one patient who had cerebral damage following multiple episodes of ventricular fibrillation, a balloon pump was inserted rapidly, roentgenographic and hemodynamic improvement ensued, but the patient eventually died of noncardiac causes after being weaned from the balloon pump, never having recovered from a state of deep coma. Two patients sustained hemodynamic and clinical improvement but did not improve radiographically. They were weaned from the balloon pump but subsequently relapsed into severe LVPF and expired.

DISCUSSION

Roentgenographic Evaluation of LVPF

That chest roentgenographic findings correlate relatively accurately with cardiac hemodynamic status has been established [14–17]. Several investigators have reported series of cases in which there was good correlation between hemodynamic data and the chest film following acute myocardial infarction [6, 7]. When left ventricular enddiastolic pressure is elevated, a concomitant rise in pulmonary capillary wedge pressure is reflected by pulmonary vascular changes as visualized on the chest x-ray. Mean wedge pressures in the range of 15–18 mm Hg give rise to constriction of vessels in the lung bases with a resultant increase in flow to the upper lobes. When the mean wedge pressure begins to exceed the colloid osmotic pressure of normal serum (22–30 mm Hg), plasma transudates begin to collect in the interstitial tissues of the lungs. This interstitial fluid is shown on the x-ray as Kerley A, B, and C lines, perivascular blurring or "cuffing," loss of margination of the lung roots, and bronchial wall thickening. Transudate accumulates in large amounts in the interstitial and alveolar compartments of the lungs when mean wedge pressures are elevated above 25–28 mm Hg. This produces the x-ray picture of alveolar pulmonary edema.

TABLE 3

RELATIONSHIP OF INITIAL CHEST X-RAY FINDING AND SURVIVAL

INITIAL CHEST X-RAY FINDING	SURVIVAL		DEATH
	No.	%	
Pulmonary venous hypertension	2	22.2	7
Interstitial pulmonary edema	5	37.5	9
Alveolar pulmonary edema	2	16.6	10
Total	9	25.7	26

NOTE.—Patients who underwent cardiac surgery are excluded.

TABLE 4

RELATIONSHIP OF SEQUENTIAL CHEST X-RAY FINDINGS, RESPONSE TO BALLOON PUMPING, AND SURVIVAL

SEQUENTIAL CHEST X-RAY FINDING*	RESPONSE TO BALLOON PUMPING†		TOTAL
	+	−	
Improved:			
Survivors	7	0	7 (63.6)
Deaths	2	2	4
No change:			
Survivors	1	0	1 (8.3)
Deaths	2	9	11
Deterioration:			
Survivors	1	0	1 (10)
Deaths	0	9	9

NOTE.—Data excludes eight patients who underwent cardiac surgery. Numbers in parentheses are percentages.

* Determined by comparison of chest x-ray before and after 24 hr of balloon pumping.

† Ability to reduce the dose of vasopressors and wean from the support of balloon pumping.

Measurement of the cardiac silhouette size is another adjunct in the evaluation of left ventricular performance. However, Stein et al. [18] have shown that cardiac size should be considered only secondarily in evaluating the presence of left ventricular failure, since 24% of their patients had mild to moderate elevation of the pulmonary capillary wedge pressure in the face of a normal transverse cardiac diameter. The presence of pleural effusions is a rough indicator of the presence of left ventricular failure but does not accurately quantitate the degree of congestive heart failure [4].

There are difficulties in estimating left ventricular failure from chest x-rays alone,

especially in patients in whom upper lobe pulmonary vascular distention is the only indicator of failure. The portable technique, recumbent or semirecumbent position, poor degree of inspiration, and the general clinical situation all contribute to the difficulty in estimating the degree of cardiac failure. However, when the failure is severe enough to produce pulmonary edema, the diagnosis becomes more definite.

Other investigators [5, 7, 19] have reported that changes in chest x-ray findings may fail to parallel the changes in the patient's hemodynamic status. This "diagnostic lag" is not surprising, inasmuch as hemodynamic measurements performed directly in the vascular space reflect only one moment in time, whereas the roentgenographic estimation of cardiovascular status is based upon changes in the lung fields which evolve more slowly and represent cumulative effects of hemodynamic events of recent hours and days.

The severity of the chest x-ray abnormalities is less directly correlated with the degree of dysfunction as determined by direct hemodynamic measurement in patients with acute myocardial infarction complicated by severe LVPF than in those without LVPF. Our study failed to demonstrate any statistical difference in the mean systolic brachial artery pressures, mean pulmonary capillary wedge pressures, or mean pulmonary artery pressures among patients with pulmonary venous hypertension or interstitial or alveolar pulmonary edema. A clinical discrepancy between the degree of congestive heart failure and the severity of hemodynamic measurement abnormality has been noted by others [6, 20, 21]. In particular, low, normal, or severely elevated left ventricular end-distolic pressures occur in patients with cardiogenic shock [21–23]. These pressure variations have been attributed to differences in left ventricular compliance or changing degrees of left ventricular dilatation perhaps related to variations in rates of venous return [20]. This variability of pressure abnormality in the left ventricle in turn causes inconsistent changes in the pulmonary vasculature, which is an additional factor that reduces the predictability of pulmonary roentgenographic changes when patients meet criteria of LVPF. Nevertheless, relative changes of improvement or deterioration can be identified with certainty when radiographs are technically satisfactory.

Chest X-rays in Acute Myocardial Infarction and Severe LVPF

Previous studies indicate that the x-ray incidence of congestive heart failure following acute myocardial infarction varies from 55% to 76% [5, 7, 8]. The roentgenographic detection of mild pulmonary venous hypertension and early interstitial pulmonary edema is of particular significance since there are often no clinical symptoms or physical signs of heart failure [3, 4, 9]. The frequency of pulmonary edema has been reported to vary from 24% to 73%, with 20% of the patients presenting in alveolar pulmonary edema. In our series of 43 patients who fit criteria of severe LVPF, all were in congestive heart failure, 44% were in interstitial pulmonary edema, and 35% had deteriorated to the point of alveolar pulmonary edema. The higher percentage of x-ray abnormalities in this group probably is correlated with their much poorer prognosis since patients in severe LVPF who are treated with conventional methods have a mortality rate estimated at 85%, whereas that of patients with uncomplicated acute myocardial infarction or infarction complicated by congestive heart failure is 4% and 15%, respectively [24, 25].

Chest X-rays as Guide to Prognosis

At present there is no accurate method of predicting which patients in LVPF supported by intraaortic balloon pumping will survive. In general, patients whose positive response to balloon pumping is rapid and sustained, eliminating the need for vasopressors and permitting gradual weaning from the balloon pump, have the best chance of survival [10, 26, 27]. If the amount of viable, contracting myocardium

is inadequate to support the circulation, patients will respond less favorably or not at all. If it is not possible to stop or substantially reduce the doses of adjunctive vasopressor drugs and if weaning from balloon support is not tolerated after 6–12 hr of pumping, then the likelihood of survival becomes remote (J. S. Krakauer, personal communication).

Sequential improvement in heart failure as assessed roentgenographically following 12–24 hr of balloon pumping is evidence which suggests that myocardial reserve is adequate. This is borne out by the markedly higher survival rate in such patients compared to those who do not undergo such improvement. Conversely, those whose chest x-rays do not improve have a small chance of survival, probably because they lack a critical volume of contracting myocardium. In patients with delayed-onset LVPF or in whom balloon pumping is delayed, the usefulness of the chest x-ray as a predictor of survival is diminished; survival rates do not rise despite the documented improvement on chest x-rays. The deleterious effects of delayed LVPF and delayed balloon pumping have been previously reported [28–30].

The ability to predict survival on the basis of chest x-ray evaluation is closely related to that based on an early positive clinical response to intraaortic balloon pumping. In seven patients who survived, the patients responded radiographically, clinically, and hemodynamically. Two papatients improved radiographically but did not respond clinically or hemodynamically and subsequently died. On the other hand, two patients responded clinically and hemodynamically but not radiographically, and after removal of the balloon pump they relapsed into LVPF and died. Two additional patients were predicted to survive on the basis of all three factors but died, in one instance of noncardiac causes. The remaining patients who died without surgery deteriorated gradually in radiographic, clinical, and hemodynamic regards despite balloon pumping.

Patients who do not exhibit rapid clinical, hemodynamic, and radiographic responses to balloon pumping should in our view be treated more aggressively. Our group as well as others [2, 16, 26, 31, 32] have reported increased survival rates in patients who undergo surgery for lesions demonstrated to be correctable at cardiac catheterization. When patients do not respond in the first 6 hr of diastolic assistance, or when weaning from balloon pumping is not completed in the first day, and if there is a lack of improvement on serial chest x-rays after 24 hr of pumping even though weaning has begun, then cardiac catheterization should be considered.

REFERENCES

1. Bialostozky D, Dorbecker N: Radiological diagnosis of left ventricular failure in acute myocardial infarction. *Arch Inst Cardiol Mex* 44:407–420, 1974
2. Bolooki H, Lemberg L, Ghahramani A, Economides C, Caldwell T, Jude JR: Clinical, surgical, and pathological correlation in patients with acute myocardial infarction and pump failure. *Circulation* 44:1034–1042, 1971
3. Grainger, RG: Interstitial pulmonary edema and its radiological diagnosis: sign of pulmonary venous and capillary hypertension. *Br J Radiol* 31:201–217, 1958
4. Harrison MO, Conte PM, Heitzman ER: Radiological detection of clinically occult cardiac failure following myocardial infarction. *Br J Radiol* 44:265–272, 1971
5. Kostuk W, Barr JW, Simon AL, Ross J: Correlations between the chest film and hemodynamics in acute myocardial infarction. *Circulation* 48:624–632, 1973
6. Lassers BW, George M, Anderton JL, Higgins MR, Philip T: Left ventricular failure in acute myocardial infarction. *Am J Cardiol* 25:511–522, 1970
7. McHugh TJ, Forrester JS, Alder L, Zion D, Swan HJC: Pulmonary vascular congestion in acute myocardial infarction; hemodynamic and radiologic correlations. *Ann Intern Med* 76:29–33, 1972
8. Tattersfield AE, McNichol MW, Shawdon H, Rolfe D: Chest x-ray film in acute myocardial infarction. *Br Med J* 3:332–335, 1969
9. Wolk MJ, Scheidt S, Killip T: Heart failure complicating acute myocardial infarction. *Circulation* 45:1125–1138, 1972
10. Cohn LH, Lamberti J, Lesch M, Collins JJ Jr: Intra-aortic balloon counterpulsation and coro-

nary revascularization for left ventricular power failure. *Eur Surg Res* 6:129–136, 1974
11. Cascade PN, Rubenfire M, Kantrowitz A: Radiographic aspects of phase-shift balloon pump. *Radiology* 103:299–302, 1972
12. Kantrowitz A, Tjønneland S, Freed PS, Phillips SJ, Butner AN, Sherman JL Jr: Initial clinical experience with intraaortic balloon pumping in cardiogenic shock. *JAMA* 203:113–118, 1968
13. Kantrowitz A, Krakauer JS, Zorzi G, Rubenfire M, Freed PS, Phillips S, Lipsius M, Titone C, Cascade P, Jaron D: Current status of intraaortic balloon pump and initial clinical experience with aortic patch mechanical auxiliary ventricle. *Transplant Proc* 3:1459–1472, 1971
14. Milne ENC: Physiological interpretation of the plain radiograph in mitral stenosis, including a review of criteria for the radiological estimation of pulmonary arterial and venous pressures. *Br J Radiol* 36:902–913, 1963
15. Milne ENC: Correlation of physiologic findings with chest roentgenology. *Radiol Clin North Am* 11:17–47, 1973
16. Ormond RS, Poznanski AK: Pulmonary veins in rheumatic heart disease. *Radiology* 74:542–549, 1960
17. Simon M: The pulmonary vessels: their hemodynamic evaluation using routine radiographs. *Radiol Clin North Am* 2:363–375, 1963
18. Stein PD, Lewison H, Potts KH: Cardiac size and left ventricular performance. *JAMA* 229: 1614–1620, 1974
19. Fluck DC, Valentine PA, Treister B, Higgs B, Reid DN, Steiner RE, Mounsey JPD: Right heart pressures in acute myocardial infarction. *Br Heart J* 29:748–757, 1967
20. Hamosh P, Cohn JN: Left ventricular function in acute myocardial infarction. *J Clin Invest* 50:523–533, 1971
21. Kirby BJ, McNichol MW, Tattersfield A: Left ventricular pressures in two patients with myocardial infarction. *Lancet* 1:944–946, 1968
22. Nixon PGF: Pulmonary edema with low left ventricular diastolic pressure in acute myocardial infarction. *Lancet* 2:146–147, 1968
23. Swan HJC, Danzig R, Sukumalchantra V, Allen H: Current status of treatment of power failure of the heart in acute myocardial infarction with drugs and blood volume replacement. *Circulation* 39–40, suppl 4:270–291, 1969
24. Scheidt S, Scheim R, Killip T III: Shock after myocardial infarction. *Am J Cardiol* 26:556–564, 1970
25. Sjogren A: Left heart failure in acute myocardial infarction. *Acta Med Scand* [*Suppl*] 510:7–22, 1970
26. Dunkman WB, Leinbach RC, Buckley MJ, Mundth ED, Kantrowitz AR, Austen WG, Sanders CA: Clinical and hemodynamic results of intraortic balloon pumping and surgery for cardiogenic shock. *Circulation* 46:465–477, 1972
27. Sanders CA, Buckley MJ, Leinbach RC, Mundth ED, Austen WG: Mechanical circulatory assistance. *Circulation* 45:1292–1313, 1972
28. Buckley MJ, Leinbach RC, Kastor JA, Laird JD, Kantrowitz AR, Madras PN, Sanders CA, Austen WG: Hemodynamic evaluation of intraaortic balloon pumping in man. *Circulation* 41–42, suppl. 2:130–136, 1970
29. Kantrowitz A, Krakauer JS, Butner AN, Freed PS, Jaron D, Rosenbaum A, Goodman PM: Phase-shift balloon pumping in cardiogenic shock. *Prog Cardiovasc Dis* 12:293–301, 1969
30. Krakauer JS, Rosenbaum A, Freed PS, Jaron D, Kantrowitz A: Clinical management ancillary to phase-shift balloon pumping in cardiogenic shock: preliminary comments. *Am J Cardiol* 27:123–128, 1971
31. Cascade PN, Wajszczuk WJ, Rubenfire M, Pursel SE, Kantrowitz A: Patient selection for cardiac surgery in left ventricular power failure. *Arch Surg* 110:1363–1367, 1975
32. Parker FB Jr, Neville JF, Hanson EL, Webb WR: Intraaortic balloon counterpulsation and cardiac surgery. *Ann Thorac Surg* 17:144–151, 1974

Am J Roentgenol 126:1155–1158, 1976

ABNORMAL LEFT VENTRICULAR CATHETER MOTION: AN ANCILLARY ANGIOGRAPHIC SIGN OF LEFT ATRIAL MYXOMA

J. M. Rausch,[1] R. T. Reinke,[1] K. L. Peterson,[2] and C. B. Higgins[1]

ABSTRACT:

The normal motion of a left ventricular catheter parallels that of the aortic root; it moves anterior during systole and posterior during diastole. In contrast, a prolapsing left atrial myxoma causes paradoxical motion of the catheter; posterior during systole and anterior during diastole. Paradoxical motion was found in each of five cases of prolapsing left atrial myxoma (no false negatives), and in six out of 61 controls (six false positives). In the false positive cases, the catheter was not positioned on the ventricular floor and usually only minor degrees of abnormal motion were present. Paradoxical motion of the left ventricular catheter is an ancillary angiographic finding in prolapsing left atrial tumor.

The initial angiographic diagnosis of a left atrial myxoma was made over 2 decades ago [1]. False positive diagnoses due to atrial thrombus [2] and false negative diagnoses due to inadequate opacification of cardiac chambers still occur [3]. A recent review of myxomas indicated that preoperative angiography failed to detect left atrial myxomas in three of 13 cases [4]. In recent years, echocardiography has greatly enhanced diagnostic potential [5, 6], but it is still imperative to angiographically confirm the diagnosis and define the anatomical relationships prior to surgical intervention. We have recently noted that the prolapsing atrial tumor may impinge on the left ventricular catheter during diastolic filling of the left ventricle and thereby provide the angiographer with an important clue to the presence of a left atrial myxoma during catheterization.

SUBJECTS AND METHODS

To assess specificity of left ventricular catheter motion in left atrial myxoma, 61 adult patients undergoing left ventricular catheterization were evaluated. Five had left atrial myxomas, 20 had coronary artery disease, and 36 had various valvular lesions (five mitral stenosis, 17 mitral insufficiency, one aortic insufficiency, and 13 multivalvular disease).

A no. 7 French Lehman catheter was used. Catheter motion was measured in the lateral projection at three points along the vertical catheter axis during end-systole and end-diastole. To avoid artifactual motion, measurements of motion were taken only after contrast injection had ceased. In addition, anterior-posterior motion of the aortic root in the lateral projection was measured in 25 patients. Any anterior catheter motion during diastole was considered to be abnormal motion.

RESULTS

In the patients without left atrial myxoma, the entire catheter moved anteriorly in systole and posteriorly in diastole (fig. 1). This movement closely approximated the movement of the aortic root. The influx of blood from the left atrium during rapid filling and during the atrial contraction had little effect on the movement of the catheter, even in patients with mitral stenosis and mitral insufficiency.

On the other hand, abnormal catheter motion was demonstrated in each patient with left atrial myxoma. This abnormal motion was characterized by posterior rather than anterior motion during systole

[1] Division of Cardiovascular Radiology, University Hospital, University of California at San Diego, and Veterans Administration Hospital, San Diego, California 92161. Address reprint requests to R. T. Reinke at the Veterans Administration Hospital.
[2] Division of Cardiology, University Hospital, University of California at San Diego.

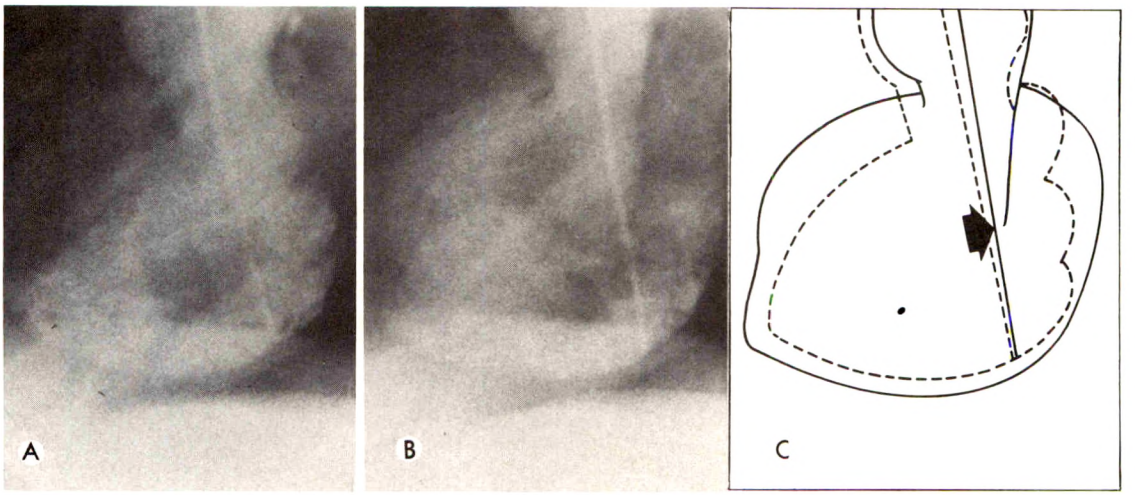


FIG. 1.—Systolic (*A*) and diastolic (*B*) frames from lateral cineangiogram of normal patient. Composite line drawing of systolic (*dashed lines*) and diastolic (*solid lines*) frames. Catheter normally moves posteriorly during diastole (*arrow*).

and anterior movement or bowing of the catheter in diastole (paradoxical motion) (fig. 2).

There were no false negative cases. Of the six false positive cases, all occurred among patients with valvular disease. Closer scrutiny of these cases indicated that the catheter was not positioned on the ventricular floor, which resulted in its apparently abnormal anterior motion in diastole. The amount of catheter motion and aortic root motion seemed to parallel the ejection fraction. Thus the false positive cases were associated with only a minor amount of abnormal catheter motion.

CASE REPORT

Case 1, a 64-year-old male (AE-603072), presented with a 1-year history of irregular heartbeat and increasing shortness of breath. He had

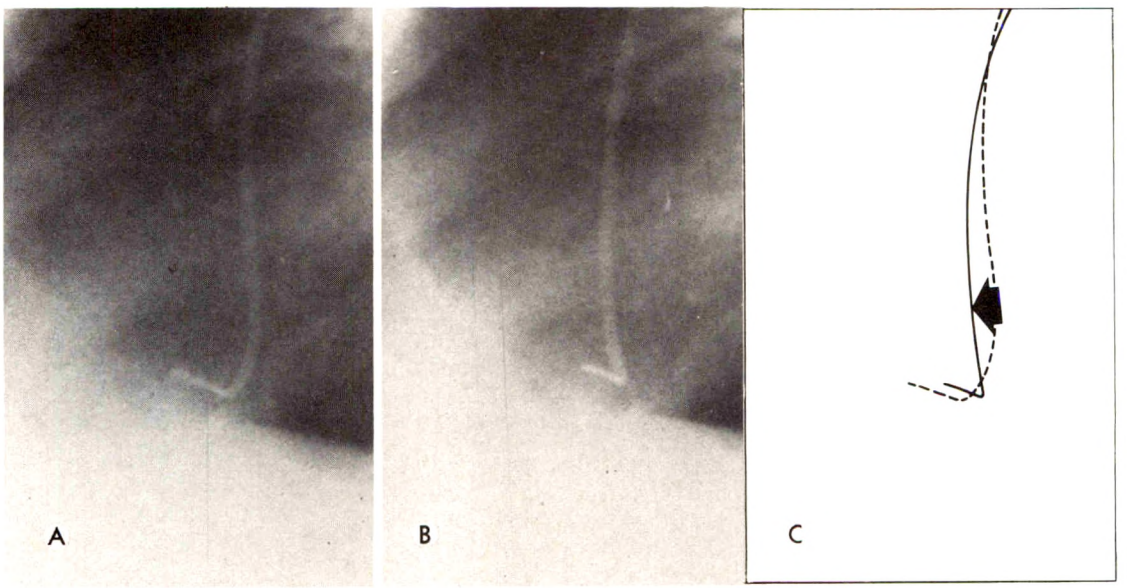


FIG. 2.—Systolic (*A*) and diastolic (*B*) frames from lateral cineangiogram of patient with left atrial myxoma. *C*, Composite line drawing of systolic (*dashed lines*) and diastolic (*solid lines*) frames. During diastole catheter moves anteriorly (*arrow*; cf. fig. 1*C*); this represents paradoxical motion of catheter.

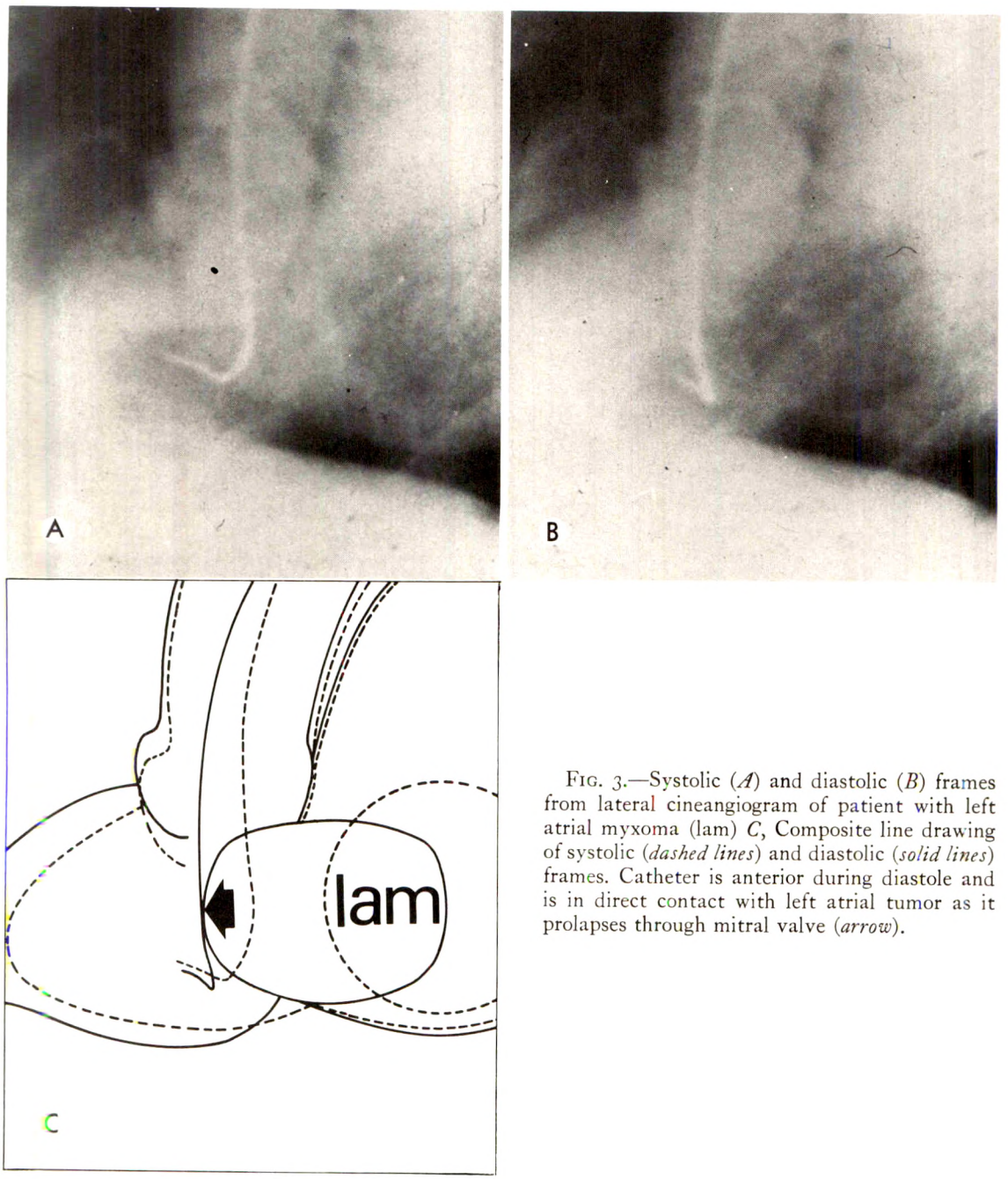


FIG. 3.—Systolic (*A*) and diastolic (*B*) frames from lateral cineangiogram of patient with left atrial myxoma (lam) *C*, Composite line drawing of systolic (*dashed lines*) and diastolic (*solid lines*) frames. Catheter is anterior during diastole and is in direct contact with left atrial tumor as it prolapses through mitral valve (*arrow*).

had three transient ischemic attacks in the previous year. On physical examination, the patient was in congestive heart failure with a mitral regurgitant murmur. A cardiac ultrasound examination was consistent with the presence of a left atrial myxoma.

Right heart catheterization revealed a mean pulmonary artery wedge pressure of 17 mm. At cineangiography, the catheter demonstrated paradoxical motion, moving posteriorly in systole and showing localized bowing anteriorly (particularly in its lower portion) during diastole (fig. 2). During left ventriculography (and after the injection had ceased), the area of anterior bowing of the catheter demonstrated proximity to the prolapsing left atrial myxoma (fig. 3). There was moderate mitral insufficiency, and a large prolapsing left atrial myxoma was demonstrated. There was no abnormal tumor vascularity at coronary angiography. At surgery, a

55 g left atrial myxoma was confirmed.

DISCUSSION

Myxomas are the most common primary cardiac tumor; 75% occur in the left atrium. Since approximately 10% of these tumors calcify, plain films may reveal calcification within the left atrium. [4] Echocardiography may reveal dense echoes originating within the left atrium, which is almost pathognomonic for a left atrial myxoma [7]. When left atrial myxoma is suggested clinically or by echocardiography, confirmatory preoperative angiography is essential. Opacification of left-side cardiac chambers after injection of contrast into the pulmonary artery usually reveals a characteristic filling defect in the left atrium. Antegrade (transeptal) catheterization for a suspected left myxoma is hazardous because of potential embolization [8]. The left atrium should therefore be visualized, preferably by pulmonary angiography [9].

However, many patients with myxoma will have an intial left ventriculogram because of the erroneous diagnosis of mitral stenosis, and the correct diagnosis may not be made in the catheterization laboratory or even later. Catheter motion analysis at this stage of the investigation process would increase the suspicion of a left atrial myxoma while the patient was still in the catheterization laboratory.

With a Lehman ventriculography catheter positioned on the left ventricular floor, the normal motion of the catheter is anterior during systole and posterior during diastole. The motion usually involves the whole catheter and is not significantly affected by the inflow of blood from the left atrium during rapid filling or atrial systole. The catheter motion probably results from aortic root motion and the fact that the catheter is "trapped" by the aortic root. The catheter motion exactly parallels the motion of the aortic root demonstrated by echocardiography.

In contrast, a prolapsing myxoma pushes a portion of the catheter forward during diastole. As the tumor returns toward the atrial cavity, the ventricular catheter moves posteriorly. This paradoxical motion was found in each of the five cases in the current report and thus provides an ancillary sign of a prolapsing mass. It must be emphasized that the ventricular catheter should be well seated on the ventricular floor. False positive anterior diastolic movement can be caused by the unseated catheter and also if the tip of the catheter is located high under the posterior mitral valve leaflet.

A prolapsing atrial myxoma may produce only minimal mitral regurgitation when a left ventriculogram is performed. However, if paradoxical catheter displacement is observed at the time of catheterization, myxoma should be immediately suspected. Pulmonary angiography should be performed to confirm the diagnosis. In summary, abnormal motion of a portion of the left ventricular catheter is a useful ancillary angiographic finding in a prolapsing atrial tumor.

ACKNOWLEDGMENT

We express our appreciation to Mrs. Marge Billman for her assistance in preparation of the manuscript.

REFERENCES

1. Goldberg HP, Glenn F, Dotter CT, Steinberg I: Myxoma of the left atrium: diagnosis made during life with operative and post-mortem findings. *Circulation* 6:762–767, 1952
2. Goodwin JF: Diagnosis of left atrial myxoma. *Lancet* 1:464–467, 1963
3. Aldridge HE, Greenwood WF: Myxoma of the left atrium. *Br Heart J* 22:189–200, 1960
4. Peters MN, Hall RJ, Cooley DA, Leachman RD, Garcia E: The clinical syndrome of atrial myxoma. *JAMA* 230:695–701, 1974
5. Bass NM, Sharratt GP: Left atrial myxoma diagnosed by echocardiography with observations on tumour movement. *Br Heart J* 35:1332–1335, 1973
6. Martinez EC, Giles TD, Burch GE: Echocardiographic diagnosis of left atrial myxoma. *Am J Cardiol* 33:281–285, 1974
7. Feigenbaum H, Chang S: *Echocardiography*. Philadelphia, Lea & Febiger, 1972
8. Marpole DG, Kloster FE, Bristow JD, Griswold HE: Atrial myxoma, a continuing diagnostic challenge. *Am J Cardiol* 23:597–601, 1969
9. Steiner RE: Radiologic aspects of cardiac tumors. *Am J Cardiol* 21:344–355, 1968

Am J Roentgenol 126:1159–1163, 1976

EVALUATION OF ROUTINE DOUBLE CONTRAST VIEWS OF THE ANTERIOR WALL OF THE STOMACH

MARTIN R. GOLDSMITH,[1] ROBERT E. PAUL, JR., WILLIAM E. POPLACK, JEFFERY P. MOORE, HIROTO MATSUE,[2] AND STEPHEN BLOOM

ABSTRACT:

Since June 1974, we have performed over 1,500 consecutive double contrast upper gastrointestinal examinations. The double contrast study of the anterior wall has been a useful adjunct to conventional mucosal relief and dosed compression studies. Nevertheless, the low diagnostic yield of the anterior wall examination does not appear to justify including it as part of the routine double contrast upper gastrointestinal study.

Recent papers published in the United States on the double contrast upper gastrointestinal examination have not emphasized that separate study of the anterior and posterior walls of the stomach can be achieved utilizing this technique [1–3]. On the other hand, Japanese researchers have stressed the importance of separate study of the anterior and posterior gastric walls [4, 5]. In an attempt to evaluate the usefulness of the anterior wall examination, we performed such examinations routinely as part of the double contrast upper GI series in over 1,500 consecutive patients.

MATERIALS AND METHODS

The technique utilized for the double contrast examination of the anterior wall has been reported [4]. Gastric relaxation is achieved by intravenous administration of 0.25–0.50 mg of Glucagon [6]. The erect patient is given 20–30 cm^3 of barium.* (Larger amounts will produce pooling when the patient is prone and should therefore be avoided.) Air insufflation is provided by gas-releasing granules to distend the fundus in the upright position to approximately the size of an orange. The table is then lowered to the horizontal position and the patient turned prone. Coating of the anterior wall is achieved by rotating the patient back and forth into high degrees of obliquity dictated by the shape and position of the stomach. Low kilovoltage (80–100 kV) spot films can now be obtained.

Antrum. The prone patient is placed in a 15° Trendelenburg position with the right side elevated. A small soft pillow is placed under the left side to prevent excess barium from pooling in the antrum. The patient is then slowly rotated to a flat, face-down position until the antrum is no longer superimposed on the body. The spot film of the anterior wall of the antrum is then taken (fig. 1).

Body. The table is elevated until gaseous distension of the body is achieved. A small soft pillow positioned over the antrum helps in obtaining optimal distension of the body (fig. 2).

With experience, the fluoroscopic time neces-



FIG. 1.—Normal double contrast anterior wall view of antrum.

[1] All authors: Department of Diagnostic Radiology, Tufts–New England Medical Center Hospital, Boston, Massachusetts 02111.
[2] Visiting Professor from the National Cancer Center Hospital, Tokyo, Japan.

* E-Z-EM high density (65% wt/wt) or Lafayette HD200 (60% wt/wt) with ½ teaspoon DOW-Corning Antifoam C emulsion added per 200 cm^3 of barium.

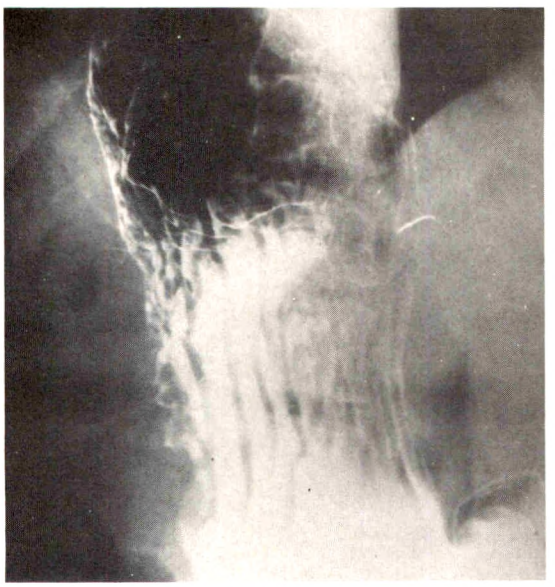


FIG. 2.—Normal double contrast anterior wall view of body.

sary to properly demonstrate the anterior wall will be less than 1 min. After obtaining the anterior wall views, the patient is turned supine and then erect. Additional barium is given to a total of 200 cm^3, and double contrast views of the posterior wall are then obtained in the usual manner [4].

DISCUSSION

In approximately 1,500 consecutive cases of double contrast upper gastrointestinal examinations, we detected 105 gastric ulcers. Locations of these ulcers are shown in table 1. Since only 4% were detected on the anterior wall and since some of these could be suspected on routine posterior wall views, there is serious question as to whether routine anterior wall views are necessary for the detection of gastric ulcers. We had only two cases in which gastric ulcers were seen exclusively on anterior wall views (figs. 3 and 4).

TABLE 1

LOCATION OF GASTRIC ULCERS

Location	No.
Lesser curvature	47
Greater curvature	12
Anterior wall	4
Posterior wall	42
Total	105

We detected 11 gastric carcinomas in our series, but all of these were fairly large lesions and were diagnosable on the posterior wall views. Shirakabe et al. [5] reported the diagnosis of 84 *early* gastric cancers in the period 1954–1965; 21% were limited to the anterior wall. Nevertheless, as they note,

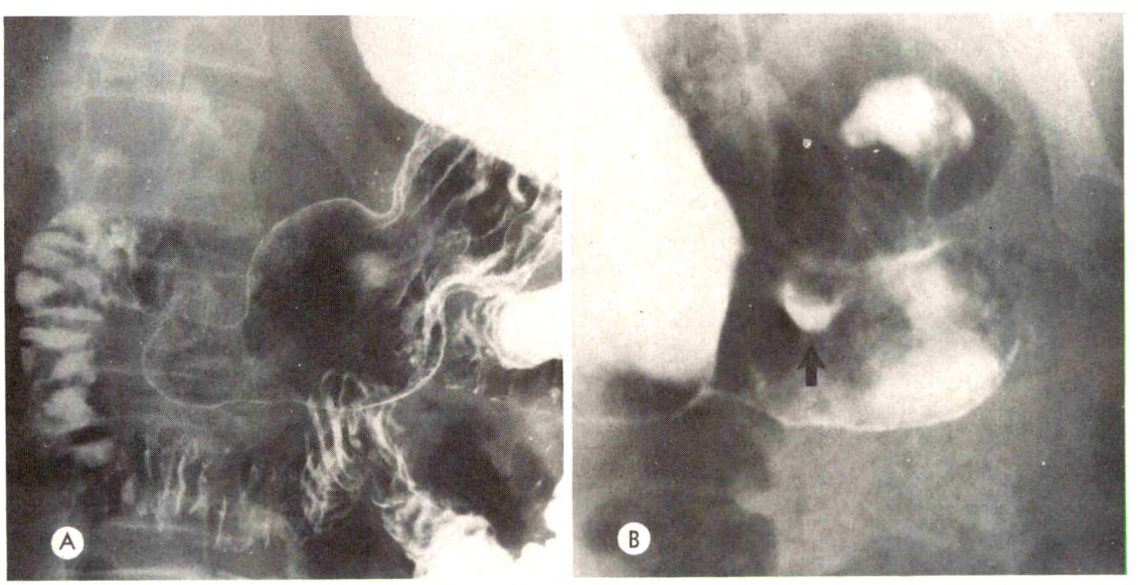


FIG. 3.—*A*, Normal supine double contrast view. *B*, Double contrast anterior wall view of antrum of same case showing 10×5 mm gastric ulcer (*arrow*). It was confirmed at endoscopy.

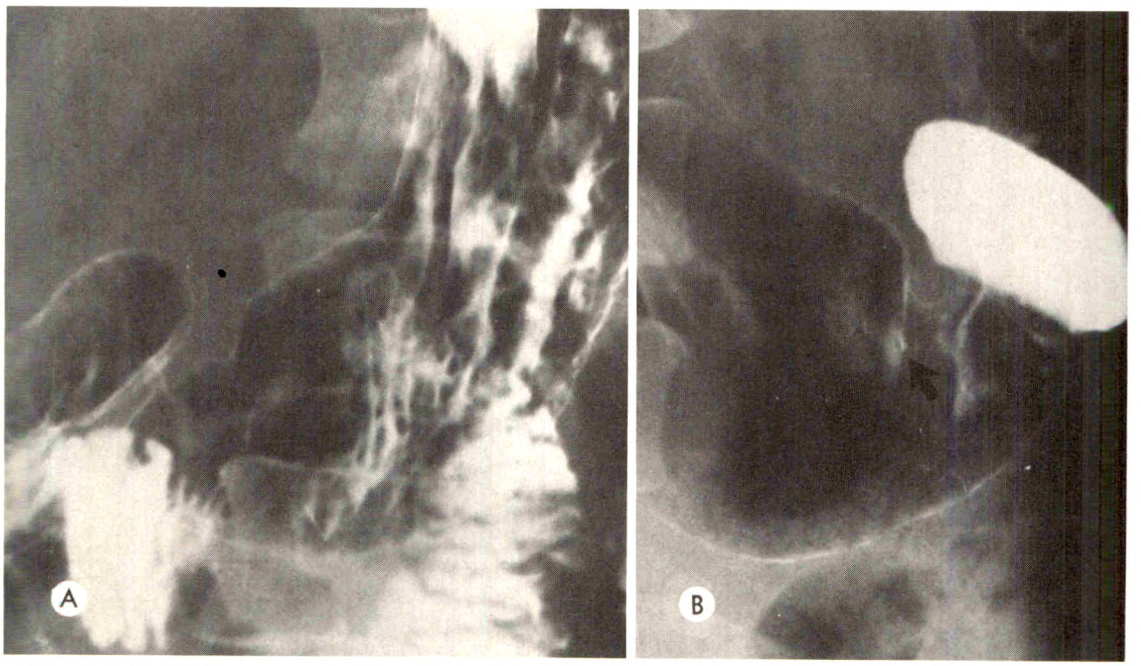


FIG. 4.—*A*, Double contrast supine view of the antrum; no ulcer evident. *B*, Double contrast anterior wall view of same case demonstrating 4 mm ulcer (*arrow*). At endoscopy 1 week later, scarring of anterior wall seen corresponding to site of radiographic demonstration of ulcer.

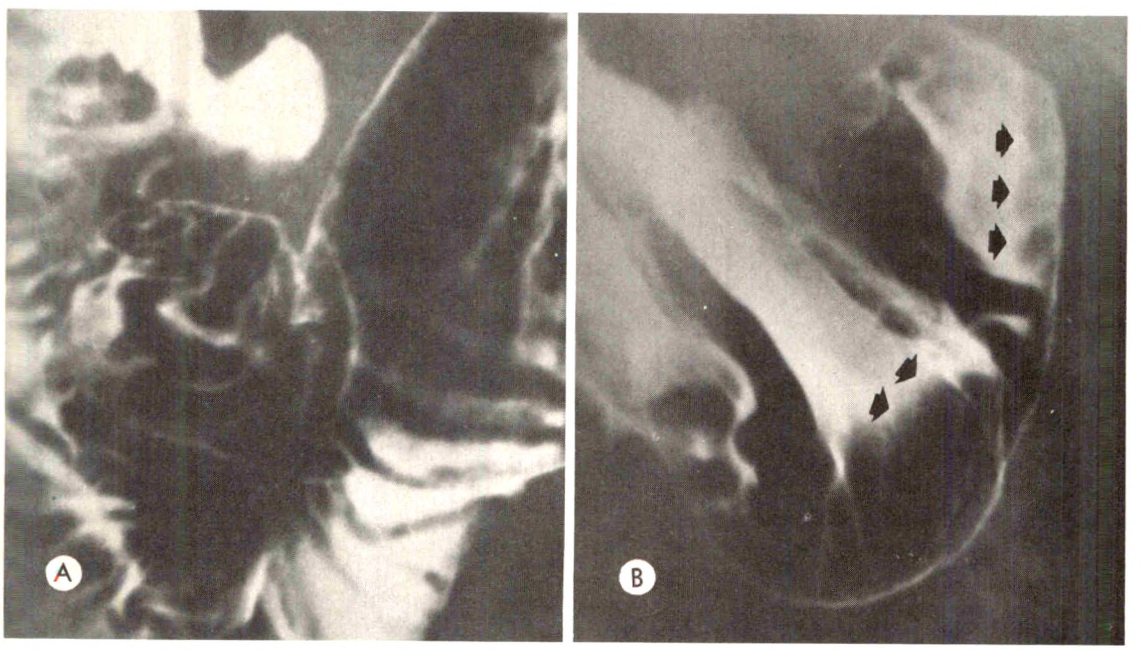


FIG. 5.—*A*, Supine double contrast view of antrum demonstrating prominent gastric folds. *B*, Anterior wall view of same case demonstrating groups of nodules with central erosions (*arrows*) characteristic of erosive gastritis [8].

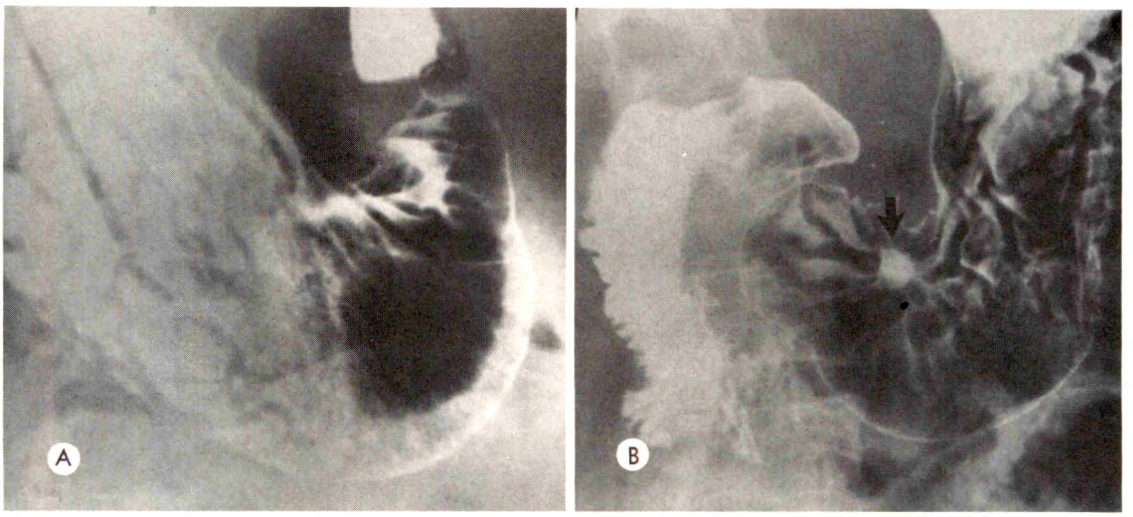


FIG. 6.—*A*, Normal double contrast anterior wall view. *B*, Supine double contrast view of same case demonstrating 1 cm gastric ulcer (*arrow*).

anterior wall pathology can be suspected on posterior wall views.

In our series, positive cases other than gastric carcinoma or ulcers (e.g. polyps, scars, erosive gastritis) were usually adequately detected on posterior wall views [7]. In two cases, however, erosive gastritis was best demonstrated on the anterior wall views. One of these is shown in figure 5.

That the double contrast examination allows separate examination of the anterior and posterior gastric walls is not being challenged. In fact, this point is nicely demonstrated in figure 6, where a large *posterior* wall ulcer cannot be diagnosed on proper *anterior* wall views. Nevertheless, since only four of 140 positive cases would have been missed without anterior wall views, the necessity for including anterior wall views in the routine examination is doubtful.

On the basis of our analysis and experience thus far, it would appear that including views of the anterior wall with their attendant added fluoroscopy time and patient exposure is not necessary to the performance of the proper double contrast examination in this country. In Japan, where the death rate from gastric carcinoma is eight times that in the United States and is the leading cancer in Japanese males, every technique for the detection of early gastric cancer would seem justified [9].

We recommend that the anterior wall study be reserved for patients with strongly suspected gastric pathology clinically whose routine double contrast examination proves negative, or for those patients who are a priori thought highly likely to have gastric pathology on clinical grounds. It could also be utilized to reexamine an area of abnormality suspected on routine posterior wall examination but thought to lie on the anterior wall.

Although the double contrast anterior wall examination of the stomach is useful in specific instances, including it as a part of the routine double contrast upper gastrointestinal examination does not appear warranted on the basis of our experience to date.

REFERENCES

1. Kawai K, et al: Double contrast radiograph on routine examination of stomach. *Am J Gastroenterol* 53:147–153, 1970
2. Kreel L, Herlinger H, Glanville J: Technique of the double contrast barium meal with examples of correlation with endoscopy. *Clin Radiol* 24: 307–314, 1973

3. Obata WG: Double contrast technique for examination of the stomach using barium sulfate with simethicone. *Am J Roentgenol* 115:275–280, 1973
4. Shirakabe H (ed): *Double Contrast Studies of the Stomach*. Tokyo, Bunkodo Co., Ltd., 1971
5. Shirakabe H, Ichikawa H, Kumakura K, Nishizawa M. Higurashi K, Hayakawa H, Murakami T: *Atlas of X-ray Diagnosis of Early Gastric Cancer*. Tokyo, Igaku Shoin Ltd., 1966
6. Miller RE, Chernish SM, Skucas J, Roscnak BD, Rodda BE: Hypotonic roentgenography with glucagon. *Am J Roentgenol* 121:264–274, 1974
7. Paul R, Poplack W, Goldsmith M, Moore J, Matsue H, Norton R: Evaluation of routine double contrast examination of upper gastrointestinal tract. In preparation
8. Poplack W, Paul R, Goldsmith M, Matsue H, Moore J, Norton R: The demonstration of erosive gastritis by the double contrast technique. *Radiology* 117:519–521, 1975
9. World Health Organization: World health statistics: annual report, 1968–1969. Cancer 25:16–17, 1975

Am J Roentgenol 126:1164–1168, 1976

INTUSSUSCEPTION OF THE APPENDIX IN CHILDREN

GEORGE O. ATKINSON,[1] BRIT B. GAY, JR.,[1] AND DARIUS NAFFIS[2]

ABSTRACT:

Intussusception of the appendix is uncommon and an unusual cause of ileocolic intussusception. The pediatric age group is most often affected. Appendiceal intussusception may present as primary appendiceal invagination but more commonly leads to secondary intussusception. Two cases of partial appendiceal intussusception leading to secondary intussusception are presented. Classification, symptomatology, radiographic appearance, and differential diagnosis are discussed.

Intussusception of the appendix is an unusual cause of ileocolic intussusception. The diagnosis is rarely made prior to surgery. Although a review of the literature reveals only about 140 cases of intussusception of the appendix, two cases leading to ileocolic intussusception were seen at the Henrietta Egleston Hospital for Children within a 2 month period. Experience gained from the first case led to the correct diagnosis preoperatively in the second case. This report summarizes the two cases and presents a brief review of the literature.

CASE REPORTS

Case 1

A 2½-year-old white female was admitted to Henrietta Egleston Hospital on June 27, 1974, with a 1 month history of daily cramping and intermittent abdominal pain. Three weeks before admission she was treated for constipation with an enema, and a marked increase in pain with vomiting developed 3 days prior to admission. There was no history of blood in the stools. Prior to transfer to Henrietta Egleston Hospital, a barium enema at another hospital revealed an intussusception which could not be reduced.

Physical examination revealed dehydration, right lower quadrant abdominal tenderness, but no mass. On repeat barium enema examination, ileocolic intussusception was reduced to the cecum where there was free reflux of barium into the terminal ileum. A lobular filling defect persisted in the base of the cecum, and no appendiceal filling was seen (fig. 1). The filling defect at the base of the cecum persisted on repeat filling of the colon.

At surgery total inversion of the appendix was present and could not be reduced. The mesoappendix was divided and ligated. After further inverting the base of the appendix into the cecum, the base was closed by encircling sutures. The patient did well following surgery and was discharged 3 days later without complications.

Case 2

This 4½-year-old white female had onset of intermittent cramping pain and vomiting 3 weeks prior to admission. There was occasional diarrhea, but no blood in the stools. On physical examination there was no abdominal tenderness or palpable mass.

Roentgenograms of the abdomen revealed a soft tissue mass in the region of the transverse colon, suggesting an intussusception. On barium enema examination, an intussusception was readily reduced to the cecum, with reflux of contrast into the terminal ileum. A persistent filling defect was seen at the base of the cecum with absence of appendiceal filling. Appendiceal intussusception was suspected roentgenographically (fig. 2).

At surgery a partially inverted appendix was found with several enlarged lymph nodes showing benign inflammatory change pathologically. The intussuscepted appendix could not be reduced. A right hemicolectomy was performed with an end-to-end anastomosis between distal ileum and ascending colon. During exploration

[1] Department of Radiology, Emory University School of Medicine, and Henrietta Egleston Hospital for Children, Atlanta, Georgia 30322.

[2] Surgical Service, Henrietta Egleston Hospital for Children, Atlanta, Georgia 30322.

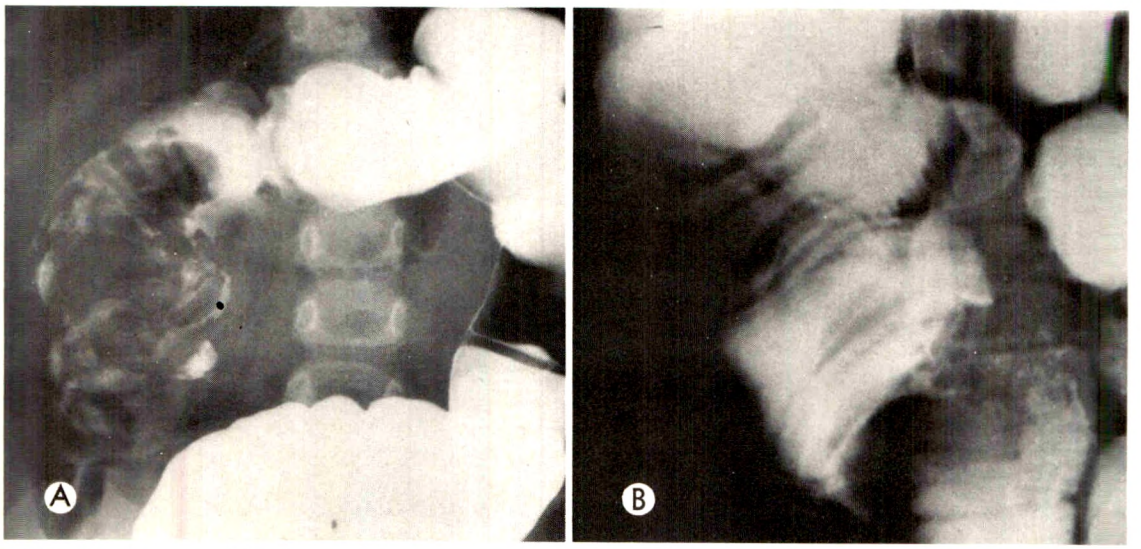


FIG. 1.—Case 1. *A*, Barium enema examination revealing filling defect in ascending colon representing an ileocecal intussusception. *B*, Persistent filling defect at base of cecum with no appendiceal filling after reduction of ileocecal intussusception and reflux of barium into ileum.

a Meckel's diverticulum was found and removed. There were no complications. The final pathology report revealed focal ulceration and acute inflammation of the inverted appendiceal surface, lymphoid hyperplasia, and subacute inflammatory changes (fig. 3).

DISCUSSION

Approximately 140 cases of intussusception of the appendix have been reported, more than half in children below the age of 10 [1–3]. Only three cases have been reported in children younger than 2½ years: these were girls 16, 17, and 10 months of age [3–5]. The average age of occurrence is 16 years, with the oldest reported case in a 75-year-old patient [2]. As in intussusception in general, intussusception of the appendix is four to five times more frequent in males than females [2, 3, 6].

Of 66 patients with intussusception seen in this department since January 1963, 10 have had organic causes: two patients had lymphoma of the distal ileum, six had Meckel's diverticulum, and two (present cases) had intussusception of the appendix. One of these latter patients also had a Meckel's diverticulum. Both patients were older than the average patient with uncomplicated intussusception. Abdominal symptoms in both patients were intermittent and present 3–4 weeks prior to admission, which is consistent with other reported cases.

The etiology of most appendiceal intussusceptions is unknown; however, certain predisposing conditions are thought to make intussusception more likely. Most workers theorize that abnormal appendiceal peristalsis secondary to local irritation is the chief factor. Local irritants such as worms, fecaliths, foreign bodies, polyps, hypertrophic lymphoid follicles, mucoceles, endometrial implants, and postinflammatory scars have been implicated. [1–8]. A fetal type of cecum with the appendix originating from its tip has also been suggested as an etiological factor, particularly if the proximal lumen of the appendix has a much greater diameter than the distal lumen [2, 3, 6].

Appendiceal intussusceptions have been classified as primary and compound or secondary (fig. 4) [3]. Of the five types of primary intussusception, only partial invagination of the base of the appendix into the cecum and complete invagination of the appendix into the cecum have been

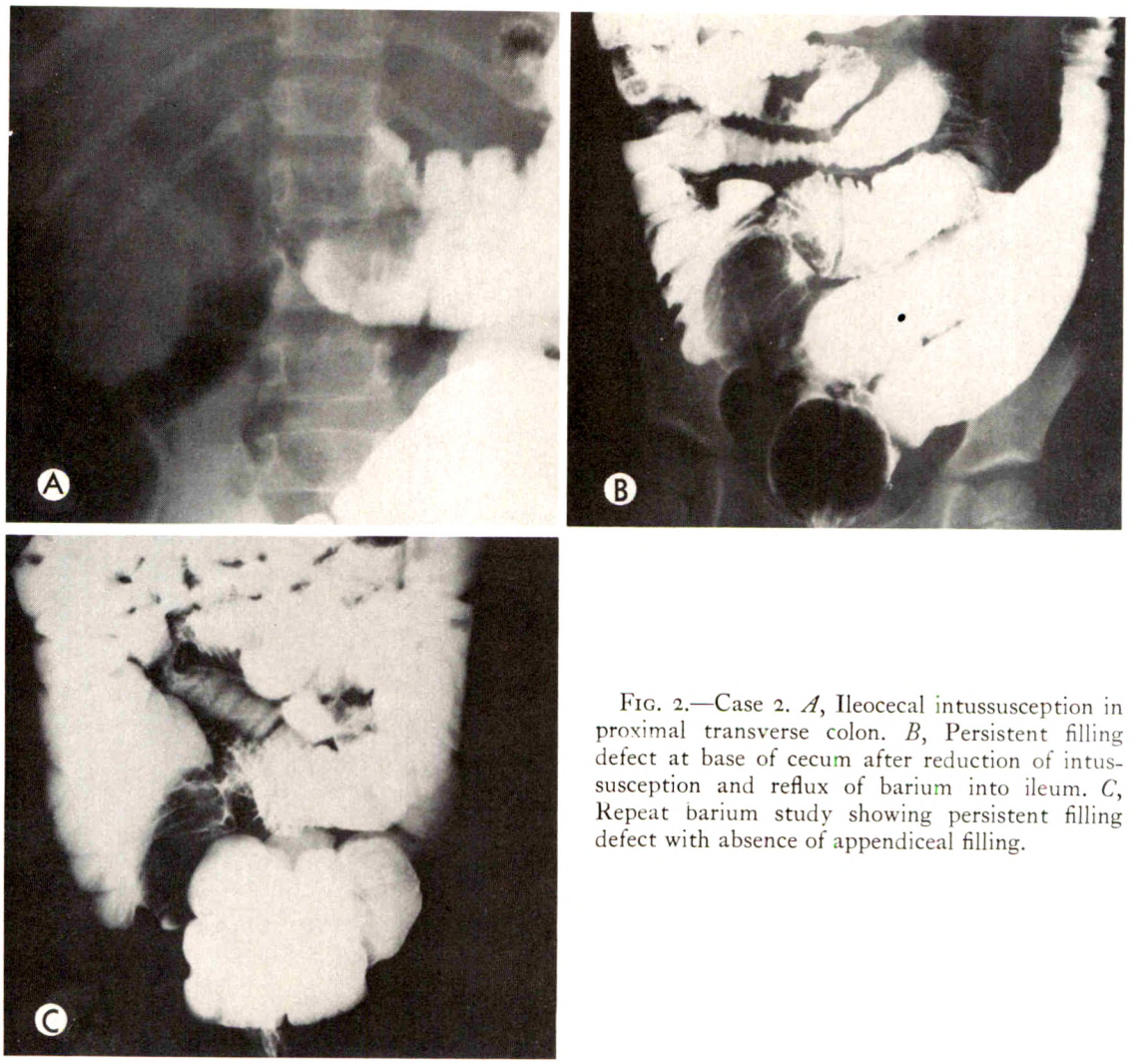


FIG. 2.—Case 2. *A*, Ileocecal intussusception in proximal transverse colon. *B*, Persistent filling defect at base of cecum after reduction of intussusception and reflux of barium into ileum. *C*, Repeat barium study showing persistent filling defect with absence of appendiceal filling.

demonstrated roentgenographically [1]. Partial invagination of the appendix into the cecum is by far the most common type [1–3].

All types of primary appendiceal intussusception, possibly with the exception of type D, can initiate a secondary intussusception. In over half the recorded cases, a secondary intussusception was found at surgery. The question of whether the intussuscepted appendix initiates a secondary intussusception presumably depends upon both the degree of irritation that the appendix causes by its presence inside the cecum and the anatomy of the cecum. A fixed cecum is unlikely to intussuscept, whereas a mobile cecum with a rotational anomaly may be more likely to produce intussusception [2, 3, 6].

Symptoms have classically been divided into four groups. In the first group, onset is acute as in acute appendicitis. These cases are frequently taken to surgery with the diagnosis of acute appendicitis. At operation partial or complete intussusception of the appendix is found [2, 3, 6, 8].

In the second group, the symptoms are consistent with intussusception. Abdominal pain and vomiting usually occur for several days. Bowel movements may be normal. Less commonly there may be constipation, diarrhea, or melena. Examination fre-

quently reveals an abdominal mass which is recognized as an intussusception. These cases have a compound intussusception, and the appendiceal invagination is discovered only after the main intussusception has been reduced either at surgery or by barium enema examination [2, 3, 6, 8].

A third group includes cases with a prolonged history of repeated intermittent severe attacks of right lower quadrant abdominal pain. Vomiting and melena may be present. The interval between the attacks is quite variable. Physical examination between attacks is unrevealing. The acute pain can be due to intermittent secondary intussusception which follows intussusception of the appendix. A child with a history of multiple attacks of intermittent abdominal pain, even if he appears perfectly well, deserves a barium enema examination with the possibility of primary appendiceal intussusception considered in the differential diagnosis [2, 3, 6, 7].

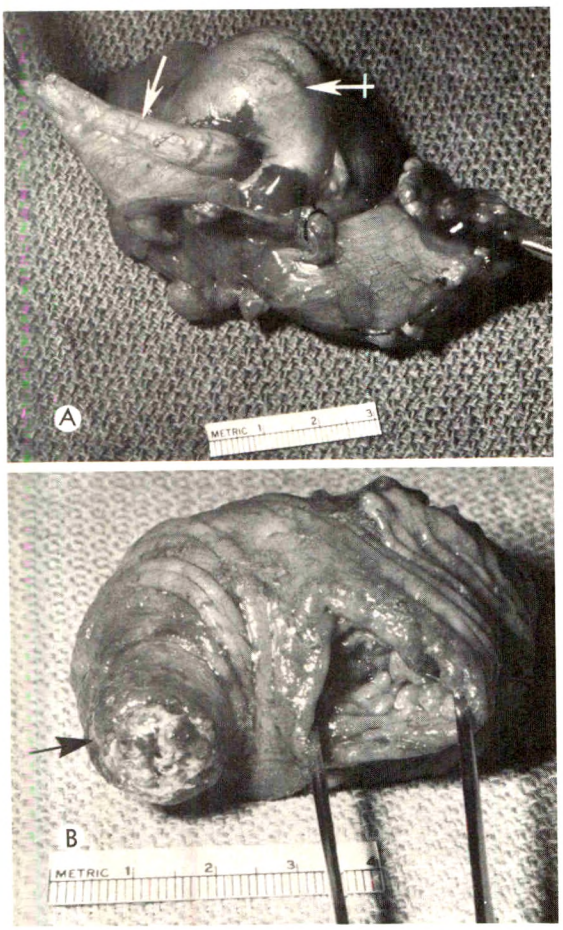


FIG. 3.—Gross specimen of case 2. *A*, Partial invagination of appendix into base of cecum with resultant mass. Hatched arrow points to cecum; arrow points to appendix invaginated into cecum. Forceps holds ascending colon right and distal appendix left. *B*, Opened cecum showing partially invaginated appendix within. Arrow points to invaginated appendix. Forceps opens ileocecal valve.

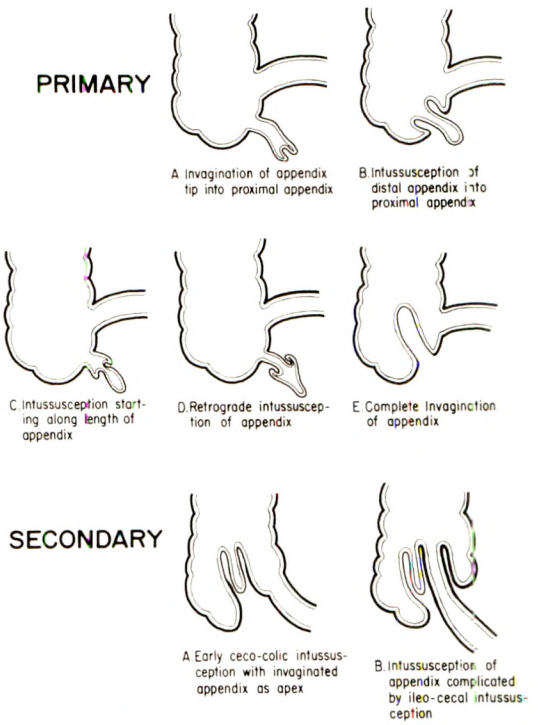


FIG. 4.—Schematic portrayal of types of appendiceal intussusception.

There is a fourth group in which primary appendiceal intussusception is asymptomatic. There have been nine reported cases, but none were in the pediatric age group [1, 5, 9, 10].

Brewer and Wangenstein [11] suggest a fifth group in which intermittent bleeding is found in otherwise asymptomatic patients. They report one case of their own and describe four others from the literature. One of these was in the pediatric age group, a 13-year-old male with a 1 month history of rectal bleeding [9].

Roentgenograms of the abdomen are un-

remarkable unless a secondary intussusception has occurred. Only partial and complete appendiceal intussusception (fig. 4, *B* and *E*, respectively) have been demonstrated by barium enema [1]. Partial appendiceal invagination appears on barium enema as an oval or round intraluminal filling defect presenting at the usual site of origin of the appendix with nonfilling of the appendix. Complete invagination of the appendix presents as a fingerlike intraluminal filling defect in the cecum arising at the usual site of the appendix. This latter appearance has been reported as pathognomonic [1, 13]. If a compound intussusception has occurred, the appendiceal intussusception will not be discovered until the secondary intussusception has been reduced and the persistent filling defect identified [1, 6, 7, 13].

In only four cases has reduction of a primary appendiceal invagination been demonstrated roentgenographically [1]. In two of these patients the normal appendices were seen to partially invaginate and the lumen completely reduce during the course of the same barium enema study. In the other two, a filling defect in the cecum at the site of the expected location of the nonvisualized appendix was seen on the initial barium enema examination. A repeat study showed a normal cecum and filling of a normal appendix. All four patients were over 50 years of age and asymptomatic. There have been no reports of reduction of a primary appendiceal intussusception by barium enema in a pediatric patient.

To differentiate appendiceal intussusception from other causes of cecal filling defects, an attempt should be made to fill the appendix and, if it cannot be visualized, to determine if the lesion is located at the expected site of appendiceal origin. Filling of the appendix excludes appendiceal intussusception. If the appendix does not fill with contrast, a positive differentiation between irreducible appendiceal intussusception, masses of appendiceal origin, or cecal masses cannot be made [1, 10].

Differential diagnosis includes appendiceal abscess, duplication cyst, and inverted appendiceal stump. Of the malignant tumors, lymphoma is most common. Carcinoma and carcinoid are unusual in the pediatric age group. Benign tumors including lipoma, leiomyoma, fibroma, and hemangioma are uncommon. Mucoceles of the appendix are more common in females and occur at a later age [4, 5, 7–9, 12].

ACKNOWLEDGMENT

We are indebted to Dr. H. Gibbs Andrews for supplying the surgical findings in case 1 of this report.

REFERENCES

1. Bachman AL, Clemett AR: Roentgen aspects of primary appendiceal intussusception. *Radiology* 101:531–538, 1971
2. Fink JH, Santos AL, Goldberg SL: Intussusception of the appendix: case reports and reviews of the literature. *Am J Gastroenterol* 42:431–441, 1964
3. Forshall I: Intussusception of the vermiform appendix with a report of seven cases in children. *Br J Surg* 40:305–312, 1953
4. Mitchell RG: Intussusception of vermiform appendix in allergic children. *Br Med J* 1:265–266, 1955
5. Paul GJ, Ferraro LR: Intussusception of appendix. *NY State J Med* 67:2625–2629, 1963
6. Fraser K: Intussusception of the appendix. *Br J Surg* 31:23–33, 1943
7. Banerjee AK, MacPherson RI: A cecal mass in a five year old child—a case for diagnosis. *J Can Assoc Radiol* 22:187–190, 1971
8. Schmidt FR, McCarthy JD: Intussusception of the appendix with endometriosis presenting as a cecal tumor. *Arch Surg* 103:515–517, 1971
9. Day WA: Appendiceal intussusception simulating cecal tumor: case report. *Dis Colon Rectum* 6:118–120, 1963
10. DeGerome JH, Rodriguez HP: Primary appendiceal intussusception. *Am J Dig Dis* 18:704–708, 1973
11. Brewer RJ, Wangenstein SL: Appendiceal intussusception: an unusual cause of painless rectal bleeding. *Am Surg* 4:319–320, 1974
12. Meyers MA, Abrams J: Intussusception of the appendix. *Br J Radiol* 43:485–486, 1970
13. Hill J, Schmidt KD, Economous SG: The "inside-out" appendix: a review of the literature and report of two cases. *Radiology* 95:613–617, 1970

Am J Roentgenol 126:1169–1174, 1976

PLAIN FILM FINDINGS OF GASTRIC VOLVULUS HERNIATING INTO THE CHEST

LESLIE MENUCK[1]

ABSTRACT:

When confronted with a chest radiograph demonstrating two large air-fluid levels, one in the retrocardiac mediastinum and the other beneath the left hemidiaphragm, the possibility of gastric volvulus herniating into the thorax should be strongly considered. These patients should have an immediate contrast study for further evaluation.

Acute obstructing gastric volvulus herniating into the chest is a life-threatening situation due to impairment of the blood supply to the stomach and the danger of aspiration. The radiographic features are specific early in the course, allowing prompt diagnosis at a time when the clinical symptoms and findings may still be quite vague. The characteristic plain film findings of two large air-fluid levels, one beneath the left hemidiaphragm and the other in the retrocardiac mediastinum, demand an immediate contrast examination for definitive diagnosis.

CASE REPORTS

Case 1

A 64-year-old man had a 3 year history of vague intermittent dull pain and fullness in the epigastrium. In December 1972, a gastrointestinal exam demonstrated a small sliding esophageal hiatus hernia. In April 1973, he experienced sudden onset of dull, aching chest pain, intermittent nausea, and vomiting which resolved 1 day later. A chest roentgenogram at that time showed two large air-fluid levels, one in the retrocardiac mediastinum and the other beneath the left hemidiaphragm. On November 30, 1973, he returned with recurrence of his previous symptoms. A repeat chest radiograph again demonstrated the two large air-fluid levels (fig. 1). On December 9, 1973, he became acutely ill with severe chest pain, intermittent vomiting, diaphoresis, and hypotension. An upper gastrointestinal examination showed the distal esophagus displaced by a homogenous soft tissue mass, with the esophagogastric junction beneath the left hemidiaphragm. An obstructing gastric volvulus demonstrated a "beak" extending upward toward the esophageal hiatus, though no barium passed distally into it (fig. 2). The patient was immediately taken to the operating room where a gastric volvulus was found. The distal half of the obstructed, twisted stomach had passed through the esophageal hiatus into a retrocardiac position within the mediastinum. The antrum was resected because of gangrene. Postoperatively, the patient did well.

Case 2

A 61-year-old man had nausea, vomiting, and nonspecific chest and abdominal pain of 1 week's duration. He had previously experienced similar symptoms which regressed spontaneously. Admission chest roentgenogram (November 24, 1974) showed two large air-fluid levels, leading to a presumptive diagnosis of gastric volvulus with herniation of the distal stomach into the chest (figs. 3*A* and 3*B*). Two days later a repeat chest radiograph showed an additional air-containing structure in the left hemithorax (fig. 3*C*). An upper gastrointestinal exam demonstrated a large paraesophageal hiatus hernia of the proximal stomach and an associated gastric volvulus of the distal stomach. The esophagogastric junction was in a normal position. The rotated distal stomach extended through the esophageal hiatus and occupied a retrocardiac position. Barium passed through the inlet of the twisted segment to fill the distal stomach. The outlet of the rotated antrum was obstructed as it reentered the abdomen through the esophageal hiatus (fig. 4). Surgery confirmed the findings of a proximal large para-

[1] Department of Radiology, University Hospital, University of California at San Diego, and Veterans Administration Hospital, San Diego, California 92161

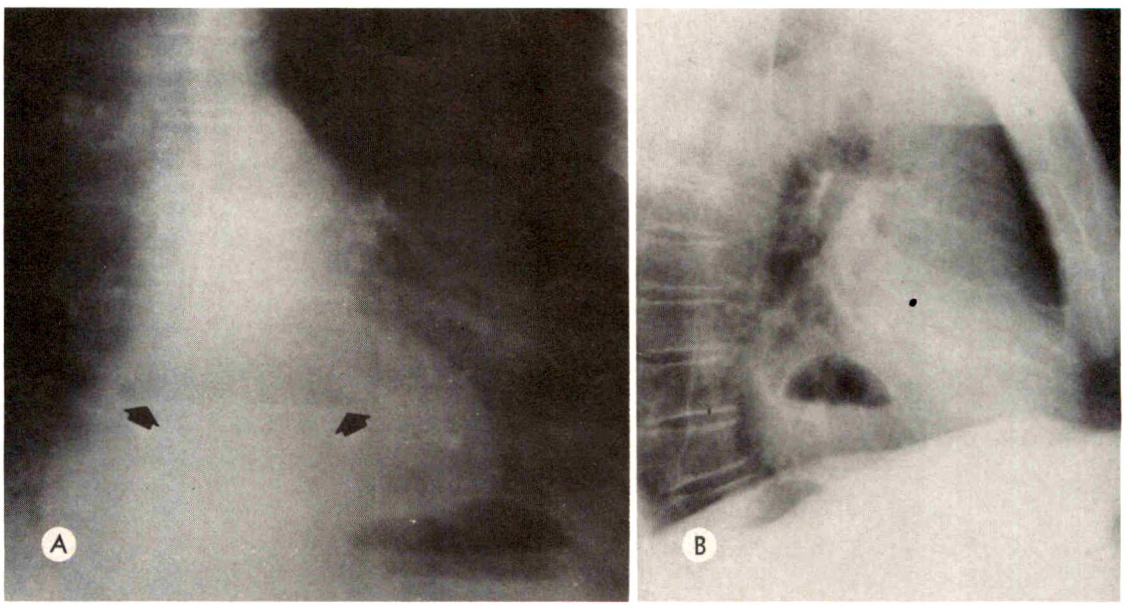


FIG. 1.—Chest radiographs of case 1 demonstrating two large air-fluid levels, one beneath left hemidiaphragm and other in retrocardiac mediastinum (best seen on lateral exam).

esophageal hiatus hernia with distal gastric volvulus. Both the inlet and outlet of the volvulus passed through the esophageal hiatus. Gangrenous changes had not occurred, and gastric resection was not necessary.

DISCUSSION

Gastric volvulus is not a rare phenomenon. Several types are recognized (table 1). Over 265 cases have been reported; at least two-thirds are of the chronic or recurring type [1]. Volvulus of the stomach can only occur when there is an abnormality in the laxity or the length of the gastric suspensory ligaments. The chance of this occurring increases with a cascade gastric configuration or an atonic, dilated, fluid-filled stomach [2].



FIG. 2.—Contrast barium study of case 1 showing "beak" with complete obstruction at inlet of gastric volvulus as it herniates into chest.

Most cases of gastric volvulus occur in association with eventration of the left hemidiaphragm or a hiatus hernia. In a review of 500 autopsies of patients with hiatus hernia, Payer [3] found 12 cases of partial gastric volvulus. Da Costa [4] stated that one-third of the cases of gastric volvulus were associated with diaphragmatic hernia. Where volvulus is associated with an esophageal hiatus hernia, the twisted distal gastric antrum may be drawn up into the chest as an associated paraesophageal component [5]. The mixed and organoaxial type of volvulus tend more frequently to herniate, while the mesenteroaxial tend to be associated with eventration.

Acute gastric volvulus is a life-threatening situation necessitating immediate surgical intervention [6–8]. Many of the acute cases of volvulus occur in patients with chronic recurring gastric volvulus, since the past history is highly suggestive of mild, repetitive episodes [5, 8, 9, 10]. The clinical manifestations of gastric volvulus

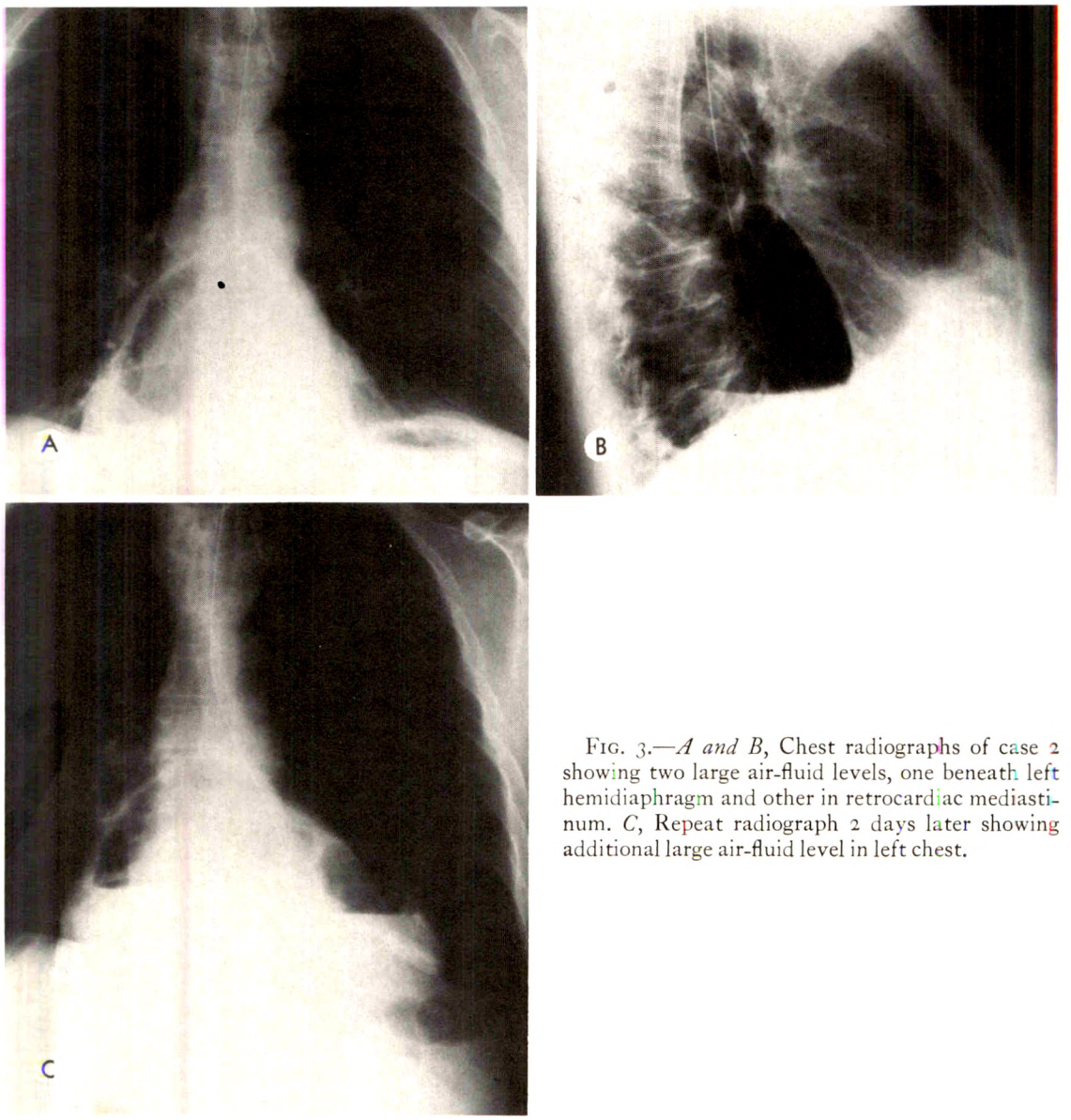


FIG. 3.—*A and B*, Chest radiographs of case 2 showing two large air-fluid levels, one beneath left hemidiaphragm and other in retrocardiac mediastinum. *C*, Repeat radiograph 2 days later showing additional large air-fluid level in left chest.

will depend upon how much of the stomach is involved, the degree of rotation of the twisted segment, and how long the volvulus is present. When the torsion is less than 180°, there is often incomplete gastric outlet obstruction since the pylorus becomes narrowed early [7]. If the torsion is greater than 180°, impairment of gastric blood supply and subsequent necrosis are likely to occur unless the volvulus is reduced [7, 8].

The diagnosis of gastric volvulus is readily made on radiographic examination of the upper gastrointestinal tract [7, 11–15]. Because of the often confusing clinical nature of chronic volvulus [5, 8, 9, 12], a contrast exam is often delayed until late in the course or until the volvulus has become acutely incarcerated. These patients, however, often have chest radiographs from which the diagnosis can be suspected before an acute incarceration develops.

When a patient with a hiatus hernia develops symptoms suggesting gastric ob-

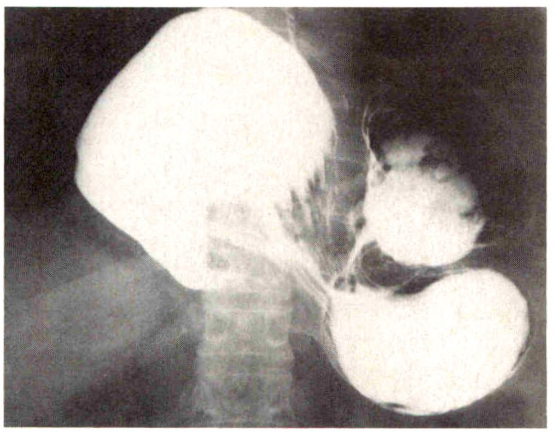


FIG. 4.—Barium examination of case 2 demonstrating gastric volvulus with obstruction at outlet of rotated herniated segment.

struction, gastric volvulus has to be considered as a possible etiology. Blatt et al. [12] reviewed nine patients with hiatal hernias who subsequently developed gastric obstruction secondary to gastric volvulus. All but one of these patients developed a reversal of the previous anatomical relationships so that the rotated, dilated distal stomach herniated into the chest through the esophageal hiatus. The fundus and the esophagogastric junction then returned to a normal position beneath the left hemidiaphragm. This subsequently led to dilatation of both the infradiaphragmatic fundus and the twisted supradiaphragmatic distal gastric segment.

When gastric volvulus herniates into the chest, two basic radiographic patterns may be seen. Early, there are two large air-fluid levels. The one in the retrocardiac mediastinum represents the dilated, herniated distal stomach with partial or complete obstruction of its outlet. The second, beneath the left hemidiaphragm, represents an air-fluid level in the normally positioned fundus which may partially be obstructed at the inlet to the twisted herniated segment. At this time, symptoms suggesting gastric outlet obstruction usually occur. When the rotation increases so that both the inlet and outlet of the rotated, herniated distal stomach become obstructed, the retrocardiac air-fluid level is replaced

TABLE 1

ANATOMIC CLASSIFICATION OF GASTRIC VOLVULUS

Classification	Description
Location:	
Abdominal	Entire volvulus in abdominal cavity; most commonly associated with eventration of left hemidiaphragm
Thoracic	Entire rotated stomach in intrathoracic position
Abdominal-thoracic	Rotated gastric segment extending into chest through hiatus (usually esophageal) in diaphragm
Direction:	
Organoaxial	Stomach rotates along longitudinal axis
Mesenteroaxial	Stomach rotates in axis of mesentery perpendicular to longitudinal axis
Mixed	Probably most common form
Extent:	
Complete	Entire stomach involved in twist
Segmental	Most commonly involves segmental twist of distal stomach

TABLE 2

RADIOGRAPHIC FINDINGS IN PATIENTS WITH UNCOMPLICATED HIATAL HERNIA

Finding	No.
Small hiatal hernia:	
Normal chest	55
Small retrocardiac mass:	
Without air	13
With small amount of air	3
Total	71*
Large hiatal hernia:	
Normal chest	0
Large retrocardiac mass:	
With small amount of air	3
With large amount of air	11
Total	14†

* All had normal infradiaphragmatic gastric bubbles.

† 12 had no infradiaphragmatic gastric bubble and two had very small ones.

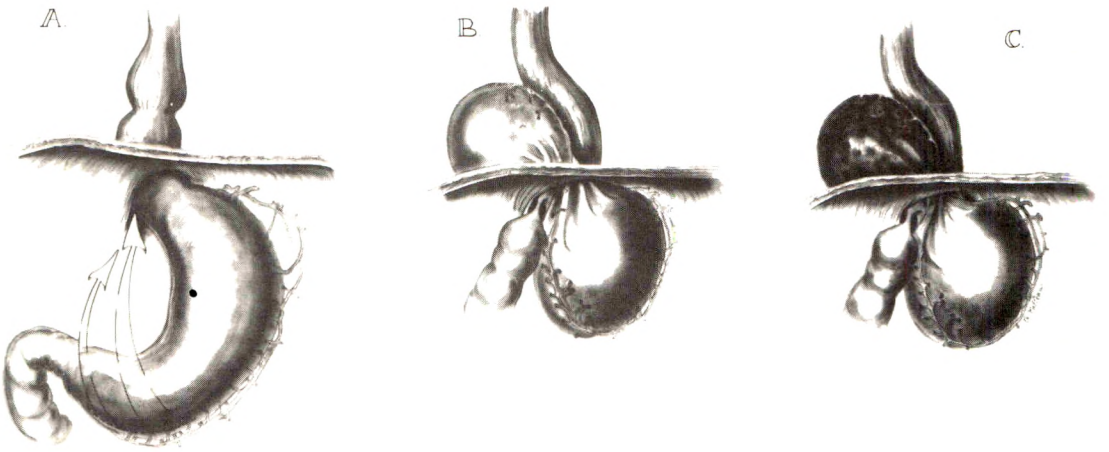


FIG. 5.—*A*, Simple esophageal hiatus hernia. *B*, Segmental volvulus of gastric antrum herniating through esophageal hiatus. Esophageal gastric junction has returned to normal position. Note obstruction at outlet of volvulus. *C*, Obstruction of both inlet and outlet of herniated gastric volvulus with secondary ischemic changes of involved segment.

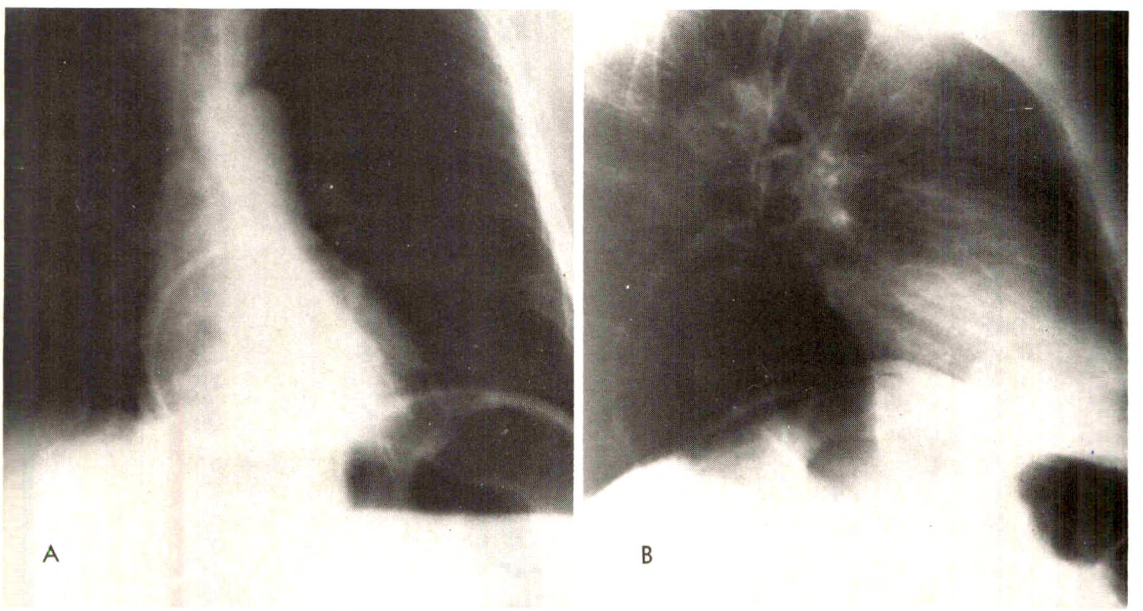


FIG. 6.—Chest radiographs of case 3 demonstrating large retrocardiac air bubble associated with large air-fluid collection beneath left hemidiaphragm.

by a homogenous soft tissue mass, the fluid-filled antrum. It is at this point that the ischemic changes have usually occurred and immediate surgical intervention is needed (fig. 5). A barium study will then confirm the diagnosis of gastric volvulus herniating into the chest.

The roentgenographic findings of a distal gastric volvulus herniating into the chest are distinct. They differ from that of an uncomplicated large esophageal hiatal hernia. A review of chest radiographs from 85 patients with documented hiatal hernia failed to reveal a single case with both a large retrocardiac air-fluid level and a normal or large infradiaphragmatic gastric air bubble (table 2). Of the 14 cases having a large hiatal hernia with a large retro-



FIG. 7.—Barium study of case 3 demonstrating distal segmental volvulus herniating into chest through esophageal hiatus with poor emptying but without any high grade obstruction.

cardiac air-containing component, 12 had an absent gastric bubble and two had very small collections of air in the small gastric remnant beneath the left hemidiaphragm. When a large simple paraesophageal hiatus hernia is present, the herniated segment usually is found in the left hemithorax, and the infradiaphragmatic gastric component is absent or quite small. Other diagnostic considerations include a giant epiphrenic diverticulum or other unrelated causes of pulmonary or mediastinal air-fluid levels (abscess, sequestration, etc.). A barium examination of the upper gastrointestinal tract will confirm the diagnosis.

ACKNOWLEDGMENT

I wish to acknowledge the assistance of Dr. John Amberg.

NOTE ADDED IN PROOF

Since submission of this paper, a third case, a 54-year-old male with a history of "hiatal hernia" diagnosed by previous upper GI, presented with a history of nonspecific recurrent chest pain. A routine chest radiograph showed a large retrocardiac air bubble associated with a large left infradiaphragmatic air-fluid level (fig. 6). A diagnosis of a distal segmental gastric volvulus herniating into the chest was made, and a barium study was performed for confirmation (fig. 7). The patient has subsequently refused surgical correction. •

REFERENCES

1. Camblos JFB: Acute volvulus of stomach. *Am Surg* 35:505–509, 1969
2. Dalgaard JB: Volvulus of the stomach. *Acta Chir Scand* 103:131–153, 1952
3. Payer A: Volvulus ventriculi und die Achsendrelung des Magens. *Mitt Grenzab Med Chir* 20:686–694, 1907
4. Da Costa JC: *Modern Surgery*. Philadelphia, Saunders, 1931
5. Raffin S: Diverticula, rupture and volvulus, in *Gastrointestinal Disease*, edited by Sleisenger MH, Fordtran JS, Philadelphia, Saunders, 1973, pp 612–614
6. Guernsey JM, Connolly JE: Acute complete gastric volvulus. *Arch Surg* 86:423–428, 1963
7. Sawyer KC, Hammer RW, Fenton WC: Gastric volvulus as a cause of obstruction. *Arch Surg* 72:764–772, 1956
8. Tanner NC: Chronic and recurrent volvulus of stomach. *Am J Surg* 115:505–515, 1968
9. Deitel M: Chronic or recurring organoaxial rotation of the stomach. *Can J Surg* 16:195–205, 1973
10. Wastell C, Ellis H: Volvulus of the stomach. *Br J Surg* 58:557–562, 1971
11. Beranbaum SL, Gottlieb C, Lefferts D: Gastric volvulus, secondary gastric volvulus. *Am J Roentgenol* 72:609–614, 1954
12. Blatt ES, Schneider HJ, Wiot JF, Felson B: Roentgen findings in obstructed diaphragmatic hernia. *Radiology* 79:648–657, 1962
13. Gottlieb C, Lefferts D, Beranbaum S: Gastric volvulus. *Am J Roentgenol* 72:609–615, 1954
14. Lefferts D, Beranbaum S, Gottlieb C: Gastric volvulus; idiopathic gastric volvulus. *Am J Roentgenol* 72:616–624, 1954
15. Singleton AC: Chronic gastric volvulus. *Radiology* 34:53–61, 1940

Am J Roentgenol 126:1175–1177, 1976

CHONDROSARCOMA OF THE ESOPHAGUS

Issa Yaghmai[1] and Gary G. Ghahremani[1]

ABSTRACT:

A 46-year-old man had a large noncalcified tumor in the wall of the thoracic esophagus narrowing its lumen by projection of numerous firm nodular masses. The pathologic diagnosis was chondrosarcoma. Malignant degeneration of a tracheobronchial cartilaginous remnant is the main consideration in this first recorded case of esophageal chondrosarcoma.

Sarcomas account for 0.5%–1.0% of all malignant esophageal neoplasms [1]. In a series of 59 cases reviewed by Thorek and Neiman [2], there were 30 fibrosarcomas, eight leiomyosarcomas, five lymphosarcomas, five melanosarcomas, four rhabdomyosarcomas, and seven unclassified sarcomas. A few mixed tumors of the esophagus known as carcinosarcoma have contained cell aggregates resembling chondrosarcoma [3, 4]. However, we wish to report the first instance of a primary esophageal chondrosarcoma and review the pertinent literature to explain its pathogenesis.

CASE REPORT

A 46-year-old Iranian farmer was referred to the University of Tehran-Tadj Pahlavi Cancer Hospital with a 6 month history of progressive dysphagia induced by solid food and a 4.5 kg weight loss. Chest roentgenograms showed widening of the mediastinum due to a large middle mediastinal tumor with ill-defined margins. An upper gastrointestinal series demonstrated marked irregularity of the wall of the distal two-thirds of the esophagus (figs. 1*A* and 1*B*). Numerous nodular masses projected into the narrowed and indistensible lumen. The peristaltic activity was absent so that the passage of barium distally was slow and dependent on the force of gravity. The diagnosis entertained was sarcoma or carcinoma of the esophagus presenting as a varicoid tumor due to submucosal infiltration.

Esophagoscopy revealed numerous firm polypoid masses in the esophageal wall that were covered by grossly intact mucosa. The pathologic report on the biopsy was "chondrosarcoma, site undetermined." Possibility of mistaken identification of the specimen led to repeat esophagoscopy. On this occasion three biopsies were taken from different sites of the involved esophagus. It was also noted that the esophageal mucosa exhibited unusual mobility over the firm submucosal mass and that a crunching sound was produced by insertion of the biopsy forceps and separation of tumor fragments. Microscopic evaluation of the biopsies confirmed the presence of a differentiated chondrosarcoma (fig. 2). The intact elements of esophageal mucosa contained in the specimens indicated the intramural location of the tumor.

Subsequently tomograms of the mediastinum and additional views with barium in the esophagus (fig. 1*C*) demonstrated the extent of the tumor which did not have visible calcifications. Other radiologic studies, including a complete bone survey, failed to reveal any lesion as a possible primary source of origin of the chondrosarcoma. Since radical resection appeared difficult, a palliative procedure such as intraesophageal insertion of a Celestin tube or gastrostomy were considered. However, the patient refused any surgical intervention and died 8 months later from complications of local extension of the tumor. Autopsy permit was not granted.

DISCUSSION

A unique feature of this chondrosarcoma is its origin in an organ that is normally devoid of the necessary cartilage-forming matrix. Metaplasia of the mesenchymal cells of the esophageal wall could conceivably account for its atypical site [5, 6]. This is an explanation for the cell aggregates of chondrosarcoma that are occasionally found within the esophageal carcinosarcomas [3,

[1] Department of Radiology, Virginia Commonwealth University–Medical College of Virginia, Richmond, Virginia 23298.

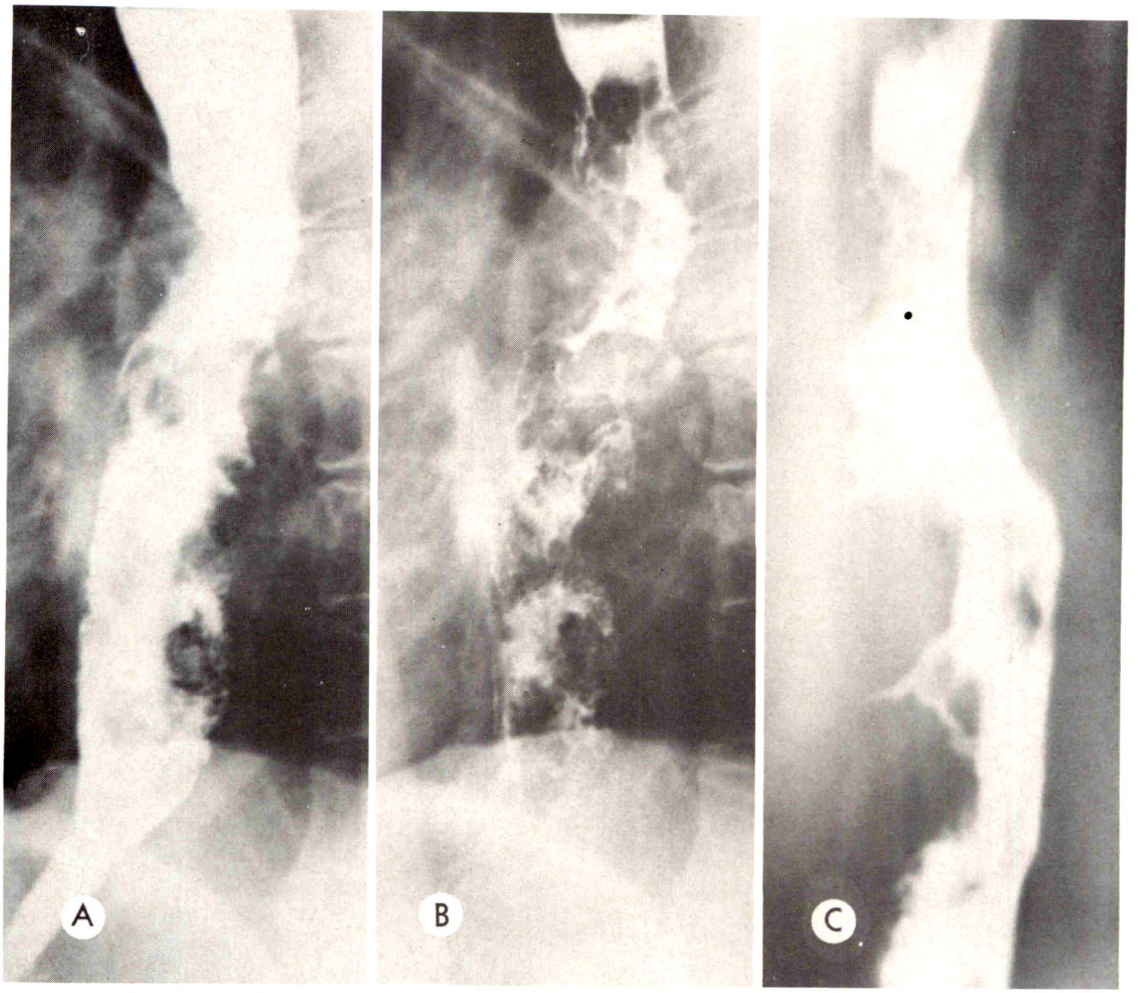


FIG. 1.—*A and B*, Views of esophagus with patient upright demonstrating extensive infiltration of wall resulting in irregular filling defects. *C*, Midline tomogram of chest with barium in esophagus showing large noncalcified tumor with mediastinal and intraluminal polypoid components.

4]. The absence of any carcinomatous tissue in our patient appears to eliminate the latter diagnosis. However, a real possibility is malignant degeneration of a cartilaginous tracheobronchial remnant in the esophagus. Several recent reports indicate that defective separation of the embryonic respiratory tract from the primitive foregut leaves behind clusters of tracheobronchial precursor cells [7, 8]. These sequestrated cells may later form cartilaginous nodules and rings causing segmental stenosis of the esophagus in children and adults [6–9]. This congenital abnormality has also been implicated in the development of various unusual tumors of the esophagus such as osteochondroma, oat-cell carcinoma, and cylindroma [6, 9]. This hypothesis also appears to provide an interesting explanation for the pathogenesis of the lesion herein described.

The roentgenographic features of our case are very similar to those described in other types of esophageal sarcoma [1, 2, 10]. These tumors commonly present as an infiltrative and polypoid lesion resulting in irregular narrowing of the esophageal lumen (fig. 1). A large extraluminal component (fig. 1) is often associated with esophageal sarcomas [1, 10]. The usual sites of involvement are the middle and lower third of the esophagus [1–3, 10]. Grossly visible calcifications have not been reported in any

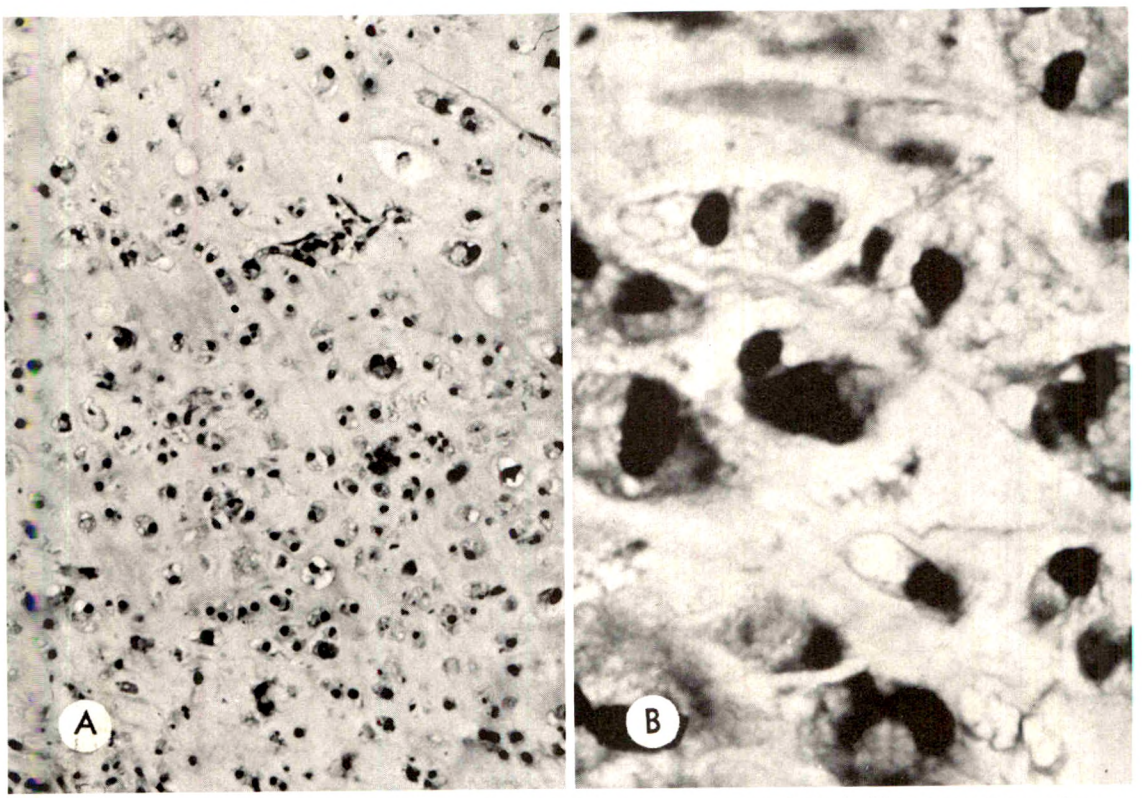


FIG. 2.—Photomicrographs at ×120 (*A*) and ×600 (*B*) of two separate fields in biopsy specimens demonstrating chondrosarcoma. Note abundance of bizarre multinucleated malignant cartilage cells.

case of sarcoma or carcinoma of the esophagus.

The prognosis of esophageal sarcoma is less favorable than carcinoma, and the majority of patients succumb within 6 months after appearance of the symptoms, usually from complications associated with esophageal obstruction and perforation of the tumor into adjacent organs [2].

ACKNOWLEDGMENT

We are indebted to Prof. A. Zia Shamsa of the University of Tehran, Iran, for providing figure 2 and the biopsy reports.

REFERENCES

1. Goodner JT, Miller TR, Watson WL: Sarcoma of the esophagus. *Am J Roentgenol* 89:132–139, 1963
2. Thorek P, Neiman BH: Rhabdomyosarcoma of the esophagus. *J Thorac Surg* 20:77–89, 1950
3. McCort JJ: Esophageal carcinosarcoma and pseudosarcoma. *Radiology* 102:519–524, 1972
4. Stener B, Kock NG, Pettersson S, Zetterlund B: Carcinosarcoma of the esophagus. *J Thorac Cardiovasc Surg* 54:746–750, 1967
5. Lichtenstein L, Goldman RL: Cartilage tumors in soft tissues, particularly in the hand and foot. *Cancer* 17:1203–1208, 1964
6. Mahour GH, Harrison EG Jr: Osteochondroma (tracheo-bronchial choristoma) of the esophagus. Report of a case. *Cancer* 20:1489–1493, 1967
7. Anderson LS, Shackelford GD, Mancilla-Jimenez R, McAlister WH: Cartilaginous esophageal ring: a cause of esophageal stenosis in infants and children. *Radiology* 108:665–666, 1973
8. Rose JS, Kassner EG, Jurgens KH, Farman J: Congenital oesophageal strictures due to cartilagenous rings. *Br J Radiol* 48:16–18, 1975
9. Bergmann M, Charnas RM: Tracheobronchial rests in the esophagus; their relation to some benign strictures and certain types of cancer of the esophagus. *J Thorac Surg* 35:97–104, 1958
10. Wolfel DA: Leiomyosarcoma of the esophagus. *Am J Roentgenol* 89:127–131, 1963

Am J Roentgenol 126:1178–1180, 1976

LOCALIZED GIANT PSEUDOPOLYPOSIS IN ULCERATIVE COLITIS

JAMES W. KEATING, JR.[1] AND HOWARD J. MINDELL[1]

ABSTRACT:

A case of localized giant pseudopolyposis in ulcertative colitis is discussed in which a mass effect mimicked tumor. The fulminant collection of pseudopolyps was palable in the epigastrium on physical exam and caused a partial obstruction to the retrograde flow of barium. Carcinoma is a worrisome possibility in ulcerative colitis, but localized giant pseudopolyposis may also present as a mass.

Pseudopolyposis is a frequent sequella of ulcerative colitis [1]. There have been some reports of localized giant pseudopolyposis producing a radiographic "masslike effect" on barium enema [2, 3]. In addition to the appearance of a mass on a barium enema, this case report demonstrates two other features of localized giant pseudopolyposis in ulcerative colitis which can mimic tumor. These features are (1) a palpable mass and (2) partial obstruction to the retrograde flow of barium.

CASE REPORT

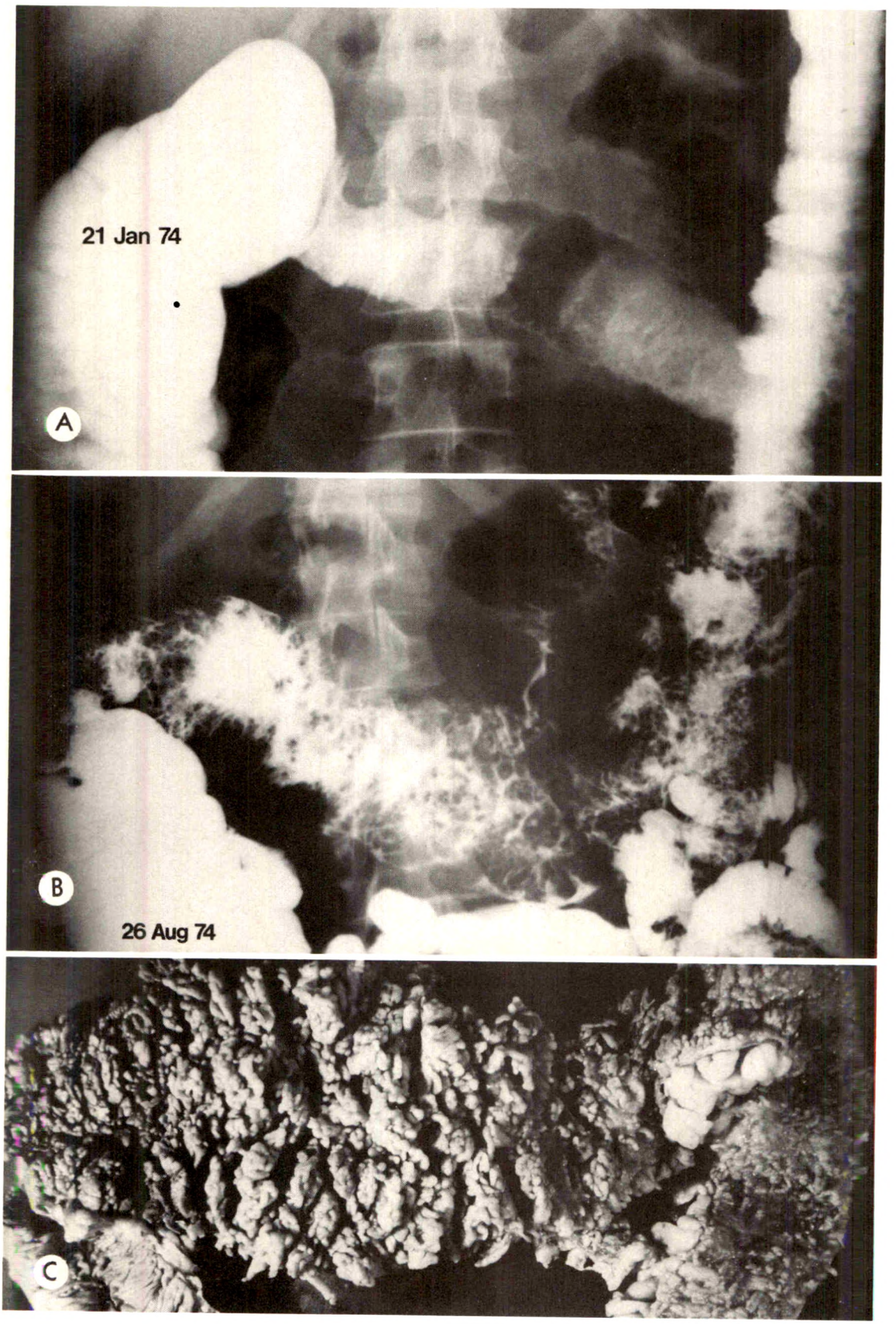
R. S. is a 40-year-old white man with a 10 year history of bloody diarrhea. A previous workup, which included a biopsy, produced a diagnosis of ulcerative colitis. The patient had been followed by barium enema examination, and intermittent exacerbations were treated with azulfidine, lomotil, and prednisone. Eight months prior to admission a barium enema demonstrated diffuse colonic mucosal disease consistent with a diagnosis of ulcerative colitis (fig. 1*A*). Approximately 6 weeks prior to admission the patient reported increasing right upper quadrant pain; a mass was palpated in the epigastrium on physical examination. A barium enema demonstrated an abnormality in the transverse colon that had developed since the last examination 8 months previously. It consisted of a partial obstructing lesion to the retrograde flow of barium with a "mass effect" containing bizarre, irregular, streaky collections of barium (fig. 1*B*), which suggested a villous adenoma or even transmural fissuring as might be seen in granulomatous colitis. The colitis would not respond to aggressive medical therapy, and a colectomy was performed. The entire colon was observed to be involved with ulcerative colitis with marked pseudopolyposis. The area of the right transverse colon was the most severely involved with extravagant "frondlike" pseudopolyposis. Some individual pseudopolyps measured as much as 2 cm in length (fig. 1*C*). This accumulation of pseudopolyposis produced a localized mass effect noticed on the physical exam and the partial obstruction to the retrograde flow of barium. However, no fissures were found in the wall of the pathological specimen, and no occult neoplasm was found in the area of extravagant pseudopolyposis. The patient has done well postoperatively.

DISCUSSION

Pseudopolyposis may be seen in either the active or quiescent state of ulcerative colitis and may be diffuse or focal in distribution. This phenomenon occurs most frequently in the transverse and descending colon. Collections of pseudopolyps may occasionally attain giant size mimicking a

FIG. 1.—*A*, Barium enema examination demonstrating diffuse inflammatory ulceration with some pseudopolyp formation. *B*, Follow-up barium enema 7 months later showing development of "mass effect" in transverse colon with fulminant pseudopolyposis. *C*, Gross specimen of colon showing many smooth-surfaced fingerlike projections which are coalesced giant pseudopolyps.

[1] Department of Radiology, University of Vermont College of Medicine, Burlington, Vermont 05401.


21 Jan 74
A
B
26 Aug 74
C

villous adenoma or carcinoma [4].

Although there is extensive documentation of the occurrence of carcinoma in patients with ulcerative colitis and pseudopolyposis [1, 5] there is some debate about the malignant potential of the pseudopolyps themselves [6].

The development of carcinoma in ulcerative colitis is not usually characterized by a polypoid mass but rather, at least in the early stages, by a constrictive, flat, ulcerating type of lesion. While the development of any colonic mass lesion in ulcertaive colitis should be of concern because of the malignant potential of ulcerative colitis, some radiographic features of localized giant pseudopolyposis might alert the examiner to the correct diagnosis. In localized giant pseudopolyposis there may be frondlike irregular linear streaking of barium amidst a mass effect causing partial obstruction to the retrograde flow of barium. Elsewhere in the colon there may be associated pseudopolyp formation of the mucosa. These features pose a problem for the clinician since they mimic tumor but can represent only a benign form of this disease.

REFERENCES

1. de Dombal FT, Watts JMcK, Watkinson G, Goligher JC: Local complications of ulcerative colitis: stricture, pseudopolyposis, and carcinoma of colon and rectum. *Br Med J* 1:1442–1447, 1966
2. Hinrichs HR, Goldman H: Localized giant pseudopolyps of the colon. *JAMA* 205:248–249, 1968
3. Ferrucci JF, Vickery AL Jr: Case records of the Massachusetts General Hospital, case 3-1972. *N Engl J Med* 286:147–153, 1972
4. Schneider R, Dickersin GR, Patterson JF: Localized giant pseudopolyposis: a complication of granulomatous colitis. *Am J Dig Dis* 18:265–270, 1973
5. Jalan KN, Walker RJ, Sircus W, McManus JPA, Prescott RJ, Card WI: Pseudopolyposis in ulcerative colitis. *Lancet* 2:555–559, 1969
6. Goldgraber MB: Pseudopolyposis in ulcerative colitis. *Dis Colon Rectum* 8:355–363, 1965

Am J Roentgenol 126:1181–1188, 1976

CLINICAL AND RADIOGRAPHIC "REANKYLOSIS" FOLLOWING HIP SURGERY IN ANKYLOSING SPONDYLITIS

DONALD RESNICK,[1] ISAAC L. DWOSH,[2] THOMAS G. GOERGEN,[1] ROBERT F. SHAPIRO,[3] AND ROBERT D'AMBROSIA[4]

ABSTRACT:

Eleven patients with ankylosing spondylitis underwent reconstructive hip surgery (21 hips). In 10 of these hips multiple surgical procedures had been performed. The final procedure included total hip arthroplasties (16 hips), femoral cup arthroplasties (four hips) and an Austin-Moore prosthetic replacement (one hip). A clinical and radiographic evaluation in the postoperative period revealed a high incidence of decreased joint motion and heterotopic ossification. Clinically moderate to severe restriction of motion was noted in 12 hips, and in six of these "reankylosis" was present. Radiographically moderate to severe new bone formation was seen in 11 hips, and in nine of these "reankylosis" was suggested. An association of excessive ossification and multiple surgical procedures was evident. It would appear that when the prime indication for hip surgery in patients with ankylosing spondylitis is restricted motion, the operation may not be beneficial.

Total hip replacement arthroplasty is being utilized extensively for the treatment of patients with osteoarthritis. Preliminary results have been encouraging, and the procedure has been extended to include individuals with other arthritic disorders. In the postoperative evaluation of several patients with ankylosing spondylitis, a surprisingly high incidence of heterotopic ossification was noted. Consequently, a more complete investigation of the role of hip surgery in patients with this disease was undertaken.

SUBJECTS AND METHODS

The clinical records and radiographs of 102 patients with definite ankylosing spondylitis (Rome criteria) were reviewed. Of this group, 11 patients were found who had undergone reconstructive hip surgery. When possible, these individuals were recalled for further clinical and x-ray examination. The clinical parameters emphasized included current age, age of onset, site of disease, extent of peripheral joint involvement, and pre- and postoperative symptoms and signs in the involved hips with particular attention to the range of motion. The number and dates of all previous surgical procedures on these hips were recorded. Pre- and postoperative hip radiographs were studied to determine the pattern of initial joint involvement and the incidence and extent of heterotopic ossification following surgery.

RESULTS

A summary of patient data is given in table 1. All 11 patients were males with an average age of 49 years (range 24–73); average age at disease onset was 21 years (range 14–36). Hip involvement was generally bilateral and symmetrical and occurred early during the course of the disease. Additional peripheral joint abnormalities were present in nine of 11 patients.

Preoperative clinical examination of the hips frequently revealed local pain on motion, regional muscle atrophy, and flexion contractures of varying severity. A univer-

[1] Department of Radiology, University Hospital, University of California at San Diego, and the Veterans Administration Hospital, San Diego, California 92161.
[2] Department of Medicine, University Hospital, University of California at San Diego, and the Veterans Administration Hospital, San Diego, California 92161. I. Dwosh is a Fellow of the Canadian Arthritis Society.
[3] Department of Medicine, Sacramento Medical Center, University of California, Sacramento, California 95817.
[4] Department of Orthopedic Surgery, Sacramento Medical Center, University of California, Sacramento, California 95817.

TABLE 1

PATIENT ANALYSIS

Patient No.	Age (Yr)	Age of Onset (Yr)	Peripheral Joint Disease	Side	Prior Hip Surgery	Final Hip Surgery		Clinical Follow-up		X-ray Follow-up	
						Date	Type	Interval (Mo)	Assessment*	Interval (Mo)	Assessment†
1	49	18	+	R	−	1970	THR	54	++	54	+++
				L	−	1970	THR	54	++	54	+++
2	54	23	−	R	+	1972	THR	30	++	30	+++
				L	+	1972	THR	30	+++	30	++
3	54	20	+	R	+	1971	THR	40	+++	20	+++
				L	+	1972	THR	36	+++	18	+++
4	61	20	−	R	+	1973	THR	24	++	21	+
				L	+	1973	THR	24	++	20	++
5	63	36	+	R	−	1973	THR	12	+	4	−
				L	−	1974	THR	9	+	1	−
6	50	36	+	R	−	1971	THR	42	+	31	−
				L	−	1972	THR	30	+	18	−
7	44	14	+	R	+	1973	THR	24	+	3	−
				L	−	1973	THR	24	+	1	−
8	24	18	+	R	−	1972	THR	20	+	20	−
				L	−	1969	Femoral cup	51	+	21	−
9	73	16	+	R	+	1970	Revised femoral cup	29	++	29	+++
				L	−	1972	THR	1	+	1	−
10	38	16	+	R	−	1968	Femoral cup	75	+++	75	+++
				L	+	1970	Austin-Moore	59	+++	59	+++
11	28	16	+	R	+	1969	Femoral cup	72	+++	72	+++

NOTE.—All patients were males. THR = total hip arthroplasty.
* + = mild symptoms and signs; ++ = moderate; +++ = clinical "reankylosis" of joint.
† − = absent new bone formation; + = mild new bone formation; ++ = moderate; +++ = apparent "reankylosis" of joint.

sal finding was decreased range of motion, particularly in internal and external rotation and flexion. Preoperative radiographs were available for nine hips in six patients. The radiographic abnormalities in seven of these hips were characteristic of the disorder [1] including axial migration of the femoral head in relation to the acetabulum, concentric joint space loss, mild to severe protrusio deformity, subchondral cysts, and "ring" osteophytes about the femoral neck. Complete bony ankylosis was noted in one hip.

A total of 35 surgical procedures of the hip were required in these patients. Initial cup arthroplasties had to be revised in three patients (nos. 2, 3, and 9) due to persistent discomfort or restricted motion with heterotopic ossification. An additional patient (no. 4) had extensive bone formation about bilateral femoral prostheses, and subsequent total hip arthroplasties were performed. The final surgical procedure in the 11 patients (21 hips) included total hip arthroplasties (16 hips), femoral cup arthroplasties (four hips), and an Austin-Moore prosthetic replacement (one hip).

Clinical and x-ray follow-up after the

final procedure averaged 35 months (range 1–75 months) and 29 months (range 1–75 months), respectively. Postoperative pain and loss of joint motion were graded from mild to severe (table 1). In the severe category, apparent "reankylosis" of the hip joint was suggested by extensive loss of active and passive motion. The extent of heterotopic bone formation on postoperative radiographs is also shown in table 1. In the severe category, "reankylosis" of the joint was suggested by complete paraarticular osseous bridging. In five of the nine hips in which heterotopic ossification was absent, follow-up was 4 months or less. There was generally good correlation between the extent of radiographically evident heterotopic bone formation and the degree of joint immobility.

Multiple surgical procedures had been performed on 10 hips in seven patients. In these patients, clinically moderate or severe restriction of motion was frequent following the final operation (table 2). In addition in these joints, radiographic "reankylosis" was noted in six hips. Thus of nine hips with severe ectopic ossification on x-ray, six had been sites of multiple procedures.

TABLE 2

POSTOPERATIVE ABNORMALITIES AFTER SINGLE OR MULTIPLE SURGICAL PROCEDURES

Abnormality	Surgical Procedure	
	Single	Multiple
Clinical symptoms and signs:		
Mild	8	1
Moderate	2	4
Severe	1	5
Heterotopic ossification:		
Absent	8	1
Mild	0	1
Moderate	0	2
Severe	3	6

NOTE.—Multiple surgical procedures performed on 10 hips in seven patients.

Superficial or deep wound infections, present in three patients (nos. 2, 5, and 7) were not associated with a higher incidence of clinical or radiographic "reankylosis."

No association between the extent of postoperative paraarticular ossification and

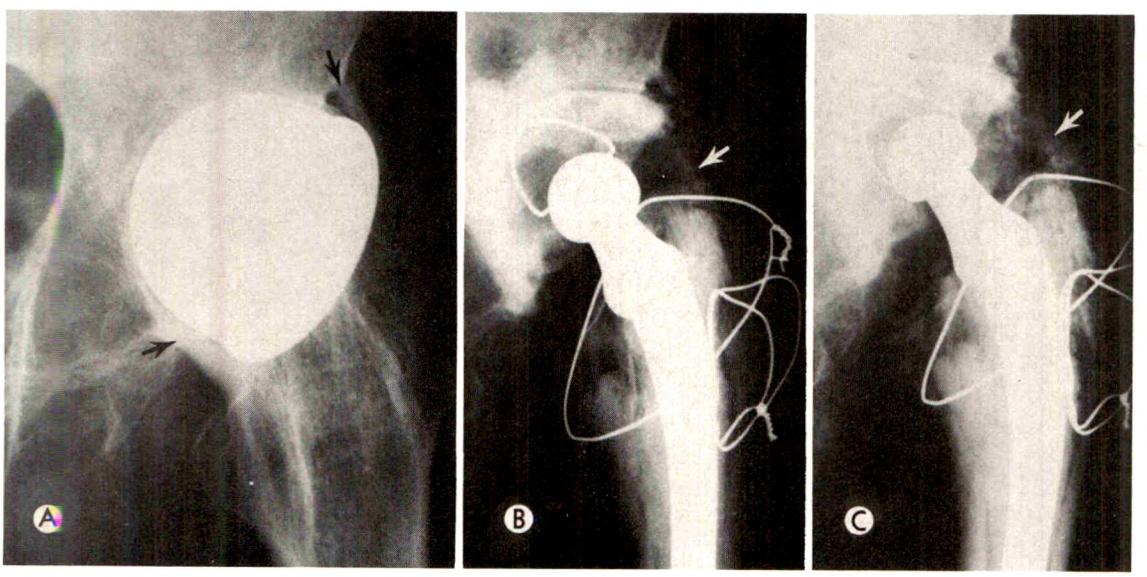


FIG. 1.—Patient 3: reankylosis following cup arthroplasty and subsequent total hip replacement. *A*, Considerable bone formation about superior and inferior aspects of left femoral cup (*arrows*) resulting in apparent ankylosis of joint. *B*, Two months after total hip replacement, ectopic ossification is apparent (*arrow*). Minimal radiolucency is seen between acetabular cement and subjacent bone. *C*, Radiographic evaluation 6 months postoperatively demonstrating almost complete paraarticular bony bridging (*arrow*).

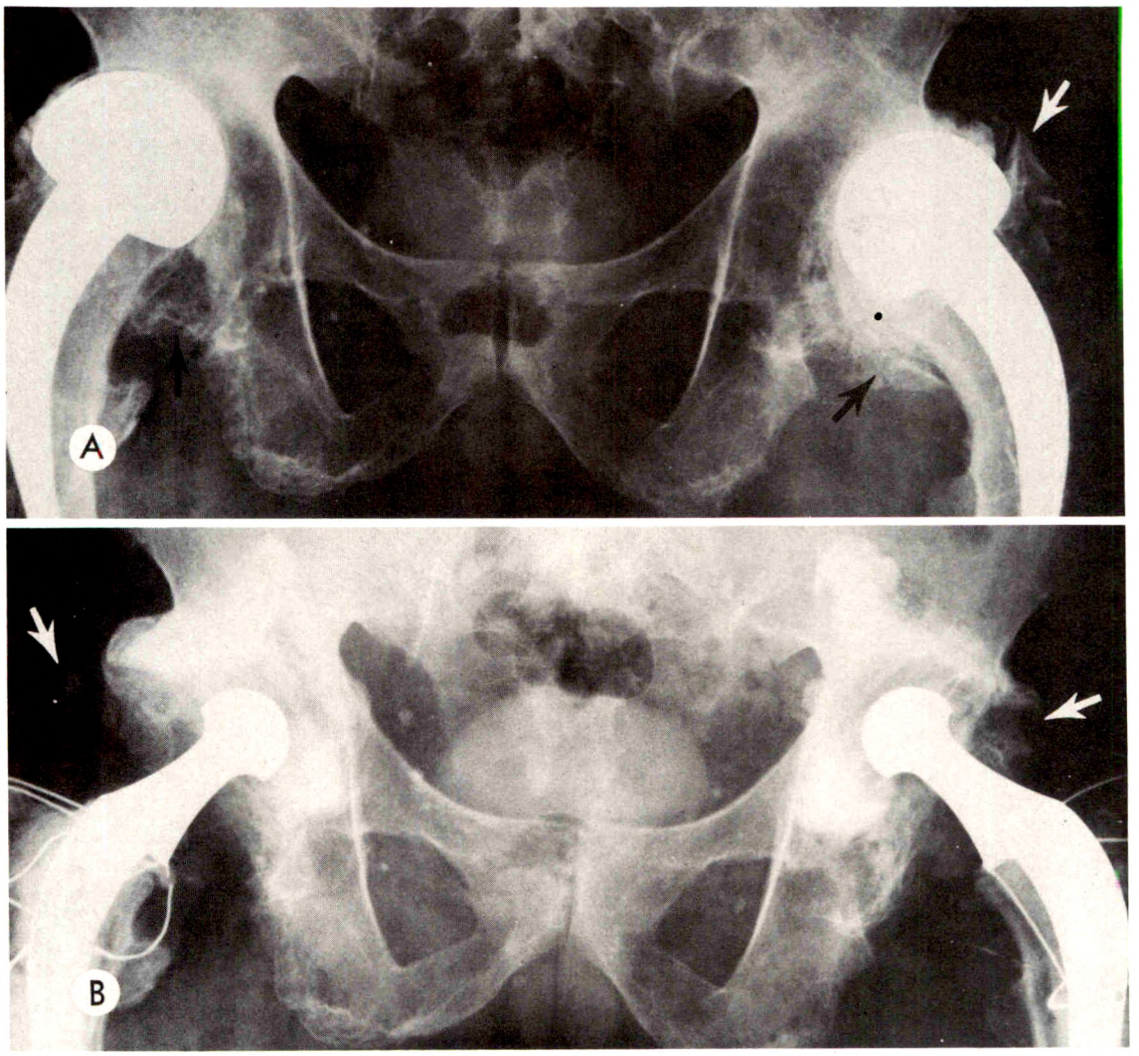


FIG. 2.—Patient 4: heterotopic ossification following femoral prosthetic replacements and total hip arthroplasties. *A*, Moderate to extensive new bone formation about femoral prostheses on both sides (*arrows*). *B*, Evaluation 2 years postoperatively showing mild (right side) and moderate (left side) heterotopic ossification about total hip arthroplasties (*arrows*).

that of new bone formation or "whiskering" about the pelvis could be established.

CASE REPORTS

Patient 3

This 54-year-old man had the onset of ankylosing spondylitis with involvement of his lower back, hips, and neck at age 20. In 1947 he had a right femoral cup prosthetic replacement, and in 1948 a similar operation on the left. Due to persistent pain, he had a revision of his right femoral cup arthroplasty in 1967. Radiographs

FIG. 3.—Patient 10: reankylosis following cup arthroplasty and Austin-Moore prosthetic replacement. *A*, Mild to moderate bone formation about right femoral cup (*arrow*). Left hip demonstrates symmetrical joint space loss, sclerosis, and acetabular osteophytosis. *B*, Moderate new bone formation (*arrowhead*) seen 3 months after Austin-Moore prosthesis used to replace previous left femoral cup arthroplasty. Tilting of right femoral cup and mild protrusio deformity evident with adjacent new bone formation (*arrow*). *C*, Apparent ankylosis about femoral cup arthroplasty (*arrow*) and protruding and loosened Austin-Moore prosthesis (*arrowhead*) $4\frac{1}{2}$ years later.

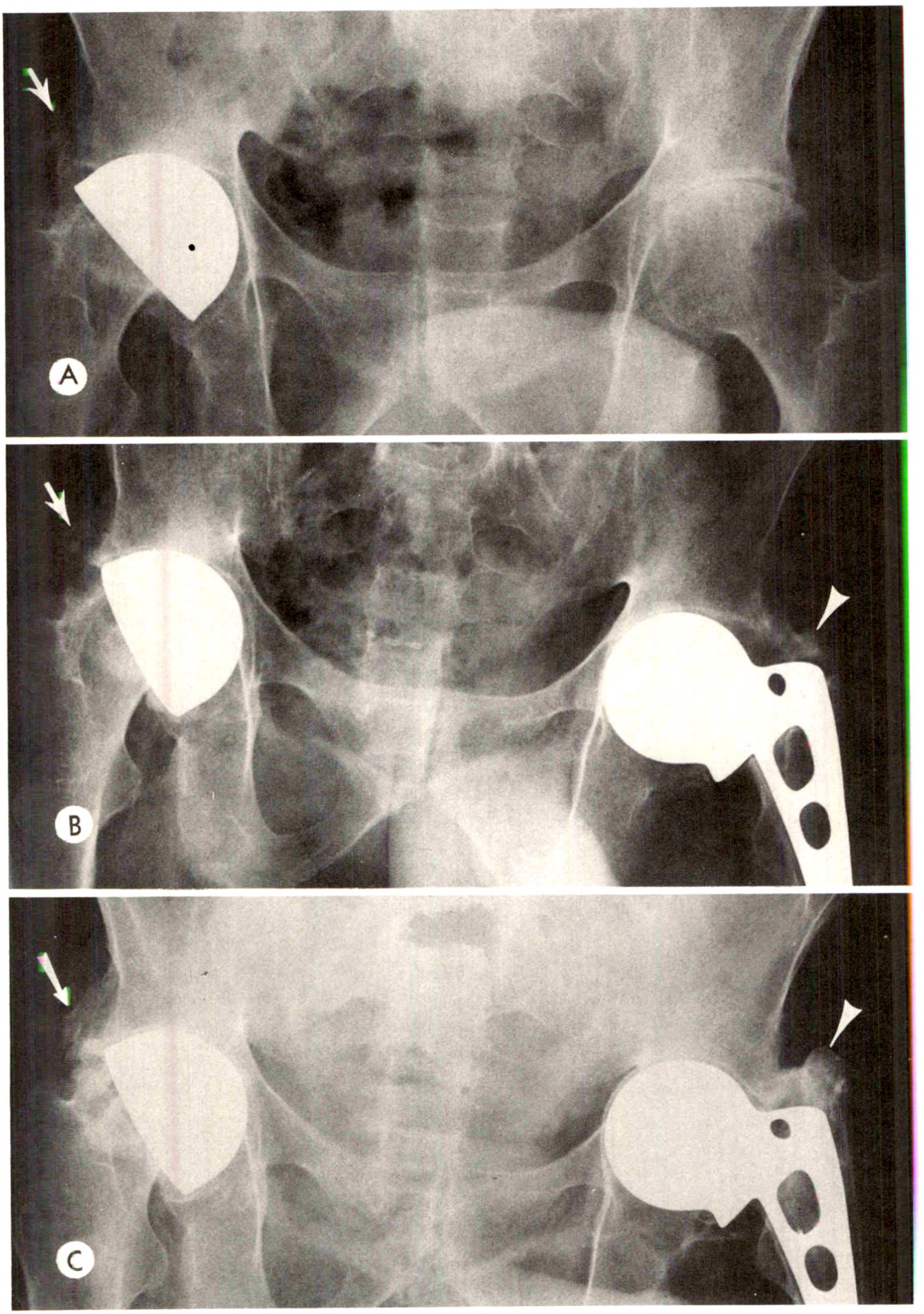

A
B
C

TABLE 3

HETEROTOPIC OSSIFICATION AFTER TOTAL HIP ARTHROPLASTY

Reference	Incidence (%)	Comment
Charnley [2]	5	Study of 379 hip replacements
Amstutz [3]	8	Noted in four of 50 hips followed more than 1 year
Patterson and Brown [4]	8.7	More frequent following multiple procedures or infection
Mendes [5]	10	Indicated those cases with "extensive" ossification only; more frequent following multiple procedures and infection or loosening
Harris [6]	14	Affected joint motion in only 3%
Hamblen et al. [7]	20	Severe joint restriction in only 3%
Brooker et al. [8]	21	Complete "reankylosis" in 2%; more frequent following multiple procedures
Nollen and Slooff [9]	53	Complete "reankylosis" in only 7%

in 1971 revealed extensive new bone formation about both cups (fig. 1*A*). In November 1971 and February 1972 he underwent total hip arthroplasties on the right and left side, respectively (fig. 1*B*). Radiographs 6 months postoperatively (fig. 1*C*) revealed apparent "reankylosis" about both hips. In 1975 his hip movement in degrees right over left was flexion 20/10, abduction 20/15, adduction 10/15, internal rotation 5/0, and external rotation 20/30. His left leg was externally rotated 20°. At present he is severely disabled and uses a special reclining wheelchair.

Patient 4

The onset of ankylosing spondylitis in this 61-year-old man was at age 20. Because of severe hip involvement he underwent bilateral femoral prosthetic replacements in 1952. In 1973 he had recurrent hip pain and was ambulating with crutches. Hip movement at that time in degrees right over left was flexion 85/70, abduction 10/5, adduction 20/10, external rotation 0/0, and internal rotation 0/0. He had bilateral flexion contractures and widespread periarticular bone formation (fig. 2*A*). He underwent bilateral total hip replacements. On a postoperative evaluation 6 months later the patient demonstrated mild to moderate bilateral heterotopic ossification. Hip movement in degrees right over left was flexion 90/80, abduction 15/15, adduction 5/0, external rotation 20/10 and internal rotation 0/0. An additional examination 2 years postoperatively revealed no change in range of hip motion (fig. 2*B*). More recently he has complained of increasing pain in his left hip.

Patient 10

This 38-year-old man had onset of ankylosing spondylitis at age 16 with pain and swelling in his ankles. Eventual involvement of other peripheral joints and the lower spine occurred. Progressive pain and decreased motion in his hips developed, and in 1968 a right femoral cup arthroplasty was performed. There was no increase of hip motion following the surgery (fig. 3*A*). In 1969 he underwent a left femoral cup arthroplasty. His left hip pain increased postoperatively and was associated with a "grating" sensation. An Austin-Moore prosthetic replacement of the left hip was accomplished in 1970, but continuous pain developed thereafter (fig. 3*B*). Evaluation $4\frac{1}{2}$ years later showed extensive heterotopic ossification about the femoral cup and Austin-Moore prosthesis (fig. 3*C*). Currently the patient has pain in both hips and no measurable joint motion.

DISCUSSION

Paraarticular ossification of the hip is a recognized complication following total joint arthroplasty. Its reported incidence has varied from 5% to 53% (table 3). Some of this variation has related to the length of follow-up and method of classification. No definite association between the incidence of heterotopic ossification and the type of prosthesis has been established [8], although a higher incidence of soft tissue bone formation is noted in hips which have been infected or sites of multiple surgical procedures [4, 5, 8]. Ectopic ossification

following cup arthroplasty has been reported in 30% of cases [7].

There have been fewer reports indicating the incidence of new bone formation following arthroplasty of the hip in ankylosing spondylitis. In a long-term follow-up study of cup arthroplasties in rheumatic patients, Edstrom and Fellander [10] noted that although the range of motion was definitely improved in the postoperative period, marked new bone formation occurred in nine of 37 hips. It cannot be determined whether this ectopic ossification was present in patients with ankylosing spondylitis or rheumatoid arthritis. Freeman [11] studied the results of McKee-Farrar total hip arthroplasty in patients with rheumatic diseases, including four patients with ankylosing spondylitis, and noted one individual with "ectopic calcification." It is not clear in this study what criteria were used for determining the presence of such calcification and whether the patient with this complication had ankylosing spondylitis or another rheumatic disease. In a report of 33 total hip arthroplasties in patients with ankylosing spondylitis, Welch and Charnley [12] found none with clinical "reankylosis" postoperatively, although ectopic bone formation was occasionally noted. Duration of disease and hip symptomatology in these patients was shorter than in ours, and the number of individuals with multiple hip operations cannot be determined. Arden et al. [13], in an evaluation of total hip replacements in juvenile chronic polyarthritis and ankylosing spondylitis, included 10 patients with the latter disease who underwent 14 arthroplasties. Although one cannot be certain whether these investigators searched for postoperative new bone formation, it is significant that some patients with ankylosing spondylitis had only "fair" results regarding increased range of motion following surgery. The only case of complete "reankylosis" following total hip replacement in a patient with ankylosing spondylitis was reported by Wilde et al. [14]. The patient, a 57-year-old man who developed bony ankylosis following bilateral cup arthroplasties, subsequently ankylosed again after a unilateral Charnley-Muller prosthetic replacement.

In our patients clinical "reankylosis" occurred in six of 20 hips (30%) followed postoperatively for longer than 6 months. Similarly, radiographic "reankylosis" was suggested in nine of 16 hips (56%) followed for at least 6 months, although in some patients limited motion was still present in joints which were interpreted as ankylosed on x-ray.

The etiology of this apparent high incidence of heterotopic bone formation following hip surgery in patients with ankylosing spondylitis is obscure, although it is particularly common following multiple surgical procedures. Bony proliferation leading to intraarticular ankylosis and "whiskering" at sites of ligament attachment is frequent in this disorder. Perhaps surgical intervention in these patients, by changing the local environment around the joint, accentuates osteoblastic activity leading to excess ossification. Although we have noted mild heterotopic ossification following hip arthroplasty in patients with osteoarthritis or aseptic necrosis of the femoral head, this finding is relatively infrequent and generally unassociated with clinical abnormality. Since heterotopic ossification appears to be a significant problem postoperatively in some patients with ankylosing spondylitis, hip arthroplasty may not be a useful procedure in this disorder when the prime indication for such surgery is restricted motion of the joint.

REFERENCES

1. Dwosh IL, Resnick D, Becker MA: Hip involvement in ankylosing spondylitis. *Arthritis Rheum.* In press, 1976
2. Charnley J: The long-term results of low-friction arthroplasty of the hip performed as a primary intervention. *J Bone joint Surg* 54B:61–76, 1972
3. Amstutz HC: Complications of total hip replacement. *Clin Orthop* 72:123–137, 1970
4. Patterson FP, Brown CS: The McKee-Farrar total hip replacement. Preliminary results and complications of 368 operations performed in

five general hospitals. *J Bone Joint Surg 54A*: 257–275, 1972
5. Mendes DG: Roentgenographic evaluation in total hip replacement. A study of 100 McKee-Farrar prosthetic replacements. *Clin Orthop* 95:104–110, 1973
6. Harris WH: Clinical results using the Muller-Charnley total hip prosthesis. *Clin Orthop* 86:95–101, 1972
7. Hamblen DL, Harris WH, Rottger J: Myositis ossificans as a complication of hip arthroplasty. *J Bone Joint Surg* 53B:764, 1971
8. Brooker AF, Bowerman JW, Robinson RA, Riley LH Jr: Ectopic ossification following total hip replacement. Incidence and a method of classification. *J Bone Joint Surg* 55A:1629–1632, 1973
9. Nollen AJG, Slooff TJJH: Para-articular ossifications after total hip replacement. *Acta Orthop Scand* 44:230–241, 1973
10. Edstrom B, Fellander M: Cup arthroplasty of the hip in rheumatic patients. A follow-up study. *Acta Orthop Belg* 40:113–125, 1974
11. Freeman PA: McKee-Farrar total replacement of the hip joint in rheumatoid arthritis and allied conditions. *Clin Orthop* 72:106–114, 1970
12. Welch RB, Charnley J: Low-friction arthroplasty of the hip in rheumatoid arthritis and ankylosing spondylitis. *Clin Orthop* 72:22–32, 1970
13. Arden GP, Ansell BM, Hunter MJ: Total hip replacement in juvenile chronic polyarthritis and ankylosing spondylitis. *Clin Orthop* 84:130–136, 1972
14. Wilde AH, Collins R, Mackenzie AH: Reankylosis of the hip joint in ankylosing spondylitis after total hip replacement. *Arthritis Rheum* 15:493–496, 1972

Am J Roentgenol 126:1189–1193, 1976

MEDIAL DEVIATION OF THE UPPER POLE CALYX ON THE INTRAVENOUS UROGRAM AS AN INDICATION OF VESICOURETERAL REFLUX

R. Brent Harrison,[1] Stuart S. Howards,[2] and Bruce R. Thomas[1]

ABSTRACT:

Eighty-three intravenous pyelograms were studied to evaluate thinning of the parenchyma on the medial edge of the superior pole of the kidney as an indicator of vesicoureteral reflux. The data indicate that this finding is suggestive of reflux: the greater the difference between the two sides, the more likely the patient is to reflux.

The association of vesicoureteral reflux, infection, and parenchymal scarring is well established [1]. Evidence of scarring or parenchymal loss is widely accepted as an indication for cystography. However, minimal parenchymal scarring in children may not be readily appreciated on the intravenous urogram. Filly et al. [2] suggest that renal parenchyma be compared on a point-by-point basis from side to side and from one examination to the next. Such measurements are often difficult or impossible in children due to overlying gas and fecal material.

Several observers have noted that the kidney moves closer to midline when scarring is present [3; 4, p. 148]. Friedland et al. [3] documented this with measurements of the distance from the upper pole calyx to the spine in 177 female children. They also found a remarkable consistency in this measurement between the two sides in normal children. The difference between the two sides averaged slightly over 1 mm, with the greatest difference being 2.9 mm in 11-year-olds.

We recently observed several cases of unilateral reflux in which the upper pole calyx on the refluxing side was closer to midline than its nonrefluxing counterpart. In some of these cases other signs of reflux were present, such as ureteropyelocaliectasis (fig. 1*A*) or atrophy of the kidney (fig. 1*B*). In others, there were few if any additional radiographic stigmata of reflux (fig. 2).

We therefore initiated a retrospective study to document the frequency of medial deviation of the upper pole calyx in normal and refluxing patients.

MATERIALS AND METHODS

A total of 83 intravenous pyelograms from 82 patients were selected for study. All patients had at least one cystogram. Cases with gross distortion of the upper tracts were excluded from the study, as were patients with spine or rotation anomalies which would distort measurements. The distance from the medialmost tip of each superior calyx to the interpedicular point was measured. We selected the supine film without compression on which the upper tracts were best seen. Films with significant rotation were excluded. There was usually good correlation when several films from the same patient were evaluated.

The series was divided into three groups: 30 patients with normal cystograms, 33 with unilateral reflux, and 19 with bilateral reflux. The type reflux was also noted (i.e., high pressure or low pressure). Low pressure cystograms are done with the meniscus 15 cm above the pubic symphysis, and high pressure cystograms were done with the patient straining, voiding, or with the meniscus 30 cm above the pubic symphysis. The high pressure–low pressure terminology has been used in this institution for many years. We agree with Williams [5, p. 117] and C. J.

[1] Department of Radiology, University of Virginia School of Medicine, Charlottesville, Virginia 22901. Address reprint requests to R. B. Harrison, Department of Radiology, Box 170, University of Virginia Hospital, Charlottesville, Virginia 22901.
[2] Department of Urology, University of Virginia School of Medicine, Charlottesville, Virginia 22901.

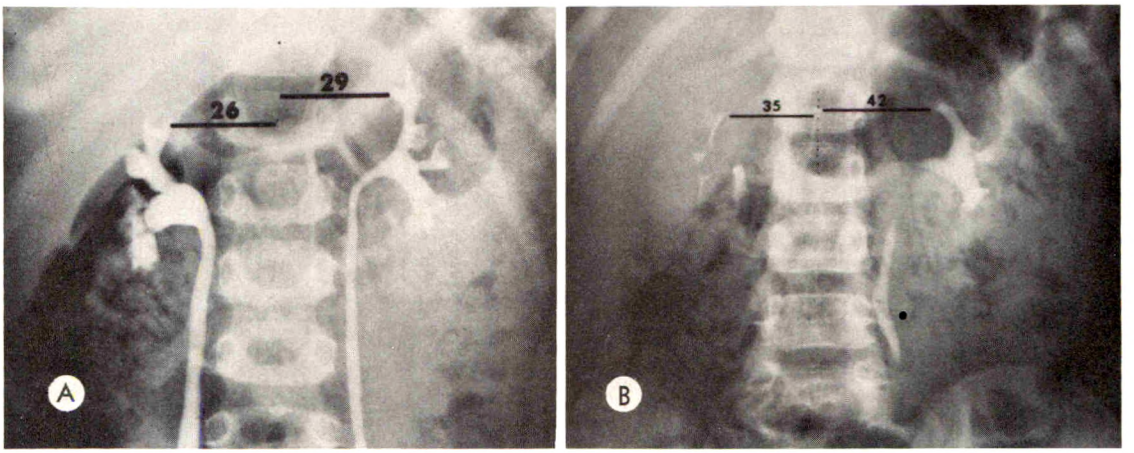


FIG. 1.—*A*, IVP showing mild ureteropyelocaliectasis on right with right upper pole calyx 3 mm closer to midline. Cystogram demonstrated right reflux. *B*, IVP showing right kidney smaller than left and right superior calyx 7 mm closer to midline. Cystogram demonstrated right reflux.

Hodson (personal communication) that this terminology is somewhat confusing since the low pressure reflux is actually a more severe reflux than high pressure reflux. Thus in this discussion, high pressure reflux should be considered the milder form of reflux.

RESULTS

The data are expressed both as the absolute difference in distance between the two sides and the relative difference. The relative difference is expressed as a percentage of the average distance from each superior calyx to midline:

$$\frac{\text{difference in mm}}{(R + L \text{ distance})/2} \times 100.$$

Normal Group

Of the 30 patients with normal cystograms, 23 (77%) had absolute differences

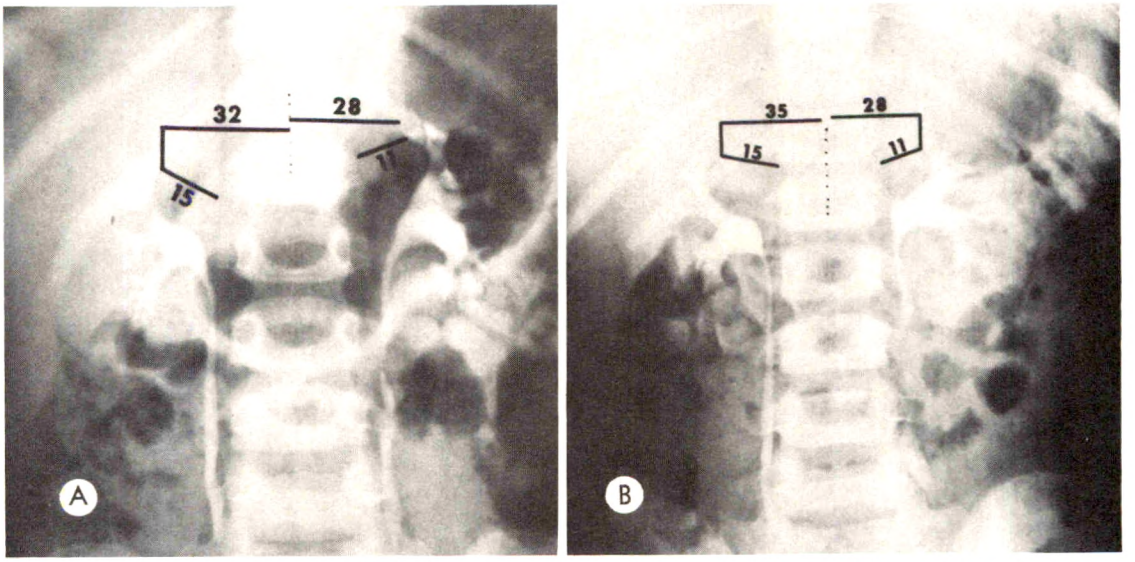


FIG. 2.—*A*, Normal-appearing IVP except parenchyma thinner on left and left superior calyx 4 mm closer to midline. Cystogram demonstrated left reflux. *B*, Normal-appearing IVP except parenchyma thinner on left with medial deviation of left superior calyx. Cystogram showed left reflux.

of 2 mm or less between the two sides and a relative difference of 8% or less. Only one case showed a relative difference of over 17%.

Unilateral Reflux Group

Among 33 patients with unilateral reflux, 12 (36%) had absolute differences of 2 mm or less and relative differences of 8% or less; 10 (30%) had relative differences of 17% or more (table 1). The absolute differences in this group (>17% relative difference) ranged from slightly over 4 mm to 17 mm. The refluxing side was closer to midline in 85% of patients. The nonrefluxing side was closer to midline with a relative difference of 8% or greater in only two cases (6%).

Bilateral Reflux Group

Of the 19 patients with bilateral reflux, six (32%) showed absolute differences of less than 2 mm and relative differences of 8% or less. Six (32%) showed relative differences of 17% or greater. The absolute differences in this group (>17%) ranged from 6 mm to 13 mm.

High Pressure versus Low Pressure Reflux

Of the 30 patients with normal cystograms, only 23% had relative differences of over 8%. However, of the 21 patients with low pressure reflux, 81% had relative differences of over 8%. Of the 31 patients with high pressure reflux, 42% had relative differences of over 8%.

Statistical Analyses

The data were subjected to extensive statistical analyses including the Wilcoxan, χ^2, and quantile tests as well as goodness of fit.

The normal and unilateral reflux populations as well as the normal and low pressure reflux populations were found to be statistically different with a high degree of confidence. The normal and high pressure reflux populations were also statistically different. The greater the difference, the more likely the patient is to reflux (table 2). With relative differences of 17% or more, the probability of reflux ranges between 2:1 and 6:1, depending on the method of analysis used. With relative differences between 8% and 17%, the probability of reflux ranges from 7:5 to 2:1, again, depending on the method used.

TABLE 1

RELATIVE DIFFERENCE IN DISTANCE FROM SUPERIOR CALYX TO MIDLINE

GROUP	RELATIVE DIFFERENCE (%)				TOTAL
	0–8	8–13	13–17	17–55	
Normal	23	4	2	1	30
Unilateral reflux	12	6	5	10	33

TABLE 2

PROBABILITY OF ABNORMALITY BASED ON RELATIVE DIFFERENCE IN DISTANCE FROM SUPERIOR CALYX TO MIDLINE

Method of Analysis and Relative Difference (%)	Probability (Abnormal:Normal)
Liberal:	
8	2:1
13	4:1
17	6:1
Conservative:	
11	7:5
17	2:1

DISCUSSION

Vesicoureteral reflux is one of the most controversial problems in pediatric urology. The diagnosis of reflux in the young child is often difficult because the symptoms are usually nonspecific [6]. The pathophysiology of reflux is poorly understood, although the work of Stephens and Lenaghan [7] and Tanagho et al. [8] has shed considerable light on the problem. There are conflicting reports as to whether reflux is primary or secondary and whether reflux alone produces renal damage or must be associated with infection [9–14]. There is also disagreement over the proper management of this condition [14–16].

Little confusion exists over the signifi-

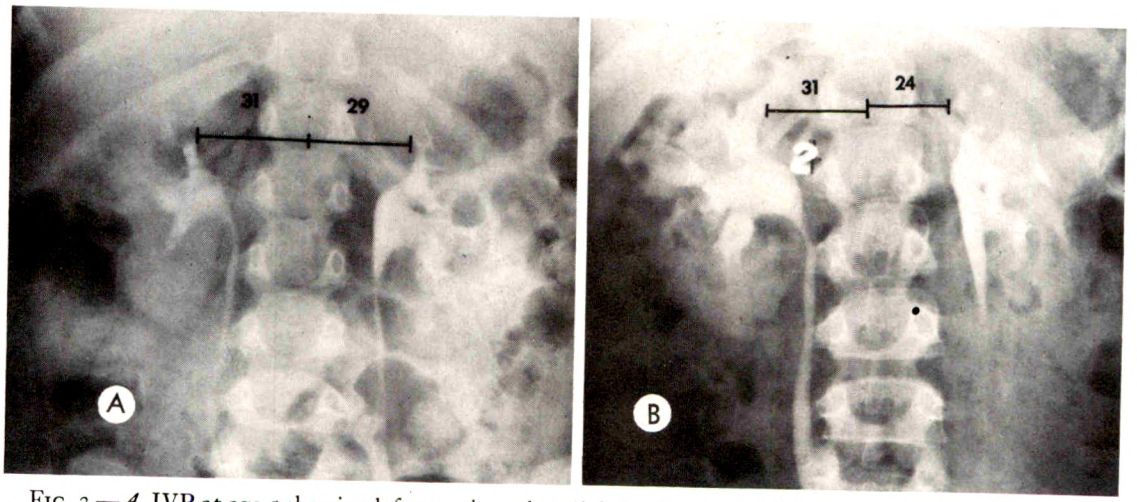


FIG. 3.—*A*, IVP at age 5 showing left superior calyx slightly closer to midline. *B*, IVP 3 years later showing left caliectasis and medial deviation of left superior calyx. Cystogram showed left low pressure reflux.

cance of vesicoureteral reflux. Reflux is associated with infection and renal damage in a high percentage of cases. Scott and Stansfield [1] found parenchymal scarring in 61% of kidneys with refluxing ureters and in only 7% with ureters that did not reflux. They also found reflux in 35% of children with infection [1]. The work of Hodson and Wilson [17] indicates a fatal outcome in the majority of cases with bilateral scarring, except when the scarring is minimal. Both Hodson [18] and Rolleston et al. [19] feel that the young kidney is particularly vulnerable to reflux. Therefore the importance of early diagnosis of vesicoureteral reflux is clear. The potential hazards of instrumenting the lower GU tract make most clinicians hesitant to submit every child with fever, failure to thrive, or feeding problems to cystography. The IVP is usually preferred as a screening procedure. This report is an attempt to add one more finding, asymmetry of position of the upper pole calyces, to the list of indications for cystography.

In the review of case material, we were able to document change in the position of the upper pole calyx over a period of time in only one case (fig. 3). Since this is largely a referral center, changes were usually present when the patient was first seen. However, this case would support the suggestion of Filly et al. [2] that fixed points be compared from study to study to evaluate renal damage.

This sign is based on the fact that renal damage associated with reflux is more likely to occur first in the upper poles. There is considerable support for this concept in the literature. Hodson and Wilson [17] found intrarenal reflux and focal scarring to occur more commonly in the upper poles. In normal individuals, the renal substance was found to be thicker in the upper poles and remarkably constant in all four poles [18]. Rolleston et al. [20] have further confirmed that the area of intrarenal reflux correlates well with the area of focal scarring. Ransley and Risdon [21] have recently reported that papillary-duct orifices in the pig are more open in the upper and lower poles and therefore more subject to intrarenal reflux. Preliminary observations suggest that such "refluxing papilla" also occur in the upper and lower poles in humans [21]. Fibrosis of the papillae have been described in hydronephrotic kidneys. This is presumed to be the result of pyelotubular backflow [9]. However, this conclusion has been questioned [22].

In our review of case material, we found several instances in which reflux occurred on only one of two sequential cystograms obtained within weeks or months of each

other. This confirms the observations of others that reflux may be an intermittent phenomenon [23–25]. This raises the possibility that perhaps some of our "normals" with wide differences in measurements could be intermittent refluxers.

CONCLUSIONS

From these data we conclude that renal damage associated with reflux and possibly infection frequently occurs first in the upper poles. This results in a loss of parenchyma on the medial edge of the kidney and medial deviation of the upper calyx. Such parenchymal damage may occur with minimal distortion of the calyceal architecture. Relative differences of 8%–17% (3–6 mm) should be viewed as suspicious and correlated with other findings in deciding whether to obtain cystography. Relative differences of over 17% should be an indication for cystography and probably is an indication for delayed or voiding cinecystography if the initial study is negative. Patients with low pressure reflux had renal damage more frequently than those with high pressure reflux.

ACKNOWLEDGMENTS

We thank Drs. Theodore E. Keats and Jay Y. Gillenwater for reviewing the manuscript. We also thank Drs. Donald Ramirez and Suresh Agarwal for the statistical analyses.

REFERENCES

1. Scott JES, Stansfield JM: Ureteric reflux and kidney scarring in children. *Arch Dis Child* 43:468–470, 1968
2. Filly R, Friedland GW, Govan DE, Fair WR: Development and progression of clubbing and scarring in children with recurrent urinary tract infections. *Radiology* 113:145–153, 1974
3. Friedland GW, Filly R, Brown BW: Distance of upper pole calyx to spine and lower pole calyx to ureter as indications of parenchymal loss in children. *Pediatr Radiol* 2:29–38, 1974
4. Williams DI: Urology in childhood, in *Encyclopedia of Urology* xv, Berlin, Springer-Verlag, 1958, p 148
5. Williams DI: *Urology in Childhood*, 2d ed. New York, Springer-Verlag, 1974
6. Smellie JM, Hodson CJ, Edwards D, Hormond ICS: Clinical and radiological features of urinary infection in childhood. *Br Med J* 2:1222–1226, 1964
7. Stephens FD, Lenaghan D: The anatomical basis and dynamics of vesicoureteral reflux. *J Urol* 87:669–680, 1962
8. Tanagho EA, Guthrie TH, Lyon RP: The intravesical ureter in primary reflux. *J Urol* 101:824–832, 1969
9. Green H, Fingerhut AG, French S: Mechanism of renovascular backflow—a pathophysiologic study. *Radiology* 92:531–536, 1972
10. King LR, Idriss FS: The effect of vesicoureteral reflux on renal function in dogs. *Invest Urol* 4:419–427, 1967
11. Pawlowsky JM: Peripelvic urine granuloma. *Am J Clin Pathol* 34:64–67, 1960
12. Redman JF, Scribner LJ, Bissade NK: Apparent failure of renal growth secondary to vesicoureteral reflux. *Urology* 3:704–707, 1974
13. Rolleston GL: Vesico-ureteric reflux in infancy on radiological aspects, in *Proceedings International Symposium on Renal Infection and Renal Scarring*, Melbourne, Mercedes Publishing Co., 1970, pp. 246–256
14. Shopfner CE: Vesicoureteral reflux. *Radiology* 95:637–648, 1970
15. Devine PC, Davis CS, Devine CD, Fiveash JG: Vesicoureteral reflux in children. *Urology* 3:315–318, 1974
16. Scott JES, Stansfield JM: Treatment of vesicoureteric reflux in children. *Arch Dis Child* 43:323–328, 1968
17. Hodson CJ, Wilson S: Natural history of chronic pyelonephritic scarring. *Br Med J* 2:191–194, 1965
18. Hodson CJ: Radiology in pyelonephritis. *Curr Probl Radiol* 2:1–32, 1972
19. Rolleston GL, Shannon FT, Utley WLF: Relationship of infantile vesicoureteral reflux to renal damage. *Br Med J* 1:460–463, 1970
20. Rolleston GL, Maling TMJ, Hodson CJ: Intrarenal reflux and the scarred kidney. *Arch Dis Child* 49:531–539, 1974
21. Ransley PG, Risdon RA: Renal papillae and intrarenal reflux in the pig. *Lancet* 2:1114–1115, 1974
22. Hodson CJ, Craven JD, Lewis DG, Matz LR, Clarke RJ, Ross EJ: Experimental obstructive nephropathy in the pig. *Br J Urol* 41, suppl: 5–51, 1969
23. Bunge RG: Further observations with delayed cystograms. *J Urol* 71:427–434, 1954
24. Stewart CM: Delayed cystograms. *J Urol* 70:588–593, 1953
25. Stewart CM: Cystography and voiding cystoureterography. *J Urol* 74:749–759, 1955

Am J Roentgenol 126:1194–1196, 1976

ULTRASOUND DIAGNOSIS OF POSTTRANSPLANT RENAL LYMPHOCELE

JOSEPH F. PHILLIPS,[1,2] HARVEY L. NEIMAN,[1,3] AND THOMAS L. BROWN[1,4]

ABSTRACT:

Two cases of posttransplant renal lymphoceles were diagnosed and followed by ultrasound. Lymphocele formation is a significant but often not thought of cause in a rejectionlike picture. Because of its noninvasive nature, ultrasound is an ideal method to detect and follow this complication.

The development of a lymphocele is an uncommon but serious complication of renal transplant surgery. A lymphocele can present with signs mimicking rejection of the kidney, and it is frequently diagnosed only after considerable host insult and damage has occurred. Ultrasound is an extremely useful tool to detect the presence of a lymphocele because it readily distinguishes the fluid collection from the surrounding soft tissue. Ultrasound avoids the use of contrast material or instrumentation of the genitourinary system, and it can be performed even in the absence of renal function. Ultrasound can also be used to determine the approximate volume of fluid collection and to follow its progression or resolution.

METHOD

A commercially available Picker Echoview VIIIA ultrasonic scanner with a 2.25 MHz, 1.2 cm diameter, 10 cm focus transducer was used for the examinations. The patients were examined in the supine position with transverse, longitudinal, and oblique cross sections. The bladder was emptied prior to examination.

CASE REPORTS

Patient 1

R. M. is a 15-year-old female whose first transplant had been removed because of rejection and a complicating lymphocele. Fifteen days after her second renal transplant, she developed hypertension and an elevation of creatinine and BUN. Ultrasound examination of the second kidney showed a fluid-filled mass superior to the transplant (fig. 1*A*). Surgical drainage of 2.5 liters of fluid was followed by internal marsupialization with a peritoneal window. The patient's renal function returned to normal. The collection recurred, and multiple percutaneous aspirations of up to 2,500 ml of fluid were performed. Serial ultrasound studies showed progressive increase in size with development of a huge retroperitoneal lymphocele (fig. 1*B*). A second operation was performed $1\frac{1}{2}$ months posttransplant confirming the presence of a huge retroperitoneal lymphocele. It was loculated with multiple adhesions. Lysis of adhesions was performed and closed-tube sump drainage was instituted. This resulted in complete obliteration of the lymphocele. An ultrasound study 4 months posttransplant showed a normal-appearing transplant bed (fig. 1*C*).

Patient 2

S. M. is a 25-year-old black male who developed a right hydrocele 3 weeks after transplant surgery. The hydrocele persisted although renal function remained excellent. Percutaneous aspiration of the fluid collection was performed. The chemistry determinations revealed lymphatic fluid. Ultrasound examination showed a collection of fluid lateral to the transplant (fig. 2). Surgical exploration disclosed a lymphocele surrounding the transplanted kidney. Sump tube suction drainage was instituted. Initially 200–300 ml of fluid per day were drained. Over a period of 6–8 weeks drainage progressively decreased and then stopped. A repeat ultrasound examination showed oblitera-

[1] Department of Radiology, Walter Reed Army Medical Center, Washington D.C. 20012.
[2] Present address: Department of Radiology, University of South Alabama School of Medicine, 2451 Fillingim Street, Mobile, Alabama 36617. Address reprint requests to J. F. Phillips.
[3] Present address: Department of Radiology, Northwestern Memorial Hospital, Northwestern University School of Medicine, Chicago, Illinois 60611.
[4] Present address: Department of Radiology, Sacred Heart Hospital, Pensacola, Florida 32504.

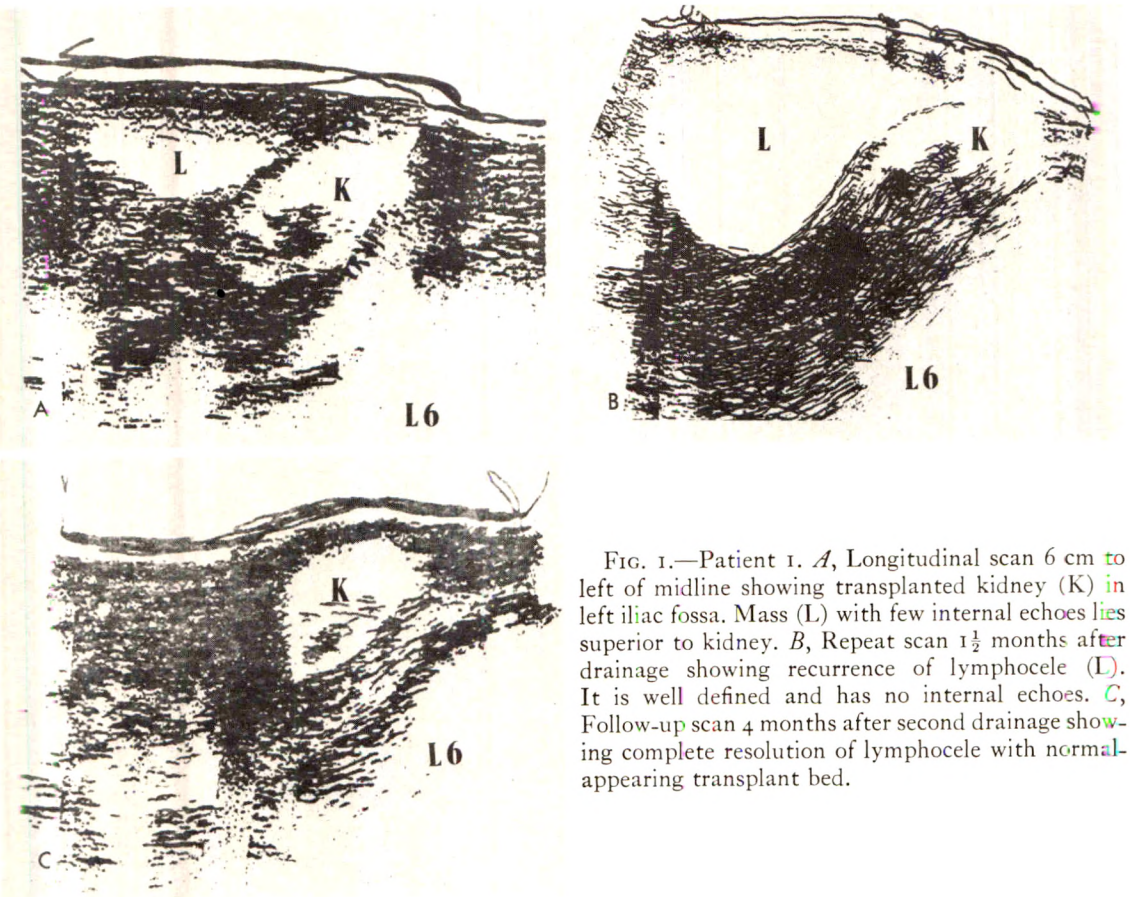


FIG. 1.—Patient 1. *A*, Longitudinal scan 6 cm to left of midline showing transplanted kidney (K) in left iliac fossa. Mass (L) with few internal echoes lies superior to kidney. *B*, Repeat scan 1½ months after drainage showing recurrence of lymphocele (L). It is well defined and has no internal echoes. *C*, Follow-up scan 4 months after second drainage showing complete resolution of lymphocele with normal-appearing transplant bed.

tion of the cystic space and a normal-appearing transplant bed. The renal function remained excellent throughout the course of the disease.

DISCUSSION

Disturbance of renal function in the posttransplant period can be caused by immunologic rejection, compromise of the renal artery or vein, and obstruction or disruption of the ureter. Another important possibility to consider is the formation of a lymphocele.

There is a 1%–8% incidence of lymphocele formation following renal transplantation [1, 2]. The time of onset is from 1 to 17 months after surgery [1]. Prior rejection episodes and postoperative or postdialysis renal hematoma are thought to be predisposing factors [3]. A lymphocele can present with various symptoms. It can mimic rejection by compromising renal function, probably secondary to compression of the renal parenchyma, and/or by displacement and kinking of the renal vessels and ureter. Some patients experience leg pain and swelling most likely secondary to venous compression or thrombosis. A palpable mass is frequently present in the larger lymphoceles. A hydrocele can also occur.

Two possible sources are reported for the site of production of the lymphatic fluid. Cutting of the recipient's lymphatics during the transplant surgery could lead to extravasation of lymphatic material; this has been documented by lymphography [4]. The second source is probably the transplant kidney itself, with lymph leakage occurring from the pericapsular and hilar branches. Rejection may aggravate formation of a lymphocele because the ensuing edema of the kidney increases intrarenal pressure and therefore increases lymph flow [3]. Perirenal hematoma pro-



FIG. 2.—Transverse scan 7 cm above symphysis showing collection of lymphatic fluid (L) lateral and posterior to transplanted kidney (K).

duces a dead space and a potential site for collection of lymphatic fluid.

Excretory urography is useful in the diagnosis of a lymphocele when it reveals displacement of the transplant or impression on the bladder or ureter [1]. Its disadvantages are that significant renal function must be present and it necessitates injection of contrast material. Retrograde cystography can reveal similar information, but it requires instrumentation of the bladder.

Ultrasound is ideally suited for the diagnosis of lymphoceles because of its ability to detect fluid-tissue interfaces. It is noninvasive and can be performed in the absence of renal function. Typically a lymphocele appears as a well-defined echo-free area adjacent to the renal transplant. It may extend in any direction. The differential diagnosis includes urinoma, abscess, and hematoma. Hematoma and abscess would be expected to show some internal echoes not seen in the entirely fluid collections of a lymphocele or urinoma. Percutaneous aspiration will yield fluid for the analysis of urea nitrogen and thus distinguish a lymphocele from a urinoma. Following exclusion of a urinoma, ultrasound can be used to follow progression or resolution of the lymphocele.

Possible treatment regimens include repeat percutaneous aspiration, but this runs the risk of complicating infection and almost certain recurrence. External drainage or marsupialization of a lymphocele has been advocated and is curative, although there is a risk of infection. Internal marsupialization avoids most of the risks of infection; however, the lymphocele may recur [5]. Satisfactory results have also been obtained with continuous closed-suction drainage to obliterate the dead space until the collection of lymphatic fluid has ceased [3]. A small asymptomatic lymphocele can be followed and not treated surgically, since there can be spontaneous resolution [6].

Lymphocele formation can be prevented by careful ligation of all the recipient lymphatics and by avoiding postoperative hematoma formation through careful hemostasis and careful anticoagulation [3].

The unsuspected lymphocele may mimic symptoms of renal transplant rejection. Ultrasound, because of its noninvasive nature, can be easily applied to all transplant patients to exclude this possibility.

REFERENCES

1. Mott C, Schreiber MH: Lymphoceles following renal transplantation. *Am J Roentgenol* 122:821–827, 1974
2. Starzl TE, Groth CG, Putnam CW, Penn I, Halgrimson CG, Flatmark A, Gecelter L, Brettschneider L, Stonington OG: Urologic complications in 216 human recipients of renal transplants. *Ann Surg* 172:1–22 1970
3. Roshid A, Posen G, Couture R, McKay O, Wallington J: Accumulation of lymph around the transplanted kidney (lymphocele) mimicking renal allograft rejection. *J Urol* 3:145–147, 1974
4. Koeher PR: Injuries and complications of the lymphatic system following renal transplantation. *Lymphology* 5:61–67, 1972
5. Zincke H, Woods JE, Aguilo JJ, Leary FJ, DeWeerd JH, Frohnert PP, Hattery RR: Experience with lymphoceles after renal transplantation. *Surgery* 77:444–450, 1975
6. Dodd GD, Rutledge F, Wallace S: Postoperative pelvic lymphocyst. *Am J Roentgenol* 108:312–323, 1970

Am J Roentgenol 126:1197–1202, 1976

PSEUDOTUMOR OF THE KIDNEY: A SEQUEL TO REGIONAL GLOMERULONEPHRITIS

THOMAS A. DEPNER,[1] KEVIN G. RYAN,[2] AND HIROSHI YAMAUCHI[1,2]

ABSTRACT:

An unusual case of chronic renal failure associated with an abnormal intravenous urogram simulating renal neoplasm is discussed. Extensive radiographic and histologic studies support the contention that the observed mass lesion resulted from a segmental or regional compensatory hypertrophy. It is likely that this case represents a variant of unilateral glomerulonephritis with sparing of a segment or lobe of one kidney and subsequent hypertrophy of that segment as the remaining renal mass atrophied.

INTRODUCTION

Mass lesions of the kidney formed by local overgrowth of otherwise normal renal parenchyma may simulate renal tumors when viewed by intravenous urography or renal angiography [1–5]. The cause of these pseudotumors is presumed to be compensatory hypertrophy or a developmental anomoly involving only one segment or lobe of the kidney. The following case documents the development of such a compensatory hypertrophy in a patient with clinical and biopsy evidence for glomerulonephritis.

CASE REPORT

A 35-year-old construction worker was referred to the Woodland Clinic on December 12, 1973, for evaluation of chronic renal failure. Exactly 10 years previously, asymptomatic pyuria was noted after a routine examination, and an intravenous urogram was obtained (fig. 1*A*). This study showed normal kidneys in all respects. Urinalysis revealed 2+ white cells, no red cells, and no protein. Urine cultures, including TB cultures, were negative, and cystoscopy was unremarkable. In July 1971, hypertension was first noted and the patient was treated with diuretics. Subsequent blood pressures were normal or mildly elevated, and urinalyses revealed 1–2+ albumin. At the time of referral his blood pressure was 130/90 mm Hg, BUN was 59 mg/100 ml, serum creatinine 4.5 mg/100 ml, and creatinine clearance 19 cm^3/min per 1.73 m^2 body surface area. His physical examination was unremarkable.

An intravenous urogram demonstrated a mass at the lower pole of the left kidney with marked contraction of the remainder of the left kidney and the entire right kidney (figs. 1*B* and 2). A subsequent aortogram and selective renal arteriograms showed a normal vascular supply with marked hypertrophy of the interlobar arteries supplying the left lower pole. There was a generalized decrease in caliber of the remaining arteries and marked cortical atrophy involving all but the left lower pole which was noted to have increased in size since the 1963 study (figs. 3 and 4). With guidance from the angiographic nephrogram and fluoroscopy, a right percutaneous renal biopsy was obtained. This revealed crowding of numerous sclerotic acellular glomeruli with numerous senechiae but minimal periglomerular fibrosis. (fig. 5*A*). A rare partially perfused glomerulus showed wrinkled and collapsed basement membranes on PAS stain but no proliferative changes (fig. 5*B*). The arterioles, which were also crowded closely together, showed slight to moderate medial and intimal hypertrophy. There was also a mild interstitial round cell infiltrate and numerous atrophic cast-filled tubules simulating a thyroid appearance. Sections for immunofluorescence and electron microscopy contained no perfused glomeruli.

Treatment for hypertension was begun with 25 mg hydrochlorothiazide, 50 mg triamterene,

[1] Department of Medicine, University of California School of Medicine, Davis, and Sacramento Medical Center, 2315 Stockton Boulevard, Sacramento, California 95817. Address reprint requests to T. A. Depner at the Sacramento Medical Center.
[2] Departments of Medicine and Radiology, Woodland Clinic Medical Group, Woodland, California 95695.

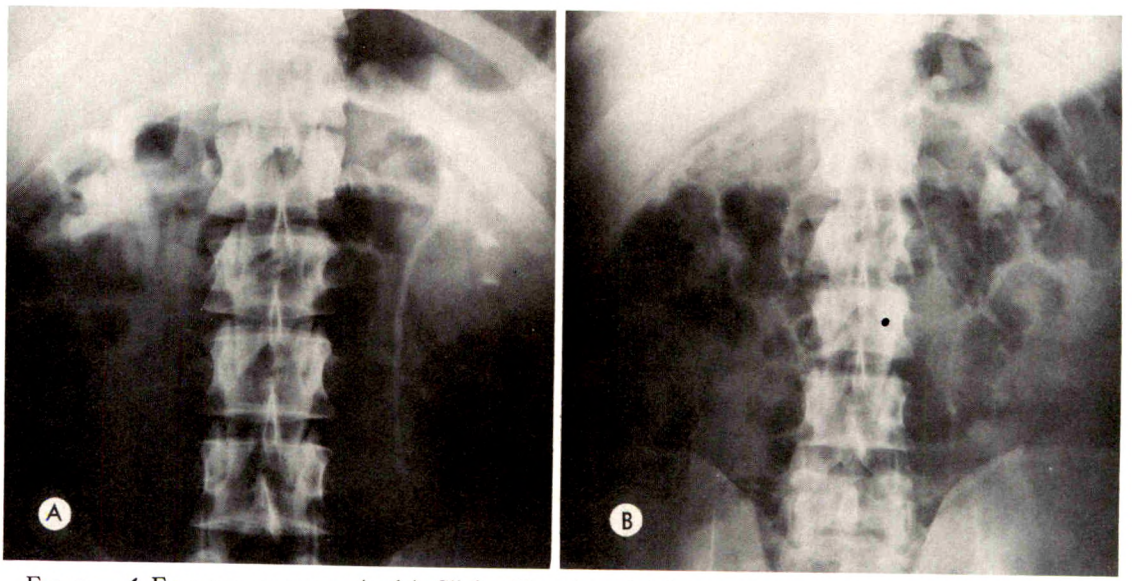


FIG. 1.—*A*, Excretory urogram (1963). Slight dilatation of right renal collecting system can be attributed to abdominal compression used during examination. Right and left kidneys measure 12.0 and 13.1 cm in length, respectively. Complete urogram interpreted as normal. *B*, Excretory urogram 10 years later. No contrast material visible within right kidney. Concentration within the left collecting system is normal, and, except for enlargement at lower pole, cortical outline is markedly contracted.

and 125 mg alpha-methyl dopa twice per day. His blood pressure subsequently fell to an average of 120/80 mm, and renal function remained stable with a serum creatinine of 4.8 mg/100 ml 1½ years after initial evaluation.

DISCUSSION

Initial interpretation of the second urogram was that of tumor at the left lower pole with coincident atrophy of the right



FIG. 2.—Excretory urography with nephrotomogram. Right kidney is small, measuring 9.5 cm in length. Note marked contraction of parenchyma of upper two-thirds of left kidney. Left lower pole is hypertrophied, measuring 8 cm in transverse diameter compared to 6 cm on 1963 urogram.

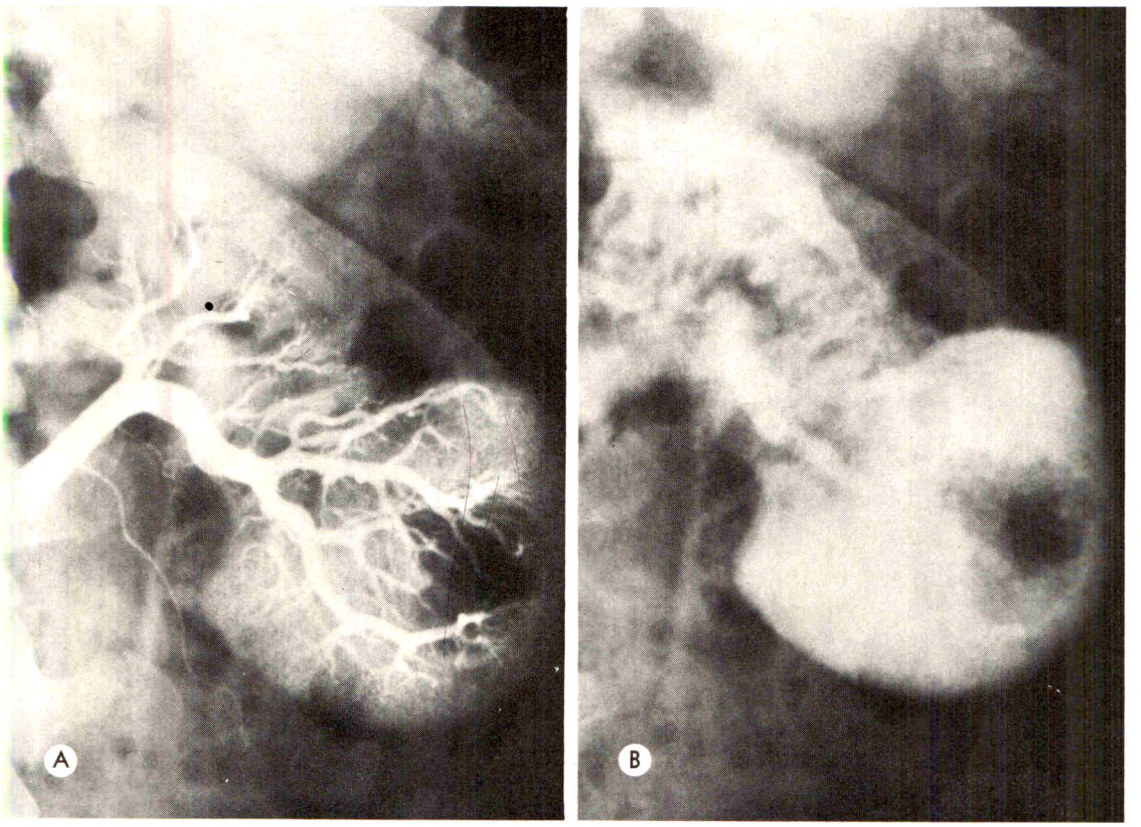


FIG. 3.—*A*, Selective left renal arteriogram. Upper two-thirds shows pruning of interlobular arteries and general decrease in caliber of arteries supplying this region. Interlobular arteries supplying lower pole are markedly hypertrophied. *B*, Nephrogram phase.

kidney. However, closer scrutiny disclosed that all of the "nontumor-involved" renal mass was atrophic and led to a suspicion that the "tumor" was actually a hypertrophied segment of the kidney at the left lower pole. This suspicion was confirmed by arteriography which, in addition, revealed patent vessels to all renal segments. The tumorlike expansion of the left lower pole resulted from compensatory hypertrophy, a process which is well described in unilaterally nephrectomized patients under 30 years of age [6]. Furthermore, the hypertrophy observed attests to the complete protection or noninvolvement of that segment of the kidney by a disease process which is no longer active.

The urographic finding of nonuniform atrophy suggests pyelonephritis as the underlying pathology. This inflammatory disease is notorious for its propensity to involve the kidney in a patchy distribution often resulting in an irregular cortical outline with skip areas and focal scarring [7]. Indeed, asymmetric hypertrophy resulting from chronic pyelonephritis and simulating renal tumor has been described [2, 4]. However, this patient's clinical course is highly inconsistent with classic pyelonephritis, and there have been a significant number of negative urine cultures. The observations of minimal or no blunting of calyces and uniform involvement of the entire right kidney and upper two-thirds of the left kidney do not support the diagnosis of chronic pyelonephritis. Furthermore, the renal biopsy showed very little interstitial inflammation with no acute inflammatory cells and very little periglomerular fibrosis, all of which are prominent features of chronic pyelonephritis [8].

Severe hypertension may lead to uniform

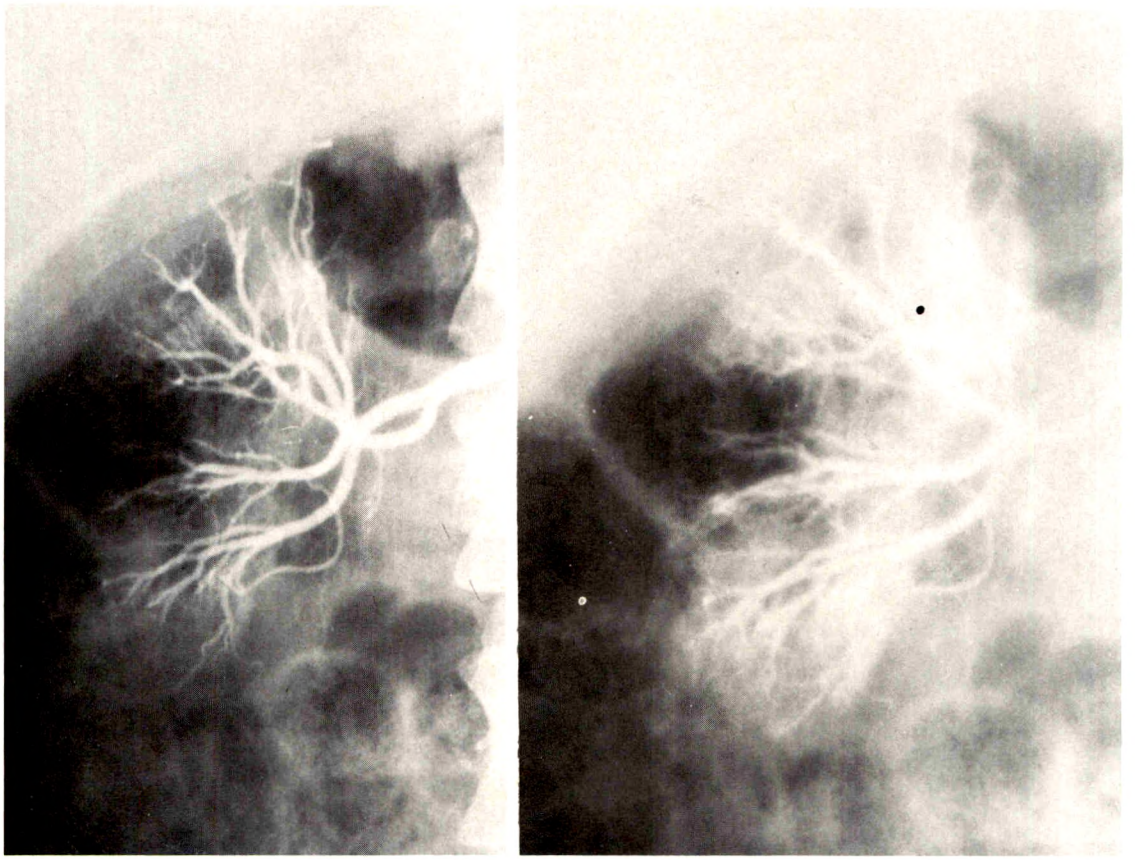


FIG. 4.—Selective right renal arteriogram. Note marked pruning of interlobular arteries and remarkably thin cortex. Corticomedullary junction is preserved and medulla has maintained relatively normal size compared to 1963 visualization.

diminution in kidney size secondary to arteriolar nephrosclerosis, a process which is often not found in the kidney protected by unilateral main renal artery stenosis [9, 10]. However, such severe renal atrophy is unlikely to have resulted from this patient's mild hypertension, which was of relatively short duration and well controlled with medications. The finding of only mild to moderate intimal and medial hypertrophy of the arterioles in the right renal biopsy specimen fails to support this diagnosis. Furthermore, the selective left renal arteriograms demonstrated no evidence for the conjectured stenosis.

Cortical necrosis which can result from severe ischemia or intravascular coagulation is also a patchy process but is unlikely to have occurred in this patient since he did not recall a period of risk for this type of injury. The lack of cortical calcification and crowding of sclerotic glomeruli with minimal scarring seen in the biopsy fails to support this etiology.

Diffuse cortical atrophy is most commonly caused by chronic glomerulonephritis which characteristically involves the kidneys in a uniform distribution resulting in smooth cortical outlines [8, 10, 11]. These findings, together with the history of sterile pyuria, proteinuria, and the renal biopsy, point to a primary glomerular disorder.

Reports of unilateral glomerulonephritis, however, raise the important question of whether a protective mechanism is acting which might spare an entire kidney or segment of kidney, resulting in a nonuniform radiographic appearance [12–15]. In studies of rabbit kidneys subjected to chronic

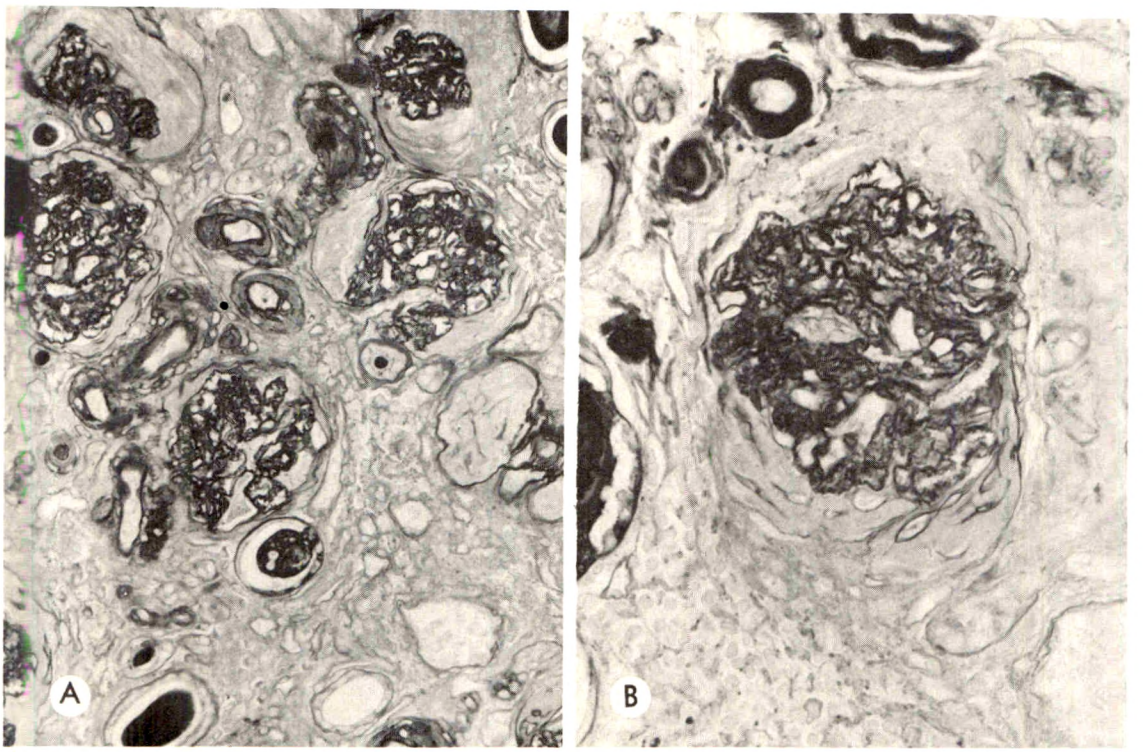


FIG. 5.—PAS-stained renal biopsy at ×200 (*A*) and ×400 (*B*). *A*, Glomeruli obsolescent and crowded together due to marked tubular atrophy. Note numerous synechiae between the glomerular tufts and Bowman's capsule. *B*, Single glomerulus revealing few patent capillary loops, loss of Bowman's capsule, wrinkled and collapsed basement membranes, and moderate amount of fibrous connective tissue adjacent to glomerular tuft.

serum sickness glomerulonephritis, Germuth et al. [16] observed that despite the presence of advanced disease, an occasional normal glomerulus was found associated with a greatly expanded Bowman's space and an obstructing proteinaceous cast found distally in the same nephron. This observation led to further studies which showed that constriction of the main renal artery or ligation of a ureter reduces or abolishes development of glomerulonephritis [17]. Presumably the combination of high hydrostatic pressure and high filtration rate at the glomerulus are necessary for the entrapment there of immune complexes and may explain why the kidney is often the only organ damaged by immune complex disease. There is no biopsy evidence for immune complex deposition in this patient's kidney, but the tissue was observed at a late state in the evolution of the glomerulonephritis when these elements may have disappeared. Whether a protective mechanism such as that suggested by Germuth and co-workers or an as yet unknown process may preserve the kidney from other destructive injuries remains to be established.

This case, therefore, is a striking demonstration of the development of a segmental compensatory hypertrophy mimicking renal tumor. Clinical, radiographic, and histological evidence implicates glomerulonephritis as the primary underlying insult which resulted in near total loss of renal function. This process, which later ended, spared the left lower pole allowing that subsequently hypertrophied segment to maintain the patient's vital renal functions.

ACKNOWLEDGMENTS

We are extremely grateful for the meticu-

lous scrutiny of this patient's renal biopsy by Drs. Charles N. Gamble and John C. Lee from Sutter Memorial Hospital.

REFERENCES

1. Azimi F, Bryan PJ: Familial occurrence of renal pseudotumours due to enlarged column of Bertin in two brothers and their first cousin. *Clin Radiol* 25:467–474, 1974
2. Felson B, Moskowitz M: Renal pseudotumors: the regenerated nodule and other lumps, bumps and dromedary humps. *Am J Roentgenol* 107:720–729, 1969
3. Kyaw MM: Renal pseudotumor due to infolding column of Bertin. *JAMA* 219:1634, 1972
4. Lopez FA: Renal pseudotumors. *Am J Roentgenol* 109:172–184, 1970
5. King MC, Friedenberg RM, Tena LB: Normal renal parenchyma simulating tumor. *Radiology* 91:217–222, 1968
6. Heideman HD, Rosenbaum HD: A study of renal size after contralateral nephrectomy. *Radiology* 94:599–601, 1970
7. Friedenberg MJ, Eisen S, Kissane J: Renal angiography in pyelonephritis, glomerulonephritis, and arteriolar nephrosclerosis. *Am J Roentgenol* 95:349–363, 1965
8. Braude AI: Current concept of pyelonephritis. *Medicine* 52:257–264, 1973
9. Brown JJ, Peart WS, Owen K, Robertson JI, Sutton D: The diagnosis and treatment of renal artery stenosis. *Br Med J* 2:327–338, 1960
10. Mena E, Bookstein JJ, Gikas PW: Angiographic diagnosis of renal parenchymal disease. *Radiology* 108:523–532, 1973
11. Ekelund L, Kaude J, Lindholm T: Angiography in glomerular disease of the kidney. *Am J Roentgenol* 119:739–747, 1973
12. Clinicopathological Conference: A case of aortitis with nephrotic syndrome. *Br Med J* 2:359–365, 1969
13. Fahr T: Die Funktionsbehinderung der Niere als hemmendes Moment bei der Entwicklung von Glomerulonephritis und maligner Nephrosklerose. *Dtsch Arch Klin Med* 191:52–59, 1943
14. Palmer JM, Eversole SL, Stamey TA: Unilateral glomerulonephritis. *Am J Med* 40:816–822, 1966
15. Salyer WR, Salyer DC: Unilateral glomerulonephritis. *J Pathol* 113:247–251, 1974
16. Germuth FC, Senterfit LB, Pollack AD: Immune complex disease. I. Experimental acute and chronic glomerulonephritis. *Johns Hopkins Med J* 120:225–241, 1967
17. Germuth FG, Kelemen WA, Pollack AD: Immune complex disease. II. The role of circulatory dynamics and glomerular filtration in the development of experimental glomerulonephritis. *Johns Hopkins Med J* 120:252–257, 1967

Am J Roentgenol 126:1203–1210, 1976

TORTUOSITY OF THE CAVERNOUS CAROTID ARTERIES CAUSING SELLAR EXPANSION SIMULATING PITUITARY ADENOMA

RICHARD D. ANDERSON[1]

ABSTRACT:

Tortuous, medially-displaced cavernous carotid arteries may cause sellar enlargement which simulates pituitary adenoma. Systemic hypertension appears to account for this tortuosity in some cases, while a congenital anomaly is probably responsible in others. Medical position of the carotid sulci may be demonstrated on sellar tomography. Cerebral arteriography provides the correct diagnosis. Surgery, particularly transsphenoidal hypophysectomy, should be avoided in such patients.

When skull films demonstrate sellar expansion with an intact lamina dura, pituitary adenoma is the most likely diagnosis. In some instances surgery or radiation therapy has been undertaken without obtaining cerebral arteriography. The variety of other lesions which can cause these sellar changes, among them aneurysms of the internal carotid artery, makes this approach unwise. We wish to report a vascular anomaly which causes sellar enlargement and for which peremptory surgery, particularly transsphenoidal hypophysectomy, could have an unfortunate result. In the following patients, tortuosity and deviation of the cavernous carotid arteries into the sellar midline caused sellar expansion which on plain films was indistinguishable from pituitary adenoma. Tomography suggested the entity in two cases. Cerebral arteriography was necessary for diagnosis and should be obtained before treatment of suspected pituitary neoplasm.

CASE REPORTS

Case 1

This 39-year-old white female was referred by her family physician for evaluation of severe hypertension of 3 years duration. She complained of headaches. Her past history included hysterectomy and bilateral oophorectomy for carcinoma of the cervix 13 years prior to admission. On admission her blood pressure was 190/100.

Skull films demonstrated that the sella was elongated in the AP dimension, measuring 19.5 mm; the superoinferior dimension was 8 mm. Frontal tomograms demonstrated a convex sellar floor approximately 15 mm in width. The left carotid sulcus lay 3.5 mm from the midline in the midportion of the sellar floor (fig. 1*C*; more posteriorly the left carotid sulcus grooved the sphenoid 6 mm from the midline (fig. 1*D*). Lateral tomograms demonstrated thinning and posterior displacement of the dorsum with loss of the lamina dura along the inner aspect of the dorsum (fig. 1*A*) and a deep left carotid sulcus (fig. 1*B*). The posterior clinoid processes were preserved. Estimated sellar volume was 1,170 mm^3.

Neurological examination, including visual fields, was negative. Papilledema was not present. Vanillylmandelic acid and catecholamine determinations were normal. The patient was thought to have essential hypertension.

Although there was no clinical or endocrinological evidence of pituitary disease, the sellar changes were consistent with pituitary adenoma. Additional studies were obtained. CT scan with contrast medium was negative. Cerebral arteriography demonstrated that the left cavernous carotid artery was tortuous, slightly ectatic, and extended into the sella within 2 mm of the midline (fig. 2). The left internal carotid at the level of the anterior clinoid was 3 mm from the midline. The right cavernous carotid was also tortuous and

Received January 3, 1976; revised February 17, 1976.
[1] Department of Diagnostic Radiology, University of Alabama School of Medicine, Birmingham, Alabama 35233.

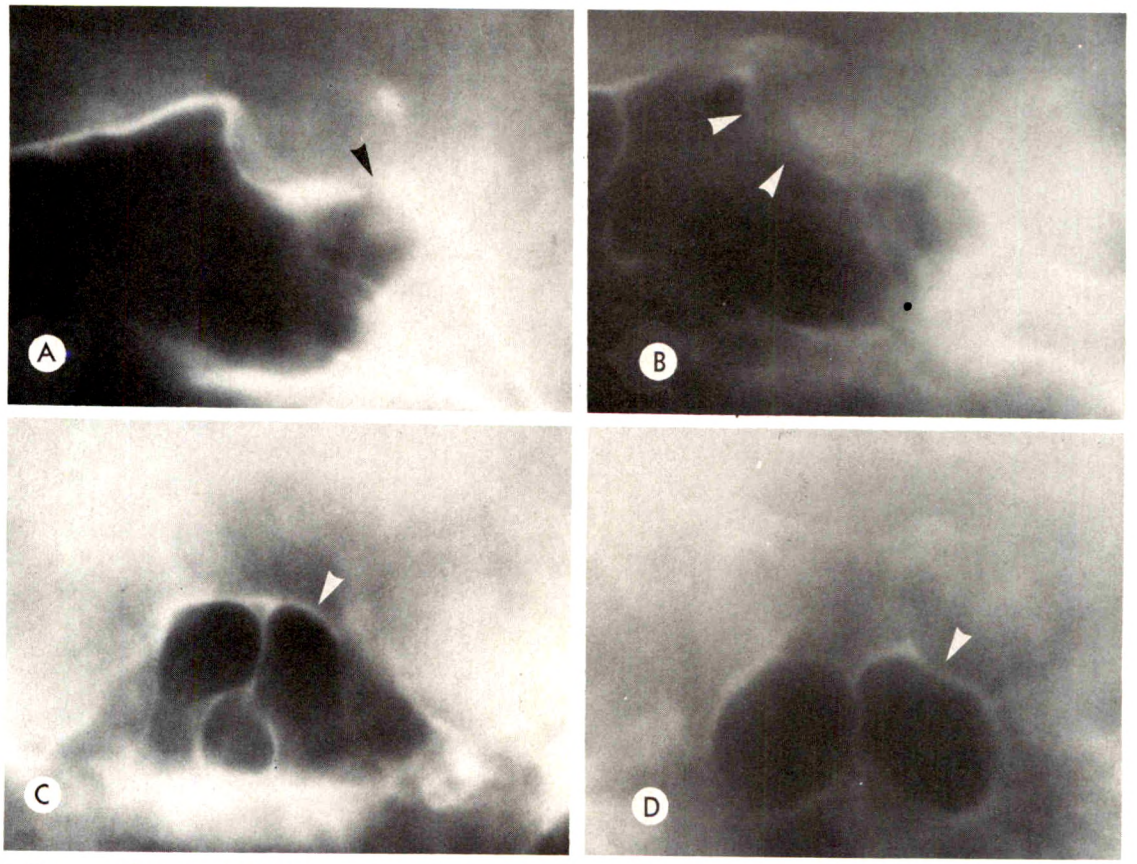


FIG. 1.—Case 1. *A*, Midline tomography in lateral projection showing localized erosion of lamina dura (*arrow*). *B*, Tomographic section 6 mm to left of midline showing left carotid sulcus. *C*, Frontal tomogram through sellar floor demonstrating left carotid sulcus 3.5 mm from midline (*arrow*). *D*, Frontal tomogram at level of dorsum demonstrating left carotid sulcus (*arrow*).

slightly ectatic but lay 6 mm from the midline in the cavernous segment and 5 mm from the midline in the clinoid segment. No other abnormalities were demonstrated. There were no angiographic signs of pituitary adenoma [1] or ventricular enlargement.

Case 2

This 50-year-old black male presented with a 3 month history of low grade fever, muscle pain, and headache. Physical examination demonstrated proximal muscle tenderness in the upper and lower extremities. Neurological examination, including visual field testing, was normal. There were no chiasmal signs or papilledema. His blood pressure was 110/60; there was no history of hypertension. Erythrocyte sedimentation rate was elevated (46). Temporal artery biopsy was negative; muscle biopsy showed type 2 fiber atrophy.

Plain skull films and lateral tomograms showed the sella to be enlarged, measuring 17 mm in the AP and 12 mm in the superoinferior dimensions. The lamina dura was intact (figs. 3*A* and 3*B*). Frontal and lateral tomograms showed deep carotid sulci separated by only 1 mm (fig. 3*D*). Sellar volume was calculated at 102 mm^3. Even though no clinical or endocrinologic evidence of pituitary disease was present, additional studies were requested because of the sellar changes. A pneumoencephalogram was negative (fig. 4). Cerebral arteriography demonstrated that both cavernous carotid arteries were tortuous and extended to within 1–2 mm of the midline at the level of the sella turcica (figs. 5 and 6). Bilateral selective external carotid arteriograms were negative. A CT scan with contrast medium demonstrated vascular structures consistent with the cavernous carotid arteries abutting and extending into

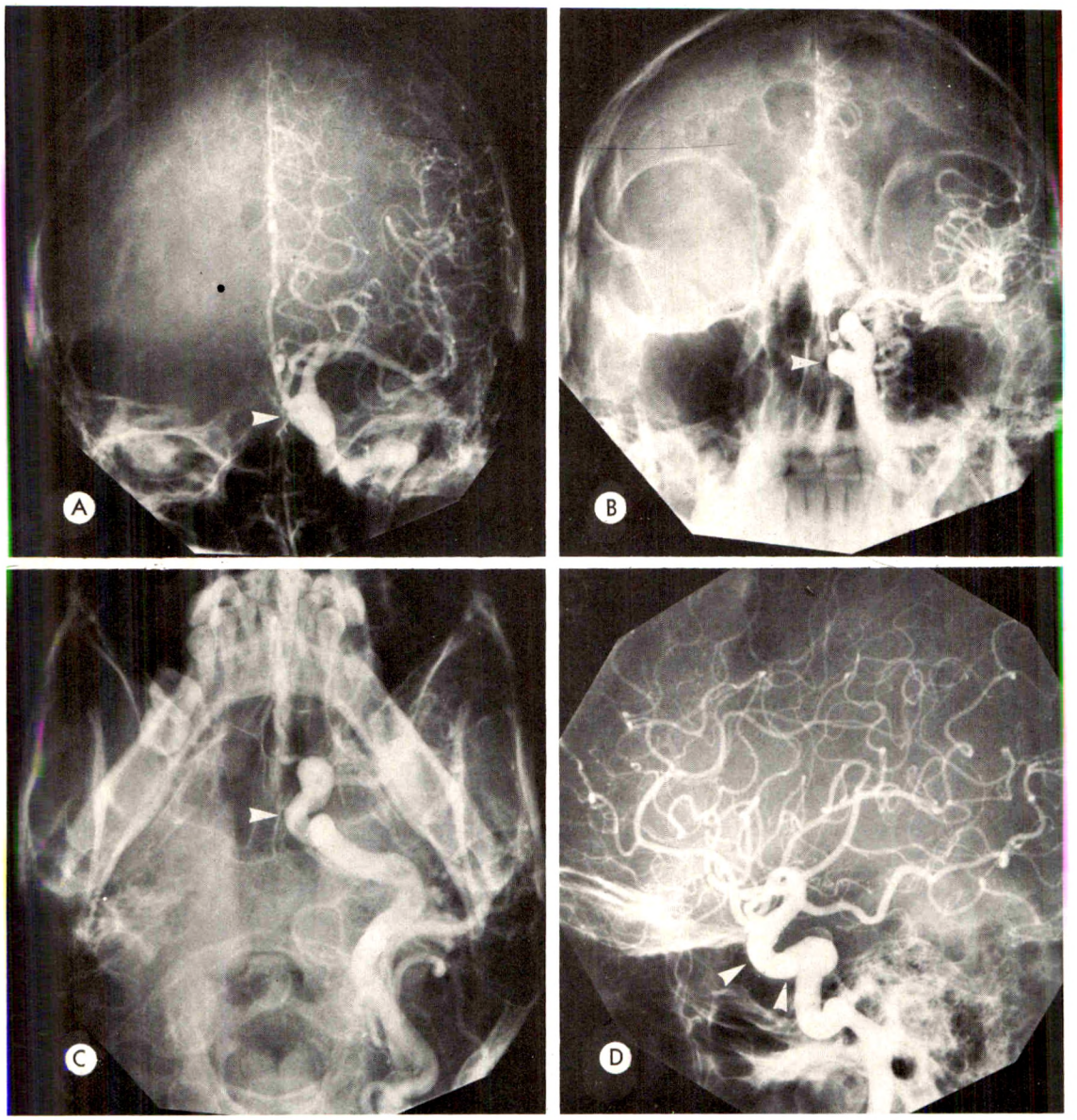


FIG. 2.—Left carotid arteriogram of case 1. *A*, Frontal projection demonstrating left cavernous carotid artery (*arrow*) extending to within 2 mm of midline. *B*, Water's projection. *C*, Base projection. *D*, Lateral projection demonstrating slight ectasia and tortuosity of left cavernous artery (*arrow*).

the sella turcica (fig. 7); the scan was otherwise negative. Since the clinical impression was polymyalgia rheumatica, the patient was placed on steroids, with subjective improvement.

Case 3

This 43-year-old black male complained of headaches following a fall. Seven years prior to admission a skull series after head trauma had shown sellar enlargement, but no additional workup was obtained. Physical examination on the present admission demonstrated a horizontal jerk nystagmus. Visual fields were normal; there were no chiasmal signs or papilledema. Blood pressure was intermittently elevated while in the hospital, varying from 120/70 to 150/110. There was no prior history of hypertension; normal blood pressure readings had been obtained 7 years and 2 years previously.

Skull series and lateral tomograms showed an enlarged sella turcica measuring 18 mm in the AP and 12 mm in the superoinferior dimen-

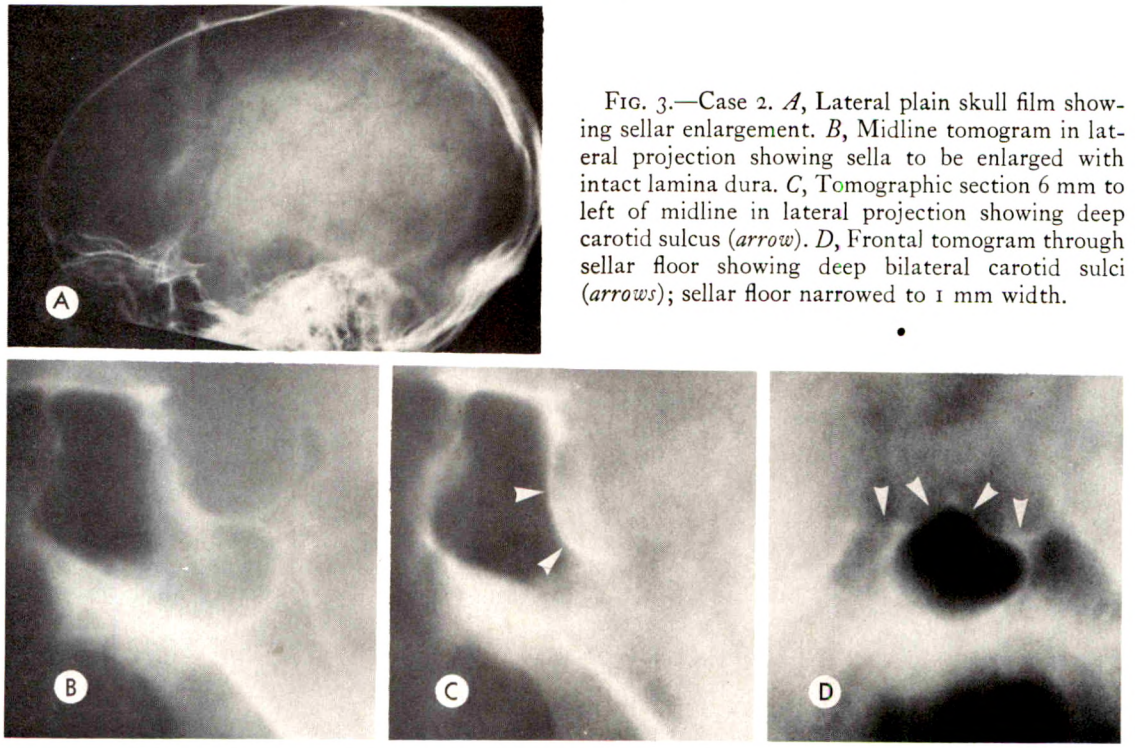


FIG. 3.—Case 2. *A*, Lateral plain skull film showing sellar enlargement. *B*, Midline tomogram in lateral projection showing sella to be enlarged with intact lamina dura. *C*, Tomographic section 6 mm to left of midline in lateral projection showing deep carotid sulcus (*arrow*). *D*, Frontal tomogram through sellar floor showing deep bilateral carotid sulci (*arrows*); sellar floor narrowed to 1 mm width.

sions (figs. 8*A* and 8*B*). The skull was slightly asymmetric. Frontal tomograms showed the sellar floor to be concave, approximately 11 mm in width; portions of the right superolateral aspect of the sella floor were not visualized (fig. 8*D*). This was felt to represent either erosion or the anomaly noted by Renn and Photon [2] in 4% of autopsy specimens in which certain segments of the cavernous carotid artery were in direct contact with sphenoid sinus mucosa. The dorsum sella had a narrow waist measuring 4 mm, with deep lateral grooves caused by the cavernous carotid arteries (fig. 8*E*). On lateral tomograms the dorsum was thinned, but the lamina dura was intact (fig 8*B*); along the lateral aspect of the dorsum deep grooves were demonstrated (fig. 8*C*). Sellar volume was calculated at 1,188 mm^3.

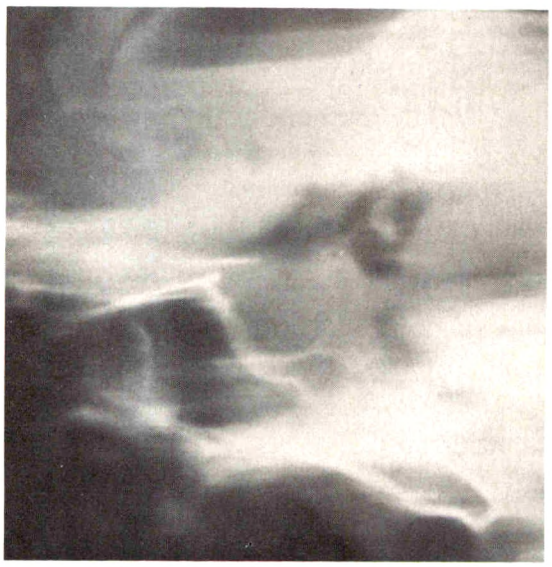


FIG. 4.—Pneumoencephalogram of case 2 showing no evidence of mass extending superior to sella.

In spite of the absence of appropriate clinical and endocrinologic findings, it was thought that the sellar enlargement could be caused by a pituitary neoplasm; additional studies were obtained. The CT scan with contrast medium proved negative. Carotid arteriography demonstrated that both cavernous carotid arteries extended to within 1 mm of the midline at the level of the sella turcica (fig. 9*A*). In the lateral view the cavernous carotid arteries demonstrated a flat contour (fig. 9*B*). Arteriography was otherwise negative; in particular there were no angiographic signs of pituitary adenoma or middle fossa lesions. It was the clinical

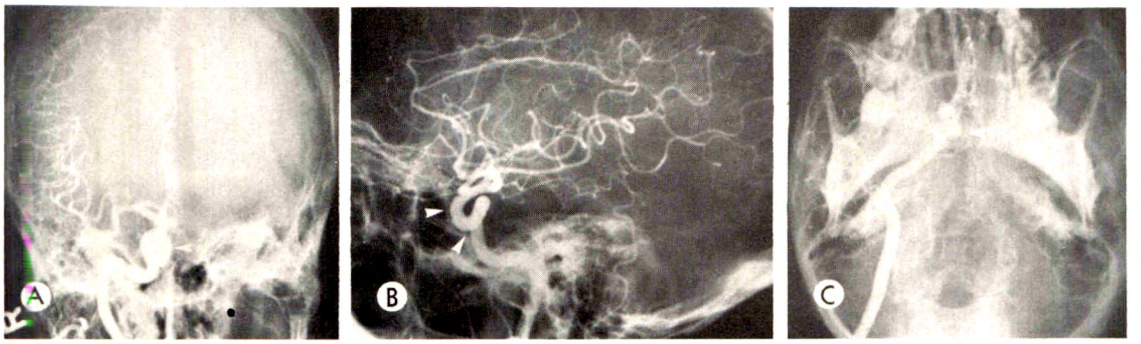


FIG. 5.—Right carotid arteriogram of case 2. *A*, Frontal projection showing right cavernous carotid artery (*arrow*) extending to within 1 mm of midline. *B*, Lateral projection showing tortuosity of right cavernous carotid artery (*arrows*). *C*, Base projection showing medial deviation of cavernous carotid artery (*arrow*).

impression that the patient's horizontal nystagmus was caused by a traumatic brain stem lesion.

DISCUSSION

When pituitary neoplasms expand the sella, the lamina dura usually remains intact initially. As the intrasellar pressure increases, the lamina dura may be eroded; often this is an asymmetrical erosion [3]. In all the above cases the AP midline dimension of the sella was increased. In cases 2 and 3 the lamina dura was intact, while in case 1 it showed localized erosion. Cerebral arteriography excluded pituitary adenoma in each case. Sellar expansion was caused by medial deviation of tortuous cavernous carotid arteries.

Sellar volume determinations covered a wide range in these patients. The normal range cited by Di Chiro and Nelson [4] is 233–1,092 mm^3 (mean 594 mm^3). Cases 1 and 3 showed increased volume, suggesting pituitary neoplasm. Case 2 showed decreased volume because the carotid sulci narrowed the sellar floor to a 1 mm width. Since the cavernous carotid arteries extended medial to the carotid sulci in cases 2 and 3, actual sellar volumes were obviously less than those calculated in these cases.

The floor of the sella is commonly de-

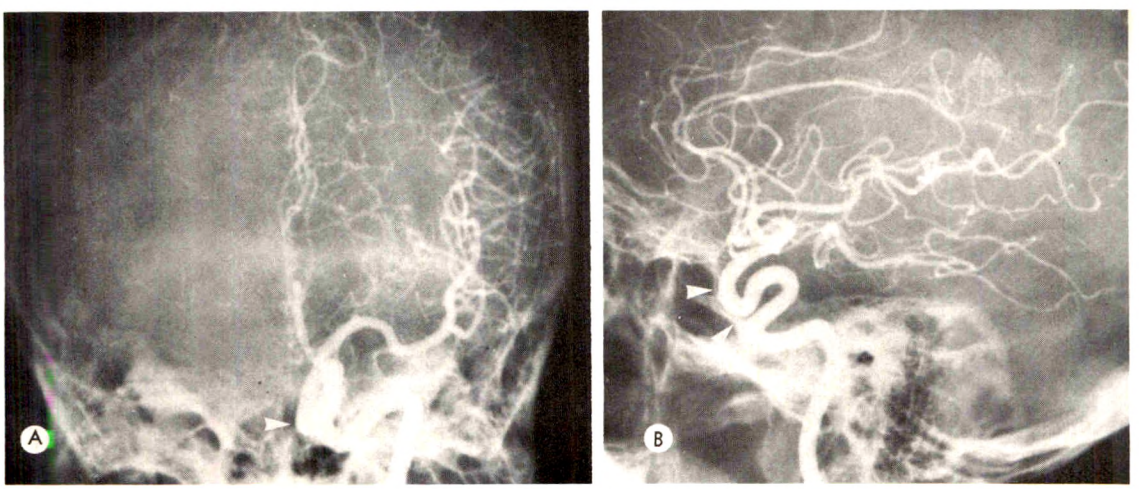


FIG. 6.—Left carotid arteriogram of case 2. *A*, Frontal projection showing left cavernous carotid artery (*arrow*) extending to within 2 mm of midline. *B*, Lateral projection showing tortuosity of left cavernous carotid artery (*arrows*).

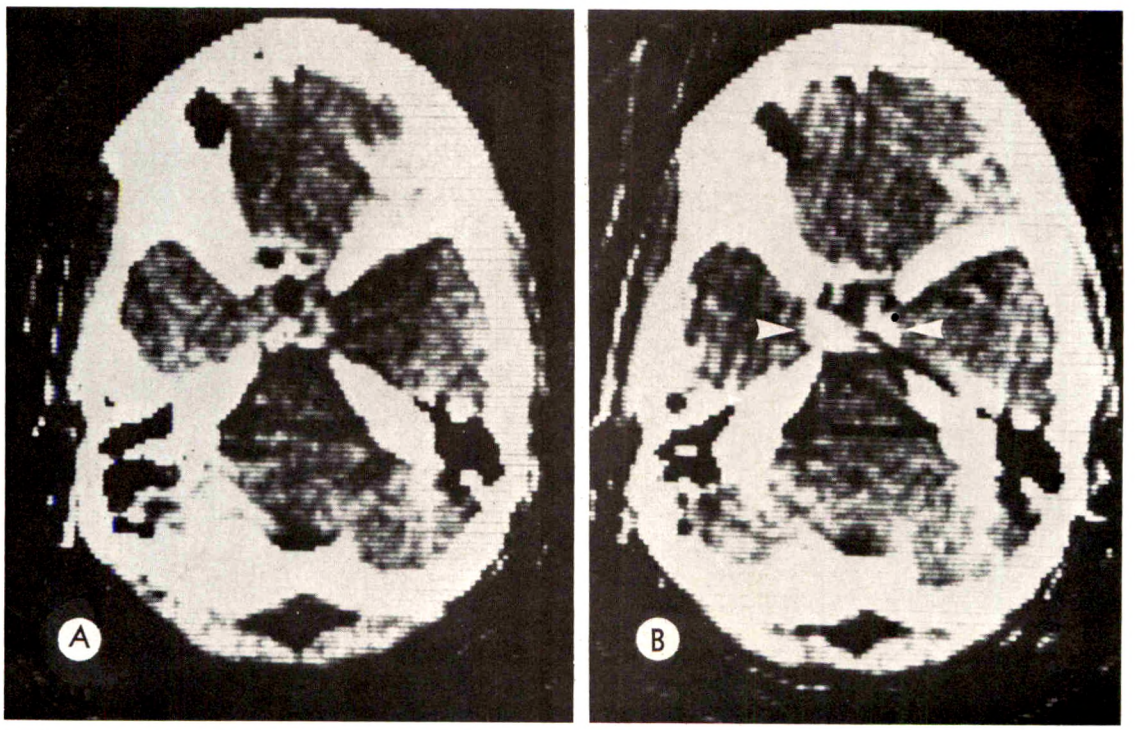


FIG. 7.—CT scans of case 2. *A*, Normal scan without contrast at level of sella, 20° to $\widetilde{OM}$ line. *B*, Scan with contrast at same level demonstrating structures which enhance with contrast (cavernous carotid arteries) and extend into sella bilaterally (*arrows*).

pressed and widened by pituitary adenomas. Although they may expand asymmetrically, depressing the floor on one side only, we found no instance in the literature of adenomas causing the bilateral notched defects in the floor and dorsum demonstrated on tomography in cases 2 and 3. In case 2 the carotid sulci caused deep bilateral grooves in the sella floor, reducing its width to 1 mm; the normal width, taken as the distance between carotid sulci, is 10–16 mm [5]. In case 3 the carotid sulci caused deep bilateral grooves in the lateral pillars of the dorsum sella, narrowing the waist of the dorsum to 4 mm side to side. The correct diagnosis was suggested after tomography in these cases. In the remaining patient (case 1), tomographic findings were interpreted as consistent with pituitary neoplasm.

Pituitary neoplasms often displace the cavernous carotid arteries laterally. In case 1, one cavernous carotid artery was medially deviated, while the opposite cavernous carotid was a normal distance from the midline. In a study of 400 normal cerebral arteriograms, Bernasconi and Pagni [6] found only two instances in which the medial aspect of the cavernous carotid artery was less than 6 mm from the midline (3 and 5 mm). On the other hand, in their study of 50 autopsy specimens, Renn and Photon [2] found five cases (10%) in which the cavernous carotid arteries lay within 4 mm of the midline.

Judging from angiographic studies [6, 7], the latter probably does not reflect the true premorbid anatomy. Medial displacement of the cavernous carotid occurs in extracerebral tumors of the middle fossa [7, 8] and rarely in intraparenchymal middle fossa lesions [6, 7]. Bull and Shunk [7] reported a single case of chromophobe adenoma causing medial displacement of the cavernous carotid. The large dumbbell-shaped mass extended from the sella into the middle fossa, causing marked elevation of the ipsilateral middle cerebral group.

In cases 2 and 3, both cavernous carotid

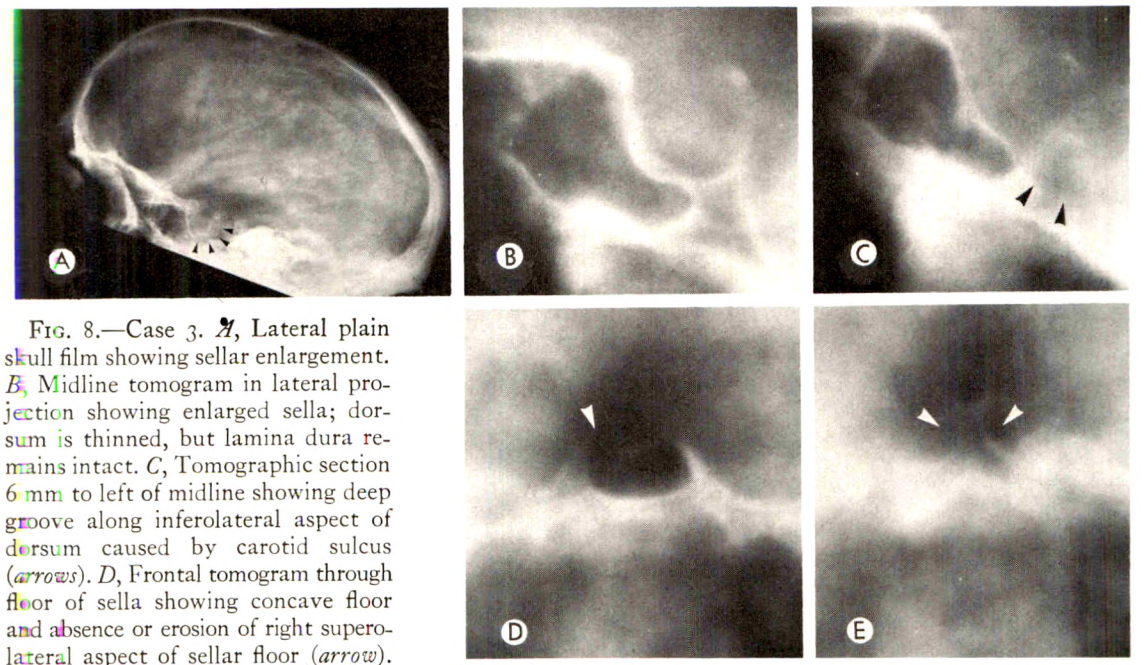


FIG. 8.—Case 3. *A*, Lateral plain skull film showing sellar enlargement. *B*, Midline tomogram in lateral projection showing enlarged sella; dorsum is thinned, but lamina dura remains intact. *C*, Tomographic section 6 mm to left of midline showing deep groove along inferolateral aspect of dorsum caused by carotid sulcus (*arrows*). *D*, Frontal tomogram through floor of sella showing concave floor and absence or erosion of right superolateral aspect of sellar floor (*arrow*). *E*, Frontal tomogram through dorsum showing dorsum deeply grooved on each side by carotid sulci (*arrows*). Superior to this, note markedly thinned posterior clinoid processes.

arteries met in the sellar midline. The literature gives no clear statement on the incidence of apposition of the cavernous carotid arteries within the sella turcica. In a study of 225 autopsy specimens, Bergland et al. [9] cite a single case in which the cavernous carotid arteries were separated only 4 mm at the level of the sella, with corresponding lateral compression of the pituitary gland. In a study of 50 autopsy specimens, Renn and Photon [2] make the statement that in "some" of their cases the cavernous carotid arteries were separated only 4 mm within the sella turcica. It is uncertain whether these postmortem findings correspond to the anatomy in life. Evidently none of these autopsy specimens showed sellar enlargement.

Whether uncomplicated systemic hypertension causes demineralization of the sellar lamina dura has been debated [10–12]. One difficulty is that the patients studied are often elderly individuals in whom demineralization may occur on the basis of age alone [10, 11]. Another problem is that systemic hypertension can cause increased intracranial pressure, which itself results in sellar demineralization. Jefferson [11] studied skull radiographs in 33 hypertensive patients without papilledema and found sellar demineralization in 10%. Malmound [12] examined autopsy specimens and radiographs in 13 severe hypertensive patients and found no evidence of sellar demineralization. In a study of radiographs in 56 hypertensive patients, Fry and du Boulay [10] found sellar demineralization in 7%. None of these patients showed sellar enlargement.

It has been suggested that excessive pulsation of the cavernous carotid arteries could be a mechanism of sellar demineralization in systemic hypertension [10]. To our knowledge this has not been verified. However, the findings in case 1 tend to confirm this: the patient's left cavernous carotid artery was tortuous and extended into the sella within 2 mm of the midline, expanding the sella and demineralizing the inner aspect of the dorsum.

Two different etiologic factors seem to be involved in these cases. Patient 1 had a history of protracted hypertension, which probably accounted for tortuosity and

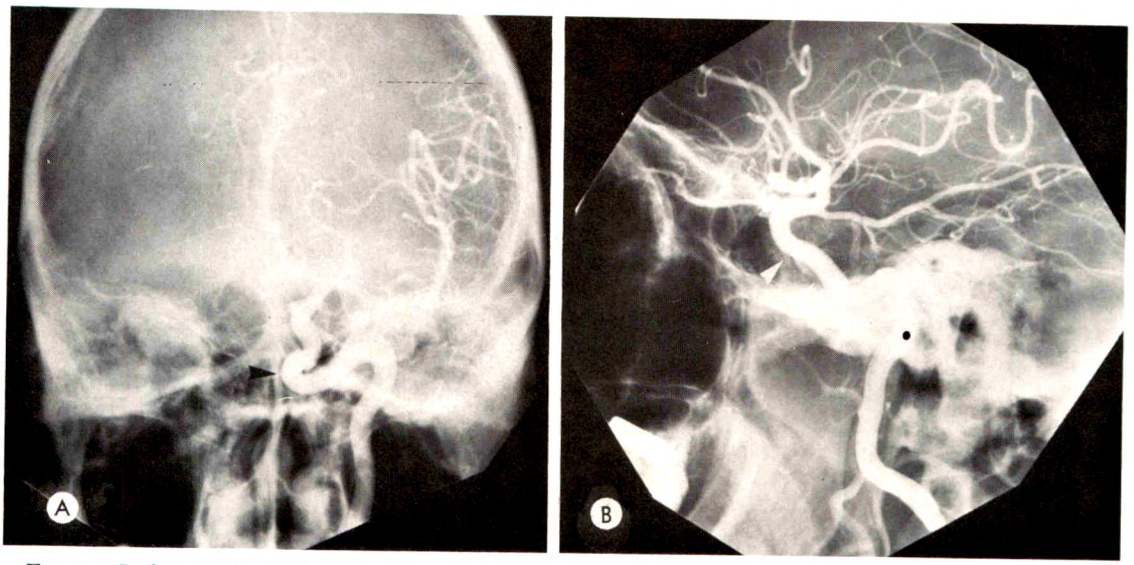


FIG. 9.—Left carotid arteriogram of case 3. *A*, Frontal projection demonstrating medial deviation of left cavernous carotid artery (*arrows*) to within 1 mm of midline. *B*, Lateral projection demonstrating flattened contour of cavernous carotid (*arrows*).

medial deviation of the cavernous carotid artery. Patients 2 and 3, on the other hand, had no history of hypertension, and their angiograms showed no evidence of arteriosclerosis. Most likely the bilateral medial deviation of the cavernous carotid arteries and the deep bilateral grooves in the sellar floor and dorsum were the result of a congenital anomaly.

None of these patients had clinical or laboratory evidence of pituitary disease. This is not a valid point for differentiation, however, since pituitary neoplasms may be manifest by sellar enlargement only [12].

ACKNOWLEDGMENT

I wish to thank Dr. David Witten for his helpful suggestions.

REFERENCES

1. Powell DF, Baker HL, Laws ER: The primary angiographic findings in pituitary adenomas. *Radiology* 110:589–595, 1974
2. Renn WH, Photon AL: Microsurgical anatomy of the sellar region. *J Neurosurg* 43:288–298, 1975
3. Pribram HW, du Boulay GH: Radiology of the skull and brain, in *Sella Turcica*, edited by Newton TH, Potts DG, St. Louis, Mosby, 1971, pp. 357–405
4. Di Chiro G, Nelson KB: The volume of the sella turcica. *Am J Roentgenol* 87:989–1008, 1962
5. Di Chiro G: The width (third dimension) of the sella turcica. *Am J Roentgenol* 84:26–37, 1960
6. Bernasconi V, Pagni CA: Medical displacement of the cavernous portion of the internal carotid artery—its diagnostic significance. *Acta Neurochir* (Wien) 20:15–29, 1969
7. Bull JWD, Schunk H: The significance of displacement of the cavernous portion of the internal carotid artery. *Br J Radiol* 35:801–814, 1962
8. Chase NE, Taveras JM: Carotid angiography in the diagnosis of extradural parasellar tumors. *Acta Radiol [Diagn]* (Stockh) 1:214–224, 1963
9. Bergland RM, Ray BS, Tarack RM: Anatomic variations in the pituitary gland and adjacent structures in 225 human autopsy cases. *J Neurosurg* 28:93–99, 1968
10. Fry IK, du Boulay G: Some observations on old age and arterial hypertension. *Br J Radiol* 38: 16–22, 1965
11. Jefferson A: Hypertensive cerebral vascular disease and intracranial tumor. *Q J Med* 95:245–268, 1955
12. Malmound MES: The sella in health and disease. *Br J Radiol* 8, suppl.:1–100, 1958
13. Daughaday WH: The adenohypophysis, in *Textbook of Endocrinology*, edited by Williams RH, Philadelphia, Saunders, 1974, pp 31–77

Am J Roentgenol 126:1211–1218, 1976

SERIAL CEREBRAL ANGIOGRAPHY IN STEREOSCOPIC MAGNIFICATION

MUTSUMASA TAKAHASHI,[1] YOSHIHARU TAMAKAWA,[1] KATSUYA GOTO,[1] AND MITSUO KOSAKA[2]

ABSTRACT:

A ceiling x-ray tube support with synchronous up and down movements is described for obtaining two parallel x-ray beams with a short focal-film distance. Stereoscopic cerebral angiography is performed with direct serial magnification using a heavy-duty anode tube with a 0.1 mm focus. This technique combines the advantages of magnification and stereoscopic angiography. Small arterial and venous changes can be observed clearly in three dimensions. The usefulness and limitations of this method are discussed using clinical and experimental data.

The value of stereoscopic angiography [1, 2] and serial magnification angiography [3–10] has been established in neuroradiology, and these technical modalities have been utilized in many medical centers. However, there have been no reports on combined stereoscopic magnification angiography in neuroradiology, although the simultaneous use of both techniques is apparently valuable. This is partly due to the fact that conventional x-ray tube housings do not permit sufficiently close approximation of the x-ray focal spots for small-angle divergence of the beams at short focal-film distances. Special housings for two tube inserts for stereography are available but, lacking these, some other means must be found.

To solve this problem, we have manufactured a ceiling x-ray tube support with synchronous up and down movements, thus obtaining two parallel x-ray beams with a short focal-film distance. The purpose of this communication is to report the merits and limitations of this method in the diagnosis of cerebral diseases.

MATERIALS AND METHODS

Equipment

The synchronous movements of the x-ray tube are obtained with a small rotating disc 68 mm in diameter mounted at the end of the ceiling tube support. The ceiling tube support is a special spring balancing system for the vertical travel of the x-ray tube. The unit can travel vertically subject to little inertia (fig. 1). The rotating movements of the disc are changed into the linear up and down movements of the ceiling tube support by means of a bar between the body of the ceiling support and the hole of the disc. The disc can turn 180° in 0.64 sec and comes to a complete stop immediately, during which time x-ray exposures are made. The disc can turn 180° every second or every other second.

The disc has eight small holes at a distance of 2.5 mm from the center, to which the bar of the ceiling x-ray tube support is fixed. Thus in one 180° turn the disc can produce eight different linear movements from 20 mm to 55 mm in 5-mm intervals (fig. 2). The electric current to the motor of the disc is taken from the main switch of the x-ray generator, which in turn is controlled by the AOT film changer.

A heavy-duty rotating anode tube with 0.1 mm focus [11] was mounted on the ceiling support, which can perform synchronous up and down movements, thus producing two parallel x-ray beams (fig. 3). The magnification factor routinely utilized is 2.5. Exposure factors include 70–75 kVp, 30 mA, and 0.14 sec, with a 90 cm focus-film distance [6–8]. An ordinary high speed film screen combination is used.

Method

Image deterioration by motion of the ceiling support was tested by the modulation transfer

Presented at the annual meeting of the American Roentgen Ray Society, Atlanta, Georgia, October 1975.
[1] Department of Radiology, Akita University School of Medicine, 6–10, Senshu Kubota-machi, Akita, Japan 010.
[2] Radiation Division, Shimadzu Seisakusho, Ltd., Kyoto, Japan 640.

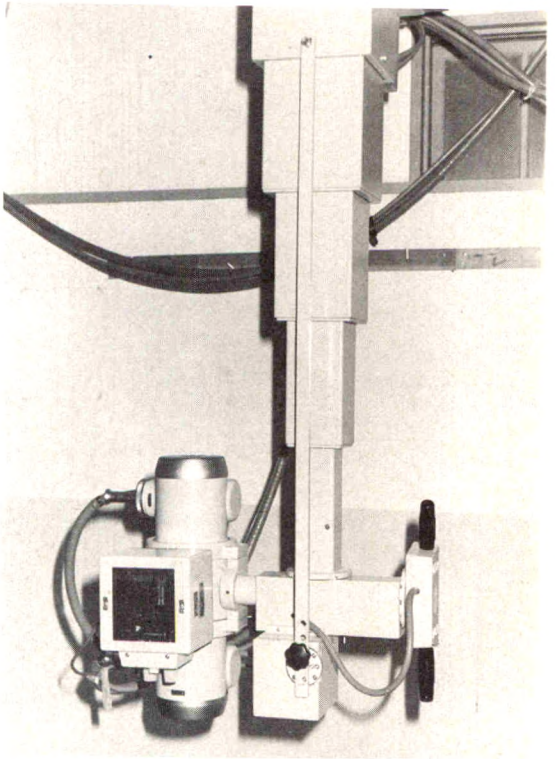


FIG. 1.—Ceiling x-ray tube support mounted with heavy-duty anode tube with a 0.1 mm focus.

function. The coordination of the x-ray exposures and the movements of the ceiling support was recorded on a multichannel recorder. Adequate distance of the tube shifts was assessed using a skull phantom.

Serial cerebral angiography in stereoscopic magnification was performed in the lateral projection with use of transfemoral catheter techniques. Frontal, Towne, and oblique projections were obtained with the usual magnification technique, using the same x-ray tube [6–8]. In most cases selective catheterization of the internal carotid, external carotid, and vertebral arteries was performed.

For serial stereoscopic magnification, injection was made with an automatic injector (Cisal 1). Eight or nine films were loaded in the cassette, and the first film was exposed just before the injection of contrast media. This was followed in 3 sec by simultaneous injection of contrast media and serial x-ray exposures. The second film was also a scout film without contrast media in the cerebral arteries. The remaining films were exposed one per second for 3 sec, followed by one film every 2 sec (fig. 4). Therefore, two base films with different beam angles were available for subsequent subtraction and accurate reading. Injection speed of contrast media was slightly prolonged to 7–8 cm^3 in 2.5 sec, using slightly lower injection pressure, so that at least two different arterial phases were available.

A total of 200 cerebral angiograms, including those of 20 brain tumors and 30 vascular lesions, were performed on this unit.

RESULTS

Experimental Data

The movements of the x-ray tube and the exposures, recorded on the multichannel recorder, revealed good synchronicity with the speed of one movement per second (fig. 5). At higher speeds, synchronous motion was disturbed. Deterioration of x-ray images was compared using the modulation transfer function. There was slight image deterioration with the use of the present technique (fig. 6). The most appropriate tube shift for good stereoscopic viewing was a 5.5 cm shift with a magnification factor of 2.5 and a focus-film distance of 90 cm.

Clinical Data

This technique combined the advantages of both magnification and stereoscopic angiography. In most cases excellent magnified stereoscopic images were obtained in both arterial and venous phases. The tumor vessels and displaced small arteries and veins were clearly shown, providing easier evaluation of the extent of lesions compared to conventional cerebral angiograms.

Stereoscopic images separated the overlapping vessels, clearly showing the lesion. The neck of the aneurysm, particularly, could be seen without overlapping adjacent arteries. The origin and course of small arteries and arterial branches, such as the meningohypophyseal artery, lenticulostriate arteries, thalmoperforate arteries, and anterior choroidal arteries, were shown to good advantage in three dimensions. Minor

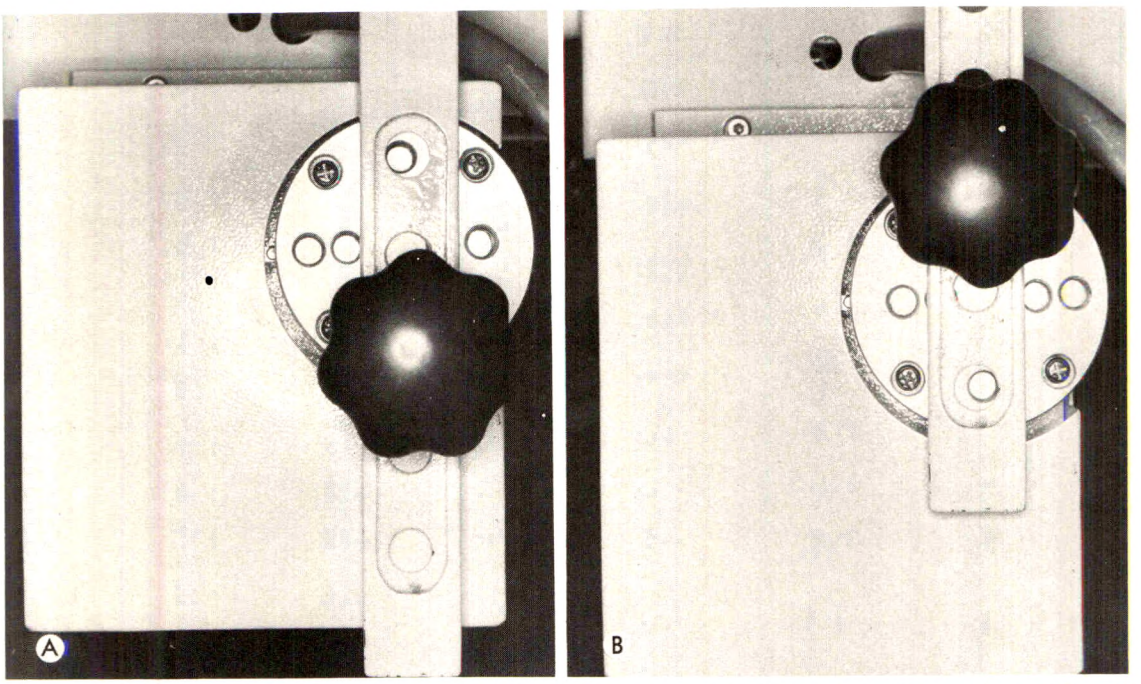


FIG. 2.—Rotating disc installed at end of ceiling support showing higher (*A*) and lower (*B*) position of the tube.

changes of these vessels could be convincingly demonstrated in some cases. On the vertebral angiograms there was good stereoscopic demonstration of nodular and choroidal branches of the posterior inferior cerebellar artery, pontine branches of the basilar artery, as well as the thalamoperforate arteries.

CASE REPORTS

Case 1

This 26-year-old female with right thalamic tumor was admitted because of a 4-month history of headache, nausea, and vomiting. Physical examination revealed moderate papilledema, left abducence palsy, and slightly disturbed consciousness. A left vertebral angiogram was performed by the transfemoral catheter technique. The arterial phase showed the right lateral posterior choroidal artery markedly displaced posteriorly in an arcuate fashion, while the medial posterior choroidal artery was displaced anteriorly on the right. The findings placed a large tumor in the right thalamus. In addition, the left medial posterior choroidal artery and the right thalamoperforate arteries were displaced anteriorly (fig. 7). These findings were clearly discernible on stereoscopic magnification angiograms.

Brain scan using ^{99m}Tc showed increased uptake in the pulvinar of the right thalamus. Pneumoencephalography also revealed a large lobulated tumor in the right pulvinar projecting into the trigone and elevating the floor of the dilated right lateral ventricle. There was slight midline shift of the third ventricle to the right.

Case 2

Case 2 was a 32-year-old male with right thalamic tumor. He gradually developed progressive weakness of the left lower and upper extremities 3 months prior to the present admission. Neurological examination revealed left-sided hemiparesis and hemihypesthesia. There was no papilledema. Internal carotid angiogram showed superior displacement in an arcuate fashion of one of the lenticulostriate arteries (fig. 8). This finding was not observed on conventional angiograms. On stereoscopic viewing, the remaining lenticulostriate arteries were all displaced anteriorly, although the lat-

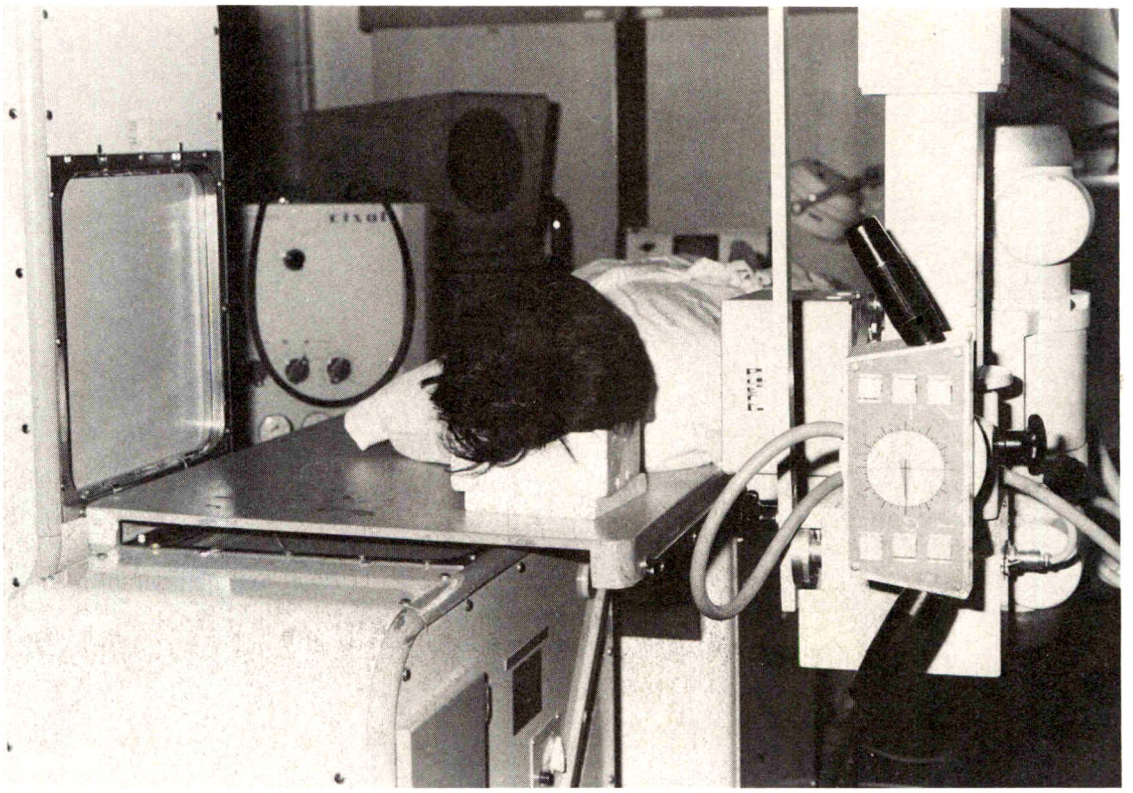


FIG. 3.—Setup for cerebral angiography in stereoscopic magnification.

ter findings were not seen clearly on magnification angiograms alone. Therefore, the diagnosis of a large thalamic tumor was made.

Brain scan showed no abnormal uptake in the basal ganglia. Pneumoencephalography showed elevation and medial displacement of the body and frontal horn of the right lateral ventricle. The temporal horn was displaced laterally and inferiorly.

Case 3

This 46-year-old male with a porencephalic cyst in the left frontoparietal area underwent left frontoparietal craniectomy for removal of a mass lesion 23 years prior to admission. After this surgery he had epileptic seizures once or twice a month. He recently developed numbness of the right extremities. On physical examination there was slight weakness of the right upper and lower extremities with positive Babinski sign. The arterial phase of the left internal carotid angiogram showed the sylvian triangle to be markedly depressed with stretching and arcuate displacement of the branches of the callosomarginal artery (fig. 9). On stereoscopic viewing, the lesion was clearly localized and appeared to be small. There was slight ventricular dilatation, evidenced by visualization of long segments of the subependymal veins.

Brain scan with ^{99m}Tc revealed a small area of increased uptake in the left frontoparietal area. RI cisternography using ^{169}Yb showed accumulation of isotope in the lateral ventricle with marked accumulation in the left frontoparietal area. There was poor accumulation of isotope over the cerebral convexity with dilatation of both sylvian fissures.

Pneumoencephalography showed the left lateral ventricle slightly enlarged with a 3-cm porencephalic cyst extending superiorly. No midline shift was noted. There was little air over the cerebral convexities.

Case 4

Case 4 was a 50-year-old male with multiple mycotic aneurysms of the supraclinoid portion of the right internal carotid artery. He complained of severe headaches for a week. Following generalized tonic seizures, he went into a semicomatous state. Neurologic examination revealed early papilledema and mild left hemi-

paresis. Body temperature was 38.5°C. Laboratory examination showed C-reactive protein and rheumatoid factor to be markedly positive. Erythrocyte sedimentation rate was 58 mm in 1 hr, and the white cell count was markedly increased.

With the magnification angiogram alone, only one saccular aneurysm was demonstrated in the lateral projection. However, stereoscopic viewing revealed at least three saccular aneurysms with broad stalks on the internal carotid artery (fig. 10). On the frontal projection the aneurysms were superimposed and seen as irregularities and lobulation of the wall of the internal carotid artery.

DISCUSSION

With the increased use of angiography and stereoscopic radiography for various parts of the body, many attempts have been made to obtain stereoscopic views of blood vessels. The apparatus utilized for this purpose has usually consisted of two x-ray tubes with a short focal-film distance and a rapid film changer [1, 2, 12]. Another technique for single tube stereoscopy requires change in position of the patient at the time of sequential filming on a rapid film changer. Stereoscopic cineradiography is obtained with two x-ray tubes with a short focal-film distance and one image intensifier [1]. In this system two alternating x-ray beams are recorded by cine. In order to avoid the delay in obtaining two stereoscopic pairs of the angiographic series, Tobe et al. [2] made simultaneous exposures by two x-ray tubes projected on the same film, thus obtaining a good stereoscopic view of the blood vessels on the same film. However, all of these techniques harbor some disadvantages and have not been used as much as their clinical value would warrant.

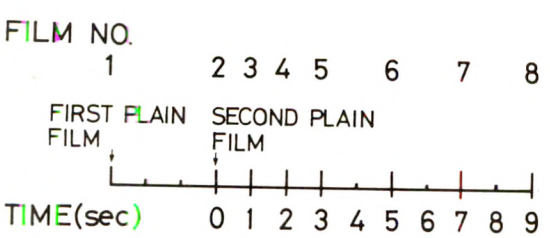


FIG. 4.—Program of serial cerebral angiogram.

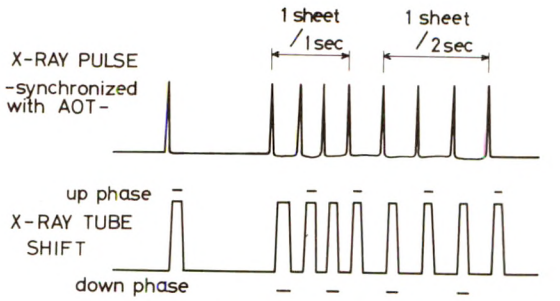


FIG. 5.—Synchronicity of AOT-synchronized exposure and x-ray tube shift.

On the other hand, magnification angiography has received widespread acceptance in cerebral angiography. In some medical centers cerebral magnification angiography is performed routinely [4, 8, 9], and conventional serial angiography is only performed when clinically indicated [8]. Application of magnification to cerebral angiography is a new development in the diagnosis of neurological diseases.

We have developed a system which incorporates the advantages of both stereoscopy and magnification in cerebral angiography. With our system the small cerebral vessels can be observed clearly in three dimensions, so that space-taking and vascular lesions can be diagnosed with increased accuracy. The technique has three disadvantages. First, the movements of the x-ray

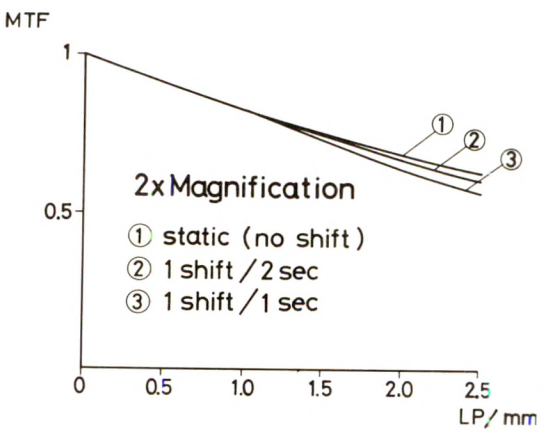


FIG. 6.—Image deterioration by x-ray tube movement as compared by modulation transfer function.

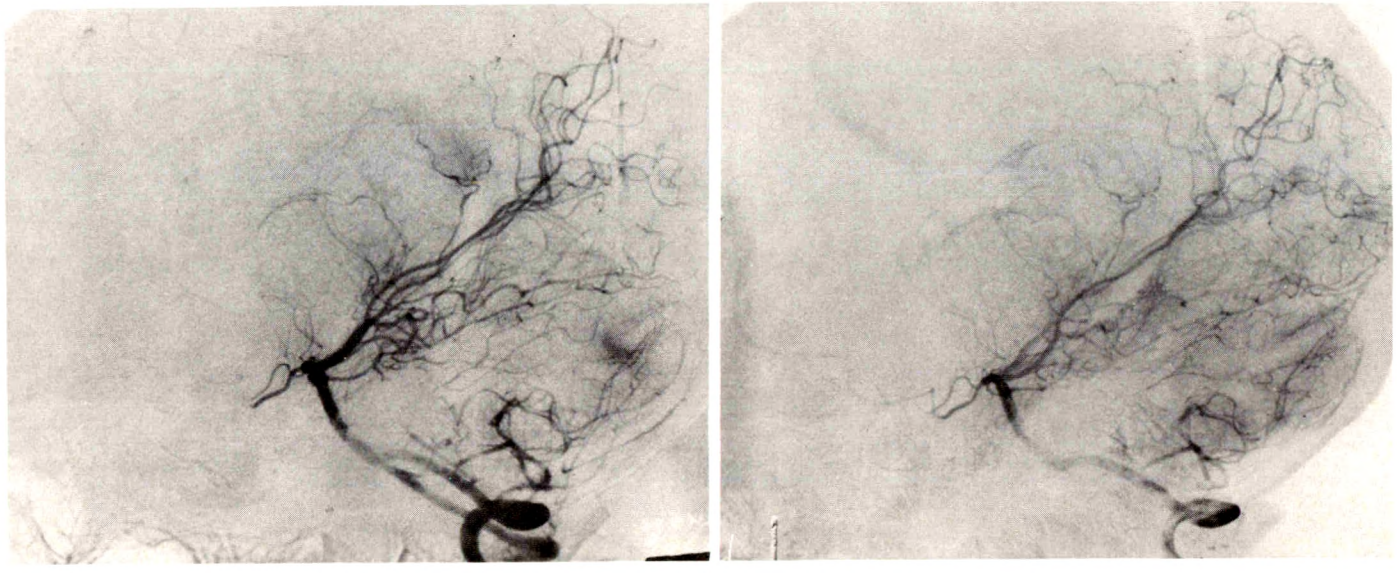


FIG. 7.—Case 1. Stereoscopic magnification of left vertebral angiogram showing right thalamic tumor.

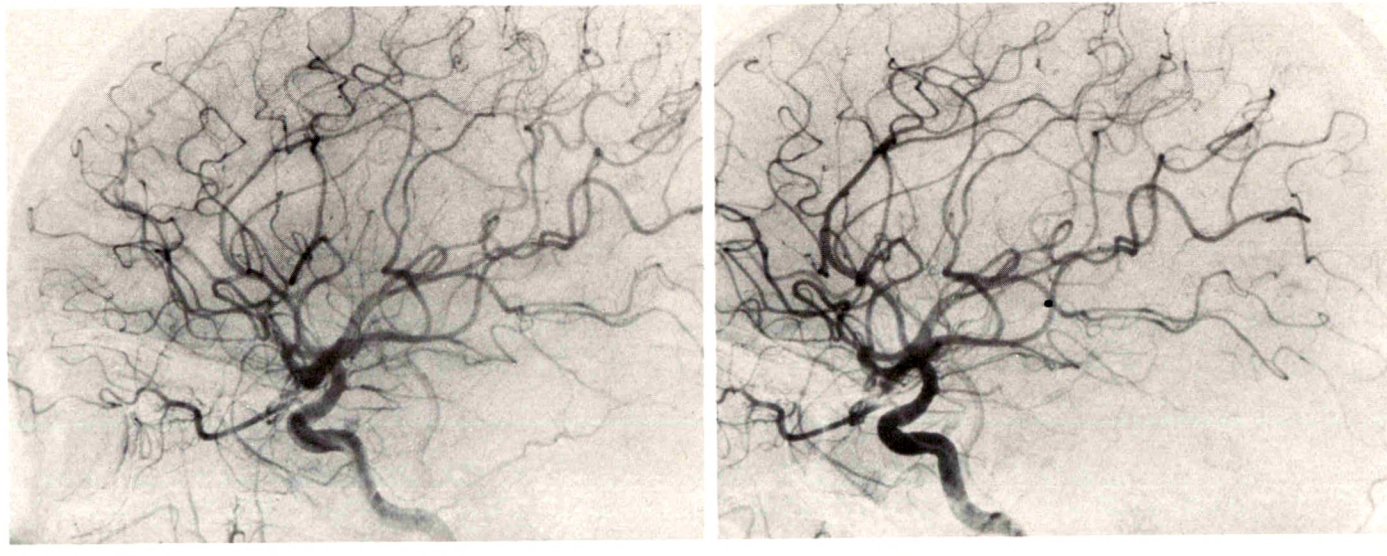


FIG. 8.—Case 2. Stereoscopic magnification of right internal carotid angiogram showing right thalamic tumor.

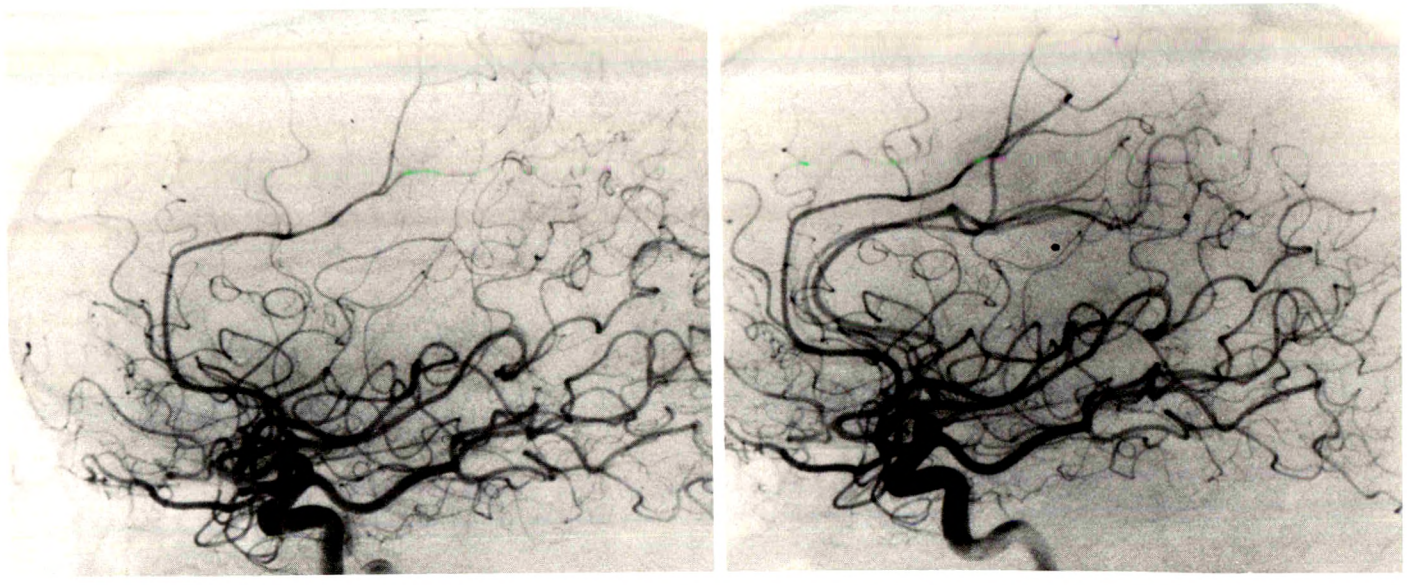


FIG. 9.—Case 3. Stereoscopic magnification of left internal carotid angiogram showing left frontoparietal porencephalic cyst.

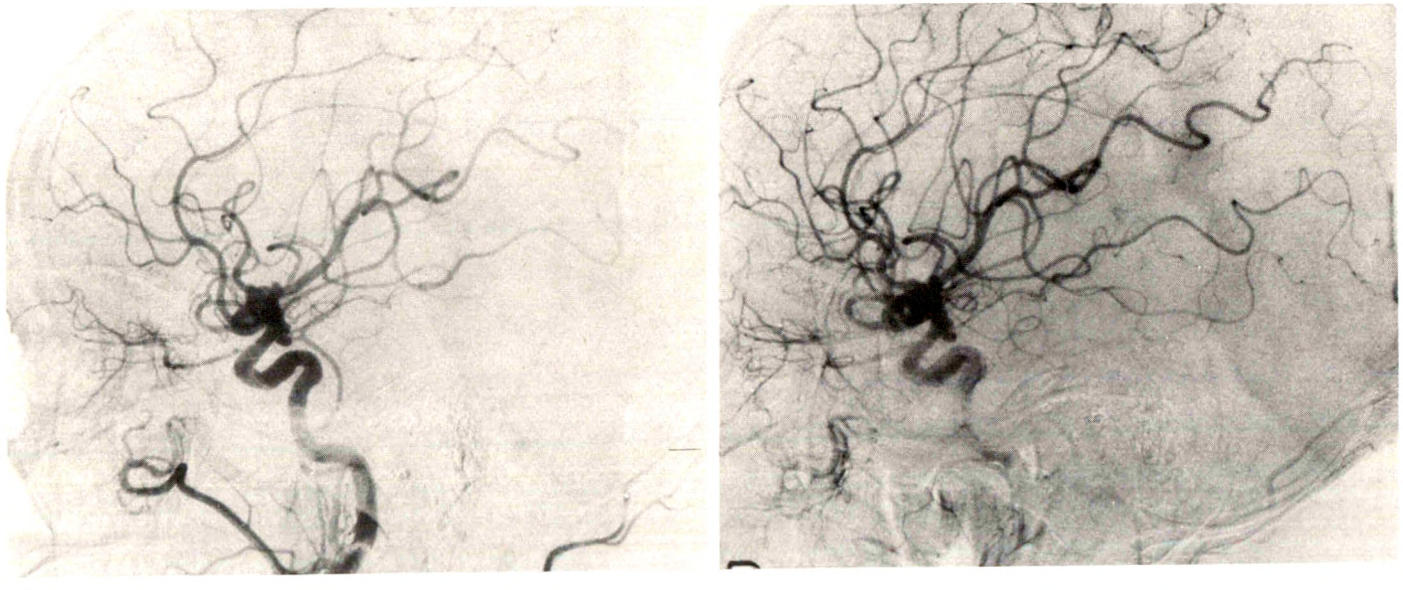


FIG. 10.—Case 4. Right internal carotid angiogram in stereoscopic magnification showing multiple mycotic aneurysms of the internal carotid artery.

tube cause slight image deterioration as demonstrated by the modulation transfer function. Second, the fastest film sequence is one exposure per second, so that the speed of injection of contrast media should be prolonged to 7–8 cm^3 over 2.5 sec to obtain good stereoscopic arterial phases. Therefore this technique cannot be applied to the diagnosis of several conditions such as arteriovenous malformation and arteriovenous fistula. Third, a portion of the carotid system is excluded from the film when the magnification factor is more than 2.0, although evaluation of the whole vascular bed is possible when sequential films are observed together.

In our hands, magnification cerebral angiography together with stereoscopic magnification has given consistently excellent results. We routinely perform serial magnification angiography in all carotid and vertebral angiograms, supplemented by lateral stereoscopic magnification angiography if indicated [8]. Standard serial angiography is used only in cases when rapid blood flow is anticipated (e.g., arteriovenous malformation, arteriovenous fistula, or angiography in small children and infants).

Because of the increased diagnostic information obtained from stereoscopic magnification in the lateral projections, we are now developing a system in which stereoscopic magnification can be achieved in the frontal projection.

REFERENCES

1. Dümmling K, Maass W: Stereoscopic television and stereoscopic cinematography with modern x-ray units. *Electromedica* 43:35–39, 1975
2. Tobe T, Saito S, Toda N, Sato S, Hatori N, Ishimoto M: Simultaneous stereoroentgenography. *Gunma J Med Sci* 15:23–31, 1966
3. Baker HL Jr: Clinical usefulness of magnification cerebral angiography. *Radiology* 98:587–594, 1971
4. Gold LHA, Krause D, Anplatz K: Routine biplane magnification cerebral angiography. *Radiology* 106:321–324, 1972
5. Leeds NE, Isard HJ, Goldberg H, Cullinan JE Jr: Serial manification cerebral angiography. *Radiology* 90:1171–1175, 1968
6. Takahashi M: Evaluation of small branches of the vertebrobasilar system by magnification vertebral angiography. *Nippon Acta Radiol* 34:479–484, 1974
7. Takahashi M: Evaluation of the small arterial branches of carotid siphon by magnification carotid angiography. *Nippon Acta Radiol* 34: 485–490, 1974
8. Takahashi M, Toyama T, Tamakawa Y, Kowada M: Clinical value of magnification cerebral angiography. *Neurol Surg* 3:297–304, 1975
9. Vignaud J, Hasso AN, Lasjaunias P, Clay C: Orbital vascular anatomy and embryology. *Radiology* 111:617–626, 1974
10. Wende S, Schindler K: Technique and use of x-ray magnification in cerebral arteriography. *Neuroradiology* 1:117–120, 1970
11. Kagawa T, Kambe K, Nishioka H: Heavy duty rotating anode x-ray tube with ultra fine focus for enlargement radiography. *Shimadzu Rev* 30:155–165, 1973
12. Fernström I, Lindblom K: Simultaneous stereoangiography. *Acta Radiol* 44:230–232, 1955

Am J Roentgenol 126:1219–1222, 1976

RADIOLOGIC CHANGES IN THE THYMOMA-HYPOGAMMAGLOBULINEMIA SYNDROME

ROBERT E. MOFFAT[1]

ABSTRACT:

Radiologic findings in the thymoma-hypogammaglobulinemia syndrome are encountered in three stages reflecting the natural history of the syndrome. Initially, a mediastinal mass is apparent on chest x-ray in an asymptomtaic patient. At this stage a failing immune system has apparently induced compensatory thymic hyperplasia which progresses to frank neoplasia. In 55% of the cases this thymic tumor is paracardiac in location. With progressive failure of immunoglobulin production, acute and chronic pulmonary infiltrates occur secondary to infection. Markedly decreased IgA in the bowel may eventually be manifested by radiologic changes of exudative enteropathy.

INTRODUCTION

The first case of primary acquired hypogammaglobulinemia in association with thymoma was reported by Good in 1954 [1] and was considered by him to represent an "experiment of nature." Since that time the immunologic role of the thymus has been extensively investigated, and 27 cases of the thymoma-hypogammaglobulinemia syndrome have been reported.

Radiographic findings have not been emphasized in the previous reports. However, it appears that any combination of a paracardiac or anterior mediastinal mass, pulmonary infiltrates, or small bowel changes of exudative enteropathy should suggest the diagnosis.

CASE REPORT

The patient was a 69-year-old white man who entered the Kansas University Medical Center with the following problems: diarrhea with up to 20 stools per day, chronic cough with purulent sputum, intermittent episodes of high fever, 65 pound weight loss, weakness, and anorexia. These symptoms had progressed over a 3 year period.

On physical examination the patient appeared markedly cachectic. Diffuse coarse rales and rhonchi were heard on auscultation of the chest. The abdomen was unremarkable to palpation. Proctosigmoidoscopy to 16 cm revealed friable hyperemic mucosa.

The following laboratory determinations were normal on admission: urinalysis, fasting blood sugar, blood urea nitrogen, creatinine, serum electrolytes, folic acid, carotene, and prothrombin time. The hemoglobin was 12.9 g/100 ml with a hematocrit of 39. The white blood cell count was 9,200/mm^3 with 59% polymorphonuclear leukocytes, 11% band forms, 19% lymphocytes, and 5% monocytes. Immunoglobulin assay revealed the following (normal values in parenthesis): IgG 210 mg (700–1,400); IgA 10 mg (170–400); and IgM 0 mg (60–250). The presence of cell-mediated immunity was evidenced by positive *Tricophyton* and *Candida* skin tests. Fecal fat determinations averaged 7 g per day with a fat intake of 50 g, indicating mild steatorrhea. *Proteus*, *Hemophilus*, and *Candida* were grown on sputum cultures. Stool cultures showed only *Candida*, *Proteus*, and *Klebsiella* and were negative for ova and parasites.

Chest x-ray (fig. 1) revealed changes of chronic pulmonary disease with scattered infiltrates. A mediastinal mass was present adjacent to the right heart border. The small bowel series (fig. 2) showed mild dilatation and markedly increased fluid within the bowel. No abnormality of lymph node morphology was present on the lymphangiogram. The intravenous pyelogram and barium enema were also normal.

Major therapeutic measures included antibiotics, anticholinergics, gluten- and fiber-free

[1] Department of Diagnostic Radiology, Kansas University Medical Center, Kansas City, Kansas 66103.

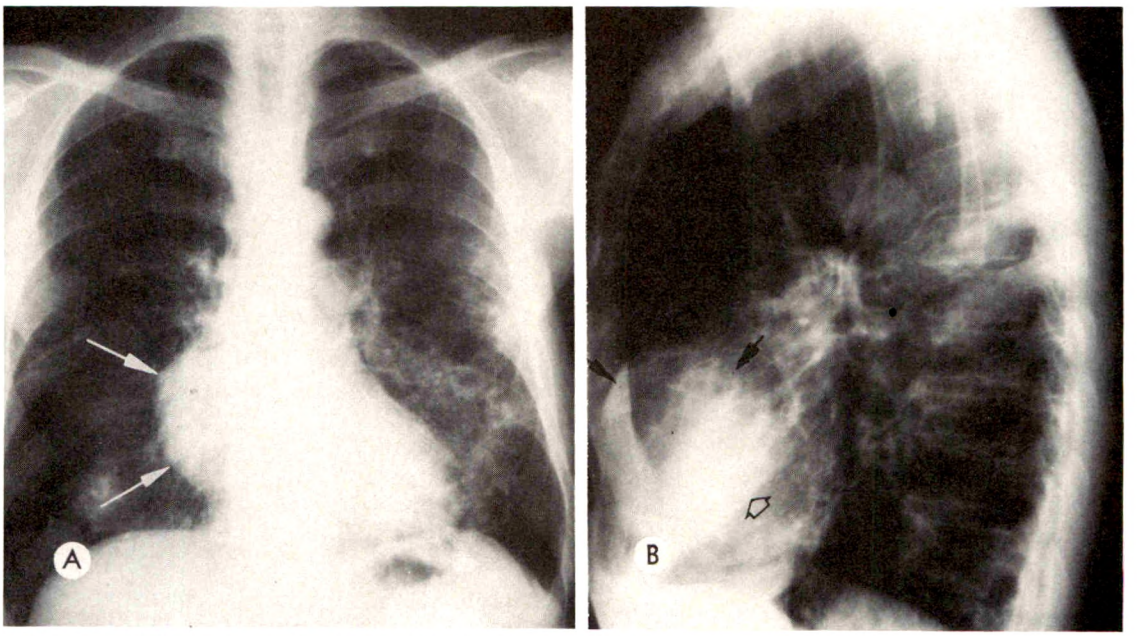


FIG. 1.—*A*, Chest x-ray showing mediastinal mass contiguous with right heart border (*arrows*). Multiple pulmonary infiltrates and mild emphysema involve both lungs. *B*, Lateral view showing superior aspect of mass (*closed arrows*). Lingular pneumonia (*open arrow*) overlies portion of mass.

diet, immune globulin injections, and, finally, parenteral hyperalimentation. The patient continued to lose weight and have frequent stools. He died of septicemia 2 months following admission.

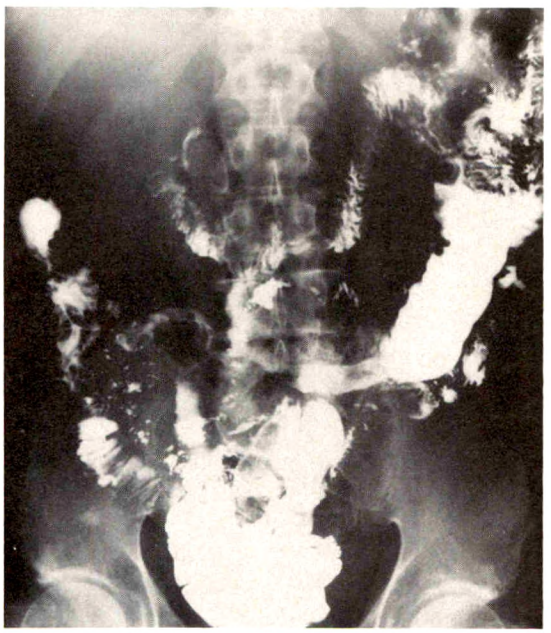


FIG. 2.—Radiograph ($3\frac{3}{4}$ hr) showing flocculation, segmentation, and localized jejunal dilatation.

At autopsy an ovoid mass measuring 8 cm in greatest dimension was found to be adherent to the right pericardium. Histologic examination revealed a thymoma of the spindle-cell type. Lung parenchymal changes consisted of mild panacinar emphysema and organizing pneumonia with superimposed acute multifocal pneumonia and abscess formation. All lymph nodes examined were characterized by absence of germinal centers and plasma cells, depletion of lymphocytes, and hyperplasia of reticulum cells. Although the sections of jejunum revealed normal villus-crypt architecture, only a small number of lymphocytes and no plasma cells were present in the lamina propria (fig. 3). Cytomegalic inclusion bodies were present in the lungs and bronchi, adrenals, liver, and colon.

DISCUSSION

The age range of patients presenting with the thymoma-hypogammaglobulinemia syndrome was 25–77 years with an average age of 57 years. The typical clinical history was that of chronic bronchitis and pneumonia in a previously healthy adult. Diarrhea was the initial or primary symptom in three patients [2–4]. In eight others the interval between the onset of respiratory

and subsequent gastrointestinal manifestations ranged up to 2–3 years [5–7].

Hypogammaglobulinemia was detected at some time during the clinical course of 6% of the 598 patients with thymoma reviewed by Souadjian et al. [8]. Conversely, approximately 10% of the patients with the primary acquired form of hypogammaglobulinemia have a thymoma [9]. Pathogenetically, the initial failure in the thymoma-hypogammaglobulinemia syndrome may be that of immunoglobulin-producing plasma cells and the B (bursal-equivalent) lymphocytes from which they are derived [10]. As with other lymphocytes, the B cells are derived from hematopoietic stem cells. However, differentiation into the B lymphocyte is determined by the human analogue of the lymphoid organ known as bursa of Fabricius in the chicken. Possible bursal equivalents in man include intestinal lymphoid tissue, bone marrow, and liver. Histologic studies of small bowel in patients with this syndrome consistently revealed diminished or absent plasma cells and lymphocytes. No case of lymphoid hyperplasia was present. Plasma cells were only rarely found in lymph nodes and bone marrow.

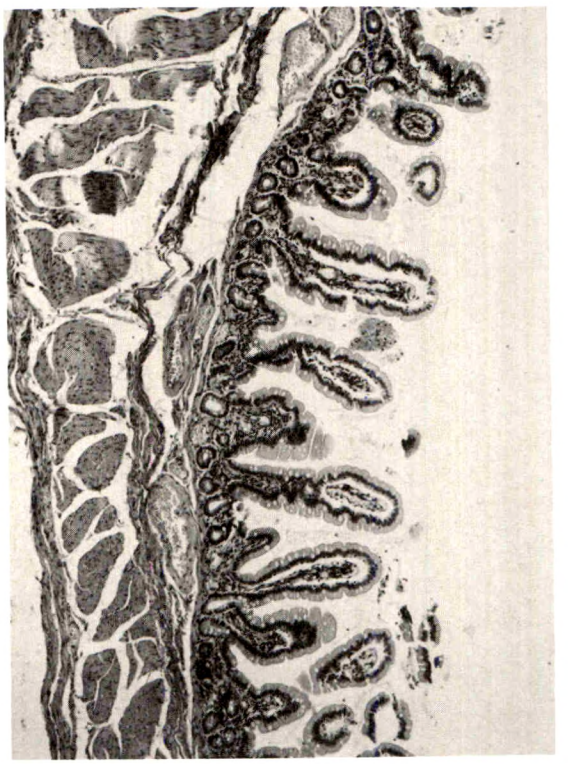


FIG. 3.—Photomicrograph of jejunum at autopsy showing normal crypt and villus architecture. Only an occasional inflammatory cell is present within lamina propria. Hematoxylin and eosin stain, ×60.

In response to the declining peripheral lymphocyte population and falling immoglobulin levels, the thymus perhaps undergoes stromal hyperplasia on a compensatory basis. Continued stromal stimulation eventually results in a thymic neoplasm of the spindle-cell type as was documented in 22 of the 28 reported cases. However, this proliferative response does not prevent the complete failure of humoral immunity.

The thymic tumors were apparent on the initial chest x-rays in 27 cases. The location of the thymic tumors could be seen on published chest x-rays in 15 cases or inferred from descriptions of radiologic or anatomic findings in seven more instances. Right and left paracardiac masses occurred in eight and four cases, respectively [2–4, 7, 11–17; present case]. Thus approximately 55% of the thymomas in this series presented in a paracardiac location compared to an expected 10%–20% [18]. Twelve patients demonstrated a mediastinal mass on chest x-ray up to 12 years before the onset of symptoms of immune deficiency. This is compatible with the concept of a failing bursal-dependent system inducing thymic hyperplasia.

Pulmonary changes secondary to infection were present at some time during the clinical course of all patients with this syndrome. Multiple episodes of pneumonia were seen on chest radiographs as well as chronic changes mainly interpreted as diffuse fibrosis and bronchiectasis.

Of the 11 patients with diarrhea, reports of small bowel series would indicate that three were normal and four showed flocculation of barium [2, 6, 19; present case]. Of the four small bowel patterns in immunoglobulin deficiency syndromes described by Marshak et al. [20], this would be considered as a sprue (malabsorption)

pattern. However, none of the patients in whom intestinal absorption data are available showed evidence of primary malabsorption. The highest fecal fat value in these patients were 7–9 g/day, indicating only mild steatorrhea. In the seven cases where small bowel histology was investigated, no case of villous atrophy was found. No enteric bacterial pathogens or ova and parasites were recovered on stool examinations to account for the diarrhea and roentgenologic small bowel findings. The decreased IgA in intestinal secretions may have caused the bowel to be less resistant to the flora normally present. The bowel reaction consisted of efflux of fluid as would occur in infectious diarrhea. The radiologic manifestations of this exudative enteropathy cannot be distinguished from primary malabsorption.

Operative thymectomy was performed in 14 cases and radiation therapy in one. In no instance did immunologic function improve. However, some patients responded well to gammaglobulin injections up to 3 years following thymectomy [1, 2, 11]. The treatment of many of these patients was complicated by other diseases of possible immunologic origin, including hypoplastic and hemolytic anemias, leukopenia and agranulocytosis, pancytopenia, limited myasthenia gravis, astrocytoma, and atrophic gastritis.

ACKNOWLEDGMENT

I wish to thank Dr. Francis E. Cuppage for reviewing the autopsy material and for providing figure 3.

REFERENCES

1. Good RA: Agammaglobulinemia—a provocative experiment of nature. *Bull Univ Minn Hosp Minn Med Found* 26:1–19, 1954
2. Kirk BW, Freedman SO: Hypogammaglobulinemia, thymoma and ulcerative colitis. *Can Med Assoc J* 96:1272–1277, 1967
3. Lehar TJ, Heard JL: Agammaglobulinemia and thymoma associated with nonthymic cancer. *Cancer* 25:875–879, 1970
4. Ramos AJ: Diagnostic problems: presentation of a case. *JAMA* 160:1317–1319, 1956
5. Conn HO, Quintiliani R: Severe diarrhea controlled by gamma globulin in a patient with agammaglobulinemia, amyloidosis and thymoma. *Ann Intern Med* 65:528–541, 1966
6. Sherman JD, Banas JS, Edwards TL, MacMahon HE, Patterson JF: A syndrome of diarrhea, thymoma and hypogammaglobulinemia. *Gastroenterology* 51:681–688, 1966
7. te Velde K, Huber J, van der Slikke LB: Primary acquired hypogammaglobulinemia, myasthenia and thymoma. *Ann Intern Med* 65:554–559, 1966
8. Souadjian JV, Enriquez P, Silverstein MN, Pepin J: The spectrum of diseases associated with thymoma: coincidence or syndrome? *Arch Intern Med* 134:374–379, 1974
9. Peterson ROA, Cooper MD, Good RA: The pathogenesis of immunologic deficiency diseases. *Am J Med* 38:579–604, 1965
10. Jeunet FS, Good RA: Thymoma, immunologic deficiencies and hematological abnormalities. *Birth Defects: Orig Art Ser* 4:192–206, 1968
11. Brasher GW, Howard PH Jr., Brindley GV: Thymoma and hypogammaglobulinemia (Good's syndrome). *Surg Clin North Am* 52:429–438, 1972
12. Gafni J, Michaeli D, Heller H: Idiopathic acquired agammaglobulinemia associated with thymoma. *N Engl J Med* 263:536–541, 1960
13. Gehrmann G, Engstfeld G: Thymoma and agammaglobulinemia. *Ger Med Mon* 10:281–283, 1965
14. Jacox RF, Mongan ES, Hanshaw JB, Leddy JP: Hypogammaglobulinemia with thymoma and probable pulmonary infection with cytomegalovirus. *N Engl J Med* 271:1091–1096, 1964
15. Jeunet F: Thymome de syndrome de carence en immunoglobulines. *Schweiz Med Wochenschr* 95: 1419–1420, 1965
16. MacLean LD, Zak SJ, Varco RL, Good RA: Thymic tumor and acquired agammaglobulinemia: a clinical and experimental study of the immune response. *Surgery* 40:1010–1017, 1956
17. Rubin M, Strauss B, Allen L: Clinical disorders associated with thymic tumors. *Arch Intern Med* 114:393–398, 1964
18. Harper RAK, Guyer PB: The radiological features of thymic tumors: a review of 65 cases. *Clin Radiol* 16:97–105, 1965
19. Mallinson WJW: Hypogammaglobulinemia with thymoma. *Proc R Soc Med* 64:53–54, 1971
20. Marshak RH, Hazzi C, Lindner AE, Maklansky D: Small bowel in immunoglobulin deficiency syndromes. *Am J Roentgenol* 122:227–240, 1974

Am J Roentgenol 126:1223–1228, 1976

CEREBRO-COSTO-MANDIBULAR SYNDROME: LONG TERM FOLLOW-UP OF A PATIENT AND REVIEW OF THE LITERATURE

HUGH J. WILLIAMS[1] AND SHASHIKANT M. SANE[2]

ABSTRACT:

The cerebro-costo-mandibular syndrome is a rare disorder, and most afflicted infants die during the first few months of life. The pertinent features of the syndrome are reviewed, and a hitherto undescribed finding in the pelvis is described. A case is reported in which vigorous treatment permitted survival. Serial roentgenograms subsequently demonstrated a progressive diminution of the characteristic posterior rib-gap defects.

The association of severe rib defects with micrognathia and other anomalies was first described by Smith and co-workers in 1966 [1]. The patient, who died from respiratory distress shortly after birth, demonstrated abrupt termination of the ossified posterior ribs a short distance beyond the posterior rib angle. A tissue defect was present between the posterior ossified segments of the ribs and the ventral cartilaginous portions which extended normally to the sternum. In addition, the infant also exhibited micrognathia, malformed tracheal cartilages, and pterygium colli. In 1970 McNicholl et al. [2] reported three infants with palatal defects, micrognathia, rib-gap defects, and mental deficiency; only one survived. They aptly named this combination of findings the cerebro-costo-mandibular syndrome. In 1972 Miller et al. [3] reported two infants with a Pierre Robin-like syndrome and associated posterior rib-gap defects, both of whom died early in life.

The purpose of this report is to describe another infant with this syndrome who survived because of prompt diagnosis and vigorous treatment.

CASE REPORT

This full-term male infant was delivered normally, and no drug ingestion during pregnancy was reported. There was no family history of a similar malformation, and consanguinity was denied. Two previous male siblings were normal. At 11 days of age, he was admitted to St. Paul Children's Hospital because of apneic spells and numerous episodes of cyanosis aggravated by feedings.

On physical examination micrognathia, glossoptosis, and an incomplete cleft palate were noted. The degree of respiratory difficulty was disproportionately severe for the micrognathia present; this was felt due to a coexistent flail chest. The only other demonstrable external physical abnormality was a medially displaced right great toe with a broad deformed distal phalanx. All laboratory data, including a chromosomal study, was normal.

A chest roentgenogram (fig. 1) demonstrated bony defects of varying length in the right third to ninth ribs and the left fifth to eighth ribs. The transverse processes of many of the corresponding vertebral bodies were absent and the involved ribs fused with these vertebrae rather than articulating normally. The vertebral ends of the left seventh, ninth, and tenth ribs as well as the right tenth rib were rather bulbous. The anterior portions of all the ribs terminated somewhat more laterally than normal. A skull film demonstrated a moderate degree of micrognathia. A skeletal survey revealed fusion between the fourth and fifth sacral segments and internal rotation of the ilia resulting in a flask-shaped configuration of the pelvis (fig. 2). The iliac angles were increased while the acetabular angles were normal. Serial chest films demonstrated considerable motion between the opposing ends of some of the ribs with the widest defects, thereby explaining the

[1] Children's Hospital, 311 Pleasant Avenue, St. Paul, Minnesota 55102. Address reprint requests to H. J. Williams.
[2] Children's Health Center and Hospital, Minneapolis, Minnesota 55404.



FIG. 1.—Chest roentgenogram at 11 days of age demonstrating posterior rib defects in right third to ninth ribs and left fifth to eighth ribs. Transverse processes are absent in many corresponding vertebrae and there is fusion of bodies to corresponding ribs rather than normal type of articulation. Note bulbous termination of posterior portion of several of involved ribs bilaterally. All anterior ribs terminate more laterally than usual.

clinically present flail chest.

Treatment of the apneic spells with elastic scalp traction applied to the thorax was inadequate, and a fascial sling mandibular glossopexy was performed. While this procedure did reduce the frequency of the apneic spells, it did not eliminate them. A tracheostomy tube was inserted under local anesthesia. Because of protracted feeding difficulties due to defective swallowing, a gastrostomy was also performed. The infant did well subsequently and was discharged at 4 months of age. The cleft palate was repaired at 1 year of age, and the tracheostomy and gastrostomy sites were later closed.

A follow-up chest roentgenogram at 5 years of age demonstrated a diminution in extent of most of the posterior rib defects (fig. 3). Fusion of the previously noted bulbous posterior rib terminations with their corresponding transverse vertebral processes had occurred. Clinically the child was doing quite well at this time and, although of limited intelligence, was functioning adequately in school.

DISCUSSION

This patient represents the seventh reported case of the cerebro-costo-mandibular syndrome, a disorder characterized by rib-gap defects, micrognathia, and mental deficiency [2]. It is a familial syndrome, probably with an autosomal recessive pattern of inheritance. No detectable chromosomal abnormality has been associated with the disorder. The father of one of the cases reported by Miller et al. [3] had a cleft palate, suggesting the possibility of variable expressivity of the syndrome.

The syndrome bears a resemblance to the Pierre Robin syndrome, inasmuch as the affected infants demonstrate mandibular hypoplasia and glossoptosis with resultant feeding and respiratory difficulties. However, it differs by virtue of the associated rib-gap defects. Although the number of ribs involved in the reported cases has varied from a few to almost all, both sides have always been involved, although not necessarily symmetrically. The extent of involvement has varied from a very short defect resembling the pseudarthrosis encountered in neurofibromatosis to complete absence of the anterior three-fourths of the ribs.

Embryologically the most posterior portion of the rib is derived from the somite. Whether the remainder of the rib develops as a direct ventral extension of the somite [4] or from mesenchymal cells of the lateral mesodermal plate [5] is controversial. The cause of the rib defects cannot therefore

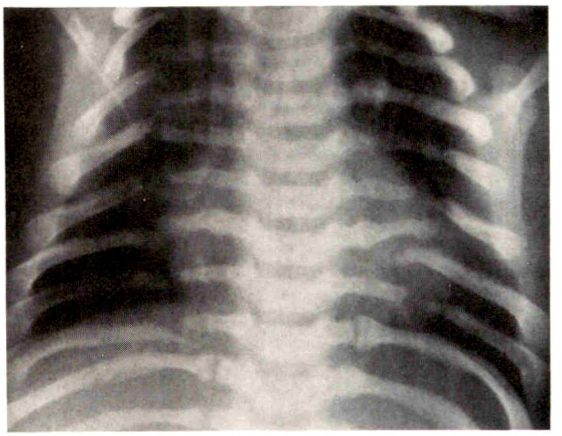


FIG. 2.—Flask-shaped configuration of iliac wings due to internal rotation. Iliac angles are increased while acetabular angles are normal.

be stated with certainty. Histologic examination of the posterior gaps in the patient of Smith et al. [1] failed to demonstrate any foci of cartilage or bone, although in several ribs the intercostal vessels bridged the gap. Microscopic studies by Miller et al. [3] show the defective areas to contain undifferentiated fibroconnective tissue, striated muscle, and small foci of cartilage undergoing calcification, which suggest a defect in the transition of the primitive mesenchyme to cartilage.

The rib gaps present in this syndrome may produce varying degrees of clinical flail chest. Review of the numerous films obtained during the first few months of life in our patient revealed varying degrees of motion between the short posterior rib segments and the longer anterior portions. Although these areas were not biopsied in our patient, this observation would suggest that the defects were initially composed primarily of fibrous or mesenchymal tissue rather than a solid substance such as cartilage. Serial chest roentgenograms during the 5 year period in which we have followed this patient demonstrate a progressive diminution in several of the rib defects, evidently secondary to formation of calcified cartilage or bone, with resultant pseudarthrosis formation in some areas. While no change was observed in some of the rib gaps, in no instance did enlargement of the rib defects occur. In the only other reported surviving infant with the cerebro-costo-mandibular syndrome, similar rib changes were observed in films obtained at the age of 4 years, at which time disappearance of several rib defects had occurred. In our patient most posterior segments of the involved ribs were fused to the corresponding vertebrae instead of exhibiting normal costovertebral articulations. This fusion may have represented a spontaneous attempt to compensate for the flail chest present in our infant. The salient clinical and roentgenologic features in all reported cases of this syndrome are included in table 1.

Micrognathia has been a constant feature in all cases, including our own, and in conjunction with glossoptosis has caused varying degrees of respiratory and feeding distress. The additional burden of diminished respiratory excursions secondary to the associated rib defects may be responsible for the high mortality reported in infants with this syndrome. Palatal defects have been present in all patients in which the palate has been described (five of six cases) and have varied from a cleft palate to a short palate with absent uvula. Less constant findings reported have been abnormalities of the brain, tracheal cartilages, skin, skeleton, and kidneys. In addition, our case demonstrated an unusual internal rotation of the iliac bones which caused a reduction in the iliac angles and gave a flask-shaped configuration to the ilia.

The combination of micrognathia, glossoptosis, and rib-gap defects in the cerebro-costo-mandibular syndrome is a formidable one and constitutes a life-threatening situ-

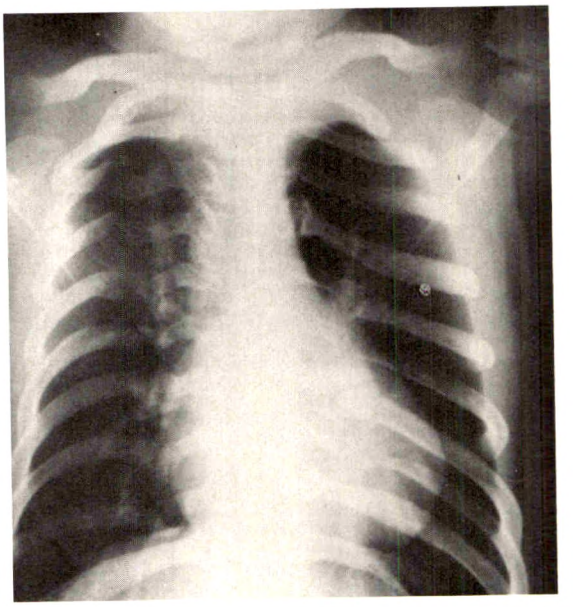


FIG. 3.—Chest roentgenogram at 5 years of age demonstrating decrease in extent of most posterior rib defects. Pseudarthrosis is demonstrable in several areas. This spontaneous improvement eliminated clinical flail chest present in infancy. Fusion of previously noted bulbous posterior rib terminations with their corresponding vertebral transverse processes has occurred.

TABLE 1

SUMMARY OF FINDINGS IN CEREBRO-COSTO-MANDIBULAR SYNDROME

	Cases						
	1	2	3	4	5	6	7
Reference	[1]	[2]	[2]	[2]	[3]	[3]	Present report
Sex and age	M, newborn	M, newborn	F, newborn	M, newborn	M, 3 mo	F, newborn	M, 11 days
Obstetric history	Full term; normal pregnancy and delivery; no drugs	41 wk gestation; 2,475 g; prolonged second stage	Full term; 2,900 g; normal pregnancy and delivery	42 wk gestation; 2,920 g; diagnosis made in utero from rib defects visible on x-ray	Full term; 2,425 g; mother had "flu" in first trimester; normal delivery	40 wk gestation; 2,700 g; induced labor; normal vaginal delivery	Full term; normal pregnancy and delivery; no drugs
Family history	No consanguinity; 1 normal female sibling	2 siblings affected; 1 male sibling abnormal; 2 abortions; 1 stillbirth at 6½ mo	See case 2	See case 2	Father had cleft palate	1 normal sibling; 1 abortion	2 normal male siblings
Chromosomes	Normal	...	...	...	Not done	Not done	Normal
Clinical symptoms and course	Respiratory distress and cyanosis; lungs could not be inflated in spite of high pressure through ET tube; died, autopsy performed	Respiratory distress treated with pharyngeal suction and gavage; died at 14 days	Moderate respiratory distress; retraction in lower anterior transverse sulcus; treated as Case 2; high-pitched barking cough; recurrent respiratory tract infections in first year; glossopharyngopalatal dysphagia and aspiration in lungs; diarrhea, folate deficiency, megoblastic anemia	Severe respiratory distress; inspiratory retraction and expiratory grunting; same treatment as case 2	Respiratory stridor; recurrent lung aspiration; pneumonia, right lung; died on day 10, autopsy performed	Resuscitation at birth; feedings caused aspiration; endotracheal intubation; died on day 4, autopsy performed	Apneic spells and episodes of cyanosis; treated with elastic scalp traction, mandibular glossopexy, and tracheostomy; gastrostomy due to protracted feeding difficulties; did well and discharged at 4 mo; clinically well at 5 years
Clinical signs:*							
Facial features	Micrognathia	Micrognathia and small maxilla; glossoptosis; short, hard palate with hole; absent soft palate	Micrognathia; glossoptosis; short, taut soft palate; absent uvula; large low-set ears; prominent eyes and epicanthal folds; absent lower lateral incisors; small maxilla; small larynx on laryngoscopy	Micrognathia; first molar absent; cleft palate; slight epicanthal folds; glossoptosis	Asymmetrical hypoplasia of mandible (left side more involved); high, arched, short hard palate	Small mandible with cleft soft palate; glossoptosis with forked lip	Micrognathia; partial cleft palate

* Radiographic and autopsy findings.

TABLE 1—(*Continued*)

	Cases						
	1	2	3	4	5	6	7
Tracheobronchial tree	Tracheal cartilages collapsed, abnormal shape	...	...	...	Normal	Normal	Normal
Ribs	Bell-shaped thorax; rib defects 0.5–2 cm beyond post rib angle involving 10 pairs; 11th ribs normal, 12th ribs absent; microscopically no cartilage or any other bridging tissue	Gaps in posterior portions of 4th–10th ribs	1st rib on left absent; 1, 2, and 12th ribs on right and 3, 6, and 12th on left were rudimentary; defects in posterior portion of right 3, 4, 5, 6, and 7th ribs and left 2, 3, 4, 5 and 7th ribs; pseudarthrosis of 7th right rib between ventral and dorsal segments	Rib defects (right 2–9, left 4–9); 12th ribs rudimentary	Rib defects in first 9 pairs of ribs bilaterally; 12th ribs rudimentary or absent; microscopically, defects were filled with fibrocartilaginous tissue and a few islands of cartilage	Multlple rib defects involving at least first 7 pairs; pseudarthrosis of left 4, 5, and 6th and right 4th and 6th ribs; microscopically, defects composed of fibrous tissue, skeletal muscle, and normal cartilage with some calcification	Multiple rib defects (right 3–9, left 5–8); vertebral ends of left 7, 9, and 10th ribs and right 10th ribs were bulbous (fused with corresponding vertebrae at 5 years)
Spine	...	...	Neural arch defect of C_4–C_5; spina bifida, T_3–T_4; hypoplastic neural arches, T_7–T_8; anterior wedging of T_2–T_5 with kyphosis; rudimentary S_3–S_5	Absent transverse processes of T_2–T_5 on right and T_3 on left	...	...	Many absent transverse processes at T_3–T_9 level bilaterally
Head and brain	...	...	Mild microcephaly; bone age $3\frac{1}{2}$ yr at 5 yr; mental age 1 yr at 5 yr; no speech	Microcephaly; diminished brain weight; poor myelinization; absent internal capsule and some tracts	No mental or motor abnormalities; brain normal on gross and microscopic exam	No mental or motor abnormalities; brain normal on gross and microscopic exam	Retarded mental growth but functioning adequately in school at age 5 years
Miscellaneous	Loose subcutaneous tissues especially around neck	Hemorrhagic and aspiration pneumonia	Subluxation of left elbow; hypoplasia of bones at left elbow; coxa valga	Hemorrhagic and aspiration pneumonia; undescended testis	Small medullary cysts of kidneys seen only on microscopic exam	Hemorrhagic and aspiration pneumonia; fatty infiltration of liver	Internal rotation of iliac bones with flask-shaped configuration

ation. Prompt and vigorous medical and surgical treatment can be life saving, as in our case, and should be employed. This is particularly appropriate since spontaneous reduction in the extent of rib defects may occur with the passage of time, thereby enhancing the patient's chance of survival.

ACKNOWLEDGMENT

We thank Mrs. Norma Brandon for her devoted technical assistance.

REFERENCES

1. Smith DW, Theiler K, Schachenmann G: Rib-gap defect with micrognathia, malformed tracheal cartilages, and redundant skin: a new pattern of defective development. *J Pediatr* 69:799–803, 1966
2. McNicholl B, Egan-Mitchell BE, Murray JP, Doyle JF, Kennedy JD, Crome L: Cerebro-costo-mandibular syndrome: a new familial developmental disorder. *Arch Dis Child* 45:421–424, 1970
3. Miller KE, Parker Allen R, Davis WS: Rib gap defects with micrognathia. *Am J Roentgenol* 114: 253–256, 1972
4. Strau WL Jr, Rawles ME: An experimental study of the origin of the trunk musculature and ribs in the chick. *Am J Anat* 92:471–509, 1953
5. Seno T: An experimental study of the formation of the body wall in the chick. *Acta Anat* 45:60–82, 1961

Am J Roentgenol 126:1229–1232, 1976

INTESTINAL PERFORATION SECONDARY TO NASOJEJUNAL FEEDING TUBES

ROBERT L. SIEGLE,[1] JACK G. RABINOWITZ, AND CHARLES SARASOHN

ABSTRACT:

Infant alimentation by nasojejunal tube feeding has been successfully used since 1973. A significant complication is small bowel perforation by the tube: three cases are presented. The differential diagnosis includes spontaneous gastric perforation and necrotizing enterocolitis.

Nasojejunal tube perforation almost always occurs in the distal duodenum. It is likely the result of peristaltic activity which propels the tube along the relatively rigid duodenal loop. Thus it is preferable to position the tube end distal to the ligament of Treitz.

Since its introduction in 1973, nasojejunal feeding has become an efficient and successful method of alimenting premature infants [1]. As with many other medical advances, potential hazards have arisen. The most significant is duodenal perforation caused directly by the tube. Three single case reports of this complication have appeared recently in the pediatric literature [2–4]. During the past year, we have experienced three duodenal perforations among premature infants on nasojejunal feeding. As a result, we would like to stress the radiographic features since the radiologist is in the position to establish an early diagnosis and possibly prevent such perforations.

CASE REPORTS

Case 1

A 730 g infant was placed on peripheral hyperalimentation on the fifth day of life and changed to nasojejunal feeding on the eleventh day. Tube position was verified radiographically to be in the distal duodenum (fig. 1*A*). There was no manipulation of the tube once it was in place. Two days later abdominal distention occurred suddenly with a marked drop in white count and platelets. An abdominal radiograph demonstrated that the tube had progressed into the left lower quadrant (fig. 1*B*). A minimal amount of free air was also seen under the left diaphragm. The tube was removed, and a radiograph in the erect position showed extensive free air (fig. 1*C*). Laparotomy revealed a 1.5 mm perforation in the third portion of the duodenum without other intestinal abnormality. Recovery was uneventful.

Case 2

A 1,300 g infant was placed on nasojejunal feeding on the sixth day. The tip of the tube was in the distal duodenum (fig. 2*A*). On the eighteenth day the infant showed abdominal distention, lethargy, and falling white count and platelets. There had been no tube manipulation. An upright abdominal radiograph demonstrated free air under the diaphragm and only minimal change in tube position (fig. 2*B*). Long dilated loops of small bowel with a mottled appearance on the right suggested the diagnosis of necrotizing enterocolitis. After removal of the tube and initiation of gastric suction, surgery revealed a pinpoint perforation of the third portion of the duodenum with otherwise normal bowel. Recovery was uneventful.

Case 3

An 1,150 g premature infant, the first of twins, was started on nasojejunal feeding on the sixth day of life. This followed resolution of hyaline membrane disease and successful treatment of a right-sided pneumothorax. Feedings were well tolerated until the fourth day when the patient had several episodes of vomiting and bradycardia. Radiographs first demon-

Received December 22, 1975.

[1] All authors: Department of Diagnostic Radiology and the Newborn Center, University of Tennessee Center for the Health Sciences, Memphis, Tennessee 38163.

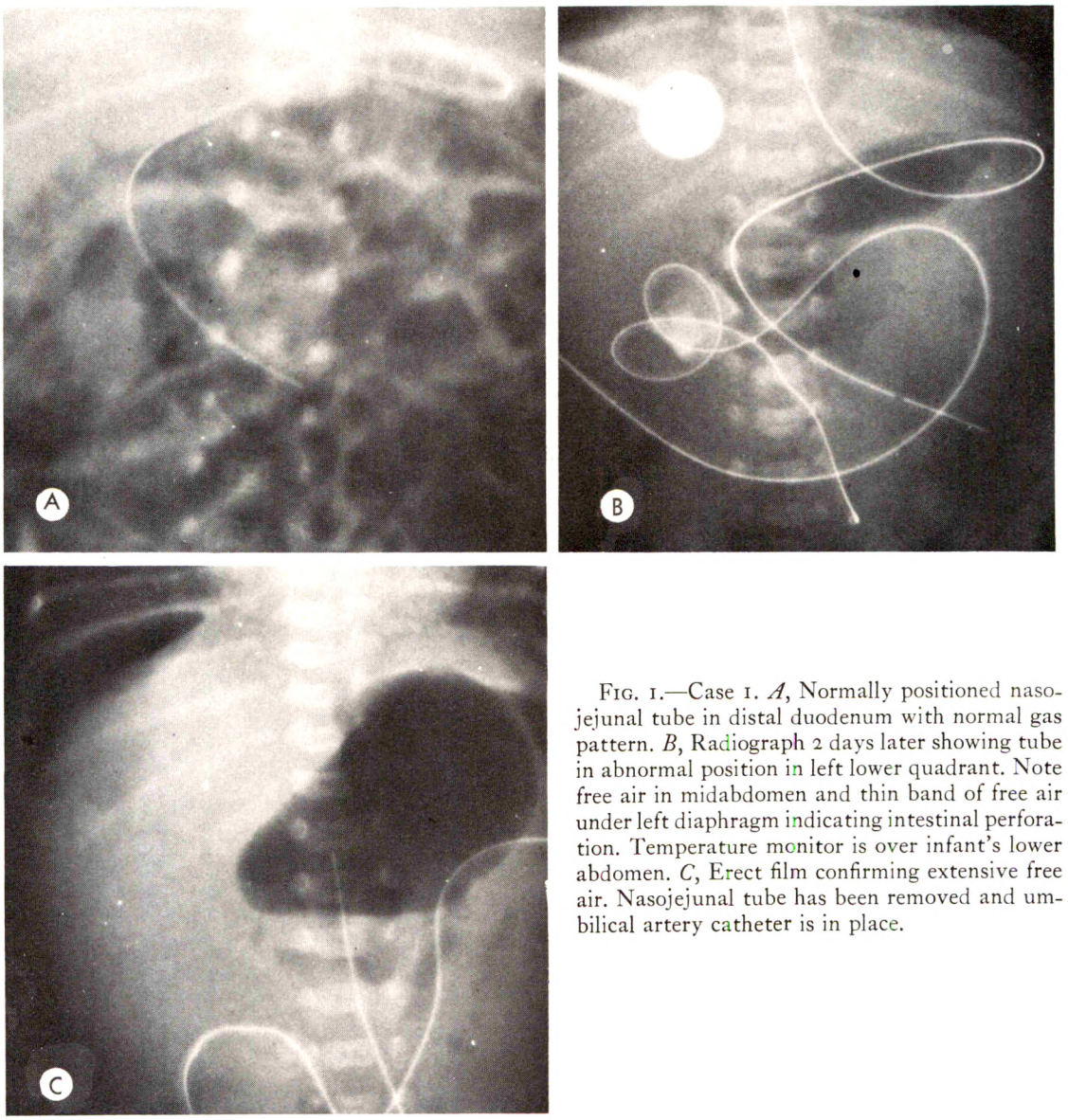


FIG. 1.—Case 1. *A*, Normally positioned nasojejunal tube in distal duodenum with normal gas pattern. *B*, Radiograph 2 days later showing tube in abnormal position in left lower quadrant. Note free air in midabdomen and thin band of free air under left diaphragm indicating intestinal perforation. Temperature monitor is over infant's lower abdomen. *C*, Erect film confirming extensive free air. Nasojejunal tube has been removed and umbilical artery catheter is in place.

strated long dilated loops of small bowel and free air under the diaphragm. The infant was started on therapy for necrotizing enterocolitis, the tube was withdrawn, and laparotomy was performed. A pinpoint perforation in the third part of a healthy duodenum was located and closed, and the postoperative course was uneventful.

DISCUSSION

Nasojejunal tubes present a unique problem. They are made of a polyvinyl material that appears to change consistency after as little as 6–12 hr in the small bowel. Instead of remaining a soft pliable plastic, they harden and become rigid. Thus they convert from a life-supporting tube to a potential hazard. The sudden appearance of free air in the abdomen of an otherwise healthy baby being fed through a nasojejunal tube should immediately suggest duodenal perforation.

Perforation can easily result if the tube is manipulated after being in the duodenum for more than 12 hr. Consequently, re-

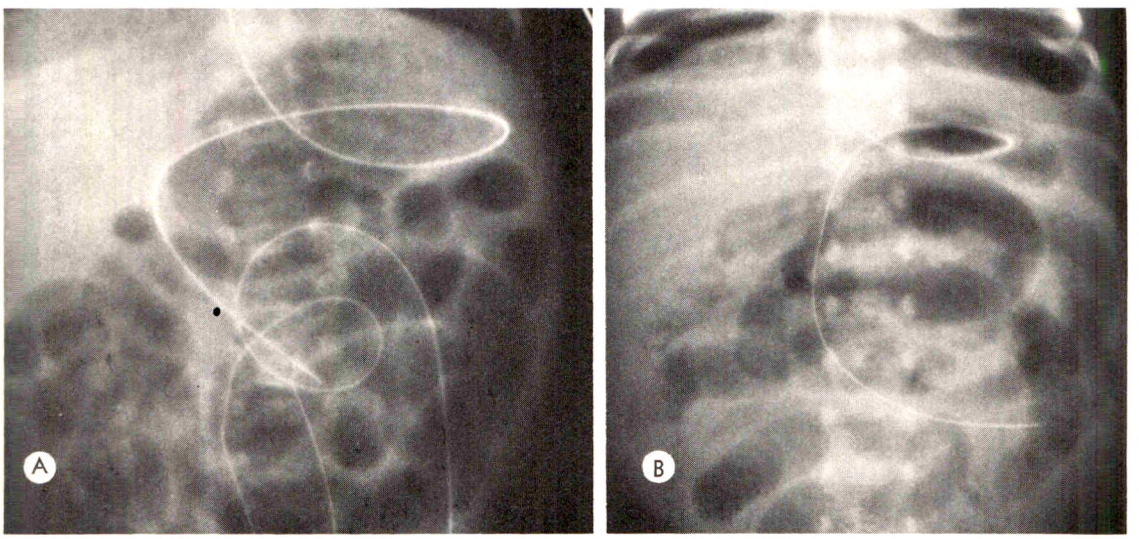


FIG. 2.—Case 2. *A*, Nasojejunal tube ending in distal duodenum with umbilical artery catheter ending just below it. *B*, Erect film 12 days later showing little change in position of nasojejunal tube. Free air is evident under diaphragm indicating bowel perforation. Separation of bowel loops and mottling, especially on right, is result of intraperitoneal infant formula.

positioning of the tube should be avoided whenever possible. If there is need for repositioning, the tube should be removed and a fresh one inserted. Unfortunately, normal peristaltic activity propels the tube and, as in our cases, results in spontaneous perforations.

It has been previously reported that nasojejunal tubes harden in the intestine [2, 3]. Why this occurs is not clear. We have been unable to duplicate this transition in vitro. Incubation of the tubes in nine buffered solutions ranging from pH 5.5 to 9.5 for 5 day periods at body temperature and at room temperature failed to produce any change in consistency. The addition of infant formula to the buffered solution also had no effect. We have not as yet challenged the tube with neonatal enzymatic secretions.

Radiographically it may not be possible to distinguish perforation caused by the nasojejunal tube from other causes such as necrotizing enterocolitis or spontaneous gastric perforation (see cases 2 and 3). At surgery, the distinction between puncture caused by the tube and necrotizing enterocolitis is obvious. In all instances of tube perforation, the adjacent bowel was entirely normal, whereas in necrotizing enterocolitis the bowel is ischemic, edematous, and often necrotic. The site of involvement is an important diagnostic feature since duodenal involvement is usual for perforations caused by a nasojejunal tube but rare in enterocolitis. While the differential diagnosis also includes idiopathic gastric perforation, we have seen no cases of gastric perforation in which the infant had a nasojejunal tube in place.

An attempt was made to diagnose perforations caused by a nasojejunal tube based on abnormal position of the distal end of the tube. Unfortunately this method is not very helpful since normally positioned tubes can end anywhere in the left upper quadrant or the midabdomen. Little change in position was observed following perforation (fig. 2*B*).

Visual proof of perforation caused by the tubes is lacking; thus the diagnosis is one of exclusion and inference. In all three cases presented, the tube was removed and replaced by a nasogastric tube for suction when the diagnosis of small bowel perforation was first suspected. Clear signs of

perforation in an infant on nasojejunal tube feeding should be adequate for the diagnosis.

The sites of perforation are uniformly within the duodenum. The increasingly rigid tube probably has difficulty negotiating the curving course of the duodenum which is relatively fixed to the retroperitoneum. Consequently, it would be preferable to initially place the tube beyond the duodenum into the more freely movable jejunum. However, such distal manipulation is not always possible. Clinicians should be warned of the potential hazard of a tube located in the duodenum. Tubes in this position should be removed to prevent possible perforation.

REFERENCES

1. Cheek JA, Staub GF: Nasojejunal alimentation for premature and full-term newborn infants. *J Pediatr* 82:955–958, 1973
2. Boros SJ, Reynolds JW: Duodenal perforation: a complication of neonatal nasojejunal feeding. *J Pediatr* 85:107–108, 1974
3. Cheu JW, Wong PWK: Intestinal complications of nasojejunal feeding in low-birth-weight infants. *J Pediatr* 85:109–110, 1974
4. Sun SC, Samuels S, Lee J, Marquis JR: Duodenal perforation: a rare complication of neonatal nasojejunal tube feeding. *Pediatrics* 55:371–375, 1975

Am J Roentgenol 126:1233–1238, 1976

LESION CONSPICUITY, STRUCTURED NOISE, AND FILM READER ERROR

HAROLD L. KUNDEL[1] AND GEORGE REVESZ[1]

ABSTRACT:

The concept of conspicuity is introduced in an attempt to objectively quantitate radiographic observational error. Defined as a ratio between lesion contrast and surround complexity, the measure correlates well with the probability of detecting faint nodular lesions in chest radiographs. The concept helps in understanding why abnormalities are missed by radiologists. It is also used to explain why image-processing techniques advocated in the past did not yield improvements in diagnostic accuracy and to outline directions for the future. Preliminary results are presented which show that photographic subtraction can increase the conspicuity of simulated early lung lesions and improve their detection.

INTRODUCTION

The visibility of a lesion such as a nodule on a chest film depends not only on the physical properties of the lesion such as size, shape, and density but also on the properties of the structures that surround it. For example, contrast is a joint property of the lesion and the surround: the greater the difference in density between the two, the greater the visibility. Additional factors affect visibility. One is the complexity of the normal anatomic structures that form the surround or background of the lesion. In the chest, this structural complexity is due for the most part to ribs and blood vessels. A commonly encountered example of structural complexity obscuring a lesion is the pulmonary nodule that is superimposed on the vascular shadow of the pulmonary hilum. The effect of structural complexity is illustrated in figure 1*A*, where four nodules of identical size, contrast, and edge sharpness were photographically superimposed on a chest film. Figure 1*B* was included to verify the presence and location of the nodules and was made by photographically subtracting the original normal film from the same film containing the simulated nodules.

Clearly, the nodule in the upper part of the right hilum is less visible than the one in the left upper lung, while the other two are intermediate in visibility. It seems logical to assume that the probability of detecting the lesion in the left upper lung is greater than the probability of detecting the nodule in the upper right hilum.

DEFINITION OF CONSPICUITY

To explore the relationship between the probability of detection of a nodule on the chest film and the complexity of the normal structures that surround it, a quantitative measure called conspicuity was developed [1]:

$$\text{conspicuity} = \frac{\text{lesion contrast}}{\text{surround complexity}}. \quad (1)$$

The technique for measuring complexity has been described [1]. In brief it consists of making a series of densitometric measurements with a small aperture (1 mm) along the inside and the outside of the border of the lesion. The density change *across* the lesion border is used to calculate contrast, and the rate of fluctuation of the density *around* the lesion border is used as a measure of complexity.

Presented at the annual meeting of the American Roentgen Ray Society, Atlanta, Georgia, October 1975.
This work was supported in part by U.S. Public Health Service grant CA 16491 from the National Cancer Institute.
[1] Diagnostic Radiology Research Laboratory, Temple University School of Medicine, Philadelphia, Pennsylvania 19140.

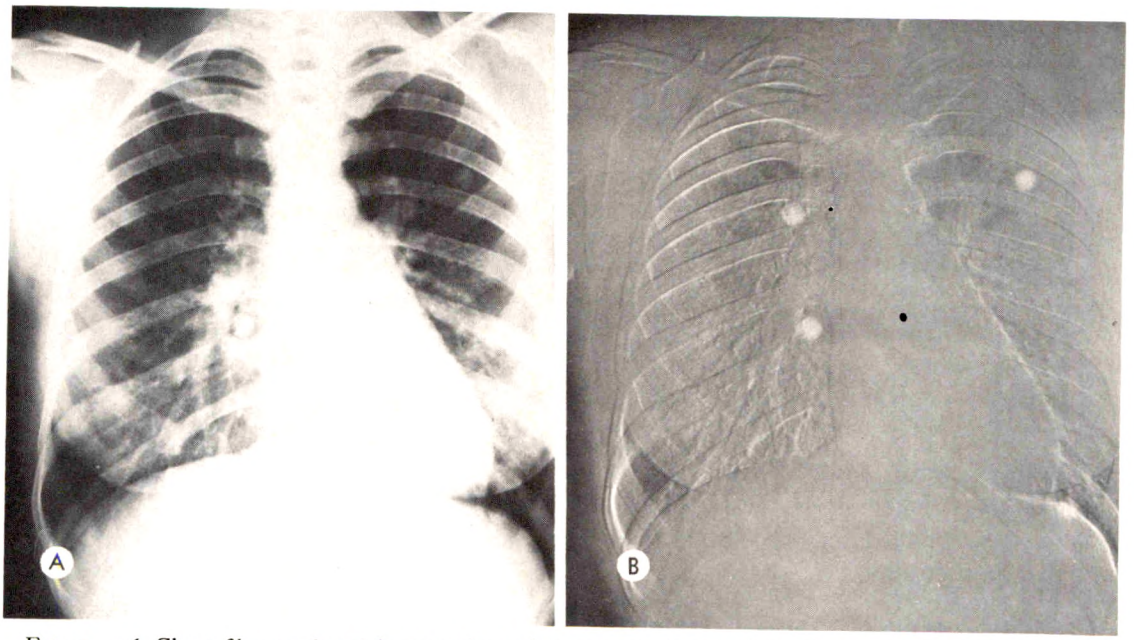


FIG. 1.—*A*, Chest film produced by superimposing grey mask containing four nodules of identical size, shape, and contrast. *B*, Result of subtracting original film from film with superimposed nodules.

To study the relationship between detection and conspicuity, the numerical value of conspicuity was measured for lung nodules on 25 different films. After 25 normal films were added to the series, they were shown in random sequence to 10 film readers who were asked to determine the presence and location of any nodules. Based on the responses, the probability of detection was calculated for each nodule. For the purposes of this experiment, false positives were neglected. A plot of the probability of detection $P(d)$ against the logarithm of conspicuity K is shown in figure 2. The logarithmic relationship seems to hold over a range of conspicuities from 0.5 to 1.5. That is, in a first approximation

$$P(d) = C(\log K), \qquad (2)$$

where C is a constant. Equation (2) is not complete. Factors such as size, the resolving ability of the human eye–brain system, the total background luminance, and factors related to visual search must be included. A more complete equation is in development. The purpose of this discussion is to present the concept of conspicuity and relate it to detection.

IMPROVING FILM READER ERROR

The study of conspicuity was undertaken to develop a rational basis for the use of image processing in radiology. Error rates are known to be high in reading chest films, approaching 30% in surveys for tuberculosis [2] or lung cancer [3]. Image processing techniques such as contrast enhancement, edge enhancement, density-to-color conversion, and others have been uniformly unsuccessful in improving error rates [4]. In our opinion, the importance of the structures that surround a lesion has not been recognized during picture processing. When using contrast or edge enhancement, the contrast or edges of both the lesion and the background structures are affected. If they are affected equally, conspicuity remains unchanged; if surrounding complexity increases faster than contrast, conspicuity will actually decrease. The latter appears to be what generally happens.

Engineers discuss this problem in terms

of signal and noise. Equation (1) is analogous to a signal-to-noise ratio except that the noise is not the traditional random graininess or mottle seen in images but rather consists of structures that interfere with the visibility of the signal. Therefore we have referred to this as structural noise [1].

The image processing problem now becomes one of either selectively enhancing contrast or selectively reducing structural complexity. The use of contrast material is an example of a technique to produce images with enhanced contrast, while planigraphy is a technique to decrease structural complexity. Subtraction is an image processing technique to reduce structural complexity or structural noise [4].

Reducing Structured Noise by Subtraction

Photographic subtraction is used increasingly in angiography: a preliminary film is subtracted from a film made after the injection of contrast material. Both films contain identical anatomic structures (structural noise), but the postinjection film also contains the contrast-filled vessels (the signal). Subtraction will then reduce complexity without affecting the signal contrast. Angiography is an ideal field for use of this technique because the major condition necessary for good results can be met, namely, accurate anatomic registration between the two films being subtracted. The structures to be subtracted must superimpose precisely to achieve good results, and in an angiogram with rapid serial filming this is possible.

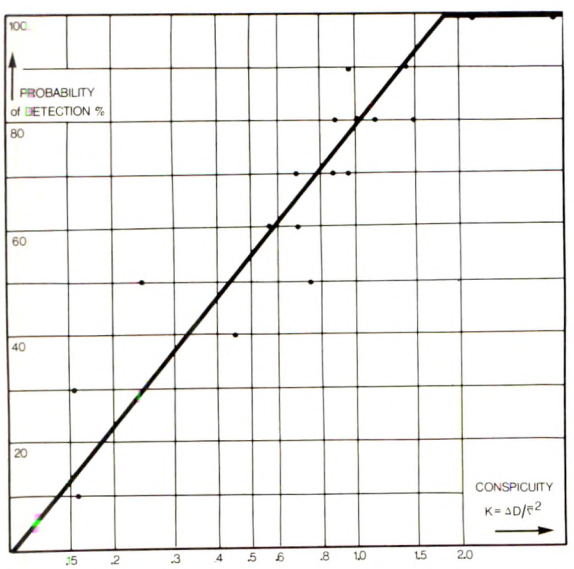


FIG. 2.—Probability of detecting nodule on chest film plotted against conspicuity on semilogarithmic scale. (Reprinted with permission from Revesz G, Kundel HL, Graber M: The influence of structured noise on the detection of radiologic abnormalities. *Invest Radiol* 9:479, 1974)

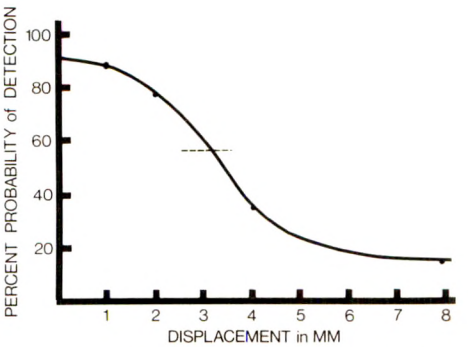


FIG. 3.—Probability of detecting nodule on subtraction film plotted against displacement (improper registration) of film containing nodule and film without nodule. Dashed line = average probability of detection for unsubtracted displays.

To improve detection of early lung lesions, particularly small cancers, ideally one would like to subtract films taken at some longer interval such as 6–12 months. The problem of image registration then becomes a major limiting factor. Two approaches are being studied: (1) positioning the patient in a reproducible way and (2) using computer programs to stretch or move anatomic structures on one film in order to achieve registration with the other [5].

To determine how close registration has to be to improve detection, the following experiment was done. A series of nodules ranging in size from 0.5 to 3 cm in diameter were artificially superimposed on 25 normal chest films at various locations in the lungs using a photographic technique [6] and

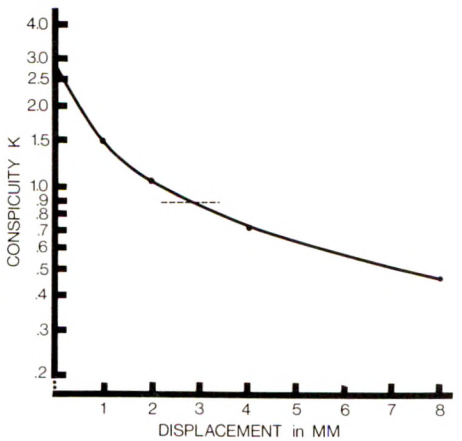


FIG. 4.—Effect of displacement of two subtracted radiographs on conspicuity of nodular lesion. Dashed line = average conspicuity for unsubtracted displays.

Kodak RP-D film. A reversal film was produced for each normal film on Kodak RP-SU film. The nodule films were then superimposed on the normal reversal films with horizontal displacements of 0, 1, 2, 4, and 8 mm. They were photographed on 35 mm slides, taking great care to maintain density ranges and contrasts during copying. This resulted in a series of 300 slides, half normal and half with nodules, in six modes of display: unsubtracted, perfect subtraction, and 1, 2, 3, 4, and 8 mm of displacement. These slides were projected on a rear view screen to standard 14×17 inch size and displayed in random order to five film readers. Each film reader was shown the series two times so that each nodule film was seen 10 times. The probability of detection of the nodule was then calculated.

Figure 3 shows the probability of detection of the subtracted films plotted against displacement. The average probability of detection of the unsubtracted films is also shown. With lesions in the 5–30 mm range, detection is improved by subtraction as long as registration error is limited to less than 3 mm. Otherwise detection is worse.

As a further check of the conspicuity hypothesis, K was measured for each of the nodules on both subtracted and unsubtracted films. Figure 4 shows the conspicuity plotted against displacement in millimeters on a semilogarithmic scale compared to the average conspicuity value for unsubtracted films. Again the crossover value is at about 3 mm.

Practical Application

After establishing a theoretical limit for registration, an attempt was made to realize that limit in practice. A simple device to position a patient in the erect position in front of a film cassette was constructed of aluminum tubing. Shown in figure 5, it consists of a chin rest on the top of the cassette and two cradles acting like crutches with an extended support running from the axilla to the elbow to hold the arms in a horizontal position. A volunteer was radiographed and returned 1 week later for a second frontal chest film. This time three plastic nodules 1 cm in diameter were attached to the skin of his back so that they would superimpose on the lungs. Figure 6 shows the "nodule film" and the result of subtracting the original film from that

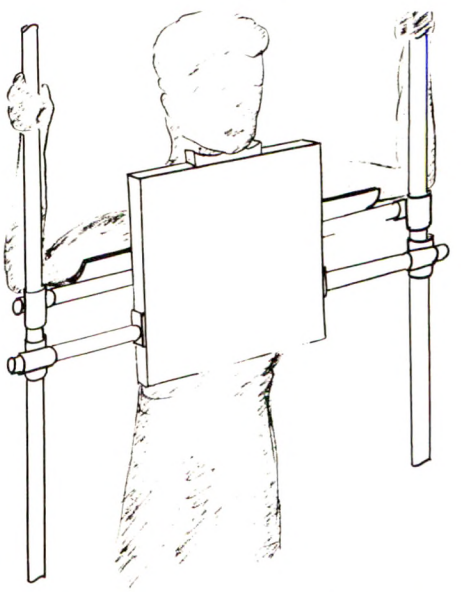


FIG. 5.—Simple device used to position patient. Patient is restrained by chin rest atop screen/film cassette, arm supports, and hand grip. Pictures are taken at full inhalation.

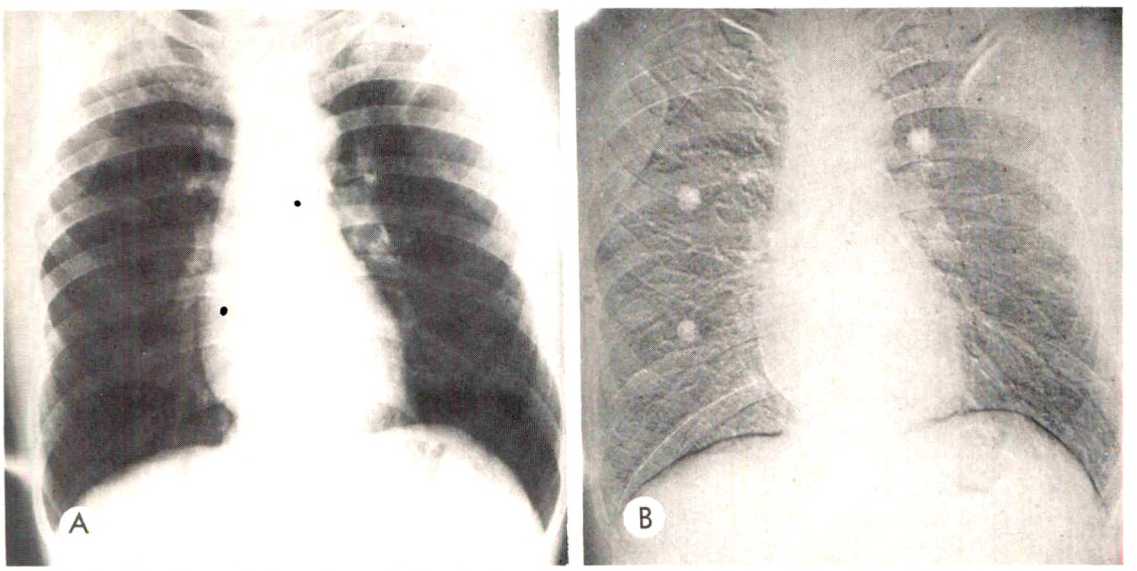


FIG. 6.—*A*, Film of person with three plastic nodules taped to back. *B*, Result of subtracting normal chest film of same person obtained at different time.

taken a week later. Clearly the visibility of the nodules has improved. Conspicuity was measured for each nodule in the subtracted and unsubtracted image (table 1). The K value has increased, and since it has been shown that the probability of detection increases with increased conspicuity, it follows that subtraction *can* work for the chest under clinical conditions.

DISCUSSION AND CONCLUSIONS

The fact that a technique works is a necessary demonstration but is not sufficient to even begin a clinical study. A highly motivated group of volunteers who understand exactly what to do is not representative of any patient population. Much more effort needs to be directed to the positioning device, particularly with respect to controlling the level of the hemidiaphragms at the time of exposure. Electronic devices using an image intensifier have been suggested but not tested [5].

We believe that the most important aspect of this work is the development of a rational mathematical basis for describing radiographic observational error. A process that is not understood is difficult to improve by any means but serendipity. The concept of conspicuity has been used to describe the effect of both random noise [7] and structural noise [8] on the detection of targets by peripheral vision and may be of value in the description of the effect of the visual search process on detection [9]. At present the mathematical formulation is only valid for circumscribed lesions where the border can be either definitely identified or extrapolated with a high level of confidence. Generalization of the concept to other abnormalities is essential. Nevertheless, it does provide a firm rationale for further subtraction studies and may provide an analytical technique for evaluating the potential usefulness of various patient

TABLE 1

CONSPICUITY VALUES OF SIMULATED NODULES FOR UNSUBTRACTED AND SUBTRACTED FILMS

Location	Original Film	Subtracted Film
Right lobe:		
Middle	1.43	2.18
Upper	1.91	2.58
Left upper lobe	1.17	2.66

positioning apparatuses without resorting to subjective appraisals or clinical trials which should be reserved for techniques where the expectation of success is high.

REFERENCES

1. Revesz G, Kundel HL, Graber M: The influence of structured noise on the detection of radiologic abnormalities. *Invest Radiol* 9:479–486, 1974
2. Yerushalmy J: The statistical assessment of the variability in observer perception and description of roentgenographic pulmonary shadows. *Radiol Clin North Am* 7:381–392, 1969
3. Guiss LW, Kuenstler P: A retrospective view of survey photofluorograms of persons with lung cancer. *Cancer* 13:91–95, 1960
4. Kundel HL, Ziskin MC: The evaluation of television image processing for diagnostic radiology. *CRC Crit Rev Clin Radiol Nucl Med* 1(3):435–457, 1970
5. Kinsey JH, Vannelli BD, Fontana RS, Miller WE, Johnson SA, Gilbert BK: Application of digital image change detection to diagnosis and follow-up of cancer involving the lungs, in *Proceedings of the Meeting on Application of Optical Instruments in Medicine*, Atlanta, Georgia, September 1975, vol 4, pp 99–112
6. Kundel HL, Revesz G, Stauffer HM: Evaluation of a television image processing system. *Invest Radiol* 3:44–50, 1968
7. Engel FL: Visual conspicuity, directed attention, and retinal locus. *Vision Res* 11:563–576, 1971
8. Kundel HL: Peripheral vision, structured noise, and film reader error. *Radiology* 114:269–273, 1975
9. Engel FL, Bos TM: Visual conspicuity and eye movements, in *Annual Progress Report of the Institute for Perception*, Eindhoven, Netherlands, vol 6, 1971, pp 45–52

Am J Roentgenol 126:1239–1245, 1976

A CIRCULAR TEST PATTERN FOR EVALUATING X-RAY TUBE FOCAL SPOTS

G. H. Zeman,[1] G. U. V. Rao,[1] and R. J. Doyle[2]

ABSTRACT:

The design and use of a circular x-ray resolution test pattern is presented. This pattern is shown to yield equivalent focal spot dimensions equal to those obtained with the more commonly used star pattern. The advantage of using the circular pattern is that it obviates the necessity of positioning the pattern strictly along the x-ray beam central axis. A major source of experimental error in making focal spot measurements is therefore circumvented, especially in the case of x-ray tubes with a small target angle.

One of the important causes of loss of resolution in a radiographic imaging system is the finite size of the x-ray focal spot. Traditionally the size of an x-ray focal spot has been determined by making a pinhole image of it at some convenient magnification [1]. Recent recognition that the resolution limitations imposed by an x-ray focal spot are not only a function of focal spot size but also its shape and intensity distribution have led to a number of methods to determine what is now referred to as the equivalent focal spot size [2–5]. The equivalent focal spot size of an x-ray tube is defined as the size of a homogeneously irradiating rectangular focal spot that yields the same resolution as the tube in question.

Two types of test patterns are currently in use for the determination of equivalent focal spot size: the line-bar pattern and the star pattern [3, 5, 6]. The major difficulty associated with the use of these test patterns, and in fact with the pinhole method also, is that the measured focal spot dimensions are critically dependent on the position of the pattern with respect to the x-ray beam central axis. This difficulty arises because of the line-focus principle employed in the design of the anodes of many diagnostic x-ray tubes. For x-ray tubes with small anode target angles, it is especially important to ensure proper alignment of the test patterns along the x-ray beam central axis. This paper presents a discussion of this difficulty and proposes to circumvent most alignment problems through use of a circular test pattern.

BACKGROUND

Line Focus Principle

The line focus principle used in most x-ray tubes is illustrated in figure 1. The x-ray beam originates over an area of length l of the tube anode, which is positioned at target angle ϕ with respect to the x-ray beam central axis. Along the central axis ($\theta = 0$), the projected focal spot size $a_{pa}(0)$ parallel to the anode-cathode axis is equal to AB and is given by the equation

$$a_{pa}(0) = l \sin \phi. \qquad (1)$$

At an angle θ toward the anode from the central axis, the projected focal spot size DC is equal to $l \sin (\phi - \theta)$. In the plane of the test object, the projected focal spot length $a_{pa}(\theta)$ is equal to CE and is given by the equation

$$a_{pa}(\theta) = l \sin (\phi - \theta)/\cos \theta. \qquad (2)$$

By substituting the value for $a_{pa}(0)$ from equation (1) in equation (2),

$$a_{pa}(\theta) = a_{pa}(0)\left(1 - \frac{\tan \theta}{\tan \phi}\right). \qquad (3)$$

The equivalent width a_{pe} of the focal

[1] Department of Radiology and Radiological Sciences, Johns Hopkins University School of Medicine, Baltimore, Maryland 21205.
[2] CGR Medical Corporation, Baltimore, Maryland 21203.

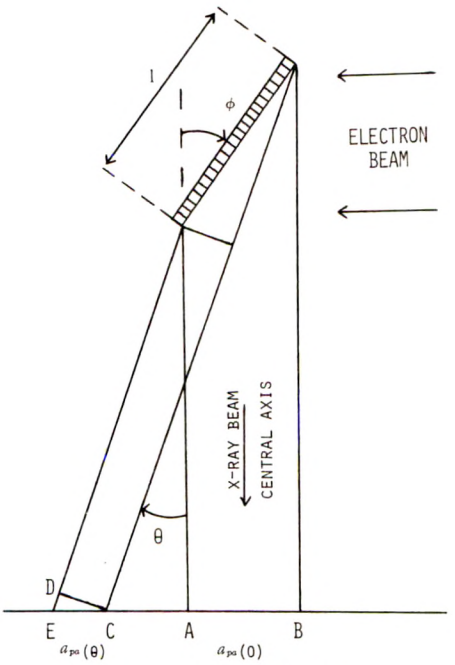


FIG. 1.—Line focus principle.

spot along a direction perpendicular to the anode cathode axis is practically independent of the angle of projection [7]. Equivalent focal spot dimensions are usually specified by the lengths $a_{pa}(\circ)$ and a_{pe}.

Equivalent Focal Spot Measurements

The measurement of equivalent focal spot dimensions using resolution test patterns has traditionally been done as follows. First a magnified radiographic image of the test pattern is formed. The lowest spatial frequency f_0 of the lines at which complete loss of resolution occurs is then visually estimated. This frequency represents the first zero of the focal spot modulation transfer function [3] and may be used to calculate the equivalent focal spot size a from the equation

$$a = \frac{1}{f_0}\left(\frac{m}{m-1}\right), \qquad (4)$$

where m is the radiographic magnification factor.

For measurements of a_{pe}, a line-bar pattern is positioned so that the line pairs are parallel to the anode-cathode axis. Conversely, to measure $a_{pa}(\circ)$, the pattern is positioned so that the line pairs are perpendicular to the anode-cathode axis. Thus at least two images are required to measure the effective focal spot dimensions with a line-bar pattern.

The star test pattern allows measurement of both a_{pe} and $a_{pa}(\circ)$ from a single image. This is because the radial spokes of the star pattern form spatial frequency line pairs oriented in all directions. Therefore to measure a_{pe} and $a_{pa}(\circ)$, the lowest disappearance frequencies of the radial spokes oriented parallel and perpendicular, respectively, to the anode-cathode axis are used.

It must be emphasized that for either of the above test patterns, accurate knowledge of the location of the x-ray beam central axis is required for measurement of $a_{pa}(\circ)$. If the test pattern is not located strictly along this axis, then the measured length will be $a_{pa}(\theta)$ as given by equation (3). The amount of error involved in such measurements depends on both the positioning error θ and the x-ray tube target angle ϕ. The smaller the target angle, the more significant the positioning error. For example, a 2° positioning error results in an 11% error in the focal spot size for tubes in which $\phi = 17°$ and 28% error when $\phi = 7°$.

CIRCULAR TEST PATTERN METHOD

The problem of positioning the resolution test pattern strictly along the x-ray beam central axis can be circumvented by using two adjacent line-bar patterns along the anode-cathode axis (fig. 2) or a circular pattern* (fig. 3). With such patterns the equivalent length $a_{pa}(\theta)$ of the focal spot determines the value of the disappearance frequency observed along the anode-cathode axis rather than perpendicular to it as in the case of the star pattern. Due to the

* Prototype made by Emil Funk Optik (West Germany) following our specifications.

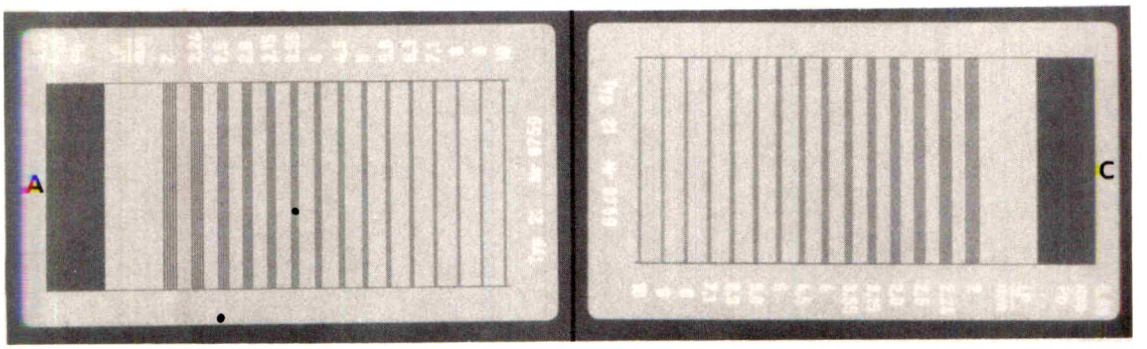


FIG. 2.—Double line-bar test pattern oriented along anode-cathode (A-C) axis for determination of equivalent focal spot lengths. Because of line focus principle, a different disappearance frequency is observed in each pattern.

line focus principle (eq. 3), the value of $a_{pa}(\theta)$ varies along the anode-cathode axis. Therefore the images of the double line-bar and circular test patterns will be asymmetrical since the disappearance frequency observed in one direction along the anode cathode axis is different from that observed in the other. This asymmetry, which does not arise in images of star test patterns, forms the basis for measuring $a_{pa}(o)$ using the double line-bar or circular test patterns.

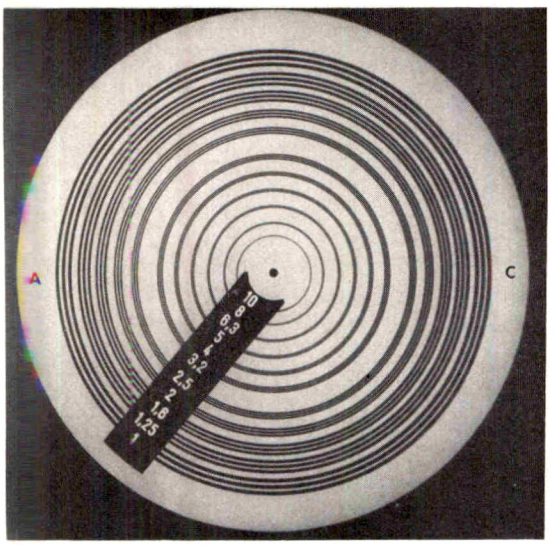


FIG. 3.—Circular test pattern for determination of equivalent focal spot dimensions. In this image the disappearance frequencies along the anode-cathode (A-C) axis were 3.2 mm^{-1} toward the cathode and 6.3 mm^{-1} toward the anode. Disappearance frequency perpendicular to the anode-cathode axis was 5 mm^{-1}.

If the two disappearance frequencies f_1 and f_2 observed along the anode-cathode axis occur at angles θ_1 and θ_2 from the x-ray beam central axis, then two effective focal spot lengths $a_{pa}(\theta_1)$ and $a_{pa}(\theta_2)$ can be calculated from equation (4). The distances S_1 and S_2 (see fig. 4) from the x-ray beam central axis to the observed disappearance frequencies are related to the angles θ_1 and θ_2 as follows:

$$S_1 = d \tan \theta_1$$
$$S_2 = -d \tan \theta_2, \qquad (5)$$

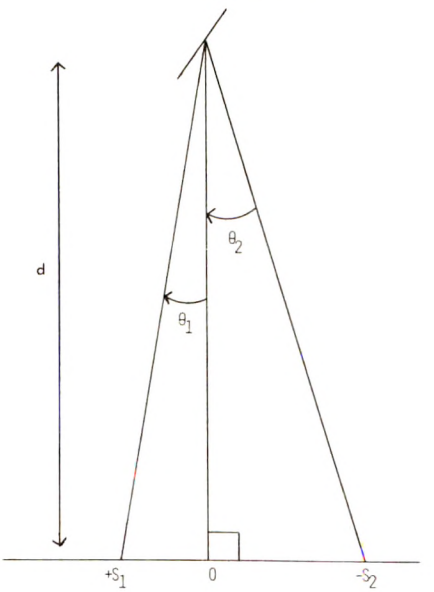


FIG. 4.—Relationship between distances of disappearance frequencies from central axis as measured in the image plane and corresponding angular displacements.

where d is the focus-to-film distance. (The minus sign indicates that S_2 is measured in the opposite direction.) The effective focal spot lengths can be related to S_1 and S_2 by combining equations (3) and (5) as follows:

$$a_{pa}(\theta_1) = a_{pa}(0)\left(1 - \frac{S_1}{d \tan \phi}\right)$$
$$a_{pa}(\theta_2) = a_{pa}(0)\left(1 + \frac{S_2}{d \tan \phi}\right). \quad (6)$$

By subtracting $a_{pa}(\theta_2)$ from $a_{pa}(\theta_1)$, we arrive at the following equation:

$$a_{pa}(0) = [a_{pa}(\theta_1) - a_{pa}(\theta_2)]\frac{d \tan \phi}{S_1 + S_2}. \quad (7)$$

Equation (7) can be rewritten in terms of the disappearance frequencies f_1 and f_2 as follows:

$$a_{pa}(0) = \left(\frac{1}{f_1} - \frac{1}{f_2}\right)\frac{m}{m - 1}\left(\frac{d \tan \phi}{S_1 + S_2}\right). \quad (8)$$

Equation (7) provides a method for determining the central axis equivalent focal spot size parallel to the anode-cathode axis without the requirement of an accurate knowledge of the position of the x-ray beam central axis. This is because the total distances S_1+S_2 between the disappearance frequencies f_1 and f_2 can be measured directly from the pattern image, even though the individual distances S_1 and S_2 remain unknown. Also required to measure $a_{pa}(0)$ are the magnification factor m, the focus-film distance d, and the x-ray tube target angle ϕ. Generally the manufacturer provides the value of ϕ for a given x-ray tube. However, ϕ can also be determined by an experimental method (see later).

The above analysis applies equally well to two adjacent line-bar patterns or to the circular pattern. The advantage of using the circular pattern is that the value of a_{pe} can be determined from the same image used to determine $a_{pa}(0)$. This is accomplished by observing the disappearance frequency along the pattern direction perpendicular to the anode-cathode axis.

EXPERIMENTAL RESULTS

Two types of experiments were performed to evaluate the circular test pattern. First, equivalent focal spot dimensions of three x-ray tubes were measured using both the star and circular test patterns to compare the two methods. Second, the equivalent focal spot dimensions of a single x-ray tube were measured using the circular test pattern positioned at several locations with respect to the x-ray beam central axis to determine if unique values of a_{pe} and $a_{pa}(0)$ would be obtained.

In each experiment the x-ray beam central axis was located by a parallax method. The device used consisted of two identical aluminum discs 3 mm thick in which a rectangular array of holes 1.5 mm in diameter had been drilled at 6.5 mm intervals. The discs were mounted on the parallel ends of a hollow plexiglass cylinder 16 cm in diameter and 15 cm in height. The cylinder was positioned directly above an x-ray film and aligned so that the optical cross hairs of the x-ray collimater coincided with the axes of the rectangular array of holes. The focus-film distance most often used was 80 cm. At this distance the 6.5 mm spacing between the holes in the lower aluminum plate represents an angular displacement of 0.5°. A photograph of the parallax cylinder and a typical radiographic image are shown in figures 5 and 6, respectively. The line joining the upper and lower holes which coincide in the processed image determines the x-ray beam central axis. Using this method, the location of the central axis was determined within ±0.25°.

The target angle of each x-ray tube used was measured by observing the position at which anode cutoff occurred in the same image used to locate the x-ray beam central axis. The distance S_a from the central axis to the position of anode cutoff was measured (see fig. 6) and the target angle calculated from the equation

$$\phi = \tan^{-1}\frac{S_a}{d}, \quad (9)$$

TABLE 1

X-RAY TUBE DATA FOR FOCAL SPOT MEASUREMENTS

	X-RAY TUBE		
	1	2	3
Focal spot, nominal (mm)	0.3	0.3	0.6
Target angle, nominal (°)	10	11	11
Target angle, measured (°)	9.8	12.0	11.8
kVp	50	80	85
mA	100	150	200

where d is the focus-to-film distance. The results of these measurements are shown in table 1 along with other physical data on the three x-ray tubes used for focal spot measurements.

Measurements of equivalent focal spot dimensions using both the star and circular patterns positioned along the x-ray beam central axis are shown in table 2. For each x-ray tube the values of a_{pe} and a_{pa} obtained by the two methods were equal within the limits of experimental error. Table 3 presents results of a series of focal spot measurements for a 10° target angle x-ray tube with the circular test pattern positioned at various locations with respect to the x-ray beam central axis. The calculated value of a_{pe} was identical over a range of ±2° with respect to the central axis either along or perpendicular to the anode-cathode axis. The values of $a_{pa}(o)$ varied from 0.34 to 0.38 mm at the various positions, with the central axis position yielding 0.36 mm. These variations are within the experimental error of estimating the disappearance frequencies. Similar displacements of a star test pattern resulted

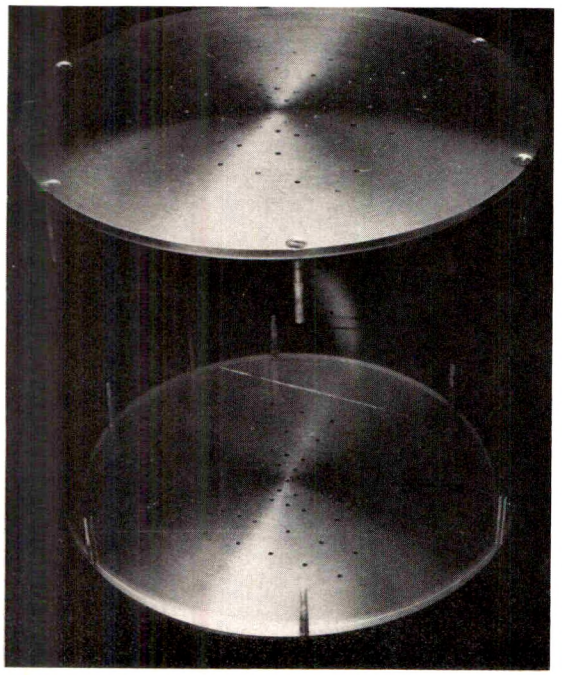


FIG. 5.—Cylindrical parallax device used to locate position of x-ray beam central axis.

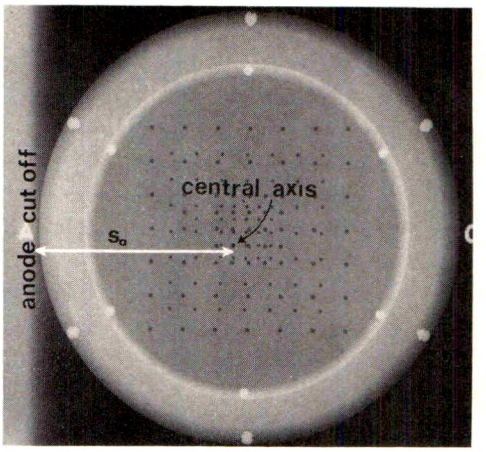


FIG. 6.—Typical radiographic image obtained with cylindrical parallax device. Location of x-ray beam central axis is determined by position at which images of an upper and lower grid hole coincide. Target angle ϕ of x-ray tube is calculated from equation $\phi = \tan^{-1}(S_a/d)$, where d is focus-to-film distance and S_a is distance measured on image from central axis to position of anode cutoff. A-C = anode-cathode axis.

TABLE 2

COMPARISON OF STAR AND CIRCULAR PATTERN FOCAL SPOT MEASUREMENTS

	a_{pa}		$a_{pa}(o)$	
X-RAY TUBE	Star	Circle	Star	Circle
1	0.34	0.34	0.35	0.36
2	0.56	0.56	0.48	0.46
3	0.88	0.76	1.02	1.09

NOTE.—Values shown in mm.

TABLE 3

OFF-AXIS MEASUREMENTS WITH CIRCULAR PATTERN

ANGLE FROM CENTRAL AXIS (°)		FOCAL SPOT MEASUREMENT (mm)	
Along A-C	Perpendicular to A-C	a_{pe}	$a_{pa}(o)$
o	o	0.34	0.36
+2	o	0.34	0.35
+2	±2	0.34	0.38
−2	o	0.34	0.34
−2	±2	0.34	0.34

NOTE.—A-C= anode-cathode axis.

in measured equivalent focal spot lengths ranging from 0.29 to 0.45 mm.

DISCUSSION

The circular test pattern proposed in this paper has been shown to yield equivalent focal spot dimensions equal to those obtained by the more commonly used star test pattern. The advantage of using the circular test pattern is that it need not be accurately aligned along the x-ray beam central axis. Therefore use of this pattern will obviate a major source of error in the measurement of equivalent focal spot dimensions, especially for small target angle x-ray tubes for which the projected focal spot size depends strongly on the angle of projection.

The simple parallax device described in this report can be used to locate the x-ray beam central axis within ±0.25°, which is sufficiently accurate for most applications. Additionally, the parallax device was found useful in measuring x-ray tube target angles. We have used this device to evaluate a number of diagnostic x-ray tubes and have generally found that while nominal target angle values are accurate within 1.0°, the location of the x-ray beam central axis may be displaced from the optical cross hairs of the tube collimator by as much as ±2°. These variations represent a major source of error in evaluating x-ray tube equivalent focal spot dimensions.

The circular test pattern is especially applicable to small target angle x-ray tubes. This is because the calculation of $a_{pa}(o)$ is based on the difference $a_{pa}(\theta_1) - a_{pa}(\theta_2)$ between the projected focal lengths at two different positions along the anode-cathode axis. With small target angle tubes this difference is accentuated more so than with large target angle tubes. Therefore measurement of $a_{pa}(o)$ with the circular pattern will be more accurate for small than for large target angle tubes. The star and circular patterns can be used complementarily, with the former applicable to large target angle tubes where accurate positioning is not critical and the latter to small target angle tubes for which it allows accurate measurements without the requirement of accurate positioning.

One drawback to the use of resolution test patterns for evaluating equivalent focal spot dimensions is that with some tubes a disappearance frequency cannot be observed. This will be the case if the intensity distribution from the focal spot happens to be a Gaussian or exponential distribution. Special methods have been devised to specify the equivalent focal spot size in these cases [8]. Another possibility in this area lies in the recently proposed use of a Fresnel zone plate test pattern for focal spot measurements [9]. This method may allow direct reconstruction of the focal spot intensity distribution from a test pattern image.

ACKNOWLEDGMENT

We thank Mrs. Ellen Ellis for typing the manuscript. G. Zeman expresses appreciation to the U.S. Navy Bureau of Medicine and Surgery for sponsoring his educational program.

REFERENCES

1. International Commission on Radiological Units and Measurements: *Methods of Evaluating Radiological Equipment and Materials*, NBS Handbook 89, Washington, D.C., Government Printing Office, 1962
2. Rao GUV, Bates LM: Effective dimensions of roentgen tube focal spots based on measurement of the modulation transfer function. *Acta Radiol* 9:362–368, 1970
3. Rao GUV: A new method to determine the focal

spot size of x-ray tubes. *Am J Roentgenol* 111: 628–633, 1971
4. Rao GUV: Effective focal spot size. *Invest Radiol* 7:352–353, 1972
5. Rao GUV: Evaluation of the focal spot characteristics of diagnostic x-ray tubes. *Proc Soc Photo-Optical Instrumentation Engineers* 56:139–149, 1975
6. Spiegler P, Breckinridge WC: Imaging of focal spots by means of the star test pattern. *Radiology* 102:679–684, 1972
7. Moores BM, Roeck W: The field characteristics of the focal spot in the radiographic imaging process. *Invest Radiol* 8:53–57, 1973
8. Rao GUV, Soong A: Physical characteristics of modern microfocus x-ray tubes. *Am J Roentgenol* 119:626–634, 1973
9. Braun M, Stoner WW: Zone plate: a new resolution test pattern for focal spots. Paper presented at the annual meeting of the American Association of Physicists in Medicine, San Antonio, Texas, August 1975

Am J Roentgenol 126:1246–1248, 1976

LACK OF GALLIUM UPTAKE IN PRIMARY HEPATIC AMYLOIDOSIS

THOMAS G. GOERGEN,[1] ANDREW TAYLOR, AND NAOMI ALAZRAKI

ABSTRACT:

^{99m}Tc-sulfur colloid and ^{67}Ga citrate hepatic scintigrams showed matching defects in a patient with diffuse primary amyloidosis. Amyloidosis should be added to the usual differential diagnosis of such matching lesions which includes cysts, fibrosis, most benign tumors, and occasional metastatic lesions which do not concentrate gallium.

Liver scanning with ^{67}Ga citrate is often helpful for evaluation of focal abnormalities detected on the routine ^{99m}Tc-sulfur colloid scan. Increased gallium uptake in an area of decreased sulfur colloid activity generally suggests tumor or abscess, while decreased gallium uptake matching a focal abnormality on the sulfur colloid scan suggests a benign process such as a cyst, fibrosis, or benign tumor. This report presents a case of focally decreased gallium uptake in the liver matching the sulfur colloid scan in a patient with primary amyloidosis.

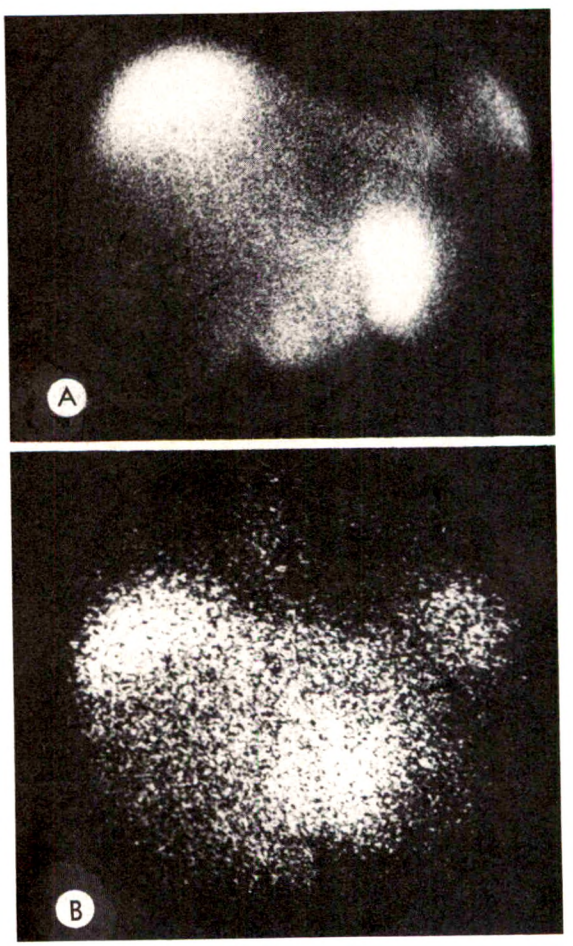


FIG. 1.—*A*, ^{99m}Tc-sulfur colloid images of anterior liver showing hepatomegaly with large areas of decreased activity. There is more normal uptake in dome and inferior left lobe. *B*, Same view with ^{67}Ga citrate showing large areas of decreased activity corresponding to colloid images.

CASE REPORT

A 65-year-old alcoholic was admitted with progressive chest pain, abdominal pain, and increasing abdominal girth. The abdomen was distended by a large palpable liver. Pertinent laboratory values (normal range in parentheses) included: SGOT, 66 (8–300); serum alkaline phosphatase, 105 (4.5–11); and bilirubin, 2.1 mg/100 ml. An upper gastrointestinal examination revealed esophageal varices and mural or submucosal mass without ulceration in the left anterior gastric fundus. A ^{99m}Tc-sulfur colloid scan showed hepatosplenomegaly with large focal defects in both the liver and spleen (figs. 1*A* and 2). A ^{67}Ga citrate scan showed a matching pattern of decreased accumulation in the liver (fig. 1*B*). Sonography of the right upper abdomen revealed an enlarged liver with multiple internal echoes, suggesting an infiltrating process such as fibrosis or diffuse hepatoma

Received February 6, 1976.

[1] All authors: Department of Radiology, University of California at San Diego, and Nuclear Medicine Service, Veterans Administration Hospital, 3350 La Jolla Village Drive, San Diego, California 92161. Address reprint requests to N. Alazraki at the Veterans Administration Hospital.

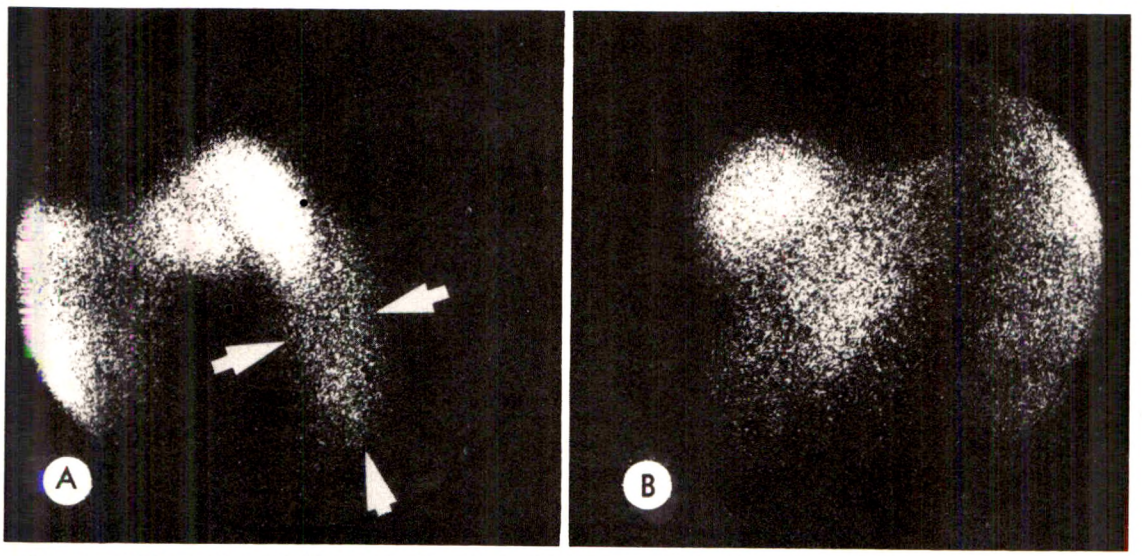


FIG. 2.—^{99m}Tc-sulfur colloid images of anterior (*A*) and posterior (*B*) spleen showing splenomegaly with markedly decreased counts in lower pole (*arrows*).

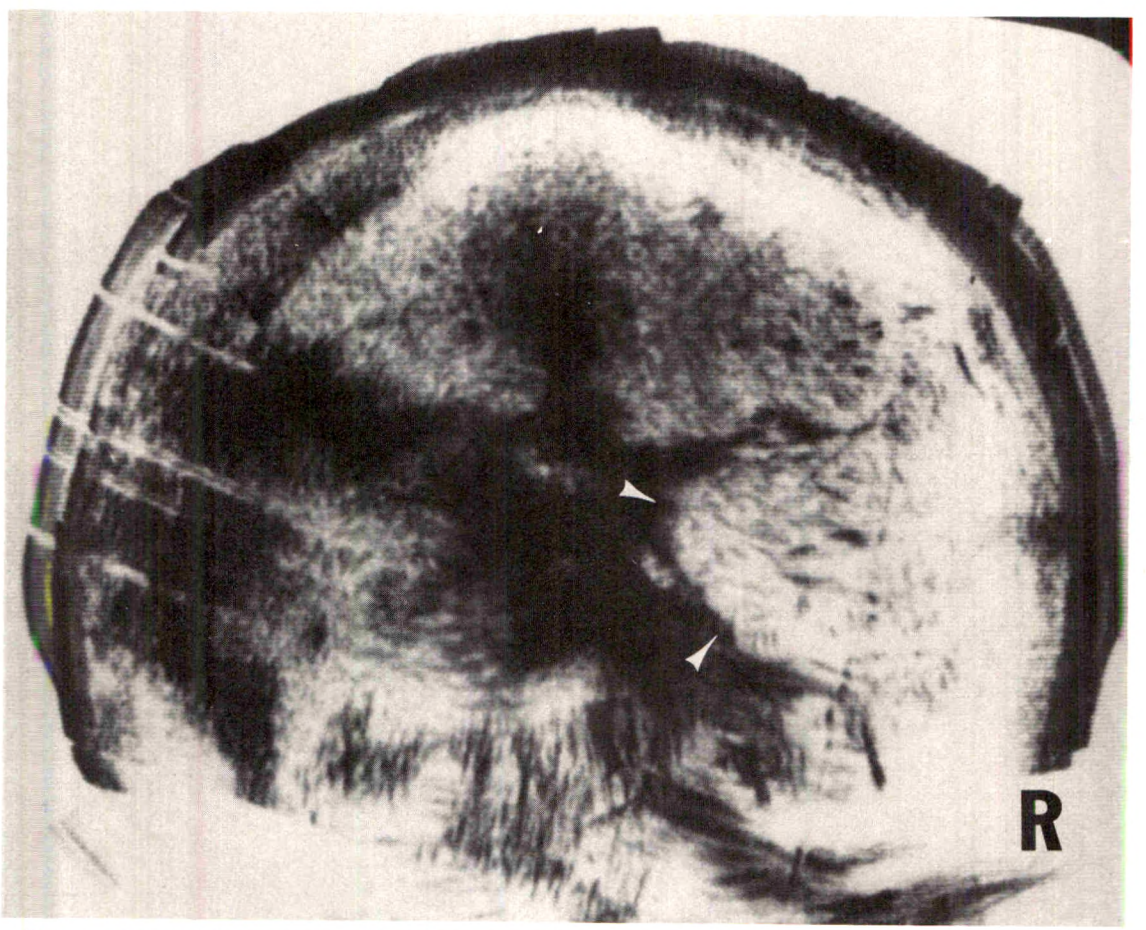


FIG. 3.—Gray-scale sonogram of liver (transverse, 6 cm above umbilicus) showing generalized hepatomegaly, including the caudate lobe (*arrows*), and generalized increase in internal echoes.

U. S. • UNIVERSITY • LIBRARY

(fig. 3). A liver biopsy and biopsy of the gastric mass revealed massive amyloid deposition. Subsequent evaluation has failed to establish a diagnosis of myeloma.

DISCUSSION

Amyloidosis is a disease of unknown etiology which in its primary or secondary form may affect a variety of organ systems. The basic pathologic abnormality is characterized by accumulation of abnormal protein mucopolysaccharide in various tissues and around blood vessels. In a patient with widespread primary amyloid infiltrates in the liver, large focal areas of decreased radionuclide accumulation were identified on the ^{99m}Tc-sulfur colloid scan. Liver scanning with ^{67}Ga citrate revealed areas of decreased gallium accumulation matching the sulfur colloid images.

In a small series of multisystem scanning in primary amyloidosis, ^{99m}Tc-sulfur colloid liver scan abnormalities included hepatomegaly with either homogeneous or heterogeneous uptake [1]. Spleen scans in the same patients ranged from normal to enlarged with either increased or decreased uptake. There was one case of absent spleen uptake with diffuse splenic amyloidosis. Experience with gallium or other tumor scanning agents has not been reported.

Uniform gallium activity is expected in the normal liver; the site of uptake is thought to be the hepatocyte. It has been postulated that hepatic metabolism of the citrate liberates free gallium which can form proteinate complexes within the liver [2]. Since hepatic involvement is common in amyloidosis, the appearance of large focal defects on the ^{67}Ga citrate scan is not surprising. Presumably, residual functioning hepatocytes were displaced by large areas of amyloid deposition. Thus the differential diagnosis of matching focal defects in the liver on liver scans with ^{99m}Tc-sulfur colloid and ^{67}Ga citrate should include amyloid infiltrates, in the proper clinical setting. This is added to the usual differential diagnosis of matched defects which includes cysts, fibrosis, most benign tumors, and occasional metastatic lesions which do not concentrate gallium.

REFERENCES

1. Sostre S, Martin ND, Lucas RN, Strauss HW: Scintigraphic findings in primary amyloidosis. *Radiology* 115:675–677, 1975
2. Winchell HS, Sanchez PD, Watanabe CK, et al: Visualization of tumors in humans using ^{67}Ga-citrate and the Anger whole body scanner, scintillation camera and tomographic scanner. *J Nucl Med* 11:459–466, 1970

Am J Roentgenol 126:1249–1250, 1976

INCIDENTALLY DETECTED THROMBOSED VEIN DURING ^{67}GA CITRATE SCANNING

CHAN H. PARK,[1,2] FRANKLIN J. MILLER,[1] ALLAN LIPTON,[3] AND HAROLD HARVEY[3]

ABSTRACT:

A patient with stage IVA Hodgkin's disease developed thrombosis of the right cephalic vein at the site of an indwelling catheter. A few weeks later, 72 and 96 hr scans after injection of ^{67}Ga citrate revealed an increased linear uptake where the thrombosed vein was palpated. As far as we know, this is the first case showing abnormal uptake of this agent in a thrombosed vein. It is postulated that residual chronic inflammatory cells are responsible for ^{67}Ga citrate uptake in this case.

In 1968 Edwards and Hayes [1] discovered that ^{67}Ga citrate localized in certain human neoplasms. This was subsequently verified in a number of papers [2–8]. A variety of nonneoplastic lesions also showed a localized accumulation of this agent, including abscesses [9], pulmonary sarcoidosis [10] and tuberculosis, pneumonia [11, 12], empyema of the gall bladder [13], and acute myocardial infarction [14]. There has been no previous report of a thrombosed vein secondary to an indwelling catheter taking up ^{67}Ga intensely. One such instance is now described.

CASE REPORT

R. E. is a 34-year-old Caucasian male who was admitted for the third time to Hershey Medical Center Hospital on February 6, 1975, for recurrent malignant lymphoma and jaundice. He had Hodgkin's disease, stage IVA, previously treated by chemotherapy. In 1973 he had a splenectomy: liver and bone marrow biopsies also were positive for Hodgkin's disease. He responded well to multiple chemotherapeutic agents and radiation therapy to the left axilla. In December 1974 he developed progressive pain in lower abdomen and back with vomiting, dark urine, and jaundice. A Rose Bengal liver scan strongly suggested an extrahepatic biliary obstruction. At laparotomy, a large multinodular mass was found in the region of the porta hepatis as well as nodal enlargement in the celiac and paraaortic regions. A cholecystojejunostomy was carried out. An intravenous catheter was inserted in the right antecubital vein and subsequently removed because of thrombophlebitis. Approximately 1 month after the laparotomy, a ^{67}Ga scan was performed. At that time, the patient was receiving intravenous fluid through an indwelling catheter in the left antecubital vein. Carrier free ^{67}Ga citrate was injected through the cathe-

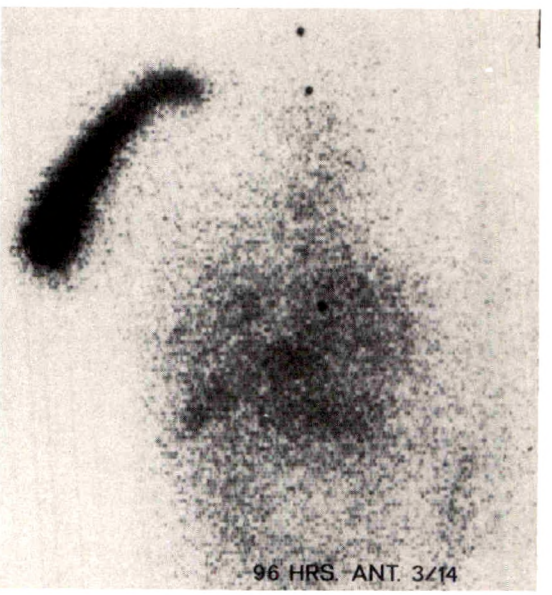


FIG. 1.—^{67}Ga scan showing anterior view of whole trunk. Note intense uptake along lateral aspect of right arm and abnormal uptakes in liver and abdomen. Dots indicate chin, suprasternal notch, and xyphoid process.

[1] Department of Radiology, Milton S. Hershey Medical Center, Hershey, Pennsylvania 17033.
[2] Present address: Division of Nuclear Medicine, Thomas Jefferson University Hospital, Philadelphia, Pennsylvania 19107. Address reprint requests to C. H. Park.
[3] Division of Oncology, Milton S. Hershey Medical Center, Hershey, Pennsylvania 17033.



FIG. 2.—Venogram of right arm revealing occlusion of cephalic vein (*arrow*).

ter, and rectilinear scans were performed at 72 and 96 hr. These showed intense activity along the thrombosed vein in his right arm (fig. 1) as well as abnormal activity in both hili, liver, and abdomen. Physical examination revealed a hard linear mass where thrombophlebitis was noted previously along the lateral aspect of the right upper arm. Bilateral venograms were performed, and occlusion of the right cephalic vein was demonstrated (fig. 2). The left side was normal. The patient later expired, and an autopsy (excluding the extremities in accordance with family wishes) confirmed the diagnosis of stage IVA recurrent malignant lymphoma, Hodgkin's disease, lymphocyte-depleted type.

REFERENCES

1. Edwards CL, Hayes RL: Tumor scanning with ^{67}Ga citrate: preliminary note. *J Nucl Med* 10: 103–105, 1969
2. Edwards CL, Hayes RL: Scanning malignant neoplasms with gallium-67. *JAMA* 212:1182–1190, 1970
3. Higasi T, Nakayama Y, Murata A, Nakamura K, Sugiyama M, Kawaguchi T, Suzuki S: Clinical evaluation of gallium-67 citrate scanning. *J Nucl Med* 13:196–201, 1972
4. Johnston GS, Jones AE: *Atlas of Gallium-67 Scintigraphy*. New York, Plenum, 1973
5. Langhammer H, Glaubitt G, Grebe SF, Hampe JF, Hauhold H, Hor G, Kaul A, Koeppe P, Koppenhagen J, Roedler HD, Van der Schoot JB: Gallium-67 for tumor scanning. *J Nucl Med* 13:25–30, 1972
6. Larson SM, Milder MS, Johnston GS: Interpretation of the gallium-67 photoscan. *J Nucl Med* 14:208–214, 1973
7. Lomas A, Dipos PE, Wagner HN: Increased specificity of liver scanning with the use of gallium-67 citrate. *N Engl J Med* 286:1323–1329, 1972
8. Nelson B, Hayes RL, Edwards CL, Kinseley RM, Andrews GA: Distribution of gallium in human tissues after intravenous administration. *J Nucl Med* 13:92–100, 1972
9. Gelrud LG, Arseneau JC, Johnston GS: Gallium-67 localization in experimental and clinical abscesses. *Clin Res* 21:600, 1973
10. McKusick KA, Soin JS, Ghiladi A, Wagner HN: Gallium-67 accumulation in pulmonary sarcoidosis. *JAMA* 223:688, 1973
11. Ito Y, Okuyama S, Awano T, Takahashi K, Sato T, Kanno I: Diagnostic evaluation of gallium-67 scanning of lung cancer and other diseases. *Radiology* 101:355–362, 1971
12. Kamada M, Oshima S, Kobara Y, Izumi T: Clinical evaluation of gallium-67 citrate scintigraphy in pulmonary diseases (abstr.). *Jpn J Nucl Med* 9:215, 1972
13. Lomas A, Wagner HN: Accumulation of ionic gallium-67 in empyema of the gallbladder. *Radiology* 105:689–692, 1972
14. Kramer RJ, Goldstein RE, Hirshfeld JW, Johnston GS, Epstein SE: Visualization of acute myocardial infarction by the radionuclide gallium-67. *Circulation* 46, suppl. 2:11–20, 1972

Am J Roentgenol 126:1251–1255, 1976

ELECTRON BEAM THERAPY IN HEAD AND NECK TUMORS

DANIEL A. TOBIN,[1] WILLIAM HALL, AND RALPH M. SCOTT

ABSTRACT:

Electron beam therapy with its high energy capabilities appears promising as a therapeutic modality in head and neck neoplasms. Over a 10-year period, 153 cases of head and neck neoplasms involving the alveolar ridge, floor of mouth, buccal mucosa, retromolar trigone, tonsil, parotid, tongue, and pharynx were treated. The pharyngeal group was removed from consideration because of the unsuitability of this lesion for single port therapy. Normal standard doses and time-dose fractions are included as a basis for treatment comparison, and the influence of stage on survival is noted. Survival and tolerance of this form of treatment is comparable to photon therapy and may in fact result in fewer complications.

High energy electron beam therapy, considered in the 1950s and 1960s as potentially promising for unilateral head and neck tumors, is emerging in the 1970s as an acceptable treatment modality for these lesions. The beam characteristics of high surface dose from rapid buildup and fast falloff in the tissue depths seemed promising in the treatment of head and neck neoplasms confined to one side of these structures (fig. 1). If electron beam therapy could approach photon therapy in the effective control of these unilateral lesions and at the same time offer some skin-sparing effect, preserve salivary function, and preserve the normal tissue and bone on the opposite side of the head and neck, it would indeed prove a valuable addition to the armamentarium of the radiation oncologist.

In 1965 the Radiation Center of the University of Louisville instituted a study of electron therapy as applied to certain head and neck lesions. A report of that study in 1973 [1] suggested that high energy electron therapy could indeed be adapted to approach the survival rates of photon therapy. Further, the use of the electron beam resulted in significant reduction of normal tissue and bone reaction and preserved more salivary gland function, thus improving the dental hygiene of the post-radiation patient. The study has now been in progress for 10 years. Results are summarized in this paper.

SUBJECTS AND METHODS

Study Design

During the first years of the study, tumors from the oral, oropharyngeal, and pharyngeal areas were considered for admission. However, short-term survival rates soon demonstrated the inability of this modality to encompass the

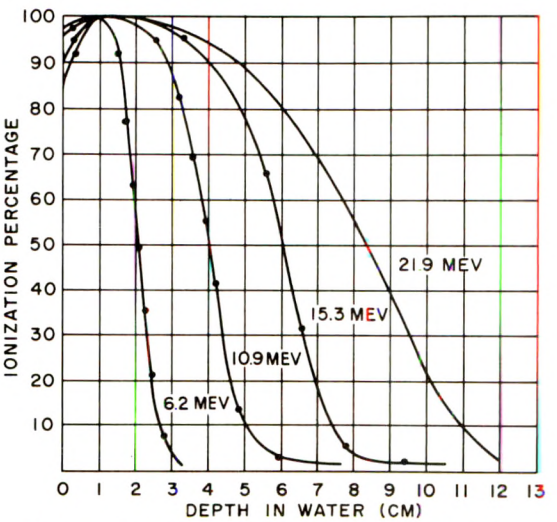


FIG. 1.—Depth dose distribution for direct electron beam.

Presented at the annual meeting of the American Roentgen Ray Society, Atlanta, Georgia, October 1975.
[1] All authors: University of Louisville Radiation Center, Louisville, Kentucky 40202.

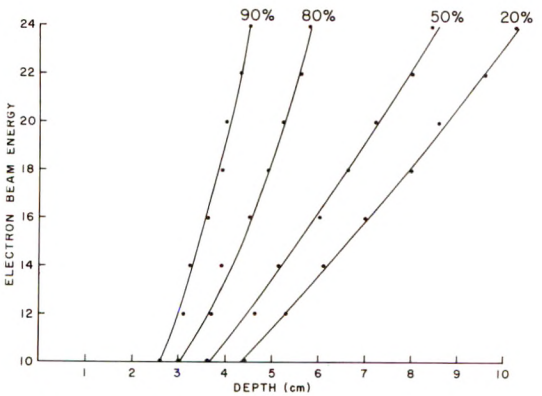


FIG. 2.—Percentage depth dose versus betatron electron beam energy. 10×12 cm FS at 100 cm SSD.

entire disease area of such lesions as the lateral wall of the pharynx with its many lymphagitic and vascular pathways of spread. Subsequent admissions to the study were confined to the oral and oropharyngeal areas and included unilateral lesions of the buccal mucosa, floor of the mouth, alveolar ridge, retromolar trigone, tonsil, tongue, and parotid. All treatment plans were instituted with curative intent. Staging of the tumors followed that of the Joint Committee for Cancer and End Results Reporting for Oral Cavity (1967), and Pharynx (1965). Staging was accomplished whenever necessary by both direct and indirect laryngoscopy and included soft tissue radiographic studies. Tissue diagnoses were obtained in all cases.

A 25-meV betatron provided the electron beam in suitable energies from 10 to 24 meV. The energy of the electrons selected was that necessary to encompass the tumor and nodes, if present, and permit "falloff" in the adjacent normal tissue behind the tumor. Depth dose determinations, described previously [2], were employed in planning the patient's treatment (fig. 2). The rapid buildup of the surface dose reaches 90% in the first 2 mm of tissue. The tissue dose remains uniformly high and, depending on the energy employed, falls off very rapidly in the lower energies (10–12 meV) and less rapidly as the energy level rises. Even at 24 meV the 80% depth dose level obtained was maintained to 5.8 cm, fell to 50% at 8.2 cm, and to 20% at 10.4 cm.

Because the asymmetry of fields perpendicular and parallel to the axis of the beam was thought to be significant at low and high energies [1], large normal tissue margins were presumed necessary at all energies. Subsequent film dosimetry showed this asymmetry to be significant only at energies above 18 meV, requiring large normal tissue margins above that energy. The problem of tissue nonhomogeneity (particularly bone) in an electron beam field continues to be studied intensively. Single treatment portals were used, and field size varied from 48–120 cm squares or rectangles to 4–8 cm circles. A wax bolus was used when maximum doses were needed at the skin surface. Treatment distance was 100 cm. Tumor doses employed varied from 5,500 rad in 30 days to 7,000 in 68 elapsed days, utilizing both straight and "split course" techniques in 20–35 fractions.

The time-dose relationship utilized in the study included four treatment plans. Eighty-one patients were treated with a total tumor dose of 6,000–6,600 rad in 40–44 days utilizing "straight" therapy technique, and 53 patients were treated to 6,500–7,000 rad in 63–67 days with the "split course" 3 weeks rest technique. Both of these groups received 200 rad/day. Ten cases were treated to 5,500 rad in 32 days at 250 rad/day, and nine to 6,000 rad in 49 days at 300 rad/day. The time-dose fraction values of Ellis [3] and Orton and Ellis [4] revealed comparable values of 108, 109, 102, and 107 for these plans and ret values of 1,770, 1,876, 1,804, and 1,808.

Patients Investigated

In the past 10 years, 6,150 new patients were seen at the radiation center; 153 patients with head and neck cancer fulfilled criteria for admission to the study, were treated, and have remained available to us for follow-up. All have had a minimum of 2 years follow-up. Table 1 shows the location and extent of disease in these patients. The highest number of cases (29) had tumors in the tonsillar portion of the oropharyngeal area, followed by 28 cases with tumors in the anterior two-thirds of the tongue.

In reviewing the patients at each stage of the disease, the tongue lesions were the only ones seen in any number at the earlier stages. The utilization of the tongue in eating and in speech may explain the early detection. Among the tonsillar cases, 55% were recognized by the time stage II was reached. This stage lesion does not involve spread to the adjacent nodes. Only cancer of the pharyngeal area had over 50% of cases with lymph node involvement (stages III

TABLE 1

EXTENT OF DISEASE

Area	No. Cases	Stage I	Stage II	Stage III	Stage IV
		T1N0	T2N0	T3N0, T123N1	T123N23
Oral area:					
Tongue	28	9	6	8	5
Buccal mucosa	16	3	7	3	3
Floor of mouth	18	3	8	6	1
Alveolar ridge	13	2	6	5	0
Retromolar trigone	13	3	8	2	0
		T1N0	T23N0	T123N1	T123N2
Oropharyngeal area:					
Tonsil	29	2	14	5	8
Pharynx	8	0	3	2	3
Parotid	28	...	...	...	...
Total	153	22	52	31	20

NOTE.—1965–1973.

and IV), another reason why treatment proved ineffective.

Lesions of the buccal mucosa, floor of mouth, alveolar ridge, and retromolar trigone were not recognized early (stage I) but were noted by patients when the primary tumor advanced to dimensions sufficient to produce symptoms. Only two of 13 cases with retromolar trigone lesions had adenopathy, the least adenopathy, for any of the types investigated. Tonsillar lesions, traditionally the best responders to curative attempt by radiation therapy, were not recognized early; 52% were recognized by the T2N0 stage, but 45% presented with nodes (23% with N2 nodes). Parotid tumors have no widely accepted staging system to categorize them at this time.

RESULTS OF THERAPY

Table 2 shows the survival data following electron beam therapy. Of the 153 patients,

TABLE 2

SURVIVAL AFTER ELECTRON BEAM THERAPY

AREA	No. CASES	2-YEAR SURVIVAL	AT RISK			
			Stage I	Stage II	Stage III	Stage IV
Tongue	28	14	4	3	0	0
Buccal mucosa	16	9	1	3	2	0
Floor of mouth	18	12	0	2	2	0
Alveolar ridge	13	3	1	0	0	0
Retromolar trigone	13	7	1	6	0	0
Tonsil	29	16	1	4	2	0
Pharynx	8	1	0	0	0	1
Parotid	28	17*	...	...	...	...
Total	153	79	8	18	6	1

NOTE.—1965–1973.
* 13 are long-term survivors (not staged).

79 survived 2 years; 45 of these are still at risk. There were no long-term survivors with stage IV disease. Of the 45 patients at risk, only six have mobile adenopathy; none survived with N2 lesions (fixed nodes). Of the 108 deaths, 94 were from cancer (six demonstrated second primaries) and 14 from nonmalignant disease or accidents.

Of the 28 with disease of the anterior two-thirds of tongue, 14 survived 2 years: none with adenopathy remain alive. Of the seven patients at risk, all had primary disease but without adenopathy. Among the 29 patients with tonsillar disease, 16 survived 2 years and seven of these remain at risk. In the buccal mucosa group nine of 16 patients survived 2 years with six patients presently at risk, two with non-fixed nodes. Of 28 patients with parotid tumors, 17 survived 2 years, and 13 are now long-term survivors. Of the 18 patients with tumor in floor of mouth, 12 survived 2 years; however, only four are at risk, two with N1 disease. Among 13 cases with retromolar trigone lesions, seven survived 2 years and are still at risk. Among 13 cases cases of alveolar ridge lesions, only three survived to 2 years and only one remains at risk.

The eight patients with pharyngeal lesions were included for a short time and then dropped from the study because of very poor survival with electron beam therapy. Only one stage IV patient remains at risk and is considered a most unusual case.

DISCUSSION

Our original inquiry into the use of electron beam therapy for patients with selected unilateral tumors of the head and neck, initiated in 1965, indicated that this modality had potential. The hope that the electron beam might produce less permanent damage to normal tissue and still produce survival rates approaching those of photon therapy has been sustained by review of our experience from 1965 to 1975. The 2-year survival rates of patients treated with electron beam therapy for lesions of the tongue (50%), buccal mucosa (56%), retromolar trigone (53%), tonsil (56%), and floor of mouth (66%) compare favorably with our experience using photon therapy in treating these areas.

Our experience also demonstrates the necessity for careful selection of patients for electron beam therapy. Failure to achieve any long-term survival in patients with lateral pharyngeal lesions led to the exclusion of this group of patients from the study and suggests probable failure of the electron beam to satisfactorily treat any cancer which even approaches the midline of head or neck areas. Lesions of the anterior two-thirds of tongue not on the lateral edge and the anterior alveolar ridge should be carefully evaluated for approach to midline and could better be treated with opposed photon fields.

The presence of adenopathy was again demonstrated to markedly compromise survival. Of 31 patients with nonfixed small lymph nodes (N1), only six survived past 2 years; none of the patients with N2 large fixed nodes survived past 2 years. The stage of the primary tumor, always a critical factor in survival, is even more crucial when electron beam by single field is utilized. Of 52 cases classified T2N0, 35% remain at risk.

Tolerance of electron beam therapy by the patient remains the significant reason for its continued utilization by the radiation oncologist. During therapy, erythema and dry desquamation occur in the treatment schedule at approximately the same time as with photon therapy. A total of 19% of cases demonstrated wet desquamation which responded in all cases to conservative management. Those cases treated with "straight" therapy to a total tumor dose of 5,500 rad at 250 rad/day demonstrated wet desquamation in a higher percentage of cases, as would be expected.

Mucosal reactions were comparable to those encountered with photon therapy. Confluent mucositis occurs more frequently in those patients treated to a high total dose in "straight" therapy. Thus patients with high stage disease treated with "split

course" therapy did not develop confluent mucositis as frequently.

Hyperpigmentation was noted as a late skin reaction in 16 of the patients surviving 2 years. Three of the patients presently at risk demonstrated fibrosis in the tissues, but this reaction could not be associated with any particular time-dose relationship and occurred at the same frequency as with photon therapy.

The ability of the patients to complete the entire treatment plan in the correct time sequence with adequate nutrition and with lower incidence and severity of skin and mucosal reactions emerges as the significant advantage of electron therapy. There was a lesser tendency to posttherapy dental problems, and mandibular necrosis has not been encountered.

In the cases where surgical attempts at salvage postradiation therapy were made, the surgeons reported that tissue handling and postoperative healing were similar to those encountered following rescue after photon therapy.

As the result of this on-going study we conclude that (1) single-field electron beam therapy of selected areas of head and neck cancer is well tolerated by patients; (2) planning and administration of therapy is simplified by use of the electron beam; and (3) complications in patients treated with electron therapy appear diminished, survival comparable, and quality of life improved compared to photon therapy of similar lesions.

REFERENCES

1. Tobin DA, Byrd SL, Scott RM: Electron beam therapy of head and neck tumors. *Am J Roentgenol* 120:617–623, 1974
2. Jacobson A: Practical aspects of betatron electron beam dosimetry. *Acta Radiol* [*Ther*] (Stockh) 9:545–554, 1970
3. Ellis F: in *Current Topics in Radiation Research*, edited by Ebert M, Howard A, New York, Wiley, 1968, pp 359–395
4. Orton CG, Ellis F: Simplification in use of NSD concept in practical radiotherapy. *Br J Radiol* 46:529–537, 1973

Am J Roentgenol 126:1256–1259, 1976

SURGICAL TREATMENT OF ADVANCED CARCINOMA OF THE FLOOR OF THE MOUTH

OSCAR M. GUILLAMONDEGUI[1] AND RICHARD H. JESSE[1]

ABSTRACT:

The anterior arch of the mandible is essential for satisfactory oral function and appearance. It can be preserved in surgical treatment of advanced cancers of the floor of the mouth by partial thickness resection. Surgery and radiation are approximately equally effective in the control of advanced (T_3) primary lesions. A treatment plan is proposed which employs a combination of nondisabling surgical resection followed by immediate postoperative radiation. Of 19 patients with T_2, T_3, and T_4 lesions treated and followed 1 year or more, 11 were free of cancer, including six who had positive lymph nodes. Of those dying of cancer, only one had local recurrence, while recurrence in the neck occurred in four. This report further strengthens the need for postsurgical radiation in certain situations.

The floor of the mouth can be arbitrarily divided into an anterior or sublingual area and a lateral or gingivolingual sulcus. The results of treatment of advanced carcinomas are similar in both areas; however, the functional, cosmetic, and psychological effects of the various modalities of treatment employed are strikingly different for the two areas.

The surgical treatment of many large tumors requires the resection of a segment of mandible and has been traditionally considered a necessary means of obtaining "adequate" surgical margins. Resection of the lateral or horizontal ramus of the mandible produces only moderate disability and usually does not need prosthetic or surgical repair. Resection of the anterior arch of the mandible, the notorious "Andy Gump" deformity, creates a formidable disability and an overwhelming cosmetic problem. The patient becomes unable to masticate, speak intelligibly, and frequently is incontinent of saliva and unable to swallow.

Reconstruction of the anterior arch in patients who have had advanced lesions removed is often unsuccessful due to the concomitant loss of large amounts of soft tissue in the tongue, floor of the mouth, and upper neck necessary to cover the prosthesis. In addition, radiation therapy either pre- or postoperatively almost uniformly results in failure of any prosthetic device.

Invasion of the periosteum by tumor, or even superficial invasion into the lingual aspect of the mandible, is not a mandatory indication for resecting a segment of the

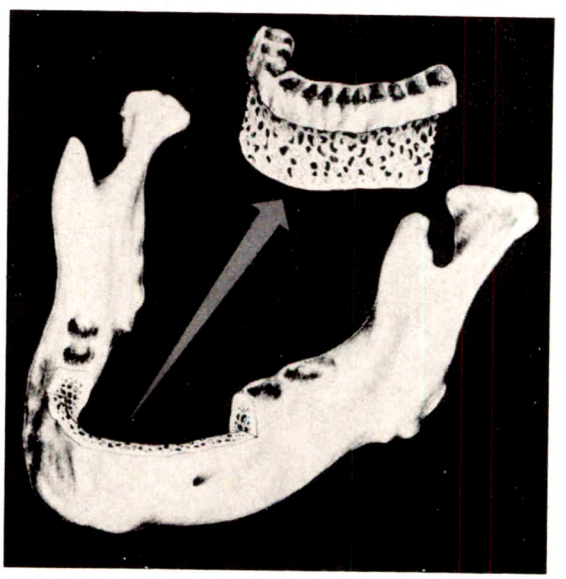


FIG. 1.—Anterior view of horizontal-coronal resection of anterior arch of mandible.

Presented at the annual meeting of the American Radium Society, San Juan, Puerto Rico, May 1975.

[1] Department of Surgery, Head and Neck Section, University of Texas System Cancer Center, M. D. Anderson Hospital and Tumor Institute, 6723 Bertner Avenue, Houston, Texas 77025. Address reprint requests to O. M. Guillamondegui.

mandibular arch. The dense, solid bone of the anterior mandible offers a good barrier to the local growth of cancer. In the midline, the mandible is penetrated or destroyed only very late in the course of the disease, unless infection due to decayed teeth with periodontal infection softens the bone to the extent that the tumor can infiltrate the alveoli with ease.

In some patients, therefore, it is possible to remove a cancer of the anterior floor of the mouth with adequate margins by resecting only a portion of the thickness of the mandible and leaving enough bone to preserve the continuity of the anterior arch. The surgeon must make a careful decision in selecting candidates for this type of procedure, usually without the aid of immediate histopathological studies. The inner table of the mandible can be removed with the tumor (fig. 1), or, if necessary, a more complex horizontal resection of the alveolar ridge can be performed in addition (figs. 2 and 3).

The root of the tongue and the muscles of the floor of the mouth, genioglossus, geniohyoid, and mylohyoid can also be removed. This can be accomplished intraorally, or in continuity, bilateral, partial, or complete neck dissections en bloc can be added. The defect is covered with a skin graft or local flaps. In summary, this procedure makes possible the removal of some large tumors of the anterior floor of the mouth with limited invasion of the anterior arch of the mandible and sublingual structures. The functional and cosmetic results are indeed acceptable, and the postoperative disability is minimal.

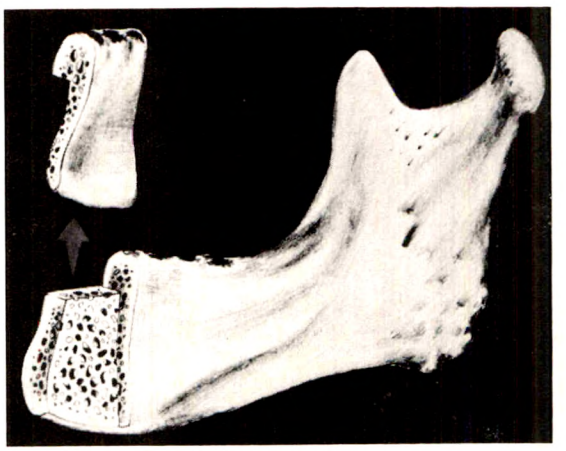


FIG. 2.—Medial view of horizontal-coronal resection of anterior arch of mandible.

Advanced cancers of the floor of the mouth are classified as T3 and T4 according

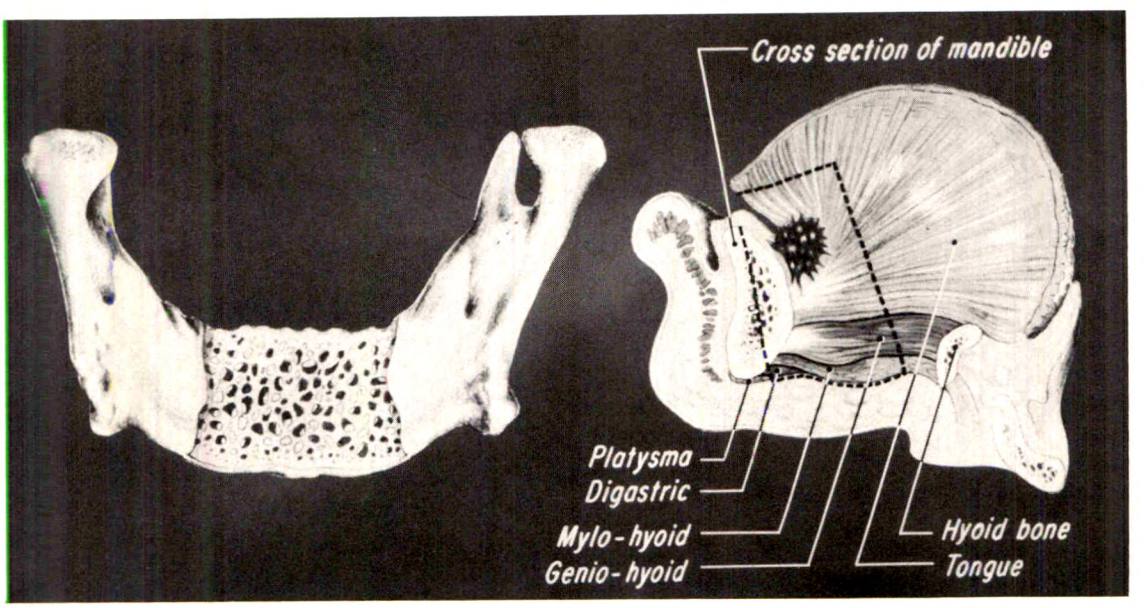


FIG. 3.—Coronal resection of anterior arch of mandible.

TABLE 1

STAGING CRITERIA FOR FLOOR OF MOUTH

Stage	Description
UICC–AJC* (1973):	
T2	Tumor 2 cm but <4 cm
T3	Tumor >4 cm
M. D. Anderson Hospital (1974):	
T2	Tumor 2–4 cm
T3	Tumor >4 cm; fixation to periosteum or pressure defect in bone
T4	Massive tumor or bone involvement of root of tongue

* UICC = International Union Against Cancer; AJC = American Joint Committee for Cancer Staging and End Result Reporting.

to the primary lesion. The currently used staging criteria are shown in table 1 [1]. At the M. D. Anderson Hospital in Houston, about 60% of the patients with cancers of the floor of the mouth are classified in the T3–T4 group. The results of treatment are shown in table 2. Table 3 shows the absolute survival figures for the advanced stages. It must be noted that the patients were individually selected for each modality of treatment and that the combination of treatment modalities was seldom used before 1968. The number of failures is similar in the group of patients treated by surgery or those treated by radiation alone. The difference in control of the primary lesion is striking when stages T3 and T4 are compared.

It has been proved in the past that the surgical salvage of radiation failures is far more successful than the reverse [2]. Thus if the patients are treated initially by radiation therapy, many of the failures in stage T3 can still be salvaged by surgical resection (table 4). However, radiation in therapeutic doses reduces the blood supply of the tissues, including the mandible, and increases the incidence of infection and necrosis when the trauma of surgery is added. Therefore, after radiation therapy, surgical procedures which attempt the resection of less than the entire segment of mandible adjacent to the tumor will usually fail due to necrosis or fractures. However, surgical procedures employed alone for T3 and T4 cancers have a reasonably high local failure rate and are even less effective in controlling regional lymph node metastasis [3].

From the above considerations, a treatment plan has evolved which employs a combination of a nondisabling surgical resection followed by immediate postoperative irradiation. This plan improves both the control rate of the cancer and the quality of the patient's life.

From January 1970 to July 1973, 20 selected patients with squamous cell carcinoma of the anterior floor of the mouth and gingiva, staged T2, T3, or T4, were treated with surgical procedures that included partial resections of bone and preservation of the arch of the mandible. All of these pa-

TABLE 2

SURVIVAL AFTER TREATMENT BY SURGERY OR X-RAY THERAPY FOR CANCER OF FLOOR OF MOUTH

	Surgery		X-ray Therapy	
Stage	No.	%	No.	%
T1	11/14	78.6	30/34	88.2
T2	12/15	80	42/58	72.4
T3	9/16	56.3	28/46	60.9
T4	1/8	12.5	0/10	0.0
Total	33/53	62.3	100/148	67.6

NOTE.—Determinate survival data, 5 years with NED. Data from M. D. Anderson Hospital, 1948–1965.

TABLE 3

SURVIVAL AFTER TREATMENT OF PRIMARY LESION BY X-RAY THERAPY OR SURGERY ALONE

	Surgery		X-ray Therapy	
Stage	No.	%	No.	%
T3	12/22	54.5	28/50	56.0
T4	1/11	9.0	0/8	0

NOTE.—Absolute survival data, 5 years with NED. Data from M. D. Anderson Hospital, 1954–1968.

TABLE 4

SURGICAL SALVAGE OF X-RAY THERAPY FAILURES IN CANCER OF FLOOR OF MOUTH

STAGE	X-RAY THERAPY FAILURES		SALVAGE BY SURGERY	ULTIMATE FAILURE
	No.	%		%
T_3	14/60	23	11/14	5
T_4	19/24	79	0/19	79

NOTE.—Local control for a minimum of 30 months. Data from M. D. Anderson Hospital, 1954–1967.

tients had cancer extending at least into the periosteum, while seven had evidence of bone invasion. Ten patients also had cancer in the cervical nodes.

Of the 20 patients, one died shortly after returning home from his operation. The 19 remaining patients could be followed 1 year or more. (In our experience, 85% of the recurrences above the clavicle will occur during the first year.) Eleven of the 19 patients were free of cancer, six of these having had positive lymph nodes. Seven patients died of cancer: one recurred at the primary site, four recurred in the neck, and two had distant metastasis while free of cancer in the local and regional area. The remaining patient died of other causes (table 5).

If survival is evaluated according to the T stage of the disease, all six patients with T_2 cancers survived, while only four patients of nine with T_3 lesions and one of four with T_4 lesions survived. Most of the recurrences were in the neck, but it is interesting to note that only for one of these patients with recurrence in the neck was lymph node metastasis found in the surgical specimen.

TABLE 5

RESULTS OF TREATMENT FOR CANCER OF ANTERIOR GUM AND FLOOR OF MOUTH

Result	No.
NED (1 yr)	11*
Died:	
Primary recurrence	1
Node recurrence	4
Distant metastasis	2
Other causes	1
Total	8

NOTE.—1970–1973; patients followed 1 year or more.
* Six N+.

In our opinion, these considerations strengthen the necessity of postoperative radiation therapy in the following situations: presence of gross residual disease; aggressive tumors including large infiltrating tumors (nerves, etc.), carcinoma in situ at margins, and multiple foci of carcinoma; subclinical disease in regional lymphatics; and suspected microscopic disease (surgical margins histologically "clear").

REFERENCES

1. Fletcher GH: Oral cavity and oropharynx, in *Textbook of Radiotherapy*, 2d ed, edited by Fletcher G, Philadelphia, Lea & Febiger, 1973, pp 232–237
2. Byers RM: Surgical salvage for radiation failures, in *Neoplasia of Head and Neck*, Proceedings 17th Annual Clinical Conference on Cancer, M. D. Anderson Hospital and Tumor Institute, Chicago, Year Book Medical Publishers, 1974, pp 75–84
3. Perez CA, Jesse RH, Fletcher GH: Metastatic carcinoma in cervical lymph nodes: unknown primary site, in *Neoplasia of Head and Neck*, Proceedings 17th Annual Clinical Conference on Cancer, M. D. Anderson Hospital and Tumor Institute, Chicago, Year Book Medical Publishers, 1974, pp 289–302

Am J Roentgenol 126:1260–1265, 1976

CENTRAL AXIS DEPTH DOSE FOR A 2.5 MV VAN DE GRAAFF GENERATOR

David W. Anderson,[1] David E. Raeside,[1] Reba I. Adams,[1] and Myron R. Goede[1,2]

ABSTRACT:

Central axis percentage depth dose values and isodose curves for the bremsstrahlung beam from a 2.5 MV Van de Graaff generator were measured with a water phantom at 100 cm target-to-surface distance. Tissue-air ratios were calculated from the central axis depth dose data. Use of the 2.5 MV percentage depth dose values are necessary for treatment planning since they are substantially larger than the values given in compilations for 2.0 MV beams.

INTRODUCTION

Increased output and increased percentage depth dose are two advantages to operation of a Van de Graaff bremsstrahlung generator at 2.5 MV rather than 2.0 MV. The generator used for radiation therapy at the University of Oklahoma Health Sciences Center was recently modified for 2.5 MV operation with the result that the dose rate was increased by a factor of 1.8. Subsequent to the modification, measurements required for obtaining central axis percentage depth dose tables and isodose curves for a variety of fields were made. The complete tables and several of the isodose curves are presented here since they may prove useful in other institutions anticipating similar modifications.

EXPERIMENTAL APPARATUS AND TECHNIQUE

The generator used as the radiation source was an electrostatic electron accelerator (Van de Graaff) manufactured by High Voltage Engineering Corporation (Burlington, Massachusetts) and operated at 2.5 MV. A tungsten transmission target 2.3 mm thick and mounted on a 1.8 mm copper backing in the end of the accelerator tube was used to produce the radiation beam. No field flattener was used, but additional filtration due to cooling water jacket, an exposure rate monitor, and a light field mirror was sufficient to produce a beam with a half-value thickness of 7.65 ± 0.05 mm of lead.

The maximum energy of the bremsstrahlung photons was calibrated using the threshold for the $D(\gamma,n)H$ reaction at 2.226 MeV [1]. A sample of 25 g of heavy water was irradiated at various indicated terminal voltages with a silver sheet wrapped around the teflon sample holder. The β activity induced in the silver was counted after the irradiation as the indicator of reaction yield. A linear plot of yield versus indicated voltage was easily extended to zero yield to verify threshold terminal voltage to within ± 10 kV.

The focal spot size for the accelerator beam was measured using a device made of laminated strips of lead alternating with paper spacers in a holder 15 cm long with a film packet placed at the end. The first exposure was followed by a second with the lamination direction rotated through 90°. The effective focal spot size was 2.5×3.0 mm on the film.

Dose profile measurements for the bremsstrahlung beam were made at 100 cm target-to-surface distance for a 10×10 cm field and a 25×25 cm field. In separate measurements, lithium borate thermoluminescent dosimeters and later a low sensitivity nonscreen radiographic film were sandwiched between pieces of plexiglass 0.5 cm thick. Film density measurements were corrected using the characteristic curve for the film for ^{60}Co radiation. The

[1] Department of Radiological Sciences, University of Oklahoma Health Sciences Center, Oklahoma City, Oklahoma 73190.
[2] Present address: St. Francis Hospital, Tulsa, Oklahoma 74136.

measurements both showed a narrow penumbra region at the field edges with the dose falling from 90% to 10% of the central axis value within 1 cm of lateral distance. A tail on the dose profile extended laterally from the field edge with relative dose less than 2% of the central axis value at 4 cm lateral distance. Since the transmission of the 7.6 cm lead collimator blocks was less than 1%, the tail must be partially attributed to scatter from the collimator block faces.

Since no flattening filter was used, the dose profile was noticeably forward peaked. At central axis and laterally to within 1 cm of the field edge, the dose was well described by the form

$$D(x) = D(0) \exp(-ax^2).$$

The variable x is defined here as the radial distance in centimeters from the central axis at the usual treatment distance. The coefficient a is the peaking parameter. A least square fit of the 2.5 MV data to this function gave the value

$$a_{VDG} = (6.5 \pm 0.8)10^{-4}.$$

This is substantially larger than the peaking parameter for our ^{60}Co teletherapy machine obtained in a similar manner at 80 cm without trimmers. For that machine,

$$a_{Co} = (5.0 \pm 0.6)10^{-4}.$$

The effects of the forward peaking on the isodose curves are discussed later.

Determination of the depth necessary for electron buildup was accomplished using thermoluminescent dosimeters made of lithium borate imbedded in teflon. The dosimeters were 10.0 mm in diameter and only 0.1 mm thick. They were placed in a phantom consisting of plexiglass sheets of 1.0 mm thickness. The arrangement for irradiation was such that no two dosimeters overlapped. Irradiation at 2.5 MV and 100 cm distance with a 10×10 cm field was chosen. The dosimeter response showed a maximum at a depth of 3.8±0.1 mm. Under the assumption that the depth of the dose maximum is proportional to electron range in the medium, a value of 4.4±0.1 mm was calculated for the buildup depth in water [2].

Dose versus depth data were taken with a computer controlled system (Artonix, Inc., St. Louis, Missouri). A pair of ionization chambers 0.5 cm in diameter and 1.5 cm in length with tissue-equivalent walls were used. The chambers used meet the recommended standards of the ICRU [3]. Mounting rods were made of teflon. One chamber served as the beam intensity monitor and was located at the periphery of the field. The other chamber served as the underwater probe and was moved about in a plexiglass water tank with a surface area of 52×53 cm and a depth of 50 cm. This volume was sufficient to allow ample peripheral water even for our largest field (20×20 cm) and deepest measurement (28 cm). The water temperature was 21° C (density = 0.998 g/cm^3).

Two shielded preamplifiers were used to drive the chamber signals to the electrometer located outside of the radiation room. Data points were taken as the ratio of the response of the underwater probe to that of the monitor probe to minimize the effects of fluctuating exposure rates. With the automated scan several minutes were required to acquire a full set of data for a given field. The true probe depths (controlled remotely) were found to be within 1.5 mm of the desired depths in all situations. The target-to-surface distance for the irradiations was determined to be 100.0±0.5 cm.

The effects of scattered radiation on the preamplifiers and cables were tested by placing the movable probe near the bottom of the tank and outside the field limits for a 15×15 cm field. The response was small but measurable with the beam on. A similar reading taken with a thick cylindrical lead cap over the chamber was reduced substantially. This indicated that the preamplifier and cable response due to scattered radiation was very small. The magnitude of the preamplifier and cable response during operation is estimated to be less than 1% of central axis values at com-

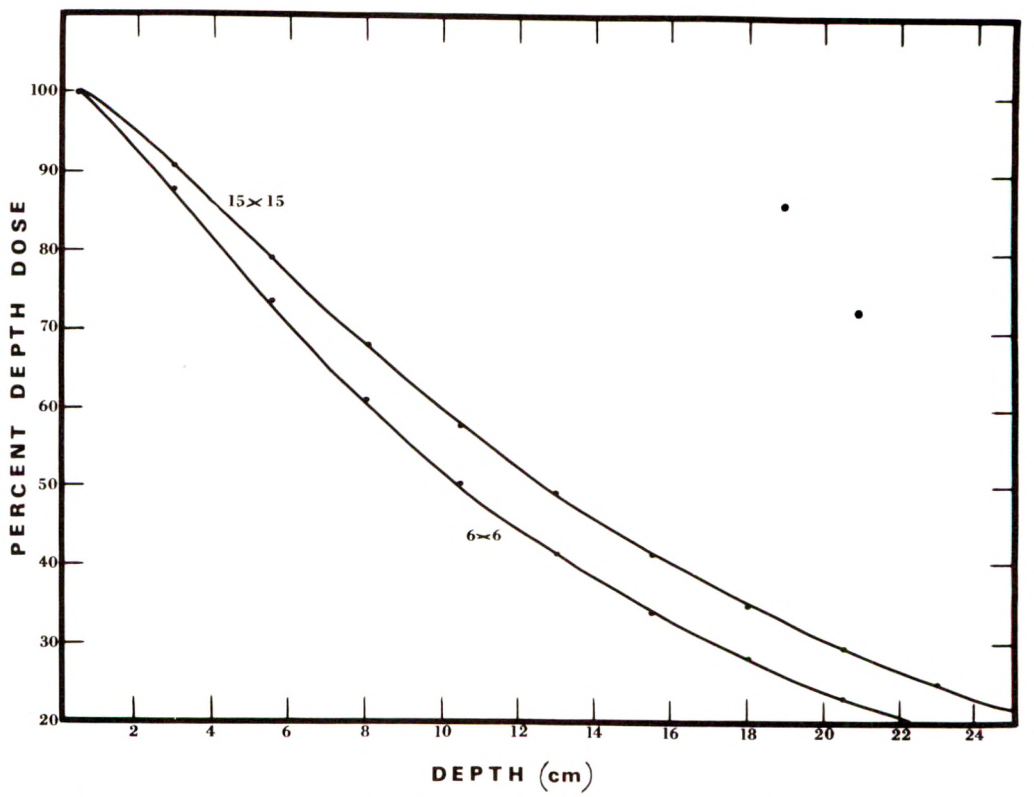


FIG. 1.—Central axis percentage depth doses calculated from functional fit. Radius of data points indicates standard deviation.

parable depths for moderate field size and depth.

As an overall check on the experimental technique, several runs were made at 2.0 MV. The central axis percentage depth dose data obtained were similar to values in standard compilations [4]. The magnitude of the deviations between our raw values and the accepted values was 1.4% of the local dose for depths between 1 and 20 cm for a 10×10 cm field.

The data runs at 2.5 MV were then made. A total of 40 separate and complete isodose curves were obtained with 1,440 individual measurements for central axis response ratios. The standard deviations for the central axis values for a single field and depth were less than 1% on the average.

RESULTS

The ion chamber response ratios obtained at the central axis were averaged at each depth for each field size investigated and normalized to 100.0% at the depth of 0.45 cm to produce the percentage depth dose values $P(d)$.

To minimize subjective errors, a regression analysis technique was used to generate smooth curves from the data. When such an analysis is performed with a computer, a quantitative measure of the precision of the fit can easily be calculated as part of the program. A similar measure of the precision of the fit has rarely been given when curves are drawn by hand through raw data points.

In this case, the values were fit by computer to a smooth curve with the form

$$P(d) = 100\left(\frac{d+\alpha}{m+\alpha}\right)^{\beta} \exp\left[-\gamma(d-m)\right],$$

where d is the depth in water, m is the depth of the maximum dose, and α, β, and

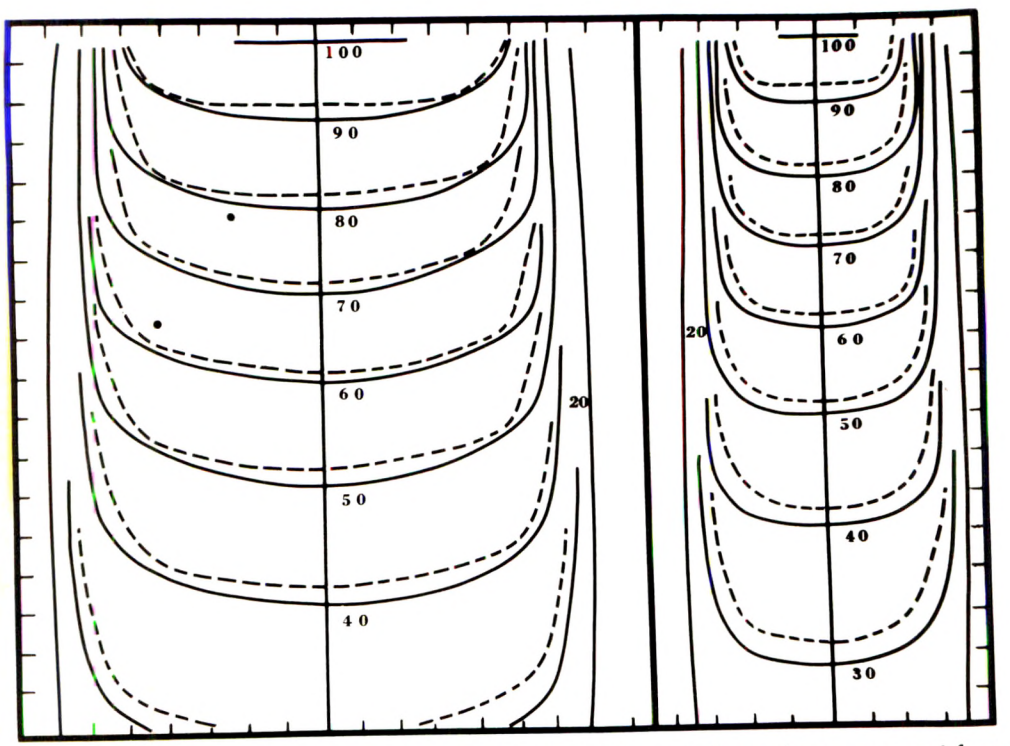


FIG. 2.—Isodose curves for 12×12 cm and 6×6 cm fields. Solid lines indicate shapes measured for 2.5 MV beam. Dashed curves indicate shapes for beam from ^{60}Co machine at 80 cm without trimmers. Details in edge-of-field effects masked on these curves because ionization chamber used in measurement had 0.5 cm diameter.

γ are constants determined by the computer analysis for each field.

Scattered radiation in the field at central axis is known to be a function of the area–perimeter ratio [5–7] defined as $(A/P)_d$= field area at deph d/field perimeter at depth d. Because of this, the values of α, β, and γ were fit by computer to a power series in A/P so that all field sizes could be represented. Using the results of this procedure, the final percentage depth dose values, defined as $P[d, (A/P)_m]$, are calculable for all depths and fields. Values of this percentage depth dose are tabulated in table 1 for common square fields. It should be noted that the depth dose values for the 0×0 cm field in table 1 are the result of extrapolation to A/P=0 of measurements for several small fields.

To check the analysis technique, the calculated values taken from the table were compared with the data for each field. The precision of the fit was indicated by the average magnitude of the difference between these quantities. For our data the average deviation was only 0.8% of the local values, and the largest deviation was 1.5% of the local value. Thus the fitting procedure was adequate for the data obtained.

Figure 1 shows two of the continuous central axis percentage depth dose curves plotted from the calculated points in table 1 and from the function. The experimental data points are also given on the figure for comparison. The functional form and fitting technique is shown to be adequate.

Table 2 contains the values of the central axis tissue-air ratios for the 2.5 MV beam. These numbers were calculated from the smooth curves for percentage depth dose. For this calculation, the following expres-

TABLE 1

PERCENTAGE DEPTH DOSES AT 2.5 MV

DEPTH (CM)	FIELD (CM) AND BACKSCATTER FACTOR								
	0×0 1.000	4×4 1.025	5×5 1.028	6×6 1.031	8×8 1.036	10×10 1.041	12×12 1.045	15×15 1.051	20×20 1.059
0.45	100.0	100.0	100.0	100.0	100.0	100.0	100.0	100.0	100.0
1.0	96.0	97.1	97.4	97.7	98.1	98.4	98.6	98.7	98.8
2.0	89.7	90.8	91.6	92.3	93.4	94.1	94.6	95.1	95.4
3.0	82.4	84.5	85.6	86.6	88.1	89.2	90.0	90.7	91.5
4.0	75.1	78.4	79.7	80.8	82.8	84.1	85.2	86.1	87.2
5.0	68.5	72.5	74.0	75.3	77.5	79.1	80.3	81.5	82.8
6.0	62.8	67.1	68.7	70.0	72.4	74.1	75.5	76.8	78.4
7.0	57.1	62.0	63.6	65.0	67.5	69.4	70.8	72.3	74.1
8.0	52.2	57.2	58.9	60.3	62.9	64.8	66.3	67.9	70.0
9.0	47.8	52.8	54.4	55.9	58.5	60.5	62.1	63.7	65.9
10.0	43.3	48.6	50.3	51.8	54.4	56.4	58.0	59.7	62.0
11.0	39.5	44.8	46.5	48.0	50.6	52.6	54.2	55.9	58.3
12.0	36.0	41.3	42.9	44.4	46.9	48.9	50.6	52.3	54.8
13.0	32.8	38.1	39.6	41.1	43.6	45.5	47.2	48.9	51.5
14.0	29.8	35.1	36.6	38.0	40.4	42.4	44.0	45.7	48.3
15.0	27.2	32.3	33.8	35.1	37.5	39.4	40.9	42.7	45.3
16.0	24.8	29.7	31.1	32.5	34.8	36.6	38.1	39.9	42.4
17.0	22.6	27.4	28.7	30.0	32.2	34.0	35.5	37.2	39.8
18.0	20.6	25.2	26.5	27.7	29.8	31.6	33.0	34.7	37.2
19.0	18.8	23.2	24.4	25.6	27.7	29.3	30.7	32.4	34.9
20.0	17.1	21.3	22.5	23.6	25.6	27.2	28.6	30.2	32.6
21.0	15.6	19.6	20.8	21.8	23.7	25.3	26.6	28.1	30.5
22.0	14.2	18.0	19.1	20.1	22.0	23.5	24.7	26.2	28.6
23.0	13.0	16.6	17.6	18.6	20.3	21.8	23.0	24.4	26.7
24.0	11.8	15.3	16.2	17.2	18.8	20.2	21.3	22.7	25.0
25.0	10.8	14.0	15.0	15.8	17.4	18.7	19.8	21.2	23.4

NOTE.—100 cm. target-to-surface distance.

sion was used [8]:

$$T[d, (A/P)_d] = \left(\frac{TSD + d}{TSD + m}\right)^2 B[(A/P)_m] \left\{\frac{P[d, (A/P)_m]}{100}\right\}.$$

In this equation the tissue-air ratio (T) is a function of depth d and the area perimeter ratio at that depth, $(A/P)_d$. The symbol TSD denotes the target-to-surface distance (100 cm), and m is the depth of the maximum dose. Note that the relationship between the area–perimeter ratios is

$$(A/P)_d = (A/P)_m \left(\frac{100 + d}{100 + m}\right).$$

The backscatter factors $B[(A/P)_m]$ were measured with the chamber described previously.

The results in tables 1 and 2 can be compared with the published results for 2.0 MV beams [4] and ^{60}Co beams at 100 cm. Central axis percentage depth dose values at 2.5 MV are generally from 1% to 5% larger than those for 2.0 MV beams for most fields at substantial depths. However, the 2.5 MV percentage depth dose values generally are not as large as values for ^{60}Co beams at 100 cm distances.

Figure 2 shows isodose curves obtained for a 6×6 cm field and a 12×12 cm field. As expected, the ^{60}Co curves show considerably more penumbra than the 2.5 MV curves. However, the 2.5 MV isodose lines show more forward peaking than the ^{60}Co lines. As depth increases, the effects of penumbra and forward peaking become more difficult to distinguish, and compa-

TABLE 2

TISSUE-AIR RATIOS AT 2.5 MV

	FIELD (CM)								
DEPTH (CM)	0×0	4×4	5×5	6×6	8×8	10×10	12×12	15×15	20×20
0.45	1.000	1.025	1.028	1.031	1.036	1.041	1.045	1.051	1.059
1.0	0.971	1.005	1.012	1.017	1.027	1.034	1.040	1.047	1.056
2.0	0.925	0.958	0.970	0.979	0.996	1.008	1.018	1.028	1.040
3.0	0.866	0.908	0.923	0.935	0.957	0.973	0.986	0.999	1.015
4.0	0.805	0.858	0.875	0.889	0.915	0.934	0.949	0.966	0.985
5.0	0.748	0.808	0.827	0.843	0.871	0.893	0.910	0.929	0.951
6.0	0.699	0.760	0.780	0.797	0.828	0.851	0.870	0.891	0.916
7.0	0.648	0.714	0.735	0.753	0.785	0.810	0.830	0.853	0.880
8.0	0.603	0.670	0.691	0.710	0.743	0.769	0.790	0.814	0.843
9.0	0.563	0.629	0.650	0.669	0.702	0.729	0.751	0.776	0.807
10.0	0.519	0.589	0.610	0.629	0.663	0.690	0.713	0.738	0.771
11.0	0.482	0.551	0.572	0.591	0.625	0.653	0.676	0.702	0.735
12.0	0.448	0.516	0.537	0.555	0.589	0.617	0.640	0.666	0.701
13.0	0.415	0.483	0.503	0.521	0.555	0.582	0.605	0.632	0.667
14.0	0.383	0.451	0.471	0.489	0.522	0.549	0.572	0.599	0.634
15.0	0.357	0.422	0.441	0.459	0.491	0.517	0.540	0.567	0.602
16.0	0.331	0.394	0.412	0.430	0.461	0.487	0.510	0.537	0.572
17.0	0.307	0.368	0.386	0.402	0.433	0.459	0.481	0.507	0.542
18.0	0.284	0.343	0.360	0.377	0.406	0.432	0.453	0.479	0.514
19.0	0.264	0.320	0.337	0.353	0.381	0.406	0.427	0.453	0.487
20.0	0.244	0.299	0.315	0.330	0.357	0.381	0.402	0.427	0.461
21.0	0.226	0.278	0.294	0.308	0.335	0.358	0.378	0.403	0.436
22.0	0.209	0.259	0.274	0.288	0.314	0.336	0.356	0.380	0.412
23.0	0.195	0.242	0.256	0.269	0.294	0.316	0.335	0.358	0.389
24.0	0.180	0.225	0.239	0.251	0.275	0.296	0.314	0.337	0.368
25.0	0.167	0.210	0.223	0.235	0.258	0.278	0.295	0.317	0.347

rable isodose lines from the two sources have similar curvature.

ACKNOWLEDGMENT

Our thanks to Dr. Joseph C. Giarratano for suggesting the use of heavy water in the machine energy calibration.

REFERENCES

1. Mattauch L, Thiele J, Wapstra A. Mass excess values. *Nucl Phys* 67:1–40, 1974
2. Pages L, Bertel E, Joffre H, Sklavenitis L: Energy loss, range, and bremsstrahlung yield for 10 keV to 100 MeV electrons. *Atomic Data* 4:69–125, 1972
3. International Commission on Radiation Units and Measurements: Report 23, Measurement of absorbed dose in a phantom irradiated by a single beam of x or gamma rays, 1973, p 3
4. Cohen M, Jones DEA, Green D: Central axis depth dose data for use in radiotherapy. *Br J Radiol* 11, suppl: 47–51, 1972
5. Sterling TD, Perry H, Katz L: Automation of radiation treatment planning. *Br J Radiol* 37: 544–550, 1964
6. Wrede DE: Practical aspects of area/perimeter. *Bull Am Assoc Phys Med* 6:73–74, 1972
7. Wrede DE: Central axis tissue-air ratios as a function of area/perimeter at depth. *Phys Med Biol* 17:548–554, 1972
8. Johns HE, Cunningham JR: *The Physics of Radiology*. Springfield, Thomas, 1969

Am J Roentgenol 126:1266–1314, 1976

THIRD INTERNATIONAL CONFERENCE ON BONE MINERAL MEASUREMENT

Edited by Richard B. Mazess

METHODS

General Methods

A Two-Energy Densitometry Method for Measuring Bone Mineral Concentrations and Bone Densities In-Vitro and In-Vivo. J. Rassow 1268
Concurrent X-ray Photodensitometric and Gamma-Ray Absorptiometric Measurements of Bone Mineral in the Radius in Patients. H. E. Meema, D. R. Taves, D. G. Oreopoulos 1269
Experiences with the X-ray Bone Scanner, Developed in Bonn. M. Gebhardt, K. D. Hermanutz 1269
An Electronic Device for Direct Readout of Bone Mineral Content from Roentgenograms Scanned with a Microphotodensitometer. K. R. Wing, E. Birring 1269
The Relationships between Bending Stiffness, Mineral Content, Geometry, and Strength of the Human Ulna. A. S. Foltz, D. J. Rolnick, J. M. Jurist 1270

Imaging and Area Scanning

Bone Mineral Distribution in the Immediate Vicinity of Implants. P. Rüegsegger, T. Hinderling 1272
A New Detector for Absorptiometric Measurement. R. E. Zimmerman, R. C. Lanza, T. Tanaka, G. G. Bolon, H. J. Griffiths, P. F. Judy 1272
Bone Imaging Using a Gadolinium-153 Source and a Xenon-filled Multiwire Proportional Counter as Detector. A. Horsman, D. H. Reading, J. Connolly, W. Glasgow, M. S. F. McLachlan 1273
Bone Densitometry with the Aid of Computerized Transaxial Tomography. U. Elsasser, P. Rüegsegger 1275
Regional and Whole-Body Bone Mineral Content Measurement with a Rectilinear Scanner. R. R. Price, J. Wagner, K. Larsen, J. Patton, A. B. Brill 1277
Recent Advances in Skeletal Trans-imaging. A. M. Strash, R. W. Bright 1278

Compton Scattering

Absolute Bone Density Measurement Using Compton Scattered Radiation. D. G. Piper, L. E. Preuss 1279
Measurement of Bone Mineral Density Using Coherent and Compton Scattering. H. Olkkonen, P. Puumalainen, P. Karjalainen, E. M. Alhava 1279
Experience with Photon Scattering Measurements of Bone Density. C. E. Webber 1280
Quantitative Density Longitudinal Section through the Spine. K. H. Reiss, B. Conrad, K. Killig 1281

BIOMEDICAL

Normative Studies

Bone Mineral Mass and Width in Normal White Women and Men. R. A. Schlenker, B. G. Oltman, T. J. Kotek 1282
Bone Mineral Content of the Growing Skeleton. T. Klemm, D. H. Banzer, U. Schneider 1283
Bone Mineral Content in Full-Term Infants Measured by Direct Photon Absorptiometry. J. J. Steichen, B. Kaplan, N. Edwards, R. C. Tsang 1284
Validity of the Absorptiometric Measurement of Bone Mineral Content of the Radius. S. H. Cohn, K. J. Ellis, N. F. Goldsmith 1286

Transactions of a conference presented in New Orleans, Louisiana, 26–28 January 1976, sponsored by the University of Wisconsin Bone Mineral Laboratory. Chairmen were: George Bailey, Uriel Barzel, John R. Cameron, Charles Chesnut III, C. Conrad Johnston, Jr., Bo Nilsson, A. M. Parfitt, Karl H. Reiss, J. van der Sluys Veer. Financial assistance for travel was provided by: Ayerst Laboratories, Marion Laboratories, Norland Instruments, Proctor & Gamble Miami Valley Laboratories, and Upjohn Company. Support for reprints provided by the National Institute of Arthritis and Metabolic Diseases. Reprints of this section available from R. B. Mazess, University of Wisconsin, Madison, Wisconsin 53706. Randie Wealton aided substantially with the organization of the meeting and preparation for publication.

Influence of Skeletal Size on Bone Mineral Content: Skeletal Size–Adjusted National and International Normative Trend Lines. J. Dequeker, Fr. Gielen 1288

Renal Disease

Bone Demineralization in Renal Failure: A Longitudinal Study of the Distal Femur Using Photon Absorptiometry. T. R. Overton, D. S. Silverberg 1289
Bone Mineral Analysis in Renal Osteodystrophy. L. H. Diamond, R. Smith, L. Pierce 1291
The Effect of Chronic Renal Failure and Maintenance Hemodialysis on Bone Mineral Content of the Radius. A. M. Parfitt, I. Oliver, N. Walczak, N. Levin, G. Santiago, C. Cruz 1292
The Need for Differential Bone Mineral Standards for Blacks. G. H. Mayor, S. M. Garn, T. V. Sanchez, H. A. Shaw 1293

Osteoporoses

Effect of Combined Therapy with Sodium Fluoride, Calcium, and Vitamin D on the Lumbar Spine in Osteoporosis. T. Hansson, B. Roos 1294
Bone Mineral Content Changes in the Skylab Astronauts. J. M. Vogel, M. W. Whittle 1296
Physical Activity—A Modality for Bone Accretion in the Aged. E. L. Smith, W. Reddan 1297
Changes of Bone Mineral in Healthy Menopausal and Premenopausal Women: Two Year Preliminary Results of a Longitudinal Study. K. R. Heer, K. Alexandrow, Th. Lauffenburger, H. G. Haas 1298
The Slowing of the Rate of Mineral Loss with Aging. D. M. Smith, M. R. A. Khairi, C. C. Johnston, Jr., J. Norton 1298
Prediction of Femoral Neck Fracture from a Pelvic X-ray. B. E. Nilsson, L. Hagberg 1299

Clinical

Effects of Corticosteroids on Bone Mineral in Rheumatoid Arthritis and Asthma. M. N. Mueller 1300
Bone Mineral Determinations on Long-Term Diabetics. J. D. Ringe, F. Kuhlencordt, H. P. Kruse 1300
An Overview of Clinical Applications of Photon Absorptiometry. H. J. Griffiths, R. E. Zimmerman 1301
Bone Mineral Content in Patients with Gonadal Dysfunction. W. D. Risch, D. H. Banzer, L. Moltz, U. Schneider, R. Rudloff 1302
Bone Mineral Content in Anticonvulsant Osteomalacia. C. Christiansen, P. Rodbro 1302
Quantitative Bone Mineral Analyses in Patients with Inflammatory Bowel Disease. H. K. Genant, J. C. Mall, L. H. Lanzl, J. Vander Horst, J. B. Wagonfeld 1303
The Proximal End of Tibia, a Sensitive Site for Measurement of the Bone Mineral Content in Lower Limb Dysfunction. B. E. Nilsson, S. Andersson 1304
Skeletal Mass in Rheumatoid Arthritis: A Comparison with Forearm Bone Mineral Content. I. Zanzi, M. S. Roginsky, K. J. Ellis, S. Blau, S. H. Cohn 1305
Roentgen Signs of Vertebral Demineralization and Mineral Content of Peripheral Cancellous Bone. D. H. Banzer, U. Schneider, W. D. Risch, H. Botsch 1306
Partial Body Calcium Measurements by In Vivo Neutron Activation Analysis. J. E. Harrison, K. G. McNeill 1308

Miscellaneous

Experimental Use of Photon Absorptiometry in Animal Research Models. H. Griffiths, R. E. Zimmerman, R. D. Hunt, H. H. Wolfe 1309
Percentages of Cortical and Trabecular Bone Mineral Mass in the Radius and Ulna. R. A. Schlenker 1309
Comparison of Bone Mineral Content (BMC) in Different Skeletal Sites. U. Schneider, D. Banzer, M. Bange 1312
A Rectilinear Scanning Technique for Bone Mineral Measurements in Animals. J. A. Bevan, H. E. Black, L. A. Oliver 1313

METHODS

General Methods

A Two-Energy Densitometry Method for Measuring Bone Mineral Concentrations and Bone Densities In-Vitro and In-Vivo. Juergen Rassow (Institut fur Medizinische Strahlenphysik und Strahlenbiologie, Hufelandstr. 55, D 4300 Essen 1, West-Germany)

Our absorptiometric method[1,2] is used to determine both mineral and tissue concentrations. The results are given as attenuation equivalents of a bone reference standard according to Reiss/Siemens consisting of four steps of different concentrations of hydroxy apatite (ha) in epoxy resin ($\rho_r = 1.169$ g/cm³).

Measurements were made with a macerated calcaneus which had been embedded in epoxy resin by Heuck and used for an international comparison of mineral content measuring procedures. Figure 1

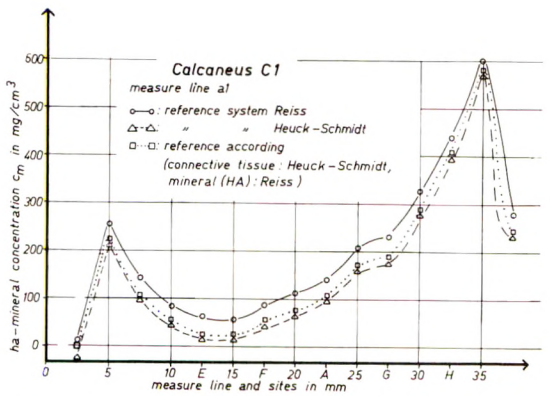


FIG. 1.—Dependence of c_m on the bone reference system used and on the site.

shows that the ha-mineral concentrations (c_m) varied strongly with positions. The absolute values, not the relative course, depended on the composition of the reference standard. The sites we used for in-vivo measurements are situated in the most uniform regions of the calcaneus. The connective tissue concentration (c_{ct}) at any site was largely complementary to the ha-concentration. Therefore the bone density ($\rho = c_m + c_{ct}$) varied only slightly. Filling of the macerated bone with paraffin as fat substitute instead of epoxy resin reduced the results for the c_m greatly.

We measured two location on each calcaneous and averaged the four values on subjects in vivo.

The c_m (Fig. 2) and the ρ increased significantly with age in healthy children ($n = 76$) up to 15 years. No age dependence was seen from 18 to 54 years(70 male and 50 female healthy adults). The standard deviation in adults was 12% for c_m and 14% for ρ. The mean for all adults was $\bar{c}_m = 198$ mg/cm³ (with Reiss/Siemens bone reference system) with a 17% standard deviation. The low absolute bone density

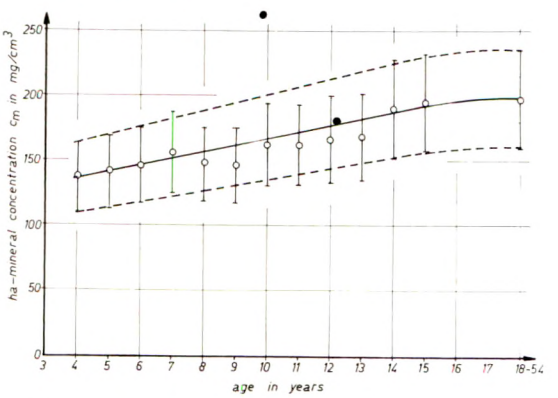


FIG. 2.—Dependence of c_m on the age of healthy children.

values for in-vivo measurements are a consequence of an erroneous bone reference system, chiefly the connective tissue substitute. A noticeably higher mean value ($\bar{c}_m = 217$ mg/cm³) was found for athletes compared with less active individuals.

Follow-up measurements with several children having chronic renal disease showed a good correlation of the relative change of the c_m and ρ with the clinical course. The absolute value for the c_m was lower than the mean for healthy children of the same age (e.g. 50–100 compared to 140 mg/cm³), while the ρ is slightly increased. A 68-year-old patient with symptoms of osteoporosis showed reduced bone values c_m and a higher ρ too. Twelve nursing mothers, 9 days after giving birth, had a significantly lower c_m (151 versus 198 mg/cm³). The $\bar{\rho}$ was increased (1,141 versus 1,010 mg/cm³).

I thank Miss I. Klaskala, Dr. W. Bachmann, Prof. Dr. H. Olbing, Dr. H. G. Wolf, and Prof. Dr. H. Ludwig. Supported by The Deutsche Forschungsgemeinschaft.

REFERENCES

1. RASSOW, J., H.D. STRUETER: Ueber ein verfahren zur quantitativen bestimmung des mineralgehaltes der knochen mit radioaktiven isotopen. II. Mitteilung: Zwei Isotopenmethode. *Fortschr. Roentgenstr.* 1969, 111:155–163.
2. RASSOW, J.: Systematic errors in determinations of bone mineral content in-vivo. Proceedings of the Symposium on Bone Mineral Determinations held in Stockholm-Studsvik, Sweden, 27–29 May, 1974, Vol. 2:131–147. Aktiebolaget Atomenergi, Studsvik, Nykoping, Sweden, AE-489.

Concurrent X-Ray Photodensitometric and Gamma-Ray Absorptiometric Measurements of Bone Mineral in the Radius in Patients. H. E. Meema, D. R. Taves, D. G. Oreopoulos (Departments of Radiology and Medicine, The Toronto Western Hospital, and Department of Toxicology and Pharmacology, University of Rochester, Rochester, New York)

X-ray photodensitometric[2] and gamma ray absorptiometric[3] measurements of bone mineral in the radius were made independently but concurrently by two investigators in 52 patients suffering from chronic renal failure. The sites and units of measurements in the radius were different; the x-ray method determining bone mineral mass of a longitudinal scan in g/cm², and the gamma ray method measuring it along a transverse scan in g/cm. However, moderately good correlations were found between the two techniques (for gamma ray diaphyseal site $r=0.61$, $p<0.001$; for epiphyseal site $r=0.68$, $p<0.001$).

Direct radiogrammetric measurements of the combined cortical thickness (C) and the external bone width (W) at the site of photodensitometric measurements permitted calculations of the bone mineral mass per unit length (M_2 in g/cm) using the following equation: $M_2=0.785\ M_1(2W-C)$, where M_1 is the photodensitometrically measured bone mineral mass (in g/cm²). This conversion improved the correlation between the two techniques considerably (for diaphyseal site $r=0.78$, for epiphyseal site $r=0.79$). The correlation for gamma ray absorptiometry between the two sites was only slightly higher ($r=0.84$, $p<0.001$).

The correlations between the different measuring sites in the radius are of similar order as those reported recently between radial photodensitometry and in vivo neutron activation analysis of partial-body calcium content in a heterogenous group of patients[1] ($r=0.76$, $p<0.01$).

Supported by the Medical Research Council of Canada, grants MA 3889 and MA 4142, and by U.S. Public Health Service grant no. A.M. 11992.

REFERENCES

1. Harrison, J.E., McNeill, K.G., Meema, H.E., Fenton, S., Oreopoulos, D.G., and Sturtridge, W.C. Partial-body calcium measurements by in vivo neutron activation analysis: comparisons with x-ray photo-densitometry measurements of the radius. *J. Nucl. Med.* 1974, 15:929–934.
2. Meema, H.E., and Meema, S. Cortical bone mineral density versus cortical thickness in the diagnosis of osteoporosis: a roentgenologic—densitometric study. *J. Am. Geriatr. Soc.* 1969, 17:120–141.
3. Sorenson, J.A., and Cameron, J.R. A reliable in vivo measurement of bone mineral content. *J. Bone Joint Surg.* 1967, 49A:481–497.

Experiences with the X-ray Bone Scanner, Developed in Bonn. M. Gebhardt, K. D. Hermanutz (Mineralogisch-Petrologisches Institut und Museum der Universität Bonn, Poppelsdorfer Schloss, D-5300 Bonn, West Germany)

The dual photon technique using x-ray generators and monochromators was discontinued, because in practical use with patients the adjustment of the two monochromators was too critical. Now we use a single-photon technique and make scans of the finger in two perpendicular directions. The thickness of the soft tissue and all intensity values of the scans were evaluated by a computer (IBM 370/90).

The essential results are: a) the largeness of compacta and spongiosa ellipses (x- and y-axis); b) the shifting of spongiosa ellipse relative to the compacta ellipse; c) the linear absorption coefficient (μ) of compacta, spongiosa and bone; d) the apatite content (mg/cm³) of compacta, spongiosa and bone; e) the remaining volume (that means the volume which does not consist of apatite) in compacta, spongiosa and bone.

Results were obtained on 100 normal persons and 60 osteoporotic patients.

An Electronic Device for Direct Readout of Bone Mineral Content from Roentgenograms Scanned with a Microphotodensitometer. K. R. Wing, E. Birring (Department of Oral Roentgenology and Biophysics Laboratory, University of Umeå School of Dentistry, Umeå, Sweden)

We have developed a method for measuring bone mineral content (BMC) from the alveolar crest of the maxilla and the second phalanx of the middle finger of the nondominant hand. We use a conventional dental x-ray apparatus (50 kVp, total filtration increased to about 4 mm Al) and fine-grained, no-screen film to make periodically "identical" roentgenograms at these sites. The films are analyzed in a Joyce-Loebl Mark III microphotodensitometer.

The method was basically described by Colbert.[1,2] Since we do not have the on-line computer facilities for the Colbert method, we must estimate contributions to the film density from the film base, fog, and scattered radiation. We have eliminated the soft tissue contribution by using an even thickness of soft tissue equivalent, and we have designed and

built a simple inexpensive instrument for translation and integration of the film density readings from the microdensitometer to BMC.

Translation of film density to BMC involves five steps. First, the background film density (D_b)due to film base fog and scattered radiation (assumed to be evenly distributed over the film) must be subtracted from the measured film density (D). The corrected film density ($D-D_b$) is almost directly proportional to the exposure if this density does not exceed 20% of the maximum corrected density of the film (for direct film, between $D_{1.0}$ and $D_{2.0}$): $D-D_b=K\cdot X$. Second, taking the logarithm of both sides of the above equation does not affect this direct relationship: $\log (D-D_b)=\log K+\log X$. Log X is in turn directly proportional to the attenuation coefficient: $\log X=\log X_0^*-\mu d$, where $\log X_0^*$ is the exposure through the soft tissue layer. Third, by subtracting the logarithm of the corrected film density from a constant log K and a measured quantity $\log X_0^*$, we obtain

$$\mu d=\log K+\log X_0^*-\log (D-D_b),$$

where $\log K+\log X_0^*=\log (D_0^*-D_b)$ and D_0^* = soft tissue density. Fourth, the μd must be related to that of a reference in order to obtain the d of bone mineral. And, finally, these values must be integrated over one or more scans.

In order to estimate D_b, we placed a lead cylinder approximately 1 mm in diameter in a hole through the plastic plate closest to the x-ray source. The radiation producing the image of the lead is assumed to contain little primary radiation but nearly all of the scattered radiation from the surrounding material and the film density there should be close to D_b. The first step in our electronic device subtracts a voltage proportional to D_b and gives a zero density reading at this spot on the film. The second step is a logarithmic amplifier which is adjusted to maximum input—maximum output while the image of the soft tissue is being viewed. At maximum output of this amplifier, the final output voltage of the next stage is zero due to its subtraction from a constant voltage representing $\log K+\log X_0^*$. In the last amplifier stage the output is adjusted to a reference value while the reference object is being viewed. Finally, the signal is applied to a voltage/frequency converter, the pulses (100 Hz–100 kHz) from which are gated to 0–2 decade divider and then to a 5-decade counter. A clock signal of 1 kHz is gated simultaneously to a second 5-decade counter as a measure of scan length. The results are displayed on 5 LEDs. Gating may be done mechanically or triggered electronically at a given bone mineral value. There are unavoidable systematic errors in this system due to hardening of the radiation and to the assumptions of even distribution of the scattered radiation and linearity of the film exposure curve. Fortunately these errors are not all in the same direction.

Simplified schematics are available on request.

REFERENCES

1. Colbert, C., Garrett, C. Photodensitometry of bone roentgenograms with an on-line computer. *Clin. Orthop.*, 1969, 65:39–45.
2. Colbert, C., Bachtell, R. S. Progress in radiographic photodensitometry. International Conference on Bone Mineral Measurement 1973. Ed. R. B. Mazess. DHEW Publ. No. (NIH) 75–683, 1974, 169–176.

The Relationships between Bending Stiffness, Mineral Content, Geometry, and Strength of the Human Ulna. A. S. Foltz, D. J. Rolnick, J. M. Jurist (Division of Orthopedic Surgery, University of Wisconsin Medical Center, Madison, Wisconsin 53706)

Our laboratory is studying relationships between ulnar resonant frequency, mineral content, and geometry as a function of the severity of osteoporosis Since methods are being developed to non-invasively estimate the bending stiffness of long bones from measurements of driving-point mechanical impedance,[4,5] resonant frequency,[1,9] or response to a transient impulse,[2,3] we studied the predictability of ulnar strength from measurements of bending stiffness, mineral content, and geometry.

Forty-five randomly selected, embalmed ulnae were obtained. The length of each ulna was measured from the tip of the styloid to the olecranon. The standard measurement site was $\frac{1}{3}$ of the ulnar length proximal to the styloid. Depth (in the anteroposterior direction) was measured with a vernier caliper. Width (in the mediolateral direction) and bone mineral content (BMC) were determined by direct monoenergetic photon absorptiometry.[8]

Individual load-deflection curves were recorded with a modified Comten Industries materials tester. Each ulna was tested in bending at the standard site by three-point loading over a 4 inch span with the posterior surface under tension. The deflection rate was 4 inches per minute. The average slope of the load-deflection curve was computed between 10% and 50% of the yielding load to determine bending stiffness. The load and deflection at failure were also recorded.

Regressions between the various parameters of interest were obtained in order to develop least-squares power series regression line for each pair of significantly associated parameters. Each pair-wise combination of the following parameters was tested: BMC, width, depth, cross-sectional area calculated from width and depth assuming an elliptical section, length, the ratios of BMC to width, depth, and cross-sectional area, load and deflection at failure, and bending stiffness.

Highly significant associations between the load

at failure and the bending stiffness ($r=0.958$) and between load at failure and BMC ($r=0.947$) were found. The associations between load at failure and the geometrical measurements were somewhat lower but still significant: $r=0.637$, 0.697, 0.743, and 0.754 for length, width, depth, and cross-sectional area, respectively. The deflection of the ulna at failure was not significantly associated with the geometrical measurements. The deflection at failure was correlated weakly with BMC ($p<0.1$). The association between deflection at failure and bending stiffness was somewhat stronger with a correlation coefficient of 0.416 ($p<0.01$).

This implies that stiffer bones deflect more before they fail than less rigid bones. As expected, the associations of BMC with bone size were all highly significant with correlation coefficients of 0.693, 0.756, 0.830, and 0.832 for length, width, depth, and cross-sectional area, respectively.

The best predictors of load at failure were bending stiffness and BMC. We attempted to improve the strength estimate by multiple power series regression analysis with the remaining parameters. The residuals of the regression of strength on stiffness had the highest correlation with width ($r=0.310$). Accordingly, a multiple power series regression equation was developed relating load at failure to both bending stiffness and bone width. The r between observed breaking strength and that estimated from stiffness and width together was 0.962. The corresponding standard error of estimate (SEE) was 37 pounds or 11% of the mean strength. Residuals of the regression of strength on BMC did not correlate significantly with any of the other parameters. Strength estimated by BMC yielded a SEE of 44 pounds or 13%.

The prediction ability of geometrical measurements alone was lower than that of the stiffness or BMC measurements. The highest association between load at failure and a geometrical factor was with cross-sectional area: $r=0.754$ and SEE = 90 pounds or 27%. Residuals of the regression of strength on cross-sectional area did not correlate significantly with the remaining geometrical parameters. Residuals of strength on stiffness were not significantly correlated with BMC. This suggests that stiffness and BMC determinations are essentially equivalent over the range of values obtained for intact bones.

Although these findings are valid for intact bones only, the implications are clear. Noninvasive methods of estimating bone stiffness from dynamic measurements are justified because of the high correlation between strength and stiffness. Furthermore, BMC is justified as a noninvasive index of intact bone strength although the utility of BMC in estimating strength of healing fractures or abnormal bone (Paget's disease, fluorosis, osteopetrosis, and avascular necrosis) has not been established.[6,7,10] Finally, estimates of bone strength based on the geometrical factors described in the report are of limited value.

Supported by NIH grants AM-16514 and AM-17804.

REFERENCES

1. Jurist, J., and Kianian, K. Three models of the vibrating ulna. *J. Biomech.*, 1973, 6:331–342.
2. Lewis, J. A dynamic model of a healing fractured long bone. *J. Biomech.*, 1975, 8:17–25.
3. Lewis, J. Goldsmith, W., Lewis, M., and Wong, A. Impact response of long bones as a diagnostic tool for fracture healing. *In Proceedings of the 26th ACEMB Conference*, 1973.
4. Orne, D. The in vivo, driving-point mechanical impedence of the human ulna—a viscoelastic beam model. *J. Biomech.*, 1974, 7:249–257.
5. Orne, D., and Mandke, J. The influence of musculature on the mechanical impedance of the human ulna, an in vivo simulated study. *J. Biomech.*, 1975, 8:143–149.
6. Riggins, R., Zeman, F., and Moon, D. The effects of sodium fluoride on bone breaking strength. *Calc. Tiss. Res.*, 1974, 14: 283–289.
7. Riggins, R., Rucker, R. Chan, M., Seman, F., and Beljan, J. The effect of sodium fluoride on bone strength: An experimental study with clinical implications. *J. Bone Jt. Surg.*, 1975, 57A:575.
8. Sorenson, J., and Cameron, J. A reliable in vivo measurement of bone-mineral content. *J. Bone Jt. Surg.*, 1967, 49A:481–497.
9. Spiegl, P., and Jurist, J. Prediction of ulnar resonant frequency. *J. Biomech.*, 1975, 8:213–217.
10. Yu, W., Siu, C., Shim, S., Hawthorne, H., and Dunbar, J. Mechanical properties and mineral content of avascular and revascularizing cortical bone. *J. Bone Jt. Surg.*, 1975, 57A: 692–695.

Imaging and Area Scanning

Bone Mineral Distribution in the Immediate Vicinity of Implants. P. Rüegsegger, T. Hinderling (Institut für biomedizinische Technik der Universität und der ETH Zürich, Moussonstr. 18, CH-8044, Zurich, Switzerland)

Post operative complications after implantations of artificial joint endoprostheses are still a serious problem. Long term studies on patients with total hip joint replacements indicate that the major cause for these complications is a loosening of the implant. For an early detection and a study of the processes leading to them we need detailed information on the bone mineral distribution in the immediate vicinity of the prostheses. Computerized transaxial tomography. seems to lend itself as a suitable tool for such investigations. However it can not be applied without modifications. As the linear absorption coefficient for steel at 30 keV is more than one hundred times higher than that for spongy bone the conventionally reconstructed cross sectional images are spoiled by artefacts which render a quantitative description of the bone material of interest impossible. A self consistent interpolation procedure has been developed to overcome the effects of the excessive photon absorption by the implant. Results obtained from computer simulations, model studies, and implanted endoprostheses show that the method promises to be a useful tool in orthopedics.

A New Detector for Absorptiometric Measurement. R. E. Zimmerman, R. C. Lanza, T. Tanaka, G. G. Bolon, H. J. Griffiths, P. F. Judy (Department of Radiology, Harvard Medical School, Boston, Massachusetts 02115)

Photon absorptiometry is the preferred technique for rapid, accurate, and precise determinations of bone mineral content (BMC). The usual system has a point source and sodium iodide detector with narrow beam collimation which is scanned across a peripheral bone, usually the forearm.[1] The precision is determined by the source strength and photon detector efficiency,[3] but experience has shown that in vivo measurements consistently give lower precision than measurements on inanimate objects. We attribute this to repositioning errors and patient movement during measurement. There is a clinical demand for high precision in order to quickly measure changes of BMC with various diseases and therapies. To improve precision we are developing an area detector which counts at high rates (30×10^6CPS) to provide rapid determination of BMC using a high intensity source and fan beam geometry, i.e., a slit collimator on the source and detector.

The prototype area detector is a sealed, one-dimensional, gas-filled, multiwire proportional counter 30 cm×6.4 cm×2.5 cm with the wires running the length of the chamber. Wire spacing is 2 mm. The filling gas was $Ar-CO_2$ or $Kr-CO_2$ at atmospheric pressure. Each of 32 active wires are connected to an amplifier, discriminator, and scaler. Very high count rates are obtained because of the parallel wire readout. An on-line computer reads each scaler contents after the measurement, performs a normalization, and computes the BMC. The source was ^{125}I, unfiltered, with a slit collimator 0.78 mm wide placed 47.5 cm from the central plane of the chamber. The measured object was placed in a water bath 6 mm above the entrance window of the chamber.

A calibration study was performed using an aluminum step wedge 1.59 cm wide with 1 mm steps covering the nominal range from 1 mm to 20 mm. The results are shown in Figure 1 for both argon and krypton. The corrected curves were obtained with a deconvolution formula which adjusted for the spatial resolution of the chamber.

The uncorrected curves shown in Figure 1 indicated that for small amounts of BMC, the system is linear. However, for large amounts of absorber, the curve shows no change with increasing amounts. The

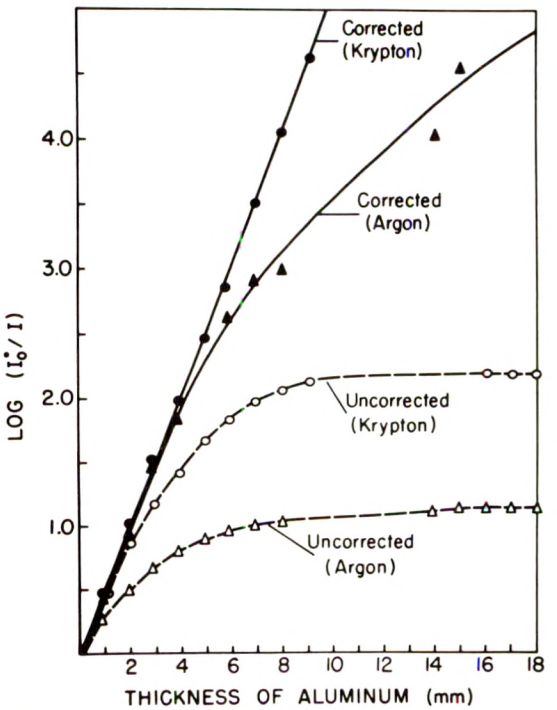


FIG. 1.—Beam attenuation versus the amount of aluminum for the argon and krypton filled detectors. The effects of chamber resolution are removed in the corrected curves.

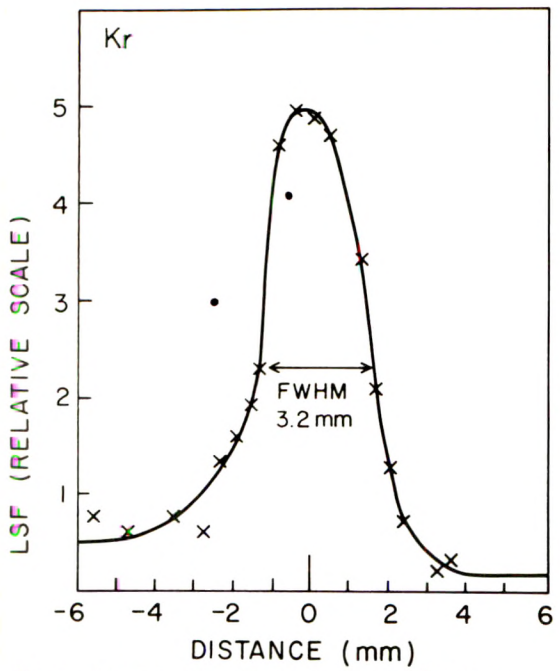


FIG. 2.—Line spread function for the krypton filled chamber.

two most significant reasons for this are system spatial resolution and spectral hardening. The corrected curves show the result of deconvolution to adjust for spatial resolution limitations. The effects of beam hardening[2] are being evaluated.

Resolution was measured by calculating the line spread function from the edge response function. The edge response function was obtained by placing a thin lead edge in the beam and moving the edge in 0.1 mm increments. The derivative was the line spread function, shown in Figure 2, for the chamber filled with krypton. The line spread function for the argon filling was similar but was somewhat broadened.

The resolution was not determined by the wire spacing but primarily by the range of the photo-electron. In argon at 1 atmosphere, the range is 3.0 mm and in krypton the range is 1.6 mm. The line spread function (Fig. 2) for the krypton-filled chamber showed resolution consistent with the wire spacing and electron range. Resolution with argon was better than expected from simple electron range considerations because of a significant amount of conversion in the front and back windows of the chamber which accounts for as much as 65% of the detected photons. Further studies are in progress to quantify the resolution with various gas fillings.

The calculated efficiency of the argon and krypton filled chamber was 1.0% and 14.3%. This compared with measured values of 3% and 11%. The value for argon was high because of the conversion process described above.

The in-vivo precision of the system should be limited by the time to produce an image of the BMC. This cannot be adequately measured on this prototype. Improved design will permit measurement along the length of the arm and formation of a BMC image which will give high precision. A computed tomographic section could be determined by rotating the source-chamber.

REFERENCES

1. CAMERON, J.R., and SORENSON, J. Measurement of bone mineral *in vivo:* An improved method. *Science*, 1963:230–232.
2. SANDRIK, J.M., and JUDY, P.F. Effects of the polyenergetic character of the spectum of ^{125}I on the measurement of bone mineral content. *Invest. Radiol.*, 1973, 8:143–149.
3. JUDY, P.F. The theoretical accuracy and precision in the photon attenuation measurement of bone mineral. Proceedings of Bone Mineral Conference, ed. Cameron, J.R., U.S. Atomic Energy Conf. 700515, U.S. Dept. of Commerce (CFSTI), Springfield, Va., 1970, 1–21.

Bone Imaging Using a Gadolinium-153 Source and a Xenon-filled Multiwire Proportional Counter as Detector. A. Hörsman, D. H. Reading, J. Connolly, W. Glasgow, M. S. F. McLachlan (M. R. C. Mineral Metabolism Unit, Leeds General Infirmary, Leeds, England)

An important factor limiting the precision of bone mineral content (BMC) measured in vivo by photon absorptiometry is the difficulty in identifying the measurement site from external landmarks. This problem would be reduced if BMC could be measured over an area sufficiently large for the bone outline to be delineated. Two-dimensional images of bones have been constructed by computer processing the results of rectilinear transmission scans.[3] However, rectilinear scanning is inefficient, and the increased measurement time increases the probability of patient movement. A large area detector such as the multiwire proportional counter (or multiwire chamber)[2] is desirable and we have done preliminary testing.

The chamber has an active diameter of about 20 cm, and is filled with xenon gas containing 30% isobutane at atmospheric pressure. It contains three planes of wires (Fig. 1), the central plane forming the anode. The outer planes (cathodes, or "induction planes") are used to locate events within the chamber. The wire spacing is 2 mm in all three planes. When an x-ray photon interacts with a xenon atom, the ionization trail produced by the photo-electron is accelerated towards the anode (the anode potential is approximately 5 kV) and an

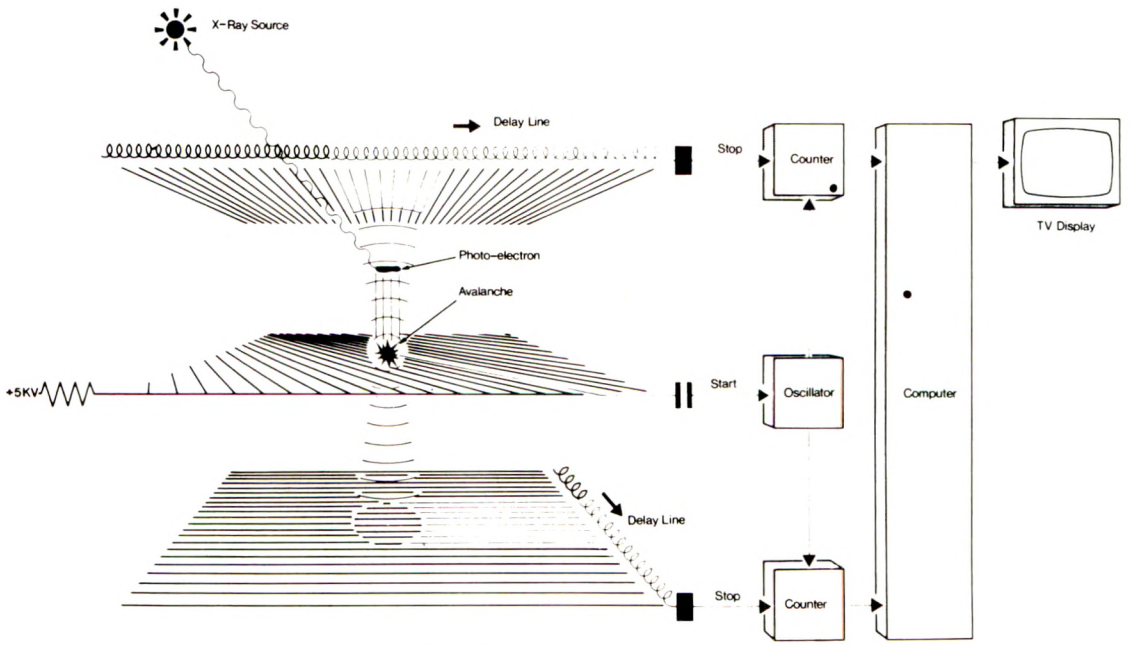


FIG. 1.—Schematic diagram of the multiwire chamber.

avalanche is produced on one of the wires. The avalanche causes pulses to be induced in the induction plane wires which are coupled into two delay lines, one for each induction plane. The x-y coordinates of the avalanche are converted by the delay lines into two time intervals (measured with respect to the anode signal). The coordinates are recovered from the time intervals by time to digital converters and transferred to a PDP-11 computer with disc store and color TV monitor.

The binding energy of the K shell electrons in xenon is about 35 keV. Thus photoelectrons with low kinetic energy can be produced by photons in the energy band suitable for the examination of the limbs. The energy of the photoelectrons critically determines their range and thus the spatial resolution of the chamber. ^{153}Gd, which emits 42 keV x-rays with a half-life of 242 days, is a suitable source, and causes photoelectrons to be emitted from the K shell with an initial kinetic energy of about 7 keV and a range of less than 0.5 mm.[1]

Fig. 2a shows a "baseline" exposure containing 10^7 events reconstructed by the PDP-11. The picture is non-uniform due to the varying sensitivity of the chamber over the image area and to the inverse square law effect. Fig. 2b shows the effect of inserting the proximal end of a femur in the beam. In Fig. 2c, the log of the ratio of the counts in the baseline and object pictures is displayed. Cursors can be superimposed on the display in order to define the region over which a two dimensional summation of the log-ratio is to be performed. The resulting sum should be

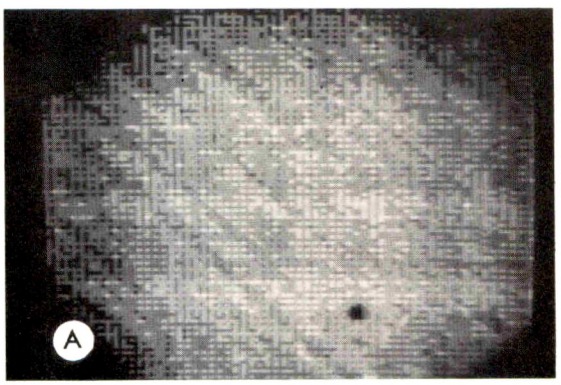
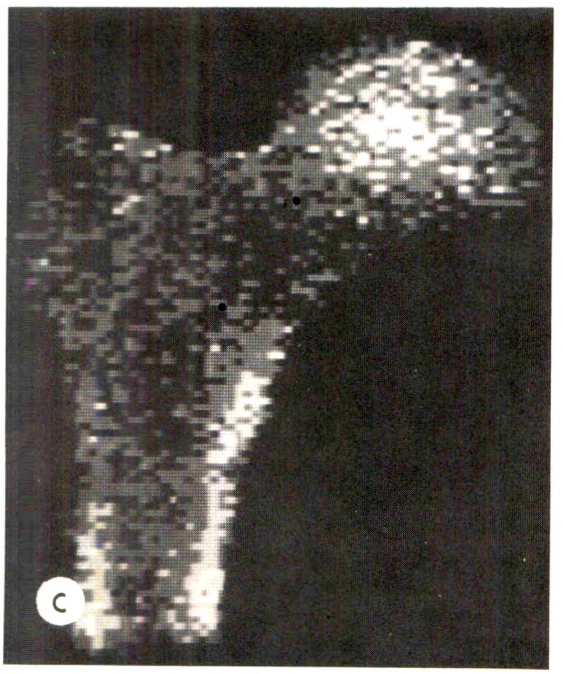


FIG. 2a.—Baseline exposure to a ^{153}Gd source. The image contains 10^7 counts. There is no object in path of the beam.



2b.—Effect of inserting the proximal end of a femur in the beam. The image contains 10^7 counts.



2c.—Femur image extracted from a) and b) by evaluating and displaying the logarithm of the ratio of the counts in each image cell.

proportional to the mass of absorbing material within the area defined by the cursors.

Twenty clean, dry 4 cm long sections from the shafts of five femora were exposed in pairs in contact with the chamber window to a 0.5 mCi ^{153}Gd source until 10^6 counts had been accumulated. Each exposure took approximately 6 minutes. From the baseline and object images, the log-ratio image was constructed and, using the cursors, the sum of all the log-ratio values of each image cell within the object, Q, was computed. The weights of the sections, W, were also determined. The correlation coefficient between Q and W is 0.97 (Fig. 3) and the standard error of estimate (SE) of W from Q is 0.70 g (approximately 4% of the mean specimen weight).

Twenty-four 4 cm lengths of bone from the shafts of eight clean, dry radii were studied in the same way. The samples were exposed six at a time. A longer exposure (5×10^6 counts) was used in order to compensate for the worsened signal to noise ratio due to the smaller specimen mass. The correlation coefficient between Q and W was 0.93, and the SE 0.25 g.

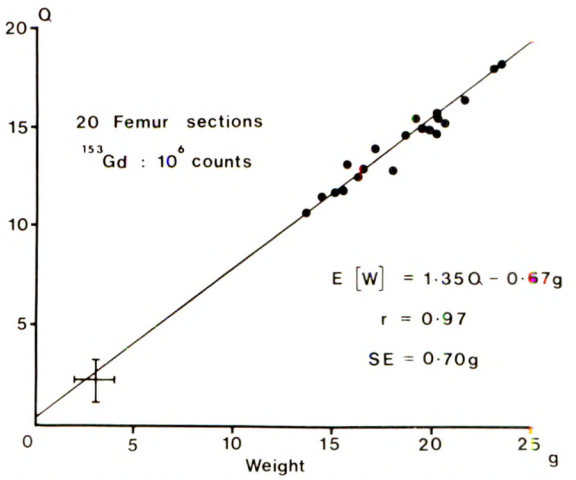


FIG. 3.—The relationship between the value of the log-ratio summated in two dimensions over the image of each specimen, Q, and the weight, W of 20 sections from the shafts of five femora. The cross marks the range of the data on 24 similar sections from the shafts of eight radii. The regression line is shown only for the femur data.

The range of the radius data is shown in Figure 3.

The xenon-filled multiwire chamber shows promise as a detector for transmission measurements of BMC. It opens up the possibility of accurate measurement combined with a low resolution image of sufficient detail to allow measurement sites to be located from the bone outline.

We acknowledge the active interest and support of Professor R. Ellis, Head of the Department of Medical Physics at Leeds University, in the design, construction and applications of the multiwire chamber.

REFERENCES

1. BATEMAN, J.E., WATERS, M.W. and JONES, R.E. Spatial resolution in a xenon-filled MWPC x-ray imaging detector—a computing physics approach. Rutherford Laboratory Report RL 75–140, 1975.
2. KAPLAN, S.N., KAUFMAN, L., PEREZ-MENDEZ, V. and VALENTINE, K. Multi-wire proportional chambers for biomedical application. *Nuclear Instruments and Methods* 1973, 106:397–406.
3. VOGEL, J.M. and ANDERSON, J.T. Rectilinear transmission scanning of irregular bones for quantification of mineral content. *J. Nucl. Med.*, 1972, 13:13–18.

Bone Densitometry with the Aid of Computerized Transaxial Tomography. U. Elsasser, P. Rüegsegger (Institut fur Biomedizinische Technik der Universitat Zurich und der ETHZ Moussonstr. 18, CH-8044 Zurich, Switzerland)

Trabecular bone shows a more rapid change of the mineralization than does compact bone,[1,2,6] so a method for detection of minute alterations in mineralization must allow for separate quantification of compact and spongy bone. With the aid of the techniques of computerized transaxial tomography[3]

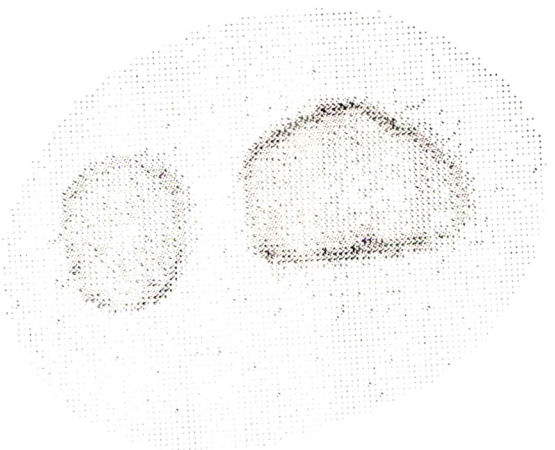


FIG. 1.—Cross sectional image through the distal metaphysis of the forearm of an 18-year-old boy with slightly reduced mineralization. Local linear absorption coefficients are represented by 10 different grey levels.

an image can be reconstructed of the bone cross section on the basis of the local linear absorption coefficients. If monoenergetic isotopes are used, these coefficients can be determined with sufficient accuracy to allow for the quantification of the mineral distribution.

The multi-scan photon absorptiometry technique developed for determination of compact bone density in human long bones[4] forms the basis of the method. The object is linearly scanned with a highly collimated beam (^{125}I) and a NaI scintillation detector. The transmitted photons are counted during 128 equal time intervals. The linear scanning process is repeated 48 times with the beam rotated by 3.75° after each scan. The scanning is effected by stepping motors which are computer-controlled to assure uniform time and space intervals. One entire measurement lasts 5 minutes and the radiation dose is less than 5 mrad.

From the 48 projections the mineral distribution in the plane of the scans is calculated by means of a convolution algorithm[5] as is used in brain tomography. The resulting matrix of 128×128 local linear absorption coefficients can be visualized in the form of a color TV image or a matrix plot (Fig. 1). The cross section through the distal region of a human forearm is built up from more than 16,000 matrix elements or pixels, each of them measuring .58×.58 mm. The corresponding values for the linear absorption coefficients are divided into 10 classes and are represented by 10 different grey levels. Whereas qualitative visual evaluation of the mineralization is possible from the image, the computer permits a precise quantification of various parameters defining the cross sectional geometry, the total mineral content, and the compact as well as the spongy bone density.

The validation of the method was carried out in

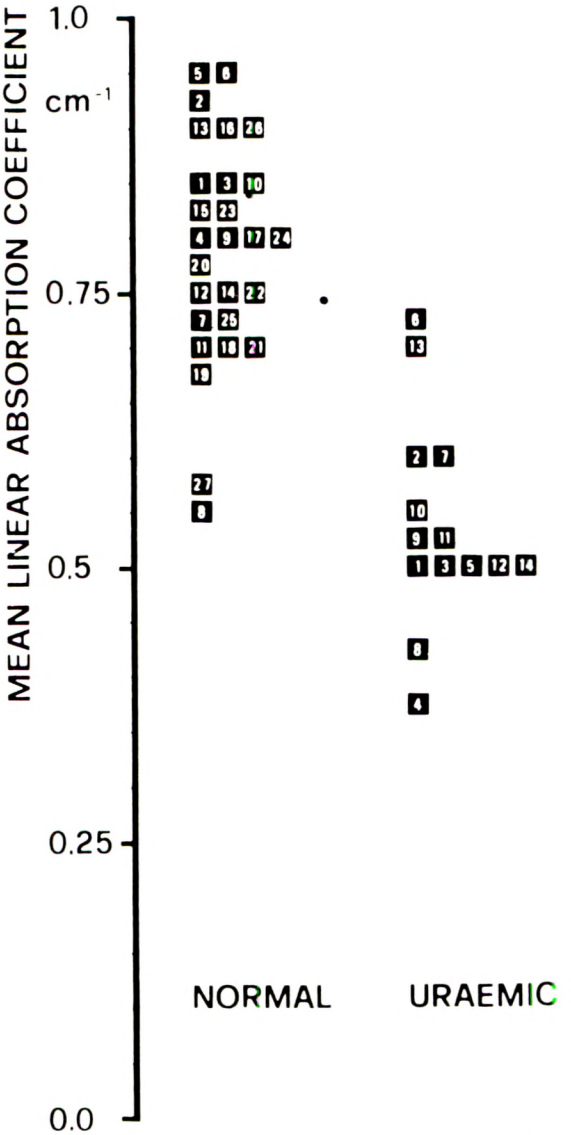


FIG. 2.—Comparison between the spongy bone densities of a group of patients suffering from uraemia and a control group.

three steps: reconstructions from computer-simulated transmission data, transmission measurements of physical models, and measurements of macerated bone. The mathematical and physical models simulated in principle the in-vivo measurements at a position in the distal region of the forearm.

To determine the bone mineral content and the cross-sectional area of the bone, the surrounding soft tissue is computationally subtracted. Subsequently, concentric rings with a thickness of one matrix unit are peeled off beginning at the outer contour of the bone until a region of purely trabecular bone is left. The innermost 50% of the total cross section of the bone is identified as spongy bone do-

main. The average linear absorption coefficient of this area is defined as the mean spongy bone density.

The model studies indicated that individual differences in the thickness of the compacta and the soft tissue at the human forearm did not affect the value of the mean linear absorption coefficient for spongiosa by more than 2%. A detailed study of the mineral distribution in various sections of the distal metaphysis of the radius showed that an appropriate site for our in vivo measurements was at 10% of the ulna length measured from its distal end. There the variation in the spongy bone density, due to shifts in the measuring site of ±1.5 mm was on the order of ±2%. Similar variations were observed on the right and left radius of the same patient or when the measurement was repeated on a subsequent day. Ten determinations of the spongy bone density on the same healthy subject over a period of 60 days showed a reproducibility of 1% (s.d.).

Initial results of a 6 week study on patients suffering from uraemia and controls showed a significant difference in the mean spongy bone densities and also relatively large variance within each group (Fig. 2). Longitudinal studies of changes of bone mineralization due to endocrinological and nephrological factors as well as immobilization are in progress.

Supported in part by the Swiss National Science Foundation under grant no. 4.140–0–74.

REFERENCES

1. Gustafsson, L., Jacobson, B., Kusoffski, L. X-ray spectrophotometry for bone-mineral determinations. *Med Biol Eng*, 1974, 12:113–119.
2. Hahn, T.J., Boisseau, V.C., Avioli, L.V. Effect of chronic corticosteroid administration on diaphyseal and metaphyseal bone mass. *J Clin Endocrinol Metab*, 1974, 39:274–281.
3. Hounsfield, G.N., Ambrose, J. Computerized transverse axial scanning. *Brit J Radiol*, 1973, 46:1016–1047.
4. Ruegsegger, P., Niederer, P., Anliker, M. An extension of classical bone mineral measurements. *Ann Biomed Eng*, 1974, 2:194–205.
5. Shepp, L.A., Logan, B.F. Reconstructing interior head tumor from x-ray transmission. *IEEE Trans NS*, 1974, 21:228–236.
6. Smith, D.M., Johnston, C.C., Yu, P.L. In-vivo measurement of bone mass, its use in demineralization states such as osteoporoses. *JAMA*, 1972, 291:325–329.

Regional and Whole-Body Bone Mineral Content Measurement with a Rectilinear Scanner.
R. R. Price, J. Wagner, K. Larsen, J. Patton, A. B. Brill (Departments of Radiology and Physics, Vanderbilt University Medical Center, Nashville, Tennessee 37232)

Accurate bone mineral content (BMC) of lumbar vertebrae is needed as a measure of demineralization in weight-bearing bones in addition to the more routinely performed measurements of the extremities. For this reason, we used the two photon attenuation technique with a modified dual-headed whole-body clinical scanner to make rectilinear scans of the vertebral column. Others[1,2,3] have shown the feasibility of the method using profile type scans and have demonstrated a precision of 3%–6%. With our system, signals from the scanner's x and y position encoders, the single channel analyzer pulses from the two photopeaks, a third energy window, and the pulses from a high frequency oscillator are monitored via CAMAC modules driven by a PDP-9 computer. The data are buffered into core and then dumped to disk at the end of each line. The recorded oscillator pulses make it possible to correct for scanner speed instabilities. The third energy window was for studying the effects of scattered radiation or system dead-time characteristics (both sources of error were found to be negligible).

The source/detector system consisted of a 2-Ci Gd-153 source (obtained from the Isotopes Development Group at Oak Ridge National Laboratory) and a 2×½ inch thin window NaI crystal mounted as an integral unit with the photomultiplier tube. The 44- and 100-Kev lines of Gd-153 have been shown to be optimum for the measurement of the vertebral bone mineral content.[2] The source/detector separation for the vertebral measurement is 15-inches with both source and detector collimated to 0.63-cm by cylindrical cadmium collimators. Cadmium was chosen instead of lead to minimize the production of lead x-rays (75-Kev). The vertebral scans are collected in 64×64 image matrix corresponding to a 1.5-mm×1.5-mm square spatial element. Scan time for a 10-cm segment of the spine is approximately 10-minutes and delivers an average radiation dose of <10-mrad per scan.

We first measured the BMC of the ulna and radius. Using a 256×16 image matrix corresponding to a 0.5-mm×1.5-mm spatial element and found a precision of 1%–2%. Recently we calibrated our system with University of Wisconsin BMC standard. The results of patient studies are reported as the mean g/cm as measured along a 1-inch segment at the middle of the forearm. The bone width in each line is determined by an edge cut off criterion and then carrying out a least squares fit of the edge coordinates to a second order polynomial, thus imposing continuity along the bone edge and allowing a means of interpolating between data cell boundaries. It is our hypothesis that the mean BMC determined from a number of parallel scan lines will be a more stable estimator by being less sensitive to repositioning errors.

Rectilinear scanning is most important for the

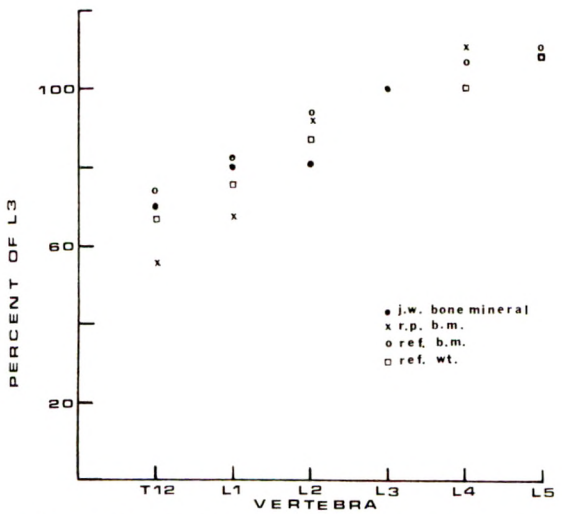


FIG. 1.—Normalized bone mineral content for two volunteers (J.W. and R.P.) and reference vertebrae plotted for the T12 to L5 region.

measurement of irregular objects such as the vertebral column. For such irregular objects accurate and reproducible repositioning is essential since small variations in position result in large changes in the BMC. Rectilinear scans allow visualization of the vertebrae, thus allowing use of internally recognizable and relocatable fiducial structures for location. With this technique the linear density (g/cm), which presents some difficulty in interpretation when applied to irregular objects, should be replaced by an estimate of the total BMC in the sampled region.

Repeated scans on humans and on a reference disarticulated spine, showed precision of the vertebral measurements to be $\pm 5\%$ independent of orientation. Estimates of BMC were made for six vertebrae from our reference spine placed in a 10 cm scattering medium. BMC was highly correlated ($r=0.98$) with the dry weight of the vertebrae.

Figure 1 shows plots of the BMC of each vertebrae in the T12–L4 region of the spine for two volunteers and the reference spine. The measurements are presented as a percent of the L_3 vertebrae. For comparison the dry weight of the reference vertebrae was plotted normalized in the same manner. We are refining the vertebral scan technique and extending it to estimate the total-body BMC.

REFERENCES

1. JACOBSON, B. Bone salt determination by x-ray spectrophotometry. *Proc Bone Meas Conf* AEC CONF 700515, 1970, 237.
2. MAZESS, R.B., WILSON, C.R., HANSON, J., KAN, W., MADSEN, M., PELC, N. and WITT, R. Progress in dual photon absorptiometry of bone. In: P. Schmeling (ed)—Symp. on Bone Mineral Determinations, AE-489, Vol. 2. Aktiebologet Atomenergi, Studsvik, Sweden 1974, 40–52.
3. ROOS, B. and SKOLDBORN, H. Dual photon absorptiometry. I. Theory and Method. *Acta Radiologica*, 1975, 13, 3–18.

Recent Advances in Skeletal Trans-imaging. A. M. Strash, R. W. Bright (Department of Radiology, Medical College of Virginia, Richmond, Virginia 23298)

Trans-imaging as a technique for determining bone mineral content (BMC) has been used to delineate the progression of bone graft incorporation or resorption in dogs over a 3-year period. We were concerned with the variation in BMC along the length of the graft as well as the temporal changes at each position. Recently, trans-imaging was applied to the BMC distribution in resected human metatarsals. A complete profile of BMC distribution along the metatarsal was required for 200 specimens. The data would then be correlated with the biomechanical properties of whole bone. These projects required BMC over several centimeters of bone length. Although a photon absorptiometric bone scanning device was available, sequential parallel linear scans along the region of interest was prohibitively time consuming. Trans-imaging, which requires the simple adaptation of equipment already available in many institutions, rapidly provides regional BMC.

The area of bone to be studied by trans-imaging was placed between a source of gamma or x-rays and the large surface scintillation detector of a gamma camera. The entire bone region of interest was "illuminated" by a broad beam of radiation and a shadow image of this region was displayed by the gamma camera system. Trans-images formed by the gamma camera were stored in a 64 by 64 element array by a dedicated computer connected to the gamma camera. Each array element is associated with the transmitted radiation through a small section of the bone, and a row of matrix elements corresponds to a single traverse of a linear scanning device. Thus, for our system, 64 linear parallel scans are collected simultaneously. Distance between the radiation source and the detector surface was usually greater than 3 m with the bone positioned to provide a magnified but relatively undistorted image and to adjust the spatial resolution of the absorption data. Thus, a bone of only a few centimeters in length could be magnified to make maximum use of the 64 by 64 image array. With this geometry and the large area of the gamma camera detector, relatively small radiation sources could be used. Incident radiation intensity was adjusted to the maximum count rate of the gamma camera system by varying

source to detector distance or by changing or adding filters to the radiation beam.

To define the BMC of resected metatarsals, the bones were trans-imaged in groups of three. Each group was imaged with a total detector count of 4×10^6 in about 6 minutes, thus providing approximately 1,000 counts per array element. At regular intervals "flood" images were made to determine the response of the gamma camera system. In addition, a bone of known mineral density was scanned as a reference standard and a lead bar grid was imaged to establish dimensions within the stored matrix.

All of the metatarsals were trans-imaged with ^{125}I. Since most gamma cameras are designed to operate with the 140 keV ^{99m}Tc gamma radiation, the relatively low energy ^{125}I radiation created a noticeable variation in response over the surface of the scintillation detector as well as a loss in resolution. The latter problem was partially offset by the magnification of the bone region at the detector surface. Variations in response over the detector surface were corrected with a flood image. Selected metatarsals were also imaged with 60 keV radiation of ^{241}Am. Although the higher energy gamma-rays would be expected to provide better resolution and better uniformity of camera response, flood corrections were still required as well as higher total counts to offset the greater penetration of the higher energy gamma-rays through bone.

All trans-images, including those of a reference standard, grid and flood were stored on magnetic tape and were analyzed with the aid of a large batch-processing computer. Images could therefore be reprocessed from original data as experimental needs dictated. Images formed by an electrostatic printer and histograms formed from the equivalent of over 10,000 linear scans have thus delineated the distribution of BMC in over 200 metatarsals.

Compton Scattering

Absolute Bone Density Measurement Using Compton Scattered Radiation. D. G. Piper, L. E. Preuss (Department of Physics and Biophysics, Edsel B. Ford Institute for Medical Research, Detroit, Michigan 48202)

The Compton scattering method for determining bone density offers the advantage of measuring absolute density (g/cm³), independent of sample size and thickness of surrounding tissue. This may be accomplished by measuring the electron density at the intersection of monoenergetic photon beams emitted by radioactive sources with appropriate energies.

A laboratory device has been constructed for use with ^{153}Gd (100 keV) and ^{170}Tm (84 keV) using a scattering angle of 86°. Various organic and inorganic materials with densities ranging from 0.665 g/cm³ (petroleum ether) to 2.65 g/cm³ (quartz) have been measured accurately and reproducibly. Twenty samples of trabecular bone from the distal tibia of cattle, with densities between 1.13 g/cm³ and 1.58 g/cm³, were measured repeatedly, with precision generally better than 3% and a correlation coefficient with Archimedean measurement of 0.97.

Measurement of Bone Mineral Density Using Coherent and Compton Scattering. H. Olkkonen, P. Puumalainen, P. Karjalainen, E. M. Alhava (University Central Hospital, Kuopio, Finland)

Density distributions of body tissues have been evaluated for many years using scattered radiation. Modifications which enable the measurement of bone density in the presence of varying quantities of surrounding tissues were introduced recently.[1,4] Clinical measurements with the Compton technique are complicated requiring four time-consuming procedures. We have introduced a simplified photon scattering method[6] based on the measurement of coherently and Compton scattered photons. This paper describes the preliminary results from application of the method in vitro and outlines the advantages in clinical use.

The measuring procedure consists of the detection of the scattered photons in a narrow beam geometry using a semiconductor detector and a multichannel analyzer. In the scattering spectrum the peaks due to coherently and Compton scattered photons are well separated by the fine energy resolution of the detector. For the ratio of the peak areas the following expression is valid:[6]

$$A_{coh}/A_{Compt} = \text{const.}\frac{\overline{Z^3}}{\overline{Z}}\bar{A},$$

where $\overline{Z}$ and $\bar{A}$ are the average charge and mass numbers of the target atoms. The A_{coh}/A_{Compt} ratios have been calculated for some substances contained in bone (Table 1). The $\overline{Z}$ and $\bar{A}$ are considerably higher for hydroxyapatite than for organic components (collagen, fat). Therefore, the A_{coh}/A_{Compt} ratio is strongly related to the mineral content of bone.

Twenty-eight distal radii taken at autopsy from females were fixed in 30% ethyl alcohol. The measuring site was about 15 mm from the dorsal end of the distal radius in the region of trabecular bone. The scattering angle was 90° and a hole collimator (length 30 mm, diameter 6 mm) and a slit collimator (length 30 mm, aperture 6×20 mm) were used in the source and the detector side. The detector was a

TABLE 1.—A_{coh}/A_{Compt} ratios relative to water (= 1).

Material	Chemical formula	$\bar{Z}$	$\bar{Z^3}$	$\bar{A}$	A_{coh}/A_{Compt}
calciumhydroxy-apatite	$Ca_{10}O_{26}P_6H_2$	11.36	2581	22.82	16.82
water	H_2O	3.33	171	6.00	1.00
triglyc.palm. acid	$H_{98}C_{51}O_6$	2.92	91.5	5.20	0.53
fat	-	3.00	107.4	5.36	0.62
paraffin	$(H_2C)_n$	2.67	72.7	4.67	0.41

200 mm² intrinsic germanium semiconductor crystal and the radiation source a 45 mCi ^{241}Am point source. The mineral density of the specimens was also determined by the gamma transmission method.[3] After that, 6–8 mm long segments were cut from the specimens by sawing and the cortical parts were removed. The mineral density was determined by ashing at a temperature of 550°C for 24 hours.

The following linear regression was found between bone mineral density and the A_{coh}/A_{Compt} ratio:

$$\rho(g/cm^3) = -0.181 + 0.107\, A_{coh}/A_{Compt}.$$

The correlation coefficient was 0.96. The mineral density values measured by the scattering technique correlated well ($r = 0.75$) with the mineral density values yielded by the gamma transmission method. The correlation equation was

$$\rho_{scatt}(g/cm^3) = -0.522 + 2.880\, \rho_{transm}(g/cm^3).$$

The decrease in bone mineral density with age was also well reflected in the results.

The principal source of error in the present method is the difference in the attenuation of the coherently and Compton scattered photons. In practice, however, the error is negligible when measuring peripheral bones. By using the ^{241}Am source, the 90° scattering angle results in energy difference of 6.1 keV between the coherent and Compton peaks. A 10 cm thick soft tissue layer placed in the scattered beam yields about 15% increase in the A_{coh}/A_{Compt} ratio. This equals only about 3% increase in the bone density value.

Clinically the present method has the following unique features: (1) It measures the density of trabecular bone where changes occur sooner than in compact bone[2]; (2) it is based on the coherent to Compton scattering ratio, which is not affected by the tissue layers overlying the measuring site. Hence, slight involuntary movements do not introduce errors as in other methods.

We also think the method is applicable to the density determinations of central bones. In applications, where a more intensive incoming beam is needed, the quasidiscrete beam of the x-ray tube has given successful results. Also we replaced the semiconductor detector by two NaI probes. However, the accuracy of the last method was found to be poorer than with the semiconductor detector.

REFERENCES

1. GARNETT, E.S., KENNETT, T.J., KENYON, D.B., and WEBBER, C.E. A photon scattering technique for the measurement of absolute bone density. *Radiology*, 1973, 106:209–212.
2. JOHNSTON JR, C.C. Measurement of bone mass in the radius. *Conf-680211*, 1968, 283.
3. KARJALAINEN, P. A method for determination of the mineral content and mineral density in the distal radius using gamma ray attenuation. *Annals of Clinical Research*, 1973, 5:231–237.
4. OLKKONEN, H., and KARJALAINEN, P. A ^{170}Tm gamma scattering technique for the determination of absolute bone density. *Br. J. Radiol.*, 1975, 48:594–597.

Experience with Photon Scattering Measurements of Bone Density. C. E. Webber (Department of Nuclear Medicine, McMaster University Medical Centre, Hamilton, Ontario, Canada)

The density of a selected volume within a bone can be measured from the number of gamma rays scattered by the bone from a monoenergetic photon beam.[1,3–5] The result is independent of attenuation within the bone and within surrounding tissues when the transmission of both the primary and secondary photon beams is measured. The secondary beam energy must equal that of the photons scattered from the primary beam. In vitro studies have established the accuracy of this procedure and have also shown that the optimum energy of the primary photon beam is about 90 keV.[2]

To design a system for density measurement of the os calcis several factors had to be considered. The sources selected should possess an intense component of the desired photon energy with no significant gamma rays of higher energy which would unnecessarily increase the dose. The source half-lifes should be long: activities of the order of 1 Ci are required. ^{153}Gd (242 day $T_{\frac{1}{2}}$) which emits 103.2 keV and 97.5 keV photons is an ideal primary source, but large quantities are expensive. ^{153}Sm, which decays to the same daughter product as ^{153}Gd, emits the 103.2 keV gamma ray with an intensity of 28.2%. The availability of highly enriched ^{152}Sm and the relatively short half-life of ^{153}Sm (47 hours) mean that large quantities can be produced in a reactor with relatively short irradiation times. Therefore ^{153}Sm was used as our primary source.

The choice of scattering angle is determined by the angular distribution of scattered photons, the availability of a suitable secondary source, and the physical arrangement of the sources and detectors with respect to both the bone and the patient. At an inci-

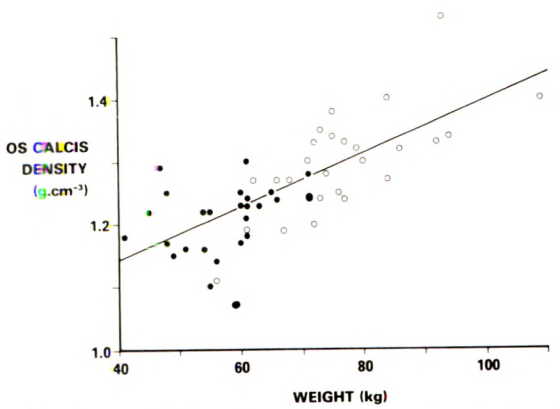


FIG. 1.—The normal relation between os calcis density and body weight for 25 females (closed circle) and 27 males (open circle). The straight line is the least squares best fit to the data.

dent energy of about 100 keV scattered photons produce an almost isotropic distribution, so a large angle entails little loss of intensity. Ninety degree scattering of 103.2 keV photons produces photons of 85.9 keV; 90° is a convenient angle for the foot and provides the most symmetrical scattering volume within the os calcis. Since ^{170}Tm emits gamma rays at 84.3 keV and is conveniently produced in a reactor, the 90° configuration was selected.

With a 1.7 Ci ^{153}Sm source, the scattered count rate for the foot phantom was approximately 32,000 cpm. A density measurement of the os calcis could be made in 3 minutes and the calculated dose was 160 mrad. The precision of density for 26 phantom determinations over a period of 6 months was 1.5%. In addition, in two human subjects, os calcis density was measured five times for each foot during a single day. The mean variation for the measurements was 1.3%.

The os calcis density was measured on the side of hand preference in 52 normal human volunteers. A good correlation (Fig. 1) was found between density and body weight ($r=0.74$; $p<0.001$). Os calcis density was also measured in 16 patients with radiological evidence of osteoporosis. For each patient the density was less than that predicted from their body weight, and 75% were more than 1 S.D. below the predicted density.

The differences between transmission and scattering measurements should be stressed. A transmission measurement yields the mineral mass within a cylinder of bone. A scattering measurement yields the average density within a selected volume which will include both the inorganic and organic phases of bone. Most importantly, the selected volume can be restricted to trabecular bone. Consequently, scattering techniques are tools for the accurate and precise measurement of changes in density within trabecular bone.

REFERENCES

1. CLARKE, R.L. and VAN DYK, G. A new method for the measurement of bone mineral content using both transmitted and scattered beams of gamma rays. *Phys. Med. Biol.*, 1973, 18:532–539.
2. GARNETT, E.S., KENNETT, T.J., KENYON, D.B., and WEBBER, C.E. A photon scattering technique for the measurement of absolute bone density in man. *Radiology*, 1973, 106:209–212.
3. KENNETT, T.J., GARNETT, E.S., and WEBBER, C.E. An in-vivo measurement of absolute bone density. *J. Can. Assoc. Radiol.*, 1972, 23:168–170.
4. OLKKONEN, H., and KARJALAINEN, P. A ^{170}Tm gamma scattering technique for the determination of absolute bone density. *Brit. J. Radiol.*, 1975, 48:594–597.
5. WALFORD, G.V., and FENTON, T.R. The remote measurement of principal elemental concentration and electron density in dense bodies. *I.E.E.E. Trans. Nucl. Sci.*, 1975, NS-22:428–436.

Quantitative Density Longitudinal Section Through the Spine. K. H. Reiss, B. Conrad, K. Killig (Siemens Medical Division, Henkstrasse 127, D-8520 Erlangen, West Germany)

The measurement of Compton scatter gives absolute tissue densities in vivo provided that corrections for absorption and multiple scatter are precise. We previously used a ^{137}Cs source and NaI scintillation detector for measurement of os calcis density and of lung density. We are now using an x-ray beam and a 5 inch detector with a collimator for 8 mm resolution for measurement of the spine. By using two different energies, for example 300 and 150 kVp, a correction for absorption can be calculated. Multiple scatter was measured on a phantom and amounted to 50%. These procedures allowed accurate density determination along a spinal phantom.

BIOMEDICAL

Normative Studies

Bone Mineral Mass and Width in Normal White Women and Men. R. A. Schlenker, B. G. Oltman, T. J. Kotek (Center for Human Radiobiology, Argonne National Laboratory, Argonne, Illinois 60439)

Bone mineral content (BMC) and width (W) have been measured in approximately 600 white women and 100 white men ranging from the teens to the 80s. Measurements were made using the ^{125}I photon absorptiometric method at five pairs of contralateral sites with the arm in the prone position: the midshafts of the right and left radii and ulnae, the distal metaphyses of the right and left radii and ulnae, and the distal diaphyses of the right and left third proximal phalanges.

Most subjects were from a group who had abnormally high body burdens of ^{226}Ra. A large fraction of radium intake to the body is deposited in the skeleton and these subjects were studied to determine if irradiation of bone by radium alpha particles affected the BMC. There was no relation of BMC to radiation dose, although for very high doses there were depressions in BMC when scanning across osteolytic lesions. The data here are for subjects who had ^{226}Ra body burdens less than 100 nCi plus persons who were unexposed to radium. Body burdens of 100 nCi ^{226}Ra cause no radiographic skeletal abnormalities. This and the absence of a correlation between BMC and radiation dose, indicated that our radium-exposed subjects had normal skeletons.

Von Roth et al[3] noted significant differences between BMC/W in normal Germans and in the U.S. We made comparisons to evaluate if such differences were due to procedures or population. First we grouped data for a given sex, site, and parameter into decade age intervals and then compared (t-test with $p<.01$) against the means from other laboratories. This showed differences between decade subsets but not for entire data sets. Second, we counted the number of decades in which a significant difference was observed, and computed the probability of significant differences by chance. If the probability was 0.01 or less, we concluded that our data set and the comparison data set differed significantly and that the populations and/or the measurement procedures differed.

The comparisons are summarized in Table 1. They fall naturally into four groupings which are indicated in the table: (1) comparisons with U.S. data at the radius midshaft[2] (C. C. Johnson, personal communication, 1972), (2) comparisons with Mazess and Cameron[2] data at the ulna midshaft, (3) comparisons with U.S. data[1,2] at the distal radius, and (4) comparisons with German data at several sites. Significant differences are noted in the second, third, and fourth groups. The + and − signs in the latter groups indicated if our data values were greater or less than the comparison values.

Some of the observed differences can be explained by unrecognized differences in measurement procedures. Consider the midshaft ulna. If procedures were identical in our laboratory and in Mazess's and Cameron's laboratory except that the rotation of the ulna during measurement was different, we would expect the W to be smaller, the BMC to be the same, and the BMC/W to be greater in one laboratory. Ulna rotation would not affect measurements in the radius. Such rotation could occur if the arm were raised higher with respect to the body in one laboratory than in the other, or if the arm were further from the trunk during measurement thus causing the upper arm to make a different angle with respect to the trunk in the two laboratories. This may be the explanation.

Our W and BMC values in the distal radius are larger than reported values, although the differences are not significant in some cases. Both W and BMC increase rapidly moving distally on the radius, and the comparison can be explained if our measurement site is more distal than sites used in other laboratories. Since W and BMC both increase distally the BMC/W should be similar in all laboratories. The small differences noted in BMC/W were not significant. Thus a small difference in scan site is a plausible explanation.

The phalanx site differs in our laboratory and in Von Roth's laboratory. Procedural differences cannot be evaluated for the German data, as W and BMC data were not available. The differences observed at sites other than the phalanx could be due to differences in the populations.

We have attempted to explain our comparisons first on the basis of procedure and second on the basis

Table 1.—Intercomparisons among laboratories.

	SEX	SITE	BMC	W	BMC/W
U.S. WHITES	F	Mid Radius*	NS	NS	--
	F	Mid Radius[2]	NS	NS	NS
	M	Mid Radius[2]	NS	NS	NS
	F	Mid Ulna[2]	NS(−)	S(−)	S(+)
	F	Distal Radius[1]	S(+)	NS(+)	NS(−)
	F	Distal Radius*	S(+)	S(+)	--
	F	Distal Radius[2]	NS(+)	S(+)	NS(+)
GERMANY	F	Mid Radius[3]	--	--	S(+)
	M	Mid Radius[3]	--	--	S(+)
	F	Mid Ulna[3]	--	--	S(+)
	F	Phalanx[3]	--	--	NS(+)

*C. C. Johnson, personal communication, 1972.

of population. Until procedural intercomparisons are made and calibrations standardized, each laboratory must collect its own data on normals.

Work performed under the auspices of the U.S. Energy Research and Development Administration.

REFERENCES

1. Goldsmith, N.F., Johnston, J.O., Picetti, G., and Garcia, C. Bone mineral in the radius and vertebral osteoporosis in an insured population. *J. Bone Jt. Surg.*, 1973, 55-A, 1276–1293.
2. Mazess, R.B. and Cameron, J.R. Bone mineral content in normal U.S. whites. In: International Conference on Bone Mineral Measurement (Mazess, R.B., ed.), 228–238. Washington: U.S. Department of Health, Education, and Welfare Publication No. (NIH) 75-683, 1974.
3. V. Roth, A., Ringe, J.D., Kruse, H.P. and Kuhlencordt, F. Bestinmung des Knochenmineral gehalts durch ^{125}I—Photonenabsorptions messung bei Gesunden. *Fortschr. Rontgenstr.* 1974, 121:597–603.

Bone Mineral Content of the Growing Skeleton. T. Klemm, D. H. Banzer, U. Schneider (Universitätskinderklinik and the Klinik fur Radiologie und Nuklearmedizin, Klinikum Steglitz, Freie Universität Berlin, Berlin, West Germany)

Bone mineral content (BMC) in children seems to be of special interest, because growing bone often responds to treatment better than adult bone. Thus, an early diagnosis may determine the prognosis of the child's future life. Standard values of bone mineral content have been reported by Mazess et al[2] and by Schuster et al[4] for radius and ulna. The aim of this work is to get normal values of BMC for the more cancellous os calcis.

The BMC of 66 boys ages 3–16 years and of 71 girls ages 3–20 years was measured. These were children of the hospital staff and others who were examined in the course of a field study on chronic lead incorporation. In none of them were signs of elevated lead concentration found in blood, hair or bone. All were healthy children of normal height and weight. There was no history of diseases which might affect calcium-phosphate metabolism. The investigations were carried out by a method[3] we developed following the principles of photon absorptiometry.[1] The BMC was expressed in g/cm length unit and in g/cm^3 bone volume, indicating the bone density.

In childhood the mineral content of the os calcis increased with age in both sexes. In Table 1 the mean values and standard deviation of BMC are listed; the body height and weight and the width and thickness of the os calcis are specified for each age group. Expressing the BMC and bone density values as a percentage of the normal standard for adults 20–30 years of age makes values for both comparable (Figure 1). While the BMC at the age of 6 years amounts to only 1/3 of that of normal adults, the bone density is 2/3. The bone density curve shows a flatter course in comparison to that representing the BMC. Starting from the same value at 6 years of age, girls at the age of 15 show 90% and boys only 80% of the adult bone density. A comparison of the standard values of the os calcis with those of the radius midshaft reported by Mazess et al[2] indicated a corresponding percentage increase of mineral content in the compact and cancellous portions of the growing skeleton in normal children.

The increase of the bone volume with age has to be considered in children. In order to get comparable values independent of bone diameter at different ages, it is suggested that one determine the bone density (g/cm^3) rather than the bone mineral values per length unit (g/cm). A similar increase of BMC in different parts of the skeleton up to the adult state can be expected in healthy children. On the other hand, generalized disorders of bone metabolism often become manifest first in cancellous portions of the skeleton. Therefore, the os calcis seems to be indicated for measuring pathological demineralization.

REFERENCES

1. Cameron, J.R., and Sorenson, J.A. Measurement of bone mineral in vivo: an improved method. *Science*, 1963, 142:230.
2. Mazess, R.B., and Cameron, J.R. Bone mineral content in normal U.S. whites. Internat. Conf. on Bone Mineral Measurement, Chicago 1973, DHEW Publ. No. (NIH) 75-683, 228–237.
3. Schneider, U., and Banzer, D. A computerized method of determination of bone mineral con-

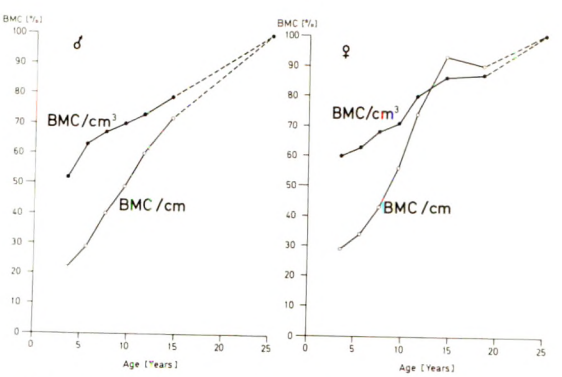


Fig. 1.—Normal values of BMC expressed as percentage of standard for normal adults.

TABLE 1.—Bone mineral content (BMC) of the os calcis in children.

AGE (YEARS) ♂	n	BMC		C–WIDTH	C–THICKNESS	HEIGHT	WEIGHT
		M ± SD (mg/cm³)	M ± SD (g/cm)	M ± SD (mm)	M ± SD (mm)	M ± SD (cm)	M ± SD (kg)
3 – 4	6	145 ± 24	0.82 ± 0.23	32.0 ± 1.8	24.8 ± 1.9	108 ± 4.0	16.8 ± 2.1
5 – 6	10	176 ± 36	1.07 ± 0.21	35.5 ± 1.6	25.6 ± 4.0	117 ± 8.2	21.3 ± 2.5
7 – 8	17	188 ± 20	1.48 ± 0.26	39.3 ± 2.8	29.2 ± 2.5	132 ± 5.9	27.0 ± 4.2
9 – 10	13	195 ± 28	1.83 ± 0.39	43.6 ± 5.3	32.0 ± 3.3	139 ± 9.2	34.4 ± 7.1
11 – 12	8	206 ± 26	2.23 ± 0.38	47.3 ± 4.3	33.9 ± 2.6	152 ± 5.6	42.3 ± 5.9
13 – 16	12	222 ± 31	2.68 ± 0.40	49.8 ± 2.6	36.3 ± 2.7	161 ± 9.6	51.0 ± 9.1

AGE (YEARS) ♀	n	BMC		C–WIDTH	C–THICKNESS	HEIGHT	WEIGHT
		M ± SD (mg/cm³)	M ± SD (g/cm)	M ± SD (mm)	M ± SD (mm)	(cm)	(kg)
3 – 4	6	165 ± 34	0.90 ± 0.18	33.0 ± 4.1	24.0 ± 3.7	108 ± 5.4	17.7 ± 1.0
5 – 6	17	172 ± 37	1.05 ± 0.25	34.3 ± 4.0	26.2 ± 3.3	118 ± 7.0	21.4 ± 3.7
7 – 8	12	186 ± 26	1.33 ± 0.28	37.1 ± 3.6	27.9 ± 2.6	129 ± 6.6	26.9 ± 4.1
9 – 10	11	195 ± 24	1.74 ± 0.32	43.1 ± 3.1	30.8 ± 1.9	142 ± 6.5	32.6 ± 4.1
11 – 12	6	221 ± 36	2.29 ± 0.42	45.7 ± 4.1	33.5 ± 1.8	149 ± 12.5	37.5 ± 6.0
13 – 16	6	236 ± 34	2.88 ± 0.50	49.3 ± 1.2	36.3 ± 2.7	165 ± 8.3	50.3 ± 8.0
17 – 20	13	239 ± 35	2.80 ± 0.38	48.7 ± 3.4	35.7 ± 1.8	165 ± 7.5	53.2 ± 6.7

BMC OF THE OS CALCIS IN CHILDREN – NORMAL VALUES (n = 137)

tent by a transmission-scanner: description of the system. Internat. Conf. on Bone Mineral Measurement, Chicago 1973, DHEW Publ. No. (NIH) 75–683, 142–150.

4. SCHUSTER, W., REISS, K.H., and KRAMER, K. Quantitative mineralsalzbestimmung am kindlichen skelett. *Dtsch. med. Wschr.*, 1969, 94: 1983–1987.

Bone Mineral Content in Full-term Infants Measured by Direct Photon Absorptiometry. J. J. Steichen, B. Kaplan, N. Edwards, R. C. Tsang (Fels Division of Pediatric Research, University of Cincinnati College of Medicine, Cincinnati, Ohio)

The determination of bone mineral content (BMC) in young infants is of clinical importance, particularly for premature infants who often have decreased intake of vitamin D and calcium and occasionally developed nutritional rickets.[4] Photodensiotometric methods are imprecise and expose the infant to excessive radiation. BMC measurement by direct photon absorptiometry[1,2] is a precise and accurate method in adults, but had not been used previously in newborn and premature infants. Thus, normal standard values were not available. We adapted photon absorptiometry for use in young infants and established normal values for BMC in the newborn.

Sixty-two full term (38–42 weeks gestation) infants were studied during the first 3 days of life. Gestational age was calculated from the first day of the last menstrual period according to the history obtained from the mother and was verified by clinical assessment of physical and neuromuscular maturity.[3] Measurements were performed on the left ulna and radius at the 1/3 and 1/10 distal site of both bones (Table 1).

Analysis of variance did not show any significant difference in BMC measured at the different sites. No differences were found in BMC between male or

TABLE 1.—Normal values for BMC in full term newborn infants, appropriate for gestational age (AGA).

					RADIUS				ULNA			
					1/3		1/10		1/3		1/10	
BLACK MALE n=12	WT	LENGTH	H C	MATERN AGE	BMC	BW	BMC	BW	BMC	BW	BMC	BW
$\bar{X}$	3211	49.47	34.1	22.92	.0964	.484	.1144	.720	.0833	.475	.0797	.552
SE	96.43	.515	.375	1.124	.0083	.027	.0114	.065	.0074	.040	.0092	.045
SD	373.46	1.995	1.454	4.051	.0248	.082	.0302	.172	.0210	.114	.0245	.119
WHITE MALE n=18												
$\bar{X}$	3311	50.14	34.17	24.231	.1006	.497	.1178	.707	.0857	.482	.0752	.643
SE	83.84	.387	.256	1.602	.0056	.024	.0071	.038	.0034	.023	.0067	.040
SD	365.44	1.643	1.085	5.776	.0239	.105	.0274	.148	.0137	.093	.0201	.122
BLACK FEMALE n=20												
$\bar{X}$	3067	49.75	33.61	21.08	.1069	.574	.1088	.652	.0804	.443	.0690	.548
SE	60.12	.37	.2	1.059	.0097	.063	.0178	.085	.0045	.023	.0055	.041
SD	275.52	1.737	.938	3.818	.0432	.284	.0617	.296	.0190	.099	.0182	.137
WHITE FEMALE n=12												
$\bar{X}$	3313	51.35	33.95	26.2	.1081	.502	.1230	.815	.0953	.416	.1010	.581
SE	89.12	.236	.311	1.772	.0071	.045	.0151	.118	.0038	.018	.0205	.077
SD	282.1	.747	.985	3.962	.0202	.129	.0369	.291	.0100	.049	.0410	.155

WT = weight in gm; LENGTH in cm; HC = head circumference in cm;

BW = bone width in cm; BMC = bone mineral content in gm/cm

female babies as a group nor between black and white babies. Paired t-test analysis matching black and white babies for birth weight and exact gestation, did not reveal any statistical difference between black and white babies. BMC did not correlate with head circumference or length. However, there was a significant positive correlation ($p<.01$, $r=.484$) between birth weight and BMC.

The average BMC for all term infants was .103 g/cm (SEM $\pm$.007, SD $\pm$.020) for the 1/3 distal radius and .117 g/cm (SEM $\pm$.012, SD $\pm$.039) for the 1/10 distal radius. BMC of the ulna was .085 g/cm (SEM $\pm$.004, SD $\pm$.015) at the 1/3 distal site, and .078 g/cm (SEM $\pm$.009, SD $\pm$.026) at the 1/10 distal site.

The Norland Analyzer has been shown to be linear when BMC is measured in the range of 0.6 to 1.4 g/cm, but the BMC of infants was in the much lower range of 0.03 to .145 g/cm. Correlation between BMC of small phantom standards and the measured BMC was excellent ($r=.96$). The precision was less (7%) in infants than in adults (3%).

As BMC correlated well with birth weight, we propose that dividing BMC by birth weight will allow us to normalize BMC and to compare term and preterm infants. When we divided BMC by birth weight the normal value was 2.75×10^{-8} g/cm/kg body weight ($\pm 2.1\times10^{-9}$) for 1/3 radius. Preliminary data in preterm infants also showed a significant correlation between birth weight and BMC ($r=.739$).[5]

Supported in part by the Fels Research Institute and a grant by Ross Laboratories.

REFERENCES

1. CAMERON, J.R. and SORENSON, J.A. Measurement of bone mineral in vivo. An improved method. *Science, 1963*, 142:230.
2. CAMERON, J.R., MAZESS, R.B. and SORENSON, J.A. Precision and accuracy of bone mineral determination by direct photon absorptiometry. *Invest. Radiol.* 1968, 3:141–150.
3. DUBOWITZ, L. DUBOWITZ, V., and GOLDBERG, C. Clinical assessment of gestational age in the newborn infant. *J. Pediatr. 1970*, 77:1–10.
4. LEWIN, P.K., REID, M., REILLY, B.J., SWYER, P.R., and FRASER, D. Iatrogenic rickets in low-birth-weight infants. *J. Pediatr. 1971*, 78:207–210.
5. STEICHEN, J.J., MINTON, S.D., CHEN, I-W., DISNEY, T. and TSANG, R.C. Bone Mineral Content (BMC) and 25 hydroxy D in preterm (AGA) and small for gestational age (SGA) infants. *Pediatr. Res.* (in press).

Validity of the Absorptiometric Measurement of Bone Mineral Content of the Radius. S. H. Cohn, K. J. Ellis, N. F. Goldsmith (Medical Department, Brookhaven National Laboratory, Upton, New York 11973)

Photon absorptiometry usually measures bone mineral content (BMC) in the appendicular skeleton, but is often interpreted with the implicit assumptions that (1) BMC is directly proportional to total body Ca and (2) the total skeleton reacts similarly to influences such as diet, drugs, and disease. Serial BMC measurements on a single patient are useful in reflecting changes, but when intercomparisons among individuals are required, there is a problem of normalization for the influences of age, sex, and body habitus. The common method of normalization has been to take the ratio of the BMC to the bone width (W)[9,10]. We investigated the underlying assumptions above and normalization.

The total body calcium (TBCa), as measured by neutron activation,[2] and BMC correlate well. The predicted value of BMC (BMC_p), can be obtained by a modification of the algorithm for prediction of total-body calcium.[3] The BMC_p provides a normalization based on parameters which influence TBCa.[5] Body habitus is reflected by measurement of height (H) and lean body mass (inferred from measurement of ^{40}K).

Females:

$BMC = 0.00112 TBCa - 0.0664$

$TBCa = \alpha HK^{1/2}$

$BMC_p = 0.0635 HK^{1/2} - 0.0664$, for age < 55 years

$BMC_p = 0.0635 - 0.00043$ (age $- 55$ $HK^{1/2} - 0.0664$, for age > 55 years)

Males:

$BMC = 0.00091$ TBCa $+ 0.233$ where:

BMC, BMC_p = g/cm

$BMC_p = 0.0496\ HK^{1/2} + 0.233$ TBCa = g

K = g

H = m

BMC varied widely in a population measured at Brookhaven National Laboratory (BNL); the mean values were markedly below U.S. white standards (Table 1). The BMC/W tends to decrease the variability, but may not provide satisfactory normalization since radius width is poorly correlated ($r = 0.383$) with skeletal size (height). In this population BMC/BMC_p was close to 1.00, except for the two oldest groups of men. The correlation coefficient between individual BMC and BMC_p was 0.75, $p < .001$ for males, and 0.71, $p < .001$ for females. This method of normalization was also tested on BMC data (732 men and 826 women) for the distal radius.[8] Since TBK (total body potassium) data were not available, the BMC_p was calculated on the basis of weight, height, and sex, using a previously derived relationship.[7] A constant was used to transform the distal radius data into equivalent values for the 8 cm radius site (see Table 2). The BMC and BMC_p values were highly correlated ($r = 0.82$). The SD for the distal radius BMC_p was considerably larger in each age group than for the radial shaft BMC in the BNL normals. This larger variation in distal radius BMC_p was most likely the result of using body weight rather than lean body weight for obtaining the BMC_p.

One common assumption is that different portions of the skeletal system are well correlated and have the same rate of change. For normal adults, the assumption holds up fairly well. BMC measurements were compared with TBCa and the correlation coefficients were 0.78 and 0.74 for women and men, respectively ($p < .001$). However, studies in patients with metabolic disorders of the bone, particularly those that involve a differential rate of remodelling in compact and trabecular bone, indicated that caution must be used in extrapolating from BMC.[4,6]

We thank Don Feeney for his computational assistance.

REFERENCES

1. Cameron, J.R., Mazess, R.B., Sorenson, J.A. Precision and accuracy of bone mineral deter-

Table 1.—BMC in the radius shaft in the BNL population (±coeff. variation).

Age	No.	BMC	W	BMC/BMC_p	TBCa
FEMALES					
30-39	6	0.819 ±7.2	1.102 ±6.4	1.023 ±4.9	785. ±4.5
40-49	18	0.891 ±10.2	1.197 ±8.6	0.995 ±10.8	880. ±10.5
50-59	39	0.873 ±10.4	1.249 ±9.5	1.011 ±8.2	822. ±11.1
60-69	5	0.766 ±10.1	1.184 ±6.9	1.046 ±7.5	716. ±11.6
70-79	4	0.605 ±11.6	1.104 ±5.1	0.940 ±8.7	637. ±16.2
	72			1.003 ±8.6	
MALES					
30-39	13	1.229 ±15.1	1.495 ±10.5	0.983 ±8.4	1150. ±12.4
40-49	12	1.166 ±10.6	1.543 ±9.7	0.939 ±9.4	1078. ±14.8
50-59	8	1.199 ±11.4	1.494 ±3.8	1.007 ±7.4	988. ±15.6
60-69	7	1.189 ±11.1	1.508 ±8.2	0.981 ±11.4	1047. ±10.8
70-79	6	1.189 ±10.2	1.492 ±8.3	1.092 ±10.4	1075. ±10.8
80-89	8	1.103 ±16.0	1.593 ±6.8	1.109 ±14.9	1005. ±20.7
	54			1.019 ±10.0	

TABLE 2.—BMC in the distal radius of Goldsmith's population.[8]

	Age	No.	W (kg')	Ht (cm)	BMC (g)	BMC_p (g)	$\frac{BMC}{BMC_p}$
Male	30-39	207	81.2	176.5	1.317 ±16.6	1.351	0.975 ±17.9
	40-49	199	80.6	175.3	1.301 ±17.8	1.325	0.982 ±17.7
	50-59	199	81.4	173.7	1.285 ±17.4	1.292	0.995 ±17.0
	60-69	95	78.7	171.9	1.233 ±20.1	1.257	0.981 ±19.6
	70-79	32	73.2	168.7	1.154 ±21.3	1.195	0.966 ±19.4
		732					0.980 ±17.9
Female	30-39	198	63.1	163.6	0.936 ±18.8	0.945	0.991 ±14.8
	40-49	249	65.2	162.0	0.949 ±17.7	0.919	1.033 ±16.7
	50-59	220	64.3	160.0	0.883 ±22.3	0.874	1.010 ±20.1
	60-69	117	64.0	157.7	0.767 ±24.3	0.793	0.967 ±25.5
	70-79	42	61.7	157.5	0.710 ±24.4	0.720	0.986 ±21.3
		826					0.997 ±18.6

mination by direct photon absorptiometry. *Invest. Radiol.* 1968, 3:141–150.

2. COHN, S.H., SHUKLA, K.K., FAIRCHILD, R.G.: Design and calibration of a "broad-beam" ^{238}Pu, Be source for total-body neutron activation analysis. *J. Nucl. Med.* 1972, 13:487–492.
3. COHN, S.H., SHUKLA, K.K., ELLIS, K.J. A multivariate predictor for total body calcium in man based on activation analysis. *Int. J. Nucl. Med. Biol.* 1974, 1:131–134.
4. COHN, S.H., ELLIS, K.J., WALLACH, S., ZANZI, I., ATKINS, H.L., and ALOIA, J.F., Absolute and relative deficit in total-body skeletal calcium and radial bone mineral in osteoporosis. *J. Nucl. Med.* 1974, 15:428–435.
5. COHN, S.H., and ELLIS, K.J. Predicting radial bone mineral content in normal subjects. *Int. J. Nucl. Med. & Biol.* 1975, 2:53–57.
6. COHN, S.H., ELLIS, K.J., CASELNOVA, A.C., ASAD, S.N. and LETTERI, J.M. Correlation of radial mineral content with total body calcium in chronic renal failure. *J. Lab. Clin. Med.* 1975, 86:910–919.
7. ELLIS, K.J., SHUKLA, K.K. and COHN, S.H. A predictor for total-body potassium in man based on height, weight, sex and age: Application in metabolic disorders. *J. Lab. Clin. Med.* 1974, 83:716–727.
8. GOLDSMITH, N.F. Normative data from the osteoporosis prevalence survey, Oakland, California, 1969–70. Bone mineral at the distal radius: variation with age, sex, skin color, and exposure to oral contraceptive and exogenous hormones. In Int. Conf. on Bone Mineral Measurement, pp. 239–266, Ed. R. B. Mazess, HEW. Publication No. NIH 75–683, 1974.
9. JOHNSTON, C.C., SMITH, D.M., YU, P.L., et al: In vivo measurement of bone mass in the radius. *Metabolism*, 1968, 17:1140–1153.
10. SMITH, D.M., JOHNSTON, C.C., YU, P.L. In vivo measurement of bone mass. *J. Amer. Med. Assoc.* 1972, 219:325–336.

Influence of Skeletal Size on Bone Mineral Content: Skeletal Size–Adjusted National and International Normative Trend Lines. J. Dequeker, Fr. Gielen (Rheumatology Unit, Academic Hospitals Leuven and Pellenberg, Belgium)

This study is based on photon absorption data of 248 subjects from Belgium[1] and on data from four additional populations: U.S.A. white and black from California,[2] U.S.A. white from Wisconsin,[3] and North Alaskan Eskimos.[4] In the Belgian population over 40 years old, bone width of the radius 8 cm from distal end was significantly correlated with BMC/W in women and with BMC in men. These indices were expressed in relation to bone size using linear regression analysis for each age-sex group sepa-

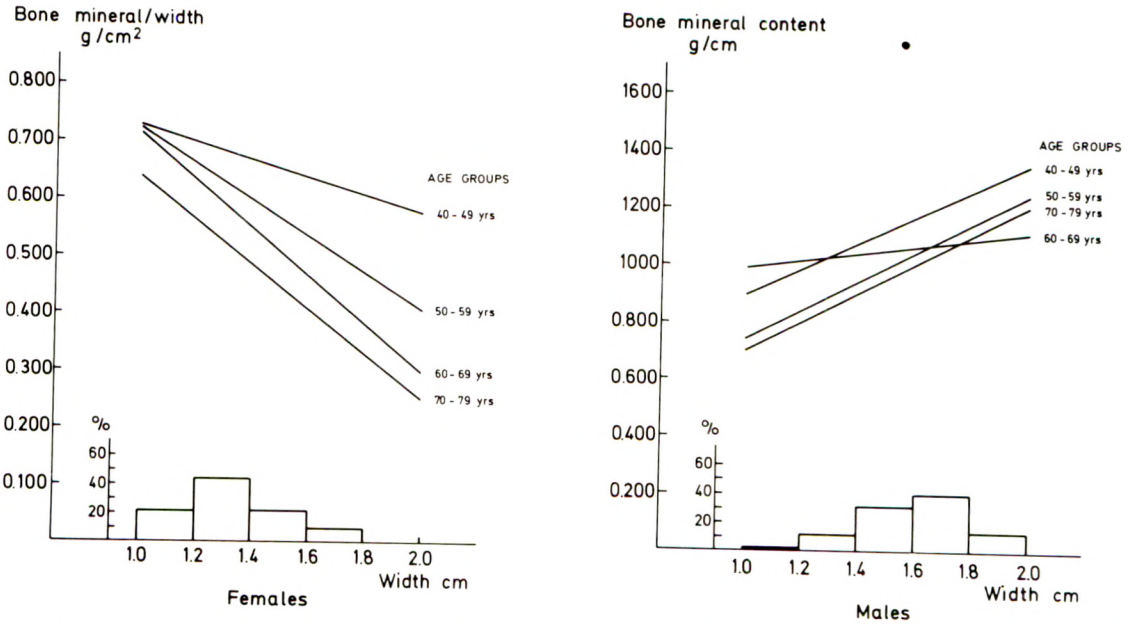


FIG. 1.—Skeletal size adjusted normative trend lines for bone mineral concentration (females), bone mineral content (males), and percentage distribution of bone width of the radius 8 cm distal end (248 Belgian subjects).

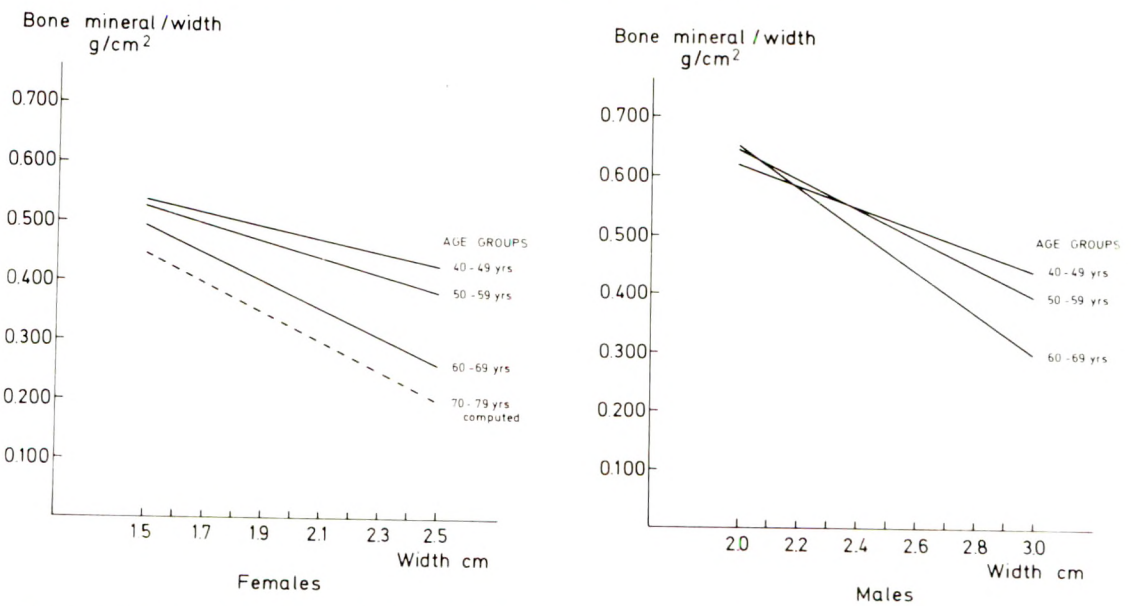


FIG. 2.—Skeletal size adjusted international normative trend lines for bone mineral concentration of the radius 3 cm from distal end (five populations).

TABLE 1.—Percentage difference BMC (g/cm²) radius distal end from international trend line skeletal size adjusted at age 40 and at age 60.

	FEMALES		MALES	
	Age 40	Age 60	Age 40	Age 60
USA Black Calif.	+ 5.58	+ 3.96	+ 3.60	+ 11.22
USA White Wisconsin	+ 1.64	+ 0.24	+ 2.42	- 1.18
North Alaskan Eskimo	0.00	- 1.25	+ 0.27	- 1.12
USA White Calif.	- 1.39	+ 4.12	- 0.16	+ 2.62
Belgium	- 5.06	- 6.41	- 6.06	- 11.53

rately. Important differences in bone mineral index per bone size were noted (Fig. 1).

Using the same procedure normative trend lines were obtained from the mean values of W and BMC 3 cm from the distal end of the radius of the five populations. Between bone width and BMC/W a negative slope was found in all age-sex subgroups (Fig. 2). With these normative trend lines we compared BMC/W values of the populations adjusted for skeletal size (Table 1). The U.S. whites and blacks have a larger BMC/W for a given skeletal size than the Belgian and the North Alaskan Eskimo population. The U.S.A. blacks compared to U.S.A. whites also have a larger BMC/W.

REFERENCES

1. DEQUEKER, J., ROH, Y.S., VAN DESSEL, D., GAUTAMA, K., and BURSSENS, A. Bone mineral estimation in vivo by photon absorptiometry. *J. Belge Rhum. Med. Phys.*, 1973, 28:293–301.
2. GOLDSMITH, N.F., JOHNSTON, J.O., PICETTI, G., and GARCIA, C. Bone mineral in the radius and vertebral osteoporosis in an insured population. *J. Bone Jt. Surg.*, 1973, 55 A, 1276–1293.
3. MAZESS, R.B., and CAMERON, J.R. Bone mineral content in normal U.S. whites. In International Conference on bone mineral measurement, 1974, DHEW Publication No. (NIH) 75–683, 228–238.
4. MAZESS, R.B., and MATHER, W. Bone mineral content of North Alaskan Eskimos. *Amer. J. Clin. Nutr.*, 1974, 27:916–926.

Renal Disease

Bone Demineralization in Renal Failure: A Longitudinal Study of the Distal Femur Using Photon Absorptiometry.

T. R. Overton, D. S. Silverberg (Division of Biomedical Engineering and Department of Medicine, University of Alberta, Edmonton, Alberta T6G, 2G3, Canada)

Variable results have been obtained in renal patients using photon absorptiometry measurement of the bone mineral content (BMC) of the lower radius and ulna,[6,8,11,13,14] os calcis,[3,4] and lower end of the femur.[1,2]

Using a measurement apparatus constructed in this laboratory,[12] with ^{241}Am as the photon source, we studied BMC in the distal femur of 87 chronic renal failure patients: 21 pre-dialysis patients (CRF), 45 chronic hemodialysis patients (CHD), and 21 renal transplant patients (RT).

The CRF patients had serum creatinine concentrations of 3 to 14 mg/100 ml. The CHD patients received dialysis for 3 to 8 hours, 2 to 3 times weekly. The dialysis fluid was deionized; Ca was 6.5 mg/100 ml and Mg was 1.5 mg/100 ml.

Both the CRF and CHD patients received 0.125 mg dihydrotachysterol (Hytakerol^{R}) twice daily and sufficient aluminum hydroxide to maintain a normal serum phosphorus concentration. Two CHD patients received 0.5 to 2 μg. of 1,25 dihydroxycholecalciferol (1,25 DHCC) parenterally 3 times weekly while on dialysis, and two received 0.5 to 2 μg. daily of oral 1∝ hydroxycholecalciferol (1∝ HCC).

BMC was measured in the distal femur at a site approximately ⅕ of the shaft length from the lateral tubercle. Measurements were made at about 2 month intervals over an average period of 12 months (range 8–24 months).

Group comparisons of mean BMC using a two-tailed "t" test were made after determining that no significant differences existed in age, height or weight between groups. For the longitudinal study a weighted linear regression[16] (BMC vs time in months) was made for eight normals (five males, three females, each with a minimum of five measurements in the study period), and for each individual patient. In all cases the slope of the regression line was tested for a difference from zero slope. In the reported cases where patients changed groups or type of treatment, a comparison was also made between the regression slopes before and after the change.

We used data obtained in long-term studies of BMC measurement precision to define a BMC "trend" threshold in terms of the slope of the regression line (BMC vs time) for normal subjects. This threshold value was 0.0005 g/cm/day which corresponds to a rate of change in BMC between 1 and 2 percent per year depending upon the particular group (normal or patient) considered.

The three patient groups (CRF, CHD and RT) had significantly lower BMC than the normal group with the exception of the male CRF group.

TABLE 1.—Numbers of subjects with change in BMC for normal and renal disease groups.

		NORMAL	CRF	CHD	RT
Total Number in Group*		8	26	42	21
BMC Increase		0	3 (1 child)	2 (children)	0
BMC Decrease		0	0	2 (1 child)	0
TREND	Positive	0	5	9	6
	Zero	8	13	18	7
	Negative	0	5	11	8

* Includes 9 children and six patients with therapy change (5 CRF → 4 CHD + 1 RT; 1 CHD → 1 RT)
Excludes 4 CHD patients with special therapy (two receiving 1,25 DHCC and 2 receiving 1-HCC)

BMC comparisons between the three patient groups showed no significant differences.

In the longitudinal study, significant BMC increases ($p<0.05$) were found in five patients (Table 1). Three were children aged 11 to 14 years. The increase in BMC was attributed to normal growth during the study period. Two CHD patients (one adult and one child) showed significant loss of BMC during this study ($p<0.05$). A test of proportions (Table 1) comparing each group for positive vs zero and negative trends showed that the patient groups were significantly different from normal ($P<0.05$) but not from each other.

Six patients (included in Table 1) underwent a therapy change during the period of this study (4 CRF→CHD, 1 CHD and 1 CRF→RT). No change in BMC was observed following this therapy change.

Four additional patients, not included in Table 1, were initially on Hytakerol but this agent was replaced by 1,25 DHCC (in two cases) and 1∝HCC (in two cases). One patient who received 1,25 DHCC showed a negative trend in BMC before receiving the drug and a significant increase in BMC during treatment;[15] the other showed a zero trend before and during treatment with this agent. One of the two who received 1∝HCC showed a significant loss of BMC before receiving the drug and a zero trend during treatment; the other showed a zero trend before and during treatment.

In the CHD patients on Hytakerol the mean values for serum Ca were 9.6 ± 0.15 mg/100 ml (normal 8.5–10.5), and serum phosphorus 6.0 ± 0.29 mg/100 ml (normal 2.5–4.5), and serum alkaline phosphatase 137 ± 35 I.U. (normal 20–90). No significant changes in these values occurred during the study period.

Radiological skeletal surveys were performed before and after this study. No evidence of change in bone demineralization was observed for any patient included in the CRF, CHD or RT groups (Table 1). Of the two patients who received 1,25 DHCC, the one who showed improvement in BMC also showed radiological improvement in osteitis fibrosa and osteomalacia during treatment. Of the two who received 1∝HCC, the one who showed improvement in BMC also showed radiological evidence of healing of fractures of two metatarsal bones during treatment. In both patients the serum alkaline phosphatase fell significantly during the treatment with these two Vitamin D analogs. All four patients receiving these analogs showed symptomatic improvement.

The lack of change in BMC in the majority of the patients may have been related to use of Hytakerol,[10] fluoride-free dialysate,[8] a dialysate calcium concentration sufficient to create a positive calcium balance[17] and to control of hyperphosphatemia.[14]

The improvement in BMC that occurred in one of the two patients receiving 1∝HCC is consistent with the findings of others.[5,17]

This BMC measurement technique, with a long term precision of better than 2% permits early detection of bone mineral loss and is, we believe, a valuable method in following renal osteodystrophy.

REFERENCES

1. ATKINSON, P.J., HANCOCK, D.A., ACHARYA, V.N., PARSONS, F.M., PROCTOR, E.A., REED, G.W. Changes in skeletal mineral in patients on prolonged maintenance dialysis. *Brit. Med. J.*, 1973, 4:519–522.
2. ATKINSON, P.J., WEST, R.R., PARSONS, F.M., REED, G.W. Loss of skeletal calcium by patients on maintenance dialysis. *Brit. Med. J.*, 1970, 3:490–492.
3. BANZER, D., SCHNEIDER, U. A computerized method of determination of bone mineral content by a transmission scanner. *In Proceedings of International Conference on Bone Mineral Measurement, DHEW Publ., 1974, (NIH) 75–683*, 206–213.
4. BANZER, D., SCHNEIDER, U., KRAFT, D. Special application of a transmission scanner for bone mineral determination in normal and osteoporotic rats. *In Proceedings of Symposium of Bone Mineral Determinations, Aktiebolaget Atomergi, 1974, 489*:75–87.
5. BRICKMAN, A.S., SHERRARD, D.J., JOWSEY, J. 1,25 dihydroxycholecalciferol. *Arch. Int. Med.*, 1974, 134:883–888.
6. CATTO, G.R.D., MCINTOSH, J.A.R., MACDONALD, A.F., MACDONALD, M. Hemodialysis therapy and changes in skeletal calcium. *Lancet*, 1973, 1:1150–1153.
7. CHALMERS, T.M., HUNTER, J.O., DAVIE, M.W., SZAZ, K.F., PELC, B., KODICEK, E. 1-alpha-hydroxycholecalciferol as a substitute for 1,25 dihydroxycholecalciferol in chronic renal failure. *Lancet*, 1973, 3:696–699.

8. David, D.S. Calcium metabolism in renal failure. *Amer. J. Med.*, 1975, 58:48–56.
9. Griffiths, H. J., Zimmerman, R.E., Bailey, G., Snyder, R. The use of photon absorptiometry in the diagnosis of renal osteodystrophy. *Radiology*, 1973, 109:277–281.
10. Kaye, M., Chatterjee, G., Cohen, G.F., Sagar, S. Arrest of hyperparathyroid bone disease with dihydrotachysterol in patients undergoing chronic hemodialysis. *Ann. Int. Med.*, 1970, 73:225–233.
11. Meema, H.E., Rabinovich, D., Orepoulos, D.G., Lloyd, G.J., Meema, S. Changes in bone mineral content of radius in chronic renal disease. *In Proceedings of Bone Measurement Conference, U.S. Atomic Energy Commission Conference*, 1970, 700515, 383–396.
12. Overton, T. R., Silverberg, D.S., Rigal, W.M., Friedenberg, L.W. University of Alberta bone mineral analysis system—performance and clinical applications. *In Proceedings of International Conference on Bone Mineral Measurements. DHEW Publ.*, 1974, (NIH) 75–683, 11–29.
13. Schuster, W. Follow-up examination of the mineral salt content in the skeleton with various Vitamin D resistant forms of rickets of renal origin. *Proceedings of International Conference on Bone Mineral Measurement*, 1974, (NIH) 75–683, 317–324.
14. Ringe, J.D., Kruse, H.P., Kuhlencordt, F. Repeated bone mineral measurements in patients with primary and secondary hyperparathyroidism by photon absorptiometry. *Aktiebolaget Atomergi*, 1974, 489:102–111.
15. Silverberg, D.S., Bettcher, K.B., Dossetor, J.B., Overton, T.R., Holick, M.F., DeLuca H.F. Effect of 1,25 dihydroxycholecalciferol in renal osteodystrophy. *Can. Med. Assoc. J.*, 1975, 112:190–195.
16. Snedecor, G.W., Cochran, W.G. Statistical methods. *Iowa State University Press*, 1967, 6th Edition.
17. Wing, A.J. Optimum calcium concentration of dialysis fluid for maintenance hemodialysis. *Brit. Med. J.*, 1968, 4:145–149.

Bone Mineral Analysis in Renal Osteodystrophy. L. H. Diamond, R. Smith, L. Pierce (Division of Nephrology, Department of Medicine and Department of Radiology, Georgetown School of Medicine, Washington, D.C.)

Renal patients (n=161) have been studied with the Norland Bone Mineral Analyzer, 53 on two or more occasions. All patients were hemodialyzed for 6 hours, three times a week with a dialysate calcium of 6.5 mg%. No calcium supplements were administered. Amphojel, for hyperphosphatemia, was used at a variable and individualized dosage so as to maintain the pre-dialysis serum phosphorous below 6.5 mEq/L. The group comprised 24 females and 29 males (16 Caucasians and 37 Negroes) with a mean age of 53 years. (Range 28–77 years.) The followup period ranged from 3 to 14 months ($\bar{x}$=7.9 months). The bone mineral content (BMC) of the majority of the 161 patients fell below the reported mean for age and sex matched controls.[1]

In a smaller group of patients, no correlation between BMC and serum Ca, PO_4, Ca×PO_4 product nor alkaline phosphatase was found.

Fifteen patients had radiological osteopenia; 23 had radiological changes compatible with osteitis fibrosa cystica, and 16 had normal radiological evaluations.

The range of BMC change for the entire group was −7.0%–+11.3%/month ($\bar{x}$=−0.23%/month). If two patients, who demonstrated a 6.5% gain and 7% loss followed by an 11% gain, respectively, are excluded, the range for the entire group was −4.2%–+4.3%/month. Of patients studied sequentially a BMC change of less than 1.0%/month occurred in 53%; of 1%–2%/month in 19%, of 2%–3%/month in 16.5%; of 3%–4%/month in 1.5% and >4%/month in 10%, respectively. Thus 72% of patients demonstrated a change of BMC of under 2%/month and 88% of patients a change of less than 3%/month.

Of the 53 patients analyzed sequentially, 22 (41.5%) demonstrated persistent loss of BMC (−1.6%/month; SD 1.3%/month), while 22 (41.5%) gained BMC (+1.5%/month; SD 1.9%/month); the difference between these groups was highly significant ($P<0.0001$). Three (5.7%) patients demonstrated no change, while 6 (11.3%) demonstrated fluctuations in BMC.

Of the 22 patients with BMC loss, six (27%) had a normal radiological evaluation, eight (36%) had osteopenia and eight (36%) demonstrated osteitis fibrosa cystica; of the 22 patients who gained BMC, six (27%), five (22%) and 11 (50%) had normal, osteopenia or fibrosa cystica, respectively, diagnosed by radiologic evaluations.

The rate of BMC change in males ranged from −2.8%–+4.3%/month ($\bar{x}$=−0.53%/month) and for females from −4.2%–+2.9%/month ($\bar{x}$=−0.14%/month); the difference was not statistically significant. ($P>0.3$).

In Caucasians, the rate of change ranged from −2.6%–+1.8%/month ($\bar{x}$=+0.11%/month), whereas for Negroes, the range was −4.2%–+4.3%/month ($\bar{x}$=−0.56%/month); the difference between the groups was not statistically significant. ($P>0.3$).

The rate of change of BMC, measured in the forearm with vascular access, when compared to the forearm without vascular access, was found not to be significantly different ($P>0.2$) when compared to the rate of change in the opposite forearm.

The BMC measurement is helpful in the manage-

ment of renal osteodystrophy, especially in the identification of a group of patients in whom further evaluation is both justified and mandatory.

Supported in part with a Grant from the Public Health Service (PR-5360). We acknowledge technical assistance from Nancy Wilson, Mike Smith and administrative assistance from Laundretta Grant, Dorothy Powell and Carol Singleton.

REFERENCE

1. MAZESS, R.B. AND CAMERON, J.R. Bone mineral content in normal U.S. whites. Int. Conf. on Bone Mineral Measurement. Ed. Mazess, Chicago. U.S. Depart. of HEW 1974, 228–237.

The Effect of Chronic Renal Failure and Maintenance Hemodialysis on Bone Mineral Content of the Radius. A. M. Parfitt, I. Oliver, N. Walczak, N. Levin, G. Santiago, C. Cruz (Mineral Metabolism Research Laboratory and Department of Nephrology, Henry Ford Hospital, Detroit, Michigan 48202)

Loss of cortical bone occurs both in primary and in uremic secondary hyperparathyroidism.[4,5] Studies by radiographic morphometry suggest that metacarpal cortical thickness declines in early chronic renal failure (CRF), remains stable in late CRF, and declines further with poorly controlled maintenance hemodialysis (MHD). In this study, photon absorptiometry was carried out by using the Norland Analyzer on 132 patients with CRF. Quadruplicate scans of the radius were made at one-third of the distance from the ulnar styloid to the olecranon process, and the results expressed as bone mineral over bone width (BM/BW) in g/cm.[2] Scans at this site reflect predominantly cortical bone, although a low value may be due to increased intracortical porosity, osteomalacia, osteitis fibrosa or accumulation of incompletely mineralized bone as well as to reduced cortical thickness.[6,7] For white patients, age and sex specific normal values were obtained from published values.[3] For black patients, provisional normal values were obtained by multiplying white male values by 1.06 and white female values by 1.10 (factors based on the data of Johnston et al[2]). Both absolute differences between actual and expected values for BM/BW and z scores were computed. (z = absolute difference/SD). Fine detail x-rays of the scanned forearm and of both hands on industrial film were obtained immediately after scanning. The films were examined under eight fold magnification[1,7] after completion of the study without knowledge of the scan results.

In 102 patients (group A) the first scan was performed less than 6 months (mean 1.1 months) after the start of MHD (Table 1). A highly significant reduction in BM/BW was found in the group as a whole (9.6%) and when subdivided on the basis of sex and race. Subperiosteal erosion in the phalanges due to osteitis fibrosa was detected in 47 patients (46%), and arterial calcification in the hands or forearm in 27 (26%).

The remaining 30 patients (group B) had received MHD and/or renal transplantation for 6 months or more (mean 2 years) prior to commencement of the study. Their management had been defective in several respects by current standards with too low a dialysate calcium level and inadequate control of hyperphosphatemia. The mean deficit in BM/BW was 16.6%. Subperiosteal erosion was detected in 16 (53%) but was more often severe than in group A. In group B, but not in group A, the BM/BW deficit was significantly greater in those with moderate to severe subperiosteal erosion than in those with slight or none. In each grade of subperiosteal erosion the deficit in BM/BW was more severe in group B than in group A. Arterial calcification was detected in seven of these patients (23%).

TABLE 1.—Bone mineral measurements in patients scanned less than six months after (group A) or more than six months after (group B) the start of maintenance hemodialysis.

		BM/BW (g/cm^2)					
Group A	n	Expected	Actual	Δ (Abs)	Δ %	z	p
All Subjects	102	0.833	0.753	−0.080	− 9.6	−1.20	< 0.001
Black Male	33	0.914	0.834	−0.080	− 8.7	−1.11	< 0.001
White Male	32	0.860	0.779	−0.081	− 9.4	−1.16	< 0.001
Black Female	20	0.772	0.697	−0.075	− 9.7	−1.116	< 0.001
White Female	17	0.699	0.611	−0.088	−12.6	−1.47	< 0.001
Group B							
All Subjects	30	0.859	0.716	−0.143	−16.6	−2.18	< 0.001
Black Male	12	0.918	0.777	−0.145	−15.8	−1.90	< 0.001
White Male	9	0.862	0.702	−0.160	−18.6	−2.30	< 0.005
Black Female	3	0.841	0.725	−0.116	−13.8	−2.12	< 0.05
White Female	6	0.742	0.611	−0.131	−17.7	−2.62	< 0.025

In 85 patients serial measurements were obtained during MHD (Table 2). The dialysate Ca level was 7.0 mg% and predialysis plasma Ca and phosphate levels were maintained as close to normal as possible by Ca supplementation and phosphate restriction. Only three patients received DHT and none received vitamin D or its metabolites. No significant change in mean BM/BW occurred either in the group as a whole or when subdivided on the basis of sex, race, age, initial BM/BW or duration of MHD. However, an apparent loss of greater than 10% occurred in three patients and an apparent gain of greater than 10% occurred in four patients, one of whom developed extensive radial artery calcification between the two scans. The significance of these changes was uncertain since too few serial measurements were obtained to compute individual regression lines. Because of uremic twitching and signifi-

TABLE 2.—Changes in bone mineral measurement during maintenance hemodialysis (MHD).

	n	BM/BW (g/cm²) Initial	Final	Δ	Duration (months)	p
All subjects	85	0.739	0.737	-0.002	11.6	> 0.9
Black Male	28	0.839	0.837	-0.002	11.2	> 0.6
White Male	25	0.756	0.750	-0.006	10.0	> 0.2
Black Female	16	0.692	0.697	+0.005	16.0	> 0.6
White Female	16	0.583	0.580	-0.003	10.3	> 0.6
Age ≤ 45 (F) ≤ 55 (M)	37	0.795	0.789	-0.006	11.7	> 0.2
Age > 45 (F) >55 (M)	48	0.695	0.696	+0.001	11.5	> 0.8
Initial z > -1.5	46	0.798	0.796	-0.002	12.3	> 0.6
Initial z ≤ -1.5	39	0.669	0.668	-0.001	11.0	> 0.6
Months of MHD, 1–6	20	0.749	0.747	-0.002	4.1	> 0.7
Months of MHD, 7–12	37	0.736	0.736	0	9.7	> 0.9
Months of MHD, 13–18	15	0.717	0.707	-0.010	15.7	> 0.1
Months of MHD, 19+	13	0.754	0.754	0	23.2	> 0.9

cant patient discomfort for a variety of reasons, the repositioning error was considerably greater in these patients than in normal subjects. The overall severity of subperiosteal erosion did not change, but significant improvement occurred in four patients and significant worsening in five.

Bone biopsies were performed in 10 of 27 patients whose initial z score was less than −2.0. Significant abnormalities in classic histological appearances, static morphometric measurements and dynamic tetracycline labelling indices were found in each case.

A substantial loss of radial mineral occurs in CRF before the initiation of MHD, the magnitude of which does not vary significantly with sex or race. The therapeutic regimen prior to initiation of this study probably caused further loss of radial mineral. The present therapeutic regimen seemingly prevented further loss in most patients for up to 2 years. Bone mineral loss in the radius and severity of osteitis fibrosa in the hands can vary independently.

Bone mineral measurement appeared of value in indicating the efficacy of treatment regimen and for selecting patients for more detailed study (such as bone biopsy) but its value in following the course of individual patients with renal failures was uncertain.

REFERENCES

1. GENANT, H.K., HECK, L.L., LANZL, L.H., ROSSMAN, K., VANDERHOST, J., PALOYAN, E. Primary hyperparathyroidism. *Radiology*, 109:513–524, 1973.
2. JOHNSTON, C.C., SMITH, D.M., YU, P.L., DEISS, W.P. In vivo measurement of bone mass in the radius. *Metabolism*, 17:1140–1154, 1968.
3. MAZESS, R.B., CAMERON, J.R. Bone mineral content in normal U.S. whites. In: *International Conference on Bone Mineral Measurement*, ed. R.B. Mazess, U.S. Dept. HEW Publ. No. (NIH) 75—683, 1974.
4. PARFITT, A.M. The actions of parathyroid hormone on bone. Relation to bone remodelling and turnover, calcium homeostasis and metabolic bone disease. III. PTH and osteoblasts, the relationship between bone turnover and bone loss, and the state of the bones in the primary hyperparathyroidism. *Metabolism* (In Press).
5. PARFITT, A.M. The actions of parathyroid hormone on bone. Relation to bone remodelling and turnover, calcium homeostatsis and metabolic bone disease. IV. The state of the bones in uremic hyperparathyroidism. The mechanisms of skeletal resistance to PTH in renal failure and pseudohypoparathyroidism and the role of PTH in osteoporosis, osteopetrosis and osteofluorosis. *Metabolism* (In Press).
6. PARFITT, A.M., DUNCAN, H. Metabolic bone disease affecting the spine. In: The Spine, ed. Rothman, R., Simeone, F., 1975, 599–720.
7. PARFITT, A.M., The clinical and radiographic manifestations of renal osteodystrophy. *Perspectives in Hypertension and Nephrology* (In Press).

The Need for Differential Bone Mineral Standards for Blacks. G. H. Mayor, S. M. Garn, T. V. Sanchez, H. A. Shaw (Departments of Internal Medicine and Surgery, Michigan State University, East Lansing, Michigan and the Center for Human Growth and Development, University of Michigan, Ann Arbor, Michigan)

There is considerable evidence that American blacks have a larger skeletal mass than whites of comparable age and sex. This has been demonstrated over the entire life span by Trotter et al[3,4] using gravimetric techniques on skeletons, and by Garn et al[1] using radiogrammetric techniques on more than 25,000 subjects. Comparable black-white differerences would be expected in both normal individuals and in osteodystrophies using direct photon absorptiometry.

Bone mineral content, BMC (g/cm), bone width, BW (cm), and bone density, BMC/BW (g/cm²), were measured in vivo by direct photon absorptiometry using the Norland Bone Mineral Analyzer. The radius of all subjects was scanned four times at a site 1/3 the distance from the ulnar styloid to the olecrenon where the bone is predominately compact.

We studied 150 white and 30 black chronic renal failure, transplant, or hemodialysis patients as well as 153 black and 62 white normal controls. In 150

white patients with renal disease, the BMC generally fell well below the white standards for the left radius compiled by Mazess and Cameron.[2] Of the 82 white male patients studied, 12 fell above the white standard, while 70 were below ($p<.01$). Similar findings were noted for the white female patients studied with 17 falling above the white standards and 51 falling below ($p<.01$). Many of the white patients exhibited less than 75% of their expected BMC and some had values as low as 30%. These observations indicated osteopenia associated with end-stage renal disease. Virtually identical findings were noted for BMC/BW.

Unlike whites, black renal patients of both sexes do not generally fall below the white standards. The vast majority of black patients have normal BMC and BMC/BW by the white standards. Matching 24 black and 24 white patients for age, sex, creatinine, and treatment category to rule out differences in the severity of disease demonstrated that black patients have greater BMC/BW than matched whites. This tendency for greater BMC/BW among black patients was found in chronic renal disease, transplant, and dialysis patients. The magnitude of these highly significant ($p<.001$) differences approached 12.5%.

BMC and BMC/BW were determined on 25 white male and 37 white female controls. The means for these groups were generally below the Wisconsin standards. A Chi-squared test indicated that the distribution below the standard was significant ($p<.05$). These differences could be explained by technique or could reflect differences in the populations. The 74 black female controls tend to exceed published standards for BMC and BMC/BW for whites in the 4th, 5th, 6th and 7th decade (but not the 3rd. Similar findings are noted for 79 black male controls. The Black male controls also exceeded white norms for the 4th, 5th, 6th and 7th decade). In both the male and female black controls the distribution above the standards for whites was significant ($p<.05$) by the Chi-squared test.

The clinically normal blacks showed levels of bone mass higher than both those of Wisconsin whites and our normal whites. Black patients showed considerably greater bone mass than do comparable white patients, both on an individual and a group basis. Black and white renal patients demonstrated similar patterns of bone loss. A problem arises because normal blacks have more bone than whites. As the osteopenia of renal diseases evolves, black patients begin to approach the white norms. Consequently, their severe osteopenia could often be overlooked. To correct this, we are establishing race specific norms against which black patients may be more effectively compared.

Supported by the Michigan Association for Regional Medical Programs; Ms. Amy Bessire kindly aided in preparation of this manuscript.

REFERENCES

1. Garn, S.M., Poznanski, A.K. and Larson, K. Standards for bone size and mass. Workshop on bone morphometry. Edited by Jaworski, Z.F.J. Ottawa, in press.
2. Mazess, R.B. and Cameron, J.R. Bone mineral content in normal U.S. whites. *Int. Conf. on Bone Mineral Measurement.* Edited by Mazess, R.B., Chicago, U.S. Dept. of Health, Education and Welfare, 1974, 228–237.
3. Trotter, M., Broman, G.E. and Peterson, R.R. Densities of bones of white and Negro skeletons. *J. Bone and Joint Surg., 1960, 42A*:50–58.
4. Trotter, M. and Peterson, R.R. The relationship of ash weight and organic weight of human skeletons. *J. Bone and Joint Surg., 1962, 44A*: 669–681.

Osteoporoses

Effect of Combined Therapy with Sodium Fluoride, Calcium, and Vitamin D on the Lumbar Spine in Osteoporosis. T. Hansson, B. Roos (Department of Orthopedic Surgery and Radiation Physics, Sahlgren Hospital, University of Gothenburg, Gothenburg, Sweden)

In 1972 Jowsey et al[1] reported that the combination of calcium, fluoride, and vitamin D increased bone formation in osteoporotic patients and that the newly-formed bone was normal by microradiography. We treated nine osteoporotic women (51–65 years) for 1.5–2 years with the Jowsey combination and measured their lumbar vertebrae by dual-photon absorptiometry. All of the women had at least one vertebral fracture and spinal x-ray with apparent low density. X-ray of the spine and hip as well as stature were taken before, during, and after treatment. No one in the group had any known disease which interfered with bone metabolism, and all had constant back pain. The women in the group got 30 or 50 mg of sodium fluoride and 1 g Ca (gluconate-lactate and bicarbonate) daily. They also got 0.6 mg of dihydrotachysterol daily.

In our absorptiometer[2,3] the radionuclide sources (^{241}Am and ^{137}Cs) are so arranged that emitted gamma radiation passes the vertebra in a common collimated beam. The patient lies on a couch which is moved transversally. Reproducibility on normal subjects was better than 6%.

No signs of hypercalcemia, hyperphosphatemia, or hypercalciuria were seen. Five patients became painless and four had only slight complaints of back pain.

TABLE 1.—Vertebral BMC changes in osteoporotics.

Subject	n	t_n (days)	Regression line: BMC_0	BMC_n	Increase (per cent)	$b \cdot 10^4$	$1.96 \cdot \sigma_b \cdot 10^4$	Significance
M. E.	6	496	3.31	4.22	27.7	18.5	10.8	Sign.
A. G.	7	663	2.52	3.65	44.9	17.1	7.6	Sign.
G. G.	6	593	3.08	3.41	10.6	5.5	8.7	Non-sign.
V. H.	6	600	1.84	2.37	29.1	8.9	8.5	Sign.
S. H.	6	593	2.25	2.66	18.5	7.0	8.8	Non-sign.
I. L.	6	480	3.35	4.08	21.8	15.2	11.4	Sign.
H. L.	7	504	3.56	4.35	22.2	15.7	9.5	Sign.
M. W.	6	639	3.04	3.38	11.4	5.4	8.0	Non-sign.
S. Å.	6	363	2.76	2.76	- 0.1	- 0.1	13.5	Non-sign.

n= no.of measurements, t = time, days, BMC(bone mineral content) = gram HA/cm,
b= slope, gram HA/(cm·day)

$$\sigma_b = \sqrt{\frac{\sigma^2_{BMC}}{(t - \bar{t})^2}}, \quad \sigma_{BMC} = 0.22 \text{ gram HA/cm}, \quad 1{,}96 \cdot \sigma_b = 95\ \% \text{ conf. interval}$$

Patient SÅ (Table 1) took treatment for only 2 months, but was kept in the group. One new vertebral compression fracture was visible on x-ray and in two patients further compression of one vertebra occurred. No visible changes in density occurred on x-ray of the spine or femoral neck. No change in body height was registered. Joint pain occurred in two patients. The symptoms disappeared on with-

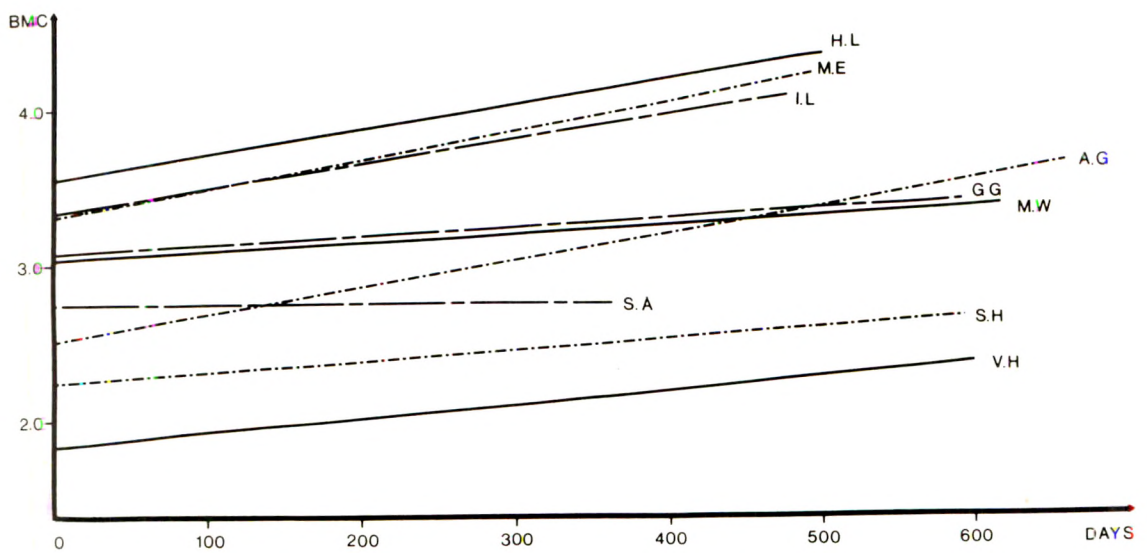


FIG. 1.—Change of vertebral BMC with the Jowsey combination.

drawal of the therapy and has not reoccurred when started again.

Absorptiometric results of the scans of the third or fourth lumbar vertebrae (Figure 1) showed that an increase of bone mineral content was achieved in eight treated women; the one case without an increase terminated treatment after only 2 months. In five, the increase was significant at the 0.95 level. The statistical calculations were made with the highest standard deviation ever determined experimentally (0.22 g/cm) and the significance has not been underestimated.

REFERENCES

1. Jowsey, J., Riggs, B.L., Kelly, P.J. and Hoffman, D.L. Effect of combined therapy with sodium fluoride, vitamin D and calcium in osteoporosis. *Am. J. Med.*, 1972, 53:43–49.
2. Roos, B. and Skoldborn, H. Dual photon absorptiometry in lumbar vertebrae. II. Precision and reproducibility. *Acta Radiologica*, 1975, 14:3.
3. Roos, B. and Skoldborn, H. Dual photon absorptiometry in lumbar vertebrae. I. Theory and method. *Acta Radiologica*, 1974, 13:3.

Bone Mineral Content Changes in the Skylab Astronauts. J. M. Vogel, M. W. Whittle (University of California School of Medicine, Davis, California and NASA, Lyndon B. Johnson Space Center, Houston, Texas)

Significant bone loss could occur in extended periods of weightlessness based on observations in bedrest and immobilization. Radiographic estimates of bone mineral on the crewmen of Gemini 4, 5, and 7 led to even greater concern since the os calcis losses ranged from 2–15%, the radius from 3%–25% and the ulna from 3%–16%.[2] Subsequent reevaluation showed there had been an approximate 6.7% overestimation of loss due to the inherent difficulties with the photodensitometric technique employed.[4] Nevertheless, these losses for 4–14 day missions suggested that longer Skylab missions could prove hazardous both in terms of potential fractures or of production of renal stones.

Bone mineral content (BMC) was determined in the central left os calcis and the distal 2 cm of the right radius and ulna using the photon absorptiometric technique.[3] Measurements were carried out preflight at about 30, 15, and 5 days before launch. Postflight measurements were made on recovery day, 1 and 7 days after recovery, and at variable times thereafter. The crews of Skylab 2 and Skylab 3 were studied until each had returned to baseline. The Skylab 4 study was terminated before two of the crewmen had returned to baseline levels. A series of seven control subjects were studied during Skylab 2 and Skylab 4, and six control subjects during Skylab 3. No losses were observed in either the radius or ulna. Os calcis BMC loss was observed only in the scientist pilots of Skylab 3 and 4 and the pilot of Skylab 4. The scientist pilot of Skylab 3 regained his os calcis mineral by day 87 postflight whereas the scientist pilot and pilot of Skylab 4 had not returned to preflight levels by day 95 postflight (table 1).

The above losses generally followed the loss patterns observed in a heterogeneous group of bedrested subjects. A prediction equation for BMC loss has been developed based upon the ratio of baseline os calcis BMC to baseline urinary hydroxyproline levels.[1] The prediction for four of the Skylab 2 and Skylab 3 crewmen fell within the limits observed in the bedrested subjects. BMC loss was predicted and seen only in the scientist pilot of Skylab 3. The two crewmen who had higher prediction terms did not lose BMC. The Skylab 4 crew had high prediction terms outside the limits set by the bedrest data and therefore predictions were not possible. It was expected, however, that losses in the os calcis would not exceed 5%. The 7.9% loss seen in the Pilot cannot be explained on this basis.

Table 1.—BMC changes as a percentage of baseline values in Skylab studies.

	Mission, Duration	Crewmen	Left Os Calcis	Right Radius	Right Ulna
Skylab	Skylab 2	Commander	+0.5	-0.5	-0.9
		Scientist Pilot	-0.9	+1.4	+1.9
	28 days	Pilot	+2.7	+0.2	+3.1
	Skylab 3	Commander	+2.3	-1.4	+0.4
		Scientist Pilot	-7.4	+0.2	-1.6
	59 days	Pilot	+1.4	-1.6	-0.4
	Skylab 4	Commander	+0.7	-1.1	-1.7
		Scientist Pilot	-4.5	+1.0	0.0
	84 days	Pilot	-7.9	-0.6	+1.4

		Left Os Calcis	Right Radius	Right Ulna
Control	Skylab 2	+0.8±1.6	-0.6±0.9	+0.2±1.5
	Skylab 3	+1.0±1.1	+0.1±0.8	-1.5±1.8
	Skylab 4	+1.0±1.2	-0.6±1.2	-0.7±1.5

The support of John Ullman, Scott Brown, Fred Kolb, and Alan Silverstein in the performance of the measurements and the support of Dr. Victor Schneider and the metabolic unit laboratory staff of the U.S.P.H.S. Hospital, San Francisco, is gratefully acknowledged.

REFERENCES

1. Lockwood, D.R., Lammert, J.E., Vogel, J.M. and Hulley, S.B. Bone mineral loss during bedrest. *Proceedings of the Clinical Aspects of Metabolic Bone Disease, Excerpta Medica Foundation (Amsterdam), 1972*, 148–151.
2. Mack, P.B., La Chance, P.A., Vose, G.P. and Vogt, F.B. Bone demineralization of foot and hand of Gemini-Titan IV, V and VII astronauts

during orbital flight. *Amer. J. Roentgen., 1967, 100*:503–511.
3. Vogel, J.M. and Whittle, M. Bone Mineral Changes: The second manned skylab mission. *Aviat. Space Environ. Med., 1976*, in press.
4. Vose, G.P. Review of roentgenographic bone demineralization studies of the gemini space flight. *Amer. J. Roentgen., 1974, 121*:1–4.

Physical Activity—A Modality for Bone Accretion in the Aged. E. L. Smith, W. Reddan (Department of Preventive Medicine, University of Wisconsin, Madison, Wisconsin 53706)

Physical activity has been used as a preventive and rehabilitative therapy for osteoporosis, but there is not conclusive data in an aged population to justify the therapy. This investigation studied the effects of physical activity on bone in an aged female nursing-home population. Bone mineral content (BMC) at the distal one-third of the radius was determined by photon absorptometry on 40 subjects (age 69–95) at 3 month intervals over a 36 month period. Twenty subjects regularly participated in a 30 minute/day, 3 day/week activity program consisting of light to moderate physical activity (1.5–3.0 METS). The remaining 20 subjects made no change in their activities of daily living. The data was analyzed for all subjects starting the study and for surviving subjects. All subjects lost were by natural causes. Seventeen control and 12 exercise subjects completed the 36-month investigation. A student t-test was used to determine bone mineral and bone width changes within and between the groups completing the study. Both control and exercise groups averaged 82 years of age at the beginning of the study and weighed 58.5 kg. The control survivors demonstrated a bone mineral loss of 2.5% during the 36 months but this was not significant ($P>.05$). The exercise survivors demonstrated a 4.2% bone mineral increase ($P<.05$) during the study. A linear regression was performed on the 10 mean values of the control group and the exercise group (Fig. 1). The control group demonstrated a negative slope consistent with the 2% loss over the 36 months. The exercise group demonstrated a positive slope slightly greater than the percentage increase demonstrated over the 36 months. All subjects starting the study within and between groups were compared by the use of a multiple regression analysis with dummy variable. No significance ($P>.05$) was observed within either the control or the exercise group, but a significant difference ($P=.02$) was present between the two groups. Bone width, while increasing somewhat more in the exercise than the control, was not significant within or between the groups. The rate of bone mineral loss in the control group is consistent with that seen by Garn[3] and Mazess and Cameron[4] in longitudinal and cross sectional studies. The physical activity program slowed bone loss in the aged subjects and even demonstrated bone accretion.

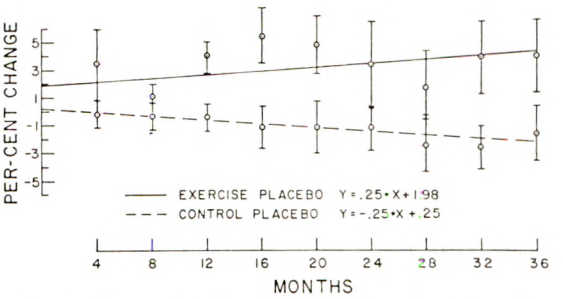


Fig. 1.—Bone mineral change at the mid-shaft of the radius over 36 months.

This accretion indicated that even aged bone is responsive to additional stress. The results are consistent with animal studies by Chamey and Tschantz[1] and human studies by Dalen[2] which showed that bone responds to increased stress with accretion. This study specifically indicated that bone in the "normal" aged female can respond to increased stress, and suggests that physical activity could influence prevention and rehabilitation of fractures in the elderly.

REFERENCES

1. Chamey, A. and P. Tschantz: Mechanical influences in bone remodeling, experimental research on Wolff's law. *J. Biomech.* 5:173–180, 1972.
2. Dalen, N. and K.E. Olsson: Bone mineral content and physical activity. *Acta Orthop. Scand.*, 45:170–174, 1974.
3. Garn, S.M., C.G. Rohmann, and P. Nolan: The developmental nature of bone changes during aging. *Relations of Development and Aging*, edited by James E. Birren. Springfield, Ill. Charles C Thomas, 41–60, 1964.
4. Mazess, R.B. and J.R. Cameron: Bone mineral content in normal U.S. whites In. R.B. Mazess (ed)—Intern. Conf. Bone Mineral Measurement, DHEW Publ. 75–683, 1974.
5. Sorenson, J.A., and J.R. Cameron: A reliable *In Vivo* measurement of bone mineral content. *Journal Bone and Joint Surgery*, Vol. 49–A:481–486, 1967.

Changes of Bone Mineral in Healthy Menopausal and Premenopausal Women: Two Year Preliminary Results of a Longitudinal Study. K. R. Heer, K. Alexandrow, Th. Lauffenburger, H. G. Haas (Division of Metabolism and Endocrinology, Department of Medicine, Kantonspital, 4004 Basle, Switzerland)

Two groups of healthy working women were studied: (1) 'premenopausal' (n=39), comprised of subjects 38–44 years of age with regular menstruation; and (2) 'menopausal' (n=77), consisting of women aged 48–54 years, either with regular menstruation or in early menopause (last menstruation not more than 4 months before starting the study). The bone mineral (BMC, g/cm) was measured at the proximal site (1/3) of the right radius by means of photon absorptiometry.

A decrease of BMC was recorded in both groups after two years of followup: (1) $-.024 \pm .030$ g/cm ($p<.01$), and (2) $-.045 \pm .031$ g/cm ($p<.001$). The decrease of group 2 is significantly higher than of group 1 ($p<.001$). In addition, a significant correlation between the change of BMC and the total BMC was found in both age groups (group 1: $r=-.49$, $p<.01$, group 2: $r=-.50$, $p<.001$). Furthermore, some individuals lost either more or less bone mineral than the average women. This is independent of the total BMC.

These data are interpreted as indicating that: (a) the loss of bone mineral begins before the age of 40, (b) it is more rapid in women aged 50, (c) there is a correlation between the total amount of bone mineral and the absolute loss of BMC, and (d) some individuals lose more bone mineral than the average women.

The Slowing of the Rate of Mineral Loss with Aging. D. M. Smith, M. R. A. Khairi, C. C. Johnston Jr., J. Norton (Departments of Medicine and Psychiatry, Indiana University School of Medicine, Indianapolis, Indiana)

Previous cross-sectional and longitudinal studies have developed models which assume that bone mineral loss after menopause is a linear function.[1,4,5] This assumption was examined by measurement of bone mineral content (BMC) of the midshaft radius in postmenopausal women with the photon absorption technique.[3] Regression analysis of BMC values of 588 Caucasian women, ages 50 to 96 (mean, 69), against age was performed. A quadratic function gave a significantly better fit to the data than a linear function suggesting a slowing of the loss rate in later years. To compare the results with a longitudinal study, the sample was divided into two age groups: 50 to 67 years (mean 59; N=292) and 68 to 96 years (mean 81; N=296). The linear regression coefficient of BMC against age was computed for these subgroups. The change of BMC in the younger group ($-0.0119 \pm .0017$ g/cm/yr) was significantly ($p<.001$) greater than that for the older group ($-0.0056 \pm .0013$). This suggested that the younger group was losing mineral about twice as fast as the older group. Similar rates of loss in younger and older postmenopausal women have been reported for cross-sectional data.[3]

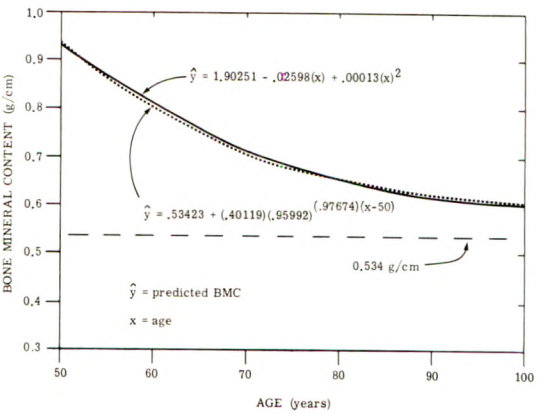


FIG. 1.—The relationship of BMC and age in a population of 588 females. The curve (——) for the quadratic equation is practically superimposible on the curve (----) for the exponential decay. The quadratic function has a minimum value of 0.602 g/cm at 100.1 and thereafter increases. The exponential approaches a value of 0.534 g/cm asymptotically.

Longitudinal rates of mineral loss were estimated from repeated measurements in postmenopausal women. The mean rate of loss in 24 women, ages (at the start of the study) 50 to 65 (mean, 57), after 16 visits over 3.8 years was $-0.0108 \pm .0015$ g/cm/yr. In an older group of 32 women, age 71 to 91 (mean, 82), after 23 visits over 2.4 years, the mean rate was $-0.0043 \pm .0026$ g/cm/yr. The mean rate for the younger group was significantly ($p<.05$) faster than that of the older group.

Previous longitudinal studies have shown that inactivity such as bed rest promotes bone loss[2] and inactivity could contribute to aging bone loss. The activity status of the 55 women in the longitudinal study was graded. The older group was significantly less active than the younger group, and yet the older group had the slower rate of bone loss.

A quadratic may not be the most appropriate function for aging bone loss since it predicts an eventual increase in BMC at ages beyond that which we have studied. A more appropriate function may be an exponential decay curve where BMC approaches an asymptote. This possibility was examined in our cross-sectional data (Fig. 1). The closeness of fit (multiple R^2) for the quadratic was 0.3846 and for the exponential 0.3850. Thus the quadratic and the

exponential appear to fit equally well, but the exponential probably better reflects the true biological phenomenon since no increase in BMC is anticipated, as would occur with a quadratic function. The rate of loss at any point in time from either equation is the first derivative. The first derivative of the quadratic is dependent on the variable age whereas the first derivative (rate) of the exponential is dependent on the level of BMC at a particular age.

REFERENCES

1. Doyle, F., Involutional osteoporosis. *Clin. Endocrinol. Metab.*, 1972, 1:143–167.
2. Hulley, S.B., Vogel, J.M., Donaldson, C.L., Bayers, J.H., Friedman, R.J., and Rosen, S.N. The effect of supplemental oral phosphate on the bone mineral changes during prolonged bed rest. *J. Clin. Invest.*, 1971, 50:2506–2518.
3. Mazess, R.B. and Cameron, J.R. Bone mineral content in normal U.S. whites. In: R.B. Mazess (ed).—International Conference on Bone Mineral Measurement. DHEW Publ. 75–683, U.S. Dept. H.E.W., Washington, D.C., 1974, 228–237.
4. Newton-John, H.F., and Morgan, D.B. The loss of bone with age, osteoporosis, and fractures. *Clin. Orthop. Relat. Res.*, 1970, 71:229–252.
5. Smith, D.M., Khairi, M.R.A., and Johnston, C.C., Jr. The loss of mineral with aging and its relationship to risk of fracture. *J. Clin. Invest.*, 1975, 56:311–318.

Prediction of Femoral Neck Fracture from a Pelvic X-ray. B. E. Nilsson, L. Hagberg (Department of Orthopedic Surgery, Mälmo General Hospital, University of Lund, Mälmo, Sweden)

Our study investigated the possibility of predicting femoral neck fracture from a pelvic x-ray. Radiograms of 137 women (age 59–62) were selected. All films were taken 1950–1960. Later, but prior to 1975, 39 of the women sustained 41 fractures of the upper end of the femur (21 trochanteric and 20 cervical fractures). The remaining women, who survived through 1974 without fracture, were age matched with the fracture cases and served as controls.

The films were evaluated by two investigators without knowing whether or not the patient on the film would later have a fracture or not. Two methods were used: 1) Singh's trabecular pattern. This is an evaluation of the trabecular pattern in the upper end of the femur ranking from normal (grade 6) to severe osteoporosis (grade 1). (2) Measurement of femoral-neck cortex. The medial cortex was measured on an antero-posterior film of the upper end of the femur immediately proximal to the lesser trochanter. The thickness was corrected for the size of the patient by dividing by the total width of the neck of the femur (cortical ratio). Ten of the control hips had radiological signs of hip osteoarthritis. Since these cases could be demonstrated to have a greater than normal cortical thickness they were excluded and only radiologically healthy hips were used for the comparison between fracture cases and control cases.

There were no cases with the most severe degrees of osteoporosis on Singh's scale. The trabecular patterns were distributed from grade 6 to 3 as demonstrated in Table 1. There was a highly significant difference between fracture and control cases in that the fracture cases were represented more often in lower ranks of trabecular pattern. The table illustrates the results in all hips separately but since there is a partial dependence between the two hips in one patient the analysis was repeated for left hips and right hips separately. The difference was significant in both instances.

The cortical ratio was compared between fracture

Table 1.—Singh index of femoral neck in Swedish females.

	Singh's Grade			
	3	4	5	6
Fracture	5	21	29	23
Control	11	11	73	81

χ^2 (3 df) = 22.3

$p < 0.001$

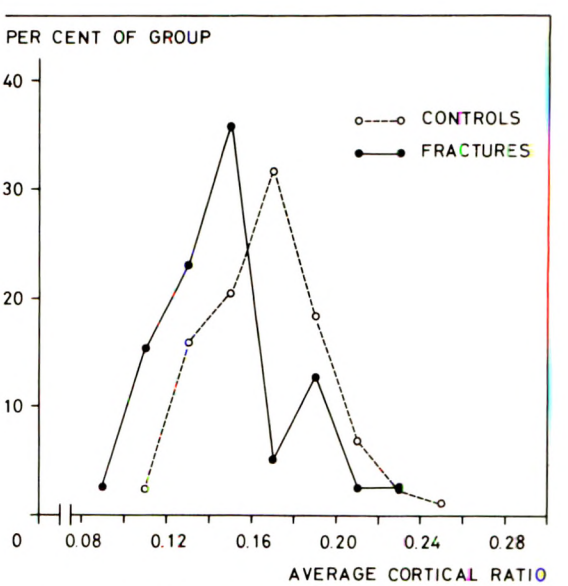


Fig. 1.—Distribution of cortical ratio in the femoral neck.

and control cases. There was a highly significant difference between the two groups although the data over-lap considerably. Nevertheless there seems to be a dividing line at about 0.16 which could be used for selection of cases with a higher than average risk for femoral neck fracture (Fig. 1).

In Sweden today, about 20% of all women will have a fracture of the upper end of the femur at some time in their lives. Measurements of the femoral neck cortex on a standard radiogram of the hips make it possible to select a set of women, 50% of whom will have a fracture of the upper end of the femur within the next two decades. Such a subset would be most appropriate for therapeutic trials.

Clinical

Effects of Corticosteroids on Bone Mineral in Rheumatoid Arthritis and Asthma. M. N. Mueller (Department of Medicine, University of Wisconsin Hospitals, 1300 University Avenue, Madison, Wisconsin 53706)

Previous studies at the University of Wisconsin have established that in adult Wisconsin women with rheumatoid arthritis there is a modest amount of bone mineral loss when patients have not been exposed to corticosteroid therapy. Using the Cameron-Sorenson monoenergetic absorptiometric method with measurements at midshaft and distal sites of the non-dominant radius, skeletal demineralization is correlated with duration and severity of disease. Rheumatoid women treated with corticosteroid therapy, when matched for age, duration, and severity of disease, demonstrated a dramatic and severe amount of demineralization which is related to total dose of corticosteroid exposure. The impact of steroids on the skeleton was equally severe in pre- and postmenopausal women; moreover the demineralization was equally severe at distal and midshaft sites of the radius, implying similar rates of loss of cortical and trabecular bone.

To further study some of the pharmacologic effects of corticosteroids, 114 adult subjects with severe asthma were studied in the same way. No detectable bone mineral loss was associated with asthma, whether or not corticosteroids had been used for therapy. There was no relationship of corticosteroid dose to bone mineral at the sites of measurement.

Thus corticosteroid therapy appears to have a unique catabolic effect on the skeleton of subjects with rheumatoid arthritis. An alternative or adjunctive hypothesis would be that the disease asthma or some other aspect of its therapy has a protective effect on the skeleton which may block the catabolic influence of corticosteroids.

Bone Mineral Determinations on Long-Term Diabetics. J. D. Ringe, F. Kuhlencordt, H. P. Kruse (Abteilung Klinische Osteologie I. Medizinische Univ.—Klinik, Martinistrasse 52, 2 Hamburg 20, W. Germany)

At present one does not know the frequency of osteopathies in diabetes, or how often osteopathies are direct or indirect consequences of the metabolic disorder in diabetes. We generally distinguish between localized and generalized skeletal findings in diabetes. Localized osteopathies have been described for the foot, vertebrae, and skull. Part of the generalized diabetic osteopathies develop secondary to well-known diabetic complications. For example osteodystrophy in chronic renal failure due to Kimmelstiel-Wilson lesions and to the common pyelonephritis. Our work was to find out whether there is any other diabetic osteopathy which is a direct derivative of the diabetic metabolic disorder aside from those osteopathies due to secondary complications.

Insulin dependent long-term diabetics (21 men and 36 women) were examined. Because of the high incidence of osteoporosis at advanced age we excluded women older than 45 years and men older than 50 years. We also excluded diabetics who suffered from diabetic nephropathy or other diseases which were apt to cause an osteopathy. The male and female groups averaged about 33 years of age: the duration of diabetes averaged 19.4 years (10–41 years) and the average onset was 13.7 years (0–31 years). In all cases a detailed history was taken. Calcium, phosphorus, alkaline phosphatase, blood urea nitrogen, and creatinine were analysed in a blood sample and the bone mineral content (BMC) of the peripheral skeleton was measured using photon absorptiometry with a Norland apparatus. We measured radius and ulna of the left arm at 1/3 the distance from the lower end of the radius.

In Table 1 the individual data of radius and ulna have been calculated in per cent of the normal values corresponding to age and sex of the patient. The cases were divided into groups of lowered, normal, and increased BMC. For women the BMC loss within the group of lowered values is 11.2% in the radius and in the ulna 16.8%. If one compares the BMC of the different groups to the mean duration and the mean onset of diabetes, no significant differences in the women can be noticed. In the group with lowered BMC the mean duration of diabetes is only two years longer than in the normals. For the men the same

TABLE 1.—Mean values in percent for BMC of radius and ulna in correlation to duration and onset of diabetes mellitus.

36 ♀		NUMBER OF PATIENTS n	%	MEAN BMC (%)	MEAN DURATION OF DIAB. (years)	MEAN ONSET OF DIAB. (age)
BMC OF RADIUS	↓	11	31	- 11.2	19.7	15.7
	↔	23	64	- 1.9	18.0	13.7
	↑	2	5	+ 14.5	20.0	2.0
BMC OF ULNA	↓	14	39	- 16.9	19.3	13.8
	↔	21	58	- 0.7	17.3	14.7
	↑	1	3	+ 15.2	19.0	0

21 ♂		NUMBER OF PATIENTS n	%	MEAN BMC (%)	MEAN DURATION OF DIAB. (years)	MEAN ONSET OF DIAB. (age)
BMC OF RADIUS	↓	10	48	- 13.1	24.7	10.1
	↔	9	43	+ 0.7	17.9	16.1
	↑	2	9	+ 9.8	13.0	22.0
BMC OF ULNA	↓	10	48	- 17.3	23.1	12.5
	↔	11	52	+ 0.7	18.5	14.9
	↑	0	0	—	—	—

calculations lead to the following conclusions: BMC loss in the group with lowered BMC is 17.3% in the ulna and 13.1% in the radius. What was only a slight tendency in the women can be recognized more clearly in the men: in the group with lowered BMC the duration of diabetes is considerably longer than in the group with normal values. The group with lowered BMC has on the average an earlier onset.

In our examination, 31% of the women and 48% of the men had a pathologically reduced BMC. As the cases with diabetic nephropathy and other diseases were excluded, the mineral loss must be considered as a direct consequence of the diabetic disorder of metabolism. There was not a significant correlation between BMC and duration of diabetes, but the mean values of the groups demonstrated some association between loss and duration. Therefore it seems justified to consider the measured BMC losses as another complication secondary to diabetes mellitus. The frequency of diabetic retinopathy and polyneuropathy in our cases is within the same range as the demonstrated lowered mineral values (between 30–40%). The coincidence of retinopathy and polyneuropathy with lowered BMC is always more than 50%.

Up to now none of the cases with measured mineral loss have shown pathological fracture. It is also remarkable that in none of the cases were there notable complaints of skeletal pains. As these patients averaged only 31 years old skeletal complications might be expected to occur as they age.

Supported by the Deutsche Forschungsgemeinschaft, Sonderforschungsbereich 34 "Endokrinologie."

An Overview of Clinical Applications of Photon Absorptiometry. H. J. Griffiths, R. E. Zimmerman (Tufts New England Medical Center, 171 Harrison Avenue, Boston, Massachusetts 02111)

Photon absorptiometry provides the most precise and accurate measurement of bone mineral content (BMC) and has been used in a variety of diseases. In acromegaly, the bones enlarge but the BMC is normal. BMC is reduced by acidosis of various types including that due to starvation. This can be corrected by control of the acidosis. Alcoholics develop osteomalacia and show decreased BMC, which may also reflect an osteoporosis due to lack of activity. Anticonvulsants, particularly phenytoin and primidone, cause an osteomalacia in which there is a decreased BMC, decreased serum Ca, and increased alkaline phosphatase. Treatment with vitamin D returns BMC to normal. In hyperparathyroidism there is decreased BMC before radiographs are positive. Cortical striations, osteoporosis, and erosions occur. Parathyroidectomy corrects this and BMC tends to return toward normal. Bone loss is an iatrogenic consequence of several drugs. Corticosteroids reduce BMC especially in the central (vertebral) bone, similar to Cushings disease. Glutethimide over the long-term causes an osteomalacia with a decreased BMC. In long-term heparin treatment, bone resorption increases and there is osteoporosis with decreased BMC.

Immobilization has been shown to decrease BMC. Bedrest and space flight reduce lower limb, but not upper limb BMC and there is full recovery when ambulated. However, in chronic disease with immobilization, there can be a general decrease of BMC. Conversely, activity increases BMC even in the elderly. BMC is greater in athletes than non-athletes, particularly in the dominant side.

Aging osteoporosis seems to be a normal process due to decreased bone formation. It occurs from age 45 in females and from 65 in males. In females, bone loss is related to early menopause and to lactation. Bone loss can be arrested by estrogens; fluoride (with calcium and vitamin D); and possibly calcium carbonate. Osteoporosis is associated with widening of the bone and alteration in trabeculae. It is first evident in regions of trabecular bone but eventually affects areas of compact and trabecular bone at similar rates.

There is decreased BMC at all stages of renal failure. There is rapid BMC loss in azotemia and during dialysis, and slower loss after transplant. Parathyroidectomy does not affect BMC in renal osteodystrophy because there is not only secondary hyperparathyroidism, but a mixture of osteomalacia, osteoporosis and even osteosclerosis. Treatment with vitamin D and Ca supplements is suggested until

transplant. Spinal cord injury shows normal BMC in compact bone but decreased BMC in trabecular areas. This is also seen in leprosy and diabetes. In hemiplegia there is decreased BMC on the paralyzed side associated with decreased activity.

In thyrotoxicosis there is increased formation and resorption of bone. Over the long-term, BMC is reduced but returns to normal with therapy. The bone shows cortical striations.

Bone Mineral Content in Patients with Gonadal Dysfunction. W. D. Risch, D. H. Banzer, L. Moltz, U. Schneider, R. Rudloff (Department of Radiology, Free University Berlin, Klinikum Steglitz, Hindenburgdamm 30, 1000 Berlin 45, West Germany)

The bone mineral content (BMC) of the os calcis was determined in 233 patients with gonadal dysfunction. Measurements were performed with a transmission-scanner for photon absorptiometry. The patients were being treated for primary or secondary amenorrhea or had been castrated 1–3 years before the measurement because of ovarial or uterine cancer. The BMC was in the normal range in Stein-Leventhal syndrome with secondary amenorrhea and in postcontraceptive amenorrheas (Fig. 1). The BMC was decreased in Stein-Leventhal syndrome with primary amenorrhea, gonadal dysgenesis, testicular feminization, anorexia, castration, gonadal hypogenesis, and adrenogenital syndrome. The first BMC-value available in each patient was used for this figure, even if hormonal substitution had been used previously in other hospitals.

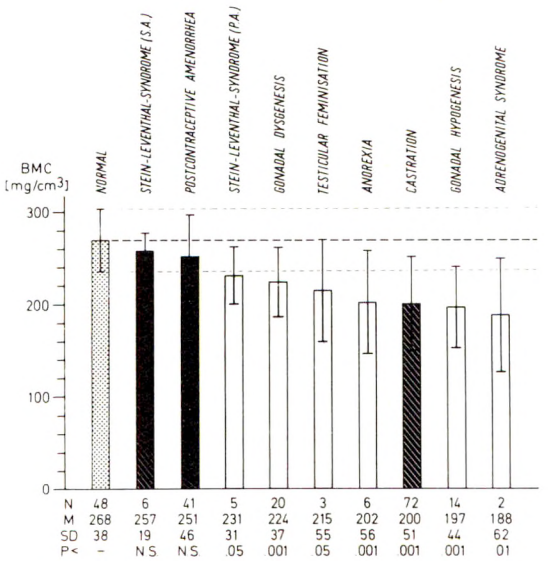


FIG. 1.—Bone mineral content per volume in the os calcis of patient groups. Error bars show standard deviation.

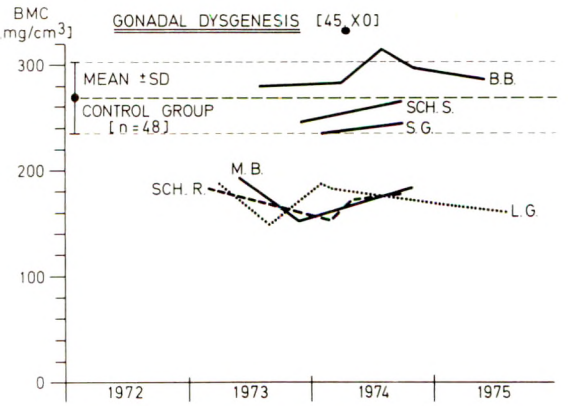


FIG. 2.—Bone mineral content in Turners syndrome.

In the group of 20 patients with gonadal dysgenesis six subjects with Turner syndrome (45, X) were found. The mean age was 22.5 years (17–28) height 148.5 cm (142–155), and weight 50.4 kg (40–59). The BMC of three subjects was normal. In the other three patients the BMC was greatly decreased (see Fig. 2). Only one of the latter subjects (Sch. R.) showed a retardation of the skeleton development (bone age 13.0 years, chronological age 18.4 years).

In some patients with primary or secondary amenorrhea the relation between BMC and secretion of gonadotropic hormones was studied. In 34 hypergonadotrope patients (>32 MUU) the BMC in mg/cm³ (M ± 1SD) was 214.8 ± 39.1. In 28 eugonadotrope subjects (4–32 MUU) and 25 hypogonadotrope patients (<4 MUU) the BMC amounted to 247.2 ± 38.8 and 234.2 ± 43.3. The difference in BMC between eugonadotrope and hypergonadotrope subjects was significant ($p < 0.005$).

Bone Mineral Content in Anticonvulsant Osteomalacia. C. Christiansen, P. Rodbro (Department of Clinical Chemistry, Glostrup Hospital, Glostrup, Denmark)

Reports over the last decade have indicated that epileptic patients on long-term anticonvulsant therapy develop biochemical signs of osteomalacia. The degree of osteomalacia, however, was not known until recently nor was the effect of vitamin D treatment.

In previous publications we have shown the mean bone mineral content (BMC) value is 87%–88% of normal for large numbers of epileptics on anticonvulsants. This indicates that "anticonvulsant osteomalacia" usually is only slight or moderate.

Patients initially were treated with vitamin D_2.

On this treatment the patients' mean BMC value rose significantly compared to controls. Eventually, it was possible to normalize the mean BMC on 4,000 IU vitamin D_2 daily and to maintain this level with a daily dose of 1,000 IU.

Others have found low serum levels of 25-hydroxycholecalciferol (25–OH–D_3) in epileptics on anticonvulsants, and it was suggested that induction of liver enzymes concerned with the primary hydroxylation of vitamin D_3 could explain the findings in anticonvulsant osteomalacia. Were this the case, then 25–OH–D_3 should be the drug of choice in this condition. We tested this by giving various doses of D_3 and 25–OH–D_3 to epileptic patients on anticonvulsants. With this treatment no BMC change was found. These findings indicate that vitamin D_2, on one hand, and vitamins D_3 and 25–OH–D_3, on the other, act in different manners in anticonvulsant osteomalacia, presumably because their metabolism is affected differently by anticonvulsant drugs. The use of BMC measurement has thus shed new light upon the metabolism of vitamin D.

Quantitative Bone Mineral Analyses in Patients with Inflammatory Bowel Disease. H. K. Genant, J. C. Mall, L. H. Lanzl, J. Vander Horst, J. B. Wagonfeld (Department of Radiology, University of California, San Francisco, California, and Department of Radiology, University of Chicago, Chicago, Illinois)

The effect of inflammatory bowel disease (IBD) on linear growth in children has been the subject of numerous reports,[2,6,7] but the effect on skeletal mineralization has not been previously reported. In this study, 54 patients (26 males and 28 females) with documented ulcerative colitis, regional enteritis or granulomatous ileocolitis were examined. Clinical and biochemical parameters of disease were assessed and conventional radiographs reviewed. The bone mineral content was determined by the technique of Lanzl and Strandjord[5] which measures the linear attenuation coefficient of phalangeal bone by means of collimated 125-I source and sodium iodide scintillation detector. The combined cortical thickness of the left second metacarpal was determined in all patients by the technique of Garn.[3] The skeletal age was determined following Greulich-Pyle. A mineralization index[4] was derived by combining the cortical thickness measurement with bone mineral value and normalizing for age and sex.

The results of the metacarpal cortical measurements showed values at least 1 SD below normal in 65% of males and 64% of females. The cortical thickness of the patients with IBD was 3.99 mm compared to 5.07 mm in controls ($p<.001$). The linear attenuation coefficient values were at least 1 SD below normal in 35% of males and 22% of females with IBD. Patients with IBD had a mean absorption coefficient of 1.99 cm^{-1} compared to 211 cm^{-1} for controls ($p<.001$). The mineralization indices in 30 of 54 patients were below the 90% value (which corresponds to a decrease of approximately 1 SD in both cortical thickness and linear absorption coefficient). In all but 10 patients the indices were below the 100% normal value. Demineralization was present at all ages but was more common and more severe in the adolescents. The mineralization index in this group was 82.2% compared to 91.8% in adults with IBD. The percent mineralization correlated closely with roentgenographic appearance of osteopenia in the spine. There was no correlation between this index and the duration of disease, biochemical parameters of malabsorption, duration of disease, or nature and extent of surgery. The percent mineralization correlated with corticosteroid treatment in adolescent patients but not in adults. In the adolescents the demineralization paralleled closely the degree of skeletal retardation which was in part steroid induced.[1,6,8] However, the demineralization exceeded that which could be explained solely on the basis of retardation of skeletal maturation.

In conclusion, we demonstrated a high incidence of osteopenia as a complication of IBD. The finding was particularly evident in adolescents where osteopenia correlated well with skeletal retardation and corticosteroid therapy. In adults, demineralization was common but less severe, and correlated poorly with other parameters of disease.

REFERENCES

1. Blodgett, F.M., Burgin, L., Iezzoni, D., et al.: Effects of prolonged cortisone therapy on the statural growth, skeletal maturation and metabolic status of children. *N. Engl. J. Med.* 254: 636–641, April 5, 1956.
2. Ehrenpreis, T., Ericsson, N.O. Surgical treatment of ulcerative colitis in childhood. *Surg. Clin. N. Am.* 44:1521–1535, Dec. 1964.
3. Garn, S. The earlier gain and the later loss of cortical bone, in nutritional perspective. Springfield, Ill., Charles C Thomas, 1970.
4. Genant, H.K., Vander Horst, J., Lanzl, L.H., et al.: Skeletal demineralization in primary hyperparathyroidism. Proc. International Conference on Bone Mineral Measurement, Chicago 1973, ed. by R.B. Mazess. National Institute of Arthritis, Metabolism and Digestive Diseases. DHEW Publication No. (NIH) 75–683, pp. 177–194, 1974.
5. Lanzl, L.H., Strandjord, N. Radioisotopic device for measuring bone mineral. Proc. of Symposium on Low-energy X- and Gamma Sources and Application, Illinois Institute, Chicago, October 20, 1964. AEC Report ORNL–II C–5, pp. 257–276.
6. McCaffery, T.D., Nasr, R., Lawrence, A.M.,

et al.: Severe growth retardation in children with inflammatory bowel disease. *Pediatrics* 45:386–393, March 1970.
7. Sobel, E.H., Silverman, F.N., Lee, C.M. Jr. Chronic regional enteritis and growth retardation. *Am. J. Dis. Child.* 103:569–576, April 1962.
8. Thorn, G.W. The effects of glucocorticoids upon growth and development. *Schweiz Med Wochenschr.* 100:1625–1635, Sept. 26, 1970.

The Proximal End of Tibia, a Sensitive Site for Measurement of the Bone Mineral Content in Lower Limb Dysfunction. B. E. Nilsson, S. Andersson (Department of Orthopedic Surgery, Mälmo General Hospital, University of Lund, Mälmo, Sweden)

For our studies on local osteoporosis, we have modified our standard method of gamma absorptiometry previously used on forearms for application to the proximal end of the tibia. The radiation source is Am-241. The site usually chosen for these measurements is the proximal end of the tibia and the fibula 4.5 cm distal to the bone joint surface on the lateral tibia condyle. This site is located by means of an x-ray image intensifier. The precision of the method is about 4%.

Figure 1 records the measurements of a patient with fractures of the shaft of the tibia and the fibula distal to the measuring site during the first 60 weeks after injury.

Our present investigation, however, focuses on changes following a joint sprain, with or without ligamental injury. All sprains seen either in outpatients or in the emergency room, in which a tear or rupture of the knee ligament cannot be clinically excluded, are taken to the operating room and reexamined under general anaesthesia so that any pathological instability may be revealed. Thirty-seven consecutive patients (age 31 ± 13) were measured with tibia absorptiometry from the day of the injury and then successively for about 12 weeks. Seventeen of the 37 were operated on with repair of one or more ligaments. They were kept in plaster casts for 6 weeks but were allowed to bear weight on the injury. The remaining cases, without ligamental lesions, were treated for several weeks only with an elastic bandage. We found a significant decrease in bone mineral content between operated and non-operated cases. The average loss in the operated cases was 14% and in the non-operated, 7% (Fig. 2). The last value is most surprising because none of these cases had bone injury and the time period of dysfunction and pain very short. In contrast, those with the more severe injuries who were operated on were immobilized for a considerable time and also had a period of knee dysfunction after removal of cast. Nevertheless, a measurable loss appears in the successive measurements. This latter finding could be of clinical importance for football players and other athletes who are subjected to repeated knee injuries.

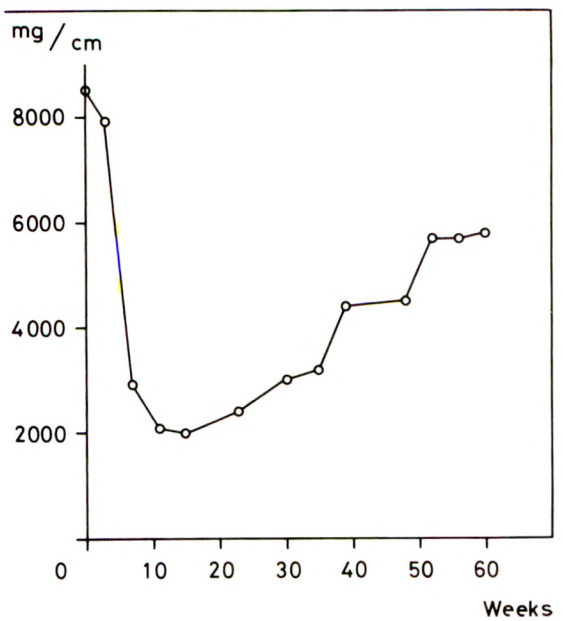


Fig. 1.—Application to tibia shaft fracture. Measurements in one patient from the day of injury.

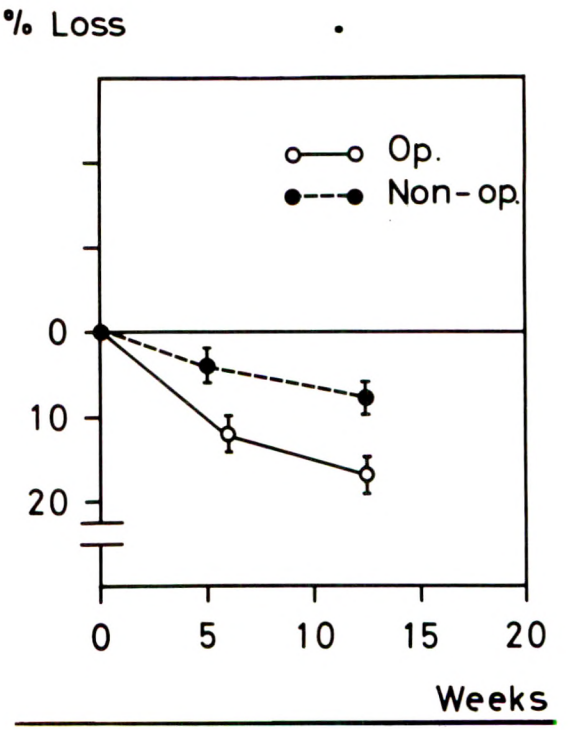


Fig. 2.—Changes in bone mineral content of the tibia in patients with knee injuries, without fractures.

Skeletal Mass in Rheumatoid Arthritis: A Comparison with Forearm Bone Mineral Content.
I. Zanzi, M. S. Roginsky, K. J. Ellis, S. Blau, S. H. Cohn (Medical Department, Brookhaven National Laboratory, Upton, New York 11973)

The evaluation of diffuse osteoporosis in rheumatoid arthritis (RA) remains controversial.[5] An important associated problem is the compounded effect of osteopenia secondary to chronic corticosteroid treatment. Most of the studies have consisted of radiographic evaluations. Recently, photon-absorptiometric techniques have been used for measurements of selected sites of the skeleton, such as the distal femur,[1] and the distal radius.[7,8,9] The development of the technique of in-vivo total body neutron activation analysis (TBNAA) along with whole body counting, has made possible the direct measurment of skeletal mass (total body calcium, TBCa).[2] In the present study, TBCa and radial bone mineral content (BMC) were evaluated in 19 Caucasian women with RA, with and without a history of corticosteroid treatment.

All patients were definite or classic according to the ARA criteria, and all were ambulatory. In all of them plasma calcium, adjusted for albumin level,[10] and phosphorus values were normal. In four patients, alkaline phosphatase values were above the upper normal range. The seven patients without corticosteroid treatment were receiving variable doses of salicyclic or gold therapy. The average daily dose of the variable steroid treatment of the other 12 patients was equivalent to 13 mg of prednisone and had been given an average of 3.7 years. Two patients who had received high doses of steroids for long periods of time had clear cushingoid characteristics.

The BMC was measured with a Norland Bone Mineral Analyzer. Measurements were made at the 8 cm site from the distal end of the radius. The details of the technique of TBNAA and the Brookhaven whole-body counter have been described previously.[3] Calibration with an anthropormorphic phantom indicated an accuracy of $\pm 5\%$ and a precision of $\pm 1.0\%$ for the measurement of Ca. The skeletal mass for an individual patient was evaluated as a ratio between the measured TBCa and the predicted value (Ca_p) for that individual calculated from empirically derived equations based on observations on normal human subjects.[4] Lean body mass was evaluated by whole body counting of ^{40}K.

The skeletal mass, as measured by TBNAA, was within normal limits in the seven patients with no steroid treatment: $TBCa/Ca_p = 0.993 \pm 0.106$ (S.D.), and was decreased in the patients following steroid therapy: $TBCa/Ca_p = 0.848 \pm 0.128$ (S.D.). The difference between the groups is significant at the level of $p < 0.025$. An even greater difference ($P < 0.001$) was observed in $TBCa/Ca_p$ when comparing the same population divided into pre- and post-menopausal groups (48y). Below 48y, $TBCa/Ca_p$ was 1.003 ± 0.068 while above age 48y $TBCa/Ca_p$ was 0.789 ± 0.100 (Fig. 1).

There was a highly significant correlation between TBCa and BMC in the total population under study and in the group receiving corticosticosteroids ($r = 0.89$ and $r = 0.88$ respectively, $p < 0.001$). The correlation observed between these two parameters in the seven patients not receiving steroids was $r = 0.82$ ($p = < 0.05$).

No correlation was obtained between TBCa and the estimated duration of the disease, or the duration and dosage of the steroid treatment.

A slightly significant difference ($p < 0.05$) was observed when comparing the lean body mass as evaluated by the ratio TBK/K_p, (measured/predicted K). The patients with corticosteroid therapy had a $TBK/K_p = 0.853 \pm 0.136$), and patients without the therapy had a ratio of 0.987 ± 117. Further, the relationship between TBK and TBCa in this population of patients was normal, a finding previously noted in other metabolic disorders.[6]

The results of this study indicate that age has an important effect on the development of osteoporosis in RA. In our patients, the detrimental effect of corticosteroids were pronounced only in the postmenopausal group of women.

Supported by the U.S. Energy Research and Development Administration.

REFERENCES

1. Bjelle, A.O., and Nilsson, B.E. Osteoporosis in rheumatoid arthritis. *Calc. Tiss. Res.*, 1970, 5:327–332.
2. Cohen, S.H., Shukla, K.K., Dombrowski,

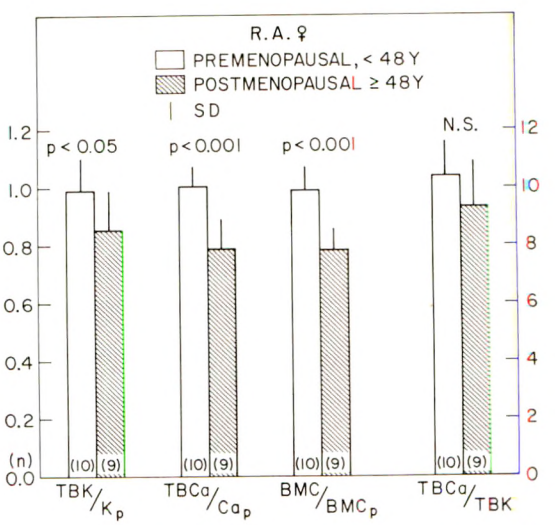


Fig. 1.—Deviation from predicted vales (1.0 is normal) in younger and older women with rheumatoid arthritis.

C.S., and FAIRCHILD, R.G. Design and calibration of a "broad beam" ^{238}Pu, Be neutron source for total body neutron activation analysis. *J. Nucl. Med.*, 1972, 13:487–492.
3. COHN, S.H., ELLIS, K.J., WALLACH, S., ZANZI, I., ATKINS, H.L., and ALOIA, J.F. Absolute and relative deficit in total-skeletal calcium and radial bone mineral in osteoporosis. *J. Nucl. Med.*, 1974, 15:428–435.
4. COHN, S.H., ELLIS, K.J., and GOLDSMITH, N.F. Validity of the absorptiometric measurement of bone mineral content of the radius. Presented at the International Conference on Bone Mineral Measurements, New Orleans, January 1976.
5. DUNCAN, H. Osteoporosis in rheumatoid arthritis and corticosteroid-induced osteoporosis. *Orthop. Clin. N.A.*, 1972, 3:571–583.
6. ELLIS, K.J., and COHN, S.H. Correlation between skeletal calcium mass and muscle mass in man. *J. Appl. Physiol.*, 1975, 38:455–460.
7. HAHN, T.J., BOISSEAU, V.C., and AVIOLI, L.V. Effect of chronic corticosteroid administration on diaphyseal and metaphyseal bone mass. *J. Clin. Endocrinol. Metab.*, 1974, 39:274–282.
8. MUELLER, M.N., and JURIST, J.M. Skeletal status in rheumatoid arthritis. A preliminary report. *Arthritis Rheum.*, 1973, 16:66–70.
9. MUELLER, M.N., MAZESS, R.B., and CAMERON, J.R. Corticosteroid therapy accelerated osteoporosis in rheumatoid arthritis. International Conference on Bone Mineral Measurement. Edited by R.B. Mazess, U.S. DHEW Publication No. (NIH)75–683, 1974, p. 195.
10. PAYNE, R.B., LITTLE, A.J., WILLIAMS, R.B., and MILNER, J.R. Interpretation of serum calcium in patients with abnormal serum proteins. *Brit. Med. J.*, 1973, 4:643–646.

Roentgen Signs of Vertebral Demineralization and Mineral Content of Peripheral Cancellous Bone. D. H. Banzer, U. Schneider, W. D. Risch, H. Botsch (Department of Radiology, Freie Universitat Berlin, Klinikum Steglitz, Hindenburgdamm 30, 1000 Berlin 45, Germany)

Of 4000 subjects measured in our laboratory between 1971–1975, 250 male and female patients were diagnosed on spinal roentgenograms as having osteoporosis. Lateral and antero-posterior roentgenograms of the thoracolumbar spine were available for 155 subjects for subsequent evaluation. The roentgenograms of the remaining patients were either incomplete or were preserved as microfilms and not suitable for detailed analysis. In addition the spinal roentgenograms of 52 patients on regular dialysis

TABLE 1.—Mean values of BMC (os calcis) in normal adults (N= 192).

AGE (YEARS) ♂	N	BMC		C–WIDTH	C–THICKNESS	HEIGHT	WEIGHT
		M ± SD (g/cm)	M ± SD (mg/cm^3)	(cm)	(cm)	(cm)	(kg)
21 – 30	18	3.87 ± 0.37	269 ± 39	54 ± 4	40 ± 4	179 ± 7	79 ± 12
31 – 40	30	3.70 ± 0.48	266 ± 31	53 ± 4	39 ± 2	177 ± 6	77 ± 10
41 – 50	12	3.32 ± 0.30	248 ± 30	54 ± 3	37 ± 2	171 ± 5	75 ± 8
51 – 60	13	3.35 ± 0.56	255 ± 30	56 ± 5	36 ± 4	172 ± 3	73 ± 8
61 – 70	11	3.08 ± 0.57	245 ± 46	54 ± 4	35 ± 3	170 ± 4	68 ± 8
71 – 80	9	3.67 ± 0.50	262 ± 24	59 ± 5	36 ± 3	168 ±10	77 ± 7

AGE (YEARS) ♀	N	BMC		C–WIDTH	C–THICKNESS	HEIGHT	WEIGHT
		M ± SD (g/cm)	M ± SD (mg/cm^3)	(cm)	(cm)	(cm)	(kg)
21 – 30	29	3.26 ± 0.48	277 ± 41	49 ± 4	36 ± 3	167 ± 7	68 ± 19
31 – 40	23	3.01 ± 0.41	260 ± 33	48 ± 3	35 ± 3	167 ±10	69 ± 8
41 – 50	18	2.94 ± 0.43	256 ± 26	50 ± 3	34 ± 2	165 ± 7	69 ± 14
51 – 60	20	2.77 ± 0.46	255 ± 28	48 ± 4	34 ± 2	162 ± 6	70 ± 15
61 – 70	9	2.77 ± 0.43	246 ± 18	50 ± 4	34 ± 5	162 ± 5	68 ± 7
71 – 80	1	(2.56)	(237)	(48)	(34)	(162)	(56)

TABLE 2.—Mean values of os calcis—BMC in g/cm (upper table) and BMC in mg/cm³ (lower table) in different states of vertebral osteopenia.

GROUP	$N_{0\text{-}3}$	0				1				2				3			
		N_0	M_0	SD	CV	N_1	M_1	SD	CV	N_2	M_2	SD	CV	N_3	M_3	SD	CV
OSTEOPOROSIS	56	5	2.44	0.35	15	29	2.28	0.46	20	4	2.13	0.49	23	18	2.00	0.79	39
ENTEROPATHY	27	2	2.83	0.77	27	11	2.46	0.45	18	7	2.26	0.48	21	7	1.45	0.40	27
RHEUMATOID ARTHRITIS	35	8	2.51	0.35	13	15	2.23	0.34	15	2	2.01	0.32	15	10	1.55	0.23	14
CASTRATION	20	3	2.68	0.58	21	9	2.42	0.30	12	2	1.68	0.1	0.5	6	1.68	0.31	18
HYPER-THYROIDISM	17	4	2.45	0.30	12	7	1.79	0.31	17	2	2.02	0.21	10	4	1.80	0.13	7
DIALYSIS	52	20	2.74	0.72	26	29	2.22	0.56	25	2	1.92	0.60	31	1	(2.09)	–	–

GROUP	$N_{0\text{-}3}$	0				1				2				3			
		N_0	M_0	SD	CV	N_1	M_1	SD	CV	N_2	M_2	SD	CV	N_3	M_3	SD	CV
OSTEOPOROSIS	56	5	191	19	9	29	179	33	18	4	159	22	13	18	142	44	30
ENTEROPATHY	27	2	220	16	7	11	184	20	10	7	169	24	14	7	115	33	28
RHEUMATOID ARTHRITIS	35	8	229	22	9	15	185	19	10	2	168	18	10	10	124	17	13
CASTRATION	20	3	219	41	18	9	194	18	9	2	176	16	9	6	140	27	19
HYPER-THYROIDISM	17	4	209	5	2	7	167	29	17	2	168	6	3	4	142	6	4
DIALYSIS	52	20	204	27	13	29	169	30	17	2	155	16	10	1	(150)	–	–

with histologically proven renal osteopathy were evaluated. A total of 140 women and 67 men were examined within an age group of 21–78 years. These subjects were divided into six groups:

1. Idiopathic osteoporosis of the senescent or postmenopausal state.
2. Gastroenteric disorders including total or subtotal gastrectomy, chronic duodenal ulcers, cholangitic cirrhosis, and chronic pancreatitis.
3. Rheumatoid arthritis.
4. Castration including ovarectomy and irradiation.
5. Hyperthyroidism.
6. Hemodialysis patients with renal osteopathy.

The varying stages of disease were not regarded for this study. The films were graded into four classes by three radiologists independently on the basis of a system modified after Goldsmith.[3]

The distinction between classes 0 and 1 was sometimes difficult to determine. In case of discrepancies the choice of the majority was followed. All class 0 patients of this study were proven as osteoporotic in follow-up roentgenograms 1 to 3 years later. The bone mineral content (BMC) of the os calcis was measured on the right side by a method based on the principles of photon absorptiometry.[2]

In comparison to normal adults (Table 1) the osteoporotic groups showed decreased BMC in all classes. Even in radiographically inconspicuous patients of class 0 the mean BMC of the heel bone showed deviations of 9%–25% in the different groups when compared to sex and age corresponding subjects (Table 2).

All groups of class 1 showed mean BMC significantly different from the normals (p in all groups <0.001). If we follow Babaiants,[1] who postulated a 30% demineralisation of the vertebral column in class 1, a corresponding percentage of bone demineralization can be measured in the os calcis. Classes 2 and 3 showed even greater losses that decreased in the gastroenteric group to an extreme of 54%. Class 2 (with compression signs of one vertebral body) was associated with a loss at a minimal average of 28% in the castration group, and a maximal average of 37% in the idiopathic osteoporosis group. No significant differences were found in BMC between class 1 and class 2 patients, but the number of subjects in the latter class was too small for accurate interpretation. Significant differences were seen between class 1 and 3 in the gastro-enteric, rheumatic, castration, and dialysis group ($p<0.001$), while in the osteoporotic and hyperthyreotic group significant differences were found between class 0 and class 3 ($p<0.05$ and $p<0.01$ respectively). All dialysis patients had histologically proven osteopathy with changes due to osteomalacia, secondary hyperparathyroidism and osteoporosis. Remarkable is the

fact that in 20 patients without roentgen signs of spinal osteoporosis or osteomalacia (class 0) an average demineralization of 22% was found in the heel bone.

The early detection of BMC loss in patients with axial osteoporosis seems to be possible by measuring the os calcis. Exact positioning of the measuring site in the central part of the bone (nearly rectangular dimensions), x-ray controls of the scan path, and of bone thickness are necessary. Patients with history of local disorders affecting the leg have to be excluded.

REFERENCES

1. Babaiants, L. Les osteoporoses. *Radiol. Clin.*, 1947, 16:291.
2. Cameron, J.R. and Sorenson, J.A. Measurement of bone mineral in vivo: an improved method. *Science*, 1963, 142:230.
3. Goldsmith, N.F., Johnston, J.O., Ury, H., Vose, G., and Colbert, C. Bone-mineral estimation in normal and osteoporotic women. *J. Bone Joint Surg.*, 1971, 53:83–100.

Partial Body Calcium Measurements by In Vivo Neutron Activation Analysis. J. E. Harrison, K. G. McNeill (Departments of Medicine and Physics, University of Toronto, Toronto, Ontario, Canada)

The calcium bone index (CaBI) based on measurements of Ca of the trunk and upper thighs by in vivo neutron activation analysis (IVNAA) has proved to be very useful in the study of metabolic bone disease. Reproducibility is $\pm 5.5\%$. The CaBI is expressed in terms of the measured ^{49}Ca count and the cube of a person's height and relates the measured Ca content to that of 23 normal adults less than 55 years old, all the same height. In these normals, the range of values is 0.82–1.2 (mean 1.00 ± 0.096) irrespective of sex. Twenty-seven elderly subjects (>55 years of age) had lower CaBI (mean 0.90 ± 0.14) in agreement with the reported aging loss of bone mineral. In 92 adults with idiopathic osteoporosis, CaBI varied from 0.9–0.4. In more than 85% of these subjects, CaBI were below 0.80. Mean CaBI was 0.65 (35% below mean values for normals <55 years of age).

Measurements were done on 35 patients with hyperthyroidism all under 55 years of age. Ten of the patients had significantly low CaBI (<0.8), indicating Ca loss in this disease. Six of the 35 patients have had repeat measurements, 6 to 19 months after treatment had produced a euthyroid state. There was no evidence of increased Ca following treatment. An insignificant mean decrease of 8% was observed.

In contrast to the data on osteoporotic patients, two patients with osteopetrosis and five cases with widespread Paget's disease had high CaBI (up to 2.5) in agreement with radiological assessment.

Patients with adult-onset osteomalacia had low CaBI in agreement with expectations, but a group of 14 adults with familial hypophosphatemic rickets had normal or above normal CaBI values despite their severe osteomalacia as shown by bone biopsy. This osteosclerosis appeared unrelated to vitamin D and phosphate therapy, but may be due to long-term mineralization of excess osteoid which continues to be produced. Sequential measurements on a 23-year-old male with vitamin D dependent rickets perhaps throws further light on this. He had never received adequate vitamin D therapy and had severe osteomalacia by radiological and histological assesssment as well as a low CaBI (0.55) value at the time of initial investigation. He was then treated with massive doses (100,000 IU/day) of vitamin D. After six months, he had radiological evidence of complete healing, and his CaBI doubled to 1.07. Over the next 18 months CaBI further increased to 1.52. This rapid increase can in part be attributed to the mineralization of excess osteoid. Subsequently (after 2–4 years of treatment) his CaBI decreased to normal values. The increase in Ca content was also shown by x-ray densitometry of the radius. However, these changes occurred over different time intervals. Whereas CaBI doubled in 6 months, the bone mineral mass (by x-ray densitometry) increased 40% in the same period, and doubled at 2 years.

In 34 subjects with renal osteodystrophy (ROD) (all <55 years of age) CaBI varied from well below to above normal (0.62–1.3). The high or normal values were in many cases associated with radiological and histological evidence of ROD and osteosclerosis. Five patients with low values studied sequentially had persistently low values over periods of up to 3 years. In three of these cases vertebral deformity and fractures developed during the 3 year period confirming the severe deficit of bone mineral. In other cases CaBI increased over 3 years on hemodialysis. The increased CaBI were in some cases associated with improvement in ROD and, in others, associated with progression of ROD and osteosclerosis.

Analysis of the trunk by IVNAA appears to show changes in Ca more quickly than does x-ray densitometry of the radius. CaBI provides useful diagnostic information on the skeletal status of patients and sequential measurements are useful in assessing progression of disease or response to therapy.

This work has been supported in part by the W. Garfield Weston Charitable Foundation.

Miscellaneous

Experimental Use of Photon Absorptiometry in Animal Research Models. H. Griffiths, R. E. Zimmerman, R. D. Hunt, H. H. Wolfe (Tufts New England Medical Center, 171 Harrison Avenue, Boston, Massachusetts 02111)

Twenty-two Rhesus monkeys were fed purified diets varying in calcium and fluoride content for 5 years. These animals were studied using routine radiography, and magnification studies (utilizing a 120μ RSI microfocal spot tube). The bone mineral content was measured by photon absorptiometry at the midshaft of the left radius and ulna. Biopsies of the iliac crest, tail (vertebral bodies), and ribs were taken following injections of tetracycline and DCAF. Undecalcified frozen tissue sections and decalcified paraffin sections were stained with H and E, von Kossa method, and basic fuchsin. Unstained sections were examined under ultraviolet light to determine the relative position of tetracycline and DCAF. Calcification fronts were determined by measuring the distance between the two fluorescent labels. The thickness of the osteoid seams and the osteoid index were determined. More recently, tissue culture techniques, spectrophotometry and electronmicroscopy have been added to our routine investigations. The results suggested that: 1) the addition of fluoride (50 ppm) to a diet containing 1% calcium resulted in a reduction in bone growth rate and resorption, without affecting bone size or density nor resulting in fluorosis; 2) a diet containing 0.15% calcium resulted in osteoporosis due to an increase in bone resorption; and 3) fluoride added to a similar low calcium diet prevented osteoporosis by reducing bone growth rate and resorption resulting in bones with normal density, but at the same time fluoride interfered with mineralization of osteoid leading to osteomalacia.

A group of 20 Cebus monkeys received diets either deficient in Vitamin D or with alterations of the Ca/PO_4 ratio. The animals were investigated using the techniques outlined above. Calcium deficient animals with high phosphate intake (1:4 ratio) and normocalcium/high phosphate animals (1:2 ratio) appeared to have a relatively normal skeleton by radiography, photon absorptiometry, and histology when compared to the control group of animals who have a calcium/phosphate ratio of 5:1.

A group of 30 rabbits were implanted with a VX_2 thyroid carcinoma in their left leg. This tumor secretes prostaglandin PGE_2 which is suppressable by Indocin. Preliminary results showed a marked resorption of bone in implanted animals who did not receive Indocin which could be demonstrated both by routine and magnification radiography as well as photon absorptiometry.

Finally a group of dogs is being investigated using radiographic, photon absorptiometric, and morphometric methods to ascertain if castration affects the bone in both male and female animals.

In the investigation of metabolic bone disease many parameters have to be used apart from the routine radiographic techniques. Magnification radiography is useful in determining alterations in morphological structures. Photon absorptiometry is also essential as a noninvasive technique for measuring the peripheral skeleton. Histological techniques should include the routine staining procedures as well as morphometric studies and studies of ultra structure.

REFERENCE

1. Griffiths, H.J., Hunt, R.D., Zimmerman, R.E., Finberg, H., Cuttino, J. The role of calcium and fluoride in osteoporosis in Rhesus monkeys. *Investigative Radiology* 10:3:263–268, 1975.

Percentages of Cortical and Trabecular Bone Mineral Mass in the Radius and Ulna. R. A. Schlenker (Center for Human Radiobiology, Argonne National Laboratory, Argonne, Illinois 60439)

Bone mineral content (BMC) by photon absorptiometry is often measured in the midshaft and the distal end of the radius. The midshaft site is recognized to be cortical bone. However, the distal site is often described ambiguously.[1,4] We measured the cortical and trabecular mass along the lengths of the distal halves of the radius and ulna in order to resolve this issue.

The subjects were four white females aged 21, 43, 63, and 85 years. The causes of death were suicide, internal hemorrhage, heart attack, and stroke respectively. Medical records showed that the 43-year-old fractured the left femoral neck with minimal trauma 4 months prior to death and that the 63-year-old was hemiplegic and confined to a nursing home for at least 22 months before she died.

Four adjacent segments, approximately 3 cm long, were cut from the radius and ulna. The segments were embedded in polymethyl methacrylate and cut serially into 2 mm thick sections. The sections were ashed to remove the embedding plastic, and the cortical and trabecular fractions were separated under a magnifying lens with tweezers. The separate fractions were re-ashed and weighed with an accuracy better than ± 1 mg.

The total bone mineral content (ash weight ÷ section thickness) and the percentage trabecular mass in the radii and ulnae are plotted as functions of percentage bone length in Figs. 1 and 2. (Percentage length may be converted to distance along the bone

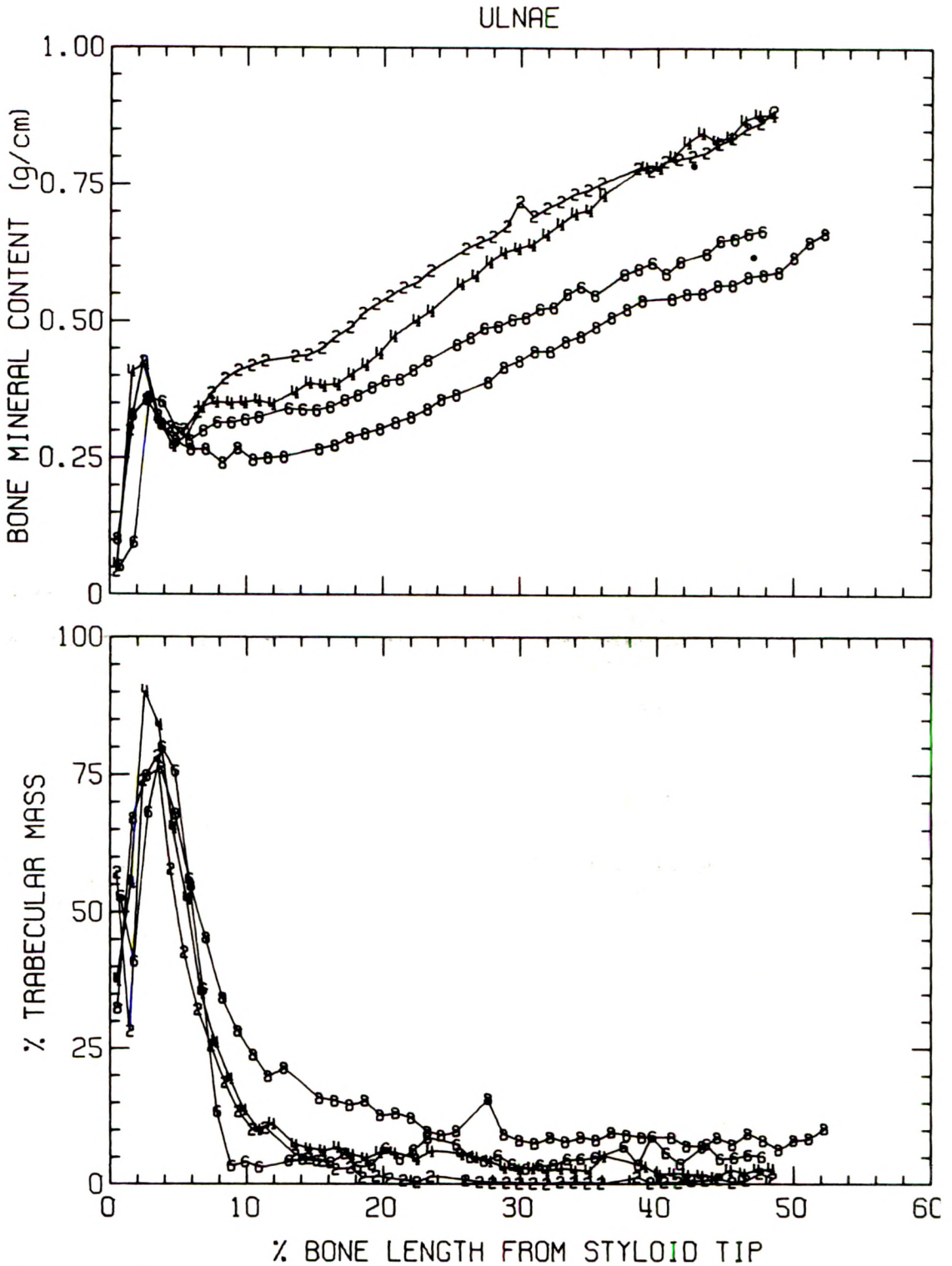


FIG. 1.—Bone mineral content and percentage trabecular bone in the radii as functions of percentage bone length. The numbers 2, 4, 6, and 8 show the actual data points and signify the 21, 43, 63, and 85 year olds respectively.

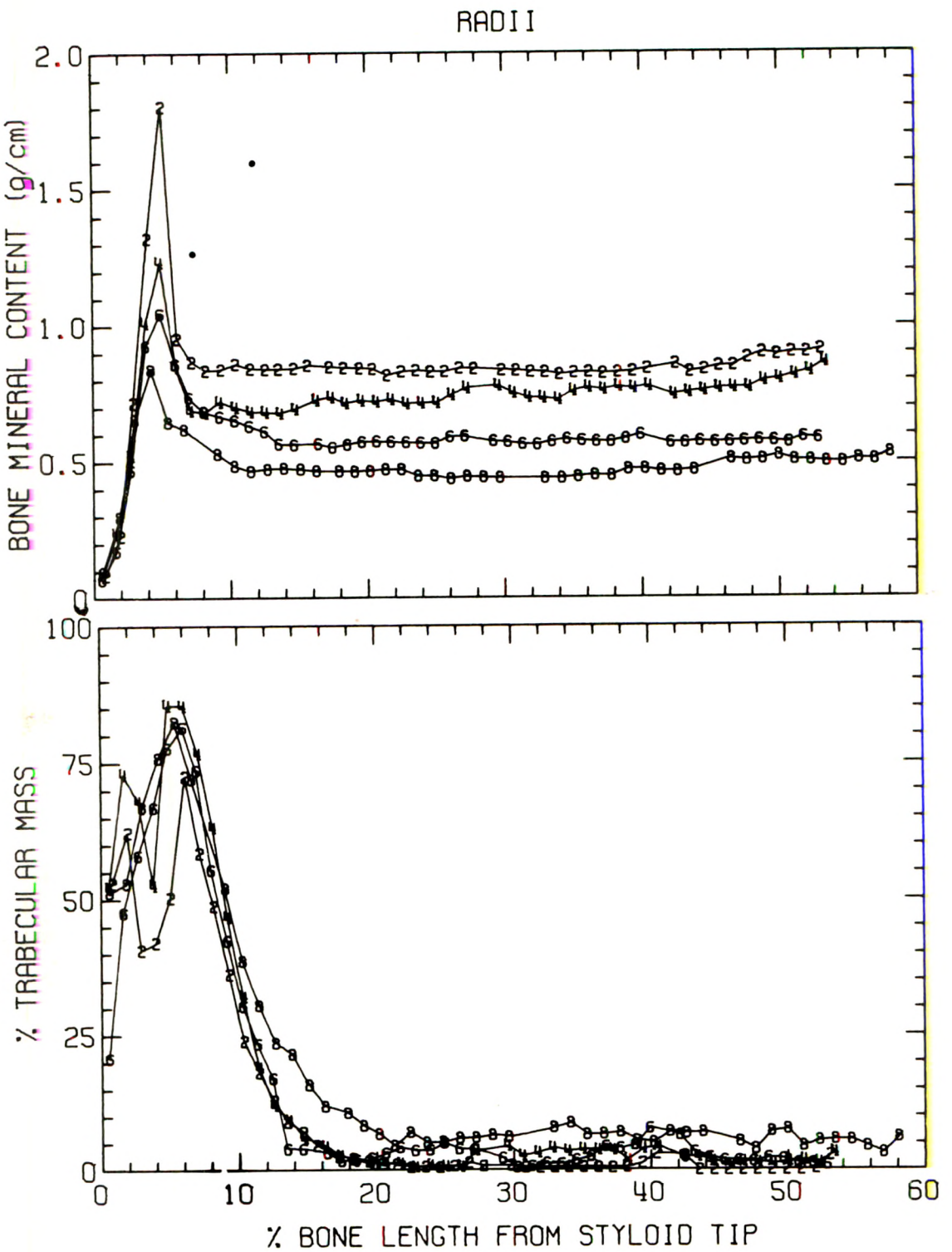


FIG. 2.—Bone mineral content and percentage trabecular bone in the ulnae as functions of percentage bone length. The numbers 2, 4, 6, and 8 show the actual data points and signify the 21, 43, 63, and 85 year olds respectively.

TABLE 1.—Trabecular bone mass at various sites on the distal radius and ulna.

Site Description	Percentage trabecular bone: Radius average (range)	Ulna average (range)
A band 7 mm wide, 1 cm from the ulnar styloid tip[5]	53 (42—61)	52 (45—58)
2 cm from the ulnar styloid tip[2]	24 (17—30)	21 (11—30)
1/10 of the length of the ulna from the ulnar styloid tip[3]	13 (6—24)	13 (4—26)
1/10 of the distance between the radial styloid tip and the olecranon of the ulna measured from the radial styloid tip[6]	27 (21—34)	24 (17—33)
3 cm from the radial styloid tip[4]	13 (10—18)	12 (4—20)

by multiplying by the bone length. In order of increasing age, the lengths are: 22.9, 22.7, 23.2, and 20.6 cm for the radii and 24.5, 24.1, 24.6, and 22.3 cm for the ulnae.) Trends in the data for all ages are: (1) a rapidly increasing and then decreasing BMC throughout the first 8% of the length of the radius and a nearly constant value thereafter; (2) a rapidly increasing and then decreasing BMC throughout the first 5% of the length of the ulna and a steadily increasing value thereafter; (3) a rapidly increasing and then decreasing percentage trabecular mass throughout the first 10–15% of the radius and ulna and a small value which fluctuates about a constant mean thereafter. Age related trends in the data are: (1) a loss of bone mass with increasing age; (2) an increase in the percentage trabecular mass in the radius and ulna at distances greater than about 20% of the bone length.

The data have been used to estimate the percentage trabecular mass in the radius and ulna at distal measurement sites (Table 1) used by five groups of investigators.[2,6] All sites are assumed to be 2 mm wide unless otherwise noted. The percentage trabecular mass in the radius at the most distal site averaged 53% (42%–61%). It was between 6% and 34% at the other four sites. The percentages in the ulna are about the same as in the radius at all sites. Thus the radius and ulna are predominantly cortical bone at the four most proximal measurement sites and are about equally divided between cortical and trabecular bone at the most distal site.

The ages, bone mineral contents, and bone lengths for the four subjects in this study span the normal range. Each of these parameters affects the percentage trabecular mass at distal measurement sites. The observed percentages of trabecular mass may also span a large part of the normal range and our conclusions could hold for the large normal populations in which BMC has been measured.[2,6] By far the greatest number of subjects have been measured at the four most proximal sites in Table 1. Thus the distal radius measurements in the literature have been made at sites which are predominantly cortical bone.

Work supported by the U.S. Energy Research and Development Administration.

REFERENCES

1. BEVAN, J.A. Bone mineral measurements in the clinical situation. Bone mineral determinations (Schmeling, P., ed.), Vol. 1, p. 89. Studsvik, Sweden: Aktiebolaget Atomenergi Publications No. AE–489, 1974.
2. GOLDSMITH, N.F., JOHNSTON, J.O., URY, H., VOSE, G., and COLBERT, C. Bone-mineral estimation in normal and osteoporotic women. *J. Bone Jt. Surg.* 1971, 53A:83–100.
3. HEER, K.R., ROSLI, A., LAUFFENBURGER, TH., GUNCAGA, J., DAMBACHER, M.A., and HAAS, H.G. Bone mineral loss in the pre-menopause. International Conference on Bone Mineral Measurement (Mazess, R.B., ed.), 214–221. Washington: U.S. Department of Health, Education and Welfare Publication No. (NIH) 75–683, 1974.
4. JOHNSTON, C.C., SMITH, D.M., YU, P., and DEISS, W.P. In vivo measurement of bone mass in the radius. *Metabolism*, 1968, 17:1140–1153.
5. NILSSON, B.E., and WESTLIN, N.E. Bone mass and Colle's fracture. International Conference on Bone Mineral Measurement (Mazess, R.B., ed.), p. 362–368. Washington: U.S. Department of Health, Education and Welfare Publication No. (NIH) 75–683, 1974.
6. SMITH, D.M., JOHNSTON, C.C., and YU, P. Bone mass in the radius, a reflection of the axial skeleton. Proceedings of Bone Measurement Conference (Cameron, J.R., ed.), 398–404. Washington: AEC CONF–700515, 1970.

Comparison of Bone Mineral Content (BMC) in Different Skeletal Sites. U. Schneider, D. Banzer, M. Bange (Klinik fur Radiologie und Nuklearmedizin, Klinikum Steglitz der Freien Universitat Berlin, Berlin, West Germany)

We used a photon absorptiometric[1] linear scanner and a computer-based data evaluation system to perform more than 4,000 measurements on the calcaneus. Luther[2] reported a poor correlation (0.3 for $n = 50$) between the os calcis and the vertebral body. He used a chemical method and the Compton backscatter method and studied small cylindrical samples of approximately 1 cm^3 volume, so in fact he made point measurements. We wanted to determine the correlation between the os calcis and other bones by our usual scanning method. We assumed that measurement of the whole cross-section area of a bone might give better results, since these bones are not very homogeneous. We measured the humerus, the

calcaneus, and the second lumbar vertebra in 10 cases.

The vertebral bodies were measured both in the saggital plane and in the horizontal plane. The saggital scans gave better correlations with the other bones. Since the determination of the cross-section area of the vertebral body is difficult, we used the BMC values per cm. The correlations were significant ($p<0.05$). The os calcis seemed to reflect the BMC of the vertebral body ($r=0.83$) and the humerus ($r=0.82$). The correlation between the humerus and vertebra was somewhat lower ($r=0.72$). Wilson[3] found a correlation of 0.6 to 0.7 between radius and vertebra. The comparison of our results with the poor correlation obtained with the Compton backscatter method suggested that results obtained with such point measurements may not be representative although they may be precise.

REFERENCES

1. Cameron, J.R. and Sorenson, J.A. Measurement of bone mineral in vivo: an improved method. *Science*, 1963, 142:230–232.
2. Luther, R. Correlation of os calcis and spinal bone by compton scattering. Intern. Conf. on Bone Mineral Measurement, Chicago 1973, DHEW Publ. No. (NIH)75–683, 161–618.
3. Wilson, C.R. Prediction of femoral neck and spine bone mineral content from the BMC of the radius or ulna and the relationship between bone strength and BMC. Intern. Conf. on Bone Mineral Measurement, Chicago 1973, DHEW Publ. No. (NIH)75–683, 51–59.

A Rectilinear Scanning Technique for Bone Mineral Measurements in Animals. J. A. Bevan, H. E. Black, L. A. Oliver (Miami Valley Laboratories, Procter & Gamble, Cincinnati, Ohio 45247)

Sequential measurements of bone mineral content (BMC) by means of the linear scan photon absorptiometry are often adversely affected by repositioning errors. This problem significantly reduces the sensitivity of the method except in the uniform regions of the long bones where the response to factors which affect bone may be slow compared to the situation at less uniform skeletal sites. Various repositioning aids have been devised in this and other laboratories but the need arose for a more versatile technique for animal studies and for a more general method of reducing repositioning errors. The area scanning principle[1,2,3] accomplishes this, partly by measuring a greater volume of bone than the linear technique, so that the non-overlapping regions in sequential measurements are a small fraction of the whole, and partly because the process of overlapping the area scans results in better repositioning, per se.

A small rectilinear scanner was constructed by mounting a Norland Bone Mineral Analyzer on a motorized dovetail slide. A control unit produces the rectilinear scanning pattern by sequentially operating the Norland drive system and the dovetail slide motor. An area of up to 10×10 cm may be covered although, in practice, it is usual to scan a 2–3 cm length of bone. The animal is anaesthetized during the procedure and lies on the scanning table with the chosen limb enclosed in soft-tissue equivalent material. In the continuous mode of operation the logarithm of the count rate is plotted on an integrating chart recorder which simultaneously records the absorption profile and its corresponding area during each successive traverse across the bone. Since the area is proportional to the BMC for each traverse, one obtains a record of the distribution of BMC along the bone. Alternatively, the Norland unit (slightly modified) may be operated in its usual manner to provide direct readout of BMC and bone width. The dovetail slide must be incremented between scans in order to produce the area scan.

The BMC data is calibrated and a smooth curve is fitted through the points by means of the computational technique known as the spline function.[4] In order to compare sequential measurements, the curves are overlaid by matching prominent features. It is then possible to measure changes in BMC, either point-by-point along the bone axis, or by integrating the curves between limits which may be based on anatomical considerations. Bone width data may also be analyzed in a similar manner.

Area scanning was used in a study on the short-term effects of cortisol on the rabbit skeleton. Previous histological studies[5,6] have established that high doses of corticosteroids produce an increase in osteoclastic resorption. Twenty-four 4 kg adult female New Zealand white rabbits were randomly assigned to four dose groups of six animals each. Three of the groups received daily subcutaneous injections of cortisol at levels of 0.1, 0.4, and 1.6 mg/kg body weight for 7 weeks. The fourth control group re-

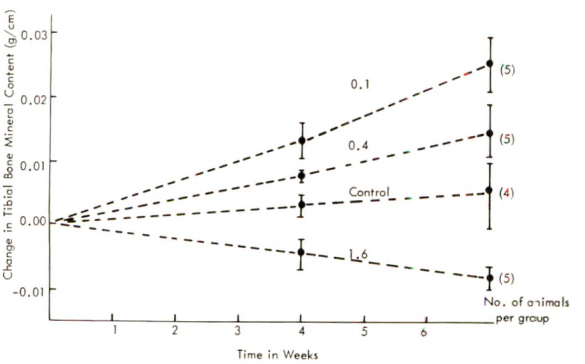


FIG. 1.—Bone mineral content (tibia). Change in BMC compared to baseline values for rabbits treated with cortisol (doses in mg/kg/day).

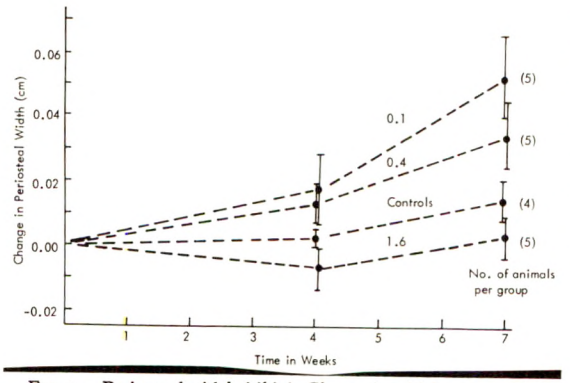


FIG. 2.—Periosteal width (tibia). Change in width compared to baseline values for rabbits treated with cortisol (doses in mg/kg /day).

ceived saline injections. BMC was measured in vivo at baseline and at four weeks with the animals anaesthetized. The final measurements were obtained on limbs excised immediately after sacrifice. The scanning site consisted of a 2 cm region of the distal tibia measured proximally from the epiphyseal plate. This included all of the distal metaphysis and a portion of uniform diaphysis. Judging from radiographs, there was little trabecular bone in this region.

Except for a dense area at the epiphyseal plate, BMC was quite uniform in the distal tibia. The average BMC was calculated over this uniform region for the 19 rabbits remaining in the study. Figure 1 shows the mean changes in BMC for each treatment group relative to baseline. There was a significant ($p<.01$) increase in BMC in the 0.1 mg/kg dose group, and a significant ($p<.05$) decrease in the 1.6 mg/kg dose group, compared to controls. Figure 2 shows the changes in periosteal width as measured by this technique. There was a significant ($p<.05$) increase in periosteal width in the 0.1 mg/kg group. The group that received the lowest dose level of cortisol showed increase periosteal apposition, whereas, as the dose was increased to its highest level, periosteal apposition was halted and there was a loss of bone from within the cortical-endosteal region.

REFERENCES

1. VOGEL, J.M., and ANDERSON, J.T. Rectilinear transmission scanning of irregular bones for quantification of mineral content. *J. Nucl. Med.*, 1972, 13:13–18.
2. SPURRELL, F.A., BRENES, J., and WARBEL, P. Tibial bone mineral distribution as influenced by calcium, phosphorus, and vitamin D feeding levels in the growing turkey. *Proc. Int. Bone Mineral Conf.*, 1974, DHEW Publ. No. (NIH) 75–683, 282–284.
3. FISHER, G.L., SCHWIND, J.A., and GOLDMAN, M. A photon absorptiometer for in vivo and in vitro measurement of small animal bone density. *Biomed. Eng.*, 1974, 9, 5:196–199.
4. GREVILLE, T.N.E. Functions, Interpolation, and Numerical Quadrature, John Wiley, New York, 1967, 156–168.
5. JEE, W.S.S., BLACKWOOD, E.L., DOCKUM, N.L., HASLAM, R.K., and KINCL, F.A. Bio-assay of responses of growing bones to cortisol. *Clin. Orthop.* 1966, 49:39–63.
6. DUNCAN, H. Osteoporosis in rheumatoid arthritis and corticosteroid induced osteoporosis., *Orthop. Clin. of North Am.*, 1972, 3, 3:571–583.

EDITORIAL

BONE MINERAL MEASUREMENT

This issue contains a section of abstracts of 44 papers from the "Transactions of the Third International Conference on Bone Mineral Measurement" held January 26–28, 1976, in New Orleans, Louisiana. These have been carefully edited and condensed without sacrificing essential information. A favorable response to this section will encourage the Journal to consider reporting other scientific programs in a similar manner.

These abstracts contain a wide range of information on the techniques of bone mineral measurement and their practical clinical application. They further indicate new developments and trends in this field. As with any publication of nonreviewed articles, defects in conclusions based on faulty material and methods may occur, or discussions may not be appropriate for the experimental evidence advanced. The advantages, however, of prompt publication of current and comprehensive information on such an important subject are thought to outweigh this possible objection.

Accurate measurement of bone mineral content may be an important tool in the early clinical diagnosis of certain metabolic bone diseases, in particular, osteoporosis. Further, a sensitive method is important in the treatment of metabolic bone disease and detecting abnormality early enough for appropriate management in such diseases as renal osteodystrophy. Such detection methods also become important in the study of the pathogenesis of many disease processes and their effects on bone, whether direct or indirect.

For example, when we attempted to identify patients with osteopenia in an attempt to link spinal osteopenia with alveolar bone osteopenia (periodontal disease) [1], we gathered cases from the New York Hospital with the diagnosis of osteopenia. An astonishing number of these patients also were found to have diabetes mellitus. It was not clear whether the osteopenia was secondary to some complication of diabetes, a direct effect of the disease on bone, or due to treatment of the disease (i.e., insulin or diet). The abstract by Rinje et al. seems to indicate that it is a direct effect of disease or its treatment. In studying the bone mineral content in patients treated with anticonvulsants or various forms of vitamin D, Christiansen and Rodbro have shed new light on the mechanism of the production of osteomalacia and also on the metabolism of vitamin D. These are just a few examples in which the technique of bone mineral measurement may give new insights into the pathogenesis of disease processes.

With expanding applications of computed tomography, it is of particular interest to discover work being done on the place of CT scanning in determining bone composition and the "density" of the components of bone. Elsasser and Ruegsegger offer some preliminary results.

This section of abstracts if offered as an overview of bone mineral technology; its application to various clinical situations; and its relationship to certain disease processes and the mechanisms by which they affect bone. Hopefully reader interest in these reports will justify their presentation here.

JOSEPH P. WHALEN

REFERENCE

1. Krook L, Whalen JP, Lesser GV, Berens DL: Experimental studies on osteoporosis, in *Methods and Achievements in Experimental Pathology*, edited by Jasman G and Cantin M, Basel, Karger, 1975

AMERICAN ROENTGEN RAY SOCIETY ANNUAL MEETING

The 77th annual meeting of the society (ARRS) will feature an expanded program of 96 papers when it opens in Washington, D.C. The meeting will run September 21–24 with double sessions each day to accommodate the enlarged scientific program.

Papers have been grouped into categories, so that radiologists seeking a series of reports on a subject will find them in an appropriate cluster. The ARRS program committee has also tried to keep the needs of the general radiologist in mind, according to Seymour F. Ochsner, ARRS president-elect.

The meeting will formally open Tuesday, September 21, at 8:30 a.m. with the installation of the new president by outgoing president Ted F. Leigh and Hymer L. Friedell, chairman of the executive council. Ochsner will deliver a presidential address before the scientific sessions begin. The following day Elias G. Theros, professor of radiology at the University of California, Los Angeles, will deliver the 1976 Caldwell Lecture. His topic is "The Varying Manifestations of Pulmonary Neoplasms." Theros previously was chief and registrar, American Registry of Radiologic Pathology of the Armed Forces Institute of Pathology.

"Instruction courses under the able direction of Eugene Gedgaudas, will be presented as usual during the meeting," Ochsner adds. A course program and registration information will be published in the July issue. At least a dozen courses will be offered daily on a variety of subjects. Courses 1½ hr in length will be held September 20–24. A special categorical course on bone and joint radiology will begin the afternoon of Sunday, September 19, and continue afternoons through Thursday, concluding on Friday morning. A number of experts will be involved in the 16 hr of concentrated bone and joint instruction.

As in past years, there will be award paper presentations. Societies sponsoring the awards include the Society for Pediatric Radiology, the Society for Neuroradiology, and the Society of Gastrointestinal Radiologists. Also scheduled is the ARRS President's Award paper, the paper judged by the research and education committee to be the best submitted by a resident (coauthors permitted) on a clinical application of radiology. The winner receives a $1,000 honorarium, a certificate, and the opportunity to present the paper at the annual meeting.

Scientific and technical exhibits will be open throughout the meeting. Richard C. Pfister heads the scientific exhibits committee while George A. Kling is in charge of technical exhibits.

Ochsner reports that a number of societies will hold meetings sequential to the ARRS, including the Societies for Pediatric Radiology, Uroradiology, Photo-optical Instrumentation Engineers, and the American Thermographic Society.

Social events will include the annual golf tournament, a tennis tournament, ladies' program, and reception for all registered physicians and wives. The golf and tennis tournaments are open to nonsociety members. Information and registration forms for the golf tourney are available from Ralph M. Caulk, Department of Radiology, Washington Hospital, 110 Irving Street, N.W., Washington, D.C. 20010. Tennis information and forms may be obtained from Bruce L. McClennan, Department of Radiology, George Washington University Hospital, Washington, D.C. 20006. All ARRS members will receive tournament information.

ARRS registration and housing forms follow the preliminary program information at the end of this article.

Preliminary Program

77th ANNUAL MEETING AMERICAN ROENTGEN RAY SOCIETY

September 21–24, 1976

Washington Hilton Hotel

Tuesday, Sept. 21
8:30 a.m.

Call to order 77th annual meeting: Ted F. Leigh, Atlanta, Georgia, president
Installation of President-Elect Seymour Fiske Ochsner, New Orleans, Louisiana by Ted F. Leigh and Hymer L. Friedell, Cleveland, Ohio, chairman, executive council
Presidential Address: Seymour F. Ochsner

9 a.m.

I. Pediatric Radiology/Mammography

Award Paper, **John Caffey Award,** Society of Pediatric Radiology

Problem of low radiation doses in radiologic practice. GV Dalrymple, ML Baker, J Vandergrift, Little Rock, Arkansas

Infantile and juvenile cerebral aneurysms. S Batnitzky, J Muller, Indianapolis, Indiana

Horner's syndrome in children, protean roentgenographic manifestions. AS Tucker, MW Levinsohn, Cleveland, Ohio

Persistence of the fetal circulation: radiological considerations. EF Silverstein, K Ellis, WJ Casarella, WM Gersony, CN Steeg, New York, New York

The effect of breathing 100% oxygen on the angiographic demonstration of left to right shunts in the pediatric age group. H Spindola-Franco, R Eisenberg, Bronx, New York

Necrotizing enterocolitis following open heart surgery employing hypothermia and cardiopulmonary bypass. PK Kleinman, P Winchester, PW Brill, New York, New York

Acute bowing fractures of the forearm in children—a frequently missed injury. JE Crowe, Winston-Salem, North Carolina, LE Swischuk, Galveston, Texas

Morning-glory disc and defect of the base of skull. HY Yune, FD Ellis, Indianapolis, Indiana

Low-dose radiography in pediatric radiology. RL Wesenberg, R Rossi, S Hilton, Denver, Colorado

Min-R mammography. RH Mintzer, HJ Matthies, HL Neiman, LF Rogers, PJP Lin, Chicago, Illinois

Dose reduction in Xeroradiography of the breast. JN Wolfe, W Van de Riet, Detroit, Michigan

9 a.m.

II. Urologic Radiology/Oncology

Emergency percutaneous nephropyelostomy—experience with 30 patients. ZL Barbaric, BP Wood, Rochester, New York

Percutaneous (antegrade) pyelography in the adult. RC Pfister, JH Newhouse, IC Yoder, Boston, Massachusetts

The spectrum of urologic disease in regional enteritis. GD Kruglik, HL Neiman, LF Rogers, EJ Nudelman, Chicago, Illinois

Complications of renal cyst puncture and aspiration (a survey). E Lang, Shreveport, Louisiana

Roentgenologic manifestations of renal carcinoma bone metastases. GS Forbes, RA McLeod, RR Hattery, Rochester, Minnesota

High dose urography: instance and relationship to spontaneous peripelvic extravasation. ME Bernadino, BL McClennan, Washington, D.C.

The role of roentgenology, nuclear medicine and ultrasound in the diagnosis of urine extravasation following renal transplantation. D Spigos, W Tan, A Roddy, D Pavel, W Kaplan, O Jonasson, V Capek, Chicago, Illinois

The application of newer screen-film systems to excretion urography. DF Stables, R Rossi, Denver, Colorado

Renal transitional-cell carcinomas—how diagnostic is the angiogram? SM Goldman, CH Meng, RI White Jr, RC Naraval, SS Siegelman, AB Diamond, SL Kaufman, DR Harrington, Baltimore, Maryland

A modified radiation therapy regimen for Hodgkin's disease in the third trimester of pregnancy. JG Conley, A Jacobson, Louisville, Kentucky

Clinically occult vs. mammographically occult breast cancers: a comparative study of 117 lesions detected on screening 16,754 women. SA Feig, GF Schwartz, GS Shaber, HI Libshitz, J Edeiken, R Newlinger, R Curley, JD Wallace, Philadelphia, Pennsylvania

Growth arrest of pulmonary metastases in papillary thyroid carcinoma. HY Kressel, GL Kalifa, WR Webb, G Gamsu, San Francisco, California

Redistribution and regeneration patterns of bone marrow after extended field radiation in Hodgkin's disease. P Rubin, RE O'Mara, D Nelson, C Scarantino, Rochester, New York

Computerized tomography scanning and computerized radiation therapy treatment planning. GL Jelden, Cleveland, Ohio

Wednesday, Sept. 22

8:30 a.m.

I. Chest Radiology

Breast thermography: demonstration of differential vascular patterns in breast carcinoma. CHJ Chang, JL Sibala, NL Martin, Kansas City, Kansas

The effect of energy (kVp) on the detectability of pulmonary nodules. EE Christensen, GW Dietz, RC Murry, JG Moore, EM Stokely, Dallas, Texas

Air in the esophagus: a frequent roentgen finding. AV Proto, EJ Lane, Syracuse, New York

Accuracy and specimen adequacy of percutaneous lung biopsy. WR Boyd, GL Ballard, Loma Linda, California

Non-malignant lymphoid disorders of the chest (a radiologic-pathologic correlation study). DS Feigin, FM King, Washington, D.C., SS Siegelman, Baltimore, Maryland, EG Theros, Los Angeles, California

The course of methotrexate induced lung disease. CE Putman, HD Sostman, RA Matthay, GJ Walker Smith, New Haven, Connecticut

PEEP: radiographic features and associated complications. TC McLoud, PG Barash, CE Ravin, New Haven, Connecticut

The pulmonary manifestations of adult leukemia. S Ulreich, TC McLoud, CE Putman, New Haven, Connecticut

Mediastinitis from odontogenic and deep cervical infections: anatomical pathways of propagation. R Moncada, R Warpeha, J Pickleman, M Spak, M Cardosa, O Stuteville, H White, Maywood, Illinois

Factors predisposing to dissecting aneurysm of the aorta. JA Michal III, RB Jaffe, Salt Lake City, Utah

Radiology of the respiratory diaphragm. AF Govoni, JP Whalen, New York, New York

8:30 a.m.

II. Angiography

Award Paper, American Society of Neuroradiology

Fluoroscopically aided femoral artery puncture. CT Dotter, J Rösch, M Robinson, Portland, Oregon

Hemodynamically significant anomalies of the coronary arteries. DC Levin, K Fellows, HL Abrams, Boston, Massachusetts

Collateral circulation and regional myocardial contractility. TA Sos, Boston, Massachusetts

The combined use of roentgen angiography and radioisotope (computer processed) angiography in the diagnosis of great vessel diseases. DG Pavel, DG Spigos, E Byron, V Capek, Chicago, Illinois

Predictors of success and survival in the treatment of variceal bleeding by selective intra-arterial vasopressin infusion. SL Kaufman, DP Harrington, KH Barth, WC Maddrey, RI White Jr, Baltimore, Maryland

Importance of arteriography in preoperative evaluation of pancreatic pseudocysts. DC Levin, H Eisenberg, R Wilson, Boston, Massachusetts

The role of subselective angiography in the diagnosis of islet cell tumors of the pancreas. ME Clouse, P Costello, Boston, Massachusetts

The value of hepatic venography and wedge hepatic vein pressure measurements in diffuse liver disease. JA Cavaluzzi, DP Harrington, SL Kaufman, KH Barth, WC Maddrey, RI White Jr, Baltimore, Maryland

Selective renal occlusion phlebography with a balloon catheter. D Novak, J Weber, Hamburg, West Germany

Therapeutic balloon occlusion of the inferior vena cava. JP Petasnick, JA Hunter, R Sessions, Chicago, Illinois

Wednesday, Sept. 22

11:30 a.m.

Caldwell Lecture: The varying manifestations of pulmonary neoplasms: a roentgenologic-pathologic correlative study. Elias G. Theros, Los Angeles, California

Thursday, Sept. 23

8:30 a.m.

I. Gastro-Intestinal/Biliary Radiology

Award Paper. The Society of Gastrointestinal Radiologists

The radiologic manifestations of idiopathic intestinal pseudoobstruction. MD Schuffler, FE Templeton, CA Rohrmann, Seattle, Washington

Calcified primary tumors of the gastrointestinal tract. GG Ghahremani, MA Meyers, RB Port, Richmond, Virginia

Gastrointestinal manifestations of adult hepatorenal polycystic disease. S Ulreich, M Burrell, R Lowman, New Haven, Connecticut

Bleeding pyloroduodenal ulcers and intraarterial vasopressin: clinical results. AC Waltman, D Schaffer, CA Athanasoulis, RA Novelline, WC Wood, LW Ottinger, Boston, Massachusetts

Inflammatory manifestations and gangrene of the transverse colon secondary to pancreatitis. WM Thompson, FM Kelvin, RP Rice, Durham, North Carolina

Cathartic colon. Seuk Ky Kim, TR Simon, R Rozanski, Syracuse, New York

The effect of bile salts on the biliary excretion of radiographic contrast materials. RN Berk, PM Loeb, A Coco-Frankel, J Lee Barnhart, Dallas, Texas

8:30 a.m.

II. Angiography/Orthopedic Radiology

President's award paper

Saralasin infusion: a screening test for renal vascular hypertension. CJ Tegtmeyer, EA Latour, CR Ayers, D Vaughan Jr, RM Carey, Charlottesville, Virginia

A method to determine the minimal visualizable blood vessel diameter in magnification angiography. T Sandor, DF Adams, Boston, Massachusetts

Transcatheter pressure sensor—clinical application. CT Dotter, TB Hutchins IV, Portland, Oregon

Electromagnetic rheo-angiometry: an extension of selective angiography. A Kolin, RN MacAlpin, RJ Steckel, Los Angeles, California

Radiology in surgical decompression of exophthalmos. GD Potter, New York, New York

Supine myelography in patients with spinal dysraphism. PJ Sones, Atlanta, Georgia

Aspects of cervical spine trauma: the mach effect at C-2. RH Daffner, Louisville, Kentucky

10:30 a.m.

Announcement of Scientific Exhibits Awards

Infusion tomography of the gallbladder: a clinical and experimental assessment of its value. R Moncada, M Cardosa, R Danley, J Rodriguez, K Kimura, J Pickleman, H Byun, Maywood, Illinois

Systemic absorption of Diatrizoate during endoscopic retrograde cholangiopancreatography (ERC). FX Bride, P Mayer Loeb, RN Berk, J Manton, Dallas, Texas

Choledochal cyst in adults. GG Ghahremani, CT Lu, RM Woodlief, VP Chuang, Richmond, Virginia

Fine needle transhepatic cholangiography: a new approach to obstructive jaundice. JT Ferrucci Jr, J Wittenberg, R Sarno, JR Dreyfuss, Boston, Massachusetts

10:30 a.m.

Announcement of Scientific Exhibits Awards

Discogenic vertebral sclerosis. DD Sauser, A Beth Goldman, JJ Kaye, New York, New York

Radiology of shoulder joint prostheses. F Jaffer SM Wyman, Boston, Massachusetts

Osteitis deformans of the hip joint. AB Goldman, P Bullough, S Kammerman, M Ambos, New York, New York

Myositis ossificans: value of angiography in the differential diagnosis. I Yaghmai, Richmond, Virginia

Injuries of the medial epicondylar ossification center of the humerus. LF Rogers, J Chessare, MO Tachdjian, Chicago, Illinois



The endoscopic retrograde intrahepatic cholangiogram, radiographic findings in intrahepatic disease. CA Rohrmann Jr, HJ Ansel, EA Ayoola, SE Silvis, JA Vennes, Seattle, Washington

Correlation of pathology, angiography and radioisotope scanning in the diagnosis of benign liver tumors. WJ Casarella, PM Johnson, D Knowles, M Wolf, New York, New York

Visualization of the lateral surface of the liver (Hellmer's sign) secondary to extra-peritoneal fluid collections. D Wixson, E Kazam, JP Whalen, New York, New York

Subchondral bone cysts (geodes) in arthritic disorders: pathogenesis and roentgen appearance. D Resnick, G Niwayama, RD Coutts, San Diego, California

Parosteal (juxta-cortical) osteogenic sarcoma—roentgen findings in a series of 30 patients. J Smith, S Ahuja, A Villaein, P Bullough, A Huvos, R Marcove, New York, New York

Friday, Sept. 24

8:30 a.m.

I. Computerized Tomography/General Radiology

A statistical description of the "normal" computerized brain scan. DF Reese, PC O'Brien, GW Beeler Jr, EC McCullough, Rochester, Minnesota

Computerized tomography of brain abscess. LC Chiu, JC Jensen, SH Cornell, JH Christie, Iowa City, Iowa

Computerized tomography in diseases of the chest. SLG Rothman, WE Allen III, CE Putman, HC Redman, New Haven, Connecticut

CAT in the diagnosis of obstructive jaundice. HL Stein, JB Naidich, RA Hyman, Manhasset, New York

Computerized tomography of the spine. SLG Rothman, A Iosue, WE Allen III, SC Orphanoudakis, New Haven, Connecticut

Computed tomography in the evaluation of genitourinary tract pathology. SA Kieffer, ET Dailey, WM Dinn, Syracuse, New York

Computerized tomography with the GE five-second body scanner. M Korobkin, D Boyd, San Francisco, California

Hyperthyroidism: does radioiodine therapy represent a health hazard? GV Dalrymple, CM Boyd, Little Rock, Arkansas

Radiological diseases in exotic animals which have human equivalents. M Bush, AE James Jr, Nashville, Tennessee

8:30 a.m.

II. Ultrasonography/General Radiology

Combined mammographic-sonographic evaluation of breast masses. HS Teixidor, E Kazam, New York, New York

Diagnosis of gynecologic pelvic masses by grey scale ultrasonography. An analysis of criteria, accuracy and specificity. TL Lawson, JN Albarelli, Washington, D.C.

Combined radionuclide and ultrasonic assessment of abdominal masses in children. GF Gates, JH Miller, Los Angeles, California

Evaluation of the non-functioning kidney by sonography. M Behan, E Kazam, D Wixson, WR Pitts Jr, New York, New York

The role of grey-scale ultrasonography in the diagnosis of medullary cystic disease of the kidney. A Ted Rosenfield, NJ Siegel, KJW Taylor, New Haven, Connecticut

Comparison of ultrasound and isotope examination of the liver. KJW Taylor, D Sullivan, AT Rosenfield, New Haven, Connecticut

Ultrasound of biliary duct system, a comparison with percutaneous transhepatic cholangiography. HL Neiman, RA Mintzer, Chicago, Illinois

Methods for pre- and post-operative radiologic evaluation of the pancreatic ducts. MK Bilbao, Portland, Oregon

Radionuclide perfusion lymphangiography: a follow-up report. RJ Steckel, S Furmanski, JD Collins, N Poe, Los Angeles, California

Advance Registration: 77th Annual ARRS Meeting

Washington, D.C., Sept. 21–24, 1976

If you plan to attend, please fill out the following form.
Official badges and program booklets will be available at the registration desk in the Washington Hilton Hotel at the time of the meeting.

Preregistration by mail will be accepted only until September 3, 1976.

MAIL TO: THE AMERICAN ROENTGEN RAY SOCIETY

20 North Wacker Drive, Suite 2920, Chicago, Illinois 60606

Check one box, and include the proper fee in your envelope:

☐ Member of the American Roentgen Ray Society (no fee).
☐ Non-member (registration fee $25.00).
☐ Physician in training (registration fee $15.00). Be sure to include the certification on bottom of this form.

Please print or type:

Name _____

Street _____

City _____

State or Province and zip _____

☐ Check here if you wish a program of events for ladies. Indicate the address to which this is to be sent.

Name _____

Street _____

City _____

State or Province and zip _____

FOR PHYSICIANS IN TRAINING:

_____ is in training in my department.

_____
Department Chief

_____
Date

_____
Institution

APPLICATION FOR HOTEL RESERVATIONS

AMERICAN ROENTGEN RAY SOCIETY—SEPTEMBER 19–24, 1976

PARTICIPATING HOTELS AND RATES

	Singles starting at	Doubles starting at (2 people)	Twins starting at (2 people)
Washington Hilton	$32	$44	$44
Statler Hilton	$32	$44	$44
Embassy Row	$38	$48	$48

RETURN APPLICATION BEFORE SEPTEMBER 1, 1976 to:

ARRS Housing Bureau
1129 20th Street, N.W.
Washington, D.C. 20036

NOTE: All changes and cancellations must be made through housing bureau.

Please reserve the following accommodations:

____ Single room ____ Double-bed room ____ Twin-bed room

____ Parlor and bedroom suite ____ Parlor and two bedroom suite

First choice, hotel _____ Second choice, hotel _____

Third choice, hotel _____

Arrival date _____ Hour (A.M.) _____ (P.M.) _____

Departure date _____ Hour (A.M.) _____ (P.M.) _____

(Reservations will be held until 6 P.M., unless requested otherwise.)

Names and addresses of all occupants of rooms: Incomplete information will delay hotel assignment.

Name _____ Name _____

Address _____ Address _____

City _____ State _____ Zip _____ City _____ State _____ Zip _____

Name _____ Name _____

Address _____ Address _____

City _____ State _____ Zip _____ City _____ State _____ Zip _____

Individual Requesting Reservations:

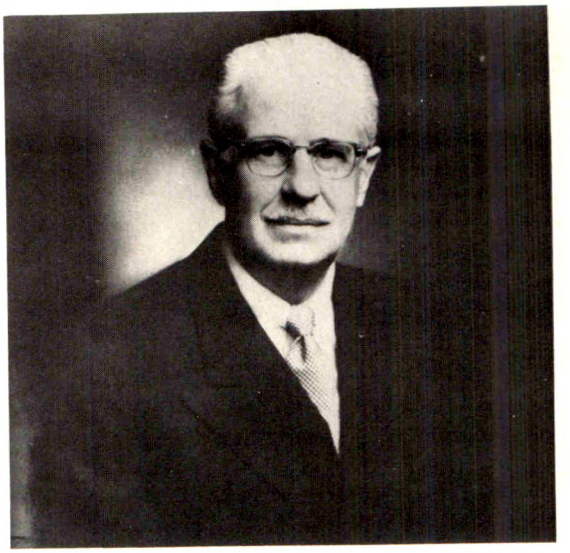
Name _____

Address _____

City _____ State _____ Zip _____

IN MEMORIAM

PAUL A. BISHOP MEMORIAL



1896–1976

Paul A. Bishop, a superior physician who made numerous contributions to the literature of obstetrical and urographic radiology, died January 6, 1976 at the age of 79.

Dr. Bishop received his premedical training in Indiana and in Philadelphia, Pennsylvania at Jefferson Medical College. He was awarded his medical degree from Jefferson Medical College in 1920. After graduating from Jefferson, he accepted a two-year internship at Episcopal Hospital, Philadelphia, 1920–1922. Later he served as chief resident physician, Episcopal Hospital, 1922–1924. Dr. Bishop served his preceptorship in roentgenology under David R. Bowen at Pennsylvania Hospital, Eighth and Spruce streets, Philadelphia, 1925–1928. That period was one of "continuing inquiry and achievement" in several Philadelphia medical institutions and the local, state, and national medical societies. The "practice of roentgenology" in particular was on a high level and was capturing world-wide attention. In Philadelphia, there was an excellent esprit de corps among the senior roentgenologists and other leaders in the fields of medicine and surgery.

Dr. Bishop was certified as a "diplomate" of the American Board of Radiology in 1934. Also that year, he became director of the Department of Radiology, Pennsylvania Hospital, a position he held until retirement 28 years later in 1962. From 1951–1953, he also was president of the medical staff at Pennsylvania Hospital, and from 1934–1949 he was chief radiologist at Delaware County Hospital. Between 1955–1966, Dr. Bishop was professor of radiology at the University of Pennsylvania School of Medicine and its graduate School of Medicine. On retirement, he became professor emeritus.

Dr. Bishop was active in numerous professional and civic organizations, serving at various times as president of the Philadelphia Roentgen Ray Society (1933), first vice president of the American Roentgen Ray Society (1941), member of the executive council of the American Roentgen Ray Society (1948–1951), and in his later years, as secretary of the Philadelphia Lyric Opera Company (1965–1976). He excelled in a variety of activities, including photography and golf. In 1950, he and Gene Pendergrass shared the Willis Manges trophy of the American Roentgen Ray Society's annual golf tournament.

Paul Bishop was a superior physician. On many occasions, his searching inquiry provided diagnostic information where others using the same tools had failed. Examples of his explorations include studies of chronic draining sinuses and of bone changes in fluorine intoxification. He also made numerous contributions to the literature of obstetrical and urographic radiology. Perhaps the crowning achievement of his career was the 1965 publication of his book *Radiologic Studies of the Gravid Uterus*, a summation of more than 35 years of painstaking observation.

Paul Bishop was a distinguished physician who was blessed with charm and a good dis-

position. His attributes were enhanced by his lovely wife, Ruth Baxter Bishop. A visit to their home was an experience cherished by their friends. Dr. Bishop's explorations in the vineyards of education, science, and day-to-day living provide a challenge for those of us who follow him.

Eugene P. Pendergrass
William J. Truddenham

BOOKS RECEIVED

Receipt of books is acknowledged as a courtesy to the sender. Books that appear of sufficient interest will be reviewed as space permits.

Cancer of the Head and Neck (Proceedings of an International Symposium, Montreux-Switzerland, April 2–4, 1975). Edited by R. G. Chambers, A. M. P. Jansen de Limpens, D. A. Jaques, R. T. Routledge. New York: American Elsevier Publishing Co., paper, 365 pp., illustrated, 1975. $53.95

Fundamentals of Abdominal and Pelvic Ultrasonography. By George R. Leopold and W. Michael Asher. Philadelphia: W. B. Saunders Co., 267 pp., 254 illustrations plus 12 color plates, 1975. $21.50

Fundamentals of Radiology. By Lucy Frank Squire. Cambridge, MA: Harvard University Press, 366 pp., numerous illustrations, 1975. $17

Diagnostic Nuclear Medicine. Edited by Alexander Gottschalk. Baltimore: Williams & Wilkins Co., 590 pp., numerous illustrations, 1976. $40

Flash Radiography. By Francis Jamet and Gustav Thomer. New York: Elsevier Scientific Publishing Co., 192 pp., illustrated, 1976. $33.95

Oral Roentgenographic Diagnosis, fourth edition. By Edward C. Stafne and Joseph A. Gibilisco. Philadelphia: W. B. Saunders Co., 478 pp., 670 illustrations, 1975. $20

Panoramic Dental Radiography. By Lincoln R. Manson-Hing. Springfield, IL: Charles C Thomas Co., 183 pp., numerous illustrations, 1975. $32.50

Pediatric Nuclear Medicine. Edited by Leonard M. Freeman and Donald M. Blaufox. New York: Grune & Stratton, Inc., 211 pp., illustrated, 1975. $15

Radioimmunoassay. Edited by Leonard M. Freeman and M. Donald Blaufox. New York: Grune & Stratton, Inc., 162 pp., illustrated, 1975. $14.50

Radiology of the Orbit. By Glyn A. S. Lloyd. Philadelphia: W. B. Saunders Co., 216 pp., 288 illustrations, 1975. $22.50

Radionuclide Studies of the Genitourinary System. Edited by Leonard M. Freeman and M. Donald Blaufox. New York: Grune & Stratton, Inc., 220 pp., illustrated, 1975. $14.50

NEWS ITEMS

NUCLEAR MEDICINE MEETING

Western regional chapters of the Society of Nuclear Medicine will sponsor the Society's first annual meeting October 1–3 at the Fairmont Hotel in San Francisco, California. General chairman is Leon Kaufman, Ph.D., Stanford University Medical Center. Administrative coordinator is Jean Lynch, P. O. Box 40279, San Francisco, California 94140.

NUCLEAR MEDICINE PRINCIPALS

A special summer program "Principals of Nuclear Medicine" will be July 12–16 at the Massachusetts Institute of Technology, Cambridge, Massachusetts. Topics will include instrumentation, radiopharmaceuticals, dosimetry, data processing, plus specific organ studies and therapy. The program is sponsored jointly by M.I.T. and the Harvard Medical School. For more information, write: Director Summer Sessions, Room E10–356, Massachusetts Institute of Technology, Cambridge, Massachusetts 02139.

COMPUTERIZED AXIAL TOMOGRAPHY

A course, "Physical Aspects of Computerized Axial Tomography," will be offered by the Massachusetts Institute of Technology and the Harvard Medical School, July 19–23 at M.I.T. Topics are the physics of radiation interaction with biological tissues, instrumentation, algorithm development and computer systems for image reconstruction, use of contrast agents, artifacts—cause and cure, and specialized areas of imaging. Additional information is available from the Director of Summer Sessions, Room E10–356, Massachusetts Institute of Technology, Cambridge, Massachusetts 02139.

ULTRASOUND COURSES

A series of three 10-week postgraduate courses in sonic medicine will be offered at Bowman Gray School of Medicine. These courses are designed to provide background, techniques, experience, and knowledge to enable an individual to set up both an ultrasonic laboratory and a training program. Courses will be offered September 27–December 3, 1976; January 10–March 18, 1977; and April 11–June 17, 1977. Participants may attend the entire course or portions. Graduates receive 30 credit hours per week in Category I.

The program will cover acoustics, instrumentation, scanning, and applications to obstetrics, gynecology, ophthalmology, adult and pediatric cardiology, abdomen, breast, radiation therapy planning, urinary tract, and nervous system.

For further information, write: Dr. James F. Martin, director, Postgraduate Medical Sonics, Bowman Gray School of Medicine, Winston-Salem, North Carolina 27103.

BONE AND JOINT RADIOLOGY

An intensive three-day course which reviews radiologic, physiologic, and orthopedic aspects of bone and joint disease will be October 25–27 in Cambridge, Massachusetts. Metabolic bone disease, bone tumors, arthritis, trauma, arthrography, arthroscopy, and joint replacement will be discussed. Sponsored by the Department of Radiology, Harvard Medical School, the course is designed primarily to suit the needs of general radiologists, radiologists specializing in bone and joint problems, and orthopedic surgeons. The course is accredited for 19.5 hours of Category I credit for the AMA's Physicians' Recognition Award.

Information is available by writing the Associate Dean, Department of Continuing Education, Harvard Medical School, 25 Shattuck Street, Boston, Massachusetts 02115.

ANGIOGRAPHY 1976

A course designed for radiologists who

participate in or intend to perform interventional and angiographic studies will be October 11–14 at the Copley Plaza Hotel in Boston, Massachusetts. Sponsored by the Department of Radiology in cooperation with the Department of Continuing Education, Harvard Medical School, the course is titled "Angiography 1976: Interventional Radiology." The course is accredited for 26 hours of Category I credit toward the AMA's Physicians' Recognition Award.

Additional information is available from: the Associate Dean, Department of Continuing Education, Harvard Medical School, 25 Shattuck Street, Boston, Massachusetts 02115.

SKELETAL SYSTEM COURSE

An international faculty will present courses on the skeletal system September 13–15 at the Queen Elizabeth Hotel in Montreal, Canada. The International Skeletal Society will sponsor the refresher course conducted by eminent specialists in skeletal disorders encompassing radiology, pathology, orthopaedic surgery, rheumatology, endocrinology, and epidemiology. Registration fees are $175 for consultant physicians; $125 for those with trainee status. Direct inquiries to Dr. Jack Edeiken, secretary-treasurer, International Skeletal Society, Radiology Department, Thomas Jefferson University Hospital, 11th and Walnut Streets, Philadelphia, Pennsylvania 19107.

CANCER CHEMOTHERAPY SYMPOSIUM

A symposium titled "Progress, Promise, and Controversy in Cancer Chemotherapy" will take place in New York City October 22 and 23 at the Barbizon Plaza Hotel. Panel members include G. Bonadonna, Paul Carbone, Bernard Fisher, James Holland, Lucien Israel, and Leonard Price. The Chemotherapy Foundation is symposium sponsor. For registration information, contact: Dr. Ezra M. Greenspan, Mount Sinai Medical Center, Fifth Avenue and 100th Street, New York, New York 10029.

CHEST DISEASE COURSE

"Chest Disease: 1976, an Interdisciplinary Approach with Emphasis on Radiology" will be October 18–22 at the Hyatt Regency Hotel in Cambridge, Massachusetts. The course is designed for radiologists, chest physicians, internists, thoracic surgeons, and other practitioners who deal with chest diseases. Sponsor is the Harvard Medical School Department of Radiology. Course aim is to provide a multi-disciplinary integrated review of pulmonary abnormalities with special emphasis on the radiologic method. The course is accredited for 30 hours of Category I credit for the AMA's Physicians' Recognition Award.

Additional information is available from the Associate Dean, Department of Continuing Education, Harvard Medical School, 25 Shattuck Street, Boston, Massachusetts 02115.

PAEDIATRIC NEUROSURGERY MEETING

The International Society for Paediatric Neurosurgery will hold its annual meeting in Wurzburg, West Germany, September 25–28. Information is available from Dr. Karl Bushe, Director of the Neurosurgery Clinic, Josef Schneider Strasse II, 87 Wurzburg BRD, West Germany.

NUCLEAR MEDICINE REFRESHER COURSE

The Central Chapter of the Society of Nuclear Medicine will present a graduate refresher course in Chicago, Illinois August 21–25, 1976. The course is designed to provide comprehensive review of the basic science and clinical aspects of nuclear medicine and to discuss the most current applications of nuclear medicine techniques. Registration fee is $200. Technologists who wish to attend only the basic science section August 21–22 will be accepted on a space available basis for a fee of $75. Additional information is available from Dr. Robert E. Henkin, Department of Nuclear Medicine, Loyola University Medical Cen-

ter, 2160 South First Avenue, Maywood, Illinois 60153.

DIAGNOSTIC RADIOLOGY POST-GRADUATE COURSE

The Department of Radiology, University of California, San Diego, will present a postgraduate course on recent advances in diagnostic radiology. The course is slated for October 26–29 at Vacation Village Hotel and Convention Center, Mission Bay, San Diego, California. Designed for the practicing radiologist, the sessions will cover ultrasound (abdominal and real time) and head and body computed tomography. Registration fee is $250. Information is available from Nomi Feldman, Box 705, La Jolla, California 92038.

Subscription Form

AMERICAN JOURNAL OF ROENTGENOLOGY

Please enter my subscription as follows:

Beginning with _____ (month), _____ (year).

Name _____

Street Address _____

City and State _____ Zip Code _____

My specialty is _____

Send gift subscription for _____ years to:

Beginning with _____ (month), _____ (year).

Name _____

Address _____

City and State _____ Zip Code _____

Specialty: _____

Enclosed is $ _____

Subscription rates are: $30 for the United States and possessions; $35 for all other countries.

Please send this form and remittance to:

Charles C Thomas, Publisher
301–327 East Lawrence Avenue
Springfield, Illinois 62717

ABSTRACTS OF RADIOLOGIC LITERATURE

INDEX TO ABSTRACTS

Chest

Cardiac rotation in left lower lobe collapse: "the flat waist sign." Kattan KR, Wiot JF 1332

Cardiovascular

Adrenal venography and ultrasound in the investigation of the adrenal gland: an analysis of 58 cases. Davidson JK, Morley P, Hurley GD, Holford GH 1332

Renal artery dissection: a complication of catheter arteriography. Talner LB, McLaughlin AP, Bookstein JJ 1332

Radiographic appearance of the thorax in systolic click-late systolic mumur syndrome. Bon Tempo CP, Ronan JA Jr, de Leon AC Jr, Twigg HL 1332

Comparison of angiographic and postmortem findings in patients with coronary artery disease. Schwartz JN, Kong Y, Hackel DB, Bartel AG 1333

Gastrointestinal

Angiographic patterns in experimental obstruction of the small bowel. Wojtowicz J, Wirga Z, Wirga E 1333

The normal endoscopic pancreatogram. Varley PF, Rohrmann CA Jr, Silvis SE, Vennes JA 1333

Adenomyomatosis of the gallbladder. Ram MD, Midha D 1333

Plain-film findings in severe pseudomembranous colitis. Stanley RJ, Melson GL, Tedesco FJ, Saylor JL 1334

Genito-Urinary

Reflux and trapping. Weiss RM, Schiff M Jr, Lytton B 1334

Investigation of ureteric function with simultaneous intraureteric pressure recordings and ureteropyelography. Ulmsten U, Diehl J 1334

Uterine artery calcification: its association with diabetes. Fisher MS, Hamm R 1334

Uriniferous perirenal pseudocyst: new observations. Meyers MA 1334

The radiographic size of renal transplants. Burgener FA, Schabel SI 1334

Musculoskeletal

Fat-fluid level due to compression fractures of upper tibia. Schwegler N, Hug I 1334

Chondroblastoma of bone. Nolan DJ, Middlemiss H 1335

Angiographic appearances of osteoid osteoma. Lechner G, Riedl P, Knahr K, Salzer M 1335

Nervous System

Cerebral circulation after cardiac arrest: angiographic and carbon black perfusion studies. Lin SR 1336

Recent ischemic brain infarcts at computed tomography: appearances pre- and post-contrast infusion. Yock DH Jr, Marshall WH Jr 1336

Computed tomography in the detection of juxtasellar lesions. Reich NE, Zelch JV, Alfidi RJ, Meaney TF, Duchesneau PM, Weinstein MA 1336

Pediatric Radiology

"Burned-out" pyloric stenosis: an elusive gastric outlet obstruction. Swischuk LE, Pyson KR 1336

Asymmetric lung involvement in bronchopulmonary dysplasia. Sickles EA, Gooding CA 1336

Staphylococcal osteomyelitis, sepsis, and pulmonary disease: observations of 10 patients with combined osseous and pulmonary infections. Felman AH, Shulman ST 1336

Miscellaneous

Air-fluid levels in the sphenoid sinus in epistaxis and nasal packing. Ogawa TK, Bergeron RT, Whitaker CW, Miles JW, Rumbaugh CL 1337

Ultrasonics

Value of echocardiography in the diagnosis of myxoma of the left atrium: 2 cases. Laurenceau JL, Dagenais GR, Gagné S 1337

Nuclear Medicine

Accuracy of brain scanning in pediatric craniocerebral neoplasms. Gilday DL, Eng B, Ash J 1337

Radiation Oncology

Radiation-related eosinophilia: correlation with delayed hypersensitivity, lymphocyte count, and survival in patients treated by curative radiotherapy. Ghossein NA, Bosworth JL, Stacey P, Muggia FM, Krishnaswamy V 1337

Postirradiation atrophic changes of bone and related complications. Howland WJ, Loeffler RK, Starchman DE, Johnson RG 1338

Chest

Cardiac rotation in left lower lobe collapse: "the flat waist sign." Kattan KR, Wiot JF (Cincinnati General Hospital, Cincinnati, Ohio 45229). *Radiology* 118:275–276, Feb 1976

Some cases of left lower lobe collapse show slight right anterior oblique rotation of the heart, manifested by loss of the concavity of the left heart border on a perfectly symmetrical posterior-anterior or anterior-posterior projection. This is a useful differential diagnostic sign, because it is not present when the left lower lobe is compressed secondary to left upper lobe emphysema.—*Author's Abstract*

Cardiovascular

Davidson, J. K., Morley, P., Hurley, G. D., and Holford, G. H. Adrenal venography and ultrasound in the investigation of the adrenal gland: an analysis of 58 cases. *Brit. J. Radiol.*, June, 1975, *48*, 435–450. (From: Department of Radiology and the M.R.C. Blood Pressure Unit, Western Infirmary, Glasgow G11 6NT, Scotland.)

Adrenal venography has been carried out in 58 patients with the left adrenal vein being successfully catheterized in 91 percent and the right in 77 percent.

Of the 30 patients with primary hyperaldosteronism, eleven adenomas (12–35 mm diameter) have been demonstrated at venography and two of 15 mm suspected, all of which were confirmed surgically. Aldosterone levels in the adrenal vein plasma were raised on the affected side. In the group of proved micronodular hyperplasia, two patients had surgically confirmed macronodules and venography demonstrated one of 12 mm diameter. Two adenomas of 11 mm and one macronodule of 15 mm have been demonstrated at venography in the remainder who have not had an operation.

Ultrasound was carried out in twelve patients with primary hyperaldosteronism, ten of which had tumors at venography. Two adenomas measuring 30 and 31 mm were outlined by ultrasound and confirmed surgically. Seven adenomas, including one macronodule (10–25 mm in diameter) were not defined. Three intra-adrenal pheochromocytomas (45–90 mm) and one extra-adrenal (80–85 mm) were demonstrated at arteriography, identified by ultrasound and confirmed surgically.

Of the ten patients with Cushing's syndrome three had enlarged glands at venography, this was confirmed surgically.

Cumulative experience from this analysis and published reports indicate that venography will demonstrate tumors of 10 mm or more in diameter and outline enlarged glands; aldosterone assays will lateralize tumors as small as 3 mm; ultrasound will outline tumors of 30 mm and selective adrenal arteriography will demonstrate tumors of 10 mm.

One patient developed acute adrenal cortical insufficiency with intra-adrenal extravasation on one side and thrombosis of the central vein on the opposite side. A second case developed temporary adrenocortical insufficiency. Published reports indicate that the risk of complication is about one percent.

The report includes an anatomical study of the efferent adrenal veins in 50 patients paying particular attention to the diameter, number of accessory hepatic veins, and the angle of entry and position of the right adrenal vein.—*E. Frederick Lang, M.D.*

Renal artery dissection: a complication of catheter arteriography. Talner LB, McLaughlin AP, Bookstein JJ (University of California–San Diego School of Medicine, San Diego, California 92115). *Radiology* 117:291–295, Nov 1975

Renal artery dissection is a rare complication of catheter arteriography. Predisposing factors include atherosclerosis and fibromuscular dysplasia. Optimum management requires aortographic documentation of the extent of vascular obstruction. Dissections causing incomplete obstruction of blood flow can be treated with systemic anticoagulation to prevent downstream thrombosis and should be followed with serial isotope blood flow studies and LDH measurements. Dissection causing complete vascular obstruction usually requires immediate surgery, although spontaneous reestablishment of flow may occur. The 3 patients discussed illustrate a spectrum of findings, including the acute development of renovascular hypertension.—*Author's Abstract*

Radiographic appearance of the thorax in systolic click-late systolic murmur syndrome. Bon Tempo CP, Ronan JA Jr, de Leon AC Jr, Twigg HL (Georgetown University Hospital, Washington, DC 20007). *Am J Cardiol* 36:27, July 1975

The posteroanterior and lateral chest X-ray films of 64 consecutive patients with an isolated systolic click (55 patients) or a systolic click with a late systolic murmur (9 patients) showed a striking frequency of thoracic skeletal abnormalities. There were 50 female and 14 male subjects. The average age of the female subjects was 36.7 years (range 13 to 67), that of the male subjects 39.7 years (range 17 to 56). Seventy-two percent of the female and 78 percent of the male subjects had an anteroposterior/transverse thoracic ratio less than the mean ratio in a normal population. Bony abnormalities such as pectus excavatum, straight thoracic spine and scoliosis occurred alone or in combination in 31 of the 50 female patients (62 percent) and in 8 of the 14 male patients (57 percent). Overall, 39 of the 64 patients (61 percent) had at least one of the skeletal abnormalities. Scoliosis occurred in 25 subjects (39 percent) and was mild in 19. A "straight back" was

found in 15 (23 percent) and pectus excavatum in 7 patients (11 percent). The explanation for these findings is not apparent. Thoracic cage abnormalities should be included as one of the nonauscultatory features of the systolic click-late systolic murmur syndrome.—*Author's Abstract*

Comparison of angiographic and postmortem findings in patients with coronary artery disease. Schwartz JN, Kong Y, Hackel DB, Bartel AG (Duke University Medical Center, Durham, North Carolina 27710). *Am J Cardiol* 36:174, Aug 1975

The accuracy of coronary cineangiography in predicting the degree of stenosis in coronary arteries was evaluated by comparing autopsy and premortem cineangiographic findings in 25 patients. Coronary cineangiograms and autopsy specimens were reviewed independently by two cardiologists and two pathologists. Identical diagrams dividing the coronary arteries into 12 segments were used by both groups to record the location and degree of stenosis observed. Cineangiographic findings were in agreement with pathologic findings (less than 25 percent difference in cross-sectional luminal area) in 178 (79 percent) of the 226 segments examined, but overestimated the degree of stenosis in 13 (6 percent) and underestimated it in 34 (15 percent). Thus, cineangiography appears to be a reliable tool in evaluating coronary artery disease. When diagnostic errors are made, they are usually underestimations of the degree of disease; common causes of error are circumferential stenosis, eccentric lesions, obstruction of view by artificial valves and poor opacification due to severe proximal stenosis.—*Author's Abstract*

Gastrointestinal

Angiographic patterns in experimental obstruction of the small bowel. Wojtowicz J, Wirga Z, Wirga E (Institute of Diagnostic Radiology, Poznan Medical School, Poznan 61–833, Szkolna 8/12, Poland). *Invest Radiol* 10:583–594, Nov–Dec 1975

This study was designed to study the dynamics of arterial changes in the intestinal wall and mesentery caused by several types of mechanical obstruction. The exteriorized loop of small intestine of 79 experimental rabbits was examined using microscopic, microangiographic, and angiographic methods at fixed time intervals following mechanical obstruction.

The type and rate of progression of peripheral arterial changes is dependent on the specific mechanism of intestinal obstruction. Within the first 6 hours arterial changes in the obstructed loop are similar in all obstructions and consist of stretching and displacement of the arteriae rectae and their branches proportional to the degree of bowel distention. In strangulation and volvulus, mural arterial branches of the involved loop are subject to rapidly progressive obstruction culminating in extensive bowel wall necrosis. This differs from the slowly progressive mucosal necrosis in simple obstruction and intussusception, in which effects on vascular elements are less intense. The mechanism of these changes is not entirely clear. An earlier theory, that increased intraluminal pressure simply diminishes mucosal perfusion, is attractive but lacks substantiation.—*Rosalind H. Troupin*

The normal endoscopic pancreatogram. Varley PF, Rohrmann CA Jr, Silvis SE, Vennes JA (Veterans Administration Hospital, Minneapolis, Minnesota 55417). *Radiology* 118:295–300, Feb 1976

Pancreatograms of 102 patients with proved normal pancreatic status were reviewed to establish normal standards of pancreatic ductal morphology. Precise details of ductal course, position, length, caliber, and variant anatomy were analyzed. The ampulla was found at the level of the second lumbar vertebra in 75% of cases, while the pancreatic duct crossed the spine at L1 in most cases. Mean ductal diameters were 3.1, 2.0, and 0.9 mm in the head, body, and tail of the pancreas, respectively.—*Author's Abstract*

Adenomyomatosis of the gallbladder. Ram MD, Midha D (Huron Road Hospital, 13951 Terrace Road, Cleveland, Ohio 44112). *Surgery* 78:224–229, Aug 1975

Adenomyomatosis of the gallbladder is an entity that is being recognized increasingly, chiefly by radiologists. The pathogenesis, pathology, and indications for surgery are not well understood. This report is a study of 27 patients seen in the last 6 years, all of whom had proved histologic features. Patients ranged from 21 to 72 years of age, with a preponderance of women. Thirteen patients had no gallstones. The disease was confined to the fundus in 15 patients, to the neck in one patient, and was generalized in 11 patients. Bile cultures were obtained in the last six consecutive patients and all were negative. Histologically there was evidence of thickening of the gallbladder wall, glandular elements in the mucosa, and invagination of glands into the muscularis. The clinical, radiological, and pathologic features supported a hyperplastic and degenerative disorder which should be distinguished from cholecystitis. Associated with these morphologic changes is a dyskinesia similar to that seen in diverticular disease of the colon. Follow-up studies after cholecystectomy have shown that over 90 percent of all patients were completely relieved of symptoms. Adenomyomatosis should be identified as a distinct entity, probably of a degenerative nature. Cholecystectomy is indicated and beneficial when the symptoms suggest biliary tract disease.—*Author's Abstract*

Plain-film findings in severe pseudomembranous colitis. Stanley RJ, Melson GL, Tedesco FJ, Saylor JL (Mallinckrodt Institute of Radiology, St. Louis, Missouri 63110). *Radiology* 118: 7–11, Jan 1976

Plain-film abdominal changes in 5 patients with severe antibiotic-related pseudomembranous colitis were found to be strikingly similar and distinct from those seen in other colitides. These consisted of moderate gaseous distention of the colon and unusual wide transverse bands of thickened bowel wall associated with giant "thumbprinting" which was universal in distribution, with minimal or absent small-bowel abnormalities. While the radiographic findings were not pathognomonic, they were highly suggestive of advanced pseudomembranous colitis when combined with the clinical data. Prompt recognition of this entity by the radiologist is extremely helpful in management, since such patients frequently present with physical findings of an acute abdomen requiring surgery.—*Author's Abstract*

Genito-Urinary

Reflux and trapping. Weiss RM, Schiff M Jr, Lytton B (Yale University School of Medicine, New Haven, Connecticut 06510). *Radiology* 118: 129–131, Jan 1976

Although functional ureteral obstruction results in a decrease in the rate of antegrade urine flow, urine may still traverse the obstructed segment in a retrograde direction. Decreased musculature is found in the obstructing area. The combination of these processes results in reflux with trapping. This process has been demonstrated radiographically at both the unterovesical and the ureteropelvic junctions.—*Author's Abstract*

Investigation of ureteric function with simultaneous intraureteric pressure recordings and ureteropyelography. Ulmsten U, Diehl J (General Hospital of Malmö, University of Lund, Malmö, Sweden). *Radiology* 117:283–289, Nov 1975

Ureteric function was investigated by simultaneous intraureteric pressure recording (ureterometry) and retrograde ureteropyelography. With a multichannel catheter, intraluminal pressures can be recorded simultaneously at three levels in the ureter. The catheter can also be used to inject contrast medium. In normal antegrade peristalsis, an interval of 0.5–1.5 sec. was observed from the disappearance of the urine bolus to the recording of the maximal contraction pressure. In cases of long-lasting retroperistalsis, the urinary flow was impaired. Combined ureterometry and ureteropyelography appears to be a valuable method for detailed studies of ureteric function.—*Author's Abstract*

Uterine artery calcification: its association with diabetes. Fisher MS, Hamm R (Temple University Medical School, Philadelphia, Pennsylvania 19140). *Radiology* 117:537–538, Dec 1975

Uterine artery calcification was observed in 26 patients. Fourteen of the 22 with adequate clinical information had diabetes mellitus. This is considered a significant association by the authors and calcification should raise the question of diabetes.—*Author's Abstract*

Uriniferous perirenal pseudocyst: new observations. Meyers MA (The New York Hospital–Cornell University Medical Center, New York, New York 10021). *Radiology* 117:539–545, Dec 1975

The chronic encapsulated extravasation of urine, most accurately designated as uriniferous perirenal pseudocyst, causes urine to collect within the cone of renal fascia. This results in a characteristic complex of radiographic findings including an elliptical soft-tissue mass in the flank oriented inferomedially with upward and lateral displacement of the lower renal pole, medial displacement of the ureter, obstructive hydronephrosis, and perhaps evidence of extravasation into the mass. Since the clinical recognition of the mass is typically delayed several weeks following the original traumatic episode, prompt radiological diagnosis is essential before irreparable damage to the kidney occurs.—*Author's Abstract*

The radiographic size of renal transplants. Burgener FA, Schabel SI (University of Rochester School of Medicine, Rochester, New York 14620). *Radiology* 117:547–550, Dec 1975

The lengths of 55 renal transplants outlined by metallic clips were measured on serial abdominal radiographs up to 3 years after operation. The range of normal transplant size was defined as the mean value ±2 standard deviations. Using this definition, the maximum increase in length was 5% at 10 days, 10% at 1 month, and 1% additional for each month in the first year. The normal maximum rate of increase in renal length was 0.5% per day, found only in the immediate postoperative period. Sixty per cent of transplants with severe rejection had either an abnormal length or growth rate or both. In chronic rejection and other complications, size and growth rate were rarely abnormal. An abnormal decrease in renal length was not seen with any complication.—*Author's Abstract*

Musculoskeletal

Schwegler, N., and Hug, I. Fettflüssigkeitsspiegel bei Tibiakopf-Impressionsfraktur. (Fat-fluid level due to compression fractures of upper tibia.) *Fortschr. a. d. Geb. d. Rönt-*

genstrahlen u. d. Nuklearmedizin, April, 1975, *122* 301–302. (Address: Dr. N. Schwegler, CH-4122 Neuallschwil, Marsstrasse 16, Switzerland.)

Compression fractures of the upper portion of the tibia are sometimes obscure, particularly if the compression is limited to the central portion of the tibial articular surface.

In most individuals who have suffered this type of fracture there is an effusion in the knee joint and there is a significant amount of fat mixed with blood in the effusion. This fluid distends the suprapatellar recess of the joint. In a lateral view exposed with the central ray horizontal there is a fluid level visible marking the interface between supernatant fat and the underlying bloody effusion. This fluid level develops rapidly in the short period of immobilization which occurs because of pain. This visible interface disappears in a few days following absorption of the fat.

If the fracture is not compound and if the joint has not been entered surgically, the possibility of air can be excluded. Air is less dense than fat and the difference between the two lateral views is apparent. Occasionally, the normal fat pad between the femur and the quadriceps tendon may simulate a fat-fluid interface, but this is a much shorter interface and is less sharp.

Such a fluid-fat interface was demonstrated in 24 of 28 consecutive fractures of the upper tibia which were examined with this technique. This indicates the usefulness of the technique when there is an obscure fracture.—*E. Frederick Lang, M.D.*

Nolan, D. J., and Middlemiss, Howard. Chondroblastoma of bone. *Clin. Radiol.*, July, 1975, *26*, 343–350. (From: Department of Radiology, University of Bristol, Bristol, England.)

The authors chart the findings in ten cases of chondroblastoma. There were nine males and one female. The age range was 14–41 years, eight in the 14–18 age group. Nine tumors were located in long bones and one in the ilium (age 41). Chondoblastoma in unusual sites is usually found in the older age group. All of these patients had pain of two to nine months' duration and most had limitation of motion. There was localized swelling in four.

The roentgenological findings are well illustrated. In these patients the lesion was a round or oval radiolucency, 1×2 to 4×8 cm in size. All but one defect had a thin sclerotic rim separating tumor from adjacent normal bone, and the remaining case had a less well-defined margin. Typically, the lesion involves the epiphysis and may extend into the metaphysis. In one patient, the tumor was initially in the epiphysis but recurred twice in the metaphysis. Two lesions showed stippled calcification and two had bony trabeculation. Periosteal new bone was present adjacent to the lesion in four cases. The chondroblastoma extended to the cortex in five patients and in two others, there was expansion of bone with thinning of the cortex. Curettage and placement of bone chips was the treatment in nine cases, although in the patients with loss of cortex of the femoral head they used a Thompson prosthesis.

The differential diagnosis is briefly considered and includes osteosarcoma, chondrosarcoma, chondromyxoid-fibroma, giant-cell tumor, aneurysmal bone cyst and inflammatory lesions. The most difficult to exclude is chondromyxoid-fibroma which is metaphyseal in origin and rarely shows periosteal new bone. It also tends to be more expansive and often causes destruction of the cortex as well as showing a greater degree of reactive sclerosis.—*Martha Mottram, M.D.*

Lechner, G., Riedl, P., Knahr, K., and Salzer, M. Das angiographische Bild des Osteoid-Osteoms. (The angiographic appearances of osteoid osteoma.) *Fortschr. a. d. Geb. d. Röntgenstrahlen u. d. Nuklearmedizin*, April, 1975, *122*, 323–326. (Address: OA Dr. G. Lechner, Leiter der Röntgenstation der I. Chirurg. Univ.-Klinik, Allgemeines Krankenhaus, A-1097 Wien IX, Alserstrasse 4, Austria.)

Although the clinical and roentgenographic appearance of osteoid osteoma is usually clear-cut, occasionally there are questions, and angiographic study was carried out in an attempt to permit a more certain diagnosis in questionable cases. Of 17 patients with histologically verified osteoid osteoma, 17 were subjected to angiography. Of these, 14 were successful, but in three, each with a tibial lesion, spasm prevented a satisfactory study.

In each of the 14 cases there was a homogeneous blush of variable density corresponding to the area of the nidus. In some which were richly vascularized the nidus became visualized early and the blush lasted during the entire venous phase. In others with poorer vascularization, the demonstration was more fleeting. No definite increase in adjacent vascularity was demonstrated nor was early filling of the veins present.

Photographic subtraction was useful particularly when the surrounding sclerotic bone was dense and the nidus was only fairly well vascularized.

The characteristic appearance on angiography permits easy differentiation from those conditions with which osteoid osteoma is occasionally confused on plain film studies, such as osteomyelitis, Ewing's sarcoma, osteogenic sarcoma, cystic lesions, osteoma, as well as others. In addition, angiography permits clear demonstration of the entire extent of the nidus in preparation for the surgical treatment of the lesion.—*E. Frederick Lang, M.D.*

Nervous System

Cerebral circulation after cardiac arrest: angiographic and carbon black perfusion studies. Lin SR (University of Pennsylvania School of Medicine, Philadelphia, Pennsylvania 19104). *Radiology* 117:627–632, Dec 1975

Cardiac arrest of 2–15 minutes was induced in 14 dogs. When circulatory arrest lasted longer than 5 minutes, abnormal cerebral angiographic findings were seen 3–4 hours after resuscitation, consisting of (*a*) marked prolongation of the arterial phase in both intracranial and extracranial arteries, and (*b*) faint (poor) visualization of the venous phase. No significant abnormalities were noted in dogs arrested less than 5 minutes, or in the control group. Carbon black perfusion studies showed multiple focal areas of small patchy and diffuse coarse reperfusion defects at the arteriolar-capillary levels in dogs arrested longer than 5 minutes. A combination of vascular and parenchymal changes during ischemia may be the cause for these findings.—*Author's Abstract*

Recent ischemic brain infarcts at computed tomography: appearances pre- and postcontrast infusion. Yock DH Jr, Marshall WH Jr (Stanford University School of Medicine, Stanford, California 94305). *Radiology* 117:599–608, Dec 1975

Thirty-seven cranial computed tomography (CCT) scans of proved or highly probable recent ischemic brain infarcts were analyzed visually and numerically, with results organized by infarct age. The lesions typically appeared as homogeneous low density abnormalities, with no significant difference in scan characteristics between infarct age groups, *i.e.*, it was not possible to determine the age of an infarct by its noninfused, CCT appearance alone. Eight infarcts showed "mass effect," and 4 of the 20 contrast-infused cases demonstrated marked density augmentation or "blush," indicating that infarcts may resemble tumor in both of these properties.—*Author's Abstract*

Computed tomography in the detection of juxtasellar lesions. Reich NE, Zelch JV, Alfidi RJ, Meaney TF, Duchesneau PM, Weinstein MA (Cleveland Clinic Foundation, Cleveland, Ohio 44106). *Radiology* 118:333–335, Feb 1976

One thousand consecutive computed tomograms were reviewed to determine the accuracy of the procedure in the detection of juxtasellar lesions. The detection rate was compared to those of plain skull films, radionuclide studies, angiography, and pneumoencephalography. Computed tomography was slightly superior to angiography and was surpassed only by pneumoencephalography, both of which are invasive procedures which carry a definite risk. The data indicate that computed tomography is the screening method of choice in the detection of juxtasellar masses.—*Author's Abstract*

Pediatric Radiology

"Burned-out" pyloric stenosis: an elusive gastric outlet obstruction. Swischuk LE, Pyson KR (University of Texas Medical Branch, Galveston, Texas 77550). *Radiology* 117:373–379, Nov 1975

Four cases of infantile pyloric stenosis are presented to illustrate the difficulties found in diagnosing pyloric stenosis. Clinical, histological, surgical, and roentgenologic examination must be combined to determine the optimum treatment. All patients exhibited failure to thrive and gain weight normally, but few showed palpable tumors upon abdominal examination. The results of upper gastrointestinal examination are often more confusing than helpful, but previously performed GI studies have been rewarding. The main problem is to rule out pylorospasm, and a trial of treatment with antispasmodics is essential. The presence or absence of a residual muscle mass at surgery would call for pylorotomy or pyroplasty, respectively.—*Author's Abstract*

Asymmetric lung involvement in bronchopulmonary dysplasia. Sickles EA, Gooding CA (University of California School of Medicine, San Francisco, California 94132). *Radiology* 118:379–383, Feb 1976

The radiographic distribution of pulmonary abnormalities in bronchopulmonary dysplasia (BPD) in all previously reported cases has been bilateral and generalized. The authors studied 11 premature infants who had BPD that was primarily unilateral. The striking feature in each of these patients was the occurrence of an episode of prolonged unilateral atelectasis or tension pneumothorax. Few, if any, radiographic manifestations of BPD developed. Results of a detailed analysis of oxygen exposure and respirator therapy during the periods of unequal lung ventilation further characterizes the protective effect of atelectasis and tension pneumothorax in the development of BPD.—*Author's Abstract*

Staphylococcal osteomyelitis, sepsis, and pulmonary disease: observations of 10 patients with combined osseous and pulmonary infections. Felman AH, Shulman ST (University of Florida, Gainesville, Florida 32601). *Radiology* 117:649–655, Dec 1975

The clinical and roentgenographic findings in 10 patients with combined staphylococcal infection of the bones, joints, and lungs are reviewed. Chest roentgenograms early in the course of the illness suggested septic embolic disease, but in most cases the

associated osseous infections were overlooked. Primary therapy, directed toward the sepsis and pulmonary complications, was often unsuccessful until the associated osteomyelitis was recognized and treated. The radiologist and clinician should recognize the roentgen pattern of septic pulmonary emboli and be alert to the possibility of associated skeletal infection. Surgical drainage is often necessary.—*Author's Abstract*

Miscellaneous

Air-fluid levels in the sphenoid sinus in epistaxis and nasal packing. Ogawa TK, Bergeron RT, Whitaker CW, Miles JW, Rumbaugh CL (LAC-USC Medical Center, Los Angeles, California 90033). 118:351–354, Feb 1976

Air-fluid levels in the sphenoid sinus have been described in association with skull fracture, cerebrospinal fluid rhinorrhea, and sinusitis. The authors have observed this sign in the absence of significant trauma in patients with epistaxis and nasal packing. The fluid is probably normal sinus secretion retained due to prolonged recumbency, although other explanations for its accumulation are discussed.—*Author's Abstract*

Ultrasonics

Laurenceau, J.-L., Dagenais, G. R., and Gagné, S. Diagnostic des myxomes auriculaires gauches par échocardiographie: deux observations. (Value of echocardiography in the diagnosis of myxoma of the left atrium: 2 cases.) *Presse méd.*, Oct., 1975, *36*, 2563–2566. (From: Institut de Cardiologie, Hôpital Laval, 2725 Chemin Sainte-Foy, C. Québec GIV 4G5, Canada.)

The echocardiograms of two patients, each with a myxoma of the left atrium, are presented. In each case there was an abnormal echo, as from a mass, shown in diastole behind the greater cusp of the mitral valve. In addition, in one of the cases, the mass was seen in the left atrium in projections designed to show the tricuspid and aortic valves.

The diagnosis in each was not suspected clinically and it was the ultrasound examination, carried out on a routine basis, which led to the discovery of the myxoma. This noninvasive technique is thus a valuable study in the demonstration of left atrial myxomas.—*Published English Abstract*

Nuclear Medicine

Gilday, David L., Eng, B., and Ash, Judith. Accuracy of brain scanning in pediatric craniocerebral neoplasms. *Radiology*, Oct., 1975, *117*, 93–97. (Address: David L. Gilday, M.D., Division of Nuclear Medicine, The Hospital for Sick Children, 555 University Avenue, Toronto, Ontario, Canada M5G 1X8.)

Previous reports had indicated a lower tumor detection rate in children, as opposed to adults, with radionuclide scanning procedures. Prior series had been relatively small also. This 34 month review of 2,536 cases points up the improvement in results using meticulous cerebral-radionuclide angiography, blood pool imaging, and two to four hour delayed images.

The methodology is important. Potassium perchlorate (10 mg/kg) is given ten minutes prior to injection of Tc-99m pertechnetate (8.3 mCi/m^2, body surface). Posterior radionuclide angiography is routinely employed. Anterior radionuclide angiography is performed when indicated, however. Rapid bolus intravenous injection is necessary for quality flow studies. Blood pool images in the posterior, vertex, and right and left lateral positions are obtained immediately postinjection. Delayed images are obtained three to four hours postinjection on the rectilinear scanner. Positioning is critical, requiring strict immobilization of the child. This calls for proper sedation and the utilization of sundry restraining devices.

Interpretation of all images was correlated with skull roentgenograms. Final statistical analysis was based on surgical or autopsy findings.

The detection rate for supratentorial neoplasms was 86 percent, and 96 percent for infratentorial neoplasms. Ependymonas and medulloblastomas were detected most readily, and craniopharyngiomas, germinomas, and histiocytosis X were difficult to detect.

Categorically, three basic patterns were detected with radionuclide angiography: normal, increased flow to the tumor, and decreased flow to the tumor due to its edematous, cystic, or necrotic structure. The immediate postinjection blood-pool images may reveal identifying accumulations in the cases of decreased flow, or present patterns of confirmation when compared with the delayed scans. The increased detection rate with delayed imaging (up to six hours) has been confirmed by many. Individualizing studies is also important, *e.g.*, Waters position for suspected facial or orbital abnormalities.—*F. C. Petty, M.D.*

Radiation Oncology

Ghossein, Nemetallah A., Bosworth, J. L., Stacey, Patricia, Muggia, Franco M., and Krishnaswamy, Vasudevasastri. Radiation-related eosinophilia: correlation with delayed hypersensitivity, lymphocyte count, and survival in patients treated by curative radiotherapy. *Radiology*, Nov., 1975, *117*, 413–417. (Address: Nemetallah A. Ghossein, M.D., The Hospital of the Albert

Einstein College of Medicine, 1825 Eastchester Road, Bronx, N. Y. 10461.)

The association of eosinophilia with malignancy has been noted for years but little attention has been paid to its prognostic significance. Abdominal irradiation has been known to give rise to eosinophilia and preliminary observations in these patients suggested a better prognosis for those who demonstrated radiation-related eosinophilia (RRE) compared to those who did not. Recent experiments have indicated that the ability to produce an eosinophilic response depends on the integrity of the cell-mediated and humoral immune mechanisms. This prospective study was undertaken to determine the correlation between RRE, delayed skin reactivity to 2–4 dinitrochlorobenzene (DNCB), initial total peripheral lymphocyte count, and short-term prognosis in patients undergoing curative irradiation for tumors located below the diaphragm.

Ninety-eight consecutive patients were evaluated; all had received 3,000 rads curative abdominal and or pelvic radiation therapy as the only treatment modality for biopsy proved malignant tumor located below the diaphragm. Delayed hypersensitivity was determined by skin reactivity to DNCB prior to treatment according to the method described by Johnson *et al.* The total lymphocyte and eosinophil counts was calculated from routine hematologic determinations of total white cell and differential counts obtained prior to and during treatment. All patients were assessed at six months for the presence or absence of disease manifestations; and those who had no disease were considered controlled.

Of 61 patients who were positive DNCB reactors, 41 (67 percent) had no evidence of disease at six months. Of the 37 nonreactors, 15 (40 percent) were free of disease. Within the two groups, there was a significantly higher rate of control in patients who had RRE. The highest control rate (almost 80 percent) was obtained in patients who had sensitivity to DNCB and also developed RRE. Positive DNCB reactors without RRE had a control rate of slightly greater than 60 percent; similar to the rates seen in nonreactors who demonstrated RRE during treatment. Of 15 patients who did not react to DNCB and did not have RRE, only one patient (seven percent) was disease free. The failure rate for patients who had a pretreatment lymphocytic count of less than 1,500 was significantly higher than for those who had a higher count. Regardless of total lymphocytic count, patients who demonstrated RRE had a higher tumor control.

It was concluded that the ability to produce an eosinophilic response is an important prognostic factor, independent of other parameters indicative of intact cell-mediated immunity.—*Paul M. Kroening, M.D.*

Postirradiation atrophic changes of bone and related complications. Howland WJ, Loeffler RK, Starchman DE, Johnson RG (Aultman Hospital, Canton, Ohio 44710). *Radiology* 117:677–685, Dec 1975

The sequence of radiographically visible changes about the shoulder girdle following irradiation was analyzed in 49 patients who received 200 kV irradiation, in 50 who received 25 MeV betatron photon irradiation, and in 20 who received cobalt-60 irradiation. The changes were dose related and were most evident in the kilovoltage group, but also occurred following megavoltage therapy. Atrophic changes may be complicated by fracture, true necrosis, true osteitis or sarcoma. These atrophic changes have clinical significance similar to the atrophic changes that occur in skin and mucous membranes. The terms radionecrosis and radiation osteitis as applied to these changes should be abandoned since they imply a more serious process than is actually present. Biopsy should be avoided if possible since trauma and secondary infection could lead to true necrosis.—*Author's Abstract*

SUBJECT INDEX TO VOLUME 126

(E) = editorial (B) = book review (M) = memorial

Academic radiology, organizing a community department, 761
American Radium Society
  58th annual meeting, 446
  meeting agenda, 447
American Roentgen Ray Society
  meeting announcement, 1316
  preliminary program, 1317
Angiography and ultrasonography, comparative study of abdominal aortic aneurysms, 95
Aorta, coarctation of, roentgenographic assessment after operative correction, 101
Aorto-enteric fistulae, roentgen findings, 714
Appendicitis, retrocecal, presenting with air in the subhepatic space, 416
Atrial myxoma, catheter motion in, 1155
Arachnoid cyst, intra- and extracerebral, 629
Arterial occlusion due to Pitressin infusion, 829
Ascariasis, biliary, in children, 352
Ascitic fluid distribution, 974
Atlas, isolated fracture of medial portion of, 1053

Barrett esophagus, postesophageal narrowing, 638
Bile duct stones, tomographic technique, 63
Bladder anomalies, multichambered, 642
Bloedorn, Fernando (M), 441
Bone mineral measurement, (E), 1315
Bone mineralization conference, abstracts of, 1266
Books reviewed
  Atlas of Hand Radiographs, 913
  Atlas of Tumor Radiology, 192
  Diagnostic Uses of Ultrasound, 656
  Radiologic and Other Biophysical Methods in Tumor Diagnosis, 915
  Technology and Interpretation, 914
  Thoracic and Cardiovascular, 192
Breast cancer
  surgery and irradiation, 216
  treatment selection in primary, 135
Breast carcinoma, extra-abdominal desmoid of the axillary tail mimicking, 903
Breast pathology, computerized tomography in, 406
Breast patterns as an index of risk, 1130
Bronchopulmonary foregut malformations, a unifying etiological concept, 46

Cardiac pacemaker, 1017
Carotid tortuosity causing sellar expansion, 1203
Carpal navicular, isolated rotatory subluxation of, 601
Catheter angiography, complication rate, 814
Cavitating lung nodules and pneumothorax in children with metastatic Wilms' tumor, 728
Cecal vasculature in vascular malformations, 394
Cerebral angiography, serial, in stereoscopic magnification, 1211
Cerebral artery, embolic occlusion, 576
Cerebral blood volume in fractional pneumoencephalography, 582
Cerebro-costo-mandibular syndrome, 1223
Changing of the guard (E), 188
Charnley hip arthroplasty, complications, 1061
Chiba percutaneous transhepatic cholangiography, 755
Cholecystocholangiography in the jaundiced patient, 70
Chondrosarcoma of esophagus, 1175
Colitis, pseudopolyposis in ulcerative, 1178
Colonic haustration loss in progressive systemic sclerosis, 704
Community cancer control activities, role of clinician, 471
Computed tomography, new frontier for radiology, 1117
Crohn's disease, angiography, 941
Crossed renal ectopia, angiographic findings, 1035
C_7, notched articular process, 612
CT and the planners (E), 1095

Disc herniations, lumbar epidural venography in diagnosis of, 992
"Doughnut" sign in brain scanning, 842
Ductus venosus, congenital absence, 892

Endometrial cancer, irradiation of, 148
Epidural venography, diagnosis of herniated lumbar intervertebral disc, 1010
Epithelial tumors, malignant, reduced fractionation, 268
Esophageal varices, optimal visualization, 512

Femur, grooves of distal articular surface, 751
Film screening by physician assistants, 1069
Fractionation, experience with twice-a-day, in clinical radiotherapy, 155
Frontal ventricular dimensions on normal computed tomography, 593

Gallium-67 scans in children with solid tumors, 179
Gastric lymphoma, "bull's eye" lesions in, 965
Gastric volvulus herniating into chest, 1169
Glioblastoma, radiation therapy treatment, 481
Glucagon and barium enema examinations, 981
Griffiths' point, critical anastomosis at the splenic flexure, 77
Guidelines for the modern cardiac catheterization–angiocardiographic laboratory (E), 652

Head and neck cancer patients, immunocompetence, 880
Head and neck tumors, electron beam therapy, 1251
Head and neck lesions, adjuvant chemoimmunotherapy, 1082
Head trauma, computerized tomography in, 765
Hemangiopercytoma, radiation therapy, 887
Hemochromatosis, silent but not invisible, 343
Hemoptysis, bronchography in patients with, 597
Hepatic amyloidosis, lack of gallium uptake, 1246
Hip prosthesis complications, arthrography, 743
Hodgkin's disease, mediastinal, 123

Immune responses, effect of therapeutic irradiation on, 313
Intensive care unit, hazards, 423
Interstitium
  gamma-ray therapy, volume, time factors, 163
  implantation, low energy radionuclides for, 171
Intestine
  malrotation in adults, assessment with emphasis on complete and partial nonrotations, 358
  perforation from feeding tubes, 1229
Intraaortic balloon pumping, chest x-ray in acute left ventricular power failure, 1147

Intracranial astrocytomas, failure patterns, 279
Intussusception of appendix in children, 1164
Islet cell tumors and the alimentary tract, 933

Kidney
  ultrasonic evaluation of unilateral nonvisualized, 853
  pseudotumor of, following glomerulonephritis, 1197
Knee, localized nodular synovitis, 649

Lesion conspicuity, structured noise, film reader error, 1233
Lobe, systemic arterial supply to left lower, 817
Lumbar epidural venography, 1003
Lymphoma, arteriography of retroperitoneal, 368

Malignancies, immunotherapy, 1088
Megacystis-microcolon–intestinal hypoperistalsis syndrome, 957
Mastectomy, elective irradiation with electron beam, 127
Measuring device for roentgenographic structures, 432
Menetrier's disease, involvement of gastric antrum, 524
Micrometastases, treatment concept in murine systems, 500
Mitral insufficiency, non-rheumatic acute, 336
Meyer-Rokitansky-Kuster-Hauser syndrome, pneumogynecography in diagnosis, 413
Mouth carcinoma, surgical treatment, 1256
Myocardium, computed tomography of normal and infarcted, 786
Myositis ossificans circumscripta, 32

Nasopharynx cancer, factors modifying radioresponse, 863
Nelson's syndrome in childhood, 550
Neonatal small left colon syndrome, fat thickness, 538
Neovascularity, roentgenology-pathology, 376
Neuroblastoma, Tc-diphosphonate uptake, 1077
Neuroepithelial (colloid) cysts, 56
Nuclear medicine, is it in trouble? (E), 908

Occipital bone, embryogenesis of human, 1063
Oral tongue, carcinoma, radiation therapy, 107
Orbit, aneurysmal bone cyst of, 896
Oropharynx, carcinoma, 236
Osteoblastoma, spectrum of, 321
Osteolysis, iodiopathic multicentric, 23
Ovarian cancer, multifarious therapy and therapists, 205

Pancreas, gray-scale echography, 624
Pancreas simulating suprarenal and renal tumors, 530
Pancreatic pseudocysts, spontaneous internal drainage, 985
Pelvic hemorrhage, embolic control, 1028
Percutaneous transaxillary catheterization, 386
Peterson, Charles Hanson (M), 444
Pheochromocytoma, arteriographic manifestations, 567
Pons, caudal dislocation, in adult Arnold-Chiari malformation, 798
Pulmonary metastases from intracerebral meningioma, 419
Pulmonary thromboembolic disease, iliocaval thrombi in, 1019

Radiation therapy bronchogenic carcinoma, 116
Radiologic research, James Picker foundation (E), 439
Radionuclide detection of thrombosed vein, 1249
Radiopharmaceuticals, pharmaco-kinetics of current skeletal-seeking, 293
Reankylosis after hip surgery, 1181
Rectum carcinoma, definitive treatment by intracavitary radiation therapy, 877
Renal failure, angiographically induced, 1039
Renal infarction, peripheral embolization, 1033
Renal lymphocele, ultrasound diagnosis, 1194
Renovascular hypertension, radiation-induced, 634
Rhabdomyosarcoma in pediatric age group, 542
Rheumatoid arthritis, lesions resembling gout, 41

Salivary gland tumors, growth analysis of pulmonary metastases, 493
Scleroderma, spotted nephrogram of renal, 734
Skeletal inflammatory and ischemic disease in children, radionuclide imaging, 832
Skeleton, iatrogenic lesions, 5
Skin response to pions and x-rays, 261
Skull, computed tomography, 779
Spinal neurofibromatosis, 617
Squamous cell carcinoma
  oral cavity, radiation and 5-fluorouracil therapy, 229
  oral tongue and floor of mouth, evaluation of interstitial radium therapy, 223
Stomach, double contrast views, 1159
Superior mesenteric artery, iatrogenic embolization, 822

Test pattern for evaluating x-ray tube focal spots, 1239
Testicular tumors metastasizing to the lungs, radiation therapy, 475
Testis, cancer of undescended or maldescended, 302
Thumb, arthrography, 1047
Thymoma-hypogammaglobulinemia syndrome, 1219
Tonsil carcinoma, management of, 248
Trauma, value of repeat cerebral arteriography, 792
Tuberous sclerosis, abdominal angiographic spectrum, 807

Ulcerative colitis and Crohn's disease, hepatic angiography, 952
Upper pole calyx, medial deviation, 1189
Ureteral fibrous polyps, multiple benign, 723
Urography, emergency excretory, in abdominal trauma, 739
Uterine sarcomas, treatment results and prognostic factors in stage I and II, 139

Van de Graaff generator, central axis depth dose, 1260
Vascular impressions of gut, 970
Venography in injuries of extremities, 1023
Ventricular aneurysms, left, on lateral chest film, 1140
Vertebral sarcoidosis, 900
Virus diseases of bone: do they exist? 677

Wilms' tumor, angiographic manifestation of bilateral, 802

AUTHOR INDEX TO VOLUME 126

Abbate J, 880
Abe M, 481
Abell MR, 704
Abrams HL, 652, 786
Acker JJ, 336
Ackerman LV, 248
Adams DF, 786
Adams RI, 1260
Akerman M, 952
Alavi A, 179
Alazraki N, 1246
Allan TNK, 63
Altemus LR, 567
Amplatz K, 432
Anderson DW, 1260
Anderson RD, 1203
Ansfield FJ, 229
Antonovic R, 386
Asher WM, 624
Atkinson GO, 1164
Azar-kia B, 56
Azimi F, 853

Baer JW, 394
Bagshaw MA, 236
Baker DH, 957
Balkov IM, 413
Balthazar EJ, 358
Barker, EG Jr, 1053, 1069
Barkley HT Jr, 163
Barnes JE, 261
Batata MA, 302
Beabout JW, 321
Beachley MC, 95
Becker JA, 368
Berdon WE, 957
Berg D, 842
Berger PE, 538
Bergreen P, 1033
Blahd WH, 293
Blake HA, 336
Blanc WA, 957
Bloom S, 1159
Bohorquez J, 863
Bradbury JN, 261
Brandenburg JH, 229
Bradley EL III, 985
Brahme F, 941
Brennon W, 46
Brodey PA, 900
Brown TL, 1194
Bryan PJ, 853
Bryson MF, 550
Buonocore E, 336
Burko H, 567

Cacciarelli AA, 642
Campbell RE, 1059
Caragol WJ, 601
Carney JA, 406
Carr DT, 116
Carter J, 46
Casecade PN, 1147
Chan EK, 107
Chang SF, 704
Cheatham WC, 1010
Chernak E, 877
Chernish SM, 512
Childs DS Jr, 116
Chiu CL, 779
Christenson R, 567
Christie JH, 779
Clapp PR, 1019
Clements JL Jr, 985
Coan JD, 1003
Cockerill EM, 512
Coel M, 970
Compton WR, 807
Constable WC, 634
Cooley CW, 914
Cooper PH, 524
Cornell SH, 779
Cox JD, 268
Cremin BJ, 352

Daffner RH, 1010
Dahlin DC, 321
D'Ambrosia R, 1181
Danzig LA, 1046
Davis CS Jr, 723
Davis HL, 229
Davis HT, 261
Dedrick CG, 419
Deignan JM, 1017
Delclos L, 148, 223
Dencker H, 952
Depner TA, 1197
Deutsch V, 1035
Dhaliwal R, 877
Diankov LA, 413
Dicello JF, 261
Di Fazio LT, 70
Dobrowolski F, 261
Dokumov SI, 413
Donaldson M, 179
Donovan C, 957
Dotter CT, 386
Doyle RJ, 1239
Drasin GF, 1010
Dunnick NR, 965
Dwosh IL, 1181

Earampamoorthy S, 70
Eaton SB Jr, 985
Eilber FR, 1082, 1088
Eisenberg RL, 814
Eisert DR, 268
Ekelund L, 952
Elguezabal A, 728
Evens RG, 1117

Fajman W, 842
Fazio V, 877
Feldstein ML, 279
Fellows RA, 892
Ferris EJ, 1019
Figley MM, 188, 339
Fisher CM, 576
Fisher RM, 352
Fletcher GH, 148, 155, 163, 216, 223, 441
Forbes GB, 550
Forrest JV, 597
Frankel RS, 832
Free EA, 817
Freimanis AK, 624
Fu KK, 107

Gallager HS, 135
Gamboa B, 1140
Gammill SL, 376
Gay B, 957
Gay BB Jr, 1164
Gelman MI, 743
Gerlock AM Jr, 1023
Gershater R, 992
Gertler AN, 70
Ghahremani GG, 1175
Gisvold JJ, 406
Goede MR, 1260
Goergen TG, 647, 1181, 1246
Goffinet DR, 236
Goldman AB, 32
Goldman HS, 728
Goldsmith MR, 1159
Gollin FF, 229
Goode RL, 236
Gordon DH, 368
Goto K, 1211
Grabstald H, 302
Green JP, 123
Greenberg M, 268
Greitz T, 582
Guillamondegui OM, 1256

Haber K, 624
Hahn FJY, 593
Hall W, 1251
Handel SF, 1003
Hanelin LG, 755
Harell GS, 965
Harned RK, 416, 981
Harrison RB, 751, 1189
Harvey H, 1249
Heithoff KB, 46
Henderson D, 1069
Henderson MD, 915
Hertz M, 1035
Hessel SJ, 786
Higgins CB, 1155
Hilaris BS, 171, 302
Hildell J, 941
Hildner JH, 1069
Himmelfarb EH, 376
Hoff JT, 792
Holgate RC, 992
Holmes EC, 1088
Holt JF, 538
Hornback NB, 542
Howards SS, 1189
Hudon G, 432
Hudson TM, 601
Huebotter RJ, 293
Hughes FA, 723

Jackson DC, 1039
Jacobs RP, 739
Jacobson HG, 617
Jahshan AE, 1028
Janzen EM, 761
Jarvis CJ, 46
Jelden G, 877
Jensen PS, 343
Jesse RH, 1256
Johnson RO, 229
Johnsrude IS, 1039
Judy PF, 786

Kalisher L, 903
Kane P, 46
Kane PE, 817
Kantrowitz A, 1147
Karlen JR, 139
Karsell PR, 406
Kassner EG, 728
Kattan KR, 612
Katzen BT, 802
Kay JJ, 601
Keating JW Jr, 1178
Keats TE, 751
Kemp HG, 1140
Kerman R, 880
Khanna NN, 887
Kim JH, 171
Kim S, 432
Kinkhabwala M, 368
Kirkham TH, 896
Kirks DR, 817
Kittredge RD, 1140
Kligerman MM, 261
Knapp EA, 261
Koff RS, 70
Kohout ND, 900
Kollins SA, 406
Korobkin M, 739
Kosaka M, 1211
Krishnamurthy GT, 293
Krumpelman J, 1053
Kuhl DE, 179
Kuhns LR, 538
Kundel HL, 1233
Kyaw MM, 807

Lal H, 887
Lande A, 822
Landgren RC, 148
Lane EJ, 974
Lane TF, 261
Lang EF, 192
Latchaw RE, 629
Lau BHS, 313
Lee FA, 248
Lee RE, 116
Leeds NE, 617
Leonidas JC, 892
Lepanto PB, 179

Lester PD, 807
Levin DC, 368
Lewis DB, 761
Lewis GC, 205
Lim GHK, 550
Lindberg RD, 223
Lindstrom RL, 755
Lipton A, 1249
Littman P, 179
Lo TCM, 229, 475
Loeffler RK, 261
Long JA, 903
Long JM, 1053
Loop JW, 63
Lucas B, 642
Lunderquist A, 952

Madewell JE, 524
Madsen JA, 807
Mahon PF, 761
Majd M, 832
Mani RL, 814
Mann WJ, 1028
Marangola JP, 853, 974
Marc J, 842
Marcial VA, 471
Markowitz M, 802
Martel W, 704
Martin JA, 444
Marvel JP Jr, 1059
Matsue H, 1159
Mazess RB, 1266
McAfee JG, 908
McAlister WH, 642
McCartney W, 1077
McDonald EJ Jr, 739, 792, 814
McDonald JV, 279
McLaughlin GC III, 512
McLeod RA, 321
McLoud TC, 423
Meaney TF, 1095
Menuck L, 970, 1169
Merino-deVillansante J, 765
Messina AV, 56
Meyers MA, 77, 822
Miller FJ Jr, 1028, 1249
Miller JP, 1039
Miller MH, 1003
Miller RE, 512
Minagi H, 739
Mindell JH, 1178
Moffatt RE, 1219
Montague ED, 127, 155, 216
Moore JP, 1159
Moore R, 432
Moore RH, 139
Mortel R, 1028
Morton DL, 1082, 1088
Moskowitz SA, 123
Murray RO, 5
Musallam JJ, 779

Nadell J, 629
Naffis D, 1164
Nazat B, 1077
Neiman HL, 101, 1194
Nelson AJ, 216
Newton TH, 798
Ngo E, 313
Nishidai T, 481
Niwayama G, 647
Nusynowitz ML, 1077

Oestreich AE, 638
O'Gorman AM, 896
Ogura JH, 248
Older RA, 1039
Olmsted WW, 524
Omell GH, 597
Onoyama Y, 481

Palacios E, 56
Palubinskas AJ, 734
Pant GC, 887
Park CH, 1249
Parker BR, 965
Parvey LS, 376
Paul RE Jr, 1159
Peck AG, 419
Perez CA, 248
Pessin M, 576
Petersen DF, 261
Peterson KL, 1155
Peyster RG, 903
Pfisterer WF, 755
Phillips JF, 1194
Phillips TL, 107
Piver SM, 139
Poplack WE, 1159
Poznanski AK, 538
Powers WE, 248
Prather J, 1077
Pripstein S, 900
Proto AV, 974
Putman CE, 423

Rabinowitz JF, 376, 1229
Raeside DE, 1260
Ramirez G, 229
Ramming KP, 1088
Ranniger K, 95
Rao AKR, 530
Rao GUV, 1239
Rappoport A, 41
Rastogi BL, 887
Rauchway M, 714
Rausch JM, 1155
Ravin CE, 423
Ray JW, 107
Reese DF, 406
Reimann BEF, 1077
Reinke RT, 1155
Resnick D, 647, 1046, 1181
Revesz G, 1233
Rim K, 593
Roberson GH, 576
Robbins AH, 70
Robinson F, 1063
Rodda BE, 512
Rodriguez-Antunez A, 877
Rösch J, 386
Rosenbaum HD, 1069
Rosenstock J, 179
Rubenfire M, 1147
Rubin P, 279
Rubinstein ZJ, 1035
Rudikoff JC, 1019
Ryan KG, 1197
Ryan S, 394

Sagel SS, 597
Sakamoto T, 481
Salazar OM, 279
Sane SM, 46, 1223
Santulli TV, 957
Sanyal B, 887
Sarasohn C, 1229
Sarkanyatz AM, 413
Schabel FM Jr, 500
Schimmel DH, 734
Schwarz H, 1033
Scott RM, 1251
Selke AC Jr, 1069
Sexton RF, 1010
Shahin N, 1035
Shannon M, 56
Shapiro R, 1063
Shapiro RF, 1181
Sherrick DW, 761
Shidnia H, 542
Shipkey FH, 376
Shukovsky LJ, 155
Siegle RL, 1229
Silver TM, 530
Silverman FN, 677
Simon AB, 101
Sklaroff DM, 493
Slater JM, 313
Smith CD, 444
Smith CW, 567
Smith GR, 63
Snead JA, 444
Snyder WH III, 1023
Son YH, 475
Sosman JL, 41
Sparks FC, 1088
Spitz HB, 714
Spasov SA, 413
Staab GE, 634
Stefani S, 880
Stein JA, 786
Stelling CB, 981
Sternhagen CJ, 261
Strange G, 900

Tabrisky J, 755
Taft PD, 419
Takahashi M, 1211
Tamakawa Y, 1211
Talpey ND, 127
Tarcan YA, 842
Taveras JM, 765
Taybi H, 817
Taylor A, 1246
Tegtmeyer CJ, 634, 1017
Thal ER, 1023
Thomas BR, 1189
Thompson WM, 1039
Tobin DA, 1251
Tokita N, 171, 302
Troupin RH, 188
Tsukada Y, 139
Tubis M, 293
Turnbull R, 877
Twardzik FG, 493
Tyler T, 23

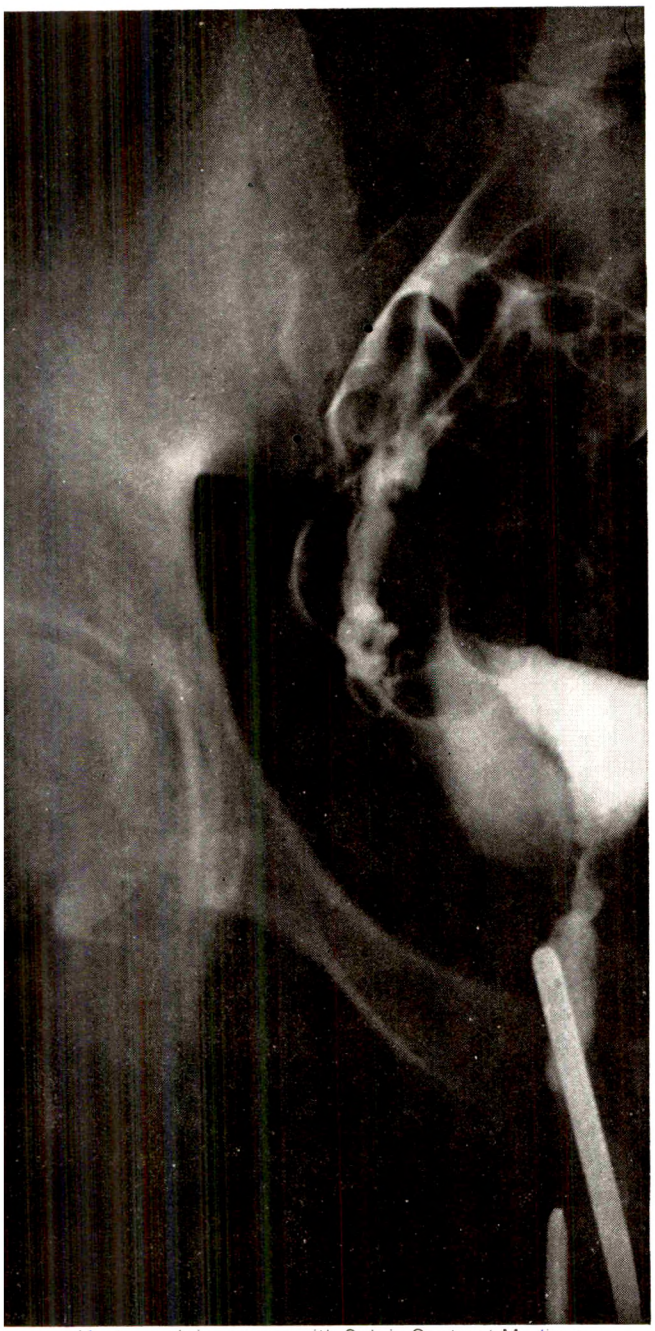
Udupa KN, 887

Vaeth JM, 123
Vermund H, 229
Voigt K, 582
Vongtama V, 139

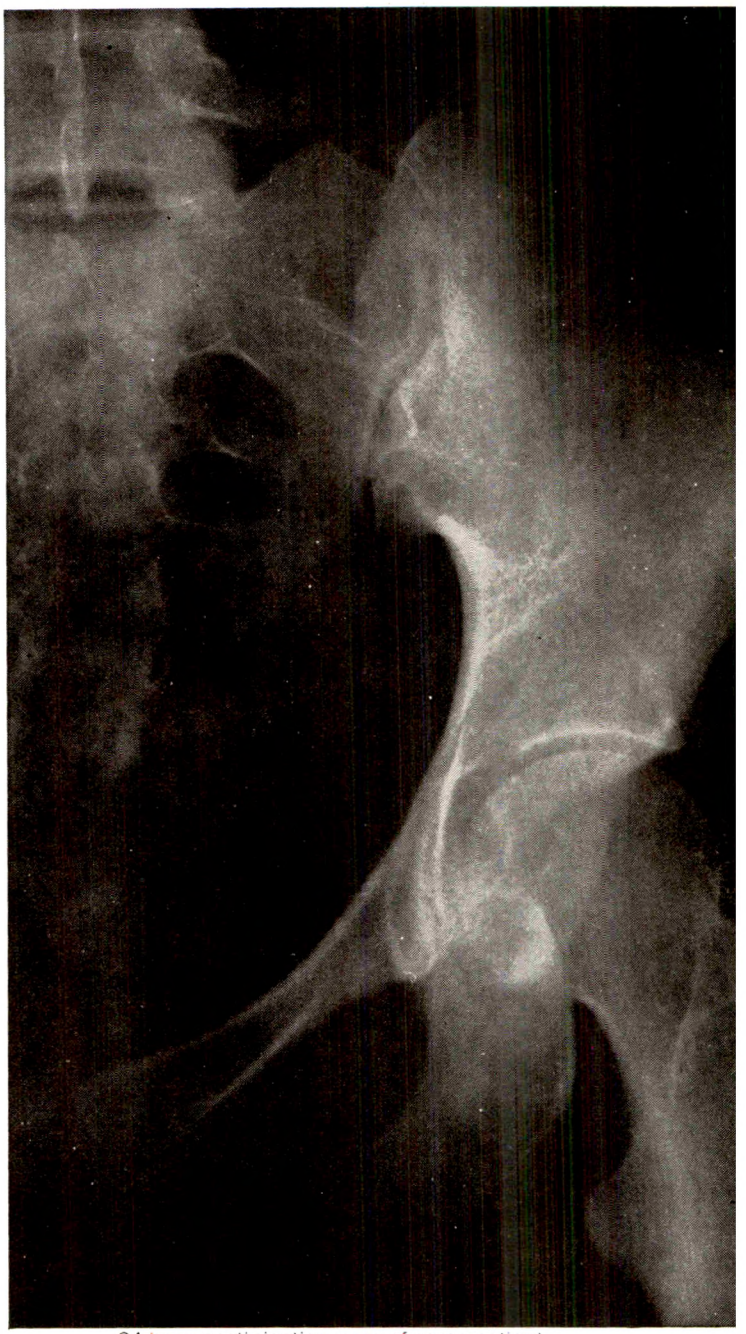
Wajszczuk WJ, 1147
Weakley F, 877
Weinstein M, 798
Weissman BN, 41
Weller SA, 236
West G, 261
Whalen JP, 1315
Wharton JT, 148
Wheeler WE, 95
Whitmore WF Jr, 302
Wickis EA, 70
Wiley AL Jr, 229
Williams HJ, 46, 1223
Williams S, 981
Winestock DP, 792
Winograd J, 734
Withers HR, 155
Wolfe GL, 981
Wolfe JN, 1130
Wood, MB, 751
Woodside J, 1033
Wyatt GM, 714

Yabumoto E, 481
Yaghmai I, 1175
Yamauchi H, 1197
Young LW, 550

Zeman GH, 1239
Zingas AP, 656
Zollinger RM, 933



Hysterosalpingogram with Salpix Contrast Medium.



24-hour postinjection x-ray of same patient.

now you see it

now you don't

With Salpix as your contrast medium, your gynecologic patient needn't undergo the 24-hour postinjection x-ray usually required with iodized oils. Water-soluble Salpix leaves virtually no irritating radiopaque residue to produce foreign-body reactions, yet it provides the viscosity needed for adequate visualization.

Contraindications: Contraindications to hysterosalpingography include the presence of severe vaginal or cervical infections, existing or recent pelvic infection, marked cervical erosion or endocervicitis, and pregnancy. The procedure is contraindicated during the immediate pre- or post-menstrual phase.

Sensitivity Test: If indicated in the patient's history, an intracutaneous skin test or sublingual absorption observation may be done with 0.1 cc Salpix.

Warning: Not for intravenous use.

© ORTHO PHARMACEUTICAL CORPORATION 1970

CONTRAST MEDIUM

Salpix

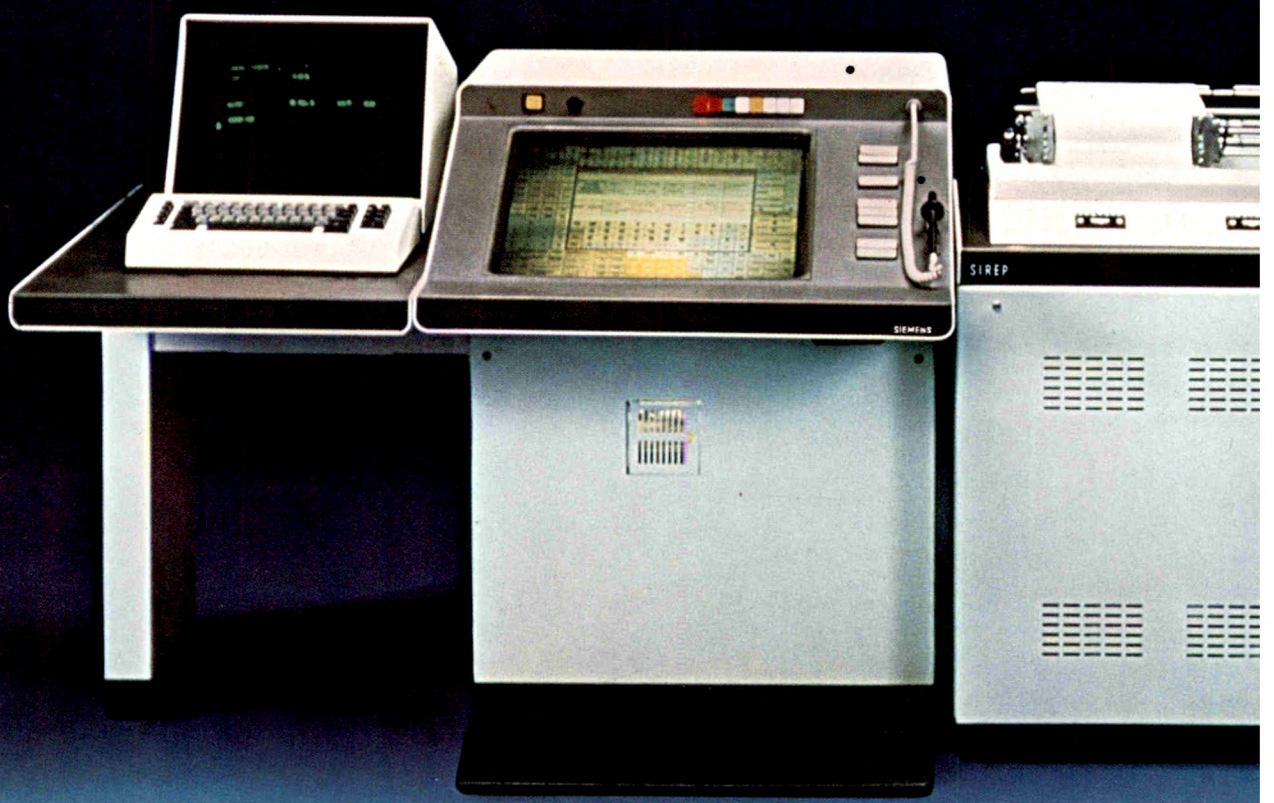
TRADEMARK

EACH CC CONTAINS:
sodium acetrizoate 0.53 g and
polyvinylpyrrolidone 0.23 g

Ortho

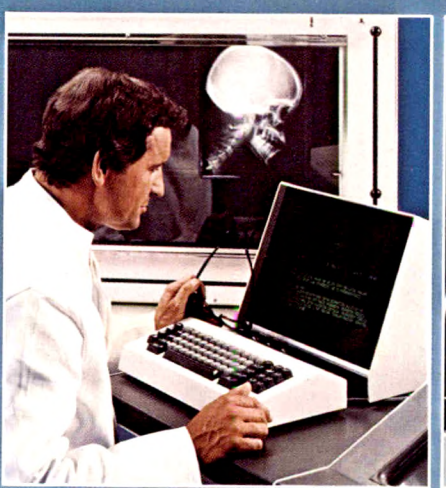
ORTHO PHARMACEUTICAL CORPORATION • RARITAN, NEW JERSEY 08869

For computerized radiological reporting.

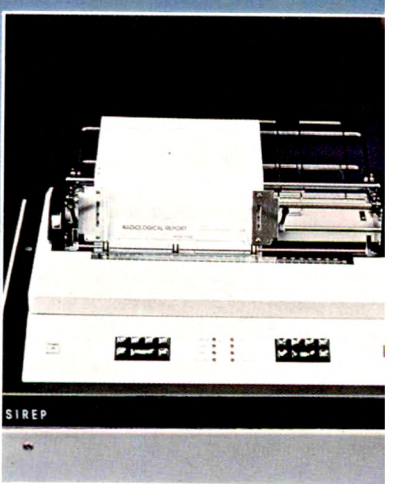




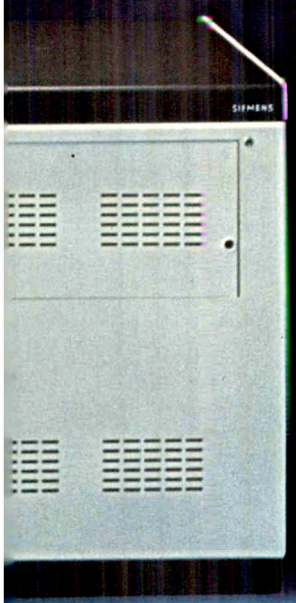
The Terminal
Reports are easily composed at The Terminal which has access to over 6500 anatomical, pathological and descriptive terms and illustrations.



The Keyboard/Display
All entries appear here for review. Corrections, cancellations or insertions can be made at any time before final printout.



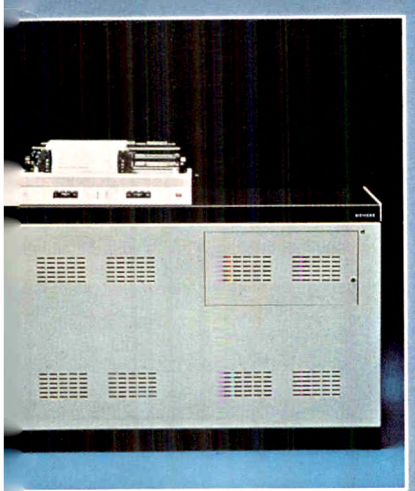
The Printer
After completing all entries, the radiologist activates The Printer and the report is printed quickly and accurately.



SIREP makes radiological reporting easier, while allowing data to reach the referring physician sooner. In addition to real savings in time and labor, SIREP serves as the basis for an improved system of information processing and communication. The result is a more efficient radiology department.

SIREP offers the speed, flexibility and depth of a conventionally dictated report. Clinical findings are entered with the touch of a finger—multi-copy finished reports are printed in seconds. The content is precise, abbreviated and free of clerical errors. The many advantages of SIREP are applicable to any size hospital, clinic or private practice.

Investigate the Siemens SIREP and ask about convenient lease financing arrangements. For detailed information, a comprehensive brochure is available from your Siemens representative, or you may write to Siemens Corporation, Iselin, New Jersey 08830.

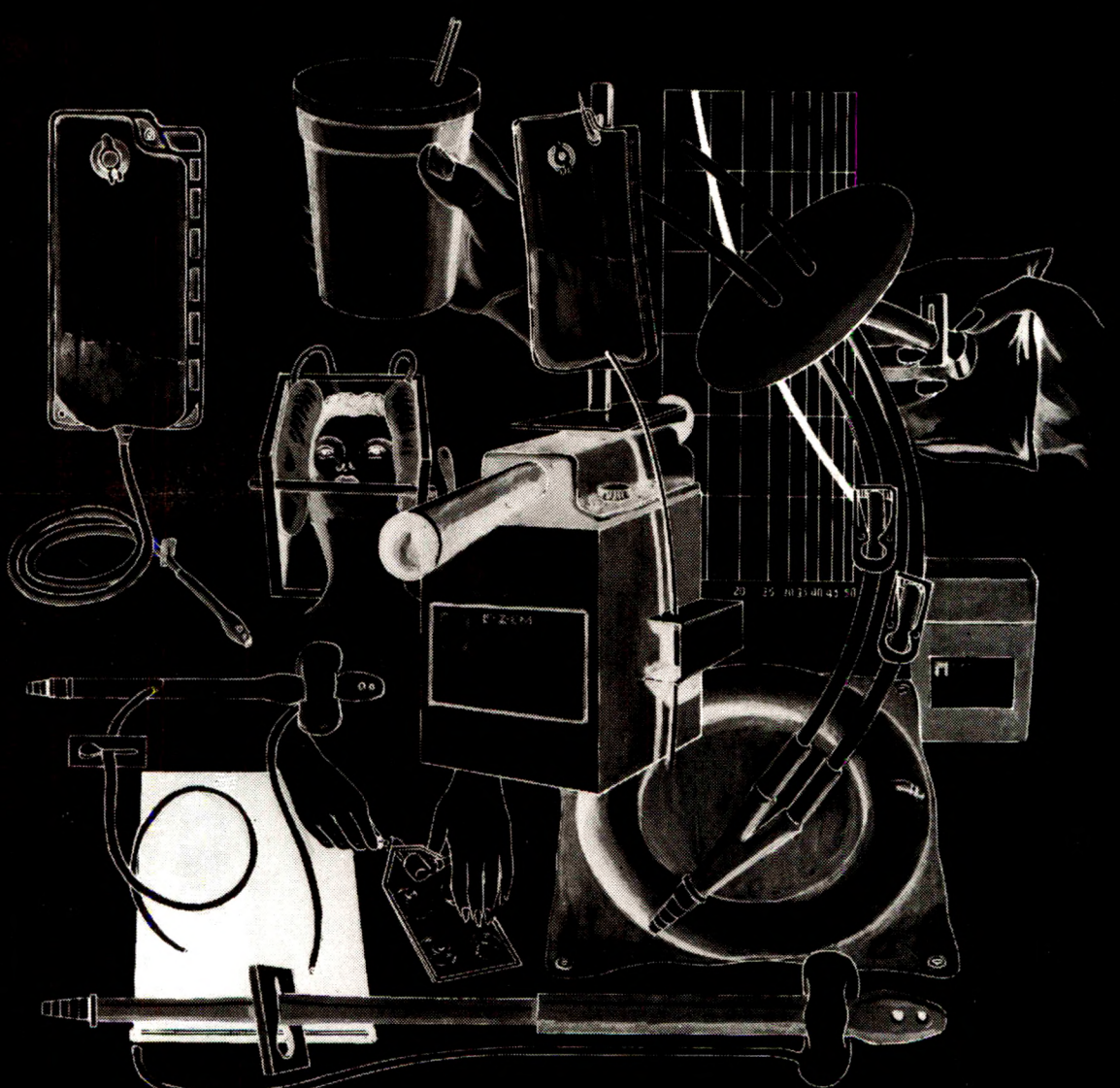


Control Unit
processor-controlled for
l and accuracy, this computer
porates the functions of a
rn data processing system.

SIEMENS

Barium, Barium Systems, and Ancillary Products

...formulated and designed to meet the realistic needs of the Modern Radiology Department



E-Z-EM

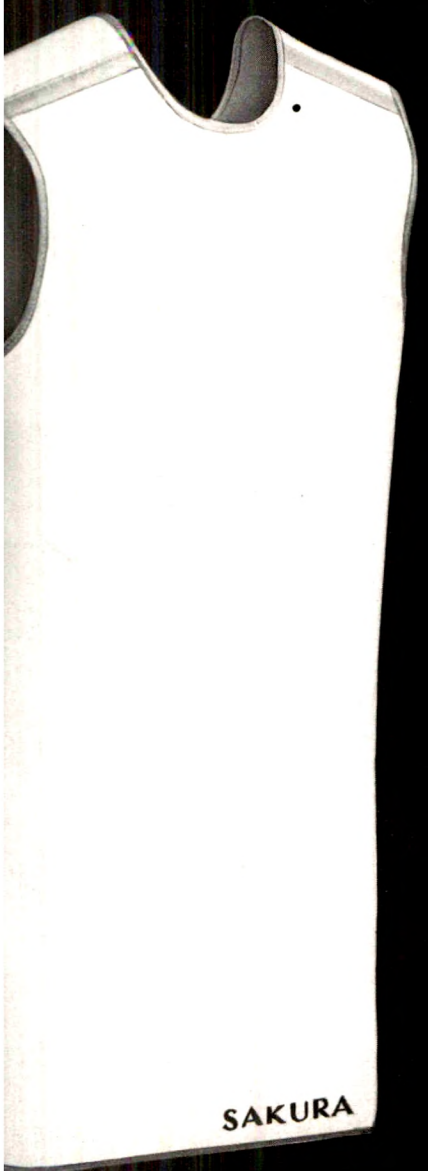
System of your choice

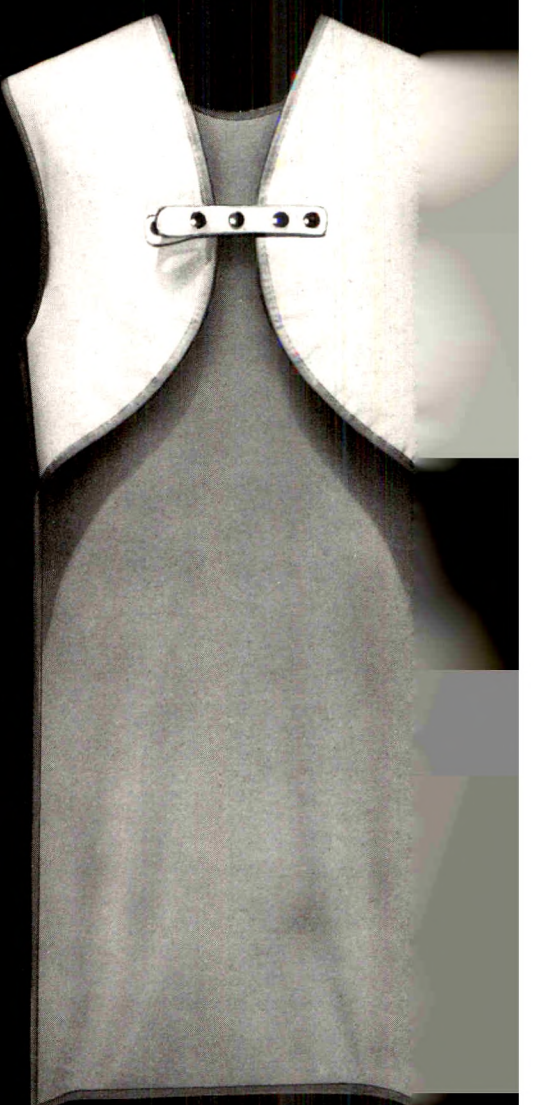
111 SWALM STREET

Westbury, N.Y. 11590 (516) 333-8230

International Affiliates: E-Z-EM Rooster B. V., Infirmeriestraat 6-8, Rotterdam 16, Netherlands

Sakura X-ray Aprons make heavy protection a little lighter.





And the first time you wear one you'll know what we mean. Sakura X-ray aprons offer maximum protection at minimum weight. A combination that means greater assurance, comfort and mobility. Far less strain and general fatigue.

Designed for a more natural feel and balance, Sakura X-ray aprons are made of the finest materials. Multi-layered, lead compounded rubber on the inside. High-strength, washable vinyl on the outside. A combination that adds up to years of carefree wear and maintenance.

And to meet a variety of apron needs, Sakura offers a variety of options. A choice of models: Standard Physician's, Technicians and Special Procedures. And choice of closures: Strings or snaps. All in Bristol blue. We also make special sizes and thicknesses on request.

Sakura X-ray aprons. They make heavy protection a little lighter.

Available for immediate delivery. Write for details.

Sakura Medical Corporation
Radiographic Film and Instrumentation
57 Bushes Lane, Elmwood Park, New Jersey 07407

Mammorex® II can see it before she can feel it.

If she's concerned enough to sk you about breast cancer— nd more women are—there's a ood chance that a quick course n self-examination may not ive her the confidence she ieeds. She probably knows here's a better way.

Mammorex II is a better way. Because the Mammorex II Xerox/film mammography ystem visualizes all breast issue from nipple to chest wall nd can reveal microcalcifications he could never feel.

The versatile Mammorex II ises both conventional film nd Xerox 125®*—virtually ll filming techniques. Changeover takes only seconds.

A capacitor-smoothed, constant-potential generator allows exact incremental adjustments of kilovoltage to help you produce high contrast studies despite the low contrast nature of breast tissue.

Precise selection of focal distances and a contoured radio-translucent breast compressor which averages thickness variations and comfortably immobilizes the breast, help assure sharp image definition.

And because Mammorex II is easy to operate, your patient's examination is quick besides being thorough.

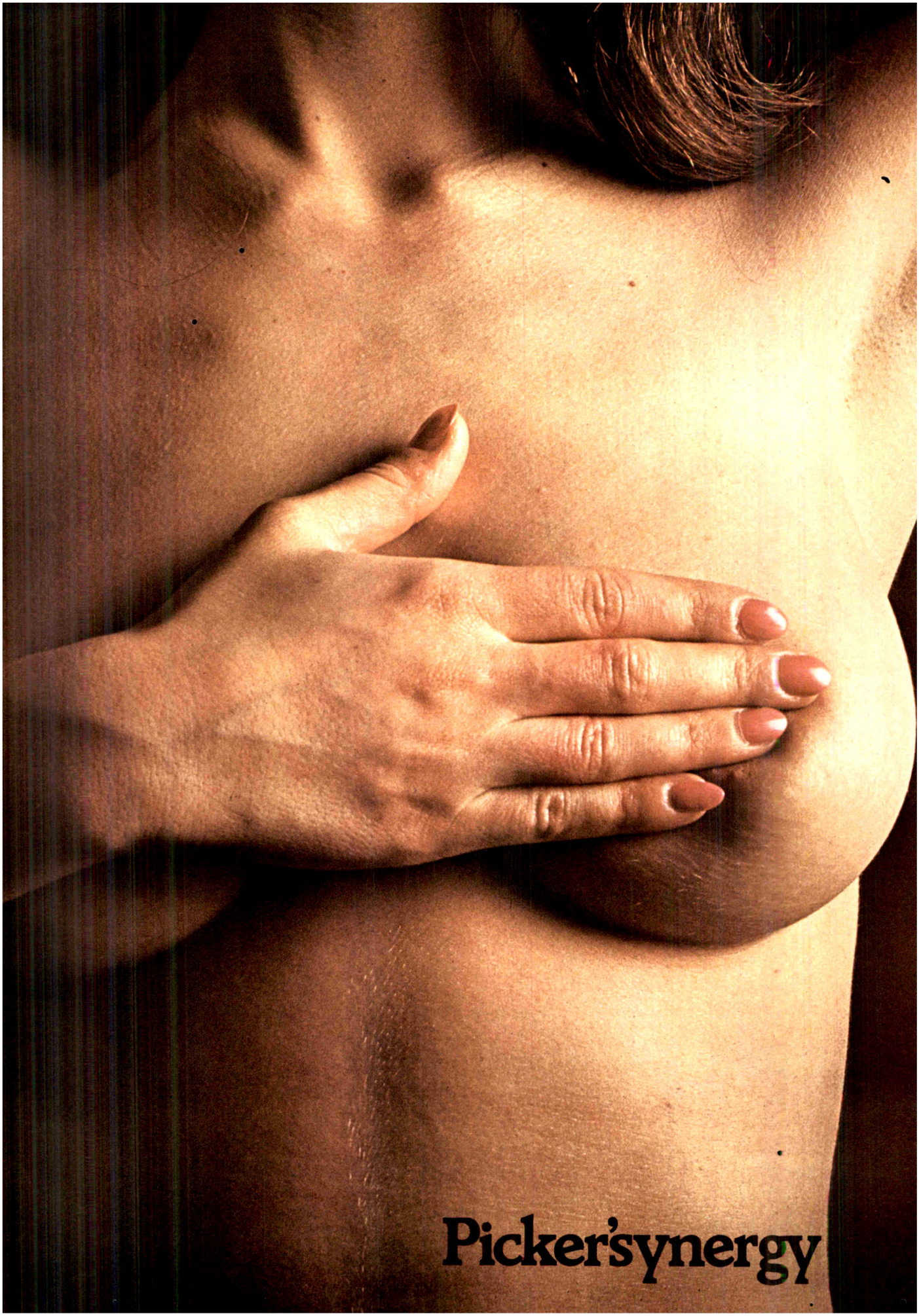
Give your patients the confidence of a complete breast image. Mammorex II is the only system that pictures the entire breast structure from the nipple to the chest wall and the axillary area.

Mammorex II is another example of Picker synergy—the complete interfacing of systems and services for better diagnostic results.

For an informative brochure on Mammorex II and answers to any questions you might have, contact your local Picker representative. Or write Picker Corporation, 595 Miner Road, Cleveland, OH 44143.

PICKER®

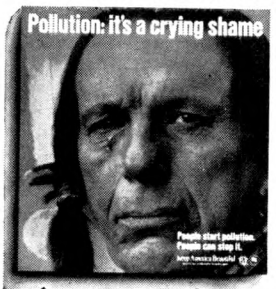
ONE OF THE C.I.T. COMPANIES


Picker'synergy

We've made our mark.

The symbol you see in the center of this page is the new mark of The Advertising Council.

It was made to identify the public service advertising campaigns provided to scores of worthwhile organizations.

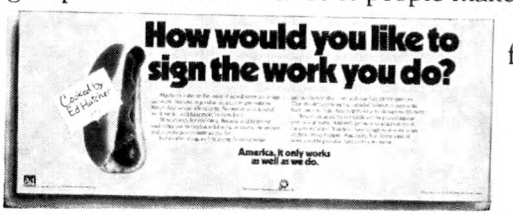


Through these Advertising Council campaigns, the men and women of the American business and communications community are working to make their mark on America's future.

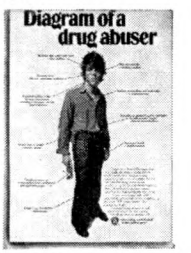


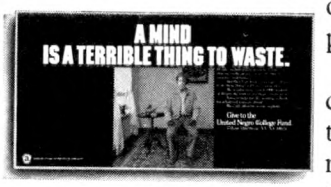


Creative and marketing experts at advertising agencies make their mark. By donating the services it takes to plan and execute these campaigns.



Television/radio networks and local stations, newspapers, business publications, consumer magazines, outdoor and transit media make their mark. By donating the space it takes to run them on the air and in print.





Concerned corporations make their mark. By donating the cash contributions it takes for The Advertising Council to coordinate all these resources and focus them where they are most urgently needed.

In short, every time The Advertising Council stamps its new mark on public service advertising, a lot of people make their mark.

And that mark counts for a lot.

A Public Service of
This Magazine &
The Advertising Council

CHARLES C THOMAS • PUBLISHER

ADMINISTRATION OF A RADIOLOGY DEPARTMENT: Hints for Day-to-Day Operation *by* **Murray L. Janower**, *St. Vincent Hospital, Worcester, Massachusetts.* Various systems which can be applied to the radiology department to insure efficient functioning are presented in this book. In addition to a general overall look at a totally functioning diagnostic radiology department, the various subunits in a department are dissected and discussed in detail. All of these discussions are supplemented by a great deal of statistical data. Specific attention has been given to the methods used in handling patients, the establishment of a quality control program, efficient production of radiological reports, methods of film interpretation, and darkroom operations. *'76, 72 pp., 8 il., 7 tables, $7.50*

"TRAUMA" AND "NO-TRAUMA" OF THE CERVICAL SPINE *edited by* **Kenneth R. Kattan**, *Univ. of Cincinnati College of Medicine, Cincinnati, Ohio. (11 Contributors)* This complete volume on the topic of cervical spine trauma includes descriptions and excellent illustrations on the anatomy of the cervical spine and numerous varieties of trauma, their assessment and management. Discussed are the many symptoms attributed to cervical spine trauma as well as diseases which provoke this malfunction. The authors deal not only with trauma, but also with how to differentiate it from other conditions including the normal. *'75, 328 pp., 292 il., $24.50*

HEALTH PROTECTION OF RADIATION WORKERS *by* **W. Daggett Norwood**, *Hanford Environmental Health Foundation, Richland, Washington.* Acute and chronic, somatic and genetic effects are discussed with emphasis on prevention. Radiation protection standards and regulations are outlined, and methods for maintaining these standards are described. Diagnosis and treatment of radiation injury from external radiation or internally deposited radionuclides are considered generally as well as specifically for each radioisotope. The medical supervision of radiation workers, radiation accidents, atomic power plants and medicolegal problems are also covered. *'75, 468 pp., 16 il., 16 tables, $27.50*

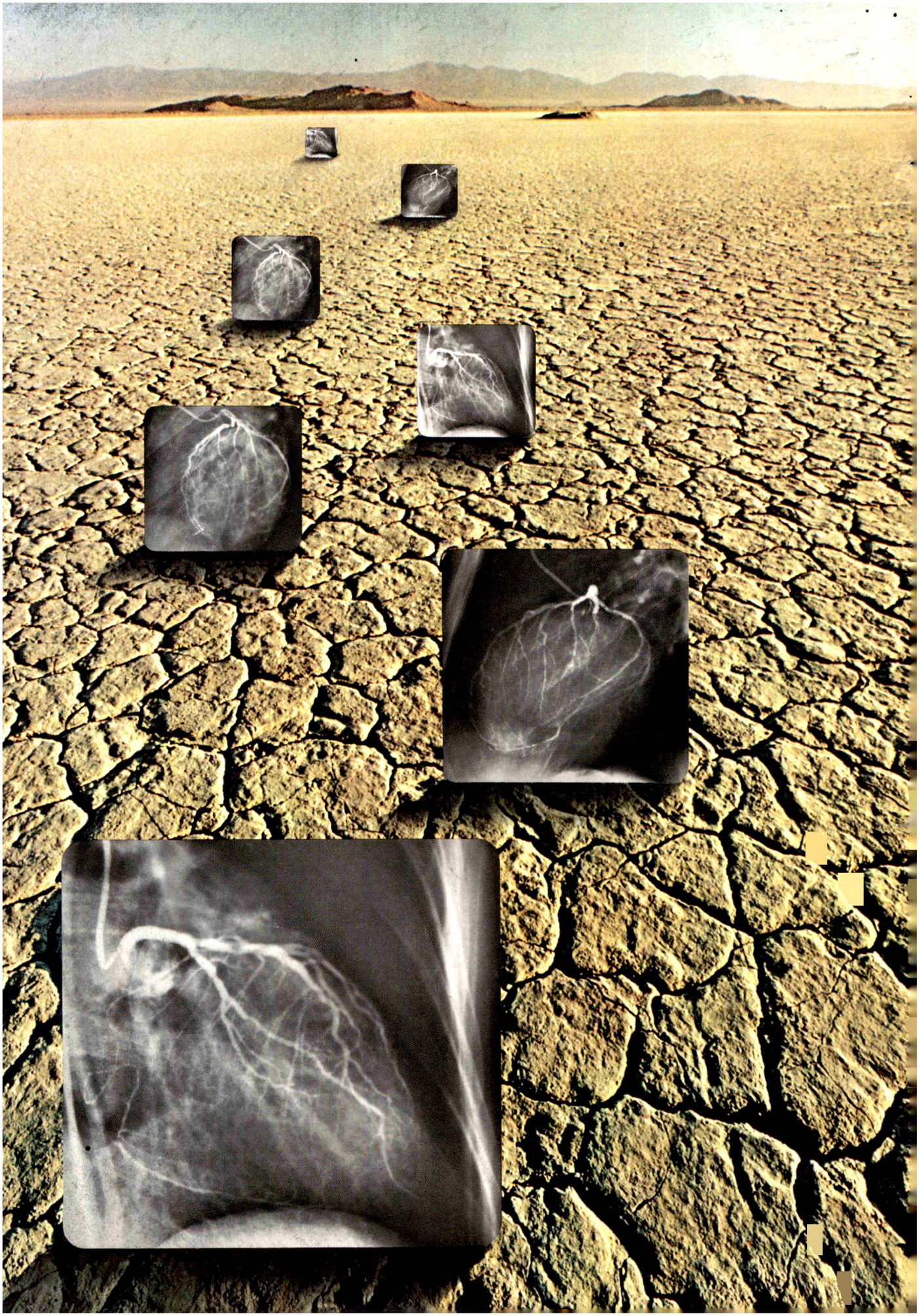
AN ATLAS OF POLYTOME PNEUMOGRAPHY *by* **Taher El Gammal** *and* **Marshall B. Allen, Jr.**, *both of Medical College of Georgia, Augusta. Assisted by* **Paul Dyken.** This atlas presents a large number of studies which supplement the study of normal anatomy of the cerebrospinal fluid pathways, and provides comparison for the identification of abnormal structures. Concentration is on the findings of polytome pneumography, but where possible, correlations are made with angiography, positive contrast ventriculography, and CAT examinations. Relative values of these different examinations are demonstrated. *'76, 480 pp. (8 1/2 x 11), 729 il., $39.50*

THE FUNDAMENTALS OF RADIOLOGICAL SCIENCE *by* **John Hale**, *Hospital of the Univ. of Pennsylvania, Philadelphia.* Training programs in radiology have recently been restructured in that the subject matter is now being divided into the two areas of basic radiological science and clinical applications. This text is devoted to the first area of basic radiology and the fundamentals of mathematics and physics common to all specialties. Chapters on such subjects as radiation-producing machines or interaction of radiation with matter are offered. With the rapidly evolving technology in clinical application, students should have an understanding of the basic principles of radiology found in this text. *'74, 356 pp., 172 il., 3 tables, $14.75*

BRONCHIAL CARCINOMA *by* **Thomas W. Shields**, *Northwestern Univ. Medical School, Chicago.* **Section on Immunologic Features and Immunotherapy** *by* **Roy E. Ritts, Jr.** In this monograph, the incidence and etiology of the disease are discussed and the pathologic, clinical and roentgenographic features of these tumors are presented. The various groups of patients are defined and a philosophy of their management is presented. Appropriate diagnostic studies are emphasized to classify the extent of the patient's disease. The indications and contraindications of surgical resection, radiation therapy, chemotherapy and immunotherapy are outlined. *'74, 200 pp., 48 il., 22 tables, $12.75*

Orders with remittance sent, on approval, postpaid

301-327 East Lawrence Avenue • Springfield • Illinois • 62717



Rare Earth Imaging products from Kodak: they offer greater technic and equipment flexibility.

Kodak Lanex regular screen and Kodak ortho G film let you make more efficient use of your exposure equipment. They provide higher speed—so you can shorten exposure time, or reduce kilovoltage, or decrease milliamperage.

The advantage is speed—2 to 4 times that of calcium tungstate screens exposed with Kodak *RP* X-Omat film. Exposure time can be minimized, helping to cut the number of retakes. This is a special advantage where motion is a problem—whether voluntary or involuntary.

The benefit is flexibility. For one thing, you can vary technic to get the image you require. For example, you can use a smaller focal spot for improved image sharpness because the high speed lets you reduce milliamperage.

Or you can reduce kilovoltage to provide increased subject contrast in contrast studies or tomographic examinations.

Another benefit: when milliamperage is decreased, or kilovoltage is reduced, or exposure time is shortened, these products can help you get more use out of your equipment.

That is, you can distribute your work load to utilize low-powered units or portable units.

All of which can help extend your radiographic capabilities, as well as the efficiency of the equipment you now have.

There's probably a lot more you want to know about rare earth imaging. Contact your Kodak Technical Sales Representative or your medical x-ray products dealer, or...

WRITE TODAY: Eastman Kodak Company, Dept. 740, Rochester, N.Y. 14650.

Kodak

A commitment to quality

Your knowledge... the film of your choice and... HUNT X-RAY CHEMISTRY for maximum information in automatic film processing

With broad years of experience in radiology, you recognize the importance of achieving more readable films.

Hunt Chemistry will increase the diagnostic value of any film you process. Hunt formulas maximize informational content, producing the full range of densities inherent in the films.

For medium to long scale contrast, **Hunt Universal 90 Developer & Replenisher** offers optimum results. If high contrast characteristics are desired, use **Hunt Type 2 Premium 90/90 Developer & Replenisher.**

Hunt chemical processing systems are respected for their consistent high quality. These concentrates come to your X-ray department full-strength and in "factory-fresh" containers.

HUNT **The Image Maker**
Photographic Industry Group

Because Hunt markets its products on a direct basis, you can save up to 33% over other major chemical manufacturers' systems.

For more information, call Hunt today.

Philip A. Hunt Chemical Corporation, Palisades Park, N.J. 07650
Philip A. Hunt Company (Canada) Ltd., Toronto




100 8 x 10 in.
KODAK
RP ROYAL X-OMAT
Medical X-ray film
Not Interleaved
RP/R14
CURIX
GEVAR POLYESTER BASE
RP 2
125 / 8 x 10 in
25539046
2 1977
IR 2000
High Resolution
Medical X-Ray Film
IN-INTERLEAVED
MS
8 x 10 INCHES
GAF Corporation
140 West 51 Street
New York, N.Y. 10020
8 x 10 inches
20.3 x 25.4 cm
100 NIF
RAPID R
TYPE S
Cronex 4 MEDICAL X-RAY FILM
125 SHEETS
9½ x 9½ IN.
24 x 24 cm
FEB76
FUJI X-RAY FILM
Medical
A TEXT-BOOK OF X-RAY DIAGNOSIS
EDITED BY
S. C. SHANKS
P. KERLEY
THIRD EDITION
ABDOMEN
CHEST
SAUNDERS
JOHN CAFFEY
EDIATRIC
X-RAY
IAGNOSIS
5th EDITION
Diagnostic
Neuro-
Radiology
TAVERAS
WOOD
WILLIAMS & WILKINS
YEAR BOOK
HUNT
PREMIUM
90/90
DEVELOPER & REPLENISHER
20 U.S. Gallon Size
PHILIP A. HUNT CHEMICAL CORPORATION
Palisades Park, New Jersey 07650 • Made in U.S.A.
HUNT
UNIVERSAL
90
DEVELOPER & REPLENISHER
20 U.S. Gallon Size
PHILIP A. HUNT CHEMICAL CORPORATION
Palisades Park, New Jersey 07650 • Made in U.S.A.

CGR's Stratomatic U gives you 240°s of positioning for fast, superb tomography.

The Stratomatic U is CGR's newest sophisticated tomography system.

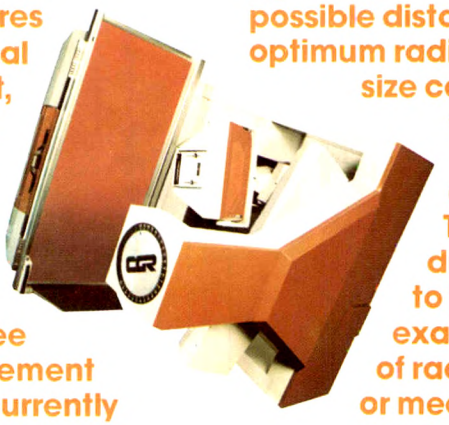


Based on the highly successful Stratomatic H, the new system brings new dimensions to tomography.

Now you can position patients easily and quickly throughout a 240° spectrum. Opening new techniques and new opportunities for examination. The large table top also features a wide range of longitudinal and transverse motions for fast, accurate patient centering.

Stratomatic U features linear, circular and tri-spiral tomography. Electronic and mechanical advances now reduce complex tomographic motion times to three seconds or less. A 50% improvement in exposure time over other currently available tomography systems.

The Stratomatic U also performs conventional radiography, stereoradiography and zonography.



The new system uses the same magnification factor in all modes for both tomography and Bucky radiography. Film is always at the shortest possible distance from the patient for optimum radiographic quality. And any size cassette from 5 x 7" to 14 x 17" can be used.

Stratomatic U is a completely remote system. Table side controls are duplicated at the generator to insure fast, accurate examinations with a minimum of radiation to your patient or medical team.

Stratomatic U. —A new dimension in tomography. Call or write your CGR representative for complete details.

CGR

CGR MEDICAL CORPORATION
2519 Wilkens Avenue
Baltimore, Maryland 21223
(301) 233-2300

CGR CANADA Ltée-Ltd.
500 Boulevard de l'Aéroparc
Lachute, Québec, Canada
(514) 562-8806

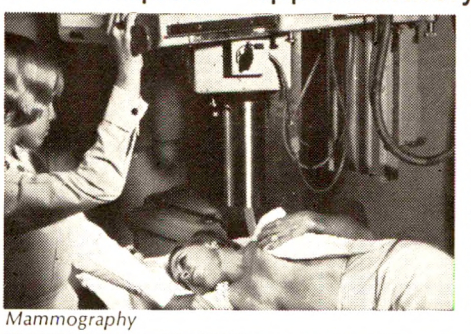




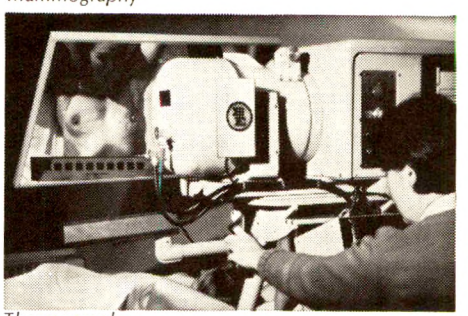
Breast Cancer: earlier warning system

Futility and frustration beset the physician confronted with breast cancer. For the last 35 years, the survival rate has not significantly changed despite intensive educational programs aimed at earlier detection, and improvement in treatment techniques.

What is the outlook? We know the key to reducing mortality from breast cancer is in the *earliest possible* diagnosis. The stage at which breast cancer is detected is *crucial* to the outcome of treatment. By the time a lump is discovered through BSE or clinical examination, critical time may have been lost.



Mammography



Thermography

And we *do* have the means to achieve earlier diagnosis. We do have an *earlier* warning system. Mammography and thermography can detect breast cancer *before* a lump is discernible by palpation. To demonstrate that it is practical and feasible to detect breast cancer earlier by using these modalities, the American Cancer Society and the National Cancer Institute are funding a network of breast cancer demonstration projects. Supported by grants of $2-million from the ACS and $4-million from the NCI, 20 such centers are expected to be operative across the country by the end of the year. Each will screen at no charge, approximately 5,000 women annually, in what is considered to be the ideal detection program — to include clinical examination, mammography and thermography. Each of these detection methods contributes independently to the detection of breast cancer, and none can be dispensed with in the search for early disease.

At present we cannot prevent breast cancer, but the potential for saving more lives is immense. The five-year survival rate changes dramatically from 53% when axillary nodes are positive, to 85% when the disease is localized, to nearly 100% for in-situ cancer.

We have an earlier warning system. Let's use it.



american cancer society®



Your Heart Association can help you help your patients

Your patients and their families might have questions about the heart and blood vessel diseases. Your Heart Association has prepared a variety of pamphlets to assist you in answering their questions in simple non-technical language.

Produced under the guidance of leading cardiovascular specialists, these pamphlets deal with such subjects as heart attack, stroke, hypertension, rheumatic fever, congestive failure, inborn heart defects, varicose veins and other disorders. There are also pamphlets advising on risk factors related to heart attack.

Booklets on therapeutic sodium-restricted or cholesterol-lowering diets are also available on a physician's prescription only.

Ask your local Heart Association for a catalogue listing all these free materials and order a supply.

American Heart Association®

44 EAST 23rd ST., NEW YORK, N.Y. 10010

Contributed by the Publisher

Philips Polytome an

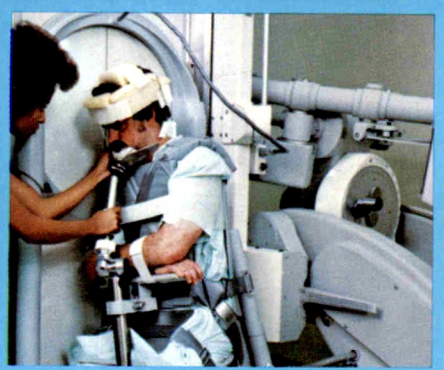
Multi-Directional Tomography for Pneumoencephalography n a fully integrated system.

Now the Polytome—world's mos sophisticated tomographic system—has its own snap-on examination chair for pneumo-encephalography. It's never beer easier or more efficient to use multi-directional tomography in pneumo studies!

Isocentric patient positioning keeps the patient's head in the fulcrum for all projections. And Polytome and chair are fully syn-chronized for proper filling of ventricles and temporal horns.

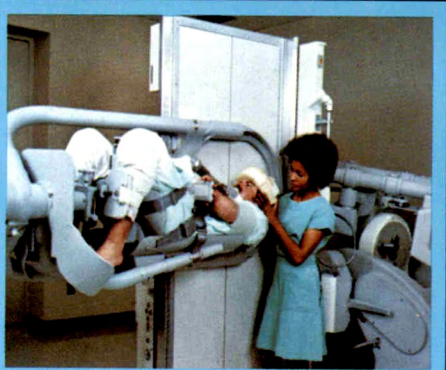
Selected patient positions and visualizations in a common pneumo procedure

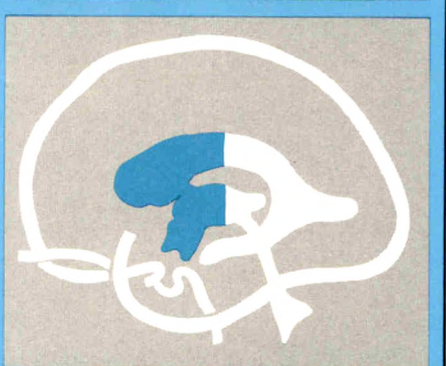
ERECT: LATERAL



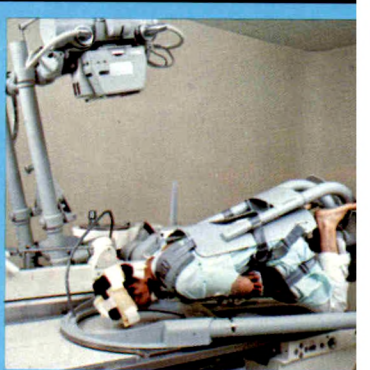


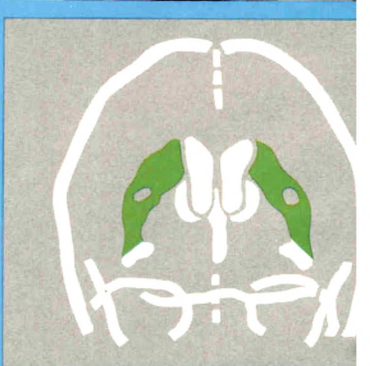
BROW-UP: LATERAL





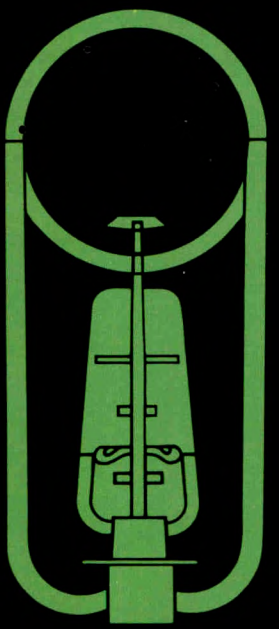
BROW-DOWN: PA





Dedicated Pneumo Chair

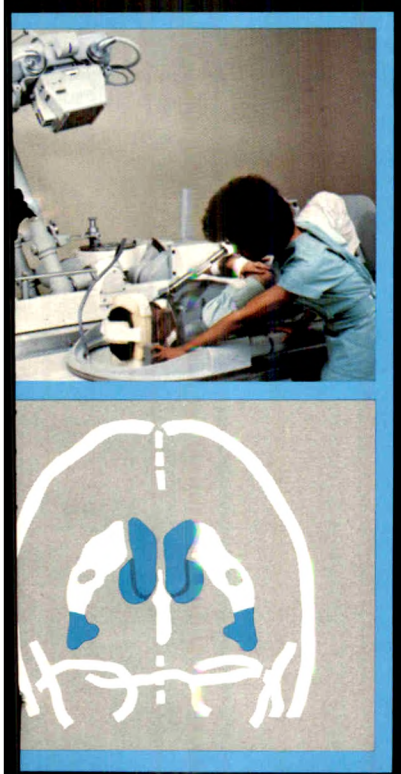
Compact, lightweight, easily and quickly attached, dismounted and stored in the Polytome room, the new chair gives you full use of *all* the Polytome's capabilities: from linear to the famous hypocycloidal blurring motions... layer height adjustment... superb image quality in every exposure... constant enlargement for every layer... optimum visibility of the patient throughout the examination.



Add a Pneumo Chair to any new or existing Polytome for a dedicated neuroradiological system at a fraction of the cost. Detach the Chair and return the Polytome to its role as top department performer!

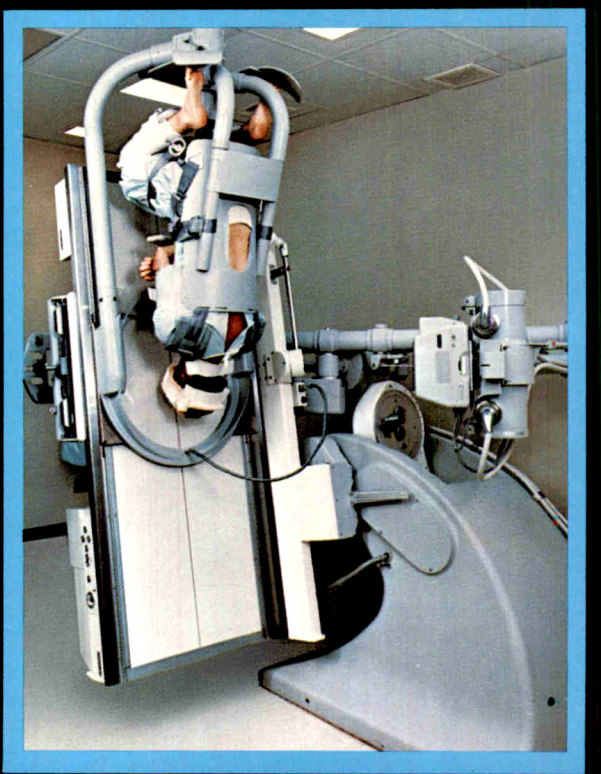
Now let *us* "pull up a chair" and show you how it works.

BROW-UP: AP*



*After sequential filling of temporal horns

A STAGE IN FILLING THE TEMPORAL HORNS



For additional information, contact your Philips representative. Or, call or write:

PHILIPS MEDICAL SYSTEMS, INC.
710 Bridgeport Avenue, Shelton, Conn. 06484

WHERE WOULD THE CAMERA HAVE BEEN, WITHOUT A COLLEGE EDUCATION?

Still making Daguerreotypes, probably.

Instead, photography is a billion-dollar business today. Because inquiring minds, trained and honed on college campuses, started looking into chemicals and film and lens.

Life-saving pharmaceuticals. Hunger-fighting new rice and new wheat. Petrochemicals. Radio. Television. The list of billion dollar industries that got their start in college-trained minds is startling.

You don't want the flow of college-bred new ideas, improvements, inventions to stop. Ever. Not if you're a *good* businessman.

So perhaps you'd better take a good hard look at how much your company is giving to higher education. Because inflation has hit colleges and universities even harder than most.

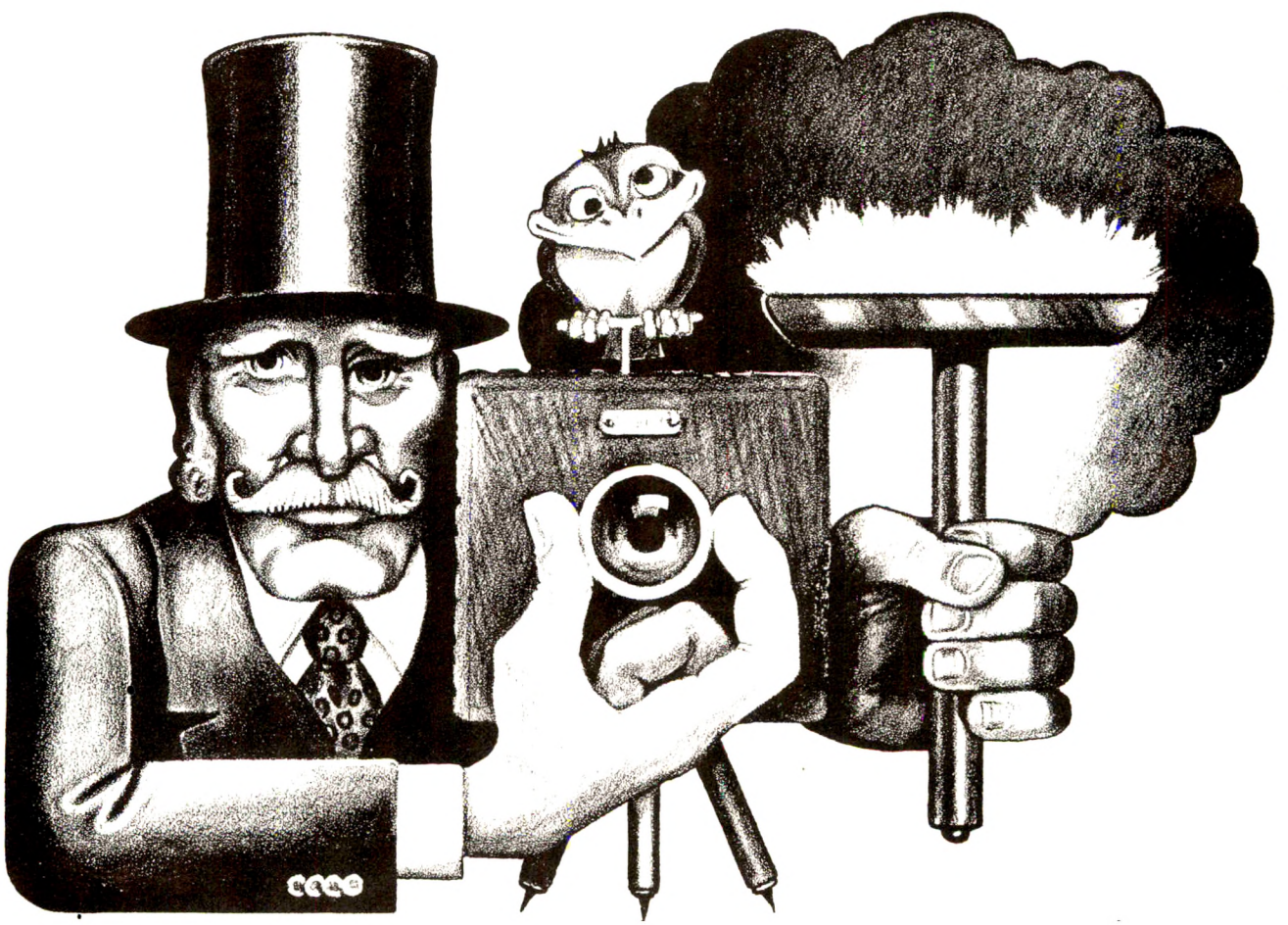
Freedom to experiment is the first casualty of tight budgets.

For the sake of the future, "Give to the college of your choice. Now." Who knows what billion-dollar business of tomorrow is germinating on some college campus today.

CFAE Council for Financial Aid to Education, Inc.
680 Fifth Avenue, New York, N.Y. 10019

A Public Service of This Magazine &
The Advertising Council

Ad Council



LIFESAVING PARTNERSHIP... AGAINST CANCER QUACKERY

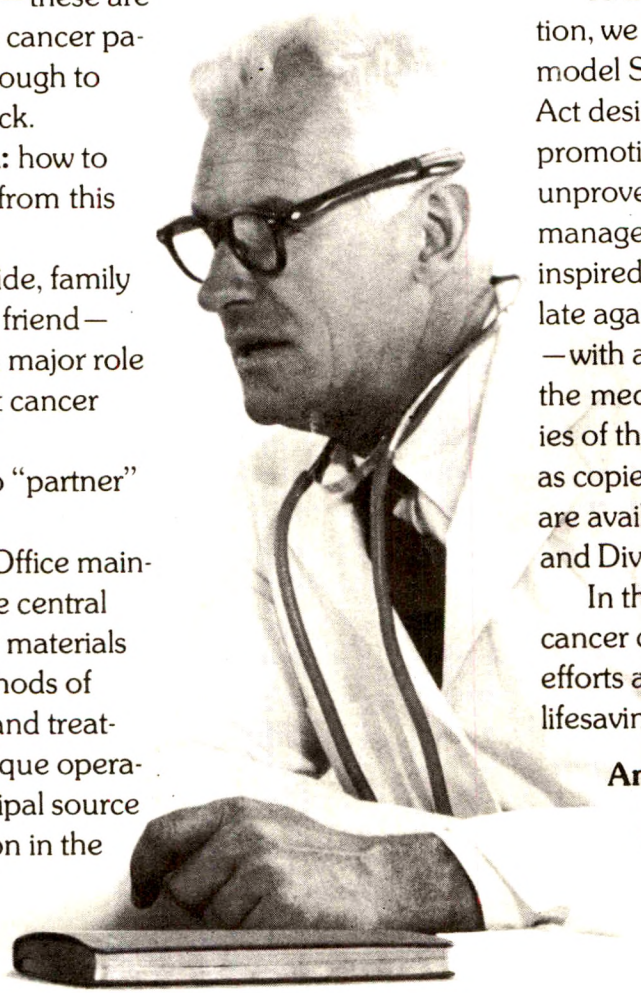
The anguish associated with cancer is compounded by the cancer quack. False hopes—harmful delays—shattering expenses—deceptive diagnoses—loss of life—these are hazards facing the cancer patient desperate enough to seek a cancer quack.

The problem: how to divert the patient from this tragic encounter.

As medical guide, family counselor, trusted friend—you, doctor, play a major role in the fight against cancer quackery.

We are here to "partner" you.

Our National Office maintains an up-to-date central clearing house for materials on unproven methods of cancer diagnosis and treatment. This is a unique operation and the principal source of such information in the country. Its services are widely used. Hundreds of inquiries are received and answered from all segments of the community, from coast to coast.



To trigger grass-roots action, we have formulated a model State Cancer Remedy Act designed to control the promotion and sale of unproven methods of cancer management. This has already inspired nine states to legislate against cancer quackery—with active support from the medical community. Copies of the model act, as well as copies of the laws in effect, are available in our National and Division offices.

In these actions against cancer quackery, as in all our efforts against cancer, ours is a lifesaving partnership.

American Cancer Society

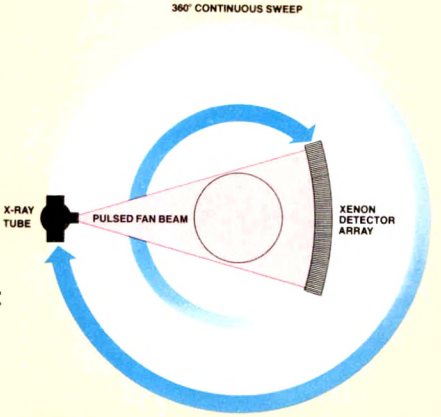
THIS SPACE CONTRIBUTED BY THE PUBLISHER

CT/T fast-scanner: the third generation computed tomography system that's versatile, efficient and consistent.

CT/T system: 4.8-second scans, consistently sharp images.

The CT/T total body scanner has established the third generation of computed tomography: GE fast-scan. With this system, one 360° sweep yields the scan information for a full 320 pixel diameter image in just 4.8 seconds.

This unprecedented speed solves the primary problem of slower units: motion unsharpness caused by patients' respiratory motion. First and second generation systems, using an incremental rotate-and-translate principle, take from 18 seconds to 5½ minutes per scan. But the new GE fast-scan unit features a rotating pulsed fan beam with a 320 element xenon detector array. The tube and detectors rotate around the body in one, smooth 360° motion, taking only 4.8 seconds. Most patients can comfortably hold their breath during the GE fast-scan procedure, with improved resulting image quality.





The CT/T system offers many other diagnostic advantages. Here are just some of the key features:

Versatile viewing capability. The viewing console allows precise selection of the range of CT numbers displayed. A special feature on the CT/T system is an IDENTIFY button, which causes the CT numbers at the center of the CT range to "blink." This provides rapid identification of picture elements at a selected CT number without changing window widths.

Photographic recording of selected images is provided by a multi-format camera which accommodates three standard film sizes.

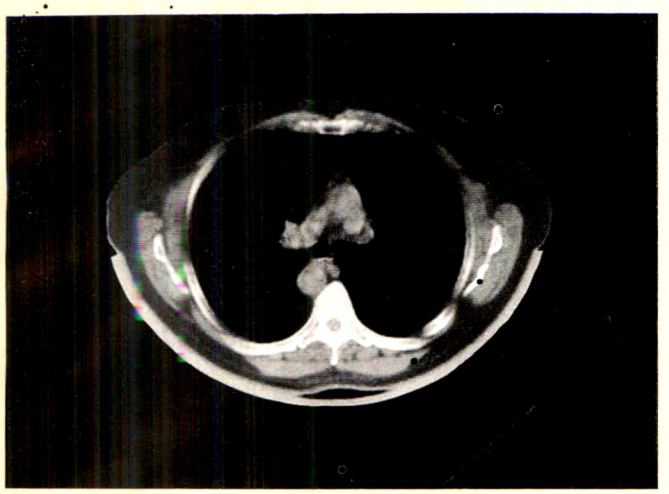
Advantages of GE xenon detectors

After studying many different detector options for the rotating pulsed fan beam fast-scan system, GE researchers found high-pressure xenon offered numerous advantages over other types of detectors. Here are some of the most important considerations:

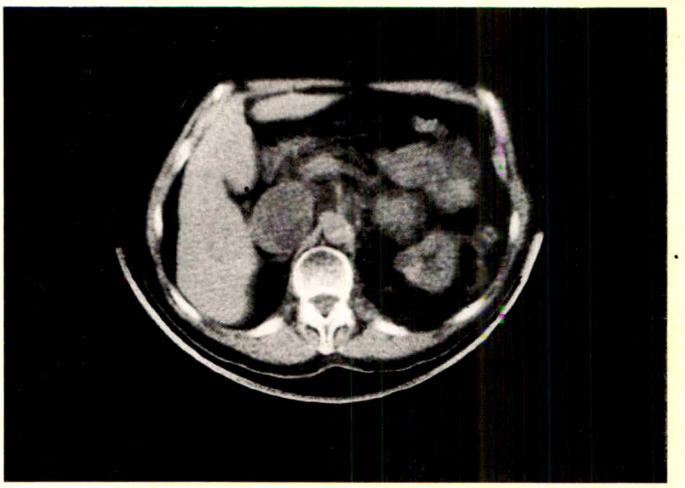
Necessary Characteristics. The multi-element xenon detector array possesses the most important requirements for a CT detector: reliability, complete response to x-radiation, and a wide linear dynamic range. Advanced fabricating techniques provide for reliable, consistent detector manufacturing. The detectors are operated in a stable range of voltage and pressure to ensure consistent performance. Unlike vacuum components, impurity contamination is not a problem, and the uniform high pressure of xenon gas within the detector chamber ensures that the response is uniform throughout the detector, and remains so with time. The pulsed mode of operation provides sufficient time for complete response to the incoming x-ray photons. And, the response of the xenon detector is linear over the range of digitization used within the system.

Overall Efficiency. The overall efficiency of the GE rotating fan beam x-ray source and detector system is a product of two main factors: the detection efficiency and the collimation efficiency. The noise equivalent absorption (NEA) for the xenon detector is about sixty percent that of the best possible scintillator crystal/ photomultiplier tube combination. But the collimation efficiency possible with this system is superior to that of any other. Because of this, at least twice as many unscattered x-rays emerging from the patient actually reach the active area of the detector as in other systems. Also, because the scan is carried out through 360° rather than 180°, the reduction in skin dose required for the same integral dose is calculated to be a factor of about 1.6.

Putting these three factors together (detection efficiency, collimation efficiency and 360° scan) provides an approximate 2X reduction in the skin dose requirement over those systems using a broad x-ray tube focal spot and scintillator crystal/ photomultiplier tube detectors. Thus the pulsed fan beam/multi-element xenon detector array provides the design option of keeping the dose low or increasing the dose to improve resolution. There is considerable latitude in changing the system mAs through changes in the pulse, the pulse mA, and the number of pulses. For the typical patient on the CT/T system, it is expected that the skin dose will be approximately 2-4R, although diagnostic quality images have been produced with skin doses substantially under 1R.



Scan of lung area—Level setting is 0; window setting is 200, ranging from +100 to −100. Soft tissue—muscle, heart and subcutaneous fat—is emphasized.



Abdominal scan—Level setting is +27; window setting is 160, ranging from −53 to +107. Scan shows lobulated liver; round tumor near liver; top of right kidney; displaced spleen.



A fast look: fast-scan CT/T system

Scanning speeds—4.8 seconds and 9.6 seconds.

Image reconstruction time—200 seconds.

Matrix dimensions—320 pixel dia. matrix. Each pixel corresponds to a volume element measuring 1.3 mm x 1.3 mm x 10 mm.

Main disc storage—over 200 images.

Archival storage—magnetic tape unit is standard with the system.

Multi-format camera—images may be positioned on film in any order for diagnostic convenience. Film sizes: 8 x 10; 11 x 14; 14 x 17.

Gantry—60 cm opening; 42 cm field of view; ±15° gantry angulation; no water bag required.

X-ray tube—Maxiray™ 125.

Generator—3-phase MSI™ 850 II.

Simultaneous reconstruction and viewing.

The display monitor in the viewing console is "refreshed" by a separate high-speed memory, to provide flicker-free images that may be viewed and manipulated without interrupting the computer's image reconstruction. This dual capability allows faster, more efficient diagnosis and speeds patient flow.

Holds more than 200 images.

The CT/T system's main memory disc can hold more than 200 images, 320 pixels in diameter. High-speed random access capability of this disc permits image retrieval in a matter of seconds, compared to minutes for tape systems. All computer functions are directed from a "conversational" keyboard/CRT display to simplify operation. A magnetic tape system for archival storage is included with the system.

If you'd like our new brochure with all the facts on the CT/T system, contact your GE representative or write GE Medical Systems, P.O. Box 414, Milwaukee, Wisconsin 53201. We want you to know more about CT/T: the fast-scan total body system backed by General Electric's corporate commitment to technology, product quality and service.

General Electric Medical Systems,
Milwaukee, Toronto, Madrid.

GE: leading the way in diagnostic imaging.

GENERAL ELECTRIC

Improving productivity is important to radiology departments. GE equipment can help make it happen.

GE: committed to helping x-ray departments do more.

The prime concern of any radiology department is serving patients. And the more efficient that service, the more everyone benefits. That's why GE is committed to providing systems that help your x-ray department make optimum use of time, space, resources and personnel. Here are some examples:

MMX system...optimum capability and efficiency for breast exams, with minimum patient apprehension.

This dedicated, self-contained system offers a wide variety of tube angulations and compression positions for virtually any breast projection. Today, in hundreds of hospitals, MMX™ is delivering high quality images of the entire area of interest, using xeroradiography or mammography, including new fast screen/low dose film procedures. The technologist can perform exams quickly and confidently, assured of minimum retakes.



Axillary view

Patient confidence is also increased, because the patient can maintain visual contact with the technologist throughout the exam.

Quantamat™ automatic exposure control provides correct exposure, regardless of breast size or firmness. This control assures consistent image density from one exam to the next. Resulting image quality is excellent, from craniocaudad views to axillary and mediolateral.

With this specialized system, any radiology room can become a dedicated breast examination area. Since no wall, ceiling or floor supports are needed, installation is fast and inexpensive. If departmental layout changes at a later date, the MMX system can be easily moved to a different room.

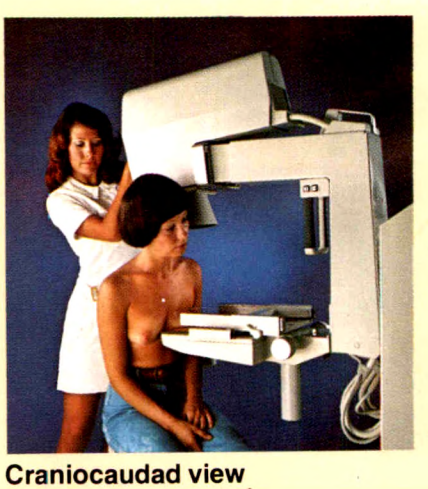
If seeing is believing, here's your opportunity to do so. Now, the ease and versatility of positioning and operating the MMX system are demonstrated in a new desk-top motion picture and related application guide. Featured are positioning directions, suggested technics, a critique of actual films and more. Ask your GE medical systems representative to arrange for a showing and a supply of application guides for your department.



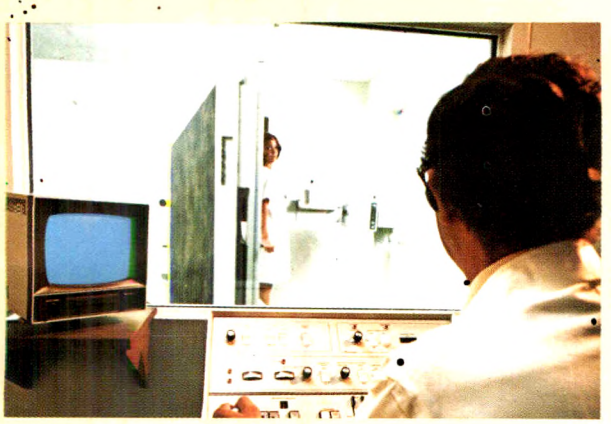
Mediolateral view



Supine mediolateral view



Craniocaudad view

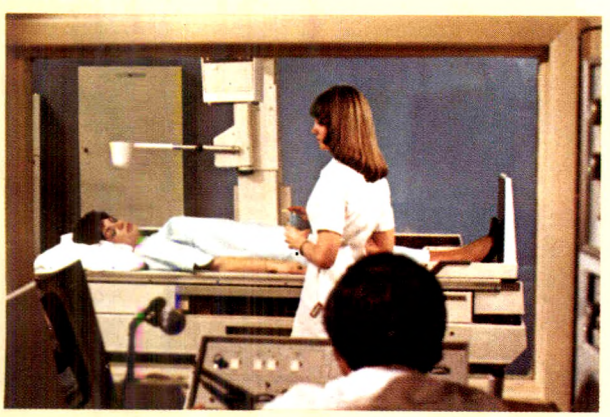


Televix remote control system... technic versatility provides more image information; improves patient flow.

Versatile, proven performance makes the Televix™ system the logical alternative to classical approaches. Any tableside R&F procedure can be handled by Televix remote control, with some very real advantages.

Maximum image information—plus better image quality—result from the system's optimized geometry (43-inch SID). And, there's greater convenience because of integrated multi-procedural capability... immediate changeover between fluoroscopy, Bucky radiography and true linear tomography. This significantly improves patient flow and, in many hospitals, results in operational cost savings up to 25%. In addition, there's reduced radiation exposure to the radiologist, because of total remote control. And, fewer retakes, less total time per examination means less exposure to patients too... the result of sharp fluoro images and immediate recording of precisely what has been viewed, as well as Quantamat™ automatic exposure control that provides the desired density in every image.

Televix system smoothly handles the full range of morning GI studies, including longitudinal oblique angle fluoroscopy in any scanning position, with 105 mm photospotting that can record up to 10 images per second, plus Bucky radiography. Then, in the afternoon, Televix takes on the department's high volume of radiographic and tomographic procedures.

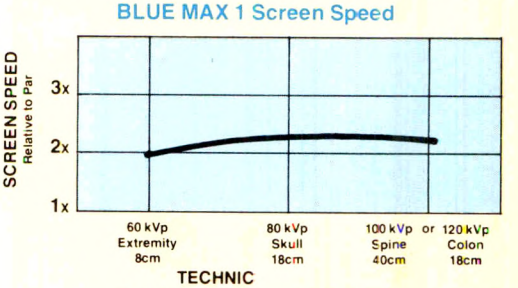


Blue Max screens... precise image quality and reduced radiation without drastic changes in equipment or technic.

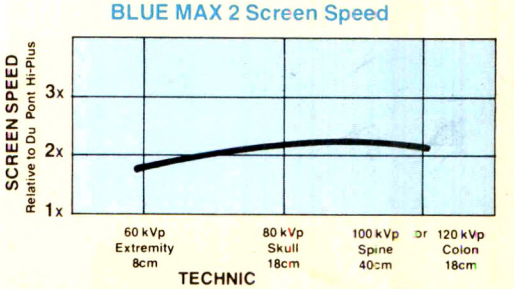


GE Blue Max™ screens provide maximum image quality and diagnostic data at much lower radiation levels than standard screens. Blue Max 1 and 2 intensifying screens feature GE-developed lanthanum oxybromide phosphors which absorb twice the x-rays, compared to standard calcium tungstate screens. Thus, Blue Max screens deliver the same image quality at half the mAs. This allows shorter exposure times, reducing motion unsharpness. Standard cassettes and any blue-sensitive film can be used. Blue Max screens are blue-emitting, so they require no unusual darkroom lighting or special processing techniques.

BLUE MAX 1 Screen Speed



BLUE MAX 2 Screen Speed



Blue Max screens' consistent 2x speed over the diagnostic kVp range makes modification of technic charts simple.

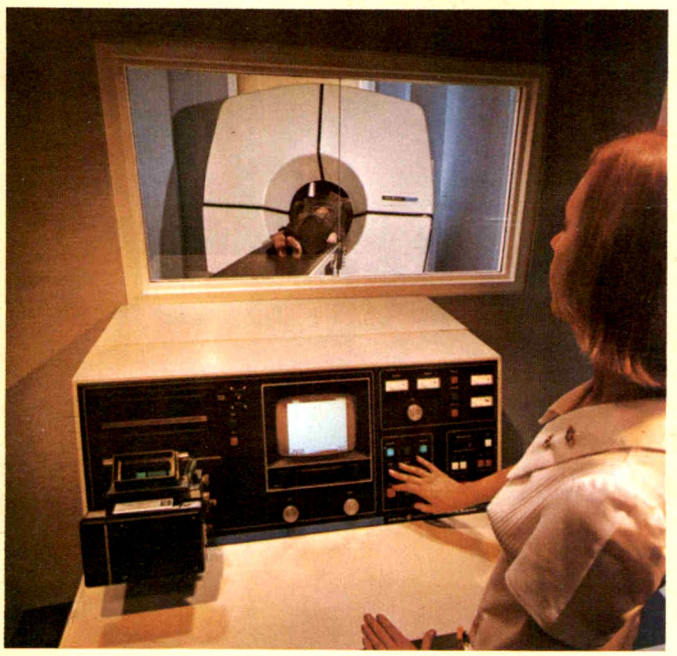
General Electric has many other time-saving, cost-saving systems to improve radiology productivity. Find out how these systems can help your x-ray department do more. Talk to your GE representative.
General Electric Medical Systems
Milwaukee, Toronto, Madrid

GE: leading the way in diagnostic imaging.

GENERAL ELECTRIC

Computed tomography from GE that combines image quality with ease of operation and patient·handling.

CT/N system: dedicated neurological scanning at moderate cost.





The CT/N system by General Electric provides quality images at moderate cost for institutions where the neurological case load justifies a dedicated head scanner. This GE computed tomography unit uses a pencil beam rectilinear scanning principle to accomplish 180° scans over a 24cm field. Since the anatomy is adequately immobilized during the procedure, image quality is high.

Efficient patient handling. The CT/N system allows convenient and precise patient positioning with a programmed two-way top. The table moves exact pre-selected distances between scans, minimizing patient handling. The angulating scanning gantry assembly facilitates proper plane alignment while comfortable patient head position is maintained; an especially important point with children.

Quick, easy image manipulation and recall. A window width control chooses the range of CT numbers (measure, 8, 16, 32, 64, 128 and 256); and a window level control sets the center of the range, between +512 and —512. CT/N system features Individual Patient Discs which store up to 8 images for permanent records. These scans can be displayed and manipulated at the console or at an optional independent viewing unit at any time.

Like all GE medical equipment, the CT/N system is backed by General Electric's corporate commitment to quality and service. If you'd like more details on how the CT/N system can give your institution dedicated neuro scanning at a realistic price, contact your GE representative.

General Electric Medical Systems, Milwaukee, Toronto, Madrid.

GE: leading the way in diagnostic imaging.

GENERAL ELECTRIC



Keep it up.

To the thousands of employers who have signed the Statement of Support for the Guard and Reserve, our sincere thanks. To those who haven't, please think it over. It's one of the best investments you can make. And a commitment to your own conscience.

A strong Guard and Reserve is an absolute must for America. Perhaps more so now than at anytime in our history. Today, this vital volunteer force represents almost 30% of our total military personnel needs—at a cost of only 5% of our entire defense budget.

You, as an employer, can help keep the Guard and Reserve trained and ready. This means *all* employers —the large, small, and those in between. Everyone who knows and values the freedom we live in.

Your signature on the Statement of Support is a pledge to back your employees who serve in the Guard and Reserve. It's an assurance that a couple of weeks on military duty won't limit their job opportunities. And for you, it means more productive, more responsible employees. Because in the Guard and Reserve they'll sharpen acquired skills and learn new ones, develop a real sense of leadership, add to their earnings and retirement benefits.

To receive your Statement of Support, or more information, write: EMPLOYER SUPPORT, Arlington, VA 22202.

Ad Council

A Public Service of This Magazine & The Advertising Council

ESGR
EMPLOYER SUPPORT OF
THE GUARD & RESERVE

The Clinac® 6X

Now A Solid 6MV Success!

A breakthrough in its own right as the first straight-through-beam rotational 6MV therapy machine, the Clinac 6X is winning immediate acceptance by clinicians. The reasons are clear–superb 6MV X-ray beam characteristics, proven reliable performance, low initial cost and excellent operational economy.

These unequalled benefits are possible because the Clinac 6X incorporates all the advanced human engineering features and major electronic sub-systems of the widely acclaimed Clinac 4. More than six years of clinical experience and engineering refinements are built into the new Clinac 6X right from the beginning.

See for yourself why the Clinac 6X is a solid success. Call or write Varian Radiation Division, 611 Hansen Way, Palo Alto, CA 94303. Tel: 415-493-4000. Worldwide sales and service.

varian

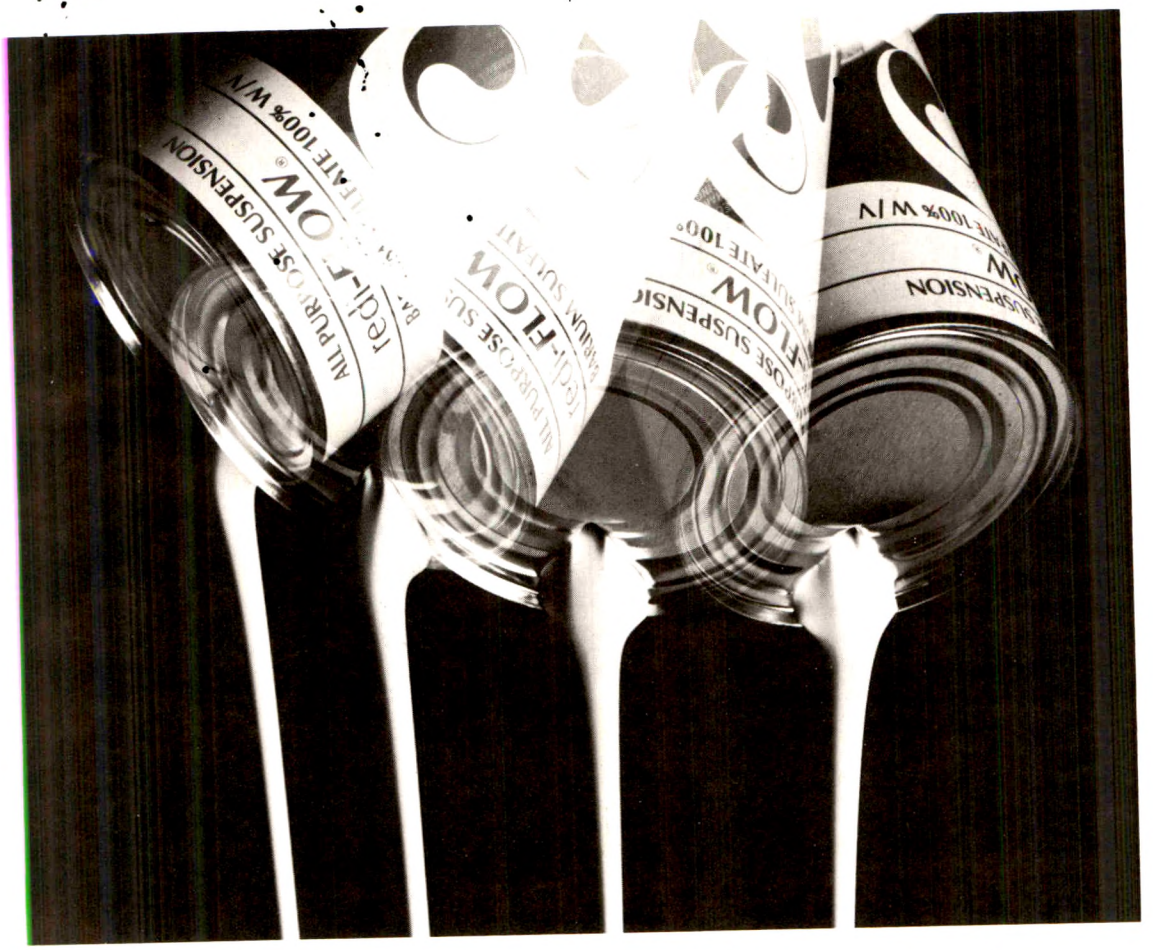


clinac 6X
120 130 140 150 160 170 180 190 200 210 220 230 240 250 260 270 280 290 300 310

INDEX TO ADVERTISERS

Atomic Energy of Canada xii
Barnes-Hind Pharmaceuticals ..... xxii, xxiii
CGR Medical Corporation ..... xlii, xliii
Eastman Kodak ..... xxxviii, xxxix
Elema-Schonander, Inc. vi
EMI Medical, Inc. ..... xvi, xvii
E-Z-EM Company xxxii
C. B. Fleet ..... xxiv, xxv
Flow Pharmaceuticals ..... Cover 3
The General Electric Company ..... l, li, lii, liii, liv
Hanley Medical Equipment Company xxiii
Philip A. Hunt Chemical Corporation ..... xl, xli
The Liebel-Flarsheim Company ii
Machlett Laboratories vii
Donald McElroy, Inc. x
C. V. Mosby Company xxi
Ortho Pharmaceutical Corporation xxix
Philips Medical Systems, Inc. ..... xlvi, xlvii
Picker Corporation ..... xxxiv, xxxv
The Purdue-Frederick Company v
Sakura Medical Corporation xxxiii
Searle Radiographics ..... i, xiii
Siemens Corporation ..... xxx, xxxi
E. R. Squibb & Sons, Inc. ..... viii, ix, xiv, xv, xviii, xix, xx, xxvi, xxvii, xxviii
Charles C Thomas · Publisher ..... xx, xxxvii
Union Carbide ..... x, xi
Universal Voltronics Corporation ..... Cover 2
University of Minnesota xxiii
Varian Associates ..... lvi, lviii

We try to present an accurate index. Occasionally this may not be possible because of a last-minute change or an omission.



redi-*FLOW*® puts convenience on tap-with four studies from one source.

Now—a presuspended, prehydrated barium preparation that's easy and economical to use in all gastro-intestinal radiological studies:

esophageal **upper G.I.** **routine enema** **air contrast enema**

Time-saving redi-Flow is flavored, concentrated, prehydrated, autoclaved, and homogenized.

Ready to use—with simple dilution directions for each type of study (no blender needed).

Produces consistent, uniform coating in all radiological examinations, including excellent readings in post-evacuation films.

Available in individual 16 fl. oz. cans; for added thrift, a plastic top is included to facilitate refrigeration for later use.

All-purpose Suspension redi-Flow (barium sulfate 100% W/V).

Simplifying without compromising



FLOW PHARMACEUTICALS, INC.
Palo Alto, CA. 94303

American Journal of Roentgenology

Vol. 126 June 1976 No. 6

DIAGNOSTIC RADIOLOGY

Hickey Lecture: New Frontier for Radiology: Computed Tomography. *R. G. Evens* 1117
Breast Patterns as an Index of Risk for Developing Breast Cancer. *J. N. Wolfe* 1130
Radiographic Visualization of Left Ventricular Aneurysms on Lateral Chest Film. *R. D. Kittredge, B. Gamboa, and H. G. Kemp* 1140
The Chest X-ray in Acute Left Ventricular Power Failure: An Aid to Determining Prognosis of Patients Supported by Intraaortic Balloon Pumping. *P. N. Cascade, A. Kantrowitz, W. J. Wajszczuk, and M. Rubenfire* 1147
Abnormal Left Ventricular Catheter Motion: An Ancillary Angiographic Sign of Left Atrial Myxoma. *J. M. Rausch, R. T. Reinke, K. L. Peterson, and C. B. Higgins* 1155
Evaluation of Routine Double Contrast Views of the Anterior Wall of the Stomach. *M. R. Goldsmith, R. E. Paul, Jr., W. E. Poplack, J. P. Moore, H. Matsue, and S. Bloom* 1159
Intussusception of the Appendix in Children. *G. O. Atkinson, B. B. Gay, Jr., and D. Naffis* 1164
Plain Film Findings of Gastric Volvulus Herniating into the Chest. *L. Menuck* 1169
Chondrosarcoma of the Esophagus. *I. Yaghmai and G. G. Ghahremani* 1175
Localized Giant Pseudopolyposis in Ulcerative Colitis. *J. W. Keating, Jr., and H. J. Mindell* 1178
Clinical and Radiographic "Reankylosis" Following Hip Surgery in Ankylosing Spondylitis. *D. Resnick, I. L. Dwosh, T. G. Goergen, R. F. Shapiro and R. D'Ambrosia* 1181
Medial Deviation of the Upper Pole Calyx on the Intravenous Urogram as an Indication of Vesicoureteral Reflux. *R. B. Harrison, S. S. Howards, and B. R. Thomas* 1189
Ultrasound Diagnosis of Posttransplant Renal Lymphocele. *J. F. Phillips, H. L. Neiman, and T. L. Brown* 1194
Pseudotumor of the Kidney: A Sequel to Regional Glomerulonephritis. *T. A. Depner, K. G. Ryan, and H. Yamauchi* 1197
Tortuosity of the Cavernous Carotid Arteries Causing Sellar Expansion Simulating Pituitary Adenoma. *R. D. Anderson* 1203
Serial Cerebral Angiography in Stereoscopic Magnification. *M. Takahashi, Y. Tamakawa, K. Goto, and M. Kosaka* 1211
Radiologic Changes in the Thymoma-Hypogammaglobulinemia Syndrome. *R. E. Moffat* 1219
Cerebro-Costo-Mandibular Syndrome: Long Term Follow-up of a Patient and Review of the Literature. *H. J. Williams and S. M. Sane* 1223
Intestinal Perforation Secondary to Nasojejunal Feeding Tubes. *R. L. Siegle, J. G. Rabinowitz, and C. Sarasohn* 1229
Lesion Conspicuity, Structured Noise, and Film Reader Error. *H. L. Kundel and G. Revesz* 1233
A Circular Test Pattern for Evaluating X-ray Tube Focal Spots. *G. H. Zeman, G. U. V. Rao, and R. J. Doyle* 1239

NUCLEAR MEDICINE

Lack of Gallium Uptake in Primary Hepatic Amyloidosis. *T. G. Goergen, A. Taylor, and N. Alazraki* 1246
Incidentally Detected Thrombosed Vein during ^{67}Ga Citrate Scanning. *C. H. Park, F. J. Miller, A. Lipton, and H. Harvey* 1249

RADIATION ONCOLOGY

Electron Beam Therapy in Head and Neck Tumors. *D. A. Tobin, W. Hall, and R. M. Scott* 1251
Surgical Treatment of Advanced Carcinoma of the Floor of the Mouth. *O. M. Guillamondegui and R. H. Jesse* 1256
Central Axis Depth Dose for a 2.5 MV Van de Graaff Generator. *D. W. Anderson, D. E. Raeside, R. I. Adams, and M. R. Goede* 1260

SPECIAL SECTION: International Bone Mineralization Conference Abstracts 1266

Editorial: Bone Mineral Measurement. *J. P. Whalen* 1315
77th ARRS Meeting Announcement and Preliminary Program 1316
Memorial: Paul A. Bishop 1325
News 1327
Literature Abstracts 1331
Volume Index 1339